The McGraw-Hill Companies

POWER SYSTEM ENGINEERING

Second Edition

About the Authors

D P Kothari is Professor, Centre for Energy Studies, Indian Institute of Technology, Delhi. He has been Head of the Centre for Energy Studies (1995–97) and Principal (1997–98) Visvesvaraya Regional Engineering College, Nagpur. He has been Director-incharge, IIT Delhi (2005), Deputy Director (Admn.) (2003–2006). Earlier (1982–83 and 1989), he was a visiting fellow at RMIT, Melbourne, Australia. He obtained his BE, ME and Ph.D degrees from BITS, Pilani. A fellow of the Institution of Engineers (India), fellow of National Academy of Engineering, fellow of National Academy of Sciences, Senior Member IEEE, Member IEE, Life Member ISTE, Professor Kothari has published/presented around 500 papers in national and international journals/conferences. He has authored/co-authored more than 18 books, including *Power System Optimization, Modern Power System Analysis, Electric Machines, Power System Transients, Theory and Problems of Electric Machines and Basic Electrical Engineering*. His research interests include power system control, optimization, reliability and energy conservation. He has received the National Khosla award for Lifetime Achievements in Engineering for 2005 from IIT Roorkee.

I J Nagrath is Adjunct Professor, BITS, Pilani, and retired as Professor of electrical engineering and Deputy Director of Birla Institute of Technology and Science, Pilani. He obtained his BE with Hons. in electrical engineering from the University of Rajasthan in 1951 and MS from the University of Wisconsin in 1956. He has co-authored several successful books which include *Electric Machines, Modern Power System Analysis* and *Systems: Modelling and Analysis*. He has also published several research papers in prestigious national and international journals.

Other books by the same authors

978 007 0435896	KOTHARI & NAGRATH	Basic Electrical Engineering, 2e
978 007 0583771	KOTHARI & NAGRATH	Electric Machines, 3e
978 007 0494893	KOTHARI & NAGRATH	Modern Power System Analysis, 3e
978 007 0616660	KOTHARI & NAGRATH	Electric Machines (Sigma Series)

The McGraw-Hill Companies

POWER SYSTEM ENGINEERING

Second Edition

D P KOTHARI
Professor, Centre for Energy Studies
Former Deputy Director (Admn.)
Indian Institute of Technology
New Delhi
Former Principal, V.R.C.E., Nagpur
Former Director-Incharge, IIT Delhi

I J NAGRATH
Adjunct Professor, BITS
Professor of Electrical Engineering and Deputy Director (Retd.)
Birla Institute of Technology and Science
Pilani

Tata McGraw-Hill Publishing Company Limited
NEW DELHI

McGraw-Hill Offices

New Delhi New York St Louis San Francisco Auckland Bogotá Caracas
Kuala Lumpur Lisbon London Madrid Mexico City Milan Montreal
San Juan Santiago Singapore Sydney Tokyo Toronto

The McGraw-Hill Companies

Tata McGraw-Hill

Published by the Tata McGraw-Hill Publishing Company Limited,
7 West Patel Nagar, New Delhi 110 008.

Power System Engineerng, 2e

ISBN-13: 978-0-07-0647916

ISBN-10: 0-07-0647917

General Manager—Publishing: SEM & Tech Ed: *Vibha Mahajan*
Asst. Sponsoring Editor: *Shalini Jha*
Executive—Editorial Services: *Sohini Mukherjee*

General Manager—Marketing : Higher Education & School: *Michael J. Cruz*
Product Manager—SEM & Tech Ed.: *Biju Ganesan*

Controller—Production: *Rajender P. Ghansela*
Asst. General Manager—Production: *B. L. Dogra*
Senior Proof Reader—*Suneeta S. Bohra*

Typeset at Script Makers, 19, A1-B, DDA Market, Paschim Vihar, New Delhi 110 063, text and cover printed at Rashtriya Printers, M-135, Panchsheel Garden, Naveen Shahdara, Delhi -110 032

RBXCRRQYDDQCD

The McGraw-Hill Companies

To my wife
Shobha

—D P Kothari

To my wife
Pushpa

—I J Nagrath

Contents

Preface to the Second Edition

The excellent response to the first edition of the book by students and faculty of Indian and foreign universities and the practicing engineers has motivated the authors to venture for the second edition. The main aim was to include the latest developments in the field of power system engineering.

A large number of teaching appendices of the first edition has now been rewritten as full-fledged chapters, since all these topics continue to be important and are part of the curriculum. We hope students and teachers will welcome this.

This edition covers a wide variety of topics in power system engineering which are normally not found in a single volume. Since the appearance of the first edition in 1994, the overall energy situation has changed considerably and this has generated great interest in nonconventional and renewable energy sources, energy conservation, energy management, power reforms and restructuring and distributed/dispersed generation. Chapter 1 has been therefore, enlarged and completely re-written. In addition, the influences of environmental constraints are also discussed.

In Chapter 6, load flow under power electronic control, that is, AC-DC-LF has been added. In Chapter 7, maintenance scheduling, power system reliability, have been included. For the first time, unit commitment has been further elaborated as an appendix to Chapter 7 In Chapter 8, AGC of restructured power system is added, keeping in line with the latest changes in the power sector.

In Chapter 4, a few more sections/topics such as power transformer have been added. In chapters 2 and 3, magnetic field induction and electrostatic induction have been added, respectively. In Chapter 5, voltage control topic has been boosted by including control by midline boosters. Two appendices, K and I of the first edition on lightning phenomenon and neutral grounding, have now been brought in the main chapters as per the wishes of readers for completeness and clarity. In Chapter 14, new topics such as isolators, fuses and contractors, kilometric faults have now been included as per the review reports. In Chapter 15, numerical (digital) relay has now been introduced along with new trends.

The present edition, like the earlier one, is designed for a two-semester course at the undergraduate level or for first-semester postgraduate study.

With all these features, this is an indispensable text for electrical engineering students. AMIE, GATE, and UPSC Engineering services and IAS candidates along with practicing engineers would also find this book extremely valuable as a text/reference book.

A first-level PG course may be taught from sections (1.17, 1.18) chapters 6, 7, 8, sections 9.6, 9.7, 11.7, chapters 12, 13, 15, 20, 22. For UG courses a combination of chapters may be chosen depending on the syllabus of a university and type of the course.

Salient Features

- Recent developments in various power system topics included
- Computational algorithm for various system studies presented
- Large number of solved examples and unsolved problems with answers presented at the end of each chapter for practice and self-evaluation
- New chapter added on voltage stability
- Old appendices of the first edition have been enlarged into full-fledged chapters 16–21 such as HVDC and Distribution Systems
- New appendices on:
  MATLAB and SIMULINK demonstrating their use in problem solving
  Real time computer control of power systems
  Power Quality

MATLAB and SIMULINK ideal programs for power system analysis are included in this book as an appendix along with 18 solved examples illustrating their use in solving representative power system problems.

A new chapter on voltage stability has been added. A new appendix on real time computer control of power systems has also been added to more students aware of latest methods of power system control and monitoring in load dispatch centers. A new appendix on power quality has also been included.

Tata McGraw-Hill and the authors would like to thank the following reviewers of this edition: Prof. S. Dasgupta of S.I.T. Siliguri, Prof. P. R. Bijwe of I.I.T. Delhi, Prof. S. Roy of B.I.T.S. Pilani, PG and doctoral students of the first author, Mr. Sunil Bhat of VNIT Nagpur, Mr. Jayaprakash of GCEK Kerala, Mr. Praveen Verma, Mr. Abhishek Rathore, Mr. Jitender Malik, Mr. Vijay Pratap, Mr. Rajeev Ranjan Kumar, Mr. Sivananda, Dr. Subir Sen of Power Grid, Dr. Shekhar of Alstrom, Mr. K.P. Singh of NPTI Guwahati for their help in preparing the manuscript.

We would also like to express our heartfelt thanks to Dr. R.N. Patel of IIT Roorkee, Dr. S. N. Tiwari of Motilal Nehru National Institute of Technology, Allahabad, Prof. Subhasish Banerjee and Prof. Ashok Kumar Basu of Calcutta Institute of Engineering and Management, Kolkata, Prof. K. Chandra Sekhar of RVR and JC College of Engineering, Guntur, Dr. M.R. Mohan of College of Engineering, Guindy, Anna University, Dr. K. Shanthi Swarup of IIT Madras and Prof. Hiren Dinker Mehta of Government Engineering College, Gandhinagar, for their valuable feedback.

While revising the text, we have been greatly encouraged by many colleagues, students and practicing engineers, reviewers who used the earlier edition of this book. All these individuals have influenced this edition. We express our thanks and appreciation to them. We hope this support/response would continue in the future also.

We also thank TMH personnel and our families who supported us during this period and given all possible help so that this book can see the light of the day.

New Delhi
June 2007

D.P. Kothari
I.J. Nagrath

Preface to the First Edition

Mathematical modelling and solutions on digital computers constitute an extremely viable approach to system analysis and planning studies for a modern-day power system with its large size and complex and integrated nature. A stage has, therefore, been reached where an undergraduate must be trained in the latest techniques of analysis of large-scale power systems. A similar need also exists in the industry where a practicing power system engineer is constantly faced with the challenge of the rapid advances in the field. This book has been designed to fulfil this need by integrating the basic principles of power system analysis illustrated through the simplest system structure with analysis techniques for practical size systems. In this book large-scale system analysis follows as a natural extension of the basic principles. The form and level of some of the well-known techniques are presented in such a manner that undergraduates can easily grasp and appreciate them.

The book covers a wide variety of topics in power system engineering which are normally not found in a single volume. The book is written in such a comprehensive manner that at least three courses on power systems can be designed—one at the postgraduate level and a two-semester sequence at the undergraduate level.

The reader is expected to have a prior grounding in circuit theory and electrical machines. He should also have been exposed to Laplace transform, linear differential equations, elementary optimization techniques and a first course in control theory. Matrix analysis is applied throughout the book. However, a knowledge of simple matrix operations would suffice and these are summarized in an appendix for quick reference.

The digital computer is an indispensable tool for power system analysis, and therefore, computational algorithms for various system studies such as load flow, fault level analysis, stability, etc. have been included at appropriate places in the book. The students should be encouraged to design computer programs for these studies using the algorithms provided. Further, the students can be asked to pool the various programs for more advanced and sophisticated studies such as optimal scheduling. A novel feature of the book is the inclusion of current trends that are practically useful such as unit commitment, generation reliability, optimal thermal scheduling, optimal hydrothermal scheduling and decoupled load flow.

The introductory chapter presents a discussion of various methods of electrical energy generation including renewable energy sources and their techno-economic comparison. The reader is also exposed to the Indian power scenario.

Chapters 2 and 3 provide the transmission line parameters and these are included for the sake of completeness of the text. Chapter 4 on the representation of power system components highlights the steady state model of the synchronous machine and the circuit models of composite power systems along with the per unit method.

Chapter 5 deals with the performance of transmission lines. The load flow problem is introduced at this stage through the simple two-bus system and basic concepts of watt and var control are illustrated. A brief treatment of circle diagrams is included as this forms an excellent teaching aid for putting across the concept of load flow and line compensation.

Chapter 6 elaborates on power network modelling and important techniques of load flow analysis like Gauss–Siedel, Newton–Raphson and decoupled load flow. Chapter 7 deals with optimal system operation for both thermal and hydrothermal systems. A rigorous treatment for thermal system is also presented.

Chapter 8 deals with load frequency control wherein both conventional and modern control approaches have been adopted for analysis and design. The chapter also covers the treatment of generation rate constraint.Voltage control is also discussed briefly.

Chapters 9–11 discuss fault studies (abnormal system operation). The synchronous machine model for transient studies is heuristically introduced to the reader. Z_{BUS} algorithm is presented and its use illustrated for both symmetrical and unsymmetrical faults.

Chapter 12 elaborates upon the concepts of various types of stability in power system. In particular, the concept of transient stability is well illustrated through the equal area criterion. The classical numerical solution technique of the swing equation as well as the algorithm for large system stability are also dealt with. A step-by-step solution of a 3-machine stability problem is presented.

Chapter 13 deals with power system transients. Topics such as traveling waves or propagation of surges, generation of over-voltages on lines, insulation coordination are discussed at length.

Chapter 14 presents a detailed account of various types of circuit breakers including HVDC breakers. Methods of testing circuit breakers are also explained.

Chapter 15 covers the important topic of power system protection. It includes an exhaustive survey of relaying schemes and also deals with the different types of protective relays used for the protection of various parts of power systems along with their theory, threshold characteristics as well as their merits and demerits. Microprocessor based relaying is also briefly explained.

A large number of appendices have been provided to deal with topics such as Cables, Insulators, Sag and Tension, Neutral Grounding, Corona, Lightning Phenomena, HVDC and Distribution Systems. These topics are still being taught and continue to be very important.

Every concept and technique presented is supported through examples employing a two-bus structure while at times, three- and four-bus illustrations have also been used. A large number of unsolved problems with their answers are included at the end of each chapter. These have been so selected that apart from providing a drill they help the reader to develop a deeper insight and illustrate some points beyond what is directly covered by the text.

The organization of various chapters is flexible and permits the teacher to mould them to the particular needs of the class and curriculum. If desired, some of the advanced level topics could be bypassed without loss of continuity. The style of writing is amenable to self-study.

We are indebted to our colleagues at the Birla Institute of Technology and Science, Pilani, and the Indian Institute of Technology, Delhi, for their encouragement and various useful suggestions. We are also grateful to the authorities at BITS, Pilani, and IIT, Delhi, for providing the facilities necessary for writing this book. Further, we would like to thank the National Book Trust for subsidizing the production of the book and thereby facilitating its availability at an affordable price. We welcome any constructive criticism and will be grateful for any appraisal by the readers.

I.J. Nagrath
D.P. Kothari

Chapter 1
Introduction

1.1 ELECTRIC POWER SYSTEM

We are in need of energy for our industrial, commercial and day-to-day activities, and we use energy in different forms. Out of all the forms of energy, electric energy is the most important one as it can be generated (actually converted from other forms of energy) efficiently, transmitted easily and utilized ultimately at a very reasonable cost. The ease of transmission of electric energy gives rise to a possibility of generating (converting) electric energy in bulk at a centralized place and transmit it over a long distance to be used ultimately by a large number of users. If we generate in small scale, say for example, just to light a house, we can perhaps intutively make the connections needed for a reasonably reliable and efficient operation. But when we have generation in bulk, transmission over a long distance and utilization by a number of distributed users; we cannot do by intution. We need to follow systematic methodology to have reliable, efficient, economic and safe use of electric energy. The components needed for generation, transmission and large-scale distribution of electric energy form a huge complex system termed as **Electric Power System**. Power system is the branch of Electrical Engineering where we study in depth for its design, operation, maintenance and analysis.

Electric power systems are a technical wonder and as per one opinion [27], electricity and its accessibility are the greatest engineering achievements of the 20th century, ahead of computers and airplanes. A modern society cannot exist without electricity. As will be explained in Secs 1.17 and 1.18, todays centralized (regulated) utilities will be distributed (deregulated) when tomorrow utilities (SEBs) have been forced to breakup in separate generation, and T/D companies. There is DG (distributed generation) by IPP (independent power producers), who can generate electric power by whatever means and must be allowed access (open access) to the power grid to sell power to consumers. The breakup has been encouraged by tremendous benefits of deregulation in communication and airline industries resulting in fierce competition leading to economy and better consumer service. In India, some

states are pursuing this deregulation and unbundling aggressively and some more cautiously. The aim is that the independent Transmission System Operators (TSO) wheel power for a charge from anywhere and anyone to the customer site.

Reliable Operation is ensured by the TSOs and the financial transactions are governed by real time bidding to buy and sell power to earn profit in the spot market. (Buying at lower prices and selling at higher prices).

1.2 INDIAN POWER SECTOR

Historical Background

More than 100 years back in 1890s first hydro power plant was commissioned in Darjeeling. At the time of independence, total installed capacity was 1360 MW (mostly owned by private companies in cities). After the enactment of Electricity (Supply) Act in 1948, barring few licenses, the entire Power Sector was owned by State Governments and largely managed by vertically integrated State Electricity Boards (SEBs). In 1975, Central Government, through Central Public Sector Undertakings, (NTPC etc.) also entered in the field of Generation and Transmission to supplement the efforts of cash starved State Electricity Boards. In 1989 Power Grid Corporation of India was formed to develop the transmission network and grid. In 1990 first HVDC bi-pole line was made operative. In 1990, power generation was opened to private sector. In 1998 Electricity Regulatory Commission Act was enacted for establishing Regulatory Commissions. Tariff is now obtained through competitive bidding to be adopted by the regulator. Congestion is managed by e-bidding.

In 1998 first 765 kV Transmission line was erected which was initially charged at 400 kV. In 2003 Electricity Act 2003 was enacted to have open access in transmission. In 2005–06 National Electricity Plan was finalized. In 2006 a big step was taken for formulation of national grid [Fig. 1.1(a)] by way of synchronization of NR with ER-NER-WR. In 2007, 765 kV transmission will be a reality. In 2010–11, 800 kV HVDC bi-pole line will start operating. Challenge is evacuation of power along with generation addition and also from surplus to deficit area. As of today (2007) India has an energy shortage of 7.8% and peak shortage of 11.23%.

1.3 A CONTEMPORARY PERSPECTIVE

Electric energy is an essential ingredient for the industrial and all-round development of any country. It is a coveted form of energy, because it can be generated centrally in bulk and transmitted economically over long distances. Further, it can be adapted easily and efficiently to domestic and industrial

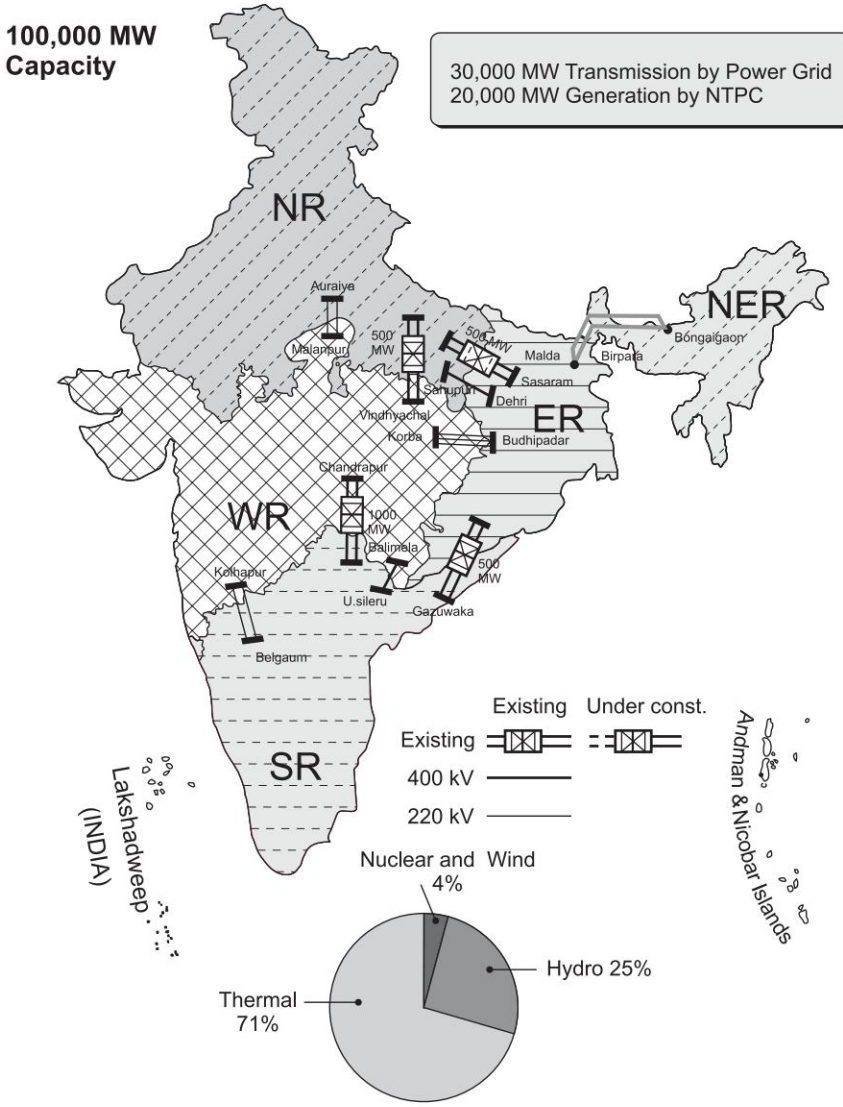

	Power grid	SEBs	Total
HVDC	1,632	1,504	3,136
800 kV	550	400	950
400 kV	32,500	13,000	45,500
220/132 kV	9,000	206,000	215,000

Figures in Circuit kms

Fig. 1.1(a) Development of Indian Grid (*Courtesy ALSTOM*)

applications, particularly for lighting purposes and mechanical work*, e.g. drives. The per capita consumption of electrical energy is a reliable indicator of a country's state of development—figures for 2006 are 650 kWh for India and 5600 kWh for UK and 15000 kWh for USA, world average is 3000 kWh.

Conventionally, electric energy is obtained by conversion from fossil fuels (coal, oil, natural gas), nuclear and hydro sources. Heat energy released by burning fossil fuels or by fission of nuclear material is converted to electricity by first converting heat energy to the mechanical form through a thermocycle and then converting mechanical energy through generators to the electrical form. Thermocycle is basically a low efficiency process—highest efficiencies for modern large size plants range up to 40%, while smaller plants may have considerably lower efficiencies. The earth has fixed non-replenishable resources of fossil fuels and nuclear materials, with certain countries overendowed by nature and others deficient. Hydro energy, though replenishable, is also limited in terms of power. The world's increasing power requirements can only be partially met by hydro sources. Furthermore, ecological and biological factors place a stringent limit on the use of hydro sources for power production. (The USA has already developed around 50% of its hydro potential and hardly any further expansion is planned because of ecological considerations.)

With the ever increasing per capita energy consumption and exponentially rising population, technologists already see the end of the earth's non-replenishable fuel resources.† The oil crisis of the 1970s has dramatically drawn attention to this fact. In fact, we can no longer afford to use oil as a fuel for generation of electricity. In terms of bulk electric energy generation, a distinct shift is taking place across the world in favour of coal and in particular nuclear sources for generation of electricity. Also, the problems of air and thermal pollution caused by power generation have to be efficiently tackled to avoid ecological disasters. A coordinated worldwide action plan is, therefore, necessary to ensure that energy supply to humanity at large is assured for a long time and at low economic cost. Some of the factors to be considered and actions to be taken are:

Curtailment of Energy Consumption

The energy consumption of most developed countries has already reached a level, which this planet cannot afford. There is, in fact, a need to find ways and means of reducing this level. The developing countries, on the other hand, have

* Electricity is a very inefficient agent for heating purposes, because it is generated by the low efficiency thermocycle from heat energy. Electricity is used for heating purposes for only very special applications, say an electric furnace.

† Varying estimates have been put forth for reserves of oil, gas and coal and fissionable materials. At the projected consumption rates, oil and gases are not expected to last much beyond 50 years; several countries will face serious shortages of coal after 2200 A.D. while fissionable materials may carry us well beyond the middle of the next century. These estimates, however, cannot be regarded as highly dependable.

to intensify their efforts to raise their level of energy production to provide basic amenities to their teeming millions. Of course, in doing so they need to constantly draw upon the experiences of the developed countries and guard against obsolete technology.

Intensification of Efforts to Develop Alternative Sources of Energy Including Unconventional Sources like Solar, Tidal Energy, etc.

Distant hopes are pitched on fusion energy but the scientific and technological advances have a long way to go in this regard. Fusion when harnessed could provide an inexhaustible source of energy. A break-through in the conversion from solar to electric energy could provide another answer to the world's steeply rising energy needs.

Recycling of Nuclear Wastes

Fast breeder reactor technology is expected to provide the answer for extending nuclear energy resources to last much longer.

Development and Application of Antipollution Technologies

In this regard, the developing countries already have the example of the developed countries whereby they can avoid going through the phases of intense pollution in their programmes of energy development. Bulk power generating stations are more easily amenable to control of pollution since centralized one-point measures can be adopted.

Electric energy today constitutes about 30% of the total annual energy consumption on a worldwide basis. This figure is expected to rise as oil supply for industrial uses becomes more stringent. Transportation can be expected to go electric in a big way in the long run, when non-conventional energy resources are well developed or a breakthrough in fusion is achieved.

To understand some of the problems that the power industry faces let us briefly review some of the characteristic features of generation and transmission. Electricity, unlike water and gas, cannot be stored economically (except in very small quantities—in batteries), and the electric utility can exercise little control over the load (power demand) at any time. The power system must, therefore, be capable of matching the output from generators to the demand at any time at a specified voltage and frequency. The difficulty encountered in this task can be imagined from the fact that load variations over a day comprises three components—a steady component known as **base load**; a varying component whose daily pattern depends upon the time of day; weather, season, a popular festival, etc.; and a purely randomly varying component of relatively small amplitude. Figure 1.1(b) shows a typical daily load curve. The characteristics of a daily load curve on a gross basis are indicated by **peak load,** and the time of its occurrence and *load factor* defined as

$$\frac{\text{average load}}{\text{maximum (peak) load}} = \text{less than unity}$$

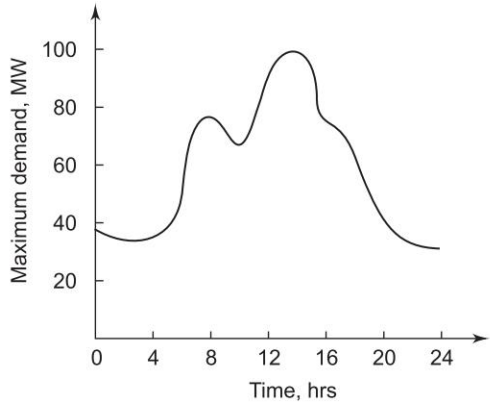

Fig. 1.1(b) Typical daily load curve

The average load determines the energy consumption over the day, while the peak load along with considerations of standby capacity determines plant capacity for meeting the load.

A high load factor helps in drawing more energy from a given installation. As individual load centres have their own characteristics, their peaks in general have a time diversity, which when utilized through transmission interconnection, greatly aids in jacking up load factors at an individual plant—excess power of a plant during light load periods is evacuated through long distance high voltage transmission lines, while a heavily loaded plant receives power.

Diversity Factor

This is defined as the sum of individual maximum demands on the consumers, divided by the maximum load on the system. This factor gives the time diversification of the load and is used to decide the installation of sufficient generating and transmission plant. If all the demands came at the same time, i.e. unity diversity factor, the total installed capacity required would be much more. Luckily, the factor is much higher than unity, especially for domestic loads.

A high diversity factor could be obtained by:

1. Giving incentives to farmers and/or some industries to use electricity in the night or light load periods.
2. Using day-light saving as in many other countries.
3. Staggering the office timings.
4. Having different time zones in the country like USA, Australia, etc.
5. Having two-part tariff in which consumer has to pay an amount dependent on the maximum demand he makes, plus a charge for each unit of energy consumed. Sometimes consumer is charged on the basis of kVA demand instead of kW to penalize loads of low power factor.

   Two other factors used frequently are:

Plant capacity factor

$$= \frac{\text{Actual energy produced}}{\text{maximum possible energy that could have been produced (based on installed plant capacity)}}$$

$$= \frac{\text{Average demand}}{\text{Installed capacity}}$$

Plant use factor

$$= \frac{\text{Actual energy produced (kWh)}}{\text{plant capacity (kW)} \times \text{Time (in hours) the plant has been in operation}}$$

Tariffs

The cost of electric power is normally given by the expression ($a + b \times \text{kW} + c \times \text{kWh}$) per annum, where a is a fixed charge for the utility, independent of the power output; b depends on the maximum demand on the system and hence on the interest and depreciation on the installed power station; and c depends on the units produced and therefore on the fuel charges and the wages of the station staff.

Tariff structures may be such as to influence the load curve and to improve the load factor.

Tariff should consider the pf (power factor) of the load of the consumer. If it is low, it takes more current for the same kWs and hence T and D (transmission and distribution) losses are correspondingly increased. The power station has to install either pf correcting (improvement) devices such as synchronous capacitors, SVC (Static Var Compensator) or voltage regulating equipment to maintain the voltages within allowed limits and thus total cost increases. One of the following alternatives may be used to avoid low pf:

(i) to charge the consumers based on kVA rather than kW.
(ii) a pf penalty clause may be imposed on the consumer.
(iii) the consumer may be asked to use shunt capacitors for improving the power factor of his installations.

Availability Based Tariffs (ABT)*

ABT comprises three main components viz. capacity charge, energy charge and charges for deviation from schedule.

1. Capacity charge, towards reimbursement of the fixed cost of the plant, linked to the plant's capacity to supply MWs.
2. Energy charge, to reimburse the fuel cost for scheduled generation and

* The term Availability Tariff, particularly in the Indian context, stands for a rational tariff structure for power supply from generating stations, on a contracted basis. In the availability tariff mechanism, the fixed and variable cost components are treated separately. The payment of fixed cost to the generation company is linked to availability of the plant, i.e. its capability to deliver MWs on a day-by-day basis.

The reader may refer to 'ABC of ABT by Mr. Bhanu Bhushan of Central Electricity Regulatory Commission (27.6.2005) for further details.

3. Payment for deviations from schedule at a rate dependent on system conditions. The last component would be negative in case the power plant is delivering less power than scheduled. For example: If a power plant delivers 600 MW while it was scheduled to supply only 500 MW, the energy charge payment would be for the scheduled generation (500 MW) only, and the excess generation (100 MW) would be paid for at a certain rate.

If the grid has surplus power at that time and frequency is above 50 Hz. The rate would be small. If the excess generation is at the time of generation deficit in the system (frequency below 50.0 Hz) the payment for extra generation would be at higher rate.

If frequency (F) is 49 Hz or below, UI (unscheduled interchange) prices is maximum (570 paise per unit), and the price is minimum (zero paisa), when frequency is 50.5 Hz or above. [see Fig. 1.2].

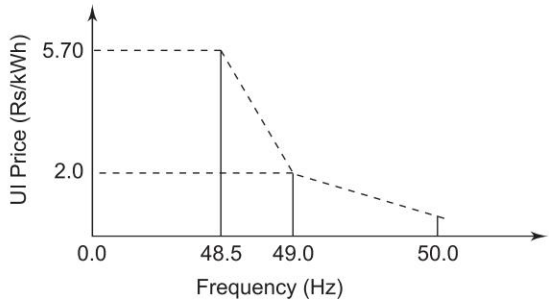

Fig. 1.2

– If frequency is in between 49.0 Hz and 50 Hz, the UI prices varies linearly as, UI rate = 187–3.7f.
– If frequency is in between 50 Hz and 50.5 Hz, the UI price is given by UI rate = 202–4.0 × f.
– Maximum value of ABT is fixed, according to the cost of generation of the costliest generating unit (diesel generating plants).

ABT has been successfully adopted for maintaining the grid discipline and already been implemented in Western Region w.e.f. 1.7.2002, in Northern Region w.e.f. 1.12.2002 and in Southern Region w.e.f. 1.1.2003.

Example 1.1 A factory to be set up is to have a fixed load of 760 kW at 0.8 pf. The electricity board offers to supply energy at the following alternate rates:
(a) LV supply at Rs 32/kVA max demand/annum + 10 paise/kWh
(b) HV supply at Rs 30/kVA max demand/annum + 10 paise/kWh
The HV switchgear costs Rs 60/kVA and switchgear losses at full load amount to 5%. Interest, depreciation charges for the switchgear are 12% of the capital cost. If the factory is to work for 48 hours/week, determine the more economical tariff.

Solution

$$\text{Maximum demand} = \frac{760}{0.8} = 950 \text{ kVA}$$

Loss in switchgear = 5%

$$\therefore \quad \text{Input demand} = \frac{950}{0.95} = 1000 \text{ kVA}$$

Cost of switchgear = 60 × 1000 = Rs 60,000

Annual charges on depreciation = 0.12 × 60,000 = Rs 7,200

Annual fixed charges due to maximum demand corresponding to tariff (b)

= 30 × 1,000 = Rs 30,000

Annual running charges due to kWh consumed

= 1000 × 0.8 × 48 × 52 × 0.10

= Rs 1,99,680

Total charges/annum = Rs 2,36,880

Max. demand corresponding to tariff (a) = 950 kVA

Annual fixed charges = 32 × 950 = Rs 30,400

Annual running charges for kWh consumed

= 950 × 0.8 × 48 × 52 × 0.10

= Rs 1,89,696

Total = Rs 2,20,096

Therefore, tariff (a) is economical.

Example 1.2 A region has a maximum demand of 500 MW at a load factor of 50%. The load duration curve can be assumed to be a triangle. The utility has to meet this load by setting up a generating system, which is partly hydro and partly thermal. The costs are as under:

Hydro plant: Rs 600 per kW per annum and operating expenses at 3p per kWh.

Thermal plant: Rs 300 per kW per annum and operating expenses at 13p per kWh.

Determine the capacity of hydro plant, the energy generated annually by each, and overall generation cost per kWh.

Solution

Total energy generated per year = 500 × 1000 × 0.5 × 8760

$= 219 \times 10^7$ kWh

Figure 1.3 shows the load duration curve. Since operating cost of hydro plant is low, the base load would be supplied from the hydro plant and peak load from the thermal plant.

Let the hydro capacity be P kW and the energy generated by hydro plant E kWh/year.

Thermal capacity = (5,00,000 – P) kW

Thermal energy = $(219 \times 10^7 - E)$ kWh

Annual cost of hydro plant

$$= 600P + 0.03E$$

Annual cost of thermal plant

$$= 300(5{,}00{,}000 - P) + 0.13 (219 \times 10^7 - E)$$

Total cost $C = 600P + 0.03E + 300(5{,}00{,}000 - P) + 0.13 (219 \times 10^7 - E)$

For minimum cost, $\frac{dC}{dP} = 0$

$$\therefore \quad 600 + 0.03 \frac{dE}{dP} - 300 - 0.13$$

$$\frac{dE}{dP} = 0$$

or $$dE = 3000\, dP$$

But $$dE = dP \times t$$

$$\therefore \quad t = 3000 \text{ hours}$$

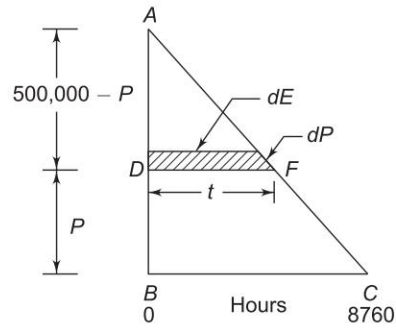

Fig. 1.3 Load duration curve

From ΔADF and ΔABC,

$$\frac{5{,}00{,}000 - P}{5{,}00{,}000} = \frac{3000}{8760}$$

$$\therefore \quad P = 328, \text{ say } 330 \text{ MW}$$

Capacity of thermal plant = 170 MW

$$\text{Energy generated by thermal plant} = \frac{170 \times 3000 \times 1000}{2}$$

$$= 255 \times 10^6 \text{ kWh}$$

Energy generated by hydro plant = 1935×10^6 kWh

Total annual cost = Rs 340.20×10^6/year

$$\text{Overall generation cost} = \frac{340.20 \times 10^6}{219 \times 10^7} \times 100$$

= 15.53 paise/kWh

Example 1.3 A generating station has a maximum demand of 25 MW, a load factor of 60%, a plant capacity factor of 50%, and a plant use factor of 72%. Find (a) the daily energy produced, (b) the reserve capacity of the plant, and (c) the maximum energy that could be produced daily if the plant, while running as per schedule, were fully loaded.

Solution

$$\text{Load factor} = \frac{\text{average demand}}{\text{maximum demand}}$$

$$0.60 = \frac{\text{average demand}}{25}$$

$$\therefore \quad \text{Average demand} = 15 \text{ MW}$$

$$\text{Plant capacity factor} = \frac{\text{average demand}}{\text{installed capacity}}$$

$$0.50 = \frac{15}{\text{installed capacity}}$$

$$\therefore \quad \text{Installed capacity} = \frac{15}{0.5} = 30 \text{ MW}$$

$\therefore$ Reserve capacity of the plant = installed capacity – maximum demand

$$= 30 - 25 = 5 \text{ MW}$$

$$\text{Daily energy produced} = \text{average demand} \times 24 = 15 \times 24$$

$$= 360 \text{ MWh}$$

Energy corresponding to installed capacity per day

$$= 24 \times 30 = 720 \text{ MWh}$$

Maximum energy that could be produced

$$= \frac{\text{actual energy produced in a day}}{\text{plant use factor}}$$

$$= \frac{360}{0.72} = 500 \text{ MWh/day}$$

Example 1.4 From a load duration curve, the following data are obtained: Maximum demand on the system is 20 MW. The load supplied by the two units is 14 MW and 10 MW. Unit No. 1 (base unit) works for 100% of the time, and Unit No. 2 (peak load unit) only for 45% of the time. The energy generated by Unit 1 is 1×10^8 units, and that by Unit 2 is 7.5×10^6 units. Find the load factor, plant capacity factor and plant use factor of each unit, and the load factor of the total plant.

Solution

$$\text{Annual load factor for Unit 1} = \frac{1 \times 10^8 \times 100}{14{,}000 \times 8760} = 81.54\%$$

The maximum demand on Unit 2 is 6 MW.

$$\text{Annual load factor for Unit 2} = \frac{7.5 \times 10^6 \times 100}{6000 \times 8760} = 14.27\%$$

Load factor of Unit 2 for the time it takes the load

$$= \frac{7.5\times10^6\times100}{6000\times0.45\times8760}$$
$$= 31.71\%$$

Since no reserve is available at Unit No. 1, its capacity factor is the same as the load factor, i.e. 81.54%. Also since Unit 1 has been running throughout the year, the plant use factor equals the plant capacity factor, i.e. 81.54%.

$$\text{Annual plant capacity factor of Unit 2} = \frac{7.5\times10^6\times100}{10\times8760\times1000} = 8.56\%$$

$$\text{Plant use factor of Unit 2} = \frac{7.5\times10^6\times100}{10\times0.45\times8760\times1000} = 19.02\%$$

$$\text{The annual load factor of the total plant} = \frac{1.075\times10^8\times100}{20{,}000\times8760} = 61.35\%$$

Comments: The various plant factors, the capacity of base and peak load units can thus be found out from the load duration curve. The load factor of the peak load unit is much less than that of the base load unit, and thus the cost of power generation from the peak load unit is much higher than that from the base load unit.

Example 1.5 There are three consumers of electricity having different load requirements at different times. Consumer 1 has a maximum demand of 5 kW at 6 p.m. and a demand of 3 kW at 7 p.m. and a daily load factor of 20%. Consumer 2 has a maximum demand of 5 kW at 11 a.m., a load of 2 kW at 7 p.m. and an average load of 1200 W. Consumer 3 has an average load of 1 kW and his maximum demand is 3 kW at 7 p.m. Determine: (a) the diversity factor, (b) the load factor and average load of each consumer, and (c) the average load and load factor of the combined load.

Solution

(a)	Consumer 1	MD 5 kW at 6 p.m.	3 kW at 7 p.m.	LF 20%
	Consumer 2	MD 5 kW at 11 a.m.	2 kW at 7 p.m.	Average load 1.2 kW
	Consumer 3	MD 3 kW at 7 p.m.		Average load 1 kW

Maximum demand of the system is 8 kW at 7 p.m.

Sum of the individual maximum demands = 5 + 5 + 3 = 13 kW

$\therefore$ Diversity factor = 13/8 = 1.625

(b) Consumer 1, Average load 0.2 × 5 = 1 kW, LF = 20%

Consumer 2, Average load 1.2 kW, LF = $\frac{1.2}{5}$ × 1000 = 24%

Consumer 3, Average load 1 kW, $\quad LF = \frac{1}{3} \times 100 = 33.3\%$

(c) Combined average load $= 1 + 1.2 + 1 = 3.2$ kW

$\therefore$ Combined load factor $= \frac{3.2}{8} \times 100 = 40\%$

Load Forecasting

As power plant planning and construction require a gestation period of four to eight years or even longer for the present day super power stations, energy and load demand forecasting plays a crucial role in power system studies.

This necessitates long range forecasting. While sophisticated probabilistic methods exist in literature [5, 16, 28], the simple extrapolation technique is quite adequate for long range forecasting. Since weather has a much more influence on residential than the industrial component, it may be better to prepare forecast in constituent parts to obtain total. Both power and energy forecasts are made. Multi factors involved render forecasting an involved process requiring experience and high analytical ability.

Yearly forecasts are based on previous year's loading for the period under consideration updated by factors such as general load increases, major loads and weather trends.

In short-term load forecasting, hour-by-hour predictions are made for the particular day under consideration. A minor forecast error on low side might necessitate the use of inefficient, oil-fired turbine generators or "peaking units" which are quite costly. On the other hand, a high side forecast error would keep excessive generation in hot reserve. Accuracy of the order of 1% is desirable. A temperature difference of 2°C can vary the total load by 1%. This indicates the importance of reliable weather forecast to a good load forecast. The short term forecast problem is not a simple one as often random factors such as unexpected storms, strikes, the sudden telecast of a good TV programme can upset the predictions. Regression analysis is often used for obtaining a short term load forecast which is very important and is required before solving unit commitment and economic load despatch problems discussed in Ch. 7. Owing to the great importance of load forecasting (an important input-before solving almost all power system problems), a full chapter is added in this book describing various methods of load forecasting (Ch. 16).

In India, energy demand and installed generating capacity are both increasing exponentially (so is population growth—a truly formidable combination). Power demand* has been roughly doubling every ten years as in many other countries.

* 38% of the total power required in India is for industrial consumption. Generation of electricity in India was around 530 billion kWh in 2000–2001 A.D. compared to less than 200 billion kWh in 1986–87.

On 31.3.06 the total installed generation capacity in India is 1,24,287 MW **. As per the present indications, by the time we enter the 2nd decade of the 21st century it would be nearing 2,00,000 MW—a stupendous task indeed. This, in turn, would require a corresponding development in coal resources. Development of a coalmine takes a little over four years.

1.4 STRUCTURE OF POWER SYSTEMS

Generating stations, transmission lines and the distribution systems are the main components of an electric power system. Generating stations and a distribution system are connected through transmission lines, which also connect one power system (grid, area) to another. A distribution system connects all the loads in a particular area to the transmission lines.

For economical and technological reasons (which will be discussed in detail in later chapters), individual power systems are organized in the form of electrically connected areas or regional grids (also called power pools). Each area or regional grid operates technically and economically independently, but these are eventually interconnected* to form a national grid (which may even form an international grid) so that each area is contractually tied to other areas in respect to certain generation and scheduling features. India is now heading for a national grid.

The siting of hydro stations is determined by the natural water power sources. The choice of site for coal fired thermal stations is more flexible. The following two alternatives are possible:

1. Power stations may be built close to coal mines (called pit head stations) and electric energy is evacuated over transmission lines to the load centres.
2. Power stations may be built close to the load centres and coal is transported to them from the mines by rail road.

**Comprisng 32,326 MW hydro, 82,411 MW thermal 33106 MW nuclear and 6,191 MW wind/RES.

* Interconnection has the economic advantage of reducing the reserve generation capacity in each area. Under conditions of sudden increase in load or loss of generation in one area, it is immediately possible to borrow power from adjoining interconnected areas. Interconnection causes larger currents to flow on transmission lines under faulty condition with a consequent increase in capacity of circuit breakers. Also, the synchronous machines of all interconnected areas must operate stably and in a synchronized manner. The disturbance caused by a short circuit in one area must be rapidly disconnected by circuit breaker openings before it can seriously affect adjoining areas. It permits the construction of larger and more economical generating units and the transmission of large chunk of power from the generating plants to major load centres. It provides capacity savings by seasonal exchange of power between areas having opposing winter and summer requirements. It permits capacity savings from time zones and random diversity. It facilitates transmission of off-peak power. It also gives the flexibility to meet unexpected emergency loads.

In practice, however, power station siting will depend upon many factors—technical, economical and environmental. As it is considerably cheaper to transport bulk electric energy over extra high voltage (EHV) transmission lines than to transport equivalent quantities of coal over rail road, the recent trends in India (as well as abroad) is to build super (large) thermal power stations near coal mines. Bulk power can be transmitted to fairly long distances over transmission lines of 400/765 kV and above. However, the country's coal resources are located mainly in the eastern belt and some coal fired stations will continue to be sited in distant western and southern regions.

As nuclear stations are not constrained by the problems of fuel transport and air pollution, a greater flexibility exists in their siting, so that these stations are located close to load centres while avoiding high density pollution areas to reduce the risks, however remote, of radioactivity leakage.

In India, as of now, about 75% of electric power used is generated in thermal plants (including nuclear). 23% from mostly hydro stations and 2% come from renewables and others. Coal is the fuel for most of the steam plants, the rest depends upon oil/natural gas and nuclear fuels.

Electric power is generated at a voltage of 11 to 25 kV which then is stepped up to the transmission levels in the range of 66 to 765 kV (or higher). As the transmission capability of a line is proportional to the square of its voltage, research is continuously being carried out to raise transmission voltages. Some of the countries are already employing 765 kV. The voltages are expected to rise to 800 kV in the near future. In India, several 400 kV lines are already in operation. Several 765 kV lines have been built so far in India.

For very long distances (over 600 km), it is economical to transmit bulk power by DC transmission (see Ch. 20.) It also obviates some of the technical problems associated with very long distance AC transmission. The DC voltages used are 400 kV and above, and the line is connected to the AC systems at the two ends through a transformer and converting/inverting equipment (silicon controlled rectifiers are employed for this purpose). Several DC transmission lines have been constructed in Europe and the USA. In India several HVDC transmission line (bipolar) have already been commissioned and several others are being planned. Four back to back HVDC systems are in operation (for details, see Ch. 20).

The first stepdown of voltage from transmission level is at the bulk power substation, where the reduction is to a range of 33 to 132 kV, depending on the transmission line voltage. Some industries may require power at these voltage levels. This stepdown is from the transmission and grid level to subtransmission level.

The next stepdown in voltage is at the distribution substation. Normally, two distribution voltage levels are employed: (see Ch. 21).

1. The primary or feeder voltage (11 kV).
2. The secondary or consumer voltage (415 V three phase/230 V single phase).

The distribution system, fed from the distribution transformer stations, supplies power to the domestic or industrial and commercial consumers.

Thus, the power system operates at various voltage levels separated by transformer. Figure 1.4 depicts schematically the structure of a power system.

Though the distribution system design, planning and operation are subjects of great importance, we are compelled, for reasons of space, to exclude them from the scope of this book.

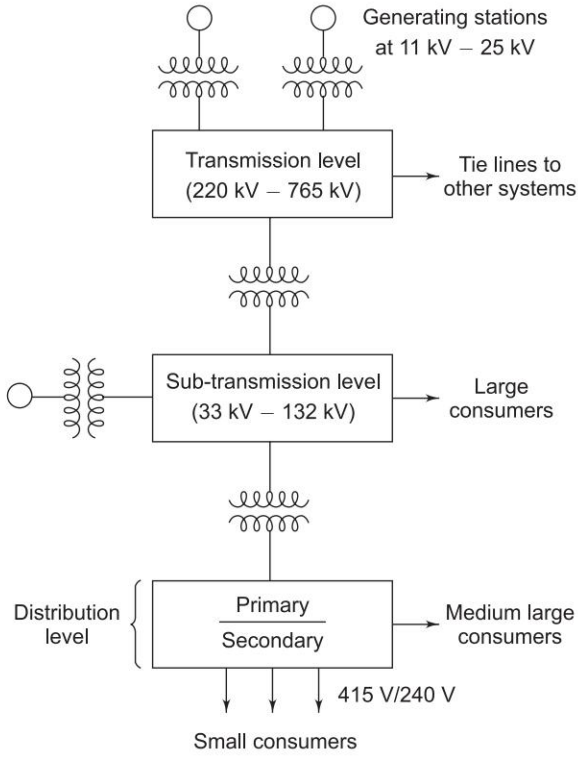

Fig. 1.4 Schematic diagram depicting power system structure

1.5 CONVENTIONAL SOURCES OF ELECTRIC ENERGY

Thermal (coal, oil, nuclear) and hydro generations are the main conventional sources of electric energy. The necessity to conserve fossil fuels has forced scientists and technologists across the world to search for nonconventional sources of electric energy. Some of the sources being explored are solar, wind and tidal sources. The conventional and some of the nonconventional sources and techniques of energy generation are briefly surveyed here with a stress on future trends, particularly with reference to the Indian electric energy scenario. A panoramic view of energy conversion to electrical form is presented in Fig. 1.5.

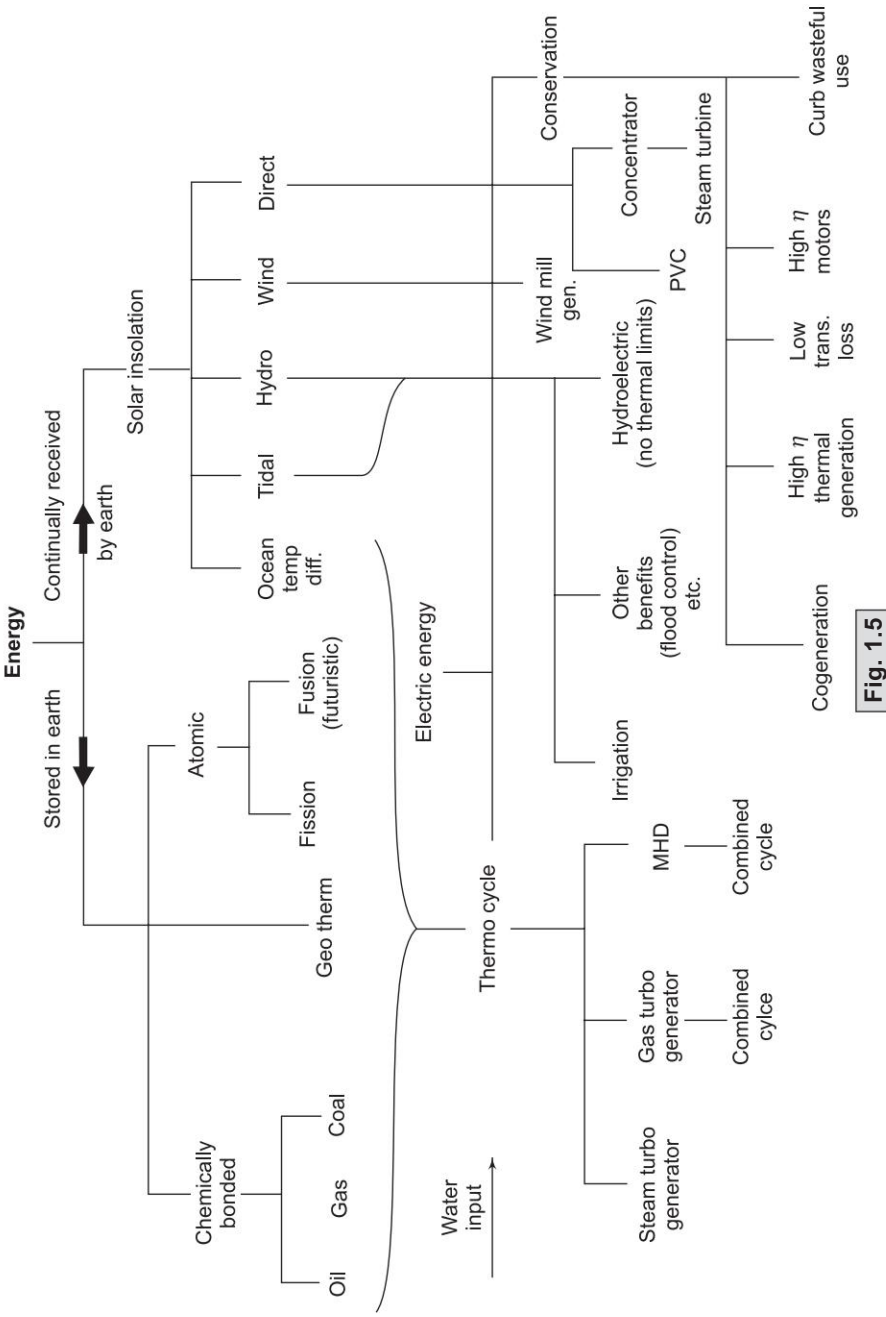
Energy
Stored in earth
Continually received by earth
Solar insolation
Direct
Wind
Hydro
Tidal
Ocean temp diff.
Atomic
Fusion (futuristic)
Fission
Geo therm
Chemically bonded
Coal
Gas
Oil
Electric energy
Water input
Thermo cycle
Steam turbo generator
Gas turbo generator
Combined cylce
MHD
Combined cycle
Irrigation
Other benefits (flood control) etc.
Wind mill gen.
Hydroelectric (no thermal limits)
Conservation
Concentrator
PVC
Steam turbine
Curb wasteful use
High η motors
Low trans. loss
High η thermal generation
Cogeneration

Fig. 1.5

Thermal Power Stations—Steam/Gas-based

The heat released during the combustion of coal, oil or gas is used in a boiler to raise steam. In India heat generation is mostly coal based except in small sizes, because of limited indigenous production of oil. Therefore, we shall discuss only coal-fired boilers for raising steam to be used in a turbine for electric generation. Natural gas is India's most important potential alternative to coal. India is planning to use natural gas in power generation and in the industrial and residential sectors. Our heavy reliance on highly polluting coal makes development and installation of clean coal technology (cct) a high priority.

The chemical energy stored in coal is transformed into electric energy in thermal power plants. The heat released by the combustion of coal produces steam in a boiler at high pressure and temperature, which when passed through a steam turbine gives off some of its internal energy as mechanical energy. The axial-flow type of turbine is normally used with several cylinders on the same shaft. The steam turbine acts as a prime mover and drives the electric generator (alternator). A simple schematic diagram of a coal fired thermal plant is shown in Fig. 1.6(a).

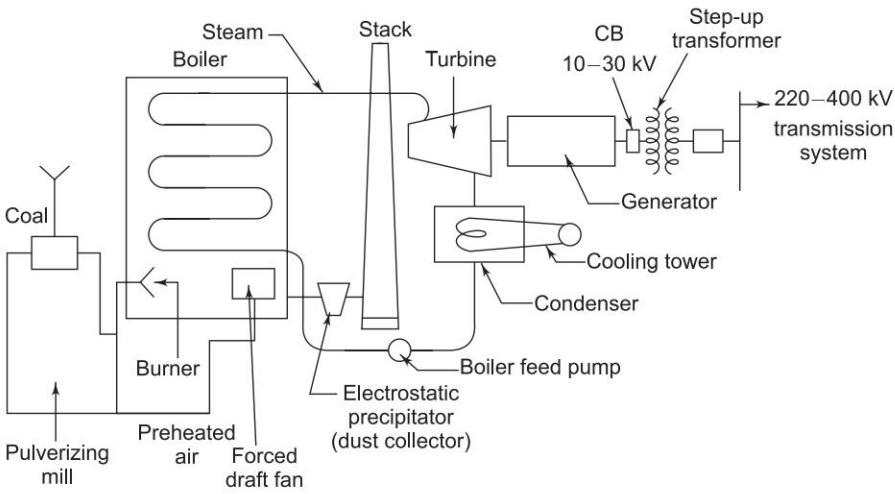

Fig. 1.6(a) Schematic diagram of a coal fired steam plant

The efficiency of the overall conversion process is poor and its maximum value is about 40% because of the high heat losses in the combustion gases and the large quantity of heat rejected to the condenser which has to be given off in cooling towers or into a stream/lake in the case of direct condenser cooling. The steam power station operates on the Rankine cycle, modified to include superheating, feed-water heating, and steam reheating as shown in Fig. 1.6(b). The thermal efficiency (conversion of heat to mechanical energy) can be increased by using steam at the highest possible pressure and

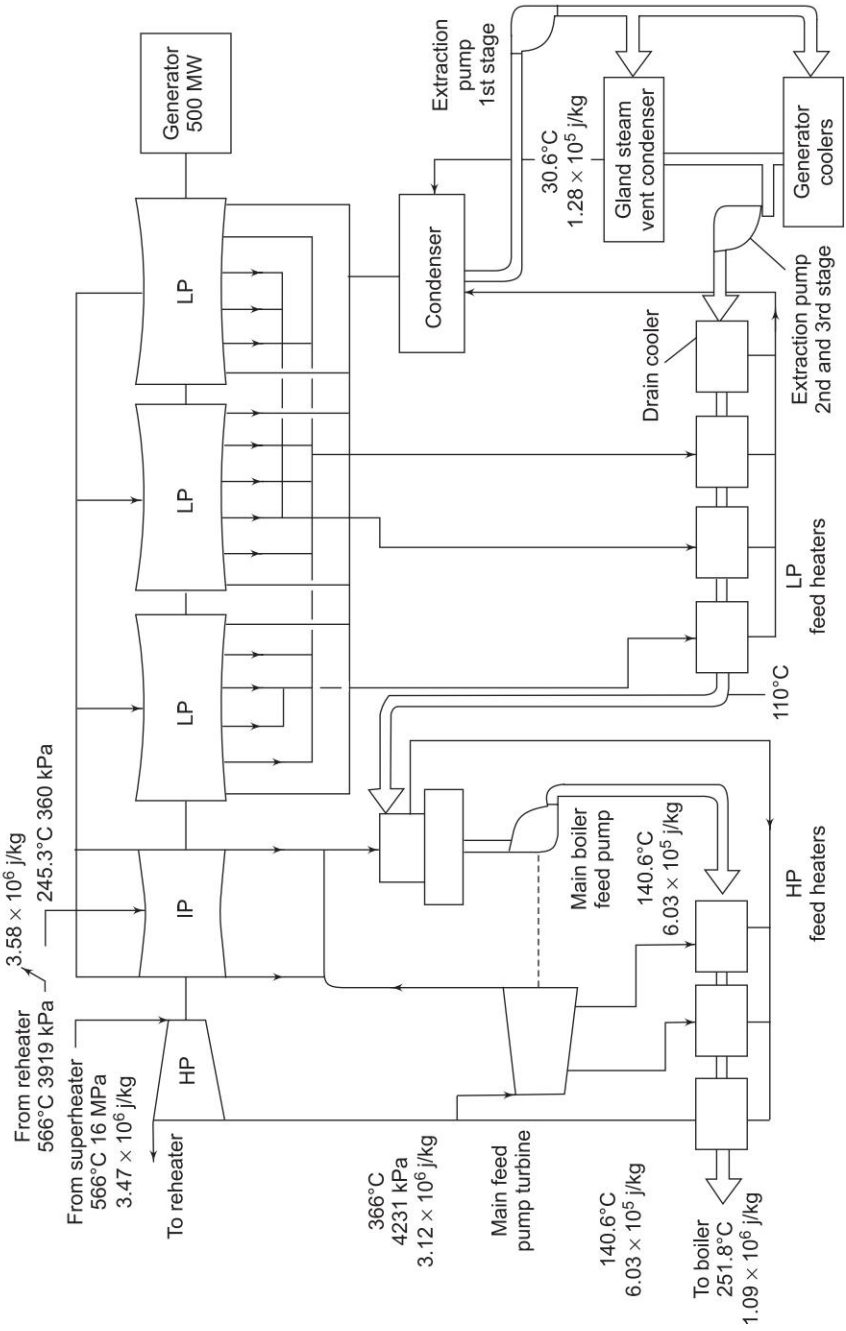

Fig. 1.6(b) Energy flow diagram for a 500 MW turbogenerator

temperature. With steam turbines of this size, additional increase in efficiency is obtained by reheating the steam after it has been partially expanded by an external heater. The reheated steam is then returned to the turbine where it is expanded through the final states of bleeding.

To take advantage of the principle of economy of scale (which applies to units of all sizes), the present trend is to go in for larger sizes of units. Larger units can be installed at much lower cost per kilowatt. They are also cheaper to operate because of higher efficiency. They require lower labour and maintenance expenditure. According to Kashkari [3] there may be a saving of as high as 15% in capital cost per kilowatt by going up from a 100 to 250 MW unit size and an additional saving in fuel cost of about 8% per kWh. Since larger units consume less fuel per kWh, they produce less air, thermal and waste pollution, and this is a significant advantage in our concern for environment. The only trouble in the case of a large unit is the tremendous shock to the system when outage of such a large capacity unit occurs. This shock can be tolerated so long as this unit size does not exceed 10% of the on-line capacity of a large grid.

In India, in 1970s the first 500 MW superthermal unit had been commissioned at Trombay. Bharat Heavy Electricals Limited (BHEL) has produced several turbogenerator sets of 500 MW capacity. Today's maximum generator unit size is (nearly 1200 MW) limited by the permissible current densities used in rotor and stator windings. Efforts are on to develop *super conducting* machines where the winding temperature will be nearing absolute zero. Extreme high current and flux densities obtained in such machines could perhaps increase unit sizes to several GWs which would result in better generating economy.

Air and thermal pollution is always present in a coal fired steam plant. The air polluting agents (consisting of particulates and gases such as NOX, CO, CO_2, SOX, etc.) are emitted via the exhaust gases and thermal pollution is due to the rejected heat transferred from the condenser to cooling water. Cooling towers are used in situations where the stream/lake cannot withstand the thermal burden without excessive temperature rise. The problem of air pollution can be minimized through scrubbers and electrostatic precipitators and by resorting to minimum emission dispatch [32] and Clean Air Act has already been passed in Indian Parliament.

Fluidized-bed Boiler

The main problem with coal in India is its high ash content (up to 40% max). To solve this, *fluidized bed combustion technology* is being developed and perfected. The fluidized-bed boiler is undergoing extensive development and is being preferred due to its lower pollutant level and better efficiency. Direct ignition of pulverized coal is being introduced but initial oil firing support is needed.

Cogeneration

Considering the tremendous amount of waste heat generated in thermal power generation, it is advisable to save fuel by the simultaneous generation of electricity and steam (or hot water) for industrial use or space heating. Now called cogeneration, such systems have long been common, here and abroad. Currently, there is renewed interest in these because of the overall increase in energy efficiencies which are claimed to be as high as 65%.

Cogeneration of steam and power is highly energy efficient and is particularly suitable for chemicals, paper, textiles, food, fertilizer and petroleum refining industries. Thus these industries can solve energy shortage problem in a big way. Further, they will not have to depend on the grid power which is not so reliable. Of course they can sell the extra power to the government for use in deficient areas. They may also sell power to the neighbouring industries, a concept called *wheeling power*.

As on 31.12.2000, total co-generation potential in India is 19,500 MW and actual achievement is 273 MW as per MNES (Ministry of Non-Conventional Energy Sources, Government of India) Annual Report 2000–01.

There are two possible ways of cogeneration of heat and electricity: (i) Topping cycle, (ii) Bottoming cycle. In the topping cycle, fuel is burnt to produce electrical or mechanical power and the waste heat from the power generation provides the process heat. In the bottoming cycle, fuel first produces process heat and the waste heat from the processes is then used to produce power.

Coal-fired plants share environmental problems with some other types of fossil-fuel plants; these include "acid rain" and the "greenhouse" effect.

Gas Turbines

With increasing availability of natural gas (methane) (recent finds in Bangladesh) primemovers based on gas turbines have been developed on the lines similar to those used in aircraft. Gas combustion generates high temperatures and pressures, so that the efficiency of the gas turbine is comparable to that of steam turbine. Additional advantage is that exhaust gas from the turbine still has sufficient heat content, which is used to raise steam to run a conventional steam turbine coupled to a generator. This is called combined-cycle gas-turbine (CCGT) plant. The schematic diagram of such a plant is drawn in Fig. 1.7.

The CCGT plant has a fast start of 2–3 min for the gas turbine and about 20 mins for the steam turbine. Local storage tanks of gas can be used in case of gas supply interruption. The unit can take up to 10% overload for short periods of time to take care of any emergency.

CCGT unit produces 55% of CO_2 produced by a coal/oil-fired plant. Units are now available for a fully automated operation for 24 h or to meet the peak demands.

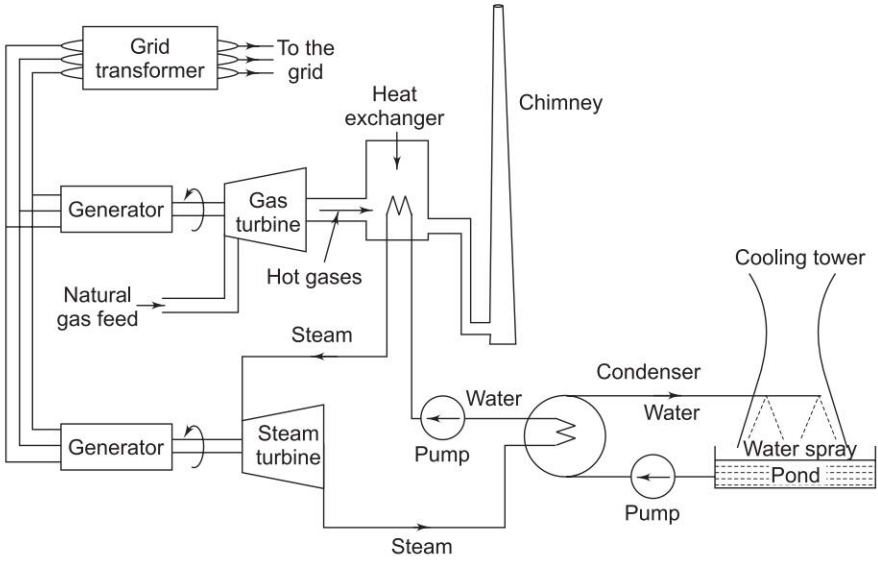

Fig. 1.7 CCGT power station

In Delhi (India) a CCGT unit of 2 × 110 MW are installed at Pragati Power Plant.

There are currently many installations using gas turbines in the world with 100 MW generators. A 6 × 30 MW gas turbine station has already been put up in Delhi. A gas turbine unit can also be used as synchronous compensator to help maintain flat voltage profile in the system.

Nuclear Power Generation

Nuclear Reaction

Considerable binding energy is released on breaking a large nucleus into smaller fragments. This process is called *fission*. Nucleus of uranium isotope ^{235}U undergoes fission when struck by a fast moving neutron. This fission is expressed in the standard nuclear reaction as

$$\underset{\text{(neutron)}}{{}^{235}_{92}\text{U(fissile)} + {}_0n^1} \rightarrow \underset{\text{(excited uranium nucleus)}}{{}^{236}_{92}\text{U}^*} \rightarrow \underset{\text{(Xenon)}}{{}^{140}_{54}\text{Xe}} + \underset{\text{(Strontium)}}{{}^{94}_{38}\text{Sr}} + 2{}_0n^1 + \text{E (20 MeV)} \qquad (1.1)$$

Nuclear Reactor

The fission of a nuclear material (Eq. (1.1)) is carried out in a nuclear reactor. A nuclear reactor is a very efficient source of energy as a small amount of fissile material produces large chunks of energy. For example 1 g of ^{235}U releases

energy at the rate of 1 MW/day, whereas 2.6 tons of coal produces the same power in a conventional thermal plant per day (this figure is much larger for Indian coal, which contains considerable amount of dust in it).

Uranium metal extracted from the base ore consists mainly of two isotopes ^{238}U (99.3% by weight) and ^{235}U (0.7% by weight). Of these only ^{235}U is fissile and when struck by slow moving neutrons, its nucleus splits into two fast moving neutrons and 3×10^{-11} J of kinetic energy. The fast moving neutrons hit the surrounding atoms, thus producing heat before coming to rest. The neutrons travel further, hitting more atoms and producing further fissions. The number of neutrons thus multiplies and under certain critical conditions a sustainable chain reaction results. For sustainability the reactor core or moderator must slow down the moving neutrons to achieve a more effective splitting of the nuclei.

The energy given off in a reactor appears in the form of heat, which is removed by a gas or liquid coolant. The hot coolant is then used in a heat exchanger to raise steam. If the coolant is ordinary water, steam could be raised inside the reactor. Steam so raised runs a turbogenerator for producing electric energy.

Fuel

Fuels used in reactors have some components of ^{238}U. Natural uranium is sometimes used and although the energy density is considerably less than that for pure isotope, it is still much better than fossil fuels. The uranium used at present comes from metal-rich areas, which have limited world resources ($\approx 2 \times 10^6$ tons). Therefore, the era of nuclear energy would be comparatively short, probably less than a century. Fortunately it is possible to manufacture certain fissile isotopes from abundant nonfissile materials like thorium by a process of conversion in a breeder reactor (details in later portion of this section). This would assure virtually an unlimited reserve of nuclear energy.

In an advanced gas-cooled reactor (AGR), whose schematic diagram is shown in Fig. 1.8, enriched uranium dioxide fuel in pellet form, encased in stainless steel cans, is used. A number of cans form a cylindrical fuel element, which is placed in a vertical hollow housing in the core. In certain reactors fuel could be in the form of rods enclosed in stainless steel.

Moderators

To slow down the neutrons the reactor elements are placed inside a moderator, a substance whose nuclei absorb energy as fast moving neutrons collide with these but do not capture the neutrons. Commonly used moderators are graphite (as in AGR of Fig. 1.8), light water and heavy water. It could also be beryllium and its oxide and possibly certain organic compounds.

Coolants

These remove the heat generated in the core by circulation and transfer it outside for raising steam. Common coolants are light ordinary water, heavy water, gas (CO_2) (this is used in AGR of Fig. 1.8) and also metals like sodium or sodium-potassium alloy in liquid form.

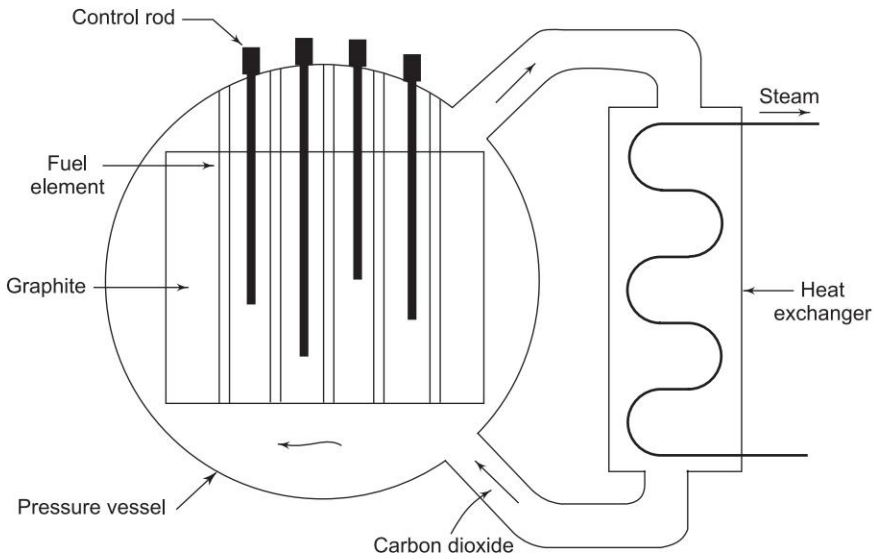

Fig. 1.8 Schematic view of a British Magnox type nuclear reactor

Control Materials

In nuclear reactors, control is achieved by means of a neutron absorbing material. The control elements are commonly located in the core in the form of either rods or plates. The control rods are moved in to decrease the fission rate or neutron flux and moved out to increase it. The most commonly used neutron absorber is *boron*. This element has a very high melting point and a large cross-section for neutron absorption.

Other control materials are cadmium and an alloy of silver 15%, iradium 15% and cadmium 5%.

Reactor Shielding

Nuclear reactors are sources of intense neutron and γ-radiation and, therefore, represent hazard to persons in the immediate vicinity of the reactor. Provisions for their health protection are made by surrounding the reactor core with a radiation shield, also called *biological shield*. It generally consists of a layer of concrete, about 1.8–2.5 m thick and capable of absorbing both γ-rays and neutrons. Part of the shield which is in immediate contact with the core heats up considerably and requires a special cooling facility to prevent it from cracking. A shield made of a 5–10 cm thick steel is located close to the core.

Power Reactor Types

The primary purpose of a power reactor is the utilization of fission energy produced in the reactor core by converting it to a useful mechanical-electrical form. The heat generated in the fission process is used to produce steam at high temperature and pressure, which runs a turbogenerator. For raising steam a heat exchanger stage is interposed between the reactor and boiler. The choice of the heat exchange fluid (or gas) is governed by three considerations:

1. It must have a high thermal conductivity so as to carry away heat efficiently and give it up in a heat exchanger.
2. It must have a low neutron capture cross-section so as not to upset the reactor characteristics.
3. It must not be decomposed by intense radiation.

Now we shall discuss some of the reactor types which are in current use in various countries. Advanced gas reactor (AGR) has already been presented earlier for discussing the various components and processes involved in a reactor.

Boiling Water Reactor (Fig. 1.9(a))

This type of power plant is designed to allow steam to be generated directly in the reactor core. This uses light water as moderator and coolant. Therefore, no external heat exchanger is required. Enriched uranium is used as fuel.

The 420 MW power station, at Tarapur (India), consists of two enriched uranium reactors of the boiling water type. These reactors were built with the help of the General Electric Company of the United States and became operational on April 1, 1969.

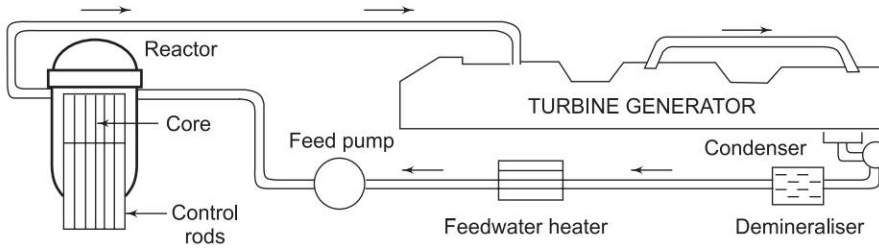

Fig. 1.9(a) Schematic diagram of a boiling water reactor (BWR)

Pressurized Water Reactor (Fig. 1.9(b))

It uses slightly enriched uranium (1.4. or 2% of U^{235}) as fuel and light water as moderator and coolant. The fuel elements are in the form of rods or plates. The core is contained in a vessel under a pressure of (6.5 to 13.8) $\times 10^6$ N/m^2.

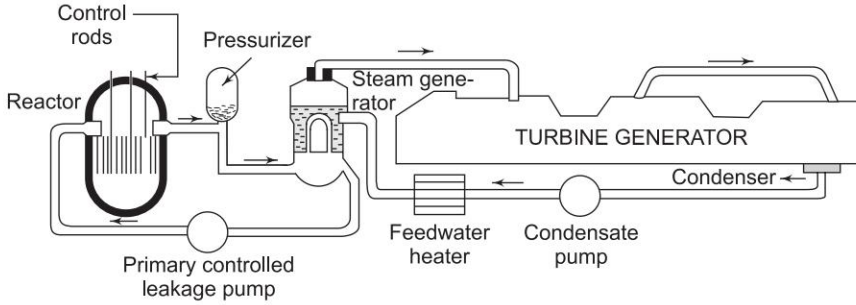

Fig. 1.9(b) Schematic diagram of a pressured water reactor (PWR)

The pressurized water is circulated through the reactor core from which it removes heat. This heat is transferred to a boiler through a heat exchanger for raising steam for turbogeneration as shown in Fig. 1.9(b).

Heavy Water (D_2O) Moderated Reactor (Fig. 1.10)

It is of the pressurized water reactor type with heavy water as moderator and coolant instead of light water. The first prototype of this type of reactor is the Nuclear Power Demonstration Reactor (NPDR) called CANDU (Canada Deuterium Uranium) type reactor completed in 1962 at Canada.

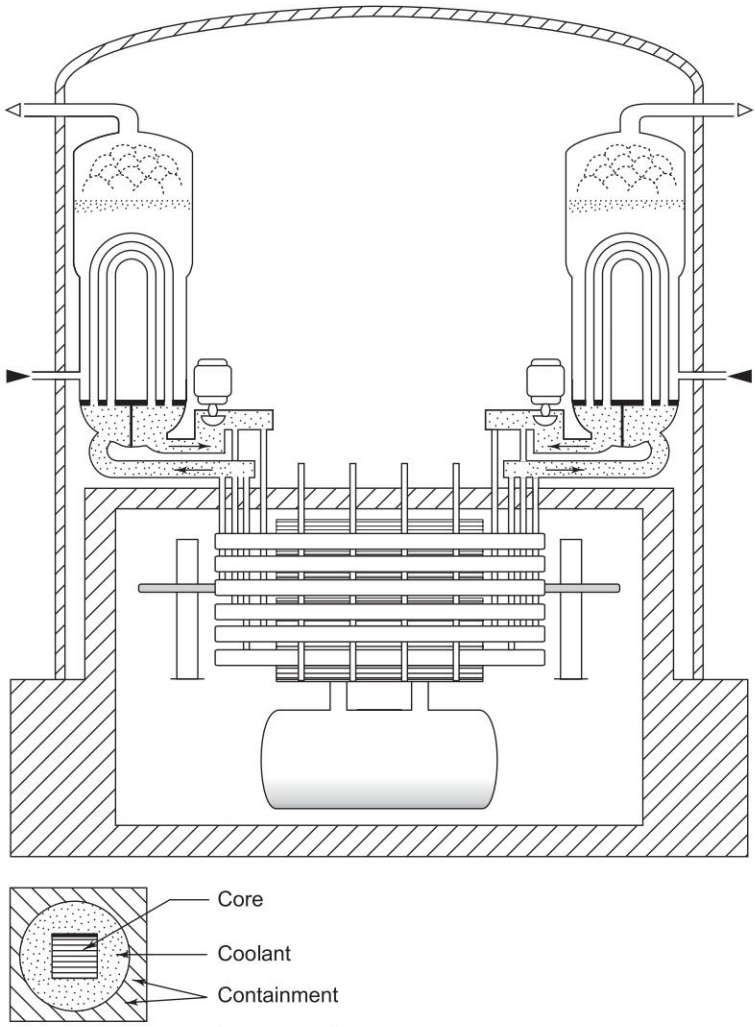

Fig. 1.10 CANDU Reactor

The 430 MW power station near Kota at Rana Pratap Sagar in Rajasthan employs a heavy water mode gated reactor using natural uranium as fuel. This

started feeding power in 1973. The other two reactors of this type are under construction, one at Kalpakham (470 MW), about 100 km away from Chennai, and the other at Narora in Uttar Pradesh (UP), Kakrapar in Gujarat. Several other nuclear power plants will be commissioned by 2012. It is planned to raise nuclear power generator to 20,000 MW by 2020.

Fast Breeder Reactor (FBR)

Such type of reactors are designed to produce more fissile material (Plutonium) than they consume (Thorium, U^{232}). The nuclear equations for breeding are as under.

$$\begin{array}{l} \qquad\qquad\qquad\qquad\quad \beta \qquad\qquad\quad \beta \\ \qquad\qquad\qquad\qquad\quad \uparrow \qquad\qquad\quad \uparrow \\ {}_0n^1 \rightarrow {}^{232}_{90}\text{Th (nonfissile)} \rightarrow {}^{233}_{90}\text{Th (22 min)} \rightarrow {}^{233}_{91}\text{Pa (27 d)} \rightarrow {}^{233}_{92}\text{U (fissile)} \quad (1.2) \end{array}$$

Bred fuel

$$\begin{array}{l} \qquad\qquad\qquad\qquad\quad \beta \qquad\qquad\quad \beta \\ \qquad\qquad\qquad\qquad\quad \uparrow \qquad\qquad\quad \uparrow \\ {}_0n^1 \rightarrow {}^{238}_{92}\text{U (nonfissile)} \rightarrow {}^{239}_{92}\text{U (24 min)} \rightarrow {}^{239}_{93}\text{Np (2.3 d)} \rightarrow {}^{239}_{94}\text{Pu (fissile)} \quad (1.3) \end{array}$$

Bred fuel
(Plutonium)

According to the above reactions there are two types of fast breeder reactors. These are:

1. A blanket of ^{232}Th surrounds ^{239}Pu and is converted to ^{233}U which is fissile (Eq. (1.2)).
2. Core 20% ^{239}Pu surrounded by a blanket of 80% ^{238}U (Thorium). About three neutrons are emitted when a ^{239}Pu nucleus fissions. Of these one is required to sustain the reaction leaving the other two to account for breeding more ^{239}Pu (Eq. 1.3).

The power density in a fast breeder reactor is considerably higher than in normal reactors. Therefore, liquid sodium which is an efficient coolant and does not moderate neutrons is used to take away heat generated in the core. Schematic diagram of an FBR reactor is shown in Fig. 1.11.

An important advantage of FBR technology, brought out through the reaction equations given above, is that it can use Thorium (as fertile material) which gets converted to ^{233}U, a fissile isotope. This holds great promise for India as we have one of the world's largest deposits of Thorium—about 450,000 tons in form of sand dunes in Kerala and along the Gopalpur Chattarpur coast of Orissa.

Typical power densities (MW/m^3) in fission reactor cores are: gas cooled 0.53, high temperature gas cooled 7.75, heavy water 18.0, boiling water 29.0, pressurized water 54.75 and fast breeder reactor 760.0.

The associated merits and problems of nuclear power plants as compared to conventional thermal plants are as follows:

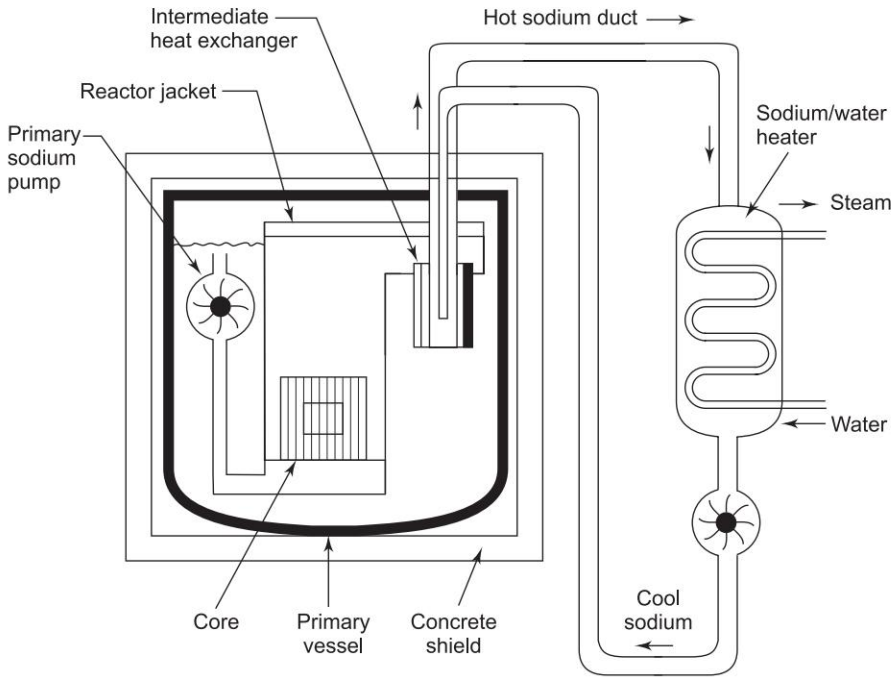

Fig. 1.11 Schematic diagram of a liquid-metal FBR

Merits

1. A nuclear power plant is totally free of air pollution. Nuclear fuel is greener than coal.
2. It requires very little fuel in terms of volume and weight, and therefore poses no transportation problems and may be sited, independently of nuclear fuel supplies, close to load centres. However, safety considerations require that these be normally located away from populated areas.
3. It lasts longer—over 45 years as against 30 in case of coal and 15 in case of gas turbines.

Problems

1. Nuclear reactors produce radioactive fuel waste, the disposal of which poses serious environmental hazards.
2. The rate of nuclear reaction can be lowered only by a small margin, so the load on a nuclear power plant can only be permitted to be marginally reduced below its full load value. Nuclear power stations must, therefore be reliably connected to a power network, as tripping of the lines connecting the station can be quite serious and may require shutting down of the reactor with all its consequences.

3. Because of a relatively high capital cost as against the running cost, the nuclear plant should operate continuously as a base load station. Wherever possible, it is preferable to support such a station with a pumped storage scheme discussed later (p. 33.)
4. There are risks in terms of fuel supplies and safety.

Safety and Environmental Considerations

The nuclei that result from fission are called fission fragments. From the nuclear reactor there is a continuous emission of β- and γ-rays, and α-particles and fission fragments. If these fission fragments cannot be retreated as a feul element, then these become the waste products, which are highly radioactive. Some of the important waste products with their half life are as follows:

$^{3}_{1}H_2$ (Tritium) – 12.26 years
^{90}Sr (Strontium) – 28.8 years
^{137}Cs (Cesium) – 32.2 years
^{131}I (Iodine) – 8 days
^{85}Kr (Krypton) – 10.76 years
^{133}Xe (Xenon) – 5.27 days

Waste products having a long life create serious problems. These are called high level wastes, e.g. ^{90}Sr. At the moment, the wastes are concentrated in the liquid form and stored in stainless steel containers. Burying nuclear wastes deep underground currently seems to be the best long-term way to dispose them off. The location should be geologically stable, should not be earthquake prone, a type of rock that does not disintegrate in the presence of heat and radiation and not near ground water that might become contaminated. At present over 15,000 tons of spent nuclear fuel is being stored on a temporary basis in United States.

In the design and construction of reactors great care is taken to cover every contingency. Many facilities, e.g. control system, are at least duplicated and have alternative electrical supplies. In March 1979, failure in its cooling system disabled one of the reactors of Three Mile Island in Pennsylvania and a certain amount of radioactive material escaped, although a catastrophe was narrowly avoided. Then in April 1986, a severe accident destroyed a 1000 MW reactor at Chernobyl, in the then Soviet Union. Much radioactive material escaped into the atmosphere and was carried around the world by winds. Tens of thousands of people were evacuated from the reactor vicinity and hundreds of plant and rescue workers died as a result of exposure to radiation. The effects of radioactive exposure of population in neighbouring regions are still showing up in the form of various incurable diseases even in the next generation offsprings.

However, the health controls in the atomic power industry have, from the very outset, been much more rigorous than in any other industry.

Fusion

Energy is produced in this process by combination of two light nuclei to form a single heavier one under sustained condition of extremely high temperature and high pressure for initiation. Neutron emission is not required in the process as the temperature (high) maintains the collisions of reacting nuclei.

The most promising fuels are isotopes of hydrogen known as deuterium (D) (mass 2) and tritium (T) (mass 3). The product of fusion is the helium isotope (mass 3), hydrogen, neutrons, and heat. As tritium is not a naturally occurring isotope, it is produced in the reactor shield by the interaction of the fusion neutrons and the lithium isotope of mass 6. The deuterium-deuterium fusion requires higher temperature than deuterium-tritium and the latter is more likely to be used initially.

Reserves of lithium have been estimated to be roughly equal to those of fossil fuels. Deuterium, on the other hand, is contained in sea-water of a concentration of about 34 parts per million. The potential of this energy resource is therefore vast. Total nuclear power will be around 10280 MW by 2012.

General Remarks

The greatest danger in a fission reactor is in the case of loss of coolant in an accident. Even with the control rods (or plates) fully lowered quickly called *scram* operation, the fission does continue for sometime and its *after-heat* may cause vaporizing and dispersal of radioactive material. This possibility does not exist in fusion process as its power density is almost 1/50th that of an FBR. The radioactive waste in fusion is the radiation damage to structural materials which would require occasional renewal. These could be recycled after 50 year period compared with centuries required for ^{90}Sr and ^{137}Cs, the fission fragments.

Intensive international research is still proceeding to develop materials and a suitable containment method, using either magnetic fields or powerful lasers to produce the high temperatures ($\approx 8 \times 10^7$ K) and pressure (above 1000 bar) to initiate a fusion reaction. It is unlikely that a successful fusion reactor will be available before 2020.

With this kind of estimated time frame for breakthrough in fusion technology, development in FBR technology and installing of power stations will continue.

France and Canada are possibly the two countries with a fairly clean record of nuclear generation. According to Indian scientists, our heavy-water based plants are most safe.

World scientists have to adopt a different reaction safety strategy-may be to discover additives to automatically inhibit reaction beyond critical rather than by mechanically inserted controlled rods, which have possibilities of several primary failure events.

Hydro Power

The oldest and cheapest method of power generation is that of utilizing the potential energy of water. The energy is obtained almost free of running cost and is completely pollution free. Of course, it involves high capital cost because of the heavy civil engineering construction works involved. Also it requires a long gestation period of about five to eight years as compared to four to six years for steam plants. Hydroelectric stations are designed, mostly, as multipurpose projects such as river flood control, storage of drinking water, irrigation and navigation. A simple block diagram of high head hydro plant is given in Fig. 1.12. The vertical difference between the upper reservoir and the tail race pond is called the *head*.

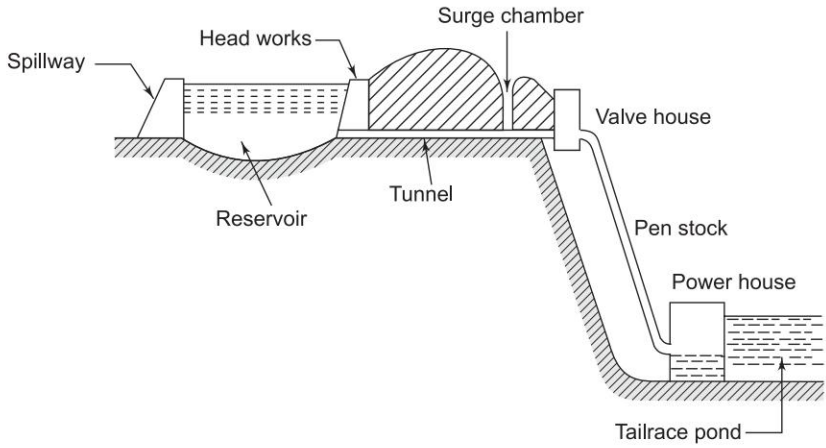

Fig. 1.12 A typical layout for a storage type hydro plant

Water falling through the head gains kinetic energy which then imparts energy to the blades of the hydraulic turbine. There are three main types of hydroelectric installations. These are

1. *High head or stored*—the storage area of reservoir fills in more than 400 hectares.
2. *Medium head or pondage*—the storage fills in 200–400 hectares.
3. *Run of river*—storage (in any) fills in less than 2 h and has a 3–15 m head.

A schematic diagram for hydroelectric schemes of Type 3 is shown in Fig. 1.13.

There can be several of these turbines on a deep and wide river.

In India mini and micro hydroelectric schemes have been installed on canals wherever 1 m or so head is available. Often cascaded plants are also constructed on the same water stream where the discharge of one plant becomes the inflow of a downstream plant.

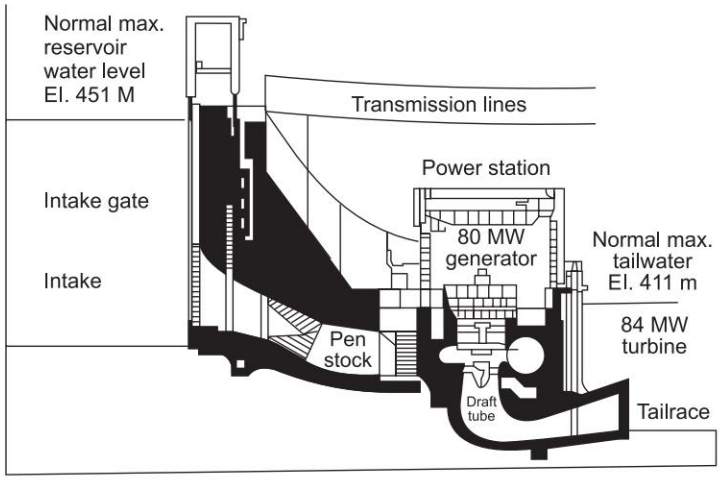

Fig. 1.13 Run of river hydroelectric scheme—80 MW Kaplan turbine, 115.41 rpm

For the three above identified heads of water level, the kind of turbines that are employed:

1. *Pelton*: This is used for heads of 184–1840 m and consists of a bucket wheel rotor with adjustable flow nozzles.
2. *Francis*: This is used for heads of 37–490 m and is of mixed flow type.
3. *Kaplan*: This is used for run-of-river and pondage stations with heads of up to 61 m. This type has an axial-flow rotor with variable-pitch blades.

Hydroelectric plants are capable of starting quickly—almost is 5 min. The rate of taking up load on the machines is of the order of 20 MW/min. Further, no losses are incurred at standstill. Thus, hydroelectric plants are ideal for meeting peak loads. The time from start up to the actual connection to the grid can be as short as 2 min.

The power available from a hydro plant is

$$P = g\,\rho\,WH \text{ W} \tag{1.4}$$

where W = discharge (m^3/s) through the turbine, ρ = density (1000 kg/m^3) and H = head (m), g = 9.81 m/s^2

$$\therefore \quad P = 9.81\,WH \text{ kW} \tag{1.5}$$

Problems peculiar to hydroelectric plants which inhibit expansion are:

1. Silting—Bhakra dead storage has reportedly silted fully in 30 years.
2. Seepage.
3. Ecological damage to region.
4. Displacement of human habitation from areas behind the dam which will fill up and become a lake.
5. These cannot provide base load and must be used for peak shaving and energy saving in coordination with thermal plants.

Typical efficiency curves of the three types of turbines are depicted in Fig. 1.14. As the efficiency depends upon the head, which is continuously fluctuating, water consumption in m^3/kWh is used instead of efficiency, which is related to water head.

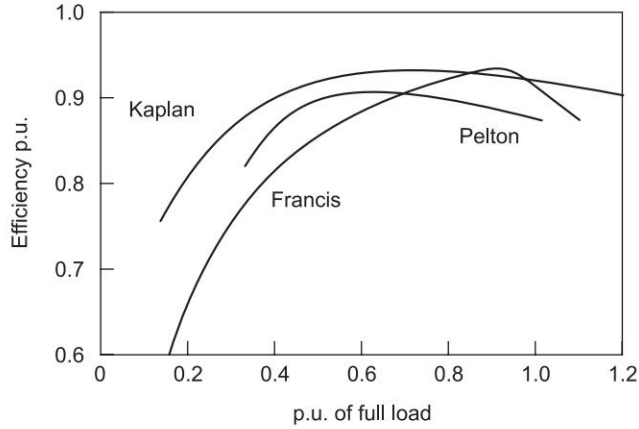

Fig. 1.14 Typical efficiency curves of hydraulic turbines

In certain periods when the water availability is low or when hydro-generation is not needed, it may be advantageous to run electric generators as motors from the grid, so as to act as synchronous condensers (these are overexcited). To reduce running losses, the water is pushed below the turbine runner by compressed air after closing the input valve. The runner now rotates in air and free running losses are low.

India also has a tremendous potential (5000 MW) of having large number of nano, pico, micro (< 1 MW), mini (< 1–5 MW) and small (< 15 MW) *hydel plants* in Himalayan region, North-East, H.P., U.P., U.K., and J.K. which must be fully exploited to generate cheap and clean power for villages situated far away from the grid power*. At present 500 MW capacity is under construction.

Pumped Storage Scheme

In areas where sufficient hydrogeneration is not available, peak load may be handled by means of pumped storage. This consists of upper and lower reservoirs and reversible turbine-generator sets, which can also be used as motor-pump sets. The upper reservoir has enough storage for about 6 h of full load generation. Such a plant acts as a conventional hydroelectric plant during the peak load periods, when production costs are the highest. The turbines are driven by water from the upper reservoir in the usual manner. During the light load period, water in the lower reservoir is pumped back into the upper one so as to be ready for use in the next cycle of the peak load period. The generators in this period change to synchronous motor action and drive the turbines which

* Existing capacity (small hydro) is 1341 MW as on June 2001, Total estimated potential is 15000 MW.

now work as pumps. The electric power is supplied to the generator sets from the general power network or an adjoining thermal plant. The overall efficiency of the generator sets is normally as high as 60–70%. The pumped storage scheme, in fact, is analogous to the charging and discharging of a battery. It has the added advantage that the synchronous machines can be used as synchronous condensers for VAR compensation of the power network, if required. In a way from the point of view of the thermal sector of the power system, the pumped storage scheme *shaves the peaks* and fills the *troughs* of the daily load-demand curve.

Some of the existing pumped storage plants are 900 MW Srisailem in AP, 80 MW of Bhiva in MS, 400 MW Kadamparai in TN.

Tidal Power

Along the shores with high tides and when a basin exists, the power in the tide can be hydroelectrically utilized. This requires a long and low dam across the basin. Two sets of turbines are located underneath the dam. As the tide comes in water flows into the basin operating one set of turbines. At low tide the water flows out of the basin operating another set of turbine.

Let tidal range from high to low be h (m) and area of water stored in the basin be A (m^2), then the energy stored in the full basin is expressed as

$$E = \rho g A \int_0^h x\,dx \qquad (1.5)$$

$$= \frac{1}{2}\,\rho g h^2 A$$

Average power, $P = \frac{1}{2}\,\rho g h^2 A/(T/2)$; T = period of tidal cycle

= 14 h 44 min, normally

$$= \rho g h^2 A/T$$

A few places which have been surveyed in the world as sites for tidal power are as follows:

Passanaquoddy Bay (N. America)	5.5 m, 262 km^2, 1,800 MW
San Jose (S. America)	10.7 m, 777 km^2, 19,900 MW
Sever (UK)	9.8 m, 70 km^2, 8,000 MW

Major sites in India where preliminary investigations have been carried out are Bhavnagar, Navalakhi (Kutch), Diamond Harbour and Ganga Sagar.

India's first Tidal Power Project is being developed by WBREDA at Durgaduani Creek in the Sunderbans delta. High tide water is stored in a reservoir and released at low tide, thus creating water flows which drive turbines that generate electricity. Total cost for 4 MW project is Rs 40 crores and will be ready by 2009.

The basin in Kandla in Gujarat has been estimated to have a capacity of 600 MW. The total potential of Indian coast is around 9000 MW, which does not compare favourably with the sites in the American continent stated above. The technical and economic difficulties still prevail.

1.6 MAGNETOHYDRODYNAMIC (MHD) GENERATION

In thermal generation of electric energy, the heat released by the fuel is converted to rotational mechanical energy by means of a thermocycle. The mechanical energy is then used to rotate the electric generator. Thus two stages of energy conversion are involved in which the heat to mechanical energy conversion has an inherently low efficiency. Also, the rotating machine has its associated losses and maintenance problems. In MHD technology electric energy is directly generated by the hot gases produced by the combustion of fuel without the need for mechanical moving parts.

In an MHD generator, electrically conducting gas at a very high temperature is passed in a strong magnetic field, thereby generating electricity. High temperature is needed to ionize the gas, so that it has good electrical conductivity. The conducting gas is obtained by burning a fuel and injecting a seeding material such as potassium carbonate in the products of combustion. The principle of MHD power generation is illustrated in Fig. 1.15. Electrically conducting gas as it flows is equivalent to electric current flowing in an imaginary conductor at 90° to the magnetic field. The result is induction of emf across an anode and cathode with current flowing through the load. About 50% efficiency can be achieved, if the MHD generator is operated in tandem with a conventional steam plant.

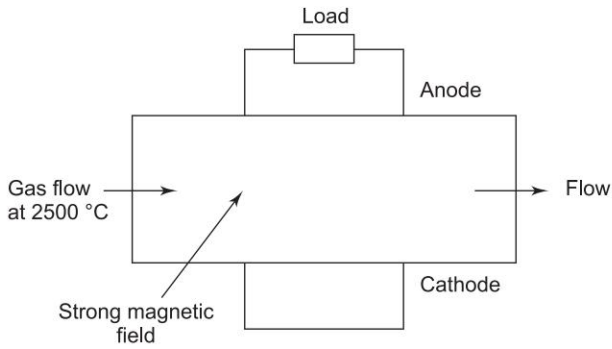

Fig. 1.15 The principle of MHD power generation

Although the technological feasibility of MHD generation has been established, its economic feasibility is yet to be demonstrated. In fact with the development of CCGT systems, which are being installed in many countries, MHD development has been put on the shelf.

1.7 GEOTHERMAL ENERGY

The outer crust of earth contains a very large reserve of energy as sensible heat. It is estimated to be one to two orders of magnitude larger than all the energy recoverable from uranium (by fission) and thorium (by breeder reactor assuming 60–70% efficiency). Fusion as and when it becomes technologically practical would represent a large energy resource than geothermal energy.

Geothermal energy is present over the entire extent of earth's surface except that it is nearer to the surface in volcanic areas. Heat transfer from the earth's interior is by three primary means:

1. Direct heat conduction;
2. Rapid injection of ballistic magma along natural rifts penetrating deep into earth's mantle; and
3. Bubble like magma that buoys upwards towards the surface.

Rift geothermal areas in sedimentary rock basins undergo repeated injection of magma, though in small amount. Over a long period of time these processes cause massive amounts of hot water to accumulate. Examples are the Imperiod Valley of Africa. The weight of the overburden in these sedimentary basins compresses the trapped water giving rise to a geopressurized geothermal resource. These high pressures serve to increase the productivity of hot-water wells, which may be natural or drilled.

Pressure released in the hot wells causes boiling and the steam and water mixture rise upwards. This mixture is passed through steam separators, which then is used to drive low-pressure steam turbines. Corrosive effects of this wet steam, because of mineral particles in it, have been tackled by advanced metallurgy. The capital cost of these plants is 40 to 60% less than that of fossil fuel and nuclear plants, because no boiler or nuclear reactor is needed to generate steam.

Geothermal plants have proved useful for base-load power plants. These kind of plants are primarily entering the market where modest sized plants are needed with low capital cost, short construction period and life-long fuel (i.e. geothermal heat).

High air-quality standards are easily attained by geothermal plants at a minimal cost such that they have an edge over clean coal-fueled plants. Considerable research and development effort is being devoted towards geothermal plants siting, designing, fabricating, installation and operation. Efforts are also on to tap the heat potential of volcanic regions and from hot volcanic rock.

No worth mentioning effort is being made in India at present. In India, feasibility studies of a 1 MW station at Peggy valley in Ladakh are being carried out. Another geothermal field has been located at Chumantang. There are a number of hot springs in India, but the total exploitable energy potential seems to be very little.

The present installed geothermal plant capacity in the world is about 500 MW and the total estimated capacity is immense provided volcanic 'regions' heat can be utilized. Since the pressure and temperatures are low, the efficiency is even less than that of the conventional fossil-fuelled plants, but the capital costs are less and the fuel is available free of cost.

1.8 ENVIRONMENTAL ASPECTS OF ELECTRIC ENERGY GENERATION

As far as environmental and health risks involved in nuclear plants of various kinds are concerned, these have already been discussed at length in Sec. 1.7. Equally the problems related to large hydroelectric plants have been dwelled upon in Sec. 1.5. Therefore, we shall now focus our attention on fossil-fuel plants including gas-based plants.

Conversion of one form of energy or another to electrical form has unwanted side effects and the pollutants generated in the process have to be disposed off. The reader may refer to Fig. 1.16, which brings out all the associated problems at a glance. Pollutants know no geographical boundary; as a result the pollution issue has become a nightmarish problem and strong national and international pressure groups have sprung up and are having a definite impact on the development of energy resources. Governmental awareness has created increasing legislation at national and international levels. The power engineers have to be fully conversant with these in their professional practice and in the survey and planning of large power projects. Lengthy, time consuming procedures at government level, PIL (public interest litigation) and demonstrative protests have delayed several projects in several countries. This has led to favouring of small size projects and redevelopment of existing sites. But with the yawning gap in electric demand and production, our country has to move forward for several large thermal, hydro and nuclear power projects.

Emphasis is being laid on conservation issues, curtailment of transmission losses, theft, subsidized power supplies and above all on *sustainable development* with *appropriate technology* wherever feasible. It has to be particularly assured that no irreversible damage is caused to the environment which would affect the living conditions of the future generations. Irreversible damages like ozone layer holes and global warming caused by increase in CO_2 in the atmosphere are already showing up.

Atmospheric Pollution

We shall treat here only pollution as caused by thermal plants using coal as feed-stock. The fossil fuel-based generating plants form the backbone of power generation in our country and also round the globe as other options (like nuclear and even hydro) have even stronger hazards associated with them. Also it should be understood that pollution in large cities like Delhi is caused more by vehicular traffic and their emission. In Delhi of course Inderprastha and Badarpur power stations contribute their share in certain areas.

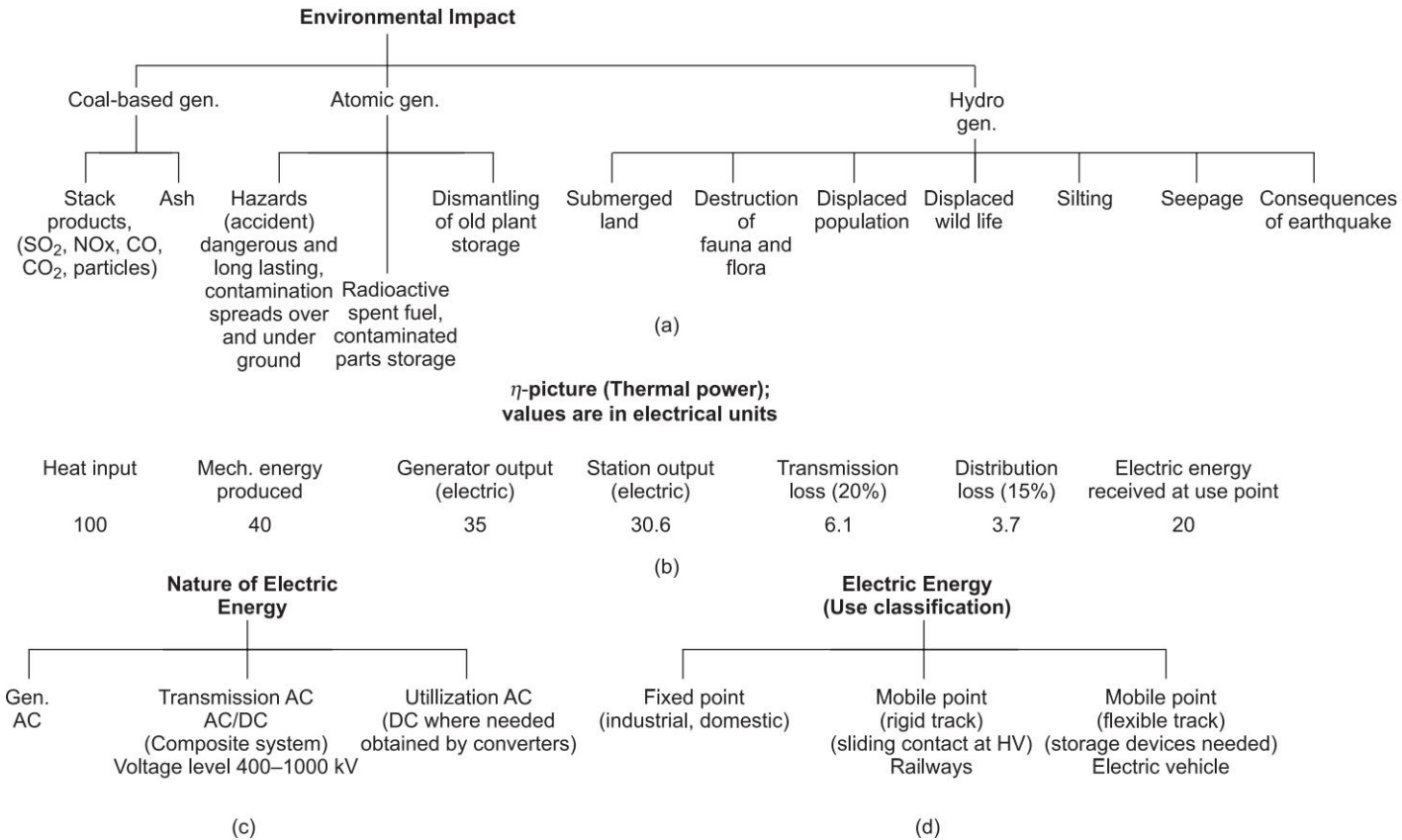

Fig. 1.16 Environmental and other aspects of electric energy production and use

Problematic pollutants in emission of coal-based generating plants are

- SO_2
- NO_x, nitrogen oxides
- CO
- CO_2
- Certain hydrocarbons
- Particulates

Although the account that follows will be general, it needs to be mentioned here that Indian coal has a comparatively low sulphur content but a very high ash content, which in some coals may be as high as 53%.

A brief account of various pollutants, their likely impact and methods of abatements are presented below.

Oxides of Sulphur (SO_2)

Most of the sulphur present in the fossil fuel is oxidized to SO_2 in the combustion chamber before being emitted by the chimney. In atmosphere it gets further oxidised to H_2SO_4 and metallic sulphates, which are the major source of concern as these can cause acid rain, impaired visibility and damage to buildings and vegetation. Sulphate concentrations of 9–10 $\mu g/m^3$ of air aggravate asthma, lung and heart disease. It may also be noted that although sulphur does not accumulate in air, it does so in soil.

Sulphur emission can be controlled by

- use of fuel with less than 1% sulphur; generally not a feasible solution;
- use of chemical reaction to remove sulphur in the form of sulphuric acid from combustion products by limestone scrubbers or fluidized bed combustion; and
- removing sulphur from the coal by gasification or floatation processes.

It has been noticed that the byproduct sulphur could off-set the cost of sulphur recovery plant.

Oxides of Nitrogen (NO_x)

Of these Nitrogen oxide, NO_2 is a major concern as a pollutant. It is soluble in water and so has adverse affect on human health as it enters the lungs on inhaling and after combining with moisture converts to nitrous and nitric acids, which damage the lungs. At levels of 25–100 parts per million, NO_x can cause acute bronchitis and pneumonia.

Emission of NO_x can be controlled by fitting advanced technology burners which can assure more complete combustion, thereby reducing these oxides from being emitted by the stack. These can also be removed from the combustion products by absorption process by certain solvents going on to the stack.

Oxides of Carbon (CO, CO_2)

CO is a very toxic pollutant, but it gets converted to CO_2 in the open atmosphere (if available) surrounding the plant. On the other hand CO_2 has been identified as a major cause of global warming. It is not yet a serious problem in developing countries.

Hydrocarbons

During the oxidation process in combustion chamber certain light weight hydrocarbons may be formed. The compounds are a major source of photo-chemical reaction that adds to depletion of ozone layer.

Particulates (Fly ash)

Dust content is particularly high in the Indian coal. Particulates come out of the stack in the form of fly ash. It comprises fine particles of carbon, ash and other inert materials. In high concentrations, these cause poor visibility and respiratory diseases.

Concentration of pollutants can be reduced by the dispersal over a wider area by use of high stacks. *Precipitators* can be used to remove particles as the flue gases rise up the stack. If in the stack a vertical wire is strung in the middle and charged to a high negative potential, it emits electrons. These electrons are captured by the gas molecules thereby becoming negative ions. These ions accelerate towards the walls, get neutralized on hitting the walls and the particles drop down the walls. Precipitators have a high efficiency, upto 99% for large particles, but they have a poor performance for particles of size less than 0.1 μm in diameter. The efficiency of precipitators is high with reasonable sulphur content in flue gases but drops for low sulphur content coals; 99% for 3% sulphur and 83% for 0.5% sulphur.

Fabric filters in form of *bag houses* also have been employed and are located before the flue gases enter the stack.

Thermal Pollution

Steam from low-pressure turbine has to be liquefied in a *condenser* and reduced to lowest possible temperature to maximize the thermodynamic efficiency. The best efficiency of steam cycle practically achievable is about 40%. It means that 60% of the heat in steam at the end of cycle must be removed. This is achieved by two methods:

1. *Once through* circulation through condenser cooling tubes of sea or river water where available. This raises the temperature of water in these two sources and threatens sea and river life around in sea and downstream in river. These are serious environmental objections and many times cannot be overruled and also there may be legislation against it.

2. *Cooling towers* Cool water is circulated around the condenser tube to remove heat from the exhaust steam in order to condense it. The circulating water gets hot in the process. It is pumped to the cooling towers and is sprayed through nozzles into a rising volume of air. Some of the water evaporates providing cooling. The latent heat of water is 2×10^6 J/kg and cooling can occur fast. But this has the disadvantage of raising the humidity to high (undesirable) levels in the surrounding areas. Of course the water evaporated must be made up in the system by adding fresh water from the source. These cooling towers are known as *wet towers*.
   Closed cooling towers where condensate flows through tubes and air is blown on these tubes avoids the humidity problem but at much higher cost. In India only wet towers are being used.

Electromagnetic Radiation from Overhead Lines

Biological effects of electromagnetic radiation from power lines and even cables in close proximity of buildings have recently attracted attention and have also caused some concern. Power frequency (50 to 60 Hz) and even their harmonies are not considered harmful. Investigations carried out in certain advanced countries have so far proved inconclusive. The electrical and electronics engineers, while being aware of this controversy, must know that many other environmental agents are moving around that can cause far greater harm to human health than does electromagnetic radiation.

As a piece of information it may be quoted that directly under an overhead line of 400 kV, the electric field strength is 11000 V/m and magnetic flux density (depending on current) may as much as 40 μT. Electric field strength in the range of 10,000–15,000 V/m is considered safe.

Visual and Audible Impacts

These environmental problems are caused by the following factors:

1. Right of way acquires land underneath. At present it is not a serious problem in India, but in future the problem will show up. This is futuristic.
2. Lines converging at a large substation mar the beauty of the landscape around. Underground cables as an alternative are too expensive a proposition except in congested city areas.
3. Radio frequency interference (RFI) has to be taken into account and countered by various means.
4. The phenomenon of *corona* (a sort of electric discharge around the high tension line) produces a hissing noise which is audible when habitation is in close proximity. At the towers great attention must be paid to tightness of joints, avoidance of sharp edges and use of earth screen shielding to limit audible noise to acceptable levels. (For details, see Ch.19)

5. Workers inside a power plant are subjected to various kinds of noise (particularly near the turbines) and vibration of floor. To reduce this noise to a tolerable level, foundations and vibration filters have to be designed properly and simulation studies carried out. The workers must be given regular medical examinations and sound medical advice.

1.9 RENEWABLE ENERGY RESOURCES

In the account that has preceded, we have concentrated mostly on those energy resources which are nonreplenishable as brought out in Fig. 1.5 (left side). These are mainly coal, oil, gas and nuclear fission. Apart from the fact that these cannot last for long, considering the galloping rate at which electricity use is rising, they have serious environmental impacts and hazards associated with electric power generation as brought out in Fig. 1.16(a). This has led to a concerted international effort in research and development of renewable energy resources. They offer viable options to address the energy security issues. India has one of the highest potential for the effective use of renewables. Special emphasis has been laid on the generation of grid quality power from them.

A major source of renewable energy is solar radiation being cyclically received by most land area of the globe. Its various manifestations are presented in Fig. 1.5 (right side) as follows:

1. Direct use;
2. Winds on land area of globe;
3. Potential energy of rain and snow at high altitudes, i.e. hydro energy;
4. Biofuel.

Gravitational pull of moon on earth 1.Tidal energy;
2. Wave energy.

Geothermal It is considered renewable because the resource is unlimited.

All the above resources, other than geothermal, pass through the environment as a *energy current or flow*. Together these energy flows are called *energy flux*. The earth's habitable surface is crossed by or accessible to an average energy flux of about 500 W/m^2. If this flux can be harnessed at just about 4% efficiency, a 10 m × 10 m surface would contribute 2 kW of power using suitable methods. Assume that an average suburban person consumes 2 kW and a population density of 500 persons/km^2. At 2 kW per person, the total energy demand of 1000 kW/km^2 could be met by using just 5% of land area for energy production. This could provide a fairly satisfactory standard of living across the globe. Realistically it is not as rosy as harnessing renewable energy is not an easy task and ridden with technological problems whose economic

solutions are yet to be found. To further complicate matters, the renewable energy flux is far from uniformally distributed round the globe.

On account of the environmental impact of harnessing hydro energy and the limitation of harnessing tidal energy, these have been treated in Sec. 1.5 Geothermal energy has also been considered alongwith thermal generation in Sec. 1.7.

We shall now study solar energy and wind energy, the methods of harnessing these and the difficulties encountered. We shall also touch up biofuel.

Wave Energy

The energy content of sea waves is very high. In India, with several hundreds of kilometers of coast line, a vast source of energy is available. The power in the wave is proportional to the square of the amplitude and to the period of the motion. Therefore, the long period (~10 s), large amplitude (~2 m) waves are of considerable interest for power generation, with energy fluxes commonly averaging between 50 and 70 kW/m width of oncoming wave. Though the engineering problems associated with wave-power are formidable, the amount of energy that can be harnessed is large and development work is in progress. Sea wave power estimated potential is 20,000 MW.

Ocean Thermal Energy Conversion (OTEC)

The ocean is the world's largest solar collector. Temperature difference of 20°C between warm, solar absorbing surface water and cooler 'bottom' water can occur. This can provide a continually replenished store of thermal energy which is in principle available for conversion to other energy forms. OTEC refers to the conversion of some of this thermal energy into work and thence into electricity. Estimated potential of ocean thermal power in India is 50,000 MW.

A proposed plant using sea temperature difference would be situated 25 km east of Miami (USA), where the temperature difference is 17.5°C.

1.10 SOLAR ENERGY AND ITS UTILIZATION

Solar energy is a free source which is not only naturally renewable but is also environment friendly and thus helps in lessening the greenhouse effects. As shall be seen in the account that follows, it can only supplement to a (very) limited extent the burgeoning need for energy across the globe. In India, with a deficient grid power and large number of sunny days across the country, solar energy as a supplement is particularly attractive.

The Sun and Solar Energy

The sun is a spherical mass of hot gases, with a diameter of about 1.39×10^9 m and at an average distance of 1.5×10^{11} m from the earth. Energy is being continuously produced in the sun through various nuclear fusion reactions, the most important one being where four protons combine to form a helium nucleus.

$$H_2 + H_2 \rightarrow He + 15 \text{ MeV}$$

The mass lost in the process is converted into energy. These reactions occur in the innermost core of the sun, where the temperature is estimated to be $(8–40) \times 10^6$ K. The various layers of differing temperatures and densities emit and absorb different wavelengths making the solar spectrum quite composite. However, the sun essentially acts as a black body having a 5800 K temperature. The spectral distribution of solar radiation at the earth's mean distance is shown in Fig. 1.17.

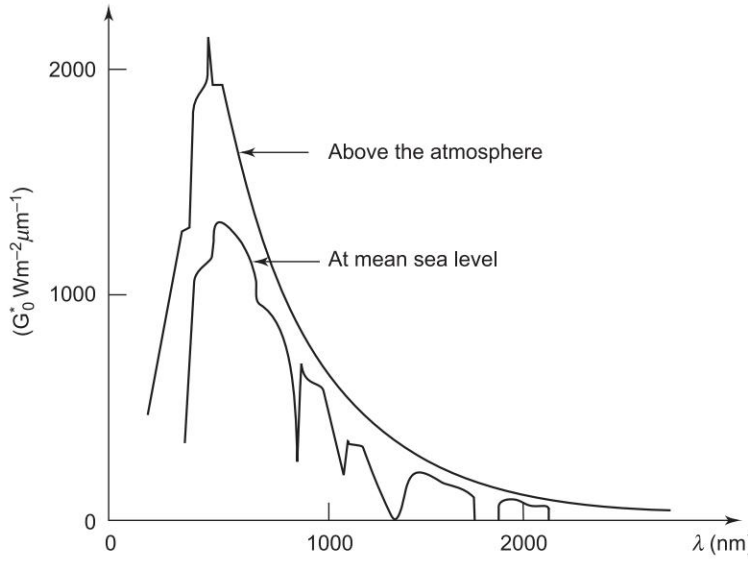

Fig. 1.17 Spectral distribution of the sun's radiation

The solar constant is the radiant flux density incident on a plane normal to the sun's rays at a distance of 1.49×10^8 km from the sun and is given by the area under the curve in Fig. 1.17. It has a value of

$$G_o^* = 1367 \text{ W/m}^2$$

The received flux density varies by ±1.5% during the day's course due to variations in the sun's output, and by about ±4% over the year due to the earth's elliptic orbit. The solar spectrum can be divided into three main regions:

1. Ultraviolet region ($\lambda < 400$ μm): 9%;
2. Visible region (400 nm $< \lambda <$ 700 nm); 45%;
3. Infrared region ($\lambda >$ 700 nm): 46%.

The radiation in the wavelengths above 2500 nm are negligible.

The earth's atmosphere absorbs various components of the radiation to different levels. The short wave UV and X-ray regions are almost completely absorbed by oxygen and nitrogen gases and ions; the ozone absorbs UV rays. The atmosphere unaffected by dust or clouds acts as an open window for the visible region. Up to 20% of the IR (Infrared) radiation is absorbed by the water vapour and CO_2. The carbon dioxide concentration in the atmosphere is about 0.03% by volume and is beginning to rise with pollutants being let off into the atmosphere. The water vapour concentration can vary greatly (upto 4% by volume). Dust, water droplets and other molecules scatter the sun's radiation.

The sun's radiation at the earth's surface is composed of two components: *beam radiation* and *diffuse radiation*. Beam or direct radiation consists of radiation along the line connecting the sun and the receiver as shown in Fig. 1.18(a). Diffuse radiation is the radiation scattered by the atmosphere without any unique direction as in Fig. 1.18(b). There is also a reflected component due to terrestrial surface. Total radiation is shown in Fig. 1.18(c).

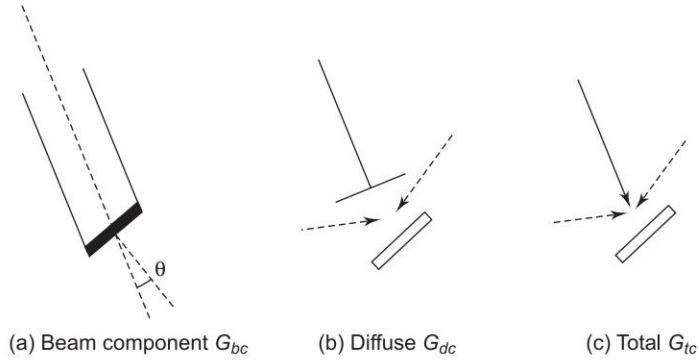

Fig. 1.18 Components of solar radiation reaching earth

It easily follows from these figures that [21]

$$G_{bc} = G^*_b \cos \theta \tag{1.6}$$

For a horizontal surface, the relation becomes

$$G_{bh} = G^*_b \cos \theta_z \tag{1.7}$$

Here θ_z (called the Zenith angle) is the angle of incidence of beam component of solar radiation for a horizontal surface. θ is shown in

Fig. 1.18(a). G_b^* is intensity of beam component of normally incident solar radiation on a surface. Adding the beam of the diffuse components, we get

$$G = G_{tc} = G_{bc} + G_{dc} \tag{1.8}$$

Variation of Insolation

Practically the earth is a sphere of radius 6400 km which rotates once in 24 h about its own axis. The axis defined by the North and South poles is shown in Fig. 1.19

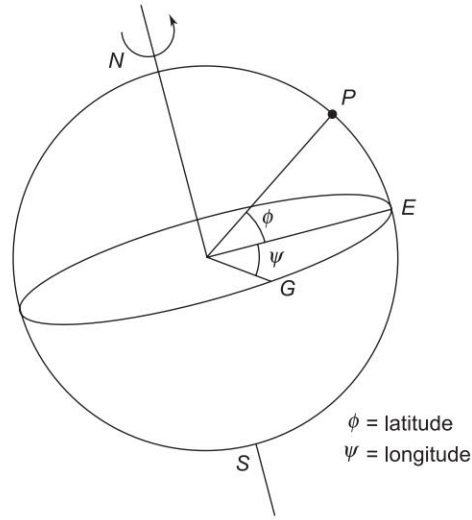

Fig. 1.19

Any point P on the earth's surface is determined by its latitude ϕ and longitude ψ. The latitude is positive in the northern hemisphere, and negative in the southern hemisphere. The longitude is measured positive eastward from Greenwich, England. The vertical North-South plane through P is called *Local Meridional Plane*. Solar noon at P and all places of the same longitude is defined, when the sun is included in the meridional plane. However, clocks do not necessarily show solar time as they are set to civil time common to time zones spanning 15° of longitude. Also the true interval between two successive solar noons is not exactly 24 h due to the elliptic orbit of the earth. The hour angle ω is the angle by which the earth has rotated since the solar noon.

$$\omega = 15°/\text{h} \times (T_{\text{solar}} - 12 \text{ h}) \tag{1.9}$$

or

$$\omega = 15° \text{ h} \times (T_{\text{zone}} - 12 \text{ h}) + (\psi - \psi_{\text{zone}}) \tag{1.10}$$

where T_{solar} is the solar time and T_{zone} is the zone time.

The earth revolves around the sun in an elliptic orbit in 365 days with its axis inclined at angle $\delta_0 = 23.5°$ to the normal to the plane of revolution around the sun.

The *declination* δ is defined as the angle between the equatorial plane and the sun's direction. It varies from +23.5° to –23.5° from 21st June to 21st December—the *summer and winter solstices in the Northern Hemisphere*. It is zero on the *equinoxes*. The declination can be expressed as

$$\delta = \delta_0 \sin\left(\frac{360°\,(284 + n)}{365}\right) \tag{1.11}$$

where n is the day of the year counted from the 1st of January.

The daily insolation is the total energy received from the sun per unit area in one day. The variation of daily insolation with latitude and season is shown in Fig. 1.20.

The variation arises due to three main factors:

(i) Variation in the length of the day;
(ii) Orientation of the receiving surface due to the earth's declination; and
(iii) Variation in atmospheric absorption.

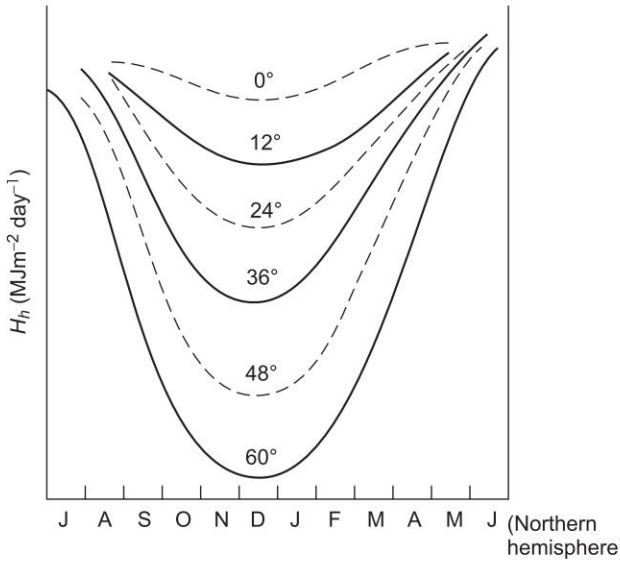

Fig. 1.20 Variation in daily insolation

Geometry of the Collector and Solar Beam

For a tilted collector surface as in Fig. 1.21, the following angles are defined. Slope β is the angle between the collector surface and the horizontal surface. *Azimuth angle* γ is the deviation of the projection of the normal to the collector surface on a horizontal plane. In the northern hemisphere for a south facing surface or horizontal surface, $\lambda = 0$. λ is positive for surface facing West of South, and negative for surfaces facing East of South. The general relation between various angles can be shown to be

$$\cos\theta = (A - B)\sin\delta + [C\sin\omega + (D + E)\cos\omega]\cos\delta \qquad (1.12)$$

where

$$A = \sin\phi\cos\beta$$
$$B = \cos\phi\sin\beta\cos\gamma$$
$$C = \sin\beta\sin\gamma$$

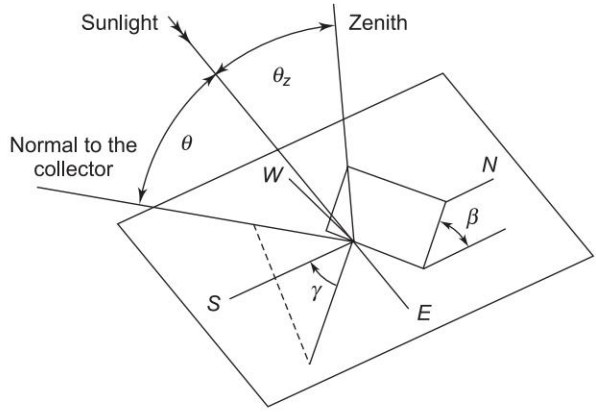

Fig. 1.21 Geometry of the collector and solar beam

$$D = \cos\phi \cos\beta$$

$$E = \sin\phi \sin\beta \cos\gamma$$

ω = hour angle given by the equation

For a horizontal plane, $\gamma = \beta = 0$; giving

$$\cos\theta = \sin\phi \sin\delta + \cos\phi \cos\omega \cos\delta \tag{1.13}$$

If the collector's slope equals the latitude, i.e. $\beta = \phi$, it will face the solar beam directly at noon. In this case:

$$\cos\theta = \cos\omega \cos\delta \tag{1.14}$$

Optimum Orientation of the Collectors

The insolation received at the collector's plane is the sum of beam and diffuse components, i.e.,

$$H_c = \int (G_b^* \cos\theta + G_d)\, dt \tag{1.15}$$

To maximize the energy collected, cos θ should be as close to 1 as possible. This is achieved by continuous *tracking*, always maintaining cos θ as 1 by letting the collector directly face the solar beam. By mounting the array on a two-axis tracker, upto 40% more energy, as compared to a fixed slope collector, can be collected. But this increases complexity and results in higher capital operation and maintenance costs. Single-axis tracking is less complex, but yields a smaller gain. However, as cos $\theta \approx 1$ for $\theta < 30°$, for most applications the collector can be kept with $\beta = \phi$ and $\gamma = 0°$. The specific tracking method to be adopted will depend on the energy demand variation. Tracking is particularly important in systems that operate under concentrated sunlight.

Applications of Solar Energy

Solar energy finds many applications, some of these being water heating, solar drying, desalination, industrial process heating and passive/active heating of buildings. However, because of the well known advantages of electrical power, the methods of converting solar radiation into electricity have attracted the greatest attention. There are two essential ways of converting solar energy into electricity.

(i) *Solar thermomechanical systems:* Here, the solar radiation is used to heat a working fluid which runs turbines.
(ii) *Solar photovoltaics*: Solar photovoltaics (SPV) convert radiant energy directly into an electric current.

In both of these systems, collecting systems are used to receive the radiant energy.

These are described below:

Flat-plate collectors are used in low efficiency photovoltaics and low medium temperature thermal systems. In thermomechanical system the flat-plate collector acts as a heat exchanger transferring the radiant energy to a working fluid. The advantages of flat-plate collectors over concentrators are as follows:

(i) Absorb the diffuse, direct and reflected components of the radiation;
(ii) Comparatively easy to fabricate and cheaper; and
(iii) Since these are usually fixed in tilt and orientation, tracking is not required—this makes them maintenance free, except for surface cleaning.

For a solar-thermal flat-plate collector the components are as follows:

(i) A flat metallic plate painted black to absorb radiation;
(ii) Channels attached to the plate where a working fluid removes the thermal energy; and
(iii) Thermal insolation at the back and sides of the collector, and a glass cover to minimize thermal losses.

Flat-plate collectors are popular in water heating systems.

Concentrating collectors are used in high temperature solar thermal systems and some high efficiency photovoltaics. There are various methods of classifying solar concentrators. They may be classified as refracting or reflecting, imaging or nonimaging, and on the basis of the type of reflecting surface as parabolic, spherical or flat. High temperatures are obtained by using central tower receivers and *heliostats*.

Solar Thermomechanical Systems

In solar thermomechanical systems, solar energy is converted to thermal energy of a working fluid. This thermal energy gets converted into shaft work

by a turbine which runs generators. Heat engines (turbine) are based on the Rankine cycle, Sterling cycle or the Brayton cycle. Usually a fossil fuel heat source is also present as standby.

A schematic flow diagram for a solar power plant operating on Rankine cycle is shown in Fig. 1.22. The maximum theoretical *thermal efficiency*, the ratio of useful work done to the heat supplied, is expressed for the Carnot cycle in terms of the temperature of the reservoirs with which it is exchanging heat.

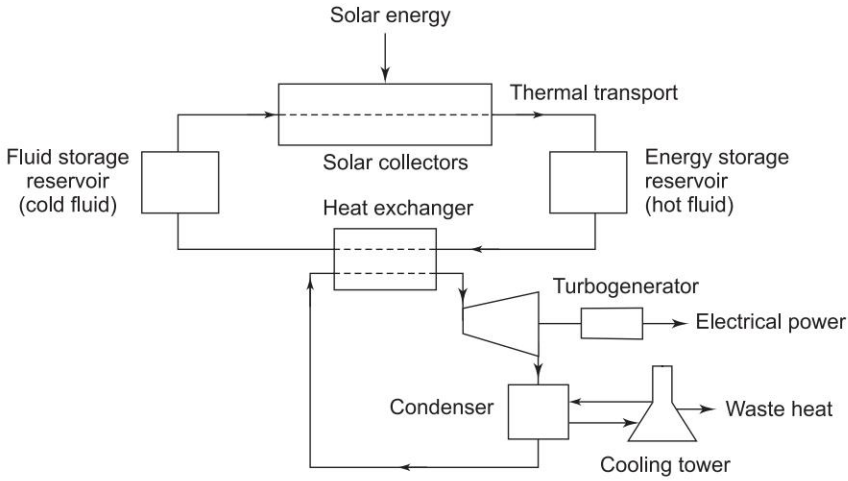

Fig. 1.22 Schematic diagram of a solar power plant operating on the Rankine cycle

$$\eta = 1 - \frac{T_L}{T_H} \tag{1.16}$$

where

η = thermal efficiency of the Carnot cycle
T_L = absolute temperature (°C + 273) of the sink
T_H = absolute temperature of the source

For a solar energy system collecting heat at 121°C, the maximum thermal efficiency of any heat engine using this heat and rejecting heat to atmosphere at a low temperature of 10°C is

$$\eta = 1 - \frac{273 + 10}{273 + 121} = 0.282 \text{ or } 28.2\%$$

The efficiency of a real engine will be considerably less.

For obtaining efficiencies close to those of fossil fuel based stations, T_H must be raised to the same order of value. This is achieved by installing an array of mirrors, called heliostats, tracking the sun. One proposed scheme is shown in Fig. 1.23 for major generation of electricity with reflectors (with concentration

factor of 30 or more) concentrating the sun's rays on to a single boiler for raising steam. A collector area of 1 km^2 would raise 100 MW of electrical power. The cost of such a scheme at present is prohibitive.

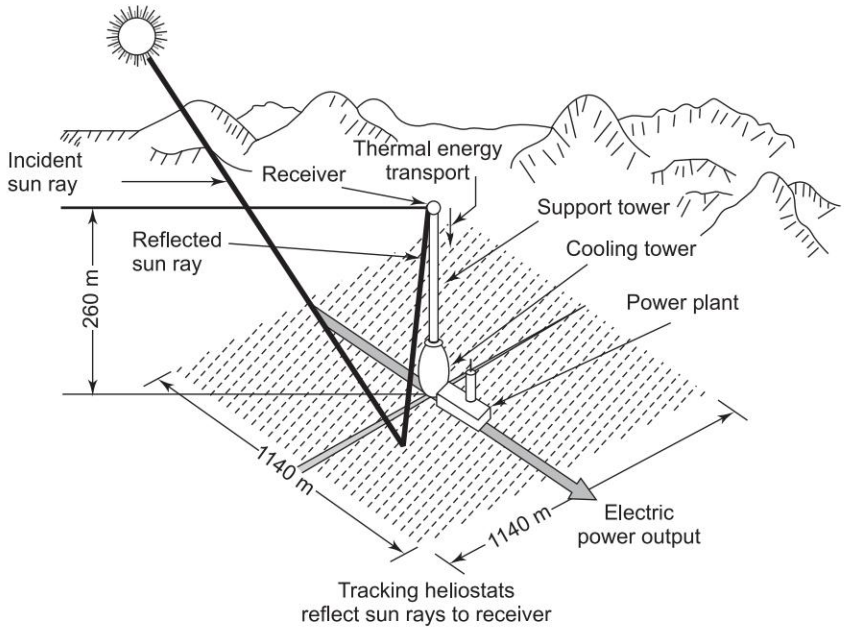

Fig. 1.23 Proposed scheme for a large central solar-thermal electric generation

A less attractive alternative to this scheme (because of the lower temperatures) is the use of many individual absorbers tracking the sun unidirectionally, the thermal energy being transferred by a fluid (water or liquid sodium) to a central boiler.

Solar-thermal electric systems have certain inherent disadvantages of a serious nature. These are as follows:

1. Low efficiency. Raising efficiency to acceptable value brings in prohibitive costs.
2. The efficiency of the collecting system decreases as its temperature increases, but the efficiency of the heat engine increases with temperature.
3. All solar-thermal schemes essentially require storage because of the fluctuating nature of the sun's energy, although it has been proposed that the schemes be used as pure fuel savers.
4. In general mechanical systems need great maintenance.
5. For a reliable system fossil fuel backup may be needed.

Because of these factors considerable research effort is being devoted to solar photovoltaics as a viable alternative.

Direct Conversion of Sunlight into Electricity

Introduction

Photovoltaic (PV) or solar cell is a semiconductor device that converts sunlight directly into electricity. Initially PV cells had very limited use, e.g., in supplying electricity to satellites in space or for meeting energy requirements of defence personnel stationed at remote areas. However, with a gradual reduction in the cost of PV cells, current international price is now between 5–10$ per peak-watt, its use has been increasing steadily and it is projected that by the year 2010 or so its share in power generation may be around 5–10%.

A PV cell can be classified

1. in terms of materials: noncrystalline silicon, polycrystalline silicon, amorphous silicon, gallium arsenide, cadmium telluride, cadmium sulphide, idium arsenide, etc.
2. in terms of technology for fabrication single crystal bonds (or cylinders), ribbon growth, thin-film, etc.

Some of the important characteristics of various types of PV cells, measured at normal temperature (25°C) and under illumination level of 100 mW/cm^2, are listed in Table 1.1

Table 1.1

PV cell	*ff**	*Short-circuit current density (Isc) (mA/cm^2)*	*Open-circuit voltage (V_{oc}) (V)*	*Conversion efficiency (%)*
Monocrystalline silicon	0.85	20–22	0.5–0.6	13-14
Polycrystalline silicon	0.85	18–20	0.5–0.6	9-12
Amorphous silicon		13–14	2.2–2.4	5–6
Gallium arsenide	0.87	–	–	20-25

* *ff* is fill-factor which is defined later.

Basic Structure of PV Cell

The basic structure of a typical PV cell is shown in Fig. 1.24(a) and (b). Various layers from top to bottom and their functions are as follows:

- Top layer is a glass cover, transparency 90–95%. Its purpose is to protect the cell from dust, moisture etc.
- The next is a transparent adhesive layer which holds the glass cover.
- Underneath the adhesive is an antireflection coating (ARC) to reduce the reflected sunlight to below 5%.
- Then follows a metallic grid (aluminium or silver) (Fig. 1.24(b)) which collects the charge carriers, generated by the cell under incidence of sunlight, for circulating to outside load.

- Under the lower side of the metallic grid lies a p-layer followed by n-layer forming a pn-junction at their interface. The thickness of the top p-layer is so chosen that enough photons cross the junction to reach the lower n-layer.
- Then follows another metallic grid in contact with the lower n-layer. This forms the second terminal of the cell.

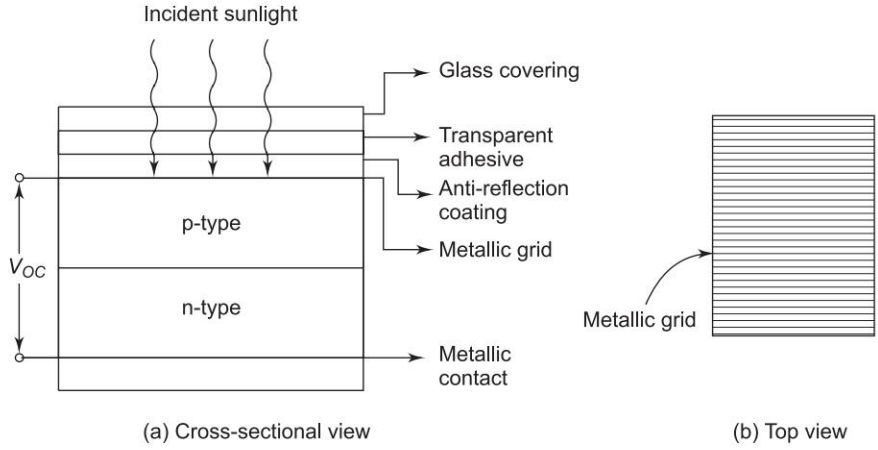

Fig. 1.24

Operation and Circuit Model

The incidence of photons (sunlight) causes the generation of electron-hole pairs in both p and n-layers. Photons generated minority carriers (electrons in p-layer and holes in n-layer) freely cross the junction. This increases the minority carrier flow manyfolds. Its major component is the light generated current I_G (when load is connected across the cell terminals). There is also the thermally generated small reverse saturation current I_s (minority carrier flow in same direction as I_G) also called *dark current* as it flows even in absence of light. I_G flows in opposite direction to I_D, the forward diode current of the junction. The cell feeds current I_L to load with a terminal voltage V.

The above operation suggests the circuit model of a PV cell as drawn in Fig. 1.25. The following Eq. (1.18) can be written from the circuit model and the well-known expression for

$$I_D = I_s\,(e^{\lambda V} - 1);\ \lambda = \frac{e}{kT} \tag{1.17}$$

where

k = Boltzmann constant,
e = electronic charge and
T = cell temperature in degree K.

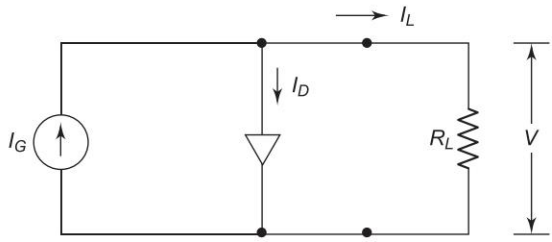

Fig. 1.25 Circuit model of PV cell

Load current $I_L = I_G - I_D$

$$= I_G - I_s\,(e^{\lambda V} - 1) \tag{1.18}$$

From this equation it easily follows that

$$V_{OC}\,(I_L = 0) = \frac{1}{\lambda}\,\ln\left(\frac{I_G}{I_s} + 1\right) \tag{1.19}$$

and $$I_{SC}\,(V = 0) = I_G \tag{1.20}$$

Solar radiation generated current I_G is dependent on the intensity of light. The I–V characteristics of the cell are drawn in Fig. 1.26(a) for various values of intensity of solar radiation. One typical I–V characteristic of the cell is drawn in Fig. 1.26(b). Each point on this curve belongs to a particular power output. The point Q indicated on the curve pertains to the maximum power output at which the cell should be operated. At this point.

$$P_{\max} = V_{P\max}\,I_{P\max} \tag{1.21}$$

The *fill-factor* (*ff*) of a cell is defined as

$$ff = \frac{P_{\max}}{I_{SC}V_{SC}} \tag{1.22}$$

The cell efficiency is given as

$$\eta = \frac{P_{\text{out}}}{P_{\text{in}}} \tag{1.23}$$

where P_{out} is the power delivered to load and P_{in} is the solar power incident on the cell.

Effect of Temperature on Solar Cell Efficiency

As the temperature increases, the diffusion of electrons and holes in the length of Si (or GaAs) increases causing an increase in the dark current and a decrease in V_{OC}. The overall effect causes a reduction in the efficiency of solar cell as the

temperature increases. The practical efficiency of Si solar cell is about 12% and that of GaAs solar cell is 25% at the normal temperature of 300 K. With each degree rise in temperature, the efficiency decreases by a factor of 0.0042%.

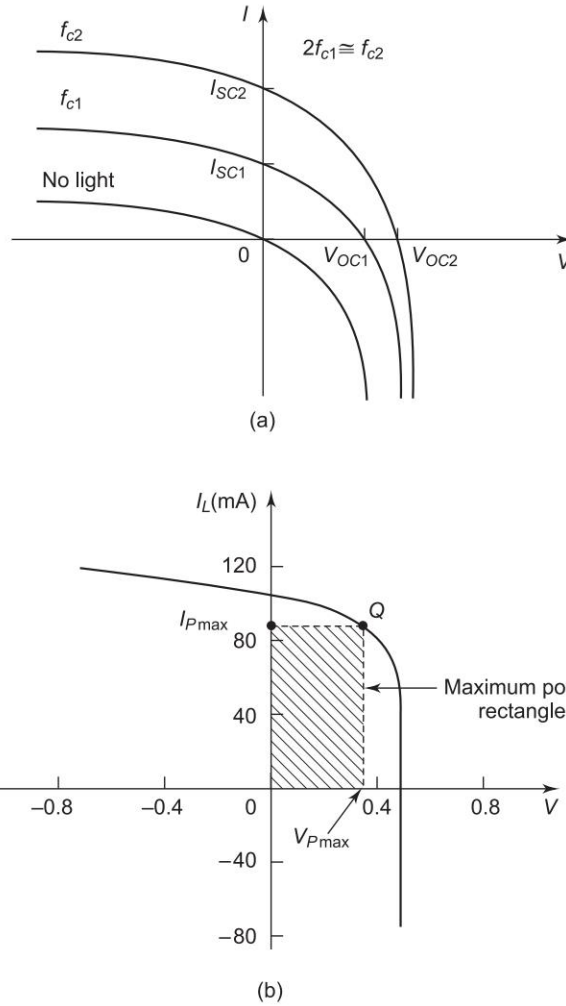

Fig. 1.26 *I–V* (current–voltage) characteristics of a PV cell

Spectral Response

It is seen from the spectral response curves of Fig. 1.27 that the Selenium cell response curve nearly matches that of the eye. Because of this fact Se cell has a widespread application in photographic equipments such as exposure meters and automatic exposure diaphragm. Silicon response also overlaps the visible spectrum but has its peak at the 0.8 μm (8000 Å) wavelength, which is in the infrared region. In general, silicon has a higher conversion efficiency and greater stability and is less subject to fatigue. It is therefore widely used for present day commercial solar cells.

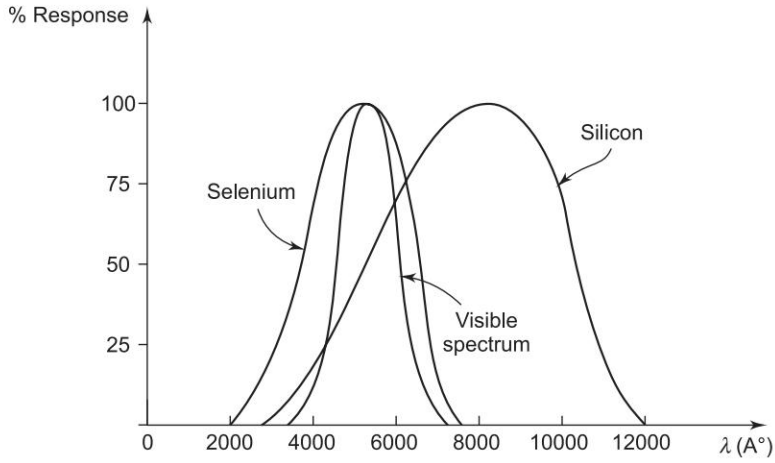

Fig. 1.27 Spectral response of Si, Se and the naked eye

Prevalent Technologies for Fabricating Silicon PV Cell

The most commonly used methods of manufacturing silicon PV cell from purified silicon feedstock are as follows:

1. Single crystal silicon with a uniform chemical structure.
2. Polycrystalline silicon-series of crystalline structures within a PV cell.
3. Amorphous silicon with a random atomic chemical structure.

The technological details of these three types of methods for manufacturing PV cells is not within the scope of this book.

In general as the atomic structure becomes more random, less energy input and manufacturing complexity is required. However, more uniform structure means increased current collection and increased efficiency.

Most PV power uses flat-plate modules of cut and polished wafer like cells of crystalline silicon, which are now about 12% conversion efficient.

Thin-film Technologies

There are two main reasons why thin film offers promise of significant cost reduction. These are as follows:

(i) Thin-film cells use only a few microns of direct material, instead of tens of mills used by crystalline, polycrystalline or *ribbon silicon modules*.

(ii) Construction of monolithic thin-film modules can be done at the same time that the cells are formatted, thus eliminating most of the cost of module fabrication. These two aspects of thin-film technology are further explained below:

- Cadmium telluride can absorb 99% of the sun's energy in less than 0.5 μm thickness as opposed to the 8 mill requirement for crystalline silicon.

- In conventional technologies, cells cut into individual parts are then circuited back together as discrete elements. Monolithic interconnection during cell fabrication eliminates labour and in addition produces a superior looking product because of its uniform finish.

Bulk Energy Conversion by SPV (Solar Photovoltaic) Cells

Bulk SPV power is feasible in bright, clear areas with sun most days of the year such that incident solar energy is about 2600 kWh/m^2 annually.

SPV cell produces DC power which is maximum at a particular point on its $I-V$ characteristics (which changes with sunlight received). There are three ways in which this power can be used:

1. Storage in batteries; this kind of storage is limited in capacity and so meant for small systems. Further reconverting equipment may be required for end use in AC form.
2. PV power is suitably conditioned to AC form for grid interactive use. This is the case with bulk power production.
3. Combined storage and conditioned AC systems.

System of the first kind with battery storage and DC load is drawn in conceptual block diagram form in Fig. 1.28. Mechanical tracking system is required to orient the SPV module at an angle 90° to the incident radiation so as to get maximum intensity. The maximum power tracking system ensures that the load draws the maximum power from the SPV module. DC voltage regulator delivers power at rated voltage despite variation in generated voltage and power. The charge controller is meant to protect the battery bank from both overcharging as well as deep discharging.

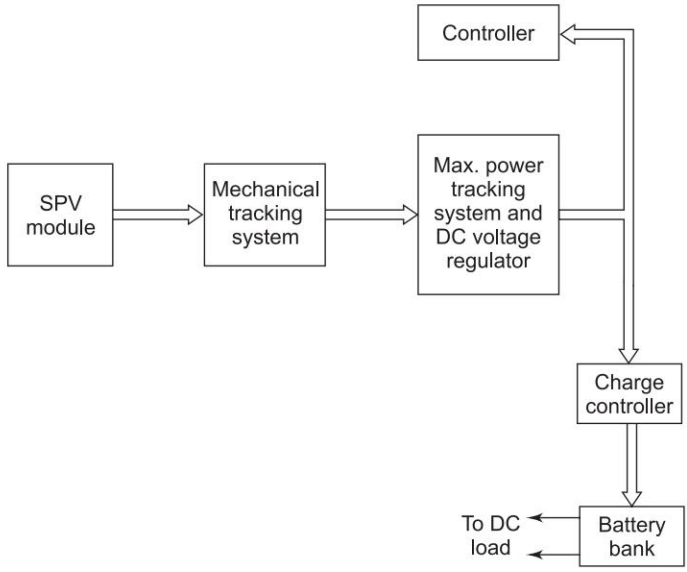

Fig. 1.28 SPV system for feeding DC load with battery storage

A grid interactive SPV system for domestic use is shown in the form of conceptual blocks in Fig. 1.29. Solar cells are connected in series–parallel and the voltage after conversion to AC form by solid state devices is not compatible with grid voltage (400 V at distribution load). This scheme, therefore, differs from that of Fig. 1.22 as the DC voltage has to be raised by the method of DC/DC high frequency chopping with an intervening inductor for raising the voltage. For grid interaction a converter–inverter is required so that power can flow either way depending upon the amount of solar power availability during the day. A battery via converter–inverter feeds the domestic load at night (or on a cloudy day) if the grid outage occurs.

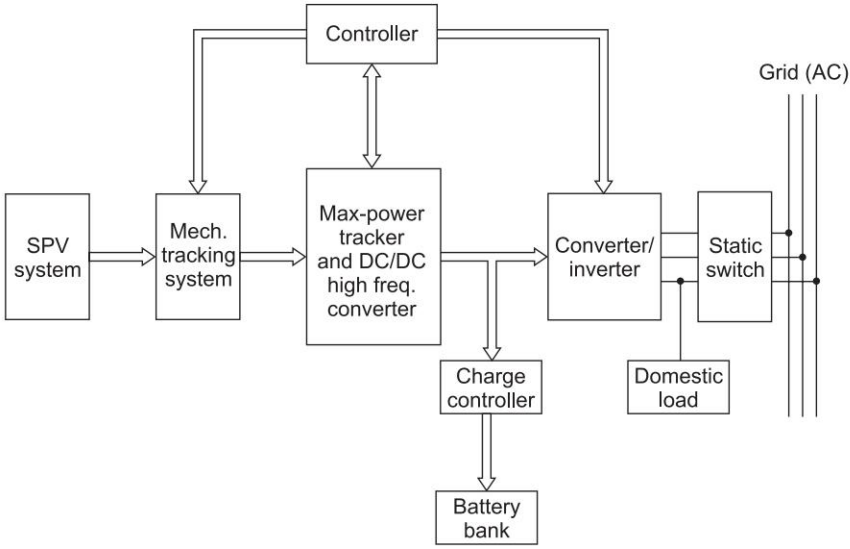

Fig. 1.29 Grid interactive SPV system

The process of conversion and reconversion with solid state devices like SCR (Silicon Controlled Rectifier) is called *power conditioning*. Such systems are already being used in cities in Japan, and are now available in India.

For bulk solar power systems the basic scheme will be similar except that it would directly feed power into the grid and no power need flow the other way.

As and when a breakthrough in SPV technology and sharp reduction in cost is achieved, domestic and bulk power systems will become common place. However, the intensity of solar insolation being low (1367 W/m^2), use of solar power requires considerable land area coverage (with shade underneath, all times, a different kind of pollution). The best estimate is that solar power will meet only 5–10% of the total electric energy need.

Total energy potential in India is 8×10^{15} kWh/yr. Upto 31.12.2005, 6,00,000 solar cookers, 55×10^4 m^2 solar thermal collector area, 47 MW of SPV power, 270 community lights, 5,38,718 solar lanterns (PV domestic lighting units), 640 TV (solar), 54,795 PV street lights and 7002 solar PV water

pumps were installed. Village power plants (stand-alone) of 1.5 MW capacity and 1.1 MW of grid connected power plants were in operation. As per one estimate [2], solar power will overtake wind in 2040 and would become the world's overall largest source of electricity by 2050. 5000 MW grid-interactive solar power could be feasible by 2032 (MNES Annual Report 2005–06). Solar water heating systems are increasingly becoming more popular for homes, hostels, hotels and industrial and domestic purposes. Research has shown that the Gallium Arsenide (GaAs) based PV cell with multijunction device could give maximum efficiency of nearly 30% and Carbon Nano Tube (CNT) based PV cell may give upto 50% efficiency.

1.11 WIND POWER

A growing concern for the environmental degradation has led to the world's interest in renewable energy resources. Wind is commercially and operationally the most viable renewable energy resource.

Worldwide, five nations—Germany, USA, Denmark, Spain and India—account for 80% of the world's installed wind energy capacity total worldwide wind power installed capacity is 79,300 MW. Kinetic energy available in the wind is converted to electrical energy by using rotor, gearbox and generator. The wind turns the blades of a windmill-like machine. The rotating blades turn the shaft to which they are attached. The turning shaft typically can either power a pump or turn a generator, producing electricity. Larger blades capture more wind. As the diameter of the circle formed by the blades doubles, the power increases four times.

Wind is air set in motion by the small amount of insolation reaching the upper atmosphere of earth. Nature generates about 1.67×10^5 kWh of wind energy annually over land area of earth and 10 times this figure over the entire globe. Wind contains kinetic energy which can easily be converted to electrical energy. Wind energy has been used in wind mills for centuries. In 1980s wind energy use received a fillip with availability of excellent wind sites and rising cost of conventionally generated electrical power. Later in 1990s interest in wind generated electrical power to displace conventional power, received further enhancement in order to reduce air pollution levels in the atmosphere. Wind is a clean power generating agent as it causes no pollution.

Power density in moving air is given by

$$P_W = KV^3 \text{ W/m}^2; \text{ Here } K = 1.3687 \times 10^{-2} \qquad (1.24)$$

or $$P_W = 0.5\, \rho\, AV^3 \text{ W}$$

where ρ = air density (1201 g/m^3 at *NTP*)

V = wind speed in km/h, mean air velocity (m/s)

A = Swept area (m^2)

Theoretically a fraction 16/27 = 0.5926 of the power in the wind is recoverable. This is called *Gilbert's limit* or *Betz coefficient*. Aerodynamical efficiency for converting wind energy to mechanical energy can be reasonably assumed to be 70%. So the mechanical energy available at the rotating shaft is limited to 40% or at the most 45% of wind energy.

Wind Characteristics

- Wind speed increases roughly as the 1/7th power of height. Typical tower heights are about 20–30 m.
- *Energy-pattern factor*: It is the ratio of actual energy in varying wind to energy calculated from the cube of mean wind speed. This factor is always greater than unity which means that energy estimates based on mean (hourly) speed are pessimistic.

Utilization Aspects

There are three broad categories of utilization of wind energy:

1. Isolated continuous duty systems which need suitable energy storage and reconversion systems.
2. Fuel-supplement systems in conjunction with power grid or isolated conventional generating units.
3. Small rural systems which can use energy when wind is available.

Category 2 is the most predominant in use as it saves fuel and is fast growing particularly in energy deficient grids. Category 3 has application in developing countries with large isolated rural areas.

Aeroturbine Types and Characteristics

Modern horizontal-axis aeroturbines (wind turbines) have a sophisticated blade design. They are installed on towers 20–30 m high to utilize somewhat high wind speed and also permit land use underneath. Cross-section view of a typical horizontal-axis wind turbine is shown in Fig. 1.30.

Tip Speed, also called *specific speed*, is by far the single most important parameter to be considered. It is defined as

$$\text{Tip speed} = \frac{\text{Peripheral speed}}{\text{wind speed}}$$

This ratio ranges from 2 to 10. Ratios less than 4 require rotor with several blades and have lower rotational speed whereas higher ratios (4 to 10) require fewer blades and have higher rotational speeds. Higher tip speed rotors have lower efficiency because of higher frictional loss. Typical blade diameters are about 20 m and rotor speeds 100–150 rpm.

Power Coefficient

C_p is defined as the fraction of wind power at the rotor shaft. It is dependent on (i) tip speed ratio and (ii) pitch angle of blades. Rather than designing for C_p (max), these factors are determined by economics.

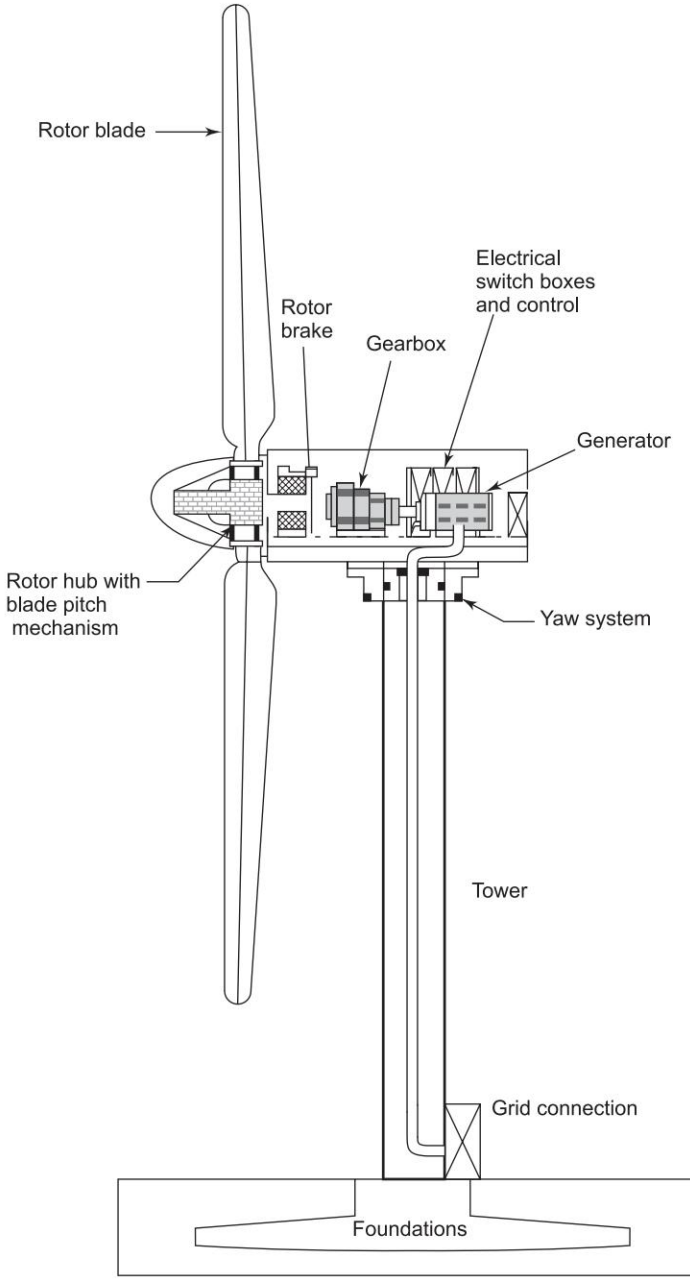

Fig. 1.30 Cross-sectional view of a typical horizontal-axis aeroturbine

Blade Arrangements

For harnessing large power, two to three blade configurations are used. Two blade arrangement is cost effective but prone to vibrations, which disappear with three blades. No unique answer on this issue has been arrived at yet.

Modern machines have metal blades based on aircraft technology. Glass reinforced plastic has also been used successfully.

Vertical-axis Wind Turbines (VAWTs)

Vertical-axis aeroturbines accept the wind from any direction and have the added advantage that the generator is located on ground. As a result the weight on tower is considerably reduced. The technology of these turbines has reached the stage where their efficiencies are comparable with those of horizontal-axis machines.

A number of vertical-axis designs have been developed and tested. We shall discuss here the one that is now commercially available—the Darrieus. The Darrieus rotor has two or more curved airfoil blades, held together at the top and the bottom. These are so positioned that they respond to wind from any direction. Physically it resembles the lower portion of an egg beater. The rotors are non-self-starting and operate at blade tip ratios of 6 to 8. These have efficiencies around 35–40%.

Wind to Electric Energy Conversion

The choice of electrical system for an aeroturbine is guided by three factors:

1. *Type of electrical output*: DC, variable-frequency AC, constant-frequency AC.
2. *Aeroturbine rotational speed*: constant speed with variable blade pitch, nearly constant speed with simpler pitch-changing mechanism or variable speed with fixed pitch blades.
3. *Utilization of electrical energy output*: in conjunction with battery or other form of storage, or interconnection with power grid.

Large scale electrical energy generated from wind is expected to be fed to the power grid to displace fuel generated kWh. For this application present economics and technological developments are heavily weighted in favour of constant-speed constant-frequency (CSCF) system with alternator as the generating unit. It must be reminded here that to obtain high efficiencies, the blade pitch varying mechanism and controls have to be installed.

Wind turbines of electrical rating of 100 kW and above normally are of constant-speed type and are coupled to synchronous generators (conventional type). The turbine rated at less than 100 kW is coupled to fairly constant speed induction generators connected to grid and so operating at constant frequency drawing their excitation VARs from the grid or capacitor compensators.

With the advent of power switching technology (high power diodes and thyristors) and chip-based associated control circuitry, it has now become possible to use variable-speed constant-frequency (VSCF) systems. VSCF wind electrical systems (WES) and its associated *power conditioning* system operates as shown in Fig. 1.31.

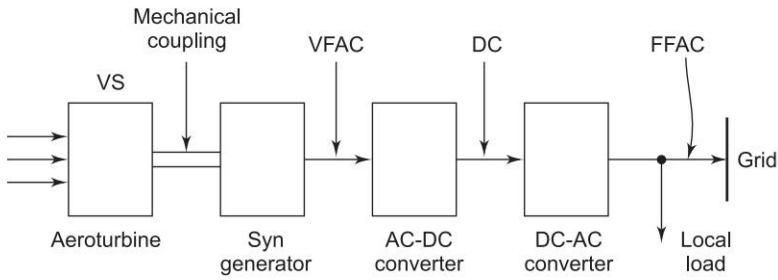

Fig. 1.31 Block schematic of VSCF wind electrical system; VF (variable frequency), FF (fixed frequency)

Various advantages of this kind of VSCF WES are:

1. No complex pitch changing mechanism is needed.
2. Aeroturbine always operates at maximum efficiency point (constant tip-speed ratio).
3. Extra energy in the high wind speed region of the speed-duration curve can be extracted.
4. Significant reduction in aerodynamic stresses, which are associated with constant-speed operation.

Operation and Control of Wind Electrical Systems (WES)

To understand the operation and control of WES, let us first consider a typical wind duration curve of Fig. 1.32(a). Any point on this curve gives the number of hours in a year for which the wind speed is higher than the value corresponding to this point.

Sensors sense the wind direction and the *yaw control* (Fig. 1.30) orients the rotor to face the wind in case of horizontal-axis machines. With reference to the wind duration curve of Fig. 1.32(a) it is seen that the wind turbine begins to deliver power at the *cut-in-speed* V_C and the plant must be shut down for wind speed at the maximum safe limit called the *furling speed* V_F. Between these two limits, mechanical power output of the turbine is determined by the power coefficient C_p. The electrical power output is determined therefrom, by the coefficients η_m and η_g of the mechanical drive and the electrical generator, respectively.

In CSCF WES the conventional synchronous generator locks into the grid and maintains a constant speed irrespective of wind speed. A suitable controller senses the generating/motoring mode of operation and makes the needed pitch adjustments and other changes for a smooth operation.

As the generator output reaches the rated value, the electrical load is held constant even though the wind speed may increase beyond this value. This extra energy in the wind is allowed to be lost as indicated in Fig. 1.32(b). This is also the case for an induction generator whose speed remains substantially constant.

With VSCF system, suitable output controls can be installed to maintain a constant tip speed ratio and so as to keep C_p at its near maximum value. This

results in somewhat more power output throughout the operating range compared to the CSCF system as shown in Fig. 1.32(b). Also there is no need to install sophisticated pitch control systems. The extra cost entailed in the power conditioning system gets more or less balanced against the cost of extra energy output. Considerable development effort is therefore being applied to CSCF system for large rating WES. These systems are yet to be proved in the field.

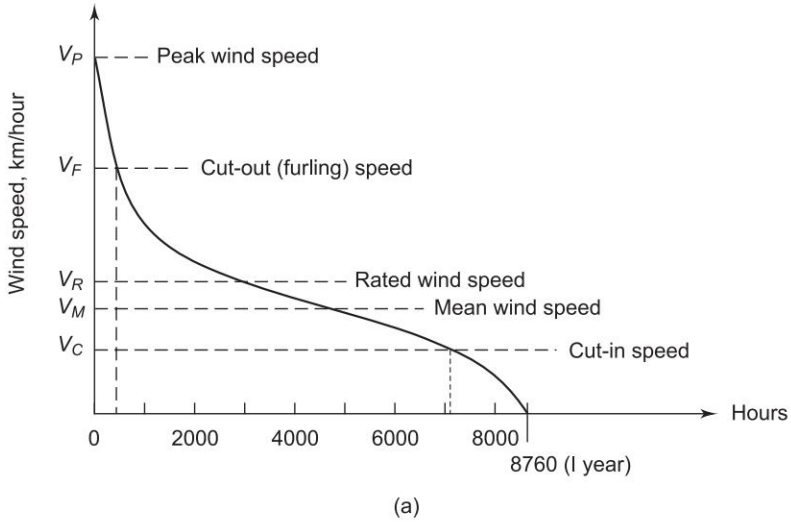

(a)

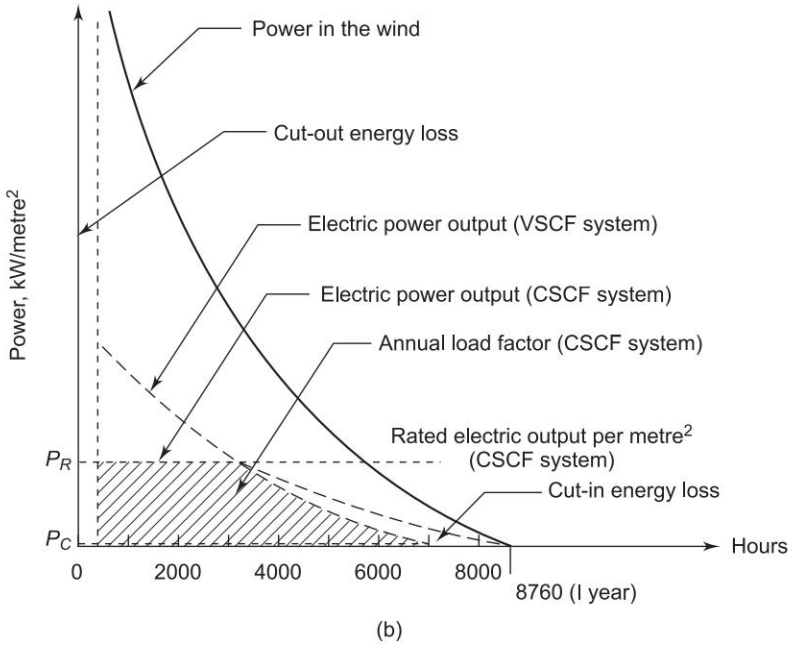

(b)

Fig. 1.32 (a) Typical wind-speed-duration curve
(b) Power-duration curve of wind-driven generator

For CSCF WES the operating curve shown shaded in Fig. 1.32(b) is redrawn in Fig. 1.33 with speed axis reversed for clarity. The aerogenerator starts to generate power at wind speed V_C, the cut-in speed. The aerogenerator produces rated power at speed V_R. At higher wind speeds the aerogenerator speed is held constant by changing the pitch of blades (part of wind energy is being lost during this part of operation). The aerogenerator must be cut-out at V_F, the furling speed.

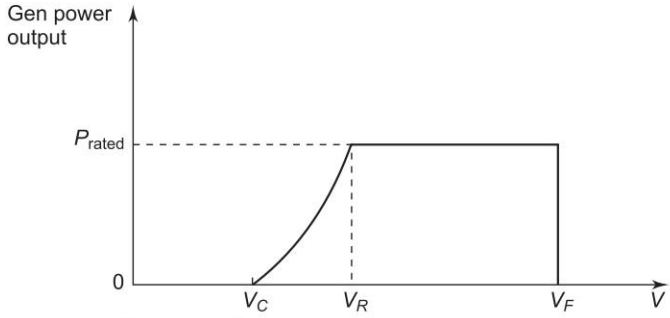

Fig. 1.33 CSCF WES characteristics

Typical wind turbine rotors of 20 m diameter rotate at 100–500 rpm and are geared up to about 750 rpm to drive an eight pole induction generator excited from 400 V, 3-phase, 50 Hz rural distribution system.

Consider as an example an area with mean wind speed of 10 km/h. Power output of 300 MW is to be produced using aeroturbines of 20 m blade diameter. Let us calculate the number of aeroturbines required.

Power in the wind is given by the relationship

$$P_W = KV^2/\text{m}^2 \text{ kW}$$

V = wind speed in km/h

$$K = 1.368 \times 10^{-2}$$

For the aeroturbine

$$P_{\text{aero}}\,(\text{mech}) = 1.368 \times 10^{-2} \times (10)^2\, \pi \left(\frac{20}{2}\right)^2$$

$$= 4290 \text{ kW}$$

$$P_{\text{gen}}\,(\text{elect}) = 4290 \times 0.4 = 1716 \text{ kW}$$

$$\approx 1.7 \text{ MW}$$

Number of aeroturbines needed

$$= \frac{300}{1.7} = 177$$

These aerogenerators will be installed in a *wind farm* with suitable X, Y spacing so that the air turbulence of one aeroturbine on the exit side and also sideways does not affect the successive turbine.

Wind Farm

It is seen from the example given above that to contribute significant power to the grid, several standard size wind turbines have to be employed at a site where there is a vast enough wind field, flat or in a valley. Such an arrangement is called a wind farm.

How closely can the individual wind turbines be located to each other in a wind farm? The operation of a wind turbine causes an air turbulence on its back as well as sides; the region of turbulence is called the *wake* of the turbine. Optimal location of wind turbines is such that no turbines are located in the wake of the forward and side turbines. Any turbine that lies in the wake of another has its power output reduced and over a period fatigue damage caused by stresses generated can occur specially for the yaw drive.

Spacing Rule

A wind turbine has to be aligned perpendicular to the direction of wind. Where wind is unidirectional all day (which is rare), the spacing between turbines of a row (side ways) is 2 D–3 D, D being the diameter of the rotor. Inter row spacing is about 10 D. Normally wind is not unidirectional in which case a uniform spacing of 5 –7D is recommended. A computer software "Micropositioning" is available for this purpose.

Internal transformers and cabling will connect the aerogenerator to the grid. Each turbine will have its own control circuitry. Grid connection requires a certain sophisticated protection scheme whose purpose is

1. to isolate the wind farm in case of any internal fault in the electrical system and
2. to disconnect the wind farm if there is a fault on any section of utility network (grid).

1.12 BIOFUELS

We shall explain the biofuels and their utilization with the help of Fig. 1.34 and explanation of certain terms.

Biomass: It is the material of all the plants and animals. The organic carbon part of this material reacts with oxygen in combustion and in the natural metabolic processes. The end product of these processes is mainly CO_2 and heat as shown in Fig. 1.34.

Biofuels: The biomass can be transformed by chemical and biological processes into intermediate products like methane gas, ethanol liquid or charcoal solid.

Agro industries: The use of biofuels when linked carefully to natural ecological cycles (Fig. 1.34) may be nonpolluting. Such systems are called agroindustries. The well established of these industries are the sugarcane and forest product industries.

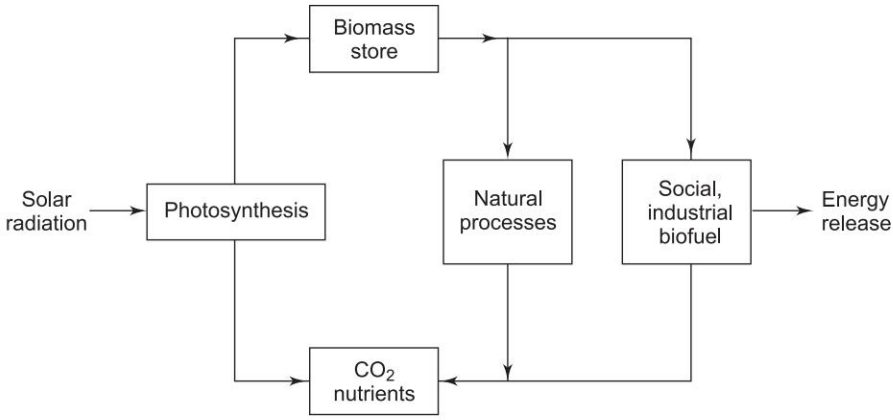

Fig. 1.34 Biomass cycle

Biofuels can be used to produce electricity in two ways:

1. By burning in a furnace to raise steam to drive turbines or
2. By allowing fermentation in landfill sites or in special anaerobic tanks, both of which produce methane gas which can be used as fuel for household stoves and in spark ignition engines or gas turbines. The CO_2 produced in this process must be recycled by cultivating next crop or planting trees as CO_2 is absorbed by photosynthesis by plants.

Biofuels have a potential to meet about 5% of the electricity requirements of an industrialized country by exploiting all forms of these household and industrial wastes, sewerage, sledge (for digestion) and agricultural waste (cow dung, chicken litter, straw, sugarcane, etc.)

1.13 GENERATING RESERVE, RELIABILITY AND CERTAIN FACTORS

Electric loads present a highly fluctuating picture and is not easily amenable to statistics and probability; moreover it is a non-stationary process as its statistics are changing with time. It is, therefore, best to interpret generation and loads in terms of certain overall factors without any direct link to probability. Some of the important factors in use and their significance is presented below.

Reserve generating capacity: Modern generating plants are stressed to limits of temperature and pressure to reduce the overall power costs. Therefore, extra generation capacity must be installed to meet the need of scheduled *downtimes* for preventive maintenance. This reserve capacity also takes care of forced equipment outages and the possibility of the actual load exceeding the forecast, while additional generating stations are in completion phase.

The amount of reserve capacity to be provided is a subjective judgement and somewhat related to the past experience. Inadequate reserve means load outages at times and excessive reserve adds to generation costs.

Reliability: It is measured by the power systems ability to serve all power demands without failure over long periods of times. Various quantitative methods have been devised for estimation of reliability.

From the point of view of generation of power, reliability is added to the system by providing *spinning reserve*. In certain stations of the system some machines are kept on line but are kept only partially loaded to meet almost instantaneously any contingency of loss of a generator feeding the load. The amount of spinning reserve is also based on generator outage statistics and subjective judgement.

Reliability is considerably increased by system interconnection or grid formation and also transmission line redundancy. A cost has to be borne for a reliable system. In India with generation and line capacity shortages reliability is not a meaningful term.

Availability (operational): It is the percentage of the time a unit is available to produce power whether needed by the system or not. It is indeed a measure of overall unit reliability.

Capacity Factor: It is defined as

$$\text{Annual capacity factor} = \frac{\text{actual annual generation (MWh)}}{\text{maximum rating (MW)} \times 8760 \text{ h}}$$

It is always lower than operational availability because of the need to provide spinning reserve and variations in hourly load.

Maximum load: The average load over half hour of maximum output.

Annual Load Factor: $$\text{Annual LF} = \frac{\text{Total annual load (MWh)}}{\text{annual peak load (MW)} \times 8760 \text{ h}}$$

LF varies with the type of load, being poor for lighting load (about 12%), and high for industrial load (80–90%).

Diversity Factor: It is already introduced earlier in Sec. 1.3. It is defined again as

$$\text{DF} = \frac{\sum \text{individual maximum demand of consumers}}{\text{maximum load on the system}}$$

This factor is more than unity. It is high for domestic load. It can be made high by adjustment of timing and kind operation in each shift in industry by providing incentives.

Diversity factor also has same meaning at HV buses where loads are fed to different time zones in a large country. Although India uses one civil time, there is half an hour of diversity between the eastern and western region.

Consider four loads which are constant at L_{max} for 6 h duration and zero for rest of the time. Now we calculate LF and DF for two imaginary cases.

Case 1. Loads occur one after another around 24 h of day. Then

$$\text{LF} = \frac{L_{max} \times 24}{L_{max} \times 24} = 1;\ \text{DF} = 4$$

Case 2. All the loads occur at the same time. Then the total load is 4 L_{max} (the capacity of supply point). Then

$$\text{LF} = \frac{4L_{max} \times 6}{4L_{max} \times 24} = 0.25;\ \text{DF} = 1$$

Local Variations: For computational purpose the yearly data can be plotted in the form of a *load-duration* curve as shown in Fig. 1.35.

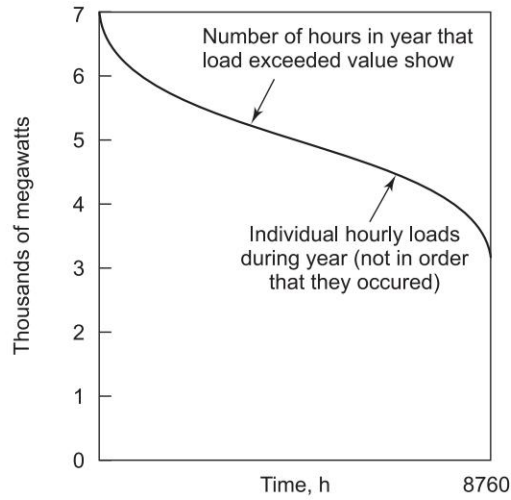

Fig. 1.35 Annual load–duration curve

Generating Capacity Mix

For economically meeting the cyclically varying load the generating capacity can be divided into three basic types (all types may not be available in a small power system):

1. Base-load capacity
2. Intermediate-load-range capacity
3. Peaking capacity

Base-load capacity runs at full rating continuously round the year (except for preventive maintenance when such capacity kept in spare is brought in). These are large units, which exploit the *economy of scale*, with all the fuel-economizing features built in; see Fig. 1.6(b).

Nuclear units have very high capital cost and very low fuel cost and thus are base-load units. Also not much underloading is permitted in these units.

For large hydroelectric dams, throughout the year, the basin is more or less full; thus, hydro unit could serve the base load purpose.

Intermediate-load-range capacity is employed to pick up the load when it rises above the base value. As this capacity does not run round the year, these units may be less efficient than base units.

Peaking capacity is run to take up the peak load of the day and the season. Since their annual output is not very high, high efficiency like in base-load unit is not a necessity. Gas turbines, small hydro units and pumped storage units are most suitable for peaking load as these are *quick start*.

These aspects of the three types of capacity are tabulated in Table 1.2

Table 1.2

Designation capacity	*Capital cost*	*Fuel cost*	*Typical annual LF%*
Base load	High	Low	65–75
Intermediate load	Intermediate	Intermediate	30–40
Peaking load	Low	High	5–15

Interconnection and Pooling: As our country is moving towards national grid formation and more private power generating companies are coming up, which can feed power in the grid, certain inherent saving and advantages result. These are as follows:

1. *Economy interchange*, which is permitted by low fuel cost stations near the coal bearing regions.
2. Each pool region needs less reserve capacity (both standby and spinning) as the reserve capacity gets pooled by interconnection.
3. *Diversity interchange* between various regions make the countrywise LF higher.

The above mentioned interchanges are possible only when strong power transporting lines link the regions into a grid.

Load Management

The procedure to modify the shape of load curve so that the load factor (LF) is raised for operational economy have been mentioned earlier here and there. These procedures and methods are as follows:

1. Offering tariff incentives in light load periods to fill in the troughs.
2. Peaking shaving by
   (i) pumped storage (hydro) and
   (ii) CCGT use at peak load.
3. In advanced countries radio-controlled means (Ripple control) are employed to cut-off comfort conditioning at the peak load hour and then to switch them on.

As mentioned earlier by various 'load management' schemes, it is possible to shift demand away from peak hours (Sec. 1.1). Remote timer controlled on/off switches help achieve adjustment of electric use by a consumer [30]. Most of the potential for load control lies in the domestic sector. Power companies are now planning the introduction of system-wide load management schemes.

Future power systems would include a transmission mix of AC and DC. Future controllers would be more and more microprocessor based, which can be modified or upgraded without requiring hardware changes, and without bringing the entire system down. While one controller is in action the duplicate controller is there as a 'hot standby' in case of sudden need.

It is by now clear that HVDC transmission is already a reliable, efficient and cost-effective alternative to HVAC for many applications. Currently a great deal of effort is being devoted to further research and development in solid state technology. This gives hope that HVDC converters and multiterminal DC (MTDC) systems will play an even greater role in the power systems of the 21st century.

1.14 ENERGY STORAGE

Because of tremendous difficulties in storage of electricity it has to be constantly generated, transmitted and utilized. Large scale storage of energy, which can be quickly converted to electrical form, can help fast changing loads. This would help to ease operation and make the overall system economical as large capacity need not be kept on line to take up short duration load surges. The options available as follows:

- pumped storage (see Sec. 1.5.3)
- compressed air storage
- heat storage
- hydrogen gas storage
- batteries
- fly wheels, superconducting coils; of doubtful promise

Most important of these is the pumped storage which has been dealt at length in Sec. 1.5.3.

Compressed Air Storage

Compressed air can be stored in natural underground caverns or old mines. The energy stored equals the volume of air multiplied by pressure. At the time of need this air can be mixed with gas fuel to run a gas turbine as shown in Fig. 1.36. Gas fuel combustion efficiency is thereby doubled compared to normal operation. A disadvantage of the scheme is that much of the energy used in compressing air appears in the form of heat and gets wasted; temperature of air is 450°C at 20 bar pressure.

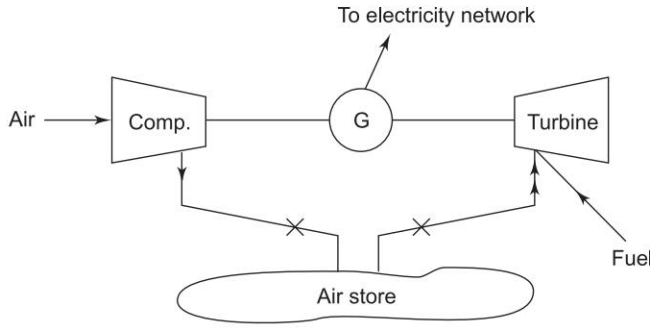

Fig. 1.36 Compressed air storage and use

Heat Storage

No large scale storage of heat has been found to be feasible. Water with good specific and latent heat has been suggested. Liquid sodium is another candidate. (It is used in FBRs for heat transfer). In a generating station, boilers can be kept ready on full steam for the turbine to pick up fast rising load. Boiler steam when not in use can heat feed-water for boilers in the station.

Secondary Batteries

These have possible use in local fluctuating loads, electric vehicles and as backup for wind and solar power (see Fig. 1.28). Considerable research and development effort is being devoted by international laboratories for secondary batteries. The present status is as in Table 1.3

Table 1.3

Battery	*Energy density*	*Operating temperature (where high)*	*Remarks*
Lead–acid cell (popular)	15 Wh/kg (low)	–	–
Nickel–Cadmium cell	40 Wh/kg	–	–
Sodium–sulphur cell	200 Wh/kg	300°C	Sodium electrolyte, liquid electrodes

A 3 MW battery storage plant has been installed in Berlin for frequency control in emergencies.

Hydrogen Energy Systems

Hydrogen can be used as a medium for energy transmission and storage. Transmission of natural gas via a network is well established. India is setting up a national gas grid; Hazira–Jagdishpur pipeline is one link of the grid being developed. The energy transmission capacity of a gas pipeline is high compared to electric energy transmission via HV lines.

Calorific value (cv) of hydrogen gas = 12×10^6 J m^{-3} (ATP)

Power transmitted = flow rate (volume) × cv (at working pressure)

For long gas pipelines pressure drop is compensated by booster compressor stations.

A typical gas system: Pipe of internal diameter = 0.914 m

Pressure = 68 atm

Gas velocity = 7 m/s

Power transferred = 12 GW (gigawatts)

Using gas, electric power can be generated by CCGT near the load centres.

A 1 m diameter pipe carrying hydrogen gas is equivalent to 4–400 kV, 3-phase transmission lines. The major advantage that hydrogen gas has is that it can be stored. The disadvantage being it is produced by electrolysis of water. An alternative method, under development, is to use heat from a nuclear station to 'crack' water for releasing hydrogen at a temperature of about 3000°C. Solar energy is also being used for water splitting to generate hydrogen which can be converted back to electricity by means of fuel cells. Also the use of hydrogen as fuel for aircraft and automobiles could encourage its large scale production, storage and distribution.

Hydrogen may prove to be a wonder element. It is non-polluting, safe and sustainable. It is most lauded alternative transportation fuel after biofuels. However, system efficiency, system cost and safety related aspects are yet to be addressed for H_2 based technology. A fuel cell run car is available in US and Japan. An H_2 and fuel cell facility is available at Solar Energy Centre, Gurgaon. Today price is Rs 150/W. Alcohol mixed petrol is tried successfully in some countries such as Brazil. Class I cities generate 27×10^6 tons of municipal waste, 4400×10^3 m^3 of sewage per year. This can be converted to energy. Estimated potential from urban, municipal and industrial waste to energy is 25000 MW or 50 million units/year of grid power. With the largest cattle population in the world of some 262 million, India holds tremendous potential for biogas development. India has 135 million hectares of wasteland (poor/semidesert) ideal for Jatropha plantation for production of **biodiesel.** It is nontoxic, 100% natural and biodegradable supplement for diesel.

India has total offshore gas hydrate resources of 1894 trillion m^3 which is 1900 times the country's current gas reserves. Even if 1% of the estimated gas hydrate reserves is tapped, our energy requirement for the coming decades can be met.

World-over hydrogen is produced from:

steam reformation of natural gas	(48%)
partial oxidation of oil	(30%)
gasification of coal	(18%)
electrolysis of water	(4%)

In India, about 2.8 MMT produced annually (fertilizer industry, petroleum refineries) for captive consumption. About 0.4 MMT by-product hydrogen

available from chlor-alkali industries. It is used in automobiles and power generation using IC engines and fuel cells. H_2 is also produced through renewable energy sources and can be stored in many ways such as hydrides, carbon nano-tubes and nano-fibres.

Fuel Cell

A fuel cell converts chemical energy to electrical form by electrochemical reaction with no intermediate combustion cycle. One electrode is continuously supplied with fuel (H_2) and the other with an oxidant (usually oxygen). A simple form of a fuel cell is shown in Fig. 1.37 where the fuel is hydrogen, which diffuses through a porous metal (nickel) electrode. This electrode has a catalyst deposited around the pores, which aids the absorption of H_2 on its surface. In this process hydrogen ions react with hydroxyl ions in the electrolyte to form water ($2H_2 + O_2 \rightarrow 2H_2O$). The cell has a theoretical emf of 1.2 V at 25°C. Other fuels are CO (1.33 V) and methanol (1.21 V) both at 25°C. Conversion efficiencies of practical cell are about 80%. The major use of the cell is in conjunction with hydrogen-oxygen system.

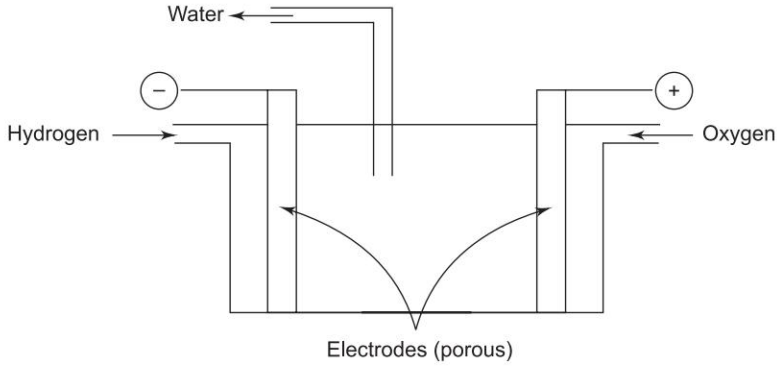

Fig. 1.37 Hydrogen-oxygen fuel cell

Intense R&D effort is on for various types of cells for power generation. Most successful of these is the phosphoric cell, which uses methane as fuel and operates at about 200 – 300°C. It has been constructed to produce 200 kW of electric power plus 200 kW heat energy with an overall efficiency of 80%. Higher temperatures give still higher efficiency. The main reason why fuel cells are not in wide use is its high cost. Global electricity generating capacity from fuel cells will grow from just 75 MW in 2001 to 15,000 MW by 2010. R&D projects on PAFC, PEMFC, DMFC, DEFC and SOFC are supported by MNES, and other funding agencies and organisations such as NTPC, IITs, BHEL, CECRI, Karaikudi. PEMFC is considered suitable for use in automobiles and also for decentralized power generation (few kW). Other FCs for higher scale (MW scale). Fuel cell based 3 kW UPS is also developed. Fuel cell-battery hybrid electric vehicle is also available.

1.15 ENERGY CONSERVATION

We shall restrict our discussion only to energy conservation associated with generation, transmission, distribution and utilization of electric energy. Some of the issues have been touched upon in previous sections. Various important conservation methods have been brought on the right most side of Fig. 1.5.

Generation

Ideal heat engine has Carnot cycle efficiency. To bring the practical efficiency as close to Carnot as possible. Rankine cycle is used by heating steam to the highest temperature (and pressure) permitted by economically feasible boiler and piping materials. This is done by *superheating* steam in upper part of the boiler. Other steps that are taken to improve the overall efficiency of the turbine set as brought out in Fig. 1.6(b) are as follows:

1. LP steam from IP and HP turbines is reheated in the boiler before feeding it to LP turbines.
2. Some of the LP steam from IP turbine and also LP turbine is used to heat feedwater to boiler.
3. Hot water from generator cooler heated by LP steam from LP turbines constitutes a part of feedwater to boiler.
4. Cooled water from cooling towers is circulated through condenser tubes to reduce the condenser pressure to the lowest possible value. This lowers the back pressure of LP ends of LP turbines.
5. Heating feedwater by the heat stored in flue gases from the combustion chamber forms the first stage of feedwater heating process.

Cogeneration

Process steam is used for generation before or after. For details see Sec. 1.3.

CCGT: Gas turbine combined with steam turbine is employed for peak load shaving. This is more efficient than normal steam turbine and has a quick automated start and shut down. It improves the load factor of the steam station. For details refer to Sec. 1.3.

T & D (*transmission and distribution*) *Loss*: Losses in transmission and distribution should be kept low while designing these lines. Of course this has to be matched against the cost factor. In any case this loss should not exceed 20%. For transporting large chunks of power over long distances, HVDC option must be considered as this method has lower transmission loss; see Ch. 20.

Energy Storage

It can play an important role where there is time or rate mismatch between supply and demand of energy. This has been discussed in Sec. 1.14. Pumped storage (hydro) scheme has been considered in Sec. 1.5.3.

Industry

In India corporate sector is required by law, to include in their annual report, the measures taken for energy conservation.

Steps for energy conservation:

- Keep an energy audit. This will put a finger on the places and items where there is wasteful use.
- Use of energy efficient electric drives. No oversize motors as these would run at low power factor and efficiency.
- Use of regenerative braking particularly the motors which require frequent start/stop operation. In regeneration, energy stored in mechanically moving parts of the machinery being driven and the rotor of the motor is fed back electrically to the mains.
- Use of high efficiency motors, which are now becoming available.

Building—Industrial, Commercial and Domestic

Heating

Electric space heating is out of question. Space heating in areas, where needed, is done by steam boiler and piping. Electric geysers are commonly used for heating water for bath in severe winter. Its thermostat should be set at the lowest acceptable temperature. In India where most areas have large number of sunny days, hot water for bath and kitchen by solar water heaters is becoming common for commercial buildings, hostels and even hospitals. For cloudy days in winter some electric support system may be necessary for essential use.

Cooling

Chilled water system saves electricity for space cooling. Air conditioning for offices and individual rooms in houses should be set at temperature of 27°C and 60% relative humidity. In dry areas in hot weather a contrivance called 'water cooler' is quite common now. The humidity and temperature are both uncontrolled except manual switching ON/OFF. In large cities in Northern India all these appliances plus refrigerators constitute more load than lighting. At present there is no other natural alternative to cool high rise buildings.

Lighting

Buildings should be designed to bring in natural light but in summer heat access has to be almost eliminated. A combination of fluorescent tube and electric lamp gives acceptable and efficient lighting for homes and even offices. In commercial buildings and street lighting, energy efficient devices as CFL (Compact Fluorescent Lamp) should be used. Their initial high cost is made up by the reduced electricity bill.

There is a lot of wasteful use of lighting prevalent in commercial buildings where the lights are kept 'on' even when not needed or the room(s) is not being used. As in corporate sector commercial buildings, energy audit must be made a requirement in educational institutions and other users where large areas are lighted. Public has to be educated that 20 units of electricity at user end require 100 units of heat input at generation end.

In India where vast regions are deficient in electric supply and are subjected to long hours of power (load) shedding (mostly random), the use of small diesel/petrol generators and inverters are very common in commercial and domestic use. These are highly wasteful energy devices for the following reasons:

- Small diesel/petrol engines (1–2 kVA) are highly inefficient. So it is a national waste. Further these cause serious noise pollution.
- Inverters are storage battery based. When the line power is ON, they draw a heavy charging current over and above the normal load. When a large number of consumers use these inverters, power load is considerably increased when the power is ON. This in fact adds to line outage. Further, pollution is caused inside the house by battery fumes.

This situation needs to be rectified speedily. By proper planned maintenance the downtime of existing large stations can be cut down. Further, HVAC and transmission lines must be installed to evacuate the excess power available in Eastern region of the country. Power Grid Corporation has already been set up for this purpose. These actions will also improve the load factor of most power stations, which would indirectly contribute to energy conservation.

Losses

There is now a movement towards estimating and monitoring AT&C (aggregate technical and commercial) loss in the country. GOI has adopted AT&C as a measure of commercial efficiency in all distribution reform programmes.

1.16 GROWTH OF POWER SYSTEMS IN INDIA

India is fairly rich in natural resources like coal and lignite; while some oil reserves have been discovered so far, intense exploration is being undertaken in various regions of the country. India has immense water power resources also of which only around 25% have so far been utilised, i.e., only 25,000 MW has so far been commissioned up to the end of 9th plan. As per a recent report of the CEA (Central Electricity Authority), the total potential of hydro power is 84,040 MW at 60% load factor. As regards nuclear power, India is deficient in uranium, but has rich deposits of thorium which can be utilised at a future date in fast breeder reactors. Since independence, the country has made tremendous progress in the development of electric energy and today it has the largest system among the developing countries.

When India attained independence, the installed capacity was as low as 1360 MW in the early stages of the growth of power system, the major portion of generation was through thermal stations, but due to economical reasons, hydro development received attention in areas like Kerala, Tamil Nadu, Uttar Pradesh and Punjab.

In the beginning of the First Five Year Plan (1951–56), the total installed capacity was around 2300 MW (560 MW hydro, 1004 MW thermal, 149 MW through oil stations and 587 MW through non-utilities). For transporting this

power to the load centres, transmission lines of up to 110 kV voltage level were constructed.

The emphasis during the Second Plan (1956–61) was on the development of basic and heavy industries and thus there was a need to step up power generation. The total installed capacity which was around 3420 MW at the end of the First Five Year Plan became 5700 MW at the end of the Second Five Year Plan in 1962, the introduction of 230 kV transmission voltage came up in Tamil Nadu and Punjab. During this Plan, totally about 1009 circuit kilometres were energized. In 1965–66, the total installed capacity was increased to 10,170 MW. During the Third Five Year Plan (1961–66) transmission growth took place very rapidly, with a nine-fold expansion in voltage level below 66 kV. Emphasis was on rural electrification. A significant development in this phase was the emergence of an inter-state grid system. The country was divided into five regions, each with a regional electricity board, to promote integrated operation of the constituent power systems. Figure 1.38 (a) shows these five regions of the country with projected energy requirement and peak load in the year 2011–12 [19].

Fig. 1.38(a) Map of India showing five regional projected energy requirement in MkWh and peak load in MW for year 2011–12

During the Fourth Five Year Plan, India started generating nuclear power. At the Tarapur Nuclear Plant 2 × 210 MW units were commissioned in April-May 1969. This station uses two boiling water reactors of American design. By August 1972, the first unit of 220 MW of the Rajasthan Atomic Power Project, Kota (Rajasthan), was added to the nuclear generating capability. The total generating capacity at Kota is 430 MW with nuclear reactors of Canadian design which use natural uranium as fuel and heavy water as a moderator and coolant. The third nuclear power station of 2 × 235 MW has been commissioned at Kalpakkam (Tamil Nadu). This is the first nuclear station to be completely designed, engineered and constructed by Indian scientists and engineers. A reactor research centre has been set up near the Madras Atomic Power Station to carry out study in fast breeder reactor technology. The fourth nuclear power plant has been set up at Narora in Uttar Pradesh. It has two units of 235 MW each. The fifth is in Kaiga in Karnataka and sixth in Gujarat near Surat, Kakrapar (440 MW). Several other nuclear power plants will be commissioned by 2012.

The growth of generating capacity so far and future projection for 2011–2012 A.D. are given in Table 1.4.

Table 1.4 Growth of installed capacity in India (in MW)

Year	*Hydro*	*Nuclear*	*Thermal*	*Diesel*	*Total*
1970–71	6383	420	7503	398	14704
1978–79	11378	890	16372	—	28640
1984–85	14271	1095	27074	—	42240
2000–01	25141	2720	71060	≈2700 MW renewable	101630
2005–06	33941	3900	84149	6190	128180

Pattern of utilization of electrical energy in 1997–98 was: Domestic 20.69%, commercial 6.91%, irrigation 30.54%, industry 35.22% and others is 6.65%. It is expected to remain more or less same in 2004–05.

To be self-sufficient in power, BHEL has plants spread out all over the country and these turn out an entire range of power equipment, viz. turbo sets, hydro sets, turbines for nuclear plants, high pressure boilers, power transformers, switch gears, etc. Each plant specializes in a range of equipment. BHEL's first 500 MW turbo-generator was commissioned at Singrauli. Today BHEL is considered one of the major power plant equipment manufacturers in the world. Figure 1.38(b) shows main powergrid lines as on 2006.

1.17 DEREGULATION

For over one hundred years, the electric power industry worldwide operated as a *regulated* industry. In any area there was only one company or government agency (mostly state-owned) that produced, transmitted, distributed and sold electric power and services. Deregulation as a concept came in early 1990s. It brought in changes designed to encourage competition.

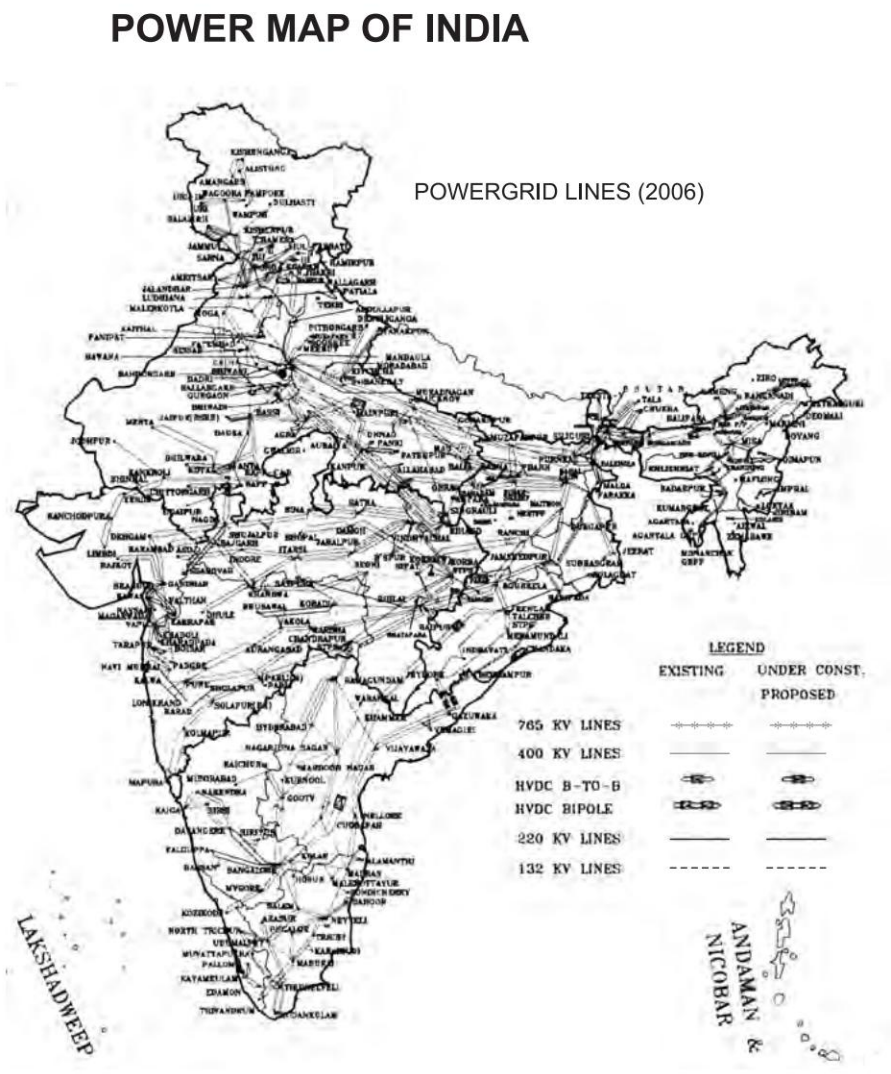

Fig. 1.38 (b) Showing main powergrid lines as on 2006

Restructuring involves disassembly of the power industry and reassembly into another form or functional organization. *Privatization* started sale by a government of its state-owned electric utility assets, and operating economy, to private companies. In some cases, deregulation was driven by privatization needs. The state wants to sell its electric utility investment and change the rules (deregulation) to make the electric industry more palatable for potential investors, thus raising the price it could expect from the sale. *Open access* is nothing but a common way for a government to encourage competition in the electric industry and tackle monopoly. The consumer is assured of good quality power supply at competitive price.

The structure for deregulation is evolved in terms of Genco (Generation Company), Transco (Transmission Company) and ISO (Independent System Operator). It is expected that the optimal bidding will help Genco to maximize its payoffs. The consumers are given choice to buy energy from different retail energy suppliers who in turn buy the energy from Genco in a power market (independent power producer, IPP).

The restructuring of the electricity supply industry that normally accompanies the introduction of competition provides a fertile ground for the growth of embedded generation, i.e. generation that is connected to the distribution system rather than to the transmission system.

The earliest reforms in power industries were initiated in Chile. They were followed by England, the USA, etc. Now India is also implementing the restructuring. Lot of research is needed to clearly understand the power system operation under deregulation. The focus of research is now shifting towards finding the optimal bidding methods which take into account local optimal dispatch, revenue adequacy and market uncertainties.

India has now enacted the Electricity Regulatory Commission's Act, 1998 and the Electricity (Laws) Amendment Act, 1998. These laws enable setting up of Central Electricity Regulatory Commission (CERC) at central level and State Electricity Regulatory Commissions (SERC) at state level. The main purpose of CERC is to promote efficiency, economy and competition in bulk electricity supply. Orissa, Haryana, Andhra Pradesh, etc. have started the process of restructuring the power sector in their respective states.

Four important terms connected with deregulated power systems are defined below:

1. ***Open Access:*** Open access is the non-discriminatory provision for the use of transmission lines or distribution system or associated facilities with such lines or system by any licensee or consumer or a person engaged in generation in accordance with the regulations specified by the Appropriate Commission. It will promote competition and, in turn, lead to availability of cheaper power.
2. ***Wheeling:*** Wheeling is the operation whereby the distribution system and associated facilities of a transmission or distribution licensee are used by another person for the conveyance of electricity on payment of charges to be determined by the Appropriate Commission.
3. ***Energy Banking:*** Energy banking is a process under which the Captive Power Plant (CPP) or a co-generator supplies power to the grid not with the intention of selling it to either a third party or to a licensee, but with the intention of exercising his eligibility to draw back this power from the grid at a prescribed time during next financial year, after deduction of banking charges.
4. ***Unbundling/Corporatization:*** Many state electricity boards have either been unbundled or corporatized. Distribution business is privatized in some states such as Delhi and Orissa.

1.18 DISTRIBUTED AND DISPERSED GENERATION

Distributed Generation (DG) entails using many small generators of 2–50 MW output, installed at various strategic points throughout the area, so that each provides power to a small number of consumers nearby. These may be solar, mini/micro hydel or wind turbine units, highly efficient gas turbines, small combined cycle plants, micro-turbines since these are the most economical choices.

Dispersed generation refers to use of still smaller generating units, of less than 500 kW output and often sized to serve individual homes or businesses. Micro gas turbines, fuel cells, diesel, and small wind and solar PV generators make up this category. The beauty is these are modular and relocatable power generating technologies.

Dispersed generation has been used for decades as an emergency backup power source. Most of these units are used only for reliability reinforcement. Nowadays inverters are being increasingly used in domestic sector as an emergency supply during black outs.

The distributed/dispersed generators can be stand alone/autonomous or grid connected depending upon the requirement.

At the time of writing this (2007) there still is and will probably always be some economy of scale favouring large generators. But the margin of economy decreased considerably in last 10 years [23]. Even if the power itself costs a bit more than central station power, there is no need of transmission lines, and perhaps a reduced need for distribution equipment as well. Another major advantage of dispersed generation is its modularity, portability and relocatability. Dispersed generators also include two new types of fossil fuel units—fuel cells and microgas turbines.

The main challenge today is to upgrade the existing technologies and to promote development, demonstration, scaling up and commercialization of new and emerging technologies for widespread adaptation. In the rural sector main thrust areas are biomass briquetting, biomass-based cogeneration, etc. In solar PV (Photovoltaic), large size solar cells/modules based on crystalline silicon thin films need to be developed. Solar cells efficiency is to be improved to 15% to be of use at commercial level. Other areas are development of high efficiency inverters. Urban and industrial wastes are used for various energy applications including power generation which was around 35 MW in 2005.

However, recently there has been a considerable revival in connecting generation to the distribution network and this has come to be known as *embedded* or dispersed generation. The term 'embedded generation' comes from the concept of generation embedded in the distribution network while 'dispersed generation' is used to distinguish it from central generation. The two terms can be used interchangeably.

There are already 35 million improved chulhas. If growing energy needs in the rural areas are met by decentralized and hybrid energy systems (distributed/dispersed generation), this can stem growing migration of rural population to urban areas in search of better living conditions. Thus, India will be able to

achieve a smooth transition from fossil fuel economy to sustainable renewable-energy based economy and bring "Energy for all" and 'Energy for ever' era for equitable, environment-friendly, and sustainable development.

1.19 POWER SYSTEM ENGINEERS AND POWER SYSTEM STUDIES

The power system engineer of the first decade of the twenty-first century has to face a variety of challenging tasks, which he can meet only by keeping abreast of the recent scientific advances and the latest techniques. On the planning side, he or she has to make decisions on how much electricity to generate—where, when, and by using what fuel. He has to be involved in construction tasks of great magnitude both in generation and transmission. He has to solve the problems of planning and coordinated operation of a vast and complex power network, so as to achieve a high degree of economy and reliability. In a country like India, he has to additionally face the perennial problem of power shortages and to evolve strategies for energy conservation and load management.

For planning the operation, improvement and expansion of a power system, a power system engineer needs load flow studies, short circuit studies, and stability studies. He has to know the principles of economic load despatch and load frequency control. All these problems are dealt within the next few chapters after some basic concepts in the theory of transmission lines are discussed. The solutions to these problems and the enormous contribution made by digital computers to solve the planning and operational problems of power systems is also investigated.

1.20 USE OF COMPUTERS AND MICROPROCESSORS

The first methods for solving various power system problems were AC and DC network analyzers developed in early 1930s. AC analyzers were used for load flow and stability studies whereas DC were preferred for short-circuit studies.

Analogue computers were developed in 1940s and were used in conjunction with AC network analyzer to solve various problems for off-line studies. In 1950s many analogue devices were developed to control the on-line functions such as generation control, frequency and tie-line control.

The 1950s also saw the advent of digital computers which were first used to solve a load flow problem in 1956. Power system studies by computers gave greater flexibility, accuracy, speed and economy. Till 1970s, there was a widespread use of computers in system analysis. With the entry of microprocessors in the arena, now, besides main frame computers, mini, micro and personal computers are all increasingly being used to carry out various power system studies and solve power system problems for off-line and on-line applications.

Off-line applications include research, routine evaluation of system performance and data assimilation and retrieval. It is mainly used for planning and analyzing some new aspects of the system. On-line and real time applications include data-logging and the monitoring of the system state.

A large central computer is used in central load despatch centres for economic and secure control of large integrated systems. Microprocessors and computers installed in generating stations control various local processes such as starting up of a generator from the cold state, etc. Table 1.5 depicts the time scale of various hierarchical control problems to be solved by computers/ microprocessors. Some of these problems are tackled in this book.

Table 1.5

Time scale	*Control problems*
Milliseconds	Relaying and system voltage control and excitation control
2 s–5 min	AGC (Automatic generation control)
10 min–few hours	ED (Economic despatch)
– do–	Security analysis
few hours–1 week	UC (Unit commitment)
1 month–6 months	Maintenance scheduling
1 year–10 years	System planning (modification/extension)

1.21 PROBLEMS FACING INDIAN POWER INDUSTRY AND ITS CHOICES

The electricity requirements of India have grown tremendously and the demand has been running ahead of supply. Electricity generation and transmission processes in India are very inefficient in comparison with those of some developed countries. As per one estimate, in India generating capacity is utilized on an average for 3600 hours out of 8760 hours in a year, while in Japan it is used for 5100 hours. If the utilization factor could be increased, it should be possible to avoid power cuts. The transmission loss in 1997–98 on a national basis was 23.68% consisting of both technical losses in transmission lines and transformers, and also non-technical losses caused by energy thefts and meters not being read correctly. It should be possible to achieve considerable saving by reducing this loss to 15% by the end of the Tenth Five Year Plan by using well known ways and means and by adopting sound commercial practices. Further, every attempt should be made to improve system load factors by flattening the load curve by giving proper tariff incentives and taking other administrative measures. As per the Central Electricity Authority's (CEA) sixteenth annual power survey of India report, the all India load factor up to 1998–99 was of the order of 78%. In future it is likely to be 71%. By 2001, 5.07 lakh of villages (86%) have been electrified and 117 lakh of pumpsets have been energized.

Assuming a very modest average annual energy growth of 5%, India's electrical energy requirement in the year 2010 will be enormously high. A difficult and challenging task of planning, engineering and constructing new

power stations is imminent to meet this situation. The government has built several super thermal stations such as at Singrauli (Uttar Pradesh), Farakka (West Bengal), Korba (Madhya Pradesh), Ramagundam (Andhra Pradesh) and Neyveli (Tamil Nadu), Chandrapur (Maharashtra) all in coal mining areas, each with a capacity in the range of 2000 MW*. Many more super thermal plants would be built in future. Intensive work must be conducted on boiler furnaces to burn coal with high ash content. National Thermal Power Corporation (NTPC) is in charge of these large scale generation projects.

Hydro power will continue to remain cheaper than the other types for the next decade. As mentioned earlier, India has so far developed only around 18% of its estimated total hydro potential of 89,000 MW. The utilization of this perennial source of energy would involve massive investments in dams, channels and generation–transmission system. The Central Electricity Authority, the Planning Commission and the Ministry of Power are coordinating to work out a perspective plan to develop all hydroelectric sources by the end of this century to be executed by the National Hydro Power Corporation (NHPC). NTPC has also started recently development of hydro and nuclear power plants.

Nuclear energy assumes special significance in energy planning in India. Because of limited coal reserves and its poor quality, India has no choice but to keep going on with its nuclear energy plans. According to the Atomic Energy Commission, India's nuclear power generation will increase to 10,000 MW by year 2010. Everything seems to be set for a take off in nuclear power production using the country's thorium reserves in breeder reactors.

In India, concerted efforts to develop solar energy and other non-conventional sources of energy need to be emphasized, so that the growing demand can be met and depleting fossil fuel resources may be conserved. To meet the energy requirement, it is expected that the coal production will have to be increased to more than 450 million tonnes in 2004–2005 as compared to 180 million tonnes in 1988.

A number of 400 kV lines are operating successfully since 1980s as mentioned already. This was the first step in working towards a national grid. There is a need in future to go in for even higher voltages (800 kV). It is expected that by the year 2011–12, 5400 circuit km of 800 kV lines and 48,000 circuit km of 400 kV lines would be in operation. Also lines may be series and shunt compensated to carry huge blocks of power with greater stability. There is a need for constructing HVDC (High Voltage DC) links in the country since DC lines can carry considerably more power at the same voltage and require fewer conductors. A 400 kV Singrauli–Vindhyachal of 500 MW capacity first HVDC back-to-back scheme has been commissioned by NPTC (National Power Transmission Corporation) followed by first point-to-point bulk

* NTPC has also built seven gas-based combined cycle power stations such as Anta and Auraiya.

EHVDC transmission of 1500 MW at ± 500 kV over a distance of 915 km from Rihand to Delhi. Power Grid recently commissioned on 14 Feb. 2003 a 2000 MW Talcher–Kolar ±500 kV HVDC bipole transmission system thus enabling excess power from East to flow to South. 7000 ckt km of ±500 kV HVDC line is expected by 2011–12.

At the time of writing, the whole energy scenario is so clouded with uncertainty that it would be unwise to try any quantitative predictions for the future. However, certain trends that will decide the future developments of electric power industry are clear.

Generally, unit size will go further up from 500 MW. A higher voltage (1200 kV) will come eventually at the transmission level. There is little chance for six-phase transmission becoming popular though there are few such lines in USA. More of HVDC lines will come in operation. As population has already touched the 1000 million mark in India, we may see a trend to go toward underground transmission in urban areas.

Public sector investment in power has increased from Rs 2600 million in the First Plan to Rs 2,42,330 million in the Seventh Plan (1985–90). Shortfall in the Sixth Plan has been around 26%. There have been serious power shortages and generation and availability of power in turn have lagged too much from the industrial, agricultural and domestic requirements. Huge amounts of funds (of the order of Rs 18,93,200 million) will be required if we have to achieve power surplus position by the time we reach the terminal year to the XI Plan (2011–2012). Otherwise achieving a target of 975 billion units of electric power will remain an utopian dream.

Power grid is planning creation of transmission highways to conserve Right-of-way. Strong national grid is being developed in phased manner. In 2001 the interregional capacity was 5000 MW. It is expected that by 2011–12, it will be 30,000 MW. Huge investment is planned to the tune of US$ 20 billion in the coming decade. Present figures for HVDC is 3136 circuit km, 800 kV is 950 circuit km, 400 kV is 45,500 circuit km and 220/132 kV is 2,15,000 circuit km. State-of-the art technologies which are, being used in India currently are HVDC bipole, HVDC back-to-back, SVC (Static Var Compensator), FACTs (Flexible AC Transmissions) devices etc. Improved O and M (Operation and Maintenance) technologies which are being used today are hotline maintenance, emergency restoration system, thermovision scanning, etc. 24 hours of supply of good-quality power would help small industries in rural areas. It will also facilitate delivery of modern health care, education, and application of information and communication technologies.

Because of power shortages, many of the industries, particularly power-intensive ones, have installed their own captive power plants.* Currently 20%

* Captive diesel plants (and small diesel sets for commercial and domestic uses) are very uneconomical from a national point of view. Apart from being lower efficiency plants they use diesel which should be conserved for transportation sector.

of electricity generated in India comes from the captive power plants and this is bound to go up in the future. Consortium of industrial consumers should be encouraged to put up coal-based captive plants. Import should be liberalized to support this activity. Now alternative fuels are increasingly being used for surface transportation. Battery operated vehicles (electric cars) are being used.

With the ever increasing complexity and growth of power networks and their economic and integrated operation, several central/regional automatic load despatch centres with real time computer control have been established. In very near future it is envisaged that using SCADA (Supervisory Control and Data Acquisition) etc. will be possible to achieve nationwide on-line monitoring and real time control of power system. It may also be pointed out that this book will also help in training and preparing the large number of professionals trained in computer aided power system operation and control that would be required to handle vast expansion planned in power system in the coming decades.

ANNEXURE 1.1

1. The Indian Electricity Rules; [25]
   The Indian Electricity Act, 1910 deals with the provisions relating to supply and use of electrical energy and the rights and obligations of persons licensed under Part II of that Act to supply energy. Under section 36A of the Act, a Board called the Central Electricity Board is constituted to exercise the powers conferred by section 37. In exercise of the powers conferred under that section, the Central Electricity Board framed the Indian Electricity Rules, 1956 for the whole or any part of the territories to which the Act extends, to regulate the generation, transmission, supply and use of energy, and generally to carry out the purposes and objects of the Act.

ANNEXURE 1.2

Table 1.6 Installed generation capacity (As on 31.03.2006)
(*Source* CEA, New Delhi)

		Thermal	MW 82411 (66%) { Coal 68519; Gas 12690; Diesel 1202
Wind	4434	Nuclear	3360 (3%)
Small Hydro	777	Hydro	32326 (26%)
Biomass/waste	980	Green	6191 (5%)
		Total	124288

Table 1.7 Growth in transmission system (2006)

132 kV	120000 ckm
220 kV	120000 ckm
400 kV	60000 ckm
HVDC bi-pole lines 5000 MW	
HVDC back to back 3000 MW	
765 kV 400 kV op 1150 ckm	
(Kishenpur-Moga, Anparo-Unnao Tehri-Meerut)	

Table 1.8 The landmark events in Indian power sector

1948	Electricity (supply) Act
1950–60	Growth of State Grid Systems
1962	First 220 kV voltage level
1964	Constitution of Regional Electricity Boards
65–73	Interconnecting State Grids to form Regional Grids
75	Central PSUs in Generation and Transmission
77	First 400 kV voltage level
80–88	Growth of Regional Grids-400 kV back-bone
89	HVDC back to back
89	Formation of Power Grid Corporation of India
90	First HVDC bi-pole line
90	Generation of electricity opened to Private Sector
98	Electricity Regulatory Commission Act
98	765 kV Transmission line (initially charged at 400 kV)
2003	Electricity Act 2003-open access in Transmission
05	The Rajiv Gandhi scheme of Rural Electricity Infrastructure and Household Electrification
5–6	National Electricity Plan
06	Synchronization of NR with ER-NER-WR
07	765 kV Transmission
10–11	800 kV HVDC bi-pole line

Table 1.9 Cumulative physical achievements as on 31.12.2005

S.No.	*Sources/Systems*	*Cumulative Achievement*
	I. Power From Renewables	
	A. *Grid-interactive renewable power*	
1.	Solar Photovoltaic Power	2.74 MW
2.	Wind Power	4433.90 MW
3.	Small Hydro Power (up to 25 MW)	1747.98 MW
4.	Biomass Power	376.53 MW
5.	Bagasse Cogeneration	491.00 MW
6.	Biomass Gasifier	1.00 MW
7.	Energy Recovery from Waste	34.95 MW
	Sub Total (A)	**7088.10 MW**
	B. *Distributed renewable power*	
8.	Biomass Gasifier	69.87 MW
9.	Energy Recovery from Waste	11.03 MW
	Sub Total (B)	**80.90 MW**
	Total (A + B)	**7169.00 MW**

(contd.)

	II. Remote Village Electrification	2195 villages 594 hamlets
	III. Decentralized Energy Systems	
10.	Family Type Biogas Plants	38 lakh
11.	Community/Institutional/Night-soil-based biogas plants	3902 nos.
12.	Improved Chulha	3.52 crore
13.	Solar Photovoltaic Programme	
	i. Solar Street Lighting System	54795 nos.
	ii. Home Lighting System	342607 nos.
	iii. Solar Lantern	538718 nos.
	iv. Solar Power Plants	1566 kW_p
14	Solar Thermal Programme	
	i. Solar Water Heating Systems	1.5 million sq.m. co
	ii. Box solar cookers	5.99 lakh
	iii. Concentrating dish cookers	2000 nos.
	iv. Community solar cookers	12 nos.
15.	Wind Pumps	1082 nos.
16.	Aero-generator/Hybrid Systems	410 kW
17.	Solar Photovoltaic Pumps	7002 nos.

MW = Megawatt; kW = kilowatt; kW_p = kilowatt peak; sq.m. = square meter

Additional Solved Examples

Example 1.6 If the average flow during the period of interest is 575 m^3/s and head is 100 m, find the power that can be developed per cubic meter per second if the efficiency of the hydraulic turbine and electric generator together is 90%.

Solution

$$P = 9.81\ \eta\rho\ W\ H \times 10^{-6}\ \text{MW}$$
$$= 9.81 \times 0.9 \times 1000 \times 575 \times 100 \times 10^{-6}\ \text{MW}$$
$$= 98.1 \times 0.9 \times 5.75 = 508\ \ \text{MW}$$

Example 1.7 How much power can be extracted from a 5 m/s wind striking a wind mill whose blades have a radius of 3 m? Assume that the efficiency of the turbine is 40%.

Solution

$$\text{Power} = \frac{1}{2}\ C_p\ \rho\ A\ V^3$$

$C_p = 0.4$ = power coefficient gives the maximum amount of wind power that can be converted into mechanical power by wind turbine

$A = \pi r^2 = 3.14 \times 3^2 = 28.26\ \text{m}^2$

$V = 5\text{m/s}\ \ \rho = 1.24\ \text{kg/m}^2$

$$\therefore \quad \text{Power} = \frac{1}{2} \times 0.4 \times 1.24 \times 28.26 \times 5^3 \times 10^{-3} = 0.876 \text{ kW}$$

Example 1.8 A wind generator whose power curve is shown in Fig. 1.39 has a blade diameter of 10 m. Find the net efficiency of the Wind Energy Converting System at a wind speed of 5 m/s.

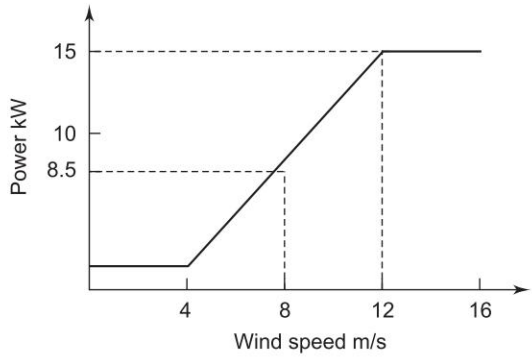

Fig. 1.39

Solution

$$A = \pi r^2 = 3.14 \times 5^2$$
$$V = 8 \text{ m/s}$$
$$\rho = 1.24 \text{ kg/m}^3$$
$$P = 1/2\ \rho\ \text{AV}^3$$
$$P_{\text{input}} = 1/2 \times 1.24 \times 3.14 \times 5^2 \times 8^3 \times 10^{-3} = 24.9 \text{ kW}$$

8 m/s wind velocity

$$P = 8.5 \text{ kW}$$
$$\eta = 8.5/24.9 \times 100 = 34.14\%$$

Example 1.9 Calculate the maximum power by a solar cell at an intensity of 200 W/m^2. Given V_{OC} = 0.24 V, I_{SC} = – 9 mA, $V_{\max}$ = 0.14 V and $I_{\max}$ = – 6 mA. Also calculate the cell efficiency if the area is 4 cm^2.

Solution

Solar cell maximum power $P_{\max} = I_{\max}\ V_{\max}$

$$P_{\max}\ (\text{output}) = -6 \times 10^{-3} \times 0.14 = -0.84 \text{ mW}$$
$$= -0.84 \times 10^{-3} \text{ W}$$
$$P_{\text{input}} = \text{Intensity} \times \text{area}$$
$$= 200 \times 4 \times 10^{-4} \text{ W}$$
$$\text{cell } \eta = \frac{0.84 \times 10^{-3}}{200 \times 4 \times 10^{-4}} \times 100 = 1.05\%$$

Problems

1.1 Maximum demand of a generating station is 200 MW, a load factor is 70%. The plant capacity factor and plant use factor are 50% and 70%, respectively. Determine
(a) daily energy produced
(b) installed capacity of plant
(c) the reserve capacity of plant
(d) maximum energy that can be produced daily if the plant is running all the time
(e) the minimum energy that could be produced daily if the plant is running at full load
(f) utilization factor

1.2 Load factor of a consumer is 40% and the monthly consumption is 500 kWh. If the rate of electricity is Rs 200 per kW of maximum demand plus Rs 2.00 per kWh. Find
(a) the monthly bill and the average cost per kWh.
(b) the overall cost per kWh if the consumption is increased by 20% with the same load factor.
(c) The overall cost per kWh if the consumption remains the same but the load factor.

References

Books

1. Nagrath, I.J. and D.P. Kothari, *Electric Machines*, Tata McGraw-Hill, New Delhi, 3rd edn, 2004.
2. Kothari, D. P., R. Ranjan and K.C. Singhal, *Renewable Energy Sources and Technology*, PHI, 2007.
3. Kashkari, C., *Energy Resources, Demand and Conservation with Special Reference to India*, Tata McGraw-Hill, New Delhi, 1975.
4. Kandpal, T. C. and H.P. Garg, *Financial Evaluation of Renewable Technologies,* Macmillian India Ltd, New Delhi, 2003.
5. Sullivan, R.L., *Power System Planning*, McGraw-Hill, New York, 1977.
6. Skrotzki, B.G.A. and W.A. Vopat, *Power Station Engineering and Economy*, McGraw-Hill, New York, 1960.
7. Car, T.H., *Electric Power Stations*, vols I and II, Chapman and Hall, London, 1944.
8. Central Electricity Generating Board, *Modern Power Station Practice*, 2nd edn, Pergamon, 1976.
9. Golding, E.W., *The Generation of Electricity by Wind Power*, Chapman and Hall, London, 1976.
10. El-Wanil, M. M., *Powerplant Technology*, McGraw-Hill, New York, 1984.
11. Bennet, D.J., *The Elements of Nuclear Power*, Longman, 1972.

12. Casazza, J. and F. Delea, *Understanding Electric Power Systems: An Overview of the Technology and Marketplace*, IEEE Press and Wiley Interscience, 2003.
13. Steinberg, M.J. and T.H. Smith, *Economy-loading of Power Plants and Electric Systems*, Wiley, New York, 1943.
14. Power System Planning and Operations: Future Problems and Research Needs, *EPRI EL-377-SR*, February 1977.
15. Twidell, J.W. and A.D. Weir, *Renewable Energy Resources*, Tailor & Francis London, 2nd edn, 2006.
16. Mahalanabis, A.K., D.P. Kothari and S.I. Ahson, *Computer Aided Power System Analysis and Control*, Tata McGraw-Hill, New Delhi, 1988.
17. Robert Noyes (Ed.), *Cogeneration of Steam and Electric Power*, Noyes Dali Corp., USA, 1978.
18. Rustebakke, H. M. (Ed.) *Electric Utility Systems and Practices*, 4th edn, Wiley New York, Aug. 1983.
19. CEA 12, *Annual Survey of Power Report*, Aug. 1985; 14th Report, March 1991; 16th Electric Power Survey of India, Sept. 2000.
20. Kothari, D.P. and D.K. Sharma (Eds), *Energy Engineering: Theory and Practice*, S. Chand, 2000.
21. Kothari, D.P. and I.J. Nagrath, *Basic Electrical Engineering*, Tata McGraw-Hill, New Delhi, 2nd edn, 2002. (Ch. 15).
22. Wehenkel, L.A., *Automatic Learning Techniques in Power Systems*, Kluwer, Norwell, MA: 1997.
23. Philipson, L. and H. Lee Willis, *Understanding Electric Utilities and Deregulation*, Marcel Dekker Inc, NY, 1999.
24. Mohan Muna Singhe, *Economics of Power Systems Reliability and Planning*, John Hopkins University Press, 1980.
25. *The Indian Electricity Rules*, 1956, Commercial Law Publishers, Delhi, 2005.
26. Nick Jenkins *et al*., *Embedded Generation*, IEE, UK, 2000.
27. Ned Mohan, *First Course on Power Systems*, MNPER, Minneapolis, 2006.

Papers

28. Kusko, A., A Prediction of Power System Development, 1968–2030, *IEEE Spectrum*, April, 1968, 75.
29. Fink, L. and K. Carlsen, *Operating under Stress and Strain, IEEE Spectrum,* Mar. 1978.
30. Talukdar, S.N., *et al*., Methods for Assessing Energy Management Options, *IEEE Trans*., Jan. 1981, PAS-100, no. 1, 273.
31. Morgen, M.G. and S.N. Talukdar, Electric Power Load Management: Some Technological, Economic, Regularity and Social Issues*, Proc. IEEE*, Feb. 1979, vol. 67, no. 2, 241.
32. Sachdev, M.S., Load Forecasting—Bibliography, *IEEE Trans.*, PAS-96, 1977, 697.
33. Sporn, P., *Our Environment—Options on the Way into the Future*, *ibid,* May 1977, 49.
34. Kothari, D.P., Energy Problems Facing the Third World, *Seminar to the Bio-Physics Workshop*, 8 Oct. 1986, Trieste, Italy.
35. Kothari, D.P., *Energy System Planning and Energy Conservation, Presented at XXIV National Convention of IIIE*, New Delhi, Feb. 1982.

36. Kothari, D.P., *et al*., Minimization of Air Pollution due to Thermal Plants, *J.I.E.* (India), Feb. 1977, 57 : 65.
37. Kothari, D.P. and J. Nanda, Power Supply Scenario in India 'Retrospects and Prospects', *Proc. NPC Cong*., *on Captive Power Generation,* New Delhi, Mar. 1986.
38. *National Solar Energy Convention*, Organized by SESI, 1–3 Dec. 1988, Hyderabad.
39. Kothari, D.P., Mini and Micro Hydropower Systems in India, invited chapter in the book, *Energy Resources and Technology*, Scientific Publishers, 1992, pp. 147–158.
40. *Power Line*, vol. 5. no. 9, June 2001.
41. United Nations*: Electricity Costs and Tariffs: A General Study*, 1972.
42. Shikha, T.S. Bhatti and D.P. Kothari, Wind as an Eco-friendly Energy Source to meet the Electricity Needs of SAARC Region", *Proc. Int. Conf. (ICME 2001)*, BUET, Dhaka, Bangladesh, Dec. 2001, pp. 11–16.
43. Bansal, R.C., D.P. Kothari and T.S. Bhatti, On Some of the Design Aspects of Wind Energy Conversion Systems", *Int. J. Energy Conversion and Management*, vol. 43, 16, Nov. 2002, pp. 2175–2187.
44. Kothari, D.P. and A. Arora, Fuel Cells in Transportation-Beyond Batteries, *Proc. Nat. Conf. on Transportation Systems*, IIT Delhi, April 2002, pp. 173–176.
45. Saxena, Anshu and D.P. Kothari, *et al*., "*Analysis of Multimedia and Hypermedia for Computer Simulation and Growth.*, EJEISA, UK, vol. 3, 1 Sept. 2001, pp. 14–28.
46. Bansal, R.C., T.S. Bhatti and D.P. Kothari, A Bibliographical Survey on Induction Generators for Application of Non-conventional Energy Systems', *IEEE Trans. on Energy Conversions*, vol. 18, Sept. 2003, pp. 433–439.
47. Kolhe, M., J.C. Joshi and D.P. Kothari, 'LOLP of stand-alone solar PV system', *Int. Journal of Energy Technology and Policy*, vol. 1, no. 3, 2003, pp. 315–323.
48. Shikha, T.S. Bhatti and D.P. Kothari, Vertical Axis Wind Rotor with Concentration by Convergent Nozzles, *Wind Engg.*, vol. 27, no. 6, 2003, pp. 555–559.
49. Shikha, T.S. Bhatti and D.P. Kothari, On Some Aspects of Technological Development of Wind Turbines, *Energy Engg.*, vol. 129, no. 3, Dec. 2003, pp. 69–80.
50. Shikha, T.S. Bhatti, and D.P. Kothari, 'Wind Energy Conversion Systems as a Distributed Source of Generation', *Energy Engg.*, vol. 129, no. 3, Dec. 2003, pp. 81–95.
51. Shikha, T.S. Bhatti and D.P. Kothari, 'Indian Scenario of Wind Energy: Problems and Solutions', *Energy Sources*, vol. 26, no. 9, July 2004, pp. 811–819.
52. Kolhe, M., J.C. Joshi and D.P. Kothari, 'Performance Analysis of a Directly Coupled PV Water Pumping Systems', *IEEE Trans.*, *on Energy Conversion*, vol. 19, no. 3, Sept. 2004, pp. 613–618.
53. Shikha, T.S. Bhatti and D.P. Kothari, 'The Power Coefficient of Windmills in Ideal Conditions', *Int. J. of Global Energy Issues*, vol. 21, no. 3, 2004, pp. 236–242.

54. Bansal, R.C., T.S. Bhatti and D.P. Kothari, 'Automatic Reactive Power Control of Isolated Wind-Diesel Hybrid Power Systems for Variable Wind Speed/Slip', *Electric Power Components and Systems*, vol. 32, 2004, pp. 901–912.
55. Shikha, T.S. Bhatti, and D.P. Kothari, 'Wind Energy in India: Shifting Paradigms and Challenges Ahead', *Energy Engg.*, vol. 130, no. 3, Dec. 2004. pp. 67–80.
56. Shikha, T.S. Bhatti and D.P. Kothari, 'New Horizons for Offshore. Wind Energy: Shifting Paradigms and Challenges', *Energy Sources*, vol. 27, no. 4, March 2005, pp. 349–360.
57. Shikha, T.S. Bhatti and D.P. Kothari, 'Development of Vertical and Horizontal Axis Wind Turbines: A Review,' *Int J. of Wind Engg.*, vol. 29, no. 3, May 2005, pp. 287–300.
58. Shikha, T.S. Bhatti and D.P. Kothari, 'A Review of Wind Resource Assessment Technology', *Energy Engg*., vol .132, no. 1, April 2006, pp. 8–14.
59. Kaushik, S.C., S. Ramesh and D.P. Kothari, 'Energy Conservation Studies in Buildings,' *Presented at PCRA Conf*, New Delhi, May 19, 2005.
60. Goyal, H., T.S. Bhatti and D.P. Kothari, 'A Novel Technique proposed for automatic control of small Hydro Power Plants,' *Special Issue of Int. J. of Global Energy Issues*, vol. 24, 2005, pp. 29–46.
61. Bansal, R.C., T.S. Bhatti, D.P. Kothari and S. Bhat, 'Reactive Power Control of Wind-diesel-microhydro Power Systems Using Matlab/Simulink', *Int. J. of Global Energy Issues*, vol. 24, no. 1, 2005, pp. 86–99.
62. Goyal, H., M. Hanmandlu and D.P. Kothari, 'A New Optimal Flow Control Approach for Automatic Control of Small Hydro Power Plants', *J.I.E. (I)*, vol. 87, May 2006, pp. 1–5.

U.S. Department of Energy (www.eia.doe.gov).
www.epa.gov/globalwarming/kids/greenhouse.html.
2004 Environment Report, www.xcellenergy.com.

Chapter 2

Inductance and Resistance of Transmission Lines

2.1 INTRODUCTION

The four parameters which affect the performance of a transmission line as an element of a power system are inductance, capacitance, resistance and conductance. Shunt conductance, which is normally due to leakage over line insulators, is almost always neglected in overhead transmission lines. This chapter deals with the series line parameters, i.e. inductance and resistance. These parameters are uniformly distributed along the line and they together form the series impedance of the line.

Inductance is by far the most dominant line parameter from a power system engineer's viewpoint. As we shall see in later chapters, it is the inductive reactance which limits the transmission capacity of a line.

2.2 DEFINITION OF INDUCTANCE

Voltage induced in a circuit is given by

$$e = \frac{\mathrm{d}\psi}{\mathrm{d}t} \text{ V} \tag{2.1}$$

where ψ represents the flux linkages of the circuit in weber-turns (Wb-T). This can be written in the form

$$e = \frac{\mathrm{d}\psi}{\mathrm{d}i} \cdot \frac{\mathrm{d}i}{\mathrm{d}t} = L\frac{\mathrm{d}i}{\mathrm{d}t} \text{ V} \tag{2.2}$$

where $L = \dfrac{\mathrm{d}\psi}{\mathrm{d}i}$ is defined as the inductance of the circuit in henry, which in general may be a function of i. In a linear magnetic circuit, i.e., a circuit with constant permeability, flux linkages vary linearly with current such that the inductance is constant given by

$$L = \frac{\psi}{i} \text{ H}$$

or

$$\psi = Li \quad \text{Wb-T} \tag{2.3}$$

If the current is alternating, the above equation can be written as

$$\lambda = LI \tag{2.4}$$

where λ and I are the rms values of flux linkages and current respectively. These are of course in phase.

Replacing $\frac{\text{d}}{\text{d}t}$ in Eq. (2.1) by $j\omega$, we get the steady state AC voltage drop due to alternating flux linkages as

$$V = j\omega LI = j\omega\lambda \text{ V} \tag{2.5}$$

On similar lines, the mutual inductance between two circuits is defined as the flux linkages of one circuit due to current in another, i.e.,

$$M_{12} = \frac{\lambda_{12}}{I_2} \text{ H} \tag{2.6}$$

The voltage drop in circuit 1 due to current in circuit 2 is

$$V_1 = j\omega M_{12} I_2 = j\omega\lambda_{12} \text{ V} \tag{2.7}$$

The concept of mutual inductance is required while considering the coupling between parallel lines and the influence of power lines on telephone lines.

2.3 FLUX LINKAGES OF AN ISOLATED CURRENT-CARRYING CONDUCTOR

Transmission lines are composed of parallel conductors which, for all practical purposes, can be considered as infinitely long. Let us first develop expressions for flux linkages of a long isolated current-carrying cylindrical conductor with return path lying at infinity. This system forms a single-turn circuit, flux linking which is in the form of circular lines concentric to the conductor. The total flux can be divided into two parts, that which is internal to the conductor and the flux external to the conductor. Such a division is helpful as the internal flux progressively links a smaller amount of current as we proceed inwards towards the centre of the conductor, while the external flux always links the total current inside the conductor.

Flux Linkages due to Internal Flux

Figure 2.1 shows the cross-sectional view of a long cylindrical conductor carrying current I.

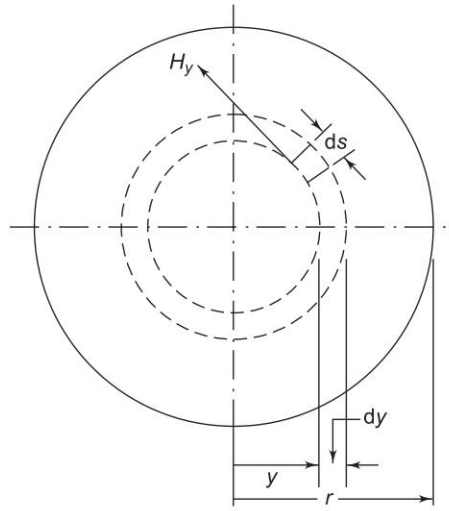

Fig. 2.1 Flux linkages due to internal flux (cross-sectional view)

The mmf round a concentric closed circular path of radius y internal to the conductor as shown in the figure is

$$\oint H_y \cdot ds\, I_y \text{ (Ampere's law)} \tag{2.8}$$

where

H_y = magnetic field intensity (AT/m)

I_y = current enclosed (A)

By symmetry, H_y is constant and is in the direction of ds all along the circular path. Therefore, from Eq. (2.8), we have

$$2\pi y H_y = I_y \tag{2.9}$$

Assuming uniform current density*

$$I_y = \left(\frac{\pi y^2}{\pi r^2}\right) I = \left(\frac{y^2}{r^2}\right) I \tag{2.10}$$

From Eqs (2.9) and (2.10), we obtain

$$H_y = \frac{yI}{2\pi r^2} \text{ AT/m} \tag{2.11}$$

The flux density B_y, y metres from the centre of the conductors, is

$$B_y = \mu H_y = \frac{\mu y I}{2\pi r^2} \text{ Wb/m}^2 \tag{2.12}$$

where μ is the permeability of the conductor.

---

* For power frequency of 50 Hz, it is quite reasonable to assume uniform current density. The effect of non-uniform current density is considered later in this chapter while treating resistance.

Consider now an infinitesimal tubular element of thickness dy and length 1m. The flux in the tubular element $d\phi = B_y\, dy$ webers links the fractional turn ($I_y/I = y^2/r^2$) resulting in flux linkages of

$$d\lambda = \left(\frac{y^2}{r^2}\right) d\phi = \left(\frac{y^2}{r^2}\right) \frac{\mu y I}{2\pi r^2} dy \quad \text{Wb-T/m} \qquad (2.13)$$

Integrating, we get the total internal flux linkages as

$$\lambda_{\text{int}} = \int_0^r \frac{\mu I}{2\pi r^4} y^3 dy = \frac{\mu I}{8\pi} \quad \text{Wb-T/m} \qquad (2.14)$$

For a relative permeability $\mu_r = 1$ (non-magnetic conductor), $\mu = 4\pi \times 10^{-7}$ H/m; therefore

$$\lambda_{\text{int}} = \frac{I}{2} \times 10^{-7} \quad \text{Wb-T/m} \qquad (2.15)$$

and

$$L_{\text{int}} = \frac{1}{2} \times 10^{-7} \quad \text{H/m} \qquad (2.16)$$

Flux Linkages due to Flux between Two Points External to Conductor

Figure 2.2 shows two points P_1 and P_2 at distances D_1 and D_2 from a conductor which carries a current of I amperes. As the conductor is far removed from the return current path, the magnetic field external to the conductor is concentric circles around the conductor and therefore all the flux between P_1 and P_2 lines within the concentric cylindrical surfaces passing through P_1 and P_2.

Magnetic field intensity at distance y from the conductor is

$$H_y = \frac{I}{2\pi y} \quad \text{AT/m}$$

The flux dϕ contained in the tubular element of thickness dy is

$$d\phi = \frac{\mu I}{2\pi y} dy \quad \text{Wb/m length of conductor}$$

The flux dϕ being external to the conductor links all the current in the conductor which together with the return conductor at infinity forms a single return, such that its flux linkages are given by

$$d\lambda = 1 \times d\phi = \frac{\mu I}{2\pi y} dy$$

Therefore, the total flux linkages of the conductor due to flux between points P_1 and P_2 is

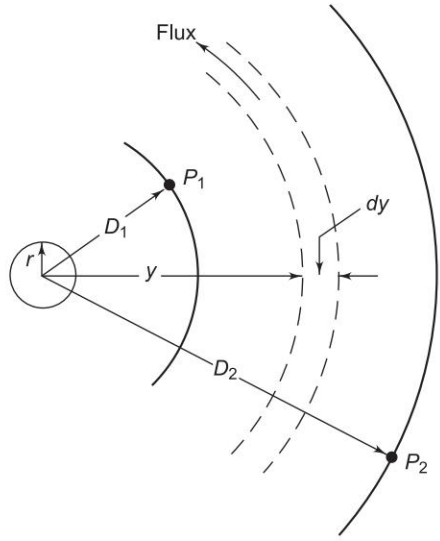

Fig. 2.2 Flux linkages due to flux between external points P_1, P_2

$$\lambda_{12} = \int_{D_1}^{D_2} \frac{\mu I}{2\pi y} dy = \frac{\mu}{2\pi} I \ln \frac{D_2}{D_1} \text{ Wb-T/m}$$

where ln stands for natural logarithm*.

Since $\mu_r = 1$, $\mu = 4\pi \times 10^{-7}$

$$\therefore \quad \lambda_{12} = 2 \times 10^{-7} I \ln \frac{D_2}{D_1} \text{ Wb/m} \tag{2.17}$$

The inductance of the conductor contributed by the flux included between points P_1 and P_2 is then

$$L_{12} = 2 \times 10^{-7} \ln \frac{D_2}{D_1} \text{ H/m} \tag{2.18}$$

or

$$L_{12} = 0.461 \log \frac{D_2}{D_1} \text{ mH/km} \tag{2.19}$$

Flux Linkages due to Flux up to an External Point

Let the external point be at distance D from the centre of the conductor. Flux linkages of the conductor due to external flux (from the surface of the conductor up to the external point) is obtained from Eq. (2.17) by substituting $D_1 = r$ and $D_2 = D$, i.e.,

* Throughout the book ln denotes natural logarithm (base e), while log denotes logarithm to base 10.

$$\lambda_{ext} = 2 \times 10^{-7} I \ln \frac{D}{r} \tag{2.20}$$

Total flux linkages of the conductor due to internal and external flux are

$$\lambda = \lambda_{int} + \lambda_{ext}$$

$$= \frac{I}{2} \times 10^{-7} + 2 \times 10^{-7} I \ln \frac{D}{r}$$

$$= 2 \times 10^{-7} I \left(\frac{1}{4} + \ln \frac{D}{r} \right)$$

$$= 2 \times 10^{-7} I \ln \frac{D}{re^{-1/4}}$$

Let

$$r' = re^{-1/4} = 0.7788r$$

$$\therefore \quad \lambda = 2 \times 10^{-7} I \ln \frac{D}{r'} \text{ Wb-T/m} \tag{2.21a}$$

Inductance of the conductor due to flux upto an external point is therefore

$$L = 2 \times 10^{-7} \ln \frac{D}{r'} \text{ H/m} \tag{2.21b}$$

Here r' can be regarded as the radius of a fictitious conductor with no internal inductance but the same total inductance as the actual conductor.

2.4 INDUCTANCE OF A SINGLE-PHASE TWO-WIRE LINE

Consider a simple two-wire line composed of solid round conductors carrying currents I_1 and I_2 as shown in Fig. 2.3. In a single-phase line,

$$I_1 + I_2 = 0$$

or

$$I_2 = -I_1$$

It is important to note that the effect of earth's presence on magnetic field geometry* is insignificant. This is so because the relative permeability of earth is about the same as that of air and its electrical conductivity is relatively small.

To start with, let us consider the flux linkages of the circuit caused by current in conductor 1 only. We make three observations in regard to these flux linkages:

1. External flux from r_1 to $(D - r_2)$ links all the current I_1 in conductor 1.

* The electric field geometry will, however, be very much affected as we shall see later while dealing with capacitance.

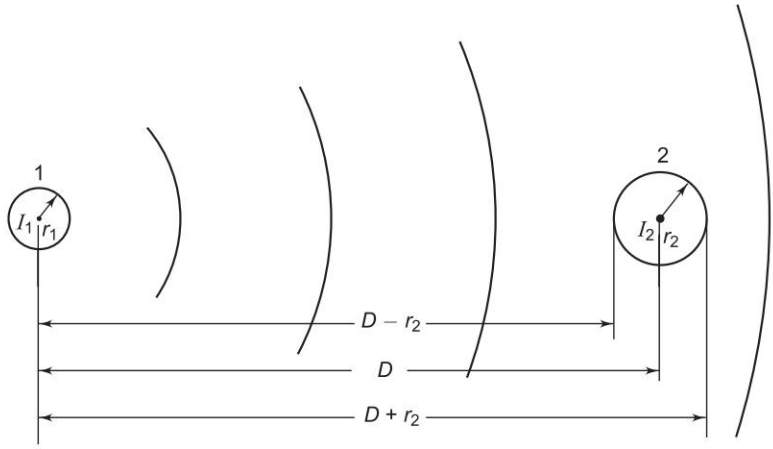

Fig.2.3 Single-phase two-wire line and the magnetic field due to current in conductor 1 only

2. External flux from $(D - r_2)$ to $(D + r_2)$ links a current whose magnitude progressively reduces from I_1 to zero along this distance, because of the effect of negative current flowing in conductor 2.
3. Flux beyond $(D + r_2)$ links a net current of zero.

For calculating the total inductance due to current in conductor 1, a simplifying assumption will now be made. If D is much greater than r_1 and r_2 (which is normally the case for overhead lines), it can be assumed that the flux from $(D - r_2)$ to the centre of conductor 2 links all the current I_1 and the flux from the centre of conductor 2 to $(D + r_2)$ links zero current*.

Based on the above assumption, the flux linkages of the circuit caused by current in conductor 1 as per Eq. (2.21a) are

$$\lambda_1 = 2 \times 10^{-7} I_1 \ln \frac{D}{r'_1} \tag{2.22a}$$

The inductance of the conductor due to current in conductor 1 only is then

$$L_1 = 2 \times 10^{-7} \ln \frac{D}{r'_1} \tag{2.22b}$$

Similarly, the inductance of the circuit due to current in conductor 2 is

$$L_2 = 2 \times 10^{-7} \ln \frac{D}{r'_2} \tag{2.23}$$

Using the superposition theorem, the flux linkages and likewise the inductances of the circuit caused by current in each conductor considered separately may be added to obtain the total circuit inductance. Therefore, for the complete circuit

* Kimbark [10] has shown that the results based on this assumption are fairly accurate even when D is not much larger than r_1 and r_2.

$$L = L_1 + L_2 = 4 \times 10^{-7} \ln \frac{D}{\sqrt{r'_1 r'_2}} \text{ H/m} \qquad (2.24)$$

If $r'_1 = r'_2 = r'$; then

$$L = 4 \times 10^{-7} \ln D/r' \text{ H/m} \qquad (2.25a)$$

$$L = 0.921 \log D/r' \text{ mH/km} \qquad (2.25b)$$

Transmission lines are infinitely long compared to D in practical situations and therefore the end effects in the above derivation have been neglected.

2.5 CONDUCTOR TYPES

So far we have considered transmission lines consisting of single solid cylindrical conductors for forward and return paths. To provide the necessary flexibility for stringing, conductors used in practice are always stranded except for very small cross-sectional areas. Stranded conductors are composed of strands of wire, electrically in parallel, with alternate layers spiralled in opposite direction to prevent unwinding. The total number of strands (N) in concentrically stranded cables with total annular space filled with strands of uniform diameter (d) is given by

$$N = 3x^2 - 3x + 1 \qquad (2.26a)$$

where x is the number of layers wherein the single central strand is counted as the first layer. The overall diameter (D) of a stranded conductor is

$$D = (2x - 1)d \qquad (2.26b)$$

Aluminium is now the most commonly employed conductor material. It has the advantages of being cheaper and lighter than copper though with less conductivity and tensile strength. Low density and low conductivity result in larger overall conductor diameter, which offers another incidental advantage in high voltage lines. Increased diameter results in reduced electrical stress at conductor surface for a given voltage so that the line is *corona free*. The low tensile strength of aluminium conductors is made up by providing central strands of high tensile strength steel. Such a conductor is known as aluminium conductor steel reinforced (ACSR) and is most commonly used in overhead transmission lines. Figure 2.4 shows the cross-sectional view of an ACSR conductor with 24 strands of aluminium and 7 strands of steel.

In extra high voltage (EHV) transmission line, *expanded* ACSR conductors are used. These are provided with paper or hessian between various layers of strands so as to increase the overall conductor diameter in an attempt to reduce electrical stress at conductor surface and prevent corona. The most effective way of constructing *corona-free* EHV lines (Ch.19) is to provide several conductors per phase in suitable geometrical configuration. These are known as *bundled conductors* and are a common practice now for EHV lines.

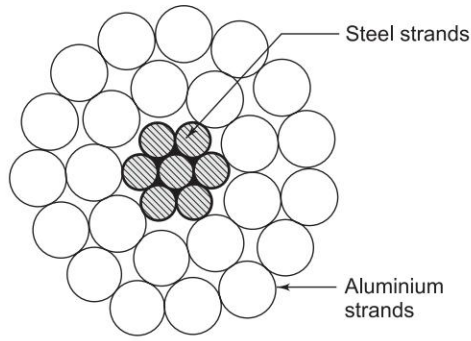

Fig. 2.4 Cross-sectional view of ACSR-7 steel strands, 24 aluminium strands

2.6 FLUX LINKAGES OF ONE CONDUCTOR IN A GROUP

As shown in Fig. 2.5, consider a group of n parallel round conductors carrying phasor currents I_1, I_2,..., I_n whose sum equals zero. Distances of these conductors from a remote point P are indicated as D_1, D_2,..., D_n. Let us obtain an expression for the total flux linkages of the ith conductor of the group considering flux upto the point P only.

The flux linkages of ith conductor due to its own current I_i (self linkages) are given by [see Eq. (2.21)]

$$\lambda_{ii} = 2 \times 10^{-7} I_i \ln \frac{D_i}{r'_i} \text{ Wb-T/m} \tag{2.27}$$

The flux linkages of conductor i due to current in conductor j [refer to Eq. (2.17)] is

$$\lambda_{ij} = 2 \times 10^{-7} I_j \ln \frac{D_j}{D_{ij}} \text{ Wb-T/m} \tag{2.28}$$

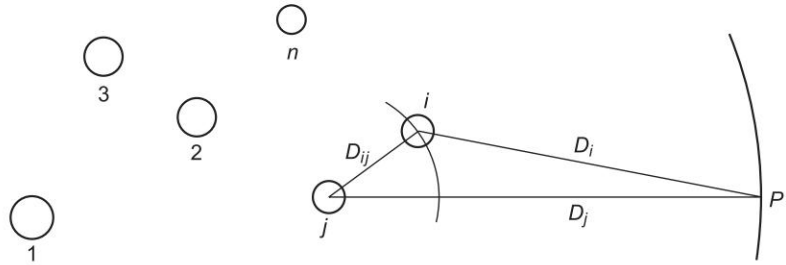

Fig. 2.5 Arbitrary group of n parallel round conductors carrying currents

where D_{ij} is the distance of ith conductor from jth conductor carrying current I_j. From Eq. (2.27) and by repeated use of Eq. (2.28), the total flux linkages of conductor i due to flux upto point P are

$$\lambda_i = \lambda_{i1} + \lambda_{i2} + \cdots + \lambda_{ii} + \cdots + \lambda_{in}$$

$$= 2 \times 10^{-7} \left(I_1 \ln \frac{D_1}{D_{i1}} + I_2 \ln \frac{D_2}{D_{i2}} + \cdots + I_i \ln \frac{D_i}{r_i'} + \cdots + I_n \ln \frac{D_n}{D_{in}} \right)$$

The above equation can be reorganized as

$$\lambda_i = 2 \times 10^{-7} \left[\left(I_1 \ln \frac{1}{D_{i1}} + I_2 \ln \frac{1}{D_{i2}} + \cdots + I_i \ln \frac{1}{r_i'} + \cdots + I_n \ln \frac{1}{D_{in}} \right) + (I_1 \ln D_1 + I_2 \ln D_2 + \cdots + I_i \ln D_i + \cdots + I_n \ln D_n) \right] \quad (2.29)$$

But, $I_n = -(I + I_2 + \cdots + I_{n-1})$.

Substituting for I_n in the second term of Eq. (2.29) and simplifying, we have

$$\lambda_i = 2 \times 10^{-7} \left[\left(I_1 \ln \frac{1}{D_{i1}} + I_2 \ln \frac{1}{D_{i2}} + \cdots + I_i \ln \frac{1}{r_i'} + \cdots + I_n \ln \frac{1}{D_{in}} \right) + \left(I_1 \ln \frac{D_1}{D_n} + I_2 \ln \frac{D_2}{D_n} + \cdots + I_i \ln \frac{D_i}{D_n} \cdots + I_{n-1} \ln \frac{D_{n-1}}{D_n} \right] \right)$$

In order to account for total flux linkages of conductor i, let the point P now recede to infinity. The terms such as $\ln D_1/D_n$, etc. approach $\ln 1 = 0$. Also for the sake of symmetry, denoting r'_i as D_{ii}, we have

$$\lambda_i = 2 \times 10^{-7} \left(I_1 \ln \frac{1}{D_{i1}} + I_2 \ln \frac{1}{D_{i2}} + \cdots I_2 \ln \frac{1}{D_{ii}} + \ldots + I_n \ln \frac{1}{D_{in}} \right) \text{ Wb-T/m} \quad (2.30)$$

2.7 INDUCTANCE OF COMPOSITE CONDUCTOR LINES

We are now ready to study the inductance of transmission lines composed of composite conductors. Figure 2.6 shows such a single-phase line comprising composite conductors A and B with A having n parallel filaments and B having m' parallel filaments. Though the inductance of each filament will be somewhat different (their resistances will be equal if conductor diameters are chosen to be uniform), it is sufficiently accurate to assume that the current is equally divided among the filaments of each composite conductor. Thus, each filament of A is taken to carry a current I/n, while each filament of conductor B carries the return current of $-I/m'$.

Applying Eq. (2.30) to filament i of conductor A, we obtain its flux linkages as

$$\lambda_i = 2 \times 10^{-7} \frac{I}{n} \left(\ln \frac{1}{D_{i1}} + \ln \frac{1}{D_{i2}} + \cdots + \ln \frac{1}{D_{ii}} + \cdots + \ln \frac{1}{D_{in}} \right)$$

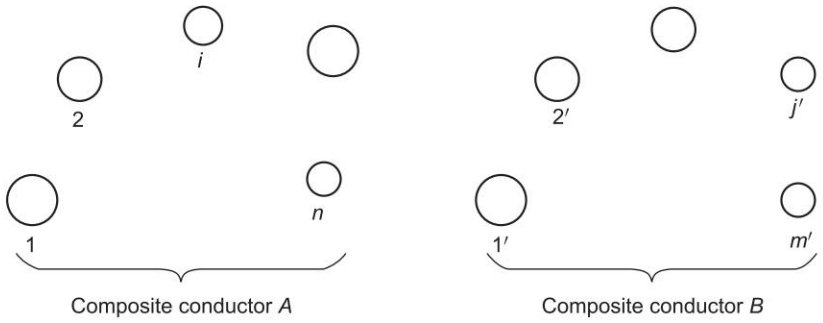

Fig. 2.6 Single-phase line consisting of two composite conductors

$$-2\times10^{-7}\frac{I}{m'}\left(\ln\frac{1}{D_{i1'}}+\ln\frac{1}{D_{i2'}}+\cdots+\ln\frac{1}{D_{im'}}\right)$$

$$=2\times10^{-7}I\ln\frac{(D_{i1'}D_{i2'}\ldots D_{im'})^{1/m'}}{(D_{i1}D_{i2}\ldots D_{ii}\ldots D_{in})^{1/n}}\ \text{Wb-T/m}$$

The inductance of filament i is then

$$L_i=\frac{\lambda_i}{I/n}=2n\times10^{-7}\ln\frac{(D_{i1'}\ldots D_{ij'}\ldots D_{im'})^{1/m'}}{(D_{i1}\ldots D_{ii}\ldots D_{in})^{1/n}}\ \text{H/m} \tag{2.31}$$

The average inductance of the filaments of composite conductor A is

$$L_{\text{avg}}=\frac{L_1+L_2+L_3+\cdots+L_n}{n}$$

Since conductor A is composed of n filaments electrically in parallel, its inductance is

$$L_A=\frac{L_{\text{avg}}}{n}=\frac{L_1+L_2+\cdots+L_n}{n^2} \tag{2.32}$$

Using the expression for filament inductance from Eq. (2.31) in Eq. (2.32), we obtain

$$L_A=2\times10^{-7}\ln\frac{[(D_{11'}\ldots D_{1j'}\ldots D_{1m'})\ldots(D_{i1'}\ldots D_{ij'}\ldots D_{im'})\ldots(D_{nl'}\ldots D_{nj'}\ldots D_{nm'})]^{1/m'n}}{[(D_{11}\ldots D_{1j}\ldots D_{1n})\ldots(D_{il}\ldots D_{ii}\ldots D_{in})\ldots(D_{n1}\ldots D_{ni}\ldots D_{nn})]^{1/n^2}}\ \text{H/m} \tag{2.33}$$

The numerator of the argument of the logarithm in Eq. (2.33) is the $m'n$th root of the $m'n$ terms, which are the products of all possible mutual distances from the n filaments of conductor A to m' filaments of conductor B. It is called *mutual geometric mean distance* (mutual GMD) between conductors A and B and is abbreviated as D_m. Similarly, the denominator of the argument of the logarithm in Eq. (2.33) is the n^2th root of n^2 product terms (n sets of n product terms each). Each set of n product term pertains to a filament and consists of $r'(D_{ii})$ for that filament and $(n - 1)$ distances from that filament to every other filament in conductor A. The denominator is defined as the *self geometric mean distance* (self GMD) of conductor A, and is abbreviated as D_{sA}. Sometimes, self GMD is also called *geometric mean radius* (GMR).

In terms of the above symbols, we can write Eq. (2.33) as

$$L_A = 2 \times 10^{-7} \ln \frac{D_m}{D_{sA}} \text{ H/m} \tag{2.34a}$$

$$= 0.4611 \log \frac{D_m}{D_{sA}} \text{ mH/km} \tag{2.34b}$$

Note the similarity of the above relation with Eq. (2.22b), which gives the inductance of one conductor of a single-phase line for the special case of two solid, round conductors. In Eq. (2.22b) r_1' is the self GMD of a single conductor and D is the mutual GMD of two single conductors.

The inductance of the composite conductor B is determined in a similar manner, and the total inductance of the line is

$$L = L_A + L_B \tag{2.35}$$

Example 2.1 A conductor is composed of seven identical copper strands, each having a radius r, as shown in Fig. 2.7. Find the self GMD of the conductor.

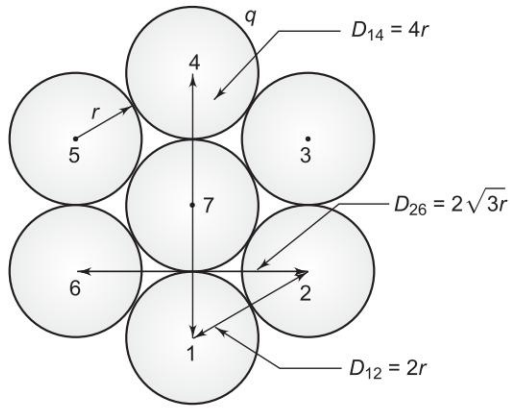

Fig. 2.7 Cross-section of a seven-strand conductor

Solution

The self GMD of the seven strand conductor is the 49th root of the 49 distances. Thus

$$D_s = ((r')^7 (D^2_{12} D^2_{26} D_{14} D_{17})^6 (2r)^6)^{1/49}$$

Substituting the values of various distances,

$$D_s = ((0.7788r)^7 (2^2 r^2 \times 3 \times 2^2 r^2 \times 2^2 r \times 2r \times 2r)^6)^{1/49}$$

or

$$D_s = \frac{2r(3(0.7788))^{1/7}}{6^{1/49}} = 2.177r$$

Example 2.2 The outside diameter of the single layer of aluminium strands of an ACSR conductor shown in Fig. 2.8 is 5.04 cm. The diameter of each strand is 1.68 cm. Determine the 50 Hz reactance at 1 m spacing; neglect the effect of the central strand of steel and advance reasons for the same.

Solution

The conductivity of steel being much poorer than that of aluminium and the internal inductance of steel strands being μ-times that of aluminium strands, the current conducted by the central strands of steel can be assumed to be zero.

Diameter of steel strand = $5.04 - 2 \times 1.68 = 1.68$ cm

Thus, all strands are of the same diameter, say d. For the arrangement of strands as given in Fig. 2.8(a),

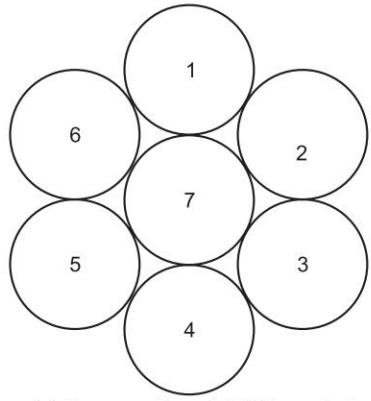

(a) Cross-section of ACSR conductor

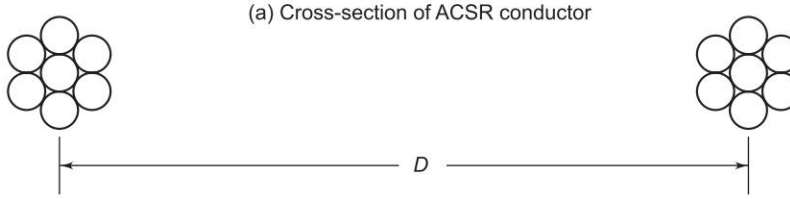

(b) Line composed of two ACSR conductors

Fig. 2.8

$$D_{12} = D_{16} = d$$
$$D_{13} = D_{15} = \sqrt{3}d$$
$$D_{14} = 2d$$
$$D_s = \left(\left[\left(\frac{d'}{2} \right) d^2 (\sqrt{3}\, d)^2 (\sqrt{2}\, d) \right]^6 \right)^{1/36}$$

Substituting $d' = 0.7788d$ and simplifying

$$D_s = 1.155d = 1.155 \times 1.68 = 1.93 \text{ cm}$$
$$D_m \approx D \quad \text{since} \quad D \gg d$$

Now, the inductance of each conductor is

$$L = 0.461 \log \frac{100}{1.93} = 0.789 \text{ mH/km}$$

Loop inductance $= 2 \times 0.789 = 1.578$ mH/km

Loop reactance $= 1.578 \times 314 \times 10^{-3} = 0.495$ ohms/km

Example 2.3 The arrangement of conductors of a single-phase transmission line is shown in Fig. 2.9, wherein the forward circuit is composed of three solid wires 2.5 mm in radius and the return circuit of two-wires of radius 5 mm placed symmetrically with respect to the forward circuit. Find the inductance of each side of the line and that of the complete line.

Solution

The mutual GMD between sides A and B is

$$D_m = ((D_{14}D_{15})\,(D_{24}D_{25})\,(D_{34}D_{35}))^{1/6}$$

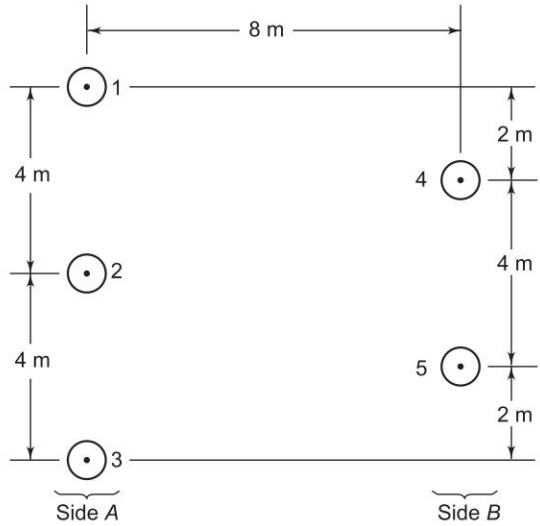

Fig. 2.9 Arrangement of conductors for Example 2.3

From the figure it is obvious that

$$D_{14} = D_{24} = D_{25} = D_{35} = \sqrt{68} \text{ m}$$
$$D_{15} = D_{34} = 10 \text{ m}$$
$$D_m = (68^2 \times 100)^{1/6} = 8.8 \text{ m}$$

The self GMD for side A is

$$D_{sA} = ((D_{11}D_{12}D_{13})(D_{21}D_{22}D_{23})(D_{31}D_{32}D_{33}))^{1/9}$$

Here,

$$D_{11} = D_{22} = D_{33} = 2.5 \times 10^{-3} \times 0.7788 \text{ m}$$

Substituting the values of various interdistances and self distances in D_{sA}, we get

$$D_{sA} = ((2.5 \times 10^{-3} \times 0.7788)^3 \times 4^4 \times 8^2)^{1/9}$$
$$= 0.367 \text{ m}$$

Similarly,

$$D_{sB} = ((5 \times 10^{-3} \times 0.7788)^2 \times 4^2)^{1/4}$$
$$= 0.125 \text{ m}$$

Substituting the values of D_m, D_{sA} and D_{sB} in Eq. (2.25b), we get the various inductances as

$$L_A = 0.461 \log \frac{8.8}{0.367} = 0.635 \text{ mH/km}$$

$$L_B = 0.461 \log \frac{8.8}{0.125} = 0.85 \text{ mH/km}$$

$$L = L_A + L_B = 1.485 \text{ mH/km}$$

If the conductors in this problem are each composed of seven identical strands as in Example 2.1, the problem can be solved by writing the conductor self distances as

$$D_{ii} = 2.177 r_i$$

where r_i is the strand radius.

2.8 INDUCTANCE OF THREE-PHASE LINES

So far we have considered only single-phase lines. The basic equations developed can, however, be easily adapted to the calculation of the inductance of three-phase lines. Figure 2.10 shows the conductors of a three-phase line with unsymmetrical spacing.

Assume that there is no neutral wire, so that

$$I_a + I_b + I_c = 0$$

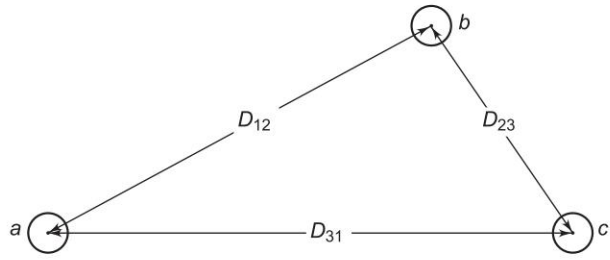

Fig. 2.10 Cross-sectional view of a three-phase line with unsymmetrical spacing

Unsymmetrical spacing causes the flux linkages and therefore the inductance of each phase to be different resulting in unbalanced receiving-end voltages even when sending-end voltages and line currents are balanced. Also voltages will be induced in adjacent communication lines even when line currents are balanced. This problem is tackled by exchanging the positions of the conductors at regular intervals along the line such that each conductor occupies the original position of every other conductor over an equal distance. Such an exchange of conductor positions is called *transposition*. A complete transposition cycle is shown in Fig. 2.11. This arrangement causes each conductor to have the same average inductance over the transposition cycle. Over the length of one transposition cycle, the total flux linkages and hence net voltage induced in a nearby telephone line is zero.

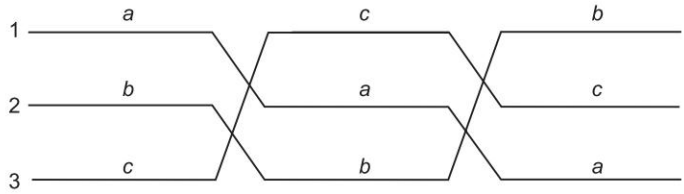

Fig. 2.11 A complete transposition cycle

To find the average inductance of each conductor of a transposed line, the flux linkages of the conductor are found for each position it occupies in the transposed cycle. Applying Eq. (2.30) to conductor *a* of Fig. 2.11, for section 1 of the transposition cycle wherein *a* is in position 1, *b* is in position 2 and *c* is in position 3, we get

$$\lambda_{a1} = 2 \times 10^{-7} \left(I_a \ln \frac{1}{r_a'} + I_b \ln \frac{1}{D_{12}} + I_c \ln \frac{1}{D_{31}} \right) \text{ Wb-T/m}$$

For the second section

$$\lambda_{a2} = 2 \times 10^{-7} \left(I_a \ln \frac{1}{r_a'} + I_b \ln \frac{1}{D_{23}} + I_c \ln \frac{1}{D_{12}} \right) \text{ Wb-T/m}$$

For the third section

$$\lambda_{a3} = 2 \times 10^{-7} \left(I_a \ln \frac{1}{r_a'} + I_b \ln \frac{1}{D_{13}} + I_c \ln \frac{1}{D_{23}} \right) \text{ Wb-T/m}$$

Average flux linkages of conductor a are

$$\lambda_a = \frac{\lambda_{a1} + \lambda_{a2} + \lambda_{a3}}{3}$$

$$= 2 \times 10^{-7} \left(I_a \ln \frac{1}{r_a'} + I_b \ln \frac{1}{(D_{12}D_{23}D_{31})^{1/3}} + I_c \ln \frac{1}{(D_{12}D_{23}D_{31})^{1/3}} \right)$$

But, $I_b + I_c = -I_a$; hence

$$\lambda_a = 2 \times 10^{-7} I_a \ln \frac{(D_{12}D_{23}D_{31})^{1/3}}{r_a'}$$

Let

$$D_{eq} = (D_{12}D_{23}D_{31})^{1/3} = \text{equivalent equilateral spacing}$$

Then

$$L_a = 2 \times 10^{-7} \ln \frac{D_{eq}}{r_a'} = 2 \times 10^{-7} \ln \frac{D_{eq}}{r_a'} \text{ H/m} \tag{2.36}$$

This is the same relation as Eq. (2.34a) where $D_m = D_{eq}$, the mutual GMD between the three-phase conductors. If $r_a = r_b = r_c$, we have

$$L_a = L_b = L_c$$

It is not the present practice to transpose the power lines at regular intervals. However, an interchange in the position of the conductors is made at switching stations to balance the inductance of the phases. For all practical purposes the dissymmetry can be neglected and the inductance of an untransposed line can be taken equal to that of a transposed line.

If the spacing is equilateral, then

$$D_{eq} = D$$

and

$$L_a = 2 \times 10^{-7} \ln \frac{D}{r_a'} \text{ H/m} \tag{2.37}$$

If $r_a = r_b = r_c$, it follows from Eq. (2.37) that

$$L_a = L_b = L_c$$

Example 2.4 Show that over the length of one transposition cycle of a power line, the total flux linkages of a nearby telephone line are zero, for balanced three-phase currents.

Solution

Referring to Fig. 2.12, the flux linkages of the conductor t_1 of the telephone line are

$$\lambda_{t1} = 2 \times 10^{-7} \left(I_a \ln \frac{1}{D_{a1}} + I_b \ln \frac{1}{D_{b1}} + I_c \ln \frac{1}{D_{c1}} \right) \text{ Wb-T/m} \qquad (2.38)$$

Similarly,

$$\lambda_{t2} = 2 \times 10^{-7} \left(I_a \ln \frac{1}{D_{a2}} + I_b \ln \frac{1}{D_{b2}} + I_c \ln \frac{1}{D_{c2}} \right) \text{ Wb-T/m} \qquad (2.39)$$

The net flux linkages of the telephone line are

$$\lambda_t = \lambda_{t1} - \lambda_{t2}$$

$$= 2 \times 10^{-7} \left(I_a \ln \frac{D_{a2}}{D_{a1}} + I_b \ln \frac{D_{b2}}{D_{b1}} + I_c \ln \frac{D_{c2}}{D_{c1}} \right) \text{ Wb-T/m} \qquad (2.40)$$

The emf induced in the telephone line loop is

$$E_t = 2\pi f \lambda_t \text{ V/m}$$

Under balanced load conditions, λ_t is not very large because there is a cancellation to a great extent of the flux linkages due to I_a, I_b and I_c. Such cancellation does not take place with harmonic currents which are multiples of three and are therefore in phase. Consequently, these frequencies, if present, may be very troublesome.

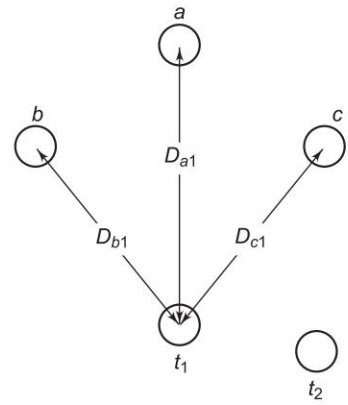

Fig. 2.12 Effect of transposition on induced voltage of a telephone line

If the power line is fully transposed with respect to the telephone line

$$\lambda_{t1} = \frac{\lambda_{t1}(\text{I}) + \lambda_{t1}(\text{II}) + \lambda_{t1}(\text{III})}{3}$$

where λ_{t1}(I), λ_{t1}(II) and λ_{t1}(III) are the flux linkages of the telephone line t_1 in the three transposition sections of the power line.

Writing for λ_{t1}(I), λ_{t2}(II) and λ_{t3}(III) by repeated use of Eq. (2.38), we have

$$\lambda_{t1} = 2 \times 10^{-7} \left(I_a + I_b + I_c \right) \ln \frac{1}{(D_{a1} D_{b1} D_{c1})^{1/3}}$$

Similarly,

$$\lambda_{t2} = \frac{\lambda_{t2}(\text{I}) + \lambda_{t2}(\text{II}) + \lambda_{t2}(\text{III})}{3}$$

$$= 2 \times 10^{-7} (I_a + I_b + I_c) \ln \frac{1}{(D_{a2} D_{b2} D_{c2})^{1/3}}$$

$$\therefore \quad \lambda_t = 2 \times 10^{-7} (I_a + I_b + I_c) \ln \frac{(D_{a2} D_{b2} D_{c2})^{1/3}}{(D_{a1} D_{b2} D_{c3})^{1/3}} \tag{2.41}$$

If $I_a + I_b + I_c = 0$, $\lambda_t = 0$, i.e. voltage induced in the telephone loop is zero over one transposition cycle of the power line.

It may be noted here that the condition $I_a + I_b + I_c = 0$ is not satisfied for

(i) power frequency L-G (line-to-ground fault) currents, where

$$I_a + I_b + I_c = 3I_0$$

(ii) third and multiple of third harmonic currents under healthy condition, where

$$I_a(3) + I_b(3) + I_c(3) = 3I(3)$$

$$\therefore \quad E_t(3) = 6\pi f \lambda_t(3)$$

The harmonic line currents are troublesome in two ways:

(i) Induced emf is proportional to the frequency.
(ii) Higher frequencies come within the audible range.

Thus there is need to avoid the presence of such harmonic currents on power line from considerations of the performance of nearby telephone lines.

It has been shown above that voltage induced in a telephone line running parallel to a power line is reduced to zero if the power line is transposed and provided it carries balanced currents. It was also shown that power line transposition is ineffective in reducing the induced telephone line voltage when power line currents are unbalanced or when they contain third harmonics. Power line transposition apart from being ineffective introduces mechanical and insulation problems. It is, therefore, easier to eliminate induced voltages by transposing the telephone line instead. In fact, the reader can easily verify that even when the power line currents are unbalanced or when they contain harmonics, the voltage induced over complete transposition cycle (called a *barrel*) of a telephone line is zero. Some induced voltage will always be present on a telephone line running parallel to a power line because in actual practice transposition is never completely symmetrical. Therefore, when the lines run parallel over a considerable length, it is a good practice to transpose both power and telephone lines. The two transposition cycles are staggered and the telephone line is transposed over shorter lengths compared to the power line.

Example 2.5 A three-phase, 50 Hz, 15 km long line has four No. 4/0 wires (1 cm dia) spaced horizontally 1.5 m apart in a plane. The wires in order are carrying currents I_a, I_b and I_c, and the fourth wire, which is a neutral, carries zero current. The currents are:

$$I_a = -30 + j50 \text{ A}$$
$$I_b = -25 + j55 \text{ A}$$
$$I_c = 55 - j105 \text{ A}$$

The line is untransposed.

(a) From the fundamental consideration, find the flux linkages of the neutral. Also find the voltage induced in the neutral wire.

(b) Find the voltage drop in each of the three-phase wires.

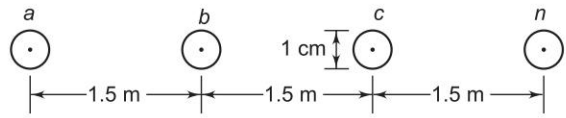

Fig. 2.13 Arrangement of conductors for Example 2.5

Solution

(a) From Fig. 2.13,

$$D_{an} = 4.5 \text{ m}, D_{bn} = 3 \text{ m}, D_{cn} = 1.5 \text{ m}$$

Flux linkages of the neutral wire n are

$$\lambda_n = 2 \times 10^{-7}\left(I_a \ln \frac{1}{D_{an}} + I_b \ln \frac{1}{D_{bn}} + I_c \ln \frac{1}{D_{cn}} \right) \text{ Wb-T/m}$$

Substituting the values of D_{an}, D_{bn} and D_{cn}, and simplifying, we get

$$\lambda_n = -2 \times 10^{-7} (1.51 I_a + 1.1 I_b + 0.405 I_c) \text{ Wb-T/m}$$

Since $I_c = -(I_a + I_b)$ (this is easily checked from the given values),

$$\lambda_n = -2 \times 10^{-7}(1.105 I_a + 0.695 I_b) \text{ Wb-T/m}$$

The voltage induced in the neutral wire is then

$$V_n = j\omega\lambda_n \times 15 \times 10^3 \text{ V}$$
$$= -j314 \times 15 \times 10^3 \times 2 \times 10^{-7}(1.105 I_a + 0.695 I_b) \text{ V}$$

or $$V_n = -j0.942 (1.105 I_a + 0.695 I_b) \text{ V}$$

Substituting the values of I_a and I_b, and simplifying,

$$V_n = 0.942 \times 106 = 100 \text{ V}$$

(b) From Eq. (2.30), the flux linkages of the conductor a are

$$\lambda_a = 2 \times 10^{-7}\left(I_a \ln \frac{1}{r_a'} + I_b \ln \frac{1}{D} + I_c \ln \frac{1}{2D} \right) \text{ Wb-T/m}$$

The voltage drop/metre in phase a can be written as

$$\Delta V_a = 2 \times 10^{-7} j\omega \left(I_a \ln \frac{1}{r_a'} + I_b \ln \frac{1}{D} + I_c \ln \frac{1}{2D} \right) \text{ V/m}$$

Since $I_c = -(I_a + I_b)$, and further since $r_a = r_b = r_c = r$, the expression for ΔV_a can be written in simplified form

$$\Delta V_a = 2 \times 10^{-7} j\omega \left(I_a \ln \frac{2D}{r'} + I_b \ln 2 \right) \quad \text{V/m}$$

Similarly, voltage drop/metre of phases b and c can be written as

$$\Delta V_b = 2 \times 10^{-7} j\omega I_b \ln \frac{D}{r'}$$

$$\Delta V_c = 2 \times 10^{-7} j\omega \left(I_b \ln 2 + I_c \ln \frac{2D}{r'} \right)$$

Using matrix notation, we can present the result in compact form

$$\begin{bmatrix} \Delta V_a \\ \Delta V_b \\ \Delta V_c \end{bmatrix} = 2 \times 10^{-7} j\omega \begin{bmatrix} \ln 2D/r' & \ln 2 & 0 \\ 0 & \ln D/r' & 0 \\ 0 & \ln 2 & \ln 2D/r' \end{bmatrix} \begin{bmatrix} I_a \\ I_b \\ I_c \end{bmatrix}$$

The voltage drop of phase a is calculated below:

$$\begin{aligned} \Delta V_a &= j2 \times 10^{-7} \times 314 \times 15 \times 10^3 \\ &\quad \left(\ln \frac{300}{0.39} (-30 + j50) + 0.693(-25 + j55) \right) \\ &= -(348.6 + j204) \text{ V} \end{aligned}$$

Example 2.6 A single-phase 50 Hz power line is supported on a horizontal cross-arm. The spacing between the conductors is 3 m. A telephone line is supported symmetrically below the power line as shown in Fig. 2.14. Find the mutual inductance between the two circuits and the voltage induced per kilometre in the telephone line if the current in the power line is 100 A. Assume the telephone line current to be zero. (see Sec. 2.13).

Solution

Flux linkages of conductor T_1

$$\lambda_{t1} = 2 \times 10^{-7} \left(I \ln \frac{1}{D_1} - I \ln \frac{1}{D_2} \right) = 2 \times 10^{-7} I \ln \frac{D_2}{D_1}$$

Flux linkages of conductor T_2

$$\lambda_{t2} = 2 \times 10^{-7} I \ln \frac{D_1}{D_2}$$

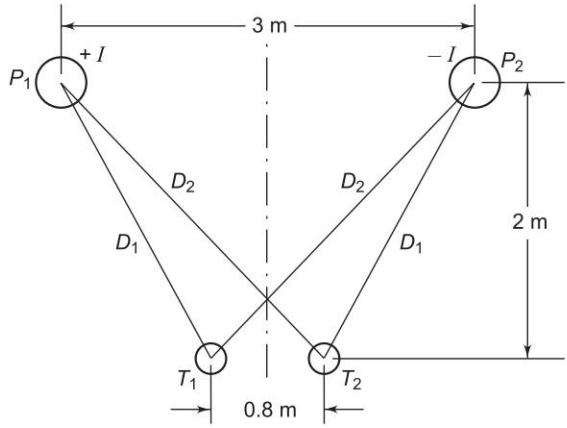

Fig. 2.14 Power and telephone lines for Example 2.6

Total flux linkage of the telephone circuit

$$\lambda_t = \lambda_{t1} - \lambda_{t2} = 4 \times 10^{-7} I \ln \frac{D_2}{D_1}$$

$$M_{pt} = 4 \times 10^{-7} \ln \frac{D_2}{D_1} \text{ H/m}$$

$$= 0.921 \log \frac{D_2}{D_1} \text{ mH/km}$$

$$D_1 = (1.1^2 + 2^2)^{1/2} = (5.21)^{1/2}$$

$$D_2 = (1.9^2 + 2^2)^{1/2} = (7.61)^{1/2}$$

$$M_{pt} = 0.921 \log \left(\frac{761}{521} \right)^{1/2} = 0.0758 \text{ mH/km}$$

Voltage induced in the telephone circuit $V_t = j\omega M_{pt} I$

$$|V_t| = 314 \times 0.0758 \times 10^{-3} \times 100 = 2.379 \quad \text{V/km}$$

2.9 DOUBLE-CIRCUIT THREE-PHASE LINES

It is common practice to build double-circuit three-phase lines so as to increase transmission reliability at somewhat enhanced cost. From the point of view of power transfer from one end of the line to the other (see Sec. 12.3), it is desirable to build the two lines with as low an inductance/phase as possible. In order to achieve this, self GMD (D_s) should be made high and mutual GMD (D_m) should be made low. Therefore, the individual conductors of a phase should be kept as far apart as possible (for high self GMD), while the distance between phases be kept as low as permissible (for low mutual GMD).

Figure 2.15 shows the three sections of the transposition cycle of two parallel circuit three-phase lines with vertical spacing (it is a very commonly used configuration).

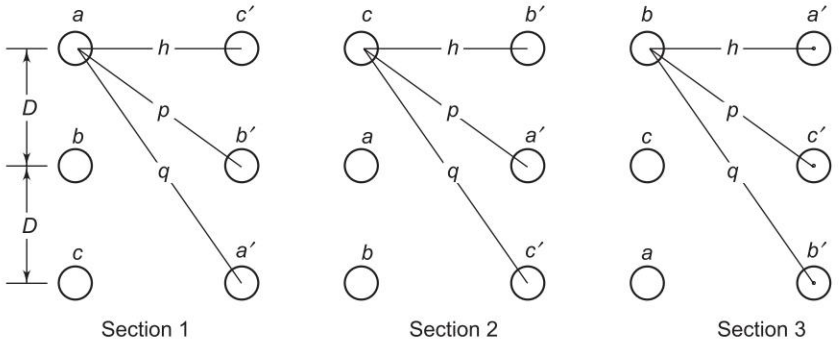

Fig. 2.15

It may be noted here that conductors a and a' in parallel compose phase a and similarly b and b' compose phase b and c and c' compose phase c. In order to achieve high D_s the conductors of two phases are placed diametrically opposite to each other and those of the third phase are horizontally opposite to each other. (The reader can try other configurations to verify that these will lead to low D_s). Applying the method of GMD, the equivalent equilateral spacing is

$$D_{eq} = (D_{ab}D_{bc}D_{ca})^{1/3} \tag{2.42}$$

where D_{ab} = mutual GMD between phases a and b in section 1 of the transposition cycle
$= (DpDp)^{1/4} = (Dp)^{1/2}$

D_{bc} = mutual GMD between phases b and c in section 1 of the transposition cycle
$= (Dp)^{1/2}$

D_{ca} = mutual GMD between phases c and a in section 1 of the transposition cycle
$= (2Dh)^{1/2}$

Hence $D_{eq} = 2^{1/6}D^{1/2}p^{1/3}h^{1/6}$ (2.43)

It may be noted here that D_{eq} remains the same in each section of the transposition cycle, as the conductors of each parallel circuit rotate cyclically, so do D_{ab}, D_{bc} and D_{ca}. The reader is advised to verify this for sections 2 and 3 of the transposition cycle in Fig. 2.15.

Self GMD in section 1 of phase a (i.e., conductors a and a') is

$$D_{sa} = (r'qr'q)^{1/4} = (r'q)^{1/2}$$

Self GMD of phases b and c in section 1 are respectively

$$D_{sb} = (r'hr'h)^{1/4} = (r'h)^{1/2}$$
$$D_{sc} = (r'qr'q)^{1/4} = (r'q)^{1/2}$$

$\therefore$ Equivalent self GMD, $D_s = (D_{sa}D_{sb}D_{sc})^{1/3}$

$$= (r')^{1/2}q^{1/3}h^{1/6} \tag{2.44}$$

Because of the cyclic rotation of conductors of each parallel circuit over the transposition cycle, D_s also remains the same in each transposition section. The reader should verify this for sections 2 and 3 in Fig. 2.15.

The inductance per phase is

$$L = 2 \times 10^{-7} \ln \frac{D_{eq}}{D_s}$$
$$= 2 \times 10^{-7} \ln \frac{2^{1/6} D^{1/2} p^{1/3} h^{1/6}}{(r')^{1/2} q^{1/3} h^{1/6}}$$
$$= 2 \times 10^{-7} \ln \left(2^{1/6} \left(\frac{D}{r'} \right)^{1/2} \left(\frac{p}{q} \right)^{1/3} \right) \text{ H/phase/m} \tag{2.45}$$

The self inductance of each circuit is given by

$$L_s = 2 \times 10^{-7} \ln \frac{(2)^{1/3} D}{r'}$$

Equation (2.45) can now be written as

$$L = \frac{1}{2} \left[2 \times 10^{-7} \ln \frac{(2)^{1/3} D}{r'} + 2 \times 10^{-7} \ln \left(\frac{p}{q} \right)^{2/3} \right] \tag{2.46}$$
$$= \frac{1}{2} (L_s + M)$$

where M is the mutual inductance between the two circuits, i.e.

$$M = 2 \times 10^{-7} \ln \left(\frac{p}{q} \right)^{2/3}$$

This is a well known result for the two coupled circuits connected in parallel (at similar polarity ends).

If $h \ll D$, $\left(\frac{p}{q} \right) \to 1$ and $M \to 0$, i.e. the mutual impedance between the circuits becomes zero. Under this condition,

$$L = 1 \times 10^{-7} \ln \frac{3\sqrt{2}\, D}{r'} \tag{2.47}$$

The GMD method, though applied above to a particular configuration of a double circuit, is valid for any configuration as long as the circuits are electrically parallel.

While the GMD method is valid for fully transposed lines, it is commonly applied for untransposed lines and is quite accurate for practical purposes.

2.10 BUNDLED CONDUCTORS

It is economical to transmit large chunks of power over long distances by employing EHV lines. However, the line voltages that can be used are severely limited by the phenomenon of *corona*. Corona, in fact, is the result of ionization of the atmosphere when a certain field intensity (about 3,000 kV/m at NTP) is reached. Corona discharge causes communication interference and associated power loss which can be severe in bad weather conditions. Critical line voltage for formation of corona can be raised considerably by the use of bundled conductors—a group of two or more conductors per phase. This increase in critical corona voltage is dependent on number of conductors in the group, the clearance between them and the distance between the groups forming the separate phases*. Reichman [11] has shown that the spacing of conductors in a bundle affects voltage gradient and the optimum spacing is of the order of 8–10 times the conductors diameter, irrespective of the number of conductors in the bundle.

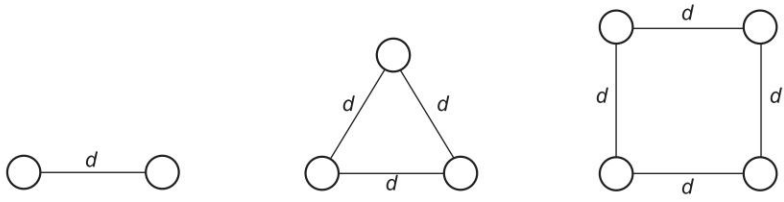

Fig. 2.16 Configuration of bundled conductors

Further, because of increased self GMD** line inductance is reduced considerably with the incidental advantage of increased transmission capacity of the line.

Example 2.7 Find the inductive reactance in ohms per kilometer at 50 Hz of a three-phase bundled conductor line with two conductors per phase as shown in Fig. 2.17. All the conductors are ACSR with radii of 1.725 cm.

* The bundle usually comprises two, three or four conductors arranged in configurations illustrated in Fig. 2.16. The current will not divide equally among them.

** The more the number of conductors in a bundle, the more is the self GMD.

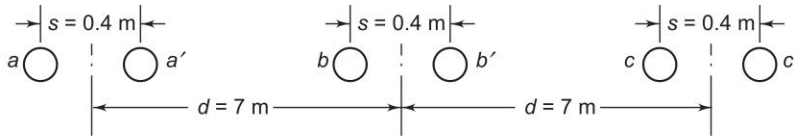

Fig. 2.17 Bundled conductor three-phase line

Even though the power lines are not normally transposed (except when they enter and leave a switching station), it is sufficiently accurate to assume complete transposition (of the bundles as well as of the conductors within the bundle) so that the method of GMD can be applied.

The mutual GMD between bundles of phases a and b

$$D_{ab} = (d\,(d+s)\,(d-s)\,d)^{1/4}$$

Mutual GMD between bundles of phases b and c

$$D_{bc} = D_{ab} \text{ (by symmetry)}$$

Mutual GMD between bundles of phases c and a

$$D_{ca} = (2d\,(2d+s\,)\,(2d-s)2d)^{1/4}$$

$$D_{eq} = (D_{ab}D_{bc}D_{ca})^{1/3}$$

$$= (4d^6(d+s)^2(d-s)^2(2d+s)(2d-s))^{1/12}$$

$$= (4(7)^6(7.4)^2(6.6)^2(14.4)(13.6))^{1/12}$$

$$= 8.81 \text{ m}$$

$$D_s = (r'sr's)^{1/4} = (r's)^{1/2} = (0.7788 \times 1.725 \times 10^{-2} \times 0.4)^{1/2}$$

$$= 0.073 \text{ m}$$

Inductive reactance per phase

$$X_L = 314 \times 0.461 \times 10^{-3} \log \frac{8.81}{0.073}$$

$$= 0.301 \text{ ohm/km}$$

In most cases, it is sufficiently accurate to use the centre to centre distances between bundles rather than mutual GMD between bundles for computing D_{eq}. With this approximation, we have for the example in hand

$$D_{eq} = (7 \times 7 \times 14)^{1/3} = 8.82 \text{ m}$$

$$X_L = 314 \times 0.461 \times 10^{-3} \log \frac{8.82}{0.073}$$

$$= 0.301 \text{ ohm/km}$$

Thus the approximate method yields almost the same reactance value as the exact method. It is instructive to compare the inductive reactance of a bundled conductor line with an equivalent (on heuristic basis) single conductor line.

For the example in hand, the equivalent line will have $d = 7$ m and conductor diameter (for same total cross-sectional area) as $\sqrt{2} \times 1.725$ cm.

$$X_L = 314 \times 0.461 \times 10^{-3} \log \frac{(7 \times 7 \times 14)^{1/3}}{0.7788 \times \sqrt{2} \times 1.725 \times 10^{-3}}$$

$$= 0.531 \text{ ohm/km}$$

This is 76.41% higher than the corresponding value for a bundled conductor line. As already pointed out, lower reactance of a bundled conductor line increases its transmission capacity.

2.11 RESISTANCE

Though the contribution of line resistance to series line impedance can be neglected in most cases, it is the main source of line power loss. Thus while considering transmission line economy, the presence of line resistance must be considered.

The effective AC resistance is given by

$$R = \frac{\text{average power loss in conductor in watts}}{I^2} \text{ ohms} \tag{2.48}$$

where I is the rms current in the conductor in amperes. Ohmic or DC resistance is given by the formula

$$R_O = \frac{\rho l}{A} \text{ ohms} \tag{2.49}$$

where ρ = resistivity of the conductor, ohm-m

l = length, m

A = cross-sectional area, m^2

The effective resistance given by Eq. (2.48) is equal to the DC resistance of the conductor given by Eq. (2.49) only if the current distribution is uniform throughout the conductor.

For small changes in temperature, the resistance increases with temperature in accordance with the relationship

$$R_t = R\,(1 + \alpha_0 t) \tag{2.50}$$

where R = resistance at temperature 0°C

α_0 = temperature coefficient of the conductor at 0°C

Equation (2.50) can be used to find the resistance R_{t2} at a temperature t_2, if resistance R_{t1} at temperature t_1 is known

$$\frac{R_{t2}}{R_{t1}} = \frac{1/\alpha_0 + t_2}{1/\alpha_0 + t_1} \tag{2.51}$$

2.12 SKIN EFFECT AND PROXIMITY EFFECT

The distribution of current throughout the cross-section of a conductor is uniform only when DC is passing through it. On the contrary when AC is flowing through a conductor, the current is non-uniformly distributed over the cross-section in a manner that the current density is higher at the surface of the conductor compared to the current density at its centre. This effect becomes more pronounced as frequency is increased. This phenomenon is called *skin effect*. It causes larger power loss for a given rms AC than the loss when the same value of DC is flowing through the conductor. Consequently, the effective conductor resistance is more for AC than for DC. A qualitative explanation of the phenomenon is given below.

Imagine a solid round conductor (a round shape is considered for convenience only) to be composed of annular filaments of equal cross-sectional area. The flux linking the filaments progressively decreases as we move towards the outer filaments for the simple reason that the flux inside a filament does not link it. The inductive reactance of the imaginary filaments therefore decreases outwards with the result that the outer filaments conduct more AC than the inner filaments (filaments being parallel). With the increase of frequency the non-uniformity of inductive reactance of the filaments becomes more pronounced, so also the non-uniformity of current distribution. For large solid conductors the skin effect is quite significant even at 50 Hz. The analytical study of skin effect requires the use of Bessel's functions and is beyond the scope of this book.

Apart from the skin effect, non-uniformity of current distribution is also caused by *proximity effect*. Consider a two-wire line as shown in Fig. 2.18. Each line conductor can be divided into sections of equal cross-sectional area (say three sections). Pairs aa', bb' and cc' can form three loops in parallel. The flux linking loop aa' (and therefore its inductance) is the least and it increases somewhat for loops bb' and cc'. Thus the density of AC flowing through the conductors is highest at the inner edges (aa') of the conductors and is the least at the outer edges (cc'). This type of non-uniform AC current distribution becomes more pronounced as the distance between conductors is reduced. Like skin effect, the non-uniformity of current distribution caused by proximity effect also increases the effective conductor resistance. For normal spacing of overhead lines, this effect is always of negligible order. However, for underground cables where conductors are located close to each other, proximity effect causes an appreciable increase in effective conductor resistance.

Fig. 2.18

Both skin and proximity effects depend upon conductor size, frequency, distance between conductors and permeability of conductor material.

2.13 MAGNETIC FIELD INDUCTION

Transmission lines are used to transmit the bulk amount of power at higher voltages. These lines establish electromagnetic and electrostatic fields of sufficient magnitude in the neighbouring vicinity. These fields induce currents and voltages in the objects that lie in the vicinity of these fields and have a considerable length parallel to the line, i.e., telephone lines, pipe lines etc. (see Example 2.6)

It is a common practice to run the communication lines in parallel or along the same route as the power lines. The induced currents, voltages in the communication lines cause, interference with communication service, e.g., damage to apparatus, hazard to person etc. In the past, researchers have shown that these fields adversely affect the blood composition, growth, immune system and neural functions.

The presence of harmonics and multiple of third harmonics is dangerous for the communication circuits.

2.14 SUMMARY

This chapter has dealt with two important series parameters of transmission lines namely resistance and inductance. Use of bundled conductors, magnetic field induction have also been discussed.

Problems

2.1 Derive the formula for the internal inductance in H/m of a hollow conductor having inside radius r_1 and outside radius r_2 and also determine the expression for the inductance in H/m of a single-phase line consisting of the hollow conductors described above with conductors spaced a distance D apart.

2.2 Calculate the 50 Hz inductive reactance at 1 m spacing in ohms/km of a cable consisting of 12 equal strands around a nonconducting core. The diameter of each strand is 0.25 cm and the outside diameter of the cable is 1.25 cm.

2.3 A concentric cable consists of two thin-walled tubes of mean radii r and R respectively, derive an expression for the inductance of the cable per unit length.

2.4 A single-phase 50 Hz circuit comprises two single-core lead-sheathed cables laid side by side; if the centres of the cables are 0.5 m apart and

each sheath has a mean diameter of 7.5 cm, estimate the longitudinal voltage induced per km of sheath when the circuit carries a current of 800 A.

2.5 Two long parallel conductors carry currents of + I and − I. What is the magnetic field intensity at a point P, shown in Fig. P-2.5?

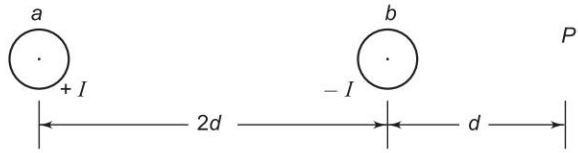

Fig. P-2.5

2.6 Two three-phase lines connected in parallel have self-reactances of X_1 and X_2. If the mutual reactance between them is X_{12}, what is the effective reactance between the two ends of the line?

2.7 A single-phase 50 Hz power line is supported on a horizontal cross-arm. The spacing between conductors is 2.5 m. A telephone line is also supported on a horizontal cross-arm in the same horizontal plane as the power line. The conductors of the telephone line are of solid copper spaced 0.6 m between centres. The distance between the nearest conductors of the two lines is 20 m. Find the mutual inductance between the circuits and the voltage per kilometre induced in the telephone line for 150 A current flowing over the power line.

2.8 A telephone line runs parallel to an untransposed three-phase transmission line, as shown in Fig. P-2.8. The power line carries balanced current of 400 A per phase. Find the mutual inductance between the circuits and calculate the 50 Hz voltage induced in the telephone line per km.

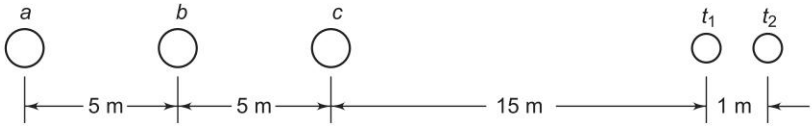

Fig. P-2.8 Telephone line parallel to a power line

2.9 A 500 kV line has a bundling arrangement of two conductors per phase as shown in Fig. P-2.9.

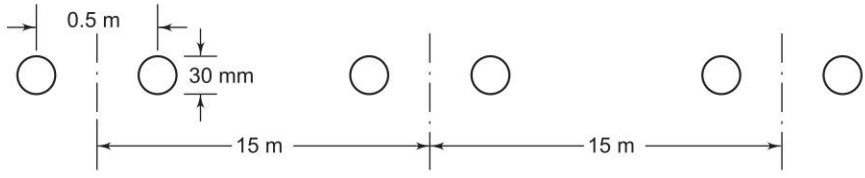

Fig. P-2.9 500 kV, three-phase bundled conductor line

Compute the reactance per phase of this line at 50 Hz. Each conductor carries 50% of the phase current. Assume full transposition.

2.10 An overhead line 50 kms in length is to be constructed of conductors 2.56 cm in diameter, for single-phase transmission. The line reactance must not exceed 31.4 ohms. Find the maximum permissible spacing.

2.11 In Fig. P-2.11 which depicts two three-phase circuits on a steel tower there is symmetry about both the horizontal and vertical centre lines. Let each three-phase circuit be transposed by replacing *a* by *b* and then by *c*, so that the reactances of the three-phases are equal and the GMD method of reactance calculations can be used. Each circuit remains on its own side of the tower. Let the self GMD of a single conductor be 1 cm. Conductors *a* and *a′* and other corresponding phase conductors are connected in parallel. Find the reactance per phase of the system.

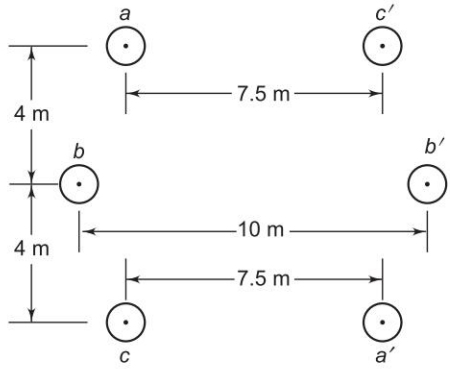

Fig. P-2.11

2.12 A double-circuit three-phase line is shown in Fig. P-2.12. The conductors *a*, *a′; b, b′* and *c*, *c′* belong to the same phase respectively. The radius of each conductor is 1.5 cm. Find the inductance of the double-circuit line in mH/km/phase.

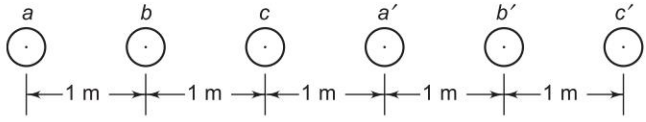

Fig. P-2.12 Arrangement of conductors for a double-circuit three-phase line

2.13 A three-phase line with equilateral spacing of 3 m is to be rebuilt with horizontal spacing ($D_{13} = D_{12} = D_{22}$). The conductors are to be fully transposed. Find the spacing between adjacent conductors such that the new line has the same inductance as the original line.

2.14 Find the self GMD of three arrangements of bundled conductors shown in Fig. 2.16 in terms of the total cross-sectional area *A* of conductors (same in each case) and the distance *d* between them.

References

Books

1. *Electrical Transmission and Distribution Book*, Westinghouse Electric and Manufacturing Co., East Pittsburgh, Pennsylvania, 1964.
2. Waddicor, H., *Principles of Electric Power Transmission*, 5th edn, Chapman and Hall, London, 1964.
3. Kothari, D.P. and I.J. Nagrath, *Electric Machines*, 3rd edn, Tata McGraw-Hill, New Delhi, 2003.
4. Stevenson, W.D., *Elements of Power System Analysis*, 4th edn, McGraw-Hill, New York, 1982.
5. *EHV Transmission Line Reference Book*, Edison Electric Institute, 1968.
6. The Aluminium Association, *Aluminium Electrical Conductor Handbook*, New York, 1971.
7. Woodruff, L.F., *Principles of Electric Power Transmission*, Wiley, New York, 1947.
8. Gross, C.A., *Power System Analysis*, Wiley, New York, 1979.
9. Weedy, B.M. and B.J. Cory, *Electric Power Systems*, 4th edn, Wiley, New York, 1998.
10. Kimbark, E.W., *Electrical Transmission of Power and Signals*, Wiley, New York, 1949.

Paper

11. Reichman, J., 'Bundled Conductor Voltage Gradient Calculations," *AIEE Trans*., 1959, pt III, 78 : 598.

Chapter 3

Capacitance of Transmission Lines

3.1 INTRODUCTION

The capacitance together with conductance forms the shunt admittance of a transmission line. As mentioned earlier the conductance is the result of leakage over the surface of insulators and is of negligible order. When an alternating voltage is applied to the line, the line capacitance draws a leading sinusoidal current called the c*harging current* which is drawn even when the line is open circuited at the far end. The line capacitance being proportional to its length, the charging current is negligible for lines less than 100 km long. For longer lines the capacitance becomes increasingly important and has to be accounted for.

3.2 ELECTRIC FIELD OF A LONG STRAIGHT CONDUCTOR

Imagine an infinitely long straight conductor far removed from other conductors (including earth) carrying a uniform charge of q coulomb/metre length. By symmetry, the equipotential surfaces will be concentric cylinders, while the lines of electrostatic stress will be radial. The electric field intensity at a distance y from the axis of the conductor is

$$\varepsilon = \frac{q}{2\pi k y} \text{ V/m}$$

where k is the permittivity* of the medium.

As shown in Fig. 3.1, consider two points P_1 and P_2 located at distances D_1 and D_2 respectively from the conductor axis. The potential difference V_{12} (between P_1 and P_2) is given by

$$V_{12} = \int \varepsilon \, \mathrm{d}y = \int \frac{q}{2\pi k y} \, \mathrm{d}y \quad \text{V}$$

* In SI units the permittivity of free space is $k_0 = 8.85 \times 10^{-12}$ F/m. Relative permittivity for air is $k_r = k/k_0 = 1$.

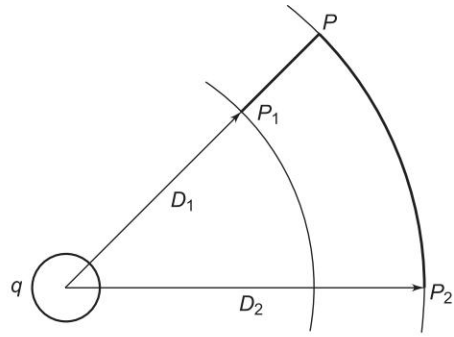

Fig. 3.1 Electric field of a long straight conductor

As the potential difference is independent of the path, we choose the path of integration as P_1PP_2 shown in thick line. Since the path PP_2 lies along an equipotential, V_{12} is obtained simply by integrating along P_1P, i.e.

$$V_{12} = \int_{D_1}^{D_2} \frac{q}{2\pi k y} \mathrm{d}y = \frac{q}{2\pi k} \ln \frac{D_2}{D_1} \quad \text{V} \tag{3.1}$$

3.3 POTENTIAL DIFFERENCE BETWEEN TWO CONDUCTORS OF A GROUP OF PARALLEL CONDUCTORS

Figure 3.2 shows a group of parallel charged conductors. It is assumed that the conductors are far removed from the ground and are sufficiently removed from each other, i.e. the conductor radii are much smaller than the distances between them. The spacing commonly used in overhead power transmission lines always meets these assumptions. Further, these assumptions imply that the charge on each conductor remains uniformly distributed around its periphery and length.

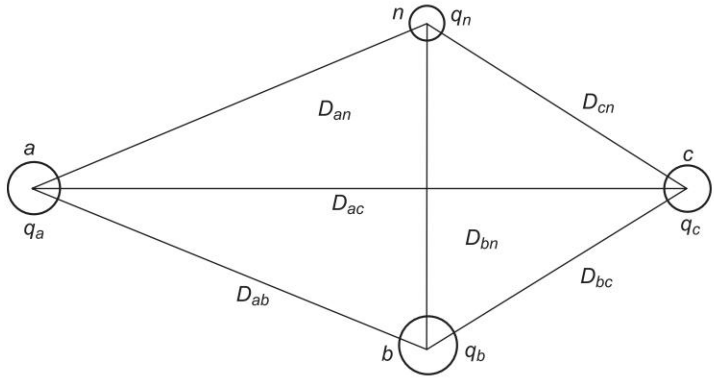

Fig. 3.2 A group of parallel charged conductors

The potential difference between any two conductors of the group can then be obtained by adding the contributions of the individual charged conductors by repeated application of Eq. (3.1). So, the potential difference between conductors a and b (voltage drop from a to b) is

$$V_{ab} = \frac{1}{2\pi k}\left(q_a \ln \frac{D_{ab}}{r_a} + q_b \ln \frac{r_b}{D_{ba}} + q_c \ln \frac{D_{cb}}{D_{ca}} + \ldots q_n \ln \frac{D_{nb}}{D_{na}} \right) \text{ V} \qquad (3.2)$$

Each term in Eq. (3.2) is the potential drop from a to b caused by charge on one of the conductors of the group. Expressions on similar lines could be written for voltage drop between any two conductors of the group.

If the charges vary sinusoidally, so do the voltages (this is the case for AC transmission line), the expression of Eq. (3.2) still applies with charges/metre length and voltages regarded as phasor quantities. Equation (3.2) is thus valid for instantaneous quantities and for sinusoidal quantities as well, wherein all charges and voltages are phasors.

3.4 CAPACITANCE OF A TWO-WIRE LINE

Consider a two-wire line shown in Fig. 3.3 excited from a single-phase source. The line develops equal and opposite sinusoidal charges on the two conductors which can be represented as phasors q_a and q_b so that $q_a = -q_b$.

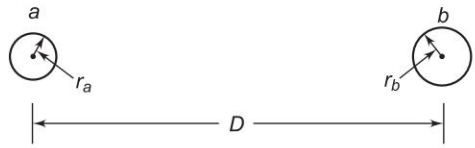

Fig. 3.3 Cross-sectional view of a two-wire line

The potential difference V_{ab} can be written in terms of the contributions made by q_a and q_b by use of Eq. (3.2) with associated assumptions (i.e. D/r is large and ground is far away). Thus,

$$V_{ab} = \frac{1}{2\pi k}\left(q_a \ln \frac{D}{r_a} + q_b \ln \frac{r_b}{D} \right) \qquad (3.3)$$

Since $q_a = -q_b$, we have

$$V_{ab} = \frac{q_a}{2\pi k} \ln \frac{D^2}{r_a r_b}$$

The line capacitance C_{ab} is then

$$C_{ab} = \frac{q_a}{V_{ab}} = \frac{\pi k}{\ln (D/(r_a r_b)^{1/2})} \text{ F/m length of line} \qquad (3.4a)$$

or

$$C_{ab} = \frac{0.0121}{\log (D/(r_a r_b)^{1/2})} \quad \mu\text{F/km} \tag{3.4b}$$

If $r_a = r_b = r$,

$$C_{ab} = \frac{0.0121}{\log (D/r)} \quad \mu\text{F/km} \tag{3.4c}$$

The associated line charging current is

$$I_c = j\omega C_{ab} V_{ab} \quad \text{A/km} \tag{3.5}$$

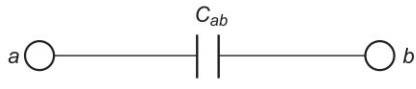

(a) Line-to-line capacitance

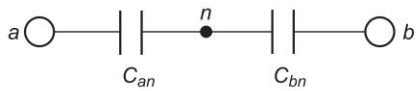

$C_{an} = C_{bn} = 2C_{ab}$

(b) Line-to-neutral capacitance

Fig. 3.4

As shown in Figs 3.4(a) and (b) the line-to-line capacitance can be equivalently considered as two equal capacitances in series. The voltage across the lines divides equally between the capacitances such that the neutral point n is at the ground potential. The capacitance of each line to neutral is then given by

$$C_n = C_{an} = C_{bn} = 2C_{ab} = \frac{0.0242}{\log (D/r)} \quad \mu\text{F/km} \tag{3.6}$$

The assumptions inherent in the above derivation are:

(i) The charge on the surface of each conductor is assumed to be uniformly distributed, but this is strictly not correct.

If non-uniformity of charge distribution is taken into account, then

$$C_n = \frac{0.0242}{\log\left(\frac{D}{2r} + \left(\frac{D^2}{4r^2} - 1\right)^{1/2}\right)} \quad \mu\text{F/km} \tag{3.7}$$

If $D/2r \gg 1$, the above expression reduces to that of Eq. (3.6) and the error caused by the assumption of uniform charge distribution is negligible.

(ii) The cross-section of both the conductors is assumed to be circular, while in actual practice stranded conductors are used. The use of the radius of the circumscribing circle for a stranded conductor causes insignificant error.

3.5 CAPACITANCE OF A THREE-PHASE LINE WITH EQUILATERAL SPACING

Figure 3.5 shows a three-phase line composed of three identical conductors of radius r placed in equilateral configuration.

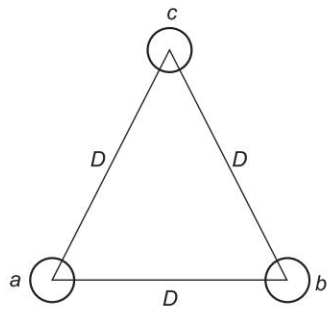

Fig. 3.5 Cross-section of a three-phase line with equilateral spacing

Using Eq. (3.2) we can write the expressions for V_{ab} and V_{ac} as

$$V_{ab} = \frac{1}{2\pi k}\left(q_a \ln\frac{D}{r} + q_b \ln\frac{r}{D} + q_c \ln\frac{D}{D}\right) \tag{3.8}$$

$$V_{ac} = \frac{1}{2\pi k}\left(q_a \ln\frac{D}{r} + q_b \ln\frac{D}{D} + q_c \ln\frac{r}{D}\right) \tag{3.9}$$

Adding Eqs (3.8) and (3.9), we get

$$V_{ab} + V_{ac} = \frac{1}{2\pi k}\left[2q_a \ln\frac{D}{r} + (q_b + q_c)\ln\frac{r}{D}\right] \tag{3.10}$$

Since there are no other charges in the vicinity, the sum of charges on the three conductors is zero. Thus $q_b + q_c = -q_a$, which when substituted in Eq. (3.10) yields

$$V_{ab} + V_{ac} = \frac{3q_a}{2\pi k}\ln\frac{D}{r} \tag{3.11}$$

With balanced three-phase voltages applied to the line, it follows from the phasor diagram of Fig. 3.6 that

$$V_{ab} + V_{ac} = 3V_{an} \tag{3.12}$$

Substituting for $(V_{ab} + V_{ac})$ from Eq. (3.12) in Eq. (3.11), we get

$$V_{an} = \frac{q_a}{2\pi k}\ln\frac{D}{r} \tag{3.13}$$

The capacitance of line to neutral immediately follows as

$$C_n = \frac{q_a}{V_{an}} = \frac{2\pi k}{\ln (D/r)} \tag{3.14a}$$

For air medium (k_r = 1),

$$C_n = \frac{0.0242}{\log (D/r)} \quad \mu\text{F/km} \tag{3.14b}$$

The line charging current of phase a is

$$I_a \text{ (line charging)} = j\omega C_n V_{an} \tag{3.15}$$

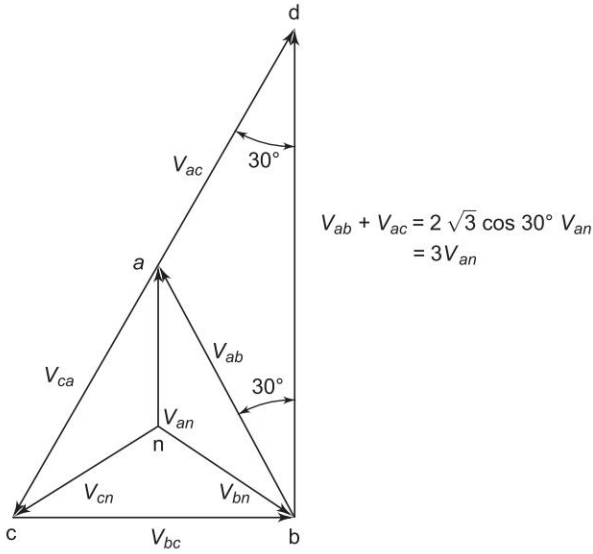

Fig. 3.6 Phasor diagram of balanced three-phase voltages

3.6 CAPACITANCE OF A THREE-PHASE LINE WITH UNSYMMETRICAL SPACING

Figure 3.7 shows the three identical conductors of radius r of a three-phase line with unsymmetrical spacing. It is assumed that the line is fully transposed. As the conductors are rotated cyclically in the three sections of the transposition cycle, correspondingly three expressions can be written for V_{ab}. These expressions are:

For the first section of the transposition cycle

$$V_{ab} = \frac{1}{2\pi k}\left(q_{a1} \ln \frac{D_{12}}{r} + q_{b1} \ln \frac{r}{D_{12}} + q_{c1} \ln \frac{D_{23}}{D_{31}} \right) \tag{3.16a}$$

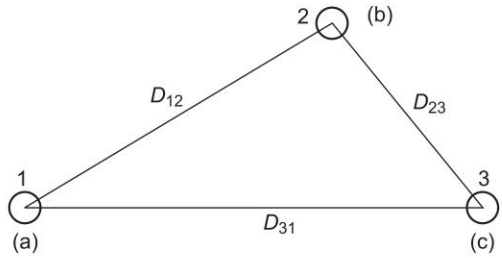

Fig. 3.7 Cross-section of a three-phase line with asymmetrical spacing (fully transposed)

For the second section of the transposition cycle

$$V_{ab} = \frac{1}{2\pi k}\left(q_{a2} \ln \frac{D_{23}}{r} + q_{b2} \ln \frac{r}{D_{23}} + q_{c2} \ln \frac{D_{31}}{D_{12}} \right) \qquad (3.16b)$$

For the third section of the transposition cycle

$$V_{ab} = \frac{1}{2\pi k}\left(q_{a3} \ln \frac{D_{31}}{r} + q_{b3} \ln \frac{r}{D_{31}} + q_{c3} \ln \frac{D_{12}}{D_{23}} \right) \qquad (3.16c)$$

If the voltage drop along the line is neglected, V_{ab} is the same in each transposition cycle. On similar lines three such equations can be written for $V_{bc} = V_{ab} \angle -120°$. Three more equations can be written equating to zero the summation of all line charges in each section of the transposition cycle. From these nine (independent) equations, it is possible to determine the nine unknown charges. The rigorous solution though possible is too involved.

With the usual spacing of conductors sufficient accuracy is obtained by assuming

$$q_{a1} = q_{a2} = q_{a3} = q_a \; ; \; q_{b1} = q_{b2} = q_{b3} = q_b ; \; q_{c1} = q_{c2} = q_{c3} = q_c \qquad (3.17)$$

This assumption of equal charges/unit length of a line in the three sections of the transposition cycle requires, on the other hand, three different values of V_{ab} designated as V_{ab1}, V_{ab2} and V_{ab3} in the three sections. The solution can be considerably simplified by taking V_{ab} as the average of these three voltages, i.e.

$$V_{ab}\,(\text{avg}) = \frac{1}{3}(V_{ab1} + V_{ab2} + V_{ab3})$$

or

$$V_{ab} = \frac{1}{6\pi k}\left[q_a \ln \left(\frac{D_{12}D_{23}D_{31}}{r^3} \right) + q_b \ln \left(\frac{r^3}{D_{12}D_{23}D_{31}} \right) + q_c \ln \left(\frac{D_{12}D_{23}D_{31}}{D_{12}D_{23}D_{31}} \right) \right]$$

$$= \frac{1}{2\pi k}\left(q_a \ln \frac{D_{eq}}{r} + q_b \ln \frac{r}{D_{eq}}\right) \tag{3.18}$$

where $D_{eq} = (D_{12}D_{23}D_{31})^{1/3}$

Similarly,

$$V_{ac} = \frac{1}{2\pi k}\left(q_a \ln \frac{D_{eq}}{r} + q_c \ln \frac{r}{D_{eq}}\right) \tag{3.19}$$

Adding Eqs (3.18) and (3.19), we get

$$V_{ab} + V_{ac} = \frac{1}{2\pi k}\left(q_a \ln \frac{D_{eq}}{r} + (q_b + q_c) \ln \frac{r}{D_{eq}}\right) \tag{3.20}$$

As per Eq. (3.12) for balanced three-phase voltages

$$V_{ab} + V_{ac} = 3V_{an}$$

and also $(q_b + q_c) = -q_a$

Use of these relationships in Eq. (3.20) leads to

$$V_{an} = \frac{q_a}{2\pi k} \ln \frac{D_{eq}}{r} \tag{3.21}$$

The capacitance of line to neutral of the transposed line is then given by

$$C_n = \frac{q_a}{V_{an}} = \frac{2\pi k}{\ln (D_{eq}/r)} \text{ F/m to neutral} \tag{3.22a}$$

For air medium ($k_r = 1$)

$$C_n = \frac{0.0242}{\log (D_{eq}/r)} \ \mu\text{F/km to neutral} \tag{3.22b}$$

It is obvious that for equilateral spacing $D_{eq} = D$, the above (approximate) formula gives the exact result presented earlier.

The line charging current for a three-phase line in phasor form is

$$I_a \text{ (line charging)} = j\omega C_n V_{an} \text{ A/km} \tag{3.23}$$

3.7 EFFECT OF EARTH ON TRANSMISSION LINE CAPACITANCE

So far, in calculating the capacitance of transmission lines, the presence of earth was ignored. The effect of earth on capacitance can be conveniently taken into account by the method of images.

Method of Images

The electric field of transmission line conductors must conform to the presence of the earth below. The earth for this purpose may be assumed to be a perfectly conducting horizontal sheet of infinite extent which therefore acts like an equipotential surface.

The electric field of two long, parallel conductors charged $+q$ and $-q$ per unit is such that it has a zero potential plane midway between the conductors as shown in Fig. 3.8. If a conducting sheet of infinite dimensions is placed at the zero potential plane, the electric field remains undisturbed. Further, if the conductor carrying charge $-q$ is now removed, the electric field above the conducting sheet stays intact, while that below it vanishes. Using these well known results in reverse, we may equivalently replace the presence of ground below a charged conductor by a fictitious conductor having equal and opposite charge and located as far below the surface of ground as the overhead conductor above it—such a fictitious conductor is the *mirror image* of the overhead conductor. This method of creating the same electric field as in the presence of earth is known as the *method of images* originally suggested by Lord Kelvin.

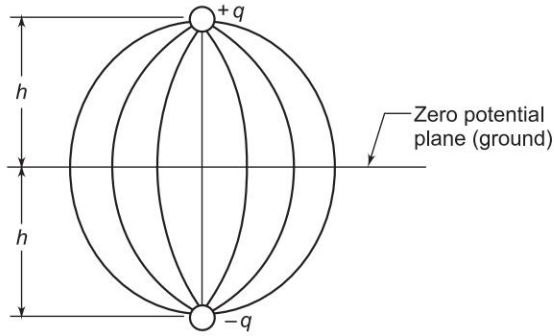

Fig. 3.8 Electric field of two long, parallel, oppositely charged conductors

Capacitance of a Single-Phase Line

Consider a single-phase line shown in Fig. 3.9. It is required to calculate its capacitance taking the presence of earth into account by the method of images described above. The equation for the voltage drop V_{ab} as determined by the two charged conductors a and b, and their images a' and b' can be written as follows:

$$V_{ab} = \frac{1}{2\pi k}\left[q_a \ln \frac{D}{r} + q_b \ln \frac{r}{D} + q_{a'} \ln \frac{(4h^2 + D^2)^{1/2}}{2h} + q_{b'} \ln \frac{2h}{(4h^2 + D^2)^{1/2}} \right] \tag{3.24}$$

Substituting the values of different charges and simplifying, we get

$$V_{ab} = \frac{q}{\pi k} \ln \frac{2hD}{r(4h^2 + D^2)^{1/2}} \tag{3.25}$$

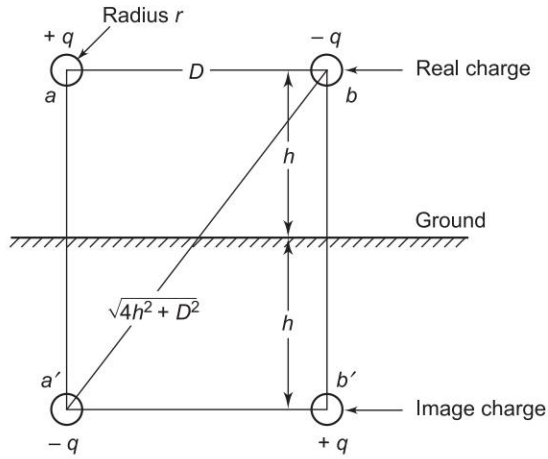

Fig. 3.9 Single-phase transmission line with images

It immediately follows that

$$C_{ab} = \frac{\pi k}{\ln \dfrac{D}{r(1+(D^2/4h^2))^{1/2}}} \text{ F/m line-to-line} \qquad (3.26a)$$

and

$$C_n = \frac{2\pi k}{\ln \dfrac{D}{r(1+(D^2/4h^2))^{1/2}}} \text{ F/m to neutral} \qquad (3.26b)$$

It is observed from the above equation that the presence of earth modifies the radius r to $r(1 + (D^2/4h^2))^{1/2}$. For h large compared to D (this is the case normally), the effect of earth on line capacitance is of negligible order.

Capacitance of a Three-Phase Line

The method of images can similarly be applied for the calculation of capacitance of a three-phase line, shown in Fig. 3.10. The line is considered to be fully transposed. The conductors *a, b* and *c* carry the charges q_a, q_b and q_c and occupy positions 1, 2, and 3, respectively, in the first section of the transposition cycle. The effect of earth is simulated by image conductors with charges $-q_a$, $-q_b$ and $-q_c$ respectively, as shown.

The equations for the three sections of the transposition cycle can be written for the voltage drop V_{ab} as determined by the three charged conductors and their images. With conductor *a* in position 1, *b* in position 2, and *c* in position 3,

$$V_{ab} = \frac{1}{2\pi k}\left[q_a\left(\ln\frac{D_{12}}{r} - \ln\frac{h_{12}}{h_1}\right) + q_b\left(\ln\frac{r}{D_{12}} - \ln\frac{h_2}{h_{12}}\right) + q_c\left(\ln\frac{D_{23}}{D_{31}} - \ln\frac{h_{23}}{h_{31}}\right)\right] \qquad (3.27)$$

Similar equations for V_{ab} can be written for the second and third sections of the transposition cycle. If the fairly accurate assumption of constant charge per unit length of the conductor throughout the transmission cycle is made, the average value of V_{ab} for the three sections of the cycle is given by

$$V_{ab} = \frac{1}{2\pi k}\left[q_a \left(\ln \frac{D_{eq}}{r} - \ln \frac{(h_{12}h_{23}h_{31})^{1/3}}{(h_1h_2h_3)^{1/3}} \right) + q_b \left(\ln \frac{r}{D_{eq}} - \ln \frac{(h_1h_2h_3)^{1/3}}{(h_{12}h_{23}h_{31})^{1/3}} \right) \right] \tag{3.28}$$

where $D_{eq} = (D_{12}D_{23}D_{31})^{1/3}$

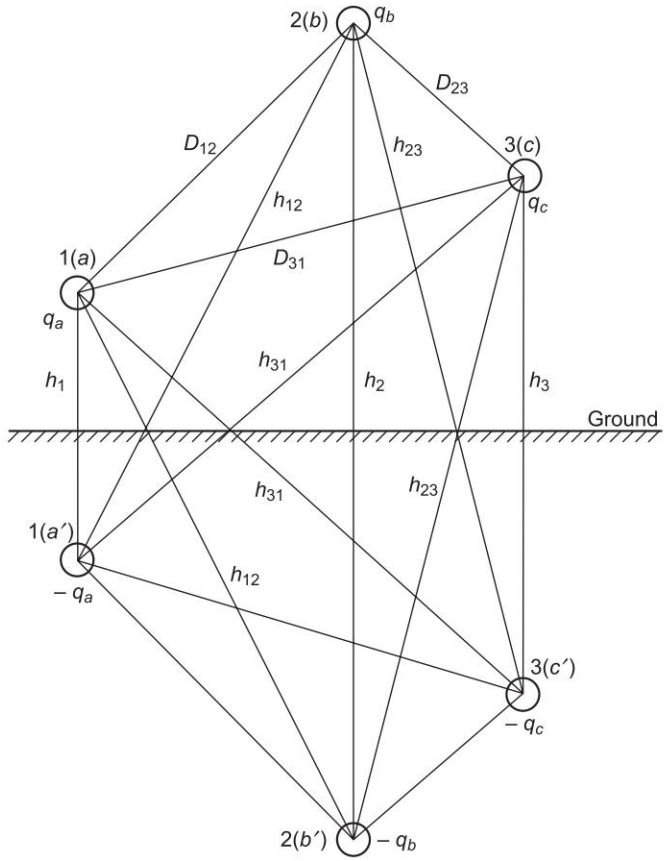

Fig. 3.10 Three-phase line with images

The equation for the average value of the phasor V_{ac} is found in a similar manner. Proceeding on the lines of Sec. 3.6 and using $V_{ab} + V_{ac} = 3V_{an}$ and $q_a + q_b + q_c = 0$, we ultimately obtain the following expression for the capacitance to neutral.

$$C_n = \frac{2\pi k}{\ln \frac{D_{eq}}{r} - \ln \left(\frac{(h_{12}h_{23}h_{31})^{1/3}}{(h_1h_2h_3)^{1/3}} \right)} \quad \text{F/m to neutral} \qquad (3.29a)$$

or

$$C_n = \frac{0.0242}{\log \frac{D_{eq}}{r} - \log \frac{(h_{12}h_{23}h_{31})^{1/3}}{(h_1h_2h_3)^{1/3}}} \quad \mu\text{F/km to neutral} \qquad (3.29b)$$

Comparing Eqs (3.22a) and (3.29a), it is evident that the effect of earth is to increase the capacitance of a line. If the conductors are high above earth compared to the distances among them, the effect of earth on the capacitance of three-phase lines can be neglected.

Example 3.1 Calculate the capacitance to neutral/km of a single-phase line composed of No. 2 single strand conductors (radius = 0.328 cm) spaced 3 m apart and 7.5 m above the ground. Compare the results obtained by Eqs (3.6), (3.7) and (3.26b).

Solution

(1) Neglecting the presence of earth [Eq. (3.6)]

$$C_n = \frac{0.0242}{\log \frac{D}{r}} \quad \mu\text{F/km}$$

$$= \frac{0.0242}{\log \frac{300}{0.328}} = 0.00817 \quad \mu\text{F/km}$$

By the rigorous relationship [(Eq. (3.7)]

$$C_n = \frac{0.0242}{\log \left(\frac{D}{2r} + \left(\frac{D^2}{4r^2} - 1 \right)^{1/2} \right)} \quad \mu\text{F/km}$$

Since $\frac{D}{r} = 915$, the effect of non-uniformity of charge distribution is almost negligible.

$\therefore \quad C_n = 0.00817 \quad \mu\text{F/km}$

(2) Considering the effect of earth and neglecting non-uniformity of charge distribution [Eq. (3.26b)]

$$C_n = \frac{0.0242}{\log \frac{D}{r(1 + (D^2/4h^2))^{1/2}}}$$

$$\frac{D}{r\sqrt{1.04}} = \frac{300}{0.328\sqrt{1.04}} = 897$$

$$C_n = \frac{0.0242}{2.953} = 0.0082 \quad \mu\text{F/km}$$

Note: The presence of earth increases the capacitance by approximately 3 parts in 800.

Example 3.2 A three-phase 50 Hz transmission line has flat horizontal spacing with 3.5 m between adjacent conductors. The conductors are No. 2/0 hard-drawn seven strand copper (outside conductor diameter = 1.05 cm). The voltage of the line is 110 kV. Find the capacitance to neutral and the charging current per kilometre of line.

Solution

$$D_{eq} = (3.5 \times 3.5 \times 7)^{1/3} = 4.4 \text{ m}$$

$$C_n = \frac{0.0242}{\log (D_{eq}/r)} = \frac{0.0242}{\log (440/0.525)}$$

$$= 0.00826 \quad \mu\text{F/km}$$

$$X_n = \frac{1}{\omega C_n} = \frac{10^6}{314 \times 0.00826}$$

$$= 0.384 \times 10^6 \quad \Omega\text{/km to neutral}$$

Charging current

$$= \frac{V_n}{X_n} = \frac{(110/\sqrt{3}) \times 1000}{0.384 \times 10^6}$$

$$= 0.17 \quad \text{A/km}$$

Example 3.3 The six conductors of a double-circuit three-phase line having an overall radius of 0.865×10^{-2} m are arranged as shown in Fig. 3.11. Find the capacitive reactance to neutral and charging current per kilometre per conductor at 110 kV, 50 Hz.

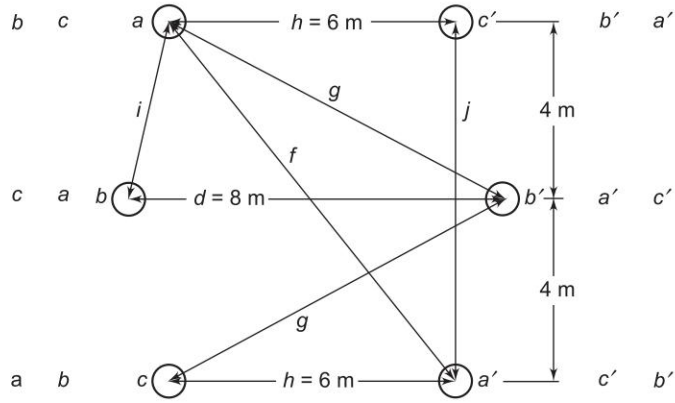

Fig. 3.11 Cross-section of a double-circuit three-phase line

Solution

As in Sec. 3.6, assume that the charge per conductor on each phase is equal in all the three sections of the transposition cycle. For section *I* of the transposition cycle

$$V_{ab}(\mathrm{I}) = \frac{1}{2\pi k}\left[q_a\left(\ln\frac{i}{r}+\ln\frac{g}{f}\right)+q_b\left(\ln\frac{r}{i}+\ln\frac{d}{g}\right) + q_c\left(\ln\frac{i}{j}+\ln\frac{g}{h}\right)\right] \tag{3.30}$$

For section II of the transposition cycle

$$V_{ab}\ (\mathrm{II}) = \frac{1}{2\pi k}\left[q_a\left(\ln\frac{i}{r}+\ln\frac{g}{d}\right)+q_b\left(\ln\frac{r}{i}+\ln\frac{f}{g}\right) + q_c\left(\ln\frac{j}{i}+\ln\frac{h}{g}\right)\right] \tag{3.31}$$

For section III of the transposition cycle

$$V_{ab}\ (\mathrm{III}) = \frac{1}{2\pi k}\left[q_a\left(\ln\frac{j}{r}+\ln\frac{h}{f}\right)+q_b\left(\ln\frac{r}{j}+\ln\frac{f}{h}\right) + q_c\left(\ln\frac{i}{j}+\ln\frac{g}{g}\right)\right] \tag{3.32}$$

Average value of V_{ab} over the transposition cycle is given by

$$V_{ab}\ (\text{avg}) = \frac{1}{6\pi k}\left[q_a \ln\left(\frac{ig\ ig\ jh}{rf\ rd\ rf}\right)+q_b \ln\left(\frac{rd\ rf\ rf}{ig\ ig\ jh}\right)\right]$$

$$= \frac{1}{2\pi k}(q_a - q_b)\ln\left(\frac{i^2g^2jh}{r^3f^2d}\right)^{1/3} \tag{3.33}$$

Similarly

$$V_{ac}\ (\text{avg}) = \frac{1}{2\pi k}(q_a - q_c)\ln\left(\frac{i^2g^2jh}{r^3f^2d}\right)^{1/3} \tag{3.34}$$

Now

$$V_{ab} + V_{ac} = 3V_{an} = \frac{1}{2\pi k}(2q_a - q_b - q_c)\ln\left(\frac{i^2g^2jh}{r^3f^2d}\right)^{1/3} \tag{3.35}$$

$$3V_{an} = \frac{3q_a}{2\pi k}\ln\left(\frac{i^2g^2jh}{r^3f^2d}\right)^{1/3}$$

$$\text{Capacitance to neutral per conductor} = \frac{2\pi k}{\ln\left(\frac{i^2 g^2 jh}{r^3 f^2 d}\right)^{1/3}} \qquad (3.36)$$

Total capacitance to neutral for two conductors in parallel

$$C_n = \frac{4\pi k}{\ln\left(\frac{i^2 g^2 jh}{r^3 f^2 d}\right)^{1/3}} \text{ F/m} \qquad (3.37)$$

Now $h = 6$ m; $d = 8$ m; $j = 8$ m. Referring to Fig. 3.12, we can write

$$i = \left[\left(\frac{j}{2}\right)^2 + \left(\frac{d-h}{2}\right)^2\right]^{1/2} = \sqrt{17} \text{ m}$$

$$f = (j^2 + h^2)^{1/2} = 10 \text{ m}$$

$$g = (7^2 + 4^2)^{1/2} = \sqrt{65} \text{ m}$$

Conductor radius (overall) $= 0.865 \times 10^{-2}$ m

Substituting the values for various distances, we have

$$C_n = \frac{4\pi \times 1 \times 8.85 \times 10^{-12} \times 10^6 \times 1000}{\ln\left[\frac{17 \times 65 \times 8 \times 6}{100 \times 8}\left(\frac{100}{0.865}\right)^3\right]^{1/3}} \ \mu\text{F/km}$$

$$= 0.0181 \ \mu\text{F/km}$$

$$\omega C_n = 314 \times 0.0181 \times 10^{-6}$$

$$= 5.68 \times 10^{-6} \ \Omega\text{/km}$$

$$\text{Charging current/phase} = \frac{110 \times 1000}{\sqrt{3}} \times 5.68 \times 10^{-6} = 0.361 \text{ A/km}$$

$$\therefore \quad \text{Charging current/conductor} = \frac{0.361}{2} = 0.1805 \text{ A/km}$$

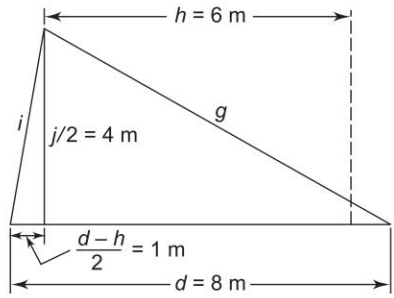

Fig. 3.12

3.8 METHOD OF GMD (MODIFIED)

A comparison of various expressions for inductance and capacitance of transmission lines [e.g. Eqs (2.22b) and (3.6)] brings out the fact that the two are similar except that in inductance expressions we have to use the fictitious conductor radius $r' = 0.7788r$, while in the expressions for capacitance actual conductor radius r is used. This fact suggests that the method of GDM would be applicable in the calculations for capacitance as well provided it is modified by using the outer conductor radius for finding D_s, the self geometric mean distance.

Example 3.3 can be conveniently solved as under by using the modified GMD method.

For the first section of the transposition cycle mutual GMD is

$$D_{ab} = ((ig)\ (ig))^{1/4} = (ig)^{1/2}$$
$$D_{bc} = (ig)^{1/2}$$
$$D_{ca} = (jh)^{1/2}$$
$$\therefore \quad D_{eq} = (D_{ab}D_{bc}D_{ca})^{1/3} = [(i^2g^2jh)^{1/3}]^{1/2}$$

In the first section of the transposition cycle, self GMD is

$$D_{sa} = (rf\ rf)^{1/4} = (rf)^{1/2}$$
$$D_{sb} = (rd)^{1/2}$$
$$D_{sc} = (rf)^{1/2}$$
$$D_s = (D_{sa}D_{sb}D_{sc})^{1/3} = [(r^3f^2d)^{1/3}]^{1/2}$$

Now
$$C_n = \frac{2\pi k}{\ln \dfrac{D_{eq}}{D_s}} = \frac{2\pi k}{\ln \left[\left(\dfrac{i^2g^2jh}{r^3f^2d}\right)^{1/3}\right]^{1/2}}$$

$$= \frac{4\pi k}{\ln \left(\dfrac{i^2g^2jh}{r^3f^2d}\right)^{1/3}} \text{ F/m}$$

This result obviously checks with the fundamentally derived expression in Example 3.3.

3.9 BUNDLED CONDUCTORS

A bundled conductor line is shown in Fig. 3.13. The conductors of any one bundle are in parallel, and it is assumed that the charge per bundle divides equally among the conductors of the bundle as $D_{12} >> d$. Also $D_{12} - d \approx D_{12} + d \approx D_{12}$ for the same reason. The results obtained with these assumptions are fairly accurate for usual spacings. Thus if the charge on phase a is q_a, the conductors a and a' have a charge of $q_a/2$ each; similarly the charge is equally divided for phases b and c.

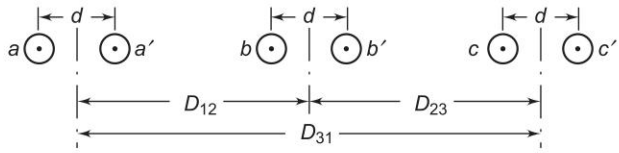

Fig. 3.13 Cross-section of a bundled conductor three-phase transmission line

Now, writing an equation for the voltage from conductor *a* to conductor *b*, we get

$$V_{ab} = \frac{1}{2\pi k}\left[0.5q_a\left(\ln\frac{D_{12}}{r} + \ln\frac{D_{12}}{d}\right) + 0.5q_b\left(\ln\frac{r}{D_{12}} + \ln\frac{d}{D_{12}}\right) + 0.5q_c\left(\ln\frac{D_{23}}{D_{31}} + \ln\frac{D_{23}}{D_{31}}\right)\right] \tag{3.38}$$

or

$$V_{ab} = \frac{1}{2\pi k}\left(q_a \ln\frac{D_{12}}{\sqrt{rd}} + q_b \ln\frac{\sqrt{rd}}{D_{12}} + q_c \ln\frac{D_{23}}{D_{31}}\right) \tag{3.39}$$

Considering the line to be transposed and proceeding in the usual manner, the final result will be

$$C_n = \frac{0.0242}{\log\left(D_{eq}/\sqrt{rd}\right)} \ \mu\text{F/km to neutral} \tag{3.40}$$

where $D_{eq} = (D_{12}D_{23}D_{31})^{1/3}$

It is obvious from Eq. (2.42) that the method of modified GMD is equally valid in this case (as it should be).

3.10 ELECTROSTATIC INDUCTION

Transmission lines as mentioned in Ch. 2, establish both magnetic and electric fields. The electric field also affects the objects that lie in the proximity of the line. Electric fields, related to the voltage of the line, are the main cause of induction to vehicles, buildings and objects of comparable size. The human body is affected adversely by the electric discharges. It has been observed that the current densities in human bodies induced by electric fields are much higher than those induced by magnetic fields.

3.11 SUMMARY

In this chapter the main shunt parameter of transmission namely capacitance has been thoroughly discussed including the effect of earth and bundled conductors and electrostatic induction is finally dealt with.

Problems

3.1 Derive an expression for the charge (complex) value per metre length of conductor *a* of an untransposed three-phase line shown in Fig. P-3.1. The applied voltage is balanced three-phase, 50 Hz. Take the voltage of phase *a* as reference phasor. All conductors have the same radii. Also find the charging current of phase *a*. Neglect the effect of ground.

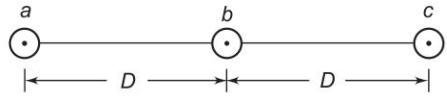

Fig. P-3.1

3.2 A three-phase double-circuit line is shown in Fig. P-3.2. The diameter of each conductor is 2.0 cm. The line is transposed and carries balanced load. Find the capacitance per phase to neutral of the line.

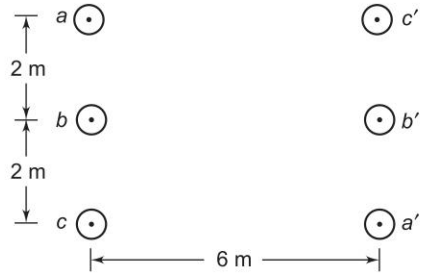

Fig. P-3.2

3.3 A three-phase, 50 Hz overhead line has regularly transposed conductors equilaterally spaced 4 m apart. The capacitance of such a line is 0.01 μF/km. Recalculate the capacitance per kilometre to neutral when the conductors are in the same horizontal plane with successive spacing of 4 m and are regularly transposed.

3.4 Consider the 500 kV, three-phase bundled conductor line as shown in Fig. P-2.9. Find the capacitive reactance to neutral in ohms/km at 50 Hz.

3.5 A three-phase transmission line has flat, horizontal spacing with 2 m between adjacent conductors. The radius of each conductor is 0.25 cm. At a certain instant the charges on the centre conductor and on one of the outside conductors are identical and voltage drop between these identically charged conductors is 775 V. Neglect the effect of ground, and find the value of the identical charge in coulomb/km at the instant specified.

3.6 Find the 50 Hz susceptance to neutral per kilometre of a double-circuit three phase line with transposition as shown in Fig. P-3.6. Given D = 7m and radius of each of the six conductors is 1.38 cm.

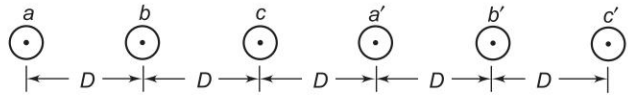

Fig. P-3.6 Double circuit three-phase line with flat spacing

3.7 A single conductor power cable has a conductor of No. 2 solid copper (radius = 0.328 cm). Paper insulation separating the conductor from the concentric lead sheath has a thickness of 2.5 mm and a relative permittivity of 3.8. The thickness of the lead sheath is 2 mm. Find the capacitive reactance per kilometre between the inner conductor and the lead sheath.

3.8 Find the capacitance of phase to neutral per kilometre of a three-phase line having conductors of 2 cm diameter placed at the corners of a triangle with sides 5 m, 6 m and 7 m respectively. Assume that the line is fully transposed and carries balanced load.

3.9 Derive an expression for the capacitance per metre length between two long parallel conductors, each of radius,*r*, with axes separated by a distance *D*, where $D \gg r$, the insulating medium being air. Calculate the maximum potential difference permissible between the conductors, if the electric field strength between them is not to exceed 25 kV/cm, *r* being 0.3 cm and $D = 35$ cm.

References

Books

1. Stevenson, W.D., *Elements of Power System Analysis*, 4th edn, McGraw-Hill, New York, 1982.
2. Cotton, H. and H. Barber, *The Transmission and Distribution of Electrical Energy*, 3rd edn, Hodder and Stoughton, 1970.
3. Starr, A.T., *Generation*, *Transmission and Utilization of Electric Power*, Pitman, 1962.

Papers

4. Parton, J.E. and A. Wright, "Electric Stresses Associated with Bundle Conductors", *International Journal of Electrical Engineering Education,* 1965, 3 : 357.
5. Stevens, R.A. and D.M. German, "The Capacitance and Inductance of Overhead Transmission Lines", *ibid*, 2 : 71.

Chapter 4

Representation of Power System Components

4.1 INTRODUCTION

A complete diagram of a power system representing all the three phases becomes too complicated for a system of practical size, so much so that it may no longer convey the information it is intended to convey. It is much more practical to represent a power system by means of simple symbols for each component resulting in what is called *a one-line diagram*.

Per unit system leads to great simplification of three-phase networks involving transformers. An impedance diagram drawn on a per unit basis does not require ideal transformers to be included in it.

An important element of a power system is the synchronous machine, which greatly influences the system behaviour during both steady state and transient conditions. The synchronous machine model in steady state is presented in this chapter. The transient model of the machine will be presented in Ch. 9.

4.2 SINGLE-PHASE REPRESENTATION OF BALANCED THREE-PHASE NETWORKS

The solution of a three-phase network under balanced conditions is easily carried out by solving the single-phase network corresponding to the reference phase. Figure 4.1 shows a simple, balanced three-phase network. The generator and load neutrals are therefore at the same potential, so that $I_n = 0$. Thus the neutral impedance Z_n does not affect network behaviour. For the reference phase a

$$E_a = (Z_G + Z_L)I_a \tag{4.1}$$

The currents and voltages in the other phases have the same magnitude but are progressively shifted in phase by 120º. Equation (4.1) corresponds to the single-phase network of Fig. 4.2 whose solution completely determines the solution of the three-phase network.

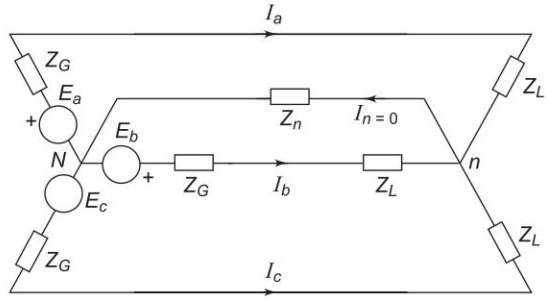

Fig. 4.1 Balanced three-phase network

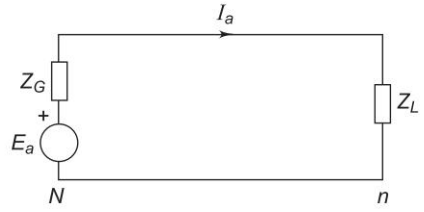

Fig. 4.2 Single-phase equivalent of a balanced three-phase network of Fig. 4.1

Consider now the case where a three-phase transformer forms part of a three-phase system. If the transformer is *Y*/*Y* connected as shown in Fig. 4.3(a), in the single-phase equivalent of the three-phase circuit it can be obviously represented by a single-phase transformer (as in Fig. 4.3(b)) with primary and secondary pertaining to phase *a* of the three-phase transformer.

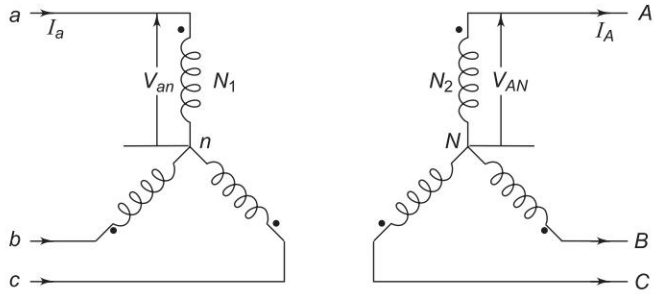

(a) Three-phase *Y*/*Y* transformer

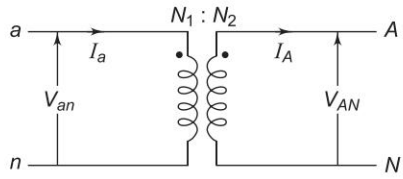

(b) Single-phase representation of three-phase *Y*/*Y* transformer

Fig. 4.3

If the transformer is Y/Δ connected as in Fig. 4.4(a), the delta side has to be replaced by an equivalent star connection as shown dotted so as to obtain the single-phase equivalent of Fig. 4.4(b). An important fact has, however, to be observed here. On the delta side the voltage to neutral V_{AN} and line current I_A have a certain phase angle shift* from the star side values V_{an} and I_a (90º for the phase labelling shown). In the single-phase equivalent (V_{AN}, I_A) are respectively in phase with (V_{an}, I_a). Since both phase voltage and line current shift through the same phase angle from star to delta side, the transformer per phase impedance and power flow are preserved in the single-phase equivalent. In most analytical studies, we are merely interested in the magnitude of voltages and currents so that the single-phase equivalent of Fig. 4.4(b) is an acceptable proposition. Wherever proper phase angles of currents and voltages are needed, correction can be easily applied after obtaining the solution through a single-phase transformer equivalent.

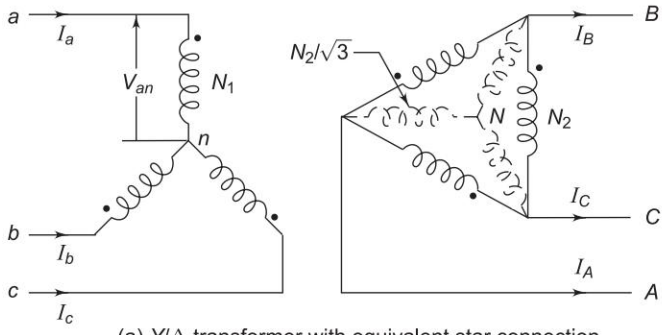

(a) Y/Δ transformer with equivalent star connection

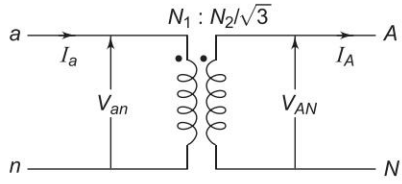

(b) Single-phase equivalent of Y/Δ transformer

Fig. 4.4

It may be noted here that irrespective of the type of connection, the transformation ratio of the single-phase equivalent of a three-phase transformer is the same as the line-to-line transformation ratio.

4.3 THE ONE-LINE DIAGRAM AND THE IMPEDANCE OR REACTANCE DIAGRAM

A one-line diagram of a power system shows the main connections and arrangements of components. Any particular component may or may not be

* See Sec. 10.3.

shown depending on the information required in a system study, e.g. circuit breakers need not be shown in a load flow study but are a must for a protection study. Power system networks are represented by one-line diagrams using suitable symbols for generators, motors, transformers and loads. It is a convenient practical way of network representation rather than drawing the actual three-phase diagram which may indeed be quite cumbersome and confusing for a practical size power network. Generator and transformer connections—star, delta, and neutral grounding are indicated by symbols drawn by the side of the representation of these elements. Circuit breakers are represented as rectangular blocks. Figure 4.5 shows the one-line diagram of a simple power system. The reactance data of the elements are given below the diagram.

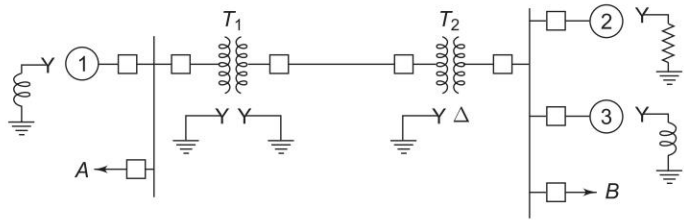

Fig. 4.5 One-line representation of a simple power system

Generator No. 1	30 MVA,	10.5 kV,	$X'' = 1.6$ ohms
Generator No. 2	15 MVA,	6.6 kV,	$X'' = 1.2$ ohms
Generator No. 3	25 MVA,	6.6 kV,	$X'' = 0.56$ ohms
Transformer T_1 (3 phase)	15 MVA,	33/11 kV,	$X = 15.2$ ohms per phase on high tension side
Transformer T_2	15 MVA, (3 phase)	33/6.2 kV,	$X = 16$ ohms per phase on high tension side
Transmission line	20.5 ohms/phase		
Load *A*	40 MW,	11 kV,	0.9 lagging power factor
Load *B*	40 MW,	6.6 kV,	0.85 lagging power factor

Note: Generators are specified in three-phase MVA, line-to-line voltage and per phase reactance (equivalent star). Transformers are specified in three-phase MVA, line-to-line transformation ratio, and per phase (equivalent star) impedance on one side. Loads are specified in three-phase MW, line-to-line voltage and power factor.

The impedance diagram on single-phase basis for use under balanced operating conditions can be easily drawn from the one-line diagram. For the system of Fig. 4.5 the impedance diagram is drawn in Fig. 4.6. Single-phase transformer equivalents are shown as ideal transformers with transformer impedances indicated on the appropriate side. Magnetizing reactances of the transformers have been neglected. This is a fairly good approximation for most power system studies. The generators are represented as voltage sources with series resistance and inductive reactance (synchronous machine model will be discussed in Sec. 4.6). The transmission line is represented by a π-model (to be

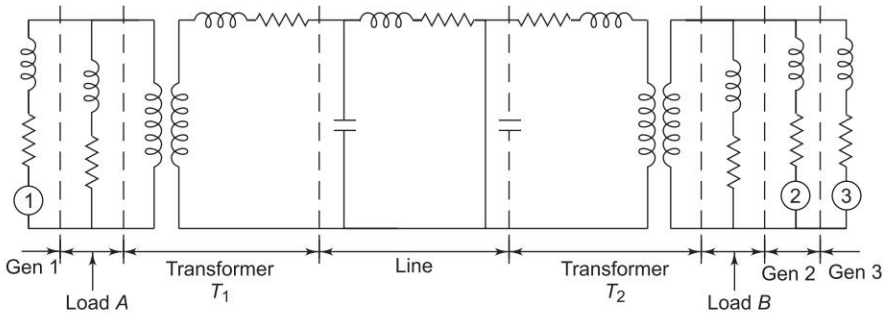

Fig. 4.6 Impedance diagram of the power system of Fig. 4.5

discussed in Ch. 5). Loads are assumed to be passive (not involving rotating machines) and are represented by resistance and inductive reactance in series. Neutral grounding impedances do not appear in the diagram as balanced conditions are assumed.

Three voltage levels (6.6, 11 and 33 kV) are present in this system. The analysis would proceed by transforming all voltages and impedances to any selected voltage level, say that of the transmission line (33 kV). The voltages of generators are transformed in the ratio of transformation and all impedances by the square of ratio of transformation. This is a very cumbersome procedure for a large network with several voltage levels. The per unit method discussed in the next section is the most convenient for power system analysis and will be used throughout this book.

4.4 PER UNIT (PU) SYSTEM

It is usual to express voltage, current, voltamperes and impedance of an electrical circuit in per unit (or percentage) of base or reference values of these quantities. The per unit* value of any quantity is defined as:

$$\frac{\text{the actual value in any units}}{\text{the base or reference value in the same units}}$$

The per unit method is particularly convenient in power systems as the various sections of a power system are connected through transformers and have different voltage levels.

Consider first a single-phase system. Let

Base voltamperes = $(\text{VA})_B$

Base voltage = V_B V

* Per cent value = per unit value × 100.
Per cent value is not convenient for use as the factor of 100 has to be carried in computations.

Then

$$\text{Base current } I_B = \frac{(\text{VA})_B}{V_B} \quad \text{A} \tag{4.2a}$$

$$\text{Base impedance } Z_B = \frac{V_B}{I_B} = \frac{V_B^2}{(\text{VA})_B} \quad \text{ohms} \tag{4.2b}$$

If the actual impedance is Z (ohms), its per unit value is given by

$$Z(\text{pu}) = \frac{Z}{Z_B} = \frac{Z(\text{ohms}) \times (\text{VA})_B}{V_B^2} \tag{4.3}$$

For a power system, practical choice of base values are:

Base megavoltamperes = $(\text{MVA})_B$

or

Base kilovoltamperes = $(\text{kVA})_B$

Base kilovolts = $(\text{kV})_B$

$$\text{Base current } I_B = \frac{1000 \times (\text{MVA})_B}{(\text{kV})_B} = \frac{(\text{kVA})_B}{(\text{kV})_B} \quad \text{A} \tag{4.4}$$

$$\text{Base impedance } Z_B = \frac{1000 \times (\text{kV})_B}{I_B}$$

$$= \frac{(\text{kV})_B^2}{(\text{MVA})_B} = \frac{1000 \times (\text{kV})_B^2}{(\text{kVA})_B} \quad \text{ohms} \tag{4.5}$$

$$\text{Per unit impedance } Z \text{ (pu)} = \frac{Z \text{ (ohms)} \times (\text{MVA})_B}{(\text{kV})_B^2} \tag{4.6}$$

$$= \frac{Z(\text{ohms}) \times (\text{kVA})_B}{(\text{kV})_B^2 \times 1000}$$

In a three-phase system rather than obtaining the per unit values using per phase base quantities, the per unit values can be obtained directly by using three-phase base quantities. Let

Three-phase base megavoltamperes = $(\text{MVA})_B$

Line-to-line base kilovolts = $(\text{kV})_B$

Assuming star connection (equivalent star can always be found),

$$\text{Base current } I_B = \frac{1000 \times (\text{MVA})_B}{\sqrt{3}(\text{kV})_B} \quad \text{A} \tag{4.7}$$

$$\text{Base impedance } Z_B = \frac{1000 \times (\text{kV})_B}{\sqrt{3}\, I_B} \quad \text{ohms}$$

$$= \frac{(\text{kV})_B^2}{(\text{MVA})_B} = \frac{1000 \times (\text{kV})_B^2}{(\text{kVA})_B} \text{ ohms} \quad (4.8)$$

$$\text{Per unit impedance } Z\,(\text{pu}) = \frac{Z\,(\text{ohms}) \times (\text{MVA})_B}{(\text{kV})_B^2} \quad (4.9)$$

$$= \frac{Z\,(\text{ohms}) \times (\text{kVA})_B}{(\text{kV})_B^2 \times 1{,}000}$$

When MVA base is changed from $(\text{MVA})_{B,\text{ old}}$ to $(\text{MVA})_{B,\text{ new,}}$ and kV base is changed from $(\text{kV})_{B,\text{ old}}$, to $(\text{kV})_{B,\text{ new}}$, the new per unit impedance from Eq. (4.9) is given by

$$Z\,(\text{pu})_{\text{new}} = Z\,(\text{pu})_{\text{old}} \times \frac{(\text{MVA})_{B,\text{ new}}}{(\text{MVA})_{B,\text{ old}}} \times \frac{(\text{kV})_{B,\text{old}}^2}{(\text{kV})_{B,\text{ new}}^2} \quad (4.10)$$

Per Unit Representation of a Transformer

It has been said in Sec. 4.2 that a three-phase transformer forming part of a three-phase system can be represented by a single-phase transformer in obtaining per phase solution of the system. The delta connected winding of the transformer is replaced by an equivalent star so that the transformation ratio of the equivalent single-phase transformer is always the line-to-line voltage ratio of the three-phase transformer.

Figure 4.7(a) represents a single-phase transformer in terms of primary and secondary leakage reactances Z_p and Z_s and an ideal transformer of ratio 1:a. The magnetizing impedance is neglected. Let us choose a voltampere base of $(\text{VA})_B$ and voltage bases on the two sides of the transformer in the ratio of transformation, i.e.

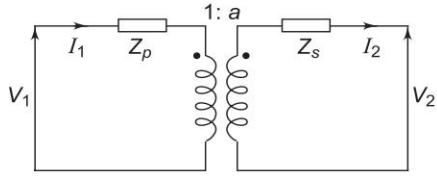

(a) Representation of single-phase transformer (magnetizing impedance neglected)

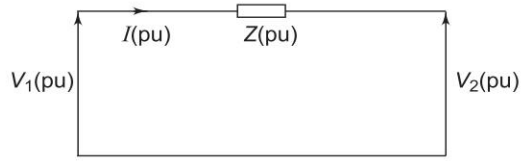

(b) Per unit equivalent circuit of single-phase transformer

Fig. 4.7

$$\frac{V_{1B}}{V_{2B}} = \frac{1}{a} \tag{4.11a}$$

Therefore, $$\frac{V_{1B}}{V_{2B}} = a \text{ (as } (VA)_B \text{ is common)} \tag{4.11b}$$

$$Z_{1B} = \frac{V_{1B}}{I_{1B}},\ Z_{2B} = \frac{V_{2B}}{I_{2B}} \tag{4.11c}$$

From Fig. 4.7(a), we can write

$$V_2 = (V_1 - I_1 Z_p)\, a - I_2 Z_s \tag{4.12}$$

We shall convert Eq. (4.12) into per unit form

$$V_2(\text{pu}) V_{2B} = [V_1(\text{pu}) V_{1B} - I_1(\text{pu}) I_{1B} Z_p(\text{pu}) Z_{1B}]$$
$$a - I_2(\text{pu}) I_{2B} Z_s(\text{pu}) Z_{2B}$$

Dividing by V_{2B} throughout and using base relations (4.11a, b, c), we get

$$V_2(\text{pu}) = V_1(\text{pu}) - I_1(\text{pu}) Z_p(\text{pu}) - I_2(\text{pu}) Z_s(\text{pu}) \tag{4.13}$$

Now $$\frac{I_1}{I_2} = \frac{I_{1B}}{I_{2B}} = a$$

or $$\frac{I_1}{I_{1B}} = \frac{I_2}{I_{2B}}$$

$\therefore$ $$I_1(\text{pu}) = I_2(\text{pu}) = I\,(\text{pu})$$

Equation (4.13) can therefore be written as

$$V_2(\text{pu}) = V_1(\text{pu}) - I(\text{pu}) Z(\text{pu}) \tag{4.14}$$

where

$$Z(\text{pu}) = Z_p(\text{pu}) + Z_s(\text{pu})$$

Equation (4.14) can be represented by the simple equivalent circuit of Fig. 4.7(b) which does not require an ideal transformer. Considerable simplification has therefore been achieved by the per unit method with a common voltampere base and voltage bases on the two sides in the ratio of transformation.

Z(pu) can be determined directly from the equivalent impedance on primary or secondary side of a transformer by using the appropriate impedance base.

On primary side:

$$Z_1 = Z_p + Z_s/a^2$$

$$Z_1(\text{pu}) = \frac{Z_1}{Z_{1B}} = \frac{Z_p}{Z_{1B}} + \frac{Z_s}{Z_{1B}} \times \frac{1}{a^2}$$

But

$$a^2 Z_{1B} = Z_{2B}$$

$$\therefore \quad Z_1(\text{pu}) = Z_p(\text{pu}) + Z_s(\text{pu}) = Z(\text{pu}) \tag{4.15}$$

On secondary side:

$$Z_2 = Z_S + a^2 Z_p$$

$$Z_2(\text{pu}) = \frac{Z_2}{Z_{2B}} = \frac{Z_s}{Z_{2B}} + a^2 \frac{Z_p}{Z_{2B}}$$

or
$$Z_2(\text{pu}) = Z_s(\text{pu}) + Z_p(\text{pu}) = Z(\text{pu}) \tag{4.16}$$

Thus the per unit impedance of a transformer is the same whether computed from primary or secondary side so long as the voltage bases on the two sides are in the ratio of transformation (equivalent per phase ratio of a three-phase transformer which is the same as the ratio of line-to-line voltage rating).

The pu transformer impedance of a three-phase transformer is conveniently obtained by direct use of three-phase MVA base and line-to-line kV base in relation (4.9). Any other impedance on either side of a transformer is converted to pu value just like Z_p or Z_s.

Per Unit Impedance Diagram of a Power System

From a one-line diagram of a power system we can directly draw the impedance diagram by following the steps given below:

1. Choose an appropriate common MVA (or kVA) base for the system.
2. Consider the system to be divided into a number of sections by the transformers. Choose an appropriate kV base in one of the sections. Calculate kV bases of other sections in the ratio of transformation.
3. Calculate per unit values of voltages and impedances in each section and connect them up as per the topology of the one-line diagram. The result is the single-phase per unit impedance diagram.

The above steps are illustrated by the following examples.

Example 4.1 Obtain the per unit impedance (reactance) diagram of the power system of Fig. 4.5.

Solution

The per phase impedance diagram of the power system of Fig. 4.5 has been drawn in Fig. 4.6. We shall make some further simplifying assumptions.

1. Line capacitance and resistance are neglected so that it is represented as a series reactance only.
2. We shall assume that the impedance diagram is meant for short circuit studies. Current drawn by static loads under short circuit conditions can be neglected. Loads *A* and *B* are therefore ignored.

Let us convert all reactances to per unit form. Choose a common three-phase MVA base of 30 and a voltage base of 33 kV line-to-line on the transmission line. Then the voltage base in the circuit of generator 1 is 11 kV line-to-line and that in the circuits of generators 2 and 3 is 6.2 kV.

The per unit reactances of various components are calculated below:

Transmission line: $\dfrac{20.5 \times 30}{(33)^2} = 0.564$

Transformer T_1: $\dfrac{15.2 \times 30}{(33)^2} = 0.418$

Transformer T_2: $\dfrac{16 \times 30}{(33)^2} = 0.44$

Generator 1: $\dfrac{1.6 \times 30}{(11)^2} = 0.396$

Generator 2: $\dfrac{1.2 \times 30}{(6.2)^2} = 0.936$

Generator 3: $\dfrac{0.56 \times 30}{(6.2)^2} = 0.437$

The reactance diagram of the system is shown in Fig. 4.8.

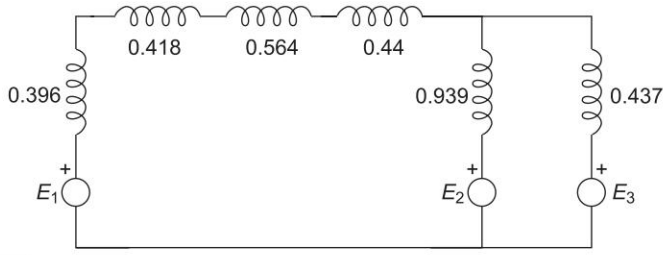

Fig. 4.8 Reactance diagram of the system of Fig. 4.5 (loads neglected)

E_1, E_2 and E_3 are per unit values of voltages to which the generators are excited. Quite often in a short circuit study, these will be taken as $1\angle 0^\circ$ pu (no load condition).

Example 4.2 The reactance data of generators and transformers is usually specified in pu (or per cent) values, based on equipment ratings rather than in actual ohmic values as given in Example 4.1; while the transmission line impedances may be given in actual values. Let us resolve Example 4.1 by assuming the following pu values of reactances

Transformer T_1:	0.209
Transformer T_2:	0.220
Generator G_1:	0.435
Generator G_2:	0.413
Generator G_3:	0.3214

With a base MVA of 30, base voltage of 11 kV in the circuit of generator 1 and base voltage of 6.2 kV in the circuit of generators 2 and 3 as used in

Example 4.1, we now calculate the pu values of the reactances of transformers and generators as per relation (4.10):

Transformer T_1: $$0.209 \times \frac{30}{15} = 0.418$$

Transformer T_2: $$0.22 \times \frac{30}{15} = 0.44$$

Generator 1: $$0.435 \times \frac{(10.5)^2}{(11)^2} = 0.396$$

Generator 2: $$0.413 \times \frac{30}{15} \times \frac{(6.6)^2}{(6.2)^2} = 0.936$$

Generator 3: $$0.3214 \times \frac{30}{25} \times \frac{(6.6)^2}{(6.2)^2} = 0.437$$

Obviously these values are the same as obtained already in Example 4.1.

4.5 COMPLEX POWER

Consider a single-phase load fed from a source as in Fig. 4.9. Let

$$V = |V| \angle \delta$$

$$I = |I| \angle (\delta - \theta)$$

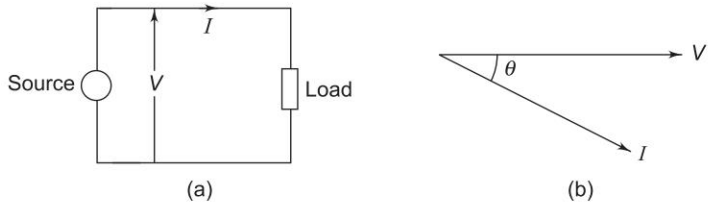

Fig. 4.9 Complex power flow in a single-phase load

When θ is positive, the current lags behind voltage. This is a convenient choice of sign of θ in power systems where loads have mostly lagging power factors.

Complex power flow in the direction of current indicated is given by

$$S = VI^*$$

$$= |V|\,|I| \angle \theta$$

$$= |V|\,|I| \cos\theta + j|V|\,|I| \sin\theta = P + jQ \qquad (4.17)$$

or

$$|S| = (P^2 + Q^2)^{1/2}$$

Here

S = complex power (VA, kVA, MVA)

$|S|$ = apparent power (VA, kVA, MVA); it signifies rating of equipments (generators, transformers)

$P = |V|\,|I| \cos\theta$ = real (active) power (watts, kW, MW)

$Q = |V|\,|I| \sin\theta$ = reactive power

= voltamperes reactive (VAR)

= kilovoltamperes reactive (kVAR)

= megavoltamperes reactive (MVAR)

It immediately follows from Eq. (4.17) that Q, the reactive power, is positive for lagging current (lagging power factor load) and negative for leading current (leading power factor load). With the direction of current indicated in Fig. 4.9, $S = P + jQ$ is supplied by the source and is absorbed by the load.

Equation (4.17) can be represented by the phasor diagram of Fig. 4.10 where

$$\theta = \tan^{-1}\frac{Q}{P} = \text{positive for lagging current} \qquad (4.18)$$

= negative for leading current

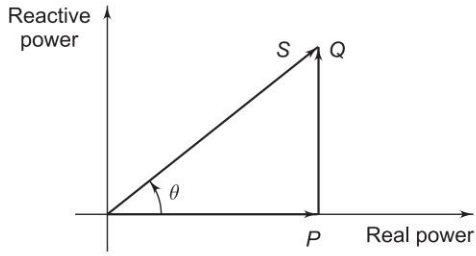

Fig. 4.10 Phasor representation of complex power (lagging pf load)

If two (or more) loads are in parallel as in Fig. 4.11

$$S = VI^* = V\left(I_1^* + I_2^*\right)$$

$$= VI_1^* + VI_2^*$$

$$= S_1 + S_2 = (P_1 + P_2) + j(Q_1 + Q_2) \qquad (4.19)$$

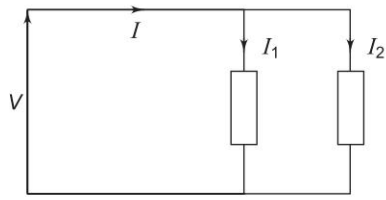

Fig. 4.11 Two loads in parallel

As per Eq. (4.19), Kirchhoff's current law applies to complex power (also applies separately to real and reactive powers).

In a series *RL* load carrying current *I*,

$$V = I(R + jX_L)$$

$$S = VI^* = I^2R + jI^2X_L$$

$\therefore$ $P = I^2R$ = active power absorbed by load

$Q = I^2X_L$ = reactive power absorbed by load

In case of a series *RC* load carrying current *I*,

$$P = I^2R$$

$$Q = -I^2X_C \text{ (reactive power absorbed is negative)}$$

Consider now a balanced three-phase load represented in the form of an equivalent star as shown in Fig. 4.12. The three-phase complex power fed into load is given by

$$S = 3V_P I_L^* = 3\,|V_P|\,\angle\delta_P I_L^* = \sqrt{3}\,|V_L|\,\angle\delta_P I_L^* \qquad (4.20)$$

if

$$I_L = |I_L|\,\angle(\delta_P - \theta)$$

then

$$S = \sqrt{3}\;|V_L|\,|I_L|\,\angle\theta$$

$$= \sqrt{3}\;|V_L|\,|I_L|\cos\theta + j\sqrt{3}\;|V_L|\,|I_L|\sin\theta = P + jQ \qquad (4.21)$$

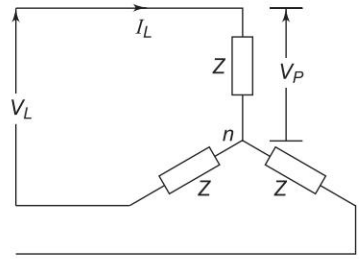

Fig. 4.12 Complex power fed to three-phase load

Here

$$|S| = \sqrt{3}\;|V_L|\,|I_L|$$

$$P = \sqrt{3}\;|V_L|\,|I_L|\cos\theta$$

$$Q = \sqrt{3}\;|V_L|\,|I_L|\sin\theta$$

where

θ = power factor angle

If V_L, the line voltage, is expressed in kV; and I_L, the line current in amperes, *S* is in kVA; and if the line current is in kiloamperes, *S* is in MVA.

In terms of load impedance *Z*,

$$I_L = \frac{V_P}{Z} = \frac{|V_L| \angle \delta_P}{\sqrt{3}Z}$$

Substituting for I_L in Eq. (4.20)

$$S = \frac{|V_L|^2}{Z^*} \tag{4.22a}$$

If V_L is in kV, S is now given in MVA. Load impedance Z if required can be calculated from

$$Z = \frac{|V_L|^2}{S^*} = \frac{|V_L|^2}{P - jQ} \tag{4.22b}$$

4.6 THE STEADY STATE MODEL OF SYNCHRONOUS MACHINE

The synchronous machine is the most important element of a power system. It converts mechanical power into electrical form and feeds it into the power network or, in the case of a motor, it draws electrical power from the network and converts it into the mechanical form. The machine excitation which is controllable determines the flow of VARs into or out of the machine. Books on electrical machines [1, 2, 4] may be consulted for a detailed account of the synchronous machine. We shall present here a simplified circuit model of the machine which with suitable modifications wherever necessary (under transient conditions) will be adopted throughout this book.

Figure 4.13 shows the schematic cross-sectional diagram of a three-phase synchronous generator (alternator) having a two pole structure. The stator has a balanced three-phase winding—aa', bb' and cc'. The winding shown is a concentrated one, while the winding in an actual machine is distributed across the stator periphery. The rotor shown is a cylindrical* one (round rotor or non-salient pole rotor) with rotor winding excited by the DC source. The rotor winding is so arranged on rotor periphery that the field excitation produces nearly sinusoidally distributed flux/pole (ϕ_f) in the air gap. As the rotor rotates, three-phase emfs are produced in stator winding. Since the machine is a balanced one and balanced loading will be considered, it can be modelled on per phase basis for the reference phase a.

In a machine with more than two poles, the above defined structure repeats electrically for every pair of poles. The frequency of induced emf is given by

$$f = \frac{NP}{120} \text{ Hz}$$

where

N = rotor speed (synchronous speed) in rpm
P = number of poles

* High-speed turbo-generators have cylindrical rotors and low-spped hydro-generators have salient pole rotors.

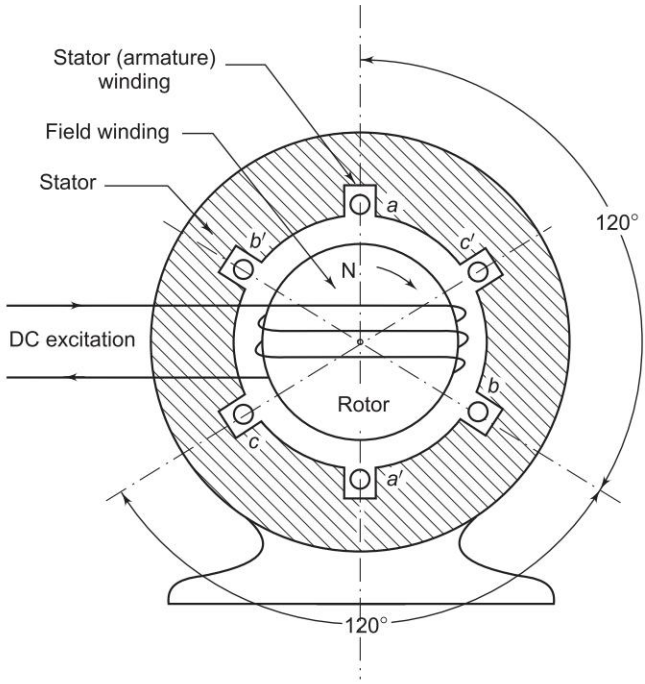

Fig. 4.13 Schematic diagram of a round rotor synchronous generator

On no load the voltage E_f induced in the reference phase a lags 90° behind ϕ_f which produces it and is proportional to ϕ_f if the magnetic circuit is assumed to be unsaturated. This phasor relationship is indicated in Fig. 4.14. Obviously the terminal voltage $V_t = E_f$.

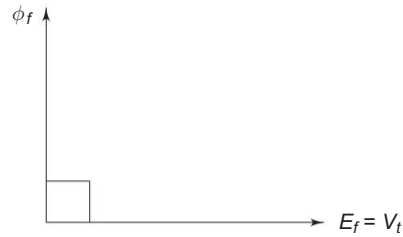

Fig. 4.14 Phasor relationship between ϕ_f and E_f

As balanced steady load is drawn from the three-phase stator winding, the stator currents produce synchronously rotating flux ϕ_a/pole (in the direction of rotation of the rotor). This flux, called *armature reaction* flux, is therefore stationary with respect to field flux ϕ_f. It intuitively follows that ϕ_a is in phase with phase a current I_a which causes it. Since the magnetic circuit has been assumed to be unsaturated, the superposition principle is applicable so that the resultant air gap flux is given by the phasor sum

$$\phi_r = \phi_f + \phi_a \tag{4.23}$$

Further assuming that the armature leakage reactance and resistance are negligible, ϕ_r induces the armature emf which equals the terminal voltage V_t. Phasor diagram under loaded (balanced) conditions showing fluxes, currents and voltages as phasors is drawn in Fig. 4.15.

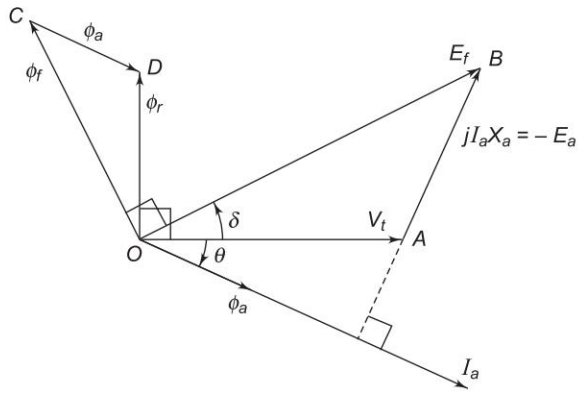

Fig. 4.15 Phasor diagram of synchronous generator

Here

θ = power factor angle

δ = angle by which E_f leads V_t called *load angle* or *torque angle*

We shall see in Sec. 5.10 that δ mainly determines the power delivered by the generator and the magnitude of E_f (i.e. excitation) determines the VARs delivered by it.

Because of the assumed linearity of the magnetic circuit, voltage phasors E_f, E_a and V_t are proportional to flux phasors ϕ_f, ϕ_a and ϕ_r, respectively; further, voltage phasors lag 90° behind flux phasors. It therefore easily follows from Fig. 4.15 that phasor $AB = -E_a$ is proportional to ϕ_a (and therefore I_a) and is 90° leading ϕ_a (or I_a). With the direction of phasor AB indicated on the diagram

$$AB = jI_aX_a$$

where X_a is the constant of proportionality.

In terms of the above definition of X_a, we can directly write the following expression for voltages without the need of invoking flux phasors.

$$V_t = E_f - jI_aX_a \tag{4.24}$$

where

E_f = voltage induced by field flux ϕ_f alone

= no load emf

The circuit model of Eq. (4.24) is drawn in Fig. 4.16 wherein X_a is interpreted as inductive reactance which accounts for the effect of armature reaction thereby avoiding the need of resorting to addition of fluxes [Eq.(4.23)].

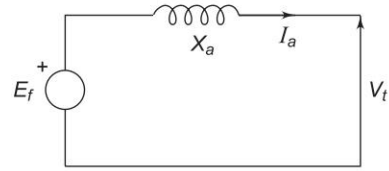

Fig. 4.16 Circuit model of round rotor synchronous generator (resistance and leakage reactance neglected)

The circuit of Fig. 4.16 can be easily modified to include

the effect of armature leakage reactance and resistance (these are series effects) to give the complete circuit model of the synchronous generator as in Fig. 4.17. The total reactance $(X_a + X_l) = X_s$ is called the *synchronous reactance* of the machine. Equation (4.24) now becomes

$$V_t = E_f - jI_a X_s - I_a R_a \tag{4.25}$$

This model of the synchronous machine can be further modified to account for the effect of magnetic saturation where the principle of superposition does not hold.

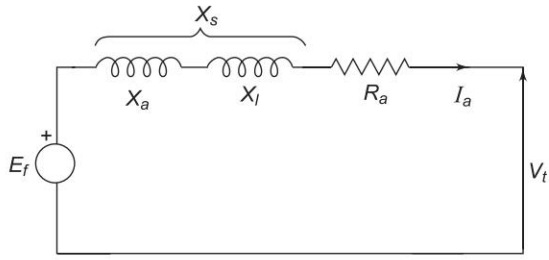

Fig. 4.17 Circuit model of round rotor synchronous generator

Armature resistance R_a is invariably neglected in power system studies. Therefore, in the place of the circuit model of Fig. 4.17, the simplified circuit model of Fig. 4.18 will be used throughout this book. The corresponding phasor diagram is given in Fig. 4.19. The field induced emf E_f leads the terminal voltage by the torque (load) angle δ. This, in fact, is the condition for active power to flow out of the generator. The magnitude of power delivered depends upon sin δ.

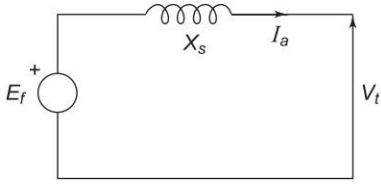

Fig. 4.18 Simplified circuit model of round rotor synchronous generator

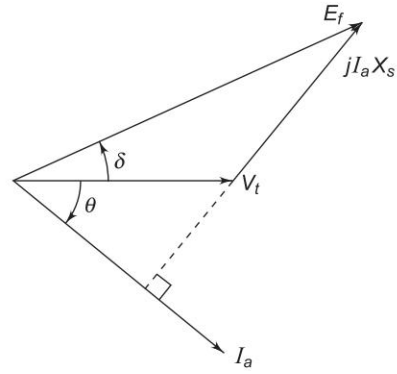

Fig. 4.19 Phasor diagram of synchronous generator

In the motoring operation of a synchronous machine, the current I_a reverses as shown in Fig. 4.20, so that Eq. (4.25) modifies to

$$E_f = V_t - jI_a X_s \tag{4.26}$$

which is represented by the phasor diagram of Fig. 4.21. It may be noted that V_t now leads E_f by δ. This in fact is the condition for power to flow into motor terminals.

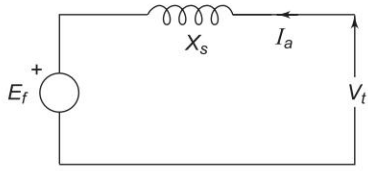

Fig. 4.20 Motoring operation of synchronous machine

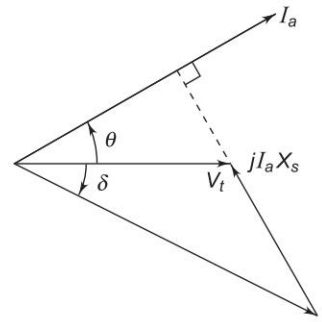

Fig. 4.21 Phasor diagram of motoring operation

The flow of reactive power and terminal voltage of a synchronous machine is mainly controlled by means of its excitation. This is discussed in detail in Sec. 5.10. Voltage and reactive power flow are often automatically regulated by voltage regulators (see Sec. 8.6) acting on the field circuits of generators and by automatic tap changing devices on transformers.

Normally, a synchronous generator operates in parallel with other generators connected to the power system. For simplicity of operation we shall consider a generator connected to an *infinite bus* as shown in Fig. 4.22. As infinite bus means a large system whose voltage and frequency remain constant independent of the power exchange between the synchronous machine and the bus, and independent of the excitation of the synchronous machine.

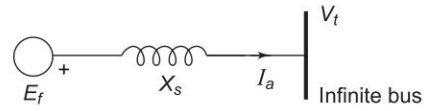

Fig. 4.22 Synchronous machine connected to infinite bus

Consider now a synchronous generator feeding constant active power into an infinite bus bar. As the machine excitation is varied, armature current I_a and its angle θ, i.e. power factor, change in such a manner as to keep

$$|V_t|\,|I_a| \cos\theta = \text{constant} = \text{active power output}$$

It means that since $|V_t|$ is fixed, the projection $|I_a| \cos\theta$ of the phasor I_a on V_t remains constant, while the excitation is varied. Phasor diagrams corresponding to high, medium and low excitations are presented in Fig. 4.23. The phasor diagram of Fig. 4.23(b) corresponds to the unity power factor case. It is obvious from the phasor diagram that for this excitation

$$|E_f| \cos\delta = |V_t|$$

This is defined as *normal excitation*. For the *overexcited* case (Fig. 4.23 (a)), i.e. $|E_f| \cos\delta > |V_t|$, I_a lags behind V_t so that the generator feeds positive reactive power into the bus (or draws negative reactive power from the bus). For the *underexcited* case (Fig. 4.23(c)), i.e. $|E_f| \cos\delta > |V_t|$, I_a leads V_t so that the generator feeds negative reactive power into the bus (or draws positive reactive power from the bus).

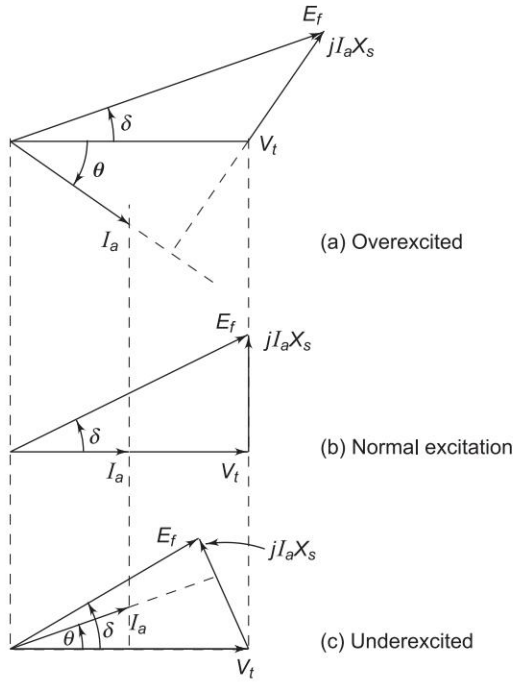

Fig. 4.23 Phasor diagrams of synchronous generator feeding constant power as excitation is varied

Figure 4.24 shows the overexcited and underexcited cases of synchronous motor (connected to infinite bus) with constant power drawn from the infinite bus. In the overexcited case, I_a leads V_t, i.e. the motor draws negative reactive power (or supplies positive reactive power); while in the underexcited case I_a lags V_t, i.e. the motor draws positive reactive power (or supplies negative reactive power).

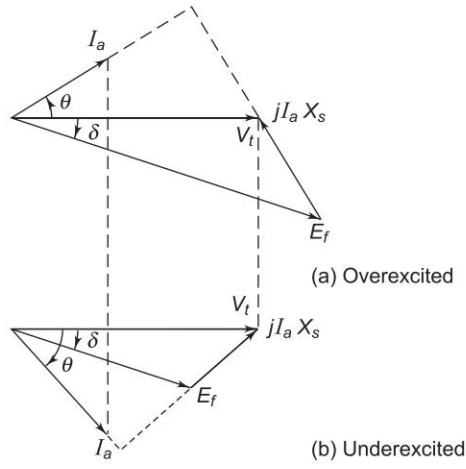

Fig. 4.24 Phasor diagrams of synchronous motor drawing constant power as excitation is varied

From the above discussion we can draw the general conclusion that a synchronous machine (generating or motoring) while operating at constant power supplies positive reactive power into the bus bar (or draws negative reactive power from the bus bar) when overexcited. An underexcited machine, on the other hand, feeds negative reactive power into the bus bar (or draws positive reactive power from the bus bar).

Consider now the power delivered by a synchronous generator to an infinite bus. From Fig. 4.19 this power is

$$P = |V_t|\,|I_a| \cos\theta$$

The above expression can be written in a more useful form from the phasor geometry. From Fig. 4.19

$$\frac{|E_f|}{\sin(90^\circ + \theta)} = \frac{|I_a| X_s}{\sin\delta}$$

or

$$|I_a| \cos\theta = \frac{|E_f|}{X_s} \sin\delta \tag{4.27}$$

$$\therefore \quad P = \frac{|E_f|\,|V_t|}{X_s} \sin\delta \tag{4.28}$$

The plot of P versus δ, shown in Fig. 4.25, is called the *power angle curve*. The maximum power that can be delivered occurs at $\delta = 90^\circ$ and is given by

$$P_{max} = \frac{|E_f|\,|V_t|}{X_s} \tag{4.29}$$

For $P > P_{max}$ or for $\delta > 90^\circ$ the generator will have stability problem. This problem (the stability) will be discussed at length in Ch. 12.

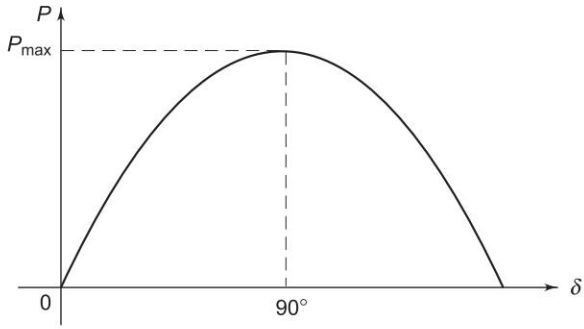

Fig. 4.25 Power angle curve of a synchronous generator

Power Factor and Power Control

While Figs 4.23 and 4.24 illustrate how a synchronous machine power factor changes with excitation for fixed power exchange, these do not give us a clue regarding the quantitative values of $|I_a|$ and δ. This can easily be accomplished by recognizing from Eq. (4.27) that

$$|E_f| \sin \delta = |I_a| X_s \cos \theta$$

$$= \frac{PX_s}{|V_t|} = \text{constant (for constant exchange of power to infinite bus bar)} \qquad (4.30)$$

Figure 4.26 shows the phasor diagram for a generator delivering constant power to infinite bus but with varying excitation. As $|E_f| \sin \delta$ remains constant, the tip of phasor E_f moves along a line parallel to V_t as excitation is varied. The direction of phasor I_a is always 90° lagging jI_aX_s and its magnitude is obtained from $(|I_a|X_s)/X_s$. Figure 4.27 shows the case of limiting excitation with $\delta = 90°$. For excitation lower than this value the generator becomes unstable.

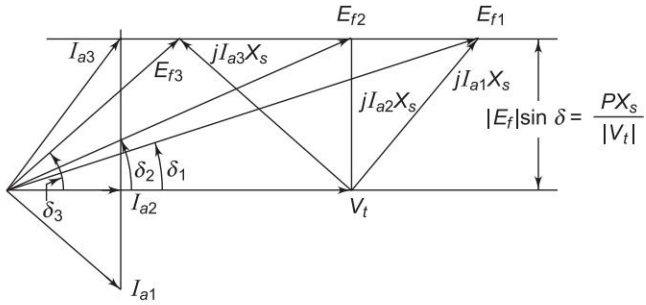

Fig. 4.26 Effect of varying excitation of generator delivering constant power to infinite bus bar

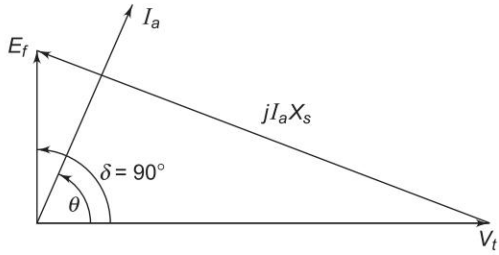

Fig. 4.27 Case of limiting excitation of generator delivering constant power to infinite bus bar

Similar phasor diagrams can be drawn for synchronous motor as well for constant input power (or constant load if copper and iron losses are neglected and mechanical loss is combined with load).

Another important operating condition is variable power and fixed excitation. In this case $|V_t|$ and $|E_f|$ are fixed, while δ and active power vary in accordance with Eq. (4.28). The corresponding phasor diagram for two values of δ is shown in Fig. 4.28. It is seen from this diagram that as δ increases, current magnitude increases and power factor improves. It will be shown in Sec. 5.10 that as δ changes, there is no significant change in the flow of reactive power.

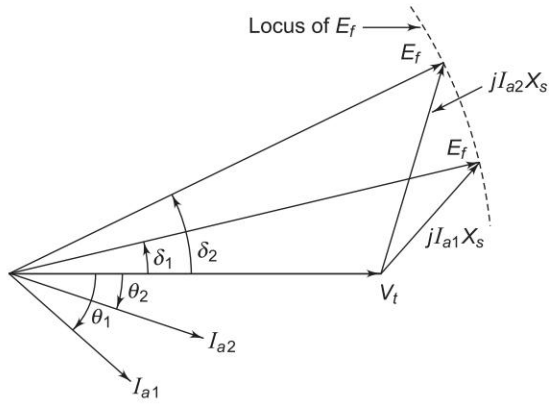

Fig. 4.28 Operation of synchronous generator with variable power and fixed excitation

Salient Pole Synchronous Generator

A salient pole synchronous machine, as shown in Fig. 4.29, is distinguished from a round rotor machine by constructional features of field poles which project with a large interpolar air gap. This type of construction is commonly employed in machines coupled to hydroelectric turbines which are inherently slow-speed ones so that the synchronous machine has multiple pole pairs as different from machines coupled to high-speed steam turbines (3,000/1,500 rpm) which have a two- or four-pole structure. Salient pole machine analysis is made through the *two-reaction theory* outlined below.

In a round rotor machine, armature current in phase with field induced emf E_f or in quadrature (at 90°) to E_f, produces the same flux linkages per ampere as the air gap is uniform so that the armature reaction reactance offered to in-phase or quadrature current is the same ($X_a + X_l = X_s$). In a salient pole machine, air gap is non-uniform along rotor periphery. It is the least along the axis of main poles (called *direct axis*) and is the largest along the axis of the interpolar region (called *quadrature axis*). Armature current in quadrature with E_f produces flux along the direct axis and the reluctance of flux path being low (because of small air gap), it produces larger flux linkages per ampere and hence the machine presents larger armature reaction reactance X_d (called direct axis reactance) to the flow of quadrature component I_d of armature current I_a.

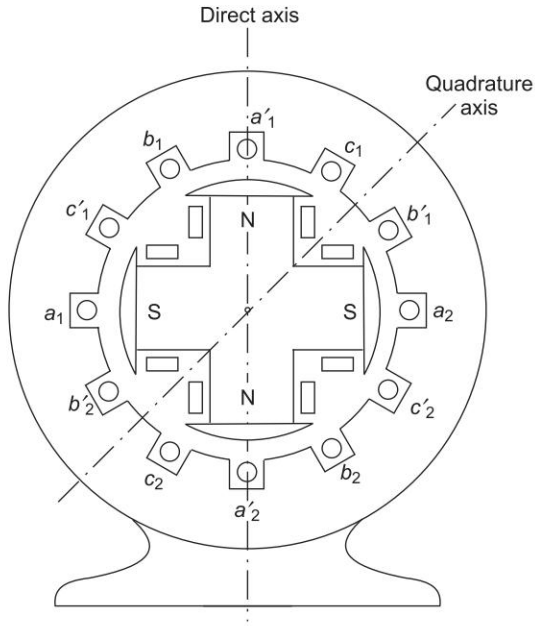

Fig. 4.29 Salient pole synchronous machine (4-pole structure)

On the other hand, armature current in phase with E_f produces flux along the quadrature axis and the reluctance of the flux path being high (because of large interpolar air gap), it produces smaller flux linkages per ampere and hence the machine presents smaller armature reaction reactance X_q (quadrature axis reactance $< X_d$) to the flow of in-phase component I_q of armature current I_a.

Since a salient pole machine offers different reactances to the flow of I_d and I_q components of armature current I_a, a circuit model cannot be drawn. The phasor diagram of a salient pole generator is shown in Fig. 4.30. It can be easily drawn by following the steps given below:

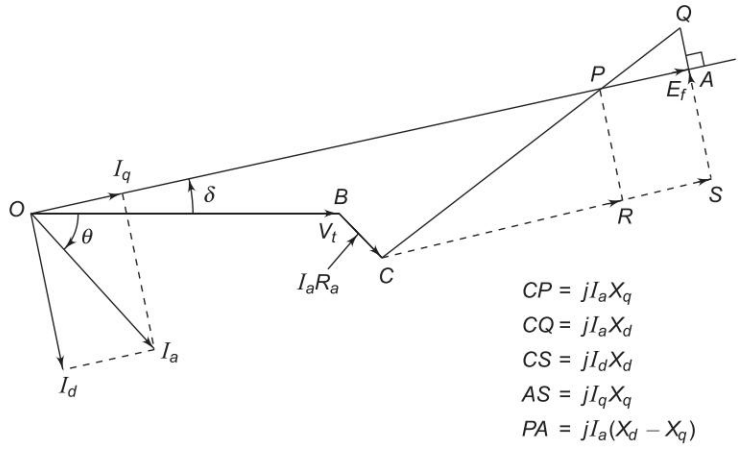

Fig. 4.30 Phasor diagram of salient pole synchronous generator

1. Draw V_t and I_a at angle θ.
2. Draw $I_a R_a$. Draw $CQ = jI_a X_d$($\perp$ to I_a).
3. Make $|CP| = |I_a| X_q$ and draw the line OP which gives the direction of E_f phasor.
4. Draw a $\perp$ from Q to the extended line OP such that $OA = E_f$.

It can be shown by the above theory that the power output of a salient pole generator is given by

$$P = \frac{|V_t||E_f|}{X_d} \sin\delta + \frac{|V_t|^2 (X_d - X_q)}{2X_d X_q} \sin 2\delta \qquad (4.31)$$

The first term is the same as for a round rotor machine with $X_s = X_d$ and constitutes the major part in power transfer. The second term is quite small (about 10–20%) compared to the first term and is known as *reluctance power.*

P versus δ is plotted in Fig. 4.31. It is noticed that the maximum power output occurs at $\delta < 90°$ (about 70°). Further $\frac{dP}{d\delta}$ (change in power per unit change in power angle for small changes in power angle), called the *synchronizing power coefficient*, in the operating region ($\delta < 70°$) is larger in a salient pole machine than in a round rotor machine.

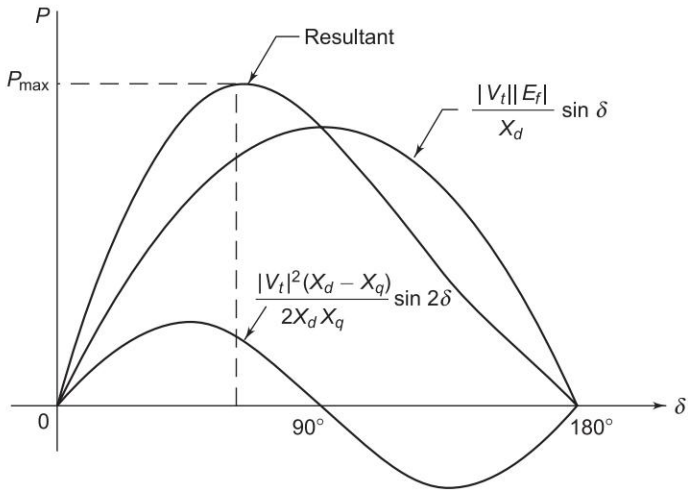

Fig. 4.31 Power angle curve for salient pole generator

In this book we shall neglect the effect of saliency and take

$$X_s = X_d$$

in all types of power system studies considered.

During a machine transient, the direct axis reactance changes with time acquiring the following distinct values during the complete transient.

X''_d = subtransient direct axis reactance
X'_d = transient direct axis reactance
X_d = steady state direct axis reactance

The significance and use of these three values of direct axis reactance will be elaborated in Ch. 9.

Operating Chart of a Synchronous Generator

While selecting a large generator, besides rated MVA and power factor, the greatest allowable stator and rotor currents must also be considered as they influence mechanical stresses and temperature rise. Such limiting parameters in the operation are brought out by means of an *operating chart* or *performance chart*.

For simplicity of analysis, the saturation effects, saliency, and resistance are ignored and an unsaturated value of synchronous reactance is considered. Consider Fig. 4.32, the phasor diagram of a cylindrical rotor machine. The locus of constant $|I_a|X_s$,$|I_a|$ and hence MVA is a circle centered at M. The locus of constant $|E_f|$ (excitation) is also a circle centered at O. As MP is proportional to MVA,QP is proportional to MVAR and MQ to MW, all to the same scale which is obtained as follows.

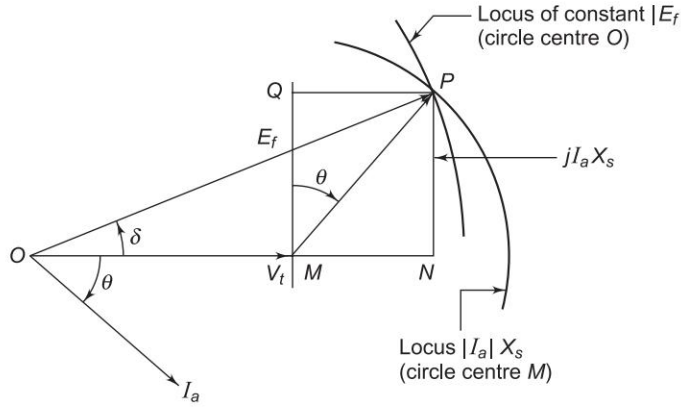

Fig. 4.32 Phasor diagram of synchronous generator

For zero excitation, i.e. $|E_f| = 0$

$$-jI_aX_s = V_t$$

or

$$I_a = jV_t/X_s$$

i.e. $|I_a| = |V_t|/X_s$ leading at 90° to OM which corresponds to VARs/phase.

Consider now the chart shown in Fig. 4.33 which is drawn for a synchronous machine having X_s = 1.43 pu. For zero excitation, the current is 1.0/1.43 = 0.7 pu, so that the length MO corresponds to reactive power of 0.7 pu, fixing both active and reactive power scales.

With centre at O, a number of semicircles are drawn with radii equal to different pu MVA loadings. Circles of per unit excitation are drawn from centre M with 1.0 pu excitation corresponding to the fixed terminal voltage OM. Lines may also be drawn from O corresponding to various power factors but for clarity only 0.85 pf lagging line is shown. The operational limits are fixed as follows.

Taking 1.0 per unit active power as the maximum allowable power, a horizontal limit-line abc is drawn through b at 1.0 pu. It is assumed that the machine is rated to give 1.0 pu unit active power at power factor 0.85 lagging and this fixes point c. Limitation of the stator current to the corresponding value requires the limit-line to become a circular arc cd about centre O. At point d the rotor heating becomes more important and the arc de is fixed by the maximum excitation current allowable, in this case assumed to be $|E_f| = 2.40$ pu (i.e. 2.4 times $|V_t|$). The remaining limit is decided by loss of synchronism at leading power factors. The theoretical limit is the line perpendicular to MO at M (i.e. $\delta = 90°$), but in practice a safety margin is brought into permit a further small increase in load before instability. In Fig. 4.33, a 0.1 pu margin is employed and is shown by the curve afg which is drawn in the following way.

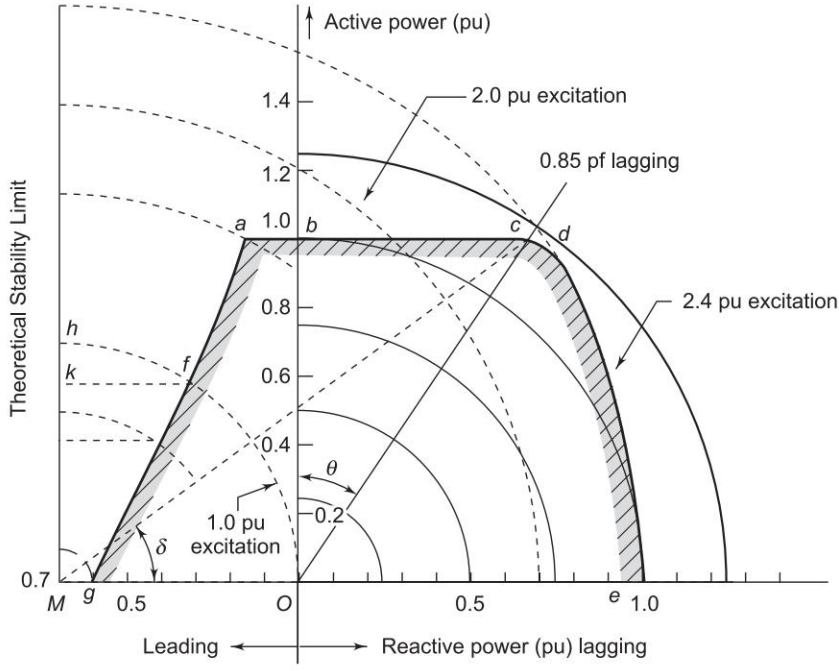

Fig. 4.33 Operating chart for large synchronous generator

Consider a point h on the theoretical limit on the $|E_f| = 1.0$ pu excitations arc, the power Mh is reduced by 0.1 pu to Mk; the operating point must, however, still be on the same $|E_f|$ arc and k is projected to f which is the required

point on the desired limiting curve. This is repeated for other excitations giving the curve *afg*. The complete working area, shown shaded, is *gfabcde*. A working point placed within this area at once defines the MVA, MW, MVAR, current, power factor and excitation. The load angle δ can be measured as shown in the figure.

4.7 POWER TRANSFORMER

Transformers are essential elements in any power system. They allow the relatively low voltages from generators to be raised to a very high level for efficient power transmission. At the load end, the transformers reduce the voltage to values suitable for various categories of loads. The detailed coverage on power transformer (Fig. 4.34) is given in Ch. 3 of Ref. 1. Single-phase equivalents and one-line diagram of three-phase transformers are given in Sec. 4.2. Any standard textbook on Electric Machines such as Ref. 1. gives detailed treatment on transformer performance such as regulation, efficiency; autotransformers and three-winding transformers voltage and phase angle control of transformers is given in Ch. 6.

4.8 TRANSMISSION OF ELECTRIC POWER

The purpose of an overhead transmission network is to transfer electric energy from power stations to the distribution system which finally supplies the load. Line parameters (R, L, G and C) have already been discussed in Chs 2 and 3. Characteristics and performance of power transmission lines are dealt with in full details in the next chapter. How power flows in a grid is the subject matter of Ch. 6. Economic operation and how optimally transmit power over lines is explained in Ch. 7. Loud frequency control and voltage control are discussed in Ch. 8. Chs 9–11 deal with faults on lines etc. Stable operation is discussed in Ch. 12. Where overhead lines cannot be used for power transmission, power is transmitted using underground cables (Ch. 16).

4.9 SYSTEM PROTECTION

Besides generators, transformers, lines and cables, other devices are required for the satisfactory operation and protection of a power system. Some of the protective devices directly connected to the circuits are called switchgear. They include instrument transformers, circuit breakers, disconnect switches, fuses and lightning arresters. These devices are required to de-energize either for normal operation or on occurrence of faults. The necessary control equipment and protective relays are kept in switchboard in control houses. These aspects are covered in Chs 14 and 15.

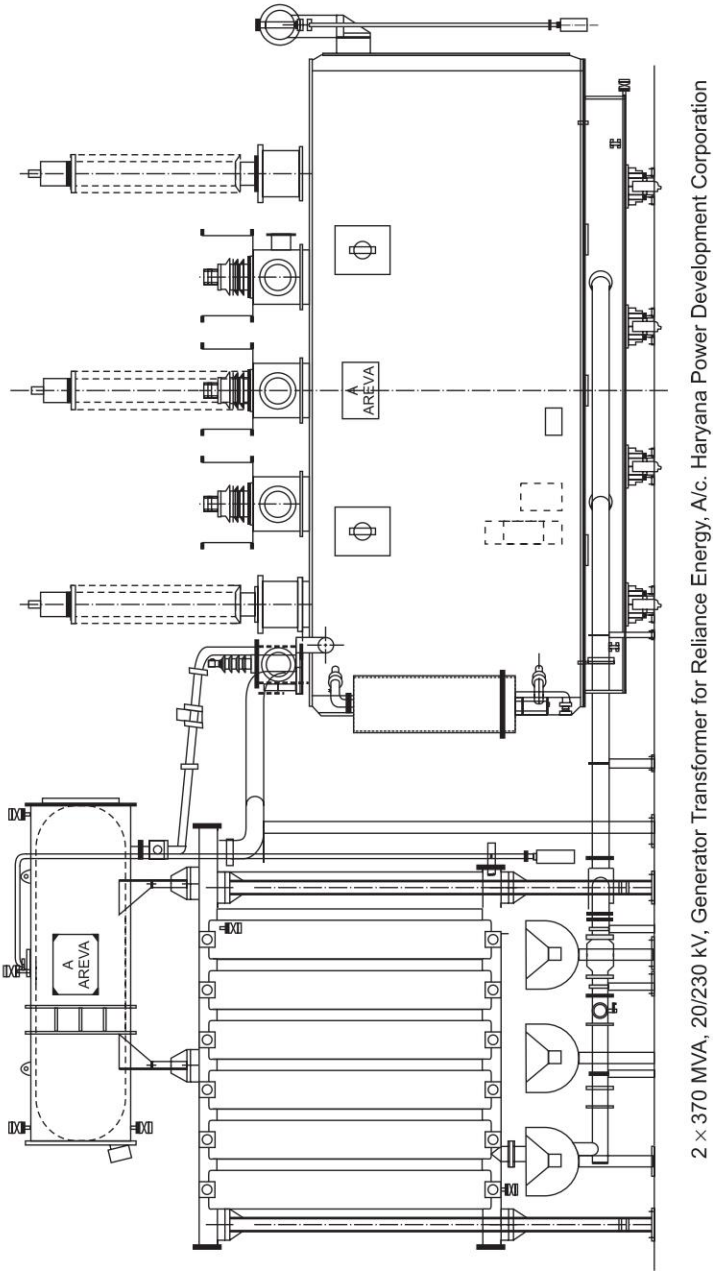

2 × 370 MVA, 20/230 kV, Generator Transformer for Reliance Energy, A/c. Haryana Power Development Corporation

Fig. 4.34 Largest generator transformer manufactured in India

4.10 REPRESENTATION OF LOADS

Load drawn by consumers is the toughest parameter to assess scientifically. The magnitude of the load, in fact, changes continuously so that the load forecasting problem is truly a statistical one. The loads are generally composed of industrial and domestic components. An industrial load consists mainly of large three-phase induction motors with sufficient load constancy and predictable duty cycle, whereas the domestic load mainly consists of lighting, heating and many single-phase devices used in a random way by householders. The design and operation of power systems both economically and electrically are greatly influenced by the nature and magnitude of loads.

In representation of loads for various system studies such as load flow and stability studies, it is essential to know the variation of real and reactive power with variation of voltage. Normally in such studies the load is of composite nature with both industrial and domestic components. A typical composition of load at a bus may be

Induction motors	55 – 75%
Synchronous motors	5 – 15%
Lighting and heating	20 – 30%

Though it is always better to consider the P – V and Q – V characteristics of each of these loads for simulation, the analytic treatment would be very cumbersome and complicated. In most of the analytical work one of the following three ways of load representation is used.

(i) Constant Power Representation

This is used in load flow studies. Both the specified MW and MVAR are taken to be constant.

(ii) Constant Current Representation

Here the load current is given by Eq. (4.17), i.e.

$$I = \frac{P - jQ}{V^*} = |I| \angle (\delta - \theta)$$

where $V = |V| \angle \delta$ and $\theta = \tan^{-1} Q/P$ is the power factor angle. It is known as constant current representation because the magnitude of current is regarded as constant in the study.

(iii) Constant Impedance Representation

This is quite often used in stability studies. The load specified in MW and MVAR at nominal voltage is used to compute the load impedance (Eq. (4.22b)). Thus

$$Z = \frac{V}{I} = \frac{VV^*}{P - jQ} = \frac{|V|^2}{P - jQ} = \frac{1}{Y}$$

which then is regarded as constant throughout the study.

4.11 SUMMARY

In this chapter representation of various power system components have been described including loads, transformer and synchronous machine.

Problems

4.1 Figure P-4.1 shows the schematic diagram of a radial transmission system. The ratings and reactances of the various components are shown therein. A load of 60 MW at 0.9 power factor lagging is tapped from the 66 kV substation which is to be maintained at 60 kV. Calculate the terminal voltage of the synchronous machine. Represent the transmission line and the transformers by series reactances only.

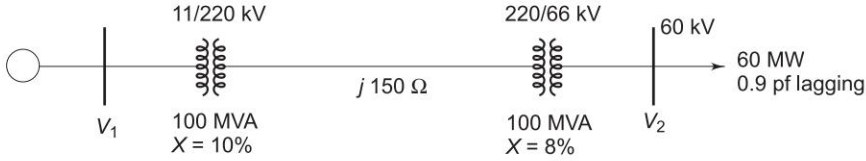

Fig. P-4.1

4.2 Draw the pu impedance diagram for the power system shown in Fig. P-4.2. Neglect resistance, and use a base of 100 MVA, 220 kV in 50 Ω line. The ratings of the generator, motor and transformers are

Generator	40 MVA,	25 kV,	$X'' = 20\%$
Motor	50 MVA,	11 kV,	$X'' = 30\%$
Y–Y transformer,	40 MVA,	33 Y–220 Y kV,	$X = 15\%$
Y–Δ transformer,	30 MVA,	11 Δ–220 Y kV,	$X = 15\%$

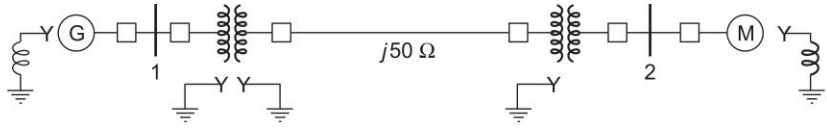

Fig. P-4.2

References

Books

1. Nagrath, I.J. and D.P. Kothari, *Electric Machines*, 3rd edn, Tata McGraw-Hill, New Delhi, 2004.

2. Van E. Mablekos, *Electric Machine Theory for Power Engineers*, Harper and Raw, New York, 1980.
3. DelToro, V., *Electric Machines and Power Systems*, Prentice-Hall,Englewood Cliffs, N.J., 1985.
4. Kothari, D.P. and I.J. Nagrath, *Theory and Problems of Electric Machines*, 2nd edn, Tata McGraw-Hill, New Delhi, 2002.
5. Ned Mohan, *First course on Power Systems*, MNPERE, Minneapolis, 2006.

Paper

6. IEEE Committee Report, "The Effect of Frequency and Voltage on Power System Load", *Presented at IEEE Winter Power Meeting*, New York, 1966.

Chapter 5

Characteristics and Performance of Power Transmission Lines

5.1 INTRODUCTION

This chapter deals primarily with the characteristics and performance of transmission lines. A problem of major importance in power systems is the flow of load over transmission lines such that the voltage at various nodes is maintained within specified limits. While this general interconnected system problem will be dealt with in Ch. 6, attention is presently focussed on performance of a single transmission line so as to give the reader a clear understanding of the principle involved.

Transmission lines are normally operated with a balanced three-phase load; the analysis can therefore proceed on a per phase basis. A transmission line on a per phase basis can be regarded as a two-port network, wherein the sending-end voltage V_S and current I_S are related to the receiving-end voltage V_R and current I_R through *ABCD* constants* as

$$\begin{bmatrix} V_S \\ I_S \end{bmatrix} = \begin{bmatrix} A & B \\ C & D \end{bmatrix} \begin{bmatrix} V_R \\ I_R \end{bmatrix} \tag{5.1}$$

Also the following identity holds for *ABCD* constants:

$$AD - BC = 1 \tag{5.2}$$

These constants can be determined easily for short- and medium-length lines by suitable approximations lumping the line impedance and shunt admittance. For long lines exact analysis has to be carried out by considering the distribution of resistance, inductance and capacitance parameters and the *ABCD* constants of the line are determined therefrom.

Equations for power flow on a line and receiving- and sending-end circle diagrams will also be developed in this chapter so that various types of end conditions can be handled.

* Refer to Appendix B

The following nomenclature has been adopted in this chapter:

z = series impedance/unit length/phase
y = shunt admittance/unit length/phase to neutral
r = resistance/unit length/phase
L = inductance/unit length/phase
C = capacitance/unit length/phase to neutral
l = transmission line length
$Z = zl$ = total series impedance/phase
$Y = yl$ = total shunt admittance/phase to neutral

Subscript S stands for a sending-end quantity
Subscript R stands for a receiving-end quantity

5.2 SHORT TRANSMISSION LINE

For short lines of length 100 km or less, the total 50 Hz shunt admittance* ($j\omega Cl$) is small enough to be negligible resulting in the simple equivalent circuit of Fig. 5.1.

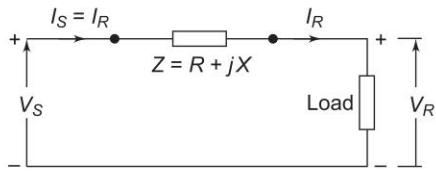

Fig. 5.1 Equivalent circuit of a short line

This being a simple series circuit, the relationship between sending-end receiving-end voltages and currents can be immediately written as:

$$\begin{bmatrix} V_S \\ I_S \end{bmatrix} = \begin{bmatrix} 1 & Z \\ 0 & 1 \end{bmatrix} \begin{bmatrix} V_R \\ I_R \end{bmatrix} \tag{5.3}$$

The phasor diagram for the short line is shown in Fig. 5.2 for the lagging current case. From this figure we can write

$$|V_S| = [(|V_R| \cos \phi_R + |I|R)^2 + (|V_R| \sin \phi_R + |I|X)^2]^{1/2}$$

$$|V_S| = [|V_R|^2 + |I|^2 (R^2 + X^2) + 2|V_R|\,|I|\,(R \cos \phi_R + X \sin \phi_R)]^{1/2} \tag{5.4}$$

$$= |V_R| \left[1 + \frac{2|I|R}{|V_R|} \cos \phi_R + \frac{2|I|X}{|V_R|} \sin \phi_R + \frac{|I|^2 (R^2 + X^2)}{|V_R|^2} \right]^{1/2}$$

* For overhead transmission lines, shunt admittance is mainly capacitive susceptance ($j\omega\, Cl$) as the line conductance (also called *leakance*) is always negligible.

The last term is usually of negligible order.

$$\therefore \quad |V_S| \simeq |V_R| \left[1 + \frac{2|I|R}{|V_R|}\cos\phi_R + \frac{2|I|X}{|V_R|}\sin\phi_R\right]^{1/2}$$

Expanding binomially and retaining first order terms, we get

$$|V_S| \simeq |V_R| \left[1 + \frac{|I|R}{|V_R|}\cos\phi_R + \frac{|I|X}{|V_R|}\sin\phi_R\right]$$

or

$$|V_S| \simeq |V_R| + |I|\,(R\cos\phi_R + X\sin\phi_R) \tag{5.5}$$

The above equation is quite accurate for the normal load range.

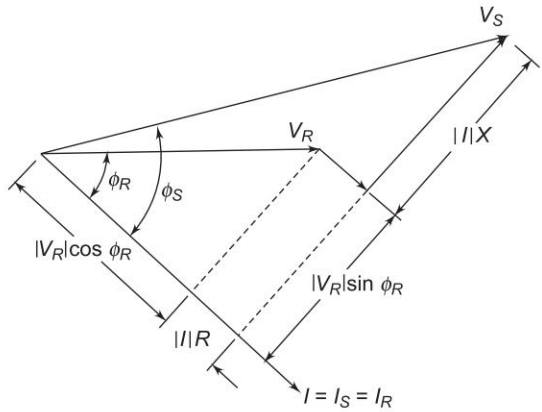

Fig. 5.2 Phasor diagram of a short line for lagging current

Voltage Regulation

Voltage regulation of a transmission line is defined as the rise in voltage at the receiving-end, expressed as percentage of full load voltage, when full load at a specified power factor is thrown off, i.e.

$$\text{Per cent regulation} = \frac{|V_{R0}| - |V_{RL}|}{|V_{RL}|} \times 100 \tag{5.6}$$

where

$|V_{R0}|$ = magnitude of no load receiving-end voltage

$|V_{RL}|$ = magnitude of full load receiving-end voltage (at a specified power factor)

For short line, $|V_{R0}| = |V_S|$, $|V_{RL}| = |V_R|$

$$\therefore \quad \text{Per cent regulation} = \frac{|V_S| - |V_R|}{|V_R|}$$

$$= \frac{|I| R\cos\phi_R + |I| X \sin\phi_R}{|V_R|} \times 100 \qquad (5.7)$$

In the above derivation, ϕ_R has been considered positive for a lagging load. It will be negative for a leading load.

$$\text{Per cent regulation} = \frac{|I| R\cos\phi_R - |I| X \sin\phi_R}{|V_R|} \times 100 \qquad (5.8)$$

Voltage regulation becomes negative (i.e. load voltage is more than no load voltage), when in Eq. (5.8)

$$X \sin \phi_R > R \cos \phi_R, \text{ or } \tan \phi_R \text{ (leading)} > \frac{R}{X}$$

It also follows from Eq. (5.8) that for zero voltage regulation

$$\tan \phi_R = \frac{R}{X} = \cot \theta$$

i.e., $$\phi_R \text{ (leading)} = \frac{\pi}{2} - \theta \qquad (5.9)$$

where θ is the angle of the transmission line impedance. This is, however, an approximate condition. The exact condition for zero regulation is determined as follows.

Figure 5.3 shows the phasor diagram under conditions of zero voltage regulation, i.e.

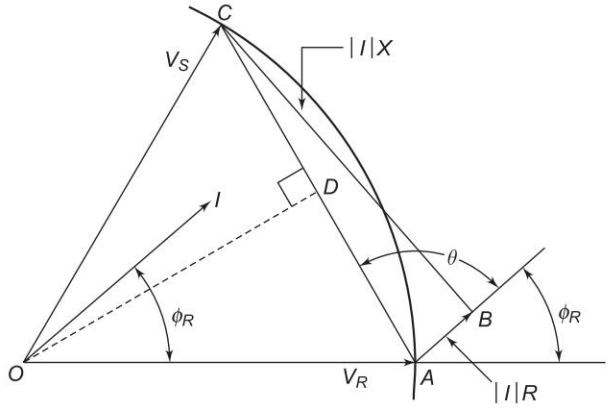

Fig. 5.3 Phasor diagram under zero regulation condition

$$|V_S| = |V_R|$$

or $$OC = OA$$

$$\sin \angle AOD = \frac{AD}{OA} = \frac{AC/2}{|V_R|} = \frac{|I||Z|}{2|V_R|}$$

or $$\angle AOD = \sin^{-1}\frac{|I||Z|}{2|V_R|}$$

It follows from the geometry of angles at A, that for zero voltage regulation,

$$\phi_R \text{ (leading)} = \left(\frac{\pi}{2} - \theta + \sin^{-1}\frac{|I||Z|}{2|V_R|}\right) \tag{5.10}$$

From the above discussion it is seen that the voltage regulation of a line is heavily dependent upon load power factor. Voltage regulation improves (decreases) as the power factor of a lagging load is increased and it becomes zero at a leading power factor given by Eq. (5.10).

Example 5.1 A single-phase 50 Hz generator supplies an inductive load of 5,000 kW at a power factor of 0.707 lagging by means of an over head transmission line 20 km long. The line resistance and inductance are 0.0195 ohm and 0.63 mH per km. The voltage at the receiving-end is required to be kept constant at 10 kV.

Find (a) the sending-end voltage and voltage regulation of the line; (b) the value of the capacitors to be placed in parallel with the load such that the regulation is reduced to 50% of that obtained in part (a); and (c) compare the transmission efficiency in parts (a) and (b).

Solution

The line constants are

$$R = 0.0195 \times 20 = 0.39\ \Omega$$
$$X = 314 \times 0.63 \times 10^{-3} \times 20 = 3.96\ \Omega$$

(a) This is the case of a short line with $I = I_R = I_S$ given by

$$|I| = \frac{5{,}000}{10 \times 0.707} = 707\ \text{A}$$

From Eq. (5.5),

$$|V_S| \simeq |V_R| + |I|\,(R\cos\phi_R + X\sin\phi_R)$$
$$= 10{,}000 + 707(0.39 \times 0.707 + 3.96 \times 0.707)\ \text{V}$$
$$= 12.175\ \text{kV}$$

Voltage regulation $$= \frac{12.175 - 10}{10} \times 100 = 21.75\%$$

(b) Voltage regulation desired $= \frac{21.75}{2} = 10.9\%$

$\therefore$ $$\frac{|V_S| - 10}{10} = 0.109$$

or

new value of $|V_S| = 11.09$ kV

Figure 5.4 shows the equivalent circuit of the line with a capacitive reactance placed in parallel with the load.

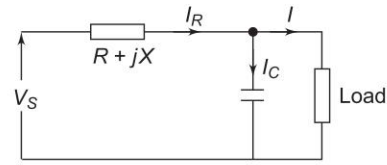

Fig. 5.4

Assuming cos ϕ_R now to be the power factor of load and capacitive reactance taken together, we can write

$$(11.09 - 10) \times 10^3 = |I_R| (R \cos \phi_R + X \sin \phi_R) \quad \text{(i)}$$

Since the capacitance does not draw any real power, we have

$$|I_R| = \frac{5{,}000}{10 \times \cos \phi_R} \quad \text{(ii)}$$

Solving Eqs (i) and (ii), we get

$$\cos \phi_R = 0.911 \text{ lagging}$$

and

$$|I_R| = 549 \text{ A}$$

Now

$$\begin{aligned} I_C &= I_R - I \\ &= 549(0.911 - j0.412) - 707(0.707 - j0.707) \\ &= 0.29 + j273.7 \end{aligned}$$

Note that the real part of 0.29 appears due to the approximation in (i). Ignoring it, we have

$$I_C = j273.7 \text{ A}$$

$$\therefore \quad X_C = \frac{1}{314 \times C} = \left|\frac{V_R}{I_C}\right| = \frac{10 \times 1000}{273.7}$$

or

$$C = 87 \ \mu\text{F}$$

(c) Efficiency of transmission;

$$\eta = \frac{\text{output}}{\text{output} + \text{loss}}$$

Case (a)

$$\eta = \frac{5{,}000}{5{,}000 + (707)^2 \times 0.39 \times 10^{-3}} = 96.2\%$$

Case (b)

$$\eta = \frac{5{,}000}{5{,}000 + (549)^2 \times 0.39 \times 10^{-3}} = 97.7\%$$

It is to be noted that by placing a capacitor in parallel with the load, the receiving-end power factor improves (from 0.707 lag to 0.911 lag), the line current reduces (from 707 A to 549 A), the line voltage regulation decreases (one half the previous value) and the transmission efficiency improves (from 96.2 to 97.7%). Adding capacitors in parallel with load is a powerful method of improving the performance of a transmission system and will be discussed further towards the end of this chapter.

Example 5.2 A substation as shown in Fig. 5.5 receives 5 MVA at 6 kV, 0.85 lagging power factor on the low voltage side of a transformer from a power station through a cable having per phase resistance and reactance of 8 and 2.5 ohms, respectively. Identical 6.6/33 kV transformers are installed at each end of the line. The 6.6 kV side of the transformers is delta connected while the 33 kV side is star connected. The resistance and reactance of the star connected windings are 0.5 and 3.75 ohms, respectively and for the delta connected windings are 0.06 and 0.36 ohms. What is the voltage at the bus at the power station end?

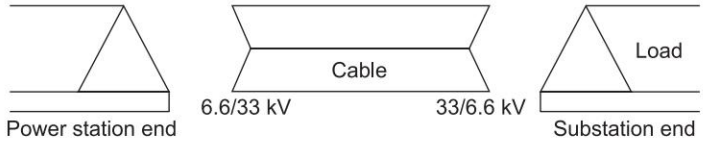

Fig. 5.5

Solution

It is convenient here to employ the per unit method. Let us choose,

$$\text{Base MVA} = 5$$

$$\text{Base kV} = 6.6 \text{ on low voltage side}$$

$$= 33 \text{ on high voltage side}$$

$$\text{Cable impedance} = (8 + j2.5)\ \Omega/\text{phase}$$

$$= \frac{(8 + j2.5) \times 5}{(33)^2} = (0.037 + j0.0115) \text{ pu}$$

Equivalent star impedance of 6.6 kV winding of the transformer

$$= \frac{1}{3}(0.06 + j0.36) = (0.02 + j0.12)\ \Omega/\text{phase}$$

Per unit transformer impedance,

$$Z_T = \frac{(0.02 + j0.12) \times 5}{(6.6)^2} + \frac{(0.5 + j3.75) \times 5}{(33)^2}$$

$$= (0.0046 + j0.030) \text{ pu}$$

Total series impedance $= (0.037 + j0.0115) + 2(0.0046 + j0.030)$

$$= (0.046 + j0.072) \text{ pu}$$

Given: Load MVA = 1 pu

$$\text{Load voltage} = \frac{6}{6.6} = 0.91 \text{ pu}$$

$$\therefore \quad \text{Load current} = \frac{1}{0.91} = 1.1 \text{ pu}$$

Using Eq. (5.5), we get

$$|V_S| = 0.91 + 1.1(0.046 \times 0.85 + 0.072 \times 0.527)$$

$$= 0.995 \text{ pu}$$

$$= 0.995 \times 6.6 = 6.57 \text{ kV (line-to-line)}$$

Example 5.3 Input to a single-phase short line shown in Fig. 5.6 is 2,000 kW at 0.8 lagging power factor. The line has a series impedance of $(0.4 + j0.4)$ ohms. If the load voltage is 3 kV, find the load and receiving-end power factor. Also find the supply voltage.

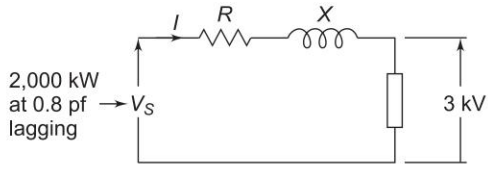

Fig. 5.6

Solution

It is a problem with mixed-end conditions—load voltage and input power are specified. The exact solution is outlined below:

Sending-end active/reactive power = receiving-end active/reactive power + active/reactive line losses

For active power

$$|V_S|\,|I| \cos \phi_S = |V_R|\,|I| \cos \phi_R + |I|^2 R \qquad \text{(i)}$$

For reactive power

$$|V_S|\,|I| \sin \phi_S = |V_R|\,|I| \sin \phi_R + |I|^2 X \qquad \text{(ii)}$$

Squaring (i) and (ii), adding and simplifying, we get

$$|V_S|^2\,|I|^2 = |V_R|^2\,|I|^2 + 2|V_R|\,|I|^2\,(|I|R \cos \phi_R + |I|X \sin \phi_R) + |I|^4\,(R^2 + X^2) \qquad \text{(iii)}$$

Note: This, in fact, is the same as Eq. (5.4) if $|I|^2$ is cancelled throughout. For the numerical values given

$$|Z|^2 = (R^2 + X^2) = 0.32$$

$$|V_S|\,|I| = \frac{2{,}000 \times 10^3}{0.8} = 2{,}500 \times 10^3$$

$$|V_S|\,|I| \cos \phi_S = 2{,}000 \times 10^3$$

$$|V_S|\,|I| \sin \phi_S = 2{,}500 \times 10^3 \times 0.6 = 1{,}500 \times 10^3$$

From Eqs (i) and (ii), we get

$$|I| \cos \phi_R = \frac{2{,}000 \times 10^3 - 0.4\,|I|^2}{3{,}000} \qquad \text{(iv)}$$

$$|I| \sin \phi_R = \frac{1{,}500 \times 10^3 - 0.4\,|I|^2}{3{,}000} \qquad \text{(v)}$$

Substituting all the known values in Eq. (iii), we have

$$(2{,}500 \times 10^3)^2 = (3{,}000)^2\,|I|^2 + 2 \times 3{,}000\,|I|^2 \left[0.4 \times \frac{2{,}000 \times 10^3 - 0.4\,|I|^2}{3{,}000} \right.$$

$$\left. + 0.4 \times \frac{1{,}500 \times 10^3 - 0.4\,|I|^2}{3{,}000} \right] + 0.32\,|I|^4$$

Simplifying, we get

$$0.32\,|I|^4 - 11.8 \times 10^6\,|I|^2 + 6.25 \times 10^{12} = 0$$

which upon solution yields

$$|I| = 725 \text{ A}$$

Substituting for $|I|$ in Eq. (iv), we get

$$\cos \phi_R = 0.82$$

$\therefore$ Load $P_R = |V_R|\,|I| \cos \phi_R = 3{,}000 \times 725 \times 0.82$

$$= 1{,}790 \text{ kW}$$

Now

$$|V_S| = |I| \cos \phi_S = 2{,}000$$

$\therefore$

$$|V_S| = \frac{2{,}000}{725 \times 0.8} = 3.44 \text{ kV}$$

5.3 MEDIUM TRANSMISSION LINE

For lines more than 100 km long, charging currents due to shunt admittance cannot be neglected. For lines in range 100 km to 250 km length, it is sufficiently accurate to lump all the line admittance at the receiving-end resulting in the equivalent diagram shown in Fig. 5.7.

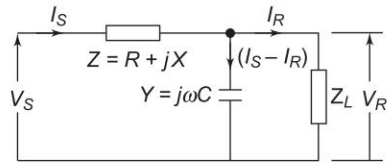

Fig. 5.7 Medium line, localized load-end capacitance

Starting from fundamental circuit equations, it is fairly straightforward to write the transmission line equations in the *ABCD* constant form given below:

$$\begin{bmatrix} V_S \\ I_S \end{bmatrix} = \begin{bmatrix} 1+YZ & Z \\ Y & 1 \end{bmatrix} \begin{bmatrix} V_R \\ I_R \end{bmatrix} \tag{5.11}$$

Nominal–*T* Representation

If all the shunt capacitance is lumped at the middle of the line, it leads to the nominal-*T* circuit shown in Fig. 5.8.

For the nominal-*T* circuit, the following circuit equations can be written:

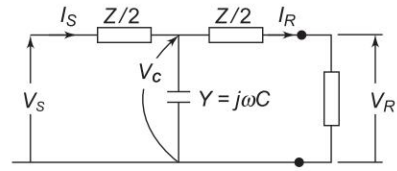

Fig. 5.8 Medium line, nominal-*T* representation

$$V_C = V_R + I_R(Z/2)$$
$$I_S = I_R + V_C Y$$
$$= I_R + YV_R + I_R(Z/2)Y$$
$$V_S = V_C + I_S(Z/2)$$

Substituting for V_C and I_S in the last equation, we get

$$V_S = V_R + I_R(Z/2) + (Z/2)\left[I_R\left(1+\frac{ZY}{2}\right) + YV_R\right]$$

$$= V_R\left(1+\frac{ZY}{2}\right) + I_R Z\left(1+\frac{YZ}{4}\right)$$

Rearranging the results, we get the following equations:

$$\begin{bmatrix} V_S \\ I_S \end{bmatrix} = \begin{bmatrix} \left(1+\frac{1}{2}ZY\right) & Z\left(1+\frac{1}{4}YZ\right) \\ Y & \left(1+\frac{1}{2}YZ\right) \end{bmatrix} \begin{bmatrix} V_R \\ I_R \end{bmatrix} \tag{5.12}$$

Nominal-π Representation

In this method the total line capacitance is divided into two equal parts which are lumped at the sending- and receiving-ends resulting in the nominal-π representation as shown in Fig. 5.9.

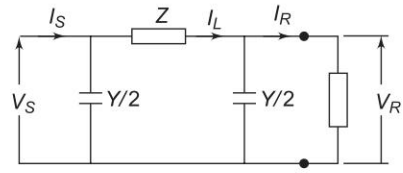

Fig. 5.9 Medium line, nominal-π representation

From Fig. 5.9, we have

$$I_S = I_R + \frac{1}{2}V_R Y + \frac{1}{2}V_S Y$$

$$V_S = V_R + (I_R + \frac{1}{2}V_R Y)Z = V_R\left(1+\frac{1}{2}YZ\right) + I_R Z$$

$$\therefore \quad I_S = I_R + \frac{1}{2}V_R Y + \frac{1}{2}Y[V_R\left(1+\frac{1}{2}YZ\right) + I_R Z]$$

$$= V_R Y\left(1+\frac{1}{4}YZ\right) + I_R\left(1+\frac{1}{2}YZ\right)$$

Finally, we have

$$\begin{bmatrix} V_S \\ I_S \end{bmatrix} = \begin{bmatrix} \left(1+\frac{1}{2}YZ\right) & Z \\ Y\left(1+\frac{1}{4}YZ\right) & \left(1+\frac{1}{2}YZ\right) \end{bmatrix} \begin{bmatrix} V_R \\ I_R \end{bmatrix} \tag{5.13}$$

It should be noted that nominal-T and nominal-π with the above constants are not equivalent to each other. The reader should verify this fact by applying star-delta transformtion to either one.

Example 5.4 Using the nominal-π method, find the sending-end voltage and voltage regulation of a 250 km, three-phase, 50 Hz, transmission line delivering 25 MVA at 0.8 lagging power factor to a balanced load at 132 kV. The line conductors are spaced equilaterally 3 m apart. The conductor resistance is 0.11 ohm/km and its effective diameter is 1.6 cm. Neglect leakance.

Solution

Now,

$$L = 0.461 \log \frac{D}{r'} = 0.461 \log \frac{300}{0.7788 \times 0.8} = 1.24 \text{ mH/km}$$

$$C = \frac{0.0242}{\log D/r} = \frac{0.0242}{\log \frac{300}{0.8}} = 0.0094 \ \mu\text{F/km}$$

$$R = 0.11 \times 250 = 27.5\ \Omega$$

$$X = 2\pi fL = 2\pi \times 50 \times 1.24 \times 10^{-3} \times 250 = 97.4\ \Omega$$

$$Z = R + jX = 27.5 + j97.4 = 101.2\ \angle 74.2^\circ\ \Omega$$

$$Y = j\omega Cl = 314 \times 0.0094 \times 10^{-6} \times 250\ \angle 90^\circ$$

$$= 7.38 \times 10^{-4}\ \angle\ 90^\circ\ \square$$

$$I_R = \frac{25 \times 1{,}000}{\sqrt{3} \times 132} \angle -36.9^\circ = 109.3\ \angle\ -36.9^\circ\ \text{A}$$

V_R (per phase) $= (132/(\sqrt{3})\ \angle 0^\circ = 76.2\ \angle 0^\circ$ kV

$$V_S = \left(1 + \frac{1}{2} YZ\right) V_R + ZI_R$$

$$= \left(1 + \frac{1}{2} \times 7.38 \times 10^{-4} \angle 90^\circ \times 101.2 \angle 74.2^\circ\right) \times 76.2$$

$$+ 101.2\ \angle 74.2^\circ \times 109.3 \times 10^{-3}\ \angle -36.9^\circ$$

$$= 76.2 + 2.85 < 164.2^\circ + 11.06 < 37.3^\circ$$

$$= 82.26 + j7.48 = 82.6 < 5.2^\circ$$

$\therefore$ $|V_S|$ (line) $= 82.6 \times \sqrt{3} = 143$ kV

$$1 + \frac{1}{2} YZ = 1 + 0.0374\ \angle 164.2^\circ = 0.964 + j0.01$$

$$|V_{R0}| \text{ (line no load)} = \frac{143}{\left|1 + \frac{1}{2} YZ\right|} = \frac{143}{0.964} = 148.3 \text{ kV}$$

$\therefore$ Voltage regulation $= \dfrac{148.3 - 132}{132} \times 100 = 12.3\%$

5.4 THE LONG TRANSMISSION LINE—RIGOROUS SOLUTION

For lines over 250 km, the fact that the parameters of a line are not lumped but distributed uniformly throughout its length, must be considered.

Figure 5.10 shows one phase and the neutral return (of zero impedance) of a transmission line. Let dx be an elemental section of the line at a distance x from the receiving-end having a series impedance z dx and a shunt admittance y dx. The rise in voltage* to neutral over the elemental section in the direction of increasing x is dV_x. We can write the following differential relationships across the elemental section:

* Here V_x is the complex expression of the rms voltage, whose magnitude and phase vary with distance along the line.

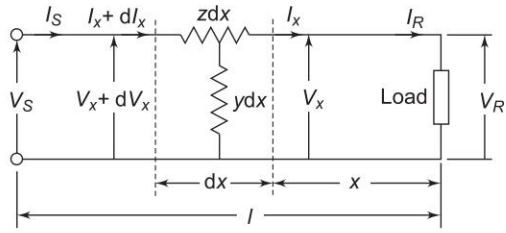

Fig. 5.10 Schematic diagram of a long line

$$dV_x = I_x z\, dx \quad \text{or} \quad \frac{dV_x}{dx} = zI_x \tag{5.14}$$

$$dI_x = V_x y\, dx \quad \text{or} \quad \frac{dI_x}{dx} = yV_x \tag{5.15}$$

It may be noticed that the kind of connection (e.g. T or π) assumed for the elemental section, does not affect these first order differential relations.

Differentiating Eq. (5.14) with respect to x, we obtain

$$\frac{d^2 V_x}{dx^2} = \frac{dI_x}{dx} z$$

Substituting the value of $\frac{dI_x}{dx}$ from Eq. (5.15), we get

$$\frac{d^2 V_x}{dx^2} = yzV_x \tag{5.16}$$

This is a linear differential equation whose general solution can be written as follows:

$$V_x = C_1 e^{\gamma x} + C_2 e^{-\gamma x} \tag{5.17}$$

where

$$\gamma = \sqrt{yz} \tag{5.18}$$

and C_1 and C_2 are arbitrary constants to be evaluated.

Differentiating Eq. (5.17) with respect to x,

$$\frac{dV_x}{dx} = C_1 \gamma e^{\gamma x} - C_2 \gamma e^{-\gamma x} = zI_x$$

$$\therefore \quad I_x = \frac{C_1}{Z_c} e^{\gamma x} - \frac{C_2}{Z_c} e^{-\gamma x} \tag{5.19}$$

where

$$Z_c = \left(\frac{z}{y}\right)^{1/2} \tag{5.20}$$

The constants C_1 and C_2 may be evaluated by using the end conditions, i.e. when $x = 0$, $V_x = V_R$ and $I_x = I_R$. Substituting these values in Eqs (5.17) and (5.19) gives

$$V_R = C_1 + C_2$$

$$I_R = \frac{1}{Z_c}(C_1 - C_2)$$

which upon solving yield

$$C_1 = \frac{1}{2}(V_R + Z_c I_R)$$

$$C_2 = \frac{1}{2}(V_R - Z_c I_R)$$

With C_1 and C_2 as determined above, Eqs (5.17) and (5.19) yield the solution for V_x and I_x as

$$V_x = \left(\frac{V_R + Z_c I_R}{2}\right)e^{\gamma x} + \left(\frac{V_R - Z_c I_R}{2}\right)e^{-\gamma x} \tag{5.21}$$

$$I_x = \left(\frac{V_R/Z_c + I_R}{2}\right)e^{\gamma x} - \left(\frac{V_R/Z_c - I_R}{2}\right)e^{-\gamma x}$$

Here Z_c is called the *characteristic impedance* of the line and γ is called the *propagation constant*.

Knowing V_R, I_R and the parameters of the line, using Eq. (5.21) complex number rms values of V_x and I_x at any distance x along the line can be easily found out.

A more convenient form of expression for voltage and current is obtained by introducing hyperbolic functions. Rearranging Eq. (5.21), we get

$$V_x = V_R\left(\frac{e^{\gamma x} + e^{-\gamma x}}{2}\right) + I_R Z_c\left(\frac{e^{\gamma x} - e^{-\gamma x}}{2}\right)$$

$$I_x = V_R\frac{1}{Z_c}\left(\frac{e^{\gamma x} - e^{-\gamma x}}{2}\right) + I_R\left(\frac{e^{\gamma x} + e^{-\gamma x}}{2}\right)$$

These can be rewritten after introducing hyperbolic functions, as

$$V_x = V_R \cosh \gamma x + I_R Z_c \sinh \gamma x \tag{5.22}$$

$$I_x = I_R \cosh \gamma x + V_R \frac{1}{Z_c} \sinh \gamma x$$

when $x = l$, $V_x = V_S$, $I_x = I_S$

$$\therefore \quad \begin{bmatrix} V_S \\ I_S \end{bmatrix} = \begin{bmatrix} \cosh \gamma l & Z_c \sinh \gamma l \\ \frac{1}{Z_c} \sinh \gamma l & \cosh \gamma l \end{bmatrix} \begin{bmatrix} V_R \\ I_R \end{bmatrix} \tag{5.23}$$

Here

$$\begin{aligned} A &= D = \cosh \gamma l \\ B &= Z_c \sinh \gamma l \\ C &= \frac{1}{Z_c} \sinh \gamma l \end{aligned} \tag{5.24}$$

In case $[V_S\ I_S]$ is known, $[V_R\ I_R]$ can be easily found by inverting Eq. (5.23). Thus

$$\begin{bmatrix} V_R \\ I_R \end{bmatrix} = \begin{bmatrix} D & -B \\ -C & A \end{bmatrix} \begin{bmatrix} V_S \\ I_S \end{bmatrix} \tag{5.25}$$

Evaluation of ABCD Constants

The *ABCD* constants of a long line can be evaluated from the results given in Eq. (5.24). It must be noted that $\gamma = \sqrt{yz}$ is in general a complex number and can be expressed as

$$\gamma = \alpha + j\beta \tag{5.26}$$

The hyperbolic function of complex numbers involved in evaluating *ABCD* constants can be computed by any one of the three methods given below:

Method 1

$$\begin{aligned} \cosh (\alpha l + j\beta l) &= \cosh \alpha l \cos \beta l + j \sinh \alpha l \sin \beta l \\ \sinh (\alpha l + j\beta l) &= \sinh \alpha l \cos \beta l + j \cosh \alpha l \sin \beta l \end{aligned} \tag{5.27}$$

Note that sinh, cosh, sin and cos of real numbers as in Eq. (5.27) can be looked up *in standard tables*.

Method 2

$$\begin{aligned} \cosh \gamma l &= 1 + \frac{\gamma^2 l^2}{2!} + \frac{\gamma^4 l^4}{4!} + \ldots \approx \left(1 + \frac{YZ}{2}\right) \\ \sinh \gamma l &= \gamma l + \frac{\gamma^3 l^3}{3!} + \frac{\gamma^5 l^5}{5!} + \ldots \approx \sqrt{YZ} \left(1 + \frac{YZ}{6}\right) \end{aligned} \tag{5.28a}$$

This series converges rapidly for values of γl usually encountered for power lines and can be conveniently approximated as above.The corresponding expressions for *ABCD* constants are

$$A = D \approx 1 + \frac{YZ}{2}$$

$$B \approx Z\left(1 + \frac{YZ}{6}\right) \tag{5.28b}$$

$$C \approx Y\left(1 + \frac{YZ}{6}\right)$$

The above approximation is computationally convenient and quite accurate for lines up to 400/500 km.

Method 3

$$\cosh(\alpha l + j\beta l) = \frac{e^{\alpha l}e^{j\beta l} + e^{-\alpha l}e^{-j\beta l}}{2} = \frac{1}{2}(e^{\alpha l} \angle \beta l + e^{-\alpha l} \angle -\beta l)$$

$$\sinh(\alpha l + j\beta l) = \frac{e^{\alpha l}e^{j\beta l} - e^{-\alpha l}e^{-j\beta l}}{2} = \frac{1}{2}(e^{\alpha l} \angle \beta l - e^{-\alpha l} \angle -\beta l) \tag{5.29}$$

5.5 THE EQUIVALENT CIRCUIT OF A LONG LINE

So far as the end conditions are concerned, the exact equivalent circuit of a transmission line can be established in the form of a *T*- or π-network.

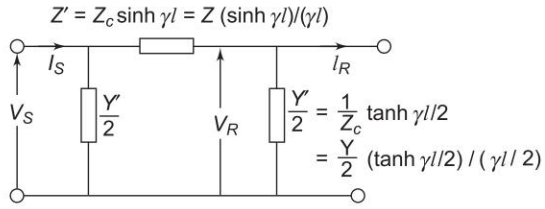

Fig. 5.11 Equivalent-π network of a transmission line

The parameters of the equivalent network are easily obtained by comparing the performance equations of a π-network and a transmission line in terms of end quantities.

For a π-network shown in Fig. 5.11 [refer to Eq. (5.13)].

$$\begin{bmatrix} V_S \\ I_S \end{bmatrix} = \begin{bmatrix} \left(1 + \frac{1}{2}Y'Z'\right) & Z' \\ Y'\left(1 + \frac{1}{4}Y'Z'\right) & \left(1 + \frac{1}{2}Y'Z'\right) \end{bmatrix} \begin{bmatrix} V_R \\ I_R \end{bmatrix} \tag{5.30}$$

According to exact solution of a long line [refer to Eq. (5.23)].

$$\begin{bmatrix} V_S \\ I_S \end{bmatrix} = \begin{bmatrix} \cosh \gamma l & Z_c \sinh \gamma l \\ \frac{1}{Z_c} \sinh \gamma l & \cosh \gamma l \end{bmatrix} \begin{bmatrix} V_R \\ I_R \end{bmatrix} \tag{5.31}$$

For exact equivalence, we must have

$$Z' = Z_c \sinh \gamma l \tag{5.32}$$

$$1 + \frac{1}{2} Y'Z' = \cosh \gamma l \tag{5.33}$$

From Eq. (5.32)

$$Z' = \sqrt{\frac{z}{y}} \sinh \gamma l = zl \frac{\sinh \gamma l}{l\sqrt{yz}} = Z\left(\frac{\sinh \gamma l}{\gamma l}\right) \tag{5.34}$$

Thus $\frac{\sinh \gamma l}{\gamma l}$ is the factor by which the series impedance of the nominal-π must be multiplied to obtain the Z' parameter of the equivalent-π.

Substituting Z' from Eq. (5.32) in Eq. (5.33), we get

$$1 + \frac{1}{2} Y'Z_c \sinh \gamma l = \cosh \gamma l$$

$$\therefore \quad \frac{1}{2} Y' = \frac{1}{Z_c}\left(\frac{\cosh \gamma l - 1}{\sinh \gamma l}\right)$$

$$= \frac{1}{Z_c} \tanh \frac{\gamma l}{2} = \sqrt{\frac{y}{z}} \tanh \frac{\gamma l}{2}$$

$$= \frac{yl}{2}\left(\frac{\tanh \gamma l/2}{\gamma l/2}\right)$$

or

$$\frac{1}{2} Y' = \frac{Y}{2}\left(\frac{\tanh \gamma l/2}{\gamma l/2}\right) \tag{5.35}$$

Thus $\left(\frac{\tanh \gamma l/2}{\gamma l/2}\right)$ is the factor by which the shunt admittance arm of the nominal-π must be multiplied to obtain the shunt parameter ($Y'/2$) of the equivalent-π.

Note that $Y'\left(1 + \frac{1}{4} Y'Z'\right) = \frac{1}{Z_c} \sinh \gamma l$ is a consistent equation in terms of the above values of Y' and Z'.

For a line of medium length $\frac{\tanh \gamma l/2}{\gamma l/2} \simeq 1$ and $\frac{\sinh \gamma l}{\gamma l} \simeq 1$ so that the equivalent-π network reduces to that of nominal-π. The equivalent-T network is shown in Fig. 5.12.

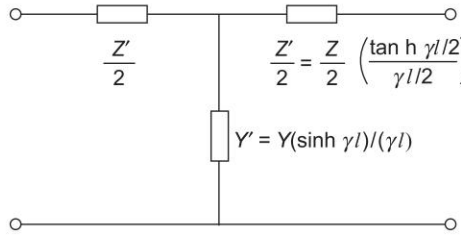

Fig. 5.12 Equivalent-T network of a transmission line

Equivalent-T network parameters of a transmission line are obtained on similar lines.

As we shall see in Ch. 6 equivalent-π (or nominal-π) network is easily adopted to load flow studies and is, therefore, universally employed.

Example 5.5 A 50 Hz transmission line 300 km long has a total series impedance of $40 + j125$ ohms and a total shunt admittance of 10^{-3} mho. The receiving-end load is 50 MW at 220 kV with 0.8 lagging power factor. Find the sending-end voltage, current, power and power factor using

(a) short line approximation,
(b) nominal-π method,
(c) exact transmission line equation [Eq. (5.27)],
(d) approximation [Eq. (5.28b)].

Compare the results and comment.

Solution

$$Z = 40 + j125 = 131.2 \angle 72.3^\circ \ \Omega$$

$$Y = 10^{-3} \angle 90^\circ \ \Omega$$

The receiving-end load is 50 MW at 220 kV, 0.8 pf lagging.

$$\therefore \quad I_R = \frac{50}{\sqrt{3} \times 220 \times 0.8} \angle -36.9^\circ = 0.164 \angle -36.9^\circ \ \text{kA}$$

$$V_R = \frac{220}{\sqrt{3}} \angle 0^\circ = 127 \angle 0^\circ \ \text{kV}$$

(a) Short line approximation:

From Eq. (5.3),

$$V_S = 127 + 0.164 \angle -36.9^\circ \times 131.2 \angle 72.3^\circ$$

$$= 145 \angle 4.9^\circ$$

$$|V_S|_{\text{line}} = 251.2 \text{ kV}$$

$$I_S = I_R = 0.164 \angle -36.9^\circ \text{ kA}$$

Sending-end power factor $= \cos(4.9^\circ + 36.9^\circ = 41.8^\circ)$

$= 0.745$ lagging

Sending-end power $= \sqrt{3} \times 251.2 \times 0.164 \times 0.745$

$= 53.2$ MW

(b) Nominal-π method:

$$A = D = 1 + \frac{1}{2}YZ = 1 + \frac{1}{2} \times 10^{-3} \angle 90^\circ \times 131.2 \angle 72.3^\circ$$

$$= 1 + 0.0656 \angle 162.3^\circ = 0.938 \angle 1.2^\circ$$

$$B = Z = 131.2 \angle 72.3^\circ$$

$$C = Y\left(1 + \frac{1}{4}YZ\right) = Y + \frac{1}{4}Y^2Z$$

$$= 0.001 \angle 90^\circ + \frac{1}{4} \times 10^{-6} \angle 180^\circ \times 131.2 \angle 72.3^\circ$$

$$= 0.001 \angle 90^\circ$$

$$V_S = 0.938 \angle 1.2^\circ \times 127 + 131.2 \angle 72.3^\circ \times 0.164 \angle -36.9^\circ$$

$$= 119.1 \angle 1.2^\circ + 21.5 \angle 35.4^\circ = 137.4 \angle 6.2^\circ$$

$$|V_S|_{\text{line}} = 238 \text{ kV}$$

$$I_S = 0.001 \angle 90^\circ \times 127 + 0.938 \angle 1.2^\circ \times 0.164 \angle -36.9^\circ$$

$$= 0.127 \angle 90^\circ + 0.154 \angle -35.7^\circ = 0.13 \angle 16.5^\circ$$

Sending-end pf $= \cos(16.5^\circ - 6.2^\circ) = 0.984$ leading

Sending-end power $= \sqrt{3} \times 238 \times 0.13 \times 0.984$

$= 52.7$ MW

(c) Exact transmission line equations (Eq. 5.29).

$$\gamma l = \alpha l + j\beta l = \sqrt{YZ}$$

$$= \sqrt{10^{-3} \angle 90^\circ \times 131.2 \angle 72.3^\circ}$$

$$= 0.0554 + j0.3577$$

$$= 0.362 \angle 81.2^\circ$$

$$\cosh(\alpha l + j\beta l) = \frac{1}{2}(e^{\alpha l} \angle \beta l + e^{-\alpha l} \angle -\beta l)$$

$$\beta l = 0.3577 \text{ (radians)} = \angle 20.49^\circ$$

$$e^{0.0554} \angle (20.49^\circ) = 1.057 \angle 20.49^\circ = 0.99 + j0.37$$

$$e^{-0.0554} \angle -20.49^\circ = 0.946 \angle -20.49^\circ = 0.886 - j0.331$$

$$\therefore \quad \cosh \gamma l = 0.938 + j0.02 = 0.938 \angle 1.2^\circ$$

$$\sinh \gamma l = 0.052 + j0.35 = 0.354 \angle 81.5^\circ$$

$$Z_c = \sqrt{\frac{Z}{Y}} = \sqrt{\frac{131.2 \angle 72.3^\circ}{10^{-3} \angle 90^\circ}} = 362.21 \angle -8.85^\circ$$

$$A = D = \cosh \gamma l = 0.938 \angle 1.2^\circ$$

$$B = Z_c \sinh \gamma l = 362.21 \angle -8.85^\circ \times 0.354 \angle 81.5^\circ$$

$$= 128.2 \angle 72.65^\circ$$

Now

$$V_S = 0.938 \angle 1.2^\circ \times 127 \angle 0^\circ + 128.2 \angle 72.65^\circ \times 0.164 \angle -36.9^\circ$$

$$= 119.13 \angle 1.2^\circ + 21.03 \angle 35.75^\circ$$

$$= 136.97 \angle 6.2^\circ \text{ kV}$$

$$|V_S|_{\text{line}} = 237.23 \text{ kV}$$

$$C = \frac{1}{Z_c} \sinh \gamma l = \frac{1}{362.21 \angle -8.85^\circ} \times 0.354 \angle 81.5^\circ$$

$$= 9.77 \times 10^{-4} \angle 90.4^\circ$$

$$I_S = 9.77 \times 10^{-4} \angle 90.4^\circ \times 127 + 0.938 \angle 1.2^\circ \times 0.164 \angle -36.9^\circ$$

$$= 0.124 \angle 90.4^\circ + 0.154 \angle -35.7^\circ$$

$$= 0.1286 \angle 15.3^\circ \text{ kA}$$

Sending-end pf = cos (15.3° – 6.2° = 9.1°) = 0.987 leading

Sending-end power = $\sqrt{3} \times 237.23 \times 0.1286 \times 0.987$

$$= 52.15 \text{ MW}$$

(d) Approximation (5.28b):

$$A = D = 1 + \frac{1}{2} YZ$$

$= 0.938 \angle 1.2°$ (already calculated in part (b))

$$B = Z\left(1 + \frac{YZ}{6}\right) = Z + \frac{1}{6}YZ^2$$

$$= 131.2 \angle 72.3° + \frac{1}{6} \times 10^{-3} \angle 90° \times (131.2)^2 \angle 144.6°$$

$$= 131.2 \angle 72.3° + 2.87 \angle -125.4°$$

$$= 128.5 \angle 72.7°$$

$$C = Y\left(1 + \frac{YZ}{6}\right) = 0.001 \angle 90° + \frac{1}{6} \times 10^{-6} \angle 180° \times 131.2 \angle 72.3°$$

$$= 0.001 \angle 90°$$

$$V_S = 0.938 \angle 1.2° \times 127 \angle 0° + 128.5 \angle 72.7° \times 0.164 \angle -36.9°$$

$$= 119.13 \angle 1.2° + 21.07 \angle 35.8° = 136.2 + j14.82$$

$$= 137 \angle 6.2° \text{ kV}$$

$$|V_S|_{\text{line}} = 237.3 \text{ kV}$$

$I_S = 0.13 \angle 16.5°$ (same as calculated in part (b))

Sending-end pf = cos (16.5° – 6.2° = 10.3°) = 0.984 leading

Sending-end power $= \sqrt{3} \times 237.3 \times 0.13 \times 0.984$

$= 52.58$ MW

The results are tabulated as:

	Short line approximation	*Nominal-π*	*Exact*	*Approximation (5.28b)*
$\|V_s\|_{\text{line}}$	251.2 kV	238 kV	237.23 kV	237.3 kV
I_s	0.164 ∠–36.9° kA	0.13 ∠16.5° kA	0.1286 ∠15.3° kA	0.13 ∠16.5° kA
pf_s	0.745 lagging	0.984 leading	0.987 leading	0.984 leading
P_s	53.2 MW	52.7 MW	52.15 MW	52.58 MW

Comments: We find from the above example that the results obtained by the nominal-π method and the approximation (5.28b) are practically the same and are very close to those obtained by exact calculations (part (c)). On the other hand the results obtained by the short line approximation are in considerable error. Therefore, for a line of this length (about 300 km), it is sufficiently accurate

to use the nominal-π (or approximation (5.28b)) which results in considerable saving in computational effort.

5.6 INTERPRETATION OF THE LONG LINE EQUATIONS

As already said in Eq. (5.26), γ is a complex number which can be expressed as

$$\gamma = \alpha + j\beta$$

The real part α is called the *attenuation constant* and the imaginary part β is called the *phase constant*. Now V_x of Eq. (5.21) can be written as

$$V_x = \left|\frac{V_R + Z_c I_R}{2}\right| e^{\alpha x} e^{j(\beta x + \phi_1)} + \left|\frac{V_R - Z_c I_R}{2}\right| e^{-\alpha x} e^{-j(\beta x - \phi_2)}$$

where

$$\phi_1 = \angle(V_R + I_R Z_c) \tag{5.36}$$

$$\phi_2 = \angle(V_R - I_R Z_c)$$

The instantaneous voltage $v_x(t)$ can be written from Eq. (5.36) as

$$v_x(t) = \text{Re}\left[\sqrt{2}\left|\frac{V_R + Z_c I_R}{2}\right| e^{\alpha x} e^{j(\omega t + \beta x + \phi_1)} + \sqrt{2}\left|\frac{V_R - Z_c I_R}{2}\right| e^{-\alpha x} e^{j(\omega t - \beta x + \phi_2)}\right] \tag{5.37}$$

The instantaneous voltage consists of two terms each of which is a function of two variables—time and distance. Thus they represent two travelling waves, i.e.

$$v_x = v_{x_1} + v_{x_2} \tag{5.38}$$

Now

$$v_{x_1} = \sqrt{2}\left|\frac{V_R + Z_c I_R}{2}\right| e^{\alpha x} \cos(\omega t + \beta x + \phi_1) \tag{5.39}$$

At any instant of time t, v_{x_1} is sinusoidally distributed along the distance from the receiving-end with amplitude increasing exponentially with distance, as shown in Fig. 5.13 ($\alpha > 0$ for a line having resistance).

After time Δt, the distribution advances in distance phase by ($\omega \Delta t/\beta$). Thus this wave is travelling towards the receiving-end and is the *incident wave*. Line losses cause its amplitude to decrease exponentially in going from the sending- to the receiving-end.

Now

$$v_{x_2} = \sqrt{2}\left|\frac{V_R - Z_c I_R}{2}\right| e^{-\alpha x} \cos(\omega t - \beta x + \phi_2) \tag{5.40}$$

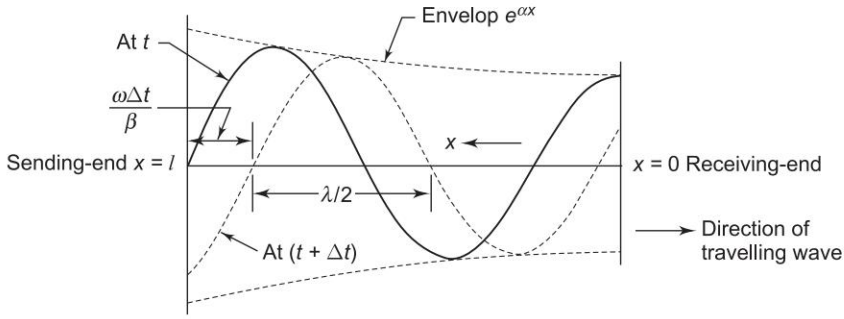

Fig. 5.13 Incident wave

After time Δt the voltage distribution retards in distance phase by $(\omega\Delta t/\beta)$. This is the *reflected wave* travelling from the receiving-end to the sending-end with amplitude decreasing exponentially in going from the receiving-end to the sending-end, as shown in Fig. 5.14.

At any point along the line, the voltage is the sum of incident and reflected voltage waves present at the point [Eq. (5.38)]. The same is true of current waves. Expressions for incident and reflected current waves can be similarly written down by proceeding from Eq. (5.21). If Z_c is pure resistance, current waves can be simply obtained from voltage waves by dividing by Z_c.

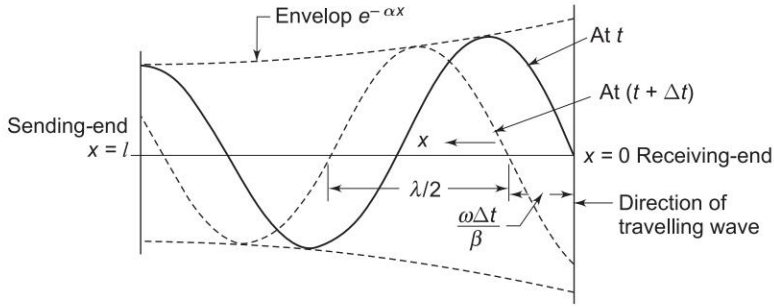

Fig. 5.14 Reflected wave

If the load impedance $Z_L = \dfrac{V_R}{I_R} = Z_c$, i.e. the line is terminated in its characteristic impedance, the reflected voltage wave is zero ($V_R - Z_c I_R = 0$).

A line terminated in its characteristic impedance is called the *infinite line*. The incident wave under this condition cannot distinguish between a termination and an infinite continuation of the line.

Power system engineers normally call Z_c the *surge impedance*. It has a value of about 400 ohms for an overhead line and its phase angle normally varies from 0° to –15°. For underground cables Z_c is roughly one-tenth of the value for overhead lines. The term surge impedance is, however, used in connection with surges (due to lightning or switching) or transmission lines, where the line loss can be neglected such that

$$Z_c = Z_s = \left(\frac{j\omega L}{-j\omega C}\right)^{1/2} = \left(\frac{L}{C}\right)^{1/2}, \text{ a pure resistance}$$

Surge Impedance Loading (SIL) of a transmission line is defined as the power delivered by a line to purely resistive load equal in value to the surge impedance of the line. Thus for a line having 400 ohms surge impedance,

$$\text{SIL} = \sqrt{3}\frac{|V_R|}{\sqrt{3}\times 400}\ |V_R| \times 1000 \text{ kW}$$

$$= 2.5\ |V_R|^2 \text{ kW} \tag{5.41}$$

where $|V_R|$ is the line-to-line receiving-end voltage in kV. Sometimes, it is found convenient to express line loading in per unit of SIL, i.e. as the ratio of the power transmitted to surge impedance loading.

At any time the voltage and current vary harmonically along the line with respect to x, the space coordinate. A complete voltage or current cycle along the line corresponds to a change of 2π rad in the angular argument βx. The corresponding line length is defined as the *wavelength*.

If β is expressed in rad/m,

$$\lambda = 2\pi/\beta \text{ m} \tag{5.42}$$

Now for a typical power transmission line

g (shunt conductance/unit length) $\simeq 0$

$r \square \omega L$

$$\therefore \quad \gamma = (yz)^{1/2} = (j\omega C(r + j\omega L))^{1/2}$$

$$= j\omega (LC)^{1/2}\left(1 - j\frac{r}{\omega L}\right)^{1/2}$$

or

$$\gamma = \alpha + j\beta \simeq j\omega(LC)^{1/2}\left(1 - j\frac{r}{2\omega L}\right)$$

$$\therefore \quad \alpha \simeq \frac{r}{2}\left(\frac{C}{L}\right)^{1/2} \tag{5.43}$$

$$\beta \simeq \omega (LC)^{1/2} \tag{5.44}$$

Now time for a phase change of 2π is $(1/f)$ sec., where $f = \omega/2\pi$ is the frequency in cycles/s. During this time the wave travels a distance equal to λ, i.e. one wavelength.

$$\therefore \quad \text{Velocity of propagation of wave, } v = \frac{\lambda}{1/f} = f\lambda \text{ m/s} \tag{5.45}$$

which is a well known result.

For a lossless transmission line ($R = 0$, $G = 0$),

$$\gamma = (yz)^{1/2} = j\omega(LC)^{1/2}$$

such that $\alpha = 0$, $\beta = \omega(LC)^{1/2}$

$$\therefore \quad \lambda = \frac{2\pi}{\beta} = \frac{2\pi}{\omega(LC)^{1/2}} = \frac{1}{f(LC)^{1/2}} \text{ m} \tag{5.46}$$

and

$$v = f\lambda = 1/(LC)^{1/2} \text{ m/s} \tag{5.47}$$

For a single-phase transmission line

$$L = \frac{\mu_0}{2\pi} \ln \frac{D}{r'}$$

$$C = \frac{2\pi k_0}{\ln D/r}$$

$$\therefore \quad v = \frac{1}{\left(\frac{\mu_0}{2\pi} \ln \frac{D}{r'} \frac{2\pi k_0}{\ln D/r}\right)^{1/2}}$$

Since r and r' are quite close to each other, when log is taken, it is sufficiently accurate to assume that $\ln \frac{D}{r'} \simeq \ln D/r$.

$$\therefore \quad v \approx \frac{1}{(\mu_0 k_0)^{1/2}} = \text{velocity of light} \tag{5.48}$$

The actual velocity of the propagation of wave along the line would be somewhat less than the velocity of light.

Wavelength of a 50 Hz power transmission is approximately given by

$$\lambda \approx \frac{3 \times 10^8}{50} = 6{,}000 \text{ km}$$

Practical transmission lines are much shorter than this (usually several hundred kilometres). **It needs to be pointed out here that the waves drawn in Figs 5.13 and 5.14 are for illustration only and do not pertain to a real power transmission line.**

Example 5.6 A three-phase 50 Hz transmission line is 400 km long. The voltage at the sending-end is 220 kV. The line parameters are $r = 0.125$ ohm/km, $x = 0.4$ ohm/km and $y = 2.8 \times 10^{-6}$ mho/km.

Find the following:

(a) The sending-end current and receiving-end voltage when there is no-load on the line.

(b) The maximum permissible line length if the receiving-end no-load voltage is not to exceed 235 kV.

(c) For part (a), the maximum permissible line frequency, if the no-load voltage is not to exceed 250 kV.

Solution

The total line parameters are:

$$R = 0.125 \times 400 = 50.0 \ \Omega$$
$$X = 0.4 \times 400 = 160.0 \ \Omega$$
$$Y = 2.8 \times 10^{-6} \times 400 \angle 90° = 1.12 \times 10^{-3} \angle 90° \ \Omega$$
$$Z = R + jX = (50.0 + j160.0) = 168.0 \angle 72.6° \ \Omega$$
$$YZ = 1.12 \times 10^{-3} \angle 90° \times 168 \angle 72.6°$$
$$= 0.188 \angle 162.6°$$

(a) At no-load

$$V_S = AV_R;\ I_S = CV_R$$

A and C are computed as follows:

$$A \simeq 1 + \frac{1}{2} YZ = 1 + \frac{1}{2} \times 0.188 \angle 162.6°$$
$$= 0.91 + j0.028$$
$$|A| = 0.91$$
$$C = Y(1 + YZ/6) = 1.12 \times 10^{-3} \angle 90° \left(1 + \frac{0.188}{6} \angle 162.6°\right)$$
$$= 1.09 \times 10^{-3} \angle 90.55°$$

Now

$$|V_R|_{\text{line}} = \frac{220}{|A|} = \frac{220}{0.91} = 242 \ \text{kV}$$
$$|I_S| = |C|\,|V_R| = 1.09 \times 10^{-3} \times \frac{242}{\sqrt{3}} \times 10^3 = 152 \ \text{A}$$

It is to be noted that under no-load conditions, the receiving-end voltage (242 kV) is more than the sending-end voltage. This phenomenon is known as the Ferranti effect and is discussed at length in Sec. 5.7.

(b) Maximum permissible no-load receiving-end voltage = 235 kV.

$$|A| = \left|\frac{V_S}{V_R}\right| = \frac{220}{235} = 0.936$$

Now

$$A \approx 1 + \frac{1}{2} YZ$$
$$= 1 + \frac{1}{2} l^2 \times j2.8 \times 10^{-6} \times (0.125 + j0.4)$$
$$= (1 - 0.56 \times 10^{-6} l^2) + j0.175 \times 10^{-6} l^2$$

Since the imaginary part will be less than $\frac{1}{10}$th of the real part, $|A|$ can be approximated as

$$|A| = 1 - 0.56 \times 10^{-6} l^2 = 0.936$$

$$\therefore \quad l^2 = \frac{1 - 0.936}{0.56 \times 10^{-6}}$$

or $$l = 338 \text{ km}$$

(c) $$|A| = \frac{220}{250} = 0.88$$

$$A \simeq 1 + \frac{1}{2} \times j1.12 \times 10^{-3} \times \frac{f}{50}\left(50 + j160 \times \frac{f}{50}\right)$$

Neglecting the imaginary part, we can write

$$|A| = 1 - \frac{1}{2} \times 1.12 \times 10^{-3} \times 160 \times \frac{f^2}{(50)^2} = 0.88$$

Simplifying, we obtain the maximum permissible frequency as

$$f = 57.9 \text{ Hz}$$

Example 5.7 If in Example 5.6 the line is open-circuited with a receiving-end voltage of 220 kV, find the rms value and phase angle of the following:

(a) The incident and reflected voltages to neutral at the receiving-end.
(b) The incident and reflected voltages to neutral at 200 km from the receiving-end.
(c) The resultant voltage at 200 km from the receiving-end.

Note: Use the receiving-end line to neutral voltage as reference.

Solution

From Example 5.6, we have following line parameters:

$$r = 0.125 \ \Omega/\text{km}; \ x = 0.4 \ \Omega/\text{km}; \ y = j2.8 \times 10^{-6} \ \Omega/\text{km}$$

$$\therefore \quad z = (0.125 + j0.4) \ \Omega/\text{km} = 0.42 \angle 72.6° \ \Omega/\text{km}$$

$$\gamma = (yz)^{1/2} = (2.8 \times 10^{-6} \times 0.42 \angle (90° + 72.6°))^{1/2}$$

$$= 1.08 \times 10^{-3} \angle 81.3°$$

$$= (0.163 + j1.068) \times 10^{-3} = \alpha + j\beta$$

$$\therefore \quad \alpha = 0.163 \times 10^{-3}; \ \beta = 1.068 \times 10^{-3}$$

(a) At the receiving-end;

For open circuit $I_R = 0$

$$\text{Incident voltage} = \frac{V_R + Z_c I_R}{2} = \frac{V_R}{2}$$

$$= \frac{220/\sqrt{3}}{2} = 63.51 \angle 0° \text{ kV (to neutral)}$$

$$\text{Reflected voltage} = \frac{V_R - Z_c I_R}{2} = \frac{V_R}{2}$$

$$= 63.51 \angle 0° \text{ kV (to neutral)}$$

(b) At 200 km from the receiving-end:

$$\text{Incident voltage} = \frac{V_R}{2} e^{\alpha x} e^{j\beta x}\Big|_{x = 200 \text{ km}}$$

$$= 63.51 \exp (0.163 \times 10^{-3} \times 200)$$

$$\times \exp (j1.068 \times 10^{-3} \times 200)$$

$$= 65.62 \angle 12.2° \text{ kV (to neutral)}$$

$$\text{Reflected voltage} = \frac{V_R}{2} e^{-\alpha x} e^{-j\beta x}\Big|_{x=200 \text{ km}}$$

$$= 63.51\, e^{-0.0326}\, e^{-j0.2135}$$

$$= 61.47 \angle -12.2° \text{ kV (to neutral)}$$

(c) Resultant voltage at 200 km from the receiving-end

$$= 65.62 \angle 12.2° + 61.47 \angle -12.2°$$

$$= 124.2 + j0.877 = 124.2 \angle 0.4°$$

Resultant line-to-line voltage at 200 km

$$= 124.2 \times \sqrt{3} = 215.1 \text{ kV}$$

5.7 FERRANTI EFFECT

As has been illustrated in Example 5.6, the effect of the line capacitance is to cause the no-load receiving-end voltage to be more than the sending-end voltage. The effect becomes more pronounced as the line length increases. This phenomenon is known as the *Ferranti effect*. A general explanation of this effect is advanced below:

Substituting $x = l$ and $I_R = 0$ (no-load) in Eq. (5.21), we have

$$V_S = \frac{V_R}{2} e^{\alpha l} e^{j\beta l} + \frac{V_R}{2} e^{-\alpha l}\, e^{-j\beta l} \tag{5.49}$$

The above equation shows that at $l = 0$, the incident (E_{i0}) and reflected (E_{r0}) voltage waves are both equal to $V_R/2$. With reference to Fig. 5.15, as l increases, the incident voltage wave increases exponentially in magnitude $\left(\frac{V_R}{2} e^{\alpha l}\right)$ and

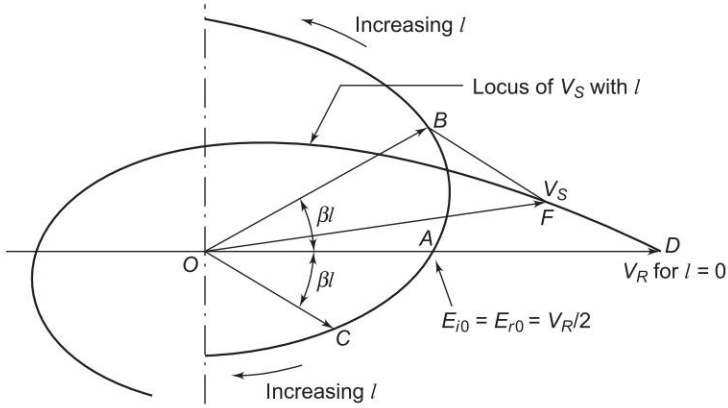

Fig. 5.15

turns through a positive angle βl (represented by phasor OB); while the reflected voltage wave decreases in magnitude exponentially $\left(\frac{V_R}{2}e^{-\alpha l}\right)$ and turns through a negative angle βl (represented by phasor OC). It is apparent from the geometry of this figure that the resultant phasor voltage $V_S\,(OF)$ is such that $|V_R| > |V_S|$.

A simple explanation of the Ferranti effect on an approximate basis can be advanced by lumping the inductance and capacitance parameters of the line. As shown in Fig. 5.16 the capacitance is lumped at the receiving-end of the line.

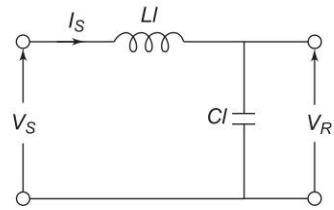

Fig. 5.16

Here
$$I_S = \frac{V_S}{\left(\frac{1}{j\omega Cl} + j\omega Ll\right)}$$

Since C is small compared to L, $\omega L\,l$ can be neglected in comparison to $1/\omega Cl$. Thus

$$I_S \simeq jV_S\omega Cl$$

Now
$$V_R = V_S - I_S(j\omega Ll) = V_S + V_S\omega^2\, CLl^2$$
$$= V_S(1 + \omega^2 CLl^2) \qquad (5.50)$$

Magnitude of voltage rise $= |V_S|\omega^2\, CLl^2$
$$= |V_S|\frac{\omega^2 l^2}{v^2} \qquad (5.51)$$

where $v = 1/\sqrt{LC}$ is the velocity of propagation of the electromagnetic wave along the line, which is nearly equal to the velocity of light.

5.8 TUNED POWER LINES

Equation (5.23) characterizes the performance of a long line. For an overhead line shunt conductance G is always negligible and it is sufficiently accurate to neglect line resistance R as well. With this approximation

$$\gamma = \sqrt{yz} = j\omega\sqrt{LC}$$

$$\cosh \gamma l = \cosh j\omega l\sqrt{LC} = \cos \omega l\sqrt{LC}$$

$$\sinh \gamma l = \sinh j\omega l\sqrt{LC} = j \sin \omega l\sqrt{LC}$$

Hence Eq. (5.23) simplifies to

$$\begin{bmatrix} V_S \\ I_S \end{bmatrix} = \begin{bmatrix} \cos \omega l\sqrt{LC} & jZ_c \sin \omega l\sqrt{LC} \\ \frac{j}{Z_c} \sin \omega l\sqrt{LC} & \cos \omega l\sqrt{LC} \end{bmatrix} \begin{bmatrix} V_R \\ I_R \end{bmatrix} \quad (5.52)$$

Now if $\omega l\sqrt{LC} = n\pi$; $n = 1, 2, 3, \ldots$

$$|V_S| = |V_R|$$

$$|I_S| = |I_R|$$

i.e. the receiving-end voltage and current are numerically equal to the corresponding sending-end values, so that there is no voltage drop on load. Such a line is called a *tuned line*.

For 50 Hz, the length of line for tuning is

$$l = \frac{n\pi}{2\pi f\sqrt{LC}}$$

Since $1/\sqrt{LC} \simeq v$, the velocity of light

$$l = \frac{1}{2}(n\lambda) = \frac{1}{2}\lambda, \lambda, \frac{3}{2}\lambda, \ldots \quad (5.53)$$

$$= 3{,}000 \text{ km}, 6{,}000 \text{ km}, \ldots$$

It is too long a distance of transmission from the point of view of cost and efficiency (note that line resistance was neglected in the above analysis). For a given line, length and frequency tuning can be achieved by increasing L or C, i.e. by adding series inductances or shunt capacitances at several places along the line length. The method is impractical and uneconomical for power frequency lines and is adopted for telephony where higher frequencies are employed.

A method of tuning power lines which is being presently experimented with, uses series capacitors to cancel the effect of the line inductance and shunt inductors to neutralize line capacitance. A long line is divided into several sections which are individually tuned. However, so far the practical method of improving line regulation and power transfer capacity is to add series capacitors to reduce line inductance; shunt capacitors under heavy load conditions; and shunt inductors under light or no-load conditions.

5.9 POWER FLOW THROUGH A TRANSMISSION LINE

So far the transmission line performance equation was presented in the form of voltage and current relationships between sending- and receiving-ends. Since loads are more often expressed in terms of real (watts/kW) and reactive (VARs/kVAR) power, it is convenient to deal with transmission line equations in the form of sending- and receiving-end complex power and voltages. While the problem of flow of power in a general network will be treated in the next chapter, the principles involved are illustrated here through a single transmission line (2-node/2-bus system) as shown in Fig. 5.17.

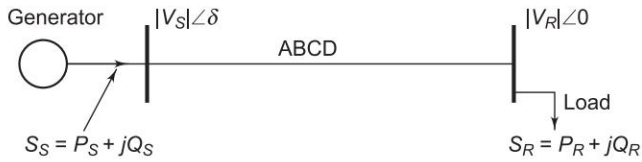

Fig. 5.17 A two-bus system

Let us take receiving-end voltage as a reference phasor ($V_R = |V_R| \angle 0^\circ$) and let the sending-end voltage lead it by an angle δ ($V_S = |V_S| \angle \delta$). The angle δ is known as the torque angle whose significance has been explained in Ch. 4 and will further be taken up in Ch. 12 while dealing with the problem of stability.

The complex power leaving the receiving-end and entering the sending-end of the transmission line can be expressed as (on per phase basis)

$$S_R = P_R + jQ_R = V_R I_R^* \tag{5.54}$$

$$S_S = P_S + jQ_S = V_S I_S^* \tag{5.55}$$

Receiving- and sending-end currents can, however, be expressed in terms of receiving- and sending-end voltages [by rearranging Eq. (5.1)] as

$$I_R = \frac{1}{B} V_S - \frac{A}{B} V_R \tag{5.56}$$

$$I_S = \frac{D}{B} V_S - \frac{1}{B} V_R \tag{5.57}$$

Let *A, B, D*, the transmission line constants, be written as

$$A = |A| \angle\alpha,\ B = |B| \angle\beta,\ D = |D| \angle\alpha \text{ (since } A = D)$$

Therefore, we can write

$$I_R = \left|\frac{1}{B}\right| |V_S| \angle(\delta - \beta) - \left|\frac{A}{B}\right| |V_R| \angle(\alpha - \beta)$$

$$I_S = \left|\frac{D}{B}\right| |V_S| \angle(\alpha + \delta - \beta) - \left|\frac{1}{B}\right| |V_R| \angle -\beta$$

Substituting for I_R in Eq. (5.54), we get

$$S_R = |V_R| \angle 0 \left[\left|\frac{1}{B}\right| |V_S| \angle(\beta - \delta) - \left|\frac{A}{B}\right| |V_R| \angle(\beta - \alpha)\right]$$

$$= \frac{|V_S||V_R|}{|B|} \angle(\beta - \delta) - \left|\frac{A}{B}\right| |V_R|^2 \angle(\beta - \alpha) \qquad (5.58)$$

Similarly,

$$S_S = \left|\frac{D}{B}\right| |V_S|^2 \angle(\beta - \alpha) - \frac{|V_S||V_R|}{|B|} \angle(\beta + \delta) \qquad (5.59)$$

In the above equations S_R and S_S are per phase complex voltamperes, while V_R and V_S are expressed in per phase volts. If V_R and V_S are expressed in kV line, then the three-phase receiving-end complex power is given by

$$S_R \text{ (three-phase VA)} = 3\left\{\frac{|V_S||V_R| \times 10^6}{\sqrt{3} \times \sqrt{3}|B|} \angle(\beta - \delta) - \left|\frac{A}{B}\right| \frac{|V_R|^2 \times 10^6}{3} \angle(\beta - \alpha)\right\}$$

$$S_R \text{ (three-phase MVA)} = \frac{|V_S||V_R|}{|B|} \angle(\beta - \delta) - 3\left|\frac{A}{B}\right| |V_R|^2 \angle(\beta - \alpha) \qquad (5.60)$$

This indeed is the same as Eq. (5.58). The same result holds for S_S. **Thus we see that Eqs (5.58) and (5.59) give the three-phase MVA if V_S and V_R are expressed in kV line.**

If Eq. (5.58) is expressed in real and imaginary parts, we can write the real and reactive powers at the receiving-end as

$$P_R = \frac{|V_S||V_R|}{|B|} \cos(\beta - \delta) - \left|\frac{A}{B}\right| |V_R|^2 \cos(\beta - \alpha) \qquad (5.61)$$

$$Q_R = \frac{|V_S||V_R|}{|B|} \sin(\beta - \delta) - \left|\frac{A}{B}\right| |V_R|^2 \sin(\beta - \alpha) \qquad (5.62)$$

Similarly, the real and reactive powers at sending-end are

$$P_S = \left|\frac{D}{B}\right| |V_S|^2 \cos(\beta - \alpha) - \frac{|V_S||V_R|}{|B|}\cos(\beta + \delta) \tag{5.63}$$

$$Q_S = \left|\frac{D}{B}\right| |V_S|^2 \sin(\beta - \alpha) - \frac{|V_S||V_R|}{|B|}\sin(\beta + \delta) \tag{5.64}$$

It is easy to see from Eq. (5.61) that the received power P_R will be maximum at

$$\delta = \beta$$

such that

$$P_R(\max) = \frac{|V_S||V_R|}{|B|} - \frac{|A||V_R|^2}{|B|}\cos(\beta - \alpha) \tag{5.65}$$

The corresponding Q_R (at max P_R) is

$$Q_R = -\frac{|A||V_R|^2}{|B|}\sin(\beta - \alpha)$$

Thus the load must draw this much leading MVAR in order to receive the maximum real power.

Consider now the special case of a short line with a series impedance Z. Now

$$A = D = 1 \angle 0;\ B = Z = |Z| \angle \theta$$

Substituting these in Eqs (5.61) to (5.64), we get the simplified results for the short line as

$$P_R = \frac{|V_S||V_R|}{|Z|}\cos(\theta - \delta) - \frac{|V_R|^2}{|Z|}\cos\theta \tag{5.66}$$

$$Q_R = \frac{|V_S||V_R|}{|Z|}\sin(\theta - \delta) - \frac{|V_R|^2}{|Z|}\sin\theta \tag{5.67}$$

for the receiving-end and for the sending-end

$$P_S = \frac{|V_S|^2}{|Z|}\cos\theta - \frac{|V_S||V_R|}{|Z|}\cos(\theta + \delta) \tag{5.68}$$

$$Q_S = \frac{|V_S|^2}{|Z|}\sin\theta - \frac{|V_S||V_R|}{|Z|}\sin(\theta + \delta) \tag{5.69}$$

The above short line equation will also apply for a long line when the line is replaced by its equivalent-π (or nominal-π) and the shunt admittances are lumped with the receiving-end load and sending-end generation. In fact, this technique is always used in the load flow problem to be treated in the next chapter.

From Eq.(5.66), the maximum receiving-end power is received, when $\delta = \theta$, so that

$$P_R\,(\max) = \frac{|V_S||V_R|}{|Z|} - \frac{|V_R|^2}{|Z|}\cos\theta$$

Now $\cos\theta = R/|Z|$,

$$\therefore \quad P_R\,(\max) = \frac{|V_S||V_R|}{|Z|} - \frac{|V_R|^2}{|Z|^2}R \tag{5.70}$$

Normally the resistance of a transmission line is small compared to its reactance (since it is necessary to maintain a high efficiency of transmission), so that $\theta = \tan^{-1} X/R \simeq 90^\circ$; where $Z = R + jX$. The receiving-end Eqs (5.66) and (5.67) can then be approximated as

$$P_R = \frac{|V_S||V_R|}{X}\sin\delta \tag{5.71}$$

$$Q_R = \frac{|V_S||V_R|}{X}\cos\delta - \frac{|V_R|^2}{X} \tag{5.72}$$

Equation (5.72) can be further simplified by assuming $\cos\delta \simeq 1$, since δ is normally small*. Thus

$$Q_R = \frac{|V_R|}{X}\,(|V_S| - |V_R|) \tag{5.73}$$

Let $|V_S| - |V_R| = |\Delta V|$, the magnitude of voltage drop across the transmission line.

$$\therefore \quad Q_R = \frac{|V_R|}{X}|\Delta V| \tag{5.74}$$

Several important conclusions that easily follow from Eqs (5.71) to (5.74) are enumerated below:

1. For $R \simeq 0$ (which is a valid approximation for a transmission line) the real power transferred to the receiving-end is proportional to $\sin\delta$ ($\simeq \delta$ for small values of δ), while the reactive power is proportional to the magnitude of the voltage drop across the line.
2. The real power received is maximum for $\delta = 90^\circ$ and has a value $|V_S||V_R|/X$. Of course, δ is restricted to values well below 90° from considerations of stability to be discussed in Ch. 12.

* Small δ is necessary from considerations of system stability which will be discussed at length in Ch. 12.

3. Maximum real power transferred for a given line (fixed X) can be increased by raising its voltage level. It is from this consideration that voltage levels are being progressively pushed up to transmit larger chunks of power over longer distances warranted by large size generating stations.

   For very long lines, voltage level cannot be raised beyond the limits placed by present-day high voltage technology. To increase power transmitted in such cases, the only choice is to reduce the line reactance. This is accomplished by adding series capacitors in the line. This idea will be pursued further in Ch. 12. Series capacitors would of course increase the severity of line over voltages under switching conditions.
4. The VARs (lagging reactive power) delivered by a line is proportional to the line voltage drop and is independent of δ. Therefore, in a transmission system if the VARs demand of the load is large, the voltage profile at that point tends to sag rather sharply. To maintain a desired voltage profile, the VARs demand of the load must be met locally by employing positive VAR generators (condensers). This will be discussed at length in Sec. 5.10.

A somewhat more accurate yet approximate result expressing line voltage drop in terms of active and reactive powers can be written directly from Eq. (5.5), i.e.

$$\begin{aligned} |\Delta V| &= |I_R|\, R\cos\phi + |I_R|\, X\sin\phi \\ &= \frac{|V_R||I_R|\, R\cos\phi + |V_R||I_R|\, X\sin\phi}{|V_R|} \\ &= \frac{RP_R + XQ_R}{|V_R|} \end{aligned} \tag{5.75}$$

This result reduces to that of Eq. (5.74) if $R = 0$.

Example 5.8 An interconnector cable links generating stations 1 and 2 as shown in Fig. 5.18. The desired voltage profile is flat, i.e. $|V_1| = |V_2| = 1$ pu. The total demands at the two buses are

$$S_{D1} = 15 + j5 \text{ pu}$$

$$S_{D2} = 25 + j15 \text{ pu}$$

The station loads are equalized by the flow of power in the cable. Estimate the torque angle and the station power factors: (a) for cable $Z = 0 + j0.05$ pu, and (b) for cable $Z = 0.005 + j0.05$ pu. It is given that generator G_1 can generate a maximum of 20.0 pu real power.

Solution

The powers at the various points in the fundamental (two-bus) system are defined in Fig. 5.18(a).

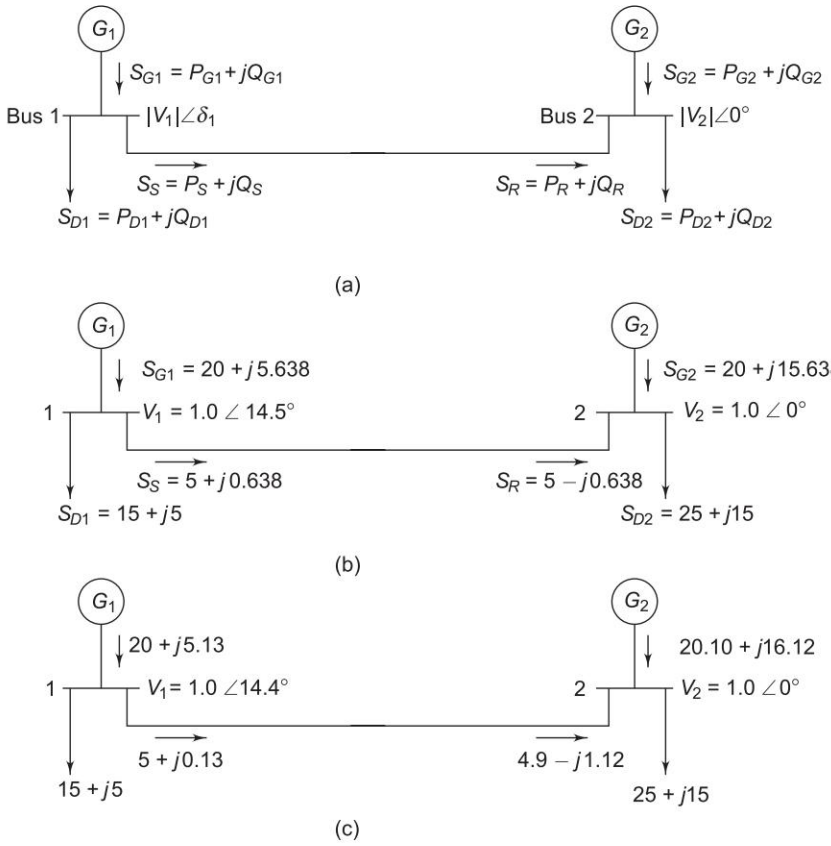

Fig. 5.18 Two-bus system

Case (a): Cable impedance = $j0.05$ pu.

Since cable resistance is zero, there is no real power loss in the cable. Hence

$$P_{G1} + P_{G2} = P_{D1} + P_{D2} = 40 \text{ pu}$$

For equalization of station loads,

$$P_{G1} = P_{G2} = 20 \text{ pu}$$

Equalization means that $P_S = P_R = 5$ MW

The voltage of bus 2 is taken as reference, i.e. $V_2 \angle 0^\circ$ and voltage of bus 1 is $V_1 \angle \delta_1$. Further, for flat voltage profile $|V_1| = |V_2| = 1$.

Real power flow from bus 1 to bus 2 is obtained from Eq. (5.58) by recognizing that since $R = 0$, $\theta = 90^\circ$.

Hence

$$P_S = P_R = \frac{|V_1||V_2|}{X} \sin \delta_1$$

$$5 = \frac{1 \times 1}{0.05} \sin \delta_1$$

or $\delta_1 = 14.5^\circ$

$\therefore$ $V_1 = 1 \angle 14.5^\circ$

From Eq. (5.69)

$$Q_S = \frac{|V_1|^2}{X} - \frac{|V_1||V_2|}{X} \cos \delta_1$$

$$= \frac{1}{0.05} - \frac{1}{0.05} \times 0.968 = 0.638 \text{ pu}$$

From Eq. (5.67)

$$Q_R = \frac{|V_1||V_2|}{X} \cos \delta_1 - \frac{|V_1|^2}{X} = -Q_S = -0.638 \text{ pu}$$

Reactive power loss* in the cable is

$$Q_L = Q_S - Q_R = 2Q_S = 1.276 \text{ pu}$$

Total load on station 1 $= (15 + j5) + (5 + j0.638)$

$$= 20 + j5.638$$

Power factor at station 1 $= \cos\left(\tan^{-1} \frac{5.638}{20}\right) = 0.963$ lagging

Total load on station 2 $= (25 + j15) - (5 - j0.638)$

$$= 20 + j15.638$$

Power factor at station 2 $= \cos\left(\tan^{-1} \frac{15.638}{20}\right) = 0.788$ lagging

The station loads, load demands, and line flows are shown in Fig. 5.18(b). It may be noted that to maintain a flat voltage profile, the generators are required to supply reactive powers $Q_{G1} = 5.638$ and $Q_{G2}=15.638$, respectively.

Case (b): Cable impedance $= 0.005 + j0.05 = 0.0502 \angle 84.3^\circ$ pu. In this case the cable resistance causes real power loss which is not known a priori. The real load flow is thus not obvious as was in the case of $R = 0$. We specify the generation at station 1 as

$$P_{G1} = 20 \text{ pu}$$

The consideration for fixing this generation is economic as we shall see in Ch. 7.

* Reactive power loss can also be computed as $|I|^2 X = \frac{5^2 + (0.638)^2}{1} \times 0.05 = 1.27$ pu.

The generation at station 2 will be 20 pu plus the cable loss. The unknown variables in the problem are

$$P_{G2},\ \delta_1,\ Q_{G1},\ Q_{G2}$$

Let us now examine as to how many system equations can be formed. From Eqs (5.68) and (5.69),

$$P_{G1} - P_{D1} = P_S = \frac{|V_1|^2}{|Z|}\cos\theta - \frac{|V_1||V_2|}{|Z|}\cos(\theta + \delta_1)$$

$$5 = \frac{1}{0.0502}\cos 84.3^\circ - \frac{1}{0.0502}\cos(84.3^\circ + \delta_1) \qquad \text{(i)}$$

$$Q_{G1} - Q_{D1} = Q_S = \frac{|V_1|^2}{|Z|}\sin\theta - \frac{|V_1||V_2|}{|Z|}\cos(\theta + \delta_1)$$

$$Q_{G1} - 5 = \frac{1}{0.0502}\sin 84.3^\circ - \frac{1}{0.0502}\sin(84.3^\circ + \delta_1) \qquad \text{(ii)}$$

From Eqs (5.66) and (5.67)

$$P_{D2} - P_{G2} = P_R = \frac{|V_1||V_2|}{|Z|}\cos(\theta - \delta_1) - \frac{|V_1|^2}{|Z|}\cos\theta$$

$$25 - P_{G2} = \frac{1}{0.0502}\cos(84.3^\circ - \delta_1) - \frac{1}{0.0502}\cos 84.3^\circ \qquad \text{(iii)}$$

$$Q_{D2} - Q_{G2} = Q_R = \frac{|V_1||V_2|}{|Z|}\sin(\theta - \delta_1) - \frac{|V_1|^2}{|Z|}\sin\theta$$

$$15 - Q_{G2} = \frac{1}{0.0502}\sin(84.3^\circ - \delta_1) - \frac{1}{0.0502}\sin 84.3^\circ \qquad \text{(iv)}$$

Thus we have four equations, Eqs (i) to (iv), in four unknowns P_{G2}, δ_1, Q_{G1}, Q_{G2}. Even though these are non-linear algebraic equations, solution is possible in this case. Solving Eq. (i) for δ_1, we have

$$\delta_1 = 14.4^\circ$$

Substituting δ_1 in Eqs (ii), (iii) and (iv), we get

$$Q_{G1} = 5.13,\ Q_{G2} = 16.12,\ P_{G2} = 20.10$$

The flow of real and reactive powers for this case is shown in Fig. 5.18 (c).

It may be noted that the real power loss of 0.1 pu is supplied by $G_2(P_{G2} = 20.10)$.

The problem presented above is a two-bus load flow problem. Explicit solution is always possible in a two-bus case. The reader should try the case when

$$Q_{G2} = j10 \text{ and } |V_2| = ?$$

The general load flow problem will be taken up in Ch. 6. It will be seen that explicit solution is not possible in the general case and iterative techniques have to be resorted to.

Example 5.9 A 275 kV transmission line has the following line constants:

$$A = 0.85 \angle 5^\circ;\ B = 200 \angle 75^\circ$$

(a) Determine the power at unity power factor that can be received if the voltage profile at each end is to be maintained at 275 kV.
(b) What type and rating of compensation equipment would be required if the load is 150 MW at unity power factor with the same voltage profile as in part (a)?
(c) With the load as in part (b), what would be the receiving-end voltage if the compensation equipment is not installed?

Solution

(a) Given $|V_S| = |V_R| = 275$ kV; $\alpha = 5^\circ$, $\beta = 75^\circ$. Since the power is received at unity power factor,

$$Q_R = 0$$

Substituting these values in Eq. (5.62), we can write

$$0 = \frac{275 \times 275}{200} \sin(75^\circ - \delta) - \frac{0.85}{200} \times (275)^2 \sin(75^\circ - 5^\circ)$$

$$0 = 378 \sin(75^\circ - \delta) - 302$$

which gives

$$\delta = 22^\circ$$

From Eq. (5.61)

$$P_R = \frac{275 \times 275}{200} \cos(75^\circ - 22^\circ) - \frac{0.85}{200} \times (275)^2 \cos 70^\circ$$

$$= 227.6 - 109.9 = 117.7 \text{ MW}$$

(b) Now $|V_S| = |V_R| = 275$ kV

Power demanded by load = 150 MW at UPF

$$\therefore \quad P_D = P_R = 150 \text{ MW};\ Q_D = 0$$

From Eq. (5.61)

$$150 = \frac{275 \times 275}{200} \cos(75^\circ - \delta) - \frac{0.85}{200} \times (275)^2 \cos 70^\circ$$

$$150 = 378 \cos (75^\circ - \delta) - 110$$

or $$\delta = 28.46^\circ$$

From Eq. (5.62)

$$Q_R = \frac{275 \times 275}{200} \sin (75^\circ - 28.46^\circ) - \frac{0.85}{200} \times (275)^2 \sin 70^\circ$$

$$= 274.46 - 302 = -27.56 \text{ MVAR}$$

Thus in order to maintain 275 kV at a receiving-end, $Q_R = -27.56$ MVAR must be drawn along with the real power of $P_R = 150$ MW. The load being 150 MW at unity power factor, i.e. $Q_D = 0$, compensation equipment must be installed at the receiving-end. With reference to Fig. 5.19, we have

$$-27.56 + Q_C = 0$$

or $$Q_C = +27.56 \text{ MVAR}$$

i.e. the compensation equipment must feed positive VARs into the line. See subsection 5.10 for a more detailed explanation.

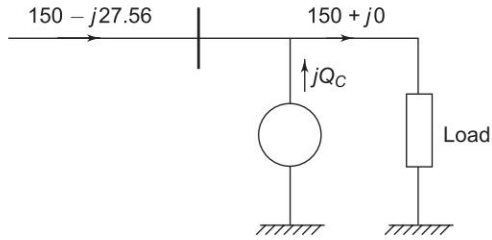

Fig. 5.19

(c) Since no compensation equipment is provided

$$P_R = 150 \text{ MW}, Q_R = 0$$

Now,

$$|V_S| = 275 \text{ kV}, |V_R| = ?$$

Substituting this data in Eqs (5.61) and (5.62), we have

$$150 = \frac{275 |V_R|}{200} \cos (75^\circ - \delta) - \frac{0.85}{200} |V_R|^2 \cos 70^\circ \quad \text{(i)}$$

$$0 = \frac{275 |V_R|}{200} \sin (75^\circ - \delta) - \frac{0.85}{200} |V_R|^2 \sin 70^\circ \quad \text{(ii)}$$

From Eq. (ii), we get

$$\sin (75^\circ - \delta) = 0.0029 |V_R|$$

$$\therefore \quad \cos (75^\circ - \delta) = (1 - (0.0029)^2 |V_R|^2)^{1/2}$$

Substituting in Eq. (i), we obtain

$$150 = 1.375\,|V_R|\,(1 - (0.0029)^2\,|V_R|^2)^{1/2} - 0.00145|V_R|^2$$

Solving the quadratic and retaining the higher value of $|V_R|$, we obtain

$$|V_R| = 244.9 \text{ kV}$$

Note: The second and lower value solution of $|V_R|$, though feasible, is impractical as it corresponds to abnormally low voltage and efficiency.

It is to be observed from the results of this problem that larger power can be transmitted over a line with a fixed voltage profile by installing compensation equipment at the receiving-end capable of feeding positive VARs into the line.

Circle Diagrams

It has been shown above that the flow of active and reactive power over a transmission line can be handled computationally. It will now be shown that the locus of complex sending- and receiving-end power is a circle. Since circles are convenient to draw, the circle diagrams are a useful aid to visualize the load flow problem over a single transmission line.

The expressions for complex number receiving- and sending-end powers are reproduced below from Eqs (5.58) and (5.59),

$$S_R = -\left|\frac{A}{B}\right| |V_R|^2 \angle(\beta - \alpha) + \frac{|V_S||V_R|}{|B|}\angle(\beta - \delta) \tag{5.58}$$

$$S_S = \left|\frac{D}{B}\right| |V_R|^2 \angle(\beta - \alpha) - \frac{|V_S||V_R|}{|B|}\angle(\beta + \delta) \tag{5.59}$$

The units for S_R and S_S are MVA (three-phase) with voltages in kV line. As per the above equations, S_R and S_S are each composed of two phasor components—one a constant phasor and the other a phasor of fixed magnitude but variable angle. The loci for S_R and S_S would, therefore, be circles drawn from the tip of constant phasors as centres.

It follows from Eq. (5.58) that the centre of receiving-end circle is located at the tip of the phasor

$$-\left|\frac{A}{B}\right| |V_R|^2 \angle(\beta - \alpha) \tag{5.76}$$

in polar coordinates or in terms of rectangular coordinates.

Horizontal coordinate of the centre

$$= -\left|\frac{A}{B}\right| |V_R|^2 \cos(\beta - \alpha) \text{ MW} \tag{5.77}$$

Vertical coordinate of the centre

$$= -\left|\frac{A}{B}\right| |V_R|^2 \sin(\beta - \alpha) \text{ MVAR}$$

The radius of the receiving-end circle is

$$\frac{|V_S||V_R|}{|B|} \text{ MVA} \tag{5.78}$$

The receiving-end circle diagram is drawn in Fig. 5.20. The centre is located by drawing OC_R at an angle $(\beta - \alpha)$ in the positive direction from the negative MW-axis. From the centre C_R the receiving-end circle is drawn with the radius $|V_S|\ |V_R|/|B|$. The operating point M is located on the circle by means of the received real power P_R. The corresponding Q_R (or θ_R) can be immediately read from the circle diagram. The torque angle δ can be read in accordance with the positive direction indicated from the reference line.

For constant $|V_R|$, the centre C_R remains fixed and concentric circles result for varying $|V_S|$. However, for the case of constant $|V_S|$ and varying $|V_R|$ the centres of circles move along the line OC_R and have radii in accordance to $|V_S|\ |V_R|/|B|$.

Similarly, it follows from Eq. (5.59) that the centre of the sending-end circle is located at the tip of the phasor

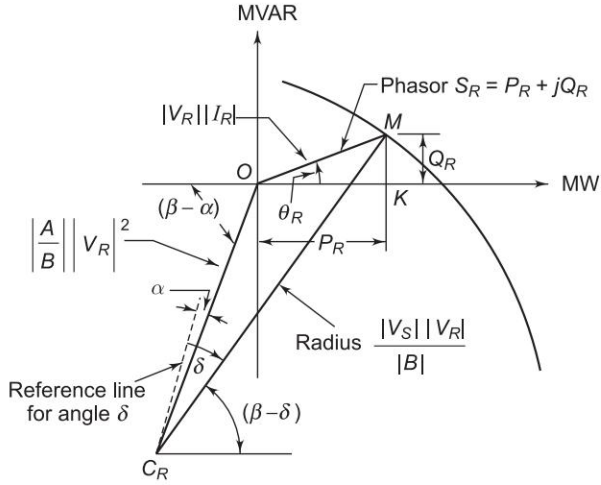

Fig. 5.20 Receiving-end circle diagram

$$\left|\frac{D}{B}\right||V_S|^2 \angle(\beta - \alpha) \tag{5.79}$$

in the polar coordinates or in terms of rectangular coordinates.

Horizontal coordinate of the centre

$$= \left|\frac{D}{B}\right||V_S|^2 \cos(\beta - \alpha) \text{ MW} \tag{5.80}$$

Vertical coordinate of the centre

$$= \left|\frac{D}{B}\right||V_S|^2 \sin(\beta - \alpha) \text{ MVAR}$$

The radius of the sending-end circle is

$$\frac{|V_S||V_R|}{|B|} \tag{5.81}$$

The sending-end circle diagram is shown in Fig. 5.21. The centre is located by drawing OC_S at angle $(\beta - \alpha)$ from the positive MW-axis. From the centre the sending-end circle is drawn with a radius $\frac{|V_S||V_R|}{|B|}$ (same as in the case of receiving-end). The operating point N is located by measuring the torque angle δ (as read from the receiving-end circle diagram) in the direction indicated from the reference line.

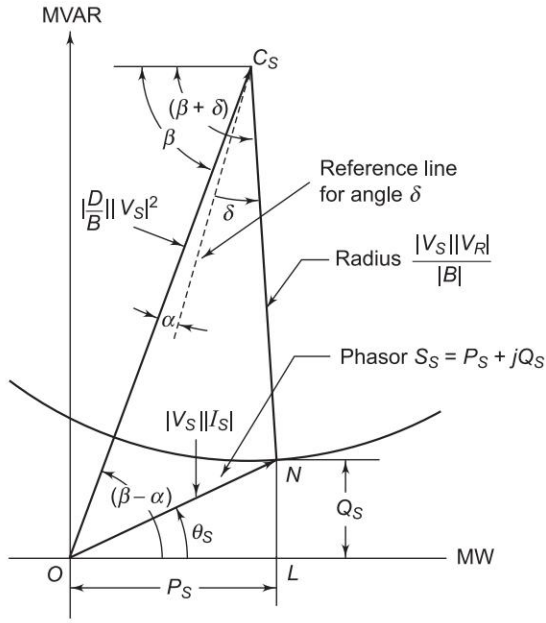

Fig. 5.21 Sending-end circle diagram

For constant $|V_S|$ the centre C_S remains fixed and concentric circles result for varying $|V_R|$. However, if $|V_R|$ is fixed and $|V_S|$ varies, the centres of the circles move along the line OC_S and have radii in accordance to $|V_S|\,|V_R|/|B|$.

For the case of a short line with a series impedance $|Z| \angle\theta$, the simplified circle diagrams can be easily drawn by recognizing

$$|A| = |D| = 1,\ \alpha = 0$$

$$|B| = |Z|, \qquad \beta = \theta$$

The corresponding receiving- and sending-end circle diagrams have been drawn in Figs 5.22 and 5.23.

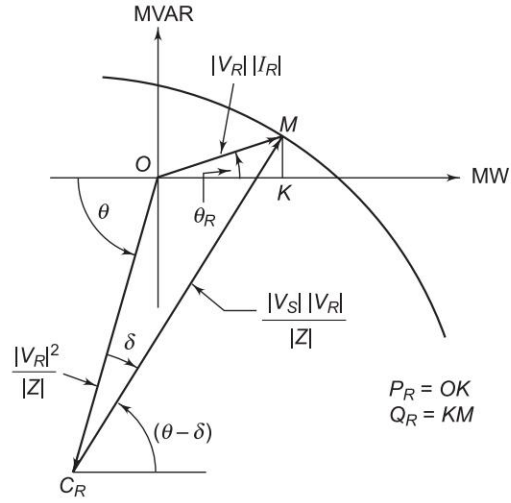

Fig. 5.22 Receiving-end circle diagram for a short line

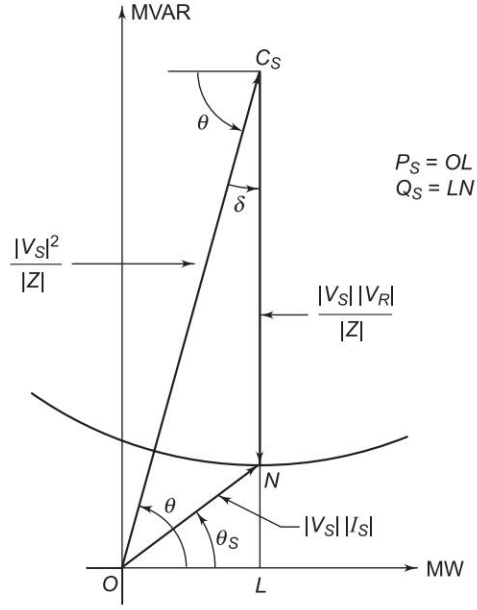

Fig. 5.23 Sending-end circle diagram for a short line

The use of circle diagrams is illustrated by means of the two examples given below:

Example 5.10 A 50 Hz, three-phase, 275 kV, 400 km transmission line has the following parameters:

Resistance = 0.035 Ω/km per phase
Inductance = 1.1 mH/km per phase
Capacitance = 0.012 μF/km per phase

If the line is supplied at 275 kV, determine the MVA rating of a shunt reactor having negligible losses that would be required to maintain 275 kV at the receiving-end when the line is delivering no load. Use nominal-π method.

Solution

$$R = 0.035 \times 400 = 14 \ \Omega$$

$$X = 314 \times 1.1 \times 10^{-3} \times 400 = 138.2 \ \Omega$$

$$Z = 14 + j138 = 138.7 \angle 84.2^\circ \ \Omega$$

$$Y = 314 \times 0.012 \times 10^{-6} \times 400 \angle 90^\circ = 1.507 \times 10^{-3} \angle 90^\circ \ \text{℧}$$

$$A = \left(1 + \frac{1}{2}YZ\right) = 1 + \frac{1}{2} \times 1.507 \times 10^{-3} \times 138.7 \angle 174.2^\circ$$

$$= (0.896 + j0.0106) = 0.896 \angle 0.7^\circ$$

$$B = Z = 138.7 \angle 84.2^\circ$$

$$|V_S| = 275 \ \text{kV}, |V_R| = 275 \ \text{kV}$$

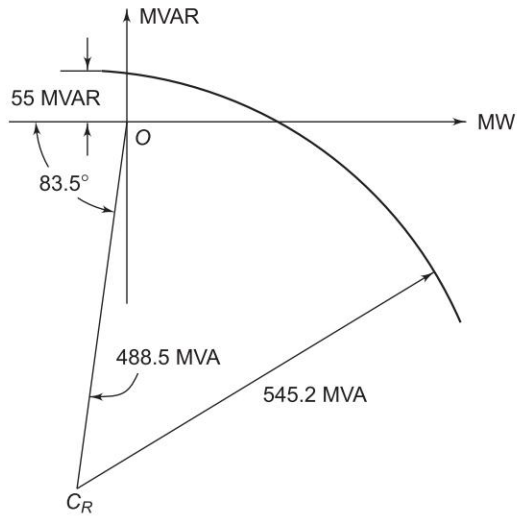

Fig. 5.24 Circle diagram for Example 5.10

Radius of receiving-end circle $= \dfrac{|V_S||V_R|}{|B|} = \dfrac{275 \times 275}{138.7} = 545.2$ MVA

Location of the centre of receiving-end circle,

$$\left|\frac{A}{B}\right||V_R|^2 = \frac{275 \times 275 \times 0.896}{138.7} = 488.5 \text{ MVA}$$

$$\angle(\beta - \alpha) = 84.2^\circ - 0.7^\circ = 83.5^\circ$$

From the circle diagram of Fig. 5.24, +55 MVAR must be drawn from the receiving-end of the line in order to maintain a voltage of 275 kV. Thus rating of shunt reactor needed = 55 MVA.

Example 5.11 A 275 kV, three-phase line has the following line parameters:

$$A = 0.93 \angle 1.5^\circ, \; B = 115 \angle 77^\circ$$

If the receiving-end voltage is 275 kV, determine:

(a) The sending-end voltage required if a load of 250 MW at 0.85 lagging pf is being delivered at the receiving-end.
(b) The maximum power that can be delivered if the sending-end voltage is held at 295 kV.
(c) The additional MVA that has to be provided at the receiving-end when delivering 400 MVA at 0.8 lagging pf, the supply voltage being maintained at 295 kV.

Solution

In Fig. 5.25 the centre of the receiving-end circle is located at

$$\left|\frac{A}{B}\right||V_R|^2 = \frac{275 \times 275 \times 0.93}{115} = 611.6 \text{ MVA}$$

$$\cos^{-1} 0.85 = 31.8^\circ$$

$$\angle(\beta - \alpha) = 77^\circ - 1.5^\circ = 75.5^\circ$$

(a) Locate OP corresponding to the receiving-end load of 250 MW at 0.85 lagging pf (+ 31.8°). Then

$$C_R P = 850 = \frac{|V_S||V_R|}{|B|} = \frac{275|V_S|}{115}$$

$$\therefore \quad |V_S| = 355.5 \text{ kV}$$

(b) Given $|V_S| = 295$ kV

$$\text{Radius of circle diagram} = \frac{295 \times 275}{115} = 705.4 \text{ MVA}$$

Drawing the receiving-end circle (see Fig. 5.25) and the line $C_R Q$ parallel to the MW-axis, we read

$$P_{R\,\max} = RQ = 556 \text{ MW}$$

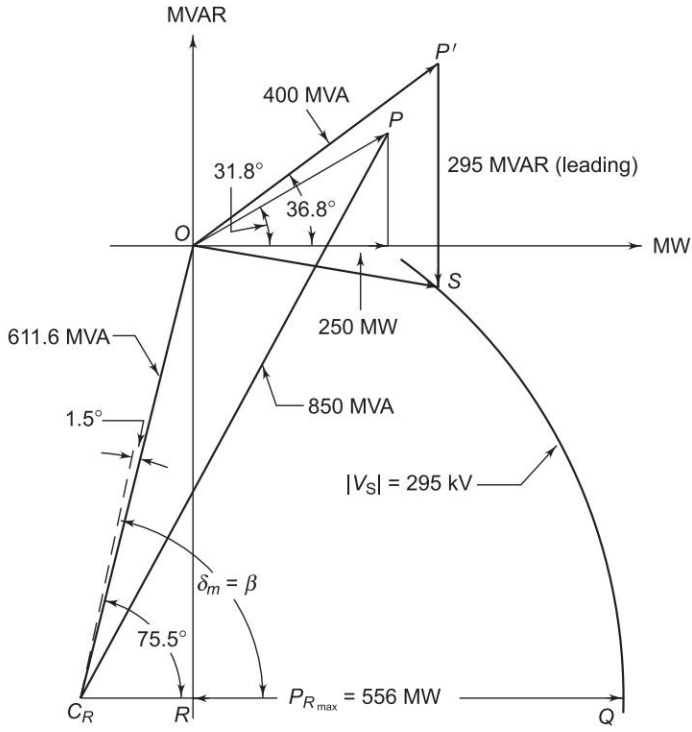

Fig. 5.25 Circle diagram for Example 5.11

(c) Locate OP' corresponding to 400 MVA at 0.8 lagging pf (+ 36.8°). Draw $P'S$ parallel to MVAR-axis to cut the circle drawn in part (b) at S. For the specified voltage profile, the line load should be OS. Therefore, additional MVA to be drawn from the line is

$$P'S = 295 \text{ MVAR or } 295 \text{ MVA leading}$$

5.10 METHODS OF VOLTAGE CONTROL

Practically all equipments used in power system is rated for a certain voltage with a permissible band of voltage variations. Voltage at various buses must, therefore, be controlled within a specified regulation figure. This article will discuss the two methods by means of which voltage at a bus can be controlled.

Consider the two-bus system shown in Fig. 5.26 (already exemplified in Sec. 5.9). For the sake of simplicity let the line be characterized by a series reactance (i.e. it has negligible resistance). Further, since the torque angle δ is small under practical conditions, real and reactive powers delivered by the line for fixed sending-end voltage $|V_S|$ and a specified receiving-end voltage $|V_R^s|$ can be written as below from Eqs (5.71) and (5.73).

$$P_R = \frac{|V_S||V_R^s|}{X} \sin \delta \qquad (5.82)$$

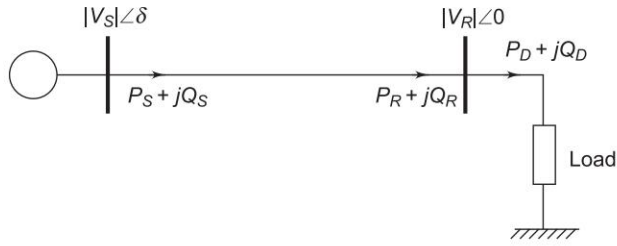

Fig. 5.26 A two-bus system

$$Q_R^s = \frac{|V_R^s|}{X}(|V_S| - |V_R^s|) \tag{5.83}$$

Equation (5.83) upon quadratic solution* can also be written as

$$|V_R^s| = \frac{1}{2}|V_S| + \frac{1}{2}|V_S|\,(1 - 4XQ_R^s/|V_S|^2)^{1/2} \tag{5.84}$$

Since the real power demanded by the load must be delivered by the line,

$$P_R = P_D$$

Varying real power demand P_D is met by consequent changes in the torque angle δ.

It is, however, to be noted that the received reactive power of the line must remain fixed at Q_R^s as given by Eq. (5.83) for fixed $|V_S|$ and specified $|V_R^s|$. The line would, therefore, operate with specified receiving-end voltage for only one value of Q_D given by

$$Q_D = Q_R^s$$

Practical loads are generally lagging in nature and are such that the VAR demand Q_D may exceed Q_R^s. It easily follows from Eq. (5.83) that for $Q_D > Q_R^s$ the receiving-end voltage must change from the specified value $|V_R^s|$ to some value $|V_R|$ to meet the demanded VARs. Thus

$$Q_D = Q_R = \frac{|V_R|}{X}\,(|V_S| - |V_R|) \text{ for } (Q_D > Q_R^s)$$

The modified $|V_R|$ is then given by

$$|V_R| = \frac{1}{2}|V_S| + \frac{1}{2}|V_S|\,(1 - 4XQ_R/|V_S|^2)^{1/2} \tag{5.85}$$

Comparison of Eqs (5.84) and (5.85) reveals that for $Q_D = Q_R = Q_R^s$, the receiving-end voltage is $|V_R^s|$, but for $Q_D = Q_R > Q_R^s$,

$$|V_R| < |V_R^s|$$

* Negative sign in the quadratic solution is rejected because otherwise the solution would not match the specified receiving-end voltage which is only slightly less than the sending-end voltage (the difference is less than 12%).

Thus a VAR demand larger than Q_R^s is met by a consequent fall in receiving-end voltage from the specified value. Similarly, if the VAR demand is less than Q_R^s, it follows that

$$|V_R| > |V_R^s|$$

Indeed, under light load conditions, the charging capacitance of the line may cause the VAR demand to become negative resulting in the receiving-end voltage exceeding the sending-end voltage (this is the Ferranti effect already illustrated in Subsection 5.7).

In order to regulate the line voltage under varying demands of VARs, the two methods discussed below are employed.

Reactive Power Injection

It follows from the above discussion that in order to keep the receiving-end voltage at a specified value $|V_R^s|$, a fixed amount of VARs (Q_R^s) must be drawn from the line.* To accomplish this under conditions of a varying VAR demand Q_D, a local VAR generator (controlled reactive source/compensating equipment) must be used as shown in Fig. 5.27. The VAR balance equation at the receiving-end is now

$$Q_R^s + Q_C = Q_D$$

Fluctuations in Q_D are absorbed by the *local VAR generator* Q_C such that the VARs drawn from the line remain fixed at Q_R^s. The receiving-end voltage would thus remain fixed at $|V_R^s|$ (this of course assumed a fixed sending-end voltage $|V_S|$). Local VAR compensation can, in fact, be made automatic by using the signal from the VAR meter installed at the receiving-end of the line.

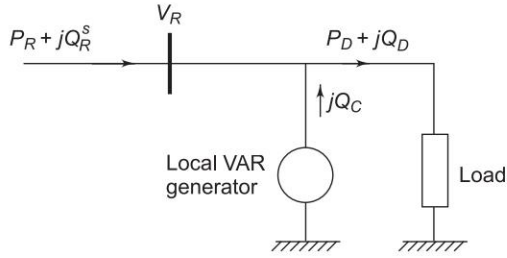

Fig. 5.27 Use of local VAR generator at the load bus

Two types of VAR generators are employed in practice—*static type* and *rotating type*. These are discussed below:

Static VAR generator

It is nothing but a bank of three-phase static capacitors and/or inductors. With reference to Fig. 5.28, if $|V_R|$ is in line kV, and X_C is the per phase capacitive

* Of course, since $|V_R^S|$ is specified within a band, Q_R^S may vary within a corresponding band.

reactance of the capacitor bank on an equivalent star basis, the expression for the VARs fed into the line can be derived as under.

$$I_C = j\frac{|V_R|}{\sqrt{3}X_C} \text{ kA}$$

$$jQ_C\,(\text{three-phase}) = 3\frac{|V_R|}{\sqrt{3}}\,(-I^*_C)$$

$$= j3 \times \frac{|V_R|}{\sqrt{3}} \times \frac{|V_R|}{\sqrt{3}X_C} \text{ MVA}$$

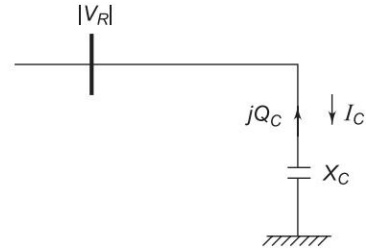

Fig. 5.28 Static capacitor bank

$$\therefore \qquad Q_C\,(\text{three-phase}) = \frac{|V_R|^2}{X_C} \text{ MVAR} \tag{5.86}$$

If inductors are employed instead, VARs fed into the line are

$$Q_L(\text{three-phase}) = -\frac{|V_R|^2}{X_L} \text{ MVAR} \tag{5.87}$$

Under heavy load conditions, when positive VARs are needed, capacitor banks are employed; while under light load conditions, when negative VARs are needed, inductor banks are switched on.

The following observations can be made for static VAR generators:

(i) Capacitor and inductor banks can be switched on in steps. However, stepless (smooth) VAR control can now be achieved using SCR (Silicon Controlled Rectifier) circuitry.

(ii) Since Q_C is proportional to the square of terminal voltage, for a given capacitor bank, their effectiveness tends to decrease as the voltage sags under full load conditions.

(iii) If the system voltage contains appreciable harmonics, the fifth being the most troublesome, the capacitors may be overloaded considerably.

(iv) Capacitors act as short circuit when switched 'on'.

(v) There is a possibility of series resonance with the line inductance particularly at harmonic frequencies.

Rotating VAR generator

It is nothing but a synchronous motor running at no-load and having excitation adjustable over a wide range. It feeds positive VARs into the line under overexcited conditions and feeds negative VARs when underexcited. A machine thus running is called a *synchronous condenser*.

Figure 5.29 shows a synchronous motor connected to the receiving-end bus bars and running at no load. Since the motor draws negligible real power from the bus bars, E_G and V_R are nearly in phase. X_S is the synchronous reactance of the motor which is assumed to have negligible resistance. If $|E_G|$ and $|V_R|$ are in line kV, we have

$$I_C = \frac{(|V_R| - |E_G|)\angle 0^\circ}{\sqrt{3} \times jX_S} \text{ kA}$$

$$jQ_C = 3\frac{|V_R|\angle 0^\circ}{\sqrt{3}}(-I^*_C)$$

$$= 3\frac{|V_R|}{\sqrt{3}}\left(-\frac{|V_R| - |E_G|}{-jX_S\sqrt{3}}\right)$$

$$= j|V_R|(|E_G| - |V_R|)/X_S \text{ MVA}$$

$$\therefore \quad Q_C = |V_R|(|E_G| - |V_R|)/X_S \text{ MVAR} \qquad (5.88)$$

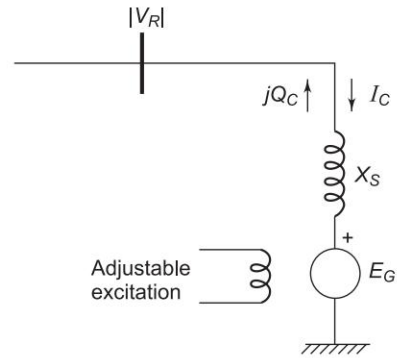

Fig. 5.29 Rotating VAR generation

It immediately follows from the above relationship that the machine feeds positive VARs into the line when $|E_G| > |V_R|$ (overexcited case) and injects negative VARs if $|E_G| < |V_R|$ (underexcited case). VARs are easily and continuously adjustable by adjusting machine excitation which controls $|E_G|$.

In contrast to static VAR generators, the following observations are made in respect of rotating VAR generators.

(i) These can provide both positive and negative VARs which are continuously adjustable.

(ii) VAR injection at a given excitation is less sensitive to changes in bus voltage. As $|V_R|$ decreases and $(|E_G| - |V_R|)$ increases with consequent smaller reduction in Q_C compared to the case of static capacitors.

From the observations made above in respect of static and rotating VAR generators, it seems that rotating VAR generators would be preferred. However, economic considerations, installation and maintenance problems limit their practical use to such buses in the system where a large amount of VAR injection is needed.

Control by Transformers

The VAR injection method discussed above lacks the flexibility and economy of voltage control by transformer tap changing. The transformer tap changing is obviously limited to a narrow range of voltage control. If the voltage correction needed exceeds this range, tap changing is used in conjunction with the VAR injection method.

Receiving-end voltage which tends to sag owing to VARs demanded by the load, can be raised by simultaneously changing the taps of sending- and receiving-end transformers. Such tap changes must be made 'on-load' and can be done either manually or automatically, the transformer being called a Tap Changing Under Load (TCUL) transformer.

Consider the operation of a transmission line with a tap changing transformer at each end as shown in Fig. 5.30. Let t_S and t_R be the fractions of the nominal transformation ratios, i.e. the tap ratio/nominal ratio. For example, a transformer with nominal ratio 3.3 kV/11 kV when tapped to give 12 kV with 3.3 kV input has $t_S = 12/11 = 1.09$.

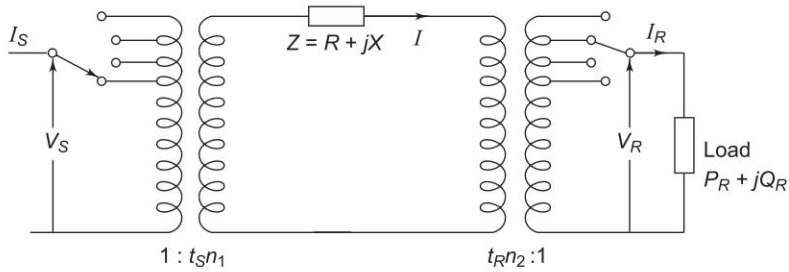

Fig. 5.30 Transmission line with tap changing transformer at each end

With reference to Fig. 5.30 let the impedances of the transformer be lumped in Z along with the line impedance. To compensate for voltage in the line and transformers, let the transformer taps be set at off nominal values, t_S and t_R. With reference to the circuit shown, we have

$$t_S n_1 V_S = t_R n_2 V_R + IZ \tag{5.89}$$

From Eq. (5.75) the voltage drop referred to the high voltage side is given by

$$|\Delta V| = \frac{RP_R + XQ_R}{t_R n_2 \,|V_R|} \tag{5.90}$$

Now $$|\Delta V| = t_S n_1 \,|V_S| - t_R n_2 |V_R|$$

$$\therefore \quad t_S n_1 |V_S| = t_R n_2 \,|V_R| + \frac{RP_R + XQ_R}{t_R n_2 \,|V_R|} \tag{5.91}$$

In order that the voltage on the HV side of the two transformers be of the same order and the tap setting of each transformer be the minimum, we choose

$$t_S t_R = 1 \tag{5.92}$$

Substituting $t_R = 1/t_S$ in Eq. (5.91) and reorganizing, we obtain

$$t_S^2 \left(1 - \frac{RP_R + XQ_R}{n_1 n_2 \,|V_S|\,|V_R|}\right) = \frac{n_2}{n_1} \frac{|V_R|}{|V_S|} \tag{5.93}$$

For complete voltage drop compensation, the right hand side of Eq. (5.93) should be unity.

It is obvious from Fig. 5.30 that $t_S > 1$ and $t_R < 1$ for voltage drop compensation. Equation (5.90) indicates that t_R tends to increase* the voltage $|\Delta V|$ which is to be compensated. Thus merely tap setting as a method of voltage drop compensation would give rise to excessively large tap setting if compensation exceeds certain limits. Thus, if the tap setting dictated by Eq. (5.93), to achieve a desired receiving-end voltage exceeds the normal tap setting range (usually not more than $\pm$ 20%), it would be necessary to simultaneously inject VARs at the receiving-end in order to maintain the desired voltage level.

Control by Mid-Line Boosters

It may be desirable on technical or economic grounds, to increase the voltage at an intermediate point in a line rather than at the ends as with tap-changing transformers. Boosters are generally used in distribution feeders where the cost of tap-changing transformers is not warranted. Fig. 5.31 shows the connection of in-phase booster transformer.

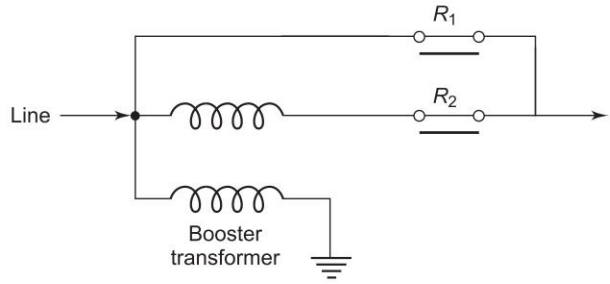

Fig. 5.31 Booster transformer

The booster can be pressed into the circuit by closure of relay R_2 and the opening of relay R_1 and vice versa.

Owing to increasing voltages and line lengths, and also the greater use of cables, the light-load reactive problem for an interconnected system becomes significant, specially with latest generators of limited VAR absorption capability. At peak load, transmission systems are required to increase their VAR generation, and as the load reduces during light load period, they need to reduce the generated VARs by the following methods listed in order of economic viability:

(i) switch out shunt capacitors,
(ii) switch in shunt reactors,
(iii) run hydro plant on maximum VAR absorption,
(iv) switch out one cable in a double-circuit link,
(v) tap-stagger transformers,
(vi) run base load generators at maximum VAR absorption.

* This is so because $t_R < 1$ increases the line current I and hence voltage drop.

Compensation of Transmission Lines

The performance of long EHV AC transmission systems can be improved by reactive compensation of series or shunt (parallel) type. Series capacitors and shunt reactors are used to reduce artificially the series reactance and shunt susceptance of lines and thus they act as the line compensators. Compensation of lines results in improving the system stability (Ch. 12) and voltage control, in increasing the efficiency of power transmission, facilitating line energization and reducing temporary and transient overvoltages.

Series capacitor compensation reduces the series impedance of the line which causes voltage drop and is the most important factor in finding the maximum power transmission capability of a line (Eq. 5.70). *A, C* and *D* constants are functions of *Z* and therefore are also affected by change in the value of *Z*, but these changes are small in comparison to the change in *B* as $B = Z$ for the nominal-π and equals Z (sinh $\gamma l / \gamma l$) for the equivalent-π.

The voltage drop ΔV due to series compensation is given by

$$\Delta V \approx IR \cos \phi_r + I(X_L - X_C) \sin \phi_r \tag{5.94}$$

Here X_C is the capacitive reactance of the series capacitor bank per phase and X_L is the total inductive reactance of the line/phase. In practice, X_C may be so selected that the factor $(X_L - X_C) \sin \phi_r$ becomes negative and equals (in magnitude) $R \cos \phi_r$ so that ΔV becomes zero. The ratio X_C/X_L is called "compensation factor" and when expressed as a percentage is known as the "percentage compensation".

The extent of effect of compensation depends on the number, location and circuit arrangements of series capacitor and shunt reactor stations. While planning long-distance lines, besides the average degree of compensation required, it is required to find out the most appropriate location of the reactors and capacitor banks, the optimum connection scheme and the number of intermediate stations. For finding the operating conditions along the line, the *ABCD* constants of the portions of line on each side of the capacitor bank, and *ABCD* constants of the bank may be first found out and then equivalent constants of the series combination of line-capacitor-line can then be arrived at by using the formulae given in Appendix B.

In India, in states like UP, series compensation is quite important since super thermal plants are located (east) several hundred kilometers from load centres (west) and large chunks of power must be transmitted over long distances. Series capacitors also help in balancing the voltage drop of two parallel lines.

When series compensation is used, there are chances of sustained overvoltage to the ground at the series capacitor terminals. This overvoltage can be the power limiting criterion at high degree of compensation. A spark gap with a high speed contactor is used to protect the capacitors under overvoltage conditions.

Under light load or no-load conditions, charging current should be kept less than the rated full-load current of the line. The charging current is approximately given by $B_C|V|$ where B_C is the total capacitive susceptance of the line

and $|V|$ is the rated voltage to neutral. If the total inductive susceptance is B_L due to several inductors connected (shunt compensation) from line to neutral at appropriate places along the line, then the charging current would be

$$I_{\text{chg}} = (B_C - B_L)\,|V| = B_C|\,V\,|\left(1 - \frac{B_L}{B_C}\right) \tag{5.95}$$

Reduction of the charging current is by the factor of $(1 - B_L/B_C)$ and B_L/B_C is the shunt compensation factor. Shunt compensation at no-load also keeps the receiving-end voltage within limits which would otherwise be quite high because of the Ferranti effect. Thus reactors should be introduced as load is removed for proper voltage control.

As mentioned earlier, the shunt capacitors are used across an inductive load so as to provide part of the reactive VARs required by the load to keep the voltage within desirable limits. Similarly, the shunt reactors are kept across capacitive loads or in light load conditions, as discussed above, to absorb some of the leading VARs for achieving voltage control. Capacitors are connected either directly to a bus or through tertiary winding of the main transformer and are placed along the line to minimize losses and the voltage drop.

It may be noted that for the same voltage boost, the reactive power capacity of a shunt capacitor is greater than that of a series capacitor. The shunt capacitor improves the pf of the load while the series capacitor has hardly any impact on the pf. Series capacitors are more effective for long lines for improvement of system stability.

Thus, we see that in both series and shunt compensation of long transmission lines it is possible to transmit large amounts of power efficiently with a flat voltage profile. Proper type of compensation should be provided in proper quantity at appropriate places to achieve the desired voltage control. The reader is encouraged to read the details about the Static Var Systems (SVS) in Refs [7, 8 , 16].

5.11 SUMMARY

In this chapter modelling, characteristics and performance of power transmission lines have been dealt with in considerable details. This is a prerequisite for future chapters and further studies in power systems.

Problems

5.1 A three-phase voltage of 11 kV is applied to a line having $R = 10\ \Omega$ and $X = 12\ \Omega$ per conductor. At the end of the line is a balanced load of P kW at a leading power factor. At what value of P is the voltage regulation zero when the power factor of the load is (a) 0.707, (b) 0.85?

5.2 A long line with $A = D = 0.9 \angle 1.5^\circ$ and $B = 150 \angle 65^\circ\ \Omega$ has at the load end a transformer having a series impedance $Z_T = 100 \angle 67^\circ\ \Omega$. The load voltage and current are V_L and I_L. Obtain expressions for V_S and I_S in form of

$$\begin{bmatrix} V_S \\ I_S \end{bmatrix} = \begin{bmatrix} A' & B' \\ C' & D' \end{bmatrix} \begin{bmatrix} V_L \\ I_L \end{bmatrix}$$

and evaluate these constants.

5.3 A three-phase overhead line 200 km long has resistance = 0.16 Ω/km and conductor diameter of 2 cm with spacing 4 m, 5 m and 6 m transposed. *Find:* (a) the *ABCD* constants using Eq. (5.28b), (b) the V_S, I_S, pf_S, P_S when the line is delivering full load of 50 MW at 132 kV and 0.8 lagging pf, (c) efficiency of transmission, and (d) the receiving-end voltage regulation.

5.4 A short 230 kV transmission line with a reactance of 18 Ω/phase supplies a load at 0.85 lagging power factor. For a line current of 1,000 A the receiving- and sending-end voltages are to be maintained at 230 kV. Calculate (a) rating of synchronous capacitor required, (b) the load current, (c) the load MVA. Power drawn by the synchronous capacitor may be neglected.

5.5 A 40 MVA generating station is connected to a three-phase line having

$$Z = 300 \angle 75^\circ\ \Omega \quad Y = 0.0025 \angle 90^\circ\ \square\ .$$

The power at the generating station is 40 MVA at unity power factor at a voltage of 120 kV. There is a load of 10 MW at unity power factor at the mid point of the line. Calculate the voltage and load at the distant end of the line. Use nominal-*T* circuit for the line.

5.6 The generalized circuit constants of a transmission line are

$$A = 0.93 + j0.016$$

$$B = 20 + j140$$

The load at the receiving-end is 60 MVA, 50 Hz, 0.8 power factor lagging. The voltage at the supply end is 220 kV. Calculate the load voltage.

5.7 Find the incident and reflected currents for the line of Problem 5.3 at the receiving-end and 200 km from the receiving-end.

5.8 If the line of Problem 5.6 is 200 km long and delivers 50 MW at 220 kV and 0.8 power factor lagging, determine the sending-end voltage, current, power factor and power. Compute the efficiency of transmission, characteristic impedance, wavelength and velocity of propagation.

5.9 For Example 5.7, find the parameters of the equivalent-π circuit for the line.

5.10 An interconnector cable having a reactance of 6 Ω links generating stations 1 and 2 as shown in Fig. 5.18(a). The desired voltage profile is $|V_1| = |V_2| = 22$ kV. The loads at the two-bus bars are 40 MW at 0.8 lagging

power factor and 20 MW at 0.6 lagging power factor, respectively. The station loads are equalized by the flow of power in the cable. Estimate the torque angle and the station power factors.

5.11 A 50 Hz, three-phase, 275 kV, 400 km transmission line has the following parameters (per phase):

Resistance = 0.035 Ω/km
Inductance = 1 mH/km
Capacitance = 0.01 μF/km

If the line is supplied at 275 kV, determine the MVA rating of a shunt reactor having negligible losses that would be required to maintain 275 kV at the receiving-end, when the line is delivering no-load. Use nominal-π method.

5.12 A three-phase feeder having a resistance of 3 Ω and a reactance of 10 Ω supplies a load of 2.0 MW at 0.85 lagging power factor. The receiving-end voltage is maintained at 11 kV by means of a static condenser drawing 2.1 MVAR from the line. Calculate the sending-end voltage and power factor. What is the voltage regulation and efficiency of the feeder?

5.13 A three-phase overhead line has resistance and reactance of 5 and 20 Ω, respectively. The load at the receiving-end is 30 MW, 0.85 power factor lagging at 33 kV. Find the voltage at the sending-end. What will be the kVAR rating of the compensating equipment inserted at the receiving-end so as to maintain a voltage of 33 kV at each end? Find also the maximum load that can be transmitted.

5.14 Construct a receiving-end power circle diagram for the line of Example 5.7. Locate the point corresponding to the load of 50 MW at 220 kV with 0.8 lagging power factor. Draw the circle passing through the load point. Measure the radius and determine therefrom $|V_S|$. Also draw the sending-end circle and determine therefrom the sending-end power and power factor.

5.15 A three-phase overhead line has resistance and reactance per phase of 5 and 25 Ω, respectively. The load at the receiving-end is 15 MW, 33 kV, 0.8 power factor lagging. Find the capacity of the compensation equipment needed to deliver this load with a sending-end voltage of 33 kV.

Calculate the extra load of 0.8 lagging power factor which can be delivered with the compensating equipment (of capacity as calculated above) installed, if the receiving-end voltage is permitted to drop to 28kV.

References

Books

1. *Transmission Line Reference Book—345 kV and Above*, 2nd edn, Electric Power Research Institute, Palo Alto CA., 1982.

2. McCombe, J. and F.J. Haigh, *Overhead-line Practice*, Macdonald, London, 1966.
3. Stevenson, W.D., *Elements of Power System Analysis*, 4th edn, McGraw-Hill, New York, 1982.
4. Arrillaga, J., High Voltage Direct Current Transmission, *IEE Power Engineering Series 6*, Peter Peregrinus Ltd., London, 1983.
5. Kimbark, E.W., *Direct Current Transmission*, vol. 1, Wiley, New York, 1971.
6. Uhlmann, E., *Power Transmission by Direct Current*, Springer-Verlag, Berlin, 1975.
7. Miller, T.J.E., *Reactive Power Control in Electric Systems*, Wiley, New York 1982.
8. Mathur, R.M. (Ed.), *Static Compensators for Reactive Power Control*, Context Pub., Winnipeg, 1984.
9. Desphande, M.V., *Electrical Power System Design*, Tata McGraw-Hill, New Delhi, 1984.

Papers

10. Dunlop, R.D., R. Gautam and D.P. Marchenko, "Analytical Development of Loadability Characteristics for EHV and UHV Transmission Lines", *IEEE Trans.*, PAS, 1979, 98: 606.
11. "EHV Transmission", (Special Issue), *IEEE Trans.*, June 1966, No. 6, PAS-85.
12. Goodrich, R.D., "A Universal Power Circle Diagram", *AIEE Trans*., 1951, 70: 2042.
13. Indulkar, C.S., Parmod Kumar and D.P. Kothari, "Sensitivity Analysis of a Multiconductor Transmission Line", *Proc. IEEE*, March 1982, 70: 299.
14. Indulkar, C.S., Parmod Kumar and D.P. Kothari, "Some Studies on Carrier Propagation in Overhead Transmission Lines", *IEEE Trans., on* PAS, no. 4, 1983, 102: 942.
15. Bijwe, P.R., D.P. Kothari, J. Nanda and K.S. Lingamurthy, "Optimal Voltage Control Using Constant Sensitivity Matrix", *Electric Power System Research*, Oct. 1986, 3: 195.
16. Kothari, D.P., *et al*., "Microprocessors Controlled Static VAR Systems", *Proc. Int. Conf. Modelling & Simulation*, Gorakhpur, Dec. 1985, 2: 139.

Chapter 6

Load Flow Studies

6.1 INTRODUCTION

With the background of the previous chapters, we are now ready to study the operational features and electrical performance of a composite power system. The symmetrical steady state is, in fact, the most important mode of operation of a power system. Three major problems encountered in this mode of operation are listed below in their hierarchical order.

1. Load flow problem
2. Optimal load scheduling problem
3. Systems control problem

This chapter is devoted to the load flow problem, while the other two problems will be treated in later chapters.

Load flow study in power system parlance is the steady state solution of the power system network. The power system is modelled by an electric network and solved for the steady-state powers and voltages at various buses. The direct analysis of the circuit is not possible, as the loads are given in terms of complex powers rather than impedances, and the generators behave more like power sources than voltage sources. The main information obtained from the load flow study comprises of magnitudes and phase angles of load bus voltages, reactive powers and voltage phase angles at generator buses, real and reactive power flow on transmission lines together with power at the reference bus, other variables being specified. This information is essential for the continuous monitoring of the current state of the system and for analyzing the effectiveness of the alternative plans for the future, such as adding new generator sites, meeting increased load demand and locating new transmission sites.

In load flow analysis, we are mainly interested in voltages at various buses and power injection into the transmission system. Figure 6.1 shows the one-line diagram of a power system having five buses.

Here $S_G s$ and $S_D s$ represent the complex powers injected by generators and complex powers drawn by the loads and Vs represent the complex voltages at the various buses. Thus, there results a net injection of power into the transmission system. In a practical system, there may be thousands of buses

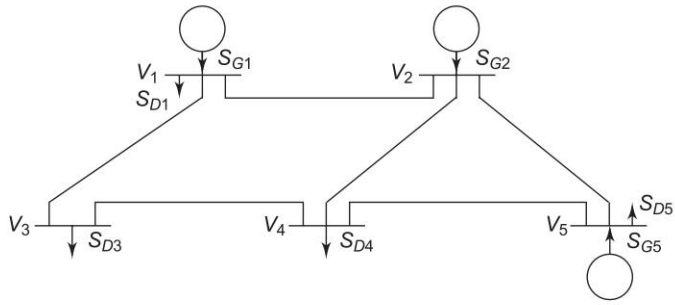

Fig. 6.1 One-line diagram of a five bus system

and transmission links. We shall concentrate mainly on the transmission system with the generators and loads modelled by the complex powers. The transmission system may be a primary transmission system, which transmits bulk power from the generators to the bulk power substation, or a subtransmission system which transmits power from substations or some old generators to the distribution substations. The transmission system is to be designed in such a manner that the power system operation is reliable and economic, and no difficulties are encountered in its operation. The likely difficulties are, one or more transmission lines becoming overloaded, generator(s) becoming overloaded, or the stability margin for a transmission link being too small, etc. Also, there may be emergencies, such as the loss of one or more transmission links, shut-down of generators, etc. which gives rise to overloading of some generators and transmission links. In system operation and planning, the voltages and powers are kept within certain limits and alternative plans are developed for easy and reliable operation. At the same time, it is also necessary to consider the economy of operation with respect to fuel costs to generate all the power needed. It may happen that each of the objectives mentioned above gives conflicting results. Usually a compromise has to be made with such results so that the system is reliable to operate in an emergency, and at the same time, is economical in operation.

The power system network of today is highly complicated consisting of hundreds of buses and transmission links. Thus, the load flow study involves extensive calculations. Before the advent of digital computers, the AC calculating board was the only means of carrying out load flow studies. These studies were, therefore, tedious and time consuming. With the availability of fast and large sized digital computers, all kinds of power system studies, including load flow study can now be carried out conveniently. In fact, some of the advanced level sophisticated studies which were almost impossible to carry out on the AC calculating board, have now become possible. The AC calculating board has been rendered obsolete.

6.2 NETWORK MODEL FORMULATION

Consider an *i*th bus of an '*n*' bus power system as shown in Fig. 6.2 below.

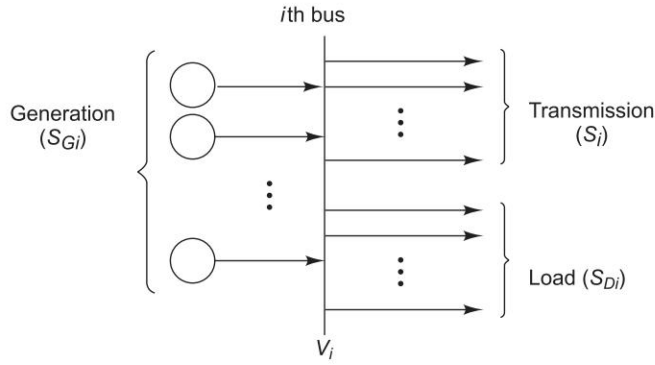

Fig. 6.2 *i* th bus in general connected to generators, loads and transmission lines

It is convenient to work with power at each bus injected into the transmission system, called the "Bus Power". The *i*th bus power is defined as

$$S_i = S_{Gi} - S_{Di}$$

The complex "Bus Power" S_i can also be visualized by splitting a bus as shown in Fig. 6.3.

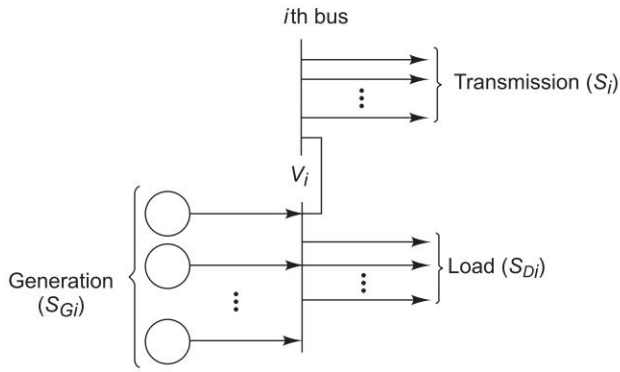

Fig. 6.3 *i*th bus split to visualize S_i which is the injected complex bus power

Writing the complex powers in terms of real and reactive powers, we have

$$\begin{aligned} S_{Gi} &= P_{Gi} + jQ_{Gi} \\ S_{Di} &= P_{Di} + jQ_{Di} \\ S_i &= P_i + jQ_i \end{aligned} \qquad (6.1a)$$

where $i = 1, ..., n$

Also

$$S_i = S_{Gi} - S_{Di}$$
$$= (P_{Gi} - P_{Di}) + j(Q_{Gi} - Q_{Di}) \quad \text{where } i = 1, ..., n \qquad (6.1b)$$

The "Bus Current" at the ith bus is defined as,

$$I_i = I_{Gi} - I_{Di}$$

Thus, the "Bus Current" I_i can also be visualized by splitting a bus as shown in Fig. 6.4.

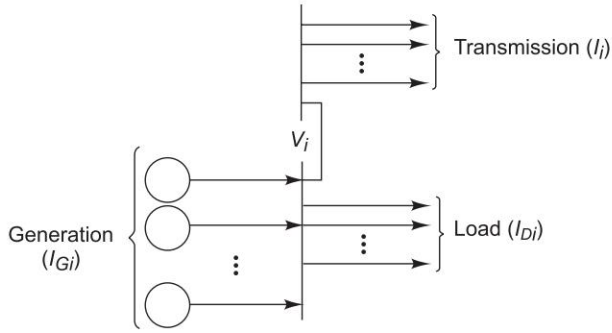

Fig. 6.4 Visualizing Bus Current I_i at the ith bus injected into the transmission system

We next develop the relation between bus currents and bus voltages under the following assumptions:

1. That there is no mutual coupling between the transmission lines, and
2. That there is an absence of regulating transformers.

Later on, we consider their presence and show that these modify the current–voltage relationship.

Let y_{ik} $(i \neq k)$ be the total admittance connected between the ith and kth buses and y_{i0} be the admittance between ith bus and the ground.

This is usually due to the capacitance present between transmission lines and the ground. The admittance y_{i0} can be realized when the transmission lines connected to the ith bus are replaced by their π-equivalent circuits. Thus each transmission line will present an admittance between the bus and the ground. The total admittance (y_{i0}) is the sum of the admittances due to all the transmission lines connected to the bus.

Also y_{ik} $(i \neq k) = 0$, if there is no transmission line between the ith and the kth bus.

By applying KCL at the ith bus, we get

$$I_i = y_{i0}V_i + y_{i1}(V_i - V_1) + y_{i2}(V_i - V_2) + \cdots$$
$$+ y_{i,\,i-1}(V_i - V_{i-1}) + y_{i,\,i+1}(V_i - V_{i+1}) + \cdots + y_{in}(V_i - V_n)$$

or

$$I_i = -y_{i1}V_1 - y_{i2}V_2 - y_{i3}V_3 - \ldots - y_{i,\,i-1}V_{i-1}$$
$$+ (y_{i0} + y_{i1} + \cdots + y_{i,\,i-1} + y_{i,\,i+1} + \cdots + y_{in})V_i$$
$$- y_{i,\,i+1}V_{i+1} - \cdots - y_{in}V_n \qquad (6.2a)$$

Thus, in general,

$$I_i = Y_{i1}\,V_1 + Y_{i2}\,V_2 + \cdots + Y_{ii}\,V_i + \cdots + Y_{in}\,V_n$$

$$= \sum_{k=1}^{n} (Y_{ik}\,V_k) \qquad (6.2b)$$

where $i = 1, \ldots, n$

where

$$Y_{ik}\,(i \neq k) = \frac{I_i}{V_k} \text{ (all } V = 0 \text{ except } V_k) \qquad (6.3)$$

= Short circuit transfer admittance between ith and kth bus

and

$$Y_{ii} = \frac{I_i}{V_i} \text{ (all } V = 0 \text{ except } V_i) \qquad (6.4)$$

= Short circuit driving point admittance or self-admittance at the ith bus

From Eqs (6.2a) and (6.3)

$Y_{ik}\,(i \neq k) = -\,y_{ik}$ = Negative of the total admittance connected between ith and kth bus (6.5a)

($Y_{ik}\,(i \neq k) = 0$ if there is no transmission line between ith and kth bus)

From Eqs (6.2a) and (6.4)

$$Y_{ii} = y_{i0} + y_{i1} + y_{i2} + \ldots + y_{i,\,i-1} + y_{i,\,i+1} + \ldots + y_{in} \qquad (6.5b)$$

= Sum of the admittances directly connected to ith bus

Writing Eq. (6.2b) for all the n buses we can write its matrix form as

$$\boldsymbol{I}_{\text{BUS}} = \boldsymbol{Y}_{\text{BUS}}\,\boldsymbol{V}_{\text{BUS}} \qquad (6.6)$$

where $\boldsymbol{I}_{\text{BUS}}$ is $n \times 1$ column vector of bus currents

$\boldsymbol{V}_{\text{BUS}}$ is $n \times 1$ column vector of bus voltages

$\boldsymbol{Y}_{\text{BUS}}$ is $n \times n$ matrix of admittances given as

$$\boldsymbol{Y}_{\text{BUS}} = \begin{bmatrix} Y_{11} & Y_{12} & \cdots & Y_{1n} \\ Y_{21} & Y_{22} & \cdots & Y_{2n} \\ \vdots & \vdots & & \vdots \\ Y_{n1} & Y_{n2} & \cdots & Y_{nn} \end{bmatrix}_{n \times n}$$

It follows that,

(1) The diagonal element of $\boldsymbol{Y}_{\text{BUS}}$ is given by Eq. (6.5b) and is the self-admittance. The off-diagonal element of $\boldsymbol{Y}_{\text{BUS}}$ is given by Eq. (6.5a) and is the transfer admittance.

(2) $\boldsymbol{Y}_{\text{BUS}}$ is $n \times n$ matrix where n is the number of buses.

(3) $\boldsymbol{Y}_{\text{BUS}}$ is a symmetric matrix ($Y_{ik} = Y_{ki}$ $(k \neq i)$) if the regulating transformers are not involved. So only $\dfrac{n \times n - n}{2} + n = \dfrac{n(n+1)}{2}$ terms are to be stored for an n-bus system.

(4) Y_{ik} $(i \neq k) = 0$ if ith and kth buses are not connected.

Since in a power network each bus is connected only to a few other buses (two or three), the $\boldsymbol{Y}_{\text{BUS}}$ of a large network is very sparse, i.e. it has a large number of zero elements.

Equation (6.6) can also be written in the form

$$\boldsymbol{V}_{\text{BUS}} = \boldsymbol{Z}_{\text{BUS}}\, \boldsymbol{I}_{\text{BUS}} \tag{6.7}$$

where $\boldsymbol{Z}_{\text{BUS}}$ (Bus Impedance Matrix) $= \boldsymbol{Y}_{\text{BUS}}^{-1}$ (6.8)

$$\boldsymbol{Z}_{\text{BUS}} = \begin{bmatrix} Z_{11} & Z_{12} \ldots Z_{1n} \\ Z_{21} & Z_{22} \ldots Z_{2n} \\ \vdots & \vdots \quad\; \vdots \\ Z_{n1} & Z_{n2} \ldots Z_{nn} \end{bmatrix}_{\substack{n \times n \text{ for } n \\ \text{bus system}}}$$

1. The diagonal elements are short circuit driving point impedances, and the off-diagonal elements are short circuit transfer impedances.
2. Symmetric $\boldsymbol{Y}_{\text{BUS}}$ yields symmetric $\boldsymbol{Z}_{\text{BUS}}$.
3. $\boldsymbol{Z}_{\text{BUS}}$ is a full-matrix, i.e. zero elements in $\boldsymbol{Y}_{\text{BUS}}$ become non-zero elements in the corresponding $\boldsymbol{Z}_{\text{BUS}}$.

$\boldsymbol{Y}_{\text{BUS}}$ is often used in solving load flow problems. It has gained widespread application owing to its simplicity in data preparation, and the ease with which it can be formed and modified for network changes. One of its greatest advantages is its sparsity, as it heavily reduces computer memory and time requirements.

The formation of a bus impedance matrix requires either matrix inversion or use of involved algorithms. $\boldsymbol{Z}_{\text{BUS}}$ is, however, most useful for short circuit studies and will be elaborated in the relevant chapter.

Note:

1. Tinney and associates at Bonnevile Power Authority were the first to exploit the sparsity feature of $\boldsymbol{Y}_{\text{BUS}}$ in greatly reducing numerical computations and in minimizing memory requirements.
2. In more sophisticated load flow studies of large power systems, it has been shown that a certain ordering of buses (nodes) produces faster convergence and solution. This ordering is known as optimal ordering.
3. $\boldsymbol{Y}_{\text{BUS}}/\boldsymbol{Z}_{\text{BUS}}$ constitute models of the passive portions of the power network.

Example 6.1 Figure 6.5(a) shows the one-line diagram of a four-bus system, which is replaced by its equivalent circuit in Fig. 6.5(b), where the equivalent power source at each bus is represented by a shaded circle. The equivalent power source at the ith bus injects currents I_i into the bus. The structure of the power system is such that all the sources are always connected to a common ground node. The transmission lines are replaced by their nominal-π equivalent. Figure 6.5(b) is redrawn in Fig. 6.5(c), after lumping the shunt admittances at the buses. The line admittance between nodes i and k is depicted by y_{ik}. Also, $y_{ik} = y_{ki}$. Further, the mutual admittances between the lines is assumed to be zero. In Fig. 6.5(c), there are five nodes, viz. the ground node zero and the nodes corresponding to the four buses. Applying KCL at nodes 1, 2, 3 and 4 respectively, we get four equations as follows:

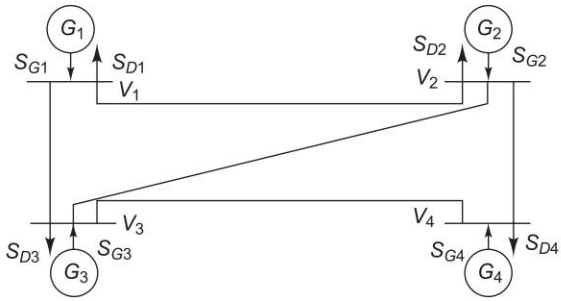

(a) One-line diagram of a four-bus system

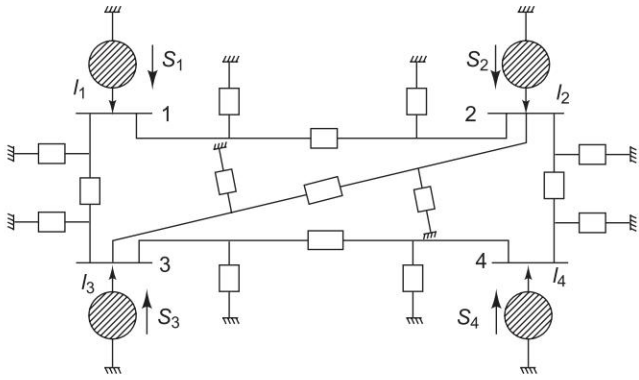

(b) Equivalent circuit of the power system of (a)

$$
\begin{aligned}
I_1 &= y_{10}\, V_1 + y_{12}\,(V_1 - V_2) + y_{13}\,(V_1 - V_3) \\
I_2 &= y_{20}\, V_2 + y_{12}\,(V_2 - V_1) + y_{23}\,(V_2 - V_3) + y_{24}\,(V_2 - V_4) \\
I_3 &= y_{30}\, V_3 + y_{13}\,(V_3 - V_1) + y_{23}\,(V_3 - V_2) + y_{34}\,(V_3 - V_4) \\
I_4 &= y_{40}\, V_4 + y_{24}\,(V_4 - V_2) + y_{34}\,(V_4 - V_3)
\end{aligned}
$$

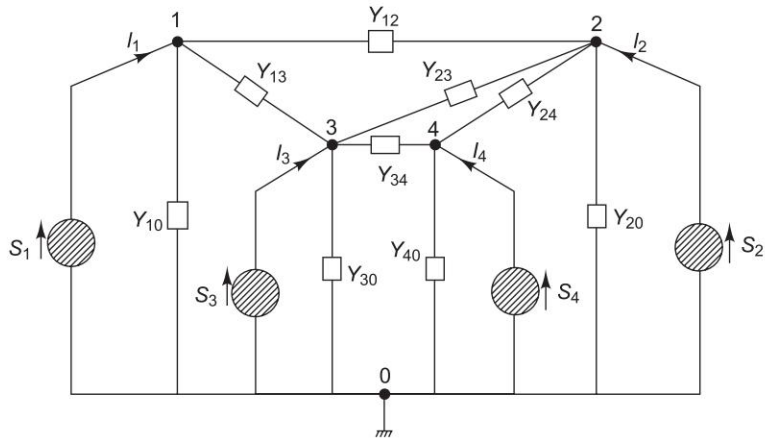

(c) Reduced circuit diagram of the power system

Fig. 6.5 (a)-(c) Sample four-bus system

Rearranging and writing in matrix form, we get

$$\begin{bmatrix} I_1 \\ I_2 \\ I_3 \\ I_4 \end{bmatrix} = \begin{bmatrix} (y_{10}+y_{12}+y_{13}) & -y_{12} & -y_{13} & 0 \\ -y_{12} & (y_{20}+y_{12}+y_{23}+y_{24}) & -y_{23} & -y_{24} \\ -y_{13} & -y_{23} & (y_{30}+y_{13}+y_{23}+y_{34}) & -y_{34} \\ 0 & -y_{24} & -y_{34}+y_{34}) & (y_{40}+y_{24} \end{bmatrix} \begin{bmatrix} V_1 \\ V_2 \\ V_3 \\ V_4 \end{bmatrix}$$

Writing in the standard form, we get

$$\begin{bmatrix} I_1 \\ I_2 \\ I_3 \\ I_4 \end{bmatrix} = \begin{bmatrix} Y_{11} & Y_{12} & Y_{13} & Y_{14} \\ Y_{21} & Y_{22} & Y_{23} & Y_{24} \\ Y_{31} & Y_{32} & Y_{33} & Y_{34} \\ Y_{41} & Y_{42} & Y_{43} & Y_{44} \end{bmatrix} \begin{bmatrix} V_1 \\ V_2 \\ V_3 \\ V_4 \end{bmatrix}$$

or

$$\boldsymbol{I}_{\text{BUS}} = \boldsymbol{Y}_{\text{BUS}}\ \boldsymbol{V}_{\text{BUS}}$$

where

$$\boldsymbol{Y}_{\text{BUS}} = \begin{bmatrix} Y_{11} & Y_{12} & Y_{13} & Y_{14} \\ Y_{21} & Y_{22} & Y_{23} & Y_{24} \\ Y_{31} & Y_{32} & Y_{33} & Y_{34} \\ Y_{41} & Y_{42} & Y_{43} & Y_{44} \end{bmatrix}$$

As already concluded in Eqs (6.5a and b), we observe that the diagonal elements of $\boldsymbol{Y}_{\text{BUS}}$ are self-admittances, and are given by

$$Y_{11} = y_{10} + y_{12} + y_{13}$$
$$Y_{22} = y_{20} + y_{12} + y_{23} + y_{24}$$
$$Y_{33} = y_{30} + y_{13} + y_{23} + y_{34}, \text{ and}$$
$$Y_{44} = y_{40} + y_{24} + y_{34}$$

The off-diagonal elements of $\boldsymbol{Y}_{\text{BUS}}$ are transfer admittances, and are given by

$$Y_{12} = Y_{21} = -y_{12}$$
$$Y_{13} = Y_{31} = -y_{13}$$
$$Y_{14} = Y_{41} = 0$$
$$Y_{23} = Y_{32} = -y_{23}$$
$$Y_{24} = Y_{42} = -y_{24}$$
$$Y_{34} = Y_{43} = -y_{34}$$

Algorithm for the Formation of Y_{BUS} Matrix

(a) Assuming no Mutual Coupling between Transmission Lines

Initially all the elements of $\boldsymbol{Y}_{\text{BUS}}$ are set to zero. Addition of an element of admittance y between buses i and j affects four entries in $\boldsymbol{Y}_{\text{BUS}}$, viz., Y_{ii}, Y_{ij}, Y_{ji}, Y_{jj}, as follows:

$$\begin{aligned} Y_{ii\ \text{new}} &= Y_{ii\ \text{old}} + y \\ Y_{ij\ \text{new}} &= Y_{ij\ \text{old}} - y \\ Y_{ji\ \text{new}} &= Y_{ji\ \text{old}} - y \\ Y_{jj\ \text{new}} &= Y_{jj\ \text{old}} + y \end{aligned} \tag{6.9a}$$

Addition of an element of admittance y from bus i to ground will only affect Y_{ii}, i.e.

$$Y_{ii\ \text{new}} = Y_{ii\ \text{old}} + y \tag{6.9b}$$

Example 6.2 Consider the sample four-bus system in Fig. 6.5. Initially, set all the elements of $\boldsymbol{Y}_{\text{BUS}}$ to zero.

1. Addition of y_{10} affects only Y_{11}

$$Y_{11\ \text{new}} = Y_{11\ \text{old}} + y_{10} = 0 + y_{10} = y_{10}$$

2. Addition of y_{12} affects Y_{11}, Y_{12}, Y_{21}, Y_{22}

$$Y_{11\ \text{new}} = Y_{11\ \text{old}} + y_{12} = y_{10} + y_{12}$$
$$Y_{12\ \text{new}} = Y_{12\ \text{old}} - y_{12} = 0 - y_{12} = -y_{12} \quad \text{(i)}$$
$$Y_{21\ \text{new}} = Y_{21\ \text{old}} - y_{12} = 0 - y_{12} = -y_{12} \quad \text{(ii)}$$
$$Y_{22\ \text{new}} = Y_{22\ \text{old}} - y_{12} = 0 + y_{12}$$

3. Addition of y_{13} affects $Y_{11}, Y_{13}, Y_{31}, Y_{33}$

$$Y_{11\ new} = Y_{11\ old} + y_{13} = y_{10} + y_{12} + y_{13} \quad \text{(iii)}$$

$$Y_{13\ new} = Y_{13\ old} - y_{13} = 0 - y_{13} = -y_{13} \quad \text{(iv)}$$

$$Y_{31\ new} = Y_{31\ old} - y_{13} = 0 - y_{13} = -y_{13} \quad \text{(v)}$$

$$Y_{33\ new} = Y_{33\ old} + y_{13} = 0 + y_{13} = y_{13}$$

4. Addition of y_{20} affects only Y_{22}

$$Y_{22\ new} = Y_{22\ old} + y_{20} = y_{12} + y_{20}$$

5. Addition of y_{23} affects $Y_{22}, Y_{23}, Y_{32}, Y_{33}$

$$Y_{22\ new} = Y_{22\ old} + y_{23} = (y_{20} + y_{12}) + y_{23} = y_{20} + y_{12} + y_{23}$$

$$Y_{23\ new} = Y_{23\ old} - y_{23} = 0 - y_{23} = -y_{23} \quad \text{(vi)}$$

$$Y_{32\ new} = Y_{32\ old} - y_{23} = 0 - y_{23} = -y_{23} \quad \text{(vii)}$$

$$Y_{33\ new} = Y_{33\ old} + y_{23} = y_{13} + y_{23}$$

6. Addition of y_{24} affects $Y_{22}, Y_{24}, Y_{42}, Y_{44}$

$$Y_{22\ new} = Y_{22\ old} + y_{24} = (y_{20} + y_{12} + y_{23}) + y_{24} \quad \text{(viii)}$$

$$= y_{20} + y_{12} + y_{23} + y_{24}$$

$$Y_{24\ new} = Y_{24\ old} - y_{24} = 0 - y_{24} = -y_{24} \quad \text{(ix)}$$

$$Y_{42\ new} = Y_{42\ old} - y_{24} = 0 - y_{24} = -y_{24} \quad \text{(x)}$$

$$Y_{44\ new} = Y_{44\ old} + y_{24} = 0 + y_{24} = y_{24}$$

7. Addition of y_{30} affects only Y_{33}

$$Y_{33\ new} = Y_{33\ old} + y_{30} = (y_{13} + y_{23}) + y_{30} + y_{13} + y_{23}$$

8. Addition of y_{34} affects $Y_{33}, Y_{34}, Y_{43}, Y_{44}$

$$Y_{33\ new} = Y_{33\ old} + y_{34} = (y_{30} + y_{13} + y_{23}) + y_{34} \quad \text{(xi)}$$

$$= y_{30} + y_{13} + y_{23} + y_{34}$$

$$Y_{34\ new} = Y_{34\ old} - y_{34} = 0 - y_{34} = -y_{34} \quad \text{(xii)}$$

$$Y_{43\ new} = Y_{43\ old} - y_{34} = 0 - y_{34} = -y_{34} \quad \text{(xiii)}$$

$$Y_{44\ new} = Y_{44\ old} + y_{34} = y_{24} + y_{34}$$

9. Addition of y_{40} affects only Y_{44}

$$Y_{44\ new} = Y_{44\ old} + y_{40} = (y_{24} + y_{34}) + y_{40} = y_{40} + y_{24} + y_{34} \quad \text{(xiv)}$$

The final values of the elements of the bus admittance matrix are given by appropriate equation from Eqs (i) through (xiv).

Further $Y_{14} = Y_{41} = 0$

(b) Assuming Mutual Coupling between Transmission Lines

The equivalent circuit of mutually coupled transmission lines is shown in Fig. 6.6. Shunt elements are omitted for simplicity; this effect can be included

in a straight forward manner as seen in Example 6.1. The mutual impedance between the transmission lines is z_m, and the series impedances are z_{s1} and z_{s2}. From Fig. 6.6, we have

$$V_i = z_{s1} I_i + z_m I_k + V_j$$
$$V_k = z_{s2} I_k + z_m I_i + V_l$$

or
$$\begin{bmatrix} V_i \\ V_k \end{bmatrix} - \begin{bmatrix} V_j \\ V_l \end{bmatrix} = \begin{bmatrix} z_{s1} & z_m \\ z_m & z_{s2} \end{bmatrix} \begin{bmatrix} I_i \\ I_k \end{bmatrix}$$

or

$$\begin{bmatrix} I_i \\ I_k \end{bmatrix} = \begin{bmatrix} y_{s1} & y_m \\ y_m & y_{s2} \end{bmatrix} \begin{bmatrix} V_i - V_j \\ V_k - V_l \end{bmatrix} \tag{6.10a}$$

Similarly, we have

$$\begin{bmatrix} I_j \\ I_l \end{bmatrix} = \begin{bmatrix} y_{s1} & y_m \\ y_m & y_{s2} \end{bmatrix} \begin{bmatrix} V_j - V_i \\ V_l - V_k \end{bmatrix} \tag{6.10b}$$

where

$$\begin{bmatrix} y_{s1} & y_m \\ y_m & y_{s2} \end{bmatrix} = \begin{bmatrix} z_{s1} & z_m \\ z_m & z_{s2} \end{bmatrix}^{-1}$$

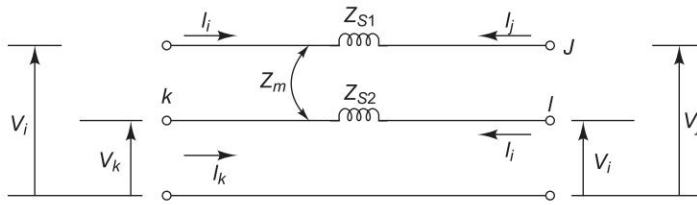

Fig. 6.6 Mutually coupled transmission lines

From Eqs 6.10(a) and (b) the elements of $\boldsymbol{Y}_{\text{BUS}}$ become

$$\left\{ \begin{aligned} Y_{ii\,\text{new}} &= Y_{ii\,\text{old}} + y_{s1} \\ Y_{jj\,\text{new}} &= Y_{jj\,\text{old}} + y_{s1} \\ Y_{kk\,\text{new}} &= Y_{kk\,\text{old}} + y_{s2} \\ Y_{ll\,\text{new}} &= Y_{ll\,\text{old}} + y_{s2} \end{aligned} \right\} \tag{6.11a}$$

$$\left\{ \begin{aligned} Y_{ij\,\text{new}} &= Y_{ji\,\text{new}} = Y_{ij\,\text{old}} - y_{s1} \\ Y_{kl\,\text{new}} &= Y_{lk\,\text{new}} = Y_{kl\,\text{old}} - y_{s2} \end{aligned} \right\} \tag{6.11b}$$

$$\left.\begin{aligned} Y_{ik\,\text{new}} = Y_{ki\,\text{new}} &= Y_{ik\,\text{old}} + y_m \\ Y_{jl\,\text{new}} = Y_{lj\,\text{new}} &= Y_{jl\,\text{old}} + y_m \end{aligned}\right\} \tag{6.11c}$$

$$\left.\begin{aligned} Y_{il\,\text{new}} = Y_{li\,\text{new}} &= Y_{il\,\text{old}} - y_m \\ Y_{jk\,\text{new}} = Y_{kj\,\text{new}} &= Y_{jk\,\text{old}} - y_m \end{aligned}\right\} \tag{6.11d}$$

Example 6.3 Figure 6.7 shows the one-line diagram of a simple four-bus system. Table 6.1 gives the line impedances identified by the buses on which these terminate. The shunt admittance at all the buses is assumed to be negligible.

(a) Find $\boldsymbol{Y}_{\text{BUS}}$, assuming that the line shown dotted is not connected.
(b) What modifications need to be carried out in $\boldsymbol{Y}_{\text{BUS}}$ if the line shown dotted is connected?

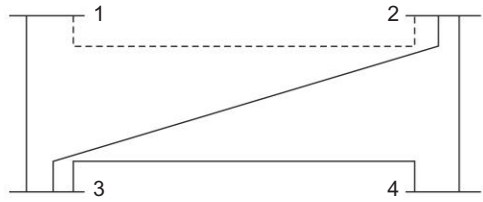

Fig. 6.7 Sample system for Example 6.3

Solution

(a) From Table 6.1, Table 6.2 is obtained from which $\boldsymbol{Y}_{\text{BUS}}$ for the system can be written as

Table 6.1

Line, bus to bus	*R, pu*	*X, pu*
1–2	0.05	0.15
1–3	0.10	0.30
2–3	0.15	0.45
2–4	0.10	0.30
3–4	0.05	0.15

Table 6.2

Line	*G, pu*	*B, pu*
1–2	2.000	– 6.0
1–3	1.000	– 3.0
2–3	0.666	– 2.0
2–4	1.000	– 3.0
3–4	2.000	– 6.0

$$\boldsymbol{Y}_{\text{BUS}} = \begin{bmatrix} Y_{11} & Y_{12} & Y_{13} & Y_{14} \\ Y_{21} & Y_{22} & Y_{23} & Y_{24} \\ Y_{31} & Y_{32} & Y_{33} & Y_{34} \\ Y_{41} & Y_{42} & Y_{43} & Y_{44} \end{bmatrix} \quad \text{(i)}$$

$$\boldsymbol{Y}_{\text{BUS}} = \begin{bmatrix} y_{13} & 0 & -y_{13} & 0 \\ 0 & (y_{23}+y_{24}) & -y_{23} & -y_{24} \\ -y_{13} & -y_{23} & (y_{31}+y_{32}+y_{34}) & -y_{34} \\ 0 & -y_{24} & -y_{34} & (y_{43}+y_{42}) \end{bmatrix} \quad \text{(ii)}$$

$$\boldsymbol{Y}_{\text{BUS}} = \begin{bmatrix} 1-j3 & 0 & -1+j3 & 0 \\ 0 & 1.666-j5 & -0.666+j2 & -1+j3 \\ -1+j3 & -0.666+j2 & 3.666-j11 & -2+j6 \\ 0 & -1+j3 & -2+j6 & 3-j9 \end{bmatrix} \quad \text{(iii)}$$

(b) The following elements of $\boldsymbol{Y}_{\text{BUS}}$ of part (a) are modified when a line is added between buses 1 and 2.

$$\begin{aligned} Y_{11\ \text{new}} &= Y_{11\ \text{old}} + (2-j6) = 3-j9 \\ Y_{12\ \text{new}} &= Y_{12\ \text{old}} - (2-j6) = -2+j6 = Y_{21\ \text{new}} \\ Y_{22\ \text{new}} &= Y_{22\ \text{old}} + (2-j6) = 3.666-j11 \end{aligned} \quad \text{(iv)}$$

Modified $\boldsymbol{Y}_{\text{BUS}}$ is written as

$$\boldsymbol{Y}_{\text{BUS}} = \begin{bmatrix} 3-j9 & -2+j6 & -1+j3 & 0 \\ -2+j6 & 3.666-j11 & -0.666+j2 & -1+j3 \\ -1+j3 & -0.666+j2 & 3.666-j11 & -2+j6 \\ 0 & -1+j3 & -2+j6 & 3-j9 \end{bmatrix} \quad \text{(v)}$$

6.3 FORMATION OF $\boldsymbol{Y}_{\text{BUS}}$ BY SINGULAR TRANSFORMATION

The matrix pair $\boldsymbol{Y}_{\text{BUS}}$ and $\boldsymbol{Z}_{\text{BUS}}$ form the network models for load flow studies. The $\boldsymbol{Y}_{\text{BUS}}$ can be alternatively assembled by the use of singular transformation given by a graph theoretical approach. This approach is of great theoretical and practical significance, and is therefore discussed here. To start with, the graph theory is briefly reviewed.

Graph

To describe the geometrical features of a network, it is replaced by single line segments called *elements*, whose terminals are called *nodes*. The resulting figure is called the *graph* of the given network. A *linear graph* depicts the geometrical interconnection of the elements of a network. A *connected graph*

is one in which there is at least one path between every pair of nodes. If each element of a connected graph is assigned a direction*, it is called an *oriented graph*.

Power networks are so structured that out of the m total number of nodes, one node (normally described by 0) is always at ground potential and the remaining $n = m - 1$ nodes are the buses at which the source power is injected. Figure 6.8 shows the oriented linear graph of the power network of Fig. 6.5(c). Here the overall line admittance between any two buses (nodes in the corresponding graph) are represented by a single line element. Also, each source and the shunt admittance connected across it are represented by a single line element. In fact, this combination represents the most general network element, and is described under the subheading Primitive Network.

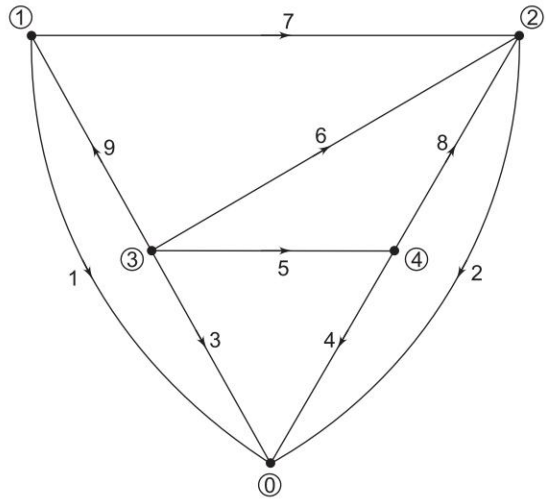

Fig. 6.8 Oriented linear graph of the circuit in Fig. 6.5(c)

A connected subgraph containing all the nodes of a graph but having no closed paths is called a *tree*. The elements of a tree are called *branches* or *tree branches*. The number of branches b that form a tree are given by

$$b = m - 1 = n \text{ (number of buses)} \tag{6.12}$$

Those elements of the graph that are not included in the tree are called *links* or *link branches*, and they form a subgraph, not necessarily connected, called *co-tree*. The number of links l of a connected graph with e elements is

$$l = e - b = e - m + 1 \tag{6.13}$$

There may be more than one possible trees (and therefore, co-trees) of a graph.

A tree and the corresponding co-tree of the graph of Fig. 6.8 are shown in Fig. 6.9. The reader should try and find some other tree and co-tree pairs.

* For convenience, direction is so assigned as to coincide with the assumed positive direction of the element current.

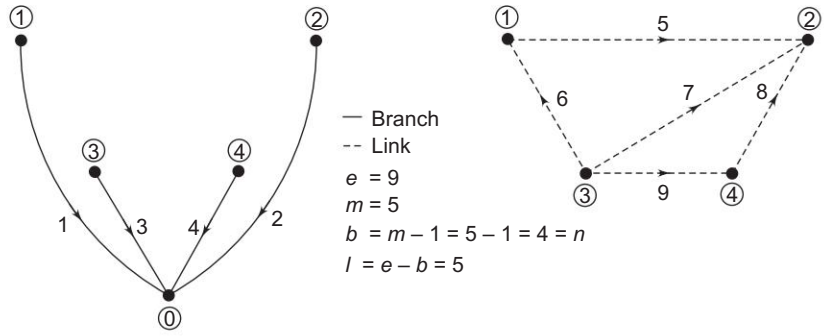

(a) Tree (b) Co-tree

Fig. 6.9 Tree and co-tree of the oriented connected graph of Fig. 6.6

If a link is added to the tree, the corresponding graph contains one closed path called a basic loop. Thus, a graph has as many basic loops as the number of links. A loop is distinguished from a basic loop, as it can be any loop in the original graph. Therefore, the number of loops is greater than, or at the most equal to, the number of basic loops in a graph.

Primitive Network

A network element may in general contain active and passive components. Figure 6.10 shows a general network element, connected between nodes r and s, with its alternative impedance and admittance form. The impedance form is a voltage source e_{rs} in series with an impedance z_{rs}, while the admittance form is a current source j_{rs} in parallel with an admittance y_{rs}. The element current is i_{rs}, and the element voltage is $v_{rs} = E_r - E_s$, where E_r and E_s are the voltages of the element nodes r and s respectively.

It may be remembered here that for steady state AC performance, all element variables (v_{rs}, E_r, E_s, i_{rs}, j_{rs}) are phasors, and the element parameters (z_{rs}, y_{rs}) are complex numbers.

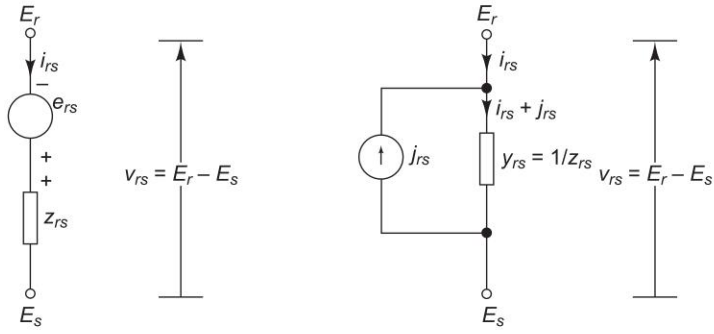

(a) Impedance form (b) Admittance form

Fig. 6.10 Representation of a network element

The voltage relation for Fig. 6.10 can be written as

$$v_{rs} + e_{rs} = z_{rs}\, i_{rs} \tag{6.14}$$

Similarly, the current relation for Fig. 6.10 can be written as

$$i_{rs} + j_{rs} = y_{rs}\, v_{rs} \tag{6.15}$$

The forms of Fig. 6.10(a) and (b) are equivalent, wherein the parallel source current in admittance form is related to the series voltage in impedance form by

$$j_{rs} = y_{rs}\, e_{rs}$$

Also

$$y_{rs} = 1/z_{rs}$$

A set of unconnected elements is defined as a primitive network. The performance equations of a primitive network are given by:

In impedance form,

$$\boldsymbol{V} + \boldsymbol{E} = \boldsymbol{ZI} \tag{6.16}$$

In admittance form,

$$\boldsymbol{I} + \boldsymbol{J} = \boldsymbol{YV} \tag{6.17}$$

Here $\boldsymbol{V}$ and $\boldsymbol{I}$ are the element voltage and current vectors respectively, and $\boldsymbol{J}$ and $\boldsymbol{E}$ are the source vectors. $\boldsymbol{Z}$ and $\boldsymbol{Y}$ are referred to as the primitive impedance and admittance matrices, respectively. These are related as $\boldsymbol{Z} = \boldsymbol{Y}^{-1}$. If there is no mutual coupling between elements, $\boldsymbol{Z}$ and $\boldsymbol{Y}$ are diagonal matrices, where the diagonal entries are the impedances/admittances of the network elements and are reciprocal.

Network Variables in Bus Frame of Reference

The linear network graph helps in the systematic assembly of a network model. The main problem in deriving mathematical models for large and complex power network is to select a minimum or zero redundancy (linearly independent) set of current or voltage variables, which is sufficient to give the information about all element voltages and currents. One set of such variables is the b tree voltages. By topological reasoning, these variables constitute a nonredundant set. The knowledge of b tree voltages allows us to compute all element voltages, and therefore, all bus currents assuming all element admittances being known.

Consider a tree graph shown in Fig. 6.9(a) where the ground node is chosen as the reference node. This is the most appropriate tree choice for the power network. With this choice, the b tree branch voltages become identical with the bus voltages as the tree branches are incidental to the ground node.

Bus Incidence Matrix

For the specific system of Fig. 6.8, we obtain the following relations between the nine element voltages and the four bus (i.e. tree branch) voltages V_1, V_2, V_3 and V_4.

$$
\begin{aligned}
V_{b1} &= V_1 \\
V_{b2} &= V_2 \\
V_{b3} &= V_3 \\
V_{b4} &= V_4 \\
V_{l5} &= V_1 - V_2 \\
V_{l6} &= V_1 - V_3 \\
V_{l7} &= V_2 - V_3 \\
V_{l8} &= V_2 - V_4 \\
V_{l9} &= V_3 - V_4
\end{aligned}
\tag{6.18}
$$

or, in matrix form

$$\boldsymbol{V} = \boldsymbol{A}\boldsymbol{V}_{\text{BUS}} \tag{6.19}$$

where $\boldsymbol{V}$ is the vector of element voltages of order $e \times 1$ (e = number of elements), $\boldsymbol{V}_{\text{BUS}}$ is the vector of bus voltages of order $b \times 1$ (b = number of branches = number of buses = n) and $\boldsymbol{A}$ is the bus incidence matrix of order $e \times b$ given by

e ↓ Bus →	1	2	3	4
1	1	0	0	0
2	0	1	0	0
3	0	0	1	0
4	0	0	0	1
5	1	–1	0	0
6	1	0	–1	0
7	0	1	–1	0
8	0	1	0	–1
9	0	0	1	–1

Elements (Branches / links) = Buses

$$\begin{bmatrix} \boldsymbol{A}_b \\ \boldsymbol{A}_l \end{bmatrix} = \begin{bmatrix} \boldsymbol{I} \\ \boldsymbol{A}_l \end{bmatrix} \tag{6.20}$$

This matrix is rectangular, and therefore, singular. Its elements a_{ik} are found as per the following rules:

a_{ik} = 1 if ith element is incident to and oriented away from the kth node (bus)

= – 1 if ith element is incident to but oriented towards the kth node

= 0 if the ith element is not incident to the kth node

Substituting Eq. (6.19) into (6.17), we get

$$\boldsymbol{I} + \boldsymbol{J} = \boldsymbol{Y}\boldsymbol{A}\boldsymbol{V}_{\text{BUS}} \tag{6.21}$$

Premultiplying by $\boldsymbol{A}^T$,

$$\boldsymbol{A}^T\boldsymbol{I} + \boldsymbol{A}^T\boldsymbol{J} = \boldsymbol{A}^T\boldsymbol{Y}\boldsymbol{A}\boldsymbol{V}_{\text{BUS}} \tag{6.22}$$

each component of the n-dimensional vector $\boldsymbol{A}^T \boldsymbol{I}$ is the algebraic sum of the element currents leaving nodes 1, 2, ..., n(n = number of buses). Therefore the application of KCL must result in

$$\boldsymbol{A}^T \boldsymbol{I} = \boldsymbol{0} \tag{6.23}$$

Similarly, each component of the vector $\boldsymbol{A}^T \boldsymbol{J}$ can be recognized as the algebraic sum of all source currents injected into nodes 1, 2, ..., n. These components are therefore the bus currents. Hence we can write

$$\boldsymbol{A}^T \boldsymbol{J} = \boldsymbol{I}_{\text{BUS}} \tag{6.24}$$

Equation (6.22) then is simplified to

$$\boldsymbol{I}_{\text{BUS}} = (\boldsymbol{A}^T \boldsymbol{YA})\, \boldsymbol{V}_{\text{BUS}} \tag{6.25}$$

Thus, following an alternative systematic approach, we obtain the same nodal current equation as Eq. (6.6). The bus admittance matrix can then be obtained from the singular transformation of the primitive $\boldsymbol{Y}$ matrix, i.e.,

$$\boldsymbol{Y}_{\text{BUS}} = \boldsymbol{A}^T \boldsymbol{YA} \tag{6.26}$$

A computer programme can be developed to write the bus incidence matrix $\boldsymbol{A}$ from the interconnected data of the directed elements of the power system. Standard matrix transpose and multiplication subroutines can then be used to compute $\boldsymbol{Y}_{\text{BUS}}$ from Eq. (6.26).

Example 6.4 Find the $\boldsymbol{Y}_{\text{BUS}}$ using singular transformation for the system of Fig. 6.5(c) whose graph is shown in Fig. 6.8.

Solution

As there is no mutual coupling between any two lines, the primitive $\boldsymbol{Y}$ matrix is diagonal and given by the following.

$\boldsymbol{Y}$ =

Elements	1	2	3	4	5	6	7	8	9
1	y_{10}								0
2		y_{20}							
3			y_{30}						
4				y_{40}					
5					y_{12}				
6						y_{13}			
7							y_{23}		
8								y_{24}	
9	0								y_{34}

Using $\boldsymbol{A}$ from Eq. (6.20), we get

$$\boldsymbol{YA} = \begin{bmatrix} y_{10} & 0 & 0 & 0 \\ 0 & y_{20} & 0 & 0 \\ 0 & 0 & y_{30} & 0 \\ 0 & 0 & 0 & y_{40} \\ y_{12} & -y_{12} & 0 & 0 \\ y_{13} & 0 & -y_{13} & 0 \\ 0 & -y_{23} & y_{23} & 0 \\ 0 & y_{24} & 0 & -y_{24} \\ 0 & 0 & y_{34} & -y_{34} \end{bmatrix}$$

Finally,

$$\boldsymbol{Y}_{\text{BUS}} = \boldsymbol{A}^T\, \boldsymbol{YA}$$

$$= \begin{bmatrix} (y_{10}+y_{12}+y_{13}) & -y_{12} & -y_{13} & 0 \\ -y_{12} & (y_{20}+y_{12}+y_{23}+y_{24}) & -y_{23} & -y_{24} \\ -y_{13} & -y_{23} & (y_{30}+y_{13}+y_{23}+y_{34}) & -y_{34} \\ 0 & -y_{24} & -y_{34} & (y_{40}+y_{24}+y_{34}) \end{bmatrix}$$

The elements of this matrix, of course, agree with those previously calculated in Example 6.1.

If there is mutual coupling between elements i and j of the network, the primitive $\boldsymbol{Y}$ matrix will not be diagonal. Thus, the element corresponding to the ith row and jth column (also, jth row and ith column) will be equal to the mutual admittance between the elements i and j. Thus $\boldsymbol{Y}_{\text{BUS}}$ is also modified as given by Eq. (6.26).

6.4 LOAD FLOW PROBLEM

The complex power injected by the source into the ith bus of a power system is

$$S_i = P_i + jQ_i = V_i I_i^*, \quad i = 1, 2, ..., n$$

Since it is convenient to work with I_i instead of I_i^*, we take the complex conjugate of the above equation,

$$P_i - jQ_i = V_i^* I_i, \; i = 1, 2, ..., n$$

Substituting $I_i = \left(\sum_{k=1}^{n} (Y_{ik} V_k) \right)$ from Eq. (6.2b) in the above equation, we have

$$P_i - jQ_i = V_i^* \left(\sum_{k=1}^{n} (Y_{ik} V_k) \right), \quad i = 1, 2, ..., n$$

Equating real and imaginary parts, we get

$$P_i \text{ (Real power)} = \text{Real}\left(V_i^*\left(\sum_{k=1}^{n}(Y_{ik}V_k)\right)\right) \tag{6.27a}$$

$$Q_i \text{ (Reactive power)} = -\text{ Imaginary}\left(V_i^*\left(\sum_{k=1}^{n}(Y_{ik}V_k)\right)\right) \tag{6.27b}$$

Let $V_i = |V_i| e^{j\delta_i}$, $V_k = |V_k| e^{j\delta_k}$

$$Y_{ik} = |Y_{ik}| e^{j\theta_{ik}}$$

then

$$P_i \text{ (Real power)} = |V_i| \sum_{k=1}^{n} |V_k||Y_{ik}| \cos(\theta_{ik} + \delta_k - \delta_i) \tag{6.28a}$$

$$Q_i \text{ (Reactive power)} = -|V_i| \sum_{k=1}^{n} |V_k||Y_{ik}| \sin(\theta_{ik} + \delta_k - \delta_i) \tag{6.28b}$$

$$(i = 1, 2, ..., n)$$

Equations 6.28(a) and (b) are called power flow equations. There are n real and n reactive power flow equations giving a total of $2n$ power flow equations.

At each bus there are four variables, viz., $|V_i|$, δ_i, P_i and Q_i, giving a total of $4n$ variables (for n buses). If at every bus two variables are specified (thus specifying a total of $2n$ variables), the remaining two variables at every bus (a total of $2n$ remaining variables) can be found by solving the $2n$ power flow Eqs 6.28(a) and (b). When a physical system is considered, specifying variables at every bus depends on what devices are connected to that bus. In general there are four possibilities giving rise to four types of buses as follows.

Slack Bus/Swing Bus/Reference Bus

This bus is distinguished from the remaining types by the fact that real and reactive powers at this bus are not specified. Instead, voltage magnitude (normally set equal to 1 pu) and voltage phase angle (normally set equal to zero) are specified. Usually, there is only one bus of this type in a given power system. The need of such a bus for a load flow study is explained in the example that follows. The slack bus is numbered 1, for convenience.

PQ Bus/Load Bus

At this type of bus, the net powers P_i and Q_i are known (P_{Di} and Q_{Di} are known from load forecasting and P_{Gi} and Q_{Gi} are specified). The unknowns are $|V_i|$ and δ_i. A pure load bus (no generating facility at the bus, i.e. $P_{Gi} = Q_{Gi} = 0$) is a PQ bus. PQ buses are the most common, comprising almost 80% of all the buses in a given power system.

PV Bus/Generator Bus

This bus has always a generator connected to it. Thus P_{Gi} and $|V_i|$ are specified. Hence the net power P_i is known (as P_{Di} is known from load forecasting). Hence the knowns are P_i and $|V_i|$ and unknowns are Q_i and δ_i. PV buses comprise about 10% of all the buses in a power system.

Voltage Controlled Bus

Frequently the PV bus and the voltage controlled bus are grouped together. But they have physical differences and slightly different calculation strategies. The voltage controlled bus has also voltage control capabilities, and uses a tap-adjustable transformer and/or a static var compensator instead of a generator. Hence $P_{Gi} = Q_{Gi} = 0$ at these buses. Thus $P_i = -P_{Di}$, $Q_i = -Q_{Di}$ and $|V_i|$ are known at these buses and the unknown is δ_i.

Example 6.5 This example will also demonstrate the need of a slack bus. Consider a simple four bus system (Fig. 6.5(a)) out of which two buses are PQ buses, one is PV bus, and the remaining one is a slack bus. The buses are numbered as shown in Table 6.3 (Refer Fig. 6.5(c)).

Table 6.3

No.	*Bus Type*	*Known*	*Unknown*
1.	Slack Bus	$\|V_1\|, \delta_1$	P_1, Q_1
2.	PQ Bus	P_2, Q_2	$\|V_2\|, \delta_2$
3.	PQ Bus	P_3, Q_3	$\|V_3\|, \delta_3$
4.	PV Bus	$P_4, \|V_4\|$	Q_4, δ_4

Total Real Power Loss, $P_L = \sum P_i = P_1 + P_2 + P_3 + P_4$

$= P_1 + K_1$

where $K_1 = P_2 + P_3 + P_4$ (known).

Total Reactive Power Loss, $Q_L = \sum Q_i = Q_1 + Q_2 + Q_3 + Q_4$

$= Q_1 + Q_4 + K_2$

where $K_2 = Q_2 + Q_3$ (known).

Since P_L and Q_L are not known prior to load flow solution, the real and reactive powers (P_i and Q_i) cannot be fixed at all the buses. In the above example, P_1, Q_1 and Q_4 cannot be fixed prior to load flow solution. After the load flow solution is complete, the total real and reactive powers, $P_L = \sum_i P_i$ and $Q_L = \sum_i Q_i$ become known and the slack bus has to supply excess real power $P_1 = P_L - K_1$, and excess reactive power $Q_1 = Q_L - Q_4 - K_2$. This is why a slack bus is needed in load flow solution.

Thus, after a load flow solution is complete, real power at the slack bus (P_1) is known, and hence the real power generation P_{G1} (as P_{D1} is known from load forecasting) is known. As V_1 is already specified for a slack bus, the slack bus must be a generator bus. It is required that the variations in real and reactive powers at the slack bus be a small percentage of its generating capacity. So, the bus connected to the largest generating station is normally selected as the slack bus.

Equations 6.28(a) and (b) which are written below for convenience are referred to as Static Load Flow Equations (SLFE).

$$P_i \text{ (Real power)} = |V_i| \sum_{k=1}^{n} (|V_k|\,|Y_{ik}| \cos(\theta_{ik} + \delta_k - \delta_i)) \tag{6.28a}$$

$$Q_i \text{ (Reactive power)} = -|V_i| \sum_{k=1}^{n} (|V_k|\,|Y_{ik}| \sin(\theta_{ik} + \delta_k - \delta_i))$$

where $i = 1, 2, \ldots, n$ (6.28b)

By transposing all the variables on one side, these equations can be written in the vector form

$$\boldsymbol{f}(\boldsymbol{x}, \boldsymbol{y}) = \boldsymbol{0} \tag{6.29}$$

where $\boldsymbol{f}$ = vector function of dimension $2n \times 1$

$\boldsymbol{x}$ = vector of dependent or state variables of dimension $2n \times 1$

($2n$ independent variables specified *a priori*)

$\boldsymbol{y}$ = vector of independent variables of dimension $2n \times 1$ (2n unspecified variables)

Some of the independent variables in $\boldsymbol{x}$ can be used to manipulate some of the state variables. These adjustable independent variables are called control variables. The remaining independent variables which are fixed are called fixed parameters. Vector $\boldsymbol{x}$ can then be partitioned into a vector $\boldsymbol{u}$ of control variables and a vector $\boldsymbol{p}$ of fixed parameters,

$$\boldsymbol{x} = \begin{bmatrix} \boldsymbol{u} \\ \boldsymbol{p} \end{bmatrix} \tag{6.30}$$

Control variables may be voltage magnitude on PV bus, P_{Gi} at buses with controllable power, etc. Fixed parameters are those which are uncontrollable.

For SLFE solution to have practical significance, all the state and control variables must be within specified practical limits. These limits are dictated by specifications of power system hardware and operating constraints, and are described below:

(1) Voltage magnitude $|V_i|$ must satisfy the inequality

$$|V_i|_{\min} \leq |V_i| \leq |V_i|_{\max} \tag{6.31a}$$

This limit arises due to the fact that the power system equipment is designed to operate at fixed voltages with allowable variations of ±(5–10)% of rated values.

(2) Certain of the δ_is (state variables) must satisfy

$$| \delta_i - \delta_k | \leq | \delta_i - \delta_k |_{\max} \tag{6.31b}$$

This constraint limits the maximum permissible power angle of transmission line connecting buses i and k and is imposed by considerations of stability.

(3) Owing to physical limitations of P and/or Q generation sources, P_{Gi} and Q_{Gi} are constrained as follows:

$$P_{Gi,\ \min} \leq P_{Gi} \leq P_{Gi,\ \max}$$

$$Q_{Gi,\ \min} \leq Q_{Gi} \leq Q_{Gi,\ \max} \tag{6.31c}$$

Also, we have

$$\sum_i P_{Gi} = \sum_i (P_{Di}) + P_L \tag{6.32a}$$

$$\sum_i Q_{Gi} = \sum_i (Q_{Di}) + Q_L \tag{6.32b}$$

where P_L and Q_L are system real and reactive power losses.

The load flow problem can now be fully defined as follows:

Assume a certain nominal bus load configuration. Specify $P_{Gi} + jQ_{Gi}$ at all PQ buses (this specifies $P_i + jQ_i$ at these buses, specify P_{Gi} (this specifies P_i) and $| V_i |$ at all PV buses; and specify $| V_1 |$ and δ_1 (= 0) at the slack bus. Thus all the $2n$ variables of vector $\boldsymbol{x}$ are specified. Thus $2n$ SLFE, which are nonlinear algebraic equations,* can be solved (iteratively) to determine the values of the $2n$ variables of the vector $\boldsymbol{y}$, comprising voltages and angles at the PQ buses; reactive powers and angles at the PV buses; and active and reactive powers at the slack bus.

The next logical step is to compute the line flows.

From the above definition we can state two versions of the load flow problem. In both the cases, bus 1 is assumed as the slack bus.

Case I: We assume all the remaining buses are PQ buses. We have:

Given: $V_1, S_2, S_3, ..., S_n$

Find: $S_1, V_2, V_3, ..., V_n$

Case II: We assume both PV and PQ buses. We number the buses so that buses 2, 3, ... m are PQ buses and $m + 1, ..., n$ are PV buses.

Thus,

Given: $V_1, S_2, ..., S_m, (P_{m+1}, | V_{m+1} |), .., (P_n, | V_n |)$

Find: $S_1, V_2, ..., V_m, (Q_{m+1}, \delta_{m+1}), ..., (Q_n, \delta_n)$

* It is because cosine and sine functions are involved in real and reactive power Eqs 6.28(a) and (b).

Since the load flow equations are essentially non-linear, they have to be solved through iterative numerical techniques. At the cost of solution accuracy, it is possible to linearize load flow equations by making suitable assumptions and approximations so that fast and explicit solutions become possible. Such techniques have value, particularly for planning studies where load flow solutions have to be carried out repeatedly but a high degree of accuracy is not needed. An approximate load flow solution is dealt in Example 6.6.

Once a load flow problem is formulated it can be seen that there exists a range of every independent variable in the vector $\boldsymbol{x}$ for which there is no solution, or there are multiple solutions. For visualizing this problem, we consider a simple two bus system in Example 6.6.

Example 6.6 In Fig. 6.11, bus 1 is the reference bus with $V_1 = 1\angle 0^\circ$ and bus 2 is PQ bus. We are to find S_1 and V_2.

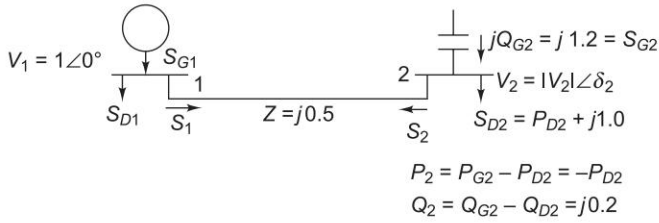

Fig. 6.11 A simple two-bus system

Solution

The complex power injected at the bus 2, S_2 is given by

$$S_2 = S_{G2} - S_{D2} = -P_{D2} + j0.2 \tag{i}$$

Also from Sec. 5.9 of Ch. 5 we have

$$S_2 = S_{21}$$

$$= \frac{|V_2|^2}{|Z|}\angle\theta - \frac{|V_2||V_1|}{Z}\angle(\theta + \delta_2 - \delta_1) \tag{ii}$$

where $$Z = |Z|\angle\theta = 0.5\angle 90^\circ \tag{iii}$$

$$\delta_1 = 0^\circ \text{ as } V_1 = |V_1|\angle\delta_1 = 1\angle 0^\circ$$

From (i), (ii) and (iii), we get

$$-P_{D2} + j0.2 = j2|V_2|^2 - 2|V_2|\cos(\theta + \delta_2) - j2|V_2|\sin(\theta + \delta_2)$$

Equating the real and the imaginary parts on both sides, we get

$$P_{D2} = 2|V_2|\cos(\theta + \delta_2)$$

$$0.2 = 2|V_2|^2 - 2|V_2|\sin(\theta + \delta_2)$$

or we get

$$\cos(\theta + \delta_2) = \frac{P_{D2}}{2|V_2|} \tag{iv}$$

$$\sin(\theta + \delta_2) = \frac{2|V_2|^2 - 0.2}{2|V_2|} = \frac{|V_2|^2 - 0.1}{|V_2|} \tag{v}$$

Squaring and adding, we get

$$1 = \frac{P_{D2}^2}{4|V_2|^2} + \frac{(|V_2|^2 - 0.1)^2}{|V_2|^2}$$

or

$$4|V_2|^4 - 4.8|V_2|^2 + (P_{D2}^2 + 0.04) = 0$$

or

$$|V_2|^2 = \frac{4.8 \pm \sqrt{4.8^2 - 16(P_{D2}^2 + 0.04)}}{8}$$

Thus, if $16(P_{D2}^2 + 0.04) > (4.8)^2$ or $P_{D2} > 1.183$, there are no real solutions. If $P_{D2} = 1.183$, $|V_2| = 0.775$, the solution is unique. If $P_{D2} < 1.183$, there are two real solutions, and hence the solution is non-unique. Let $P_{D2} = 0.5$; then $|V_2| = 0.253$ and 1.066 pu.

Thus, there may be no solution, or at least no unique solution, depending on the given data. In most cases having non-unique solutions, the practical solution is the one with voltage closest to 1 pu. Thus, with $P_{D2} = 0.5$, the desired solution is $|V_2| = 1.066$, and the angle δ_2 is given by Eq. (iv) as

$$\cos(\theta + \delta_2) = \cos(90 + \delta_2) = -\sin\delta_2 = \frac{P_{D2}}{2|V_2|}$$

or

$$\sin\delta_2 = -\frac{P_{D2}}{2|V_2|} = \frac{0.5}{2 \times 1.066} = -0.2345$$

or

$$\delta_2 = -13.56^\circ$$

Also,

$$S_1 = -S_2 = P_{D2} - j0.2 = 0.5 - j0.2$$

The solution of a load flow problem becomes simple when only two buses are present. But, in a normal power system there are large number of buses and the solution becomes quite complex, tedious and time consuming. Hence there is no choice but to use iterative methods. The most commonly used iterative methods are the Gauss–Siedel, the Newton–Raphson and fast-decoupled load flow methods.

An Approximate Load Flow Solution

Let us make the following assumptions and approximations in the load flow Eqs 6.28(a) and (b):

(1) Line resistances, being small, are neglected (shunt conductance of overhead lines is always negligible), i.e. P_L, the active power loss of the system is zero. Thus in Eqs 6.28(a) and (b), $\theta_{ik} = 90^\circ$ and $\theta_{ii} = -90^\circ$.

(2) $(\delta_i - \delta_k)$ is small [$< (\pi/6)$], so that $\sin(\delta_i - \delta_k) \approx (\delta_i - \delta_k)$. This is justified from considerations of stability (see Ch. 12).

(3) All buses other than the slack bus (numbered as 1) are PV buses, i.e. voltage magnitudes at all the buses, including the slack bus, are specified.

Equations 6.28(a) and (b) then reduce to

$$P_i = |V_i| \sum_{k=1}^{n} |V_k||Y_{ik}|(\delta_i - \delta_k) \quad i = 2, 3, ..., n \tag{6.33}$$

$$Q_i = -|V_i| \sum_{\substack{k=1 \\ k \neq i}}^{n} (|V_k||Y_{ik}| \cos(\delta_i - \delta_k)) + |V_i|^2 |Y_{ii}|, \; i = 1, 2, ..., n \tag{6.34}$$

Since $|V_i|$s are specified, Eq. (6.33) represents a set of linear algebraic equations in δ_is, which are $(n-1)$ in number as δ_1 is specified at the slack bus ($\delta_1 = 0$). The nth equation corresponding to the slack bus ($n = 1$) is redundant as the real power injected at this bus is now fully specified as $P_1 = \Sigma P_{Di} - \Sigma P_{Gi}$; ($P_L = 0$). Equation (6.33) can be solved explicitly (non-iteratively) for $\delta_2, \delta_3, ..., \delta_n$, which, when substituted in Eq. (6.34), yields Q_is, the reactive power bus injections. It may be noted that the assumptions made have decoupled Eqs (6.33) and (6.34), so that these need not be solved simultaneously but can be solved sequentially. Solution of Eq. (6.34) follows immediately upon simultaneous solution of Eq. (6.33). Since the solution is non-iterative and the dimension is reduced to $(n-1)$ from $2n$, it is computationally highly economical.

Example 6.7 Consider the four-bus sample system of Fig. 6.12, wherein line reactances are indicated in pu. Line resistances are considered negligible. The magnitudes of all four bus voltages are specified to be 1.0 pu. The bus powers are specified in Table 6.4.

Solution

Figure 6.12 indicates bus injections for the data specified in Table 6.4. As bus voltages are specified, all the buses must have controllable Q sources. It is also obvious from the data that buses 3 and 4 only have Q sources. Further, since the system is assumed lossless, the real power generation at bus 1 is known *a priori* to be $P_{G1} = P_{D1} + P_{D2} + P_{D3} + P_{D4} - P_{G2} = 2.0$ pu. Therefore, we have 7 unknowns instead of $2 \times 4 = 8$.

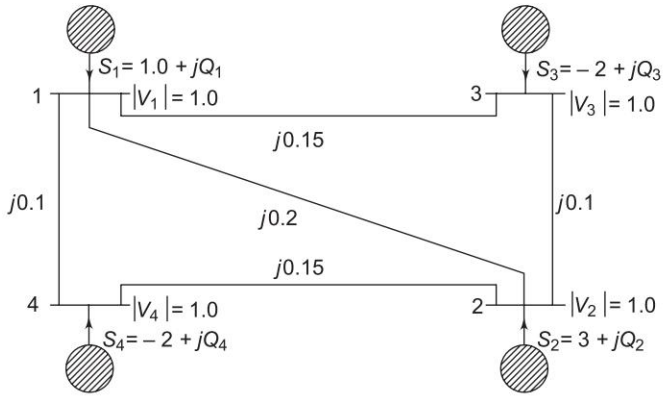

Fig. 6.12 Four bus lossless sample system

Table 6.4

Bus	*Real Demand*	*Reactive Demand*	*Real Generation*	*Reactive Generation*
1.	$P_{D1} = 1.0$	$Q_{D1} = 0.5$	$P_{G1} = ?$	Q_{G1} (unspecified)
2.	$P_{D2} = 1.0$	$Q_{D2} = 0.4$	$P_{G2} = 4.0$	Q_{G2} (unspecified)
3.	$P_{D3} = 2.0$	$Q_{D3} = 1.0$	$P_{G3} = 0.0$	Q_{G3} (unspecified)
4.	$P_{D4} = 2.0$	$Q_{D4} = 1.0$	$P_{G4} = 0.0$	Q_{G4} (unspecified)

In the present problem, the unknown state and control variables are δ_2, δ_3, δ_4, Q_{G1}, Q_{G2}, Q_{G3} and Q_{G4}.

Though the real losses are zero, the presence of the reactive losses requires that the total reactive generation must be more than the total reactive demand (2.9 pu)

From the data given, $\boldsymbol{Y}_{\text{BUS}}$ can be written as follows:

$$\boldsymbol{Y}_{\text{BUS}} = \begin{array}{c} \\ 1 \\ 2 \\ 3 \\ 4 \end{array} \begin{array}{c} \begin{array}{cccc} 1 & 2 & 3 & 4 \end{array} \\ \begin{bmatrix} -j21.667 & j5.000 & j6.667 & j10.000 \\ j5.000 & -j21.667 & j10.000 & j6.667 \\ j6.667 & j10.000 & -j16.667 & j0.000 \\ j10.000 & j6.667 & j0.000 & -j16.667 \end{bmatrix} \end{array} \quad \text{(i)}$$

Using the above $\boldsymbol{Y}_{\text{BUS}}$ and bus powers as shown in Fig. 6.12, approximate load flow Eq. (6.33) is expressed as (all voltage magnitudes are equal to 1.0 pu)

$$P_2 = 3 = 5(\delta_2 - \delta_1) + 10(\delta_2 - \delta_3) + 6.667(\delta_2 - \delta_4) \quad \text{(ii)}$$

$$P_3 = -2 = 6.667\,(\delta_3 - \delta_1) + 10(\delta_3 - \delta_2) \quad \text{(iii)}$$

$$P_4 = -2 = 10(\delta_4 - \delta_1) + 6.667(\delta_4 - \delta_2) \quad \text{(iv)}$$

Taking bus 1 as a reference bus, i.e. $\delta_1 = 0$, and solving (ii), (iii) and (iv), we get

$$\delta_2 = -0.077 \text{ rad} = 4.41^\circ$$

$$\delta_3 = -0.074 \text{ rad} = -4.23^\circ \quad \text{(v)}$$
$$\delta_4 = -0.089 \text{ rad} = -5.11^\circ$$

Substituting δs in Eq. (6.34), we have

$$Q_1 = -5 \cos 4.41^\circ - 6.667 \cos 4.23^\circ - 10 \cos 5.11^\circ + 21.667$$
$$Q_2 = -5 \cos 4.41^\circ - 10 \cos 8.64^\circ - 6.667 \cos 9.52^\circ + 21.667$$
$$Q_3 = -6.667 \cos 4.23^\circ - 10 \cos 8.64^\circ + 16.667$$
$$Q_4 = -10 \cos 5.11^\circ - 6.667 \cos 9.52^\circ + 16.667$$

or

$$Q_1 = 0.07 \text{ pu}$$
$$Q_2 = 0.22 \text{ pu} \quad \text{(vi)}$$
$$Q_3 = 0.132 \text{ pu}$$
$$Q_4 = 0.132 \text{ pu}$$

Reactive power generations at the four buses are

$$Q_{G1} = Q_1 + 0.5 = 0.57 \text{ pu}$$
$$Q_{G2} = Q_2 + 0.4 = 0.62 \text{ pu} \quad \text{(vii)}$$
$$Q_{G3} = Q_3 + 1.0 = 1.132 \text{ pu}$$
$$Q_{G4} = Q_4 + 1.0 = 1.132 \text{ pu}$$

Reactive line losses are

$$Q_L = \sum_{i=1}^{4} Q_{Gi} - \sum_{i=1}^{4} Q_{Di}$$
$$= 3.454 - 2.9 = 0.554 \text{ pu} \quad \text{(viii)}$$

Now, let us find the line flows. Equation (5.68) can be written in the form ($|Z| = X$, $\theta = 90^\circ$)

$$P_{ik} = -P_{ki} = \frac{|V_i||V_k|}{X_{ik}} \sin(\delta_1 - \delta_k)$$

where P_{ik} is the real power flow from bus i to bus k.

$$P_{13} = -P_{31} = \frac{1}{0.15} \sin(\delta_1 - \delta_3) = \sin 4.23^\circ/0.15 = 0.492 \text{ pu}$$

$$P_{12} = -P_{21} = \frac{1}{0.2} \sin(\delta_1 - \delta_2) = -\sin 4.41^\circ/0.02 = -0.385 \text{ pu} \quad \text{(ix)}$$

$$P_{14} = -P_{41} = \frac{1}{0.1} \sin(\delta_1 - \delta_4) = \sin 5.11^\circ/0.1 = 0.891 \text{ pu}$$

Real power flows on other lines can be similarly calculated. For reactive power flow, Eq. (5.69) can be written in the general form ($Z = X$, $\theta = 90°$)

$$Q_{ik} = \frac{|V_i|^2}{X_{ik}} - \frac{|V_i||V_k|}{X_{ik}} \cos(\delta_i - \delta_k)$$

where Q_{ik} is the reactive power flow from bus i to bus k.

$$Q_{12} = Q_{21} = \frac{1}{0.2} - \frac{1}{0.2} \cos(\delta_1 - \delta_2) = 0.015 \text{ pu}$$

$$Q_{13} = Q_{31} = \frac{1}{0.15} - \frac{1}{0.15} \cos(\delta_1 - \delta_3) = 0.018 \text{ pu} \qquad \text{(x)}$$

$$Q_{14} = Q_{41} = \frac{1}{0.1} - \frac{1}{0.1} \cos(\delta_1 - \delta_4) = 0.04 \text{ pu}$$

Reactive power flows on other lines can similarly be calculated. Generations and load demands at all the buses and all the line flows are indicated in Fig. 6.13.

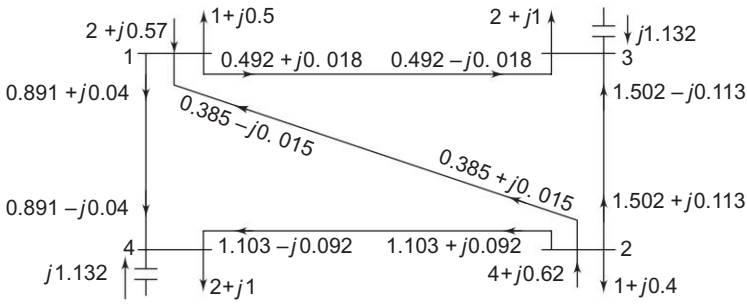

Fig. 6.13 Load flow solution for the four bus system

6.5 GAUSS–SIEDEL METHOD

The Gauss–Siedel (GS) method is an iterative algorithm for solving a set of non-linear algebraic equations. We consider a system of n equations in n unknowns $x_1, ..., x_n$. We rewrite these n equations in the form:

$$x_i = f_i(x_1, ..., x_n),\ i = 1, ..., n$$

To find the solution, we assume initial values for $x_1, ..., x_n$, based on guidance from practical experience in a physical situation. Let the initial values be $x_1^0, .., x_n^0$. Then, we get the first approximate solution by substituting these initial values in the above n equations as follows:

$$x_1^1 = f_1\left(x_1^0, x_2^0 \ldots, x_n^0\right)$$
$$\vdots$$
$$x_i^1 = f_i\left(x_1^1, x_2^1, \ldots, x_{i-1}^1, x_i^0, \ldots, x_n^0\right)$$
$$\vdots$$
$$x_n^1 = f_n\left(x_1^1, x_2^1, \ldots, x_{n-1}^1, x_n^0\right)$$

This completes one iteration. In general, we get the kth approximate solution in the kth iteration as follows:

$$x_i^k = f_i\left(x_1^k, \ldots, x_{i-1}^k, x_i^{k-1}, x_{i+1}^{k-1}, \ldots, x_n^{k-1}\right), \quad i = 1, 2, \ldots, n$$

We note that the value of x_i for the kth iteration is obtained by substituting $x_1^k, x_2^k, \ldots, x_{i-1}^k$ (obtained in kth iteration) and $x_i^{k-1}, \ldots, x_n^{k-1}$ (obtained in $(k-1)$th iteration) in the equation $x_i = f_i$. If $|x_i^k - x_i^{k-1}| < \varepsilon$ (a very small number), for all i values, then the solution is said to converge. The iterative process is repeated till the solution converges within prescribed accuracy. The convergence is quite sensitive to the starting values assumed. Fortunately, in a load flow study, a starting vector close to the final solution can be easily identified with previous experience.

To solve a load flow problem by GS method, we consider two cases depending on the type of buses present. In the first case we assume all the buses other than the slack bus are PQ buses. In the second case, we assume the presence of both PQ and PV buses, other than the slack bus. Later on we also include the presence of voltage controlled bus, whose voltage is controlled by a regulating transformer.

Case I The slack bus is numbered one, and the remaining $(n-1)$ buses are PQ buses ($i = 2, \ldots, n$). With slack bus voltage assumed, the remaining $(n-1)$ bus voltages are found through iterative process as follows:

The complex bus power injected into the ith bus is

$$S_i = P_i + jQ_i = V_i I_i^*$$

or

$$I_i = \frac{P_i - jQ_i}{V_i^*} \tag{6.35}$$

From Eq. (6.2b)

$$V_i = \frac{1}{Y_{ii}}\left(I_i - \sum_{\substack{k=1 \\ k \neq i}}^{n} (Y_{ik} V_k)\right), \quad i = 2, \ldots, n \tag{6.36}$$

Substituting I_i from Eq. (6.35) into Eq. (6.36)

$$V_i = \frac{1}{Y_{ii}} \left[\frac{P_i - jQ_i}{V_i^*} - \sum_{\substack{k=1 \\ k \neq i}}^{n} (Y_{ik} V_k) \right], \quad i = 2, ..., n \tag{6.37}$$

We assume a starting value for V_i ($i = 2, ..., n$). These values are then updated using Eq. (6.37). The voltages substituted at the right hand side of Eq. (6.37) are the most recently (updated) values for the corresponding buses. Iterations are repeated till no bus voltage magnitude changes by more than a prescribed value.

If instead of updating voltages at every step of an iteration, updating is carried out at the end of a complete iteration, the process is known as *Gauss Iterative Method*. It converges much slower and may sometimes fail to do so.

Algorithm for Load Flow Solution (Case I)

1. The slack bus voltage magnitude and angle are assumed, usually $V_1 = 1 \angle 0^\circ$ pu. With the load profile known at each bus (i.e. P_{Di} and Q_{Di} known), we allocate P_{Gi} and Q_{Gi} to all generating stations. With this step, bus injections ($P_i + jQ_i$) are known at all buses other than the slack bus.
2. Assembly of bus admittance matrix ($\boldsymbol{Y}_{\text{BUS}}$): With the line and shunt admittance data stored in the computer, $\boldsymbol{Y}_{\text{BUS}}$ is assembled by using the algorithm developed earlier. Alternatively, $\boldsymbol{Y}_{\text{BUS}}$ is assembled using $\boldsymbol{Y}_{\text{BUS}} = \boldsymbol{A}^T \boldsymbol{Y} \boldsymbol{A}$, where the input data is in the form of primitive admittance matrix $\boldsymbol{Y}$ and singular connection bus incidence matrix $\boldsymbol{A}$.
3. Iterative computation of bus voltages (V_i; $i = 2, ..., n$): To start the iteration, a set of initial voltage values is assumed. Since, in a power system the voltage spread is not too wide, it is normal practice to use a flat voltage start, i.e., initially all voltages are set equal to $(1 + j0)$, except the slack bus voltage, which is fixed. This reduces the n equations to $(n - 1)$ equations in complex numbers (Eq. (6.37)) which are to be solved iteratively for finding complex voltages $V_2, V_3, ..., V_n$. If complex number operations are not available in a computer, Eq. (6.37) can be converted into $2(n - 1)$ equations in real unknowns (e_i, f_i or $| V_i |, \delta_i$) by writing

$$V_i = e_i + jf_i = | V_i | \, \varepsilon^{j\delta_i} \tag{6.38}$$

We also define

$$A_i = \frac{P_i - jQ_i}{Y_{ii}}, \quad i = 2, ..., n \tag{6.39}$$

$$B_{ik} = Y_{ik}/Y_{ii} \quad \begin{matrix} i = 2, ..., n \\ k = 2, ..., n, \; k \neq i \end{matrix} \tag{6.40}$$

Now, for the $(r + 1)$th iteration, the voltage Eq. (6.37) becomes

$$V_i^{(r+1)} = \left[\frac{A_i}{(V_i^r)^*} - \sum_{k=1}^{i-1} (B_{ik} V_k^{(r+1)}) - \sum_{k=i+1}^{n} (B_{ik} V_k^{(r)}) \right], \quad i = 2, ..., n \qquad (6.41)$$

The iterative process is continued till the change in magnitude of bus voltage, $|\Delta V_i^{(r+1)}|$, between two consecutive iterations is less than a certain tolerance for all bus voltages, i.e.

$$|\Delta V_i^{(r+1)}| = |V_i^{(r+1)} - V_i^{(r)}| \leq \varepsilon, \quad i = 2, ..., n \qquad (6.42)$$

Also, we see if $|V_i|_{\min} \leq |V_i| \leq |V_i|_{\max}$, $i = 2, ..., n$.

If not, we fix $|V_i|$ at one of the extreme values, i.e.

$|V_i|_{\min}$ if $|V_i| \leq |V_i|_{\min}$ or $|V_i|_{\max}$ if $|V_i| \geq |V_i|_{\max}$.

Depending on the nature of the problem, we can also check

if $|\delta_i - \delta_k| \leq |\delta_i - \delta_k|_{\max}$ $(i = 1, ..., n; k = 1, ..., n; i \neq k)$

4. Computation of slack bus power: Substitution of all bus voltages computed in step 3 with V_1 in Eqs 6.28(a) and (b) with $i = 1$ yields real and reactive power at the slack bus i.e., $S_1 = P_1 + jQ_1$.
5. Computation of line flows: This is the last step in the load flow analysis wherein the power flows on the various lines of the network are computed. This also enables us to check whether any line is overloaded. Consider the line connecting buses i and k. The line and transformers at each end can be represented by a circuit with series admittance y_{ik} and two shunt admittances y_{ik0} and y_{ki0} as shown in Fig. 6.14.

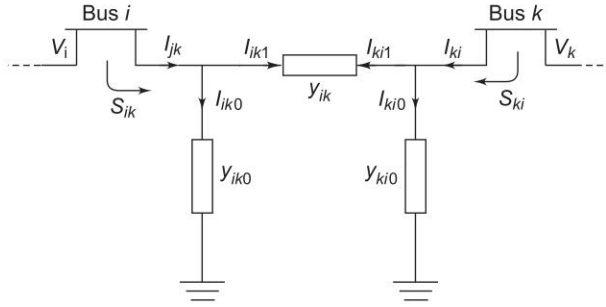

Fig. 6.14 π-representation of a line and transformers connected between two buses

The current fed by bus i into the line can be expressed as

$$I_{ik} = I_{ik1} + I_{ik0} = (V_i - V_k)\, y_{ik} + V_i y_{ik0} \qquad (6.43)$$

The power fed into the line from bus i is

$$S_{ik} = P_{ik} + jQ_{ik} = V_i I^*_{ik} = V_i(V_i^* - V_k^*)\, y_{ik}^* + V_i V_i^* y_{ik0}^* \qquad (6.44)$$

Similarly, the power fed into the line from bus k is

$$S_{ki} = V_k\,(V^*_k - V_i^*)\, y_{ik}^* + V_k V_{iko}^* y_{ki0}^* \qquad (6.45)$$

The power loss in the $(i - k)$th line is the sum of the power flows determined from Eqs (6.44) and (6.45). Total transmission loss can be computed by summing all the line flows (i.e. $S_{ik} + S_{ki}$ for all i, k).

If there are any mutually coupled transmission lines, then we use the Eqs 6.10(a) and (b) to find the currents between lines and then compute for the line flows as above.

It may be noted that the slack bus power can also be found by summing up the flows on the lines terminating at the slack bus.

Acceleration of Convergence

Convergence in the GS method can sometimes be speeded up by the use of the acceleration factor. For the ith bus, the accelerated value of voltage at the $(r + 1)$st iteration is given by

$$V_i^{(r+1)}\,(\text{accelerated}) = V_i^{(r)} + \alpha\left(V_i^{(r+1)} - V_i^{(r)}\right)$$

where α is a real number called the acceleration factor. A suitable value of α for any system can be obtained by trial load flow studies. A generally recommended value is $\alpha = 1.6$. A wrong choice of α may indeed slow down convergence or even cause the method to diverge.

This concludes the load flow analysis for PQ buses only. Next, we consider the presence of PV buses (see Example 6.9).

Case II Here we consider $(m - 1)$ PQ buses, $(n - m)$ PV buses and the slack bus.

Given: V_1, (P_2, Q_2), ..., (P_m, Q_m), $(P_{m+1}, |V_{m+1}|)$, ..., $(P_n, |V_n|)$

To find: S_1, V_2, ..., V_m, (Q_{m+1}, δ_{m+1}), ..., (Q_n, δ_n).

Algorithm (Case II) We first repeat the iteration for PQ buses as in Case I, then continue the iteration for PV buses. At the PV buses, P and $|V|$ are specified and Q and δ are unknowns to be determined. Therefore, the values of Q and δ are to be updated in every GS iteration through appropriate bus equations. This is accomplished in the following steps:

1. From Eq. (6.27b),

$$Q_i = -\,\text{Im}\left\{V_i^* \sum_{k=1}^{n} Y_{ik} V_k\right\}, \quad i = m + 1, ..., n$$

The revised value of Q_i is obtained from the above equation by substituting most updated values of voltages on the right hand side. For the $(r + 1)$th iteration we can write

$$Q_i^{(r+1)} = -\text{Im}\left\{\left(V_i^{(r)}\right)^* \sum_{k=1}^{i-1} Y_{ik}V_k^{(r+1)} + \left(V_i^{(r)}\right)^* \sum_{k=i}^{n} Y_{ik}V_k^{(r)}\right\},$$

$$i = m + 1, \ldots, n \qquad (6.46)$$

2. The revised value of δ_i is obtained from Eq. (6.41) immediately after step 1.

$$\delta_i^{(r+1)} = \angle V_i^{(r+1)}$$

$$= \text{Angle}\left[\frac{A_i^{(r+1)}}{\left(V_i^{(r)}\right)^*} - \sum_{k=1}^{i-1} B_{ik}V_k^{(r+1)} - \sum_{k=i+1}^{n} B_{ik}V_k^{(r)}\right] \qquad (6.47)$$

where

$$A_i^{(r+1)} = \frac{P_i - jQ_i^{(r+1)}}{Y_{ii}}, \qquad i = m + 1, \ldots, n \qquad (6.48)$$

Physical limitations of Q generation require that Q demand at any bus must be in the range $Q_{\min}$ to $Q_{\max}$. If at any stage during iteration, Q at any bus goes outside these limits, it is fixed at $Q_{\min}$ or $Q_{\max}$ as the case may be, and the bus voltage specification is dropped, i.e. the bus is now treated like a PQ bus. Thus Step 1 above branches out to Step 3 as follows:

3. If $Q_i^{(r+1)} \le Q_{i,\min}$, we set $Q_i^{(r+1)} = Q_{i,\min}$ or if $Q_i^{(r+1)} \ge Q_{i,\max}$, we set $Q_i^{(r+1)} = Q_{i,\max}$, and treat the bus i as a PQ bus. We compute $A_i^{(r+1)}$ and $V_i^{(r+1)}$ from Eqs (6.48) and (6.41) respectively.

Now, all the computational steps are summarized in the detailed flow chart of Fig. 6.15. It is assumed that out of n buses, the first is slack bus, then 2, 3, ..., m are PQ buses, and the remaining, $m + 1$, ..., n are PV buses.

Case III We consider here the presence of voltage controlled buses in addition to PQ and PV buses other than the slack bus. This case will be dealt in Example 6.9.

Example 6.8 For the sample system of Fig. 6.7 the generators are connected at all the four buses, while loads are at buses 2 and 3. Values of real and reactive powers are listed in Table 6.5. All buses other than the slack are PQ type.

Assuming a flat voltage start, find the voltages and bus angles at the three buses at the end of the first GS iteration.

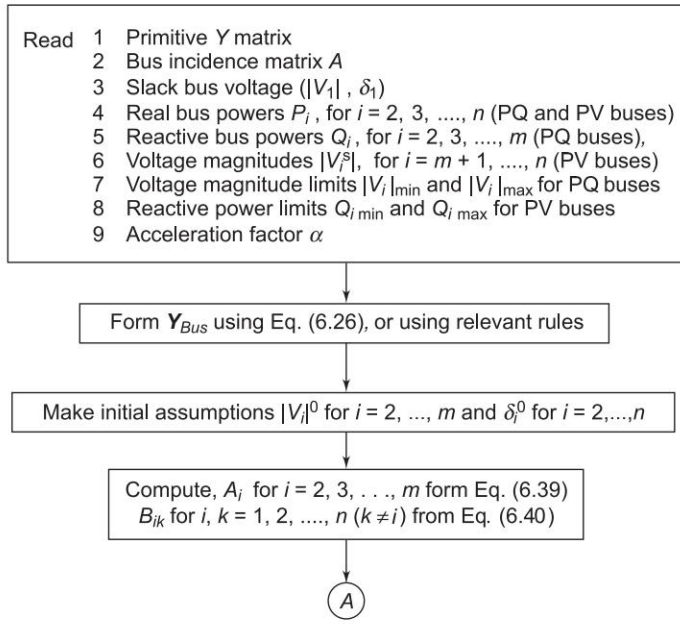

Fig. 6.15(a)

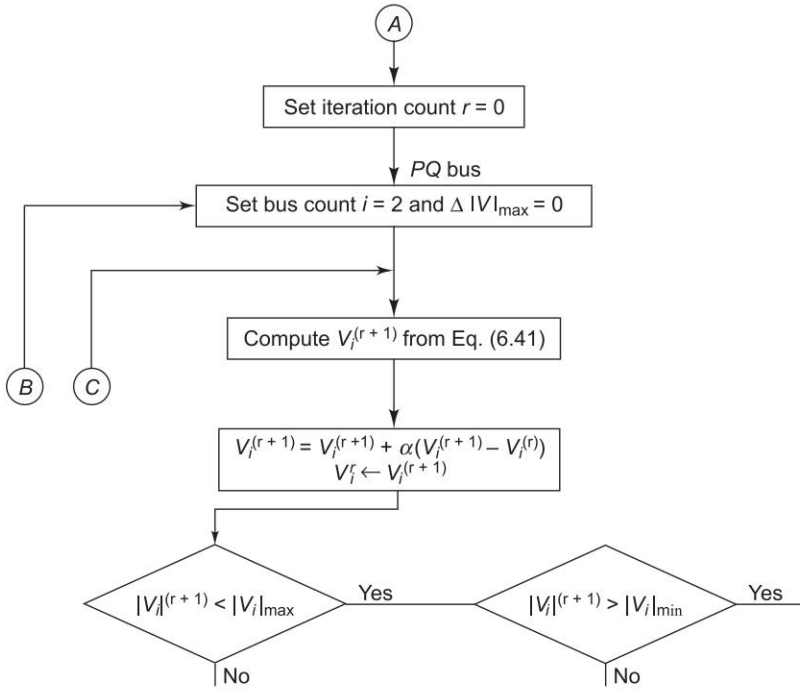

Fig. 6.15(b)

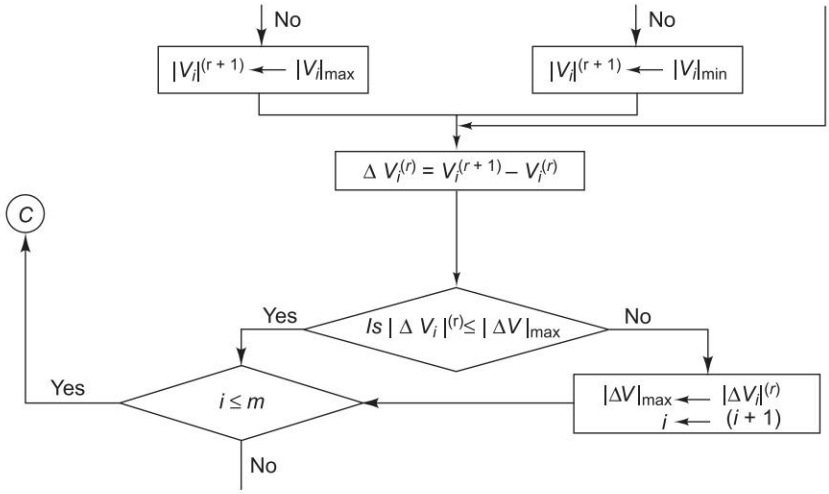

Fig. 6.15(c)

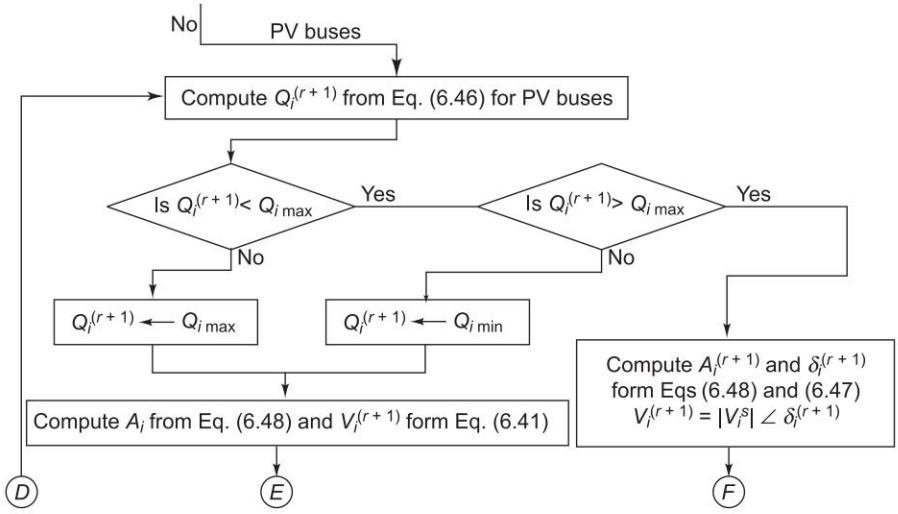

Fig. 6.15(d)

Solution

Table 6.5 Input data

Bus	P_i, *pu*	Q_i, *pu*	V_i, *pu*	*Remarks*
1	–	–	$1.04 \angle 0^o$	Slack bus
2	0.5	– 0.2	–	PQ bus
3	– 1.0	0.5	–	PQ bus
4	0.3	– 0.1	–	PQ bus

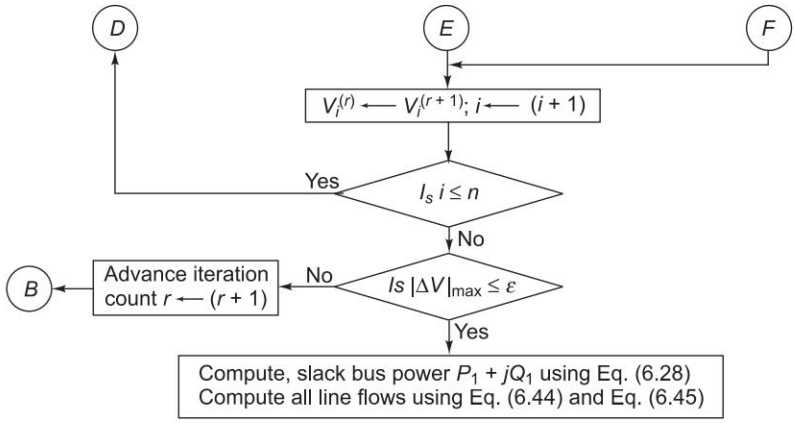

Fig. 6.15(e) Flow chart for load flow solution by the Gauss–Siedel iterative method using $\boldsymbol{Y}_{BUS}$

$$= \frac{2.991 - j9.253}{3 - j9} = 1.025 - j0.0093 \text{ pu}$$

The $\boldsymbol{Y}_{BUS}$ for the sample system has been calculated earlier in Example 6.3(b) (i.e. the dotted line is assumed to be connected). In order to approach the accuracy of a digital computer, the computations given below have been performed on an electronic calculator.

Bus voltages at the end of the first iteration are calculated using Eq. (6.41).

$$V_2^1 = \frac{1}{Y_{22}}\left[\frac{P_2 - jQ_2}{\left(V_2^0\right)^*} - Y_{21}V_1 - Y_{23}V_3^0 - Y_{24}V_4^0\right]$$

$$= \frac{1}{Y_{22}}\left[\frac{0.5 + j0.2}{1 - j0} - 1.04(-2 + j6) - (-0.666 + j2) - (-1 + j3)\right]$$

$$= \frac{4.246 - j11.04}{3.666 - j11} = 1.019 + j0.046 \text{ pu}$$

$$V_3^1 = \frac{1}{Y_{33}}\left[\frac{P_3 - jQ_3}{\left(V_3^0\right)^*} - Y_{31}V_1 - Y_{32}V_2^1 - Y_{34}V_4^0\right]$$

$$= \frac{1}{Y_{33}}\left[\frac{-1 - j0.5}{1 - j0} - 1.04(-1 + j3) - (-0.666 + j2)(1.019 + j0.046) - (-2 + j6)\right]$$

$$= \frac{2.81 - j11.627}{3.666 - j11} = 1.028 - j0.087 \text{ pu}$$

$$V_4^1 = \frac{1}{Y_{44}}\left[\frac{P_4 - jQ_4}{\left(V_4^0\right)^*} - Y_{41}V_1 - Y_{42}V_2^1 - Y_{43}V_3^1\right]$$

$$= \frac{1}{Y_{44}}\left[\frac{0.3 + j0.1}{1 - j0} - (-1 + j3)(1.019 + j0.046) - (-2 + j6)(1.028 - j0.087)\right]$$

Example 6.9 In Example 6.8, let bus 2 be a PV bus now with $|V_2| = 1.04$ pu. Once again assuming a flat voltage start, find Q_2, δ_2, V_3, V_4 at the end of the first GS iteration.

Given: $0.2 \le Q_2 \le 1$ pu

Solution

From Eq. (6.46), we get (*Note:* $\delta_2^0 = 0$, i.e. $V_2^0 = 1.04 + j0$)

$$Q_2^1 = -\text{Im}\left((V_2^0)^* Y_{21} V_1 + (V_2^0)^* (Y_{22} V_2^0 + Y_{23} V_3^0 + Y_{24} V_4^0)\right)$$

$$= -\text{Im}\,(1.04(-2 + j6)\,1.04 + 1.04((3.666 - j11)1.04 + (-0.666 + j2) + (-1 + j3)))$$

$$= -\text{Im}\,(-0.0693 - j0.2097) = 0.2079 \text{ pu}$$

From Eq. (6.47),

$$\delta_2^1 = \angle\frac{1}{Y_{22}}\left[\frac{P_2 - jQ_2^1}{\left(V_2^0\right)^*} - Y_{21}V_1 - Y_{23}V_3^0 - Y_{24}V_4^0\right]$$

$$= \angle\frac{1}{Y_{22}}\left[\frac{0.5 - j0.2079}{1.04 - j0} - (-2 + j6)(1.04 + j0) - (-0.666 + j2)(1 + j0) - (-1 + j3)(1 + j0)\right]$$

$$= \angle\left[\frac{4.2267 - j11.439}{3.666 - j11}\right] = \angle(1.0512 + j0.0339)$$

$$= 1.84658^\circ = 0.032 \text{ red}$$

$$V_2^1 = 1.04\left(\cos\delta_2^1 + j\sin\delta_2^1\right)$$

$$= 1.04\,(0.99948 + j0.0322)$$

$$= 1.03946 + j0.03351$$

$$V_3^1 = \frac{1}{Y_{33}}\left[\frac{P_3 - jQ_3}{\left(V_3^0\right)^*} - Y_{31}V_1 - Y_{32}V_2^1 - Y_{34}V_4^0\right]$$

$$= \frac{1}{Y_{33}}\left[\frac{-1-j0.5}{1-j0} - (-1+j3)1.04 - (-0.66+j2)\right.$$

$$\left.(1.03946+j0.03351) - (-2+j6)\right]$$

$$= \frac{2.7992 - j11.6766}{3.666 - j11} = 1.0317 - j0.08937$$

$$V_4^1 = \frac{1}{Y_{44}}\left[\frac{P_4 - jQ_4}{\left(V_4^0\right)^*} - Y_{41}V_1 - Y_{42}V_2^1 - Y_{43}V_3^1\right]$$

$$= \frac{1}{Y_{44}}\left[\frac{0.3+j0.1}{1-j0} - (-1+j3)\,(1.0394+j0.0335) - (-2+j6)\right.$$

$$\left.(1.0317 - j0.08937)\right]$$

$$= \frac{2.9671 - j8.9962}{3 - j9} = 0.9985 - j0.0031$$

Now, suppose the permissible limits on Q_2 (reactive power injection) are revised as follows:

$$0.25 \le Q_2 \le 1.0 \text{ pu}$$

It is clear that other data remaining the same, the calculated Q_2 (= 0.2079) is now less than the $Q_{2\ \min}$. Hence Q_2 is set equal to $Q_{2\ \min}$ i.e.

$$Q_2 = 0.25 \text{ pu}$$

Bus 2, therefore, becomes a PQ bus from a PV bus. Therefore, $|V_2|$ can no longer remain fixed at 1.04 pu. The value of V_2 at the end of the first iteration is calculated as follows. (*Note:* $V_2^0 = 1 + j0$ by virtue of a flat start).

$$V_2^1 = \frac{1}{Y_{22}}\left[\frac{P_2 - jQ_2}{\left(V_2^0\right)^*} - Y_{21}V_1 - Y_{23}V_3^0 - Y_{24}V_4^0\right]$$

$$= \frac{1}{Y_{22}}\left[\frac{0.5 - j0.25}{1-j0} - (-2+j6)1.04 - (-0.666+j2) - (-1+j3)\right]$$

$$= \frac{4.246 - j11.49}{3.666 - j11} = 1.0559 + j0.0341$$

$$V_3^1 = \frac{1}{Y_{33}}\left[\frac{P_3 - jQ_3}{\left(V_3^0\right)^*} - Y_{31}V_1 - Y_{32}V_2^1 - Y_{34}V_4^0\right]$$

$$= \frac{1}{Y_{33}}\left[\frac{-1-j0.5}{1-j0} - (-1+j3)\,1.04 - (-0.666+j2)\,(1.0559 + j0.0341) - (-2+j6)\right]$$

$$= \frac{2.8112 - j11.709}{3.666 - j11} = 1.0347 - j0.0893 \text{ pu}$$

$$V_4^1 = \frac{1}{Y_{44}}\left[\frac{P_4 - jQ_4}{\left(V_4^0\right)^*} - Y_{41}V_1 - Y_{42} - V_2^1 - Y_{43}V_3^1\right]$$

$$= \frac{1}{Y_{44}}\left[\frac{0.3+j0.1}{1-j0} - (-1+j3)\,(1.0509 + j0.0341) - (-2+j6)\,(1.0347 - j0.0893)\right]$$

$$= \frac{4.0630 - j9.4204}{3 - j9} = 1.0775 + j0.0923 \text{ pu}$$

6.6 NEWTON–RAPHSON METHOD

The Newton–Raphson (NR) method is a powerful method of solving non-linear algebraic equations. It works faster, and is sure to converge in most cases as compared to the Gauss–Siedel (GS) method. (For its convergence properties see Appendix I). It is indeed the practical method of load flow solution of large power networks. Its only drawback is the large requirement of computer memory, which can be overcome through a compact storage scheme. Convergence can be considerably speeded up by performing the first iteration through the GS method, and using the values so obtained for solving the NR iterations.

We consider a set of n nonlinear algebraic equations

$$f_i(x_1, x_2, ..., x_n) = 0 \qquad \text{where } i = 1, 2, ..., n \tag{6.49}$$

We assume initial values of unknowns as $x_1^0, x_2^0, \ldots, x_n^0$. Let $\Delta x_1^0, \Delta x_2^0, \ldots, \Delta x_n^0$ be the corrections to be found out, which on being added to the initial values, give the actual solution. Therefore,

$$f_i\left(x_1^0 + \Delta x_1^0, \ldots, x_n^0 + \Delta x_n^0\right) = 0; \qquad i = 1, 2, ..., n \tag{6.50}$$

Expanding these equations around the initial values by Taylor series, we have

$$f_i^0\left(x_1^0, ..., x_n^0\right) + \left[\left(\frac{\partial f_i}{\partial x_1}\right)^0 \Delta x_1^0 + \cdots + \left(\frac{\partial f_i}{\partial x_n}\right)^0 \Delta x_n^0\right] + \text{higher order terms} = 0 \tag{6.51}$$

where $\left(\frac{\partial f_i}{\partial x_1}\right)^0, \ldots, \left(\frac{\partial f_i}{\partial x_n}\right)^0$ are the derivatives of f_i w.r.t. $x_1, x_2, \ldots, x_n$ evaluated at $x^1_0, \ldots, x^0_n$.

Neglecting the higher order terms, Eq. (6.51) can be written in matrix form as

$$\begin{bmatrix} f_1^0 \\ \vdots \\ f_n^0 \end{bmatrix} + \begin{bmatrix} \left(\frac{\partial f_1}{\partial x_1}\right)^0 & \cdots & \left(\frac{\partial f_1}{\partial x_n}\right)^0 \\ \vdots & & \vdots \\ \left(\frac{\partial f_n}{\partial x_1}\right)^0 & \cdots & \left(\frac{\partial f_n}{\partial x_n}\right)^0 \end{bmatrix} \begin{bmatrix} \Delta x_1^0 \\ \vdots \\ \Delta x_n^0 \end{bmatrix} \cong \begin{bmatrix} 0 \\ \vdots \\ 0 \end{bmatrix} \tag{6.52}$$

or, in vector matrix form

$$\boldsymbol{f}^0 + \boldsymbol{J}^0 \Delta \boldsymbol{x}^0 = 0 \tag{6.53}$$

where $\boldsymbol{J}^0$ is the Jacobian matrix evaluated at $\boldsymbol{x}^0$.

In compact notation,

$$\boldsymbol{J}^0 = \left(\frac{\delta \boldsymbol{f}(\boldsymbol{x})}{\partial \boldsymbol{x}}\right)^0 \tag{6.54}$$

In Eq. (6.53), $\Delta \boldsymbol{x}^0$ is the vector of approximate correction. This can be written in the form

$$\Delta \boldsymbol{x}^0 = (-\boldsymbol{J}^0)^{-1} \boldsymbol{f}^0 \tag{6.55}$$

Thus, $\Delta \boldsymbol{x}^0$ can be evaluated by calculating inverse of $\boldsymbol{J}^0$. But, in practice, we do not evaluate the inverse matrix, as it is computationally expensive and not really needed. Also, the inverse has to be found for every iteration. We write Eq. (6.53) in the form

$$\boldsymbol{J}^0 \Delta \boldsymbol{x}^0 \cong -\boldsymbol{f}^0 \tag{6.56}$$

These, being a set of linear algebraic equations, can be solved for $\Delta \boldsymbol{x}^0$ efficiently by triangularization and back substitution. Updated values of $\boldsymbol{x}$ are then

$$\boldsymbol{x}^1 = \boldsymbol{x}^0 + \Delta \boldsymbol{x}^0$$

In general, for the $(r + 1)$th iteration

$$(\boldsymbol{J}(\boldsymbol{x}^r)) \Delta \boldsymbol{x}^r = -\boldsymbol{f}(\boldsymbol{x}^r)$$

or
$$(-\boldsymbol{J}(\boldsymbol{x}^r)) \Delta \boldsymbol{x}^r = \boldsymbol{f}(\boldsymbol{x}^r) \tag{6.57}$$

or
$$(-\boldsymbol{J}^r) \Delta \boldsymbol{x}^r = \boldsymbol{f}^r$$

and
$$\boldsymbol{x}^{(r+1)} = \boldsymbol{x}^r + \Delta \boldsymbol{x}^r \tag{6.58}$$

Iterations are continued till Eq. (6.49) is satisfied to any desired accuracy, i.e.,

$$|f_i(\boldsymbol{x}^r)| < \varepsilon \text{ (a specified value)}, \quad i = 1, 2, ..., n$$

Thus, each iteration involves the evaluation of $\boldsymbol{f}(\boldsymbol{x}^r)$, $\boldsymbol{J}(\boldsymbol{x}^r)$ and the correction $\Delta\boldsymbol{x}^r$. Therefore, time taken for each iteration by NR method is more compared to the GS method, but the method converges in only a few iterations and the total computation time is much less than by the GS method.

NR Algorithm for Load Flow Solution

We first consider the presence of PQ buses only apart from a slack bus. From Eq. (6.28), for an ith bus,

$$P_i = \sum_{k=1}^{n} |V_i||V_k||Y_{ik}| \cos(\theta_{ik} + \delta_k - \delta_i) = P_i(|\boldsymbol{V}|, \boldsymbol{\delta}) \tag{6.59a}$$

$$Q_i = -\sum_{k=1}^{n} |V_i||V_k||Y_{ik}| \sin(\theta_{ik} + \delta_k - \delta_i) = Q_i(|\boldsymbol{V}|, \boldsymbol{\delta}) \tag{6.59b}$$

i.e. both real and reactive powers are functions of $(|\boldsymbol{V}|, \boldsymbol{\delta})$, where

$$|\boldsymbol{V}| = (|V_1|, ..., |V_n|)^T \quad \boldsymbol{\delta} = (\delta_1, ..., \delta_n)^T$$

We write

$$P_i(|\boldsymbol{V}|, \boldsymbol{\delta}) = P_i(\boldsymbol{x})$$

$$Q_i(|\boldsymbol{V}|, \boldsymbol{\delta}) = Q_i(\boldsymbol{x})$$

where

$$\boldsymbol{x} = \begin{bmatrix} \boldsymbol{\delta} \\ |\boldsymbol{V}| \end{bmatrix}$$

Let P_i (scheduled) and Q_i (scheduled) be the scheduled powers at the load buses. In the course of iteration $\boldsymbol{x}$ should tend to that value which makes

$$P_i - P_i(\boldsymbol{x}) = 0 \text{ and } Q_i - Q_i(\boldsymbol{x}) = 0 \tag{6.60a}$$

Writing Eq. (6.60a) for all load buses, we get its matrix form

$$\boldsymbol{f}(\boldsymbol{x}) = \begin{bmatrix} \boldsymbol{P}(\text{scheduled}) - \boldsymbol{P}(\boldsymbol{x}) \\ \boldsymbol{Q}(\text{scheduled}) - \boldsymbol{Q}(\boldsymbol{x}) \end{bmatrix} = \begin{bmatrix} \Delta\boldsymbol{P}(\boldsymbol{x}) \\ \Delta\boldsymbol{Q}(\boldsymbol{x}) \end{bmatrix} \cong 0 \tag{6.60b}$$

At the slack bus (bus number 1), P_1 and Q_1 are unspecified. Therefore, the values $P_1(\boldsymbol{x})$ and $Q_1(\boldsymbol{x})$ do not enter into Eq. (6.60a), and hence (6.60b). Thus, $\boldsymbol{x}$ is a $2(n-1)$ vector ($n-1$ load buses), with each element function of $(n-1)$ variables given by the vector $\boldsymbol{x} = \begin{bmatrix} \boldsymbol{\delta} \\ |\boldsymbol{V}| \end{bmatrix}$

From Eq. (6.57), we can write

$$\boldsymbol{f}(\boldsymbol{x}) = \begin{bmatrix} \Delta \boldsymbol{P}(\boldsymbol{x}) \\ \Delta \boldsymbol{Q}(\boldsymbol{x}) \end{bmatrix} = \begin{bmatrix} -\boldsymbol{J}_{11}(\boldsymbol{x}) & -\boldsymbol{J}_{12}(\boldsymbol{x}) \\ -\boldsymbol{J}_{21}(\boldsymbol{x}) & -\boldsymbol{J}_{22}(\boldsymbol{x}) \end{bmatrix} \begin{bmatrix} \Delta \delta \\ \Delta |\boldsymbol{V}| \end{bmatrix} \tag{6.61a}$$

where $\Delta\boldsymbol{\delta} = (\Delta\delta_2, .., \Delta\delta_n)^T$

$$\Delta |\boldsymbol{V}| = (\Delta |V_2|, ..., \Delta |V_n|)^T$$

$$\boldsymbol{J}(\boldsymbol{x}) = \begin{bmatrix} -\boldsymbol{J}_{11}(\boldsymbol{x}) & -\boldsymbol{J}_{12}(\boldsymbol{x}) \\ -\boldsymbol{J}_{21}(\boldsymbol{x}) & -\boldsymbol{J}_{22}(\boldsymbol{x}) \end{bmatrix} \tag{6.61b}$$

$\boldsymbol{J}(\boldsymbol{x})$ is the Jacobian matrix, Each $\boldsymbol{J}_{11}$, $\boldsymbol{J}_{12}$, $\boldsymbol{J}_{21}$, $\boldsymbol{J}_{22}$ are $(n-1) \times (n-1)$ matrices. It follows from Eq. (6.52) and Eq. (6.60b) that

$$\begin{aligned} -\boldsymbol{J}_{11}(\boldsymbol{x}) &= \frac{\partial \boldsymbol{P}(\boldsymbol{x})}{\partial \delta} \\ -\boldsymbol{J}_{12}(\boldsymbol{x}) &= \frac{\partial \boldsymbol{P}(\boldsymbol{x})}{\partial |\boldsymbol{V}|} \\ -\boldsymbol{J}_{21}(\boldsymbol{x}) &= \frac{\partial \boldsymbol{Q}(\boldsymbol{x})}{\partial \delta} \\ -\boldsymbol{J}_{22}(\boldsymbol{x}) &= \frac{\partial \boldsymbol{Q}(\boldsymbol{x})}{\partial |\boldsymbol{V}|} \end{aligned} \tag{6.62}$$

The elements of $-\boldsymbol{J}_{11}$, $-\boldsymbol{J}_{12}$, $-\boldsymbol{J}_{21}$, $-\boldsymbol{J}_{22}$ are $\frac{\partial \boldsymbol{P}_i(\boldsymbol{x})}{\partial \delta_k}, \frac{\partial \boldsymbol{P}_i(\boldsymbol{x})}{\partial |V_k|}, \frac{\partial \boldsymbol{Q}_i(\boldsymbol{x})}{\partial \delta_k}, \frac{\partial \boldsymbol{Q}_i(\boldsymbol{x})}{\partial |V_k|}$, where $i = 2, .., n$; $k = 2, ..., n$.

From Eqs 6.59(a) and (b) we have

$$\frac{\partial \boldsymbol{P}_i(\boldsymbol{x})}{\partial \delta_k} = -|V_i||V_k||Y_{ik}| \sin(\theta_{ik} + \delta_k - \delta_i) \quad (i \neq k)$$

$$= \sum_{\substack{k=1 \\ k \neq i}}^{n} |V_i||V_k||Y_{ik}| \sin(\theta_{ik} + \delta_k - \delta_i)) \quad (i = k) \tag{6.63a}$$

$$\frac{\partial \boldsymbol{P}_i(\boldsymbol{x})}{\delta |V_k|} = |V_i||Y_{ik}| \cos(\theta_{ik} + \delta_k - \delta_i) \quad (i \neq k) \tag{6.63b}$$

$$= 2|V_i||Y_{ii}| \cos\theta_{ii} + \sum_{\substack{k=1 \\ k \neq i}}^{n} (|V_k||Y_{ik}| \cos(\theta_{ik} + \delta_k - \delta_i)) \quad (i = k)$$

$$\frac{\partial \boldsymbol{Q}_i(\boldsymbol{x})}{\partial \delta_k} = |V_i||Y_{ik}||V_k|\cos(\theta_{ik} + \delta_k - \delta_i) \quad (i \neq k)$$

$$= -\sum_{\substack{k=1 \\ k \neq i}}^{n} (|V_i||V_k||Y_{ik}|\cos(\theta_{ik} + \delta_k - \delta_i)) \quad (i = k) \tag{6.63c}$$

$$\frac{\partial \boldsymbol{Q}_i(\boldsymbol{x})}{\partial |V_k|} = |V_i||Y_{ik}|\sin(\theta_{ik} + \delta_k - \delta_i) \quad (i \neq k)$$

$$= 2|V_i||Y_{ii}|\sin\theta_{ii} + \sum_{\substack{k=1 \\ k \neq i}}^{n} (|V_k||Y_{ik}|\sin(\theta_{ik} + \delta_k - \delta_i)) \quad (i = k) \tag{6.63d}$$

An important observation can be made with respect to the elements of Jacobian matrix. If there is no connection between ith and kth bus, then $Y_{ik} = 0$, and from Eq. (6.63), the elements of the Jacobian matrix corresponding to ith and kth buses are zero. Hence, like $\boldsymbol{Y}_{\text{BUS}}$ matrix, the Jacobian matrix is also sparse. There are computational techniques to take advantage of this sparsity in the computer solution.

The Jacobian matrix in Eq. (6.61) is rearranged for obtaining the approximate correction vectors and can be written as:

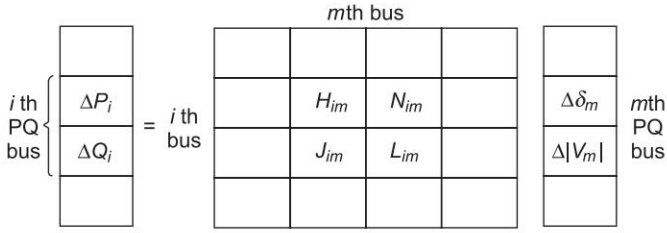

(6.64)

$i = 2, ..., n$ and $m = 2, ..., n$, where

$$H_{im} = \frac{\partial P_i}{\partial \delta_m}$$

$$N_{im} = \frac{\partial P_i}{\partial |V_m|} \tag{6.64a}$$

$$J_{im} = \frac{\partial Q_i}{\partial \delta_m}$$

$$L_{im} = \frac{\partial Q_i}{\partial |V_m|} \tag{6.64b}$$

It is to be immediately observed that the Jacobian elements corresponding to the *i*th bus residuals and *m*th bus corrections are a 2×2 matrix enclosed in the box in Eq. (6.64), where *i* and *m* are both PQ buses.

Consider now the presence of PV buses. Since Q_i is not specified and $|V_i|$ is fixed for a PV bus, ΔQ_i does not enter on the LHS of Eq. (6.64), and $\Delta |V_i|$ (= 0) does not enter on the RHS of Eq. (6.64). Let *i*th and *m*th buses be PQ buses and *j*th and *k*th buses be PV buses. Then we have

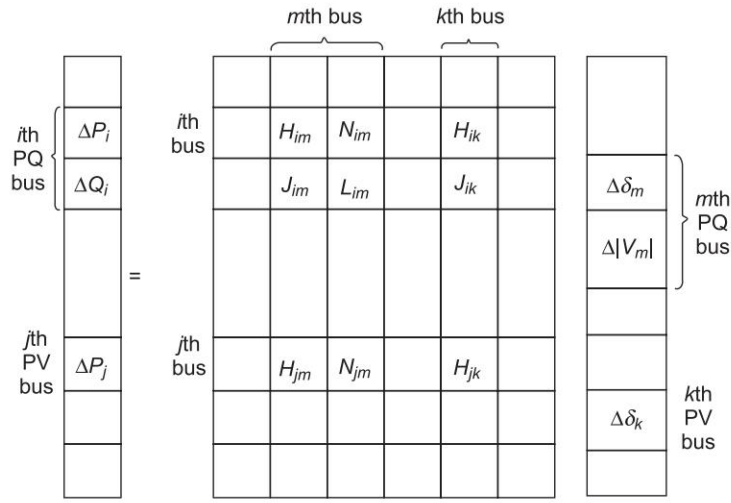

(6.65)

It is convenient for numerical solution to normalize the voltage corrections as $\Delta |V_m| / |V_m|$, as a consequence of which, the corresponding Jacobian elements become

$$N_{im} = \frac{\partial P_i}{\partial |V_m|} |V_m|$$

$$L_{im} = \frac{\partial Q_i}{\partial |V_m|} |V_m| \tag{6.66}$$

Expressions for elements of the Jacobian (in normalized form) of load flow Eq. (6.60b) are derived in Appendix D and are given below:

Case 1 $(m \neq i)$

$$H_{im} = L_{im} = a_m f_i - b_m e_i$$

$$N_{im} = -J_{im} = a_m e_i + b_m f_i \tag{6.67}$$

where

$$Y_{im} = G_{im} + JB_{im}$$

$$V_i = e_i + jf_i$$

$$a_m + jb_m = (G_{im} + jB_{im})(e_m + jf_m)$$

Case 2 $m = i$

$$\begin{aligned} H_{ii} &= -Q_i - B_{ii} |V_i|^2 \\ N_{ii} &= P_i + G_{ii} |V_i|^2 \\ J_{ii} &= P_i - G_{ii} |V_i|^2 \\ L_{ii} &= Q_i - B_{ii} |V_i|^2 \end{aligned} \tag{6.68}$$

If buses i and m are not connected, $Y_{im} = 0$ ($G_{im} = B_{im} = 0$).

Hence from Eq. (6.67) we can write

$$\begin{aligned} H_{im} &= H_{mi} = 0 \\ N_{im} &= N_{mi} = 0 \\ J_{im} &= J_{mi} = 0 \\ L_{im} &= L_{mi} = 0 \end{aligned} \tag{6.69}$$

Thus the Jacobian is as sparse as the $\boldsymbol{Y}_{\text{BUS}}$ matrix.

Formation of Eq. (6.65) of the NR method is best illustrated by a problem. Figure 6.16 shows a five bus power network with bus types indicated therein. The matrix equation for determining vector of corrections from the vector of residuals follows very soon.

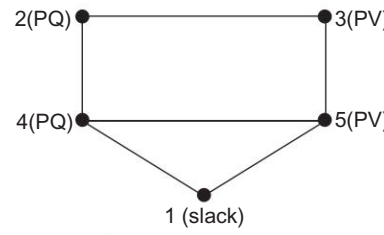

Fig. 6.16 Sample five-bus network

Corresponding to a particular vector of variables (δ_2, $|V_2|$, δ_3, δ_4, ΔQ_2, $|V_4|$, δ_5)^T, the vector of residuals is (ΔP_2, ΔQ_2, ΔP_3, ΔP_4, ΔQ_4, ΔP_5)^T and the Jacobian (6×6 in this example) are computed.

↓ bus no. | bus no. → | 2 | 3 | 4 | 5

$$\begin{array}{c|c|c|cccccc|c} & \Delta P_2 & & H_{22} & N_{22} & H_{23} & H_{24} & N_{24} & & \Delta\delta_2 \\ 2 & \Delta Q_2 & & J_{22} & L_{22} & J_{23} & J_{24} & L_{24} & & \Delta|V_2| \,/\, |V_2| \\ 3 & \Delta P_3 & = & H_{32} & N_{32} & H_{33} & & & H_{35} & \Delta\delta_3 \\ 4 & \Delta P_4 & & H_{42} & N_{42} & & H_{44} & N_{44} & H_{45} & \Delta\delta_4 \\ & \Delta Q_4 & & J_{42} & L_{42} & & J_{44} & L_{44} & J_{45} & \Delta|V_4| \,/\, |V_4| \\ 5 & \Delta P_5 & & & & H_{53} & H_{54} & N_{54} & H_{55} & \Delta\delta_5 \end{array} \tag{6.70}$$

Residuals — Jacobian (evaluated at trial values of variables) — Corrections in variables

Equation 6.70 is then solved by triangularization and back substitution procedure to obtain the vector of corrections ($\Delta\delta_2$, $\Delta \mid V_2 \mid / \mid V_2 \mid$, $\Delta\delta_3$, $\Delta\delta_4$, $\Delta \mid V_4 \mid / \mid V_4 \mid$, $\Delta\delta_5)^T$. Corrections are then added to update the vector of variables.

Iterative Algorithm

The iterative algorithm for the solution of the load flow problem by the NR method is as follows:

1. With the voltage and angle at the slack bus fixed at $V_1 \angle\delta_1$ (= $1 \angle 0^o$), we assume $\mid V \mid, \angle\delta$ at all PQ buses and δ at all PV buses. In the absence of any information flat voltage start is recommended.
2. In the rth iteration, we have (see Eqs 6.28(a) and (b))

$$P_i^r = \sum_{k=1}^{n} \mid V_i \mid^r \mid V_k \mid^r \mid Y_{ik} \mid \cos\left(\theta_{ik} + \delta_k^r - \delta_i^r\right) \tag{6.71a}$$

$$Q_i^r = -\sum_{k=1}^{n} \mid V_i \mid^r \mid V_k \mid^r \mid Y_{ik} \mid \sin\left(\theta_{ik} + \delta_k^r - \delta_i^r\right) \tag{6.71b}$$

Let $$e_i^r = \mid V_i \mid^r \cos\delta_i^r, f_i^r = \mid V_i \mid^r \sin\delta_i^r \tag{6.72}$$

$$G_{ik} = \mid Y_{ik} \mid \cos\theta_{ik}, B_{ik} = \mid Y_{ik\mid} \sin\theta_{ik} \tag{6.73}$$

Using Eqs (6.72) and (6.73) in Eqs 6.71(a) and (b), we have

$$P_i^r = \sum_{k=1}^{n} (e_i^r (e_k^r G_{ik} - f_k^r B_{ik}) + f_i^r (f_k^r G_{ik} + e_k^r B_{ik})) \tag{6.74a}$$

$$Q_i^r = \sum_{k=1}^{n} (f_i^r (e_k^r G_{ik} - f_k^r B_{ik}) - e_i^r (f_k^r G_{ik} + e_k^r B_{ik})), \; i = 2, \ldots, n \tag{6.74b}$$

We next compute

$$\Delta P_i^r = P_i \text{ (scheduled)} - P_i^r \quad \text{for PV and PQ buses} \tag{6.75a}$$

$$\Delta Q_i^r = Q_i \text{ (scheduled)} - Q_i^r \quad \text{for PQ buses} \tag{6.75b}$$

If all values of ΔP_i^r and ΔQ_i^r are less than the prescribed tolerance, we stop the iteration, calculate P_1 and Q_1 and print the entire solution, including line flows.

3. If the convergence criterion is not satisfied, we evaluate the Jacobian elements using Eqs (6.67) and (6.68).
4. We solve Eq. (6.65) for correction of voltage magnitudes $\Delta \mid V \mid^r$ and angle $\Delta\delta^r$.

5. Next we update voltage magnitudes and angles,

$$|\boldsymbol{V}|^{(r+1)} = |\boldsymbol{V}|^r + |\Delta \boldsymbol{V}|^r$$

$$\boldsymbol{\delta}^{(r+1)} = \boldsymbol{\delta}^r + \Delta \boldsymbol{\delta}^r$$

Then we return to step 2.

It is to be noted that:

(a) In step 2, if there are limits on the controllable Q sources at PV buses, Q is computed each time using Eq. (6.74b), and if it violates the limits, it is made equal to the limiting value and the corresponding PV bus is made PQ bus in that iteration. If in subsequent computation, Q comes with the prescribed limits, the bus is switched back to a PV bus. Thus if $|Q_i|^r \geq Q_{i\,\max}$, then we let $|Q_i| = Q_{i\,\max}$ and we have from Eq. (6.65)

$$\Delta Q^r{}_i = Q_i - Q^r{}_i = \sum_{k=2}^{m} \left(J^r{}_{ik}\, \Delta\delta^r{}_k + L^r{}_{ik}\, \Delta |V_k|^r \right) + \sum_{k=m+1}^{n} J^r_{ik}\ \Delta\delta^r{}_k \quad (6.76)$$

In the RHS of Eq. (6.76), all $\Delta\delta_k$s and $\Delta\ |V_k|$s are known except $\Delta |V_i|^r \cdot J_{ik}$s and L_{ik}s are calculated from Eqs (6.67) and (6.68).

Hence, from Eq. (6.76)

$$\Delta |V_i|^r = \frac{1}{L^r_{ii}} \left[\Delta Q^r_i - \sum_{\substack{k=2 \\ k \neq i}}^{n} \left(J_{ik} \Delta\delta^r_k + L^r_{ik} \Delta |V_k|^r \right) - \sum_{\substack{k=m+1 \\ k \neq i}}^{n} \left(J^r_{ik} \Delta\delta^r_k \right) - J^r_{ii} \Delta\delta^r_i \right] \quad (6.77)$$

After computing $\Delta |V_i|^r$, the new value of $|V_i|$ (scheduled) for the PV bus (now a PQ bus due to violation of the limits on Q^r_i) is

$$|V_i| = |V_i| \text{ (scheduled)} + \Delta |V_i|^r \quad (6.78)$$

With this scheduled value of $|V_i|$, the bus is restored to PV bus, and the next iteration is continued. The above procedure is repeated till Q^r_i lies within its limits.

(b) Similarly, if there are voltage limits on a PQ bus, and if any of these limits is violated, the corresponding PQ bus is made a PV bus in that iteration with voltage fixed at the limiting value.

The detailed flow chart for load flow solution by NR method is given in Fig. 6.18.

Example 6.10 Consider the three-bus system of Fig. 6.17. Each of the three lines has a series impedance of 0.02 + *j*0.08 pu and a total shunt admittance of *j*0.02 pu. The specified quantities at the buses are tabulated below:

Bus	Real load demand P_D	Reactive load demand Q_D	Real power generation P_G	Reactive Power generation Q_G	Voltage specification
1	2.0	1.0	Unspecified	Unspecified	$V_1 = 1.04 + j0$ (Slack bus)
2	0.0	0.0	0.5	1.0	Unspecified (PQ bus)
3	1.5	0.6	0.0	$Q_{G3} = ?$	$V_3 = 1.04$ (PV bus)

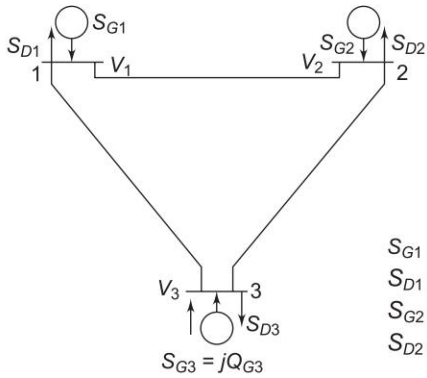

Fig. 6.17 Three-bus system for Example 6.9

Controllable reactive power source is available at bus 3 with the constraint,

$$0 \leq Q_{G3} \leq 1.5 \text{ pu}$$

Find the load flow solution using the NR method. Use a tolerance of 0.01 for power mismatch.

Solution

Using the nominal-π model for transmission lines, $\boldsymbol{Y}_{\text{BUS}}$ for the given system is obtained as follows. For each line

$$y_{\text{series}} = \frac{1}{0.02 + J\,0.08} = 2.941 - j11.764 = 12.13 \angle -75.96°$$

Each off-diagonal term $= -2.941 + j11.764$

Each self term $= 2((2.941 - j11.764) + j0.01)$

$$= 5.882 - j23.528 = 24.23 \angle -75.95°$$

$$\boldsymbol{Y}_{\text{BUS}} = \begin{bmatrix} 24.23\angle -75.95° & 12.13\angle 104.04° & 12.13\angle 104.04° \\ 12.13\angle 104.04° & 24.23\angle -75.95° & 12.13\angle 104.04° \\ 12.13\angle 104.04° & 12.13\angle 104.04° & 24.23\angle -75.95° \end{bmatrix}$$

To start iteration choose $V_2^0 = 1 + j0$ and $\delta_3^0 = 0$.

From Eqs 6.28(a) and (b)

$$P_2 = [|V_2||V_1||Y_{21}|\cos(\theta_{21} + \delta_1 - \delta_2) + |V_2|^2 |Y_{22}|\cos\theta_{22} + |V_2||V_3||Y_{23}|\cos(\theta_{23} + \delta_3 - \delta_2)]$$

$$P_3 = [|V_3||V_1||Y_{31}|\cos(\theta_{31} + \delta_1 - \delta_3) + |V_3||V_2||Y_{32}|\cos(\theta_{32} + \delta_2 - \delta_3) + |V_3|^2 |Y_{33}|\cos\theta_{33}]$$

$$Q_2 = [-|V_2||V_1||Y_{21}|\sin(\theta_{21} + \delta_1 - \delta_2) - |V_2|^2 |Y_{22}|\sin\theta_{22} - |V_2||V_3||Y_{23}|\sin(\theta_{23} + \delta_3 - \delta_2)]$$

Substituting given and assumed values of different quantities, we get the values of powers as

$$P_2^0 = -0.23 \text{ pu}$$

$$P_3^0 = 0.12 \text{ pu}$$

$$Q_2^0 = -0.96 \text{ pu}$$

Power residuals as per Eq. (6.60b) are

$$\Delta P_2^0 = P_2 \text{ (specified)} - P_2^0 \text{ (calculated)} = 0.5 - (-0.23) = 0.73$$

$$\Delta P_3^0 = -1.5 - (0.12) = -1.62$$

$$\Delta Q_2^0 = 1 - (-0.96) = 1.96$$

The changes in variables at the end of the first iteration are obtained as follows:

$$\begin{bmatrix} \Delta P_2 \\ \Delta P_3 \\ \Delta Q_2 \end{bmatrix} = \begin{bmatrix} \partial P_2/\partial\delta_2 & \partial P_2/\partial\delta_3 & \partial P_2/\partial|V_2| \\ \partial P_3/\partial\delta_2 & \partial P_3/\partial\delta_3 & \partial P_3/\partial|V_2| \\ \partial Q_2/\partial\delta_2 & \partial Q_2/\partial\delta_3 & \partial Q_2/\partial|V_2| \end{bmatrix} = \begin{bmatrix} \Delta\delta_2 \\ \Delta\delta_3 \\ \Delta|V_2| \end{bmatrix}$$

Jacobian elements can be evaluated by differentiating the expressions given above for P_2, P_3, Q_2 with respect to δ_2, δ_3 and $|V_2|$ and substituting the given and assumed values at the start of iteration. The changes in variables are obtained as

$$\begin{bmatrix} \Delta\delta_2^1 \\ \Delta\delta_3^1 \\ \Delta|V_2|^1 \end{bmatrix} = \begin{bmatrix} 24.47 & -12.23 & 5.64 \\ -12.23 & 24.95 & -3.05 \\ -6.11 & 3.05 & 22.54 \end{bmatrix}^{-1} \begin{bmatrix} 0.73 \\ -1.62 \\ 1.96 \end{bmatrix} = \begin{bmatrix} -0.0230 \\ -0.0654 \\ 0.0890 \end{bmatrix}$$

$$\begin{bmatrix} \delta_2^1 \\ \delta_3^1 \\ |V_2|^1 \end{bmatrix} = \begin{bmatrix} \delta_2^0 \\ \delta_3^0 \\ |V_2|^0 \end{bmatrix} + \begin{bmatrix} \Delta\delta_2^1 \\ \Delta\delta_3^1 \\ \Delta|V_2|^1 \end{bmatrix} = \begin{bmatrix} 0 \\ 0 \\ 1 \end{bmatrix} + \begin{bmatrix} -0.0230 \\ -0.0654 \\ +0.0890 \end{bmatrix} = \begin{bmatrix} -0.0230 \\ -0.0654 \\ 1.0890 \end{bmatrix}$$

We can now calculate, using Eq. (6.28b),

$$Q_3^1 = 0.4677$$

$$Q_{G3}^1 = Q_3^1 + Q_{D3} = 0.4677 + 0.6 = 1.0677$$

which is within limits.

If the same problem is solved using a digital computer, the solution converges in three iterations. The final results are given below:

$$V_2 = 1.081 \angle -0.024 \text{ rad}$$
$$V_3 = 1.04 \angle -0.0655 \text{ rad}$$
$$Q_{G3} = -0.15 + 0.6 = 0.45 \text{ (within limits)}$$
$$S_1 = 1.031 + j(-0.791)$$
$$S_2 = 0.5 + j1.00$$
$$S_3 = -1.5 - j0.15$$

Transmission loss = 0.031 pu

Line Flows

The following matrix shows the real part of line flows.

$$\begin{bmatrix} 0.0 & 0.191312E00 & 0.839861E00 \\ -0.184229E00 & 0.0 & 0.684697E00 \\ -0.826213E00 & -0.673847E00 & 0.0 \end{bmatrix}$$

The following matrix shows the imaginary part of line flows.

$$\begin{bmatrix} 0.0 & -0.599464E00 & -0.191782E00 \\ -0.605274E00 & 0.0 & 0.396045E00 \\ 0.224742E00 & -0.375165E00 & 0.0 \end{bmatrix}$$

Rectangular Power-Mismatch Version

Equation (6.60) represents a set of independent equations

$$\Delta P_i(|V|, \delta) = 0 \quad (i = 2, ..., n;\ n = \text{number of buses})$$
$$\Delta Q_i(|V|, \delta) = 0 \quad (i = 2, ..., m;\ m - 1 = \text{number of PQ buses})$$

each a function of $|\boldsymbol{V}| = (|V_2|, ..., |V_m|$ and

$$\delta = (\delta_2, ..., \delta_n)^T$$

Thus, this involves the solution of a total of $(m + n - 2)$ independent equations in $(m + n - 2)$ variables $|V_i| \rightarrow (m - 1)$ and $\delta_i \rightarrow (n - 1)$. In rectangular power-mismatch version, the variables used are e_i and f_i $(1 = 2, ..., n)$ giving a total of 2 $(n - 1)$ variables. Here, in addition to the independent power difference equations, we also have the independent voltage difference equations $(|V_i|^2 - (e_i^2 + f_i^2)) = 0$ for PV buses, thus giving a total of $2(n - 1)$ independent

equations in $2(n-1)$ variables. Thus, the number of equations and variables in rectangular power mismatch version is greater than for Eq. (6.60), by the number of PV buses. With sparsity programming, this increase in order is hardly of any significance. Indeed each iteration is marginally faster than for Eq. (6.60) since there are no time consuming sine and cosine terms. It may, however, be noted that even the polar version avoids these, as far as possible, by using rectangular arithmetic in constructing Eqs (6.67) and (6.68). The rectangular version seems to be slightly less reliable, but faster in convergence than the polar version.

Thus we have the following independent equations:

$$P_i\,(\text{specified}) - \sum_{k=1}^{n}(e_i(e_kG_{ik} - f_iB_{ik}) + f_i(f_kG_{ik} + e_kB_{ik})) = 0 \quad (6.79a)$$

$i = 2, \ldots, n$ for both PQ and PV buses

$$Q_i\,(\text{specified}) - \sum_{k=1}^{n}(f_i(e_kG_{ik} - f_iB_{ik}) - e_i(f_kG_{ik} + e_kB_{ik})) = 0 \quad (6.79b)$$

$i = 2, \ldots, m$ for each PQ buses

and also

$$(|V_i|\,(\text{specified}))^2 - \left(e_i^2 + f_i^2\right) = 0 \quad (6.79c)$$

$i = m+1, \ldots, n$ for each PV buses

or

$$P_i - P_i(\boldsymbol{e}, \boldsymbol{f}) = 0 \quad \text{(for both PQ and PV buses)} \quad (6.79d)$$

$$Q_i - Q_i(\boldsymbol{e}, \boldsymbol{f}) = 0 \quad \text{(for each PQ buses)} \quad (6.79e)$$

$$|V_i|^2 - (e_i^2 + f_i^2) = 0 \quad \text{(for each PV buses)} \quad (6.79f)$$

where $\boldsymbol{e} = (e_2, \ldots, e_n)^T$ and $\boldsymbol{f} = (f_2, \ldots, f_n)^T$.

In general $(e_i^2 + f_i^2)$ is also a function of $(\boldsymbol{e}, \boldsymbol{f})$. Using the NR method, the linearized equations in the rth iteration of the iterative process can be written as

$$\begin{bmatrix} \Delta \boldsymbol{P} \\ \Delta \boldsymbol{Q} \\ \Delta |\boldsymbol{V}|^2 \end{bmatrix}^{(r)} = \begin{bmatrix} \boldsymbol{J}_1 & \boldsymbol{J}_2 \\ \boldsymbol{J}_3 & \boldsymbol{J}_4 \\ \boldsymbol{J}_5 & \boldsymbol{J}_6 \end{bmatrix}^{(r)} \begin{bmatrix} \Delta \boldsymbol{e} \\ \Delta \boldsymbol{f} \end{bmatrix}^{(r)} \quad (6.80)$$

where,

For $i \neq j$

$$J_{1,ij} = -J_{4,ij} = G_{ij}e_if_i$$

$$J_{2,ij} = J_{3,ij} = -B_{ij}e_i + G_{ij}f_i \quad (6.81a)$$

$$J_{5,ij} = J_{6,ij} = 0$$

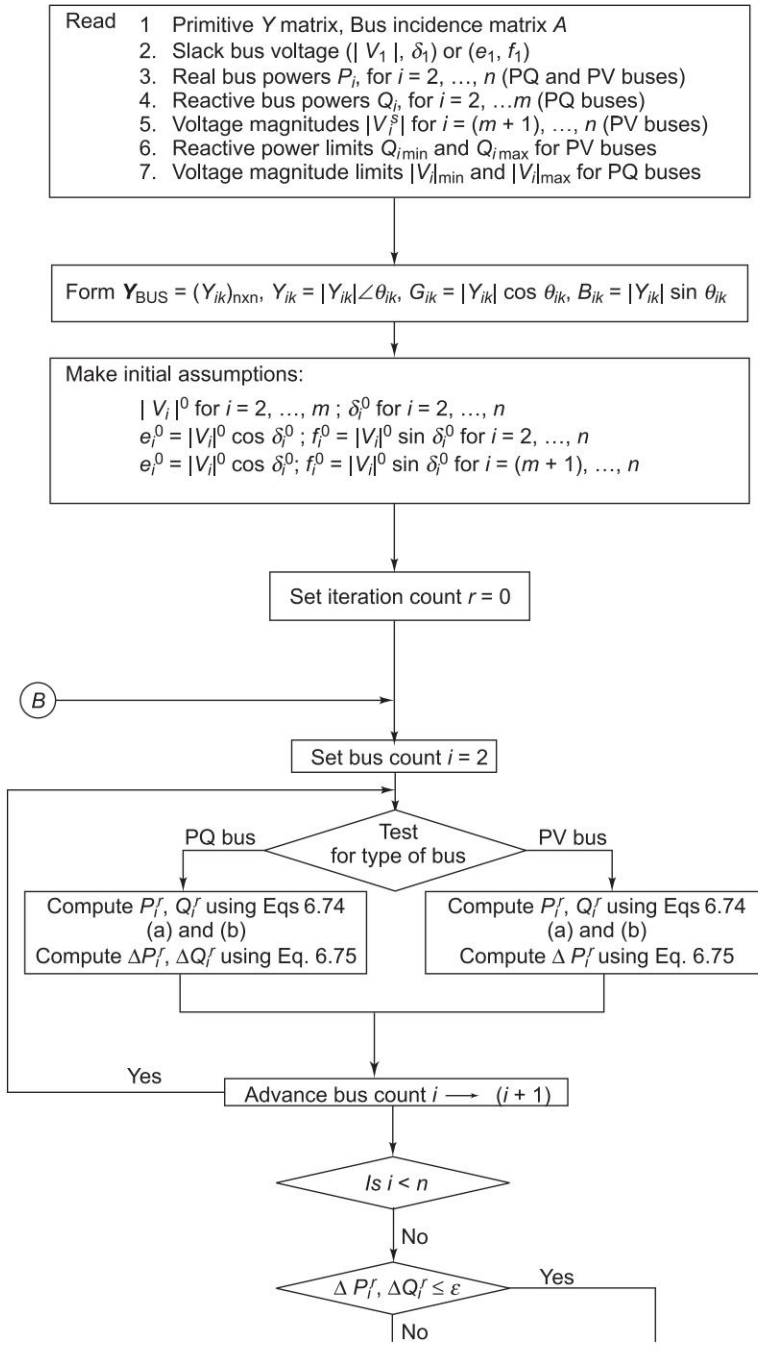

Fig. 6.18 (Contd.)

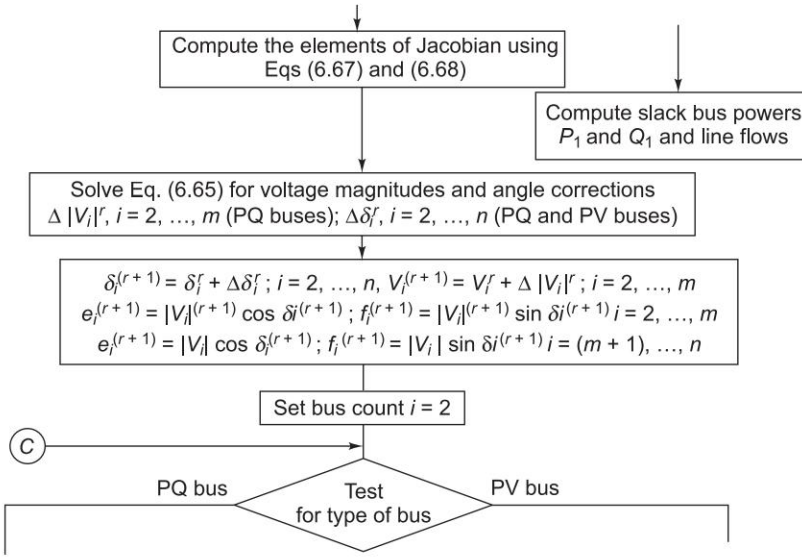

Fig. 6.18 (Contd.)

For $i = j$

$$\begin{aligned} J_{1,ii} &= a_i + G_{ii}e_i + B_{ii}f_i \\ J_{4,ii} &= a_i - G_{ii}e_i - B_{ii}f_i \\ J_{2,ii} &= b_i - B_{ii}e_i + G_{ii}f_i \\ J_{3,ii} &= b_i - B_{ii}e_i + G_{ii}f_i \\ J_{5,ii} &= 2e_i,\ J_{6,ii} = 2f_i \end{aligned} \tag{6.81b}$$

a_i and b_i are the components of the current flowing into node i, i.e. for the rth iteration

$$I^r_i = a^r_i + jb^r_i = \sum_{k=1}^{n} (G_{ik} + jB_{ik})\left(e^r_k + jf^r_k\right) \tag{6.82}$$

Steps in solution procedure are similar to the polar coordinates case, except that the initial estimates of real and imaginary parts of the voltage at the PQ buses are made, and the corrections required are obtained in each iteration, using

$$\begin{bmatrix} \Delta \boldsymbol{e}^{(r)} \\ \Delta \boldsymbol{f}^{(r)} \end{bmatrix} = \begin{bmatrix} \boldsymbol{J}_1^{(r)} & \boldsymbol{J}_2^{(r)} \\ \boldsymbol{J}_3^{(r)} & \boldsymbol{J}_4^{(r)} \\ \boldsymbol{J}_5^{(r)} & \boldsymbol{J}_6^{(r)} \end{bmatrix}^{(-1)} \begin{bmatrix} \Delta \boldsymbol{P}^{(r)} \\ \Delta \boldsymbol{Q}^{(r)} \\ \Delta |\boldsymbol{V}|^{2(r)} \end{bmatrix} \tag{6.83}$$

The corrections are then applied to $\boldsymbol{e}$ and $\boldsymbol{f}$ and the calculations are repeated till convergence is achieved. A detailed flow chart describing the procedure for

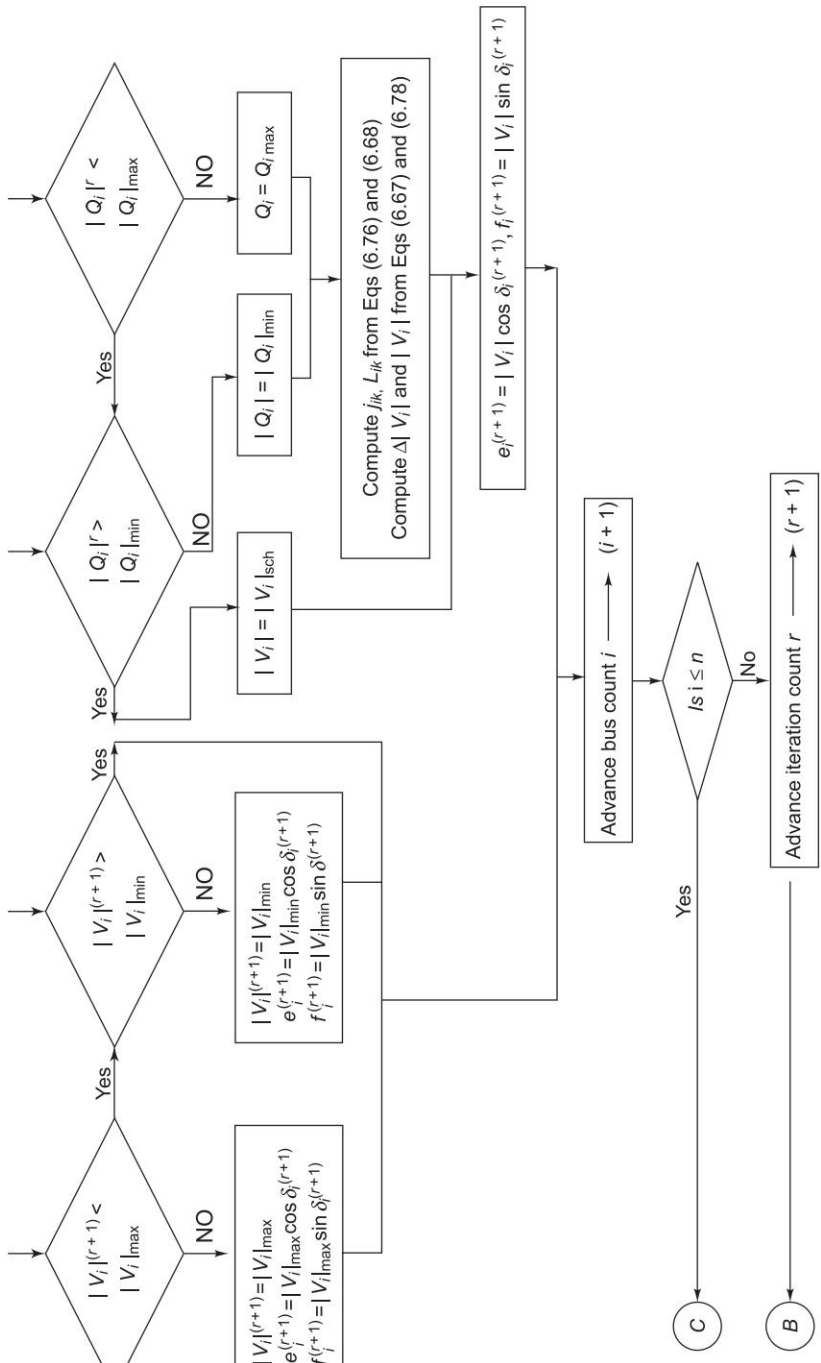

Fig. 6.18 Flow chart for load flow solution by Newton–Raphson iterative method using Y_{BUS}

load flow analysis using rectangular power-mismatch version by NR method is given in Fig. 6.19.

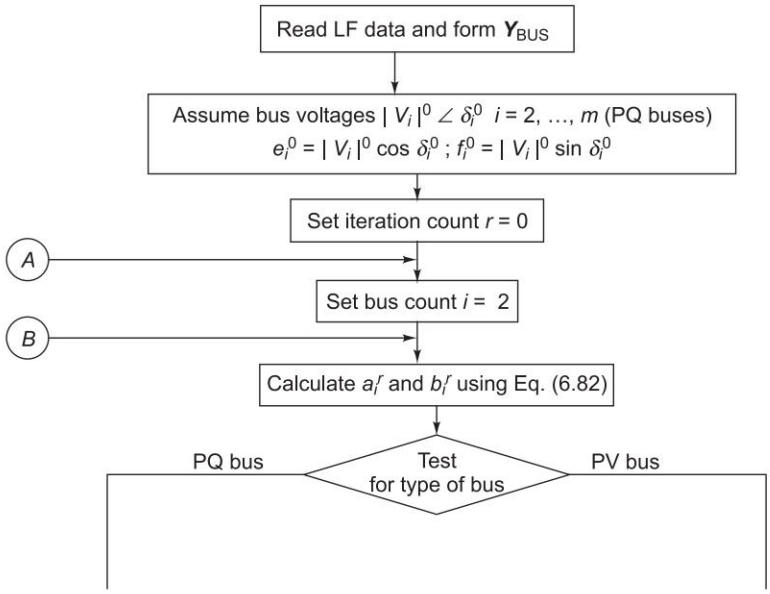

Fig. 6.19 (Contd.)

6.7 DECOUPLED LOAD FLOW STUDIES

An important characteristic of any practical power transmission system operating in steady state is that the change in real power from the specified value at a bus is more dependent on the changes in voltage angles at various buses than the changes in voltage magnitudes, and the change in reactive power from the specified value at a bus is more dependent on the changes in voltage magnitudes at various buses than the changes in voltage angles. This can be seen from Eq. (6.65) by considering the values of Jacobian elements as follows:

After normalizing the voltage corrections in Eq. (6.65), we get

$$\Delta P_i = \sum_{k=2}^{n} (H_{ik}\, \Delta\delta_k) + \sum_{k=2}^{m} (N_{ik} \Delta\, |\, V_k\, |/|\, V_k\, |) \qquad (6.84a)$$

for both PQ and PV buses

and

$$\Delta Q_i = \sum_{k=2}^{n} (J_{ik}\, \Delta\delta_k) + \sum_{k=2}^{m} (L_{ik} \Delta\, |\, V_k\, |/|\, V_k\, |) \qquad (6.84b)$$

for PQ buses

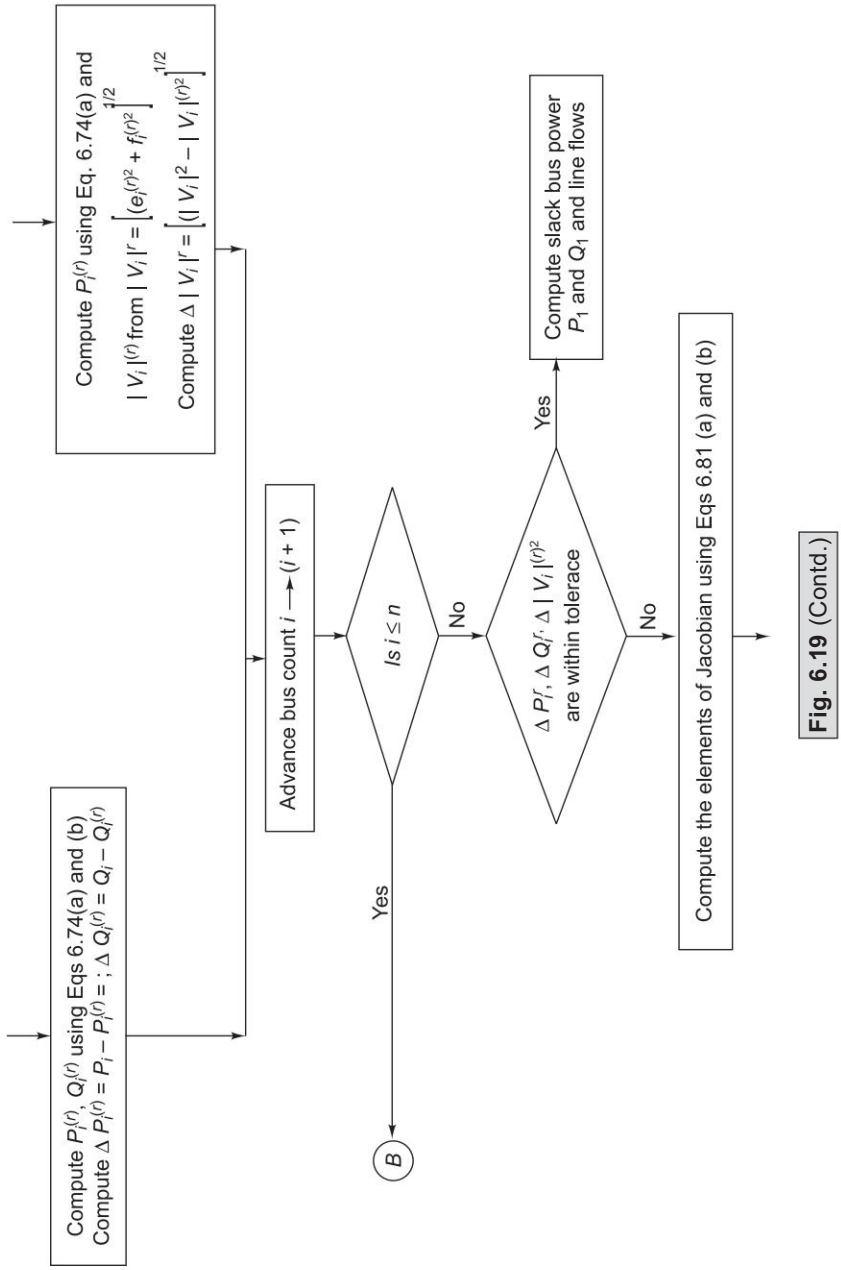

Fig. 6.19 (Contd.)

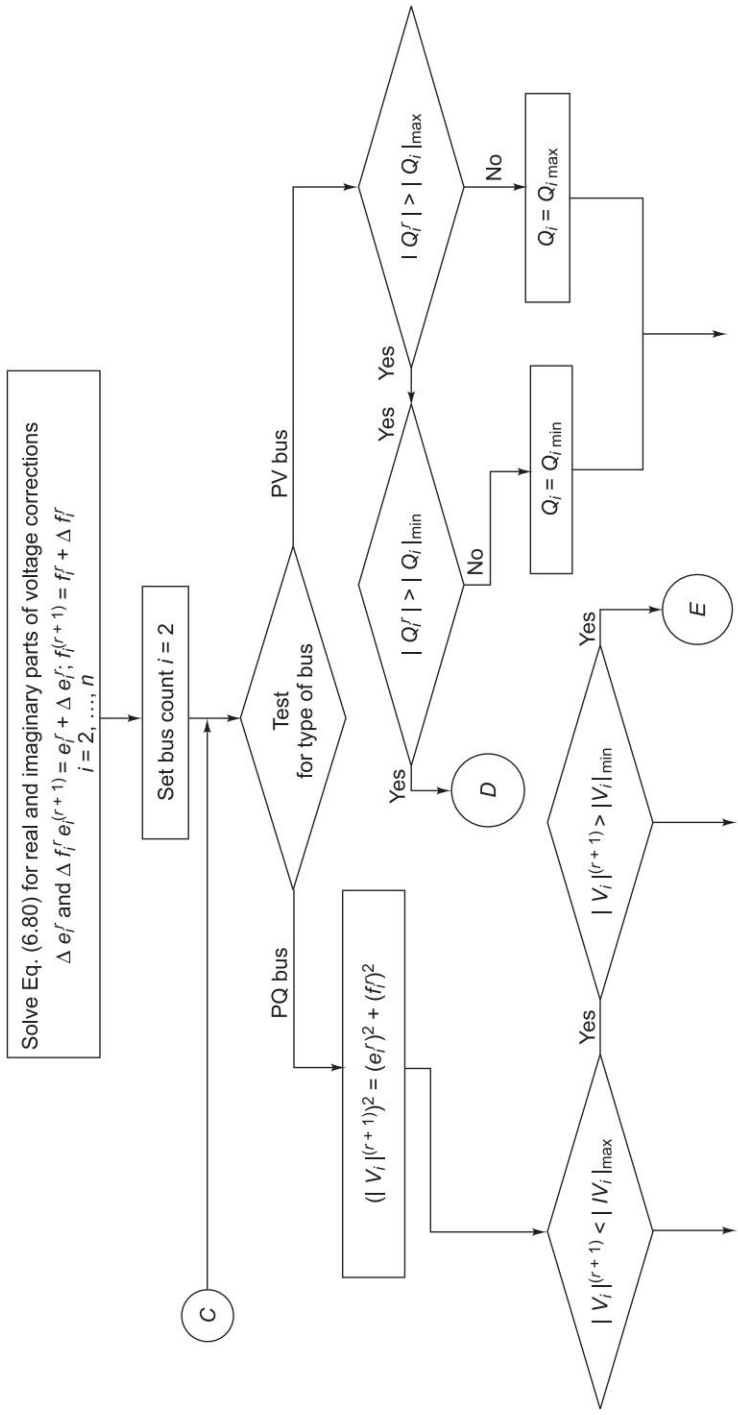

Fig. 6.19 (Contd.)

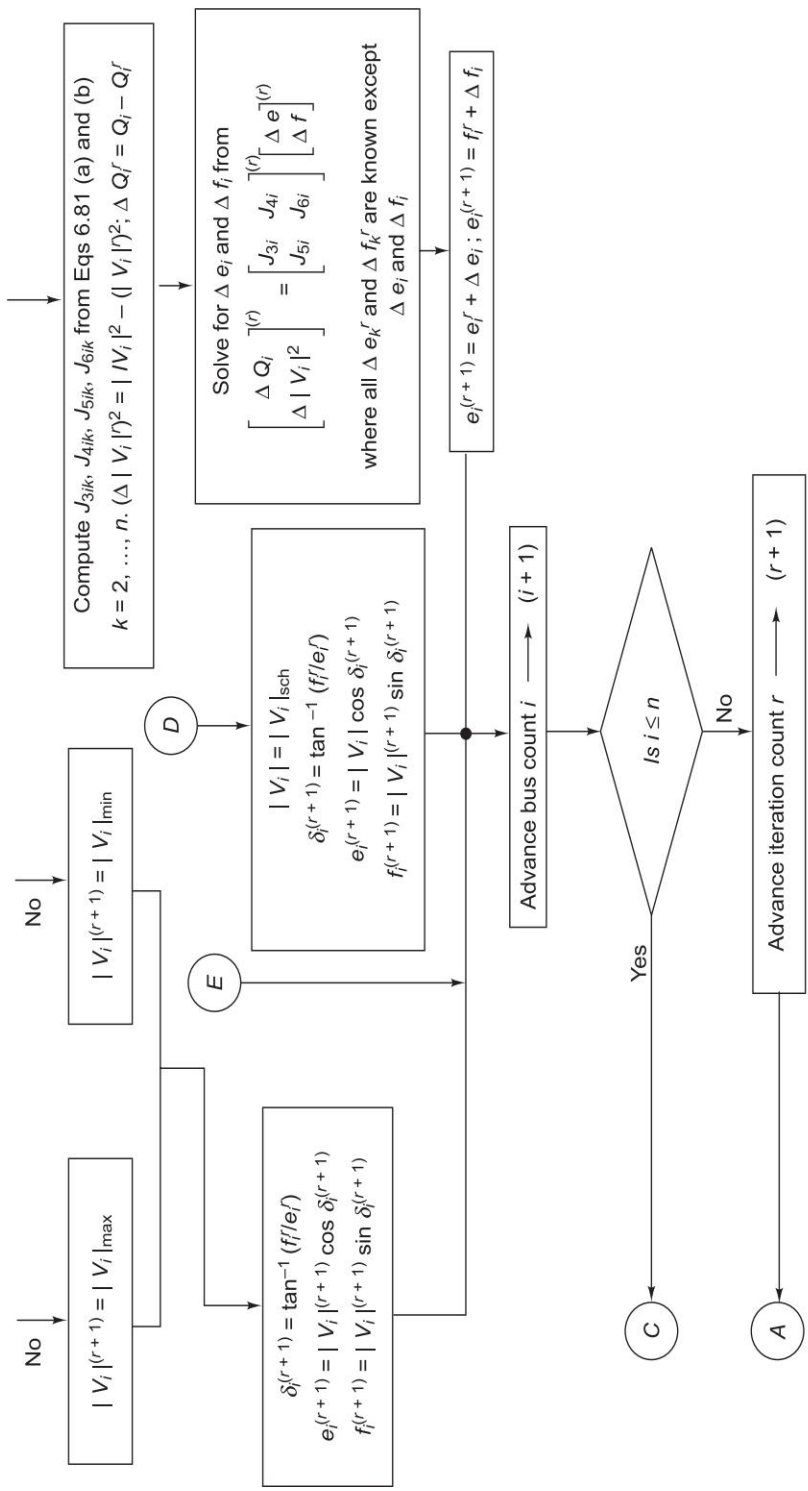

Fig. 6.19 Flow chart of load flow analysis using rectangular power mismatch version by NR method

or, in matrix form

$$\begin{bmatrix} \Delta \boldsymbol{P} \\ \Delta \boldsymbol{Q} \end{bmatrix} = \begin{bmatrix} \boldsymbol{H} & \boldsymbol{N} \\ \boldsymbol{J} & \boldsymbol{L} \end{bmatrix} \begin{bmatrix} \Delta \delta \\ \Delta |\boldsymbol{V}| / |\boldsymbol{V}| \end{bmatrix} \tag{6.85}$$

where $\boldsymbol{H}$ is a square matrix of elements H_{ik} and of order $(n-1)$,
$\boldsymbol{N}$ is a matrix of elements N_{ik} and of order $(n-1) \times (m-1)$,
$\boldsymbol{J}$ is a matrix of elements J_{ik} and of order $(m-1) \times (n-1)$,
$\boldsymbol{L}$ is a square matrix of elements L_{ik} and of order $(m-1)$.

We now proceed to show that the elements N_{ik}, J_{ik} are small compared with the elements H_{ik}, L_{ik}.

From Eq. (6.67)

$$\begin{aligned} H_{ik} = L_{ik} &= a_k f_i - b_k e_i \\ &= (G_{ik} e_k - B_{ik} f_k) f_i - (B_{ik} e_k + G_{ik} f_k) e_i \\ &= G_{ik} (e_k f_i - e_i f_k) - B_{ik} (f_i f_k + e_i e_k) \\ &= |V_i| |V_k| (G_{ik} \sin(\delta_i - \delta_k) - B_{ik} \cos(\delta_i - \delta_k)) \end{aligned} \tag{6.86a}$$

Similarly,

$$\begin{aligned} N_{ik} &= -J_{ik} = a_k e_i - b_k f_i \\ &= |V_i| |V_k| (G_{ik} \cos(\delta_i - \delta_k) + B_{ik} \sin(\delta_i - \delta_k)) \end{aligned} \tag{6.86b}$$

and from Eq. (6.68), and also from Eqs 6.28(a) and (b)

$$\begin{aligned} H_{ii} &= -Q_i - B_{ii} |V_i|^2 \\ &= -B_{ii} |V_i|^2 + \sum_{k=1}^{n} (|V_i| |V_k| |Y_{ik}| \sin(\theta_{ik} + \delta_k - \delta_i)) \\ &= -B_{ii} |V_i|^2 + \sum_{k=1}^{n} (|V_i| |V_k| (-G_{ik} \sin(\delta_i - \delta_k) + B_{ik} \cos(\delta_i - \delta_k))) \end{aligned} \tag{6.86c}$$

Similarly,

$$\begin{aligned} N_{ii} &= P_i + G_{ii} |V_i|^2 \\ &= G_{ii} |V_i|^2 + \sum_{k=1}^{n} (|V_i| |V_k| (G_{ik} \cos(\delta_i - \delta_k) + B_{ik} \sin(\delta_i - \delta_k))) \end{aligned} \tag{6.86d}$$

$$\begin{aligned} J_{ii} &= P_i - G_{ii} |V_i|^2 \\ &= -G_{ii} |V_i|^2 + \sum_{k=1}^{n} (|V_i| |V_k| (G_{ik} \cos(\delta_i - \delta_k) + B_{ik} \sin(\delta_i - \delta_k))) \end{aligned} \tag{6.86e}$$

$$\begin{aligned} L_{ii} &= Q_i - B_{ii} |V_i|^2 \\ &= -B_{ii} |V_i|^2 + \sum_{k=1}^{n} (|V_i| |V_k| (G_{ik} \sin(\delta_i - \delta_k) - B_{ik} \cos(\delta_i - \delta_k))) \end{aligned} \tag{6.86f}$$

where $Y_{ik} = G_{ik} + jB_{ik} + |\, Y_{ik} \,| \angle\theta_{ik}$.

Since transmission lines are mostly reactive, the conductances, Gs are very small compared to the susceptances, Bs. Also, under normal operating conditions the angle $(\delta_i - \delta_k)$ is small (typically less than 10°). Utilizing, these characteristics of the transmission system in Eqs 6.86(a) to (f), we find that the elements Ns and Js are small compared to the elements Hs and Ls, and hence are neglected. Thus, Eqs 6.84(a) and (b) become

$$\Delta P_i = \sum_{k=2}^{n} H_{ik}\, \Delta\delta_k \qquad i = 2, \ldots, n \tag{6.87a}$$

$$\Delta Q_i = \sum_{k=2}^{m} L_{ik} \frac{\Delta |V_k|}{|V_k|} \qquad i = 2, \ldots, n \tag{6.87b}$$

Thus, there is a fairly good decoupling between the equations for active power and reactive power. This decoupling feature can be used in simplifying the NR algorithm for load flow analysis.

Decoupled Newton Method

On neglecting the elements of N and J matrix, Eq. (6.85) reduces to

$$\begin{bmatrix} \Delta \boldsymbol{P} \\ \Delta \boldsymbol{Q} \end{bmatrix} = \begin{bmatrix} \boldsymbol{H} & \boldsymbol{0} \\ \boldsymbol{0} & \boldsymbol{L} \end{bmatrix} \begin{bmatrix} \Delta \boldsymbol{\delta} \\ \dfrac{\Delta |\boldsymbol{V}|}{|\boldsymbol{V}|} \end{bmatrix} \tag{6.88}$$

or

$$[\Delta \boldsymbol{P}] = [\boldsymbol{H}]\, [\Delta \boldsymbol{\delta}] \tag{6.89a}$$

$$[\Delta \boldsymbol{Q}] = [\boldsymbol{L}]\, [\Delta\, |\, \boldsymbol{V}\, | / |\, \boldsymbol{V}\, |] \tag{6.89b}$$

Equations 6.89(a) and (b) can be constructed and solved simultaneously with each other at each iteration, updating the $(\boldsymbol{H})$ and $(\boldsymbol{L})$ matrices in each iteration using Eqs (6.86a, c and f). A better approach is to conduct each iteration by first solving Eq. (6.89a) for $\Delta\boldsymbol{\delta}$, and use the updated $\boldsymbol{\delta}$ in constructing and then solving Eq. (6.89b) for $\Delta\, |\, \boldsymbol{V}\, |$. This will result in Eqs 6.84 (a-f) faster convergence than in the simultaneous mode.

The main advantage of the Decoupled Load Flow (DLF) as compared to the NR method is its reduced memory requirements in storing the Jacobian elements. Storage of the Jacobian and matrix triangularization is saved by a factor 4, that is an overall saving of 30–40 per cent on the formal Newton load flow. Computation time per iteration is less than the Newton method. However, the DLF takes more number of iterations to converge because of the approximation made.

Fast Decoupled Load Flow (FDLF)

The Jacobian of the decoupled Newton load flow can be made constant in value, based on physically justifiable assumptions. Hence the triangularization has to be done only once per solution. The Fast Decoupled Load Flow (FDLF) was developed by B. Stott in 1974 [20] in the process of further simplifications and assumptions. The assumptions which are valid in normal power system operation are made as follows:

$$\cos \delta_{ik} \cong 1 \tag{6.90}$$

$$\sin \delta_{ik} \cong 0 \tag{6.91}$$

$$G_{ij} \sin \delta_{ik} << B_{ik}; \text{ and}$$

$$Q_i << B_{ii} \mid V_i \mid^2$$

With these assumptions, the entries of the [$\boldsymbol{H}$] and [$\boldsymbol{L}$] submatrices become considerably simplified, and are given by

$$H_{ik} = L_{ik} = -\mid V_i \mid \mid V_k \mid B_{ik} \qquad i \neq k \tag{6.92a}$$

$$H_{ii} = L_{ii} = -B_{ii} \mid V_i \mid^2 \qquad i = k \tag{6.92b}$$

Matrices [$\boldsymbol{H}$] and [$\boldsymbol{L}$] are square matrices with dimensions (n – 1) and (m – 1), respectively, (m – 1 = number of PQ buses, and n – 1 = number of PQ and PV buses).

Equations 6.87(a and b) can now be written as (after substituting the values of H_{ik}, L_{ik}, H_{ii}, L_{ii} from Eqs 6.92(a and b)

$$\frac{\Delta P_i}{|V_i|} = -\sum_{k=2}^{n} \mid V_k \mid B_{ik} \Delta \delta_k \qquad i = 2, ..., n \tag{6.93a}$$

$$\frac{\Delta Q_i}{|V_i|} = -\sum_{k=2}^{n} B_{ik} \Delta \mid V_k \mid \qquad i = 2, ..., m \tag{6.93b}$$

Setting $\mid V_k \mid = 1$ pu on the R.H.S. of Eq. (6.93a), we get

$$\frac{\Delta P_i}{|V_i|} = \sum_{k=2}^{n} [-B_{ik}] \Delta \delta_k \qquad i = 2, ..., n$$

$$\frac{\Delta Q_i}{|V_i|} = \sum_{k=2}^{n} [-B_{ik}] \Delta \mid V_k \mid \qquad i = 2, ..., m$$

or in matrix form, after writing for all is, we get

$$\left[\frac{\Delta \boldsymbol{P}}{|\boldsymbol{V}|}\right]_{(n-1)\times 1} = [\boldsymbol{B'}]_{(n-1)\times(n-1)} [\Delta \boldsymbol{\delta}]_{(n-1)\times 1} \tag{6.94a}$$

$$\left[\frac{\Delta \boldsymbol{Q}}{|\boldsymbol{V}|}\right]_{(m-1)\times 1} = [\boldsymbol{B''}]_{(m-1)\times(m-1)} [\Delta \mid \boldsymbol{V} \mid]_{(m-1)\times 1} \tag{6.94b}$$

where $\boldsymbol{B'}$ and $\boldsymbol{B''}$ are matrices of elements $-B_{ik}$ ($i = 2, ..., n$ and $k = 2, ..., n$) and $-B_{ik}$ ($i = 2, ..., m$ and $k = 2, ..., n$)

Further simplification of the FDLF algorithm is achieved by:

1. Omitting the elements of [$\boldsymbol{B'}$] that predominantly affect reactive power flows, i.e., shunt reactances and transformer off-nominal in-phase taps.
2. Omitting from [$\boldsymbol{B''}$] the angle shifting effect of phase shifter (that which predominantly affects real power flow).
3. Ignoring the series resistance in calculating the elements of [$\boldsymbol{B'}$], which then becomes the DC approximation of the power flow matrix.

After these simplifications Eqs 6.94(a and b) are rewritten as

$$[\Delta \boldsymbol{P}/|\boldsymbol{V}|] = [\boldsymbol{B'}]\,[\Delta \boldsymbol{\delta}] \tag{6.95a}$$

$$[\Delta \boldsymbol{Q}/|\boldsymbol{V}|] = [\boldsymbol{B''}]\,[\Delta |\boldsymbol{V}|] \tag{6.95b}$$

In Eqs 6.95(a and b), both ($\boldsymbol{B'}$) and ($\boldsymbol{B''}$) are real, sparse and have the structures of [$\boldsymbol{H}$] and [$\boldsymbol{L}$], respectively. Since they contain only admittances, they are constant and need to be triangularized (or inverted) only once at the beginning of load flow analysis. If the phase shifters are not present, both [$\boldsymbol{B'}$] and [$\boldsymbol{B''}$] are always symmetrical, and their constant sparse upper triangular factors are calculated and stored only once at the beginning of the solution.

Equations 6.95(a and b) are solved alternatively, always employing the most recent voltage values. One iteration implies one solution for [$\Delta\boldsymbol{\delta}$], to update [$\boldsymbol{\delta}$], and then one solution for [$\Delta|\boldsymbol{V}|$], to update [$|\boldsymbol{V}|$] to be called $1-\delta$ and $1-V$ iteration. Separate convergence tests are applied for the real and reactive power mismatches as follows:

$$\max [\Delta \boldsymbol{P}] \le \varepsilon_P; \text{ and } \max [\Delta \boldsymbol{Q}] \le \varepsilon_Q$$

where ε_P and ε_Q are the tolerances.

In FDLF method usually two to five iterations are required for practical accuracies. The method is more reliable than the formal NR method. The speed for iterations is about five times that of the formal NR method or about two-thirds that of the GS method. Storage requirements are about 60 per cent of the formal NR method, but slightly more than the DLF method.

A flow chart giving FDLF algorithm is presented in Fig. 6.20.

Example 6.11 Consider the three-bus system of Example 6.10 (Fig. 6.17). Use (a) Decoupled NR method and (b) FDLF method to obtain one iteration of the load flow solution.

Solution

(a) *Decoupled NR method* The equations to be solved are 6.89(a) and (b). Substituting relevant values in Eqs (6.86 a, c and f), we have

$$H_{22}^{(0)} = 0.96 + 23.508 = 24.47$$

$$H_{23}^{(0)} = H_{32}^{(0)} = 1.04(-B_{23}) = -1.04 \times 11.764 = -12.23$$

$$H_{33}^{(0)} = -Q_3 - B_{33}\,(1.04)^2$$

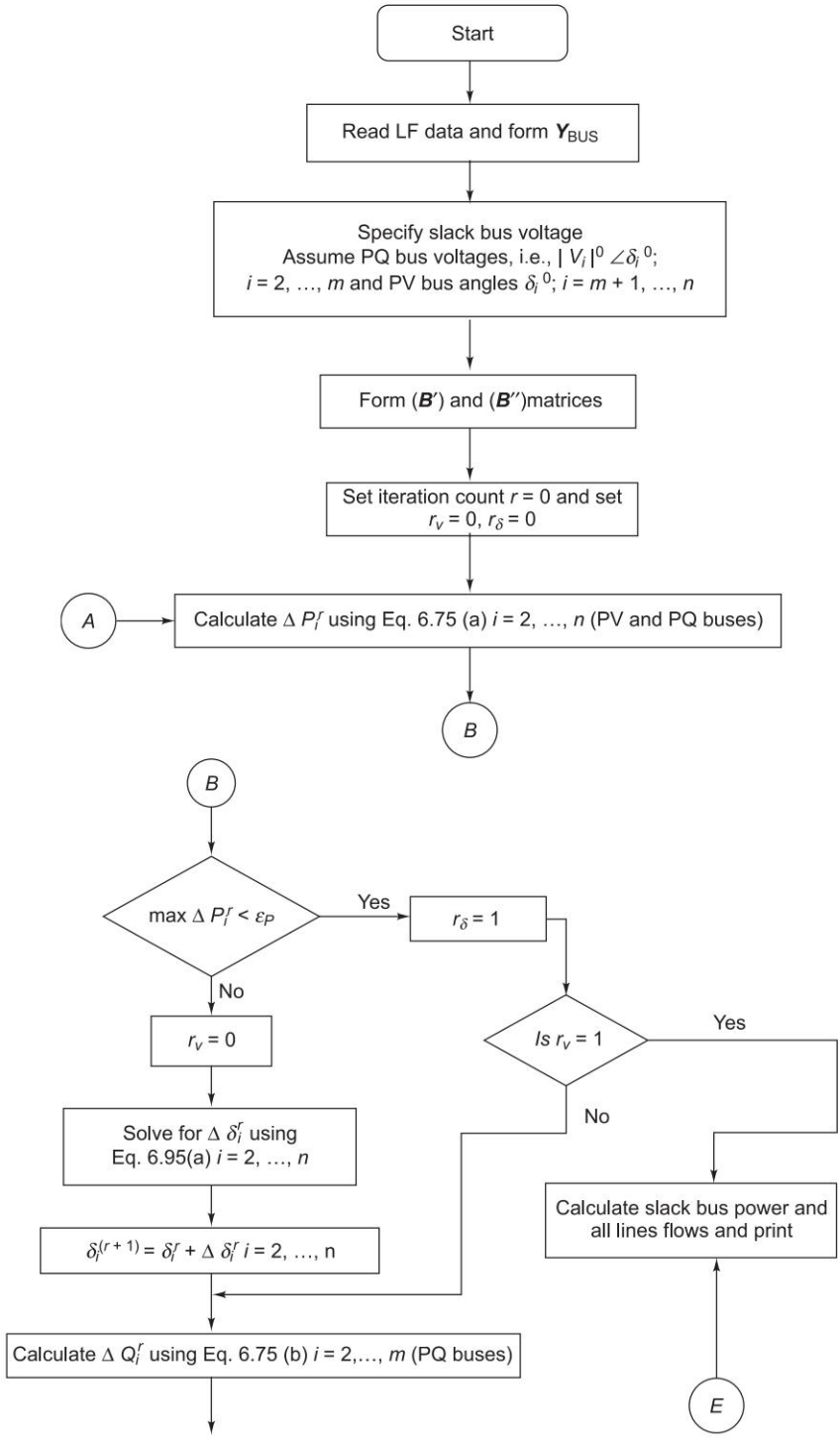

Fig. 6.20 (Contd.)

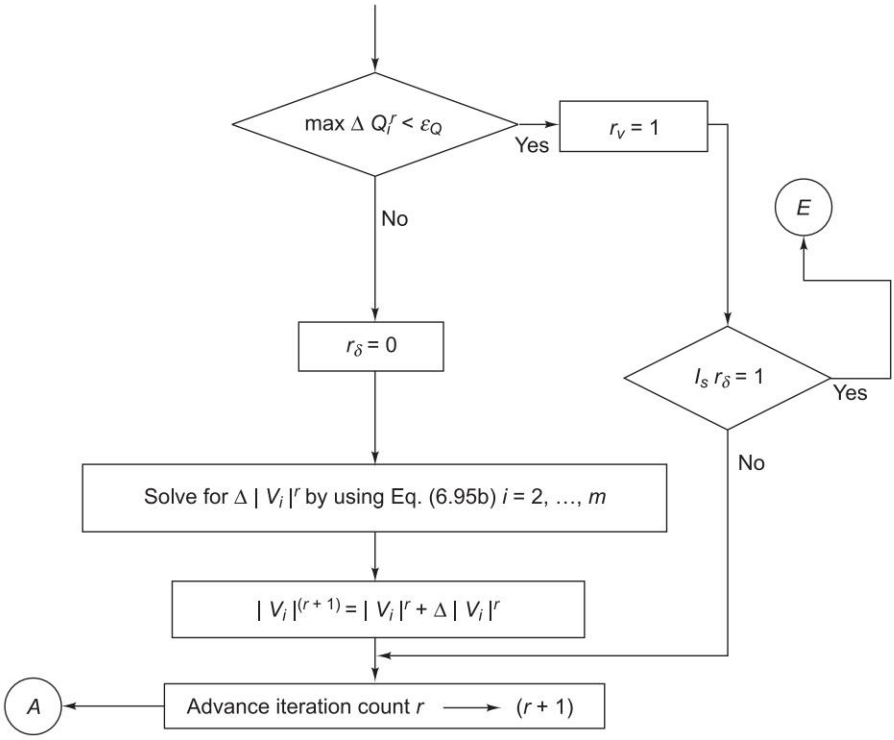

Fig. 6.20 Flow chart for FDLF algorithm

$$= (-B_{31} \mid V_3 \mid^2 - B_{32} \mid V_3 \mid^2 - B_{33} \mid V_3 \mid^2) - B_{33}\,(1.04)^2$$

$$= -11.764 \times (1.04)^2 - 11.764 \times 1.04 + (1.04)^2 \times 2 \times 23.508$$

$$= 25.89$$

$$L_{22}^{(0)} = Q_2 - B_{22} = 1 + 23.508 = 24.508$$

$$\begin{bmatrix} \Delta P_2 \\ \Delta P_3 \end{bmatrix}^{(0)} = \begin{bmatrix} H_{22} & H_{23} \\ H_{32} & H_{33} \end{bmatrix}^{(0)} \begin{bmatrix} \Delta \delta_2 \\ \Delta \delta_3 \end{bmatrix}^{(0)}$$

and

$$[\Delta Q_2]^{(0)} = [L_{22}]^{(0)} \left[\frac{\Delta |V_2|}{|V_2|} \right]^{(0)}$$

From Example 6.10,

$$\Delta P_2^{(0)} = 0.73$$

$$\Delta P_3^{(0)} = -1.62$$

Therefore,

$$\begin{bmatrix} 0.73 \\ -1.62 \end{bmatrix} = \begin{bmatrix} 24.47 & -12.23 \\ -12.23 & 25.89 \end{bmatrix} \begin{bmatrix} \Delta\delta_2^{(0)} \\ \Delta\delta_3^{(0)} \end{bmatrix}$$

$$[\Delta Q_2^{(0)}] = [24.51] \left[\frac{\Delta |V_2|^{(1)}}{|V_2|^{(1)}} \right] \qquad \text{(ii)}$$

Solving Eq. (i), we get

$\Delta\delta_2^{(0)} = -0.0082 - 0.0401 = -0.002$ rad $= -0.115°$

$\Delta\delta_3^{(0)} = -0.018 - 0.08 = -0.062$ rad $= -3.55°$

$\delta_2^{(1)} = \delta_2^{(0)} + \Delta\delta_2^{(0)} = 0 - 0.155° = -0.115°$

$\delta_3^{(0)} = \delta_3^{(0)} + \Delta\delta_3^{(0)} = 0 - 3.55° = -3.55°$

$$Q_2^{(0)} = [-|V_2||V_1||Y_{21}| \sin(\theta_{21} + \delta_1 - \delta_2^{(1)}) - |V_2|^2 |Y_{22}| \sin\theta_{22} - |V_2||V_3||Y_{23}| \sin(\theta_{23} + \delta_2^{(1)} - \delta_3^{(1)})]$$

$$Q_2^{(0)} = (-1.04 \times 12.13 \sin(104.04° + 0° - 0.115°) - 24.23 \sin(-75.95°) - 1.04 \times 12.13 \sin(104.04° + 0.115° - 3.55°))$$

$$= -12.24 + 23.505 - 12.39$$

$\therefore \quad Q_2^{(0)} = -1.125$

$\therefore \quad \Delta Q_2^{(0)} = Q_2$ (specified) $- Q_2^0 = 1 - (-1.125) = 2.125$

Substituting in Eq. (ii),

$$(2.115) = (24.51) \left[\frac{\Delta |V_2^0|}{|V_2^{(0)}|} \right]$$

$$\therefore \qquad \Delta |V_2^{(0)}| = 0.086$$

or

$$|V_2^{(1)}| = |V_2^{(0)}| + \Delta |V_2^{(0)}|$$

$$= 1.086 \text{ pu}$$

$Q_3^{(0)}$ can be similarly calculated using Eq. (6.28).

(b) *FDLF Method* The matrix equations for the solution of load flow by FDLF method are [see Eqs (6.95 a and b)]

$$\begin{bmatrix} \dfrac{\Delta P_2^{(0)}}{|V_2^{(0)}|} \\ \dfrac{\Delta P_3^{(0)}}{|V_3^{(0)}|} \end{bmatrix} = \begin{bmatrix} -B_{22} & -B_{23} \\ -B_{23} & -B_{33} \end{bmatrix} \begin{bmatrix} \Delta\delta_2^{(0)} \\ \Delta\delta_3^{(0)} \end{bmatrix} \qquad \text{(iii)}$$

and

$$\begin{bmatrix} \dfrac{\Delta Q_2^{(0)}}{|V_2^{(0)}|} \end{bmatrix} = [-B_{22}]\,[\Delta \mid V_2^{(0)} \mid] \tag{iv}$$

$$\begin{bmatrix} \dfrac{0.73}{1} = 0.73 \\ \dfrac{-1.62}{1.04} = -1.557 \end{bmatrix} = \begin{bmatrix} 23.508 & -11.764 \\ -11.764 & 23.508 \end{bmatrix} \begin{bmatrix} \Delta\delta_2^{(0)} \\ \Delta\delta_3^{(0)} \end{bmatrix} \tag{v}$$

Solving Eq. (v), we get

$$\Delta\delta_2^{(0)} = -0.003 \text{ rad}$$
$$\Delta\delta_3^{(0)} = -0.068 \text{ rad}$$
$$\delta_2^{(1)} = 0 - 0.003 = -0.003 \text{ rad}$$
$$\delta_3^{(1)} = 0 - 0.068 = -0.008 \text{ rad}$$

From Eq. (iv), we have

$$(2.125) = (23.508)\,(\Delta \mid V_2^{(1)} \mid)$$
$$\Delta \mid V_2^{(0)} \mid = 0.09$$
$$\mid V_2^{(1)} \mid = \mid V_2^{(0)} \mid + \Delta \mid V_2^{(0)} \mid$$
$$= 1 + 0.09$$
$$\mid V_2^{(1)} \mid = 1.09$$

Now Q_3 can be calculated.

These values are used to compute bus power mismatches for the next iteration. Using the values of ($\Delta \boldsymbol{P}/\mid \boldsymbol{V} \mid$) and ($\Delta \boldsymbol{Q}/\mid \boldsymbol{V} \mid$), the above equations are solved alternatively, with the most recent values, till the solution converges within the specified limits.

6.8 COMPARISON OF LOAD FLOW METHODS

In this section, GS and NR methods are compared when both use $\boldsymbol{Y}_{\text{BUS}}$ as the network model. It is experienced that the GS method works well when programmed using rectangular co-ordinates, whereas the NR method requires more memory when rectangular coordinates are used. Hence, polar coordinates are preferred for the NR method. However, to avoid time consuming sine and cosine terms in the Jacobian elements in the polar version of NR method, the elements of the Jacobian are calculated by the rectangular version. The rectangular version is faster in convergence, but slightly less reliable than the polar version.

The GS method requires the smallest number of arithmetic operations to complete an iteration. This is because of the sparsity of the network matrix and the simplicity of the solution techniques. Consequently, this method requires

less time per iteration. With the NR method, the power differences and elements of the Jacobian are to be computed per iteration and triangularization has also to be done per iteration, so that the time taken per iteration is considerably longer. For the typical large systems, the time per iteration in the NR method is roughly equivalent to 7 times that of the GS method [19]. The time per iteration in both these methods increases almost directly as the number of buses of the network.

The rate of convergence of the GS method is slow (linear convergence characteristic), requiring a considerably greater number of iterations to obtain a solution than the NR method. Due to quadratic convergence of bus voltages, in the NR method, high accuracy is obtained only in a few iterations. In addition, the number of iterations for the GS method increases directly as the number of buses of the network, whereas the number of iterations for the NR method remains practically constant, independent of the system size.The NR method needs 3 to 5 iterations to reach an acceptable solution for a large system. In the GS and other methods, convergence is affected by the choice of the slack bus and the presence of series capacitor, but the sensitivity of the NR method is minimal to these factors which cause poor convergence. Therefore, for large systems, the NR method is faster and more accurate (near exact solution) than the GS or any other known method. In fact, it works for any size and kind of problem and is able to solve a wider variety of ill-conditioned problems [22]. The NR method is also more reliable than the GS method.

The chief advantage of the GS method is the ease of programming and most efficient utilization of core memory. It is, however, restricted in use to small size systems because of its doubtful convergence and longer time needed for solution of large power networks. The programming logic of NR method is complex and it has the disadvantage of requiring a large computer memory, even when a compact storage scheme is used for the Jacobian and admittance matrices. The NR method can be made even faster by adopting the scheme of optimally renumbered buses. The method is best suited for optimal load flow studies (Chapter 7) because of its high accuracy which is restricted only by round off errors.

Thus the NR method is decidedly more suitable than the GS method for all but very small systems.

The reliability of decoupled Newton method is comparable to the formal Newton method for ill-conditioned problems. But, the decoupled method is simple and computationally efficient than the formal Newton method. Also, the storage of Jacobian elements and triangularization is saved by a factor of 4 in the decoupled method and computation time per iteration is less than the Newton method. However, the convergence characteristics of the decoupled method are geometric compared to the quadratic convergence of the Newton method. Thus, for high accuracies, more iterations are required by the decoupled Newton method.

For FDLF method, the convergence is geometric; two to five iterations are normally required for practical accuracies. This is due to the fact that the elements of $[\boldsymbol{B'}]$ and $[\boldsymbol{B''}]$ are fixed approximations to the tangents of the

defining functions $\Delta \boldsymbol{P}/|\boldsymbol{V}|$ and $\Delta \boldsymbol{Q}/|\boldsymbol{V}|$, and are not sensitive to any humps in the defining functions. If $\Delta \boldsymbol{P}/|\boldsymbol{V}|$ and $\Delta \boldsymbol{Q}/|\boldsymbol{V}|$ are calculated efficiently, then the speed for iterations of the FDLF is nearly five times that of the formal NR or about two-thirds that of the GS method. Storage requirements are around 60 per cent of the formal NR method, but slightly more than the decoupled NR method.

Because of high accuracies obtained in only a few iterations, the NR method is important for the use of load flow in short-circuit and stability studies. The method can be readily extended to include tap-changing transformers, variable constraints on bus voltages, optimal real and reactive power scheduling. Network modifications can be easily made. The FDLF can be employed in optimization studies, and is specially used for obtaining information of both real and reactive power for multiple load flow studies, as in contingency evaluation for system security assessment and enhancement analysis.

Note: When a series of load flow calculations are performed, the final values of bus voltages in each case are normally used as the initial voltages of the next case. This reduces the number of iterations, particularly when there are minor changes in system conditions.

6.9 CONTROL OF VOLTAGE PROFILE

Control by Generators

Control of voltage at the receiving bus in the fundamental two-bus system was discussed in Sec. 5.10. Though the same general conclusions hold for an interconnected system, it is important to discuss this problem in greater detail.

At a bus with generation, voltage can be conveniently controlled by adjusting generator excitation. This is illustrated by means of Fig. 6.21, where the equivalent generator at the *i*th bus is modelled by a synchronous reactance (resistance is assumed negligible) and voltage behind synchronous reactance.

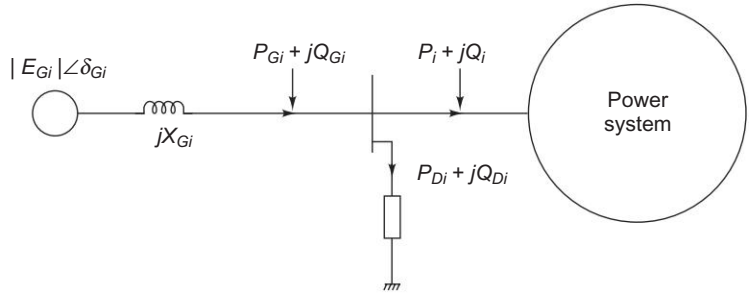

Fig. 6.21 Voltage control by adjusting generator excitation

It immediately follows upon application of Eqs (5.71) and (5.73) that

$$P_{Gi} = \frac{|V_i||E_{Gi}|}{X_{Gi}} \sin(\delta_{Gi} - \delta_i) \qquad (6.96a)$$

$$Q_{Gi} = \frac{|V_i|}{X_{Gi}} (-|V_i| + |E_{Gi}|) \tag{6.96b}$$

With $(P_{Gi} + jQ_{Gi})$ and $|V_i| \angle \delta_i$ given by the load flow solution, these values can be achieved at the bus by adjusting generator excitation to give $|E_{Gi}|$ as required by Eq. (6.96b), and by adjusting the governor setting so that the power input to generator from turbine is P_{Gi} plus losses, resulting in load angle of $(\delta_{Gi} - \delta_i)$ corresponding to Eq. (6.96a). If Q_{Gi} demand exceeds the capacity of generators, VAR generators (synchronous or static capacitor) have to be used to modify the local demand.

Control by VAR Generators (synchronous or static capacitors)

It follows from above that to control the voltage profile of an interconnected system, buses with generators are usually made PV (i.e. voltage control) buses. Load flow solution then gives the voltage levels at the load buses. If some of the load bus voltages work out to be less than the specified lower voltage limit, it is indicative of the fact that the reactive power flow capacity of transmission lines for specified voltage limits cannot meet the reactive load demand (reactive line flow from bus i to bus k is proportional to $|\Delta V| = |V_i| - |V_k|$. This situation can be remedied by installing VAR generators at some of the load buses. These buses in the load flow analysis are then regarded as PV buses with the resulting solution giving the requisite values of VAR (jQ_C) injection at these buses.

The fact that positive VAR injection at any bus of an interconnected system would help to raise the voltage at the bus is easily demonstrated as follows:

Figure 6.22(a) shows the Thevenin equivalent circuit of the power system as seen from the ith bus. Obviously, $E_{th} = V_i$. If now jQ_C from the VAR generator is injected into this bus as shown in Fig. 6.22(b), we have from Eq. (5.73)

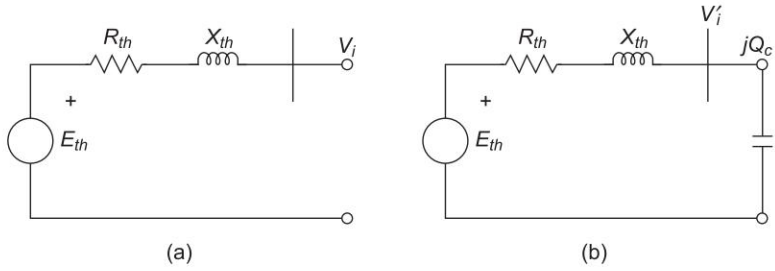

Fig. 6.22

$$|\Delta V| = |E_{th}| - |V_i'| = -\frac{X_{th}}{|V_i'|} Q_C$$

or

$$|V_i'| = |E_{th}| + \left[\frac{X_{th}}{|V_i'|}\right] Q_C = |V_i| + \left[\frac{X_{th}}{|V_i'|}\right] Q_C$$

Since we are considering a voltage rise of a few per cent, $|V_i'|$ can be further approximated as

$$|V_i'| \cong |V_i| + \left[\frac{X_{th}}{|V_i|}\right] Q_C \tag{6.97}$$

Thus the VAR injection of $+jQ_C$ causes the voltage at the ith bus to rise approximately by $(X_{th}/|V_i|)Q_C$. The voltage at other load buses will also rise owing to this injection to a varying, but smaller, extent.

Control by Transformers

Transformers provide a convenient means of controlling real power, and reactive power flow along a transmission line. As has already been clarified, real power is controlled by means of shifting the phase of voltage, and reactive power, by changing its magnitude. Voltage magnitude can be changed by transformers provided with tap changing under load (TCUL) gear. Transformers specially designed to adjust voltage magnitude or phase angle through small values are called regulating transformers.

Figure 6.23 shows a regulating transformer for control of voltage magnitude, which is achieved by adding in-phase boosting voltage in the line.

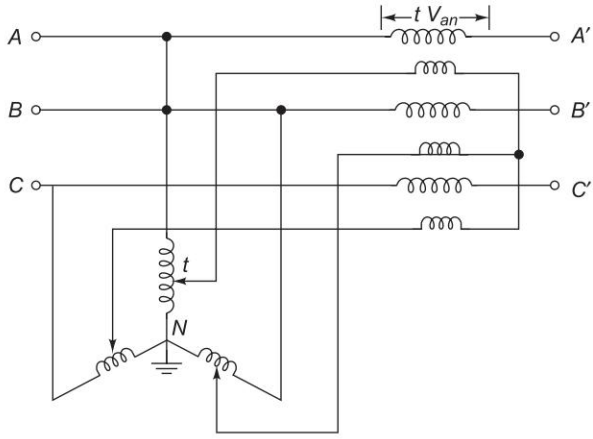

Fig. 6.23 Regulating transformer for control of voltage magnitude

Figure 6.24(a) shows a regulating transformer which shifts voltage phase angle with no appreciable change in its magnitude. This is achieved by adding a voltage in series with the line at 90° phase angle to the corresponding line to neutral voltage as illustrated by means of phasor diagram of Fig. 6.24(b). Here

$$V_{an}' = (V_{an} + tV_{bc}) = (1 - j\sqrt{3}t)V_{an} = aV_{an} \tag{6.98}$$

where

$$a = (1 - j\sqrt{3}t) \approx 1\angle -\tan^{-1}\sqrt{3}\,t$$

since t is small.

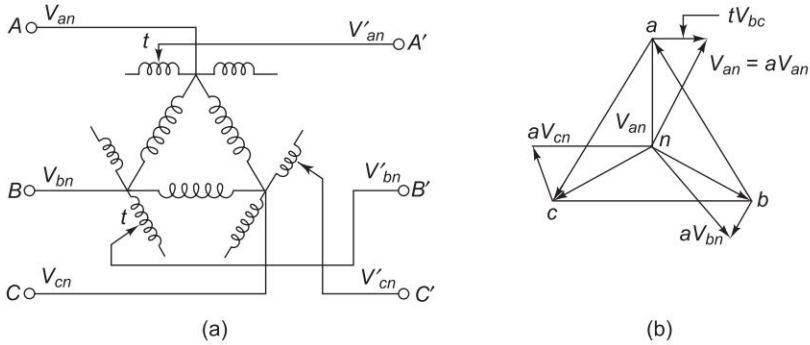

Fig. 6.24 Regulating transformer for control and voltage phase angle

The presence of regulating transformers in lines modifies the $\boldsymbol{Y}_{\text{BUS}}$ matrix, thereby modifying the load flow solution. Consider a line, connecting two buses, having a regulating transformer with off-nominal turns (tap) ratio a included at one end as shown in Fig. 6.25(a). It is quite accurate to neglect the small impedance of the regulating transformer, i.e. it is regarded as an ideal device. Figure 6.25(b) gives the corresponding circuit representation with line represented by a series admittance.

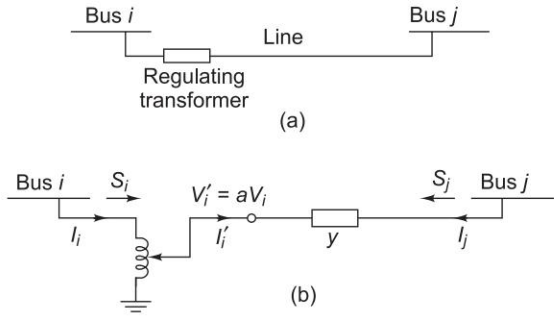

Fig. 6.25 Line with regulating transformer and its circuit representation

Since the transformer is assumed to be ideal, the complex power output from it equals complex power input,

i.e.

$$S_i = V_i I_i^* = V_i' I_i'^*$$

or

$$V_i I_i^* = a V_i I_i'^*$$

or

$$I_i = a^* I_i' \tag{6.99}$$

For the transmission line

$$I_i' = y(aV_i - V_j)$$

or

$$I_i = a^* I_i' = |a|^2 y V_i - a^* y V_j \tag{6.100a}$$

Also

$$I_j = y(V_j - aV_i) = -ayV_i + yV_j \tag{6.100b}$$

Equations (6.100a and b) cannot be represented by a bilateral network. The $\boldsymbol{Y}$ matrix representation can be written down as follows from Eqs (6.100 a and b).

$$\boldsymbol{Y} = \begin{matrix} \\ i \\ j \end{matrix} \begin{matrix} \begin{matrix} i & \quad j \end{matrix} \\ \begin{bmatrix} a^2 y & -a^* y \\ -ay & y \end{bmatrix} \end{matrix} \tag{6.101}$$

where y is the series admittance of the line. The entries of $\boldsymbol{Y}$ matrix of Eq. (6.101) would then be used in writing the $\boldsymbol{Y}_{\text{BUS}}$ matrix of the complete power network.

Equations (6.100a and b) can also be written as

$$\begin{aligned} I_i &= a^* y(V_i - V_j) - a^* y V_i + |a|^2 y V_i \\ &= a^*(a-1) y V_i + a^* y(V_i - V_j) \end{aligned} \tag{6.102a}$$

and

$$\begin{aligned} I_j &= ay(V_j - V_i) - ayV_j + yV_j \\ &= y(1 - ay)V_j + ay(V_j - V_i) \end{aligned} \tag{6.102b}$$

The above equations for I_i and I_j cannot be represented by the π-network because

$$y_{ij} = \left| \frac{I_i}{V_j} \right|_{V_i = 0, V_j \neq 0} = -a^* y$$

$$y_{ji} = \left| \frac{I_j}{V_i} \right|_{V_j = 0, V_i \neq 0} = -ay$$

i.e. because $y_{ij} \neq y_{ji}$.

For a voltage regulating transformer a is real i.e. $a^* = a$; therefore, Eqs (102 a and b) become

$$I_i = a(a-1) y V_i + ay(V_i - V_j)$$

$$I_j = (1-a) y V_j + ay(V_j - V_i)$$

which can be represented by the π-network of Fig. (6.26). Here we note that $y_{ij} = y_{ji} = -ay$.

In Fig. 6.27(a), the line shown in Fig. 6.25 is represented by a π-network with shunt admittances y_0 at each end. Also, a is real, i.e., $a^* = a$.

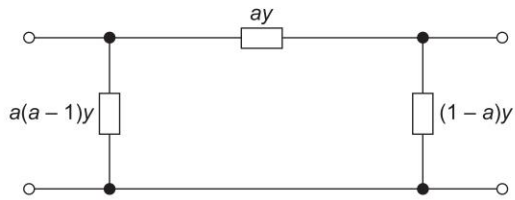

Fig. 6.26 Circuit representation of a line with off-nominal tap-setting or voltage regulating transformer

From Fig. 6.27(a)

$$I_i = a^* I_i' = aI_i' = a(aV_i y_0 + y(aV_i - V_j))$$
$$= a^2(y + y_0)V_i - ay\ V_j$$
$$= a^2 y_0 V_i + a(a-1)y\ V_i + ay\ (V_i - V_j)$$

Similarly,

$$I_j = y_0 V_j + (1-a)yV_j + ay(V_j - V_i)$$

which can be represented by the π-network of Fig. 6.27(b), where additional shunt admittances $a^2 y_0$ appears at bus j and y_0 at bus i.

The above derivations also apply for a transformer with off-nominal tap-setting $a = (kV)_{base}/(kV)_{tap}$, a real value.

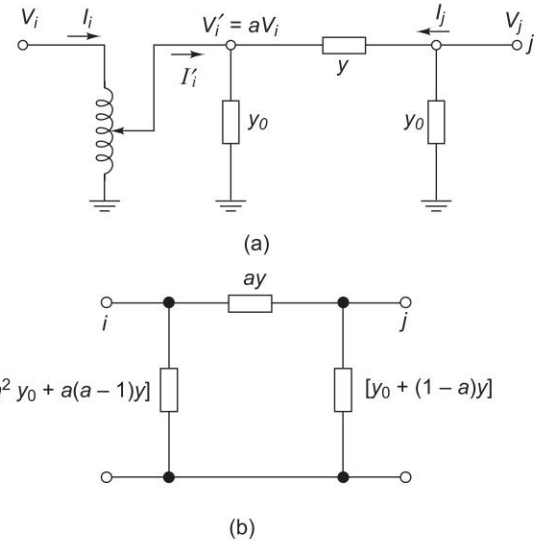

Fig. 6.27

With off-nominal tap setting transformers at each end of the line as shown in Fig. 6.28; we have

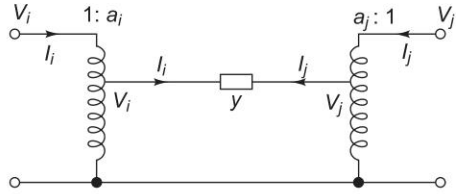

Fig. 6.28 Off-nominal transformers at both line ends (a_i, a_j are complex)

$$\begin{bmatrix} I_i' \\ I_j' \end{bmatrix} = \begin{bmatrix} y & -y \\ -y & y \end{bmatrix} \begin{bmatrix} V_i' \\ V_j' \end{bmatrix} \tag{i}$$

$$\begin{bmatrix} V_i' \\ V_j' \end{bmatrix} = \begin{bmatrix} a_i & 0 \\ 0 & a_j \end{bmatrix} \begin{bmatrix} V_i \\ V_j \end{bmatrix}; \begin{bmatrix} I_i' \\ I_j' \end{bmatrix} = \begin{bmatrix} 1/a_i^* & 0 \\ 0 & 1/a_i^* \end{bmatrix} \begin{bmatrix} I_i \\ I_j \end{bmatrix} \tag{ii}$$

Substituting (ii) in (i) and solving, we get

$$\begin{bmatrix} I_i \\ I_j \end{bmatrix} = \begin{bmatrix} |a_i|^2 y & -a_i^* a_j y \\ -a_i a_j^* y & |a_j|^2 y \end{bmatrix} \begin{bmatrix} V_i \\ V_j \end{bmatrix} \tag{iii}$$

Thus

$$\boldsymbol{Y} = \begin{bmatrix} |a_i|^2 y & -a_i^* a_j y \\ -a_i a_j^* y & |a_j|^2 y \end{bmatrix}$$

Note: When a_i, a_j are real

$$\boldsymbol{Y} = \begin{bmatrix} a_i^2 y & -a_i a_j y \\ -a_i a_j y & a_j^2 y \end{bmatrix}$$

and the π-equivalent circuit of Fig. 6.28 can now be drawn as shown in Fig. 6.29.

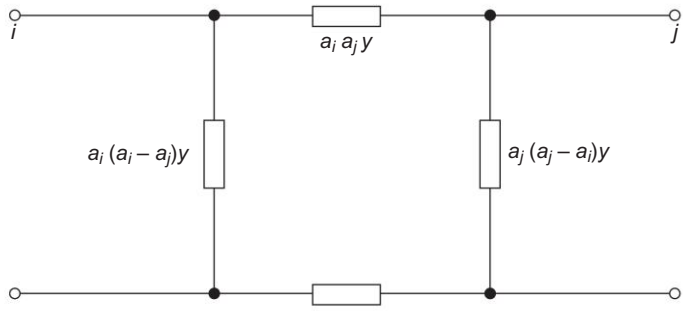

Fig. 6.29 π-equivalent of Fig. 6.28 with a_i and a_j real

Example 6.12 The four-bus system of Fig. 6.7 is now modified to include a regulating transformer in the line 3–4 near bus 3. Find the modified $\boldsymbol{Y}_{\text{BUS}}$ of the system for

(1) $V_3/V_3' = 1.04$ or $a = 1/1.04$

(2) $V_3/V_3' = e^{j3^\circ}$ or $a = e^{-j3^\circ}$ $\quad |a| = 1;\ a = V_3'/V_3$

Solution

(1) With regulating transformer in line 3–4, the elements of the corresponding submatrix in Eq. (v) of Example 6.3 are modified as under.

$$\begin{matrix} & 3 & 4 \\ 3 & (Y_{33}\,(\text{old}) - y_{34} + a^2 y_{34}) & (y_{34}\,(\text{old}) + y_{34} - a y_{34}) \\ 4 & (Y_{43}\,(\text{old}) + y_{34} - a y_{34}) & (y_{44}\,(\text{old})) \end{matrix}$$

$$\begin{matrix} & 3 & \\ 3 & (3.666 - j11) - (2 - j6) + \dfrac{1}{(1.04)^2}(2 - j6) & \\ 4 & (-2 + j6) + (2 - j6) - \dfrac{1}{(1.04)}(2 - j6) & \end{matrix}$$

$$\begin{matrix} & 4 \\ & (-2 + j6) + (2 - j6) - \dfrac{1}{(1.04)}(2 - j6) \\ & (3 - j9) \end{matrix}$$

$$\begin{matrix} & 3 & 4 \\ 3 & (3.516 - j10.547) & (-2.3113 + j5.8871) \\ 4 & (-1.683 + j6.0965) & (3 - j9) \end{matrix}$$

The old values of Y_{33}, Y_{34}, Y_{43}, Y_{44} are given in Example 6.3

(2) Modified submatrix in Eq. (v) of Example 6.3 is

$$\begin{matrix} & 3 & 4 \\ 3 & (Y_{33}\,(\text{old}) - y_{34} + |a|^2 y_{34}) & (Y_{34}\,(\text{old}) + y_{34} - a^* y_{34}) \\ 4 & (Y_{43}\,(\text{old}) + y_{34} - a y_{34}) & (Y_{44}\,(\text{old})) \end{matrix}$$

It follows from Eq. (6.101)

$$\begin{matrix} & 3 & 4 \\ 3 & (3.666 - j11) - (2 - j6) + 1(2 - j6) & (-2 + j6) + (2 - j6) - \varepsilon^{-j3^\circ}(2 - j6) \\ 4 & (-2 + j6) + (2 - j6) - \varepsilon^{j3^\circ}(2 - j6) & (3 - j9) \end{matrix}$$

$$\begin{matrix} & 3 & 4 \\ 3 & 3.666 - j11 & -2.3113 + j5.8871 \\ 4 & -1.683 + j6.0965 & 3 - j9 \end{matrix}$$

Voltage Controlled Buses

Consider a regulating transformer between *i*th and *j*th buses with the voltage at the *i*th bus to be controlled. From Eqs (6.100), it follows that

$$I_i = |a|^2 yV_i - a^* yV_j \tag{6.100a}$$

$$I_j = -ayV_i + yV_j \tag{6.100b}$$

where y is the series admittance of the line and 'a' is the complex transformer turns ratio given by

$$a = |a| \angle\alpha \tag{6.100c}$$

where $|a|$ is the turns ratio and α is the phase shift. In a regulating transformer these two parameters are independently adjustable over small ranges, such as

$$(1 - K) \le |a| \le (1 + K) \quad K << 1 \quad \text{(typically } K \le 0.1) \tag{6.103a}$$

$$-\beta^\circ \le \alpha \le \beta^\circ \quad \text{(typically } \beta \le 10^\circ) \tag{6.103b}$$

Both variables are physically adjustable in fixed steps of $\Delta|a|$ and $\Delta\alpha$, where $\Delta|a| << |a|$ and $\Delta\alpha << \alpha$ (typically $\Delta|a| \le 0.05$ and $\Delta\alpha \le 2.5^\circ$).

Let $|V_i|_{\text{spec}}$ be the voltage specified at the *i*th voltage controlled bus. Since $P_{Gi} = Q_{Gi} = 0$ for a voltage controlled bus, Q_i is specified in addition to P_i and $|V_i|$. In the *r*th iteration, $|V_i|^{(r+1)}$ is evaluated using Eq. (6.37) (for GS method) or Eq. (6.76) (for NR method). If

$$|V_i^{(r+1)}| - |V_i|_{\text{spec}} < \frac{\Delta|a|}{2} |V_i|_{\text{spec}} \tag{6.104}$$

then $|V_i^{(r+1)}| \cong |V_i|_{\text{spec}}$, so that $|V_i|$ is kept at $|V_i|^{(r+1)}$. Otherwise, $|a|$ is increased (if $|V_i|^{(r+1)}$ is high) or decreased (if $|V_i|^{(r+1)}$ is low) in steps of $\Delta|a|$ till Eq. (6.104) is satisfied.

The power flow across the line (assuming lossless transformer) is given by

$$P_{ij} = \text{Re}\,(V_i I_i^*) = \text{Re}\,(V_i^* I_i) \tag{6.105a}$$

Substituting Eq. (6.100a) in Eq. (6.105a), we get

$$\begin{aligned} P_{ij} &\cong \text{Re}\,(V_i (|a|^2 y^* V_i^* - a y^* V_j^*)) \\ &= \text{Re}\,(|a|^2 |y| |V_i|^2 \angle -\theta - |a||y||V_i||V_j| \angle(\delta_i - \delta_j + \alpha - \theta)) \end{aligned}$$

or

$$P_{ij} \cong |a|^2 |y| |V_i|^2 \cos\theta - |a||y||V_i||V_j| \cos(\delta_i - \delta_j + \alpha - \theta) \tag{6.105b}$$

where $y = |y| \angle\theta$.

Next, we estimate the change ΔP_{ij} due to the change $\Delta\alpha$. We have from Eq. (6.105b)

$$\frac{\partial P_{ij}}{\partial \alpha} = |a||y||V_i||V_j| \sin(\delta_i - \delta_j + \alpha - \theta) \tag{6.106}$$

And we approximate

$$\Delta P_{ij} = \frac{\partial P_{ij}}{\partial \alpha} \Delta\alpha \tag{6.107}$$

If

$$| P_{ij} - P_{ij,\,\text{spec}} | \le \Delta P_{ij}/\,2 \tag{6.108}$$

where $P_{ij,\ \text{spec}}$ is the specified value, then α is not changed. Otherwise, α is increased (causing more real power flow) or decreased (decreasing real power flow) depending on whether P_{ij} is low or high.

After updating the values of $| a |$ and α above, the corresponding elements in the $\boldsymbol{Y}_{\text{BUS}}$ also change and have to be updated for the next iteration. We have, therefore,

$$\begin{aligned} Y_{ii\ \text{new}} &= Y_{ii\ \text{old}} - y_{ii\ \text{old}} + y_{ii\ \text{new}} \\ Y_{ij\ \text{new}} &= Y_{ij\ \text{old}} + y_{ij\ \text{old}} - y_{ij\ \text{new}} \\ Y_{ji\ \text{new}} &= Y_{ji\ \text{old}} + y_{ji\ \text{old}} - y_{ji\ \text{new}} \\ Y_{jj\ \text{new}} &= Y_{jj\ \text{old}} - y_{jj\ \text{old}} + y_{jj\ \text{new}} \end{aligned} \tag{6.109}$$

where y_{ii}, y_{ij}, y_{ji} and y_{jj} are given by Eqs 6.100(a) and (b). By substituting the corresponding 'old' and 'new' values of $a = | a | \angle\alpha$ we get 'old' and 'new' values of y_{ii}, y_{ij}, y_{ji}, y_{jj}. From Eqs 6.100(a) and (b),

$$\begin{aligned} y_{ii} &= I_i/V_i \,|\, (V_j = 0,\ V_i \ne 0) = | a |^2 y \\ y_{ij} &= I_i/V_j \,|\, (V_i = 0,\ V_j \ne 0) = -a^* y \\ y_{jj} &= I_j/V_i \,|\, (V_j = 0,\ V_i \ne 0) = -ay \\ y_j &= I_j/V_j \,|\, (V_i = 0,\ V_j \ne 0) = y \end{aligned} \tag{6.110}$$

6.10 LOAD FLOW UNDER POWER ELECTRONIC CONTROL

Note: This section is to be read after studying Ch. 20 on HVDC transmission. The recent availability of HV power electronic switching has made it possible to develop HVDC transmission (Ch. 20) and FACTS technologies (Ch. 15 of Ref. 14). Infact, the original purpose of the former was a return to DC transmission for large distances, most of the schemes actually in use are back-to-back (interconnection of asynchronous power systems).

The FACTS technology is primarily used to enhance the controllability of the synchronous transmission system thereby improving the stability limits. In this section we will briefly describe how to incorporate these two power electronic, technologies in conventional load flow solutions wherever feasible.

It is preferable to use original full NR method described earlier to incorporate FACTS devices in the load flow solution to have better convergence.

Some FACTS devices pose no special problem, as their steady-state behaviour is properly represented by the standard load flow specifications. This is so with static VAR compensation (TCR or STATCON type). This can be specified by a zero active power and constant voltage magnitude, like the conventional synchronous condensers. Ch. 5 of Ref. 13 describes in detail the

incorporation of FACTS devices in LF solution. Static tap changing, phase-shifting, TCSC and UPFC are considered.

AC-DC Load Flow

A combined AC-DC power system with 3 buses and 4 terminals is drawn in Fig. 6.30 to bring into clarity to the procedures that follow. The label terminal (term) is given to those buses in which there is DC connection via a transformer and converter (T & C).

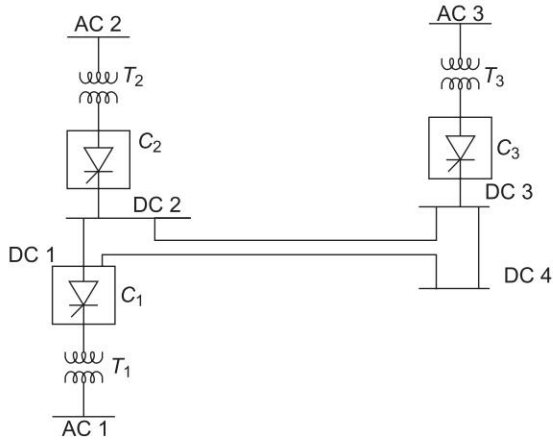

Fig. 6.30 A small size AC-DC power system

At any converter terminal the complex power flows are indicated in Fig. 6.31; this is the more general form of Fig. 6.3 for AC system. From this figure the power balance equations at the terminal are:

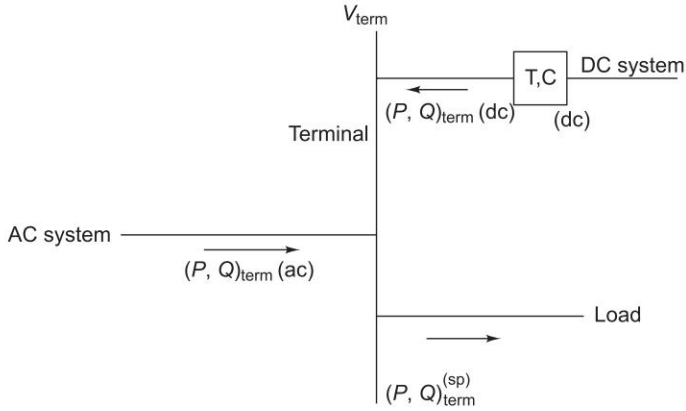

Fig. 6.31 Complex power balance at a converter terminal

$$P^{sp}_{term} - P_{term}\,(ac) - P_{term}\,(dc) = 0 \qquad (6.111)$$

$$Q^{sp}_{term} - Q_{term}\,(ac) - Q_{term}\,(dc) = 0 \qquad (6.112)$$

where

- $(P, Q)_{\text{term}}$ (ac) are injected powers (real, reactive) which are functions of AC system variables (V, δ).
- $(P, Q)_{\text{term}}$ (dc) are injected power from the DC system which are functions of DC system variables.
- $(P, Q)^{\text{sp}}_{\text{term}}$ is the AC system load at the terminal
  $(P, Q)_{\text{term}}$ (dc) are dependent on

$$P_{\text{term}}(\text{dc}) = f_p(V_{\text{term}}, x) \tag{6.113}$$

$$Q_{\text{term}}(\text{dc}) = f_q(V_{\text{term}}, x) \tag{6.114}$$

where x is a vector dc variables (converter settings).

The operating state of an AC–DC system are:

$$[V, \delta, x]^T$$

where V is vector of ac voltage magnitude
δ is vector ac system angles
x is vector of dc variables
We shall use NR formulations.

The equations derived from the specified AC system conditions may be summarized as:

$$\begin{bmatrix} \Delta \bar{P}(\bar{V}, \bar{\delta}) \\ \Delta \bar{P}_{\text{term}}(\bar{V}, \bar{\delta}, \bar{x}) \\ \Delta \bar{Q}(\bar{V}, \bar{\delta}) \\ \Delta \bar{Q}_{\text{term}}(\bar{V}, \bar{\delta}, \bar{x}) \end{bmatrix} = 0 \tag{6.115}$$

where the mismatches at the converter terminal bus bars are indicated separately.

A further set of independent equations are derived from DC system conditions. These are designated as

$$\bar{R}(V_{\text{term}}, \bar{x})_k = 0 \tag{6.116}$$

for $k = 1$, no. of converters present.

The general AC–DC load flow problem may be summarized as the solution of [Ch. 6, Ref. 11]

$$\begin{bmatrix} \Delta \bar{P}(\bar{V}, \bar{\delta}) \\ \Delta \bar{P}_{\text{term}}(\bar{V}, \bar{\delta}, \bar{x}) \\ \Delta \bar{Q}(\bar{V}, \bar{\delta}) \\ \Delta \bar{Q}_{\text{term}}(\bar{V}, \bar{\delta}, \bar{x}) \\ \bar{R}(V_{\text{term}}, \bar{x}) \end{bmatrix} = 0 \tag{6.117}$$

The DC system equations (6.113), (6.114) and (6.116) are made independent of the AC system angles δ by selecting a separate angle reference for the DC

system variable as defined in Fig. 6.32. This improves the algorithmic performance by effectively decoupling the angle dependence of AC and DC systems.

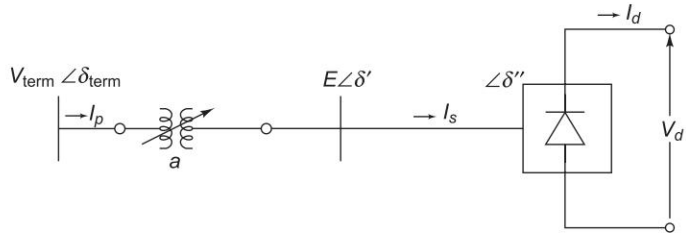

Fig. 6.32 Basic DC converter (angles refer to AC system reference)

Converter Model

Under balanced conditions, similar converter bridges, attached to the same AC terminal bus, will operate identically regardless of the transformer connection. They can, therefore, be replaced by an equivalent single bridge for the purpose of single-phase load flow analysis.

Two independent variables are sufficient to model a DC converter, operating under balanced conditions, from a known terminal voltage source.

The following set of variables allow simple relationships for all the normal control strategies

$$[\bar{x}] = [V_d, I_d, a, \cos \alpha, \phi]^T$$

variable ϕ is included to ensure a simple expression for Q_{dc}.
Here

a = transformer off-nominal tap ratio

$V_{\text{term}} \angle \phi$ converter terminal bus nodal voltage

(phase angle referred to the converter reference)

$E \angle \psi$ fundamental frequency component of the voltage waveform at the converter transformer secondary.

α = firing delay angle

V_d = average DC voltage

I_d = converter direct current

Fig. 6.33 shows an equivalent circuit for the converter

Solution Technique

The solution to a single converter connected to AC busbar is given below:
Unified Solution: The unified solution gives recognition to the interdependence of AC and DC system equations and simultaneously solves the complete

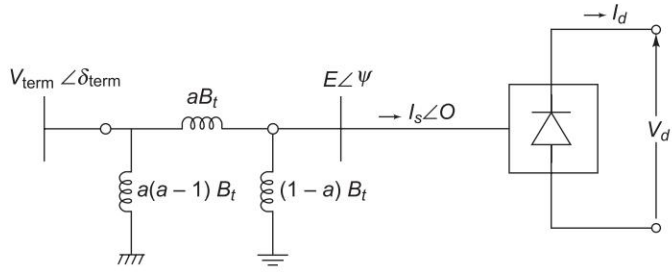

Here B_t is transformer leakage susceptance

Fig. 6.33 Single-phase equivalent circuit for basic converter (angles refer to DC reference)

system. Referring to Eq. (6.117) the standard Newton–Raphson Algorithm involves repeat solution of the matrix equations

$$\begin{bmatrix} \Delta \bar{P}(\bar{V}, \delta) \\ \Delta \bar{P}_{\text{term}}(\bar{V}, \delta, \bar{x}) \\ \Delta \bar{Q}(\bar{V}, \delta) \\ \Delta \bar{Q}_{\text{term}}(\bar{V}, \delta, \bar{x}) \\ \bar{R}(V_{\text{term}}, \bar{x}) \end{bmatrix} = [J] \begin{bmatrix} \Delta \bar{\delta} \\ \Delta \delta_{\text{term}} \\ \Delta \bar{V} \\ \Delta V_{\text{term}} \\ \Delta \bar{x} \end{bmatrix} \tag{6.118}$$

where J is the usual Jacobian.

$$\Delta P_{\text{term}} = P^{\text{sp}}_{\text{term}} - P_{\text{term}}(\text{ac}) - P_{\text{term}}(\text{dc}) \tag{6.119}$$

$$\Delta Q_{\text{term}} = Q^{\text{sp}}_{\text{term}} - Q_{\text{term}}(\text{ac}) - Q_{\text{term}}(\text{dc}) \tag{6.120}$$

and

$$P_{\text{term}}(\text{dc}) = f(V_{\text{term}}, \bar{x}) \tag{6.121}$$

$$Q_{\text{term}}(\text{dc}) = f(V_{\text{term}}, \bar{x}) \tag{6.122}$$

Applying the AC fast decoupled assumptions to all Jacobian elements related to the AC system equations, yields;

$$\begin{bmatrix} \Delta \bar{P}/\bar{V} \\ \Delta \bar{P}_{\text{term}}/V_{\text{term}} \\ \Delta \bar{Q}/\bar{V} \\ \Delta Q_{\text{term}}/\bar{V}_{\text{term}} \\ \bar{R} \end{bmatrix} = [O, B', B'', A] \begin{bmatrix} \Delta \bar{\delta} \\ \Delta \delta_{\text{term}} \\ \Delta \bar{V} \\ \Delta V_{\text{term}} \\ \Delta x \end{bmatrix} \tag{6.123}$$

where all matrix elements are zero unless otherwise indicated. The matrices [B'] and [B''] are the usual single-phase fast decoupled Jacobians and are constant in value. The other matrices [A] indicated vary at each iteration in the solution process.

In the above formulation, the DC variable x are coupled to both the real and reactive power AC mismatches. However Eq. (6.123) may be separated to enable a block successive iteration scheme to be used.

The DC mismatches and variables can be appended to the two fast decoupled AC, equations in which case the following equation results

$$\begin{bmatrix} \Delta\bar{P}/\bar{V} \\ \Delta P_{\text{term}}/V_{\text{term}} \\ \bar{R} \end{bmatrix} = \begin{bmatrix} B' & \\ & AA' \\ & A \end{bmatrix} \begin{bmatrix} \Delta\delta \\ \Delta\delta_{\text{term}} \\ \Delta x \end{bmatrix} \tag{6.124}$$

$$\begin{bmatrix} \Delta\bar{Q}/\bar{V} \\ \Delta Q_{\text{term}}/V_{\text{term}} \\ \bar{R} \end{bmatrix} = \begin{bmatrix} B'' & & \\ & B_{ii}'' & AA'' \\ & BB'' & A \end{bmatrix} \begin{bmatrix} \Delta\bar{V} \\ \Delta V_{\text{term}} \\ \Delta\bar{x} \end{bmatrix} \tag{6.125}$$

The algorithm may be further simplified by recognizing the following physical characteristics of the AC and DC systems:

- The coupling between DC variables and the AC terminal voltage is strong.
- There is no coupling between DC mismatches and AC system angles.
- Under all Practical Control Strategies, the DC power is well constrained and this implies that the changes in DC variables $\bar{x}$ do not greatly affect the real power mismatches at the terminals.

These features justify the removal of the DC equations from Eqs (6.124) and (6.125) to yield a [P, Q_{dc}] block successive iteration scheme, represented by the following two equations

$$\left[\Delta\bar{P}/\bar{V}\right] = [B']\left[\Delta\bar{\delta}\right] \tag{6.126}$$

$$\begin{bmatrix} \Delta\bar{Q}/\bar{V} \\ \Delta Q_{\text{term}}/V_{\text{term}} \\ \bar{R} \end{bmatrix} = \begin{bmatrix} B'' & & \\ & B_{ii}'' & AA'' \\ & BB'' & A \end{bmatrix} \begin{bmatrix} \Delta\bar{V} \\ \Delta V_{\text{term}} \\ \Delta\bar{x} \end{bmatrix} \tag{6.127}$$

Sequential Method

The sequential method results from a further simplification of the unified method i.e., the AC system equations are solved with the DC system modelled simply as real and reactive power injections at the appropriate terminal bus. For a DC solution, the AC system is modelled as a constant voltage at the converter AC terminal bus.

The following equations are solved iteratively till convergence:

$$[\Delta \bar{P}/\bar{V}] = [B'][\Delta\delta] \tag{6.128}$$

$$[\Delta \bar{Q}/\bar{V}] = [B''][\Delta \bar{V}] \tag{6.129}$$

$$[\bar{R}] = [A][\Delta \bar{x}] \tag{6.130}$$

6.11 SUMMARY

In this chapter, perhaps the most important power system study, viz., load flow has been introduced and discussed in detail. Important methods available have been briefly described. It is almost impossible to say which one of the existing methods is the best, because the behaviour of different load flow methods is dictated by the types and sizes of the problems to be solved, as well as the precise details of implementation. Choice of a particular method in any given situation is normally a compromise between the various criteria of goodness of the load flow methods. It would not be incorrect to say that among the existing methods, no single method meets all the desirable requirements of an ideal load flow method, viz. high speed, low storage, reliability for ill-conditioned problems, versatility in handling various adjustments and simplicity in programming. Fortunately, not all the desirable features of a load flow method are needed in all situations.

In spite of a large number of load flow methods available, it is easy to see that only the NR and FDLF load flow methods are the most important ones for general purpose load flow analysis. The FDLF method is clearly superior to the NR method from the point of view of speed as well as storage. Yet, the NR method is still in use because of its high versatility, accuracy and reliability and, as such, is being widely used for a variety of system optimization calculations. It gives sensitivity analysis and can be used in modern dynamic-response and outage-assessment calculations. Of course newer methods would continue to be developed which would either reduce the computation requirements for large systems, or would be more amenable to on-line implementation. Finally, load flow under power electronic control (FACTS/HVDC) is described.

Additional Examples

Example 6.13 Consider the two-bus system of Fig. 6.34. The line has s series impedance of $0.01 + j0.05$ pu, and a total shunt admittance of $j0.01$ pu. The specified quantities at the two buses are given in the table as follows:

Bus i	*Type*	V_i *pu*	δ_i	*Injected powers*	
				P_i *pu*	Q_i, *pu*
1.	Slack bus	1	0°	—	—
2.	PQ bus	?	?	P_2	Q_2

Determine the range of P_2 and Q_2 for which the solution of $|V_2|$ exists.

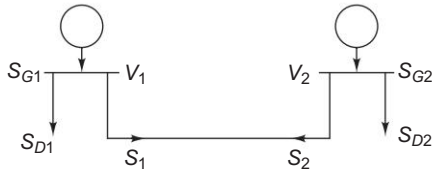

Fig. 6.34 Two-bus system

Solution

Using the nominal-π model for the transmission line $\boldsymbol{Y}_{\text{BUS}}$ is obtained as follows:

For the line,

$$y_{\text{series}} = \frac{1}{0.01 + j0.05} = 3.846 - j19.231 = 19.61 \angle -78.69° \text{ pu}$$

Therefore, in the $\boldsymbol{Y}_{\text{BUS}}$ matrix

$$\begin{aligned} \text{Each off-diagonal term} &= -3.846 + j19.231 \text{ pu} \\ &= 19.61 \angle 101.31° \text{ pu} \\ \text{Each self term} &= (3.846 - j19.231) + (j0.005)) \\ &= 3.846 - j19.226 \text{ pu} \\ &= 19.61 \angle -78.69° \end{aligned}$$

Therefore,

$$\boldsymbol{Y}_{\text{BUS}} = \begin{bmatrix} 19.61\angle -78.69° & 19.61\angle 101.31° \\ 19.61\angle 101.31° & 19.61\angle -78.69° \end{bmatrix}$$

The real and reactive powers at bus 2 are

$$P_2 = |V_2||V_1||Y_{21}| \cos(\theta_{21} + \delta_1 - \delta_2) + |V_2|^2 |Y_{22}| \cos\theta_{22}$$

$$Q_2 = |V_2||V_1||Y_{21}| \sin(\theta_{21} + \delta_1 - \delta_2) - |V_2|^2 |Y_{22}| \sin\theta_{22}$$

Substituting the value of $V_1 = 1 \angle 0°$, we get

$$\cos(\theta_{21} - \delta_2) = \frac{1}{|V_2||Y_{21}|}(P_2 - |V_2|^2 |Y_{22}| \cos\theta_{22}) \quad \text{(i)}$$

$$\sin(\theta_{21} - \delta_2) = \frac{-1}{|V_2||Y_{21}|}(Q_2 + |V_2|^2 |Y_{22}| \sin\theta_{22}) \quad \text{(ii)}$$

Squaring and adding,

$$1 = \frac{1}{|V_2|^2 |Y_{21}|^2} (P_2^2 + Q_2^2 + |V_2|^4 |Y_{22}|^2 + 2|Y_{22}||V_2|^2 (Q_2 \sin\theta_{22} - P_2 \cos\theta_{22}))$$

or

$$|Y_{22}|^2 V_2^4 + (2|Y_{22}|(Q_2 \sin\theta_{22} - P_2 \cos\theta_{22}) - |Y_{21}|^2)|V_2|^2 + (P_2^2 + Q_2^2) = 0$$

Substituting the values of $|Y_{21}|$ and $Y_{22} = |Y_{22}| \angle\theta_{22}$,

$$(384.55)|V_2|^4 + (-38.45Q_2 - 7.692P_2) - 384.55)|V_2|^2 + (P_2^2 + Q_2^2) = 0$$

or

$$|V_2|^2 = \frac{(38.45Q_2 + 7.692P_2 + 384.55) \pm \sqrt{(38.45Q_2 + 7.692P_2 + 384.55)^2 - 1538.2(P_2^2 + Q_2^2)}}{769.1} \quad \text{(iii)}$$

Therefore, real values of $|V_2|$ exists for

$$(38.45Q_2 + 7.692P_2 + 384.55)^2 \geq 1538.2(P_2^2 + Q_2^2)$$

which on simplifying yields

$$(0.196P_2 + 0.98Q_2 + 9.805)^2 \geq (P_2^2 + Q_2^2)$$

or

$$(-0.962)P_2^2 + (0.384Q_2 + 3.844)P_2 - (0.0296Q_2^2 - 19.22Q_2 - 96.138) \geq 0$$

or

$$P_2 \geq \frac{-(0.384Q_2 + 3.844) \pm \sqrt{(0.384Q_2 + 3.844)^2 - (0.1524Q_2^2 - 73.96Q_2 - 370)}}{-1.924} \quad \text{(iv)}$$

For real values of $|V_2|$, we must therefore have

$$(0.384Q_2 + 3.844)^2 \geq (0.1524\, Q_2^2 - 73.96Q_2 - 370)$$

or

$$(-4.94 \times 10^{-3})Q_2^2 + (76.91)Q_2 + 384.78 \geq 0$$

or

$$Q_2 \geq \frac{-76.91 \pm \sqrt{(76.91^2 + 4 \times 4.94 \times 384.78 \times 10^{-3})}}{-9.88 \times 10^{-3}} \quad \text{(v)}$$

$$= \frac{-76.91 \pm 76.959}{-9.88 \times 10^{-3}}$$

or

$$Q_2 \geq -4.96,\ 15.574 \times 10^3 \text{ pu}$$

Hence

$$Q_2 \geq -4.96$$

Taking

(a) $Q_2 = -2$ pu; From (iv),

$$P_2 \geq \frac{-3.078 \pm 15.196}{-1.924} = -6.3,\ 9.5 \text{ pu}$$

or

$$P_2 \geq -6.3 \text{ pu}$$

(b) $Q_2 = 0$ pu: From (iv),

$$P_2 \geq \frac{-3.844 \pm 19.616}{-1.924} = -8.198,\ 12.193 \text{ pu}$$

or

$$P_2 \geq -8.198 \text{ pu}$$

(c) $Q_2 = 2$ pu: From (iv),

$$P_2 \geq \frac{-4.612 \pm 23.21}{-1.924} = -9.67,\ 14.46 \text{ pu}$$

or

$$P_2 \geq -9.67 \text{ pu}$$

Example 6.14 Consider a three-bus system. The specifications at various buses are given in the table. Each line impedance $z_L = j0.25$ pu. Neglect shunt admittances of all lines.

Bus i	*Type*	$\lvert V_i \rvert$ *pu*	δ_i	*Injected powers*	
				P_i *pu*	Q_i, *pu*
1.	Slack bus	1	0	—	—
2.	PQ bus	?	?	–0.5	–0.4
3.	PV bus	0.9	?	0.5	—

Find $\lvert V_2 \rvert$, δ_2 and δ_3, by using small-angle approximation. Is the approximation reasonable?

Solution

Series line admittance is

$$y_L = 1/z_L = -j4.0 \text{ pu}$$

$$\therefore \quad \mathbf{Y}_{\text{BUS}} = \begin{bmatrix} -j8.0 & j4.0 & j4.0 \\ j4.0 & -j8.0 & j4.0 \\ j4.0 & j4.0 & -j8.0 \end{bmatrix}$$

Now

$$S_2^* = P_2 - jQ_2 = V_2^* \sum_{k=1}^{3} Y_{2k} V_k \quad \text{(i)}$$

$$S_3^* = P_3 - jQ_3 = V_3^* \sum_{k=1}^{3} Y_{3k} V_k \quad \text{(ii)}$$

We have

$$V_2^* V_k = |V_2||V_k|\varepsilon^{j(\delta_k - \delta_2)} = |V_2||V_k|(\cos(\delta_k - \delta_2) + j\sin(\delta_k - \delta_2))$$

$$\cong |V_2||V_k|(1 + j(\delta_k - \delta_2)) = |V_2||V_k|(1 + j\delta_{k2})$$

and similarly,

$$V_3^* V_k \cong |V_3||V_k|(1 + j(\delta_k - \delta_3)) = |V_3||V_k|(1 + j\delta_{k3})$$

Substituting in (i) and (ii),

$$P_2 - jQ_2 = |V_2|(Y_{21}|V_1|(1 + j\delta_{12}) + Y_{22}|V_2| + Y_{23}|V_3|(1 + j\delta_{32}))$$

$$= |V_2|(Y_{21}|V_1|(1 - j\delta_2) + Y_{22}|V_2| + Y_{23}|V_3|(1 + j(\delta_3 - \delta_2))) \quad \text{(iii)}$$

Similarly,

$$P_3 - jQ_3 = |V_3|(Y_{31}|V_1|(1 - j\delta_3) + Y_{32}|V_2|(1 + j(\delta_2 - \delta_3)) + Y_{33}|V_3|) \quad \text{(iv)}$$

Substituting various values in (iii) and (iv),

$$-0.5 + j0.4 = |V_2|(j4.0(1 - j\delta_2) - j8.0|V_2| + j4.0(0.9)(1 + j\delta_{32})) \quad \text{(v)}$$

$$0.5 - jQ_3 = 0.9(j4.0(1 - j\delta_3) + j4.0|V_2|(1 + j\delta_{23}) - j8.0(0.9)) \quad \text{(vi)}$$

Equating the imaginary part of (v),

$$0.4 = 4.0|V_2| - 8.0|V_2|^2 + 3.6|V_2|$$

or

$$8.0|V_2|^2 - 7.6|V_2| + 0.4 = 0$$

or

$$|V_2| = \frac{7.6 \pm \sqrt{(7.6^2 - 12.8)}}{16.0} = \frac{7.6 \pm 6.7}{16} = 0.894,\ 0.056 \text{ pu}$$

$$|V_2| = 0.894 \text{ pu}$$

Equating the real parts of (v) and (vi), we get

$$-0.5 = 0.894(4\delta_2 - 4(0.9)(\delta_3 - \delta_2))$$

$$0.5 = 0.9(4\delta_3 - 4(0.894)(\delta_2 - \delta_3))$$

or

$$6.7944\delta_2 - 3.2184\delta_3 = -0.5$$

$$-3.2184\delta_2 + 6.8184\delta_3 = 0.5$$

or

$$\delta_2 = \frac{-0.5(6.8184) + 0.5(3.2184)}{6.7944(6.8184) - 3.2184(3.2184)} = -0.05 \text{ rad}$$

or

$$\delta_3 = \frac{6.7944(0.5) + 3.2184(-0.5)}{6.7944(6.8184) - 3.2184(3.2184)} = 0.05 \text{ rad}$$

or

$$\delta_2 = -0.05 \text{ rad} = -2.85 \text{ deg}$$

$$\delta_3 = 0.05 \text{ rad} = 2.85 \text{ deg}$$

The approximation is reasonable, since

$$\delta_{12}, \delta_{23}, \delta_{31} < 10^\circ$$

so that $\cos \delta_{ij} \cong 1,$

and $\sin \delta_{ij} \cong \delta_{ij}$ rad

Example 6.15 Consider the three-bus system of Fig. 6.35. Assume negligible shunt admittances of the lines. Each line admittance is $-j10$ pu. 'a' is the complex turns ratio of the regulating transformer, RT, i.e.,

$$a = |a| \angle \alpha$$

(a) Determine $\boldsymbol{Y}_{\text{BUS}}$ for $a = 1.05\angle -2.5^\circ = 1.049 - j0.046$.

(b) Determine the changes in real and reactive power flows ΔP_{23} and ΔQ_{23} when 'a' changes from $1\angle 0^\circ$ to $1\angle -2.5^\circ$.

(c) Repeat (b) when 'a' changes from $1\angle 0^\circ$ to $1.05\angle 0^\circ$. Given, $|V_2| = 1.05$ pu, $|V_3| = 0.95$ pu, $\delta_2 = -3^\circ$, $\delta_3 = +2^\circ$, without the regulating transformer RT.

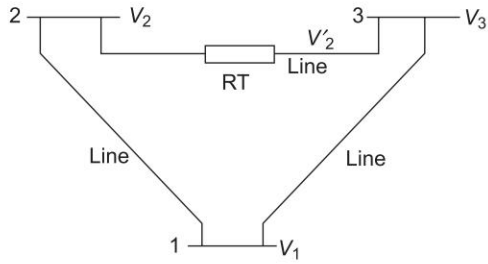

Fig. 6.35

Solution

Using Eqs (6.9) and (6.101), we get

(a)

$$\boldsymbol{Y}_{\text{BUS}} = \begin{array}{c|ccc} & 1 & 2 & 3 \\ \hline 1 & -j20 & j10 & j10 \\ 2 & j10 & -j10 + |a|^2(-j10) & -a^*(-j10) \\ 3 & j10 & -a(-j10) & -j20 \end{array}$$

$$= \begin{array}{|ccc|} \hline -j20 & j10 & j10 \\ j10 & -j21.025 & -0.46 + j10.49 \\ j10 & 0.46 + j10.49 & -j20 \\ \hline \end{array}$$

(b) We have the complex line flow from bus 2 to 3 given by

$$S_{23}^* = P_{23} - jQ_{23}$$

$$= V_2^* I_{23}$$

$$= V_2^* (|a|^2 y_L V_2 - a^* y_L V_3) \text{ from Eq. (6.100a)}$$

$$= (|V_2|^2 |a|^2 |y_L| \angle\theta_L - |V_2||V_3||a||y_L| \angle(\theta_L + \delta_3 - \delta_2 - \alpha))$$

Equating the real and imaginary parts, we have

$$P_{23} = |y_L||V_2|(|a||V_2| \cos\theta_L - |V_3| \cos(\theta_L + \delta_3 - \delta_2 - \alpha)) \quad \text{(i)}$$

$$Q_{23} = -|a||y_L||V_2|(|a||V_2| \sin\theta_L - |V_3| \sin(\theta_L + \delta_3 - \delta_2 - \alpha)) \quad \text{(ii)}$$

When $a = 1\angle 0°$,

$$P_{23} = 10(1.05)(0 - 0.95 \cos(90° + 2° + 3° - 0°)) = 0.8694 \text{ pu}$$

$$Q_{23} = -10(1.05)(1.05 - 0.95 \sin(90° + 2° + 3° - 0°)) = -1.088 \text{ pu}$$

when a is changed to $1 \angle -2.5°$

$$P_{23} = 10(1.05)(0 - 0.95 \cos(90° + 2° + 3° + 2.5°)) = 1.302 \text{ pu}$$

$$Q_{23} = -10(1.05)(1.05 - 0.95 \sin(90° + 2° + 3° + 2.5°)) = -1.135 \text{ pu}$$

$$\Delta P_{23} = (1.302 - 0.8694) \text{ pu} = 0.4326 \text{ pu}$$

$$\Delta Q_{23} = (-1.135 - (-1.088)) \text{ pu} = 0.047 \text{ pu}$$

Thus the increase in real power flow is almost 10 times that of the increase in reactive power flow. Therefore, the phase shifts varies real power flow predominantly.

(c) When a is changed to $1.05\angle 0°$

$$P_{23} = (1.05)(10)(1.05)(0 - 0.95 \cos(90 + 2° + 3°)) = 0.9128 \text{ pu}$$

$$Q_{23} = -(1.05(10)(1.05)((1.05)^2 - 0.95 \sin(90 + 2° + 3°)) = -1.7212 \text{ pu}$$

$$\Delta P_{23} = 0.9128 - 0.8694 = 0.0434 \text{ pu}$$

$$\Delta Q_{23} = -1.7212 - (-1.135) = -0.5862 \text{ pu}$$

Hence the increase in reactive power is almost 14 times that of the increase in real power flow. Therefore, the change in voltage magnitudes affects mainly reactive power flow.

Problems

6.1 For the power system shown in Fig. P-6.1, obtain the bus incidence matrix ***A***. Take ground as reference. Is this matrix unique? Explain.

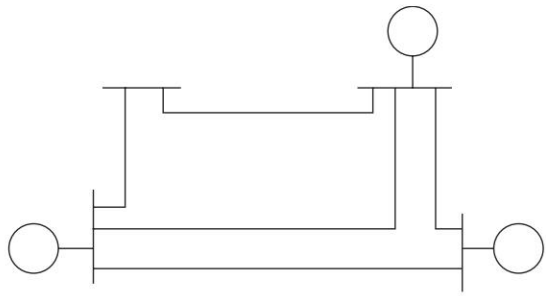

Fig. P-6.1

6.2 For the network shown in Fig. P-6.2, obtain the complex bus bar voltage at bus 2 at the end of the first iteration. Use the GS method. Line impedances shown in Fig. P-6.2 are in pu. *Given:*
Bus 1 is slack bus with $V_1 = 1.0 \angle 0°$
$P_2 + jQ_2 = -5.96 + j1.46$
$|V_3| = 1.02$
Assume: $V_3^0 = 1.02\angle 0°$ and $V_2^0 = 1\angle 0°$

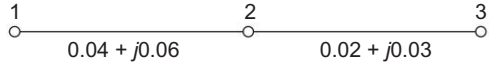

Fig. P-6.2

6.3 For the system of Fig. P-6.3 find the voltage at the receiving bus at the end of the first iteration. Load is $2 + j0.8$ pu. Voltage at the sending end (slack) is $1 + j0$ pu. Line admittance is $1.0 - j4.0$ pu. Transformer reactance is $j0.4$ pu. Off-nominal turns ratio is 1/1.04. Use the GS technique. Assume $V_R = 1\angle 0°$.

Fig. P-6.3

6.4 (a) Find the bus incidence matrix $\boldsymbol{A}$ for the four-bus system in Fig. P-6.4. Take ground as a reference.

(b) Find the primitive admittance matrix for the system. It is given that all the lines are characterized by a series impedance of $0.1 + j0.7\ \Omega$/km and a shunt admittance of $j0.35 \times 10^{-5}\ \Omega$/km. Lines are rated at 220 kV.

(c) Find the bus admittance matrix for the system. Use the values 220 kV and 100 MVA. Express all impedances and admittances in per unit.

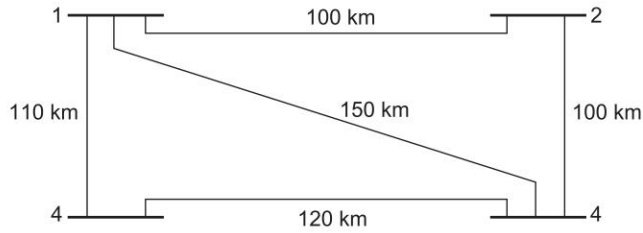

Fig. P-6.4

6.5 Consider the three-bus system of Fig. P-6.5. The pu line reactances are indicated on the figure; the line resistances are negligible. The magnitude of all the three-bus voltages are specified to be 1.0 pu. The bus powers are specified in the following table below:

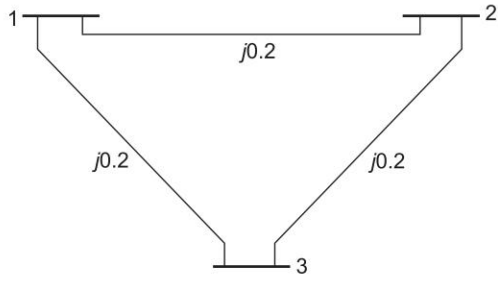

Fig. P-6.5

Bus	*Real demand*	*Reactive demand*	*Real generation*	*Reactive generation*
1	$P_{D1} = 1.0$	$Q_{D1} = 0.6$	$P_{G1} = ?$	Q_{G1} (unspecified)
2	$P_{D2} = 0$	$Q_{D2} = 0$	$P_{G2} = 1.4$	Q_{G2} (unspecified)
3	$P_{D3} = 1.0$	$Q_{D3} = 1.0$	$P_{G3} = 0$	Q_{G3} (unspecified)

Carry out the complete approximate load flow solution. Mark generations, load demands and line flows on the one-line diagram.

6.6 (a) Repeat Problem 6.5 with bus voltage specifications changed as below:

$|V_1| = 1.00$ pu
$|V_2| = 1.04$ pu
$|V_3| = 0.96$ pu

Your results should show that no significant change occurs in real power flows, but the reactive flows change appreciably as Q is sensitive to voltage.

(b) Resolve Problem 6.5 assuming that the real generation is scheduled as follows:

$P_{G1} = 1.0$ pu, $P_{G2} = 1.0$ pu, $P_{G3} = 0$

The real demand remains unchanged and the desired voltage profile is flat, i.e. $|V_1| = |V_2| = |V_3| = 1.0$ pu. In this case the results will show that the reactive flows are essentially unchanged, but the real flows are changed.

6.7 Consider the three-bus system of Problem 6.5. As shown in Fig. P-6.7 where a regulating transformer (RT) is now introduced in the line 1–2 near bus 1. Other system data remains as that of Problem 6.5. Consider two cases:

(i) RT is a magnitude regulator with a ratio = $V_1/V_1' = 0.99$,

(ii) RT is a phase angle regulator having a ratio = $V_1/V_1' = e^{j3^\circ}$

(a) Find out the modified $\boldsymbol{Y}_{BUS}$ matrix.

(b) Solve the load flow equations in cases (i) and (ii). Compare the load flow picture with one in Problem 6.5. The reader should verify that in case (i) only the reactive flow will change; whereas in case (ii) the changes will occur in the real power flow.

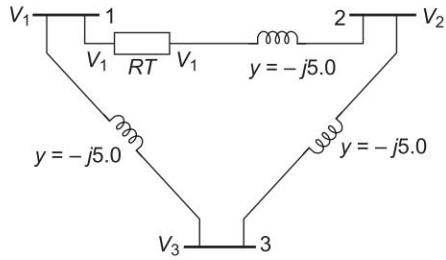

Fig. P-6.7 Three-bus sample system containing a regulating transformer

6.8 Calculate V_3 for the system of Fig. P-6.7 for the first iteration, using the data of Example 6.3. Start the algorithm with calculations at bus 3 rather than at bus 2.

6.9 For the sample system of Example 6.3 with bus 1 as slack, use the following methods to obtain a load flow solution.

(a) Gauss–Seidel using $\boldsymbol{Y}_{BUS}$, with acceleration factor of 1.6 and tolerances of 0.0001 for the real and imaginary components of voltage.

(b) Newton–Raphson using $\boldsymbol{Y}_{BUS}$, with tolerances of 0.01 pu for changes in the real and reactive bus powers.

Note: This problem requires the use of the digital computer.

6.10 Perform a load flow study for the system of Problem 6.4. The bus power and voltage specifications are given in Table P-6.10.

Table P-6.10

Bus	*Bus power, pu*		*Voltage magnitude, pu*	*Bus type*
	Real	*Reactive*		
1	Unspecified	Unspecified	1.02	Slack
2	0.95	Unspecified	1.01	PV
3	– 2.0	– 1.0	Unspecified	PQ
4	– 1.0	– 0.2	Unspecified	PQ

Compute the unspecified bus voltages, all bus powers and all line powers. Assume unlimited Q sources. Use the NR method.

References

Books

1. Mahalanabis, A.K., D.P. Kothari and S.I. Ahson, *Computer Aided Power System Analysis and Control*, Tata McGraw-Hill, New Delhi, 1988.
2. Weedy, B.M. and B.J. Cory, *Electrical Power Systems*, 4th edn, Wiley, New York, 1998.
3. Gross, C.A., *Power System Analysis*, 2nd edn, Wiley, New York, 1986.
4. Sterling, M.J.H., *Power System Control*, *IEE*, England, 1978.
5. Elgerd, O.I., *Electric Energy System Theory*: *An Introduction*, 2nd edn, McGraw-Hill, New York, 1982.
6. Stagg, G.W. and A.H. El-Abiad, *Computer Methods in Power System Analysis*, McGraw-Hill, New York, 1968.
7. Rose, D.J. and R.A. Willough (Eds), *Sparse Matrices and their Applications*, Plenum, New York, 1972.
8. Heydt, G.T., *Computer Analysis Methods for Power Systems*, Stars in a Circle Publications, 1996.
9. Brown, H.E., *Solution of Large Networks by Matrix Methods*, Wiley, New York, 1975.
10. Knight, U.G., *Power System Engineering and Mathematics*, Pergamon Press, New York 1972.
11. Arrillaga, C.P. Arnold and B.J. Harker, *Computer Modelling of Electrical Power Systems*, John Wiley, 1983.
12. Happ, H.H., *Diakoptics and Networks,* Academic Press, New York, 1971.

13. Arrillaga, J.C. and N.R. Watson, *Computer Modelling of Electrical Power Systems*, 2nd edn, Wiley, New York, 2001.
14. Kothari, D.P. and I.J. Nagrath, *Modern Power System Analysis*, 3rd edn, New York, 2006.
15. Bergen, A.R., *Power System Analysis*, Prentice-Hall, Englewood Cliffs, N.J. 1986.
16. Arrillaga, J. and C.P. Arnold, *Computer Analysis of Power Systems*, Wiley, New York, 1990.
17. Padiyar, K.R., *HVDC Power Transmission Systems*, Wiley, Eastern New Delhi, 1990.

Papers

18. Happ, H.H., 'Diakoptics—The Solution of System Problems by Tearing', *Proc. IEEE*, July 1974, 930.
19. Laughton, M.A., 'Decomposition Techniques in Power System Network Load Flow Analysis Using the Nodal Impedance Matrix', *Proc. IEE*, 1968, 115: 539
20. Stott, B., 'Decoupled Newton Load Flow', *IEEE Trans*., 1972, PAS-91, 1955.
21. Stott, B., 'Review of Load-Flow Calculation Method', *Proc. IEEE*, July 1974, 916.
22. Stott, B. and O. Alsac, 'Fast Decoupled Load Flow', *IEEE Trans*., 1974, PAS-93: 859.
23. Tinney, W.F. and J.W. Walker, 'Direct Solutions of Sparse Network Equations by Optimally Ordered Triangular Factorizations', *Proc. IEEE*, November 1967, 55:1801.
24. Tinney, W.F. and C.E. Hart, 'Power Flow Solution by Newton's Method', *IEEE Trans*., November 1967, no. 11, PAS-86: 1449.
25. Ward, J.B. and H.W. Hale, 'Digital Computer Solution of Power Problems', *AIEE Trans*., June 1956, Pt III, 75: 398.
26. Murthy, P.G., D.L. Shenoy, J. Nanda and D.P. Kothari, 'Performance of Typical Power Flow Algorithms with Reference to Indian Power Systems', *Proc. II Symp. Power Plant Dynamics and Control*, Hyderabad, 14–16 Feb. 1979, 219.
27. Tinney, W.F. and W.S. Mayer, 'Solution of Large Sparse Systems by Ordered Triangular Factorization', *IEEE Trans., Auto Control*, August 1973, vol. AC-18: 333.
28. Sato, N. and W.F Tinney, 'Techniques for Exploiting Sparsity of Network Admittance Matrix', *IEEE Trans.,* PAS, December 1963, 82: 44.
29. Sachdev, M.S. and T.K.P. Medicherla, 'A Second Order Load Flow Technique', *IEEE Trans*., PAS, Jan./Feb. 1977, 96: 189.
30. Iwamoto, S.and Y. Tamura, 'A Fast Load Flow Method Retaining Non-linearity', *IEEE Trans*., PAS, Sept./Oct. 1978, 97: 1586.
31. Roy, L., 'Exact Second Order Load Flow', *Proc. Sixth PSCC Conf. Dermstadt*, August 1978, 2: 711.
32. Iwamoto, S. and Y. Tamura, 'A Load Flow Calculation Method for III-Conditioned Power Systems', *IEEE Trans.,* PAS, April 1981, 100: 1736.
33. Happ, H.H. and C.C. Young, 'Tearing Algorithms for Large Scale Network Problems', *IEEE Trans.,* PAS, Nov./Dec. 1971, 90: 2639.

34. Dopazo, J.F., O.A. Kiltin and A.M. Sarson, 'Stochastic Load Flows', *IEEE Trans.,* PAS, 1975, 94: 299.
35. Nanda, J., D.P. Kothari and S.C. Srivastava, "Some Important Observations on FDLF Algorithm", *Proc. IEEE*, May 1987, pp. 732–33.
36. Nanda, J., P.R. Bijwe, D.P. Kothari and D.L. Shenoy, "Second Order Decoupled Load Flow', *Electric Machines and Power Systems*, vol. 12, no. 5, 1987, pp. 301–312.
37. Nanda J., D.P. Kothari and S.C. Srivastava, "A Novel Second Order Fast Decoupled Load Flow Method in Polar Coordinates", *Electric Machines and Power Systems*, vol. 14, no. 5, 1989, pp.339–351.
38. Das, D., H.S. Nagi and D.P. Kothari, "A Novel Method for Solving Radial Distribution Networks", *Proc. IEE*, ptc, vol. 141, no. 4, July 1994, pp. 291–298.
39. Das, D., D.P. Kothari and A. Kalam, "A Simple and Efficient Method for Load Flow Solution of Radial Distribution Networks", *Int. J. EPES*, 1995, pp. 335–346.
40. Power World Computer Program (www.powerworld.com).
41. ABB Website (www.ABB.com).
42. PSCAD/EMTDC.

Chapter 7
Optimal System Operation

7.1 INTRODUCTION

The optimal system operation, in general, involves the consideration of economy of operation, system security, emissions at certain fossil-fuel plants, optimal releases of water at hydro generation, etc. All these considerations may make for conflicting requirements and usually a compromise has to be made for optimal system operation. In this chapter we consider the economy of operation only, also called the *economic dispatch problem*.

The main aim in the economic dispatch problem is to minimize the total cost of generating real power (production cost) at various stations while satisfying the loads and the losses in the transmission links. For simplicity we consider the presence of thermal plants only in the beginning. In the later part of this chapter we will consider the presence of hydro plants which operate in conjunction with thermal plants. While there is negligible operating cost at a hydro plant, there is a limitation of availability of water over a period of time which must be used to save maximum fuel at the thermal plants.

In the load flow problem as detailed in Ch. 6, two variables are specified at each bus and the solution is then obtained for the remaining variables. The specified variables are real and reactive powers at PQ buses, real powers and voltage magnitudes at PV buses, and voltage magnitude and angle at the slack bus. The additional variables to be specified for load flow solution are the tap settings of regulating transformers. If the specified variables are allowed to vary in a region constrained by practical considerations (upper and lower limits on active and reactive generations, bus voltage limits, and range of transformer tap settings), there results an infinite number of load flow solutions, each pertaining to one set of values of specified variables. The 'best' choice in some sense of the values of specified variables leads to the 'best' load flow solution. Economy of operation is naturally predominant in determining the best choice, though there are other factors that should be given consideration. While an experienced operator could make a good guess of the best values of specified variables in a small system guided by past experience, the best solution would elude him in a modern complex system without the aid of powerful analytical

tools. This chapter is devoted to the study of analytical methods of arriving at the best (optimal) operating strategies in power systems. Additionally, the optimal operating strategy must meet the minimum standards of reliability or, in other words, the continuity of supply.

To start with the economic factor in power system operation, we will focus our attention on allocation of real power at generator buses. This problem can be partitioned into two sub-problems, viz. optimum allocation (commitment) of generators (units) at each generating station at various station load levels (including load sharing among committed generators), and optimum allocation of generation to each station for various system load levels. The first problem in power system parlance is called the 'unit commitment' (UC) problem and the second is called the 'load scheduling' (LS) problem. One must first solve the UC problem before proceeding with the LS problem.

Throughout this chapter we shall concern ourselves with an existing installation, so that the economic considerations are that of operating (running) cost and not the capital outlay.

7.2 OPTIMAL OPERATION OF GENERATORS ON A BUS BAR

Before we tackle the unit commitment problem, we shall consider the optimal operation of generators on a bus bar.

Generator Operating Cost

The total generator operating cost includes *fuel, labour, and maintenance costs*. For simplicity fuel cost is the only one considered to be variable. The fuel cost is meaningful in case of thermal and nuclear stations, but for hydro stations, where the energy storage is 'apparently free', the operating cost as such is not *meaningful*. A suitable meaning will be attached to the cost of hydro stored energy in Sec. 7.7. Presently we shall concentrate on fuel fired stations.

The input–output curve of a generating unit specifies the *input energy rate* $F_i(P_{Gi})$ (MKcal/h) or cost of fuel used per hour $C_i(P_{Gi})$ (Rs/h) as a function of the generator power output P_{Gi}. The input–output curve can be determined *experimentally*. A typical input–output curve is shown in Fig. 7.1 and is concave upwards. It is convenient to express the input–output curves in terms of input energy rate (MKcal/h) rather than fuel-cost per hour (Rs/h) because fuel-cost can change monthly or daily in comparison with the fuel energy used per hour or input energy rate at a given output power (generating unit efficiency). In Fig. 7.1, $(MW)_{min}$ is the minimum loading limit below which it is *uneconomical* (or may be *technically infeasible*) to operate the unit and $(MW)_{max}$ is the maximum output limit. The curve has *discontinuities at steam valve openings* which have not been indicated in the figure.

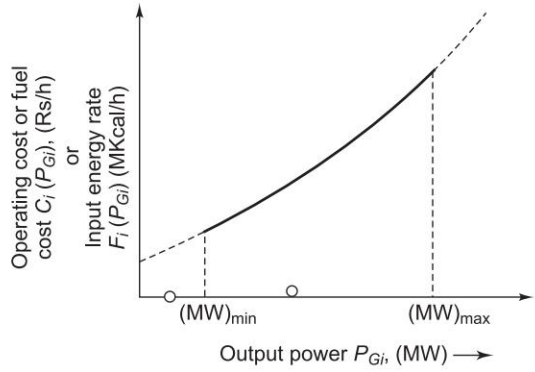

Fig. 7.1 Input-output curve of a generating unit

We next consider the heat-rate curve $H_i(P_{Gi})$ which is the heat energy (obtained by combustion of fuel) in (MKcal) needed to generate one unit of electric energy (MWh). Figure 7.2 shows the approximate shape of the heat rate curve, which can be determined experimentally. The generating unit efficiency can be defined as the ratio of electric energy output generated to fuel energy input. Thus, the generating unit is most efficient at the minimum heat-rate which corresponds to a particular P_{Gi}. The heat-rate (and hence efficiency) varies with the output power P_{Gi} and the curve indicates the increase in the heat-rate (or drop in efficiency) at low and high power limits. Typical peak efficiency heat-rates of modern fuel fired plants is around 2.5 MKcal/MWh giving a peak efficiency of $\frac{3600 \times 100}{2.5 \times 4.2 \times 1000} = 34\%$. Since all input fuel energy is not converted to electric energy output, the heat-rate indicated in Fig. 7.2 can be further reduced at all points if the conversion from input fuel energy to output electric energy is 100%. For 100% conversion, the heat rate is approximately 0.859 MKcal/MWh (1 MKcal = 1.164 MWh is the equivalent of heat).

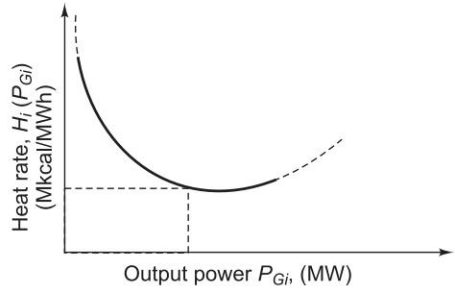

Fig. 7.2 Heat-rate curve

The input–output curve can be obtained from the heat-rate curve as

$$F_i(P_{Gi}) = P_{Gi}\, H_i(P_{Gi}) \quad \text{(MK cal/h)} \tag{7.1}$$

where $H_i(P_{Gi})$ is the heat-rate in MKcal/MWh. The graph of $F_i(P_{Gi})$ is the input–output curve (Fig. 7.1). Let the cost of the fuel be K Rs/MKcal. Then the input fuel-cost, $C_i(P_{Gi})$ is

$$C_i(P_{Gi}) = KF_i(P_{Gi}) = KP_{Gi}H_i(P_{Gi}) \quad \text{(Rs/h)} \tag{7.2}$$

The heat-rate curve (Fig. 7.2) may be approximated in the form,

$$H_i(P_{Gi}) = (a_i'/P_{Gi}) + b_i' + c_i'\, P_{Gi} \text{ (MKcal/MWh)} \tag{7.3}$$

with all coefficients positive. From Eqs (7.1) and (7.3) we get a quadratic expression for input energy rate $F_i(P_{Gi})$ with positive coefficients in the form

$$F_i(P_{Gi}) = a_i' + b_i'P_{Gi} + c_i'\, P_{Gi}^2 \quad \text{(MKcal/h)} \tag{7.4}$$

From Eqs (7.2) and (7.4), we also get a quadratic expression for fuel-cost $C_i(P_{Gi})$ with positive coefficient in the form

$$\begin{aligned} C_i(P_{Gi}) &= Ka_i' + Kb_i'P_{Gi} + Kc_i'P_{Gi}^2 \\ &= a_i + b_iP_{Gi} + c_iP_{Gi}^2 \quad \text{(Rs/h)} \end{aligned} \tag{7.5}$$

The slope of the fuel-cost curve, i.e. dC_i/dP_{Gi}, is called the incremental fuel cost (IC), and is expressed in Rs/MWh. A typical plot of the incremental fuel cost versus power output is shown in Fig. 7.3. From Eq. (7.5), the incremental fuel cost is

$$(IC)_i = dC_i/dP_{Gi} = b_i + 2c_i\, P_{Gi} \quad \text{(Rs/MWh)} \tag{7.6}$$

i.e. a linear relationship. The linearity of Eq. (7.6) arises because of the quadratic approximation for $C_i(P_{Gi})$ of Eq. (7.5). Figure 7.3 shows the actual and the linear approximation for the incremental cost curve.

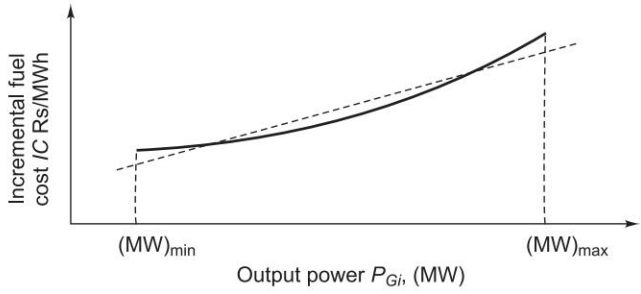

Fig. 7.3 Increment fuel cost

The fuel-cost curve and the incremental cost curve may have a number of discontinuities, as shown in Fig. 7.4(a) and (b). The discontinuities occur when the output power has to be extended by using additional boilers, steam condensers or other equipment. Discontinuities also appear if the cost represents

the operation of an entire power station, so that cost has discontinuities on paralleling of generators.

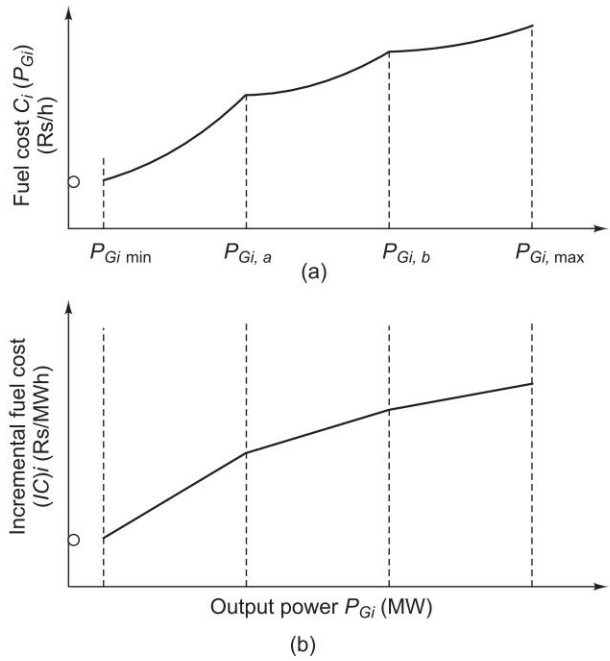

Fig. 7.4 Cost and incremental cost curves with discontinuities

Within the continuity range the incremental fuel cost may be expressed by a number of short line segments (piecewise linearization). Alternatively we can fit a polynomial of suitable degree to represent the *IC* curve in the inverse form as

$$P_{Gi} = \alpha_i + \beta_i(IC)_i + \gamma_i(IC)_i^2 + \ldots \text{ MW} \tag{7.7}$$

Example 7.1 The heat rate of a 100 MW fuel-fired generator is

10 MKcal/MWh at 25% of rating
9 MKcal/MWh at 40% of rating
10 MKcal/MWh at 100% of rating

and the cost of the fuel is Rs 2 per MKcal. Find

(a) $C(P_G)$ in the form of Eq. (7.4);
(b) the fuel input rate (heat rate) and fuel cost when 25%, 50% and 100% loaded;
(c) the incremental cost in Rs/MWh;
(d) the approximate cost and the cost using the quadratic approximation in Rs/h to deliver 101 MW.

Solution

(a) The expression for the heat rate $H(P_G)$, which leads to the expression given by Eq. (7.4), is given by Eq. (7.5) as

$$H_i(P_G) = (a'/P_G) + b' + c'P_G \quad \text{MKcal/MWh}$$

Substituting the measured values of $H(P_G)$ at different ratings, we get

$$(a'/25) + b' + c'25 = 10$$

$$(a'/40) + b' + c'40 = 9$$

$$(a'/100) + b' + c'100 = 8$$

Solving for the three unknown coefficients, a', b' and c', we get $a' = 1000/9$, $b' = 40/9$ and $c' = 2/45$. Thus

$$H(P_G) = (111.11/P_G) + 4.44 + 0.0444\ P_G \quad \text{MKcal/MWh}$$

Multiplying by P_G, we get the fuel input rate $F(P_G)$ in MKcal/h and multiplying by the cost of fuel per MKcal (Rs 2) we get fuel cost $C(P_G)$ as

$$F(P_G) = 111.11 + 4.44\ P_G + 0.0444\ P_G^2 \text{ MKcal/h}$$

$$C(P_G) = 222.22 + 8.889P_G + 0.0889P^2{}_G \text{ Rs/h}$$

(b) At 25% rating, $P_G = 25$ MW and

$$F(25) = 250.00 \text{ MKcal/h}$$

$$C(25) = 250.00 \times 2 = 500.00 \text{ Rs/h}$$

Similarly at 40% and 100% rating,

$$F(40) = 360.00 \text{ MKcal/h}$$

$$C(40) = 720.00 \text{ Rs/h}$$

$$F(100) = 1000.00 \text{ MKcal/h}$$

$$C(100) = 2000.00 \text{ Rs/h}$$

(c) The incremental cost is

$$IC = \mathrm{d}C(P_G)/\mathrm{d}P_G = 8.889 + 0.1778P_G \quad \text{Rs/MWh}$$

(d) At 100% rating (i.e. 100 MW)

$$IC = 8.889 + 0.1778 \times 100 = 26.667 \quad \text{Rs/MWh}$$

Approximate cost at 101 MW is

$$C(100) + IC(100) \times \Delta P_G = 2000 + 26.667 \times 1 = 2026.67 \quad \text{Rs/h}$$

where $\Delta P_G = 101 - 100 = 1$ MW

Cost, using the quadratic approximation, is

$$C(101) = 222.22 + 8.889(101) + 0.0889(101)$$

$$= 2026.75 \text{ Rs/h}$$

Thus, the cost calculated approximately is very close to the cost calculated by using quadratic approximation, for a small change in output power ($\Delta P_G = 1$ MW) from 100 MW.

We also note that in Eq. (7.3), if the coefficient c' is negligible, then the heat-rate may be further approximated by

$$H_i(P_{Gi}) = (a_i'/P_{Gi}) + b_i' \quad \text{(MKcal/MWh)} \tag{7.8}$$

The shape of the heat-rate curve given by Eq. (7.8) is that of rectangular hyperbola as shown in Fig. 7.5. For large values of P_{Gi}, the input energy rate $H_i(P_{Gi}) \approx b$, a constant. From Eqs (7.1), (7.2) and (7.8), we get linear approximations for the input energy rate $F_i(P_{Gi})$ and fuel cost $C_i(P_{Gi})$ in the form:

$$F_i(P_{Gi}) = a_i' + b_i' P_{Gi} \quad \text{(MKcal/h)} \tag{7.9a}$$

$$C_i(P_{Gi}) = a_i + b_i P_{Gi} \quad \text{(Rs/h)} \tag{7.9b}$$

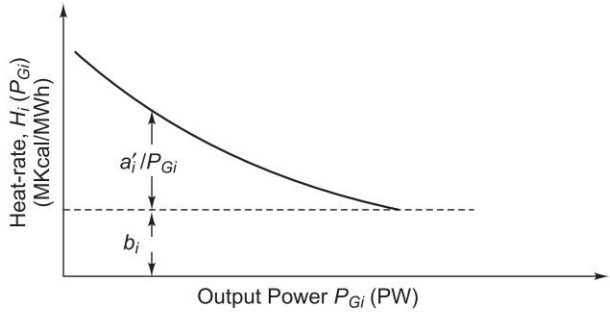

Fig. 7.5 Heat-rate curve which gives a linear input–output curve

Optimal Operation

Let us assume that it is known a *priori* which generators are to run to meet a particular load demand on the station. This is, given a station with k generators committed and the active power load P_D given, the real power generation P_{Gi} for each generator has to be allocated so as to minimize the total cost.

$$C = \sum_{i=1}^{k} C_i(P_{Gi}) \text{ (Rs/h)} \tag{7.10}$$

subject to the inequality constraint

$$P_{Gi\,\min} \le P_{Gi} \le P_{Gi\,\max}; \quad i = 1, 2, ..., k \tag{7.11}$$

where $P_{Gi\,\min}$ and $P_{Gi\,\max}$ are the lower and upper real power generation limits of the ith generator. Obviously,

$$\sum_{i=1}^{k} P_{Gi\max} \ge P_D \tag{7.12a}$$

Considerations of spinning reserve, to be explained later in this chapter, require that

$$\sum_{i=1}^{k} P_{Gi\max} > P_D \tag{7.12b}$$

In Eq. (7.10), it is assumed that the cost C is largely dependent on the real power generation P_{Gi} and is insensitive to reactive power generation Q_{Gi}.

Since $C_i(P_{Gi})$ is nonlinear, and C_i is independent of P_{Gj} $(j \neq i)$, this is a separable nonlinear programming problem.

We assume that the inequality constraint of Eq. (7.12a) is not effective, and

$$\sum_{i=1}^{k} P_{Gi} = P_D \quad \text{or} \quad \left(\sum_{i=1}^{k} P_{Gi}\right) - P_D = 0 \tag{7.13}$$

Also, for the time being we do not consider the effect of generator power limits given by Eq. (7.11).

The problem can then be solved by the method of Lagrange multipliers, which is used for minimizing (or maximizing) a function with side conditions in the form of equality constraints. Using this method we define an augmented cost function (Lagrangian) as

$$\bar{C} = C - \lambda\left(\sum_{i=1}^{k} P_{Gi} - P_D\right) \tag{7.14}$$

where λ is the Lagrangian multiplier.

Minimization is achieved by the condition

$$\frac{\partial \bar{C}}{\partial P_{Gi}} = 0$$

or

$$\mathrm{d}C_i/\mathrm{d}P_{Gi} = \lambda, \quad i = 1, 2, .., k \tag{7.15}$$

where $\mathrm{d}C_i/\mathrm{d}P_{Gi}$ is the incremental cost of the ith generator (units: Rs/MWh). Equation (7.15) can be written as

$$\mathrm{d}C_1/\mathrm{d}P_{G1} = \mathrm{d}C_2/\mathrm{d}P_{G2} = \ldots = \mathrm{d}C_k/\mathrm{d}P_{Gk} = \lambda \tag{7.16}$$

i.e., optimal loading of generators corresponds to the equal incremental cost point of all the generators. Equation (7.16), called the *coordination equation* numbering k is solved simultaneously with the load demand Eq. 7.13, to yield a solution for the Lagrange multiplier λ and the optimal generation of k generators. This is illustrated by means of Example 7.2 at the end of this section.

We now establish the procedure for determining λ in Eq. (7.16). If the cost curves are quadratic, then the problem reduces to the linear case. In general, the incremental cost curves may not be linear and λ can be determined by an iterative process. Computer solution for optimal loading of generators can be obtained iteratively by considering the incremental cost curves of Fig. 7.6 as follows:

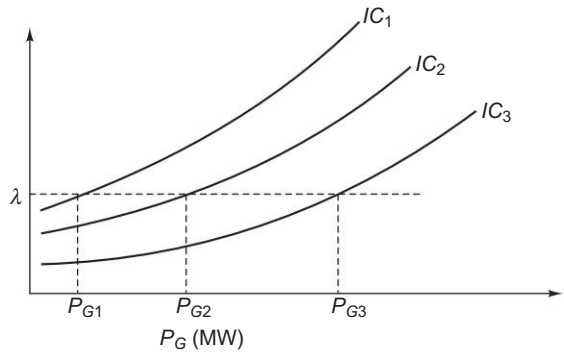

Fig. 7.6 Incremental cost curves

1. Choose a trial value of λ, i.e. $IC = (IC)°$.
2. Solve for P_{Gi} (i = 1, 2, ..., k) from Eq. (7.9).
3. If $\left|\sum_i P_{Gi} - P_D\right| < \varepsilon$ (a specified value), the optimal solution is reached. Otherwise,
4. Increment (IC) by $\Delta(IC)$, if $\left(\sum_i P_{Gi} - P_D\right) < 0$, or decrement ($IC$) by $\Delta(IC)$ if $\left(\sum_i P_{Gi} - P_D\right) > 0$ and repeat from step 2. This is possible because P_{Gi} is monotonically increasing function of (IC).

Consider now the effect of the generator limits given by the inequality constraint of Eq. (7.11). As IC is increased or decreased in the iterative process, if a particular generator loading P_{Gj} reaches the limit $P_{Gj\,\min}$ or $P_{Gj\,\max}$, its loading from then on is held fixed at this value and the balanced load is shared between the remaining generators on equal incremental cost basis. The fact that this operation is optimal can be shown by the Kuhn-Tucker theory (see Appendix E).

Example 7.2 Incremental fuel costs in rupees per MWh for a plant consisting of two units are:

$$dC_1/dP_{G1} = 0.20P_{G1} + 40 \quad \text{(i)}$$

$$dC_2/dP_{G2} = 0.40P_{G2} + 30 \quad \text{(ii)}$$

and the generator limits are as follows:

$$30 \text{ MW} \le P_{G1} \le 175 \text{ MW}$$

$$20 \text{ MW} \le P_{G2} \le 125 \text{ MW}$$

Assume that both units are operating at all times. How will the load be shared between the two units as the system load varies over the full range of the load values? What are the corresponding values of the plant incremental costs?

Solution

Figure 7.7 gives the incremental cost curves of the two units. At the lower end $P_{G1\,\min}$ (30 MW) > $P_{G2\,\min}$ (20 MW) so that P_{G1} is fixed at 30 MW and P_{G2} at 20 MW (i.e., P_D = 30 + 20 = 50 MW). For $38 \le \lambda \le 46$, $\lambda_1 < \lambda_2$ (min), and therefore as the plant load increases beyond 50 MW, the load increments are placed on unit 2 till both units have λ = 46 (P_D = 30 + 40 = 70 MW). Load sharing beyond this point is carried out on equal-λ basis till unit 1 reaches its upper limit of 175 MW. Beyond this $\lambda_2 > \lambda_1$ (max) = 75 and further load increments are carried by unit 2 till it reaches its upper limit of 125 MW (P_D = 175 + 125 = 300 MW).

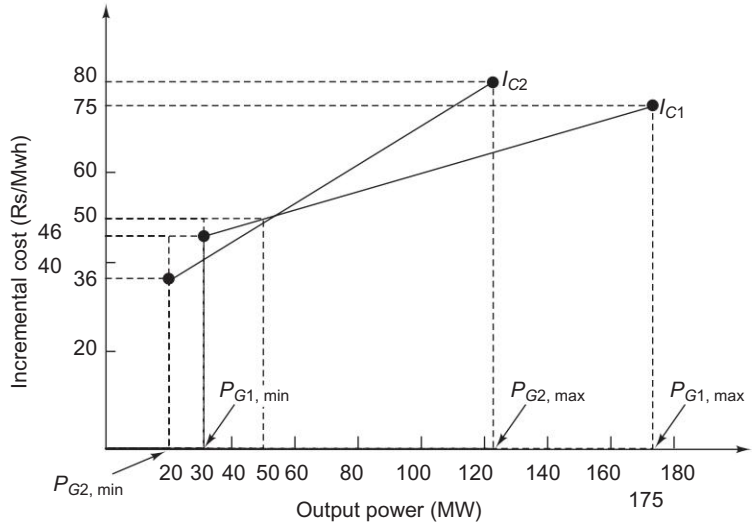

Fig. 7.7 Incremental cost curves

For $38 \le \lambda \le 46$,

$$\lambda = 0.40P_{G2} + 30 = 0.40(P_D - 30) + 30$$

$$= 0.40P_D + 18 \qquad \text{(iii)}$$

The corresponding load range is

$$50 \le P \le 70 \text{ MW}$$

For $46 \le \lambda \le 75$,

$$\lambda = 0.20P_{Gi} + 40 = 0.40P_{G2} + 30;\ P_D = P_{G1} + P_{G2}$$

or

$$\lambda = (1/3)\,(0.40P_D + 110) \qquad \text{(iv)}$$

The corresponding load range is

$$70 \le P \le 287.5 \text{ MW}$$

For $75 \le \lambda \le 80$

$$\lambda = 0.40P_{G2} + 30 = 0.40(P_D - 175) + 30$$

$$= 0.40P_D - 40 \qquad \text{(v)}$$

The corresponding load range is

$$287.5 \le P_D \le 300 \text{ MW}$$

Thus

$$\lambda = 0.40P_D + 18 \quad \text{(Rs/MWh)} \qquad (50 \le P_D \le 70) \qquad \text{(vi)}$$

$$\lambda = (4/30)P_D + (110/3) \quad \text{(Rs/MWh)} \qquad (70 < P_D \le 287.5) \qquad \text{(vii)}$$

$$\lambda = 0.40P_D - 40 \quad \text{(Rs/MWh)} \qquad (287.5 < P_D \le 300) \qquad \text{(viii)}$$

Figure 7.8 shows the plot of the plant λ versus plant output.

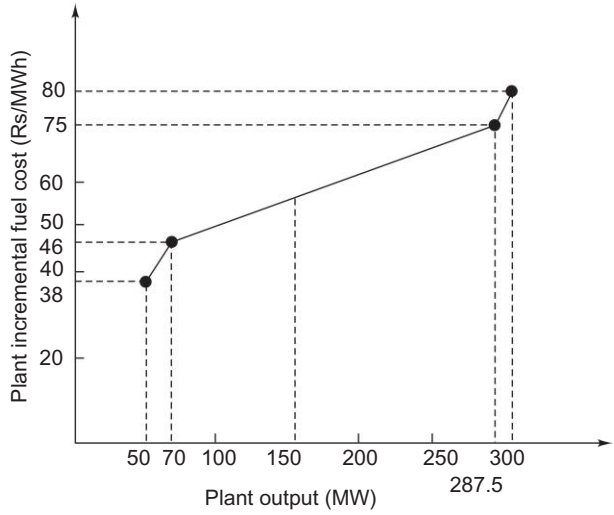

Fig. 7.8 Plant incremental fuel cost curve as found in Example 7.2.

Table 7.1

Plant Rs/MWh	*Unit 1 P_{G1}, MW*	*Unit 2 P_{G2}, MW*	*Plant output $P_D = (P_{G1} + P_{G2})$, MW*
38	30	20	50
40	30	25	55
46	30	40	70
48	40	45	85
50	50	50	100
60	100	75	175
75	175	112.5	287.5
80	175	125	300

Unit outputs for various plant outputs computed on above lines are given in Table 7.1 and are plotted in Fig. 7.9. Optimum load sharing for any plant can be directly read from this figure.

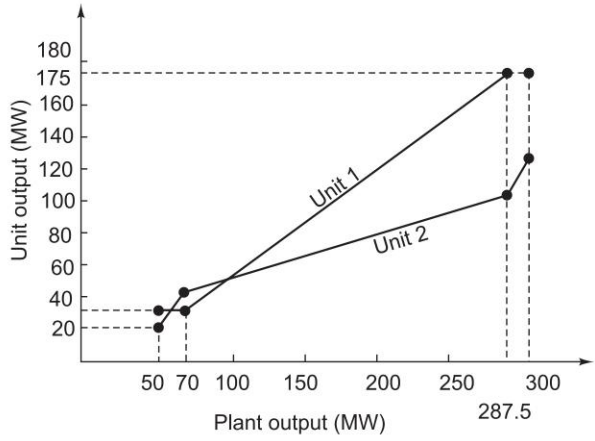

Fig. 7.9 Output of each unit versus plant output for Example 7.2

Example 7.3 For the plant described in Example 7.2, find the saving in fuel cost in rupees per hour for the optimal scheduling of a total load of 175 MW as compared to equal distribution of the same load between the two units.

Solution

Example 7.2 reveals that for a total load of 175 MW unit 1 should take up a load of 100 MW and unit 2 should supply 75 MW. For equal distribution each unit supplies 87.5 MW. The costs of generation for each unit are:

$$C_1 = \int (\mathrm{d}C_1 / \mathrm{d}P_{G1})\,\mathrm{d}P_{G1} = \int IC_1\,\mathrm{d}P_{G1}$$

$$= \int (0.20P_{G1} + 40.0)\,\mathrm{d}P_{G1}$$

$$= 0.10P_{G1}^2 + 40.0P_{G1} + k_1 \quad \text{Rs/h}$$

and

$$C_2 = \int (\mathrm{d}C_2 / \mathrm{d}P_{G1})\,\mathrm{d}P_{G2} = \int IC_2\,\mathrm{d}P_{G2}$$

$$= \int (0.40P_{G2} + 30.0)\,\mathrm{d}P_{G2}$$

$$= 0.20P_{G2}^2 + 30.0P_{G2} + k_2 \quad \text{Rs/h}$$

where k_1 and k_2 are constants.

The increase in cost for unit 1 is

$$C_1(87.5) - C_1(100) = (0.10 \times 87.5^2 + 40.0 \times 87.5 + k_1) - (0.10 \times 100^2 + 40.0 \times 100 + k_1)$$
$$= -734.375 \text{ Rs/h}$$

and the increase in cost for unit 2 is

$$C_2(87.5) - C_2(75) = (0.20 \times 87.5^2 + 30.0 \times 87.5 + k_2) - (0.20 \times 75^2 + 30.0 \times 75 + k_2)$$
$$= 1891.25 \text{ Rs/h}$$

Net saving caused by optimum scheduling is

$$-734.735 + 1891.25 = 1156.875 \quad \text{Rs/h}$$

Total yearly saving assuming continuous operation

$$= \text{Rs } 10134225.00$$

This saving justifies the need for optimal load sharing and the devices to be installed for controlling the unit loadings automatically.

Example 7.4 Let the two units of the system studied in Example 7.2 have the following cost curves:

$$C_1 = 0.1\, P^2_{G1} + 40\, P_{G1} + 120 \text{ Rs/h} \quad \text{(i)}$$
$$C_2 = 0.2\, P^2_{G2} + 30\, P_{G2} + 100 \text{ Rs/h} \quad \text{(ii)}$$

Let us assume a daily load cycle as given in Fig. 7.10. Also assume that a cost of Rs 400 is incurred in taking either unit off the line and returning it to service after 12 hours. Consider the 24 hour period from 6 a.m. one morning to 6 a.m. the next morning. Now we want to find out whether it would be more economical to keep both the units in service for this 24 hour period or to remove one of the units from service for the 12 hours of light load.

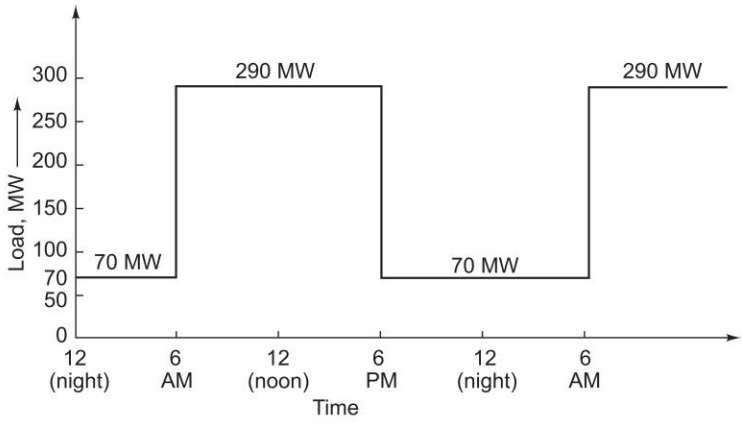

Fig. 7.10 Daily load cycle

Solution

For the twelve-hour period when the load is 290 MW, referring to Example 7.2, we get the optimum schedule as

$$P_{G1} = 175 \text{ MW}, P_{G2} = 290 - 175 = 115 \text{ MW}$$

Total fuel cost for this period is

$$[0.1 \times 175^2 + 40 \times 175 + 120 + 0.2 \times 115^2 + 30 \times 115 + 100] \times 12$$
$$= \text{Rs } 1,96,530$$

If both units operate in the light load period (70 MW from 6 p.m. to 6 a.m.) also, then from Table 7.1 of Example 7.2, we get the optimum schedule as

$$P_{G1} = 30 \text{ MW}, P_{G2} = 40 \text{ MW}$$

Total fuel cost for this period is then

$$(0.1 \times 30^2 + 40 \times 30 + 120 + 0.2 \times 40^2 + 30 \times 40 + 100) \times 12 = \text{Rs } 36,360$$

Thus the total fuel cost when both the units are operating throughout the 24 hour period is Rs 2,32,890.

If only one of the units is run during the light load period, it is easily verified from Eqs (i) and (ii) (Example 7.4) that it is economical to run unit 2 and to put off unit 1. Then the total fuel cost during this period will be

$$(0.2 \times 70^2 + 30 \times 70 + 100) \times 12 = \text{Rs } 38,160$$
$$\text{Therefore, total fuel cost for this case} = 1,96,530 + 38,160$$
$$= \text{Rs } 2,34,690$$

Total operating cost for this case will be the total fuel cost plus the start-up cost of unit 1, i.e.

$$2,34,690 + 400 = \text{Rs } 2,35,090$$

Comparing this with the earlier case, it is clear that it is economical to run both the units.

It is seen that even if the start-up cost is neglected, it is economical to run both the units.

Now consider the case when the output load is 55 MW from 6 p.m. to 6 a.m. instead of 70 MW as in the earlier case. If both units operate in this light load period, then from Table 7.1 (Example 7.2), we get the optimum schedule as

$$P_{G1} = 30 \text{ MW}, P_{G2} = 25 \text{ MW}$$

Total fuel cost for this period is

$$(0.1 \times 30^2 + 40 \times 30 + 120 + 0.2 \times 25^2 + 30 \times 25 + 100) \times 12 = \text{Rs } 28,620$$

Thus the total fuel cost when both the units are operating throughout the 24 hours period is

$$\text{Rs } (1,96,530 + 28,620) = \text{Rs } 2,25,150$$

If only one of the units is run during the light load period again it is economical to run unit 2 and to put off unit 1. The total fuel cost during this period will be

$$(0.2 \times 55^2 + 30 \times 55 + 100) \times 12 = \text{Rs } 28{,}260$$

$$\text{Therefore total fuel cost for this case} = 1{,}96{,}530 + 28{,}260$$
$$= \text{Rs } 2{,}24{,}790$$

Total operating cost for this case is

$$2{,}24{,}790 + 400 = \text{Rs } 2{,}25{,}190$$

Thus, it is clear that it is economical to run both the units.

If the start-up cost is Rs 300, then it is economical to run only unit 2 in the light load period and to put off unit 1.

Physical Significance of λ

For incremental changes in power generation it follows from Eq. (7.10) that

$$\Delta C = \sum_{i=1}^{k} (\partial C / \partial P_{Gi})^0 \Delta P_{Gi}$$

At the optimal operating point

$$(\partial C/\partial P_{Gi}) = (\mathrm{d}C/\mathrm{d}P_{Gi}) = (IC_i)^0 = \lambda$$

Therefore

$$\Delta C = \lambda \sum_{i=1}^{k} \Delta P_{Gi}$$

Now

$$\sum_{i=1}^{k} P_{Gi} = P_D$$

or

$$\sum_{i=1}^{k} \Delta P_{Gi} = \Delta P_D$$

Hence

$$\Delta C = \lambda \Delta P_D \quad \text{or} \quad \lambda = \Delta C/\Delta P_D$$

It means that λ is the incremental cost for unit incremental change in load demand.

7.3 OPTIMAL UNIT COMMITMENT (UC)

As is evident, it is not economical to run all the units available all the time. To determine the units of a plant that should operate for a particular load is the problem of unit commitment (UC). This problem is of importance for thermal

plants as for other types of generation such as hydro, the operating cost and start-up times are negligible so that their on–off status is not important.

A simple but sub-optimal approach to the problem is to impose priority ordering, wherein the most efficient unit is loaded first to be followed by the less efficient units in order as the load increases.

A straightforward but highly time-consuming way of finding the most economical combination of units to meet a particular load demand, is to try all possible combinations of units that can supply this load; to divide the load optimally among the units of each combination by use of the coordination equations, so as to find the most economical operating cost of the combination; then, to determine the combination which has the least operating cost among all these. Considerable computational saving can be achieved by using branch and bound or a dynamic programming method for comparing the economics of combinations, as certain combinations need not be tried at all.

Dynamic Programming Method

In a practical problem, the UC table is to be arrived at for the complete load cycle. If the load is assumed to increase in small but finite size steps, dynamic programming (DP) can be used to advantage for computing the UC table, wherein it is not necessary to solve the coordination equations; while at the same time the unit combinations to be tried are much reduced in number. For these reasons, only the DP approach will be advanced here.

The total number of units available, their individual cost characteristics and the load cycle on the station are assumed to be known *a priori*. Further, it shall be assumed that the load on each unit or combination of units changes in suitably small but uniform steps of size ΔMW (e.g. 1 MW).

Starting arbitrarily with any two units, the most economical combination is determined for all the discrete load levels of the combined output of the two units. At each load level the most economic answer may be to run either unit or both units with a certain load sharing between the two. The most economical cost curve in discrete form for the two units thus obtained, can be viewed as the cost curve of a single equivalent unit. The third unit is now added and the procedure repeated to find the cost curve of the three combined units. It may be noted that in this procedure the operating combinations of third and first, also third and second are not required to be worked out resulting in considerable saving in computational effort. The process is repeated, till all available units are exhausted. The advantage of this approach is that having obtained the optimal way of loading k units, it is quite easy to determine the optimal manner of loading $(k + 1)$ units.

Let a cost function $F_N(x)$ be defined as follows:

$F_N(x)$ = the minimum cost in Rs/hr of generating x MW by N units,

$f_N(y)$ = cost of generating y MW by the Nth unit

$F_{N-1}(x-y)$ = the minimum cost of generating $(x-y)$ MW by the remaining $(N-1)$ units

Now the application of DP results in the following recursive relation:

$$F_N(x) = \min_y \{f_N(y) + F_{N-1}(x-y)\} \tag{7.17}$$

Using the above recursive relation, we can easily determine the combination of units, yielding minimum operating costs for loads ranging in convenient steps from the minimum permissible load of the smallest unit to the sum of the capacities of all available units. In this process the total minimum operating cost and the load shared by each unit of the optimal combination are automatically determined for each load level.

The use of DP for solving the UC problem is best illustrated by means of an example. Consider a sample system having four thermal generating units with parameters listed in Table 7.2. It is required to determine the most economical units to be committed for a load of 9 MW. Let the load changes be in steps of 1 MW.

Now

$$F_1(x) = f_1(x)$$

$$\therefore \quad F_1(9) = f_1(9) = \frac{1}{2} a_1 P^2_{G1} + b_1 P_{G1}$$

$$= 0.385 \times 9^2 + 23.5 \times 9 = \text{Rs } 242.685/\text{h}$$

Table 7.2 Generating unit parameters for the sample system

Unit No.	Capacity (MW)		Cost curve parameters ($d = 0$)	
	Min	Max	a (Rs/MW^2)	b (Rs/MW)
1	1.0	12.0	0.77	23.5
2	1.0	12.0	1.60	26.5
3	1.0	12.0	2.00	30.0
4	1.0	12.0	2.50	32.0

From the recursive relation (7.17), computation is made for $F_2(0)$, $F_2(1)$, $F_2(2)$, ..., $F_2(9)$. Of these

$$\begin{aligned} F_2(9) = \min \{&[f_2(0) + F_1(9)], [f_2(1) + F_1(8)], \\ &[f_2(2) + F_1(7)], [f_2(3) + F_1(6)], [f_2(4) + F_1(5)], \\ &[f_2(5) + F_1(4)], [f_2(6) + F_1(3)], [f_2(7) + F_1(2)], \\ &[f_2(8) + F_1(1)], [f_2(9) + F_1(0)]\} \end{aligned}$$

On computing term-by-term and comparing, we get

$$F_2(9) = [f_2(2) + F_1(7)] = \text{Rs } 239.565/\text{h}$$

Similarly, we can calculate $F_2(8)$, $F_2(7)$, ..., $F_2(1)$, $F_2(0)$.

Using the recursive relation (7.17), we now compute $F_3(0)$, $F_3(1)$, ..., $F_3(9)$. Of these

$$F_3(9) = \min \{[f_3(0) + F_2(9)], [f_3(1) + F_2(8)], ..., [f_3(9) + F_2(0)]\}$$
$$= [f_3(0) + F_2(9)] = \text{Rs } 239.565/\text{h}$$

Proceeding similarly, we get

$$F_4(9) = [f_4(0) + F_3(9)] = \text{Rs } 239.565/\text{h}$$

Examination of $F_1(9)$, $F_2(9)$, $F_3(9)$ and $F_4(9)$ leads to the conclusion that optimum units to be committed for a 9 MW load are 1 and 2 sharing the load as 7 MW and 2 MW, respectively with a minimum operating cost of Rs 239.565/h.

It must be pointed out here, that the optimal UC table is independent of the numbering of units, which could be completely arbitrary. To verify, the reader may solve the above problem once again by choosing a different unit numbering scheme.

If a higher accuracy is desired, the step size could be reduced (e.g. $\frac{1}{2}$ MW), with a considerable increase in computation time and required storage capacity.

The effect of step size could be altogether eliminated, if the branch and bound technique [24] is employed. The answer to the above problem using branch and bound technique is the same in terms of units to be committed, i.e. units 1 and 2, but with a load sharing of 7.34 MW and 1.66 MW, respectively and a total operating cost of Rs 239.2175/h.

In fact the best scheme is to restrict the use of the DP method to obtain the UC table for various discrete load levels; while the load sharing among committed units is then decided by use of the coordination equation (7.15).

For the example under consideration, the UC table is prepared in steps of 1 MW. By combining the load range over which the unit commitment does not change, the overall result can be telescoped in the form of Table 7.3.

Table 7.3 Status* of units for minimum operating cost (Unit commitment table for the sample system)

Load range	*Unit number*			
	1	*2*	*3*	*4*
1–5	1	0	0	0
6–13	1	1	0	0
14–18	1	1	1	0
19–48	1	1	1	1

*1 = unit running; 0 = unit not running.

The UC table is prepared, once and for all, for a given set of units. As the load cycle on the station changes, it would only mean changes in starting and stopping of units with the basic UC table remaining unchanged.

Using the UC table and increasing load in steps, the most economical station operating cost is calculated for the complete range of station capacity by using

the coordination equations. The result is the overall station cost characteristic in the form of a set of data points. A quadratic equation (or higher order equation, if necessary) can then be fitted to this data for later use in economic load sharing among generating stations.

Latest developments in UC are given in Annexure 7.1.

7.4 RELIABILITY CONSIDERATIONS

With the increasing dependence of industry, agriculture and day-to-day household comfort upon the continuity of electric supply, the reliability of power systems has assumed great importance. Every electric utility is normally under obligation to provide to its consumers a certain degree of continuity and quality of service (e.g. voltage and frequency in a specified range). Therefore, economy and reliability (security) must be properly coordinated in arriving at the operational unit commitment decision. In this section, we will see how the purely economic UC decision must be modified through considerations of reliability.

In order to meet the load demand under contingency of failure (forced outage) of a generator or its derating caused by a minor defect, *static reserve capacity* is always provided at a generating station so that the total installed capacity exceeds the yearly peak load by a certain margin. This is a planning problem and is beyond the scope of this book.

In arriving at the economic UC decision at any particular time, the constraint taken into account is merely the fact that the total capacity on line is at least equal to the load. The margin, if any, between the capacity of units committed and load is incidental. If under actual operation, one or more of the units were to fail perchance (random outage), it may not be possible to meet the load requirements. To start a spare (standby) thermal unit* and to bring it on steam to take up the load will take several hours (2–8 hours), so that the load cannot be met for intolerably long periods of time. Therefore, to meet contingencies, the capacity of units on line (running) must have a definite margin over the load requirements at all times. This margin which is known as the *spinning reserve* ensures continuity by meeting the load demand up to a certain extent of probable loss of generation capacity. While rules of thumb have been used, based on past experience to determine the system's spinning reserve at any time, Patton's analytical approach to this problem is the most promising.

Since the probability of unit outage increases with operating time and since a unit which is to provide the spinning reserve at a particular time has to be started several hours ahead, the problem of security of supply has to be treated in totality over a period of one day. Furthermore, the loads are never known with complete certainty. Also, the spinning reserve has to be provided at suitable generating stations of the system and not necessarily at every

* If hydro generation is available in the system, it could be brought on line in a matter of minutes to take up the load.

generating station. This indeed is a complex problem. A simplified treatment of the problem is presented below:

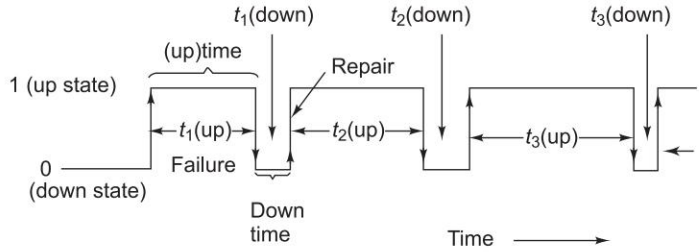

Fig. 7.11 Random unit performance record neglecting scheduled outages

A unit during its useful life span undergoes alternate periods of operation and repair as shown in Fig. 7.11. The lengths of individual operating and repair periods are a random phenomenon with operating periods being much longer than repair periods. When a unit has been operating for a long time, the random phenomenon can be described by the following parameters.

Mean time to failure (mean 'up' time),

$$\bar{T}\ (\text{up}) = \frac{\sum_j t_j (\text{up})}{\text{No. of cycles}} \tag{7.18}$$

Mean time to repair (mean 'down' time),

$$\bar{T}\ (\text{down}) = \frac{\sum_j t_j (\text{down})}{\text{No. of cycles}} \tag{7.19}$$

$$\text{Mean cycle time} = \bar{T}\ (\text{up}) + \bar{T}\ (\text{down})$$

Inverse of these times can be defined as rates [1], i.e.

$$\text{Failure rate, } \lambda = 1/\bar{T}\ (\text{up}) \quad \text{(failures/year)}$$

$$\text{Repair rate, } \mu = 1/\bar{T}\ (\text{down}) \quad \text{(repairs/year)}$$

Failure and repair rates are to be estimated from the past data of units (or other similar units elsewhere) by use of Eqs (7.18) and (7.19). Sound engineering judgement must be exercised in arriving at these estimates. The failure rates are affected by preventive maintenance and the repair rates are sensitive to size, composition and skill of repair teams.

By ratio definition of probability, we can write the probability of a unit being in 'up' or 'down' states at any time as

$$p\ (\text{up}) = \frac{\bar{T}(\text{up})}{\bar{T}(\text{up}) + \bar{T}(\text{down})} = \frac{\mu}{\mu + \lambda} \tag{7.20}$$

$$p\ (\text{down}) = \frac{\bar{T}(\text{down})}{\bar{T}(\text{up}) + \bar{T}(\text{down})} = \frac{\lambda}{\mu + \lambda} \tag{7.21}$$

Obviously,

$$p\ (\text{up}) + p\ (\text{down}) = 1$$

p (up) and p (down) in Eqs (7.20) and (7.21) are also termed as *availability* and *unavailability*, respectively.

When k units are operating, the system state changes because of random outages. Failure of a unit can be regarded as an event independent of the state of other units. If a particular system state i is defined as X_i units in 'down' state and Y_i in 'up' state ($k = X_i + Y_i$), the probability of the system being in this state is

$$p_i = \prod_{j \in Y_i} p_j(\text{up}) \prod_{l \in X_i} p_l(\text{down}) \tag{7.22}$$

Patton's Security Function

A breach of system security is defined as some intolerable or undesirable condition. The only breach of security considered here is insufficient generation capacity. The Patton's security function, which quantitatively estimates the probability that the available generation capacity (sum of capacities of units committed) at a particular hour is less than the system load at that time, is defined as [19]

$$\text{S} = \sum p_i r_i \tag{7.23}$$

where

p_i = probability of system being in state i [see Eq. (7.22)]

r_i = probability that system state i causes breach of system security.

When system load is deterministic (i.e. known with complete certainty), $r_i = 1$ if available capacity is less than load and 0 otherwise. S indeed, is a quantitative estimate of system insecurity.

Though theoretically Eq. (7.23) must be summed over all possible system states (this in fact can be very large), from a practical point of view the sum needs to be carried out over states reflecting a relatively small number of units on forced outage, e.g. states with more than two units out may be neglected as the probability of their occurrence will be too low.

Security Constrained Optimal Unit Commitment

Once the units to be committed at a particular load level are known from purely economic considerations, the security function S is computed as per Eq. (7.23). This figure should not exceed a certain maximum tolerable insecurity level (MTIL). MTIL for a given system is a management decision which is guided by past experience. If the value of S exceeds MTIL, the economic unit commitment schedule is modified by bringing in the next most economical unit as per the UC table. S is then recalculated and checked. The process is continued till $S \leq$ MTIL. As the economic UC table has some inherent spinning reserve, rarely more than one iteration is found to be necessary.

For illustration, reconsider the four unit example of Sec. 7.3. Let the daily load curve for the system be as indicated in Fig. 7.12. The economically optimal UC for this load curve is immediately obtained by use of the previously prepared UC table (see Table 7.3) and is given in Table 7.4.

Table 7.4 Economically optimal UC table for the sample system for the load curve of Fig. 7.12

Period	*Unit number*			
	1	*2*	*3*	*4*
A	1	1	1	1
B	1	1	1	0
C	1	1	0	0
D	1	1	1	0
E	1	0	0	0
F	1	1	0	0

Let us now check if the above optimal UC table is secure in every period of the load curve.

For the minimum load of 5 MW (period E of Fig. 7.12) according to optimal UC Table 7.4., only unit 1 is to be operated. Assuming identical failure rate λ of 1/year and repair rate μ of 99/year for all the four units, let us check if the system is secure for the period *E*. Further assume the system MTIL to be 0.005. Unit 1 can be only in two possible states—operating or on forced outage. Therefore,

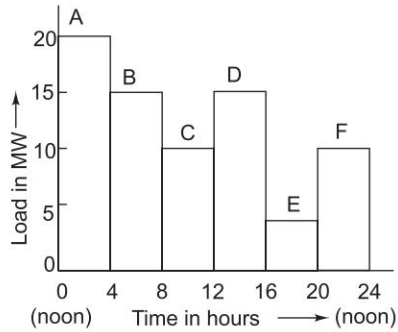

Fig. 7.12 Daily load curve

$$S = \sum_{i=1}^{2} p_i r_i = p_1 r_1 + p_2 r_2$$

where

$$p_1 = p(\text{up}) = \frac{\mu}{\mu + \lambda} = 0.99,\ r_1 = 0 \ \ (\text{unit 1} = 12\ \text{MW} > 5\ \text{MW})$$

$$p_2 = p(\text{down}) = \frac{\lambda}{\mu + \lambda} = 0.01,\ r_2 = 1 \quad \text{(with unit 1 down, load demand cannot be met)}$$

Hence

$$S = 0.99 \times 0 + 0.01 \times 1 = 0.01 > 0.005 \text{ (MTIL)}$$

Thus unit 1 alone supplying 5 MW load fails to satisfy the prescribed security criterion. In order to obtain optimal and yet secure UC, it is necessary to run the next most economical unit, i.e. unit 2 (Table 7.3) along with unit 1.

With both units 1 and 2 operating, security function is contributed only by the state when both the units are on forced outage. The states with both units operating or either one failed can meet the load demand of 5 MW and so do not contribute to the security function. Therefore,

$$S = p \text{ (down)} \times p \text{ (down)} \times 1 = 0.0001$$

This combination (units 1 and 2 both committed) does meet the prescribed MTIL of 0.005, i.e. $S <$ MTIL.

Proceeding similarly and checking security functions for periods A, B, C, D and F, we obtain the optimal and secure UC table given in Table 7.5 for the sample system for the load curve given in Fig. 7.12.

Table 7.5 Optimal and secure UC table

Period	*Unit number*			
	1	*2*	*3*	*4*
A	1	1	1	1
B	1	1	1	0
C	1	1	0	0
D	1	1	1	0
E	1	1*	0	0
F	1	1	0	0

* Unit was started due to security considerations.

Start-up Considerations

The UC table as obtained above is secure and economically optimal over each individual period of the load curve. Such a table may require that certain units have to be started and stopped more than once. Therefore, start-up cost must be taken into consideration from the point of view of overall economy. For example, unit 3 has to be stopped and restarted twice during the cycle. We must, therefore, examine whether or not it will be more economical to avoid one restarting by continuing to run the unit in period C.

Case a When unit 3 is not operating in period C.

Total fuel cost for periods B, C and D as obtained by most economic load sharing are as under (detailed computation is avoided)

$$= 1{,}690.756 + 1{,}075.356 + 1{,}690.756 = \text{Rs } 4{,}456.868$$

$$\text{Start-up cost of unit 3} = \text{Rs } 50.000 \text{ (say)}$$

$$\text{Total operating cost} = \text{Rs } 4{,}506.868$$

Case b When all three units are running in period C, i.e. unit 3 is not stopped at the end of period B.

$$\text{Total operating costs} = 1{,}690.756 + 1{,}081.704 + 1{,}690.756$$

$$= \text{Rs } 4{,}463.216 \text{ (start-up cost = 0)}$$

Clearly Case b results in overall economy. Therefore, the optimal and secure UC table for this load cycle is modified as shown in Table 7.6, with due consideration to the overall cost.

Table 7.6 Overall optimal and secure UC table

Period	*Unit number*			
	1	*2*	*3*	*4*
A	1	1	1	1
B	1	1	1	0
C	1	1	1*	0
D	1	1	1	0
E	1	1	0	0
F	1	1	0	0

*Unit was started due to start-up considerations.

7.5 OPTIMAL GENERATION SCHEDULING

From the unit commitment table of a given plant, the fuel cost curve of the plant can be determined in the form of a polynomial of suitable degree by the method of least squares fit. If the transmission losses are neglected, the total system load can be optimally divided among the various generating plants using the equal incremental cost criterion of Eq. (7.15). It is, however, unrealistic to neglect transmission losses particularly when long distance transmission of power is involved.

A modern electric utility serves over a vast area of relatively low load density. The transmission losses may vary from 5 to 15% of the total load, and therefore, it is essential to account for losses while developing an economic load dispatch policy. It is obvious that when losses are present, we can no longer use the simple 'equal incremental cost' criterion. To illustrate the point consider a simple system in which all the generators at each bus are identical. Equal incremental cost criterion would dictate that the total load should be shared equally by all the generators. But, considering line losses, it will be cheaper to draw more power from the generators which are closer to the loads.

In this section, we shall investigate how the load should be shared among various plants, when line losses are accounted for. The objective is to minimize the overall cost of generation.

$$C = \sum_{i=1}^{m} C_i (P_{Gi}) \tag{7.24}$$

at any time under equality constraint of meeting the load demand with the transmission losses, i.e.,

$$\sum_{i=1}^{m} P_{Gi} - \sum_{i=1}^{n} P_{Di} - P_L = 0 \quad \text{or} \quad \sum_{i=1}^{m} P_{Gi} - P_D - P_L = 0 \tag{7.25}$$

where

m = total number of generating plants

n = total number of buses

P_{Gi} = generation of ith plant

$P_D = \sum_{i=1}^{n} P_{Di}$ = sum of load demand at all buses (system load demand)

P_L = total system transmission loss

To solve the problem, we write the Lagrangian of cost as

$$\bar{C} = \sum_{i=1}^{m} C_i(P_{Gi}) - \lambda \left| \sum_{i=1}^{m} P_{Gi} - P_D - P_L \right| \quad \text{(Rs/h)} \tag{7.26}$$

From Eq. (7.25), it follows that, for a given real load P_{Di} at all buses, the system loss P_L is a function of active power generation at each plant. It will be shown later in this section that, if the power factor of load at each bus is assumed to remain constant, the system loss P_L can be shown to be a function of active power generation at each plant, i.e.

$$P_L = P_L(P_{G1}, P_{G2}, ..., P_{Gm}) \tag{7.27}$$

Thus in the optimization problem posed above, P_{Gi}(i = 1, 2, ..., m) are the only control variables.

For optimum real power dispatch,

$$\partial \bar{C} / \partial P_{Gi} = \mathrm{d}C_i/\mathrm{d}P_{Gi} - \lambda + \lambda \partial P_L/\partial P_{Gi} = 0, \quad i = 1, 2, ..., m \tag{7.28}$$

Rearranging Eq. (7.28) and recognizing that changing the output of only one plant can affect the cost at only that plant, we have

$$\frac{\mathrm{d}C_i / \mathrm{d}P_{Gi}}{(1 - \partial P_L / \partial P_{Gi})} = \lambda \quad \text{or} \quad (IC)_i L_i = \lambda, \quad i = 1, 2, ..., m \tag{7.29}$$

where

$$L_i = 1/(1 - \partial P_L/\partial P_{Gi}) \tag{7.30}$$

is called the *penalty factor* of the ith plant.

The Lagrangian multiplier λ has the units of rupees per megawatt-hour. Equation (7.29) implies that minimum fuel cost is obtained, when the incremental fuel cost of each plant multiplied by its penalty factor is the same for all the plants. The $(m + 1)$ variables $(P_{G1}, P_{G2}, ..., P_{Gm}, \lambda)$ can be obtained from m optimal dispatch equations (7.29) together with the power balance Eq. (7.25). From Eq. (7.29) it follows that higher the penalty factor for a given plant, lower the incremental cost at which that plant is operated.

The partial derivative $\partial P_L/\partial P_{Gi}$ is referred to as the incremental transmission loss $(\text{ITL})_i$, associated with the ith generating plant. Equation (7.29) can also be written in the alternative form

$$(IC)_i = \lambda[1 - (\text{ITL})_i]; \quad i = 1, 2, ..., m \tag{7.31}$$

This equation is referred to as the *exact coordination equation*.

Thus, it is clear that to solve the optimum load scheduling problem, it is necessary to compute ITL for each plant, and therefore, we must determine the functional dependence of transmission loss on real powers of generating plants. There are several methods, approximate and exact, for developing a transmission loss model. A full treatment of these is beyond the scope of this book.

Thus optimum generator allocation considering line losses is obtained by operating all generators such that the product $IC_i \times L_i = \lambda$ for every generator. If the generator limits are taken into account, then all generators which are not at, or beyond, their limits are operated such that $IC_i \times L_i = \lambda$ for each of them. The generators which are at, or beyond, their limits are operated at their limits as in the lossless case.

The physical significance of λ in the case of losses can be shown to be the same as was in the lossless case. From Eq. (7.24),

$$\Delta C = \sum_{i=1}^{m} (\partial C / \partial P_{Gi})^0 \Delta P_{Gi} = \sum_{i=1}^{m} (IC_i)^0 \Delta P_{Gi} \tag{7.32}$$

But from Eq. (7.29),

$$(IC_i)^0 = \lambda(1 - (\partial P_L/\partial P_{Gi})^0) \tag{7.33}$$

Substituting Eq. (7.33) in Eq. (7.32), we get

$$\Delta C = \lambda \sum_{i=1}^{m} (1 - (\partial P_L / \partial P_{Gi})^0) \Delta P_{Gi}$$

or

$$\Delta \text{C} = \lambda \left[\sum_{i=1}^{m} \Delta P_{Gi} - \sum_{i=1}^{m} (\partial P_L / \partial P_{Gi}) \Delta P_{Gi} \right] \tag{7.34}$$

We have, from Eq. (7.27)

$$P_L = P_L(P_{G1}, P_{G2}, ..., P_{Gm})$$

Then

$$\Delta P_L = \sum_{i=1}^{m} (\partial P_L / \partial P_{Gi}) \Delta P_{Gi} \tag{7.35}$$

From Eqs (7.34) and (7.35), we get

$$\Delta C = \lambda \left[\sum_{i=1}^{m} \Delta P_{Gi} - \Delta P_L \right] \tag{7.36}$$

Now

$$\sum_{i=1}^{m} P_{Gi} - P_L = P_D$$

$$\therefore \quad \sum_{i=1}^{m} \Delta P_{Gi} - \Delta P_L = \Delta P_D \tag{7.37}$$

Substituting Eq. (7.37) in Eq. (7.36),

$$\Delta C = \lambda \Delta P_D \tag{7.38}$$

Thus, λ has the same significance as in the lossless case, that is, λ represents the increment in cost (Rs/h) to the increment in load demand (MW).

Representation of Transmission Loss by *B*-Coefficients

One of the most important, simple but approximate methods of expressing transmission loss as a function of generator powers is through *B*-coefficients. This method uses the fact that under normal operating condition the transmission loss is quadratic in the injected bus real powers. The general form of the loss formula (derived later in this section) using *B*-coefficients is

$$P_L = \sum_{i=1}^{m} \sum_{j=1}^{m} P_i B_{ij} P_j \tag{7.39}$$

where

P_i, P_j = real power injection at i, jth buses,
B_{ij} = loss coefficients which are constants under certain assumed operating conditions,
m = number of generator buses.

If P_G s are in megawatts, B_{ij} are in reciprocal of megawatts. Computations, of course, may be carried out per unit*. Also, $B_{ij} = B_{ji}$.

Equation (7.39) for transmission loss may be written in the matrix form as

$$P_L = P^T BP \tag{7.40}$$

*B (in pu) = B (in MW^{-1}) × Base MVA.

We obtain the incremental cost as

$$dC_i/dP_{Gi} = b_i + 2c_iP_{Gi} \quad \text{Rs/MWh}$$

Substituting dC_i/dP_{Gi} and $\partial P_L/\partial P_{Gi}$ from Eq. (7.39) in the coordination Eq. (7.28), we have

$$b_i + 2c_i P_{Gi} + \lambda \sum_{j=1}^{m} 2B_{ij}P_j = \lambda \tag{7.41}$$

or

$$b_i + 2c_iP_{Gi} + 2\lambda B_{ii}P_i + \lambda \sum_{\substack{j=1 \\ j\neq i}}^{m} 2B_{ij}P_j = \lambda \tag{7.42}$$

Substituting $P_{Gi} = P_i + P_{Di}$ and collecting all terms of P_i we have

$$2(c_i + \lambda B_{ii})P_i = -\lambda \sum_{\substack{j=1 \\ j\neq i}}^{m} 2B_{ij}P_j - b_i + \lambda - 2c_iP_{Di} \tag{7.43}$$

or

$$P_i = \frac{1 - \dfrac{b_i}{\lambda} + 2\dfrac{c_i}{\lambda}P_{Di} - \displaystyle\sum_{\substack{j=1 \\ j\neq i}}^{m} 2B_{ij}P_j}{2\left(\dfrac{c_i}{\lambda} + B_{ii}\right)}, \quad i = 1, 2, \ldots, m \tag{7.44}$$

For any particular value of λ, Eq. (7.44) can be solved iteratively by assuming initial values of P_i (a convenient choice is $P_i = 0$, i = 1, 2, ..., m). Iterations are stopped when P_i s converge within a specified accuracy.

Equation (7.44) along with the power balance equation (7.25) for a particular load demand $P_D (= P_{D1} + P_{D2} + \ldots + P_{Dn})$ are solved iteratively on the following lines:

1. Initially choose $\lambda = \lambda_0$.
2. Assume $P_i = 0$; $i = 1, 2, \ldots, m$.
3. Solve Eq. (7.44) iteratively for P_is.
4. Calculate P_L using Eq. (7.39).
5. Check if power balance Eq. (7.25) is satisfied, i.e.,

$$\left| \sum_{i=1}^{m} P_i - P_L \right| < \varepsilon \quad \text{(a specified value)}$$

   If yes, stop. Otherwise go to step 6.
6. Increase λ by $\Delta\lambda$ (a suitable step size); if

$$\left(\sum_{i=1}^{m} P_i - P_L \right) < 0$$

   or, decrease λ by $\Delta\lambda$ (a suitable step size); if

$$\left(\sum_{i=1}^{m} P_i - P_L\right) > 0 .$$

7. Repeat from step 3.

Note: After every step of an iteration if some P_is are such that the corresponding real power generation P_{Gi} (= $P_{Di} + P_i$) is at its limit or not within its limits, then P_{Gi} is kept at its limit so that P_i (= $P_{Gi} - P_{Di}$) becomes constant for the next step of an iteration. This value is kept fixed till P_{Gi} falls within its limits.

Example 7.5 A two-bus system is shown in Fig. 7.13. If 100 MW is transmitted from plant 1 to the load, a transmission loss of 10 MW is incurred. Find the required generation for each plant and the power received by the load when the system λ is Rs 25/MWh.

The incremental fuel costs of the two plants are given below:

$$dC_1/dP_{G1} = 0.02P_{G1} + 16.00 \quad \text{Rs/MWh}$$

$$dC_2/dP_{G2} = 0.04P_{G2} + 20.00 \quad \text{Rs/MWh}$$

Fig. 7.13 A two-bus system for Example 7.5

Solution

Since the load is at bus 2 alone, P_2 will not have any effect on P_L. Therefore,

$$B_{22} = 0 \text{ and } B_{12} = 0 = B_{21}$$

Hence

$$P_L = B_{11}P_1^2$$

Since, $P_{D1} = 0$, $P_{G1} = P_1$

For $P_{G1} = 100$ MW, $P_L = 10$ MW,

i.e.,

$$10 = B_{11}(100)^2 \text{ or } B_{11} = 0.001 \quad (\text{MW})^{-1}$$

Equation (7.28) for plant 1 becomes ($\partial P_L/\partial P_{Gi} = \partial P_L/\partial P_i$)

$$0.02P_{G1} + 16.00 = \lambda(1 - \partial P_L/\partial P_1)$$

$$= \lambda(1 - 2B_{11}\, P_1) = \lambda(1 - 2B_{11}\, P_{G1}) \qquad \text{(ii)}$$

and for plant 2 becomes

$$0.04P_{G2} + 20.00 = \lambda(1 - \partial P_L/\partial P_2)$$

$$= \lambda(1 - 0) = \lambda \qquad \text{(iii)}$$

Substituting the value of B_{11} and $\lambda = 25$, we get

$$P_{G1} = 128.57 \quad \text{MW}$$

$$P_{G2} = 125.00 \quad \text{MW}$$

The transmission power loss is

$$P_L = B_{11} P_1^2 = 0.001 \times (128.57)^2 = 16.53 \quad \text{MW}$$

and the load is

$$P_{D2} = P_{G1} + P_{G2} - P_L = 128.57 + 125 - 16.53$$

$$= 237.04 \ \text{MW}$$

Example 7.6 Consider the system of Example 7.5 with a load of 237.04 MW at bus 2. Find the optimum load distribution between the two plants (1) when losses are included but not coordinated, and (2) when losses are also coordinated. Also find the savings in rupees per hour when losses are coordinated.

Solution

Case a If the transmission loss is not coordinated, the optimum schedules are obtained by equating the incremental fuel costs at the two plants. Thus

$$0.02P_{G1} + 16.00 = 0.04P_{G2} + 20.00 \qquad \text{(i)}$$

From the power balance equation we have

$$P_{G1} + P_{G2} = 0.001P_1^2 + 237.04 = 0.001P_{G1}^2 + 237.04 \qquad \text{(ii)}$$

Solving Eqs (i) and (ii) for P_{G1} and P_{G2}, we get

$$P_{G1} = 275.18 \ \text{MW and } P_{G2} = 37.59 \ \text{MW}$$

Case b This case is already solved in Example 7.5. Optimum plant generations with loss coordination are

$$P_{G1} = 128.57 \ \text{MW}; \ P_{G2} = 125 \quad \text{MW}$$

Loss coordination causes the load on plant 1 to reduce from 275.18 MW to 128.57 MW. Therefore, saving of fuel cost at plant 1 due to loss coordination is

$$\int_{128.57}^{275.18} (0.02P_{G1} + 16)\,\mathrm{d}P_{G1} = 0.01P_{G1}^2 + 16P_{G1}\Big|_{128.57}^{275.18}$$

$$= \text{Rs } 2{,}937.69/\text{h}$$

At plant 2 the load increases from 37.59 MW to 125 MW due to loss coordination. The saving at plant 2 is

$$\int_{125}^{37.59} (0.04P_{G2} + 20)\,\mathrm{d}P_{G2} = 0.02P_{G2}^2 + 20P_{G2}\Big|_{125}^{37.59}$$

$$= -\ \text{Rs } 2{,}032.43/\text{h}$$

The net saving achieved by coordinating losses while scheduling the received load of 237.04 MW is

$$2{,}937.69 - 2{,}032.43 = \text{Rs. } 905.26/\text{h}$$

Derivation of Transmission Loss Formula

An accurate method of obtaining a general formula for transmission loss has been given by Kron [4]. This, however, is quite complicated. The aim of this article is to give a simpler derivation by making certain assumptions.

Figure 7.14(c) depicts the case of two generating plants connected to an arbitrary number of loads through a transmission network. One line within the network is designated as branch p.

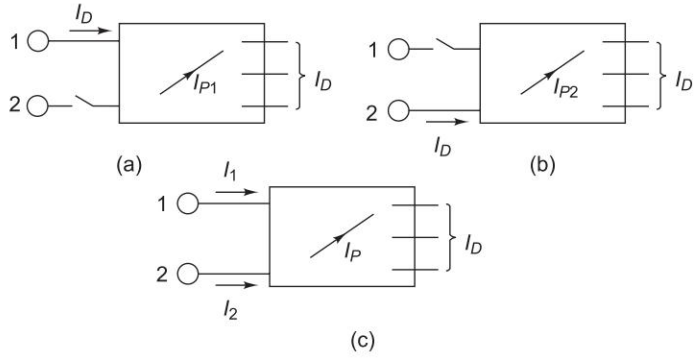

Fig. 7.14 Schematic diagram showing two plants connected through a power network to a number of loads

Imagine that the total load current I_D is supplied by plant 1 only, as in Fig. 7.14(a). Let the current in line p be I_{p1}. Define

$$M_{p1} = \frac{I_{p1}}{I_D} \tag{7.45}$$

Similarly, with plant 2 alone supplying the total load current Fig. 7.14(b) , we can define

$$M_{p2} = \frac{I_{p2}}{I_D} \tag{7.46}$$

M_{p1} and M_{p2} are called *current distribution factors*. The values of current distribution factors depend upon the impedances of the lines and their interconnection, and are independent of the current I_D.

When both generators 1 and 2 are supplying current into the network as in Fig. 7.14(c), applying the principle of superposition the current in the line p can be expressed as

$$I_p = M_{p1}I_1 + M_{p2}I_2 \tag{7.47}$$

where I_1 and I_2 are the currents injected at plants 1 and 2, respectively.

At this stage let us make certain simplifying assumptions outlined below:

(1) All load currents have the same phase angle with respect to a common reference. To understand the implication of this assumption consider the load current at the *i*th bus. It can be written as

$$|I_{Di}| \angle (\delta_i - \phi_i) = |I_{Di}| \angle \theta_i$$

where δ_i is the phase angle of the bus voltage and ϕ_i is the lagging phase angle of the load. Since δ_i and ϕ_i vary only through a narrow range at various buses, it is reasonable to assume that θ_i is the same for all load currents at all times.

(2) Ratio *X/R* is the same for all network branches.

These two assumptions lead us to the conclusion that I_{p1} and I_D [Fig. 7.14(a)] have the same phase angle and so have I_{p2} and I_D [Fig. 7.14(b)], such that the current distribution factors M_{p1} and M_{p2} are real rather than complex.

Let

$$I_1 = |I_1| \angle \sigma_1 \quad \text{and} \quad I_2 = |I_2| \angle \sigma_2$$

where σ_1 and σ_2 are phase angles of I_1 and I_2, respectively with respect to the common reference.

From Eq. (7.47), we can write

$$\begin{aligned} |I_p|^2 = {} & (M_{p1}|I_1| \cos \delta_1 + M_{p2}|I_2| \cos \delta_2)^2 \\ & + (M_{p1}|I_1| \sin \delta_1 + M_{p2}|I_2| \sin \delta_2)^2 \end{aligned} \tag{7.48}$$

Expanding and simplifying the above equation, we get

$$|I_p|^2 = M_{p1}^2 |I_1|^2 + M_{p2}^2 |I_2|^2 + 2M_{p1}M_{p2}|I_1||I_2| \cos(\delta_1 - \delta_2) \tag{7.49}$$

Now

$$|I_1| = \frac{P_1}{\sqrt{3}|V_1| \cos\phi_1}; |I_2| = \frac{P_2}{\sqrt{3}|V_2| \cos\phi_2} \tag{7.50}$$

where P_1 and P_2 are the three-phase real power injected at plants 1 and 2 at power factors of cos ϕ_1, and cos ϕ_2, and V_1 and V_2 are the bus voltages at the plants.

If R_p is the resistance of branch p, the total transmission loss is given by*

---

* The general expression for the power system with k plants is expressed as

$$\begin{aligned} P_L = {} & \frac{P_1^2}{|V_1|^2 (\cos\phi_1)^2} \sum_p M_{p1}^2 R_p + \ldots + \frac{P_k^2}{|V_k|^2 (\cos\phi_k)^2} \sum_p M_{pk}^2 R_p \\ & + 2 \sum_{\substack{m,n=1 \\ m \neq n}}^{k} \left\{ \frac{P_m P_n \cos(\sigma_m - \sigma_n)}{|V_m||V_n| \cos\phi_m \cos\phi_n} \sum_p M_{pm} M_{pn} R_p \right\} \end{aligned}$$

It can be recognized as

$$P_L = P_1^2 B_{11} + \ldots + P_k^2 B_{kk} + 2 \sum_{\substack{m,n=1 \\ m \neq n}}^{k} P_m B_{mn} P_n$$

$$P_L = \sum_p 3 |I_p|^2 R_p$$

Substituting for $|I_p|^2$ from Eq. (7.49), and $|I_1|$ and $|I_2|$ from Eq. (7.50), we obtain

$$P_L = \frac{P_1^2}{|V_1|^2 (\cos\phi_1)^2} \sum_p M_{p1}^2 R_p + \frac{2P_1P_2 \cos(\sigma_1 - \sigma_2)}{|V_1||V_2| \cos\phi_1 \cos\phi_2} \sum_p M_{p1}M_{p2}R_p + \frac{P_2^2}{|V_2|^2 (\cos\phi_2)^2} \sum_p M_{p2}^2 R_p \quad (7.51)$$

Equation (7.51) can be recognized as

$$P_L = P_1^2 B_{11} + 2P_1P_2B_{12} + P_2^2B_{22}$$

where

$$B_{11} = \frac{1}{|V_1|^2 (\cos\phi_1)^2} \sum_p M_{p1}^2 R_p$$

$$B_{12} = \frac{\cos(\sigma_1 - \sigma_2)}{|V_1||V_2| \cos\phi_1 \cos\phi_2} \sum_p M_{p1}M_{p2}R_p \quad (7.52)$$

$$B_{22} = \frac{1}{|V_2|^2 (\cos\phi_2)^2} \sum_p M_{p2}^2 R_p$$

The terms B_{11}, B_{12} and B_{22} are called *loss coefficients* or *B-coefficients*. If voltages are line to line kV with resistances in ohms, the units of *B*-coefficients are in MW^{-1}. Further, with P_1 and P_2 expressed in MW, P_L will also be in MW.

The above results can be extended to the general case of k plants with transmission loss expressed as

$$P_L = \sum_{m=1}^{k} \sum_{n=1}^{k} P_m B_{mn} P_n \quad (7.53)$$

where

$$B_{mn} = \frac{\cos(\sigma_m - \sigma_n)}{|V_m||V_n| \cos\phi_m \cos\phi_n} \sum_p M_{pm}M_{pn}R_p \quad (7.54)$$

The following assumptions including those mentioned already are necessary, if *B*-coefficients are to be treated as constants as total load and load sharing between plants vary. These assumptions are:

1. All load currents maintain a constant ratio to the total current.
2. Voltage magnitudes at all plants remain constant.

3. Ratio of reactive to real power, i.e. power factor at each plant remains constant.
4. Voltage phase angles at plant buses remain fixed. This is equivalent to assuming that the plant currents maintain constant phase angle with respect to the common reference, since source power factors are assumed constant as per assumption 3 above.

In spite of the number of assumptions made, it is fortunate that treating *B*-coefficients as constants yields reasonably accurate results, when the coefficients are calculated for some average operating conditions. Major system changes require recalculation of the coefficients.

Losses as a function of plant outputs can be expressed by other methods*, but the simplicity of loss equations is the chief advantage of the *B*-coefficients method.

Accounting for transmission losses results in considerable operating economy. Furthermore, this consideration is equally important in future system planning and, in particular, with regard to the location of plants and building of new transmission lines.

Example 7.7 Figure 7.15 shows a system having two plants 1 and 2 connected to buses 1 and 2, respectively. There are two loads and a network of four branches. The reference bus with a voltage of $1.0 \angle 0^{\circ}$ pu is shown on the diagram. The branch currents and impedances are:

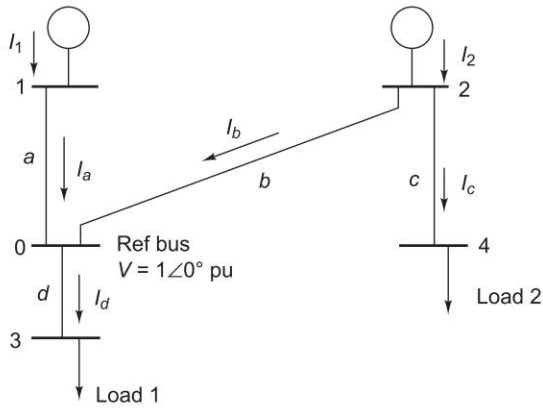

Fig. 7.15 Sample system

$I_a = 2 - j0.5$ pu $\qquad I_c = 1 - j0.25$ pu

$I_b = 1.6 - j0.4$ pu $\qquad I_d = 3.6 - j0.9$ pu

* For more accurate methods and exact expression for $\partial P_L / \partial P_{Gi}$, references [16, 17] may be consulted.

$$Z_a = 0.015 + j0.06 \text{ pu} \qquad Z_c = 0.01 + j0.04 \text{ pu}$$
$$Z_b = 0.015 + j0.06 \text{ pu} \qquad Z_d = 0.01 + j0.04 \text{ pu}$$

Calculate the loss formula coefficients of the system in pu and in reciprocal megawatts, if the base is 100 MVA.

Solution

As all load currents maintain a constant ratio to the total current, we have

$$\frac{I_d}{I_c + I_d} = \frac{3.6 - j0.9}{4.6 - j1.15} = 0.7826$$

$$\frac{I_c}{I_c + I_d} = \frac{1 - j0.25}{4.6 - j1.15} = 0.2174$$

$$\therefore \qquad M_{a1} = 1,\ M_{b1} = -0.2174,\ M_{c1} = 0.2174,\ M_{d1} = 0.7826$$
$$M_{a2} = 0,\ M_{b2} = 0.7826,\ M_{c2} = 0.2174,\ M_{d2} = 0.7826$$

Since the source currents are known, the voltages at the source buses can be calculated. However, in a practical size network a load flow study has to be made to find power factors at the buses, bus voltages and phase angles. The bus voltages at the plants are

$$V_1 = 1.0 + (2 - j0.5)(0.015 + j0.06)$$
$$= 1.06 + j0.1125 = 1.066 \angle 6.05^\circ \text{ pu}$$
$$V_2 = 1 + (1.6 - j0.4)(0.015 + j0.06)$$
$$= 1.048 + j0.09 = 1.051 \angle 4.9^\circ \text{ pu}$$

The current phase angles at the plants are ($I_1 = I_a$, $I_2 = I_b + I_c$).

$$\sigma_1 = \tan^{-1}\frac{-0.5}{2} = -14^\circ; \quad \sigma_2 = \tan^{-1}\frac{-0.65}{2.6} = -14^\circ;$$
$$\cos(\sigma_2 - \sigma_1) = \cos 0^\circ = 1$$

The plant power factors are

$$pf_1 = \cos(6.05^\circ + 14^\circ) = 0.9393$$
$$pf_2 = \cos(4.9^\circ + 14^\circ) = 0.946$$

The loss coefficients are [Eq. (7.42)]

$$B_{11} = \frac{0.015 \times 1^2 + 0.015 \times (0.2174)^2 + 0.01 \times (0.2174)^2 + 0.01 \times (0.7826)^2}{(1.066)^2 \times (0.9393)^2}$$
$$= 0.02224 \text{ pu}$$

$$B_{22} = \frac{0.015 \times (0.7826)^2 + 0.01 \times (0.2174)^2 + 0.01 \times (0.7826)^2}{(1.051)^2 \times (0.946)^2}$$
$$= 0.01597 \text{ pu}$$

$$B_{12} = \frac{(-0.2174)(0.7826)(0.015) + 0.01 \times (0.2174)^2 + 0.01 \times (0.7826)^2}{1.066 \times 1.051 \times 0.9393 \times 0.946}$$

$$= 0.00406 \text{ pu}$$

For a base of 100 MVA, these loss coefficients must be divided by 100 to obtain their values in units of reciprocal megawatts, i.e.

$$B_{11} = \frac{0.02224}{100} = 0.02224 \times 10^{-2} \quad \text{MW}^{-1}$$

$$B_{22} = \frac{0.01597}{100} = 0.01597 \times 10^{-2} \quad \text{MW}^{-1}$$

$$B_{12} = \frac{0.00406}{100} = 0.00406 \times 10^{-2} \quad \text{MW}^{-1}$$

Representation of Transmission Loss by Power Flow Equations

Earlier, the transmission loss (and hence penalty factors and incremental transmission losses) was expressed in terms of *B*-coefficients. The transmission loss (and hence penalty factors and incremental transmission losses) can also be expressed in terms of power flow equations. The transmission loss in terms of power injection at various buses is:

$$P_L = \sum_{i=1}^{n} P_i = \sum_{i=1}^{m} P_{Gi} - \sum_{i=1}^{n} P_{Di} \tag{7.55}$$

The incremental transmission loss for the ith generating unit is

$$\partial P_L / \partial P_{Gi} = \partial P_L / \partial P_i \quad i = 1, 2, \ldots, m$$

where

n = total number of buses

m = number of generator buses supplying real power

From Ch. 6, the real power injection P_i is

$$P_i = \sum_{j=1}^{n} |V_i||V_j|[G_{ij} \cos(\delta_i - \delta_j) + B_{ij} \sin(\delta_i - \delta_j)] \tag{7.56}$$

where

$Y_{ij} = G_{ij} + jB_{ij}$ = element of bus admittance matrix

$|V_i|$s = voltage magnitudes at various buses

δ_is = voltage angles at various buses

δ_1 = voltage angle at the slack bus = 0

Equation (7.56) shows that for a given voltage magnitude distribution, P_i (and hence P_L from Eq. (7.55)) depends on the bus voltage angles. From Eq. (7.55) we have

$$\partial P_L / \partial \delta_k = \partial P_1 / \partial \delta_k + \partial P_2 / \partial \delta_k + \ldots + \partial P_m / \partial \delta_k + \ldots + \partial P_n / \partial \delta_k \tag{7.57}$$

$$k = 2, \ldots, n$$

Also, since $P_L = P_L(P_1, P_2, ..., P_m)$ and each $P_i (i = 1, 2, ..., m)$ is dependent on the voltage angles, we have by the rule of differentiation,

$$\partial P_L/\partial \delta_k = (\partial P_L/\partial P_1)(\partial P_1/\partial \delta_k) + (\partial P_L/\partial P_2)(\partial P_2/\partial \delta_k) + \ldots + (\partial P_L)/\partial P_m)(\partial P_m/\partial \delta_k)$$

or
$$\partial P_L/\partial \delta_k = (\partial P_L/\partial P_1)(\partial P_1/\partial \delta_k) + (\partial P_L/\partial P_2)(\partial P_2/\partial \delta_k) + ... + (\partial P_L/\partial P_m)(\partial P_m/\partial \delta_k) \qquad k = 2, ..., n \tag{7.58}$$

since $\partial P_L/\partial P_{Gi} = \partial P_L/\partial P_i$ for a given load P_{Di}.

Subtracting Eq. (7.58) from Eq. (7.57), we get

$$(1 - \partial P_L/\partial P_{G1})(\partial P_1/\partial \delta_k) + (1 - \partial P_L/\partial P_{G2})(\partial P_2/\partial \delta_k) + ... + (1 - \partial P_L/\partial P_{Gm})(\partial P_m/\partial \delta_k) + (\partial P_m/\partial \delta_k) + ... + (\partial P_n/\partial \delta_k) = 0 \tag{7.59}$$
$$k = 2, ..., n$$

In Eqs (7.57), (7.58) and (7.59), $k \neq 1$ because for a slack bus $\delta_1 = 0 =$ constant.

Equation (7.59) can be written in matrix form as

$$\begin{bmatrix} \partial P_1/\partial \delta_2 \ldots \partial P_m/\partial \delta_2 \ldots \partial P_n/\partial \delta_2 \\ \partial P_1/\partial \delta_3 \ldots \partial P_m/\partial \delta_3 \ldots \partial P_n/\partial \delta_3 \\ \vdots \quad \vdots \quad \vdots \\ \partial P_1/\partial \delta_n \ldots \partial P_m/\partial \delta_n \ldots \partial P_n/\partial \delta_n \end{bmatrix}_{(n-1)\times n} \begin{bmatrix} (1 - \partial P_L/\partial P_{G1}) \\ \vdots \\ (1 - \partial P_L/\partial P_{Gm}) \\ \vdots \\ 1 \end{bmatrix}_{n\times 1} = 0 \tag{7.60}$$

An expression for $\partial P_i/\partial P_k$ ($i \neq k$ and $i = k$) can be written from Eq. (7.56) as follows:

$$\partial P_i/\partial \delta_k (i \neq k) = |V_i||V_k|[G_{ik} \sin(\delta_i - \delta_k) - B_{ik} \cos(\delta_i - \delta_k)] \tag{7.61a}$$

and
$$\partial P_i/\partial \delta_i = \sum_{\substack{j=1 \\ j\neq i}}^{n} |V_i||V_j|[-G_{ij} \sin(\delta_i - \delta_j) - B_{ij} \cos(\delta_i - \delta_j)] \tag{7.61b}$$

Equation (7.60) can be simplified if we assume that the incremental transmission loss for the slack bus is negligible i.e. $\partial P_L/\partial P_{G1} = 0$. Thus, Eq. (7.60) reduces to

$$\begin{bmatrix} \partial P_2/\partial \delta_2 \ldots \partial P_n/\partial \delta_2 \\ \vdots \quad \vdots \\ \partial P_1/\partial \delta_n \ldots \partial P_n/\partial \delta_n \end{bmatrix}_{(n-1)\times(n-1)} \begin{bmatrix} (1 - \partial P_L/\partial P_{G2}) \\ \vdots \\ (1 - \partial P_L/\partial P_{Gm}) \\ 1 \\ \vdots \\ 1 \end{bmatrix}_{(n-1)\times 1} = - \begin{bmatrix} \partial P_1/\partial \delta_2 \\ \vdots \\ \partial P_1/\partial \delta_n \end{bmatrix}_{(n-1)\times 1} \tag{7.62}$$

$$\text{or} \quad \begin{bmatrix} (1-\partial P_L/\partial P_{G2}) \\ 1 \\ \vdots \\ (1-\partial P_L/\partial P_{Gm}) \\ 1 \\ \vdots \\ 1 \end{bmatrix}_{(n-1)\times 1} = -\begin{bmatrix} \partial P_2/\partial \delta_2 \ldots \partial P_n/\partial \delta_2 \\ \vdots \quad\quad \vdots \\ \partial P_2/\partial \delta_n \ldots \partial P_n/\partial \delta_n \end{bmatrix}^{-1}_{(n-1)\times(n-1)} \begin{bmatrix} \partial P_1/\partial \delta_2 \\ \vdots \\ \partial P_1/\partial \delta_n \end{bmatrix}_{(n-1)\times 1} \quad (7.63)$$

The values of $\partial P_i/\partial \delta_j$ (i = 1, ..., n; j = 2, ..., n) can be calculated using (Eqs 7.61a and b). The various values of $|V_i|$, δ_i in Eqs (7.61 a and b) can be obtained from load flow solution.

7.6 OPTIMAL LOAD FLOW SOLUTION

The problem of optimal real power dispatch has been treated in the earlier section. This section presents the *more general problem of real and reactive power flow so as to minimize the instantaneous operating costs*.

Method 1: In the first method we solve the optimal load flow problem using Eq. (7.63). The algorithm for this problem is as follows (no generator limits):

1. The real loads at various buses are specified, P_{Di} (i = 1, 2, ..., n). Assume initial values for real generation, P^0_{Gi} (i = 2, ..., m) at the generator buses. From these we calculate the injected powers $P_i = P_{Gi} - P_{Di}$ (i = 2, 3, ..., n).
2. With the part of the load flow data available in step 1 and with remaining load flow data, the load flow solution is obtained, giving the voltage angles δ_i s (i = 2, ..., n) and voltage magnitudes at the PQ buses.
3. The slack bus power P_1 is calculated using Eq. (7.56) and then $P_{G1} = P_1 + P_{D1}$.
4. Using Eq. (7.61a), $\partial P_i/\partial \delta_k$ ($i \neq k$) for i = 1, 2, ..., n and k = 2, ..., n are calculated.

   Using Eq. (7.61b), $\delta P_i/\partial \delta_i$ for i = 1, 2, ..., n are calculated.
   Equation (7.63) is then solved for $(1 - \partial P_L/\partial P_{Gi})$, i = 2, ..., m.
5. Taking reciprocals we have $L_i = 1/(1 - \partial P_L/\partial P_{Gi})$, i = 2, ..., m. Also, we note that $L_1 = 1$.
6. Knowing P_{Gi}; i = 1, 2, ..., m, we calculate IC_i using $IC_i = b_i + 2c_iP_{Gi}$.
7. Next, we calculate the product $L_i \times IC_i$, i = 1, 2, ..., m. If all are equal we have the optimal generator allocation considering losses.

If one or more of the products $L_i \times IC_i$ are not equal, then we need to change P_{Gi} (i = 2, 3, ..., m) taking $L_1 \times IC_1$ as the reference. If $L_i \times IC_i$ (i = 2, ..., m) is too low (high) compared to $L_1 \times IC_1$, then P_{Gi} should be increased (decreased) by ΔP_{Gi}. The change ΔP_{Gi} can be chosen to be proportional to $(L_i \times IC_i - L_1 \times IC_1)$.

After obtaining a new set of P_{Gi} (i = 2, ..., m) the iteration is repeated from step 1.

Note: As P_{Gi} is changed during the iteration process, if one or more P_{Gi} reaches its limit, then the value of P_{Gi} is fixed at this value. The iteration is repeated for the remaining generator buses. If, at any iteration it is required to change P_{Gi} (which was earlier fixed at its limit) so that it falls within its limit, then from next iteration P_{Gi} is let free.

The flow chart for the optimal load flow solution is shown in Fig. (7.16).

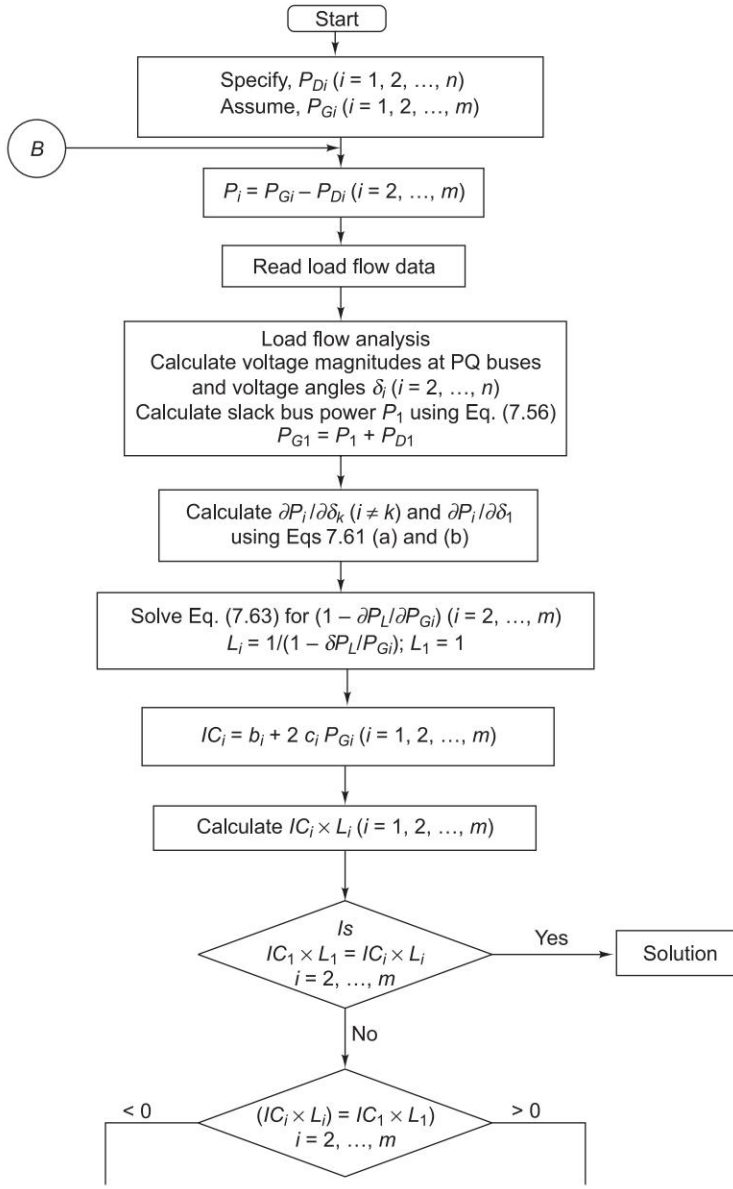

Fig. 7.16 (Contd.)

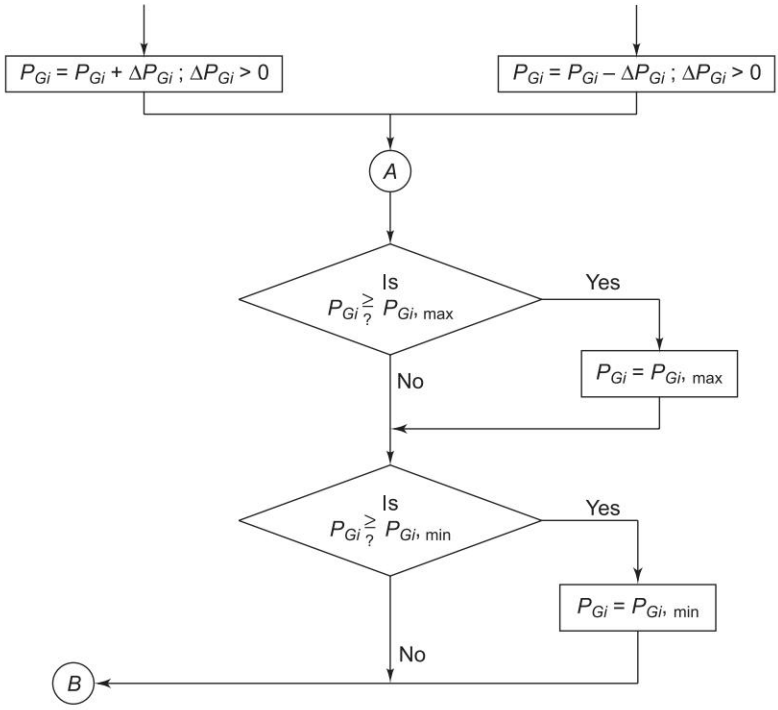

Fig. 7.16 Flowchart for optimal load flow solution (method 1)

Method 2 The solution technique given here was first given by *Dommel* and *Trinney* [34]. It is a *static optimization problem* with a scalar objective function (also called cost function). It is based on load flow solution by NR method, a first order gradient adjustment algorithm for minimizing the objective function and use of penalty functions to account for inequality constraints on dependent variables. The problem of unconstrained optimal load flow is first tackled. Later the inequality constraints are introduced, first on *control variables* and then on *dependent variables*.

Optimal Power Flow without Inequality Constraints

The objective function to be minimized is the operating cost

$$C = \sum_i C_i(P_{Gi})$$

subject to the load flow equations [see Eqs (6.28a) and (6.28b)]

$$P_i - \sum_{j=1}^{n} |V_i||V_j||Y_{ij}| \cos(\theta_{ij} + \delta_j - \delta_i) = 0 \quad \text{for each PQ bus} \qquad (7.64)$$

$$Q_i + \sum_{j=1}^{n} |V_i||V_j||Y_{ij}| \sin(\theta_{ij} + \delta_j - \delta_i) = 0 \quad \text{for each PQ bus} \qquad (7.65)$$

and

$$P_i - \sum_{j=1}^{n} |V_i||V_j||Y_{ij}|\cos(\theta_{ij} + \delta_j - \delta_i) = 0 \text{ for each PV bus} \quad (7.66)$$

It is to be noted that at the ith bus

$$\begin{aligned} P_i &= P_{Gi} - P_{Di} \\ Q_i &= Q_{Gi} - Q_{Di} \end{aligned} \quad (7.67)$$

where P_{Di} and Q_{Di} are load demands at bus i.

Equations (7.64), (7.65) and (7.66) can be expressed in vector form

$$\boldsymbol{f}(\boldsymbol{x}, \boldsymbol{y}) = \begin{bmatrix} \left\{\begin{matrix}\text{Eq. (7.64)} \\ \text{Eq. (7.65)}\end{matrix}\right\} & \text{for each PQ bus} \\ \text{Eq. (7.66)} & \text{for each PV bus} \end{bmatrix} \quad (7.68)$$

where the vector of dependent variables is

$$\boldsymbol{x} = \begin{bmatrix} \left\{\begin{matrix}|V_i| \\ \delta_i\end{matrix}\right\} & \text{for each PQ bus} \\ \delta_i & \text{for each PV bus} \end{bmatrix} \quad (7.69a)$$

and the vector of independent variables is

$$\boldsymbol{y} = \begin{bmatrix} \left\{\begin{matrix}|V_1| \\ \delta_1\end{matrix}\right\} & \text{for slack bus} \\ \left\{\begin{matrix}P_i \\ Q_i\end{matrix}\right\} & \text{for each PQ bus} \\ \left\{\begin{matrix}P_i \\ |V_i|\end{matrix}\right\} & \text{for each PV bus} \end{bmatrix} = \begin{bmatrix} \boldsymbol{u} \\ \boldsymbol{p} \end{bmatrix} \quad (7.69b)$$

In the above formulation, *the objective function must include the slack bus power*.

The vector of independent variables y can be partitioned into two parts—a vector $\boldsymbol{u}$ of control variables which are to be varied to achieve optimum value of objective function and a vector $\boldsymbol{p}$ *of fixed* or *disturbance* or *uncontrollable parameters*. Control parameters* may be voltage magnitudes on PV buses, P_{Gi} at buses with controllable power, etc.

The optimization problem** can now be restated as

---

* Slack bus voltage and regulating transformer tap setting may be employed as additional control variables. Dopazo *et al.* [25] use Q_{Gi} as control variable on buses with reactive power control.

** If the system real power loss is to be minimized, the objective function is

$$C = P_1(|V|, \delta)$$

Since in this case the net injected real powers are fixed, the minimization of the real injected power P_1 at the slack bus is equivalent to minimization of total system loss. This is known as *optimal reactive power flow problem.*

$$\min_{\boldsymbol{u}} C(\boldsymbol{x}, \boldsymbol{u}) \tag{7.70}$$

subject to equality constraints

$$\boldsymbol{f}(\boldsymbol{x}, \boldsymbol{u}, \boldsymbol{p}) = 0 \tag{7.71}$$

To solve the optimization problem, define the Lagrangian function as

$$\mathcal{L}(\boldsymbol{x}, \boldsymbol{u}, \boldsymbol{p}) = C(\boldsymbol{x}, \boldsymbol{u}) + \lambda^T \boldsymbol{f}(\boldsymbol{x}, \boldsymbol{u}, \boldsymbol{p}) \tag{7.72}$$

where λ is the vector of Lagrange multipliers of same dimension as $\boldsymbol{f}(\boldsymbol{x}, \boldsymbol{u}, \boldsymbol{p})$

The necessary conditions to minimize the unconstrained Lagrangian function are (see Appendix A for differentiation of matrix functions).

$$\frac{\partial \mathcal{L}}{\partial \boldsymbol{x}} = \frac{\partial C}{\partial \boldsymbol{x}} + \left[\frac{\partial \boldsymbol{f}}{\partial \boldsymbol{x}}\right]^T \lambda = 0 \tag{7.73}$$

$$\frac{\partial \mathcal{L}}{\partial \boldsymbol{u}} = \frac{\partial C}{\partial \boldsymbol{u}} + \left[\frac{\partial \boldsymbol{f}}{\partial \boldsymbol{u}}\right]^T \lambda = 0 \tag{7.74}$$

$$\frac{\partial \mathcal{L}}{\partial \lambda} = \boldsymbol{f}(\boldsymbol{x}, \boldsymbol{u}, \boldsymbol{p}) = 0 \tag{7.75}$$

Equation (7.75) is obviously the same as the equality constraints. The expressions for $\frac{\partial C}{\partial \boldsymbol{x}}$ and $\frac{\partial \boldsymbol{f}}{\partial \boldsymbol{u}}$ as needed in Eqs (7.73) and (7.74) are rather involved*. It may, however, be observed by comparison with Eq. (6.52) that $\frac{\partial \boldsymbol{f}}{\partial \boldsymbol{x}}$ = Jacobian matrix [same as employed in the NR method of load flow solution; the expressions for the elements of Jacobian are given in Eqs (6.67) and (6.68).

Equations (7.73), (7.74) and (7.75) are *non-linear algebraic equations* and can only be solved *iteratively*. A simple yet efficient iteration scheme, that can by employed, is the *steepest descent method* (also called *gradient method*). The basic technique is to adjust the *control vector* $\boldsymbol{u}$, so as to move from one feasible solution point (a set of values of $\boldsymbol{x}$ which satisfies Eq. (7.75) for given $\boldsymbol{u}$ and $\boldsymbol{p}$; it indeed is the load flow solution) in the direction of steepest descent (negative gradient) to a new feasible solution point *with a lower value of objective function*. By repeating these moves in the direction of the negative gradient, *the minimum will finally be reached*.

The computational procedure for the gradient method with relevant details is given below:

Step 1 Make an initial guess for $\boldsymbol{u}$, the control variables.

Step 2 Find a feasible load flow solution from Eq. (7.75) by the NR iterative method. The method successively improves the solution $\boldsymbol{x}$ as follows:

$$\boldsymbol{x}^{(r+1)} = \boldsymbol{x}^{(r)} + \Delta \boldsymbol{x}$$

* The original paper of Dommel and Trinney [35] may be consulted for details.

where $\Delta \boldsymbol{x}$ is obtained by solving the set of linear equations (6.57) reproduced below:

$$\left[\frac{\partial \boldsymbol{f}}{\partial \boldsymbol{x}}(\boldsymbol{x}^{(r)}, \boldsymbol{y})\right]\Delta \boldsymbol{x} = -\boldsymbol{f}(\boldsymbol{x}^{(r)}, \boldsymbol{y})$$

or

$$\Delta \boldsymbol{x} = -(\boldsymbol{J}^{(r)})^{-1}\boldsymbol{f}(\boldsymbol{x}^{(r)}, \boldsymbol{y})$$

The end results of step 2 are a feasible solution of $\boldsymbol{x}$ and the Jacobian matrix.

Step 3 Solve Eq. (7.73) for

$$\lambda = -\left[\left(\frac{\partial \boldsymbol{f}}{\partial \boldsymbol{x}}\right)^T\right]^{-1}\frac{\partial C}{\partial \boldsymbol{x}} \tag{7.76}$$

Step 4 Insert λ from Eq. (7.76) into Eq. (7.74), and compute the gradient

$$\nabla \mathcal{L} = \frac{\partial C}{\partial \boldsymbol{u}} + \left[\frac{\partial \boldsymbol{f}}{\partial \boldsymbol{u}}\right]^T \lambda \tag{7.77}$$

It may be noted that for computing the gradient, the Jacobian $\boldsymbol{J} = \dfrac{\partial \boldsymbol{f}}{\partial \boldsymbol{x}}$ is already known from the load flow solution (step 2 above).

Step 5 If $\nabla \mathcal{L}$ equals zero within prescribed tolerance, the minimum has been reached. Otherwise,

Step 6 Find a new set of control variables

$$\boldsymbol{u}_{\text{new}} = \boldsymbol{u}_{\text{old}} + \Delta \boldsymbol{u} \tag{7.78}$$

where

$$\Delta \boldsymbol{u} = -\alpha \Delta \mathcal{L} \tag{7.79}$$

Here $\Delta \boldsymbol{u}$ is a step in the negative direction of the gradient. The step size is adjusted by the *positive scalar* α.

Steps 1 through 5 are straightforward and pose no computational problems. Step 6 is the critical part of the algorithm, where the *choice of* α is very important. Too small a value of α guarantees the convergence but *slows down the rate of convergence*; *too high a value causes oscillations around the minimum*. *Several methods are available for optimum choice of step size*.

Inequality Constraints on Control Variables

Though in the earlier discussion, the control variables are assumed to be unconstrained, the permissible values are, in fact, always constrained,

$$\boldsymbol{u}_{\min} \le \boldsymbol{u} \le \boldsymbol{u}_{\max}$$

e.g.

$$P_{Gi,\,\min} \le P_{Gi} \le P_{Gi\,\max} \tag{7.80}$$

These inequality constraints on control variables can be easily handled. If the correction Δu_i in Eq. (7.78) causes u_i to exceed one of the limits, u_i is set equal to the corresponding limit, i.e.

$$u_{i,\text{new}} = \begin{cases} u_{i,\max} & \text{if } u_{i,\text{old}} + \Delta u_i > u_{i,\max} \\ u_{i,\min} & \text{if } u_{i,\text{old}} + \Delta u_i < u_{i,\min} \\ u_{i,\text{old}} + \Delta u_i & \text{otherwise} \end{cases} \tag{7.81}$$

After a control variable reaches any of the limits, its component in the gradient should continue to be computed in later iterations, as the variable may come within limits at some later stage.

In accordance with the Kuhn-Tucker theorem (see Appendix E), the necessary conditions for minimization of $\mathcal{L}$ under constraint (7.80) are:

$$\left.\begin{aligned} \frac{\partial \mathcal{L}}{\partial u_i} &= 0 \quad \text{if } u_{i,\min} < u_i < u_{i,\max} \\ \frac{\partial \mathcal{L}}{\partial u_i} &\le 0 \quad \text{if } u_i = u_{i,\max} \\ \frac{\partial \mathcal{L}}{\partial u_i} &\ge 0 \quad u_i = u_{i,\min} \end{aligned}\right\} \tag{7.82}$$

Therefore, now, in step 5 of the computational algorithm, the gradient vector has to satisfy the optimality condition (7.82).

Inequality Constraints on Dependent Variables

Often, the upper and lower limits on dependent variables are specified as

$$\boldsymbol{x}_{\min} \le \boldsymbol{x} \le \boldsymbol{x}_{\max}$$

e.g.

$$|V|_{\min} \le |V| \le |V|_{\max} \text{ on a PQ bus} \tag{7.83}$$

Such inequality constraints can be conveniently handled by the *penalty function method*. The objective function is augmented by penalties for inequality constraints violations. This forces the solution to lie sufficiently close to the constraint limits, when these limits are violated. The penalty function method is valid in this case, because these constraints are seldom *rigid limits* in the strict sense, but are in fact, *soft limits* (e.g. $|V| \le 1.0$ on a PQ bus really means V should not exceed 1.0 too much and $|V| = 1.01$ may still be permissible).

The penalty method calls for augmentation of the objective function so that the new objective function becomes

$$C' = C(\boldsymbol{x}, \boldsymbol{u}) + \sum_j \boldsymbol{W}_j \tag{7.84}$$

where the penalty $\boldsymbol{W}_j$ is introduced for each violated inequality constraint. A suitable penalty function is defined as

$$W_j = \begin{cases} \gamma_j (x_j - x_{j,\max})^2; & \text{whenever } x_j > x_{j,\max} \\ \gamma_j (x_j - x_{j,\min})^2; & \text{whenever } x_j < x_{j,\min} \end{cases} \tag{7.85}$$

where γ_j is *a real positive number* which controls *degree of penalty* and is called the *penalty factor*.

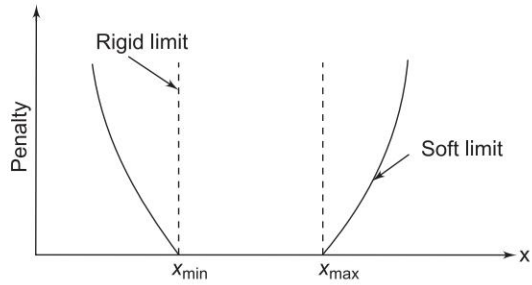

Fig. 7.17 Penalty function

A plot of the proposed penalty function is shown in Fig. (7.17), which clearly indicates how the rigid limits are replaced by soft limits.

The necessary conditions (7.73) and (7.74) would now be modified as given below, while the conditions (7.75), i.e. load flow equations, remain unchanged.

$$\frac{\partial \mathcal{L}}{\partial \boldsymbol{x}} = \frac{\partial C}{\partial \boldsymbol{x}} + \sum_j \frac{\partial \boldsymbol{W}_j}{\partial \boldsymbol{x}} + \left[\frac{\partial \boldsymbol{f}}{\partial \boldsymbol{x}}\right]^T \lambda = 0 \tag{7.86}$$

$$\frac{\partial \mathcal{L}}{\partial \boldsymbol{u}} = \frac{\partial C}{\partial \boldsymbol{u}} + \sum_j \frac{\partial \boldsymbol{W}_j}{\partial \boldsymbol{u}} + \left[\frac{\partial \boldsymbol{f}}{\partial \boldsymbol{u}}\right]^T \lambda = 0 \tag{7.87}$$

The vector $\dfrac{\partial \boldsymbol{W}_j}{\partial \boldsymbol{x}}$ obtained from Eq. (7.85) would contain only one non-zero term corresponding to the dependent variable x_j; while $\dfrac{\partial \boldsymbol{W}_j}{\partial \boldsymbol{u}} = 0$ as the penalty functions on dependent variables are independent of the control variables.

By choosing a higher value for γ_j, the penalty function can be made steeper so that the solution lies closer to the rigid limits; the convergence, however, will become poorer. A good scheme is to start with a low value of γ_j and to increase it during the optimization process, if the solution exceeds a certain tolerance limit.

This section has shown that the NR method of load flow can be extended to *yield the optimal load flow solution* that is feasible with respect to *all relevant inequality constraints*. These solutions are often required *for system planning and operation*.

7.7 OPTIMAL SCHEDULING OF HYDROTHERMAL SYSTEM

The previous sections have dealt with the problem of optimal scheduling of a power system with *thermal plants only.* Optimal operating policy in this case can be completely determined *at any instant* without reference *to operation at other times*. This, indeed, is the static *optimization problem*. Operation of a system having both hydro and thermal plants is, however, *far more complex* as hydro plants have *negligible operating cost*, but are required to operate under *constraints of the water available* for hydro generation in a *given period of time*. The problem thus belongs to, the *realm of dynamic optimization*. The problem of minimizing the operating cost of a hydrothermal system can be viewed as one of minimizing the fuel cost of thermal plants under the *constraint of water availability (storage and inflow)* for hydro generation *over a given period of operation*.

For the sake of simplicity and understanding, the problem formulation and solution techniques are illustrated through a simplified hydrothermal system of Fig. (7.18). This system consists of *one hydro* and *one thermal* plant supplying power to a *centralized load* and is referred to as a *fundamental system*.

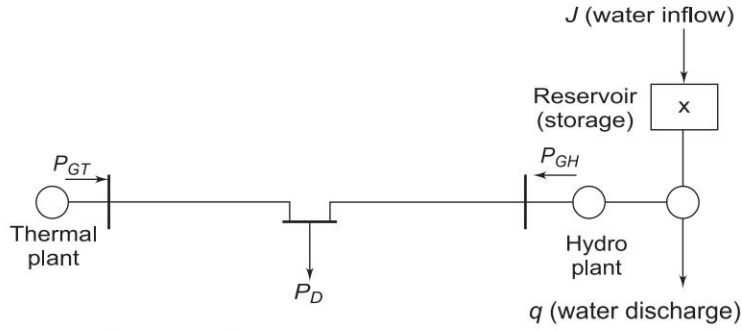

Fig. 7.18 Fundamental hydrothermal system

Optimization will be carried out with real power generation as control variable, with transmission loss accounted for by the loss formula of Eq. (7.39).

Mathematical Formulation

For a certain period of operation T (one year, one month or one day, depending upon the requirement), it is assumed that (1) storage of hydro reservoir at the beginning and the end of the period are specified, and (2) water inflow to reservoir (after accounting for irrigation use) and load demand on the system are known as functions of time with complete certainty (deterministic case). The problem is to determine $q(t)$, the water discharge (rate) so as to minimize the cost of thermal generation,

$$C_T = \int_0^T C'(P_{GT}(t))\,\mathrm{d}t \tag{7.88}$$

under the following constraints:

(i) Meeting the load demand

$$P_{GT}(t) + P_{GH}(t) - P_L(t) - P_D(t) = 0; \quad t \in [0,T] \tag{7.89}$$

This is called the *power balance equation*.

(ii) Water availability

$$X'(T) - X'(0) - \int_0^T J(t)\,dt + \int_0^T q(t)dt = 0 \tag{7.90}$$

where $J(t)$ is the water inflow (rate), $X'(t)$ water storage, and $X'(0)$, $X'(T)$ are specified water storages at the beginning and at the end of the optimization interval.

(iii) The hydro generation $P_{GH}(t)$ is a function of hydro discharge and water storage (or head), i.e.

$$P_{GH}(t) = f(X'(t), q(t)) \tag{7.91}$$

The problem can be handled conveniently by discretization. The optimization interval T is subdivided into M subintervals each of time length ΔT. Over each subinterval it is assumed that all the variables remain fixed in value. The problem is now posed as

$$\min_{q^m (m=1,2,\ldots,M)} \Delta T \sum_{m=1}^{M} C'\left(P_{GT}^m\right) = \min_{q^m (m=1,2,\ldots,M)} \sum_{m=1}^{M} C\left(P_{GT}^m\right) \tag{7.92}$$

under the following constraints:

(i) Power balance equation

$$P_{GT}^m + P_{GH}^m - P_L^m - P_D^m = 0 \tag{7.93}$$

where

P_{GT}^m = thermal generation in the mth interval

P_{GH}^m = hydro generation in the mth interval

P_L^m = transmission loss in the mth interval

$= B_{TT}(P_{GT}^m)^2 + 2B_{TH} P_{GT}^m P_{GH}^m + B_{HH}(P_{GH}^m)^2$

P_D^m = load demand in the mth interval

(ii) Water continuity equation

$$X'^m - X'^{(m-1)} - J^m \Delta T + q^m \Delta T = 0$$

where

X'^m = water storage at the end of the mth interval

J^m = water inflow (rate) in the mth interval

q^m = water discharge (rate) in the mth interval

The above equation can be written as

$$X^m - X^{m-1} - J^m + q^m = 0, \quad m = 1, 2, \ldots, M \tag{7.94}$$

where $X^m = X'^m/\Delta T$ = storage in discharge units.

In Eq. (7.94), X^0 and X^M are the specified storages at the beginning and end of the optimization interval.

(iii) Hydro generation in any subinterval can be expressed* as

$$P_{GH}^{m} = h_0\{1 + 0.5e\,(X^m + X^{m-1})\}\,(q^m - \rho) \tag{7.95}$$

where

$h_0 = 9.81 \times 10^{-3} h_0'$

h_0' = basic water head (head corresponding to dead storage)

e = water head correction factor to account for head variation with storage

ρ = non-effective discharge (water discharge needed to run hydro generator at no load).

In the above problem formulation, it is convenient to choose water discharges in all subintervals except one as independent variables, while hydro generations, thermal generations and water storages in all subintervals are treated as dependent variables. The fact, that water discharge in one of the subintervals is a dependent variable, is shown below.

Adding Eq. (7.94) for $m = 1, 2, ..., M$ leads to the following equation, known as *water availability equation*:

$$X^M - X^0 - \sum_m J^m + \sum_m q^m = 0 \tag{7.96}$$

Because of this equation, only $(M - 1)$ *qs* can be specified independently and the remaining one can then be determined from this equation and is, therefore, a dependent variable. For convenience, q^1 is chosen as a dependent variable, for which we can write

$$q^1 = X^0 - X^M + \sum_m J^m - \sum_{m=2}^{M} q^m \tag{7.97}$$

---

* $P_{GH}^{m} = 9.81 \times 10^{-3}\, h_{av}^{m}\,(q^m - \rho)$ MW

where

$(q^m - \rho)$ = effective discharge in m^3/s

h_{av}^{m} = average head in the mth interval

Now

$$h_{av}^{m} = h_0' + \frac{\Delta T(X^m + X^{m-1})}{2A}$$

where

A = area of cross-section of the reservoir at the given storage

h_0' = basic water head (head corresponding to dead storage)

$h_{av}^{m} = h_0'\{1 + 0.5e(X^m + X^{m-1})\}$

where

$$e = \frac{\Delta T}{Ah_0'};\ e \text{ is tabulated for various storage values}$$

Now

$$P_{GH}^{m} = h_0\,\{1 + 0.5e(X^m + X^{m-1})\}\,(q^m - \rho)$$

where

$$h_0 = 9.81 \times 10^{-3} h_0'$$

Solution Technique

The problem is solved here using non-linear programming technique in conjunction with the first order gradient method. The Lagrangian $\mathcal{L}$ is formulated by augmenting the cost function of Eq. (7.92) with equality constraints of Eqs (7.93–7.95) through Lagrange multipliers (dual variables) λ_1^m, λ_2^m and λ_3^m. Thus,

$$\mathcal{L} = \sum_m [C(P_{GT}^m) - \lambda_1^m (P_{GT}^m + P_{GH}^m - P_L^m - P_D^m) + \lambda_2^m (X^m - X^{m-1} - J^m + q^m) + \lambda_3^m \{P_{GH}^m - h_0 (1 + 0.5e(X^m + X^{m-1})) \times (q^m - \rho)\}] \quad (7.98)$$

The dual variables are obtained by equating to zero the partial derivatives of the Lagrangian with respect to the dependent variables yielding the following equations:

$$\frac{\partial \mathcal{L}}{\partial P_{GT}^m} = \frac{\mathrm{d}C(P_{GT}^m)}{\mathrm{d}P_{GT}^m} - \lambda_1^m \left(1 - \frac{\partial P_L^m}{\partial P_{GT}^m}\right) = 0 \quad (7.99)$$

[The reader may compare this equation with Eq. (7.29)]

$$\frac{\partial \mathcal{L}}{\partial P_{GH}^m} = \lambda_3^m - \lambda_1^m \left(1 - \frac{\partial P_L^m}{\partial P_{GH}^m}\right) = 0 \quad (7.100)$$

$$\left(\frac{\partial \mathcal{L}}{\partial X^m}\right)_{\substack{m \neq M \\ \neq 0}} = \lambda_2^m - \lambda_2^{m+1} - \lambda_3^m \{0.5h_0 e(q^m - \rho)\} - \lambda_3^{m+1} \{0.5h_0 e (q^{m+1} - \rho)\} = 0 \quad (7.101)$$

and using Eq. (7.94) in Eq. (7.98), we get

$$\left(\frac{\partial \mathcal{L}}{\partial q^1}\right) = \lambda_2^1 - \lambda_3^1 h_0 \{1 + 0.5e (2X^0 + J^1 - 2q^1 + \rho)\} = 0 \quad (7.102)$$

The dual variables for any subinterval may be obtained as follows:

(i) Obtain λ_1^m from Eq. (7.99).

(ii) Obtain λ_3^m from Eq. (7.100).

(iii) Obtain λ_2^1 from Eq. (7.102) and other values of λ_2^m ($m \neq 1$) from Eq. (7.101).

The gradient vector is given by the partial derivatives of the Lagrangian with respect to the independent variables. Thus

$$\left(\frac{\partial \mathcal{L}}{\partial q^m}\right)_{m \neq 1} = \lambda_2^m - \lambda_3^m h_0 \{1 + 0.5e (2X^{m-1} + J^m - 2q^m + \rho)\} \quad (7.103)$$

For optimality the gradient vector should be zero if there are no inequality constraints on the control variables.

Algorithm

1. Assume an initial set of independent variables $q^m (m \neq 1)$ for all subintervals except the first.
2. Obtain the values of dependent variables X^m, P^m_{GH}, P^m_{GT}, q^1 using Eqs (7.93, 7.94, 7.95 and 7.97).
3. Obtain the dual variables λ^m_1, λ^m_3, λ^m_2 $(m \neq 1)$ and λ^1_2 using Eqs (7.99–7.102).
4. Obtain the gradient vector using Eq. (7.103) and check if all its elements are equal to zero within a specified accuracy. If so, optimum is reached. If not, go to step 5.
5. Obtain new values of control variables using the first order gradient method, i.e.

$$q^m_{\text{new}} = q^m_{\text{old}} - \alpha\left(\frac{\partial \mathcal{L}}{\partial q^m}\right);\ m \neq 1 \tag{7.104}$$

where α is a positive scalar. Repeat from step 2.

In the solution technique presented above, if some of the control variables (water discharges) cross the upper or lower bounds, these are made equal to their respective bounded values. For these control variables, step 4 above is checked in accordance with the Kuhn–Tucker conditions (7.82) given in Sec. 7.6.

The inequality constraints on the dependent variables are treated conveniently by augmenting the cost function with penalty functions as discussed in Sec. 7.6.

The method outlined above is quite general and can be directly extended to a system having multi-hydro and multi-thermal plants. The method, however, has the disadvantage of large memory requirement, since the independent variables, dependent variables and gradients need to be stored simultaneously. A modified technique known as decomposition [18] overcomes this difficulty. In this technique optimization is carried out over each subinterval and the complete cycle of iteration is repeated, if the water availability equation does not check at the end of the cycle.

Example 7.8 Consider the fundamental hydrothermal system shown in Fig. (7.18). The objective is to find the optimal generation schedule for a typical day, wherein load varies in three steps of eight hours each as 7 MW, 10 MW and 5 MW, respectively. There is no water inflow into the reservoir of the hydro plant. The initial water storage in the reservoir is 100 m^3/s and the final water storage should be 60m^3/s, i.e. the total water available for hydro generation during the day is 40 m^3/s.

Basic head is 20 m. Water head correction factor e is given to be 0.005. Assume for simplicity that the reservoir is rectangular so that e does not change with water storage. Let the non-effective water discharge be assumed as 2 m^3/s. Incremental fuel cost of the thermal plant is

$$\frac{dC}{dP_{GT}} = 1.0P_{GT} + 25.0 \quad \text{Rs/h}$$

Further, transmission losses may be neglected.

The above problem has been specially constructed (rather oversimplified) to illustrate the optimal hydrothermal scheduling algorithm, which is otherwise computationally involved and the solution has to be worked on the digital computer. Steps of one complete iteration will be given here.

Since there are three subintervals, the control variables are q^2 and q^3. Let us assume their initial values to be

$$q^2 = 15 \text{ m}^3/\text{s}$$
$$q^3 = 15 \text{ m}^3/\text{s}$$

The value of water discharge in the first subinterval can be immediately found out using Eq. (7.97), i.e.

$$q^1 = 100 - 60 - (15 + 15) = 10 \quad \text{m}^3/\text{s}$$

It is given that $X^0 = 100$ m^3/s and $X^3 = 60$ m^3/s.
From Eq. (7.94)

$$X^1 = X^0 + J^1 - q^1 = 90 \quad \text{m}^3/\text{s}$$
$$X^2 = X^1 + J^2 - q^2 = 75 \quad \text{m}^3/\text{s}$$

The values of hydro generations in the subintervals can be obtained using Eq. (7.95) as follows:

$$\begin{aligned} P_{GH}^1 &= 9.81 \times 10^{-3} \times 20 \{1 + 0.5 \times 0.005 (X^1 + X^0)\} \{q^1 - \rho) \\ &= 0.1962 \{1 + 25 \times 10^{-4} \times 190\} \times 8 \\ &= 2.315 \text{ MW} \\ P_{GH}^2 &= 0.1962 \{1 + 25 \times 10^{-4} \times 165\} \times 13 \\ &= 3.602 \text{ MW} \\ P_{GH}^3 &= 0.1962 \{1 + 25 \times 10^{-4} \times 135\} \times 13 \\ &= 3.411 \text{ MW} \end{aligned}$$

The thermal generations in the three intervals are then

$$P_{GT}^1 = P_D^1 - P_{GH}^1 = 7 - 2.315 \quad = 4.685 \text{ MW}$$
$$P_{GT}^2 = P_D^2 - P_{GH}^2 = 10 - 3.602 \quad = 6.398 \text{ MW}$$
$$P_{GT}^3 = P_D^3 - P_{GH}^3 = 5 - 3.411 \quad = 1.589 \text{ MW}$$

From Eq. (7.99), we have values of λ_1^m as

$$\frac{\text{d}C(P_{GT}^m)}{\text{d}P_{GT}^m} = \lambda_1^m$$

or

$$\lambda_1^m = P_{GT}^m + 25$$

Calculating λ_1 for all the three subintervals, we have

$$\begin{bmatrix} \lambda_1^1 \\ \lambda_1^2 \\ \lambda_1^3 \end{bmatrix} = \begin{bmatrix} 29.685 \\ 31.398 \\ 26.589 \end{bmatrix}$$

Also from Eq. (7.100), we can write

$$\begin{bmatrix} \lambda_3^1 \\ \lambda_3^2 \\ \lambda_3^3 \end{bmatrix} = \begin{bmatrix} \lambda_1^1 \\ \lambda_1^2 \\ \lambda_1^3 \end{bmatrix} = \begin{bmatrix} 29.685 \\ 31.398 \\ 26.589 \end{bmatrix} \text{ for the lossless case}$$

From Eq. (7.102)

$$\lambda_2^1 = \lambda_3^1 h_0 \{1 + 0.5e (2X^0 + J^1 - 2q^1 + \rho)\}$$

$$= 29.685 \times 0.1962 \{1 + 25 \times 10^{-4} (200 - 20 + 2)\}$$

$$= 8.474$$

From Eq. (7.101) for $m = 1$ and 2, we have

$$\lambda^1{}_2 - \lambda_2^2 - \lambda_3^1 \{0.5h_0 e (q^1 - \rho)\} - \lambda_3^2 \{0.5h_0 e (q^2 - \rho)\} = 0$$

$$\lambda_2^2 - \lambda_2^3 - \lambda_3^2 \{0.5\, h_0 e (q^2 - \rho)\} - \lambda_3^3 \{0.5h_0 e (q^3 - \rho)\} = 0$$

Substituting various values, we get

$$\lambda_2^2 = 8.474 - 29.685 \{0.5 \times 0.1962 \times 0.005 \times 8\} - 31.398 \{0.5 \times 0.1962 \times 0.005 \times 13\}$$

$$= 8.1574$$

$$\lambda_2^3 = 8.1574 - 31.398 (0.5 \times 0.1962 \times 0.005 \times 13) - 26.589 (0.5 \times 0.1962 \times 0.005 \times 13) = 7.7877$$

Using Eq. (7.103), the gradient vector is

$$\left(\frac{\partial \mathcal{L}}{\partial q^2}\right) = \lambda_2^2 - \lambda_3^2 h_0 \{1 + 0.5 \times 0.005 (2 \times 90 - 2 \times 15 + 2)\}$$

$$= 8.1574 - 31.398 \times 0.1962 \{1 + 25 \times 10^{-4} \times 152\}$$

$$= -0.3437$$

$$\left(\frac{\partial \mathcal{L}}{\partial q^3}\right) = \lambda_2^3 - \lambda_3^3 h_0 \{1 + 0.5e (2X^2 + J^3 - 2q^3 + \rho)\}$$

$$= 7.7877 - 26.589 \times 0.1962 \{1 + 25 \times 10^{-4} \times 122\}$$

$$= 0.9799$$

If the tolerance for gradient vector is 0.1, then optimal conditions are not yet satisfied, since the gradient vector is not zero, i.e. (≤ 0.1); hence the second iteration will have to be carried out starting with the following new values of the control variables obtained from Eq. (7.104).

$$\begin{bmatrix} q^2_{\text{new}} \\ q^3_{\text{new}} \end{bmatrix} = \begin{bmatrix} q^2_{\text{old}} \\ q^3_{\text{old}} \end{bmatrix} - \alpha \begin{bmatrix} \dfrac{\partial \mathcal{L}}{\partial q^2} \\ \dfrac{\partial \mathcal{L}}{\partial q^3} \end{bmatrix}$$

Let us take $\alpha = 0.5$, then

$$\begin{bmatrix} q^2_{\text{new}} \\ q^3_{\text{new}} \end{bmatrix} = \begin{bmatrix} 15 \\ 15 \end{bmatrix} - 0.5 \begin{bmatrix} -0.3437 \\ 0.9799 \end{bmatrix} = \begin{bmatrix} 15.172 \\ 14.510 \end{bmatrix}$$

and from Eq. (7.97)

$$q^1_{\text{new}} = 100 - 60 - (15.172 + 14.510) = 10.318 \text{ m}^3/\text{s}$$

The above computation brings us to the starting point of the next iteration. Iterations are carried out till the gradient vector becomes zero within specified tolerance.

7.8 POWER SYSTEM SECURITY

Introduction

So far we have been primarily concerned with the economical operation of a power system. An equally important factor in the operation of a power system is the desire to maintain system security. System security involves practices suitably designed to keep the system operating when components fail. Besides economizing on fuel cost, the power system should be operationally "secure". An operationally "secure" power system is one with low probability of blackout or equipment damage. All these aspects require security constrained power system optimization (SCO).

Since security and economy are normally conflicting requirements, it is inappropriate to treat them separately. The final aim of economy is the security function of the utility-company. The Energy Management System is to operate the system at minimum cost, with the guaranteed alleviation of emergency conditions. The emergency condition will depend on severity of violations of operating limits (branch flows and bus voltage limits). The most severe violations result from contingencies. An important part of security study, therefore, moves around the power system's ability to withstand the effects of contingencies. A particular system state is said to be secure only with reference to one or more specific contingency cases, and a given set of quantities monitored for violation.

Most of the security related functions deal with static "snapshots" of the power system. They have to be executed at intervals compatible with the rate-of-change of system state. This quasi-static approach is, to a large extent, the only practical approach at present, since dynamic analysis and optimization are considerably more difficult and computationally more time consuming.

System security can be said to comprise three major functions that are carried out in an energy control centre: (i) System monitoring, (ii) contingency analysis, and (iii) corrective action analysis.

System monitoring supplies the power system operators with pertinent up-to-date information on the conditions of the power system. Telemetry systems measure and transmit the data. Voltages, currents, current flows, and the status of circuit breakers and switches in every substation in a transmission network are monitored. Further, other critical and important information such as frequency, generator outputs and transformer tap positions can also be telemetered. Digital computers in a control centre then process the telemetered data and place them in a data base form and inform the operators in case of an overload or out-of-limit voltage. Important data are also displayed on big monitors. Alarms/warnings may be given if required.

State estimation [11, 13] is normally used in such systems to combine telemetered data to give the best estimate (in a statistical sense) of the current system condition or "state". Such systems often work with supervisory control systems to help operators control circuit breakers and operate switches and taps remotely. These systems together are called SCADA (supervisory control and data acquisition) systems.

The second major security function is contingency analysis. Modern operation computers have contingency analysis programmes stored in them. These model possible system troubles (outages) before they occur. They study outage events and alert the operators to any potential overloads or serious voltage violations. For example, the simplest form of contingency analysis can be put together with a standard LF program such as studied in Ch. 6, along with procedures to set up the load flow data for each outage to be studied by the LF program. This allows the system operators to locate defensive operating states where no single contingency event will generate overloads and/or voltage violations. This analysis thus evolves operating constraints which may be employed in the ED and UC program. Thus contingency analysis carries out emergency identification and "what if" simulations.

The third major security function, corrective action analysis, permits the operator to change the operation of the power system if a contingency analysis program predicts a serious problem in the event of the occurrence of a certain outage. Thus this provides preventive and post-contingency control. A simple example of corrective action is the shifting of generation from one unit to another. This may result in change in power flows and thus can change loading on overloaded lines.

These three functions together consist of a very complex set of tools that can help in the secure operation of a power system.

System State Classification

A formal classification of power system security levels was first suggested by DyLiacco [68] and further clarified by Fink and Carlsen [69] in order to define relevant EMS functions. Stott *et al.* [70] have recently presented a more practical static security level diagram (see Fig. 7.19) by incorporating 'correctively secure' (level 2) and 'correctable emergency' (level 4) security levels. In the figure, the arrowed lines represent involuntary transitions between levels 1 to 5

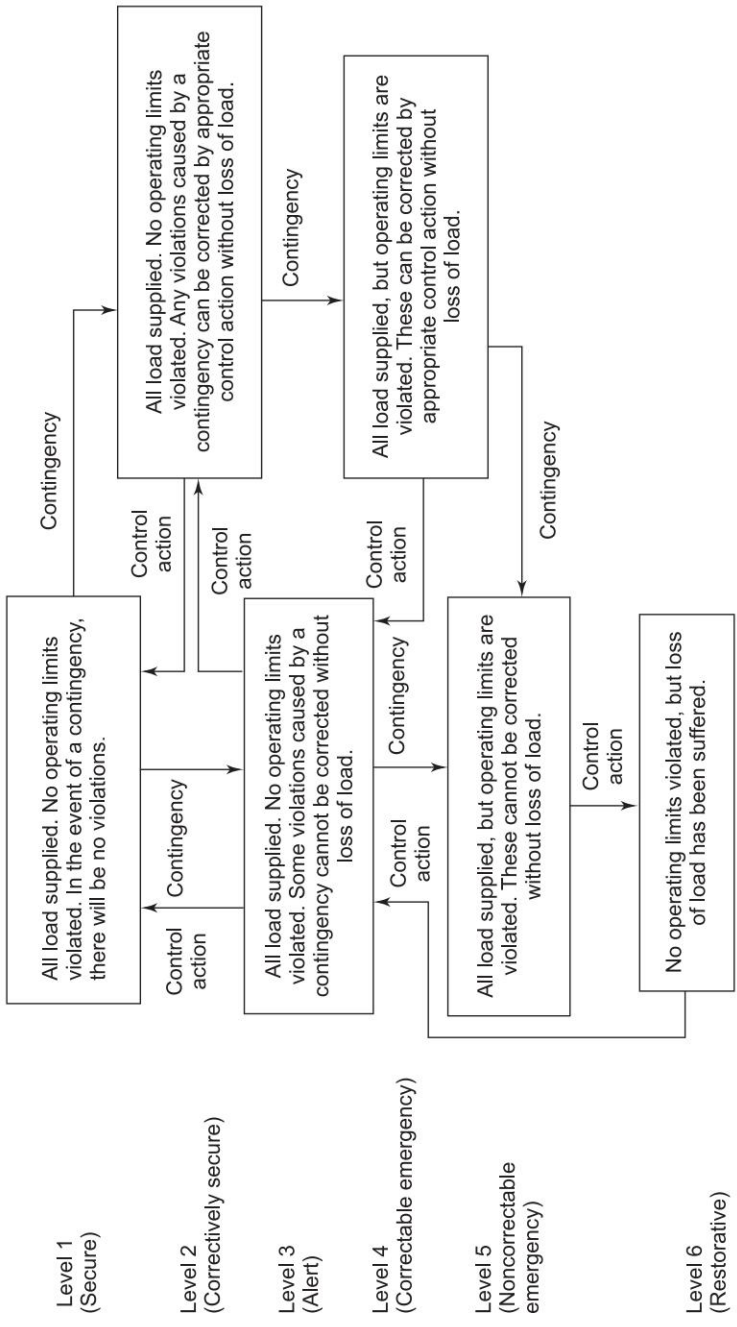

Fig. 7.19 Power system static security levels

due to contingencies. The removal of violations from level 4 normally requires EMS-directed "corrective rescheduling" or "remedial action", bringing the system to level 3, from where it can return to either level 1 or 2 by further EMS-directed "preventive rescheduling" depending upon the desired operational security objectives.

Levels 1 and 2 represent normal power system operation. Level 1 has the ideal security but is much too conservative and costly. The power system survives any of the credible contingencies without relying on any post-contingency corrective action. Level 2 is more economical, but depends on post-contingency corrective rescheduling to alleviate violations without loss of load, within a specified period of time. Post-contingency operating limits might be different from their pre-contingency values.

Security Analysis

System security can be broken down into two major functions that are carried out in an operations control centre: (i) security assessment, and (ii) security control. The former gives the security level of the system operating state. The latter determines the appropriate security constrained scheduling required to optimally attain the target security level.

The security functions in an EMS can be executed in 'real time' and 'study' modes. Real time application functions have a particular need for computing speed and reliability.

The static security level of a power system is characterized by the presence or otherwise of emergency operating conditions (limit violations) in its actual (pre-contingency) or potential (post-contingency) operating states. System security assessment is the process by which any such violations are detected.

System assessment involves two functions: (i) system monitoring, and (ii) contingency analysis. System monitoring provides the operator of the power system with pertinent up-to-date information on the current conditions of the power system. In its simplest form, this just detects violations in the actual system operating state. Contingency analysis is much more demanding and normally performed in three distinct states, i.e. contingency definition, selection and evaluation. Contingency definition gives the list of contingencies to be processed whose probability of occurrence is high. This list, which is usually large, is in terms of network changes, i.e. branch and/or injection outages. These contingencies are ranked in rough order of severity employing contingency selection algorithms to shorten the list. Limited accuracy results are required, and therefore an approximate (linear) system model is utilized for speed. Contingency evaluation is then performed (using AC power flow) on the successive individual cases in decreasing order of severity. The evaluation process is continued up to the point where no post-contingency violations are encountered. Hence, the purpose of contingency analysis is to identify the list of contingencies that, if they occur, would create violations in system operating states. They are ranked in order of severity.

The second major security function, security control, allows operating personnel to change the power system operation in the event that a contingency analysis program predicts a serious problem should a certain outage occur. Normally the security control is achieved through SCO program.

Modelling for Contingency Analysis

The power system limits of most interest in contingency analysis are those on line flows and bus voltages. Since these are soft limits, limited-accuracy models and solutions are justified. The most fundamental approximate load-flow model is the NR model discussed in Ch. 6.

$$\begin{bmatrix} \Delta P \\ \Delta Q \end{bmatrix} = [J] \begin{bmatrix} \Delta \delta \\ \Delta |V| \end{bmatrix} \tag{7.105}$$

The DC load flow model in its incremental version is normally preferred.

$$[\Delta P] = [B'] [\Delta \delta] \tag{7.106}$$

This model assumes voltages to remain constant after contingencies. However, this is not true for weak systems. The utility has to prespecify whether it wants to monitor post-contingency "steady state" conditions immediately after the outage (system intertial response) or after the automatic controls* (governor, AGC, ED) have responded. Depending upon this decision, different participation factors are used to allocate the MW generation among the remaining units. The reactive problem tends to be more nonlinear and voltages are strongly influenced by active power flows. The model often used is

$$[\Delta Q/|V|] = [B''] [\Delta |V|] \tag{7.107}$$

Contingency Selection

There are two main approaches:

Direct methods

These involve screening and direct ranking of contingency cases. They monitor the appropriate post-contingent quantities (flows, voltages). The severity measure is often a performance index.

Indirect methods

These give the values of the contingency case severity indices for ranking, without calculating the monitored contingent quantities directly. (e.g. use of sensitivity factors).

Simulation of line outage is more complex than a generator outage, since line outage results in a change in system configurations. The Inverse Matrix Modification Lemma (IMML) or "compensation" method is used throughout

* See Ch. 8 for details about these controls.

the contingency analysis field [70]. The IMML helps in calculating the effects of network changes due to contingencies, without reconstructing and refactorizing or inverting the base case network matrix. It is also possible to achieve computational economy by getting only local solutions by calculating the inverse elements in the vicinity of the contingencies. The question is how far one should go. Some form of sensitivity analysis may be used.

The problem of studying hundreds of possible outages becomes very difficult to solve if it is desired to present the results quickly so that corrective actions can be taken. One of the simplest ways of obtaining a quick calculation of possible overloads is to use network sensitivity factors. These factors show the approximate change in line flows for changes in generation on the network configuration and are derived from the DC load flow [10,13]. They are of two types:

1. Generation shift distribution factors
2. Line outage distribution factors

Reference [10] and Ch. 13 of Ref. 13 give a good account of the way they are used and derived.

In a practical situation when a contingency causing emergency occurs, control action to alleviate limit violations is always taken, if such a capability exists and a protective system (Ch. 15) permits time to do so.

The security control function (which is normally achieved by SCO) responds to each insecure contingency case (as obtained by contingency analysis), usually in decreasing order of severity by:

(i) Rescheduling the pre-contingency operating state to alleviate the emergency resulting from the contingency, and/or
(ii) Developing a post-contingency control strategy that will eliminate the emergency, or
(iii) Taking no action, on the basis that post-contingency emergency is small and/or probability of its occurrence is very low.

A specific security control function, then, is designed to:

(i) Operate in real time or study mode
(ii) Schedule active or reactive power controls or both
(iii) Achieve a defined security level
(iv) Minimize a defined operational objective.

Only a small proportion of work on optional power flow (OPF) has taken into account the security constraints. The most successful applications have been to the security constrained MW dispatch OPF sub-problem. The contingency-constrained voltage/var rescheduling problem, as of the writing of this text, still remains to be solved to a satisfactory degree.

The total number of contingency constraints imposed on SCO is enormous. The SCO or contingency constrained OPF problem is solved with or without first optimizing with respect to the base case (precontingency) constraints. The general procedure adopted is as follows:

(i) Contingency analysis is done and cases with violations or near violations are identified.
(ii) The SCO problem is solved.

(iii) the rescheduling in step (i) might have created new violations, and therefore step (i) should be repeated till no violations exist.

Hence, SCO represents a potentially massive additional computing effort. An excellent comprehensive overview of various available methods is presented by Stott *et al*. [62].

There is still great potential for further improvement in power system security control. Better problem formulations, theory, computer solution methods and implementation techniques are required.

7.9 MAINTENANCE SCHEDULING (MS)

Maintenance scheduling of generating units is a problem of great importance in both planning and designing power systems and also in operation management. High reliability requirement of power system operation has made the generator maintenance scheduling problem very important. The intricacy of this problem arises when system size relating the total number of units grows. Also the low available reserve margin and unavoidable peak demands in modern power systems render the maintenance scheduling task much more complex. The risk of systems supply being not sufficient may be increased during the scheduled maintenance outages. Furthermore there will be increase in overall system cost comprising maintenance and production cost that needs to be kept to the acceptable value.

Maintenance Scheduling problem is characterized by its conflicting multi-objective nature of several incommensurable criteria like economy and reliability. MS is treated as a constrained optimization problem.

On the whole a desirable maintenance schedule is expected to achieve the following goals:

(i) Increase the reliability and economic benefits of power system,
(ii) extend generator lifetime,
(iii) reduce and (or) postpone installations of highly capital intensive new units.

It is a long term form of UC problem discussed earlier (see 7.3). Hence Dynamic Programming can be applied successfully to solve MSP. [29, 50, 55, 49, 39]. The main objective is to maintain the prescribed capacity margins at all times or failing this, to minimize the risk of energy interruption to the customer, while minimizing production cost. System maintenance includes inspection, preventive maintenance and overhaul [7].

7.10 POWER-SYSTEM RELIABILITY

In Sec. 7.4 we considered reliability as specific to unit commitment. Here we shall examine the power system reliability as a whole. System reliability is the probability that the system will perform its intended function adequately for a specified interval of time (useful life span) under specified operating conditions.

Figure 7.20 shows a bath-tub curve which is divided into three different regions in the entire life of a component/device/system. The initial period is known as de-bugging/burn-in period/period of infant mortality during which failures may be high due to errors in design or manufacture. The region shows decreasing λ (failure or hazard rate). Then comes the useful life span. Here the failure is due to chance failures. It is more or less constant. The assumption of course in system is well maintained. The last region is the wear out period (old age).

Each region can be expressed by a probability distribution function

$$\lambda(t) = Kt^{\alpha-1} \quad \text{for } t > 0 \tag{7.108}$$

K and α are constants.

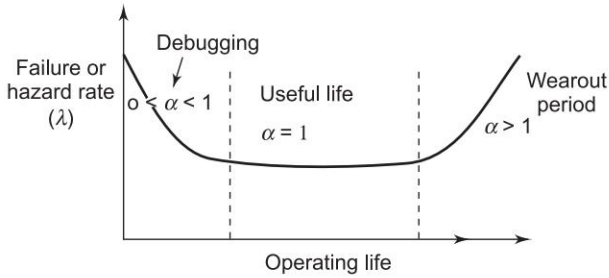

Fig. 7.20 Bath-tub curve

Outage

An outage refers to that state of component/device (say a transformer) in which it is unavailable to carry out its intended function due to some event directly linked with it such an outage may or may not cause an outage of the full system (power system) or interruption of supply depending on system and degree of redundancy built in the system. An outage may be a forced outage (emergency) or a scheduled outage (maintenance). Upon forced outage of a component, it is taken out of service immediately either automatically or through a protection scheme switching operations. Outage may also be there by malfunctioning of an equipment or human error. During scheduled outage component is preplanned to be taken out of service at selected time, normally for the sake if preventive maintenance (Sec. 7.19) or overhaul or repair. A scheduled outage if necessary, may be postponned. A momentary outage (short duration) is caused by the reclosing breaker to clear a temporary fault. The outages (forced) in T and D systems may be there due to lightning, wind, vehicle accident, tree contact etc.

Continuous Markov Process

The state space method can be used for reliability evaluation. System is represented by its states and the possible transition between states.

A set of random variables with the variables ordered in a given sequence is called stochastic process. The values assumed by the variables form the state space. In power system studies the state space is discrete but the probability index is continuous. This special class of stochastic processes is known as Markov process. A Markov process with discrete index is known as Markov chain.

Figure 7.21 shows the state space diagram of a single repairable component whose failure and repair rates are characterized by exponential distributions. Let

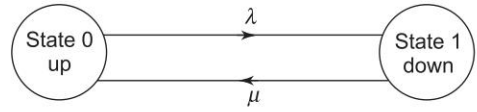

Fig. 7.21 State space diagram

$P_0(t)$ = prob. that the component is in state 0 at time t

$P_1(t)$ = prob. that the component is in state 1 at time t.

If the process starts from 0, i.e. the system is in state 0 at time 0, $P_0(0) = 1$ and $P_1(0) = 0$. It can then be shown that [1, 2, 8, 13]

$$\text{Reliability} = R(t) = P_0(t) = \frac{\mu}{\lambda+\mu} + \frac{\lambda e^{-(\lambda+\mu)t}}{\lambda+\mu} \tag{7.109}$$

$$P_1(t) = \frac{\lambda}{\lambda+\mu} + \frac{\lambda e^{-(\lambda+\mu)t}}{\lambda+\mu} \tag{7.110}$$

when $t \to \infty$, the probabilities are known as limiting state probabilities given by Eqs (7.20) and (7.21).

Planning of Generating Capacity – Loss of Load Probability (LOLP)

The outages of generating units may be ignored if they do not result in load-shedding i.e. loss of load. But if this result in insufficient generating capacity resulting in inability to supply the load fully. There is a need to evaluate the loss of load probability from the outage probability. For this we require:

(i) List of generating units with their FOR (forced outage rate)

(ii) List of forecasted daily peak loads for a period of one year (see Ch. 16 of Ref. 13)

If an outage O_k has the probability P_k and if due to outage, the peak load cannot be supplied for r_k days, the probability of loss of load is $O_k\, r_k$ days. Summing up all such probabilities of the loss of load due to all probable capacity outages, the system loss of load probability

$$\text{LOLP} = \sum_k O_k r_k \quad \text{days/year} \tag{7.111}$$

Frequency and Duration of a State

The forced outage rate O_k of a unit does not indicate anything about the duration of an outage stage or the frequency of encountering that state.

The frequency f_2 of encountering an outage state can be found out as:

$$f_2 = \frac{1}{T} = Q\mu \tag{7.112}$$

Similarly, frequency f_1 of encountering the up state can be found out as

$$f_1 = \frac{1}{T} = R\lambda \tag{7.113}$$

T = mean cycle time
R = reliability of the unit = p(up)
Q = unreliability of the unit = p(down)

Reliability Planning

The ultimate goal in power system reliability analysis is the evaluation of the total system so that overall reliability measures can be achieved. However, this is too ambitious and tough task due to large number of components and complex interconnections. Hence it is advisable to calculate reliability indices separately for the generation, transmission and distribution systems. An additional advantage is easy identification of the weakest links and components and remedial measures can be taken for reliability improvement through the use of better components and provision of redundancy. In Generation subsystem it means making available additional generation capacity. In transmission subsystem it means that stronger ties should exist between plants and load centres. This extra transmission capacity can be used to avoid overloading during normal operating conditions. Redundancy in distribution subsystem means duplication of some important components and employment of better bus schemes. Avoidance of imperfect switching devices is a must as they mainly cause unreliable operation.

Example 7.9 A radial system consists of a transformer and a distributor 0.5 km long. *Given*: $\lambda_{tr} = 0.6$ failures/year and $\lambda_{\text{distributor}} = 8$ failures per km per year; $\mu_{tr} = 5$ hours, $\mu_{\text{dist}} = 4$ hours.

Find: (i) λ_{system}, (ii) down time per outage, (iii) total outage time per year

Solution

(i) Failure rate = $0.6 + 8 \times 0.5 = 4.6$ outages/year

(ii) Down time = $\dfrac{0.6 \times 5 + 8 \times 4}{4.6} = 7.6$ hours/outage

(iii) Total outage time = $4.6 \times 7.6 = 34.96$ hours/year

Interconnected Systems

The adequacy of the generating capacity in a power system is generally improved by interconnecting the system to another power system. Each interconnected system can then operate at a given risk level with a lower reserve

than would be needed otherwise. This is possible due to diversity in the probabilistic occurrence of load and capacity outages in the different systems. There are several probabilistic methods available which provide a quantitative reliability assessment of interconnected system generation capabilities. The loss of load expectation (LOLE) approach is the most widely used technique [13]. Ref. 13 also shows evaluation techniques by considering a hypothetical example. It also discusses how the effect of load forecast uncertainty can be considered.

Composite Generation and Transmission Systems

One of the most important elements in power system planning is to find out how much generation is needed to satisfy given load requirements. A second equally important element in the planning process is the development of a suitable transmission network to provide the energy generated to the customer load points. The transmission network can be divided into the two general areas of bulk transmission and distribution facilities.

Distribution system design (Ch. 21) is normally a separate and independent process. The overall problem of assessing the adequacy of the generation and bulk power transmission systems to provide a dependable and suitable supply at the terminal load stations is called a composite system reliability evaluation.

Reliability concepts can be applied to power system network of Fig. 6.17 (three bus system). The conditional probability approach can be employed to develop the expression [13] for the probability of load point failure.

The probability of inadequate transmission capability in each configuration of Fig. 6.17 can be found after performing a load flow study on each configuration say as shown in Fig. 7.22 using the appropriate load model.

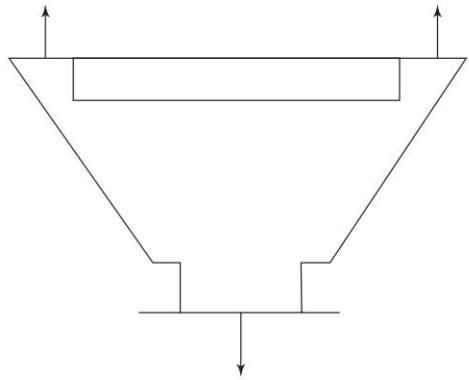

Fig. 7.22 One possible configuration of Fig. 6.17

If line overload is to be considered, then a DC load flow may be used, but if voltage is also to be included as a load point criterion, then AC load flow has to be used.

The evaluation of a composite system in a practical configuration including both generation and bulk transmission is a very complex problem. The data may be deterministic or stochastic. In view of the environmental, ecological, societal and economic constraints faced by electric companies, it is expected that the reliability evaluation will receive greater attention in future.

Quantitative assessment of each subsystem or hierarchical level to be done separately and combined appropriately to give indices of relevant systems or subsets of systems. The quantitative indices so arrived at are used in the managerial decision making process at that hierarchical level in order to find out the most appropriate expansion and reinforcement schemes, operating policies, and maintenance strategies. Quantitative reliability evaluation does not remove the decision-making process from the engineer or manager but only enhances the quality of the decision by adding quantitative measures to the decision process. With deregulation and privatization, these decisions are now left to individual private power producers in response to market forces. The values of LOLP and VOLL (value of lost load) embedded in the pool (energy trading) pricing mechanism are intended to be indicators that decide the installation of additional generation.

This short account would encourage the readers, to widen and deepen their knowledge and understanding of power system reliability by consulting the available technical papers and publications [1, 2, 8, 9, 13, 29].

7.11 SUMMARY

This chapter deals with economic operation of pure thermal system and hydrothermal system. Unit commitment and Maintenance Scheduling problems are discussed in considerable detail for pure thermal system using Dynamic Programming technique. A very important topic of power system optimal operation including economic dispatch, unit commitment, maintenance, reliability is fully and thoroughly discussed along with illustrative examples and computational algorithms. Power System Reliability and Power System Security are the important topics introduced so that interested reader can do further study using existing literature. Approximate solutions with loss coefficients and exact method for optimal load flow solution have also been discussed.

Problems

7.1 Consider the following incremental cost curves in Rs/MWh for a plant having 2 units.

$$\frac{\mathrm{d}C_1}{\mathrm{d}P_{G1}} = 0.20\,P_{G1} + 40$$

$$\frac{dC_2}{dP_{G2}} = 0.25\,P_{G2} + 30$$

Calculate the extra cost incurred in Rs/h, if a load of 220 MW is scheduled as $P_{G1} = P_{G2} = 110$ MW.

7.2 A constant load of 300 MW is supplied by two 200 MW generators, 1 and 2, for which the respective incremental fuel costs are

$$\frac{dC_1}{dP_{G1}} = 0.1\,P_{G1} + 20$$

$$\frac{dC_2}{dP_{G2}} = 0.12\,P_{G2} + 15$$

with powers P_G in MW and costs C in Rs/h. Determine (a) the most economical division of load between the generators, and (b) the saving in Rs/day thereby obtained compared to equal load sharing between machines.

7.3 Figure P-7.3 shows the incremental fuel cost curves of generators A and B. How would a load (i) more than $2P_G$, (ii) equal to $2P_G$, and (iii) less than $2P_G$ be shared between A and B if both generators are running.

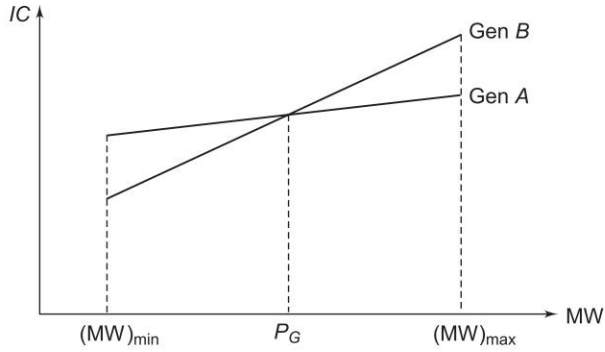

Fig. P-7.3

7.4 Consider the following three *IC* curves

$$P_{G1} = -100 + 50\,(IC)_1 - 2\,(IC)_1^2$$

$$P_{G2} = -150 + 60\,(IC)_2 - 2.5\,(IC)_2^2$$

$$P_{G3} = -80 + 40\,(IC)_3 - 1.8\,(IC)_3^2$$

where ICs are in Rs/MWh and P_Gs are in MW.

The total load at a certain hour of the day is 400 MW. Neglect transmission loss and develop a computer programme for optimum generation scheduling within an accuracy of ± 0.05 MW. (*Note*: This problem also has a direct solution.)

Note: All P_Gs must be real positive.

7.5 For a certain generating unit of a thermal power plant, the fuel input in millions of kilocalories per hour can be expressed as a function of power output P_G in megawatts by the equation

$$0.0001P_G^3 + 0.03P_G^2 + 12.0P_G + 150$$

Find the expression for incremental fuel cost in rupees per megawatt hour as a function of power output in megawatts. Also find a good linear approximation to the incremental fuel cost as a function of P_G.
Given: Fuel cost is Rs 2/million kilocalories.

7.6 For the system of Example 7.4, the system λ is Rs 26/MWh. Assume further the fuel costs at no load to be Rs 250 and Rs 350 per h, respectively for plants 1 and 2.
(a) For this value of system λ, what are the values of P_{G1}, P_{G2} and received load for optimum operation.
(b) For the above value of received load, what are the optimum values of P_{G1} and P_{G2}, if system losses are accounted for but not coordinated.
(c) Total fuel costs in Rs/h for parts (a) and (b).

7.7 Figure P-7.7 shows a system having two plants 1 and 2 connected to buses 1 and 2, respectively. There are two loads and a network of three branches. The bus 1 is the reference bus with voltage of $1.0 \angle 0^\circ$ pu. The branch currents and impedances are

$$I_a = 2 - j0.5 \text{ pu}$$
$$I_b = 1.6 - j0.4 \text{ pu}$$
$$I_c = 1.8 - j0.45 \text{ pu}$$
$$Z_a = 0.06 + j0.24 \text{ pu}$$
$$Z_b = 0.03 - j0.12 \text{ pu}$$
$$Z_c = 0.03 - j0.12 \text{ pu}$$

Calculate the loss formula coefficients of the system in per unit and in reciprocal megawatts, if the base is 100 MVA.

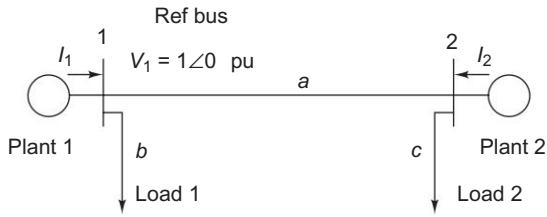

Fig. P-7.7 Sample system

7.8 For the power plant of the illustrative example used in Sec. 7.3, obtain the economically optimum unit commitment for the daily load cycle given in Fig. P-7.8. Correct the schedule to meet security requirements.

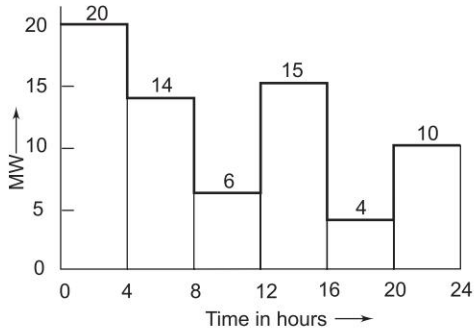

Fig. P-7.8 Daily load curve for Problem P-7.8

7.9 Repeat Example 7.3 with a load of 220 MW from 6 a.m. to 6 p.m. and 40 MW from 6 p.m. to 6 a.m.

7.10 For the system of Problem 7.7

$$IC_1 = 0.1\, P_{G1} + 20.0 \text{ Rs/MWh}$$

$$IC_2 = 0.2\, P_{G2} + 30.0 \text{ Rs/MWh}$$

Using λ = Rs 40/MWh, find the values of real power generation P_{G1} and P_{G2} at the buses 1 and 2.

[Ans. P_{G1} = 168.495 MW, P_{G2} = 46.96 MW]

7.11 Reformulate the optimal hydrothermal scheduling problem considering the inequality constraints on the thermal generation and water storage employing penalty functions. Find out the necessary equations and gradient vector to solve the problem.

References

Books

1. Billinton, R., *Power System Reliability Evaluation*, Gordon and Breach, New York, 1970.
2. Billinton, R., R.J. Ringlee and A.J. Wood, *Power System Reliability Calculations*, The MIT Press, Boston, Mass, 1973.
3. Kusic, G.L., *Computer Aided Power System Analysis*, Prentice-Hall, Englewood Cliffs, New Jersey, 1986.
4. Kirchmayer, L.K., *Economic Operation of Power Systems*, Wiley, New York, 1958.
5. Kirchmayer, L.K., *Economic Control of Interconnected Systems*, Wiley, New York, 1959.
6. Knight, U.G., *Power Systems Engineering and Mathematics*, Pergamon Press, New York, 1972.

7. Singh, C. and R. Billinton, *System Reliability, Modelling and Evaluation*, Hutchinson, London, 1977.
8. Sullivan, R.L., *Power System Planning*, McGraw-Hill, New York, 1977.
9. Wood, A.J. and B.F. Wollenberg, *Power Generation, Operation and Control*, 2nd edn, Wiley, New York, 1996.
10. Mahalanabis, A.K., D.P. Kothari and S.I. Ahson, *Computer Aided Power System Analysis and Control*, Tata McGraw-Hill, New Delhi, 1988.
11. Bergen, A.R., *Power System Analysis*, Prentice-Hall, Englewood Cliffs., New Jersey, 1986.
12. Billinton, R. and R.N. Allan, *Reliability Evaluation of Power System*, Plenum Press, New York, 1984.
13. Kothari, D.P. and I.J. Nagrath, *Modern Power System Analysis,* 3rd edn, McGraw-Hill, New York, 2006.
14. Khatib, H., "Economics of Power Systems Reliability", *Technicopy* Ltd., Stonehouse, Glasgow, U.K. 1978.
15. Warwick, K., A.E. Kwue and R. Aggarwal, (Eds), *AI Techniques in Power Systems*, *IEE*, UK, 1997.
16. Momoh, J.A., *Electric Power System Applications of Optimization*, Marcel Dekker, Inc, NY, 2001.
17. Yong-Hua Song (Ed.), *Modern Optimization Techniques in Power Systems*, Kluwer Academic Publishers, London, 1999.
18. Debs, A.S., *Modern Power Systems Control and Operation,* KAP, New York, 1988.
19. Kothari, D.P. and J.S. Dhillon, *Power System Optimization,* PHI, New Delhi, 2004.
20. Ramkumar, R., *Engineering Reliability Fundamentals and Applications,* Prentice-Hall, NJ, 1993.

Papers

21. Meyer, W.S. and V.D. Albertson, "Improved Loss Formula Computation by Optimally Ordered Elimination Techniques'" *IEEE Trans.,* PAS, 1971, 90: 716.
22. Hill, E.F. and W.D. Stevenson, Jr., "A New Method of Determining Loss Coefficients", *IEEE Trans.,* PAS, July 1968, 87: 1548.
23. Agarwal, S.K. and I.J. Nagrath, "Optimal Scheduling of Hydrothermal Systems", *Proc. IEEE*, 1972, 199: 169.
24. Ayub, A.K. and A.D. Patton, "Optimal Thermal Generating Unit Commitment", *IEEE Trans*., July-Aug. 1971, PAS-90: 1752.
25. Dopazo, J.F., *et al*., "An Optimization Technique for Real and Reactive Power Allocation", *Proc. IEEE*, Nov. 1967, 1877.
26. Happ, H.H., "Optimal Power Dispatch—A Comprehensive Survey", *IEEE Trans.,* 1977, PAS-96: 841.
27. Harker, D.C., "A Primer on Loss Formula", *AIEE Trans.,* 1958, pt. III, 77: 1434.
28. IEEE Committee Report, "Economy-Security Functions in Power System Operations", *IEEE Special Publication 75 CHO 969.6 PWR*, New York, 1975.
29. Kothari, D.P., "Optimal Hydrothermal Scheduling and Unit Commitment", *Ph. D. Thesis*, B.I.T.S, Pilani, 1975.

30. Kothari, D.P. and I.J. Nagrath, "Security Constrained Economic Thermal Generating Unit Commitment", *J.I.E.* (India), Dec. 1978, 59: 156.
31. Nagrath, I.J. and D.P. Kothari, "Optimal Stochastic Scheduling of Cascaded Hydro-thermal Systems", *J.I.E.* (India), June 1976, 56: 264.
32. Berrie, T.W., *Power System Economics*, *IEE*, London, 1983.
33. Berrie, T.W., *Electricity*, *Economics and Planning*, *IEE*, London, 1992.
34. Peschen, J., *et al.*, "Optimal Control of Reactive Power Flow", *IEEE Trans*., 1968, PAS-87: 40.
35. Dommel, H.W. and W.F. Trinney, "Optimal Power Flow Solution", *IEEE Trans*., October 1968, PAS-87: 1866.
36. Sasson, A.M. and H.M. Merrill, "Some Applications of Optimization Techniques to Power System Problems", *Proc. IEEE*, July 1974, 62: 959.
37. Wu, F., *et al*., "A Two-Stage Approach to Solving Optimal Power Flows", *Proc. 1979 PICA Conf*., pp. 126–136.
38. Nanda, J., P.R. Bijwe and D.P. Kothari, Application of Progressive Optimality Algorithm to Optimal Hydrothermal Scheduling Considering Deterministic and Stochastic Data, *Int. J. Elect. Power and Energy Syst.*, Jan. 1986, 8: 61.
39. Kothari, D.P., *et al*., "Some Aspects of Optimal Maintenance Scheduling of Generating Units", *J.I.E.* (India), August 1985, 66: 41.
40. Kothari, D.P. and R.K. Gupta, Optimal Stochastic Load Flow Studies, *J.I.E.* (India), August 1978, p. 34.
41. "Description and Bibliography of Major Economy-Security Functions—Part I, II, and III", *IEEE Committee Report*, *IEEE Trans*., Jan. 1981, PAS-100: 211–235.
42. Bijwe, P.R., D.P. Kothari, J. Nanda and K.S. Lingamurthy, "Optimal Voltage Control using Constant Sensitivity Matrix", *Electric Power System Research*, vol. II, no. 3, Dec. 1986, pp. 195–203.
43. Nanda, J., D.P. Kothari and K.S. Lingamurthy, "Economic Emission Load Dispatch through Goal Programming Techniques", *IEEE Trans*., *on Energy Conversion*, vol. 3, no. 1, March 1988, pp. 26–32.
44. Nanda, J., D.P. Kothari and S.C. Srivastava, " A New Optimal Power Dispatch Algorithm using Fletcher's QP Method", *Proc. IEE,* pte, vol. 136. no. 3, May 1989, pp. 153–161.
45. Dhillon, J.S., S.C. Parti and D.P. Kothari, "Stochastic Economic Emission Load Dispatch", *Int. J. of Electric Power System Research,* vol. 26, no. 3, 1993, pp. 179–183.
46. Dhillon, J.S., S.C. Parti and D.P. Kothari, "Multiobjective Optimal Thermal Power Dispatch", *Int. J. of EPES,* vol. 16, no. 6, Dec. 1994, pp. 383–389.
47. Kothari, D.P. and Aijaz Ahmad, "An Expert System Approach to the Unit Commitment Problem", *Energy Conversion and Management",* vol. 36, no. 4 April 1995, pp. 257–261.
48. Sen, Subir, D.P. Kothari and F.A Talukdar, "Environment Friendly Thermal Power Dispatch—An Approach", *Int. J. of Energy Sources,* vol. 19, no. 4, May 1997, pp. 397–408.
49. Kothari, D.P. and A. Ahmad, "Fuzzy Dynamic Programming Based Optimal Generator Maintenance Scheduling Incorporating Load Forecasting", in *Advances in Intelligent Systems,* edited by F.C. Morabito, IOS Press, Ohmsha, 1997, pp. 233–240.

50. Ahmad Aijaz and D.P. Kothari, "A Review of Recent Advances in Generator Maintenance Scheduling", *Electric Machines and Power Systems,* vol. 26, no. 4, 1998, pp. 373–387.
51. Sen, S. and D.P. Kothari, "Evaluation of Benefit of Inter-Area Energy Exchange of Indian Power System Based on Multi-Area Unit Commitment Approach", *Int. J. of EMPS,* vol. 26, no. 8, Oct. 1998, pp. 801–813.
52. Sen, S. and D.P. Kothari, "Optimal Thermal Generating Unit Commitment-A Review, "*Int. J. EPES,* vol. 20, no. 7, Oct. 1998, pp. 443–451.
53. Kulkarni, P.S., A.G. Kothari and D.P. Kothari, "Combined Economic and Emission Dispatch using Improved BPNN", *Int. J. of EMPS,* vol. 28, no. 1, Jan. 2000, pp. 31–43.
54. Arya, L.D., S.C. Chaude and D.P. Kothari, "Economic Despatch Accounting Line Flow Constraints using Functional Link Network," *Int. J. of Electrical Machine & Power Systems,* 28, 1, Jan. 2000, pp. 55–68.
55. Ahmad, A. and D.P. Kothari, "A Practical Model for Generator Maintenance Scheduling with Transmission Constraints", *Int. J. of EMPS,* vol. 28, no. 6, June 2000, pp. 501–514.
56. Dhillon, J.S. and D.P. Kothari, "The Surrogate Worth Trade off Approach for Multiobjective Thermal Power Dispatch Problem". *EPSR,* vol. 56, no. 2, Nov. 2000, pp. 103–110.
57. Sen, S. and D.P. Kothari, "Large Scale Thermal Generating Unit Commitment: A New Model", in *The Next Generation of Electric Power Unit Commitment Models,* edited by B.F. Hobbs *et al*., KAP, Boston, 2001, pp. 211–225.
58. Dhillon, J.S., S.C. Parti and D.P. Kothari, "Fuzzy Decision Making in Multi-objective Long-term Scheduling of Hydrothermal System", *Int. J. of EPES,* vol. 23, no. 1, Jan. 2001, pp. 19–29.
59. Brar, Y.S., J.S. Dhillon and D.P. Kothari, "Multiobjective Load Dispatch by Fuzzy Logic based Searching Weightage Pattern," *Electric Power Systems Research*, vol. 63, 2002, pp. 149–160.
60. Dhillon, J.S., S.C. Parti and D.P. Kothari, "Fuzzy Decision-making in Stochastic Multiobjective Short-term Hydrothermal Scheduling," *IEE Proc. GTD*, vol. 149, 2, March 2002, pp. 191–200.
61. Kothari, D.P., Application of Neural Networks to Power Systems (Invited Paper), *Proc. Int. Conf., ICIT 2000*, Jan. 2000, pp. 621–626.
62. Stott, B., O. Alsac and A.J. Monticelli, "Security Analysis and Optimization", *Proc. IEEE,* vol. 75, no. 12, Dec. 1987, pp. 1623–1644.
63. Bath, S.K., J.S. Dhillon and D.P. Kothari, " Stochastic Multiobjective Generation Dispatch," *Int. J. of Electric Power Component and Systems*, vol. 32, 2004, pp. 1083–1103.
64. Bath, S.K., J.S. Dhillon and D.P. Kothari, "Fuzzy Satisfying Multiobjective Generation Scheduling by Weightage Pattern Search Methods", *EPSR*, vol. 69, 2004, pp. 311–320.
65. Bath, S.K., J.S. Dhillon and D.P. Kothari, "Stochastic Multiobjective Generation Dispatch by Search Methods," *AJIT,* vol. 4(9), 2005, pp. 823–831.

66. Bath, S.K., J.S. Dhillon and D.P. Kothari," Stochastic Multobjective Generation Allocation using Pattern Search Method, *Proc. IEE GTD,* vol. 153, no. 4, July 2006, pp. 476–484.
67. Dhillon, J., J.S. Dhillon and D.P. Kothari, "Interactive Search based Stochastic Multiobjective Thermal Power Dispatch," *Asian Jounral of Inf. Tech.,* 6(3), 2007, pp. 314–322.
68. DyLiacco, T.E., The Adaptive Reliability Control Systems, *IEEE Trans., on PAS*, vol. PAS-86, no. 3., May 1967, pp. 517–531.
69. Fink, L. and K. Carlsen, 'Operating Under Stress and Strain', *IEEE Spectrum*, March 1978, pp. 48–50.
70. Stott, B., O. Alsac and A.J. Monticelli, Security Analysis and Optimization, *Proc. IEEE*, vol. 75, no. 12, Dec. 1987, pp. 1623–1644.
71. Arya, L.D., Security Constrained Power System Optimization, *Ph.D. Thesis*, IIT Delhi, 1990.
72. Nanda, J., D.P. Kothari and S.C. Srivastava, A New Optimal Power Dispatch, Algorithm using Fletcher's Quadratic Programming Method, *IEE Proc. C*, vol. 136, pt., no. 3, May 1989, pp. 153–161.
73. Dhillon, J.S., S.C. Parti and D.P. Kothari, Stochastic Economic Emission Load Dispatch, *Int. J. Electric Power System Research,* vol. 26, no. 3, 1993, pp. 179–183.
74. Bijwe, P.R., D.P. Kothari and L.D. Arya, 'Alleviation of Line Overloads and Voltage Violations by Corrective Rescheduling', *IEE Proc. C*. vol. 140, no. 4, July 1993, pp. 249–255.

Annexure 7.1

Unit Commitment

A 7.1 INTRODUCTION

There are many factors involved in the successful operation of electric power system. The system is expected to have power instantaneously and continuously available to meet customers demands. In order to meet the demands it is necessary to commit adequate generating units. The economical operation demands interaction of the major control functions such as load forecasting, unit commitment, economic dispatch, security analysis, etc. An overall solution to these set of problems must result in a continuous and reliable supply of electricity while maintaining the optimal cost of production and operation for the system.

Economic factors influenced by actions of operating personnel include the loading of generating equipment, particularly of thermal plants, where unit efficiencies and fuel costs are major factors in the cost of power production. The proper operation of hydro plants can also affect generation cost, where at times of the year the availability of water is high and at other times must be conserved. Purchase power availability, cost and the scheduling of overhaul of generating unit all affect operating costs. The system operators can have considerable control over these factors.

A 7.2 UNIT COMMITMENT

One of the most important problems in operational scheduling of electric power generation is the unit commitment. It involves determining the start-up and shut-down (ON/OFF) schedules of generating units to be used to meet forecasted demand over a short-term (24–168 hours) period. The objective is to minimize total production cost to meet system demand and reserve requirements while observing a large set of operating constraints. The unit commitment problem (UCP) is a complex mathematical optimization problem having both integer and continuous variables.

The recent trend of installing large size thermal units (660 MW and above), complexity of power network and more concern about environment pollution has further created a need for finding better approaches for determination of economic-emission unit commitment schedule. Proper scheduling ensures that better use is made of available capacity.

Prior to solving the economic dispatch problem, unit commitment problem should be solved because only those units which were allocated to generating duties by the unit commitment solution can be considered for power generation.

Traditionally, in a vertically integrated utility environment, a utility system operator, who had the knowledge of system components, constraints and operating costs of generating units, made decisions on unit commitment for minimizing the utility's generation cost. The Security constrained unit commitment (SCUC) determines generating unit schedules in a utility for minimizing the operating cost and satisfying the prevailing constraints, such as load balance, system spinning reserve, ramp rate limits, fuel constraints, multiple emission requirements as well as minimum up and down time limits over a set of time periods. The SCUC insures system transmission and voltage security including the occurrences of $n - 1$ transmission contingencies. Three elements are included in the SCUC paradigm: supplying load, maximizing security and minimizing cost. Satisfying load is a hard constraint and an obligation for SCUC. Maximizing security could often be satisfied by supplying sufficient spinning reserve at less congested regions, which could easily be accessible by loads. Cost minimization is realized by committing less expensive units while satisfying the corresponding constraints and dispatching the committed units economically.

In the restructured deregulated environment, electric power system has now moved from vertically integrated to horizontally integrated utilities. The market share the features of decentralized competitive bidding in auction markets for energy and reserves and some degree of non-discriminatory pricing as well as access to transmission. In some deregulated markets, the ISO commits generating units in the same way as system operators did in the vertically integrated structure using the SCUC. Suppliers submit their bids to supply the forecasted daily demand. The ISO uses the bid-in costs submitted by GENCOs for each generating unit to minimize the cost of operation, determine which units will be dispatched in how many hours and calculate the corresponding market clearing prices (MCP) while the system security is retained. The ISO also obtains information from TRANSCOs via the open access same time information system (OASIS) on transmission capability and availability.

In some other deregulated markets, the unit commitment is the responsibility of the individual GENCOs in order to maximize their own profit. GENCOs decision is associated with financial risks. This unit commitment has different objective than that of SCUC and is referred to as price-based unit commitment (PBUC) to emphasize the importance of price signal. In this case, satisfying load is no longer an obligation and the objective would be to maximize the profit. In this paradigm, the signal that would enforce a unit's ON/OFF status would be the price, including the fuel purchase price, energy sale price, ancillary service sale price etc. GENCOs submit single-part bids to the ISO for minimizing the risk of not knowing the number of hours that they would be dispatched or MCPs that would be paid on during dispatched hours. The ISO uses GENCOs' single-part bids, aggregates them and determines the MCP. Here, the ISOs objective is to maintain the system security. In the SCUC, demand forecast advised the system operators of the amount of power to be

generated. However, in the PBUC, bilateral contracts will make part of the system demand known *a priori* and the remaining is forecasted.

Constraints of Unit Committment Problem

The objective of UCP is to minimize the total production cost over the scheduling horizon. The total production cost consists of fuel cost, start-up cost and shut-down cost. Fuel cost is calculated by using heat rate and fuel price information. Start-up cost is expressed as a function of the number of hours the unit has been down (exponential when cooling and linear when banking). The shut-down cost is given by fixed amount for each unit shut down.

Further, UCP is a practical problem and must take into account a large number of practical constraints. These constraints are system, device/ operational and environmental type. Again, these are broadly categorized as equality and inequality constraints.

Equality constraint is described by the system power balance (demand plus loss and export) also known as demand constraint i.e.,

$$\sum_{i}^{N} P_i = P_D$$

where P_D : Load demand

N : Number of units committed at a particular hour

Inequality constraints are:

- Minimum up-time and down-time.
- Unit generation capability (upper/lower) limits.
- Ramp rate limits.
- System reserve requirement.
- Plant crew constraint.
- Unit status restrictions (must-run, fixed-MW, unavailable/available).

The most non-linear constraints are the units minimum up-time and down-time restriction. A unit is to be started up only if it will run for a minimum number of continuous hours. By contrast, minimum down-time is the number of hours a unit must be off-line before it can be brought on-line again. Violation of down-time constraint may be alleviated by banking the unit.

The upper and lower limits of generation on the generating units force them to operate within their boundaries of operation.

The rate of increasing or decreasing electrical output from the unit is restricted by the ramp rate limit.

System reserve requirement pertains to supply the load throughout the scheduling period with certain degree of reliability even during outage of some committed units.

Plant crew constraint pertains to the number of units that can be started at the same time in a particular plant due to the limited personnel (crew) available.

For multi-area unit commitment, the system constraint must be modified to take into account the interchange schedules and the tie-line limitations.

Optimization Techniques

The UCP belongs to the class of complex combinational optimization problem. They ranged from simple to complicated methods. The method adopted by different entities depends on their mix of units and operating constraints. Several mathematical programming techniques have been proposed to solve this time-dependent problem. Recent mathematical developments and advances in computing technologies have made the problem to be readily solvable. Major available methods for unit commitment can be grouped as below:

- Deterministic techniques
- Meta-heuristic techniques
- Hydrothermal coordination

Deterministic approaches include priority list, inter/mixed-integer programming method, dynamic and linear programming, branch-and-bound method, decomposition technique, and colony system and Lagrangian relaxation.

Meta-heuristic approaches include expert system, fuzzy logic, artificial neural networks, genetic algorithm, evolutionary programming, simulated annealing, tabu search and memetic algorithm (hybrid technique).

Large scale UCP can also be solved using "equivalencing" like method comprising three steps: aggregation, solution and disaggregation.

Hydrothermal Coordination

The problem of short-term hydro scheduling is to determine the optimum hourly generation production of hydro units, water flows through generating stations, reservoir releases and storage levels. The objective is to maximize the energy production from hydro resources.

In a hydrothermal system, short-term hydro scheduling is to done as part of hydrothermal coordination. The hydrothermal coordination problem requires the solution for the thermal unit commitments and generation dispatch as well as the hydro schedules. The objective here is to minimize the thermal production cost subject to meeting the load and other generation requirements. Most of the methods for solving the hydrothermal coordination problem are based on decomposition methods involving the unit commitment and hydro scheduling sub problems. The coordination procedure depends on the decomposition method used like heuristic decomposition, combined Lagrangian relaxation and network flow programming, genetic algorithm etc.

Unit Commitment in Deregulated Market

In the deregulated markets, the UCP requires a formulation similar to the PBUC that includes the electricity market in the model. The main difficulty under

deregulation is that the spot price of electricity is no longer pre-determined but set by open competition. This hourly spot prices have shown evidence of being highly volatile. The volatility of the spot prices is accounted for using a probabilistic technique to develop unit commitment schedules for continually changing loads in an interconnected power system configuration for a specified period. The SCUC programme optimizes the scheduled generation and price-sensitive load while satisfying generation, reserve requirements, transmission constraints and generator operating constraints such as minimum up and down times.

Discussion

Priority list (PL) method of solving UCP is the simplest and fastest but achieves sub-optimal solution. Dynamic programming (DP) techniques, essentially based on PLs are flexible but the computation time suffers from the "curse of dimensionality", which leads to more mathematical complexity and increase in computation time. Lagrangian relaxation (LR) methods are now among the most widely used approaches for solving UCP. The LR method provides a faster solution but it suffers from numerical convergence and existence of duality gap. Augmented LR resolves the duality gap by incorporating a penalty function with different sorts of system constraints. The integer and mixed integer methods adopt linear programming to solve and check for an integer solution. These methods fail when number of units increases because they require a large memory and suffer from great computational delay. Branch-and-bound method employs a linear function to represent fuel cost and start-up cost and obtains a lower and upper bounds. The deficiency of this method is the exponential growth in the execution time for systems of a practical size. Any colony system approach is similar to ants finding the shortest path to its destination. Ants can smell pheromone and when choosing their path, they tend to choose paths marked by strong pheromone concentrations to find their way back to the food by their nest mates.

Expert system (ES) is an intelligent technique that uses theoretical and practical knowledge inference procedures to solve the UCP. Fuzzy logic (FL) method allows a qualitative description of the behaviour of a system, the systems' characteristics, and response without the need for exact mathematical formulation. Artificial neural network (ANN) has become among the most widely used tools for solving many optimization problems. ANN parameters are estimated based on a database holding typical load curves and corresponding unit commitment optimal schedules. ANN respond to changes in operating conditions when presented with sufficient facts, even though they are trained off-line. Genetic algorithm (GA) is a general-purpose stochastic and parallel search method based on the mechanism of natural selection and natural genetics. It has the potential of obtaining near-global minimum and the capability of obtaining the solution within short time and the constraints can be easily included.

Evolutionary programming (EP)s are quite similar to the GAs with the main difference being in representing and encoding of the candidates, type of alterations to create new solutions, and mechanism of selecting new "parents". The EP has the advantages of good convergence and a significant speedup over traditional GAs and can obtain high quality solutions. The "curse of dimensionality" is surmounted and the computational burden is almost linear with the problem scale. Simulated annealing (SA) is a powerful, general-purpose stochastic optimization technique which can theoretically converge asymptotically to a global optimum solution. Tabu search (TS) is also a stochastic general-purpose optimization technique that has been successfully applied to number of combinatorial optimization problems. TS is a meta-heuristic method that iteratively explores a solution neighbourhood by incorporating adaptive memory and responsive exploration.

The hybrid methods can accommodate more complicated constraints and are claimed to have better quality solutions. Combined use of LR (Memetic Algorithm, it is GA combined with local search technique) methods provide the best result for the UCP.

Other Aspects of UCP

Other important aspects of UCP are as under:

(i) Multi-area unit commitment.
(ii) Emission constrained unit commitment.
(iii) Multi-objective unit commitment schedule.

Multi-area Constraints

Many utilities and power pools have limits on power flow between different areas/regions over tie lines. Each area/region have its own pattern of load variation and generation characteristics. They also have separate spinning reserve constraints. The techniques should select the units in each area in such a way that reserve requirements and transmission constraints will be satisfied. The techniques available to handle the multi-area constraints is based on commitment utilisation factor (CUF) in conjunction with average full-load cost (AFLC) to determine near optimal multi-area priority commitment order which are unified approach, efficient and easy to implement.

Extension of the sequential UC method that resembles 'bidding' can also be used to multi-area system employing DC power flow model to represent the inter-area transmission network. The DC power flow network model is more accurate than linear power flow model. The physical flow in transmission network is governed by the Kirchoff's current law (KCL) and Kirchoff's voltage law (KVL) which is taken care in DC model. In contrast, linear power flow model consider only the KCL. Probabilistic technique to develop a reliability constrained multi-area UC may also be used which is based on 'two risk concept'. This is useful for interconnected system with continually changing load and considering unit forced outages.

Emission Constraint

Generation of electricity from fossil fuel releases several pollutants, such as sulphur dioxide (SO_2), oxides of nitrogen (NO_x), carbon dioxide (CO_2), particulate matters etc. into the atmosphere. Reducing atmospheric pollution will be one of the major challenges for utilities with special emphasis to Kyoto protocol. One of the economic way of reducing SO_2 emission is to switch from high sulphur to low-sulphur fuels using a fast unit commitment and dispatch heuristic. Another approach is to solve the combined planning-operation optimization problem (i.e., minimize long run production costs including the cost of SO_2 control and emission) over a time horizon of interest using a fast UC and dispatch heuristic.

Multi Objective Unit Commitment

In contrast to existing UC solution, this method treats economy, security, emission and reliability as competing objectives for optimal UC solution. An operators preference in finding a compromised solution may be required in such an environment where most of these objectives are conflicting and improvement of one objective may degrade the performance of another.

A fast and efficient approach that integrates a fuzzy expert system with pattern recognition techniques for optimum generation scheduling and evaluating security transfer limits in an interconnected system has been established. The use of fuzzy logic in expert system reduces dimensionality of the input data while improving the results by taking into account operators preferences. Constraints related to the security have been incorporated using a pattern data base for different system scenarios.

Chapter 8

Automatic Generation and Voltage Control

8.1 INTRODUCTION

Power system operation considered so far was under conditions of steady load. However, both active and reactive power demands are never steady and they continually change with the rising or falling trend. Steam input to turbo-generators (or water input to hydro-generators) must, therefore, be continuously regulated to match the active power demand, failing which the machine speed will vary with consequent change in frequency which may be highly undesirable* (maximum permissible change in power frequency is ± 0.5 Hz). Also the excitation of generators must be continuously regulated to match the reactive power demand with reactive generation, otherwise the voltages at various system buses may go beyond the prescribed limits. In modern large interconnected systems, manual regulation is not feasible and therefore automatic generation and voltage regulation equipment is installed on each generator. Figure 8.1 gives the schematic diagram of load frequency and excitation voltage regulators of a turbo-generator. The controllers are set for a particular operating condition and they take care of small changes in load demand without frequency and voltage exceeding the prescribed limits. With the passage of time, as the change in load demand becomes large, the controllers must be reset either manually or automatically.

It has been shown in previous chapters that for small changes active power is dependent on internal machine angle δ and is independent of bus voltage; while bus voltage is dependent on machine excitation (therefore on reactive generation Q) and is independent of machine angle δ. Change in angle δ is caused by momentary change in generator speed. Therefore, load frequency

* Change in frequency causes change in speed of the consumers' plant affecting production processes. Further, it is necessary to maintain network frequency constant so that the power stations run satisfactorily in parallel, the various motors operating on the system run at the desired speed, correct time is obtained from synchronous clocks in the system, and the entertaining devices function properly.

and excitation voltage controls are non-interactive for small changes and can be modelled and analyzed independently. Furthermore, excitation voltage control is fast acting in which the major time constant encountered is that of the generator field; while the power frequency control is slow acting with major time constant contributed by the turbine and generator moment of inertia—this time constant is much larger than that of the generator field. Thus, the transients in excitation voltage control vanish much faster and do not affect the dynamics of power frequency control.

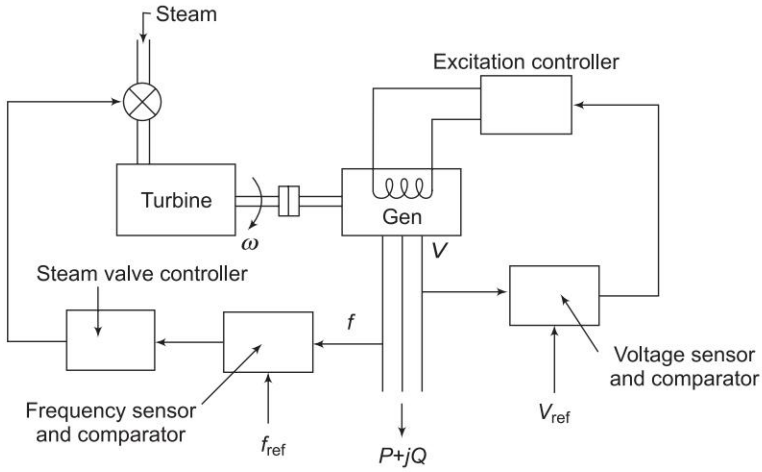

Fig. 8.1 Schematic diagram of load frequency and excitation voltage regulators of a turbo-generator

Changes in load demand can be identified as: (i) slow varying changes in mean demand, and (ii) fast random variations around the mean. The regulators must be designed to be insensitive to fast random changes, otherwise the system will be prone to hunting resulting in excessive wear and tear of rotating machines and control equipment.

8.2 LOAD FREQUENCY CONTROL (SINGLE AREA CASE)

Let us consider the problem of controlling the power output of the generators of a closely knit electric area so as to maintain the scheduled frequency. All the generators in such an area constitute a *coherent* group so that all the generators speed up and slow down together maintaining their relative power angles. Such an area is defined as a *control area*. The boundaries of a control area will generally coincide with that of an individual Electricity Board.

To understand the load frequency control problem, let us consider a single turbo-generator system supplying an isolated load.

Turbine Speed Governing System

Figure 8.2 shows schematically the speed governing system of a steam turbine. The system consists of the following components:

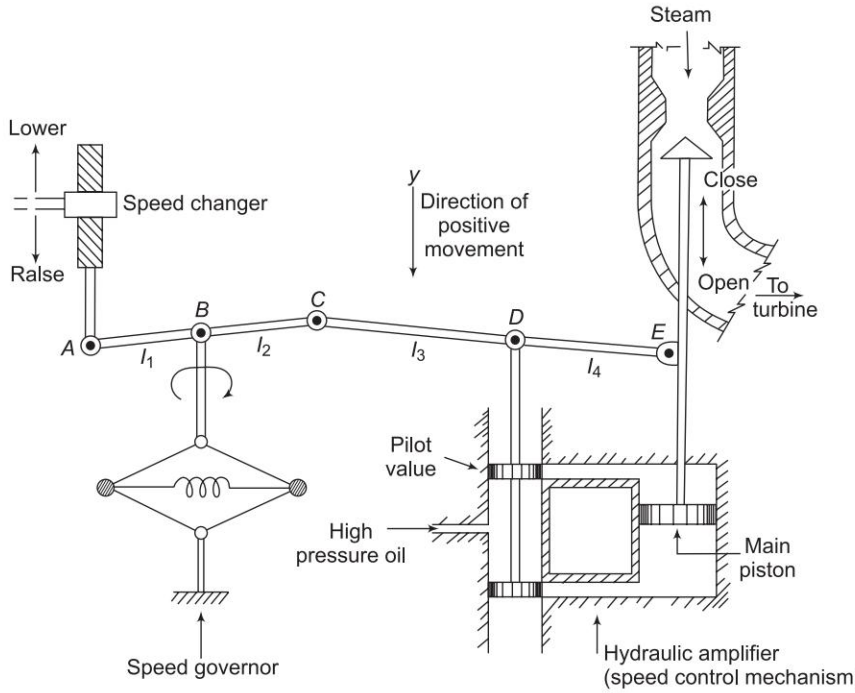

Fig. 8.2 Turbine speed governing system

(Reprinted with permission of McGraw-Hill Book Co., New York, from Olle I. Elgerd: *Electric Energy System Theory: An Introduction*, 1971, p. 322.)

(i) *Fly ball speed governor:* This is the heart of the system which senses the change in speed (frequency). As the speed increases the fly balls move outwards and the point B on linkage mechanism moves downwards. The reverse happens when the speed decreases.

(ii) *Hydraulic amplifier:* It comprises a pilot valve and main piston arrangement. Low power level pilot valve movement is converted into high power level piston valve movement. This is necessary in order to open or close the steam valve against high pressure steam.

(iii) *Linkage mechanism:* ABC is a rigid link pivoted at B and CDE is another rigid link pivoted at D. This link mechanism provides a movement to the control valve in proportion to change in speed. It also provides a feedback from the steam valve movement (link 4).

(iv) *Speed changer:* It provides a steady state power output setting for the turbine. Its downward movement opens the upper pilot valve so that more

steam is admitted to the turbine under steady conditions (hence more steady power output). The reverse happens for upward movement of speed changer.

Model of Speed Governing System

Assume that the system is initially operating under steady conditions—the linkage mechanism stationary and pilot valve closed, steam valve opened by a definite magnitude, turbine running at constant speed with turbine power output balancing the generator load. Let the operating conditions be characterized by

f^0 = system frequency (speed)
P_G^0 = generator output = turbine output (neglecting generator loss)
y_E^0 = steam valve setting

We shall obtain a linear incremental model around these operating conditions.

Let the point A on the linkage mechanism be moved downwards by a small amount Δy_A. It is a command which causes the turbine power output to change and can therefore be written as

$$\Delta y_A = k_C \Delta P_C \tag{8.1}$$

where ΔP_C is the commanded increase in power.

The command signal ΔP_C (i.e. Δy_E) sets into motion a sequence of events—the pilot valve moves upwards, high pressure oil flows on to the top of the main piston moving it downwards; the steam valve opening consequently increases, the turbine generator speed increases, i.e. the frequency goes up. Let us model these events mathematically.

Two factors contribute to the movement of C:

(i) Δy_A contributes $-\left(\frac{l_2}{l_1}\right)\Delta y_A$ or $-k_1 \Delta y_A$ (i.e. upwards) of $-k_1 k_C \Delta P_C$.

(ii) Increase in frequency Δf causes the fly balls to move outwards so that B moves downwards by a proportional amount $k'_2 \Delta f$. The consequent movement of C with A remaining fixed at Δy_A is $+\left(\frac{l_1 + l_2}{l_1}\right) k'_2 \Delta f = + k_2 \Delta f$ (i.e. downwards).

The net movement of C is therefore

$$\Delta y_C = - k_1 k_C \Delta P_C + k_2 \Delta f \tag{8.2}$$

The movement of D, Δy_D, is the amount by which the pilot valve opens. It is contributed by Δy_C and Δy_E and can be written as

$$\begin{aligned} \Delta y_D &= \left(\frac{l_4}{l_3 + l_4}\right) \Delta y_C + \left(\frac{l_3}{l_3 + l_4}\right) \Delta y_E \\ &= k_3 \Delta y_C + k_4 \Delta y_E \end{aligned} \tag{8.3}$$

The movement Δy_D depending upon its sign opens one of the ports of the pilot valve admitting high pressure oil into the cylinder thereby moving the main piston and opening the steam valve by Δy_E. Certain justifiable simplifying assumptions, which can be made at this stage, are:

(i) Inertial reaction forces of main piston and steam valve are negligible compared to the forces exerted on the piston by high pressure oil.

(ii) Because of (i) above, the rate of oil admitted to the cylinder is proportional to port opening Δy_D.

The volume of oil admitted to the cylinder is thus proportional to the time integral of Δy_D. The movement Δy_E is obtained by dividing the oil volume by the area of the cross-section of the piston. Thus

$$\Delta y_E = k_5 \int_0^k (-\Delta y_D)\,\mathrm{d}t \tag{8.4}$$

It can be verified from the schematic diagram that a positive movement Δy_D, causes negative (upward) movement Δy_E accounting for the negative sign used in Eq. (8.4).

Taking the Laplace transform of Eqs (8.2), (8.3) and (8.4), we get

$$\Delta Y_C(s) = -k_1 k_C\, \Delta P_C(s) + k_2 \Delta F(s) \tag{8.5}$$

$$\Delta Y_D(s) = k_3 \Delta Y_C(s) + k_4 \Delta Y_E(s) \tag{8.6}$$

$$\Delta y_E(s) = -k_5 \frac{1}{s}\, \Delta Y_D(s) \tag{8.7}$$

Eliminating $\Delta Y_C(s)$ and $\Delta Y_D(s)$, we can write

$$\Delta Y_E(s) = \frac{k_1 k_3 k_C \Delta P_C(s) - k_2 k_3 \Delta F(s)}{\left(k_4 + \dfrac{s}{k_5}\right)}$$

$$= \left[\Delta P_C(s) - \frac{1}{R}\Delta F(s)\right] \times \left(\frac{K_{sg}}{1 + T_{sg} s}\right) \tag{8.8}$$

where

$$R = \frac{k_1 k_C}{k_2} = \text{speed regulation of the governor}$$

$$K_{sg} = \frac{k_1 k_3 k_C}{k_4} = \text{gain of speed governor}$$

$$T_{sg} = \frac{1}{k_4 k_5} = \text{time constant of speed governor}$$

Equation (8.8) is represented in the form of a block diagram in Fig. 8.3

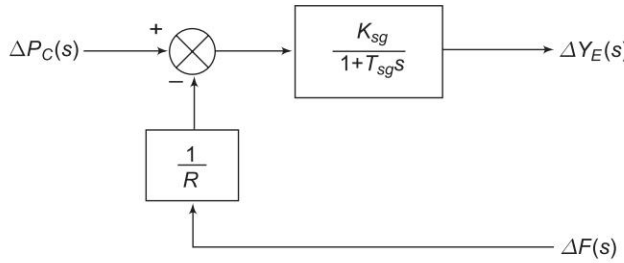

Fig. 8.3 Block diagram representation of speed governor system

The speed governing system of a hydro-turbine is more involved. An additional feedback loop provides temporary droop compensation to prevent instability. This is necessitated by the large inertia of the penstock gate which regulates the rate of water input to the turbine. Modelling of a hydro-turbine regulating system is beyond the scope of this book.

Turbine Model

Let us now relate the dynamic response of a steam turbine in terms of changes in power output to changes in steam valve opening Δy_E. Figure 8.4(a) shows a two stage steam turbine with a reheat unit. The dynamic response is largely influenced by two factors, (i) entrained steam between the inlet steam valve and first stage of the turbine, (ii) the storage action in the reheater which causes the output of the low pressure stage to lag behind that of the high pressure stage. Thus, the turbine transfer function is characterized by two time constants. For ease of analysis it will be assumed here that the turbine can be modelled to have a single equivalent time constant. Figure 8.4(b) shows the transfer function model of a steam turbine. Typically the time constant T_t lies in the range 0.2 to 2.5 s.

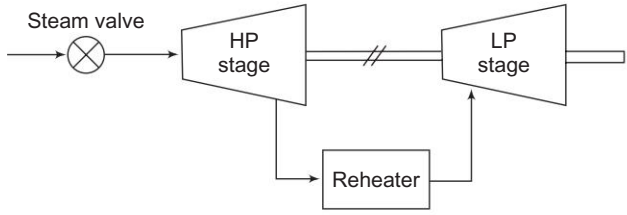

(a) Two-stage steam turbine

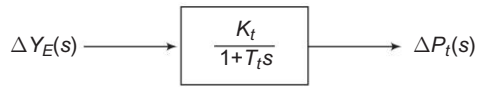

(b) Turbine transfer function model

Fig. 8.4

Generator Load Model

The increment in power input to the generator-load system is

$$\Delta P_G - \Delta P_D$$

where $\Delta P_G = \Delta P_t$, incremental turbine power output (assuming generator incremental loss to be negligible) and ΔP_D is the load increment.

This increment in power input to the system is accounted for in two ways:

(i) Rate of increase of stored kinetic energy in the generator rotor. At scheduled frequency (f^0), the stored energy is

$$W_{ke}^0 = H \times P_r \text{ kWs (kilojoules)}$$

where P_r is the kW rating of the turbo-generator and H is defined as its inertia constant.

The kinetic energy being proportional to square of speed (frequency), the kinetic energy at a frequency of ($f^0 + \Delta f$) is given by

$$W_{ke} = W_{ke}^0 \left(\frac{f^0 + \Delta f}{f^0} \right)^2$$

$$\simeq HP_r \left(1 + \frac{2\Delta f}{f^0} \right) \tag{8.9}$$

Rate of change of kinetic energy is therefore

$$\frac{\mathrm{d}}{\mathrm{d}t}(W_{ke}) = \frac{2HP_r}{f^0} \frac{\mathrm{d}}{\mathrm{d}t}(\Delta f) \tag{8.10}$$

(ii) As the frequency changes, the motor load changes being sensitive to speed, the rate of change of load with respect to frequency, i.e. $\partial P_D / \partial f$ can be regarded as nearly constant for small changes in frequency Δf and can be expressed as

$$(\partial P_D / \partial f)\ \Delta f = B\ \Delta f \tag{8.11}$$

where the constant B can be determined empirically. B is positive for a predominantly motor load.

Writing the power balance equation, we have

$$\Delta P_G - \Delta P_D = \frac{2HP_r}{f^0} \frac{\mathrm{d}}{\mathrm{d}t}(\Delta f) + B\ \Delta f$$

Dividing throughout by P_r and rearranging, we get

$$\Delta P_G(\text{pu}) - \Delta P_D(\text{pu}) = \frac{2H}{f^0} \frac{\mathrm{d}}{\mathrm{d}t}(\Delta f) + B(\text{pu})\ \Delta f \tag{8.12}$$

Taking the Laplace transform, we can write $\Delta F(s)$ as

$$\Delta F(s) = \frac{\Delta P_G(s) - \Delta P_D(s)}{B + \frac{2H}{f^0}(s)}$$

$$= [\Delta P_G(s) - \Delta P_D(s)] \times \left(\frac{K_{ps}}{1 + T_{ps}s} \right) \tag{8.13}$$

where

$$T_{ps} = \frac{2H}{Bf^0} = \text{power system time constant}$$

$$K_{ps} = \frac{1}{B} = \text{power system gain}$$

Equation (8.13) can be represented in block diagram form as shown in Fig. 8.5.

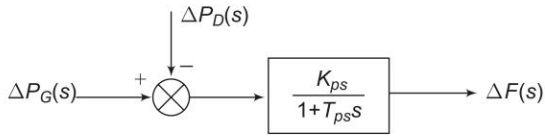

Fig. 8.5 Block diagram representation of generator-load model

Complete Block Diagram Representation of Load Frequency Control of an Isolated Power System

A complete block diagram representation of an isolated power system comprising turbine, generator, governor and load is easily obtained by combining the block diagrams of individual components, i.e. by combining Figs (8.3, 8.4 and 8.5). The complete block diagram with feedback loop is shown in Fig. 8.6.

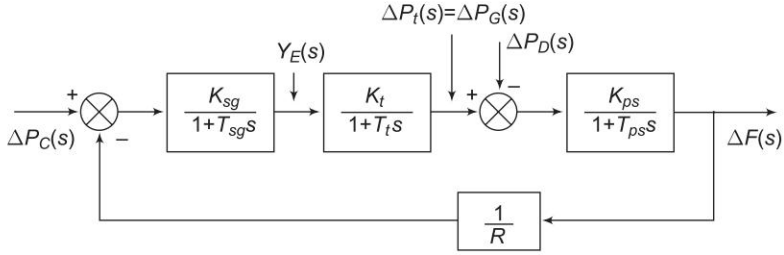

Fig. 8.6 Block diagram model of load frequency control (isolated power system)

Steady States Analysis

The model of Fig. 8.6 shows that there are two important incremental inputs to the load frequency control system – ΔP_C, the change in speed changer setting; and ΔP_D, the change in load demand. Let us consider a simple situation in which the speed changer has a fixed setting (i.e. $\Delta P_C = 0$) and the load demand changes. This is known as *free governor operation*. For such an operation the steady change in system frequency for a sudden change in load demand by an amount ΔP_D, i.e. $\Delta P_D(s) = \Delta P_D/s$ is obtained as follows:

$$\Delta F(s)\Big|_{\Delta P_C(s)=0} = -\frac{K_{ps}}{(1+T_{ps}s)+\dfrac{K_{sg}K_tK_{ps}/R}{(1+T_{sg}s)(1+T_ts)}} \times \frac{\Delta P_D}{s} \qquad (8.14)$$

$$\Delta f\Big|_{\substack{\text{steady state}\\ \Delta P_C=0}} = s\,\Delta F(s)\Big|_{\substack{s\to 0\\ \Delta P_C(s)=0}}$$

$$= -\left(\frac{K_{ps}}{1+(K_{sg}K_tK_{ps}\mid R)}\right)\Delta P_D \qquad (8.15)$$

While the gain K_t is fixed for the turbine and K_{ps} is fixed for the power system, K_{sg}, the speed governor gain is easily adjustable by changing lengths of various links. Let it be assumed for simplicity that K_{sg} is so adjusted that

$$K_{sg}K_t \approx 1$$

It is also recognized that $K_{ps} = 1/B$, where $B = \dfrac{\partial P_D}{\partial f}/P_r$ (in pu MW/unit change in frequency). Now

$$\Delta f = -\left(\frac{1}{B+(1/R)}\right)\Delta P_D \qquad (8.16)$$

The above equation gives the steady state changes in frequency caused by changes in load demand. Speed regulation R is naturally so adjusted that changes in frequency are small (of the order of 5% from no load to full load). Therefore, the linear incremental relation (8.16) can be applied from no load to full load. With this understanding, Fig. 8.7 shows the linear relationship between frequency and load for free governor operation with speed changer set to give a scheduled frequency of 100% at full load. The 'droop' or slope of this relationship is $-\left(\dfrac{1}{B+(1/R)}\right)$.

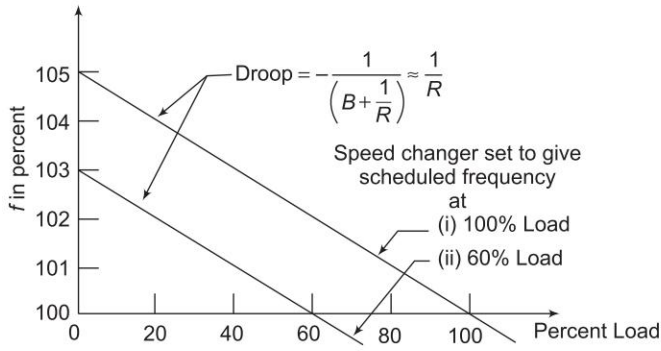

Fig. 8.7 Steady state load-frequency characteristic of a speed governor system

Power system parameter B is generally much smaller* than $1/R$ (a typical value is B = 0.01 pu MW/Hz and $1/R$ = 1/3) so that B can be neglected in comparison. Equation (8.16) then simplifies to

$$\Delta f = -R(\Delta P_D) \tag{8.17}$$

The droop of the load frequency curve is thus mainly determined by R, the speed governor regulation.

It is also observed from the above that increase in load demand (ΔP_D) is met under steady conditions partly by increased generation (ΔP_G) due to opening of the steam valve and partly by decreased load demand due to drop in system frequency. From the block diagram of Fig. 8.6 (with $K_{sg}K_t \simeq 1$)

$$\Delta P_G = -\frac{1}{R}\Delta f = \left(\frac{1}{BR+1}\right)\Delta P_D$$

Decrease in system load = $B\Delta f = \left(\frac{BR}{BR+1}\right)\Delta P_D$

Of course, the condition of decrease in system load is much less than the increase in generation. For typical values of B and R quoted earlier,

$$\Delta P_{G1} = 0.971\ \Delta P_D$$

Decrease in system load = $0.029\ \Delta P_D$

Consider now the steady effect of changing speed changer setting $\left(\Delta P_C(s) = \frac{\Delta P_C}{s}\right)$ with load demand remaining fixed (i.e. $\Delta P_D = 0$). The steady state change in frequency is obtained as follows:

$$\Delta F(s)\Big|_{\Delta P_D(s)=0} = \frac{K_{sg}K_tK_{ps}}{(1+T_{sg}s)(1+T_ts)(1+T_{ps}s)+K_{sg}K_tK_{ps}/R} \times \frac{\Delta P_C}{s} \tag{8.18}$$

$$\Delta f\Big|_{\substack{\text{steady state}\\ \Delta P_D=0}} = \left(\frac{K_{sg}K_tK_{ps}}{1+K_{sg}K_tK_{ps}/R}\right)\Delta P_C \tag{8.19}$$

If

$$K_{sg}K_t \simeq 1$$

---

* For a 250 MW machine with an operating load of 125 MW, let the change in load be 1% for 1% change in frequency (scheduled frequency = 50 Hz). Then

$$\frac{\partial P_D}{\partial f} = \frac{1.25}{0.5} = 2.5 \text{ MW/Hz}$$

$$B = \left(\frac{\partial P_D}{\partial f}\right)\Big/ P_r = \frac{2.5}{250} = 0.01 \text{ pu MW/Hz}$$

$$\Delta f = \left(\frac{1}{B + 1/R}\right)\Delta P_C \tag{8.20}$$

If the speed changer setting is changed by ΔP_C while the load demand changes by ΔP_D, the steady frequency change is obtained by superposition, i.e.

$$\Delta f = \left(\frac{1}{B + 1/R}\right)(\Delta P_C - \Delta P_D) \tag{8.21}$$

According to Eq. (8.21) the frequency change caused by load demand can be compensated by changing the setting of the speed changer, i.e.

$$\Delta P_C = \Delta P_D, \text{ for } \Delta f = 0$$

Figure 8.7 depicts two load frequency plots—one to give scheduled frequency at 100% rated load and the other to give the same frequency at 60% rated load.

Example 8.1 A 100 MVA synchronous generator operates on full load at a frequency of 50 Hz. The load is suddenly reduced to 50 MW. Due to time lag in governor system, the steam valve begins to close after 0.4 s. Determine the change in frequency that occurs in this time.
Given: $H = 5$ kWs/kVA of generator capacity.

Solution

Kinetic energy stored in rotating parts of generator and turbine

$$= 5 \times 100 \times 1000 = 5 \times 10^5 \text{ kWs}$$

Excess power input to generator before the steam valve begins to close

$$= 50 \text{ MW}$$

Excess energy input to rotating parts in 0.4 s

$$= 50 \times 1000 \times 0.4 = 20{,}000 \text{ kWs}$$

Stored kinetic energy $\propto$ (frequency)^2

$\therefore$ Frequency at the end of 0.4 s

$$= 50 \times \left(\frac{500{,}000 + 20{,}000}{500{,}000}\right)^{1/2} = 51 \text{ Hz}$$

Example 8.2 Two generators rated 200 MW and 400 MW are operating in parallel. The droop characteristics of their governors are 4% and 5%, respectively from no load to full load. Assuming that the generators are operating at 50 Hz at no load, how would a load of 600 MW be shared between them? What will be the system frequency at this load? Assume free governor operation.
Repeat the problem if both governors have a droop of 4%.

Solution

Since the generators are in parallel, they will operate at the same frequency at steady load.

Let load on generator 1 (200 MW) = x MW
and
load on generator 2 (400 MW) = (600 − x) MW

Reduction in frequency = Δf

Now

$$\frac{\Delta f}{x} = \frac{0.04 \times 50}{200} \quad \text{(i)}$$

$$\frac{\Delta f}{600 - x} = \frac{0.05 \times 50}{400} \quad \text{(ii)}$$

Equating Δf in (i) and (ii), we get

$$x = 231 \text{ MW (load on generator 1)}$$

$$600 - x = 369 \text{ MW (load on generator 2)}$$

$$\text{System frequency} = 50 - \frac{0.04 \times 50}{200} \times 231 = 47.69 \text{ Hz}$$

It is observed here that due to difference in droop characteristics of governors, generator 1 gets overloaded while generator 2 is underloaded.

It easily follows from above that if both governors have a droop of 4%, they will share the load as 200 MW and 400 MW respectively, i.e. they are loaded corresponding to their ratings. This indeed is desirable from operational considerations.

Dynamic Response

To obtain the dynamic response giving the change in frequency as function of the time for a step change in load, we must obtain the Laplace inverse of Eq. (8.14). The characteristic equation being of third order, dynamic response can only be obtained for a specific numerical case. However, the characteristic equation can be approximated as first order by examining the relative magnitudes of the time constants involved. Typical values of the time constants of load frequency control system are related as

$$T_{sg} < T_t \ll T_{ps}$$

Typically* $T_{sg} = 0.4$ s, $T_t = 0.5$ s and $T_{ps} = 20$ s.

Letting $T_{sg} = T_t = 0$ (and $K_{sg} K_t \cong 1$), the block diagram of Fig. 8.6 is reduced to that of Fig. 8.8, from which we can write

* For a 250 MW machine quoted earlier, inertia constant $H = 5$ kWs/kVA

$$T_{ps} = \frac{2H}{Bf^0} = \frac{2 \times 5}{0.01 \times 50} = 20 \text{ s}$$

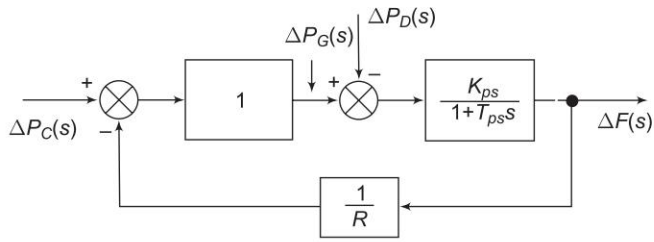

Fig. 8.8 First order approximate block diagram of load frequency control of an isolated area

$$\Delta F(s)\Big|_{\Delta P_C(s)=0} = -\frac{K_{ps}}{(1+K_{ps}/R)+T_{ps}s}\times\frac{\Delta P_D}{s}$$

$$= -\frac{K_{ps}/T_{ps}}{s\left[s+\dfrac{R+K_{ps}}{RT_{ps}}\right]}\times\Delta P_D$$

$$\Delta f(t) = -\frac{RK_{ps}}{R+K_{ps}}\left\{1-\exp\left[-\frac{t}{T_{ps}}\left(\frac{R}{R+K_{ps}}\right)\right]\right\}\Delta P_D \qquad (8.22)$$

Taking $R = 3$, $K_{ps} = 1/B = 100$, $T_{ps} = 20$, $\Delta P_D = 0.01$ pu

$$\Delta f\,(t) = -\,0.029\,(1 - e^{-1.717t}) \qquad (8.23a)$$

$$\Delta f\Big|_{\text{steady state}} = -\,0.029 \text{ Hz} \qquad (8.23b)$$

The plot of change in frequency versus time for first order approximation given above and the exact response are shown in Fig. 8.9. First order approximation is obviously a poor approximation.

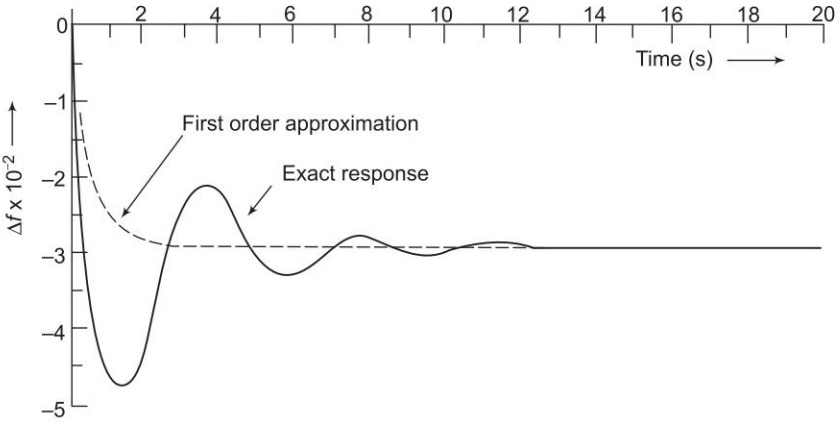

Fig. 8.9 Dynamic response of change in frequency for a step change in load (ΔP_D = 0.01 pu, T_{sg} = 0.4 s, T_t = 0.5 s, T_{ps} = 20 s, K_{ps} = 100, R = 3)

Control Area Concept

So far we have considered the simplified case of a single turbo-generator supplying an isolated load. Consider now a practical system with a number of generating stations and loads. It is possible to divide an extended power system (say, national grid) into subareas (may be, State Electricity Boards) in which the generators are tightly coupled together so as to form a *coherent* group, i.e. all the generators respond in *unison* to changes in load or speed changer settings. Such a coherent area is called a *control area* in which the frequency is assumed to be the same throughout in static as well as dynamic conditions. For purposes of developing a suitable control strategy, a control area can be reduced to a single speed governor, turbo-generator and load system. All the control strategies discussed so far are, therefore, applicable to an independent control area.

Proportional Plus Integral Control

It is seen from the above discussion that with the speed governing system installed on each machine, the steady load frequency characteristic for a given speed changer setting has considerable droop, e.g. for the system being used for the illustration above, the steady state drop in frequency will be 2.9 Hz [see Eq. (8.23b)] from no load to full load (1 pu load). System frequency specifications are rather stringent and, therefore, so much change in frequency cannot be tolerated. In fact, it is expected that the steady change in frequency will be zero. While steady state frequency can be brought back to the scheduled value by adjusting speed changer setting, the system could undergo intolerable dynamic frequency changes with changes in load. It leads to the natural suggestion that the speed changer setting be adjusted automatically by monitoring the frequency changes. For this purpose, a signal from Δf is fed through an integrator to the speed changer resulting in the block diagram configuration shown in Fig. 8.10. The system now modifies to a proportional plus integral controller, which, as is well known from control theory, gives zero steady state error, i.e. $\Delta f|_{\text{steady state}} = 0$.

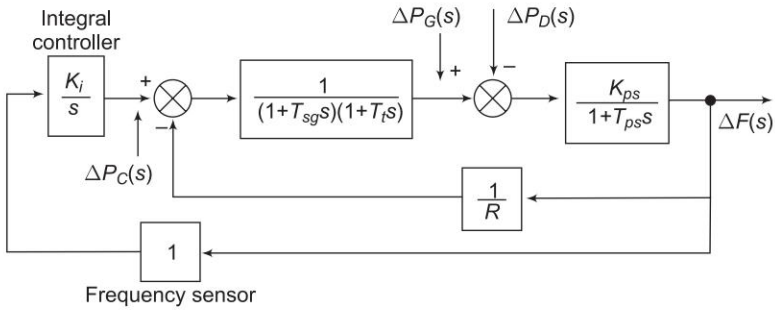

Fig. 8.10 Proportional plus integral load frequency control

The signal $\Delta P_C(s)$ generated by the integral control must be of opposite sign to $\Delta F(s)$ which accounts for negative sign in the block for integral controller. Now

$$\Delta F(s) = -\frac{K_{ps}}{(1+T_{ps}s)+\left(\frac{1}{R}+\frac{K_i}{s}\right)\times\frac{K_{ps}}{(1+T_{sg}s)(1+T_t s)}}\times\frac{\Delta P_D}{s}$$

$$= -\frac{RK_{ps}s(1+T_{sg}s)(1+T_t s)}{s(1+T_{sg}s)(1+T_t s)(1+T_{ps}s)R+K_{ps}(K_i R+s)}\times\frac{\Delta P_D}{s} \quad (8.24)$$

Obviously,

$$\Delta f|_{\text{steady state}} = \lim_{s\to 0} s\,\Delta F(s) = 0 \quad (8.25)$$

In contrast to Eq. (8.16), we find that the steady state change in frequency has been reduced to zero by the addition of the integral controller. This can be argued out physically as well. Δf reaches steady state (a constant value) only when $\Delta P_C = \Delta P_D$ = constant. Because of the integrating action of the controller, this is only possible if $\Delta f = 0$.

In central load frequency control of a given control area, the change (error) in frequency is known as *Area Control Error* (ACE). The additional signal fed back in the modified control scheme presented above is the integral of ACE.

In the above scheme ACE being zero under steady conditions*, a logical design criterion is the minimization of $\int$ ACE dt for a step disturbance. This integral is

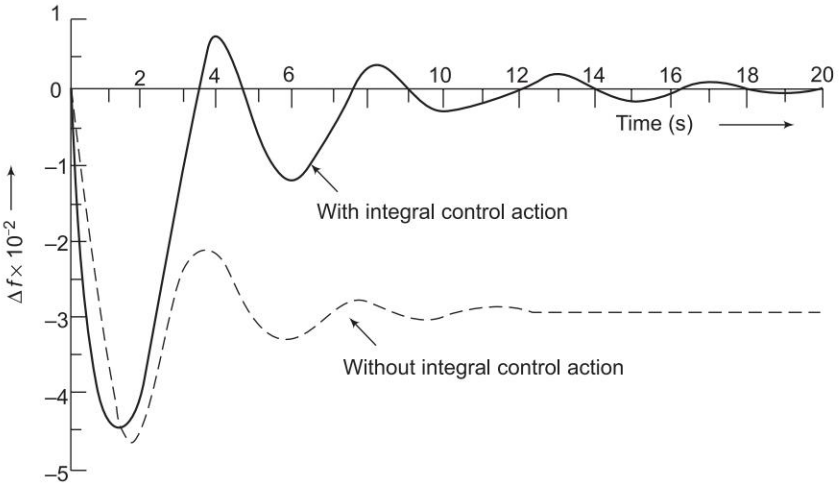

Fig. 8.11 Dynamic response of load frequency controller with and without integral control action (ΔP_D = 0.01 pu, T_{sg} = 0.4 s, T_t = 0.5 s, T_{ps} = 20 s, K_{ps} = 100, R = 3, K_i = 0.09)

* Such a control is known as *isochronous control*, but it has its time (integral of frequency) error though steady frequency error is zero.

indeed the *time error* of a synchronous electric clock run from the power supply. In fact, modern power systems keep track of integrated time error all the time. A corrective action (manual adjustment of ΔP_C, the speed changer setting) is taken by a large (preassigned) station in the area as soon as the time error exceeds a prescribed value.

The dynamics of the proportional plus integral controller can be studied numerically only, the system being of fourth order—the order of the system has increased by one with the addition of the integral loop. The dynamic response of the proportional plus integral controller with $K_i = 0.09$ for a step load disturbance of 0.01 pu obtained through digital computer are plotted in Fig. 8.11. For the sake of comparison the dynamic response without integral control action is also plotted on the same figure.

8.3 LOAD FREQUENCY CONTROL AND ECONOMIC DESPATCH CONTROL

Load frequency control with integral controller achieves zero steady state frequency error and a fast dynamic response, but it exercises no control over the relative loadings of various generating stations (i.e. *economic despatch*) of the control area. For example, if a sudden small increase in load (say, 1%) occurs in the control area, the load frequency control changes the speed changer settings of the governors of all generating units of the area so that, together, these units match the load and the frequency returns to the scheduled value (this action takes place in a few seconds). However, in the process of this change the loadings of various generating units change in a manner independent of economic loading considerations. In fact, some units in the process may even get overloaded. Some control over loading of individual units can be exercised by adjusting the gain factors (K_i) included in the signal representing integral of the area control error as fed to individual units. However, this is not satisfactory.

A satisfactory solution is achieved by using independent controls for load frequency and economic despatch. While the load frequency controller is a fast acting control (a few seconds), and regulates the system around an operating point; the economic despatch controller is a slow acting control, which adjusts the speed changer setting every minute (or half a minute) in accordance with a command signal generated by the central economic despatch computer. Figure 8.12 gives the schematic diagram of both these controls for two typical units of a control area. The signal to change the speed changer setting is constructed in accordance with economic despatch error, $[P_G\,(\text{desired}) - P_G\,(\text{actual})]$, suitably modified by the signal representing integral ACE at that instant of time. The signal P_G (desired) is computed by the central economic despatch computer (CEDC) and is transmitted to the local economic despatch controller (EDC) installed at each station. The system thus operates with economic despatch error only for very short periods of time before it is readjusted.

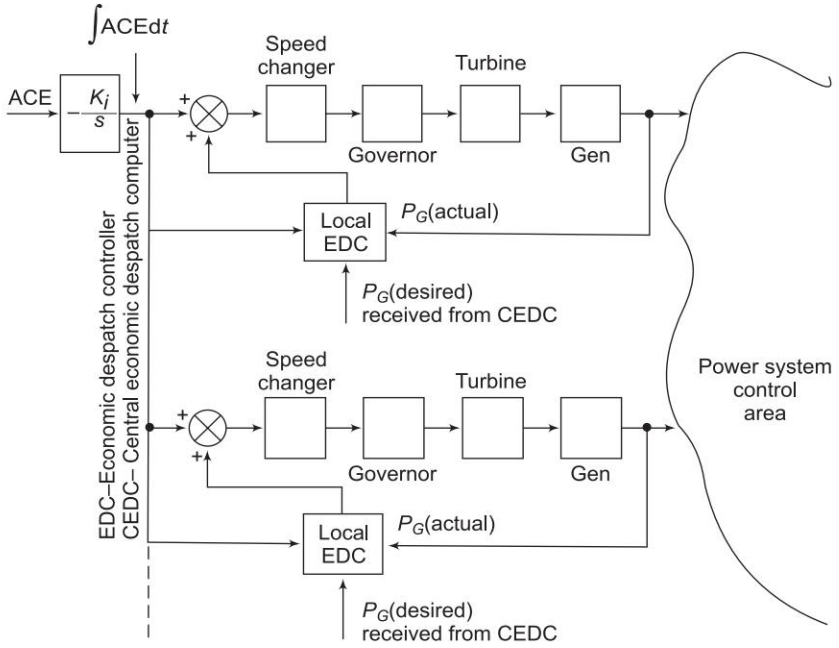

Fig. 8.12 Control area load frequency and economic despatch control (Reprinted (with modification) with permission of McGraw-Hill Book Company, New York from Olle I. Elgerd: *Electric Energy Systems Theory: An Introduction,* 1971, p. 345.)

8.4 TWO-AREA LOAD FREQUENCY CONTROL

An extended power system can be divided into a number of load frequency control areas interconnected by means of tie lines. Without loss of generality we shall consider a two-area case connected by a single tie line as illustrated in Fig. 8.13.

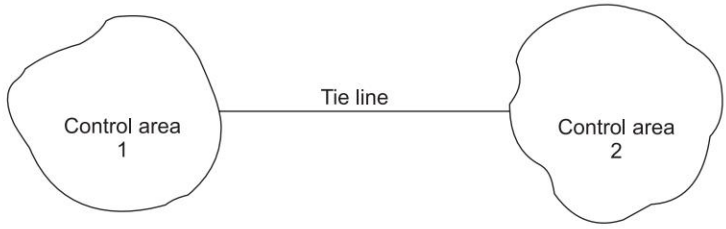

Fig. 8.13 Two interconnected control areas (single tie line)

The control objective now is to regulate the frequency of each area and to simultaneously regulate the tie line power as per inter-area power contracts. As in the case of frequency, proportional plus integral controller will be installed

so as to give zero steady state error in tie line power flow as compared to the contracted power.

It is conveniently assumed that each control area can be represented by an equivalent turbine, generator and governor system. Symbols used with suffix 1 refer to area 1 and those with suffix 2 refer to area 2.

In an isolated control area case the incremental power ($\Delta P_G - \Delta P_D$) was accounted for by the rate of increase of stored kinetic energy and increase in area load caused by increase in frequency. Since a tie line transports power in or out of an area, this fact must be accounted for in the incremental power balance equation of each area.

Power transported out of area 1 is given by

$$P_{\text{tie, 1}} = \frac{|V_1||V_2|}{X_{12}} \sin\left(\delta_1^0 - \delta_2^0\right) \tag{8.26}$$

where

δ_1^0, δ_2^0 = power angles of equivalent machines of the two areas.

For incremental changes in δ_1 and δ_2, the incremental tie line power can be expressed as

$$\Delta P_{\text{tie, 1}}(\text{pu}) = T_{12}(\Delta\delta_1 - \Delta\delta_2) \tag{8.27}$$

where

$$T_{12} = \frac{|V_1||V_2|}{P_{r1}X_{12}} \cos\left(\delta_1^0 - \delta_2^0\right) = \text{synchronizing coefficient}$$

Since incremental power angles are integrals of incremental frequencies, we can write Eq. (8.27) as

$$\Delta P_{\text{tie, 1}} = 2\pi T_{12}\left(\int \Delta f_1 \mathrm{d}t - \int \Delta f_1 \mathrm{d}t\right) \tag{8.28}$$

where Δf_1 and Δf_2 are incremental frequency changes of areas 1 and 2, respectively.

Similarly the incremental tie line power out of area 2 is given by

$$\Delta P_{\text{tie, 2}} = 2\pi T_{21}\left(\int \Delta f_2 \mathrm{d}t - \int \Delta f_1 \mathrm{d}t\right) \tag{8.29}$$

where

$$T_{21} = \frac{|V_2||V_1|}{P_{r2}X_{21}} \cos\left(\delta_2^0 - \delta_1^0\right) = \left(\frac{P_{r1}}{P_{r2}}\right) T_{12} = a_{12}T_{12} \tag{8.30}$$

With reference to Eq. (8.12), the incremental power balance equation for area 1 can be written as

$$\Delta P_{G1} - \Delta P_{D1} = \frac{2H_1}{f_1^0}\frac{\mathrm{d}}{\mathrm{d}t}(\Delta f_1) + B_1 \Delta f_1 + \Delta P_{\text{tie},1} \tag{8.31}$$

It may be noted that all quantities other than frequency are in per unit in Eq. (8.31).

Taking the Laplace transform of Eq. (8.31) and reorganizing, we get

$$\Delta F_1(s) = [\Delta P_{G1}(s) - \Delta P_{D1}(s) - \Delta P_{\text{tie},1}(s)] \times \frac{K_{ps1}}{1 + T_{ps1}s} \tag{8.32}$$

where as defined earlier [see Eq. (8.13)],

$$K_{ps1} = 1/B_1$$
$$T_{ps1} = 2H_1/B_1 f^0 \tag{8.33}$$

Compared to Eq. (8.13) of the isolated control area case, the only change is the appearance of the signal $\Delta P_{\text{tie},1}(s)$ as shown in Fig. 8.14.

Taking the Laplace transform of Eq. (8.28), the signal $\Delta P_{\text{tie},1}(s)$ is obtained as

$$\Delta P_{\text{tie},1}(s) = \frac{2\pi T_{12}}{s}[\Delta F_1(s) - \Delta F_2(s)] \tag{8.34}$$

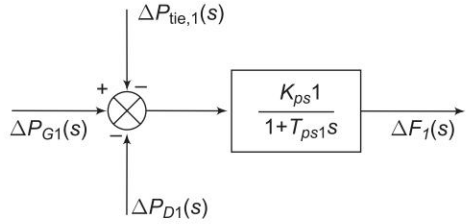

Fig. 8.14

The corresponding block diagram is shown in Fig. 8.15.

For the control area 2, $\Delta P_{\text{tie},2}(s)$ is given by [Eq. (8.29)]

$$\Delta P_{\text{tie},2}(s) = \frac{-2\pi a_{12} T_{12}}{s}[\Delta F_1(s) - \Delta F_2(s)] \tag{8.35}$$

which is also indicated by the block diagram of Fig. 8.15.

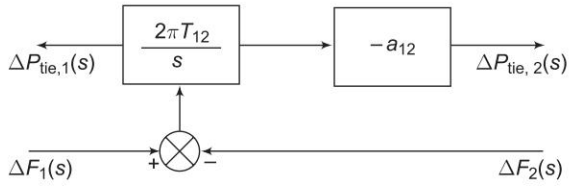

Fig. 8.15

Let us now turn our attention to ACE (area control error) in the presence of a tie line. In the case of an isolated control area, ACE is the change in area frequency which when used in integral control loop forced the steady state frequency error to zero. In order that the steady state tie line power error in a two-area control be made zero another integral control loop (one for each area) must be introduced to integrate the incremental tie line power signal and feed it back to the speed changer. This is accomplished by a single integrating block by redefining ACE as a linear combination of incremental frequency and tie line power. Thus, for control area 1,

$$\text{ACE}_1 = \Delta P_{\text{tie, 1}} + b_1 \Delta f_1 \tag{8.36}$$

where the constant b_1 is called area *frequency bias*.
Equation (8.36) can be expressed in the Laplace transform as

$$\text{ACE}_1(s) = \Delta P_{\text{tie, 1}}(s) + b_1 \Delta F_1(s) \tag{8.37}$$

Similarly, for the control area 2, ACE_2 is expressed as

$$\text{ACE}_2(s) = \Delta P_{\text{tie, 2}}(s) + b_2 \Delta F_2(s) \tag{8.38}$$

Combining the basic block diagrams of the two control areas corresponding to Fig. 8.6, with $\Delta P_{C1}(s)$ and $\Delta P_{C2}(s)$ generated by integrals of respective ACEs (obtained through signals representing changes in tie line power and local frequency bias) and employing the block diagrams of Figs 8.14 to 8.15, we easily obtain the composite block diagram of Fig. 8.16.

Let the step changes in loads ΔP_{D1} and ΔP_{D2} be simultaneously applied in control areas 1 and 2, respectively. When steady conditions are reached, the output signals of all integrating blocks will become constant and in order for this to be so, their input signals must become zero. We have, therefore, from Fig. 8.16,

$$\Delta P_{\text{tie, 1}} + b_1 \Delta f_1 = 0 \left(\text{input of integrating block} - \frac{K_{i1}}{s} \right) \tag{8.39a}$$

$$\Delta P_{\text{tie, 2}} + b_2 \Delta f_2 = 0 \left(\text{input of integrating block} - \frac{K_{i2}}{s} \right) \tag{8.39b}$$

$$\Delta f_1 - \Delta f_2 = 0 \left(\text{input of integrating block} - \frac{2\pi T_{12}}{s} \right) \tag{8.40}$$

From Eqs (8.28) and (8.29)

$$\frac{\Delta P_{\text{tie,1}}}{\Delta P_{\text{tie, 2}}} = -\frac{T_{12}}{T_{21}} = -\frac{1}{a_{12}} = \text{constant} \tag{8.41}$$

Hence Eqs (8.39) – (8.41) are simultaneously satisfied only for

$$\Delta P_{\text{tie, 1}} = \Delta P_{\text{tie, 2}} = 0 \tag{8.42}$$

and

$$\Delta f_1 = \Delta f_2 = 0$$

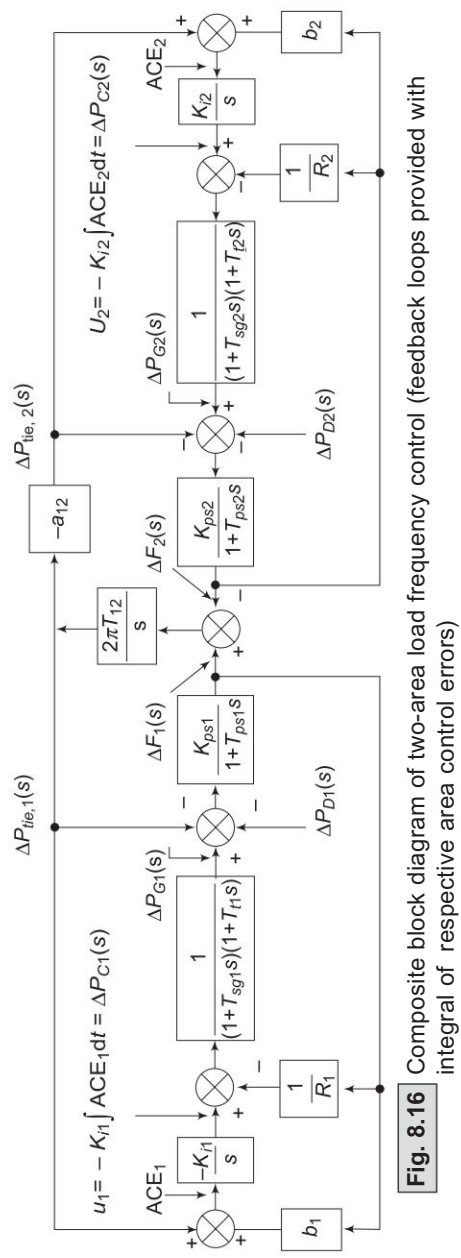

Fig. 8.16 Composite block diagram of two-area load frequency control (feedback loops provided with integral of respective area control errors)

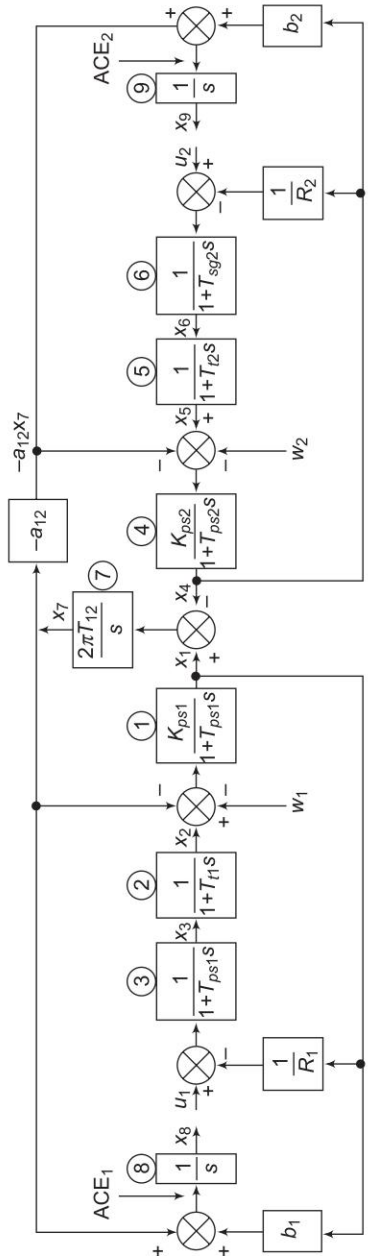

Fig. 8.17 State space model of two-area system

Thus, under steady condition, change in the tie line power and frequency of each area is zero. This has been achieved by integration of ACEs in the feedback loops of each area.

Dynamic response is difficult to obtain by the transfer function approach (as used in the single area case) because of the complexity of blocks and multi-input (ΔP_{D1}, ΔP_{D2}) and multi-output ($\Delta P_{\text{tie, 1}}$, $\Delta P_{\text{tie, 2}}$, Δf_1, Δf_2) situation. A more organized and more conveniently carried out analysis is through the state space approach (a time domain approach). Formulation of the state space model for the two-area system will be illustrated in Sec. 8.5.

The results of the two-area system (ΔP_{tie}, change in tie line power and Δf, change in frequency) obtained through digital computer study are shown in the form of a dotted line in Figs 8.18 and 8.19. The two areas are assumed to be identical with system parameters given by

$$T_{sg} = 0.4 \text{ s}, \; T_t = 0.5 \text{ s}, \; T_{ps} = 20 \text{ s}$$

$$K_{ps} = 100, \; R = 3, \; b = 0.425, \; K_i = 0.09, \; 2\pi T_{12} = 0.05$$

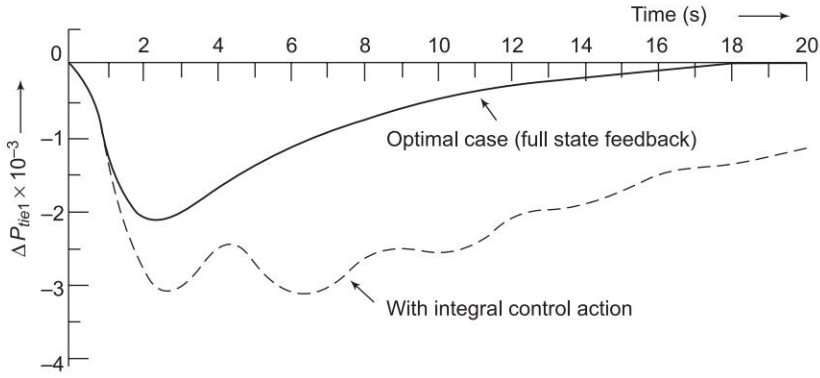

Fig. 8.18 Change in tie line power due to step load (0.01 pu) change in area 1

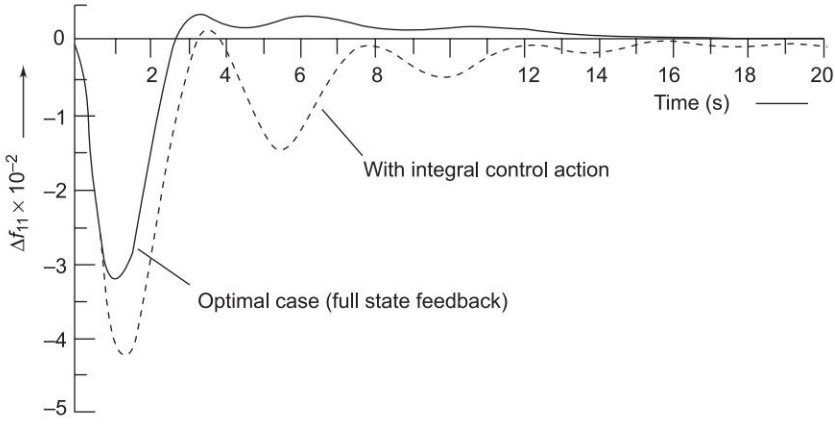

Fig. 8.19 Change in frequency of area 1 due to step load (0.01 pu) change in area 1

8.5 OPTIMAL (TWO-AREA) LOAD FREQUENCY CONTROL

Modern control theory is applied in this section to design an optimal load frequency controller for a two-area system. In accordance with modern control terminology ΔP_{C1} and ΔP_{C2} will be referred to as control inputs u_1 and u_2. In the conventional approach u_1 and u_2 were provided by the integral of ACEs. In modern control theory approach u_1 and u_2 will be created by a linear combination of all the system states (full state feedback). For formulating the state variable model for this purpose the conventional feedback loops are opened and each time constant is represented by a separate block as shown in Fig. 8.17. State variables are defined as the outputs of all blocks having either an integrator or a time constant. We immediately notice that the system has nine state variables.

Before presenting the optimal design, we must formulate the state model. This is achieved below by writing the differential equations describing each individual block of Fig. 8.17 in terms of state variables (note that differential equations are written by replacing s by d/dt).

Comparing Figs 8.16 and 8.17,

$$x_1 = \Delta f_1 \qquad x_4 = \Delta f_2 \qquad x_8 = \int \text{ACE}_1 \, dt$$

$$x_2 = \Delta P_{G1} \qquad x_5 = \Delta P_{G2} \qquad x_9 = \int \text{ACE}_2 \, dt$$

$$u_1 = \Delta P_{C1} \qquad u_2 = \Delta P_{C2}$$

$$w_1 = \Delta P_{D1} \qquad w_2 = \Delta P_{D2}$$

For block **1**

$$x_1 + T_{ps1}\dot{x}_1 = K_{ps1}(x_2 - x_7 - w_1)$$

or

$$\dot{x}_1 = -\frac{1}{T_{ps1}}x_1 + \frac{K_{ps1}}{T_{ps1}}x_2 - \frac{K_{ps1}}{T_{ps1}}x_7 - \frac{K_{ps1}}{T_{ps1}}w_1 \quad (8.43)$$

For block **2**

$$x_2 + T_{t1}\dot{x}_2 = x_3$$

or

$$\dot{x}_2 = -\frac{1}{T_{t1}}x_2 + \frac{1}{T_{t1}}x_3 \quad (8.44)$$

For block **3**

$$x_3 + T_{sg1}\dot{x}_3 = -\frac{1}{R_1}x_1 + u_1$$

or

$$\dot{x}_3 = -\frac{1}{R_1 T_{sg1}}x_1 - \frac{1}{T_{sg1}}x_3 + \frac{1}{T_{sg1}}u_1 \quad (8.45)$$

For block **4**

$$x_4 + T_{ps2}\dot{x}_4 = K_{ps2}(x_5 + a_{12}x_7 - w_2)$$

or

$$\dot{x}_4 = -\frac{1}{T_{ps2}}x_4 + \frac{K_{ps2}}{T_{ps2}}x_5 + \frac{a_{12}K_{ps2}}{T_{ps2}}x_7 - \frac{K_{ps2}}{T_{ps2}}w_2 \tag{8.46}$$

For block **5**

$$x_5 + T_{t2}\dot{x}_5 = x_6$$

or

$$\dot{x}_5 = -\frac{1}{T_{t2}}x_5 + \frac{1}{T_{t2}}x_6 \tag{8.47}$$

For block **6**

$$x_6 + T_{sg2}\dot{x}_6 = -\frac{1}{R_2}x_4 + u_2$$

or

$$\dot{x}_6 = -\frac{1}{R_2T_{sg2}}x_4 - \frac{1}{T_{sg2}}x_6 + \frac{1}{T_{sg2}}u_2 \tag{8.48}$$

For block **7**

$$\dot{x}_7 = 2\pi T_{12}x_1 - 2\pi T_{12}x_4 \tag{8.49}$$

For block **8**

$$\dot{x}_8 = b_1x_1 + x_7 \tag{8.50}$$

For block **9**

$$\dot{x}_9 = b_2x_4 - a_{12}x_7 \tag{8.51}$$

The nine equations (8.43) to (8.51) can be organized in the following vector matrix form

$$\dot{\boldsymbol{x}} = \boldsymbol{Ax} + \boldsymbol{Bu} + \boldsymbol{Fw} \tag{8.52}$$

where

$\boldsymbol{x} = [x_1 \;\; x_2 \;\; \ldots \; x_9]^T$ = state vector

$\boldsymbol{u} = [u_1 \;\; u_2]^T$ = control vector

$\boldsymbol{w} = [w_1 \;\; w_2]^T$ = disturbance vector

while the matrices $\boldsymbol{A}$, $\boldsymbol{B}$ and $\boldsymbol{F}$ are defined below:

$$
\boldsymbol{A} = \begin{array}{c} \\ 1 \\ 2 \\ 3 \\ 4 \\ 5 \\ 6 \\ 7 \\ 8 \\ 9 \end{array}
\begin{array}{c}
\begin{array}{ccccccccc} 1 & 2 & 3 & 4 & 5 & 6 & 7 & 8 & 9 \end{array} \\
\begin{bmatrix}
-\dfrac{1}{T_{ps1}} & \dfrac{K_{ps1}}{T_{ps1}} & 0 & 0 & 0 & 0 & -\dfrac{K_{ps1}}{T_{ps1}} & 0 & 0 \\
0 & -\dfrac{1}{T_{t1}} & \dfrac{1}{T_{t1}} & 0 & 0 & 0 & 0 & 0 & 0 \\
\dfrac{1}{R_1 T_{sg1}} & 0 & -\dfrac{1}{T_{sg1}} & 0 & 0 & 0 & 0 & 0 & 0 \\
0 & 0 & 0 & -\dfrac{1}{T_{ps2}} & \dfrac{K_{ps2}}{T_{ps2}} & 0 & \dfrac{a_{12}K_{ps2}}{T_{ps2}} & 0 & 0 \\
0 & 0 & 0 & 0 & -\dfrac{1}{T_{t2}} & \dfrac{1}{T_{t2}} & 0 & 0 & 0 \\
0 & 0 & 0 & -\dfrac{1}{R_2 T_{sg2}} & 0 & -\dfrac{1}{T_{sg2}} & 0 & 0 & 0 \\
2\pi T_{12} & 0 & 0 & -2\pi T_{12} & 0 & 0 & 0 & 0 & 0 \\
b_1 & 0 & 0 & 0 & 0 & 0 & 1 & 0 & 0 \\
0 & 0 & 0 & b_2 & 0 & 0 & -a_{12} & 0 & 0
\end{bmatrix}
\end{array}
$$

$$
\boldsymbol{B}^T = \begin{bmatrix}
0 & 0 & \dfrac{1}{T_{sg1}} & 0 & 0 & 0 & 0 & 0 & 0 \\
0 & 0 & 0 & 0 & 0 & \dfrac{1}{T_{sg2}} & 0 & 0 & 0
\end{bmatrix}
$$

$$
\boldsymbol{F}^T = \begin{bmatrix}
-\dfrac{K_{ps1}}{T_{ps1}} & 0 & 0 & 0 & 0 & 0 & 0 & 0 & 0 \\
0 & 0 & 0 & -\dfrac{K_{ps2}}{T_{ps2}} & 0 & 0 & 0 & 0 & 0
\end{bmatrix}
$$

In the conventional control scheme of Fig. 8.16, the control inputs u_1 and u_2 are constructed as under from the state variables x_8 and x_9 only.

$$u_1 = -K_{i1}x_8 = -K_{i1}\int \mathrm{ACE}_1 \mathrm{d}t$$

$$u_2 = -K_{i2}x_9 = -K_{i2}\int \mathrm{ACE}_2 \mathrm{d}t$$

In the optimal control scheme the control inputs u_1 and u_2 are generated by means of feedbacks from all the nine states with feedback constants to be determined in accordance with an optimality criterion.

Examination of Eq. (8.52) reverals that our model is not in the standard form employed in optimal control theory. The standard form is

$$\dot{\boldsymbol{x}} = \boldsymbol{Ax} + \boldsymbol{Bu}$$

which does not contain the disturbance term $\boldsymbol{Fw}$ present in Eq. (8.52). Furthermore, a constant disturbance vector $\boldsymbol{w}$ would drive some of the system states and the control vector $\boldsymbol{u}$ to constant steady values; while the cost function employed in optimal control requires that the system state and control vectors have zero steady state values for the cost function to have a minimum.

For a constant disturbance vector $\boldsymbol{w}$, the steady state is reached when

$$\dot{\boldsymbol{x}} = 0$$

in Eq. (8.52); which then gives

$$0 = \boldsymbol{A}\boldsymbol{x}_{ss} + \boldsymbol{B}\boldsymbol{u}_{ss} + \boldsymbol{F}\boldsymbol{w} \tag{8.53}$$

Defining $\boldsymbol{x}$ and $\boldsymbol{u}$ as the sum of transient and steady state terms, we can write

$$\boldsymbol{x} = \boldsymbol{x}' + \boldsymbol{x}_{ss} \tag{8.54}$$

$$\boldsymbol{u} = \boldsymbol{u}' + \boldsymbol{u}_{ss} \tag{8.55}$$

Substituting $\boldsymbol{x}$ and $\boldsymbol{u}$ from Eqs (8.54) and (8.55) in Eq. (8.52), we have

$$\dot{\boldsymbol{x}}' = \boldsymbol{A}\,(\boldsymbol{x}' + \boldsymbol{x}_{ss}) + \boldsymbol{B}(\boldsymbol{u}' + \boldsymbol{u}_{ss}) + \boldsymbol{F}\boldsymbol{w}$$

By virtue of relationship (8.53), we get

$$\dot{\boldsymbol{x}}' = \boldsymbol{A}\boldsymbol{x}' + \boldsymbol{B}\boldsymbol{u}' \tag{8.56}$$

This represents system model in terms of excursion of state and control vectors from their respective steady state values.

For full state feedback, the control vector $\boldsymbol{u}$ is constructed by a linear combination of all states, i.e.

$$\boldsymbol{u} = -\boldsymbol{K}\boldsymbol{x} \tag{8.57a}$$

where $\boldsymbol{K}$ is the feedback matrix.
Now

$$\boldsymbol{u}' + \boldsymbol{u}_{ss} = -\boldsymbol{K}\,(\boldsymbol{x}' + \boldsymbol{x}_{ss})$$

For a stable system both $\boldsymbol{x}'$ and $\boldsymbol{u}'$ go to zero, therefore

$$\boldsymbol{u}_{ss} = -\boldsymbol{K}\boldsymbol{x}_{ss}$$

Hence

$$\boldsymbol{u}' = -\boldsymbol{K}\boldsymbol{x}' \tag{8.57b}$$

Examination of Fig. 8.17 easily reveals the steady state values of state and control variables for constant values of disturbance inputs w_1 and w_2. These are

$$\begin{aligned}
x_{1ss} &= x_{4ss} = x_{7ss} = 0 \\
x_{2ss} &= x_{3ss} = w_1 \\
u_{1ss} &= w_1 \\
x_{5ss} &= x_{6ss} = w_2 \\
u_{2ss} &= w_2 \\
x_{8ss} &= \text{constant} \\
x_{9ss} &= \text{constant}
\end{aligned} \tag{8.58}$$

The values of x_{8ss} and x_{9ss} depend upon the feedback constants and can be determined from the following steady state equations:

$$u_{1ss} = k_{11}x_{1ss} + \ldots + k_{18}x_{8ss} + k_{19}x_{9ss} = w_1$$
$$u_{2ss} = k_{21}x_{1ss} + \ldots + k_{28}x_{8ss} + k_{29}x_{9ss} = w_2 \qquad (8.59)$$

The feedback matrix $\boldsymbol{K}$ in Eq. (8.57b) is to be determined so that a certain performance index (PI) is minimized in transferring the system from an arbitrary initial state $x'(0)$ to origin in infinitie time (i.e. $x'(\infty) = 0$). A convenient PI has the quadratic form

$$\mathbf{PI} = \frac{1}{2}\int_0^\infty (x'^T \boldsymbol{Q}\boldsymbol{x}' + \boldsymbol{u}'^T \boldsymbol{R}\boldsymbol{u}')\, \mathrm{d}t \qquad (8.60)$$

The matrices $\boldsymbol{Q}$ and $\boldsymbol{R}$ are defined for the problem in hand through the following design considerations:

(i) Excursions of ACEs about the steady values $(x'_7 + b_1x'_1;\ -a_{12}x'_7 + b_2x'_4)$ are minimized. The steady values of ACEs are of course zero.

(ii) Excursions of $\int \text{ACE}\ \mathrm{d}t$ about the steady values (x'_8, x'_9) are minimized. The steady values of $\int \text{ACE}\ \mathrm{d}t$ are, of course, constants.

(iii) Excursions of the control vector (u'_1, u'_2) about the steady value are minimized. The steady value of the control vector is, of course, a constant. This minimization is intended to indirectly limit the control effort within the physical capability of components. For example, the steam valve cannot be opened more than a certain value without causing the boiler pressure to drop severely.

With the above reasoning, we can write the PI as

$$\mathbf{PI} = \frac{1}{2}\int_0^\infty [(x'_7 + b_1x'_1)^2 + (-a_{12}x'_7 + b_2x'_4)^2 + (x'^2_8 + x'^2_9) + k(u'^2_1 + u'^2_2)]\, \mathrm{d}t \qquad (8.61)$$

From the PI of Eq. (8.61), $\boldsymbol{Q}$ and $\boldsymbol{R}$ can be recognized as

$$\boldsymbol{Q} = \begin{bmatrix} b_1^2 & 0 & 0 & 0 & 0 & 0 & b_1 & 0 & 0 \\ 0 & 0 & 0 & 0 & 0 & 0 & 0 & 0 & 0 \\ 0 & 0 & 0 & 0 & 0 & 0 & 0 & 0 & 0 \\ 0 & 0 & 0 & b_2^2 & 0 & 0 & -a_{12}b_2 & 0 & 0 \\ 0 & 0 & 0 & 0 & 0 & 0 & 0 & 0 & 0 \\ 0 & 0 & 0 & 0 & 0 & 0 & 0 & 0 & 0 \\ b_1 & 0 & 0 & -a_{12}b_2 & 0 & 0 & \left(1 + a_{12}^2\right) & 0 & 0 \\ 0 & 0 & 0 & 0 & 0 & 0 & 0 & 1 & 0 \\ 0 & 0 & 0 & 0 & 0 & 0 & 0 & 0 & 1 \end{bmatrix}$$

= symmetric matrix

$\boldsymbol{R} = \boldsymbol{kI}$ = symmetric matrix

Determination of the feedback matrix $\boldsymbol{K}$ which minimizes the above PI is the standard *optimal regulator problem*. $\boldsymbol{K}$ is obtained from solution of the *reduced matrix Riccati equation*[*] given below.

$$\boldsymbol{A}^T\boldsymbol{S} + \boldsymbol{S}\boldsymbol{A} - \boldsymbol{S}\boldsymbol{B}\boldsymbol{R}^{-1}\boldsymbol{B}^T\boldsymbol{S} + \boldsymbol{Q} = 0 \tag{8.62}$$

$$\boldsymbol{K} = \boldsymbol{R}^{-1}\boldsymbol{B}^T\boldsymbol{S} \tag{8.63}$$

The acceptable solution of $\boldsymbol{K}$ is that for which the system remains stable. Substituting Eq. (8.57b) in Eq. (8.56), the system dynamics with feedback is defined by

$$\dot{\boldsymbol{x}}' = (\boldsymbol{A} - \boldsymbol{B}\boldsymbol{K})\boldsymbol{x}' \tag{8.64}$$

For stability all the eigenvalues of the matrix $(\boldsymbol{A} - \boldsymbol{B}\boldsymbol{K})$ should have negative real parts.

For illustration we consider two identical control areas with the following system parameters:

$$T_{sg} = 0.4 \text{ s}; \; T_t = 0.5 \text{ s}; \; T_{ps} = 20 \text{ s}$$

$$\boldsymbol{R} = 3; \; \boldsymbol{K}_{ps} = 1/B = 100$$

$$b = 0.425; \; \boldsymbol{K}_i = 0.09; \; a_{12} = 1; \; 2\pi T_{12} = 0.05$$

Computer solution for the feedback matrix $\boldsymbol{K}$ is presented below, while the system dynamic response is plotted in Figs 8.18 and 8.19. These figures also give for comparison the dynamic response for the case of integral control action only. The improvement in performance achieved by the optimal controller is evident from these figures.

$$\boldsymbol{K} = \begin{bmatrix} 0.5286 & 1.1419 & 0.6813 & -0.0046 & -0.0211 & -0.0100 & -0.7437 & 0.9999 & 0.0000 \\ -0.0046 & -0.0211 & -0.0100 & 0.5286 & 1.1419 & 0.6813 & 0.7437 & 0.0000 & 0.9999 \end{bmatrix}$$

As the control areas extend over vast geographical regions, there are two ways of obtaining full state information in each area for control purposes.

(i) Transport the state information of the distant area over communication channels. This is, of course, expensive.

(ii) Generate all the states locally (including the distant states) by means of 'observer' or 'Kalman filter' by processing the local output signal. An 'observer' being itself a high order system, renders the overall system highly complex and may, in fact, result in impairing system stability and dynamic response which is meant to be improved through optimal control.

Because of the above mentioned difficulties encountered in implementation of an optimal control load frequency scheme, it is preferable to use a sub-optimal scheme employing only local states of the area. The design of such structurally constrained optimal control schemes is beyond the scope of this book. The conventional control scheme of Fig. 8.16 is, in fact, the local output feedback scheme in which feedback signal derived from changes in local frequency and tie line power is employed in each area.

---

* a set of linear algebraic equations.

8.6 AUTOMATIC VOLTAGE CONTROL

Figure 8.20 gives the schematic diagram of an automatic voltage regulator of a generator. It basically consists of a main exciter which excites the alternator field to control the output voltage. The exciter field is automatically controlled through error $e = V_{\text{Ref}} - V_T$, suitably amplified through voltage and power amplifiers. It is a type-0 system which requires a constant error e for a specified voltage at generator terminals. The block diagram of the system is given in Fig. 8.21. The function of important components and their transfer function is given below:

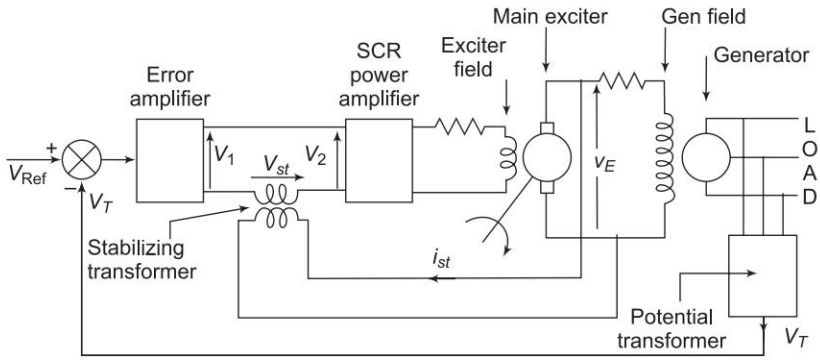

Fig. 8.20 Schematic diagram of alternator voltage regulator scheme

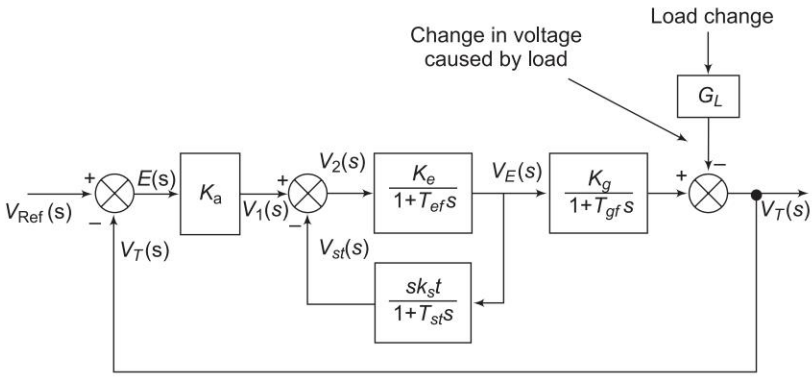

Fig. 8.21 Block diagram of alternator voltage regulator scheme

Potential transformer It gives a sample of terminal voltage V_T.

Differencing device It gives the actuating error

$$e = V_{\text{Ref}} - V_T$$

The error initiates the corrective action of adjusting the alternator excitation. Error waveform is suppressed carrier modulated, the carrier frequency being the system frequency of 50 Hz.

Error amplifier It demodulates and amplifies the error signal. Its gain is K_a.

SCR power amplifier and exciter field It provides the necessary power amplification to the signal for controlling the exciter field. Assuming the amplifier time constant to be small enough to be neglected, the overall transfer function of these two is

$$\frac{K_e}{1+T_{ef}s}$$

where T_{ef} is the exciter field time constant.

Alternator Its field is excited by the main exciter voltage V_E. Under no load it produces a voltage proportional to field current. The no load transfer function is

$$\frac{K_g}{1+T_{gf}s}$$

where

T_{gf} = generator field time constant.

The load causes a voltage drop which is a complex function of direct and quadrature axis currents. The effect is only schematically represented by block G_L. The exact load model of the alternator is beyond the scope of this book.

Stabilizing transformer T_{ef} and T_{gf} are large enough time constants to impair the systems dynamic response. It is well known that the dynamic response of a control system can be improved by the internal derivative feedback loop. The derivative feedback in this system is provided by means of a stabilizing transformer excited by the exciter output voltage V_E. The output of the stabilizing transformer is fed negatively at the input terminals of the SCR power amplifier. The transfer function of the stabilizing transformer is derived below.

Since the secondary is connected at the input terminals of an amplifier, it can be assumed to draw zero current. Now

$$V_E = R_1 i_{st} + L_1 \frac{\mathrm{d}i_{st}}{\mathrm{d}t}$$

$$V_{st} = M \frac{\mathrm{d}i_{st}}{\mathrm{d}t}$$

Taking the Laplace transform, we get

$$\frac{V_{st}(s)}{V_E(s)} = \frac{sM}{R_1 + sL_1} = \frac{sM/R_1}{1+T_{st}s}$$

$$= \frac{sK_{st}}{1+T_{st}s}$$

Accurate state variable models of loaded alternator around an operating point are available in literature using which optimal voltage regulation schemes can be devised. This is, of course, beyond the scope of this book.

8.7 LOAD FREQUENCY CONTROL WITH GENERATION RATE CONSTRAINTS (GRCS)

The load frequency control problem discussed so far does not consider the effect of the restrictions on the rate of change of power generation. In power systems having steam plants, power generation can change only at a specified maximum rate. The generation rate (from safety considerations of the equipment) for reheat units is quite low. Most of the reheat units have a generation rate around 3%/min. Some have a generation rate between 5 to 10%/min. If these constraints are not considered, system is likely to chase large momentary disturbances. This results in undue wear and tear of the controller. Several methods have been proposed to consider the effect of GRCs for the design of automatic generation controllers. When GRC is considered, the system dynamic model becomes non-linear and linear control techniques cannot be applied for the optimization of the controller setting.

If the generation rates denoted by P_{Gi} are included in the state vector, the system order will be altered. Instead of augmenting them, while solving the state equations, it may be verified at each step if the GRCs are violated. Another way of considering GRCs for both areas is to add limiters to the governors [9, 18] as shown in Fig. 8.22, i.e., the maximum rate of valve opening or closing speed is restricted by the limiters. Here $T_{sg}\, g_{\max}$ is the power rate limit imposed by valve or gate control. In this model

$$|\Delta \dot{Y}_E| < g_{\max} \tag{8.65}$$

The banded values imposed by the limiters are selected to restrict the generation rate by 10% per minute.

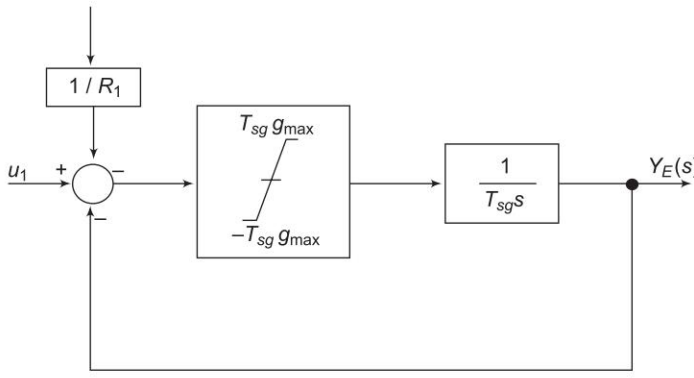

Fig. 8.22 Governor model with GRC

The GRCs result in larger deviations in ACEs as the rate at which generation can change in the area is constrained by the limits imposed. Therefore, the duration for which the power needs to be imported increases considerably as compared to the case where generation rate is not constrained. With GRCs, R should be selected with care so as to give the best dynamic response. In hydro-thermal system, the generation rate in the hydro area normally remains below the safe limit and therefore GRCs for all the hydro plants can be ignored.

8.8 SPEED GOVERNOR DEAD-BAND AND ITS EFFECT ON AGC

The effect of the speed governor dead-band is that for a given position of the governor control valves, an increase/decrease in speed can occur before the position of the valve changes. The governor dead-band can materially affect the system response. In AGC studies, the dead-band effect indeed can be significant, since relatively small signals are under considerations.

The speed governor characteristic, though non-linear, has been approximated by linear characteristics in earlier analysis. Further, there is another non-linearity introduced by the dead-band in the governor operation. Mechanical friction and backlash and also valve overlaps in hydraulic relays cause the governor dead-band. Due to this, though the input signal increases, the speed governor may not immediately react until the input reaches a particular value. Similar action takes place when the input signal decreases. Thus the governor dead-band is defined as the total magnitude of sustained speed change within which there is no change in valve position. The limiting value of dead-band is specified as 0.06%. It was shown by Concordia *et al.* [18] that one of the effects of governor dead-band is to increase the apparent steady-state speed regulation R.

The effect of the dead-band may be included in the speed governor control loop block diagram as shown in Fig. 8.23. Considering the worst case for the dead-band, (i.e., the system starts responding after the whole dead-band is traversed) and examining the dead-band block in Fig. 8.23, the following set of equations completely define the behaviour of the dead-band [19].

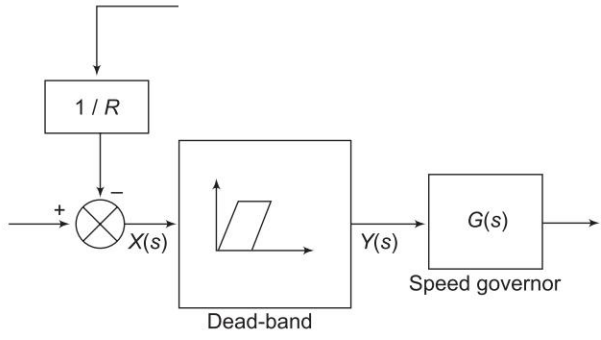

Fig. 8.23 Dead-band in speed-governor control loop

$$\begin{aligned} y^{(r+1)} &= x^{(r)} \text{ if } x^{(r+1)} - x^{r} \leq \text{dead-band} \\ &= x^{(r+1)} - \text{dead-band; if } x^{(r+1)} - x^{(r)} > 0 \\ &= x^{(r+1)}; \text{ if } x^{r+1} - x^{r} < 0 \end{aligned} \qquad (8.66)$$

(r is the step in the computation)

Reference [20] considers the effect of governor dead-band nonlinearity by using the describing function approach [11] and including the linearized equations in the state space model.

The presence of governor dead-band makes the dynamic response oscillatory. It has been seen [19] that the governor dead-band does not influence the selection of integral controller gain settings in the presence of GRCs. In the presence of GRC and dead band even for small load perturbation, the system becomes highly non-linear and hence the optimization problem becomes rather complex.

8.9 DIGITAL LF CONTROLLERS

In recent years, increasingly more attention is being paid to the question of digital implementation of the automatic generation control algorithms. This is mainly due to the facts that digital control turns out to be more accurate and reliable, compact in size, less sensitive to noise and drift and more flexible. It may also be implemented in a time shared fashion by using the computer systems in load despatch centre, if so desired. The ACE, a signal which is used for AGC is available in the discrete form, i.e., there occurs sampling operation between the system and the controller. Unlike the continuous-time system, the control vector in the discrete mode is constrained to remain constant between the sampling instants. The digital control process is inherently a discontinuous process and the designer has thus to resort to the discrete-time analysis for optimization of the AGC strategies.

Discrete-Time Control Model

The continuous-time dynamic system is described by a set of linear differential equations

$$\dot{\boldsymbol{x}} = \boldsymbol{A}\boldsymbol{x} + \boldsymbol{B}\boldsymbol{u} + \boldsymbol{\Gamma}\boldsymbol{P} \qquad (8.67)$$

where $\boldsymbol{x}$, $\boldsymbol{u}$, $\boldsymbol{p}$ are state, control and disturbance vectors respectively and $\boldsymbol{A}$,$\boldsymbol{B}$ and $\boldsymbol{\Gamma}$ are constant matrices associated with the above vectors.

The discrete-time behaviour of the continuous-time system is modelled by the system of first order linear difference equations:

$$\boldsymbol{x}(k+1) = \phi\boldsymbol{x}(k) + \Psi\boldsymbol{u}(k) + \gamma\boldsymbol{p}(k) \qquad (8.68)$$

where $\boldsymbol{x}(k)$, $\boldsymbol{u}(k)$ and $\boldsymbol{p}(k)$ are the state, control and disturbance vectors and are specified at $t = k\text{T}$, $k = 0, 1, 2, \ldots$ etc. and T is the sampling period. ϕ, ψ and γ are

the state, control and disturbance transition matrices and they are evaluated using the following relations:

$$\phi = e^{AT}$$
$$\psi = (e^{AT} - I)\, A^{-1} B$$
$$\gamma = (e^{AT} - I)\, A^{-1} \Gamma$$

where A, B and Γ are the constant matrices associated with x, u and p vectors in the corresponding continuous-time dynamic system. The matrix e^{AT} can be evaluated using various well-documented approaches like Sylvestor's expansion theorem, series expansion technique etc. The optimal digital load frequency controller design problem is discussed in detail in Ref [7].

8.10 DECENTRALIZED CONTROL

In view of the large size of a modern power system, it is virtually impossible to implement either the classical or the modern LFC algorithm in a centralized manner. In Fig. 8.24, a decentralized control scheme is shown x_1 is used to find out the vector u_1 while x_2 alone is employed to find out u_2. Thus,

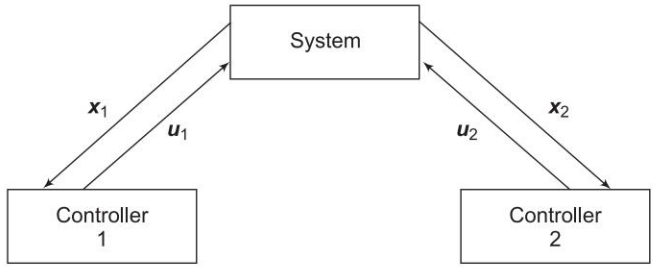

Fig. 8.24 Decentralized control

$$x = (x_1\ x_2)^T$$
$$u_1 = -k_1\, x_1$$
$$u_2 = -k_2\, x_2$$

A systematic design of the decentralized tie-line bias control solution has been shown possible using the modal control principle. Decentralized or hierarchical implementation of the optimal LFC algorithms seems to have been studied more widely for the stochastic case since the real load disturbances are truly stochastic. A simple approach is discussed in Ref. [7].

It may be noted that other techniques of model simplification are available in the literature on alternative tools to decentralized control. These include the method of "aggregation", "singular perturbation", "moment matching" and other techniques [9] for finding lower order models of a given large scale system.

8.11 DISCRETE INTEGRAL CONTROLLER FOR AGC

An interconnected power system normally consists of combination of several areas (e.g. NREB has 08 states). This facilitates smooth operation and better control. It is a normal practice to sample system data (frequency and tie line power) and transfer information over data links to the dispatch centre. These signals are updated every few seconds.

Power system along with the controller is shown in Fig. 8.25.

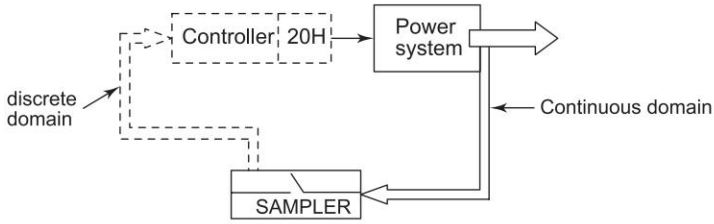

Fig. 8.25 Power system and representation of a controller

The controller is in the discrete domain though the power system is in the analogue or continuous-time domain. Discretization of the model for simulation studies must be carried out as per the Shannon's sampling theorem otherwise it would result in an error, proportional to the amount of aliasing.

A mixed system of Fig. 8.25 may be analyzed by modelling the entire system. The system output will be sampled at the normal sampling rate. If the sampling time $T = 1$ s, the controller output will be updated every second. Control input to the power system therefore, is held constant for 1 s between consecutive samples.

The control law in continuous mode is given as

$$u_i(t) = -k_{Ii} \int \text{ACE}_i(t)\, dt \tag{8.69}$$

The discrete version of Eq. (8.69) may be written as

$$u_i(kT) = u_i[(k-1)T] - k_{Ii}T\, \text{ACE}_i(kT) \tag{8.70}$$

where k is a sampling count.

8.12 AGC IN A RESTRUCTURED POWER SYSTEM

In a restructured power system, the engineering aspects of planning and operation have to be reformulated though main concepts and ideas do not change. The electric power systems currently is largely in the hands of vertically integrated utilities (VIU) Ref. [7] which own generation transmission-distribution systems that supply power to the customer at regulated rates. The electric power can be bought and sold between VIUs along the tie lines.

As explained in Ch. 1, the major change that has taken place is the emergence of IPPs (independent power producers) that can sell power to VIUs. Figure 8.26 shows the deregulated utility structure. GEN will compete in a free market to sell electricity (Electricity Bill 2003) they produce. The retail customer will continue to buy from local distribution company (DISCO). The entities that will wheel this power between GENCOs and DISCOs have been called TRANSCOs.

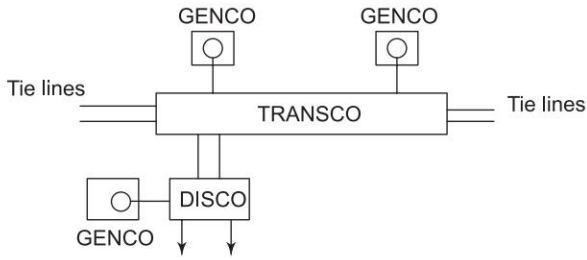

Fig. 8.26 Deregulated utility structure

A particular DISCO has the freedom to have a contract with any GENCO (may be in another control area) for transaction of power. All the transactions have to be cleared through an impartial entity called an 'independent system operator' (ISO). The ISO has to control a number of "ancillary services". AGC is one such service.

In the restructured environment, GENCOs sell power to various DISCOs at competitive prices. DISCO participation matrix (DPM) is used for easy visualization of contracts. Figure 8.27 shows a restructured two-area power system. Each area having one GENCO and one DISCO.

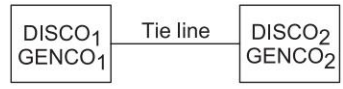

Fig. 8.27 Two interconnected control areas in a restructured power system

$$\text{DPM} = \begin{matrix} \\ \text{GENCO}_1 \\ \text{GENCO}_2 \end{matrix} \begin{bmatrix} \text{DISCO}_1 & \text{DISCO}_2 \\ cpf_{11} & cpf_{12} \\ cpf_{21} & cpf_{22} \end{bmatrix} \tag{8.71}$$

ijth entry in Eq. (8.71) corresponds to the fraction of the total load power contracted by DISCO_j from a GENCO_i. Notice $cpf_{11} + cpf_{12} = 1$ DPM shows the participation of a DISCO in a contract with a GENCO, and hence the name "DISCO participation matrix". In Eq. (8.71), cpf_{ij} refers to "contract participation factor".

$$\text{In general } \sum_i cpf_{ij} = 1.0 \tag{8.72}$$

Block Diagram Representation

Figure 8.16 shows block diagram representation of two area system for conventional AGC. Refs [27, 12] may be referred to for the complete analysis of AGC in a Restructured Power System.

Whenever a load demanded by a DISCO in an area changes, it is reflected as a local load in the area. This corresponds to the local load ΔP_{D1} and should appear in the deregulated AGC system block diagram at the point of input to the power system block. Since normally there are several GENCOs in each area, ACE signal has to be distributed between them in proportion to their participation in AGC. These coefficients that distribute ACE to several GENCOs are called "ACE participation factors".

$$\sum_{i=1}^{\text{NGENCO}_j} \alpha'_{ji} = 1.0 \tag{8.73}$$

where α'_{ji} = participation factor of ith GENCO in jth area

NGENCO_j = Number of GENCOs in jth area

Unlike the conventional AGC system, a DISCO prefers a particular GENCO for load power. As these demands should be incorporated in the dynamic models of the system, turbine and governor units must respond corresponding to this power demand. Therefore, for a specific set of GENCOs which is supposed to follow the load demanded by a DISCO, information signals must flow from a DISCO to a particular GENCO specifying corresponding demands as specified by *cpf*s and the pu MW load of a DISCO. These signals carry information as to which GENCO has to follow a load demanded by which DISCO.

The scheduled steady state power flow on the tie-line can be given as:

$$\Delta P_{\text{tie12}}^{\text{scheduled}} = \text{(Demand of DISCOs in area 2 from GENCOs in area 1) – (Demand of DISCOs in area 1 from GENCOs in area 2)}$$

$$\text{i.e. } \Delta P_{\text{tie12}}^{\text{scheduled}} = cpf_{12}\,\Delta P_{\text{L2}} - cpf_{21}\,\Delta P_{L1} \text{ for the system of Fig. 8.27.} \tag{8.74}$$

The tie-line power error at any time is defined as:

$$\Delta P_{\text{tie12}}^{\text{error}} = \Delta P_{\text{tie12}}^{\text{actual}} - \Delta P_{\text{tie12}}^{\text{scheduled}} \tag{8.75}$$

When steady state is reached, $\Delta P_{\text{tie12}}^{\text{error}}$ vanishes. However, this error signal is used to generate the respective ACE signals as in the conventional system scenario:

$$\text{ACE}_1 = B_1\,\Delta F_1 + \Delta P_{\text{tie12}}^{\text{error}} \tag{8.76}$$

$$\text{ACE}_2 = B_2\,\Delta F_2 + a_{12}\,\Delta P_{\text{tie12}}^{\text{error}} \tag{8.77}$$

For a two area power system (Refer Fig. 8.27), contracted power supplied by *i*th GENCO is given as:

$$\Delta P_i = \sum_{j=1}^{\text{NDISCO}=2} cpf_{ij}\,\Delta P_{Lj} \tag{8.78}$$

As an example, the block diagram representation of a two-area AGC system in a deregulated environment is shown in Fig. 8.28 (a) and its simplified version is described in Fig. 8.28 (b). In Fig. 8.28 (b), for $i = 1$,

$$\Delta P_1 = cpf_{11}\,\Delta P_{L1} + cpf_{12}\,\Delta P_{L2} \tag{8.79}$$

Similarly, the expression for ΔP_2 can be obtained from equation (8.78). In Fig. 8.28(b), ΔP_{uc1} and ΔP_{uc2} are uncontracted power demand, if any.

Also note that $\Delta P_{L1,\,LOC} = \Delta P_{L1}$ and $\Delta P_{L2,\,LOC} = \Delta P_{L2}$.

In this AGC scheme implementation, contracted load is fed forward through the DPM matrix to GENCO set points. The actual loads affect system dynamics via the input $\Delta P_{L,\,LOC}$ to the blocks of the power system. The difference between actual and contracted load demands may result in a frequency deviation that will drive AGC to redispatch GENCOs according to ACE participation factors. It is to note that AGC scheme does not require measurement of actual loads. The inputs $\Delta P_{L1,\,LOC}$ and $\Delta P_{L2,\,LOC}$ in the block diagram of Fig. 8.28(a) and (b) are part of the power system model, not part of AGC.

State SPACE Model of the Two Area Power System in Deregulated Environment

The state space model of the closed loop system of Fig. 8.28(b) is given as

$$\dot{\boldsymbol{x}} = \boldsymbol{Ax} + \boldsymbol{Bu} + \boldsymbol{\Gamma P} + \boldsymbol{\gamma P} \tag{8.80}$$

For determining the matrices $\boldsymbol{A}$, $\boldsymbol{B}$, $\boldsymbol{\Gamma}$ and $\boldsymbol{\gamma}$, the following equations are obtained from Fig. 8.28 (b):

Block **1** $$x_1 = (-\Delta P_{uc1} - \Delta P_{L1,LOC} - x_3 + x_4)\left(\frac{K_{P1}}{1 + ST_{P1}}\right)$$

or $$\dot{x}_1 = -\frac{x_1}{T_{P1}} - \frac{K_{P1}}{T_{P1}}x_3 + \frac{K_{P1}}{T_{P1}}x_4 + (\Delta P_{uc1} + \Delta P_{L1,LOC})\frac{K_{P1}}{T_{P1}} \tag{8.81}$$

Block **2** $$\dot{x}_2 = -\frac{x_2}{T_{P2}} - a_{12}x_3\frac{K_{P2}}{T_{P2}} + \frac{K_{P2}}{T_{P2}}x_6 + (\Delta P_{uc2} + \Delta P_{L2,LOC})\frac{K_{P2}}{T_{P2}} \tag{8.82}$$

Block **3** $$\dot{x}_3 = 2\pi\,T_{12}\,(x_1 - x_2) \tag{8.83}$$

Block **4** $$\dot{x}_4 = (x_5 - x_4)\,\frac{1}{T_{t1}} \tag{8.84}$$

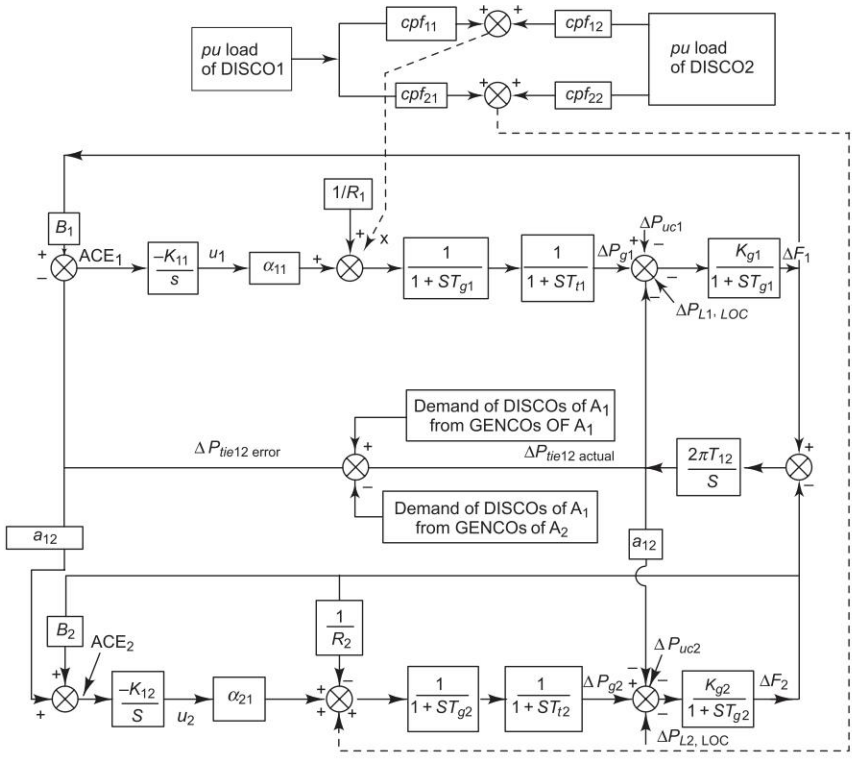

Fig. 8.28 (a) Block diagram of two area deregulated power system

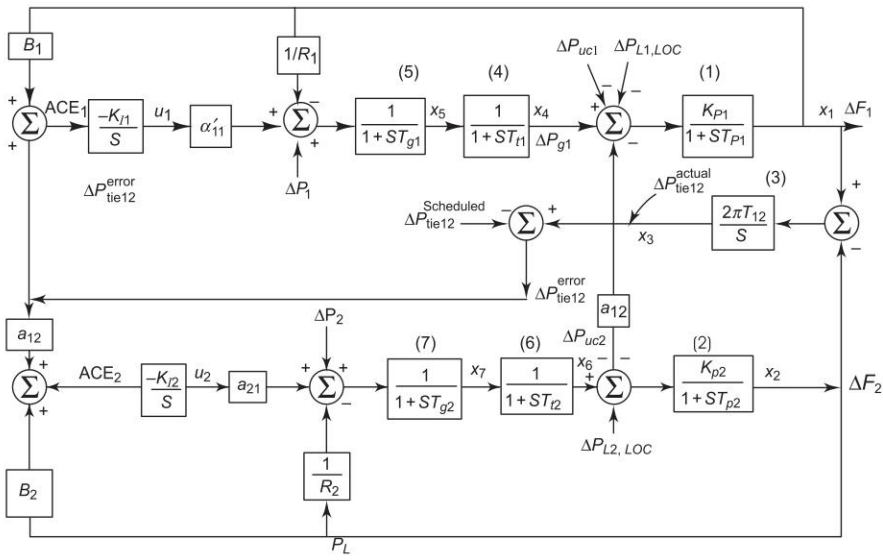

Fig. 8.28 (b) Simplified representation of Fig. 8.28 (a)

Block **5** $$\dot{x}_5 = -\frac{x_1}{T_{g1}R_1} - \frac{x_5}{T_{g1}} + (u_1\alpha'_{11} + \Delta P_1)\frac{1}{T_{g1}} \tag{8.85}$$

Block **6** $$\dot{x}_6 = \frac{x_7}{T_{t2}} - \frac{x_6}{T_{t2}} \tag{8.86}$$

Block **7** $$\dot{x}_7 = \frac{x_2}{R_{2T_{g2}}} - \frac{x_7}{T_{g2}} \ (\alpha'_2, u_2 + \Delta P_2) \ \frac{1}{T_{g2}} \tag{8.87}$$

The order of matrices $\boldsymbol{A}$, $\boldsymbol{B}$, $\boldsymbol{\Gamma}$ and γ for this case will be 11×11, 11×2, 11×2 and 11×2, respectively.

The structure of these matrices can be obtained from the differential equations (8.81)–(8.87) as

$$\boldsymbol{A} = \begin{bmatrix}
-\frac{1}{T_{P1}} & 0 & -\frac{K_{P1}}{T_{P1}} & \frac{K_{P1}}{T_{P1}} & 0 & 0 & 0 \\
0 & -\frac{1}{T_{P2}} & -a_{12}\frac{K_{P2}}{T_{P2}} & 0 & 0 & \frac{K_{P2}}{T_{P2}} & 0 \\
2\pi T_{12} & -2\pi T_{12} & 0 & 0 & 0 & 0 & 0 \\
0 & 0 & 0 & -\frac{1}{T_{t1}} & \frac{1}{T_{t1}} & 0 & 0 \\
-\frac{1}{R_1 T_{g1}} & 0 & 0 & 0 & -\frac{1}{T_{g1}} & 0 & 0 \\
0 & 0 & 0 & 0 & 0 & -\frac{1}{T_{t2}} & \frac{1}{T_{t2}} \\
0 & -\frac{1}{R_2 T_{g2}} & 0 & 0 & 0 & 0 & \frac{1}{T_{g2}}
\end{bmatrix}$$

$$\boldsymbol{B} = \begin{bmatrix}
0 & 0 \\
0 & 0 \\
0 & 0 \\
0 & 0 \\
-\frac{\alpha'_{11}}{T_{g1}} & 0 \\
0 & 0 \\
0 & -\frac{\alpha'_{21}}{T_{g2}}
\end{bmatrix}, \quad \Gamma = \begin{bmatrix}
-\frac{K_{P1}}{T_{P1}} & 0 \\
0 & \frac{K_{P2}}{T_{P2}} \\
0 & 0 \\
0 & 0 \\
\frac{cpf_{11}}{T_{g1}} & \frac{cpf_{12}}{T_{g1}} \\
0 & 0 \\
\frac{cpf_{21}}{T_{g2}} & \frac{cpf_{22}}{T_{g2}}
\end{bmatrix}, \quad \gamma = \begin{bmatrix}
-\frac{K_{P1}}{T_{P1}} & 0 \\
0 & -\frac{K_{P2}}{T_{P2}} \\
0 & 0 \\
0 & 0 \\
0 & 0 \\
0 & 0 \\
0 & 0
\end{bmatrix}$$

The structure of vectors U, P, p and x are as follows:

$$U = \begin{bmatrix} u_1 \\ u_2 \end{bmatrix}, P = \begin{bmatrix} \Delta P_{L1} \\ \Delta P_{L2} \end{bmatrix}, p = \begin{bmatrix} \Delta P_{uc1} \\ \Delta P_{uc2} \end{bmatrix}$$

$$X = [x_1, x_2\ x_3\ x_4\ x_5\ x_6\ x_7]^T$$

The integral control law for area-1 and area-2 are given as:

$$U_1 = -K_{i1} \int \text{ACE}_1\, dt$$

and

$$U_2 = -K_{i2} \int \text{ACE}_2\, dt$$

where, K_{i1} and K_{i2} are the integral gain settings of area 1 and area 2 respectively. Further analysis will be exactly as the non-regulated conventional power system.

8.13 SUMMARY

In this chapter AGC is introduced along with automatic voltage control for both conventional and deregulated power systems. Two area LFC and optimal controllers are also dealt with.

Problems

8.1 Two generators rated 200 MW and 400 MW are operating in parallel. The droop characteristics of their governors are 4% and 5% respectively from no load to full load. The speed changers are so set that the generators operate at 50 Hz sharing the full load of 600 MW in the ratio of their ratings. If the load reduces to 400 MW, how will it be shared among the generators and what will the system frequency be? Assume free governor operation.

The speed changers of the governors are reset so that the load of 400 MW is shared among the generators at 50 Hz in the ratio of their ratings. What are the no load frequencies of the generators?

8.2 Consider the block diagram model of load frequency control given in Fig. 8.6. Make the following approximation.

$$(1 + T_{sg}s)\,(1 + T_t s) \simeq 1 + (T_{sg} + T_t)s = 1 + T_{eq}s$$

Solve for $\Delta f(t)$ with parameters given below. Given $\Delta P_D = 0.01$ pu

$$T_{eq} = 0.4 + 0.5 = 0.9 \text{ s};\ T_{ps} = 20 \text{ s}$$

$$K_{sg}K_t = 1;\ K_{ps} = 100;\ R = 3$$

Compare with the exact response given in Fig. 8.9.

8.3 For the load frequency control with proportional plus integral controller as shown in Fig. 8.10, obtain an expression for the steady state error in cycles, i.e. $\int_{\lim t\to\infty}^{t} \Delta f(t)\,\mathrm{d}t$; for a unit step ΔP_D. What is the corresponding time error in seconds (with respect to 50 Hz)? Comment on the dependence of error in cycles upon the integral controller gain K_i.

$$\left[Hint: \mathcal{L}\int_0^t \Delta f(t)\mathrm{d}t = \frac{\Delta F(s)}{s};\ \int_{\lim t\to\infty}^{t} \Delta f(t)\,\mathrm{d}t = \lim_{s\to 0} s \times \frac{\Delta F(s)}{s} = \lim_{s\to 0} \Delta F(s) \right]$$

8.4 For the two area load frequency control of Fig. 8.16 assume that integral controller blocks are replaced by gain blocks, i.e. ACE_1 and ACE_2 are fed to the respective speed changers through gains $-K_{i1}$ and $-K_{i2}$. Derive an expression for the steady values of change in frequency and tie line power for simultaneously applied unit step load disturbance inputs in the two areas.

8.5 For the two area load frequency control employing integral of area control error in each area (Fig. 8.16), obtain an expression for $\Delta P_{\text{tie}}(s)$ for unit step disturbance in one of the areas. Assume both areas to be identical. Comment upon the stability of the system for parameter values given below:

$$T_{sg} = 0.4 \text{ s};\ T_t = 0.5 \text{ s};\ T_{ps} = 20 \text{ s}$$
$$K_{ps} = 100;\ R = 3;\ K_i = 1;\ b = 0.425$$
$$a_{12} = 1;\ 2\pi T_{12} = 0.05$$

[*Hint*: Apply Routh's stability criterion to the characteristic equation of the system.]

References

Books

1. Elgerd, O.I., *Electric Energy System Theory: An Introduction*, 2nd edn, McGraw-Hill, New York, 1982.
2. Weedy, B.M. and B.J. Cory, *Electric Power Systems*, 4th edn, Wiley, New York, 1998.
3. Cohn, Nathan, *Control of Generation and Power Flow on Interconnected Systems*, Wiley, New York, 1971.
4. Wood, A.J. and B.F. Woolenberg, *Power Generation, Operation and Control*, 2nd edn, Wiley, New York, 1994.
5. Nagarth, I.J. and M. Gopal, *Control Systems Engineering*, 3rd edn, New Age, New Delhi, 2001.
6. Handschin, E. (Ed.), *Real Time Control of Electric Power Systems*, Elsevier, New York, 1972.

7. Mahalanabis, A.K., D.P. Kothari and S.I. Ahson, *Computer Aided Power System Analysis and Control*, Tata McGraw-Hill, New Delhi, 1988.
8. Kirchmayer, L.K., *Economic Control of Interconnected Systems*, Wiley, New York, 1959.
9. Jamshidi, M., *Large Scale Systems: Modelling and Control*, North Holland, New York, 1983.
10. Singh, M.G. and A. Titli, *Systems Decomposition, Optimization and Control*, Pergamon Press, Oxford, 1978.
11. Siljak, D.D., *Non-Linear Systems: The Parameter Analysis and Design*, Wiley, New York, 1969.
12. Das, D., *Electrical Power Systems*, New Age Int. Pub., New Delhi, 2006.

Papers

13. Elgerd, O.I. and C.E. Fosha, "The Megawatt Frequency Control Problem: A New Approach Via Optimal Control Theory", *IEEE Trans*., April 1970, no. 4, PAS-89: 556.
14. Bhatti, T.S., C.S. Indulkar and D.P. Kothari, "Parameter Optimization of Power Systems for Stochastic Load Demands" *Proc. IFAC*, Bangalore, December 1986.
15. Kothari, M.L., P.S. Satsangi and J. Nanda, "Sampled-Data Automatic Generation Control of Interconnected Reheat Thermal Systems Considering Generation Rate Constraints", *IEEE Trans*., May 1981, PAS-100: 2334.
16. Nanda, J., M.L. Kothari and P.S. Satsangi, "Automatic Generation Control of an Interconnected Hydro-thermal System in Continuous and Discrete Modes Considering Generation Rate Constraints, *IEE Proc.,* pt D, no. 1, January 1983, 130 : 17.
17. IEEE Committee Report, 'Dynamic Models for Steam and Hydro-turbines in Power System Studies" *IEEE Trans.,* Nov./Dec. 1973, PAS-92: 1904.
18. Hiyama, T., "Optimization of Discrete-type Load Frequency Regulators Considering Generation-Rate Constraints" *Proc. IEE,* Nov. 1982, 129, pt C, 285.
19. Concordia, C., L.K. Kirchmayer and E.A. Szyonanski, "Effect of Speed Governor Dead-band on Tie Line Power and Frequency Control Performance" *AIEE Trans.,* Aug. 1957, 76: 429.
20. Nanda, J., M.L. Kothari and P.S. Satsangi, "Automatic Control of Reheat Thermal System Considering Generation Rate Constraint and Governor Dead-band", *J.I.E.* (India), June 1983, 63: 245.
21. Tripathy, S.C., G.S. Hope and O.P. Malik, "Optimization of Load-frequency Control Parameters for Power Systems with Reheat Steam Turbines and Governor Dead-band Nonlinearity", *Proc. IEE*, January 1982, 129, pt C, no. 1, 10.
22. Kothari, M.L., J. Nanda, D.P. Kothari and D. Das, "Discrete-mode AGC of a Two Area Reheat Thermal System with New Area Control Error", *IEEE Trans., on Power System*, vol. 4, no. 2 May 1989, 730.
23. Das, D., J. Nanda, M.L. Kothari and D.P. Kothari, "AGC of a Hydrothermal System with New ACE considering GRC", *Int. J. Electric Machines and Power System,* 1990, 18, no. 5, 461.
24. Das, D., M.L. Kothari, D.P. Kothari and J. Nanda, "Variable Structure Control Strategy to AGC of an Interconnected Reheat Thermal System", *Proc. IEE*, Nov. 1991, 138, pt D, 579.

25. Jalleli, Van Slycik *et al*., "*Understanding Automatic Generation Control*'' Paper no. 91 MW 229–5 PWRS, Presented at IEEE Winter Power Meeting, 1991.
26. Kothari, N.L., J. Nanda, D.P. Kothari and D. Das," Discrete Mode AGC of a Two Area Reheat Thermal System with a NACE considering GRC," *J.I.E.* (I) vol. 72, Feb. 1992, pp. 297–303.
27. Bakken, B.H. and Q.S. Grande," AGC in a Deregulated Power System", *IEEE Trans., on Power Systems,* 13, 4, Nov. 1998, pp. 1401–1406.
28. Ibraheem, P. Kumar and D.P. Kothari, "AGC Philosophies: A Review," *IEEE Trans., on Power Systems,* Feb. 2005, pp. 346–357.

Chapter 9
Symmetrical Fault Analysis

9.1 INTRODUCTION

So far we have dealt with the steady state behaviour of power system under normal operating conditions and its dynamic behaviour under small scale perturbations. This chapter is devoted to abnormal system behaviour under conditions of symmetrical short circuit (symmetrical three-phase fault*). Such conditions are caused in the system accidentally through insulation failure of equipment or flashover of lines initiated by a lightning stroke or through accidental faulty operation. The system must be protected against flow of heavy short circuit currents (which can cause permanent damage to major equipment) by disconnecting the faulty part of the system by means of circuit breakers operated by protective relaying. For proper choice of circuit breakers and protective relaying, we must estimate the magnitude of currents that would flow under short circuit conditions—this is the scope of fault analysis (study).

The majority of system faults are not three-phase faults but faults involving one line to ground or occasionally two lines to ground. These are unsymmetrical faults requiring special tools like symmetrical components and form the subject of study of the next two chapters. Though the symmetrical faults are rare, the symmetrical fault analysis must be carried out, as this type of fault generally leads to most severe fault current flow against which the system must be protected. Symmetrical fault analysis is, of course, simpler to carry out.

A power network comprises synchronous generators, transformers, lines and loads. Though the operating conditions at the time of fault are important, the loads can be neglected during fault, as voltages dip very low so that currents drawn by loads can be neglected in comparison to fault currents.

The synchronous generator during short circuit has a characteristic time-varying behaviour. In the event of a short circuit, the flux per pole undergoes dynamic change with associated transients in damper and field windings. The reactance of the circuit model of the machine changes in the first few cycles from a low subtransient reactance to a higher transient value, finally settling at a still higher synchronous (steady state) value. Depending upon the arc

*Symmetrical fault may be a solid three-phase short circuit or may involve arc impedance.

interruption time of circuit breakers, a suitable reactance value is used for the circuit model of synchronous generators for short circuit analysis.

In a modern large interconnected power system, heavy currents flowing during a fault must be interrupted much before the steady state conditions are established. Furthermore, from the considerations of mechanical forces that act on circuit breaker components, the maximum current that a breaker has to carry momentarily must also be determined. For selecting a circuit breaker we must, therefore, determine the initial current that flows on occurrence of a short circuit and also the current in the transient that flows at the time of circuit interruption.

9.2 TRANSIENT ON A TRANSMISSION LINE

Let us consider the short circuit transient on a transmission line. Certain simplifying assumptions are made at this stage.

(i) The line is fed from a constant voltage source (the case when the line is fed from a realistic synchronous machine will be treated in Sec. 9.3).
(ii) Short circuit takes place when the line is unloaded (the case of short circuit on a loaded line will be treated later in this chapter).
(iii) Line capacitance is negligible and the line can be represented by a lumped *RL* series circuit.

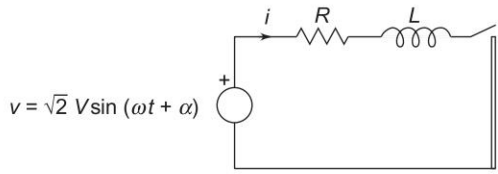

Fig. 9.1

With the above assumptions the line can be represented by the circuit model of Fig. 9.1. The short circuit is assumed to take place at $t = 0$. The parameter α controls the instant on the voltage wave when short circuit occurs. It is known from circuit theory that the current after short circuit is composed of two parts, i.e.

$$i = i_s + i_t$$

where

i_s = steady state current

$$= \frac{\sqrt{2}V}{|Z|} \sin(\omega t + \alpha - \theta)$$

$$Z = (R^2 + \omega^2 L^2)^{1/2} \angle \left(\theta = \tan^{-1} \frac{\omega L}{R}\right)$$

i_t = transient current [it is such that $i(0) = i_s(0) + i_t(0) = 0$ being an inductive circuit; it decays corresponding to the time constant L/R].

$$= -i_s(0)e^{-(R/L)t}$$

$$= \frac{\sqrt{2}V}{|Z|}\sin(\theta-\alpha)e^{-(R/L)t}$$

Thus short circuit current is given by

$$i = \underbrace{\frac{\sqrt{2}V}{|Z|}\sin(\omega t+\alpha-\theta)}_{\text{Symmetrical short circuit current}} + \underbrace{\frac{\sqrt{2}V}{|Z|}\sin(\theta-\alpha)e^{-(R/L)t}}_{\text{DC off-set current}} \qquad (9.1)$$

A plot of i_s, i_t and $i = i_s + i_t$ is shown in Fig. 9.2. In power system terminology, the sinusoidal steady state current is called the *symmetrical short circuit current* and the unidirectional transient component is called the *DC off-set current*, which causes the total short circuit current to be unsymmetrical till the transient decays.

It easily follows from Fig. 9.2 that the *maximum momentary short circuit current* i_{mm} corresponds to the first peak. If the decay of transient current in this short time is neglected,

$$i_{mm} = \frac{\sqrt{2}V}{|Z|}\sin(\theta-\alpha) + \frac{\sqrt{2}V}{|Z|} \qquad (9.2)$$

Since transmission line resistance is small, $\theta \approx 90^\circ$.

$$\therefore \quad i_{mm} = \frac{\sqrt{2}V}{|Z|}\cos\alpha + \frac{\sqrt{2}V}{|Z|} \qquad (9.3)$$

This has the maximum possible value for $\alpha = 0$, i.e. short circuit occurring when the voltage wave is going through zero. Thus

$$i_{mm\ (\text{max possible})} = 2\frac{\sqrt{2}V}{|Z|} \qquad (9.4)$$

= twice the maximum of symmetrical short circuit current (*doubling effect*)

For the selection of circuit breakers, momentary short circuit current is taken corresponding to its maximum possible value (a safe choice).

The next question is 'what is the current to be interrupted?' As has been pointed out earlier, modern day circuit breakers are designed to interrupt the current in the first few cycles (five cycles or less). With reference to Fig. 9.2 it means that when the current is interrupted, the DC off-set (i_t) has not yet died out and so contributes to the current to be interrupted. Rather than computing

the value of the DC off-set at the time of interruption (this would be highly complex in a network of even moderately large size), the symmetrical short circuit current alone is calculated. This figure is then increased by an empirical multiplying factor to account for the DC off-set current. Details are given in Sec. 9.5.

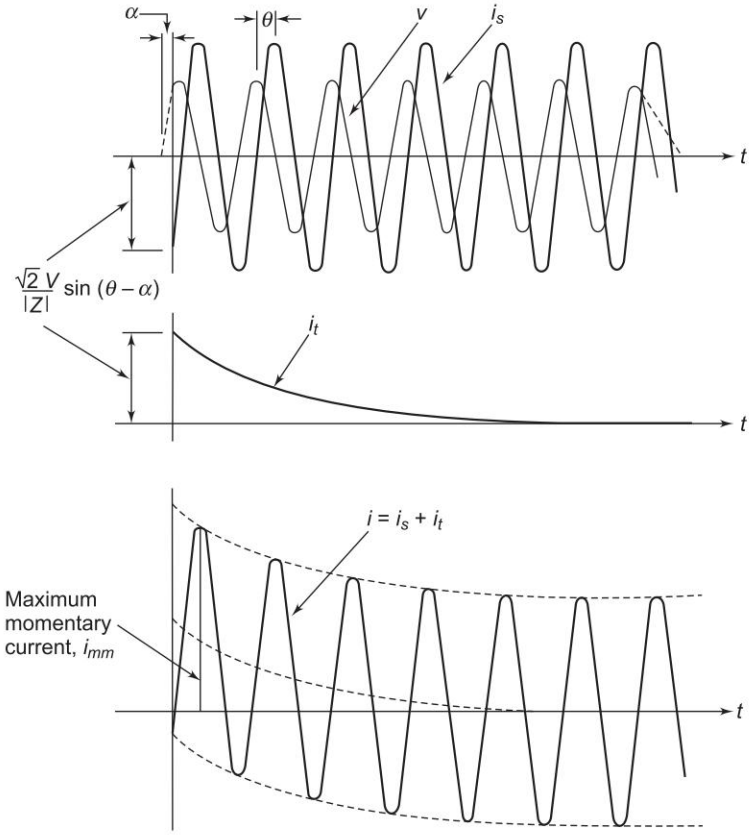

Fig. 9.2 Waveform of a short circuit current on a transmission line

9.3 SHORT CIRCUIT OF A SYNCHRONOUS MACHINE (ON NO LOAD)

Under steady state short circuit conditions, the armature reaction of a synchronous generator produces a demagnetizing flux. In terms of a circuit this effect is modelled as a reactance X_a in series with the induced emf. This reactance when combined with the leakage reactance X_l of the machine is called *synchronous reactance* X_d (direct axis synchronous reactance in the case of salient pole machines). Armature resistance being small can be neglected. The steady state short circuit model of a synchronous machine is shown in Fig. 9.3(a) on per phase basis.

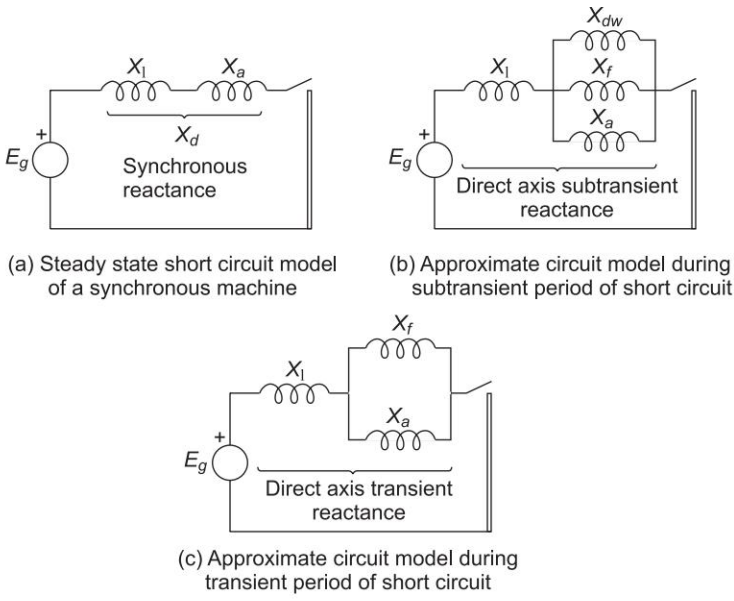

(a) Steady state short circuit model of a synchronous machine

(b) Approximate circuit model during subtransient period of short circuit

(c) Approximate circuit model during transient period of short circuit

Fig. 9.3

Consider now the sudden short circuit (three-phase) of a synchronous generator initially operating under open circuit conditions. The machine undergoes a transient in all the three phases finally ending up in steady state conditions described above. The circuit breaker must, of course, interrupt the current much before steady conditions are reached. Immediately upon short circuit, the DC off-set currents appear in all the three phases, each with a different magnitude since the point on the voltage wave at which short circuit occurs is different for each phase. These DC off-set currents are accounted for separately on an empirical basis and, therefore, for short circuit studies, we need to concentrate our attention on *symmetrical (sinusoidal) short circuit current only*. Immediately in the event of a short circuit, the symmetrical short circuit current is limited only by the leakage reactance of the machine. Since the air gap flux cannot change instantaneously (*theorem of constant flux linkages*), to counter the demagnetization of the armature short circuit current, currents appear in the field winding as well as in the damper winding in a direction to help the main flux. These currents decay in accordance with the winding time constants. The time constant of the damper winding which has low leakage inductance is much less than that of the field winding, which has high leakage inductance. Thus during the initial part of the short circuit, the damper and field windings have transformer currents induced in them so that in the circuit model their reactances—X_f of field winding and X_{dw} of damper winding—appear in parallel* with X_a as shown in Fig. 9.3(b). As the damper

*Unity turn ratio is assumed here.

winding currents are first to die out, X_{dw} effectively becomes open-circuited and at a later stage X_f becomes open-circuited. The machine reactance thus changes from the parallel combination of X_a, X_f and X_{dw} during the initial period of the short circuit to X_a and X_f in parallel (Fig. 9.3(c)) in the middle period of the short circuit, and finally to X_a in steady state (Fig. 9.3(a)). The reactance presented by the machine in the initial period of the short circuit, i.e.

$$X_l + \frac{1}{(1/X_a + 1/X_f + 1/X_{dw})} = X_d'' \tag{9.5}$$

is called the *subtransient reactance* of the machine, while the reactance effective after the damper winding currents have died out, i.e.

$$X_d' = X_1 + (X_a \,||\, X_f) \tag{9.6}$$

is called the *transient reactance* of the machine. Of course, the reactance under steady conditions is the *synchronous reactance* of the machine. Obviously $X_d'' < X_d' < X_d$. The machine thus offers a time-varying reactance which changes from X_d'' to X_d' and finally to X_d.

If we examine the oscillogram of the short circuit current of a synchronous machine after the DC off-set currents have been removed from it, we will find the current wave shape as given in Fig. 9.4(a). The envelope of the current wave shape is plotted in Fig. 9.4(b). The short circuit current can be divided into three periods—initial subtransient period when the current is large as the machine offers subtransient reactance, the middle transient period where the machine offers transient reactance, and finally the steady state period when the machine offers synchronous reactance.

If the transient envelope is extrapolated backwards in time, the difference between the transient and subtransient envelopes is the current $\Delta i''$ (corresponding to the damper winding current) which decays fast according to the damper winding time constant. Similarly, the difference $\Delta i'$ between the steady state and transient envelopes decays in accordance with the field time constant.

In terms of the oscillogram, the currents and reactances discussed above, we can write

$$|I| = \frac{Oa}{\sqrt{2}} = \frac{|E_g|}{X_d} \tag{9.7a}$$

$$|I'| = \frac{Ob}{\sqrt{2}} = \frac{|E_g|}{X_d'} \tag{9.7b}$$

$$|I''| = \frac{Oc}{\sqrt{2}} = \frac{|E_g|}{X_d''} \tag{9.7c}$$

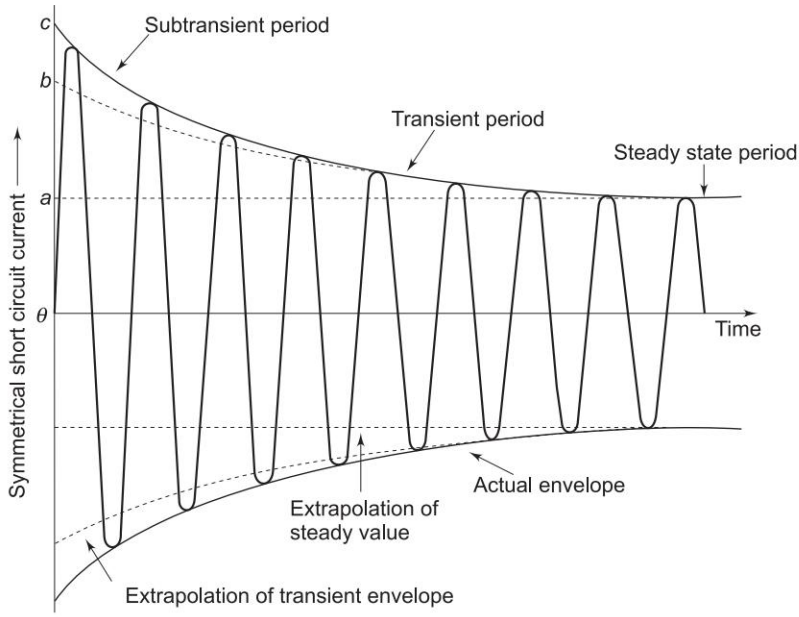

(a) Symmetrical short circuit armature current in synchronous machine

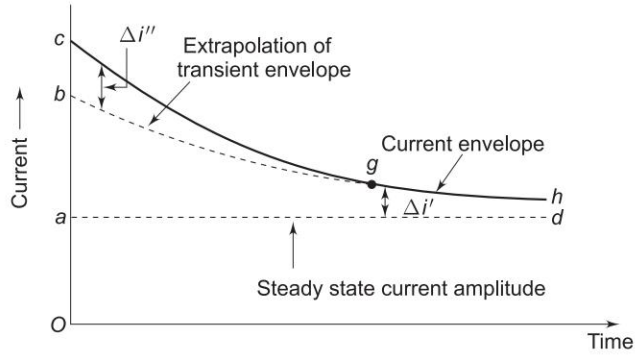

(b) Envelope of synchronous machine symmetrical short circuit current

Fig. 9.4

where

$|I|$ = steady state current (rms)
$|I'|$ = transient current (rms) excluding DC component
$|I''|$ = subtransient current (rms) excluding DC component
X_d = direct axis synchronous reactance
X'_d = direct axis transient reactance
X''_d = direct axis subtransient reactance
$|E_g|$ = per phase no load voltage (rms)
Oa, Ob, Oc = intercepts shown in Figs 9.4(a) and (b).

The intercept *Ob* for finding transient reactance can be determined accurately by means of a logarithmic plot. Both $\Delta i''$ and $\Delta i'$ decay exponentially as

$$\Delta i'' = \Delta i''_0 \exp(-t/\tau_{dw})$$

$$\Delta i' = \Delta i'_0 \exp(-t/\tau_f)$$

where τ_{dw} and τ_f are respectively damper, and field winding time constants with $\tau_{dw} \gg \tau_f$. At time $t \gg \tau_{dw}$, $\Delta i''$ practically dies out and we can write

$$\log(\Delta i'' + \Delta i')\big|_{t >> \tau_{dw}} \approx \log \Delta i'_0 - t/\tau_f = -\Delta i'_0 (-t/\tau_f)$$

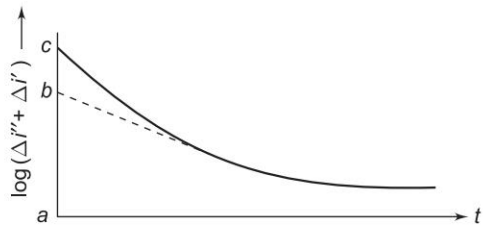

Fig. 9.5

The plot of log $(\Delta i'' + \Delta i')$ versus time for $t \gg \tau_{dw}$ therefore, becomes a straight line with a slope of $(-1/\tau_f)$ as shown in Fig. 9.5. As the straight line portion of the plot is extrapolated (straight line extrapolation is much more accurate than the exponential extrapolation of Fig. 9.4), taking inverse log of intercept corresponding to $t = 0$ is

$$\log^{-1}(ab) = \Delta i'|_{t=0} = \Delta i_0' \exp(-t/\tau_f)|_{t=0} = \Delta i'_0 = ab$$

Table 9.1 Typical values of synchronous machine reactances (All values expressed in pu of rated MVA)

Type of machine	*Turbo-alternator (Turbine generator)*	*Salient pole (Hydroelectric)*	*Synchronous compensator (Condenser/ capacitor)*	*Synchronous motors**
X_s (or X_d)	1.00–2.0	0.6–1.5	1.5–2.5	0.8–1.10
X_q	0.9–1.5	0.4–1.0	0.95–1.5	0.65–0.8
X_d'	0.12–0.35	0.2–0.5	0.3–0.6	0.3–0.35
X_d''	0.1–0.25	0.13–0.35	0.18–0.38	0.18–0.2
X_2	$= X_d''$	$= X_d''$	0.17– 0.37	0.19–0.35
X_0	0.04–0.14	0.02–0.2	0.025–0.16	0.05–0.07
r_a	0.003–0.008	0.003–0.015	0.004–0.01	0.003–0.012

r_a = AC resistance of the armature winding per phase.

* High-speed units tend to have low reactance and low-speed units high reactance.

Though the machine reactances are dependent upon magnetic saturation (corresponding to excitation), the values of reactances normally lie within certain predictable limits for different types of machines. Table 9.1 gives typical values of machine reactances which can be used in fault calculations and in stability studies.

Normally both generator and motor subtransient reactances are used to determine the momentary current flowing on occurrence of a short circuit. To decide the interrupting capacity of circuit breakers, except those which open instantaneously, subtransient reactance is used for generators and transient reactance for synchronous motors. As we shall see later the transient reactances are used for stability studies.

The machine model to be employed when the short circuit takes place from loaded conditions will be explained in Sec. 9.4.

The method of computing short circuit current is illustrated through examples given below.

Example 9.1 For the radial network shown in Fig. 9.6, a three-phase fault occurs at *F*. Determine the fault current and the line voltage at 11 kV bus under fault conditions.

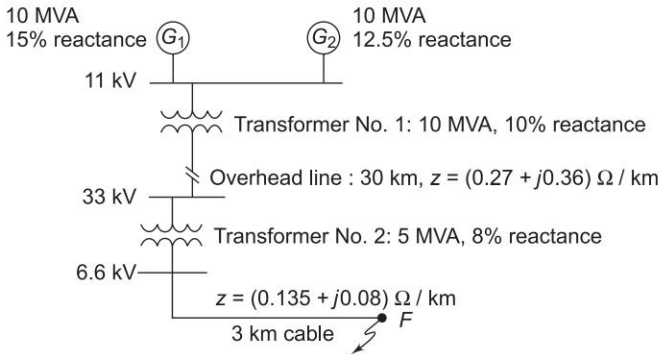

Fig. 9.6 Radial network for Example 9.1

Solution

Select a system base of 100 MVA.

Voltage bases are: 11 kV in generators, 33 kV for overhead line and 6.6 kV for cable.

$$\text{Reactance of } G_1 = j\frac{0.15 \times 100}{10} = j1.5 \text{ pu}$$

$$\text{Reactance of } G_2 = j\frac{0.125 \times 100}{10} = j1.25 \text{ pu}$$

$$\text{Reactance of } T_1 = j\frac{0.1 \times 100}{10} = j1.0 \text{ pu}$$

$$\text{Reactance of } T_2 = j\frac{0.08 \times 100}{5} = j1.6 \text{ pu}$$

$$\text{Overhead line impedance} = \frac{Z \text{ (in ohms)} \times \text{MVA}_{\text{Base}}}{(\text{kV}_{\text{Base}})^2}$$

$$= \frac{30 \times (0.27 + j0.36) \times 100}{(33)^2}$$

$$= (0.744 + j0.99) \text{ pu}$$

$$\text{Cable impedance} = \frac{3(0.135 + j0.08) \times 100}{(6.6)^2}$$

$$= (0.93 + j0.55) \text{ pu}$$

Circuit model of the system for fault calculations is shown in Fig. 9.7. Since the system is on no load prior to occurrence of the fault, the voltages of the two generators are identical (in phase and magnitude) and are equal to 1 pu. The generator circuit can thus be replaced by a single voltage source in series with the parallel combination of generator reactances as shown.

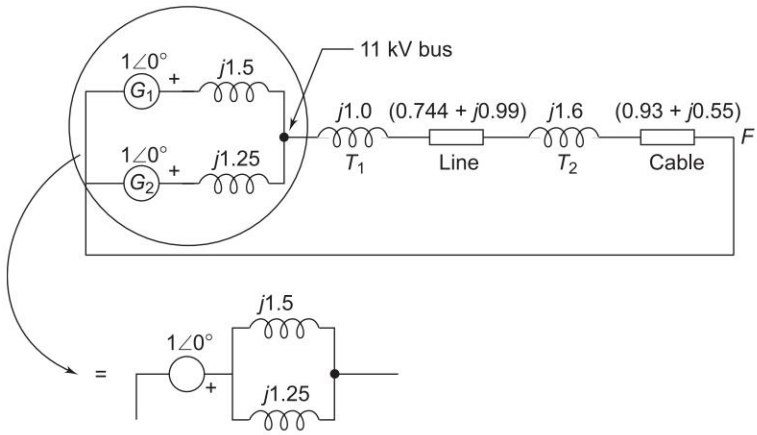

Fig. 9.7

$$\text{Total impedance} = (j1.5 \,||\, j1.25) + (j1.0) + (0.744 + j0.99) + (j1.6) + (0.93 + j0.55)$$

$$= 1.674 + j4.82 = 5.1 \angle 70.8^\circ \text{ pu}$$

$$I_{SC} = \frac{1\angle 0}{5.1\angle 70.8^\circ} = 0.196 \angle -70.8^\circ \text{ pu}$$

$$I_{\text{Base}} = \frac{100 \times 10^3}{\sqrt{3} \times 6.6} = 8750 \text{ A}$$

$$\therefore \quad I_{SC} = 0.196 \times 8750 = 1715 \text{ A}$$

Total impedance between F and 11 kV bus

$$= (0.93 + j055) + (j1.6) + (0.744 + j0.99) + (j1.0)$$

$$= 1.674 + j4.14 = 4.43 \angle 76.8^\circ \text{ pu}$$

$$\text{Voltage at 11 kV bus} = 4.43 \angle 67.8^\circ \times 0.196 \angle -70.8^\circ$$

$$= 0.88 \angle -3^\circ \text{ pu} = 0.88 \times 11 = 9.68 \text{ kV}$$

Example 9.2 A 25 MVA, 11 kV generator with $X_d'' = 20\%$ is connected through a transformer, line and a transformer to a bus that supplies three identical motors as shown in Fig. 9.8. Each motor has $X_d'' = 25\%$ and $X_d' = 30\%$ on a base of 5 MVA, 6.6 kV. The three-phase rating of the step-up transformer is 25 MVA, 11/66 kV with a leakage reactance of 10% and that of the step-down transformer is 25 MVA, 66/6.6 kV with a leakage reactance of 10%. The bus voltage at the motors is 6.6 kV when a three-phase fault occurs at the point *F*. For the specified fault, calculate

(a) the subtransient current in the fault,
(b) the subtransient current in the breaker *B*,
(c) the momentary current in breaker *B*, and
(d) the current to be interrupted by breaker *B* in five cycles.

Given: Reactance of the transmission line = 15% on a base of 25 MVA, 66 kV. Assume that the system is operating on no load when the fault occurs.

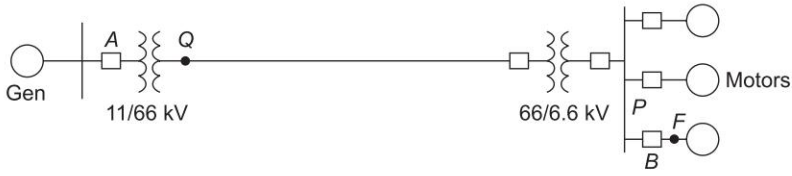

Fig. 9.8

Solution

Choose a system base of 25 MVA.
For a generator voltage base of 11 kV, line voltage base is 66 kV and motor voltage base is 6.6 kV.

(a) For each motor

$$X''_{dm} = j0.25 \times \frac{25}{5} = j1.25 \text{ pu}$$

Line, transformers and generator reactances are already given on proper base values.

The circuit model of the system for fault calculations is given in Fig. 9.9(a). The system being initially on no load, the generator and motor induced emfs are identical. The circuit can therefore be reduced to that of Fig. 9.9(b) and then to Fig. 9.9(c). Now

$$I_{SC} = 3 \times \frac{1}{j1.25} + \frac{1}{j0.55} = -j4.22 \text{ pu}$$

$$\text{Base current in 6.6 kV circuit} = \frac{25 \times 1000}{\sqrt{3} \times 6.6} = 2187 \text{ A}$$

$$\therefore \quad I_{SC} = 4.22 \times 2187 = 9229 \text{ A}$$

(b) From Fig. 9.9(c), current through circuit breaker B is

$$I_{SC}(B) = 2 \times \frac{1}{j1.25} + \frac{1}{j0.55} = -j3.42$$

$$= 3.42 \times 2187 = 7479.5 \text{ A}$$

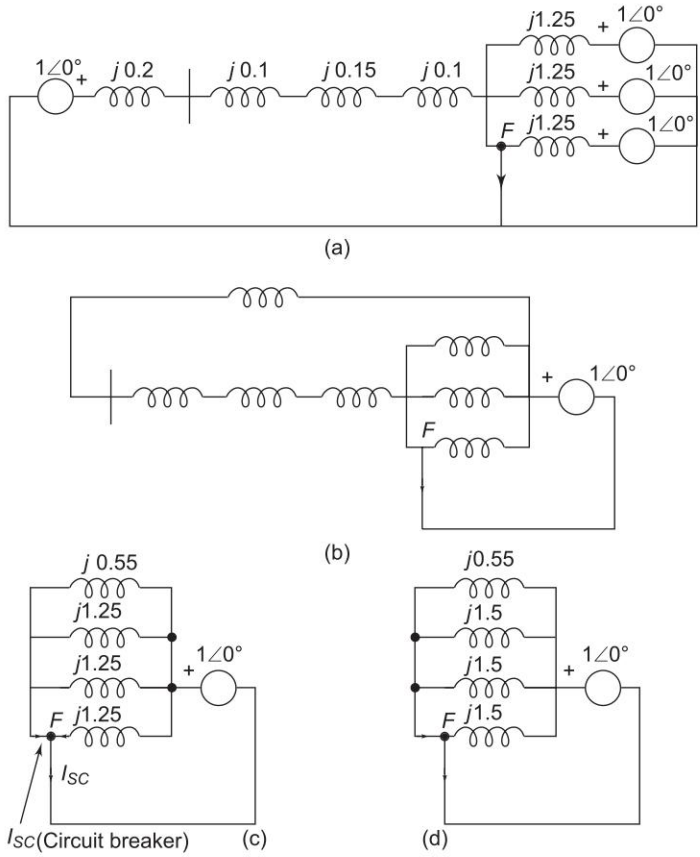

Fig. 9.9

(c) For finding momentary current through the breaker, we must add the DC off-set current to the symmetrical subtransient current obtained in part (b). Rather than calculating the DC off-set current, allowance is made for it on an empirical basis. As explained in Sec. 9.5,

Momentary current through breaker $B = 1.6 \times 7479.5$

$= 11967$ A

(d) To compute the current to be interrupted by the breaker, motor subtransient reactance ($X_d'' = j0.25$) is now replaced by transient reactance ($X_d' = j0.30$).

$$X_d' \text{ (motor)} = j0.3 \times \frac{25}{5} = j1.5 \text{ pu}$$

The reactances of the circuit of Fig. 9.9(c) now modify to that of Fig. 9.9(d). Current (symmetrical) to be interrupted by the breaker (as shown by arrow)

$$= 2 \times \frac{1}{j1.5} + \frac{1}{j0.55} = 3.1515 \text{ pu}$$

Allowance is made for the DC off-set value by multiplying with a factor of 1.1 (Sec. 9.5). Therefore, the current to be interrupted is

$$1.1 \times 3.1515 \times 2187 = 7581 \text{ A}$$

9.4 SHORT CIRCUIT OF A LOADED SYNCHRONOUS MACHINE

In the previous article on the short circuit of a synchronous machine, it was assumed that the machine was operating at no load prior to the occurrence of short circuit. The analysis of short circuit on a loaded synchronous machine is complicated and is beyond the scope of this book. We shall, however, present here the methods of computing short circuit current when short circuit occurs under loaded conditions.

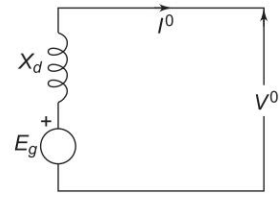

Fig. 9.10 Circuit model of a loaded machine

Figure 9.10 shows the circuit model of a synchronous generator operating under steady conditions supplying a load current I^0 to the bus at a terminal voltage of V^0, E_g is the induced emf under loaded condition and X_d is the direct axis synchronous reactance of the machine. When short circuit occurs at the terminals of this machine, the circuit model to be used for computing short circuit current is given in Fig. 9.11(a) for subtransient current, and in Fig. 9.11(b) for transient current. The induced emfs to be used in these models are given by

$$E_g'' = V^0 + jI^0X_d'' \tag{9.8}$$

$$E_g' = V^0 + jI^0X_d' \tag{9.9}$$

The voltage E_g'' is known as the *voltage behind the subtransient reactance* and the voltage E_g' is known as the *voltage behind the transient reactance*. In fact, if I^0 is zero (no load case), $E_g'' = E_g' = E_g$, the no load voltage, in which case the circuit model reduces to that discussed in Sec. 9.3.

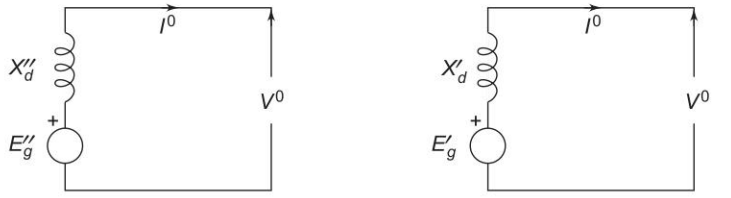

(a) Circuit model for computing subtransient current

(b) Circuit model for computing transient current

Fig. 9.11

Synchronous motors have internal emfs and reactances similar to that of a generator except that the current direction is reversed. During short circuit conditions these can be replaced by similar circuit models except that the voltage behind subtransient/transient reactance is given by

$$E''_m = V^0 - jI^0 X''_d \tag{9.10}$$

$$E'_m = V^0 - jI^0 X'_d \tag{9.11}$$

Whenever we are dealing with short circuit of an interconnected system, the synchronous machines (generators and motors) are replaced by their corresponding circuit models having voltage behind subtransient (transient) reactance in series with subtransient (transient) reactance. The rest of the network being passive remains unchanged.

Example 9.3 A synchronous generator and a synchronous motor each rated 25 MVA, 11 kV having 15% subtransient reactance are connected through transformers and a line as shown in Fig. 9.12(a). The transformers are rated 25 MVA, 11/66 kV and 66/11 kV with leakage reactance of 10% each. The line has a reactance of 10% on a base of 25 MVA, 66 kV. The motor is drawing 15 MW at 0.8 power factor leading and a terminal voltage of 10.6 kV when a symmetrical three-phase fault occurs at the motor terminals. Find the subtransient current in the generator, motor and fault.

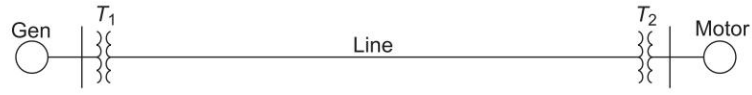

(a) One-line diagram for the system of Example 9.3

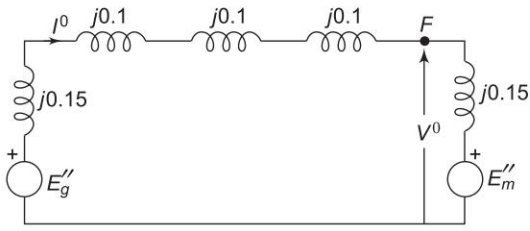

(b) Prefault equivalent circuit

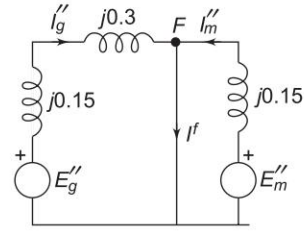

(c) Equivalent circuit during fault

Fig. 9.12

Solution

All reactances are given on a base of 25 MVA and appropriate voltages.

$$\text{Prefault voltage } V^0 = \frac{10.6}{11} = 0.9636 \angle 0^\circ \text{ pu}$$

$$\text{Load} = 15 \text{ MW, } 0.8 \text{ pf leading}$$

$$= \frac{15}{25} = 0.6 \text{ pu, } 0.8 \text{ pf leading}$$

$$\text{Prefault current } I^0 = \frac{0.6}{0.9636 \times 0.8} \angle 36.9^\circ$$
$$= 0.7783 \angle 36.9^\circ \text{ pu}$$

Voltage behind subtransient reactance (generator)

$$E_g'' = 0.9636 \angle 0^\circ + j0.45 \times 0.7783 \angle 36.9^\circ$$
$$= 0.7536 + j0.28 \text{ pu}$$

Voltage behind subtransient reactance (motor)

$$E_m'' = 0.9636 \angle 0^\circ - j0.15 \times 0.7783 \angle 36.9^\circ$$
$$= 1.0336 - j0.0933 \text{ pu}$$

The prefault equivalent circuit is shown in Fig. 9.12(b). Under faulted condition (Fig. 9.12(c))

$$I_g'' = \frac{0.7536 + j0.2800}{j0.45} = 0.6226 - j1.6746 \text{ pu}$$

$$I_m'' = \frac{1.0336 - j0.0933}{j0.15} = -0.6226 - j6.8906 \text{ pu}$$

Current in fault

$$I^f = I_g'' + I_m'' = -j8.5653 \text{ pu}$$

$$\text{Base current (gen/motor)} = \frac{25 \times 10^3}{\sqrt{3} \times 11} = 1{,}312.2 \text{ A}$$

Now

$$I_g'' = 1{,}312.2\ (0.6226 - j1.6746) = (816.4 - j2{,}197.4) \text{ A}$$
$$I_m'' = 1{,}312.2\ (-0.6226 - j6.8906) = (-816.2 - j9{,}041.8) \text{ A}$$
$$I^f = -j11{,}239 \text{ A}$$

Short Circuit (SC) Current Computation through the Thevenin Theorem

An alternate method of computing short circuit currents is through the application of the Thevenin theorem. This method is faster and easily adopted to systematic computation for large networks. While the method is perfectly general, it is illustrated here through a simple example.

Consider a synchronous generator feeding a synchronous motor over a line. Figure 9.13(a) shows the circuit model of the system under conditions of steady load. Fault computations are to be made for a fault at F, at the motor terminals. As a first step the circuit model is replaced by the one shown in Fig. 9.13(b), wherein the synchronous machines are represented by their transient reactances (or subtransient reactances if subtransient currents are of interest) in series with voltages behind transient reactances. This change does not disturb the prefault current I^0 and prefault voltage V^0 (at F).

As seen from *FG* the Thevenin equivalent circuit of Fig. 9.13(b) is drawn in Fig. 9.13(c). It comprises prefault voltage V^0 in series with the passive Thevenin impedance network. It is noticed that the prefault current I^0 does not appear in the passive Thevenin impedance network. It is therefore to be remembered that this current must be accounted for by superposition after the SC solution is obtained through use of the Thevenin equivalent.

Consider now a fault at *F* through an impedance Z^f. Figure 9.13(d) shows the Thevenin equivalent of the system feeding the fault impedance. We can immediately write

$$I^f = \frac{V^0}{jX_{Th} + Z^f} \tag{9.12}$$

Current caused by fault in generator circuit

$$\Delta I_g = \frac{X'_{dm}}{(X'_{dg} + X + X'_{dm})} I^f \tag{9.13}$$

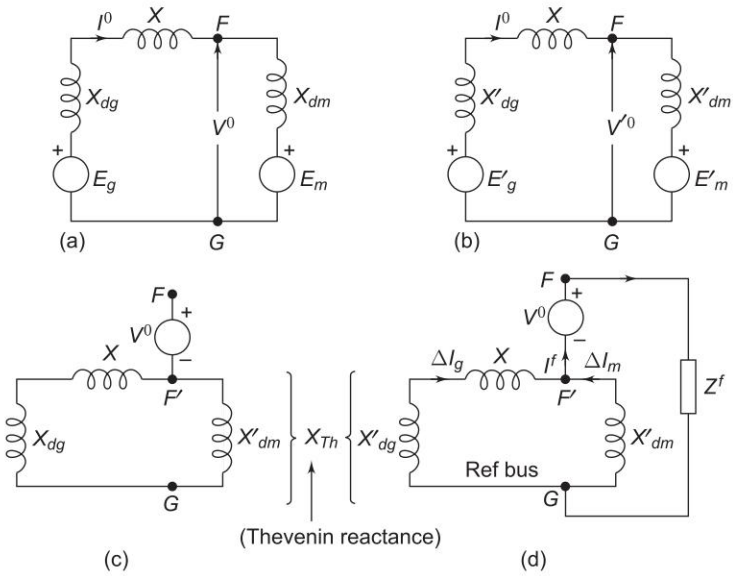

Fig. 9.13 Computation of SC current by the Thevenin equivalent

Current caused by fault in motor circuit

$$\Delta I_m = \frac{X'_{dg} + X}{(X'_{dm} + X + X'_{dg})} I^f \tag{9.14}$$

Postfault currents and voltages are obtained as follows by superposition:

$$I_g^f = I^0 + \Delta I_g$$
$$I_m^f = -I^0 + \Delta I_m \text{ (in the direction of } \Delta I_m) \tag{9.15}$$

Postfault voltage

$$V^f = V^0 + (-jX_{Th} I^f) = V^0 + \Delta V \tag{9.16}$$

where $\Delta V = -jX_{Th}I^f$ is the voltage of the fault point F' on the Thevenin passive network (with respect to the reference bus G) caused by the flow of fault current I^f.

An observation can be made here. Since the prefault current flowing out of fault point F is always zero, the postfault current out of F is independent of load for a given prefault voltage at F.

The above approach to SC computation is summarized in the following four steps:

Step 1: Obtain steady state solution of loaded system (load flow study).

Step 2: Replace reactances of synchronous machines by their subtransient/ transient values. Short circuit all emf sources. The result is the passive Thevenin network.

Step 3: Excite the passive network of step 2 at the fault point by negative of prefault voltage (see Fig. 9.13(d)) in series with the fault impedance. Compute voltages and currents at all points of interest.

Step 4: Postfault currents and voltages are obtained by adding results of steps 1 and 3.

The following assumptions can be safely made in SC computations leading to considerable computational simplification:

Assumption 1 All prefault voltage magnitudes are 1 pu.

Assumption 2 All prefault currents are zero.

The first assumption is quite close to actual conditions as under normal operation all voltages (pu) are nearly unity.

The changes in current caused by short circuit are quite large, of the order of 10–20 pu and are purely reactive; whereas the prefault load currents are almost purely real. Hence the total postfault current which is the result of the two currents can be taken in magnitude equal to the larger component (caused by the fault). This justifies assumption 2.

Let us illustrate the above method by recalculating the results of Example 9.3.

The circuit model for the system of Example 9.3 for computation of postfault condition is shown in Fig. 9.14.

$$I^f = \frac{V^0}{(j0.15 \,||\, j0.45)}$$

$$= \frac{0.9636 \times j0.60}{j0.15 \times j0.45}$$

$$= -j8.565 \text{ pu}$$

Change in generator current due to fault,

$$\Delta I_g = -j8.565 \times \frac{j0.15}{j0.60} = -j2.141 \text{ pu}$$

Change in motor current due to fault,

$$\Delta I_m = -j8.565 \times \frac{j0.45}{j0.60} = -j6.424 \text{ pu}$$

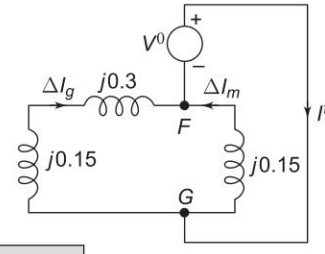

Fig. 9.14 *F* is the fault point on the passive Thevenin network

To these changes we add the prefault current to obtain the subtransient current in machines. Thus

$$I_g'' = I^0 + \Delta I_g = (0.623 - j1.674) \text{ pu}$$
$$I_m'' = -I^0 + \Delta I_m = (-0.623 - j6.891) \text{ pu}$$

which are the same (and should be) as calculated already.

We have thus solved Example 9.3 alternatively through the Thevenin theorem and superposition. This, indeed, is a powerful method for large networks.

9.5 SELECTION OF CIRCUIT BREAKERS

Two of the circuit breaker ratings which require the computation of SC current are: *rated momentary current* and *rated symmetrical interrupting current*. Symmetrical SC current is obtained by using subtransient reactances for synchronous machines. Momentary current (rms) is then calculated by multiplying the symmetrical momentary current by a factor of 1.6 to account for the presence of DC off-set current.

Symmetrical current to be interrupted is computed by using subtransient reactances for synchronous generators and transient reactances for synchronous motors—induction motors are neglected.* The DC off-set value to be added to obtain the current to be interrupted is accounted for by multiplying the symmetrical SC current by a factor as tabulated below:

Circuit Breaker Speed	*Multiplying Factor*
8 cycles or slower	1.0
5 cycles	1.1
3 cycles	1.2
2 cycles	1.4

If SC MVA (explained below) is more than 500, the above multiplying factors are increased by 0.1 each. The multiplying factor for air breakers rated 600 V or lower is 1.25.

The current that a circuit breaker can interrupt is inversely proportional to the operating voltage over a certain range, i.e.,

Amperes at operating voltage

$$= \text{amperes at rated voltage} \times \frac{\text{rated voltage}}{\text{operating voltage}}$$

Of course, operating voltage cannot exceed the maximum design value. Also, no matter how low the voltage is, the rated interrupting current cannot exceed the *rated maximum interrupting current*. Over this range of voltages, the

*In some recent attempts, currents contributed by induction motors during a short circuit have been accounted for.

product of operating voltage and interrupting current is constant. It is therefore logical as well as convenient to express the circuit breaker rating in terms of SC MVA that can be interrupted, defined as

Rated interrupting MVA (three-phase) capacity

$$= \sqrt{3}\,|V(\text{line})|_{\text{rated}} \times |I(\text{line})|_{\text{rated interrupting current}}$$

where V(line) is in kV and I (line) is in kA.

Thus, instead of computing the SC current to be interrupted, we compute three-phase SC MVA to be interrupted, where

$$\text{SC MVA (3-phase)} = \sqrt{3} \times \text{prefault line voltage in kV} \times \text{SC current in kA.}$$

If voltage and current are in per unit values on a three-phase basis

$$\text{SC MVA (3-phase)} = |V|_{\text{prefault}} \times |I|_{SC} \times (\text{MVA})_{\text{Base}} \tag{9.17}$$

Obviously, rated MVA interrupting capacity of a circuit breaker is to be more than (or equal to) the SC MVA required to be interrupted.

For the selection of a circuit breaker for a particular location, we must find the maximum possible SC MVA to be interrupted with respect to type and location of fault and generating capacity (also synchronous motor load) connected to the system. A three-phase fault though rare is generally the one which gives the highest SC MVA and a circuit breaker must be capable of interrupting it. An exception is an LG (line-to-ground) fault close to a synchronous generator.* In a simple system the fault location which gives the highest SC MVA may be obvious but in a large system various possible locations must be tried out to obtain the highest SC MVA requiring repeated SC computations. This is illustrated by the examples that follow.

Example 9.4 Three 6.6 kV generators A, B and C, each of 10% leakage reactance and MVA ratings 40, 50 and 25, respectively are interconnected electrically, as shown in Fig. 9.15, by a tie bar through *current limiting reactors*, each of 12% reactance based upon the rating of the machine to which it is connected. A three-phase feeder is supplied from the bus bar of generator A at a line voltage of 6.6 kV. The feeder has a resistance of 0.06 Ω/phase and an inductive reactance of 0.12 Ω/phase. Estimate the maximum MVA that can be fed into a symmetrical short circuit at the far end of the feeder.

Solution

Choose as base 50 MVA, 6.6 kV

$$\text{Feeder impedance} = \frac{(0.06 + j0.12) \times 50}{(6.6)^2} = (0.069 + j0.138)\ \text{pu}$$

$$\text{Gen } A \text{ reactance} = \frac{0.1 \times 50}{40} = 0.125\ \text{pu}$$

$$\text{Gen } B \text{ reactance} = 0.1\ \text{pu}$$

*This will be explained in Ch. 11.

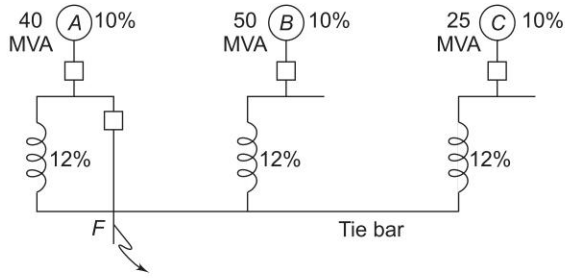

Fig. 9.15

$$\text{Gen } C \text{ reactance} = 0.1 \times \frac{50}{25} = 0.2 \text{ pu}$$

$$\text{Reactor } A \text{ reactance} = \frac{0.12 \times 50}{40} = 0.15 \text{ pu}$$

$$\text{Reactor } B \text{ reactance} = 0.12 \text{ pu}$$

$$\text{Reactor } C \text{ reactance} = \frac{0.12 \times 50}{25} = 0.24 \text{ pu}$$

Assume no load prefault conditions, i.e. prefault currents are zero. Postfault currents can then be calculated by the circuit model of Fig. 9.16(a) corresponding to Fig. 9.13(d). The circuit is easily reduced to that of Fig. 9.16(b), where

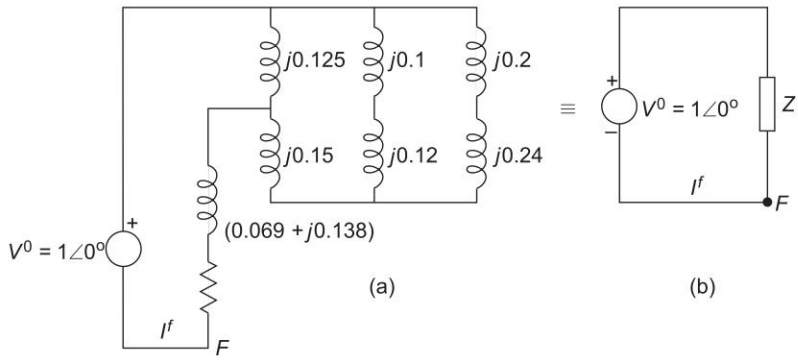

Fig. 9.16

$$Z = (0.069 + j0.138) + j0.125 \,||\, (j0.15 + j0.22 \,||\, j0.44)$$
$$= 0.069 + j0.226 = 0.236\angle 73^\circ$$

$$\text{SC MVA} = V^0 I^f = V^0 \left(\frac{V^0}{Z} \right) = \frac{1}{Z} \text{ pu (since } V^0 = 1 \text{ pu)}$$

$$= \frac{1}{Z} \times (\text{MVA})_{\text{Base}}$$

$$= \frac{50}{0.236} = 212 \text{ MVA}$$

Example 9.5 Consider the four-bus system of Fig. 9.17. Buses 1 and 2 are generator buses and 3 and 4 are load buses. The generators are rated 11 kV, 100 MVA, with transient reactance of 10% each. Both the transformers are 11/110 kV, 100 MVA with a leakage reactance of 5%. The reactances of the lines to a base of 100 MVA, 110 kV are indicated on the figure. Obtain the short circuit solution for a three-phase solid fault on bus 4 (load bus).

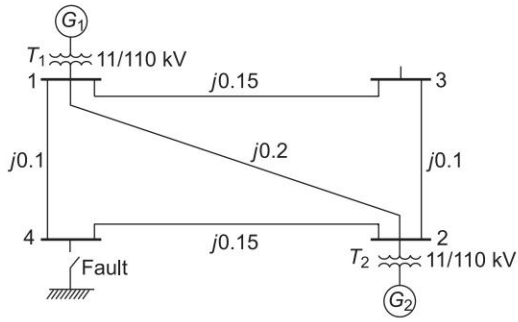

Fig. 9.17 Four-bus system

Assume prefault voltages to be 1 pu and prefault currents to be zero.

Solution

Changes in voltages and currents caused by a short circuit can be calculated from the circuit model of Fig. 9.18. Fault current I^f is calculated by systematic network reduction as in Fig. 9.19.

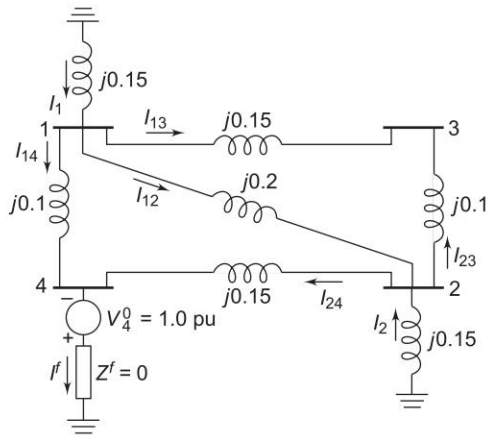

Fig. 9.18

From Fig. 9.19(e), we get directly the fault current as

$$I^f = \frac{1.0}{j0.13560} = -j7.37463 \text{ pu}$$

From Fig. 9.19(d), it is easy to see that

$$I_1 = I^f \times \frac{j0.19583}{j0.37638} = -j3.83701 \text{ pu}$$

$$I_2 = I^f \times \frac{j0.18055}{j0.37638} = -j3.53762 \text{ pu}$$

Let us now compute the voltage changes for buses 1, 2 and 3. From Fig. 9.19(b), we have

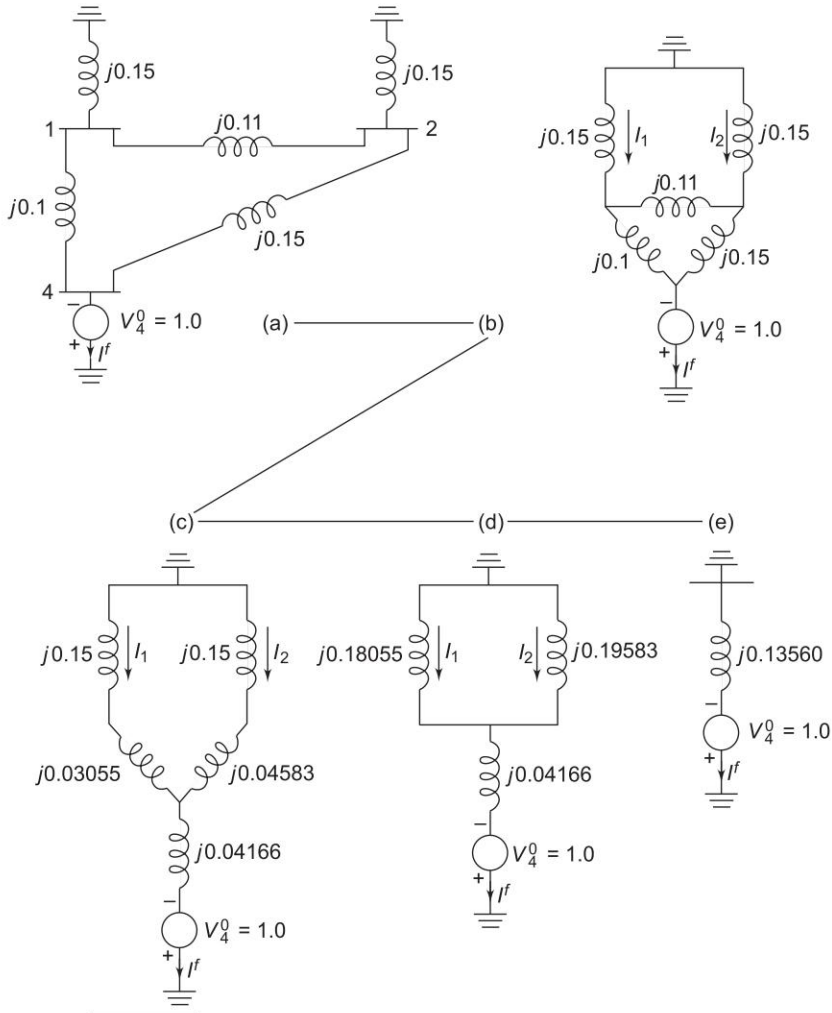

Fig. 9.19 Systematic reduction of the network of Fig. 9.18

$$\Delta V_1 = 0 - (j0.15)(-j3.83701) = -0.57555 \text{ pu}$$
$$\Delta V_2 = 0 - (j0.15)(-j3.53762) = -0.53064 \text{ pu}$$

Now

$$V_1^f = 1 + \Delta V_1 = 0.42445 \text{ pu}$$
$$V_2^f = 1 + \Delta V_2 = 0.46936 \text{ pu}$$

$$\therefore \quad I_{13} = \frac{V_1^f - V_2^f}{j0.15 + j0.1} = j0.17964 \text{ pu}$$

Now

$$\Delta V_3 = 0 - [(j0.15)(-j3.83701) + (j0.15)(j0.17964)]$$
$$= -0.54860 \text{ pu}$$
$$\therefore \quad V_3^f = 1 - 0.54860 = 0.4514 \text{ pu}$$
$$V_4^f = 0$$

The determination of currents in the remaining lines is left as an exercise to the reader.

Short circuit study is complete with the computation of SC MVA at bus 4.

$$(\text{SC MVA})_4 = 7.37463 \times 100 = 737.463 \text{ MVA}$$

It is obvious that the heuristic network reduction procedure adopted above is not practical for a real power network of even moderate size. It is, therefore, essential to adopt a suitable algorithm for carrying out short circuit study on a digital computer. This is discussed in Sec. 9.6.

9.6 ALGORITHM FOR SHORT CIRCUIT STUDIES

So far we have carried out short circuit calculations for simple systems whose passive networks can be easily reduced. In this section we extend our study to large systems. In order to apply the four steps of short circuit computation developed earlier to large systems, it is necessary to evolve a systematic general algorithm so that a digital computer can be used.

Consider an n-bus system shown schematically in Fig. 9.20 operating at steady load. The first step towards short circuit computation is to obtain prefault voltages at all buses and currents in all lines through a load flow study. Let us indicate the prefault bus voltage vector as

$$V^0_{\text{BUS}} = \begin{bmatrix} V_1^0 \\ V_2^0 \\ \vdots \\ V_n^0 \end{bmatrix} \tag{9.18}$$

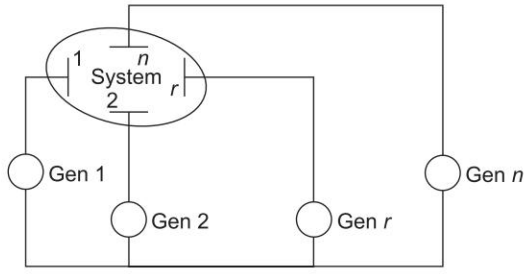

Fig. 9.20 *n*-bus system under steady load

Let us assume that the rth bus is faulted through a fault impedance Z^f. The postfault bus voltage vector will be given by

$$\boldsymbol{V}^{f}_{\text{BUS}} = V^{0}_{\text{BUS}} + \Delta \boldsymbol{V} \tag{9.19}$$

where $\Delta \boldsymbol{V}$ is the vector of changes in bus voltages caused by the fault.

As step 2, we drawn the passive Thevenin network of the system with generators replaced by transient/subtransient reactances with their emfs shorted (Fig. 9.21).

As per step 3 we now excite the passive Thevenin network with $-V^{0}_{r}$ in series with Z^{f} as in Fig. 9.21. The vector $\Delta \boldsymbol{V}$ comprises the bus voltages of this network.

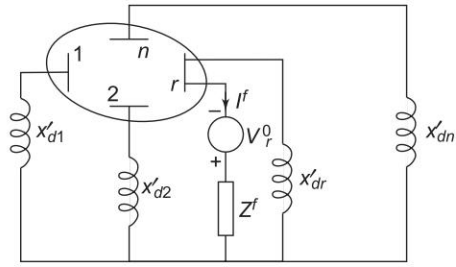

Fig. 9.21 Network of the system of Fig. 9.20 for computing changes in bus voltages caused by the fault

Now

$$\Delta \boldsymbol{V} = \boldsymbol{Z}_{\text{BUS}} \boldsymbol{J}^{f} \tag{9.20}$$

where

$$\boldsymbol{Z}_{\text{BUS}} = \begin{bmatrix} Z_{11} & \cdots & Z_{1n} \\ \vdots & & \vdots \\ Z_{n1} & \cdots & Z_{nn} \end{bmatrix} = \text{bus impedance matrix of the passive Thevenin network} \tag{9.21}$$

$\boldsymbol{J}^{f}$ = bus current injection vector

Since the network is injected with current $-I^{f}$ only at the rth bus, we have

$$J^{f} = \begin{bmatrix} 0 \\ 0 \\ \vdots \\ I^{f}_{r} = -I^{f} \\ \vdots \\ 0 \end{bmatrix} \tag{9.22}$$

Substituting Eq. (9.22) in Eq. (9.20), we have for the rth bus

$$\Delta V_{r} = -Z_{rr} I^{f}$$

By step 4, the voltage at the rth bus under fault is

$$V^{f}_{r} = V^{0}_{r} + \Delta V^{0}_{r} = V^{0}_{r} - Z_{rr} I^{f} \tag{9.23}$$

However, this voltage must equal

$$V^{f}_{r} = Z^{f} I^{f} \tag{9.24}$$

We have from Eqs (9.23) and (9.24)

$$Z^f I^f = V_r^0 - Z_{rr} I^f$$

or
$$I^f = \frac{V_r^0}{Z_{rr} + Z^f} \tag{9.25}$$

At the ith bus (from Eqs (9.20) and (9.22))

$$\Delta V_i = - Z_{ir} I^f$$

$\therefore$
$$V_i^f = V_i^0 - Z_{ir} I^f,\ i = 1, 2, ..., n \tag{9.26}$$

Substituting for I^f from Eq. (9.25), we have

$$V_i^f = V_i^0 - \frac{Z_{ir}}{Z_{rr} + Z^f} V_r^0 \tag{9.27}$$

For $i = r$ in Eq. (9.27)

$$V_r^f = \frac{Z^f}{Z_{rr} + Z^f} V_r^0 \tag{9.28}$$

In the above relationship V_i^0s , the prefault bus voltages are assumed to be known from a load flow study. Z_{BUS} matrix of the short-circuit study network of Fig. 9.21 can be obtained by the inversion of its Y_{BUS} matrix as in Example 9.6 or the Z_{BUS} building algorithm presented in Sec. 9.7. It should be observed here that the SC study network of Fig. 9.21 is different from the corresponding load flow study network by the fact that the shunt branches corresponding to the generator reactances do not appear in the load flow study network. Further, in formulating the SC study network, the load impedances are ignored, these being very much larger than the impedances of lines and generators. Of course synchronous motors must be included in Z_{BUS} formulation for the SC study.

Postfault currents in lines are given by

$$I_{ij}^f = Y_{ij} \left(V_i^f - V_j^f \right) \tag{9.29}$$

For calculation of postfault generator current, examine Figs 9.22(a) and (b). From the load flow study (Fig. 9.22(a))

Prefault generator output = $P_{Gi} + jQ_{Gi}$

$\therefore$
$$I_{Gi}^0 = \frac{P_{Gi} - jQ_{Gi}}{V_i^0} \quad (\text{prefault generator output} = P_{Gi} + jQ_{Gi}) \tag{9.30}$$

$$E'_{Gi} = V_i + jX'_{Gi} I_{Gi}^0 \tag{9.31}$$

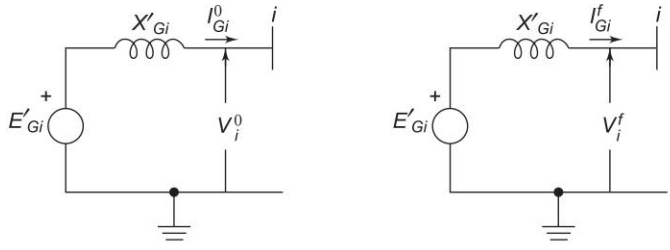

Fig. 9.22

From the SC study, V_i^f is obtained. It then follows from Fig. 9.22(b) that

$$I_{Gi}^f = \frac{E'_{Gi} - V_i^f}{jX'_{Gi}} \tag{9.32}$$

Example 9.6 To illustrate the algorithm discussed above, we shall re-compute the short circuit solution for Example 9.5 which was solved earlier using the network reduction technique.

First of all the bus admittance matrix for the network of Fig. 9.18 is formed as follows:

$$Y_{11} = \frac{1}{j0.15} + \frac{1}{j0.15} + \frac{1}{j0.1} + \frac{1}{j0.2} = -j28.333$$

$$Y_{12} = Y_{21} = \frac{-1}{j0.2} = j5.000$$

$$Y_{13} = Y_{31} = \frac{-1}{j0.15} = j6.667$$

$$Y_{14} = Y_{41} = \frac{-1}{j0.1} = j10.000$$

$$Y_{22} = \frac{1}{j0.15} + \frac{1}{j0.15} + \frac{1}{j0.1} + \frac{1}{j0.2} = -j28.333$$

$$Y_{23} = Y_{32} = \frac{-1}{j0.1} = j10.000$$

$$Y_{24} = Y_{42} = \frac{-1}{j0.15} = j6.667$$

$$Y_{33} = \frac{1}{j0.15} + \frac{1}{j0.1} = -j16.667$$

$$Y_{34} = Y_{43} = 0.000$$

$$Y_{44} = \frac{1}{j0.1} + \frac{1}{j0.15} = -j16.667$$

$$\boldsymbol{Y}_{\text{BUS}} = \begin{bmatrix} -j28.333 & j5.000 & j6.667 & j10.000 \\ j5.000 & -j28.333 & j10.000 & j6.667 \\ j6.667 & j10.000 & -j16.667 & j0.000 \\ j10.000 & j6.667 & j0.000 & -j16.667 \end{bmatrix}$$

By inversion we get $\boldsymbol{Z}_{\text{BUS}}$ as

$$\boldsymbol{Z}_{\text{BUS}} = \begin{bmatrix} j0.0903 & j0.0597 & j0.0719 & j0.0780 \\ j0.0597 & j0.0903 & j0.0780 & j0.0719 \\ j0.0719 & j0.0780 & j0.1356 & j0.0743 \\ j0.0780 & j0.0719 & j0.0743 & j0.1356 \end{bmatrix}$$

Now, the postfault bus voltages can be obtained using Eq. (9.27) as

$$V_1^f = V_1^0 - \frac{Z_{14}}{Z_{44}} V_4^0$$

The prefault condition being no load, $V_1^0 = V_2^0 = V_3^0 = V_4^0 = 1$ pu

$$V_1^f = 1.0 - \frac{j0.0780}{j0.1356} \times 1.0 = 0.4248 \text{ pu}$$

$$V_2^f = V_2^0 - \frac{Z_{24}}{Z_{44}} V_4^0$$

$$= 1.0 - \frac{j0.0719}{j0.1356} \times 1.0 = 0.4698 \text{ pu}$$

$$V_3^f = V_3^0 - \frac{Z_{34}}{Z_{44}} V_4^0$$

$$= 1.0 - \frac{j0.0743}{j0.1356} \ 1.0 = 0.4521 \text{ pu}$$

$$V_4^f = 0.0$$

Using Eq. (9.25) we can obtain the fault current as

$$I^f = \frac{1.000}{j0.1356} = -j7.37463 \text{ pu}$$

These values agree with those obtained earlier in Example 9.5. Let us also calculate the short circuit current in lines 1–3, 1–2, 1–4, 2–4 and 2–3.

$$I_{13}^f = \frac{V_1^f - V_3^f}{z_{13}} = \frac{0.4248 - 0.4521}{j0.15} = j0.182 \text{ pu}$$

$$I_{12}^f = \frac{V_1^f - V_2^f}{z_{12}} = \frac{0.4248 - 0.4698}{j0.2} = j0.225 \text{ pu}$$

$$I_{14}^f = \frac{V_1^f - V_4^f}{z_{14}} = \frac{0.4248 - 0}{j0.1} = -j4.248 \text{ pu}$$

$$I_{24}^f = \frac{V_2^f - V_4^f}{z_{24}} = \frac{0.4698 - 0}{j0.15} = -j3.132 \text{ pu}$$

$$I_{23}^f = \frac{V_2^f - V_3^f}{z_{23}} = \frac{0.4698 - 0.4521}{j.01} = -j0.177 \text{ pu}$$

For the example on hand this method may appear more involved compared to the heuristic network reduction method employed in Example 9.5. This, however, is a systematic method and can be easily adopted on the digital

computer for practical networks of large size. Further, another important feature of the method is that having computed Z_{BUS}, we can at once obtain all the required short circuit data for a fault on any bus. For example, in this particular system, the fault current for a fault on bus 1 (or bus 2) will be

$$I^f = \frac{1.000}{Z_{11}(\text{or } Z_{22})} = \frac{1.00}{j0.0903} = -j11.074197 \text{ pu}$$

9.7 Z_{BUS} FORMULATION

By Inventing Y_{BUS}

$$J_{BUS} = Y_{BUS}\, V_{BUS}$$

or $$V_{BUS} = [Y_{BUS}]^{-1} J_{BUS} = Z_{BUS}\, J_{BUS} \qquad (9.33)$$

or $$Z_{BUS} = [Y_{BUS}]^{-1}$$

The sparsity of Y_{BUS} may be retained by using an efficient inversion technique [1] and nodal impedance matrix can then be calculated directly from the factorized admittance matrix. This is beyond the scope of this book.

Current Injection Technique

Equation (9.33) can be written in the expanded form

$$\begin{aligned} V_1 &= Z_{11}I_1 + Z_{12}I_2 + \ldots + Z_{1n}I_n \\ V_2 &= Z_{21}I_1 + Z_{22}I_2 + \ldots + Z_{2n}I_n \\ &\ldots\ldots\ldots\ldots\ldots\ldots\ldots\ldots\ldots\ldots \\ V_n &= Z_{n1}I_1 + Z_{n2}I_2 + \ldots + Z_{nn}I_n \end{aligned} \qquad (9.34)$$

It immediately follows from Eq. (9.34) that

$$Z_{ij} = \left.\frac{V_i}{I_j}\right|_{\substack{I_1 = I_2 = \cdots = I_n = 0 \\ I_j \neq 0}} \qquad (9.35)$$

Also $Z_{ij} = Z_{ji}$; (Z_{BUS} is a symmetrical matrix).

As per Eq. (9.35) if a unit current is injected at bus (node) j, while the other buses are kept open circuited, the bus voltages yield the values of the jth column of Z_{BUS}. However, no organized computerizable techniques are possible for finding the bus voltages. The technique had utility in AC Network Analyzers where the bus voltages could be read by a voltmeter.

Example 9.7 Consider the network of Fig. 9.23(a) with three buses one of which is a reference. Evaluate Z_{BUS}.

Solution

Inject a unit current at bus 1 keeping bus 2 open circuit, i.e., $I_1 = 1$ and $I_2 = 0$ as in Fig. 9.22(b). Calculating voltages at buses 1 and 2, we have

$$Z_{11} = V_1 = 7$$

$$Z_{21} = V_2 = 4$$

Now let $I_1 = 0$ and $I_2 = 1$. It similarly follows that

$$Z_{12} = V_1 = 4 = Z_{12}$$

$$Z_{22} = V_2 = 6$$

Collecting the above values

$$Z_{BUS} = \begin{bmatrix} 7 & 4 \\ 4 & 6 \end{bmatrix}$$

Because of the above computational procedure, the Z_{BUS} matrix is referred to as the 'open-circuit impedance matrix'.

Z_{BUS} Building Algorithm

It is a step-by-step programmable technique which proceeds branch by branch. It has the advantage that any modification of the network does not require complete rebuilding of Z_{BUS}.

Consider that Z_{BUS} has been formulated upto a certain stage and another branch is now added. Then

$$Z_{BUS}\text{ (old)} \xrightarrow{Z_b = \text{branch impedance}} Z_{BUS}\text{ (new)}$$

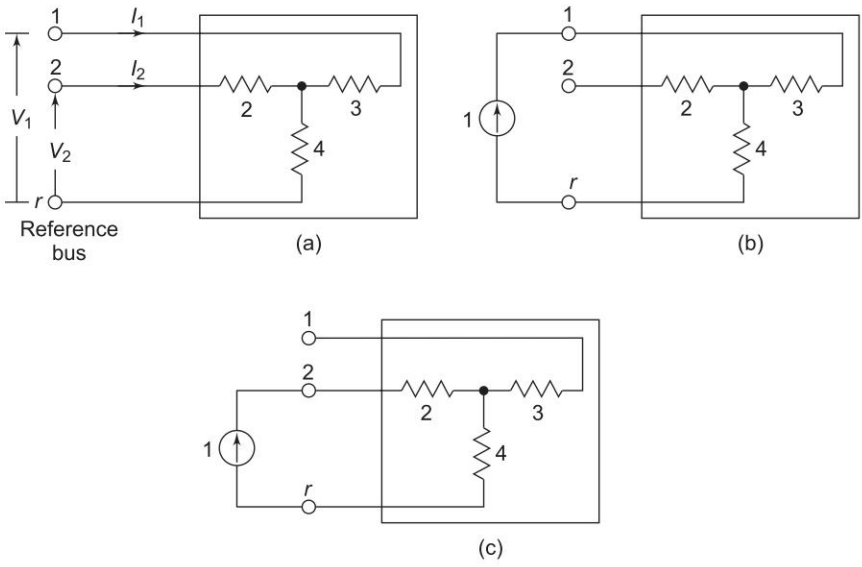

Fig. 9.23 Current injection method of computing Z_{BUS}

Upon adding a new branch, one of the following situation is presented.

1. Z_b is added from a new bus to the reference bus (i.e. a new branch is added and the dimension of Z_{BUS} goes up by one). This is *type-1 modification*.
2. Z_b is added from a new bus to an old bus (i.e., a new branch is added and the dimension of Z_{BUS} goes up by one). This is *type-2 modification*.
3. Z_b connects an old bus to the reference branch (i.e., a new loop is formed but the dimension of Z_{BUS} does not change). This is *type-3 modification*.
4. Z_b connects two old buses (i.e., new loop is formed but the dimension of Z_{BUS} does not change). This is *type-4 modification*.
5. Z_b connects two new buses (Z_{BUS} remains unaffected in this case). This situation can be avoided by suitable numbering of buses and from now onwards will be ignored.

Notation: i, j—old buses; *r*—reference bus; *k*—new bus.

Type-1 Modification

Figure 9.24 shows a passive (linear) *n*-bus network in which branch with impedance Z_b is added to the new bus *k* and the reference bus *r*. Now

$$V_k = Z_b I_k$$

$$Z_{ki} = Z_{ik} = 0;\ i = 1, 2, ..., n$$

$$\therefore \quad Z_{kk} = Z_b$$

Hence

$$Z_{BUS}\ (\text{new}) = \left[\begin{array}{c|c} Z_{BUS}(\text{old}) & \begin{matrix}0\\|\\|\\|\\0\end{matrix} \\ \hline 0\ -\ -\ -\ 0 & Z_b \end{array}\right] \tag{9.36}$$

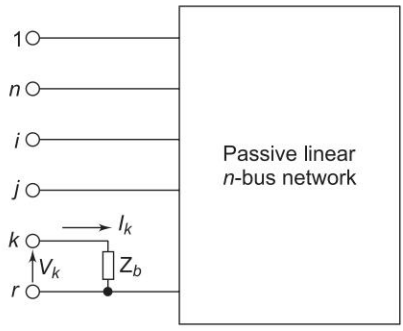

Fig. 9.24 Type-1 modification

Type-2 Modification

Z_b is added from new bus *k* to the old bus *j* as in Fig. 9.25. It follows from this figure that

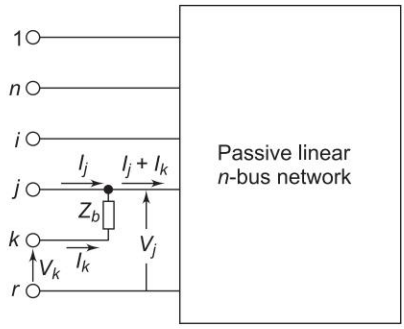

Fig. 9.25 Type-2 modification

$$V_k = Z_b I_k + V_j$$

$$= Z_b I_k + Z_{j1} I_1 + Z_{j2} I_2 + \cdots + Z_{jj} (I_j + I_k) + \cdots + Z_{jn} I_n$$

Rearranging,

$$V_k = Z_{j1} I_1 + Z_{j2} I_2 + \cdots + Z_{jj} I_j + \cdots + Z_{jn} I_n + (Z_{jj} + Z_b) I_k$$

Consequently

$$Z_{\text{BUS}}\ (\text{new}) = \left[\begin{array}{c|c} & Z_{1j} \\ & Z_{2j} \\ Z_{\text{BUS}}(\text{old}) & \vdots \\ & Z_{nj} \\ \hline Z_{ji} Z_{j2} \ldots Z_{jn} & Z_{jj} + Z_b \end{array}\right] \tag{9.37}$$

Type-3 Modification

Z_b connects an old bus (j) to the reference bus (r) as in Fig. 9.26. This case follows from Fig. 9.25 by connecting bus k to the reference bus r, i.e. by setting $V_k = 0$.

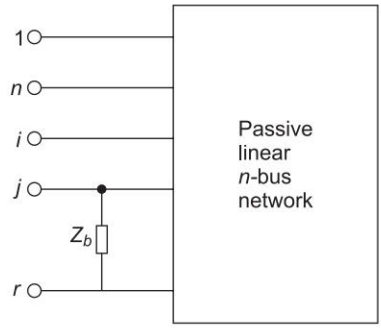

Fig. 9.26 Type-3 modification

Thus

$$\begin{bmatrix} V_1 \\ V_2 \\ \vdots \\ V_n \\ \hline 0 \end{bmatrix} = \left[\begin{array}{c|c} & Z_{1j} \\ & Z_{2j} \\ Z_{\text{BUS}}(\text{old}) & \vdots \\ & Z_{nj} \\ \hline Z_{j1}Z_{j2}\ldots Z_{jn} & Z_{jj}+Z_b \end{array}\right] \begin{bmatrix} I_1 \\ I_2 \\ \vdots \\ I_n \\ I_k \end{bmatrix} \tag{9.38}$$

Eliminate I_k in the set of equations contained in the matrix operation (9.38),

$$0 = Z_{j1}I_1 + Z_{j2}I_2 + \cdots + Z_{jn}I_n + (Z_{jj} + Z_b)I_k$$

or

$$I_k = -\frac{1}{Z_{jj}+Z_b}\,(Z_{j1}I_1 + Z_{j2}I_2 + \cdots + Z_{jn}I_n) \tag{9.39}$$

Now

$$V_i = Z_{i1}I_1 + Z_{i2}I_2 + \cdots + Z_{in}I_n + Z_{ij}I_k \tag{9.40}$$

Substituting Eq. (9.40) in Eq. (9.39)

$$V_i = \left[Z_{i1} - \frac{1}{Z_{jj}+Z_b}(Z_{ij}Z_{j1})\right]I_1 + \left[Z_{i2} - \frac{1}{Z_{jj}+Z_b}(Z_{ij}Z_{j2})\right]I_2$$

$$+\ldots+\left[Z_{in} - \frac{1}{Z_{jj}+Z_b}\left(Z_{ij}\,Z_{jn}\right)\right]I_n \tag{9.41}$$

Equation (9.37) can be written in matrix form as

$$Z_{\text{BUS}}\,(\text{new}) = Z_{\text{BUS}}\,(\text{old} - \frac{1}{Z_{jj}+Z_b}\begin{bmatrix} Z_{1j} \\ \vdots \\ Z_{nj} \end{bmatrix}[Z_{j1}\ldots Z_{jn}] \tag{9.42}$$

Type-4 Modification

Z_b connects two old buses as in Fig. 9.27. Equations can be written as follows for all the network buses.

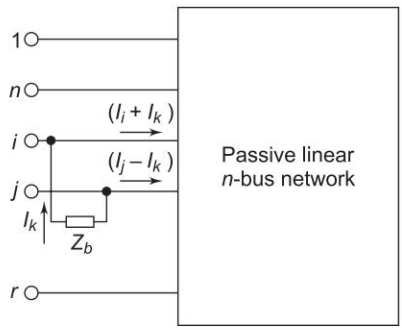

Fig. 9.27 Type-4 modification

$$V_i = Z_{i1}I_1 + Z_{i2}I_2 + \cdots + Z_{1i}\,(I_i + I_k) + Z_{ij}\,(I_j - I_k) + \cdots + Z_{in}I_n \tag{9.43}$$

Similar equations follow for other buses.

The voltages of the buses i and j are, however, constrained by the equation (Fig. 9.27)

$$V_j = Z_bI_k + V_i \tag{9.44}$$

or
$$Z_{j1}I_1 + Z_{j2}I_2 + \cdots + Z_{ji}\,(I_i + I_k) + Z_{jj}\,(I_j - I_k) + \cdots + Z_{jn}I_n$$
$$= Z_bI_k + Z_{i1}I_1 + Z_{i2}I_2 + \cdots + Z_{ii}\,(I_i + I_k) + Z_{ij}(I_j - I_k) + \cdots + Z_{in}I_n$$

Rearranging

$$0 = (Z_{i1} - Z_{j1})\,I_1 + \cdots + (Z_{ii} - Z_{ji})\,I_i + (Z_{ij} - Z_{jj})\,I_j$$
$$+ \cdots + (Z_{in} - Z_{jn})\,I_n + (Z_b + Z_{ii} + Z_{jj} - Z_{ij} - Z_{ji})\,I_k \tag{9.45}$$

Collecting equations similar to Eq. (9.43) and Eq. (9.45), we can write

$$\begin{bmatrix} V_1 \\ V_2 \\ \vdots \\ V_n \\ - \\ 0 \end{bmatrix} = \left[\begin{array}{c|c} & (Z_{1i} - Z_{1j}) \\ & (Z_{2i} - Z_{2j}) \\ Z_{\text{BUS}} & \vdots \\ & (Z_{ni} - Z_{nj}) \\ \hline (Z_{i1} - Z_{j1}) \ldots (Z_{in} - Z_{jn}) & Z_b + Z_{ii} + Z_{jj} - 2Z_{ij} \end{array}\right] \begin{bmatrix} I_1 \\ I_2 \\ \vdots \\ I_n \\ \hline I_j \end{bmatrix} \tag{9.46}$$

Eliminating I_k in Eq. (9.46) on lines similar to what was done in type-2 modification, it follows that

$$Z_{\text{BUS}}\,(\text{new}) = Z_{\text{BUS}}\,(\text{old}) - \frac{1}{Z_b + Z_{ii} + Z_{jj} - 2Z_{ij}} \begin{bmatrix} Z_{1i} - Z_{1j} \\ \vdots \\ Z_{ni} - Z_{nj} \end{bmatrix}$$

$$[Z_{i1} - Z_{j1}] \ldots (Z_{in} - Z_{jn})] \tag{9.47}$$

With the use of four relationships Eqs (9.36), (9.37), (9.42) and (9.47) bus impedance matrix can be built by a step-by-step procedure (bringing in one branch at a time) as illustrated in Example 9.8. This procedure being a mechanical one can be easily computerized.

When the network undergoes changes, the modification procedures can be employed to revise the bus impedance matrix of the network. The opening of a line (Z_{ij}) is equivalent to adding a branch in parallel to it with impedance $-Z_{ij}$ (see Example 9.8).

Example 9.8 For the three-bus network shown in Fig. 9.28 build Z_{BUS}.

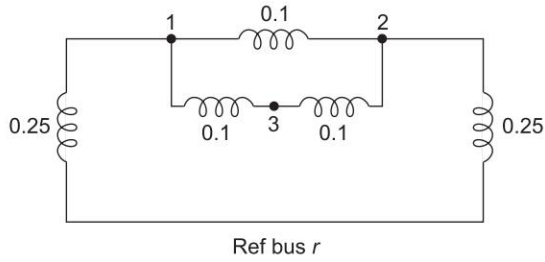

Fig. 9.28

Solution

Step 1: Add branch $z_{1r} = 0.25$ (from bus 1 (new) to bus r)

$$Z_{BUS} = [0.25] \tag{i}$$

Step 2: Add branch $z_{21} = 0.1$ (from bus 2 (new) to bus 1 (old)); type-2 modification

$$Z_{BUS} = \begin{matrix} \\ 1 \\ 2 \end{matrix} \begin{bmatrix} 0.25 & 0.25 \\ 0.25 & 0.35 \end{bmatrix} \tag{ii}$$

Step 3: Add branch $z_{13} = 0.1$ (from bus 3 (new) to bus 1 (old)); type-2 modification

$$Z_{BUS} = \begin{bmatrix} 0.25 & 0.25 & 0.25 \\ 0.25 & 0.35 & 0.25 \\ 0.25 & 0.25 & 0.35 \end{bmatrix} \tag{iii}$$

Step 4: Add branch z_{2r} (from bus 2 (old) to bus r); type-3 modification

$$Z_{BUS} = \begin{bmatrix} 0.25 & 0.25 & 0.25 \\ 0.25 & 0.35 & 0.25 \\ 0.25 & 0.25 & 0.35 \end{bmatrix} - \frac{1}{0.35 + 0.25} \begin{bmatrix} 0.25 \\ 0.35 \\ 0.25 \end{bmatrix} [0.25 \ 0.35 \ 0.25]$$

$$= \begin{bmatrix} 0.1458 & 0.1042 & 0.1458 \\ 0.1042 & 0.1458 & 0.1042 \\ 0.1458 & 0.1042 & 0.2458 \end{bmatrix}$$

Step 5: Add branch $z_{23} = 0.1$ (from bus 2 (old) to bus 3 (old)); type-4 modification

$$Z_{BUS} = \begin{bmatrix} 0.1458 & 0.1042 & 0.1458 \\ 0.1042 & 0.1458 & 0.1042 \\ 0.1458 & 0.1042 & 0.2458 \end{bmatrix} - \frac{1}{0.1 + 0.1458 + 0.2458 - 2 \times 0.1042}$$

$$= \begin{bmatrix} -0.1042 \\ 0.0417 \\ -0.0417 \end{bmatrix} \begin{bmatrix} -0.1042 & 0.0417 & -0.0417 \end{bmatrix}$$

$$= \begin{bmatrix} 0.1397 & 0.1103 & 0.1250 \\ 0.1103 & 0.1397 & 0.1250 \\ 0.1250 & 0.1250 & 0.1750 \end{bmatrix}$$

Opening a line (line 3-2): This is equivalent to connecting an impedance – 0.1 between bus 3 (old) and bus 2 (old) i.e. type-4 modification.

$$Z_{BUS} = Z_{BUS}\,(\text{old}) - \frac{1}{(-0.1) + 0.175 + 0.1397 - 2 \times 0.125}$$

$$\begin{bmatrix} 0.0147 \\ -0.0147 \\ 0.0500 \end{bmatrix} [0.0147 \;-\; 0.0147 \;\; 0.0500]$$

$$= \begin{bmatrix} 0.1458 & 0.1042 & 0.1458 \\ 0.1042 & 0.1458 & 0.1042 \\ 0.1458 & 0.1042 & 0.2458 \end{bmatrix}; \text{ (same as in step 4)}$$

Example 9.9 For the power system shown in Fig. 9.29 the pu reactance are shown therein. For a solid three-phase fault on bus 3, calculate the following

(a) Fault current
(b) V_1^f and V_2^f
(c) I_{12}^f, I_{13}^f and I_{23}^f
(d) I_{G-1}^f, and I_{G2}^f

Assume prefault voltage to be 1 pu.

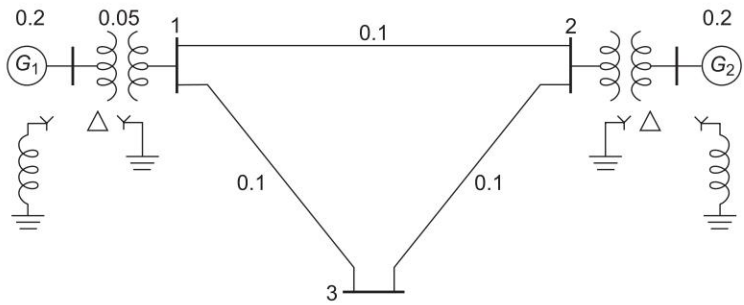

Fig. 9.29

Solution

The Thevenin passive network for this system is drawn in Fig. 9.28 with its Z_{BUS} given in Eq. (iv) of Example 9.8.

(a) As per Eq. (9.25),

$$I^f = \frac{V_r^0}{Z_{rr} + Z^f}$$

or

$$I^f = \frac{V_3^0}{Z_{33}} = \frac{1}{j0.175} = -j5.71$$

(b) As per Eq. (9.26),

$$I_i^f = V_i^0 - \frac{Z_{ir}}{Z_{rr} + Z^f} V_r^0$$

Now

$$V_1^f = \left(1 - \frac{Z_{13}}{Z_{33}}\right) = 1 - \frac{0.125}{0.175}$$

$$= 0.286$$

and

$$V_2^f = \left(1 - \frac{Z_{23}}{Z_{33}}\right) = 0.286$$

The two voltages are equal because of the symmetry of the given power network

(c) From Eq. (9.29),

$$I_{ij}^f = Y_{ij}\,(V_i^f - V_j^f)$$

$$I_{12}^f = \frac{1}{j0.1}(0.286 - 0.286) = 0$$

and

$$I_{13}^f = I^f{}_{31} = \frac{1}{j0.1}\,(0.286 - 0)$$

$$= -j2.86$$

(d) As per Eq. (9.32)

$$I_{G1}^f = \frac{E'_{G1} - V_1^f}{jX'_{iG} + jX_T}$$

But

$$E'_{G1} = 1 \text{ pu (prefault no load)}$$

$\therefore$

$$I_{G1}^f = \frac{1 - 0.286}{j0.2 + j0.05} = -j2.86$$

Similarly

$$I_{G2}^f = j2.86$$

9.8 SUMMARY

After studying modelling, characteristics and steady-state behaviour of power systems under normal operating conditions, this chapter has discussed abnormal system behaviour under symmetrical three-phase fault. Short circuit of a synchronous machine with and without loading is deliberated. Circuit breaker selection is also dealt with. Finally Z_{BUS} formulation is discussed and algorithm is presented for short circuit studies.

Problems

9.1 A transmission line of inductance 0.1 H and resistance 5 ohms is suddenly short circuited at $t = 0$ at the bar end as shown in Fig. P-9.1. Write the expression for short circuit current $i(t)$. Find approximately the value of the first current maximum (maximum momentary current).
[*Hint:* Assume that the first current maximum occurs at the same time as the first current maximum of the symmetrical short circuit current.)

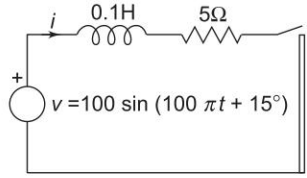

Fig. P-9.1

9.2 (a) What should the instant of short circuit be in Fig. P-9.1 so that the DC off-set current is zero?
(b) What should the instant of short circuit be in Fig. P-9.1 so that the DC off-set current is maximum?

9.3 For the system of Fig. 9.8 (Example 9.2) find the symmetrical currents to be interrupted by circuit breakers A and B for a fault at (i) P and (ii) Q.

9.4 For the system in Fig. P-9.4 the ratings of the various components are:

Generator:	25 MVA, 12.4 kV, 10% subtransient reactance
Motor:	20 MVA, 3.8 kV, 15% subtransient reactance
Transformer T_1:	25 MVA, 11/33 kV, 8% reactance
Transformer T_2:	20 MVA, 33/3.3 kV, 10% reactance
Line:	20 ohms reactance

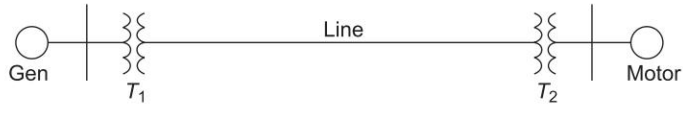

Fig. P-9.4

The system is loaded so that the motor is drawing 15 MW at 0.9 leading power factor, the motor terminal voltage being 3.1 kV. Find the subtransient current in generator and motor for a fault at generator bus.
[*Hint:* Assume a suitable voltage base for the generator. The voltage base for transformers, line and motor would then be given by the transformation ratios. For example, if we choose generator voltage base as 11 kV, the line voltage base is 33 kV and motor voltage base is 3.3 kV. Per unit reactances are calculated accordingly.]

9.5 Two synchronous motors are connected to the bus of a large system through a short transmission line as shown in Fig. P-9.5. The ratings of various components are:

Motors (each): 1 MVA, 440 V, 0.1 pu transient reactance
Line: 0.05 ohm reactance
Large system: Short circuit MVA at its bus at 440 V is 8.

When the motors are operating at 440 V, calculate the short circuit current (symmetrical) fed into a three-phase fault at motor bus.

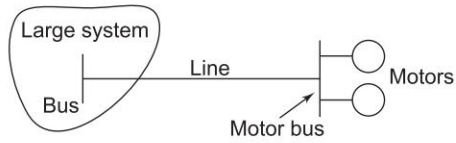

Fig. P-9.5

9.6 A synchronous generator rated 500 kVA, 440 V, 0.1 pu subtransient reactance is supplying a passive load of 400 kW at 0.8 lagging power factor. Calculate the initial symmetrical rms current for a three-phase fault at generator terminals.

9.7 A generator-transformer unit is connected to a line through a circuit breaker. The unit ratings are:

Generator: 10 MVA, 6.6 kV; $X_d'' = 0.1$ pu, $X_d' = 0.20$ pu and $X_d = 0.80$ pu
Transformer: 10 MVA, 6.9/33 kV, reactance 0.08 pu

The system is operating no load at a line voltage of 30 kV, when a three-phase fault occurs on the line just beyond the circuit breaker. Find
(a) the initial symmetrical rms current in the breaker,
(b) the maximum possible DC off-set current in the breaker,
(c) the momentary current rating of the breaker,
(d) the current to be interrupted by the breaker and the interrupting kVA, and
(e) the sustained short circuit current in the breaker.

9.8 The system shown in Fig. P-9.8 is delivering 50 MVA at 11 kV, 0.8 lagging power factor into a bus which may be regarded as infinite. Particulars of various system components are:

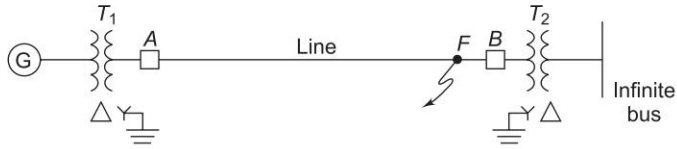

Fig. P-9.8

Generator: 60 MVA, 12 kV, $X'_d = 0.35$ pu
Transformers (each): 80 MVA, 12/66 kV, $X = 0.08$ pu
Line: Reactance 12 ohms, resistance negligible

Calculate the symmetrical current that the circuit breakers A and B will be called upon to interrupt in the event of a three-phase fault occurring at F near the circuit breaker B.

9.9 A two generator station supplies a feeder through a bus as shown in Fig. P-9.9. Additional power is fed to the bus through a transformer from a large system which may be regarded as infinite. A reactor X is included between the transformer and the bus to limit the SC rupturing capacity of the feeder circuit breaker B to 333 MVA (fault close to breaker). Find the inductive reactance of the reactor required. System data are:

Generator G_1: 25 MVA, 15% reactance
Generator G_2: 50 MVA, 20% reactance
Transformer T_1: 100 MVA; 8% reactance
Transformer T_2: 40 MVA; 10% reactance.

Assume that all reactances are given on appropriate voltage bases. Choose a base of 100 MVA.

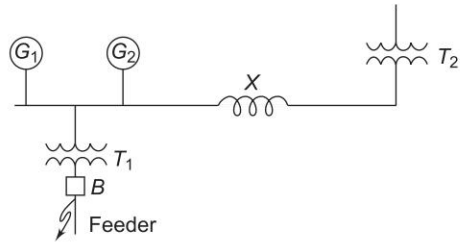

Fig. P-9.9

9.10 For the three-phase power network shown in Fig. P-9.10, the ratings of the various components are:

Generator G_1: 100 MVA, 0.30 pu reactance
Generator G_2: 60 MVA, 0.18 pu reactance
Transformers (each): 50 MVA, 0.10 pu reactance
Inductive reactor X: 0.20 pu on a base of 100 MVA
Lines (each): 80 ohms (reactive); neglect resistance.

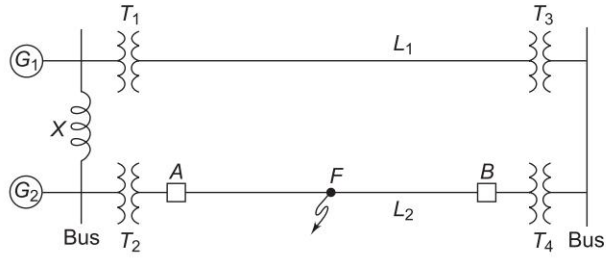

Fig. P-9.10

With the network initially unloaded and a line voltage of 110 kV, a symmetrical short circuit occurs at mid point F of line L_2.

Calculate the short circuit MVA to be interrupted by the circuit breakers A and B at the ends of the line. What would these values be, if the reactor X were eliminated? Comment.

9.11 A synchronous generator feeds bus 1 of a system. A power network feeds bus 2 of the system. Buses 1 and 2 are connected through a transformer and a transmission line. Per unit reactances of the various components are:

Generator (connected to bus bar 1):	0.25
Transformer:	0.12
Transmission line:	0.28

The power network can be represented by a generator with a reactance (unknown) in series.

With the generator on no load and with 1.0 pu voltage at each bus under operating condition, a three-phase short circuit occurring on bus 1 causes a current of 5.0 pu to flow into the fault. Determine the equivalent reactance of the power network.

9.12 Consider the three-bus system of Fig. P-9.12. The generators are 100 MVA, with transient reactance 10% each. Both the transformers are 100 MVA with a leakage reactance of 5%. The reactance of each of the lines to a base of 100 MVA, 110 kV is 10%. Obtain the short circuit solution for a three-phase solid short circuit on bus 3.

Assume prefault voltages to be 1 pu and prefault currents to be zero.

9.13 In the system configuration of Fig. P-9.12, the system impedance data is given below:

Transient reactance of each generator = 0.15 pu

Leakage reactance of each transformer = 0.05 pu

$z_{12} = j0.1$, $z_{13} = j0.12$, $z_{23} = j0.08$ pu

For a solid three-phase fault on bus 3, find all bus voltages and short circuit currents in each component.

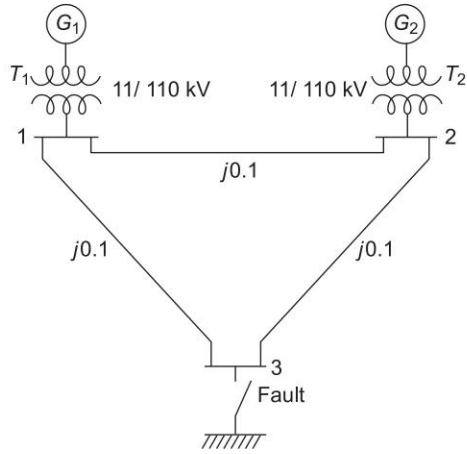

Fig. P-9.12

9.14 For the fault (solid) location shown in Fig. P-9.14. Find the short circuit currents in lines 12 and 13. Prefault system is on no-load with 1 pu voltage and prefault currents are zero. Use Z_{BUS} method and compute its elements by the current injection technique.

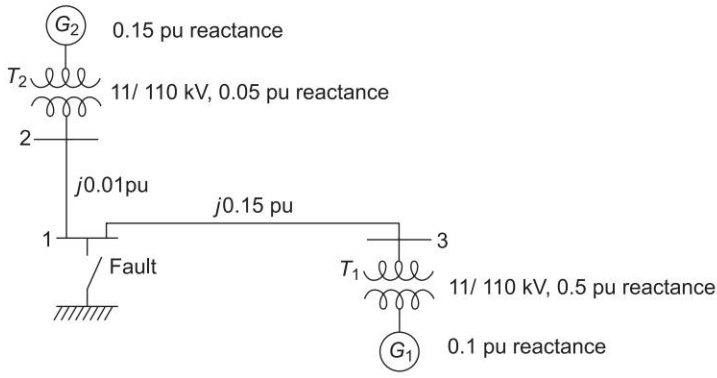

Fig. P-9.14

References

Books

1. Brown, H.E., *Solution of Large Network by Matrix Methods*, Wiley, New York, 1975.
2. Neuenswander, J.R., *Modern Power Systems*, International Textbook Company, New York, 1971.

3. Stagg, G.W. and A.H. El-Abiad, *Computer Methods in Power Systems Analysis*, McGraw-Hill, New York, 1968.
4. Anderson, P.M., *Analysis of Faulted Power Systems*, Iowa State Press, Ames, Iowa, 1973.
5. Clarke, E., *Circuit Analysis of Alternating Current Power Systems*, vol. 1, Wiley, New York, 1943.
6. Stevenson, W.D. Jr., *Elements of Power Systems Analysis*, 4th edn, McGraw-Hill, New York, 1982.
7. Glover, J.D. and M.S. Sarma, *Power System Analysis and Design*, 3rd edn, Thomson, Bangalore, 2002.

Paper

8. Brown, H.E. *et al*., "Digital Calculation of Three-Phase Short Circuits by Matrix Methods", *AIEE Trans.,* 1960, 79: 1277.

Chapter 10
Symmetrical Components

10.1 INTRODUCTION

In our work so far, we have considered both normal and abnormal (short circuit) operations of power system under completely balanced (symmetrical) conditions. Under such operation the system impedances in each phase are identical and the three-phase voltages and currents throughout the system are completely balanced, i.e. they have equal magnitudes in each phase and are progressively displaced in time phase by 120° (phase *a* leads/lags phase *b* by 120° and phase *b* leads/lags phase *c* by 120°). In a balanced system, analysis can proceed on a single-phase basis. The knowledge of voltage and current in one phase is sufficient to completely determine voltages and currents in the other two phases. Real and reactive powers are simply three times the corresponding per phase values.

Unbalanced system operation can result in an otherwise balanced system due to unsymmetrical fault, e.g. line-to-ground fault or line-to-line fault. These faults are, in fact, of more common occurrence* than the symmetrical (three-phase) fault. System operation may also become unbalanced when loads are unbalanced as in the presence of large single-phase loads. Analysis under unbalanced conditions has to be carried out on a three-phase basis. Alternatively, a more convenient method of analyzing unbalanced operation is through symmetrical components where the three-phase voltages (and currents) which may be unbalanced are transformed into three sets of balanced voltages (and currents) called symmetrical components. Fortunately, in such a transformation the impedances presented by various power system elements (synchronous generators, transformers, lines) to symmetrical components are decoupled from each other resulting in independent system networks for each

* Typical relative frequencies of occurrence of different kinds of faults in a power system (in order of decreasing severity) are:

Three-phase (3L) faults	5%
Double line-to-ground (LLG) faults	10%
Double line (LL) faults	15%
Single line-to-ground (LG) faults	70%

component (balanced set). This is the basic reason for the simplicity of the symmetrical component method of analysis.

10.2 SYMMETRICAL COMPONENT TRANSFORMATION

A set of three balanced voltages (phasors) V_a, V_b, V_c is characterized by equal magnitudes and interphase differences of 120°. The set is said to have a phase sequence *abc* (*positive sequence*) if V_b lags V_a by 120° and V_c lags V_b by 120°. The three phasors can then be expressed in terms of the reference phasor V_a as

$$V_a = V_a,\ V_b = \alpha^2 V_a,\ V_c = \alpha V_a$$

where the complex number operator α is defined as

$$\alpha = e^{j120^\circ}$$

It has the following properties:

$$\left\{\begin{array}{ll} \alpha^2 = e^{j240^\circ} = e^{-j120^\circ} & = \alpha^* \\ (\alpha^2)^* & = \alpha \\ \alpha^3 & = 1 \\ 1 + \alpha + \alpha^2 & = 0 \end{array}\right\} \qquad (10.1)$$

If the phase sequence is *acb* (*negative sequence*), then

$$V_a = V_a,\ V_b = \alpha V_a,\ V_c = \alpha^2 V_a$$

Thus a set of balanced phasors is fully characterized by its reference phasor (say V_a) and its phase sequence (positive or negative).

Suffix 1 is commonly used to indicate positive sequence. A set of (balanced) positive sequence phasors is written as

$$V_{a1},\ V_{b1} = \alpha^2 V_{a1},\ V_{c1} = \alpha V_{a1} \qquad (10.2)$$

Similarly, suffix 2 is used to indicate negative sequence. A set of (balanced) negative sequence phasors is written as

$$V_{a2},\ V_{b2} = \alpha V_{a2},\ V_{c2} = \alpha^2 V_{a2} \qquad (10.3)$$

A set of three voltages (phasors) equal in magnitude and having the same phase is said to have zero sequence. Thus a set of *zero sequence* phasors is written as

$$V_{a0},\ V_{b0} = V_{a0},\ V_{c0} = V_{a0} \qquad (10.4)$$

Consider now a set of three voltages (phasors) V_a, V_b, V_c which in general may be unbalanced. According to Fortesque's theorem* the three phasors can be expressed as the sum of positive, negative and zero sequence phasors defined above. Thus

* The theorem is a general one and applies to the case of n phasors [7].

$$V_a = V_{a1} + V_{a2} + V_{a0} \quad (10.5)$$
$$V_b = V_{b1} + V_{b2} + V_{b0} \quad (10.6)$$
$$V_c = V_{c1} + V_{c2} + V_{c0} \quad (10.7)$$

The three phasor sequences (positive, negative and zero) are called the *symmetrical components* of the original phasor set V_a, V_b, V_c. The addition of symmetrical components as per Eqs (10.5) to (10.7) to generate V_a, V_b, V_c is indicated by the phasor diagram of Fig. 10.1.

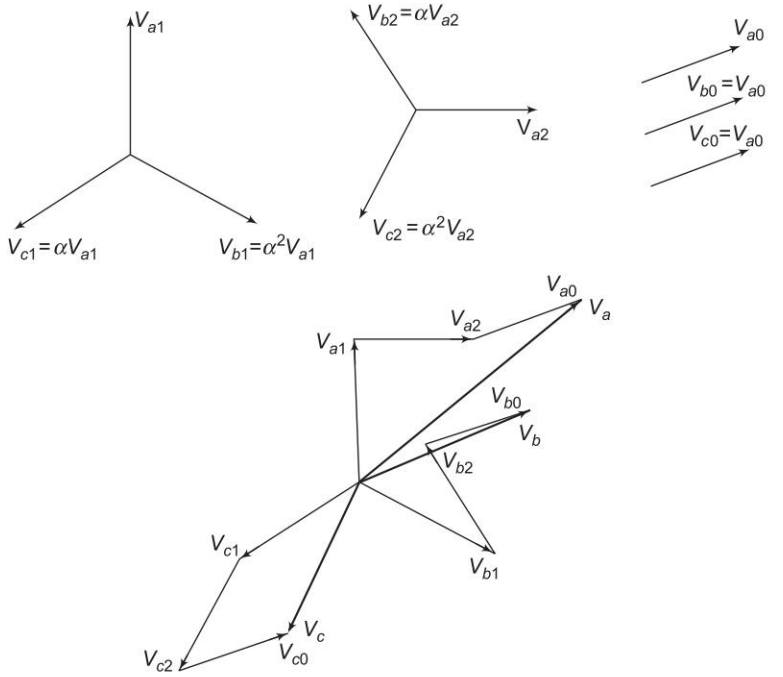

Fig. 10.1 Graphical addition of the symmetrical components to obtain the set of phasors V_a, V_b, V_c (unbalanced in general)

Let us now express Eqs (10.5) to (10.7) in terms of reference phasors V_{a1}, V_{a2} and V_{a0}. Thus

$$V_a = V_{a1} + V_{a2} + V_{a0} \quad (10.8)$$
$$V_b = \alpha^2 V_{a1} + \alpha V_{a2} + V_{a0} \quad (10.9)$$
$$V_c = \alpha V_{a1} + \alpha^2 V_{a2} + V_{a0} \quad (10.10)$$

These equations can be expressed in the matrix form

$$\begin{bmatrix} V_a \\ V_b \\ V_c \end{bmatrix} = \begin{bmatrix} 1 & 1 & 1 \\ \alpha^2 & \alpha & 1 \\ \alpha & \alpha^2 & 1 \end{bmatrix} \begin{bmatrix} V_{a1} \\ V_{a2} \\ V_{a0} \end{bmatrix} \quad (10.11)$$

or

$$\boldsymbol{V}_p = \boldsymbol{A}\boldsymbol{V}_s \tag{10.12}$$

where

$$\boldsymbol{V}_p = \begin{bmatrix} V_a \\ V_b \\ V_c \end{bmatrix} = \text{vector of original phasors}$$

$$\boldsymbol{V}_s = \begin{bmatrix} V_{a1} \\ V_{a2} \\ V_{a0} \end{bmatrix} = \text{vector of symmetrical components}$$

$$\boldsymbol{A} = \begin{bmatrix} 1 & 1 & 1 \\ \alpha^2 & \alpha & 1 \\ \alpha & \alpha^2 & 1 \end{bmatrix} \tag{10.13}$$

We can write Eq. (10.12) as

$$\boldsymbol{V}_s = \boldsymbol{A}^{-1}\boldsymbol{V}_p \tag{10.14}$$

Computing $\boldsymbol{A}^{-1}$ and utilizing relations (10.1), we get

$$\boldsymbol{A}^{-1} = \frac{1}{3}\begin{bmatrix} 1 & \alpha & \alpha^2 \\ 1 & \alpha^2 & \alpha \\ 1 & 1 & 1 \end{bmatrix} \tag{10.15}$$

In expanded form we can write Eq. (10.14) as

$$V_{a1} = \frac{1}{3}(V_a + \alpha V_b + \alpha^2 V_c) \tag{10.16}$$

$$V_{a2} = \frac{1}{3}(V_a + \alpha^2 V_b + \alpha V_c) \tag{10.17}$$

$$V_{a0} = \frac{1}{3}(V_a + V_b + V_c) \tag{10.18}$$

Equations (10.16) to (10.18) give the necessary relationships for obtaining symmetrical components of the original phasors, while Eqs (10.5) to (10.7) give the relationships for obtaining original phasors from the symmetrical components.

The symmetrical component transformations though given above in terms of voltages hold for any set of phasors and therefore automatically apply for a set of currents. Thus

$$\boldsymbol{I}_p = \boldsymbol{A}\boldsymbol{I}_s \tag{10.19}$$

and

$$\boldsymbol{I_s} = \boldsymbol{A}^{-1}\boldsymbol{I_p} \tag{10.20}$$

where

$$\boldsymbol{I_p} = \begin{bmatrix} I_a \\ I_b \\ I_c \end{bmatrix} \text{ and } \boldsymbol{I_s} = \begin{bmatrix} I_{a1} \\ I_{a2} \\ I_{a0} \end{bmatrix}$$

Of course $\boldsymbol{A}$ and $\boldsymbol{A}^{-1}$ are the same as given earlier.

In expanded form the relations (10.19) and (10.20) can be expressed as follows:

(i) Construction of current phasors from their symmetrical components:

$$I_a = I_{a1} + I_{a2} + I_{a0} \tag{10.21}$$

$$I_b = \alpha^2 I_{a1} + \alpha I_{a2} + I_{a0} \tag{10.22}$$

$$I_c = \alpha I_{a1} + \alpha^2 I_{a2} + I_{a0} \tag{10.23}$$

(ii) Obtaining symmetrical components of current phasors:

$$I_{a1} = \frac{1}{3}(I_a + \alpha I_b + \alpha^2 I_c) \tag{10.24}$$

$$I_{a2} = \frac{1}{3}(I_a + \alpha^2 I_b + \alpha I_c) \tag{10.25}$$

$$I_{a0} = \frac{1}{3}(I_a + I_b + I_c) \tag{10.26}$$

Certain observations can now be made regarding a three-phase system with neutral return as shown in Fig. 10.2.

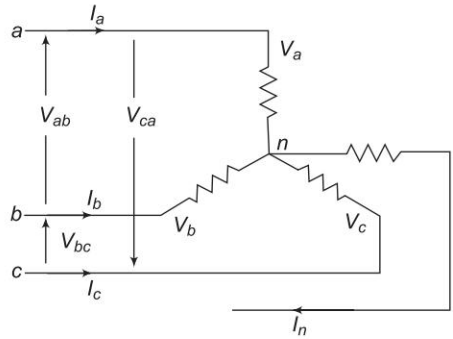

Fig. 10.2 Three-phase system with neutral return

The sum of the three line voltages will always be zero. Therefore, the *zero sequence component of line voltages is always zero*, i.e.

$$V_{ab0} = \frac{1}{3}(V_{ab} + V_{bc} + V_{ca}) = 0 \tag{10.27}$$

On the other hand, the sum of phase voltages (line to neutral) may not be zero so that their zero sequence component V_{a0} may exist.

Since the sum of the three line currents equals the current in the neutral wire, we have

$$I_{a0} = \frac{1}{3}(I_a + I_b + I_c) = \frac{1}{3} I_n \tag{10.28}$$

i.e. the current in the neutral is three times the zero sequence line current. If the neutral connection is severed,

$$I_{a0} = \frac{1}{3} I_n = 0 \tag{10.29}$$

i.e. *in the absence of a neutral connection the zero sequence line current is always zero.*

Power Invariance

We shall now show that the symmetrical component transformation is power invariant, which means that the sum of powers of the three symmetrical components equals the three-phase power.

Total complex power in a three-phase circuit is given by

$$\boldsymbol{S} = \boldsymbol{V}_p^T \boldsymbol{I}_p^* = V_a I_a^* + V_b I_b^* + V_c I_c^* \tag{10.30}$$

or

$$\begin{aligned} \boldsymbol{S} &= [\boldsymbol{A}\boldsymbol{V}_s]^T [\boldsymbol{A}\boldsymbol{I}_s]^* \\ &= \boldsymbol{V}_s^T \boldsymbol{A}^T \boldsymbol{A}^* \boldsymbol{I}_s^* \end{aligned} \tag{10.31}$$

Now

$$\boldsymbol{A}^T \boldsymbol{A}^* = \begin{bmatrix} 1 & \alpha^2 & \alpha \\ 1 & \alpha & \alpha^2 \\ 1 & 1 & 1 \end{bmatrix} \begin{bmatrix} 1 & 1 & 1 \\ \alpha & \alpha^2 & 1 \\ \alpha^2 & \alpha & 1 \end{bmatrix} = 3 \begin{bmatrix} 1 & 0 & 0 \\ 0 & 1 & 0 \\ 0 & 0 & 1 \end{bmatrix} = 3U \tag{10.32}$$

$$\therefore \quad \begin{aligned} \boldsymbol{S} &= 3 \boldsymbol{V}_s^T \boldsymbol{U} \boldsymbol{I}_s^* = 3 \boldsymbol{V}_s^T \boldsymbol{I}_s^* \\ &= 3 V_{a1} I_{a1}^* + 3 V_{a2} I_{a2}^* + 3 V_{a0} I_{a0}^* \\ &= \text{sum of symmetrical component powers} \end{aligned} \tag{10.33}$$

Example 10.1 A delta connected balanced resistive load is connected across an unbalanced three-phase supply as shown in Fig. 10.3. With currents in lines *A* and *B* specified, find the symmetrical components of line currents. Also find the symmetrical components of delta currents. Do you notice any relationship between symmetrical components of line and delta currents? Comment.

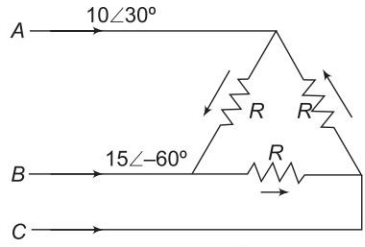

Fig. 10.3

Solution

$$I_A + I_B + I_C = 0$$

or

$$10\angle 30^\circ + 15\angle -60^\circ + I_C = 0$$

$$\therefore \quad I_C = -16.2 + j8.0 = 18\angle 154^\circ \text{ A}$$

From Eqs (10.24) to (10.26),

$$I_{A1} = \frac{1}{3}(10\angle 30^\circ + 15\angle(-60^\circ + 120^\circ) + 18\angle(154^\circ + 240^\circ))$$
$$= 10.35 + j9.3 = 14\angle 42^\circ \text{ A} \qquad \text{(i)}$$

$$I_{A2} = \frac{1}{3}(10\angle 30^\circ + 15\angle(-60^\circ + 240^\circ) + 18\angle(154^\circ + 120^\circ))$$
$$= -1.7 - j4.3 = 4.65\angle 248^\circ \text{ A} \qquad \text{(ii)}$$

$$I_{A0} = \frac{1}{3}(I_A + I_B + I_C) = 0 \qquad \text{(iii)}$$

From Eq. (10.2),

$$I_{B1} = 14\angle 282^\circ \text{ A} \qquad I_{C1} = 14\angle 162^\circ \text{ A}$$
$$I_{B2} = 4.65\angle 8^\circ \text{ A} \qquad I_{C2} = 4.65\angle 128^\circ \text{ A}$$
$$I_{B0} = 0 \text{ A} \qquad I_{C0} = 0 \text{ A}$$

Check:

$$I_A = I_{A1} + I_{A2} + I_{A0} = 8.65 + j5 = 10\angle 30^\circ$$

Converting delta load into equivalent star, we can redraw Fig. 10.3 as in Fig. 10.4.

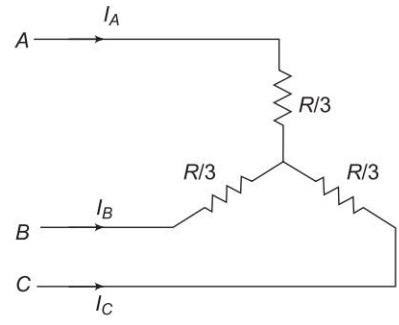

Fig. 10.4

Delta currents are obtained as follows:

$$V_{AB} = \frac{1}{3}(I_A - I_B)$$

Now

$$I_{AB} = V_{AB}/R = \frac{1}{3}(I_A - I_B)$$

Similarly,

$$I_{BC} = \frac{1}{3}(I_B - I_C)$$

$$I_{CA} = \frac{1}{3}(I_C - I_A)$$

Substituting the values of I_A, I_B and I_C, we have

$$I_{AB} = \frac{1}{3}(10\angle 30° - 15\angle -60°) = 6\angle 86° \text{ A}$$

$$I_{BC} = \frac{1}{3}(15\angle -60° - 18\angle 154°) = 10.5\angle -41.5° \text{ A}$$

$$I_{CA} = \frac{1}{3}(18\angle 154° - 10\angle 30°) = 8.3\angle 173° \text{ A}$$

The symmetrical components of delta currents are

$$I_{AB1} = \frac{1}{3}(6\angle 86° + 10.5\angle(-41.5° + 120°) + 8.3\angle(173° + 240°)) \quad \text{(iv)}$$

$$= 8\angle 72° \text{ A}$$

$$I_{AB2} = \frac{1}{3}(6\angle 86° + 10.5\angle(-41.5° + 240°) + 8.3\angle(173° + 120°)) \quad \text{(v)}$$

$$= 2.7\angle 218° \text{ A}$$

$$I_{AB0} = 0 \quad \text{(vi)}$$

I_{BC1}, I_{BC2}, I_{BC0}, I_{CA1}, I_{CA2} and I_{CA0} can be found by using Eq. (10.2).

Comparing Eqs (i) and (iv), and (ii) and (v), the following relationship between symmetrical components of line and delta currents are immediately observed:

$$I_{AB1} = \frac{I_{A1}}{\sqrt{3}}\angle 30° \quad \text{(vii)}$$

$$I_{AB2} = \frac{I_{A2}}{\sqrt{3}}\angle -30° \quad \text{(viii)}$$

The reader should verify these by calculating I_{AB1} and $I_{AB2}$from Eqs (vii) and (viii) and comparing the results with Eqs (iv) and (v).

10.3 PHASE SHIFT IN STAR-DELTA TRANSFORMERS

Positive and negative sequence voltages and currents undergo a phase shift in passing through a star-delta transformer which depends upon the labelling of terminals. Before considering this phase shift, we need to discuss the standard polarity marking of a single-phase transformer as shown in Fig. 10.5. The transformer ends marked with a dot have the same polarity. Therefore, voltage V'_{HH} is in phase with voltage V'_{LL}. Assuming that the small amount of magnetizing current can be neglected, the primary current I_1, entering the dotted end cancels the demagnetizing ampere-turns of the secondary current I_2 so that I_1 and I_2 with directions of flow as indicated in the diagram are in phase. If the direction of I_2 is reversed, I_1 and I_2 will be in phase opposition.

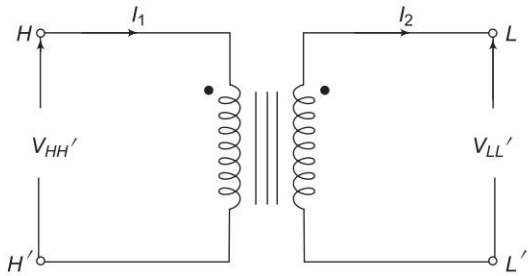

Fig. 10.5 Polarity marking of a single-phase transformer

Consider now a star/delta transformer with terminal labelling as indicated in Fig. 10.6(a). Windings shown parallel to each other are magnetically coupled. Assume that the transformer is excited with positive sequence voltages and carries positive sequence currents. With the polarity marks shown, we can immediately draw the phasor diagram of Fig. 10.7. The following interrelationship between the voltages on the two sides of the transformer is immediately observed from the phasor diagram:

$$V_{AB1} = x\, V_{ab1} \angle 30°,\ x = \text{phase transformation ratio} \qquad (10.34)$$

As per Eq. (10.34), the positive sequence line voltages on star side lead the corresponding voltages on the delta side by 30° (The same result would apply to line-to-neutral voltages on the two sides). The same also applies for line currents.

If the delta side is connected as in Fig. 10.6(b), the phase shift reverses (the reader should draw the phasor diagram); the delta side quantities lead the star side quantities by 30°.

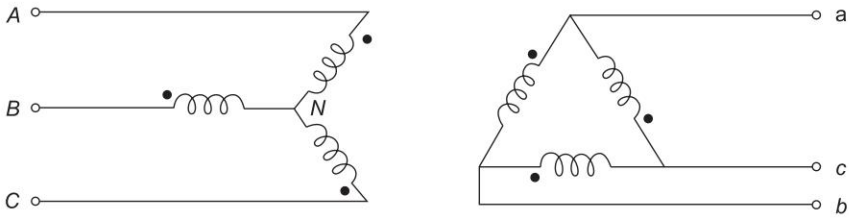

(a) Star side quantities lead delta side quantities by 30°

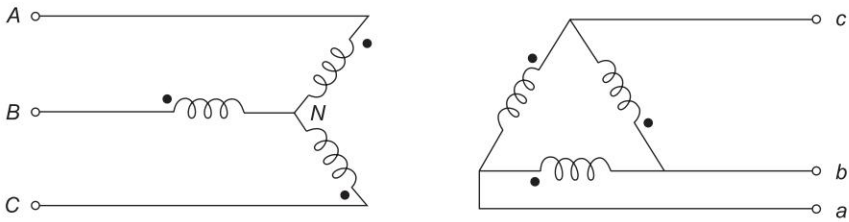

(b) Delta side quantities lead star side quantities by 30°

Fig. 10.6 Labelling of the star/delta transformer

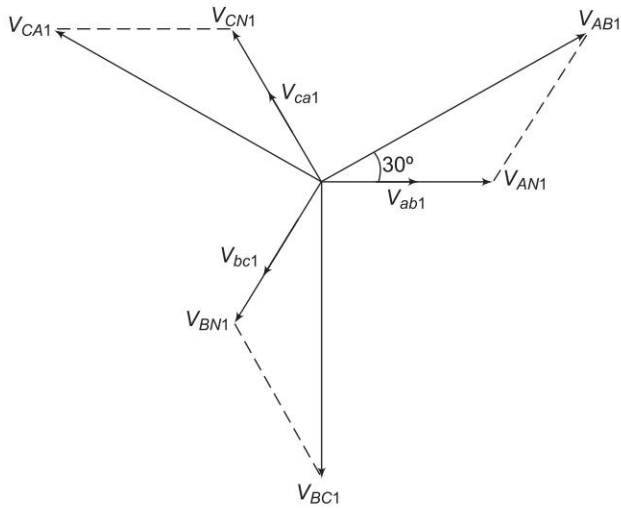

Fig. 10.7 Positive sequence voltages on a star/delta transformer

Instead, if the transformer of Fig. 10.6(a) is now excited by negative sequence voltages and currents, the voltage phasor diagram will be as in Fig. 10.8. The phase shift in comparison to the positive sequence case now reverses, i.e., the star side quantities lag the delta side quantities by 30°. The result for Fig. 10.6(b) also correspondingly reverses.

It shall from now onwards be assumed that a *star/delta transformer is so labelled that the positive sequence quantities on the HV side lead their corresponding positive sequence quantities on the LV side by 30°. The reverse is the case for negative sequence quantities wherein HV quantities lag the corresponding LV quantities by 30°.*

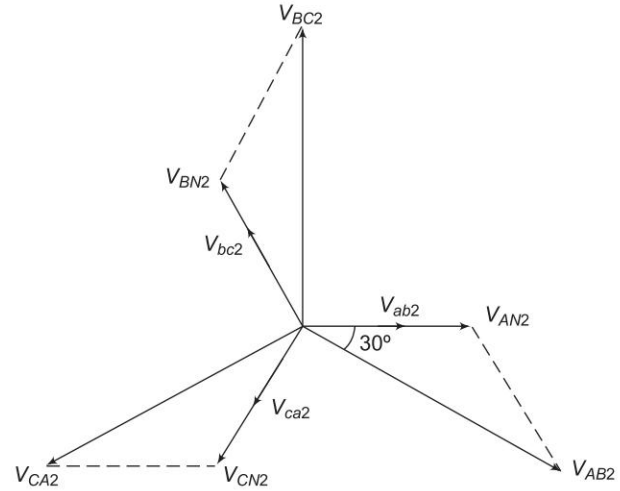

Fig. 10.8 Negative sequence voltages on a star/delta transformer

10.4 SEQUENCE IMPEDANCES OF TRANSMISSION LINES

Figure 10.9 shows the circuit of a fully transposed line carrying unbalanced currents. The return path for I_n is sufficiently away for the mutual effect to be ignored. Let

X_s = self reactance of each line

X_m = mutual reactance of any line pair

The following KVL equations can be written down from Fig. 10.9.

$$\begin{aligned} V_a - V_a' &= jX_sI_a + jX_mI_b + jX_mI_c \\ V_b - V_b' &= jX_mI_a + jX_sI_b + jX_mI_c \\ V_c - V_c' &= jX_mI_a + jX_mI_b + jX_sI_c \end{aligned} \tag{10.35}$$

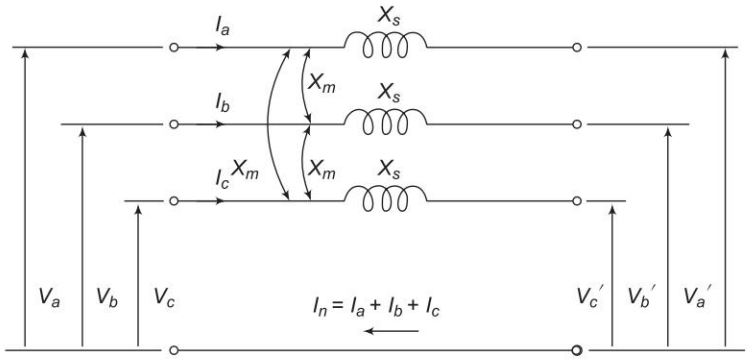

Fig. 10.9

or in matrix form

$$\begin{bmatrix} V_a \\ V_b \\ V_c \end{bmatrix} - \begin{bmatrix} V_a' \\ V_b' \\ V_c' \end{bmatrix} = j \begin{bmatrix} X_s X_m X_m \\ X_m X_s X_m \\ X_m X_m X_s \end{bmatrix} \begin{bmatrix} I_a \\ I_b \\ I_c \end{bmatrix} \tag{10.36}$$

or $$V_p - V_p' = ZI_p \tag{10.37}$$

or $$A\,(V_s - V_s') = ZAI_s \tag{10.38}$$

or $$V_s V_s' = A^{-1}ZAI_s \tag{10.39}$$

Now

$$A^{-1}ZA = \frac{1}{3}\begin{bmatrix} 1 & \alpha & \alpha^2 \\ 1 & \alpha^2 & \alpha \\ 1 & 1 & 1 \end{bmatrix} \begin{bmatrix} jX_s & jX_m & jX_m \\ jX_m & jX_s & jX_m \\ jX_m & jX_m & jX_s \end{bmatrix} \begin{bmatrix} 1 & 1 & 1 \\ \alpha^2 & \alpha & 1 \\ \alpha & \alpha^2 & 1 \end{bmatrix} \tag{10.40}$$

$$= j\begin{bmatrix} X_s - X_m & 0 & 0 \\ 0 & X_s - X_m & 0 \\ 0 & 0 & X_s + 2X_m \end{bmatrix}$$

Thus Eq. (10.37) can be written as

$$\begin{bmatrix} V_1 \\ V_2 \\ V_0 \end{bmatrix} - \begin{bmatrix} V_1' \\ V_2' \\ V_0' \end{bmatrix} = j\begin{bmatrix} X_s - X_m & 0 & 0 \\ 0 & X_s - X_m & 0 \\ 0 & 0 & X_s + 2X_m \end{bmatrix}\begin{bmatrix} I_1 \\ I_2 \\ I_0 \end{bmatrix} \quad (10.41)$$

$$= \begin{bmatrix} Z_1 & 0 & 0 \\ 0 & Z_2 & 0 \\ 0 & 0 & Z_0 \end{bmatrix}\begin{bmatrix} I_1 \\ I_2 \\ I_0 \end{bmatrix} \quad (10.42)$$

where in

$$Z_1 = j(X_s - X_m) = \textit{positive sequence impedance} \quad (10.43)$$

$$Z_2 = j(X_s - X_m) = \textit{negative sequence impedance} \quad (10.44)$$

$$Z_0 = j(X_s + 2X_m) = \textit{zero sequence impedance} \quad (10.45)$$

We conclude that a fully transposed transmission has:

(i) equal positive and negative sequence impedances.

(ii) zero sequence impedance much larger than the positive (or negative) sequence impedance (it is approximately 2.5 times).

It is further observed that the sequence circuit equations (10.42) are in *decoupled* form, i.e. there are no mutual sequence inductances. Equation (10.42) can be represented in network form as in Fig. 10.10.

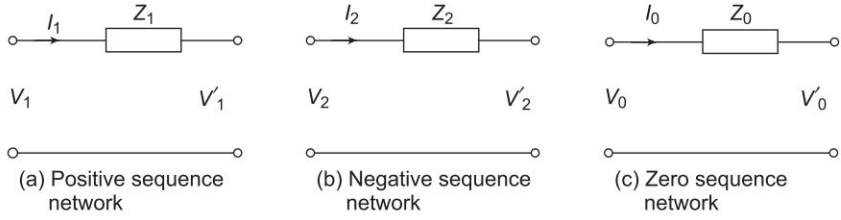

Fig. 10.10

The decoupling between sequence networks of a fully transposed transmission holds also in three-phase synchronous machines and three-phase transformers. This fact leads to considerable simplifications in the use of symmetrical components method in unsymmetrical fault analysis.

In case of three static unbalanced impedances, coupling appears between sequence networks and the method is no more helpful than a straight forward three-phase analysis.

10.5 SEQUENCE IMPEDANCES AND SEQUENCE NETWORK OF POWER SYSTEM

Power system elements—transmission lines, transformers and synchronous machines—have a three-phase symmetry because of which when currents of a particular sequence are passed through these elements, voltage drops of the same sequence appear, i.e. the elements possess only self-impedances to sequence currents. Each element can therefore be represented by three decoupled *sequence networks* (on single-phase basis) pertaining to positive, negative and zero sequences, respectively. EMFs are involved only in a positive sequence network of synchronous machines. For finding a particular sequence impedance, the element in question is subjected to currents and voltages of that sequence only. With the element operating under these conditions, the sequence impedance can be determined analytically or through experimental test results.

With the knowledge of sequence networks of elements, complete positive, negative and zero sequence networks of any power system can be assembled. As will be explained in the next chapter, these networks are suitably interconnected to simulate different unsymmetrical faults. The sequence currents and voltages during the fault are then calculated from which actual fault currents and voltages can be found.

10.6 SEQUENCE IMPEDANCES AND NETWORKS OF SYNCHRONOUS MACHINE

Figure 10.11 depicts an unloaded synchronous machine (generator or motor) grounded through a reactor (impedance Z_n). E_a, E_b and E_c are the induced emfs of the three phases. When a fault (not shown in the figure) takes place at machine terminals, currents I_a, I_b and I_c flow in the lines. Whenever the fault involves ground, current $I_n = I_a + I_b + I_c$ flows to neutral from ground via Z_n.

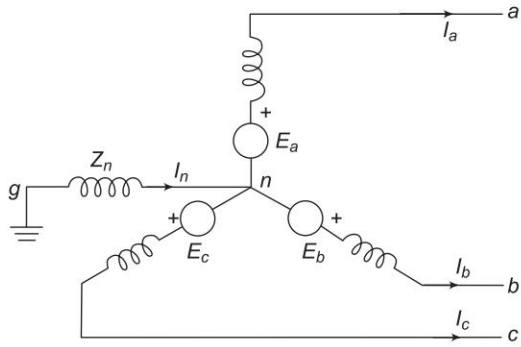

Fig. 10.11 Three-phase synchronous generator with grounded neutral

Unbalanced line currents can be resolved into their symmetrical components I_{a1}, I_{a2} and I_{a0}. Before we can proceed with fault analysis (Ch. 11), we must know the equivalent circuits presented by the machine to the flow of positive, negative and zero sequence currents, respectively. Because of winding symmetry currents of a particular sequence produce voltage drops of that sequence only. Therefore, there is a no coupling between the equivalent circuits of various sequences*.

Positive Sequence Impedance and Network

Since a synchronous machine is designed with symmetrical windings, it induces emfs of positive sequence only, i.e. no negative or zero sequence voltages are induced in it. When the machine carries positive sequence currents only, this mode of operation is the balanced mode discussed at length in Ch. 9. The armature reaction field caused by positive sequence currents rotates at synchronous speed in the same direction as the rotor, i.e., it is stationary with respect to field excitation. The machine equivalently offers a direct axis reactance whose value reduces from subtransient reactance (X_d'') to transient reactance (X_d') and finally to steady state (synchronous) reactance (X_d), as the short circuit transient progresses in time. If armature resistance is assumed negligible, the positive sequence impedance of the machine is

$$Z_1 = jX_d'' \text{ (if 1 cycle transient is of interest)} \quad (10.46)$$

$$= jX_d' \text{ (if 3 – 4 cycle transient is of interest)} \quad (10.47)$$

$$= jX_d \text{ (if steady state value is of interest)} \quad (10.48)$$

If the machine short circuit takes place from unloaded conditions, the terminal voltage constitutes the positive sequence voltage; on the other hand, if the short circuit occurs from loaded conditions, the voltage behind appropriate reactance (subtransient, transient or synchronous) constitutes the positive sequence voltage.

Figure 10.12(a) shows the three-phase positive sequence network model of a synchronous machine. Z_n does not appear in the model as $I_n = 0$ for positive sequence currents. Since it is a balanced network it can be represented by the single-phase network model of Fig. 10.12(b) for purposes of analysis. The reference bus for a positive sequence network is at neutral potential. Further, since no current flows from ground to neutral, the neutral is at ground potential.

With reference to Fig. 10.12(b), the positive sequence voltage of terminal *a* with respect to the reference bus is given by

$$V_{a1} = E_a - Z_1 I_{\alpha 1} \quad (10.49)$$

Negative Sequence Impedance and Network

It has already been said that a synchronous machine has zero negative sequence induced voltages. With the flow of negative sequence currents in the stator a

*This can be shown to be so by synchronous machine theory [5].

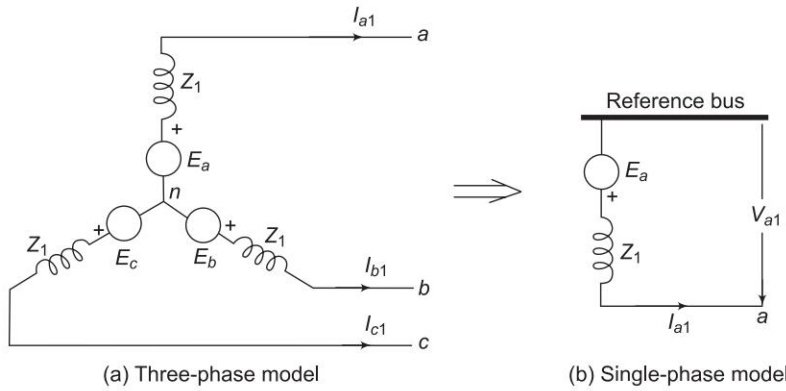

Fig. 10.12 Positive sequence network of synchronous machine

rotating field is created which rotates in the opposite direction to that of the positive sequence field and, therefore, at double synchronous speed with respect to rotor. Currents at double the stator frequency are therefore induced in rotor field and damper winding. In sweeping over the rotor surface, the negative sequence mmf is alternately presented with reluctances of direct and quadrature axes. The negative sequence impedance presented by the machine with consideration given to the damper windings, is often defined as

$$Z_2 = j\frac{X_q'' + X_d''}{2}; \; |Z_2| < |Z_1| \tag{10.50}$$

Negative sequence network models of a synchronous machine, on a three-phase and single-phase basis are shown in Figs 10.13(a) and (b), respectively. The reference bus is of course at neutral potential which is the same as ground potential.

From Fig. 10.13(b) the negative sequence voltage of terminal *a* with respect to reference bus is

$$V_{a2} = - Z_2 I_{a2} \tag{10.51}$$

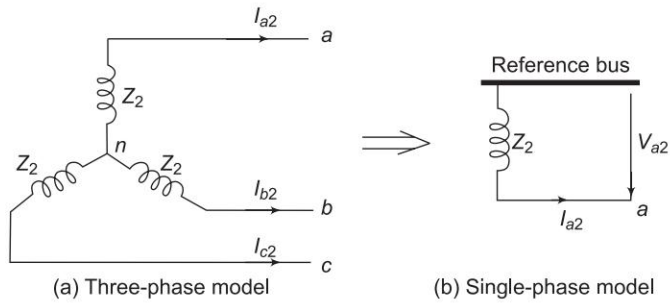

Fig. 10.13 Negative sequence network of a synchronous machine

Zero Sequence Impedance and Network

We state once again that no zero sequence voltages are induced in a synchronous machine. The flow of zero sequence currents creates three mmfs which are in time phase but are distributed in space phase by 120°. The resultant air gap field caused by zero sequence currents is therefore zero. Hence, the rotor windings present leakage reactance only to the flow of zero sequence currents ($Z_{0g} < Z_2 < Z_1$).

Zero sequence network models on a three-and single-phase basis are shown in Fig. 10.14(a) and (b). In Fig. 10.14(a), the current flowing in the impedance Z_n between neutral and ground is $I_n = 3I_{a0}$. The zero sequence voltage of terminal a with respect to ground, the reference bus, is therefore

$$V_{a0} = -3Z_nI_{a0} - Z_{0g}I_{a0} = -(3Z_n + Z_{0g})I_{a0} \qquad (10.52)$$

where Z_{0g} is the zero sequence impedance per phase of the machine. Since the single-phase zero sequence network of Fig. 10.14(b) carries only per phase zero sequence current, its total zero sequence impedance must be

$$Z_0 = 3Z_n + Z_{0g} \qquad (10.53)$$

in order for it to have the same voltage from a to reference bus. The reference bus here is, of course, at ground potential.

From Fig. 10.14(b) zero sequence voltage of point a with respect to the reference bus is

$$V_{a0} = -Z_0I_{a0} \qquad (10.54).$$

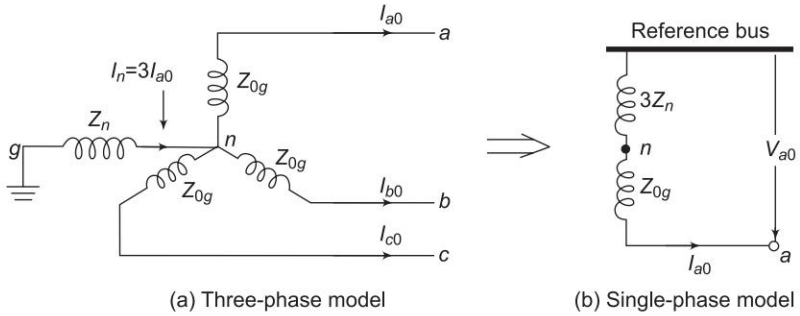

(a) Three-phase model (b) Single-phase model

Fig. 10.14 Zero sequence network of a synchronous machine

Order of Values of Sequence Impedances of a Synchronous Generator

Typical values of sequence impedances of a turbo-generator rated 5 MVA, 6.6 kV, 3,000 rpm are:

Z_1 = 12% (subtransient)

Z_1 = 20% (transient)

Z_1 = 110% (synchronous)

Z_2 = 12%

Z_0 = 5%

For typical values of positive, negative and zero sequence reactances of a synchronous machine refer to Table 9.1.

10.7 SEQUENCE IMPEDANCES OF TRANSMISSION LINES

A fully transposed three-phase line is completely symmetrical and therefore the per phase impedance offered by it is independent of the phase sequence of a balanced set of currents. In other words, the impedances offered by it to positive and negative sequence currents are identical. The expression for its per phase inductive reactance accounting for both self and mutual linkages has been derived in Ch. 2.

When only zero sequence currents flow in a transmission line, the currents in each phase are identical in both magnitude and phase angle. Part of these currents return via the ground, while the rest return through the overhead ground wires. The ground wires being grounded at several towers, the return currents in the ground wires are not necessarily uniform along the entire length. The flow of zero sequence currents through the transmission lines, ground wires and ground creates a magnetic field pattern which is very different from that caused by the flow of positive or negative sequence currents where the currents have a phase difference of 120° and the return current is zero. The zero sequence impedance of a transmission line also accounts for the ground impedance ($Z_0 = Z_{l0} + 3Z_{g0}$). Since the ground impedance heavily depends on soil conditions, it is essential to make some simplifying assumptions to obtain analytical results. The zero sequence impedance of transmission lines usually ranges from 2 to 3.5 times the positive sequence impedance*. This ratio is on the higher side for double circuit lines without ground wires.

---

* We can easily compare the forward path positive and zero sequence impedances of a transmission line with ground return path infinitely away. Assume that each line has a self inductance L and mutual inductance M between any two lines (completely symmetrical case). The voltage drop in line a caused by positive sequence currents is

$$V_{Aa1} = \omega L I_{a1} + \omega M I_{b1} + \omega M I_{c1}$$
$$= [\omega L + (\alpha^2 + \alpha)\,\omega M] I_{a1} = \omega(L - M) I_{a1}$$

$\therefore$ Positive sequence reactance = $\omega(L - M)$

The voltage drop in line a caused by zero sequence currents is

$$V_{Aa0} = \omega L I_{a0} + \omega M I_{b0} + \omega M I_{c0}$$
$$= \omega(L + 2M) I_{a0}$$

$\therefore$ Zero sequence reactance = $\omega(L + 2M)$

Obviously, zero sequence reactance is much more than positive sequence reactance. This result has already been derived in Eq. (10.45).

10.8 SEQUENCE IMPEDANCES AND NETWORKS OF TRANSFORMERS

It is well known that almost all present day installations have three-phase transformers since they entail lower initial cost, have smaller space requirements and higher efficiency.

The positive sequence series impedance of a transformer equals its leakage impedance. Since a transformer is a static device, the leakage impedance does not change with alteration of phase sequence of balanced applied voltages. The transformer negative sequence impedance is also therefore equal to its leakage reactance. Thus, for a transformer

$$Z_1 = Z_2 = Z_{\text{leakage}} \tag{10.55}$$

Assuming such transformer connections that zero sequence currents can flow on both sides, a transformer offers a zero sequence impedance which may differ slightly from the corresponding positive and negative sequence values. It is, however, normal practice to assume that the series impedances of all sequences are equal regardless of the type of transformer.

The zero sequence magnetizing current is somewhat higher in a core type than in a shell type transformer. This difference does not matter as the magnetizing current of a transformer is always neglected in short circuit analysis.

Above a certain rating (1,000 kVA) the reactance and impedance of a transformer are almost equal and are therefore not distinguished.

Zero Sequence Networks of Transformers

Before considering the zero sequence networks of various types of transformer connections, three important observations are made:

(i) When magnetizing current is neglected, transformer primary would carry current only if there is current flow on the secondary side.

(ii) Zero sequence currents can flow in the legs of a star connection only if the star point is grounded which provides the necessary return path for zero sequence currents. This fact is illustrated by Figs 10.15(a) and (b).

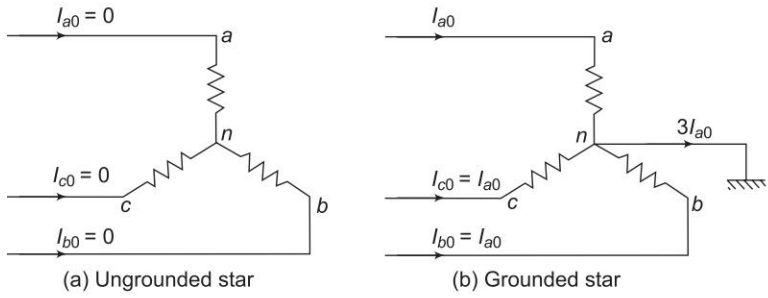

Fig. 10.15 Flow of zero sequence currents in a star connection

(iii) No zero sequence currents can flow in the lines connected to a delta connection as no return path is available for these currents. Zero sequence currents can, however, flow in the legs of a delta—such currents are caused by the presence of zero sequence voltages in the delta connection. This fact is illustrated by Fig. 10.16.

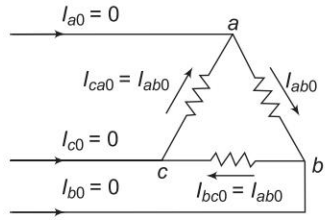

Fig. 10.16 Flow of zero sequence currents in a delta connection

Let us now consider various types of transformer connections.

Case 1: Y-Y transformer bank with any one neutral grounded

If any one of the two neutrals of a *Y-Y* transformer is ungrounded, zero sequence currents cannot flow in the ungrounded star and consequently, these cannot flow in the grounded star. Hence, an open circuit exists in the zero sequence network between *H* and *L*, i.e. between the two parts of the system connected by the transformer as shown in Fig. 10.17.

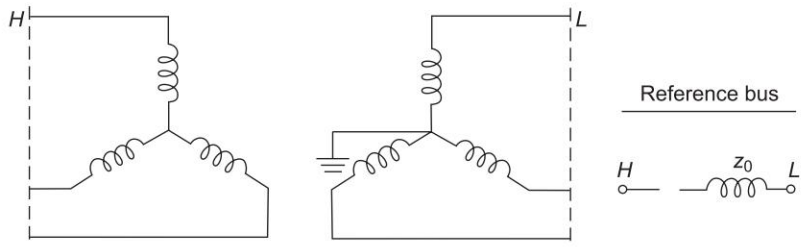

Fig. 10.17 *Y-Y* transformer bank with one neutral grounded and its zero sequence network

Case 2: Y-Y transformer bank both neutrals grounded

When both the neutrals of a *Y–Y* transformer are grounded, a path through the transformer exists for zero sequence currents in both windings via the two grounded neutrals. Hence, in the zero sequence network *H* and *L* are connected by the zero sequence impedance of the transformer as shown in Fig. 10.18.

Case 3: Y-Δ transformer bank with grounded Y neutral

If the neutral of star side is grounded, zero sequence currents can flow in star because a path is available to ground and the balancing zero sequence currents

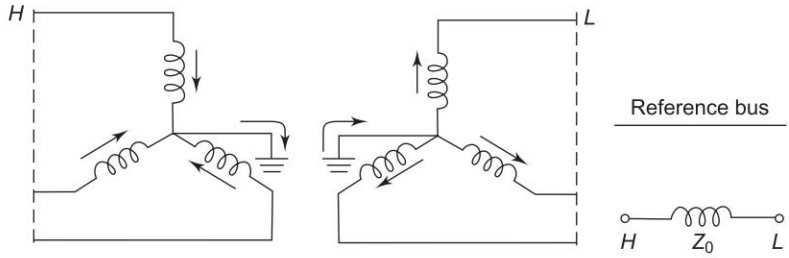

Fig. 10.18 *Y-Y* transformer bank with neutrals grounded and its zero sequence network

can flow in delta. Of course no zero sequence currents can flow in the line on the delta side. The zero sequence network must therefore have a path from the line *H* on the star side through the zero sequence impedance of the transformer to the reference bus, while an open circuit must exist on the line *L* side of delta (see Fig. 10.19). If the star neutral is grounded through Z_n, an impedance $3Z_n$ appears in series with Z_0 in the sequence network.

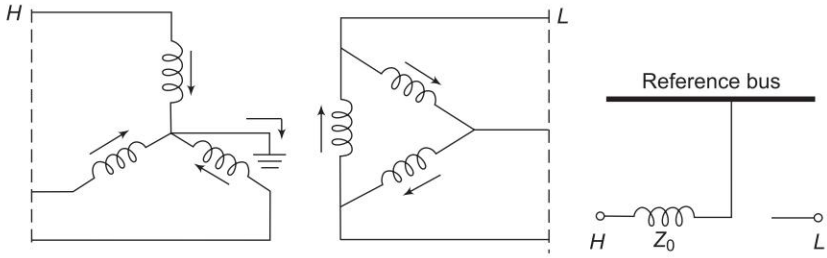

Fig. 10.19 *Y*-Δ Transformer bank with grounded y neutral and its zero sequence network

Case 4: Y-Δ transformer bank with ungrounded star

This is the special case of Case 3 where the neutral is grounded through $Z_n = \infty$. Therefore no zero sequence current can flow in the transformer windings. The zero sequence network then modifies to that shown in Fig. 10.20.

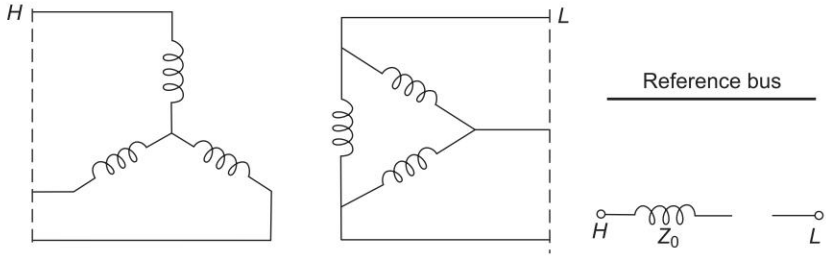

Fig. 10.20 *Y*-Δ Transformer bank with ungrounded star and its zero sequence network

Case 5: Δ-Δ transformer bank

Since a delta circuit provides no return path, the zero sequence currents cannot flow in or out of Δ-Δ transformer; however, it can circulate in the delta windings*. Therefore, there is an open circuit between H and L and Z_0 is connected to the reference bus on both ends to account for any circulating zero sequence current in the two deltas (see Fig. 10.21).

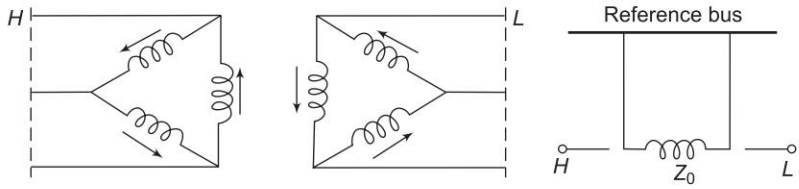

Fig. 10.21 Δ-Δ Transformer bank and its zero sequence network

10.9 CONSTRUCTION OF SEQUENCE NETWORKS OF A POWER SYSTEM

In the previous sections the sequence networks for various power system elements—synchronous machines, transformers and lines—have been given. Using these, complete sequence networks of a power system can be easily constructed. To start with, the positive sequence network is constructed by examination of the one-line diagram of the system. It is to be noted that positive sequence voltages are present in synchronous machines (generators and motors) only. The transition from positive sequence network to negative sequence network is straightforward. Since the positive and negative sequence impedances are identical for static elements (lines and transformers), the only change necessary in positive sequence network to obtain negative sequence network is in respect of synchronous machines. Each machine is represented by its negative sequence impedance, the negative sequence voltage being zero.

The reference bus for positive and negative sequence networks is the system neutral. Any impedance connected between a neutral and ground is not included in these sequence networks as neither of these sequence currents can flow in such an impedance.

Zero sequence subnetworks for various parts of a system can be easily combined to form complete zero sequence network. No voltage sources are present in the zero sequence network. Any impedance included in generator or transformer neutral becomes three times its value in a zero sequence network. Special care needs to be taken of transformers in respect of zero sequence network. Zero sequence networks of all possible transformer connections have been dealt with in the preceding section.

---

* Such circulating currents would exist only if zero sequence voltages are somehow induced in either delta winding.

The procedure for drawing sequence networks is illustrated through the following examples.

Example 10.2 A 25 MVA, 11 kV, three-phase generator has a subtransient reactance of 20%. The generator supplies two motors over a transmission line with transformers at both ends as shown in the one-line diagram of Fig. 10.22. The motors have rated inputs of 15 and 7.5 MVA, both 10 kV with 25% subtransient reactance. The three-phase transformers are both rated 30 MVA, 10.8/121 kV, connection Δ–Y with leakage reactance of 10% each. The series reactance of the line is 100 ohms. Draw the positive and negative sequence networks of the system with reactances marked in per unit.

Fig. 10.22

Assume that the negative sequence reactance of each machine is equal to its subtransient reactance. Omit resistances. Select generator rating as base in the generator circuit.

Solution

A base of 25 MVA, 11 kV in the generator circuit requires a 25 MVA base in all other circuits and the following voltage bases:

$$\text{Transmission line voltage base} = 11 \times \frac{121}{10.8} = 123.2 \text{ kV}$$

$$\text{Motor voltage base} = 123.2 \times \frac{10.8}{121} = 11 \text{ kV}$$

The reactances of transformers, line and motors are converted to pu values on appropriate bases as follows:

$$\text{Transformer reactance} = 0.1 \times \frac{25}{30} \times \left(\frac{10.8}{11}\right)^2 = 0.0805 \text{ pu}$$

$$\text{Line reactance} = \frac{100 \times 25}{(123.2)^2} = 0.164 \text{ pu}$$

$$\text{Reactance of motor 1} = 0.25 \times \frac{25}{15} \times \left(\frac{10}{11}\right)^2 = 0.345 \text{ pu}$$

$$\text{Reactance of motor 2} = 0.25 \times \frac{25}{7.5} \times \left(\frac{10}{11}\right)^2 = 0.69 \text{ pu}$$

The required positive sequence network is presented in Fig. 10.23.

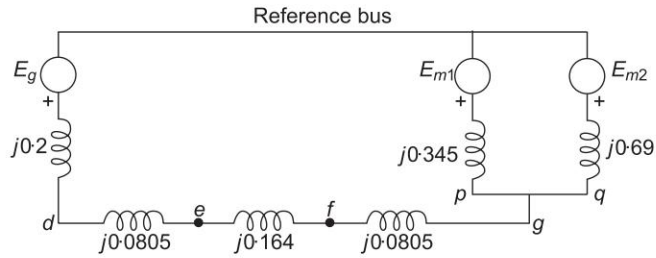

Fig. 10.23 Positive sequence network for Example 10.2

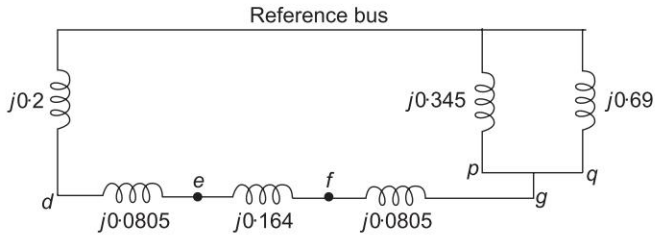

Fig. 10.24 Negative sequence network for Example 10.2

Since all the negative sequence reactances of the system are equal to the positive sequence reactances, the negative sequence network is identical to the positive sequence network but for the omission of voltage sources. The negative sequence network is drawn in Fig. 10.24

Example 10.3 For the power system whose one-line diagram is shown in Fig. 10.25, sketch the zero sequence network.

Fig. 10.25

Solution

The zero sequence network is drawn in Fig. 10.26.

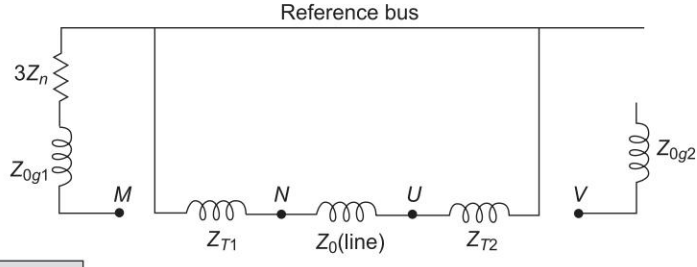

Fig. 10.26 Zero sequence network of the system presented in Fig. 10.25

Example 10.4 Draw the zero sequence network for the system described in Example 10.3. Assume zero sequence reactances for the generator and motors of 0.06 per unit. Current limiting reactors of 2.5 ohms each are connected in the neutral of the generator and motor No. 2. The zero sequence reactance of the transmission line is 300 ohms.

Solution

The zero sequence reactance of the transformer is equal to its positive sequence reactance. Hence

$$\text{Transformer zero sequence reactance} = 0.0805 \text{ pu}$$

$$\text{Generator zero sequence reactances} = 0.06 \text{ pu}$$

$$\text{Zero sequence reactance of motor 1} = 0.06 \times \frac{25}{15} \times \left(\frac{10}{11}\right)^2$$

$$= 0.082 \text{ pu}$$

$$\text{Zero sequence reactance of motor 2} = 0.06 \times \frac{25}{7.5} \times \left(\frac{10}{11}\right)^2$$

$$= 0.164 \text{ pu}$$

$$\text{Reactance of current limiting reactors} = \frac{2.5 \times 25}{(11)^2} = 0.516 \text{ pu}$$

Reactance of current limiting reactor included in zero sequence network $= 3 \times 0.516 = 1.548$ pu

$$\text{Zero sequence reactance of transmission line} = \frac{300 \times 25}{(123.2)^2}$$

$$= 0.494 \text{ pu}$$

The zero sequence network is shown in Fig. 10.27.

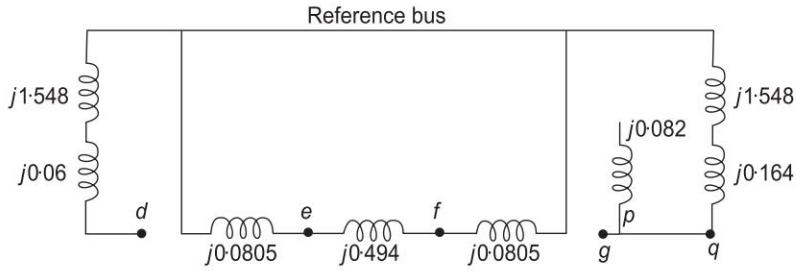

Fig. 10.27 Zero sequence network of Example 10.4

10.10 SUMMARY

For analyzing unsymmetrical (unbalanced) faults on power system (Ch. 11), this chapter has presented simple method of analysis called method of symmetrical components given by C.L. Fortescue in 1918 (Ref. 17). How different sequence networks of a power system are constructed is explained.

Problems

10.1 Compute the following in polar form

(i) $\alpha^2 - 1$ (ii) $1 - \alpha - \alpha^2$ (iii) $3\alpha^2 + 4\alpha + 2$ (iv) $j\alpha$

10.2 Three identical resistors are star connected and rated 2,500 V, 750 kVA. This three-phase unit of resistors is connected to the Y side of a Δ-Y transformer. The following are the voltages at the resistor load:

$$|V_{ab}| = 2{,}000 \text{ V}; |V_{bc}| = 2{,}900 \text{ V}; |V_{ca}| = 2{,}500 \text{ V}$$

Choose base as 2,500 V, 750 kVA and determine the line voltages and currents in per unit on the delta side of the transformer. It may be assumed that the load neutral is not connected to the neutral of the transformer secondary.

10.3 Determine the symmetrical components of three voltages

$$V_a = 200\angle 0^\circ,\ V_b = 200\angle 245^\circ \text{ and } V_c = 200\angle 105^\circ \text{ V}$$

10.4 A single-phase resistive load of 100 kVA is connected across lines bc of a balanced supply of 3 kV. Compute the symmetrical components of the line currents.

10.5 A delta connected resistive load is connected across a balanced three-phase supply of 400 V as shown in Fig. P-10.5. Find the symmetrical components of line currents and delta currents.

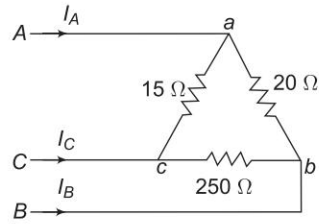

Fig. P-10.5 Phase sequence *ABC*

10.6 Three resistances of 10, 15 and 20 ohms are connected in star across a three-phase supply of 200 V per phase as shown in Fig. P-10.6. The supply neutral is earthed while the load neutral is isolated. Find the

currents in each load branch and the voltage of load neutral above earth. Use the method of symmetrical components.

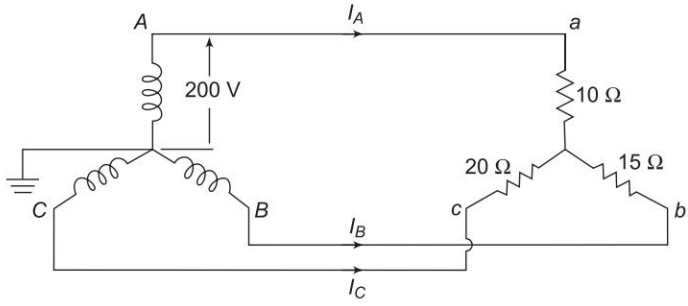

Fig. P-10.6

10.7 The voltages at the terminals of a balanced load consisting of three 20 ohm *Y*-connected resistors are 200 ∠0°, 100 ∠255.5° and 200 ∠151° V. Find the line currents from the symmetrical components of the line voltages if the neutral of the load is isolated. What relation exists between the symmetrical components of the line and phase voltages? Find the power expended in three 20 ohm resistors from the symmetrical components of currents and voltages.

10.8. Draw the positive, negative and zero sequence impedance networks for the power system of Fig. P-10.8.

Choose a base of 50 MVA, 220 kV in the 50 Ω transmission lines, and mark all reactances in pu. The ratings of the generators and transformers are:

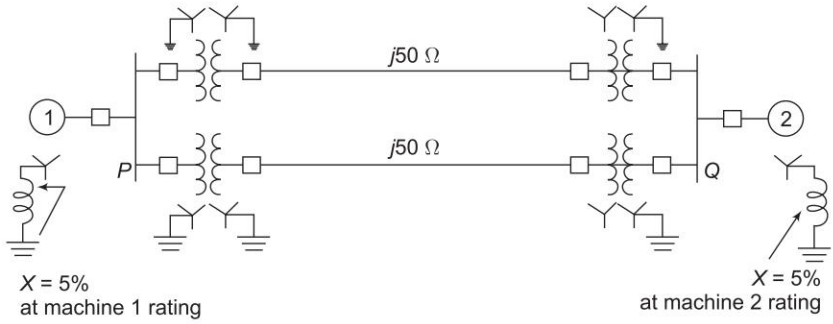

Fig. P-10.8

Generator 1: 25 MVA, 11 kV, $X'' = 20\%$
Generator 2: 25 MVA, 11 kV, $X'' = 20\%$

Three-phase transformer (each): 20 MVA, 11 *Y*/220 *Y* kV, $X = 15\%$

The negative sequence reactance of each synchronous machine is equal to its subtransient reactance. The zero sequence reactance of each

machine is 8%. Assume that the zero sequence reactances of lines are 250% of their positive sequence reactances.

10.9 For the power system of Fig. P-10.9 draw the positive, negative and zero sequence networks. The generators and transformers are rated as follows:

Generator 1: 25 MVA, 11 kV, $X'' = 0.2$, $X_2 = 0.15$, $X_0 = 0.03$ pu

Generator 2: 15 MVA, 11 kV, $X'' = 0.2$, $X_2 = 0.15$, $X_0 = 0.05$ pu

Synchronous Motor 3: 25 MVA, 11 kV, $X'' = 0.2$, $X_2 = 0.2$, $X_0 = 0.1$ pu

Transformer 1: 25 MVA, 11 Δ/120 *Y* kV, $X = 10\%$

2: 12.5 MVA, 11 Δ/120 *Y* kV, $X = 10\%$

3: 10 MVA, 120 *Y*/11 *Y* kV, $X = 10\%$

Choose a base of 50 MVA, 11 kV in the circuit of generator 1.

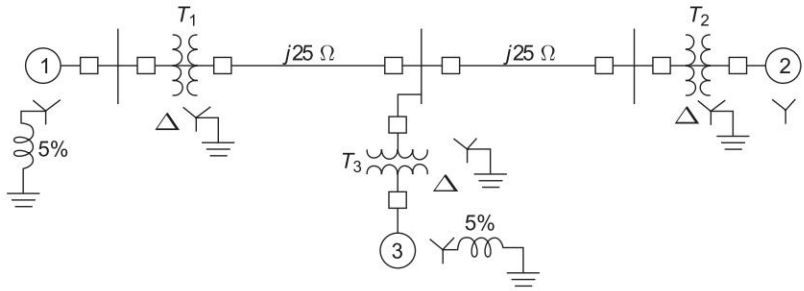

Fig. P-10.9

Note: Zero sequence reactance of each line is 250% of its positive sequence reactance.

10.10 Consider the circuit shown in Fig. P-10.10. Suppose

$V_{an} = 100 \angle 0°$ $X_s = 12\ \Omega$

$V_{bn} = 60 \angle 60°$ $X_{ab} = X_{bc} = X_{ca} = 5$ W

$V_{cn} = 60 \angle 120°$

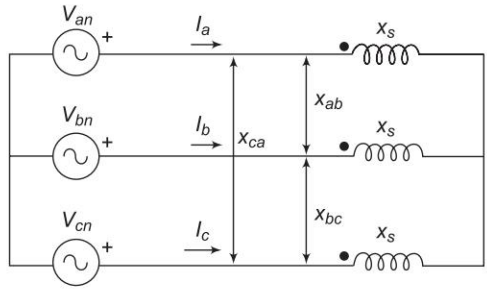

Fig. P-10.10

(a) Calculate I_a, I_b and I_c without using symmetrical component.
(b) Calculate I_a, I_b and I_c using symmetrical component.

References

Books

1. Wagner, C.F. and R.D. Evans, *Symmetrical Components,* McGraw-Hill, New York 1933.
2. Clarke, E., *Circuit Analysis of Alternating Current Power Systems*, vol. 1, Wiley, New York, 1943.
3. Austin Stigant, S., *Master Equations and Tables for Symmetrical Component Fault Studies*, Macdonald, London, 1964.
4. Stevenson, W.D., *Elements of Power System Analysis,* 4th edn, McGraw-Hill, New York, 1982.
5. Kothari, D.P. and I.J. Nagrath, *Electric Machines*, 3rd edn, Tata McGraw-Hill, New Delhi, 2004.
6. Kothari, D.P. and I.J. Nagrath, *Electric Machines*, 2nd edn, Tata McGraw-Hill, Sigma Series, New Delhi, 2006.

Paper

7. Fortescue, C.L., "Method of Symmetrical Coordinates Applied to the Solution of Polyphase Networks', *AIEE*, 1918, 37: 1027.

Chapter 11

Unsymmetrical Fault Analysis

11.1 INTRODUCTION

Chapter 9 was devoted to the treatment of symmetrical (three-phase) faults in a power system. Since the system remains balanced during such faults, analysis could conveniently proceed on a single-phase basis. In this chapter, we shall deal with unsymmetrical faults. Various types of unsymmetrical faults that occur in power systems are:

Shunt Type Faults

(i) Single line-to-ground (LG) fault
(ii) Line-to-line (LL) fault
(iii) Double line-to-ground (LLG) fault

Series Type Faults

(i) Open conductor (one or two conductors open) fault.

It was stated in Ch. 9, that a three-phase (3L) fault being the most severe must be used to calculate the rupturing capacity of circuit breakers, even though this type of fault has a low frequency of occurrence, when compared to the unsymmetrical faults listed above. There are, however, situations when an LG fault can cause greater fault current than a three-phase fault (this may be so when the fault location is close to large generating units). Apart from this, unsymmetrical fault analysis is important for relay setting, single-phase switching and system stability studies (Ch. 12).

The probability of two or more simultaneous faults (cross-country faults) on a power system is remote and is therefore ignored in system design for abnormal conditions.

The method of symmetrical components presented in Ch. 10, is a powerful tool for study of unsymmetrical faults and will be fully exploited in this chapter.

11.2 SYMMETRICAL COMPONENT ANALYSIS OF UNSYMMETRICAL FAULTS

Consider a general power network shown in Fig. 11.1. It is assumed that a shunt type fault occurs at point F in the system, as a result of which currents I_a, I_b, I_c flow out of the system, and V_a, V_b, V_c are voltages of lines *a, b, c* with respect to ground.

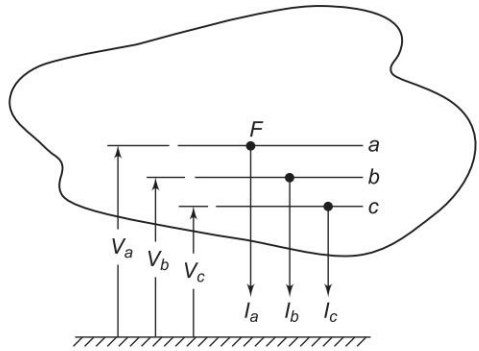

Fig. 11.1 A general power network

Let us also assume that the system is operating at no load before the occurrence of a fault. Therefore, the positive sequence voltages of all synchronous machines will be identical and will equal the prefault voltage at F. Let this voltage be labelled as E_a.

As seen from F, the power system will present positive, negative and zero sequence networks, which are schematically represented by Figs 11.2 (a), (b) and (c). The reference bus is indicated by a thick line and the point F is identified on each sequence network. Sequence voltages at F and sequence currents flowing out of the networks at F are also shown on the sequence networks. Figures 11.3 (a), (b) and (c), respectively, give the Thevenin equivalents of the three sequence networks.

Recognizing that voltage E_a is present only in the positive sequence network and that there is no coupling between sequence networks, the sequence voltages at F can be expressed in terms of sequence currents and Thevenin sequence impedances as

$$\begin{bmatrix} V_{a1} \\ V_{a2} \\ V_{a0} \end{bmatrix} = \begin{bmatrix} E_a \\ 0 \\ 0 \end{bmatrix} - \begin{bmatrix} Z_1 & 0 & 0 \\ 0 & Z_2 & 0 \\ 0 & 0 & Z_0 \end{bmatrix} \begin{bmatrix} I_{a1} \\ I_{a2} \\ I_{a0} \end{bmatrix} \tag{11.1}$$

Depending upon the type of fault, the sequence currents and voltages are constrained, leading to a particular connection of sequence networks. The

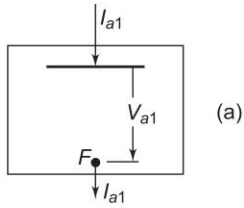

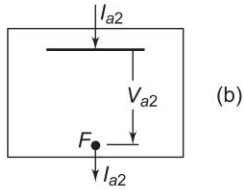

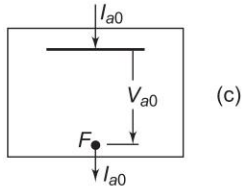

Fig. 11.2 Sequence networks as seen from the fault point *F*

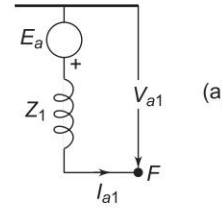

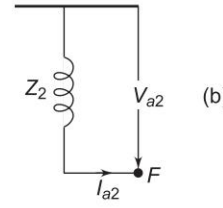

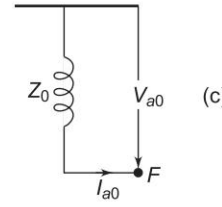

Fig. 11.3 Thevenin equivalents of the sequence networks as seen from the fault point F

sequence currents and voltages and fault currents and voltages can then be easily computed. We shall now consider the various types of faults enumerated earlier.

11.3 SINGLE LINE-TO-GROUND (LG) FAULT

Figure 11.4 shows a line-to-ground fault at *F* in a power system through a fault impedance Z^f. The phases are so labelled that the fault occurs on phase *a*.

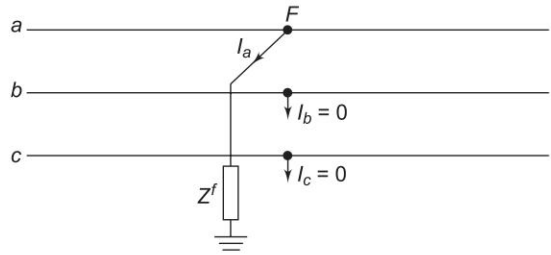

Fig. 11.4 Single line-to-ground (LG) fault at *F*

At the fault point F, the currents out of the power system and the line-to-ground voltages are constrained as follows:

$$I_b = 0 \tag{11.2}$$

$$I_c = 0 \tag{11.3}$$

$$V_a = Z^f I_a \tag{11.4}$$

The symmetrical components of the fault currents are

$$\begin{bmatrix} I_{a1} \\ I_{a2} \\ I_{a0} \end{bmatrix} = \frac{1}{3} \begin{bmatrix} 1 & \alpha & \alpha^2 \\ 1 & \alpha^2 & \alpha \\ 1 & 1 & 1 \end{bmatrix} \begin{bmatrix} I_a \\ 0 \\ 0 \end{bmatrix}$$

from which it is easy to see that

$$I_{a1} = I_{a2} = I_{a0} = \frac{1}{3} I_a \tag{11.5}$$

Expressing Eq. (11.4) in terms of symmetrical components, we have

$$V_{a1} + V_{a2} + V_{a0} = Z^f I_a = 3Z^f I_{a1} \tag{11.6}$$

As per Eqs (11.5) and (11.6) all sequence currents are equal and the sum of sequence voltages equals $3Z^f I_{a1}$. Therefore, these equations suggest a series connection of sequence networks through an impedance $3Z^f$ as shown in Figs 11.5(a) and (b).

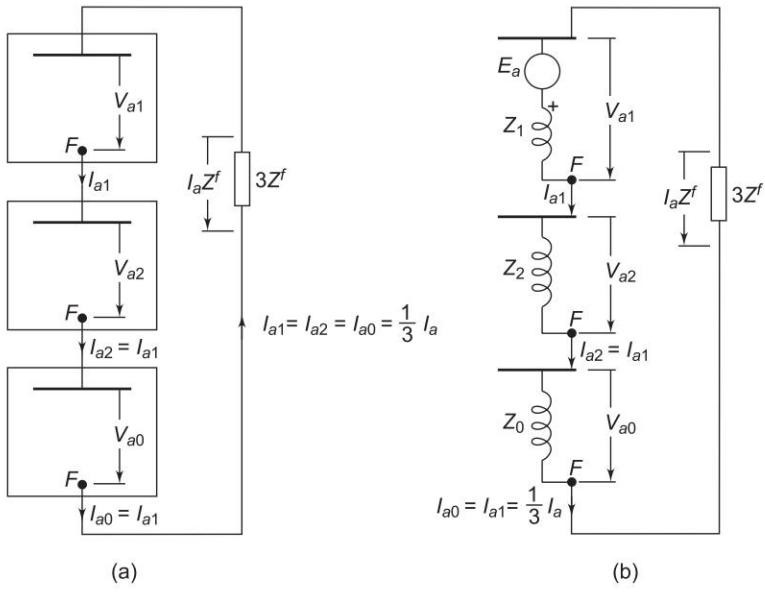

Fig. 11.5 Connection of sequence network for a single line-to-ground (LG) fault

In terms of the Thevenin equivalent of sequence networks, we can write from Fig. 11.5(b).

$$I_{a1} = \frac{E_a}{(Z_1 + Z_2 + Z_0) + 3Z^f} \tag{11.7}$$

Fault current I_a is then given by

$$I_a = 3I_{a1} = \frac{3E_a}{(Z_1 + Z_2 + Z_0) + 3Z^f} \tag{11.8}$$

The above results can also be obtained directly from Eqs (11.5) and (11.6) by using V_{a1}, V_{a2} and V_{a0} from Eq. (11.1). Thus

$$(E_a - I_{a1}Z_1) + (-I_{a2}Z_2) + (-I_{a0}Z_0) = 3Z^f I_{a1}$$

or

$$\left[(Z_1 + Z_2 + Z_0) + 3Z^f \right] I_{a1} = E_a$$

or

$$I_{a1} = \frac{E_a}{(Z_1 + Z_2 + Z_0) + 3Z^f}$$

The voltage of line b to ground under fault condition is

$$V_b = \alpha^2 V_{a1} + \alpha V_{a2} + V_{a0}$$

$$= \alpha^2 \left(E_a - Z_1 \frac{I_a}{3} \right) + \alpha \left(-Z_2 \frac{I_a}{3} \right) + \left(-Z_0 \frac{I_a}{3} \right)$$

Substituting for I_a from Eq. (11.8) and reorganizing, we get

$$V_b = E_a \frac{3\alpha^2 Z^f + Z_2(\alpha^2 - \alpha) + Z_0(\alpha^2 - 1)}{(Z_1 + Z_2 + Z_0) + 3Z^f} \tag{11.9}$$

The expression for V_c can be similarly obtained.

Fault Occurring Under Loaded Conditions

When a fault occurs under balanced load conditions, positive sequence currents alone flow in a power system before the occurrence of the fault. Therefore, negative and zero sequence networks are the same as without load. The positive sequence network must of course carry the load current. To account for load current, the synchronous machines in the positive sequence network are replaced by subtransient, transient or synchronous reactances (depending upon the time after the occurrence of fault, when currents are to be determined) and voltages behind appropriate reactances. This change does not disturb the flow of prefault positive sequence currents (see Ch. 9). This positive sequence network would then be used in the sequence network connection of Fig. 11.5(a) for computing sequence currents under fault.

In case the positive sequence network is replaced by its Thevenin equivalent as in Fig. 11.5(b), the Thevenin voltage equals the prefault voltage V_f^0 at the fault point F (under loaded conditions). The Thevenin impedance is the impedance between F and the reference bus of the passive positive sequence network (with voltage generators short circuited). This is illustrated by a two machine system in Fig. 11.6. It is seen from this figure that while the prefault currents flow in the actual positive sequence network of Fig. 11.6(a), the same do not exist in its Thevenin equivalent network of Fig. 11.6(b). Therefore, when the Thevenin equivalent of positive sequence network is used for calculating fault currents, the positive sequence currents within the network are those due to fault alone and we must superimpose on these the prefault currents. Of course, the positive sequence current into the fault is directly the correct answer, the prefault current into the fault being zero.

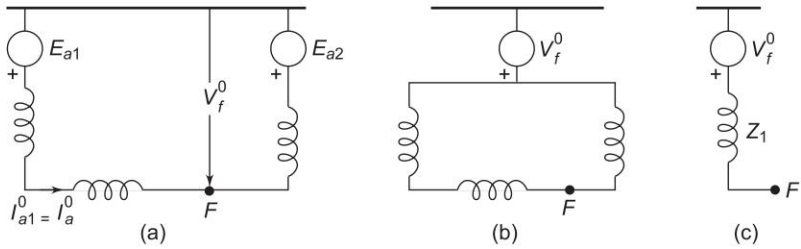

Fig. 11.6 Positive sequence network and its Thevenin equivalent before occurrence of a fault

The above remarks are valid for the positive sequence network, independent of the type of fault.

11.4 LINE-TO-LINE (LL) FAULT

Figure 11.7 shows a line-to-line fault at F in a power system on phases b and c through a fault impedance Z^f. The phases can always be relabelled, such that the fault is on phases b and c.

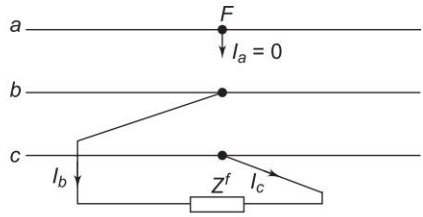

Fig. 11.7 Line-to-line (LL) fault through impedance Z^f

The currents and voltages at the fault can be expressed as

$$I_p = \begin{bmatrix} I_a = 0 \\ I_b \\ I_c = -I_b \end{bmatrix}; \; V_b - V_c = I_b Z^f \tag{11.10}$$

The symmetrical components of the fault currents are

$$\begin{bmatrix} I_{a1} \\ I_{a2} \\ I_{a0} \end{bmatrix} = \frac{1}{3} \begin{bmatrix} 1 & \alpha & \alpha^2 \\ 1 & \alpha^2 & \alpha \\ 1 & 1 & 1 \end{bmatrix} \begin{bmatrix} 0 \\ I_b \\ -I_b \end{bmatrix}$$

from which we get

$$I_{a2} = -I_{a1} \tag{11.11}$$

$$I_{a0} = 0 \tag{11.12}$$

The symmetrical components of voltages at F under fault are

$$\begin{bmatrix} V_{a1} \\ V_{a2} \\ V_{a0} \end{bmatrix} = \frac{1}{3} \begin{bmatrix} 1 & \alpha & \alpha^2 \\ 1 & \alpha^2 & \alpha \\ 1 & 1 & 1 \end{bmatrix} \begin{bmatrix} V_a \\ V_b \\ V_b - Z^f I_b \end{bmatrix} \tag{11.13}$$

Writing the first two equations, we have

$$3V_{a1} = V_a + (\alpha + \alpha^2)\, V_b - \alpha^2 Z^f I_b$$

$$3V_{a2} = V_a + (\alpha + \alpha^2)\, V_b - \alpha Z^f I_b$$

from which we get

$$3(V_{a1} - V_{a2}) = (\alpha - \alpha^2) Z^f I_b = j\sqrt{3}\; Z^f I_b \tag{11.14}$$

Now

$$I_b = (\alpha^2 - \alpha)\, I_{a1} \; (\because \; I_{a2} = -I_{a1}; \; I_{a0} = 0)$$

$$= -j\sqrt{3} I_{a1} \tag{11.15}$$

Substituting I_b from Eq. (11.15) in Eq. (11.14), we get

$$V_{a1} - V_{a2} = Z^f I_{a1} \tag{11.16}$$

Equations (11.11) and (11.16) suggest parallel connection of positive and negative sequence networks through a series impedance Z^f as shown in Figs 11.8(a) and (b). Since $I_{a0} = 0$ as per Eq. (11.12), the zero sequence network is unconnected.

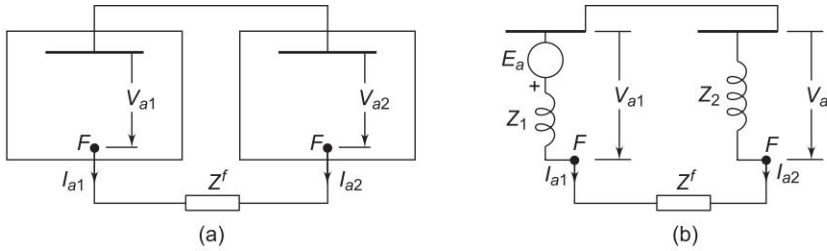

Fig. 11.8 Connection of sequence networks for a line-to-line (LL) fault

In terms of the Thevenin equivalents, we get from Fig. 11.8(b)

$$I_{a1} = \frac{E_a}{Z_1 + Z_2 + Z^f} \tag{11.17}$$

From Eq. (11.15), we get

$$I_b = -I_c = \frac{-j\sqrt{3}E_a}{Z_1 + Z_2 + Z^f} \tag{11.18}$$

Knowing I_{a1}, we can calculate V_{a1} and V_{a2} from which voltages at the fault can be found.

If the fault occurs from loaded conditions, the positive sequence network can be modified on the lines of the later portion of Sec. 11.3.

11.5 DOUBLE LINE-TO-GROUND (LLG) FAULT

Figure 11.9 shows a double line-to-ground fault at F in a power system. The fault may in general have an impedance Z^f as shown.

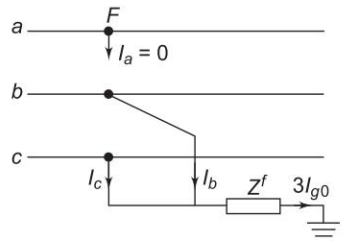

Fig. 11.9 Double line-to-ground (LLG) fault through impedance Z^f

The current and voltage (to ground) conditions at the fault are expressed as

$$\left.\begin{aligned} I_a &= 0 \\ I_{a1} + I_{a2} + I_{a0} &= 0 \end{aligned}\right\} \tag{11.19}$$

or

$$V_b = V_c = Z^f(I_b + I_c) = 3Z^f I_{a0} \tag{11.20}$$

The symmetrical components of voltages are given by

$$\begin{bmatrix} V_{a1} \\ V_{a2} \\ V_{a0} \end{bmatrix} = \frac{1}{3}\begin{bmatrix} 1 & \alpha & \alpha^2 \\ 1 & \alpha^2 & \alpha \\ 1 & 1 & 1 \end{bmatrix}\begin{bmatrix} V_a \\ V_b \\ V_b \end{bmatrix} \tag{11.21}$$

from which it follows that

$$V_{a1} = V_{a2} = \frac{1}{3}\left[\, V_a + (\alpha + \alpha^2)V_b \,\right] \tag{11.22a}$$

$$V_{a0} = \frac{1}{3}(V_a + 2V_b) \tag{11.22b}$$

From Eqs (11.22a) and (11.22b)

$$V_{a0} - V_{a1} = \frac{1}{3}(2 - \alpha - \alpha^2)\, V_b = V_b = 3Z^f I_{a0}$$

or

$$V_{a0} = V_{a1} + 3Z^f I_{a0} \tag{11.23}$$

From Eqs (11.19), (11.22a) and (11.23), we can draw the connection of sequence networks as shown in Figs 11.10(a) and (b). The reader may verify this by writing mesh and nodal equations for these figures.

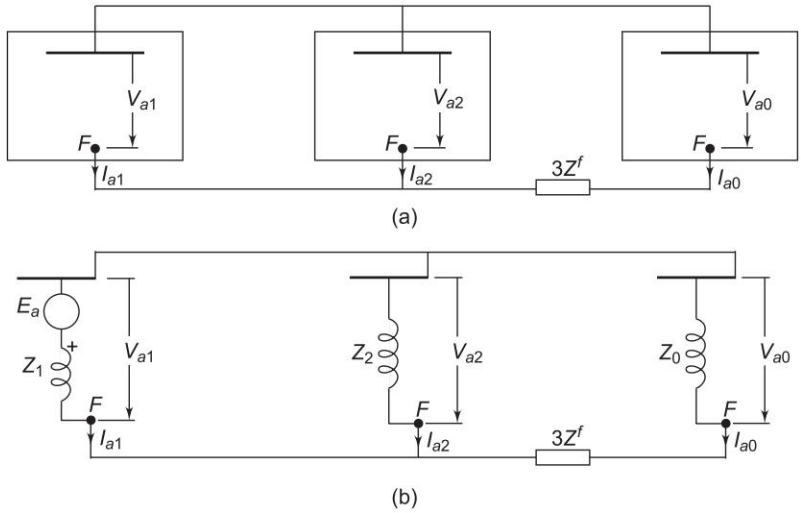

Fig. 11.10 Connection of sequence networks for a double line-to ground (LLG) fault

In terms of the Thevenin equivalents, we can write from Fig. 11.10(b)

$$I_{a1} = \frac{E_a}{Z_1 + Z_2 \,\|\, (Z_0 + 3Z^f)}$$

$$= \frac{E_a}{Z_1 + Z_2(Z_0 + 3Z^f)/(Z_2 + Z_0 + 3Z^f)} \tag{11.24}$$

The above result can be obtained analytically as follows:

Substituting for V_{a1}, V_{a2} and V_{a0} in terms of E_a in Eq. (11.1) and premultiplying both sides by Z^{-1} (inverse of sequence impedance matrix), we get

$$\begin{bmatrix} Z_1^{-1} & 0 & 0 \\ 0 & Z_2^{-1} & 0 \\ 0 & 0 & Z_0^{-1} \end{bmatrix} \begin{bmatrix} E_a - Z_1 I_{a1} \\ E_a - Z_1 I_{a1} \\ E_a - Z_1 I_{a1} + 3Z^f I_{a0} \end{bmatrix}$$

$$= \begin{bmatrix} Z_1^{-1} & 0 & 0 \\ 0 & Z_2^{-1} & 0 \\ 0 & 0 & Z_0^{-1} \end{bmatrix} \begin{bmatrix} E_a \\ 0 \\ 0 \end{bmatrix} - \begin{bmatrix} I_{a1} \\ I_{a2} \\ I_{a0} \end{bmatrix} \tag{11.25a}$$

Premultiplying both sides by row matrix [1 1 1] and using Eqs (11.19) and (11.20), we get

$$-\frac{3Z^f}{Z_0} I_{a0} + \left(1 + \frac{Z_1}{Z_0} + \frac{Z_1}{Z_2}\right) I_{a1} = \left(\frac{1}{Z_2} + \frac{1}{Z_0}\right) E_a \tag{11.25b}$$

From Eq. (11.22a), we have

$$E_a - Z_1 I_{a1} = -Z_2 I_{a2}$$

Substituting $I_{a2} = -(I_{a1} + I_{a0})$ [see Eq. (11.19)]

$$E_a - Z_1 I_{a1} = Z_2 (I_{a1} + I_{a0})$$

or

$$I_{a0} = \frac{E_a}{Z_2} - \left(\frac{Z_1 + Z_2}{Z_2}\right) I_{a1}$$

Substituting this value of I_{a0} in Eq. (11.25b) and simplifying, we finally get

$$I_{a1} = \frac{E_a}{Z_1 + Z_2(Z_0 + 3Z^f)/(Z_2 + Z_0 + 3Z^f)} \tag{11.26}$$

If the fault takes place from loaded conditions, the positive sequence network will be modified as discussed in Sec. 11.3.

Example 11.1 Figure 11.11 shows a synchronous generator whose neutral is grounded through a reactance X_n. The generator has balanced emfs and sequence reactances X_1, X_2 and X_0 such that $X_1 = X_2 \neq X_0$.

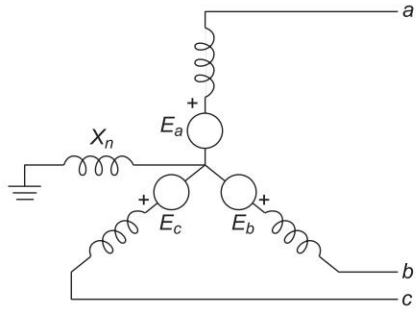

Fig. 11.11 Synchronous generator grounded through neutral reactance

(a) Draw the sequence networks of the generator as seen from the terminals.
(b) Derive expression for fault current for a solid line-to-ground fault on phase a.
(c) Show that, if the neutral is grounded solidly, the LG fault current would be more than the three-phase fault current.
(d) Write expression for neutral grounding reactance, such that the LG fault current is less than the three-phase fault current.

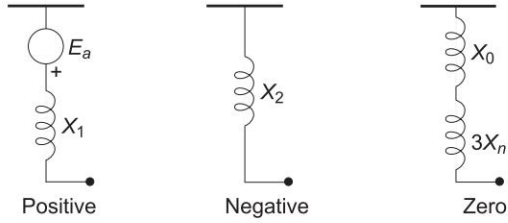

Fig. 11.12 Sequence networks of synchronous generator grounded through neutral impedance

Solution

(a) Figure 11.12 gives the sequence networks of the generator. As stated earlier voltage source is included in the positive sequence network only.

(b) Connection of sequence networks for a solid LG fault ($Z^f = 0$) is shown in Fig. 11.13, from which we can write the fault current as

$$|I_a|_{LG} = \frac{3|E_a|}{2X_1 + X_0 + 3X_n} \quad \text{(i)}$$

(c) If the neutral is solidly grounded

$$|I_a|_{LG} = \frac{3|E_a|}{2X_1 + X_0} \qquad \text{(ii)}$$

For a solid three-phase fault (see Fig. 11.14)

$$|I_a|_{3L} = \frac{|E_a|}{X_1} = \frac{3|E_a|}{3X_1} \qquad \text{(iii)}$$

Comparing (ii) and (iii), it is easy to see that

$$|I_a|_{LG} > |I_a|_{3L}$$

An important observation is made here that, when the generator neutral is solidly grounded, LG fault is more severe than a 3L fault. It is so because $X_0 \neq X_1 = X_2$ in generator. However, for a line $X_0 \neq X_1 = X_2$, so that for a fault on a line sufficiently away from generator, 3L fault will be more severe than an LG fault.

(d) With generator neutral grounded through reactance, comparing Eqs (i) and (iii), we have for LG fault current to be less than 3L fault

$$\frac{3|E_a|}{2X_1 + X_0 + 3X_n} < \frac{3|E_a|}{3X_1}$$

or

$$2X_1 + X_0 + 3X_n > 3X_1$$

or

$$X_n > \frac{1}{3}(X_1 - X_0) \qquad \text{(iv)}$$

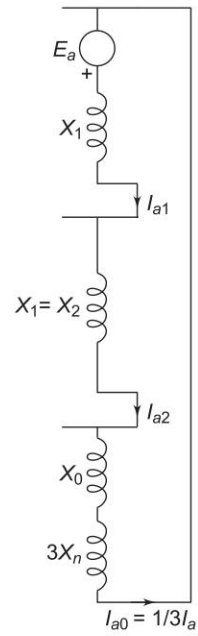

Fig. 11.13 LG fault

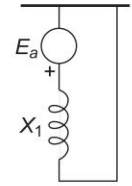

Fig. 11.14 Three-phase fault

Example 11.2 Two 11 kV, 20 MVA, three-phase, star connected generators operate in parallel as shown in Fig. 11.15; the positive, negative and zero sequence reactances of each being, respectively, *j*0.18, *j*0.15, *j*0.10 pu. The star point of one of the generators is isolated and that of the other is earthed through a 2.0 ohm resistor. A single line-to-ground fault occurs at the terminals of one of the generators. Estimate (i) the fault current, (ii) current in grounding resistor, and (iii) the voltage across grounding resistor.

Solution

(*Note*: All values are given in per unit.) Since the two identical generators operate in parallel,

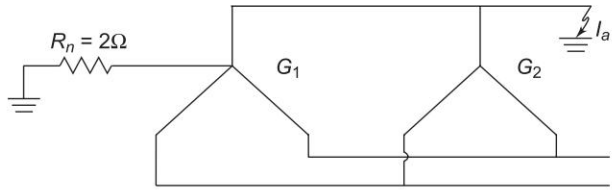

Fig. 11.15

$$X_{1eq} = \frac{j0.18}{2} = j\,0.09,\ X_{2eq} = \frac{j0.15}{2} = j0.075$$

Since the star point of the second generator is isolated, its zero sequence reactance does not come into picture. Therefore,

$$Z_{0eq} = j0.10 + 3R_n = j\,0.10 + 3 \times \frac{2 \times 20}{(11)^2} = 0.99 + j\,0.1$$

For an LG fault, using Eq. (11.8), we get

$$I_f \text{ (fault current for LG fault)} = I_a = 3I_{a1} = \frac{3E_a}{X_{1eq} + X_{2eq} + Z_{0eq}}$$

(a) $$I_f = \frac{3 \times 1}{j0.09 + j0.075 + j0.1 + 0.99} = \frac{3}{0.99 + j0.265}$$

$$= 2.827 - j0.756$$

(b) Current in the grounding resistor $= I_f = 2.827 - j0.756$

$$|I_f| = 2.926 \times \frac{20}{\sqrt{3} \times 11} = 3.07 \text{ kA}$$

(c) Voltage across grounding resistor $= \frac{40}{121}\ (2.827 - j0.756)$

$$= 0.932 - j0.249$$

$$= 0.965 \times \frac{11}{\sqrt{3}} = 6.13 \text{ kV}$$

Example 11.3 For the system of Example 10.3 the one-line diagram is redrawn in Fig. 11.16. On a base of 25 MVA and 11 kV in generator circuit, the positive, negative and zero sequence networks of the system have been drawn already in Figs 10.23, 10.24 and 10.27. Before the occurrence of a solid LG at bus *g*, the motors are loaded to draw 15 and 7.5 MW at 10 kV, 0.8 leading power factor. If prefault current is neglected, calculate the fault current and subtransient current in all parts of the system.

What voltages behind subtransient reactances must be used in a positive sequence network if prefault current is to be accounted for?

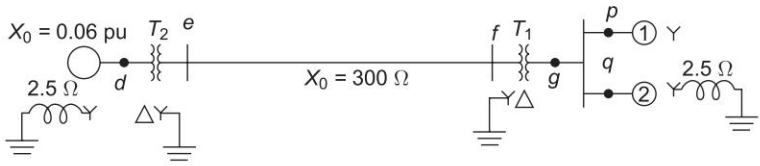

Fig. 11.16 One-line diagram of the system of Example 11.3

Solution

The sequence networks given in Figs 10.23, 10.24 and 10.27 are connected in Fig. 11.17 to simulate a solid LG fault at bus *g* (see Fig. 11.16). If prefault currents are neglected,

$$E_g'' = E_{m1}'' = E_{m2}'' = V_f^0 \text{ (prefault voltage at } g)$$

$$= \frac{10}{11} = 0.909 \text{ pu}$$

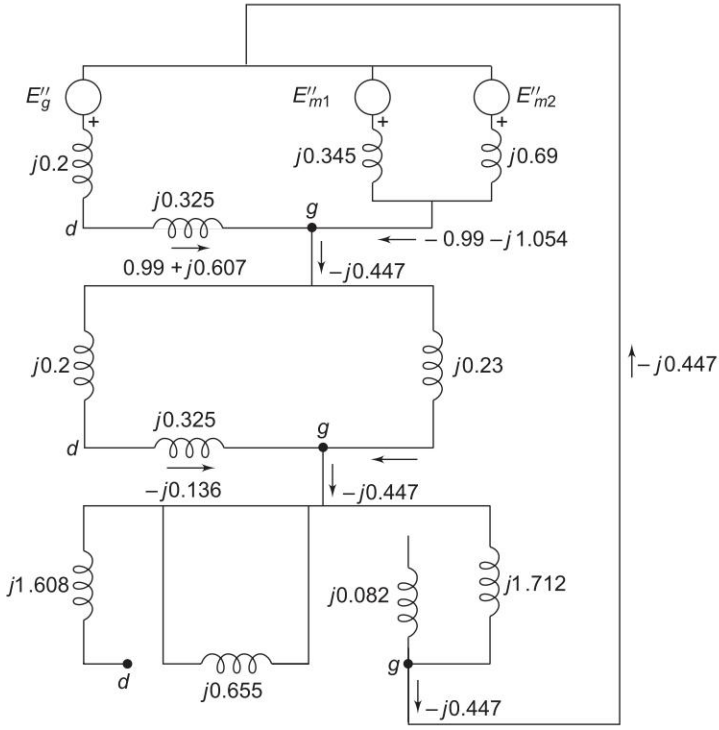

Fig. 11.17 Connection of the sequence networks of Example 11.3. Subtransient currents are shown on the diagram in pu for a solid line-to-ground fault at *g*

The positive sequence network can now be easily replaced by its Thevenin equivalent as shown in Fig. 11.18.

Now

$$Z_1 = \frac{j0.525 \times j0.23}{j0.755} = j0.16 \text{ pu}$$

$$Z_2 = Z_1 = j0.16 \text{ pu}$$

From the sequence network connection

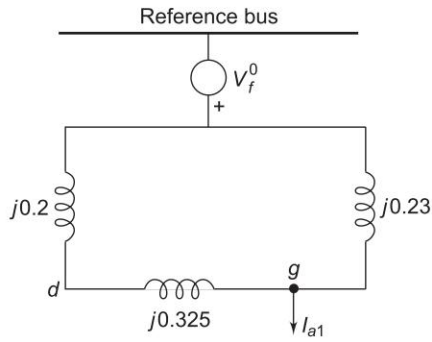

Fig. 11.18

$$I_{a1} = \frac{V_f^0}{Z_1 + Z_2 + Z_0}$$

$$= \frac{0.909}{j2.032} = -j0.447 \text{ pu}$$

$$I_{a2} = I_{a0} = I_{a1} = -j0.447 \text{ pu}$$

Fault current $= 3I_{a0} = 3 \times (-j0.447) = -j1.341$ pu

The component of I_{a1} flowing towards g from the generator side is

$$-j0.447 \times \frac{j0.23}{j0.755} = -j0.136 \text{ pu}$$

and its component flowing towards g from the motors side is

$$-j0.447 \times \frac{j0.525}{j0.755} = -j0.311 \text{ pu}$$

Similarly, the component of I_{a2} from the generator side is $-j0.136$ pu and its component from the motors side is $-j0.311$. All of I_{a0} flows towards g from motor 2.

Fault currents from the generator towards g are

$$\begin{bmatrix} I_a \\ I_b \\ I_c \end{bmatrix} = \begin{bmatrix} 1 & 1 & 1 \\ \alpha^2 & \alpha & 1 \\ \alpha & \alpha^2 & 1 \end{bmatrix} \begin{bmatrix} -j0.136 \\ -j0.136 \\ 0 \end{bmatrix} = \begin{bmatrix} -j0.272 \\ j0.136 \\ j0.136 \end{bmatrix} \text{pu}$$

and to g from the motors are

$$\begin{bmatrix} I_a \\ I_b \\ I_c \end{bmatrix} = \begin{bmatrix} 1 & 1 & 1 \\ \alpha^2 & \alpha & 1 \\ \alpha & \alpha^2 & 1 \end{bmatrix} \begin{bmatrix} -j0.311 \\ -j0.311 \\ -j0.447 \end{bmatrix} = \begin{bmatrix} -j1.069 \\ -j0.136 \\ -j0.136 \end{bmatrix} \text{pu}$$

The positive and negative sequence components of the transmission line currents are shifted –90° and +90°, respectively, from the corresponding components on the generator side to T_2, i.e.

Positive sequence current $= -j(-j0.136) = -0.136$ pu

Negative sequence current $= j(-j0.136) = 0.136$ pu

Zero sequence current $= 0$ ($\because$ there are no zero sequence currents on the transmission line, see Fig. 11.17)

$\therefore$ Line a current on the transmission line $= -0.136 + 0.136 + 0 = 0$

I_b and I_c can be similarly calculated.

Let us now calculate the voltages behind subtransient reactances to be used if the load currents are accounted for. The per unit motor currents are:

$$\text{Motor 1: } \frac{15}{25 \times 0.909 \times 0.8} \angle 36.86^\circ = 0.825 \angle 36.86^\circ = 0.66 + j0.495 \text{ pu}$$

$$\text{Motor 2: } \frac{7.5}{25 \times 0.909 \times 0.8} \angle 36.86^\circ = 0.4125 \angle 36.86^\circ = 0.33 + j0.248 \text{ pu}$$

Total current drawn by both motors $= 0.99 + j0.743$ pu

The voltages behind subtransient reactances are calculated below:

Motor 1: $E''_{m1} = 0.909 - j0.345 \times 0.825 \angle 36.86^\circ$

$= 1.08 - j0.228 = 1.104 \angle -11.92^\circ$ pu

Motor 2: $E''_{m2} = 0.909 - j0.69 \times 0.4125 \angle 36.86^\circ$

$= 1.08 - j0.228 = 1.104 \angle -11.92^\circ$ pu

Generator: $E''_g = 0.909 + j0.525 \times 1.2375 \angle 36.86^\circ$

$= 0.52 + j0.52 = 0.735 \angle 45^\circ$ pu

It may be noted that with these voltages behind subtransient reactances, the Thevenin equivalent circuit will still be the same as that of Fig. 11.18. Therefore, in calculating fault currents taking into account prefault loading condition, we need not calculate E''_{m1}, E''_{m2} and E''_g. Using the Thevenin equivalent approach, we can first calculate currents caused by fault to which the load currents can then be added.

Thus, the actual value of positive sequence current from the generator towards the fault is

$$0.99 + j0.743 - j0.136 = 0.99 + j0.607$$

and the actual value of positive sequence current from the motors to the fault is

$$-0.99 - j0.743 - j0.311 = -0.99 - j1.054$$

In this problem, because of large zero sequence reactance, load current is comparable with (in fact, more than) the fault current. In a large practical system, however, the reverse will be the case, so that it is normal practice to neglect load current without causing an appreciable error.

Example 11.4 For Example 11.2, assume that the grounded generator is solidly grounded. Find the fault current and voltage of the healthy phase for a line-to-line fault on terminals of the generators. Assume solid fault ($Z^f = 0$).

Solution

For the LL fault, using Eq. (11.17) and substituting the values of X_{1eq} and X_{2eq} from Example 11.2, we get

$$I_{a1} = \frac{E_a}{X_{1eq} + X_{2eq}} = \frac{1}{j0.09 + j0.075} = -j6.06$$

Using Eq. (11.15), we have

$$I_f \text{ (fault current)} = I_b = -j\sqrt{3}I_{a1} = (-j\sqrt{3})(-j6.06) = -10.496$$

Now

$$V_{a1} = V_{a2} = E_a - I_{a1}X_{1eq} = 1.0 - (-j6.06)\,(j0.09)$$
$$= 0.455$$
$$V_{a0} = -I_{a0}Z_0 = 0 \quad (\because \quad I_{a0} = 0)$$

Voltage of the healthy phase,

$$V_a = V_{a1} + V_{a2} + V_{a0} = 0.91$$

Example 11.5 For Example 11.2, assume that the grounded generator is solidly grounded. Find the fault current in each phase and voltage of the healthy phase for a double line-to-ground fault on terminals of the generator. Assume solid fault ($Z^f = 0$).

Solution

Using Eq. (11.24) and substituting the values of Z_{1eq}, Z_{2eq} and Z_{0eq} from Example 11.2, we get (note $Z^f = 0$, $Z_{0eq} = j0.1$)

$$I_{a1} = \frac{1 + j0}{j0.09 + \dfrac{j0.075 \times j0.10}{j0.075 + j0.10}} = -j7.53$$

$$V_{a1} = V_{a2} = V_{a0} = E_a - I_{a1}\,Z_{1eq} = 1 - (-j7.53)\,(j0.09)$$
$$= 0.323$$

$$I_{a2} = -\frac{V_{a2}}{Z_{2eq}} = -\frac{0.323}{j0.075} = j4.306$$

$$I_{a0} = -\frac{V_{a0}}{Z_{0eq}} = -\frac{0.323}{j0.10} = j3.23$$

Now

$$I_b = \alpha^2 I_{a1} + \alpha I_{a2} + I_{a0}$$
$$= (-0.5 - j0.866)\,(-j7.53) + (-0.5 + j0.866)\,(j4.306) + j3.23$$
$$= -10.248 + j4.842 = 11.334 \angle 154.74°$$
$$I_c = \alpha I_{a1} + \alpha^2 I_{a2} + I_{a0}$$

$$= (-0.5 + j0.866)(-j7.53) + (-0.5 - j0.866)(j4.306) + j3.23$$
$$= 10.248 + j4.842 = 11.334\angle 25.28^\circ$$

Voltage of the healthy phase,

$$V_a = 3V_{a1} = 3 \times 0.323 = 0.969$$

11.6 OPEN CONDUCTOR FAULTS

An open conductor fault is in series with the line. Line currents and series voltages between broken ends of the conductors are required to be determined.

Figure 11.19 shows currents and voltages in an open conductor fault. The ends of the system on the sides of the fault are identified as F, F', while the conductor ends are identified as aa', bb' and cc'. The set of series currents and voltages at the fault are

$$I_p = \begin{bmatrix} I_a \\ I_b \\ I_c \end{bmatrix};\ V_p = \begin{bmatrix} V_{aa'} \\ V_{bb'} \\ V_{cc'} \end{bmatrix}$$

The symmetrical components of currents and voltages are

$$I_s = \begin{bmatrix} I_{a1} \\ I_{a2} \\ I_{a0} \end{bmatrix};\ V_s = \begin{bmatrix} V_{aa'1} \\ V_{aa'2} \\ V_{aa'0} \end{bmatrix}$$

The sequence networks can be drawn for the power system as seen from FF' and are schematically shown in Fig. 11.20. These are to be suitably connected depending on the type of fault (one or two conductors open).

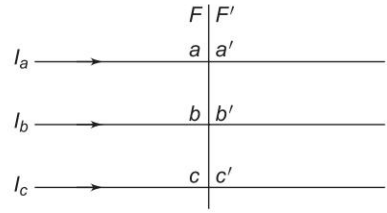

Fig. 11.19 Currents and voltages in open conductor fault

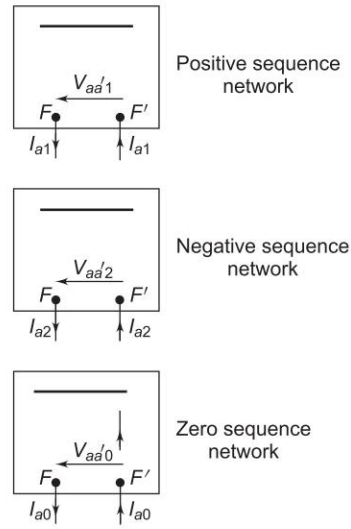

Fig. 11.20 Sequence networks for open conductor fault at FF'

Two Conductors Open

Figure 11.21 represents the fault at FF' with conductors b and c open. The currents and voltages due to this fault are expressed as

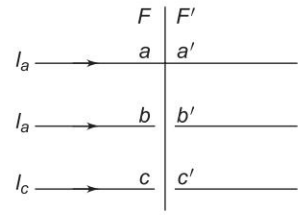

Fig 11.21 Two conductors open

$$V_{aa'} = 0 \qquad (11.27)$$

$$I_b = I_c = 0 \qquad (11.28)$$

In terms of symmetrical components, we can write

$$V_{aa'1} + V_{aa'2} + V_{aa'0} = 0 \qquad (11.29)$$

$$I_{a1} = I_{a2} = I_{a0} = \frac{1}{3} I_a \qquad (11.30)$$

Equations (11.29) and (11.30) suggest a series connection of sequence networks as shown in Fig. 11.22. Sequence currents and voltages can now be computed.

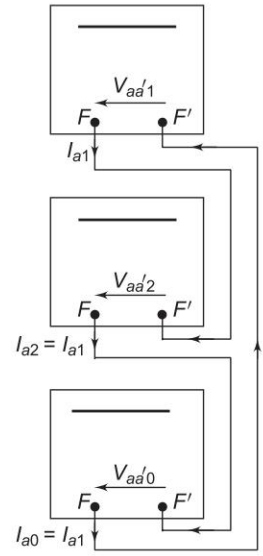

Fig. 11.22 Connection of sequence networks for two conductors open

One Conductor Open

For one conductor open as in Fig. 11.23, the circuit conditions require

$$V_{bb'} = V_{cc'} = 0 \qquad (11.31)$$

$$I_a = 0 \qquad (11.32)$$

In terms of symmetrical components these conditions can be expressed as

$$V_{aa'1} = V_{aa'2} = V_{aa'0} = \frac{1}{3} V_{aa'} \qquad (11.33)$$

$$I_{a1} + I_{a2} + I_{a0} = 0 \qquad (11.34)$$

Equations (11.33) and (11.34) suggest a parallel connection of sequence networks as shown in Fig. 11.24.

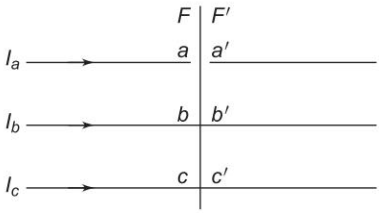

Fig. 11.23 One conductor open

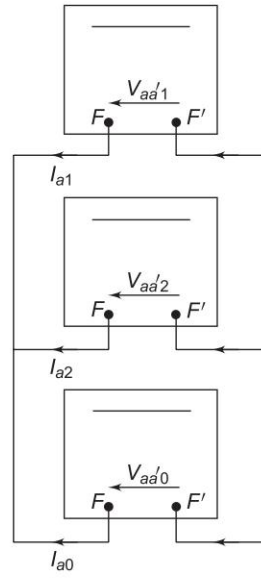

Fig. 11.24 Connection of sequence networks for one conductor open

11.7 BUS IMPEDANCE MATRIX METHOD FOR ANALYSIS OF UNSYMMETRICAL SHUNT FAULTS

Bus impedance method of fault analysis, given for symmetrical faults in Ch. 9, can be easily extended to the case of unsymmetrical faults. Consider for example an LG fault on the rth bus of a n-bus system. The connection of sequence networks to simulate the fault is shown in Fig. 11.25. The positive sequence network has been replaced here by its Thevenin equivalent, i.e. prefault voltage V_{1-r}^0 of bus r in series with the passive positive sequence network (all voltage sources short circuited). Since negative and zero sequence prefault voltages are zero, both these are passive networks only.

It may be noted that subscript a has been dropped in sequence currents and voltages, while integer subscript is introduced for bus identification. Superscripts 0 and f respectively, indicate prefault and postfault values.

For the passive positive sequence network

$$\boldsymbol{V}_{1\text{–BUS}} = \boldsymbol{Z}_{1\text{–BUS}}\, \boldsymbol{J}_{1\text{–BUS}} \tag{11.35}$$

where

$$\boldsymbol{V}_{1\text{–BUS}} = \begin{bmatrix} V_{1-1} \\ V_{1-2} \\ \vdots \\ V_{1-n} \end{bmatrix} = \text{positive sequence bus voltage vector} \tag{11.36}$$

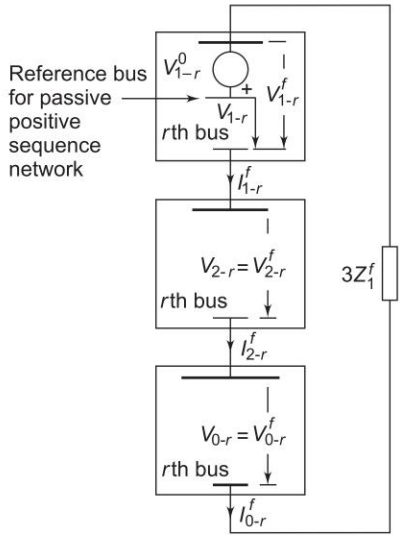

Fig. 11.25 Connection of sequence networks for LG fault on the r th bus (positive sequence network represented by its Thevenin equivalent)

$$\boldsymbol{Z}_{1\text{–BUS}} = \begin{bmatrix} Z_{1-11} & \cdots & Z_{1-1n} \\ \vdots & & \vdots \\ Z_{1-n1} & \cdots & Z_{1-nn} \end{bmatrix} = \text{postive sequence bus impedance matrix} \tag{11.37}$$

and

$$\boldsymbol{J}_{1\text{–BUS}} = \begin{bmatrix} J_{1-1} \\ J_{1-2} \\ \vdots \\ J_{1-n} \end{bmatrix} = \text{positive sequence bus current injection vector} \tag{11.38}$$

As per the sequence network connection, current $-I^f_{1-r}$ is injected only at the faulted rth bus of the positive sequence network, we have therefore

$$\boldsymbol{J}_{1\text{–BUS}} = \begin{bmatrix} 0 \\ 0 \\ \vdots \\ -I^f_{1-r} \\ \vdots \\ 0 \end{bmatrix} \tag{11.39}$$

Substituting Eq. (11.39) in Eq. (11.35), we can write the positive sequence voltage at the rth bus of the passive positive sequence network as

$$\boldsymbol{V}_{1-r} = -\boldsymbol{Z}_{1-rr}\boldsymbol{I}^f_{1-r} \tag{11.40}$$

Thus, the passive positive sequence network presents an impedance $\boldsymbol{Z}_{1-rr}$ to the positive sequence current $\boldsymbol{I}^f_{1-r}$.

For the negative sequence network

$$\boldsymbol{V}_{2-\text{BUS}} = \boldsymbol{Z}_{2-\text{BUS}}\boldsymbol{J}_{2\text{–BUS}} \tag{11.41}$$

The negative sequence network is injected with current $\boldsymbol{I}^f_{2-r}$ at the rth bus only. Therefore,

$$\boldsymbol{J}_{2\text{–BUS}} = \begin{bmatrix} 0 \\ 0 \\ \vdots \\ -I^f_{2-r} \\ \vdots \\ 0 \end{bmatrix} \tag{11.42}$$

The negative sequence voltage at the rth bus is then given by

$$\boldsymbol{V}_{2-r} = -\boldsymbol{Z}_{2-rr}\boldsymbol{I}^f_{2-r} \tag{11.43}$$

Thus, the negative sequence network offers an impedance $\boldsymbol{Z}_{2-rr}$ to the negative sequence current $\boldsymbol{I}^f_{2-r}$

Similarly, for the zero sequence network

$$\boldsymbol{V}_{0\text{–BUS}} = \boldsymbol{Z}_{0\text{–BUS}}\,\boldsymbol{J}_{0\text{–BUS}} \tag{11.44}$$

$$\boldsymbol{J}_{0\text{–BUS}} = \begin{bmatrix} 0 \\ 0 \\ \vdots \\ -I^f_{0-r} \\ \vdots \\ 0 \end{bmatrix} \tag{11.45}$$

and

$$\boldsymbol{V}_{0-r} = -\boldsymbol{Z}_{0-rr}\boldsymbol{I}^f_{0-rr} \tag{11.46}$$

That is, the zero sequence network offers an impedance $\boldsymbol{Z}_{0-rr}$ to the zero sequence current $\boldsymbol{I}^f_{0-r}$.

From the sequence network connection of Fig. 11.25, we can now write

$$I^f_{1-r} = I^f_{2-r} = I^f_{0-r} = \frac{V^0_{1-r}}{Z_{1-rr} + Z_{2-rr} + Z_{0-rr} + 3Z^f} \tag{11.47}$$

Sequence currents for other types of faults can be similarly computed using Z_{1-rr}, Z_{2-rr} and Z_{0-rr} in place of Z_1, Z_2 and Z_0 in Eqs (11.7), (11.17) and (11.24) with $E_a = V^0_{1-r}$.

Postfault sequence voltages at any bus can now be computed by superposing on prefault bus voltage, the voltage developed owing to the injection of appropriate sequence current at bus r.

For passive positive sequence network, the voltage developed at bus i owing to the injection of $-I^f_{1-r}$ at bus r is

$$V_{1-i} = -Z_{1-ir}I^f_{1-r} \tag{11.48}$$

Hence postfault positive sequence voltage at bus i is given by

$$V^f_{1-i} = V^0_{1-i} - Z_{1-ir}I^f_{1-r}; \quad i = 1, 2, ..., n \tag{11.49}$$

where

V^0_{1-i} = prefault positive sequence voltage at bus i

Z_{1-ir} = ir th component of $Z_{1\text{–BUS}}$

Since the prefault negative sequence bus voltages are zero, the postfault negative sequence bus voltages are given by

$$\begin{aligned} V^f_{2-i} &= 0 + V_{2-i} \\ &= -Z_{2-ir}I^f_{2-r} \end{aligned} \tag{11.50}$$

where

Z_{2-ir} = ir th component of $Z_{2\text{–BUS}}$

Similarly, the postfault zero sequence bus voltages are given by

$$V_{0-i}^{f} = -Z_{0-ir} I_{0-r}^{f}; \quad i = 1, 2, ..., n \tag{11.51}$$

where

$Z_{0-ir} = ir$th component of $Z_{0\text{–BUS}}$

With postfault sequence voltages known at the buses, sequence currents in lines can be computed as:

For line uv, having sequence admittances y_{1-uv}, y_{2-uv} and y_{0-uv}

$$\begin{aligned} I_{1-uv}^{f} &= y_{1-uv} (V_{1-u}^{f} - V_{1-v}^{f}) \\ I_{2-uv}^{f} &= y_{2-uv} (V_{2-u}^{f} - V_{2-v}^{f}) \\ I_{0-uv}^{f} &= y_{0-uv} (V_{0-u}^{f} - V_{0-v}^{f}) \end{aligned} \tag{11.52}$$

Knowing sequence voltages and currents, phase voltages and currents can be easily computed by the use of the symmetrical component transformation

$$\boldsymbol{V_p} = \boldsymbol{A V_s}$$

$$\boldsymbol{I_p} = \boldsymbol{A I_s}$$

It appears at first, as if this method is more laborious than computing fault currents from Thevenin impedances of the sequence networks, as it requires computation of bus impedance matrices of all the three sequence networks. It must, however, be pointed out here that once the bus impedance matrices have been assembled, fault analysis can be conveniently carried out for all the buses, which, in fact, is the aim of a fault study. Moreover, bus impedance matrices can be easily modified to account for changes in power network configuration.

Example 11.6 For Example 10.3, positive, negative and zero sequence networks have been drawn in Figs 10.23, 10.24 and 10.27. Using the bus impedance method of fault analysis, find fault currents for a solid LG fault at (i) bus *e* and (ii) bus *f*. Also find bus voltages and line currents in case (i). Assume the prefault currents to be zero and the prefault voltages to be 1 pu.

Solution

Figure 11.26 shows the connection of the sequence networks of Figs 10.23, 10.24 and 10.27 for a solid LG fault at bus *e*.

Refer to Fig. 11.26 to find the elements of the bus admittance matrices of the three sequence networks, as follows:

$$Y_{1-dd} = \frac{1}{j0.2} + \frac{1}{j0.0805} = -j17.422$$

$$Y_{1-fg} = Y_{1-de} = \frac{-1}{j0.0805} = j12.422$$

$$Y_{1-ff} = Y_{1-ee} = \frac{1}{j0.0805} + \frac{1}{j0.164} = -j18.519$$

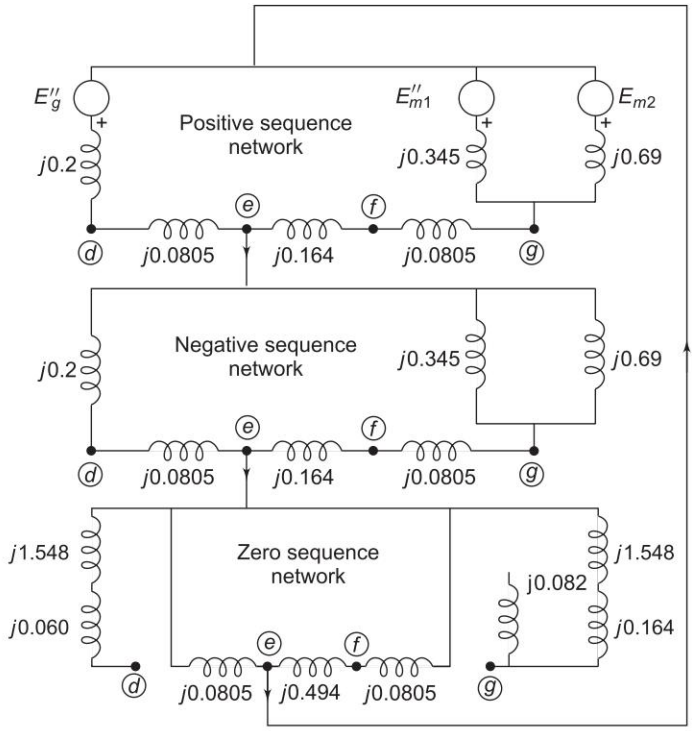

Fig. 11.26 Connection of the sequence networks of Example 11.6 for an LG fault at bus *e*

$$Y_{1-ef} = \frac{-1}{j0.164} = j6.097$$

$$Y_{1-gg} = \frac{1}{j0.085} + \frac{1}{j0.345} + \frac{1}{j0.69} = -j16.769$$

$$Y_{1-\text{BUS}} = Y_{2-\text{BUS}} = j \begin{array}{c} \\ d \\ e \\ f \\ g \end{array} \begin{array}{c} \begin{array}{cccc} d & e & f & g \end{array} \\ \begin{bmatrix} -17.422 & 12.422 & 0 & 0 \\ 12.422 & -18.519 & 6.097 & 0 \\ 0 & 6.097 & -18.519 & 12.422 \\ 0 & 0 & 12.422 & -16.769 \end{bmatrix} \end{array}$$

$$Y_{0-dd} = \frac{1}{j1.608} = -j0.621$$

$$Y_{0-ee} = Y_{0-ff} = \frac{1}{j0.0805} + \frac{1}{j0.494} = -j14.446$$

$$Y_{0-gg} = \frac{1}{j1.712} = -j0.584$$

$$Y_{0-de} = 0.0$$

$$Y_{0-ef} = \frac{-1}{j0.494} = j2.024$$

$$Y_{0-fg} = 0.0$$

$$Y_{0\text{–BUS}} = j\begin{array}{c} \\ d \\ e \\ f \\ g \end{array}\begin{array}{c} \begin{array}{cccc} d & e & f & g \end{array} \\ \begin{bmatrix} -0.621 & 0 & 0 & 0 \\ 0 & -14.446 & 2.024 & 0 \\ 0 & 2.024 & -14.446 & 0 \\ 0 & 0 & 0 & -0.584 \end{bmatrix} \end{array}$$

Inverting the three matrices above renders the following three bus impedance matrices

$$Z_{1\text{–BUS}} = Z_{2\text{–BUS}} = j\begin{bmatrix} 0.14706 & 0.12575 & 0.08233 & 0.06102 \\ 0.12575 & 0.17636 & 0.11547 & 0.08558 \\ 0.08233 & 0.11547 & 0.18299 & 0.13563 \\ 0.06102 & 0.08558 & 0.13563 & 0.16019 \end{bmatrix}$$

$$Z_{0\text{–BUS}} = j\begin{bmatrix} 1.61031 & 0 & 0 & 0 \\ 0 & 0.07061 & 0.00989 & 0 \\ 0 & 0.00989 & 0.07061 & 0 \\ 0 & 0 & 0 & 1.71233 \end{bmatrix}$$

The fault current with LG fault on bus e is

$$I_e^f = \frac{3 \times 1}{j0.17636 + j0.17636 + j0.07061} = -j7.086 \text{ pu} \qquad \text{(i)}$$

The fault current with LG fault on bus f is

$$I_f^f = \frac{3 \times 1}{j0.18299 + j0.18299 + j0.07061} = \frac{3}{j0.43659}$$

$$= -j6.871 \text{ pu} \qquad \text{(ii)}$$

Bus voltages and line currents in case (i) can easily be computed using Eqs (11.49)–(11.52). Given below is a sample calculation for computing voltage at bus f and current in line ef.

From Eq. (11.49)

$$V_{1-d}^f = V_{1-d}^0 - Z_{1-de} - I_{1-e}^f$$

$$= 1.0 - j0.12575\left(-j\frac{7.086}{3}\right) = 0.703 \text{ pu}$$

$$V_{1-f}^f = V_{1-f}^0 - Z_{1-fe} - I_{1-e}^f$$

$$= 1.0 - j0.11547\left(-j\frac{7.086}{3}\right) = 0.728 \text{ pu}$$

$$V^f_{1-e} = V^0{}_{1-e} - Z_{1-ee} - I^f_{1-e}$$
$$= 1.0 - j0.17638\ (-j2.363) = 0.584 \text{ pu}$$
$$V^f_{1-g} = V^0_{1-g} - Z_{1-ge} - I^f_{1-e}$$
$$= 1.0 - j0.08558\ (-j2.363) = 0.798 \text{ pu}$$
$$V^f_{2-f} = -Z_{2-fe} I^f_{2-e}$$
$$= -j0.11547 \times (-j2.362) = -0.272 \text{ pu}$$
$$V^f_{0-f} = -Z_{0-fe} I^f_{0-e} = -j0.00989 \times (-j2.362)$$
$$= -0.023 \text{ pu}$$
$$V^f{}_{2-e} = -Z_{2-ee} I^f{}_{2-e} = -j0.17636 \times (-j2.362)$$
$$= -0.417 \text{ pu}$$
$$V^f_{0-e} = -Z_{0-ee} I^{\mathrm{f}}_{0-e} = -j0.0706 \times (-j2.362)$$
$$= -0.167 \text{ pu}$$
$$V^f_{2-g} = -Z_{2-ge} I^f_{2-e} = -j0.08558 \times (-j2.362)$$
$$= -0.202 \text{ pu}$$
$$V^f_{0-g} = -Z_{0-ge} I^f_{0-e} = 0$$

Using Eq. (11.52), the currents in various parts of Fig. 11.26 can be computed as follows:

$$I^f_{1-fe} = y_{1-fe}\,(V^f_{1-f} - V^f_{1-fe})$$
$$= -j6.097\ (0.728 - 0.584)$$
$$= -j0.88$$
$$I^f_{1-de} = y_{1-de}\,(V^f_{1-d} - V^f_{1-e})$$
$$= -j12.422\ (0.703 - 0.584) = -j1.482$$
$$\therefore \quad I_{a1} = I^f_{1-fe} + I^f_{1-de} = -j0.88 + (-j1.482)$$
$$= -j2.362$$

which is the same as obtained earlier [see Eq. (i)] where $I^f_e = 3I_{a1}$.

$$I^f_{1-gf} = y_{1-gf}\,(V^f_{1-g} - V^f_{1-f})$$
$$= j12.422\ (-0.798 - 0.728) = -j0.88$$

Notice that as per Fig. 11.26, it was required to be the same as I^f_{1-fe}.

$$I_{2-fe} = y_{2-fe}\,(V^f_{2-f} - V^f_{2-e})$$
$$= -j6.097\ (-0.272 + 0.417) = -j0.884$$
$$I^f_{0-fe} = y_{0-fe}\,(V^f_{0-f} - V^f_{0-e})$$

$$= -j2.024\ (-0.023 + 0.167) = -j0.291 \text{ pu}$$

$$\therefore \quad I_{fe}^{f}\ (a) = I_{1-fe}^{f} + I_{2-fe}^{f} + I_{0-fe}^{f}$$

$$= -j0.88 + (-j0.88) + (-j0.291)$$

$$= -j2.05$$

Similarly, other currents can be computed.

Example 11.7 A single line-to-ground fault (on phase *a*) occurs on the bus 1 of the system of Fig. 11.27. Find

Fig. 11.27

(a) Current in the fault.
(b) SC current on the transmission line in all the three phases.
(c) SC current in phase *a* of the generator.
(d) Voltage of the healthy phases of the bus 1.

Given: Rating of each machine 1200 kVA, 600 V with $X' = X_2 = 10\%$, $X_0 = 5\%$. Each three-phase transformer is rated 1200 kVA, 600 V – Δ/3300 V–*Y* with leakage reactance of 5%. The reactances of the transmission line are $X_1 = X_2 = 20\%$ and $X_0 = 40\%$ on a base of 1200 kVA, 3300 V. The reactances of the neutral grounding reactors are 5% on the kVA and voltage base of the machine.

Note: Use Z_{BUS} method.

Solution

Figure 11.28 shows the passive positive sequence network of the system of Fig.11.27. This also represents the negative sequence network for the system. Bus impedance matrices are computed below:

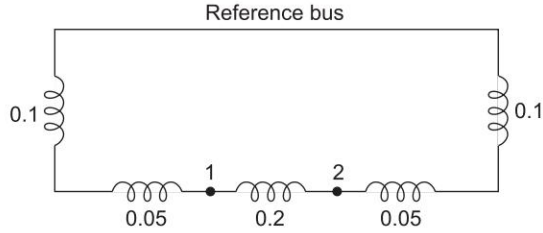

Fig. 11.28

Bus 1 to reference bus

$$Z_{1\text{–BUS}} = j[0.15]$$

Bus 2 to Bus 1

$$Z_{1\text{–BUS}} = j\begin{bmatrix} 0.15 & 0.15 \\ 0.15 & 0.35 \end{bmatrix}$$

Bus 2 to reference bus

$$Z_{1\text{–BUS}} = j\begin{bmatrix} 0.15 & 0.15 \\ 0.15 & 0.35 \end{bmatrix} - \frac{j}{0.35 + 0.15}\begin{bmatrix} 0.15 \\ 0.35 \end{bmatrix}[0.15 \quad 0.35]$$

or

$$Z_{1\text{–BUS}} = j\begin{bmatrix} 0.105 & 0.045 \\ 0.045 & 0.105 \end{bmatrix} = Z_{2\text{–BUS}} \qquad \text{(i)}$$

Zero sequence network of the system is drawn in Fig. 11.29 and its bus impedance matrix is computed below:

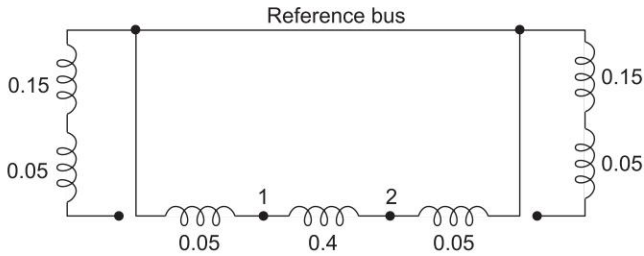

Fig. 11.29

Bus 1 to reference bus

$$Z_{0\text{–BUS}} = j[0.05]$$

Bus 2 to bus 1

$$Z_{0\text{–BUS}} = j\begin{bmatrix} 0.05 & 0.05 \\ 0.05 & 0.45 \end{bmatrix}$$

Bus 2 to reference bus

$$Z_{0\text{–BUS}} = j\begin{bmatrix} 0.05 & 0.05 \\ 0.05 & 0.45 \end{bmatrix} - \frac{j}{0.45 + 0.05}\begin{bmatrix} 0.05 \\ 0.45 \end{bmatrix}[0.05 \quad 0.45]$$

or

$$Z_{0\text{–BUS}} = j\begin{matrix} 1 \\ 2 \end{matrix}\begin{bmatrix} 0.045 & 0.005 \\ 0.005 & 0.045 \end{bmatrix} \qquad \text{(ii)}$$

As per Eq. (11.47)

$$I^f_{1-1} = \frac{V_1^0}{Z_{1\text{–}11} + Z_{2\text{–}11} + Z_{0-11} + 3Z^f}$$

But

$$V_1^0 = 1 \text{ pu (system unloaded before fault)}$$

Then

$$I_{1-1}^f = \frac{-j1.0}{0.105 + 0.105 + 0.045} = -j3.92 \text{ pu}$$

$$I_{1-1}^f = I_{2-1}^f = I_{a-1}^f = -j3.92 \text{ pu}$$

(a) Fault current, $I_1^f = 3I_{1-1}^f = -j11.7$ pu

(b) $V_{1-1}^f = V_{1-1}^0 = Z_{1-11}\, I_{1-1}^f$

$= 1.0 - j\,0.105 \times -j3.92 = 0.588$; $V_{1-1}^0 = 1$ pu

$V_{1-2}^f = V_{1-2}^0 - Z_{1-21} I_{2-1}^f$; $V_{1-2}^0 = 1.0$ (system unloaded before fault)

$= 1.0 - j0.045 \times -j\,3.92 = 0.824$

$V_{2-1}^f = -Z_{2-11} I_{2-1}^f$

$= -j\,0.105 \times -j\,3.92 = 0.412$

$V_{2-2}^f = -Z_{2-21}\, I_{2-1}^f$

$= -j\,0.045 \times -j3.92 = -0.176$

$V_{0-1}^f = -Z_{0-11} I_{0-1}^f$

$= -j\,0.045 \times -j3.92 = -0.176$

$V_{0-2}^f = -Z_{0-21}\, I_{0-1}^f$

$= -j\,0.005 \times -j\,3.92 = -0.02$

$I_{1-12}^f = y_{1-12}\,(V_{1-1}^f - V_{1-3}^f)$

$= \frac{1}{j0.2}\,(0.588 - 0.824) = j1.18$

$I_{2-12}^f = y_{2-12}\,(V_{2-1}^f - V_{2-2}^f)$

$= \frac{1}{j0.2}(-0.412 + 0.176) = j1.18$

$I_{0-12}^f = y_{0-12}\,(V_{0-1}^f - V_{0-2}^f)$

$= \frac{1}{j0.4}\,(-0.176 + 0.020) = j0.39$

$$\begin{bmatrix} I_{a-12}^f \\ I_{b-12}^f \\ I_{c-12}^f \end{bmatrix} - = \begin{bmatrix} 1 & 1 & 1 \\ \alpha^2 & \alpha & 1 \\ \alpha & \alpha^2 & 1 \end{bmatrix} \begin{bmatrix} I_{1-12}^f \\ I_{2-12}^f \\ I_{0-12}^f \end{bmatrix}$$

$$= \begin{bmatrix} 1 & 1 & 1 \\ \alpha^2 & \alpha & 1 \\ \alpha & \alpha^2 & 1 \end{bmatrix} \begin{bmatrix} j1.18 \\ j1.18 \\ j0.39 \end{bmatrix}$$

$$I^f_{a-12} = j1.18 + j1.18 + j0.39 = j2.75$$

$$I^f_{b-12} = j1.18 \angle 240° + j1.18 \angle 120° + j0.39$$
$$= -j079$$

$$I^f_{c-12} = j1.18 \angle 120° + j1.18 \angle 240° + j0.39$$
$$= j0.79$$

(c) $$I^f_{1-G} = \frac{1}{j0.15}(1 - 0.588) \angle -33°$$
$$= -1.37 - j2.38$$

$$I^f_{2-G} = \frac{1}{j0.15}[0 - (0.412)] \angle 30°$$
$$= 1.37 - j2.38$$

$$I^f_{0-G} = 0 \text{ (see Fig. 11.29)}$$

$\therefore$ $$I^f_{a-G} = (-1.37 - j2.38) + (1.37 - j2.38)$$
$$= -j4.76$$

Current in phases *b* and *c* of the generator can be similarly calculated.

(d) $$V^f_{b-1} = V^f_{1-1} + V^f_{2-1} + V^f_{0-1}$$
$$= 0.588 \angle 240° - 0.412 \angle 120° - 0.176$$
$$= -0.264 - j0.866 = 0.905 \angle -107°$$

$$V^f_{c-1} = V^f_{1-1} + V^f_{2-1} + V^f_{0-1}$$
$$= 0.588 \angle 120° - 0.412 \angle 240° - 0.176$$
$$= -0.264 + j0.866 = 0.905 \angle 107°$$

11.8 SUMMARY

Various types of unsymmetrical fault analysis have been discussed in this chapter. Both shunt and series faults are dealt with. Finally Z_{BUS} method is presented.

Problems

11.1 A 25 MVA, 11 kV generator has a X''_d = 0.2 pu. Its negative and zero sequence reactances are respectively 0.3 and 0.1 pu. The neutral of the generator is solidly grounded. Determine the subtransient current in the generator and the line-to-line voltages for subtransient conditions when

an LG fault occurs at the generator terminals. Assume that before the occurrence of the fault, the generator is operating at no load at rated voltage. Ignore resistances.

11.2 Repeat Problem 11.1 for (a) an LL fault; and (b) an LLG fault.

11.3 A synchronous generator is rated 25 MVA, 11 kV. It is star-connected with the neutral point solidly grounded. The generator is operating at no load at rated voltage. Its reactances are $X'' = X_2 = 0.20$ and $X_0 = 0.08$ pu. Calculate the symmetrical subtransient line currents for (i) single line-to-ground fault; (ii) double line fault; (iii) double line-to-ground fault; and (iv) symmetrical three-phase fault. Compare these currents and comment.

11.4 For the generator of Problem 11.3, calculate the value of reactance to be included in the generator neutral and ground, so that line-to-ground fault current equals the three-phase fault current. What will be the value of the grounding resistance to achieve the same condition?

With the reactance value (as calculated above) included between neutral and ground, calculate the double line fault current and also double line-to-ground fault current.

11.5 Two 25 MVA, 11 kV synchronous generators are connected to a common bus bar which supplies a feeder. The star point of one of the generators is grounded through a resistance of 1.0 ohm, while that of the other generator is isolated. A line-to-ground fault occurs at the far end of the feeder. Determine: (a) the fault current; (b) the voltage to ground of the sound phases of the feeder at the fault point; and (c) voltage of the star point of the grounded generator with respect to ground.

The impedances to sequence currents of each generator and feeder are given below:

	Generator (per unit)	Feeder (ohms/phase)
Positive sequence	$j0.2$	$j0.4$
Negative sequence	$j0.15$	$j0.4$
Zero sequence	$j0.08$	$j0.8$

11.6 Determine the fault currents in each phase following a double line-to-ground short circuit at the terminals of a star-connected synchronous generator operating initially on an open circuit voltage of 1.0 pu. The positive, negative and zero sequence reactances of the generator are, respectively, $j0.35$, $j0.25$ and $j0.20$, and its star point is isolated from ground.

11.7 A three-phase synchronous generator has positive, negative and zero sequence reactances per phase respectively, of 1.0, 0.8 and 0.4 Ω. The winding resistances are negligible. The phase sequence of the generator is *RYB* with a no load voltage of 11 kV between lines. A short circuit occurs between lines *Y* and *B* and earth at the generator terminals.

Calculate sequence currents in phase *R* and current in the earth return circuit, (a) if the generator neutral is solidly earthed; and (b) if the generator neutral is isolated.

Use *R* phase voltage as reference.

11.8 A generator supplies a group of identical motors as shown in Fig. P-11.8. The motors are rated 600 V, 90% efficiency at full load unity power factor with sum of their output ratings being 5 MW. The motors are sharing equally a load of 4 MW at rated voltage, 0.8 power factor lagging and 90% efficiency when an LG fault occurs on the low voltage side of the transformer.

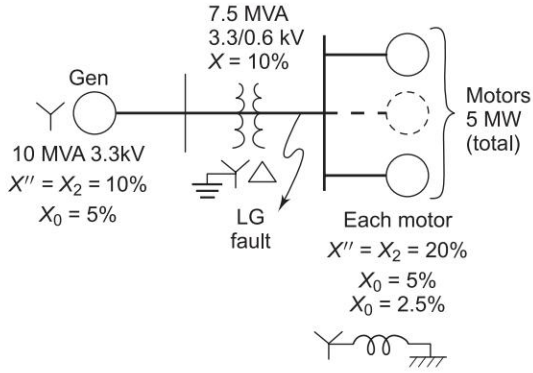

Fig. P-11.8

Specify completely the sequence networks to simulate the fault so as to include the effect of prefault current. The group of motors can be treated as a single equivalent motor.

Find the subtransient line currents in all parts of the system with prefault current ignored.

11.9 A double line-to-ground fault occurs on lines *b* and *c* at point *F* in the system of Fig. P-11.9. Find the subtransient current in phase *c* of machine 1, assuming prefault currents to be zero. Both machines are rated 1,200 kVA, 600 V with reactances of $X'' = X_2 = 10\%$ and $X_0 = 5\%$. Each three-phase transformer is rated 1,200 kVA, 600 V–Δ/3,300 V–*Y* with leakage reactance of 5%. The reactances of the transmission line are $X_1 = X_2 = 20\%$ and $X_0 = 40\%$ on a base of 1,200 kVA, 3,300V. The reactances of the neutral grounding reactors are 5% on the kVA base of the machines.

Fig. P-11.9

11.10 A synchronous machine 1 generating 1 pu voltage is connected through a Y/Y transformer of reactance 0.1 pu to two transmission lines in parallel. The other ends of the lines are connected through a Y/Y transformer of reactance 0.1 pu to a machine 2 generating 1 pu voltage. For both transformers $X_1 = X_2 = X_0$.

Calculate the current fed into a double line-to-ground fault on the line side terminals of the transformer fed from machine 2. The star points of machine 1 and of the two transformers are solidly grounded. The reactances of the machines and lines referred to a common base are:

	X_1	X_2	X_0
Machine 1	0.35	0.25	0.05
Machine 2	0.30	0.20	0.04
Line (each)	0.40	0.40	0.80

11.11 Figure P-11.11 shows a power network with two generators connected in parallel to a transformer feeding a transmission line. The far end of the line is connected to an infinite bus through another transformer. Star point of each transformer, generator 1 and infinite bus are solidly grounded. The positive, negative and zero sequence reactances of various components in per unit on a common base are:

Fig. P-11.11

	Positive	Negative	Zero
Generator 1	0.15	0.15	0.08
Generator 2	0.25	0.25	∞ (i.e. neutral isolated)
Each transformer	0.15	0.15	0.15
Infinite bus	0.15	0.15	0.05
Line	0.20	0.20	0.40

(a) Draw the sequence networks of the power system.

(b) With both generators and infinite bus operating at 1.0 pu voltage on no load, a line-to-ground fault occurs at one of the terminals of the star-connected winding of the transformer A. Calculate the currents flowing (i) in the fault; and (ii) through the transformer A.

11.12 A star connected synchronous generator feeds bus bar 1 of a power system. Bus bar 1 is connected to bus bar 2 through a star/delta transformer in series with a transmission line. The power network connected to bus bar 2 can be equivalently represented by a star-connected generator with equal positive and negative sequences

reactances. All star points are solidly connected to ground. The per unit sequence reactances of various components are given below:

	Positive	Negative	Zero
Generator	0.20	0.15	0.05
Transformer	0.12	0.12	0.12
Transmission Line	0.30	0.30	0.50
Power Network	X	X	0.10

Under no load condition with 1.0 pu voltage at each bus bar, a current of 4.0 pu is fed to a three-phase short circuit on bus bar 2. Determine the positive sequence reactance X of the equivalent generator of the power network.

For the same initial conditions, find the fault current for single line-to-ground fault on bus bar 1.

11.13 The reactance data for the three-phase system of Fig. P-11.13 is:

Generator: $X_1 = X_2 = 0.1$ pu; $X_0 = 0.05$ pu

X_g (grounding reactance) = 0.02 pu

Transformer: $X_1 = X_2 = X_0 = 0.1$ pu

X_g (grounding reactance) = 0.04 pu

Form the positive, negative and zero sequence bus impedance matrices. For a solid LG fault at bus 1, calculate the fault current and its contributions from the generator and transformer.

Hint: Notice that the line reactances are not given. Therefore it is convenient to obtain $Z_{1-\text{BUS}}$ directly rather than by inverting $Y_{1-\text{BUS}}$. Also $Y_{0-\text{BUS}}$ is singular and $Z_{0-\text{BUS}}$ cannot be obtained from it. In such situations the method of unit current injection outlined below can be used.

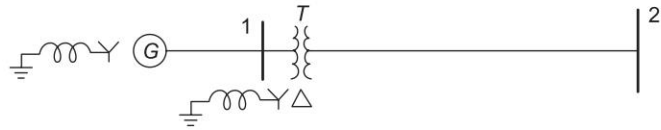

Fig. P-11.13

For a two-bus case

$$\begin{bmatrix} V_1 \\ V_2 \end{bmatrix} = \begin{bmatrix} Z_{11} & Z_{12} \\ Z_{21} & Z_{22} \end{bmatrix} \begin{bmatrix} I_1 \\ I_2 \end{bmatrix}$$

Injecting unit current at bus 1 (i.e. $I_1 = 1$, $I_2 = 0$), we get

$$Z_{11} = V_1$$
$$Z_{21} = V_2$$

Similarly injecting unit current at bus 2 (i.e. $I_1 = 0$, $I_2 = 1$), we get

$$Z_{12} = V_1$$
$$Z_{22} = V_2$$

Z_{BUS} could thus be directly obtained by this technique.

11.14 Consider the 2-bus system of Example 11.3. Assume that a solid LL fault occurs on bus *f*. Determine the fault current and voltage (to ground) of the healthy phase.

11.15 Write a computer programme to be employed for studying a solid LG fault on bus 2 of the system shown in Fig. 9.17. Our aim is to find the fault current and all bus voltages and the line currents following the fault. Use the impedance data given in Example 9.5. Assume all transformers to be Y/Δ type with their neutrals (on HV side) solidly grounded.

Assume that the positive and negative sequence reactances of the generators are equal, while their zero sequence reactance is one-fourth of their positive sequence reactance. The zero sequence reactances of the lines are to be taken as 2.5 times their positive sequence reactances. Set all prefault voltages = 1 pu.

References

Books

1. Stevenson, W.D., *Elements of Power System Analysis*, 4th edn, McGraw-Hill, New York, 1982.
2. Elgerd, O.I., *Electric Energy Systems Theory—An Introduction*, 2nd edn, McGraw-Hill, New York, 1982.
3. Gross, C.A., *Power System Analysis*, Wiley, New York, 1979.
4. Neuenswander, J.R., *Modern Power Systems*, International Textbook Co., New York, 1971.
5. Anderson, P., *Analysis of Faulted Power Systems*, IEEE Press, 1995.
6. Bergan, A.R. and V. Vittal, *Power System Analysis*, 2nd edn, Pearson Education Asia, Delhi, 2000.
7. Soman, S.A., S.A. Khaparde and Shubha Pandit, *Computational Methods for Large Sparse Power Systems Analysis*, KAP, Boston, 2002.

Papers

8. Brown, H.E. and C.E. Person, 'Short Circuit Studies of Large Systems by the Impedance Matrix Method', *Proc. PICA*, 1967, p. 335.
9. Smith, D.R., 'Digital Simulation of Simultaneous Unbalances Involving Open and Faulted Conductors', *IEEE Trans., PAS*, 1970, p. 1826.

Chapter 12

Power System Stability

12.1 INTRODUCTION

The stability of an interconnected power system is its ability to return to normal or stable operation after having been subjected to some form of disturbance. Conversely, instability means a condition denoting loss of synchronism or falling out of step. Stability considerations have been recognized as an essential part of power system planning for a long time. With interconnected systems continually growing in size and extending over vast geographical regions, it is becoming increasingly more difficult to maintain synchronism between various parts of a power system.

The dynamics of a power system are characterised by its basic features given below:

1. Synchronous tie exhibits the typical behaviour that as power transfer is gradually increased a maximum limit is reached beyond which the system cannot stay in synchronism, i.e., it falls out of step.
2. The system is basically a spring-inertia oscillatory system with inertia on the mechanical side and spring action provided by the synchronous tie wherein power transfer is proportional to sin δ or δ (for small δ, δ being the relative internal angle of machines).
3. Because of power transfer being proportional to sin δ, the equation determining system dynamics is nonlinear for disturbances causing large variations in angle δ. Stability phenomenon peculiar to non-linear systems as distinguished from linear systems is therefore exhibited by power systems (stable up to a certain magnitude of disturbance and unstable for larger disturbances).

Accordingly power system stability problems are classified into three basic types*—steady state, dynamic and transient.

* There are no universally accepted precise definitions of this terminology. For a definition of some important terms related to power system stability, refer to IEEE Standard Dictionary of Electrical and Electronic Terms, IEEE, New York, 1972.

The study of steady state stability is basically concerned with the determination of the upper limit of machine loadings before losing synchronism, provided the loading is increased gradually.

Dynamic instability is more probable than steady state instability. Small disturbances are continually occurring in a power system (variations in loadings, changes in turbine speeds, etc.) which are small enough not to cause the system to lose synchronism but do excite the system into the state of natural oscillations. The system is said to be dynamically stable if the oscillations do not acquire more than certain amplitude and die out quickly (i.e., the system is well-damped). In a dynamically unstable system, the oscillation amplitude is large and these persist for a long time (i.e., the system is underdamped). This kind of instability behaviour constitutes a serious threat to system security and creates very difficult operating conditions. Dynamic stability can be significantly improved through the use of power system stabilizers. Dynamic system study has to be carried out for 5–10 s and sometimes up to 30 s. Computer simulation is the only effective means of studying dynamic stability problems. The same simulation programmes are, of course, applicable to transient stability studies.

Following a sudden disturbance on a power system rotor speeds, rotor angular differences and power transfer undergo fast changes whose magnitudes are dependent upon the severity of disturbance. For a large disturbance, changes in angular differences may be so large as to cause the machines to fall out of step. This type of instability is known as transient instability and is a fast phenomenon usually occurring within 1 s for a generator close to the cause of disturbance. There is a large range of disturbances which may occur on a power system, but a fault on a heavily loaded line which requires opening the line to clear the fault is usually of greatest concern. The tripping of a loaded generator or the abrupt dropping of a large load may also cause instability.

The effect of short circuits (faults), the most severe type of disturbance to which a power system is subjected, must be determined in nearly all stability studies. During a fault, electrical power from nearby generators is reduced drastically, while power from remote generators is scarcely affected. In some cases, the system may be stable even with a sustained fault, whereas other systems will be stable only if the fault is cleared with sufficient rapidity. Whether the system is stable on occurrence of a fault depends not only on the system itself, but also on the type of fault, location of fault, rapidity of clearing and method of clearing, i.e., whether cleared by the sequential opening of two or more breakers or by simultaneous opening and whether or not the faulted line is reclosed. The transient stability limit is almost always lower than the steady state limit, but unlike the latter, it may exhibit different values depending on the nature, location and magnitude of disturbance.

Modern power systems have many interconnected generating stations, each with several generators and many loads. The machines located at any one point in a system normally act in unison. It is, therefore, common practice in stability studies to consider all the machines at one point as one large machine. Also

machines which are not separated by lines of high reactance are lumped together and considered as one equivalent machine. Thus a multimachine system can often be reduced to an equivalent few machine system. If synchronism is lost, the machines of each group stay together although they go out of step with other groups. Qualitative behaviour of machines in an actual system is usually that of a two machine system. Because of its simplicity, the two machine system is extremely useful in describing the general concepts of power system stability and the influence of various factors on stability. It will be seen in this chapter that a two machine system can be regarded as a single machine system connected to infinite system.

Stability study of a multimachine system must necessarily be carried out on a digital computer.

12.2 DYNAMICS OF A SYNCHRONOUS MACHINE

The kinetic energy of the rotor at synchronous machine is

$$\text{K.E.} = \frac{1}{2} J\omega^2_{sm} \times 10^{-6} \text{ MJ}$$

where J = rotor moment of inertia in kg-m^2

ω_{sm} = synchronous speed in rad (mech)/s

But $\omega_s = \left(\frac{P}{2}\right) \omega_{sm}$ = rotor speed in rad (elect)/s

where P = number of machine poles

$$\therefore \quad \text{K.E.} = \frac{1}{2}\left(J\left(\frac{2}{P}\right)^2 \omega_s \times 10^{-6}\right)\omega_s$$

$$= \frac{1}{2} M\omega_s$$

where $$M = J\left(\frac{2}{P}\right)^2 \omega_s \times 10^{-6}$$

= moment of inertia in MJ-s/elect rad

We shall define the inertia constant H such that

$$GH = \text{K.E.} = \frac{1}{2} M\omega_s \text{ MJ}$$

where G = machine rating (base) in MVA (three-phase)

H = *inertia constant* in MJ/MVA or MW-s/MVA

It immediately follows that

$$M = \frac{2GH}{\omega_s} = \frac{GH}{\pi f} \text{ MJ-s/elect rad} \qquad (12.1)$$

$$= \frac{GH}{180 f} \text{ MJ-s/elect degree}$$

M is also called the *inertia constant*.

Taking G as base, the inertia constant in pu is

$$M(\text{pu}) = \frac{H}{\pi f} \text{ s}^2\text{/elect rad} \qquad (12.2)$$

$$= \frac{H}{180 f} \text{ s}^2\text{/elect degree}$$

The inertia constant H has a characteristic value or a range of values for each class of machines. Table 12.1 lists some typical inertia constants.

Table 12.1 Typical inertia constants of synchronous machines[1]

Type of Machine		*Intertia Constant H Stored Energy in MW-s per MVA*[2]
Turbine Generator		
Condensing	1,800 rpm	9–6
	3,000 rpm	7–4
Non-Condensing	3,000 rpm	4–3
Waterwheel Generator		
Slow-speed (< 200 rpm)		2–3
High-speed (> 200 rpm)		2–4
Synchronous Condenser[3]		
Large		1.25
Small		1.00
Synchronous Motor with load varying from 1.0 to 5.0 and higher for heavy flywheels		2.00

It is observed from Table 12.1 that the value of H is considerably higher for steam turbogenerator than for water wheel generator. Thirty to sixty percent of the total inertia of a steam turbogenerator unit is that of the primemover, whereas only 4–15% of the inertia of a hydroelectric generating unit is that of the waterwheel, including water.

[1] Reprinted with permission of the Westinghouse Electric Corporation from Electrical Transmission and Distribution Reference Book.

[2] Where range is given, the first figure applies to the smaller MVA sizes.

[3] Hydrogen-cooled, 25 per cent less.

The Swing Equation

Figure 12.1 shows the torque, speed and flow of mechanical and electrical powers in a synchronous machine. It is assumed that the windage, friction and iron-loss torque is negligible. The differential equation governing the rotor dynamics can then be written as

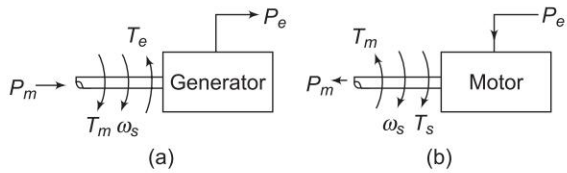

Fig. 12.1 Flow of mechanical and electrical powers in a synchronous machine

$$J\frac{\mathrm{d}^2\theta_m}{\mathrm{d}t^2} = T_m - T_e \text{ Nm} \tag{12.3}$$

where

θ_m = angle in rad (mech)

T_m = turbine torque in Nm; it acquires a negative value for a motoring machine

T_e = electromagnetic torque developed in Nm; it acquires negative value for a motoring machine

While the rotor undergoes dynamics as per Eq. (12.3), the rotor speed changes by insignificant magnitude for the time period of interest (1s) [Sec. 12.1]. Equation (12.3) can therefore be converted into its more convenient power form by assuming the rotor speed to remain constant at the synchronous speed (ω_{sm}). Multiplying both sides of Eq. (12.3) by ω_{sm} we can write

$$J\omega_{sm}\frac{\mathrm{d}^2\theta_m}{\mathrm{d}t^2} \times 10^{-6} = P_m - P_e \text{ MW} \tag{12.4}$$

where

P_m = mechanical power input in MW

P_e = electrical power output in MW; stator copper loss is assumed negligible

Rewriting Eq. (12.4)

$$\left(J\left(\frac{2}{P}\right)^2 \omega_s \times 10^{-6}\right)\frac{\mathrm{d}^2\theta_e}{\mathrm{d}t^2} = P_m - P_e \text{ MW}$$

where θ_e = angle in rad (elect)

or
$$M\frac{\mathrm{d}^2\theta_e}{\mathrm{d}t^2} = P_m - P_e \tag{12.5}$$

It is more convenient to measure the angular position of the rotor with respect to a synchronously rotating frame of reference. Let

$\delta = \theta_e - \omega_s t$; rotor angular displacement from synchronously rotating reference frame (called *torque angle/power angle*) (12.6)

From Eq. (12.6)

$$\frac{d^2\theta_e}{dt^2} = \frac{d^2\delta}{dt^2} \tag{12.7}$$

Hence Eq. (12.5) can be written in terms of δ as

$$M \frac{d^2\delta}{dt^2} = P_m - P_e \text{ MW} \tag{12.8}$$

With M as defined in Eq. (12.1), we can write

$$\frac{GH}{\pi f} \frac{d^2\delta}{dt^2} = P_m - P_e \text{ MW} \tag{12.9}$$

Dividing throughout by G, the MVA rating of the machine,

$$M(\text{pu}) \frac{d^2\delta}{dt^2} = P_m - P_e; \text{ in pu of machine rating as base} \tag{12.10}$$

where

$$M(\text{pu}) = \frac{H}{\pi f}$$

or

$$\frac{H}{\pi f} \frac{d^2\delta}{dt^2} = P_m - P_e \text{ pu} \tag{12.11}$$

This equation, Eq. (12.10)/Eq. (12.11), is called the *swing equation* and it describes the rotor dynamics for a synchronous machine (generating/motoring). It is a second-order differential equation where the damping term (proportional to $d\delta/dt$) is absent because of the assumption of a lossless machine and the fact that the torque of *damper winding* has been ignored. This assumption leads to pessimistic results in transient stability analysis—damping helps to stabilize the system. Damping must of course be considered in a dynamic stability study. Since the electrical power P_e depends upon the sine of angle δ (see Eq. (12.29)), the *swing equation is a non-linear second-order differential equation.*

Multimachine System

In a multimachine system a common system base must be chosen.
Let

G_{mach} = machine rating (base)

G_{system} = system base

Equation (12.11) can then be written as

$$\frac{G_{\text{mach}}}{G_{\text{system}}}\left(\frac{H_{\text{mach}}}{f}\frac{\mathrm{d}^2\delta}{\mathrm{d}t^2}\right) = (P_m - P_e)\ \frac{G_{\text{mach}}}{G_{\text{system}}}$$

or

$$\frac{H_{\text{system}}}{\pi f}\frac{\mathrm{d}^2\delta}{\mathrm{d}t^2} = P_m - P_e \text{ pu in system base} \tag{12.12}$$

where

$$H_{\text{system}} = H_{\text{mach}}\left(\frac{G_{\text{mach}}}{G_{\text{system}}}\right) \tag{12.13}$$

= machine inertia constant in system base

Machines Swinging Coherently

Consider the swing equations of two machines on a *common system base*.

$$\frac{H_1}{\pi f}\frac{\mathrm{d}^2\delta_1}{\mathrm{d}t^2} = P_{m1} - P_{e1} \text{ pu} \tag{12.14}$$

$$\frac{H_2}{\pi f}\frac{\mathrm{d}^2\delta_2}{\mathrm{d}t^2} = P_{m2} - P_{e2} \text{ pu} \tag{12.15}$$

Since the machine rotors swing together (coherently or in unison)

$$\delta_1 = \delta_2 = \delta$$

Adding Eqs (12.14) and (12.15),

$$\frac{H_{eq}}{\pi f}\frac{\mathrm{d}^2\delta}{\mathrm{d}t^2} = P_m - P_e \tag{12.16}$$

where

$$\begin{aligned} P_m &= P_{m1} + P_{m2} \\ P_e &= P_{e1} + P_{e2} \\ H_{eq} &= H_1 + H_2 \end{aligned} \tag{12.17}$$

The two machines swinging coherently are thus reduced to a single machine as in Eq. (12.16). The equivalent inertia in Eq. (12.17) can be written as

$$H_{eq} = H_{1\ \text{mach}}\ G_{1\ \text{mach}}/G_{\text{system}} + H_{2\ \text{mach}}\ G_{2\ \text{mach}}/G_{\text{system}} \tag{12.18}$$

The above results are easily extendable to any number of machines swinging coherently.

Example 12.1 A 50 Hz, four pole turbogenerator rated 100 MVA, 11 kV has an inertia constant of 8.0 MJ/MVA.

(a) Find the stored energy in the rotor at synchronous speed.

(b) If the mechanical input is suddenly raised to 80 MW for an electrical load of 50 MW, find rotor acceleration, neglecting mechanical and electrical losses.

(c) If the acceleration calculated in part (b) is maintained for 10 cycles, find the change in torque angle and rotor speed in revolutions per minute at the end of this period.

Solution

(a) Stored energy = $GH = 100 \times 8 = 800$ MJ

(b) $P_a = 80 - 50 = 30$ MW $= M \dfrac{d^2\delta}{dt^2}$

$$M = \frac{GH}{180f} = \frac{800}{180 \times 50} = \frac{4}{45} \text{ MJ-s/elect deg}$$

$$\therefore \quad \frac{4}{45}\frac{d^2d}{dt^2} = 30$$

or

$$\alpha = \frac{d^2\delta}{dt^2} = 337.5 \text{ elect deg/s}^2$$

(c) 10 cycles = 0.2 s

$$\text{Change in } \delta = \frac{1}{2}(337.5) \times (0.2)^2 = 6.75 \text{ elect deg}$$

$$\alpha = 60 \times \frac{337.5}{2 \times 360^\circ} = 28.125 \text{ rpm/s}$$

$\therefore$ Rotor speed at the end of 10 cycles

$$= \frac{120 \times 50}{4} + 28.125 \times 0.2$$

$$= 1505.625 \text{ rpm}$$

12.3 POWER ANGLE EQUATION

In solving the swing equation (Eq. (12.10)), certain simplifying assumptions are usually made. These are:

1. Mechanical power input to the machine (P_m) remains constant during the period of electromechanical transient of interest. In other words, it means that the effect of the turbine governing loop is ignored, being much slower than the speed of the transient. This assumption leads to pessimistic result—governing loop helps to stabilize the system.
2. Rotor speed changes are insignificant—these have already been ignored in formulating the swing equation.
3. Effect of voltage regulating loop during the transient is ignored, as a consequence the generated machine emf remains constant. This assumption also leads to pessimistic results—voltage regulator helps to stabilize the system.

Before the swing equation can be solved, it is necessary to determine the dependence of the electrical power output (P_e) upon the rotor angle.

Simplified Machine Model

For a salient pole machine, the per phase induced emf-terminal voltage equation under steady conditions is

$$E = V + jX_dI_d + jX_qI_q;\ X_d > X_q \tag{12.19}$$

where
$$I = I_d + I_q \tag{12.20}$$

and usual symbols are used.

Under transient condition

$$X_d \rightarrow X'_d < X_d$$

but

$X'_q = X_q$ since the main field is on the d-axis

$X'_d < X_q$; but the difference is small

Equation (12.19) during the transient modifies to

$$E' = V + jX'_dI_d + jX_qI_q \tag{12.21}$$

$$= V + jX_q(I - I_d) + jX'_dI_d$$

$$= (V + jX_qI) + j(X'_d - X_q)I_d \tag{12.22}$$

The phasor diagram corresponding to Eqs (12.21) and (12.22) is drawn in Fig. 12.2.

Since under transient condition, $X'_d < X_d$ but X_q remains almost unaffected, it is fairly valid to assume that

$$X'_d \approx X_q \tag{12.23}$$

Equation (12.22) now becomes

$$E' = V + jX_qI$$

$$= V + jX'_dI \tag{12.24}$$

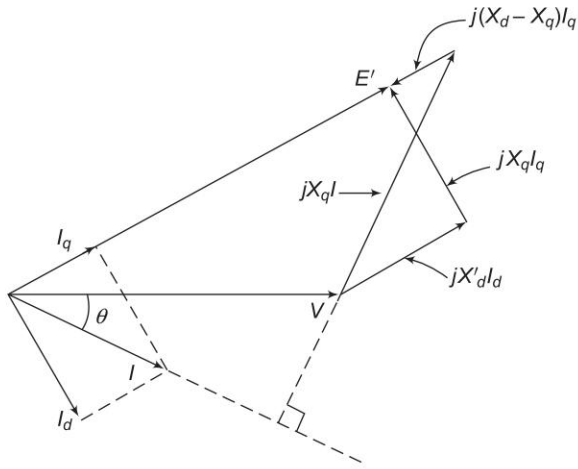

Fig. 12.2 Phasor diagram—salient pole machine

The machine model corresponding to Eq. (12.24) is drawn in Fig. 12.3 which also applies to a cylindrical rotor machine where $X_d' = X_q' = X_s'$ (transient synchronous reactance).

The simplified machine model of Fig. 12.3 will be used in all stability studies.

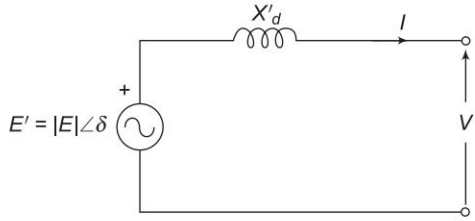

Fig. 12.3 Simplified machine model

Power Angle Curve

For the purposes of stability studies $|E'|$, transient emf of generator/motor, remains constant or is the independent variable determined by the voltage regulating loop but V, the generator determined terminal voltage is a dependent variable. Therefore, the nodes (buses) of the stability study network pertain to the emf terminal in the machine model as shown in Fig. 12.4, while the machine reactance (X_d') is absorbed in the system network as different from a load flow study. Further, the loads (other than large synchronous motors) will be replaced by equivalent static admittances (connected in shunt between transmission network buses and the reference bus). This is so because load voltages vary during a stability study (in a load flow study, these remain constant within a narrow band).

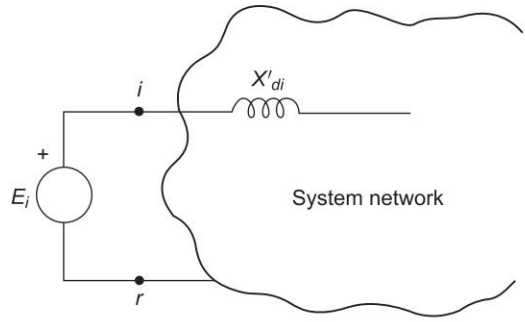

Fig. 12.4

For the two-bus system of Fig. 12.5

$$\boldsymbol{Y}_{\text{BUS}} = \begin{bmatrix} Y_{11} & Y_{12} \\ Y_{21} & Y_{22} \end{bmatrix}; \; Y_{12} = Y_{21} \tag{12.25}$$

Complex power into bus is given by

$$P_i + jQ_i = E_i I_i^*$$

At bus 1,

$$P_1 + jQ_1 = E_1'(Y_{11}E_1')^* + E_1\,(Y_{12}E_2')^* \tag{12.26}$$

But

$$E_1' = |E_1'|\,\angle\delta_1;\; E_2' = |E'_2|\,\angle\delta_2$$
$$Y_{11} = G_{11} + jB_{11};\; Y_{12} = |Y_{12}|\,\angle\theta_{12}$$

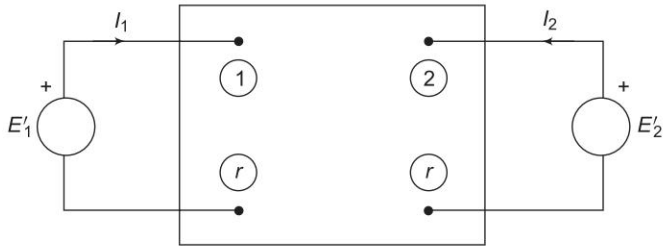

Fig. 12.5 Two-bus stability study network

Since in solution of the swing equation only real power is involved, we have from Eq. (12.26)

$$P_1 = |E_1'|^2\, G_{11} + |E_1'|\,|E_2'|\,|Y_{12}|\cos(\delta_1 - \delta_2 - \theta_{12}) \tag{12.27}$$

A similar equation will hold at bus 2.

Let

$$|E_1'|^2 G_{11} = P_c$$

$$|E_1'|\,|E_2'|\,|Y_{12}| = P_{\max}$$

$$\delta_1 - \delta_2 = \delta$$

and

$$\phi_{12} = \pi/2 - \gamma$$

Then Eq. (12.27) can be written as

$$P_1 = P_c + P_{\max} \sin(\delta - \gamma);\ \textit{Power Angle Equation} \tag{12.28}$$

For a purely reactive network

$$G_{11} = 0\ (\therefore \quad P_c = 0);\ \text{lossless network}$$

$$\theta_{12} = \pi/2, \quad \therefore \quad \gamma = 0$$

Hence

$$P_e = P_{\max} \sin \delta \tag{12.29a}$$

where

$$P_{\max} = \frac{|E_1'|\,|E_2'|}{X};\ \text{simplified power angle equation} \tag{12.29b}$$

where

X = transfer reactance between nodes (i.e., between E_1' and E_2').

The graphical plot of power angle equation (Eq.(12.29) is shown in Fig. 12.6.

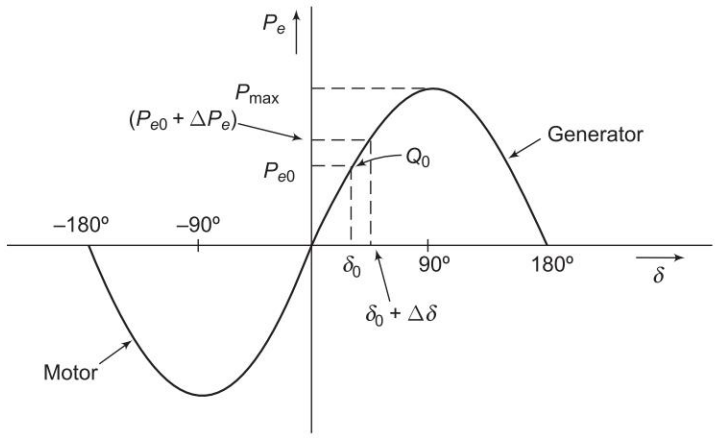

Fig. 12.6 Power angle curve

The swing equation (Eq. (12.10)) can now be written as

$$\frac{H}{\pi f}\frac{\mathrm{d}^2\delta}{\mathrm{d}t^2} = P_m - P_{\max} \sin \delta \text{ pu} \tag{12.30}$$

which, as already stated, is a non-linear second-order differential equation with no damping.

12.4 NODE ELIMINATION TECHNIQUE

In stability studies, it has been indicated that the buses to be considered are those which are excited by the internal machine voltages (transient emfs) and not the load buses which are excited by the terminal voltages of the generators. Therefore, in Y_{BUS} formulation for the stability study, the load buses must be eliminated. Three methods are available for bus elimination. These are illustrated by the simple system of Fig. 12.7(a) whose reactance diagram is drawn in Fig. 12.7(b). In this simple situation, bus 3 gets easily eliminated by parallel combination of the lines. Thus

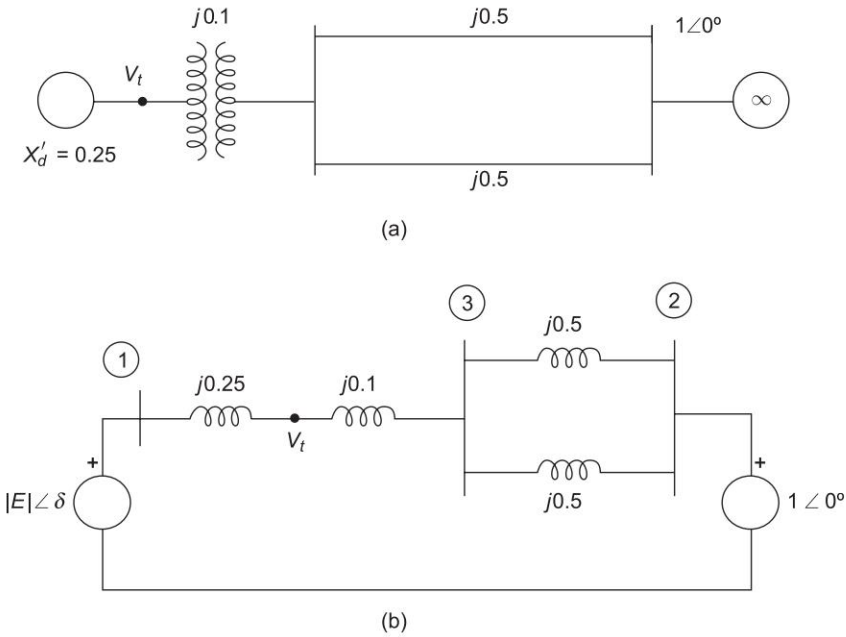

Fig. 12.7 A simple system with its reactance diagram

$$X_{12} = 0.25 + 0.1 + \frac{0.5}{2}$$

$$= 0.6$$

Consider now a more complicated case wherein a three-phase fault occurs at the midpoint of one of the lines in which case the reactance diagram becomes that of Fig. 12.8 (a).

Star-Delta Conversion

Converting the star at the bus 3 to delta, the network transforms to that of Fig. 12.8(b) wherein

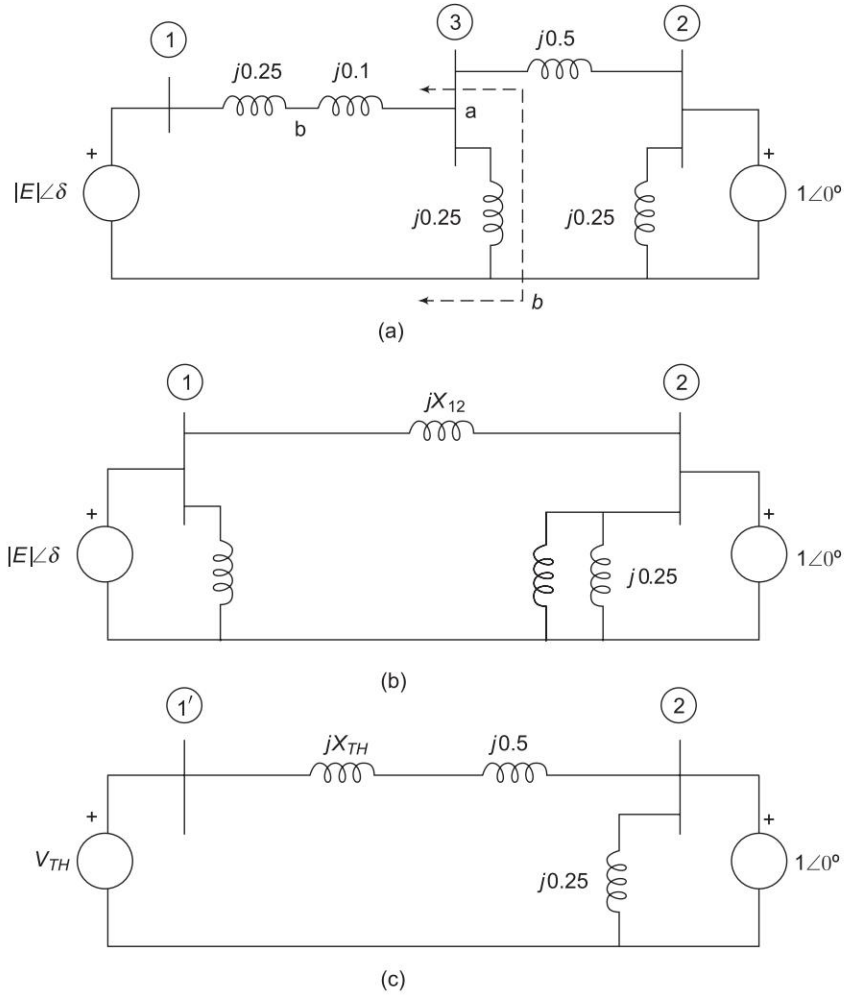

Fig. 12.8

$$X_{12} = \frac{0.25 \times 0.35 + 0.35 \times 0.5 + 0.5 \times 0.25}{0.25}$$

$$= 1.55$$

This method for a complex network, however, cannot be mechanized for preparing a computer programme.

Thevenin's Equivalent

With reference to Fig. 12.8(a), the Thevenin's equivalent for the network portion to the left of terminals *ab* as drawn in Fig. 12.8(c) wherein bus 1 has been modified to 1′,

$$V_{TH} = \frac{0.25}{0.25 + 0.35} |E'| \angle\delta$$

$$= 0.417 |E'| \angle\delta$$

$$X_{TH} = \frac{0.35 \times 0.25}{0.35 + 0.25} = 0.146$$

Now

$$X_{12} = 0.146 + 0.5 = 0.646^*$$

This method obviously is cumbersome to apply for a network of even small complexity and cannot be computerized.

Node Elimination Technique

Formulate the bus admittances for the three-bus system of Fig. 12.8(a). This network is redrawn in Fig. 12.9 wherein instead of reactance branch, admittances are shown. For this network,

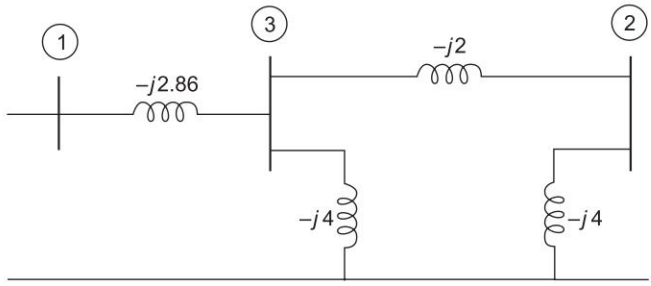

Fig. 12.9

$$Y_{\text{BUS}} = j \begin{matrix} 1 \\ 2 \\ 3 \end{matrix} \begin{bmatrix} -2.86 & 0 & 2.86 \\ 0 & -6 & 2 \\ 2.86 & 2 & -8.86 \end{bmatrix}$$

The bus 3 is to be eliminated.

In general for a three-bus system

$$\begin{bmatrix} I_1 \\ I_2 \\ I_3 \end{bmatrix} = \begin{bmatrix} Y_{11} & Y_{12} & Y_{13} \\ Y_{21} & Y_{22} & Y_{23} \\ Y_{31} & Y_{32} & Y_{33} \end{bmatrix} \begin{bmatrix} V_1 \\ V_2 \\ V_3 \end{bmatrix} \tag{12.31}$$

* This value is different from that obtained by star delta transformation as V_{TH} is no longer $|E'| \angle\delta$; in fact it is $0.417 |E'| \angle\delta$.

Since no source is connected at the bus 3,

$$I_3 = 0$$

or $$Y_{31}V_1 + Y_{32}V_2 + Y_{33}V_3 = 0$$

or $$V_3 = -\frac{Y_{31}}{Y_{33}}V_1 - \frac{Y_{32}}{Y_{33}}V_2 \tag{12.32}$$

Substituting this value of V_3 in the remaining two equations of Eq. (12.31), thereby eliminating V_3,

$$I_1 = Y_{11}V_1 + Y_{12}V_2 + Y_{13}V_3$$

$$= \left(Y_{11} - \frac{Y_{13}Y_{31}}{Y_{33}}\right)V_1 + \left(Y_{12} - \frac{Y_{13}Y_{32}}{Y_{33}}\right)V_2$$

In compact form

$$\boldsymbol{Y}_{\text{BUS}}\ (\text{reduced}) = \begin{bmatrix} Y'_{11} & Y'_{12} \\ Y'_{21} & Y'_{22} \end{bmatrix} \tag{12.33}$$

where

$$Y'_{11} = Y_{11} - \frac{Y_{13}Y_{31}}{Y_{33}} \tag{12.34a}$$

$$Y'_{12} = Y'_{21} = Y_{12} - \frac{Y_{13}Y_{32}}{Y_{33}} \tag{12.34b}$$

$$Y'_{22} = Y_{22} - \frac{Y_{23}Y_{32}}{Y_{33}} \tag{12.34c}$$

In general, in eliminating node n

$$Y_{kj}\ (\text{new}) = Y_{kj}\ (\text{old}) - \frac{Y_{kn}(\text{old})Y_{rj}(\text{old})}{Y_{nn}(\text{old})} \tag{12.35}$$

Applying Eqs (12.34) to the example in hand

$$\boldsymbol{Y}_{\text{BUS}}\ (\text{reduced}) = j\begin{bmatrix} -1.937 & 0.646 \\ 0.646 & -5.549 \end{bmatrix}$$

It then follows that

$$X_{12} = \frac{1}{0.646} = 1.548\ (\approx 1.55)$$

Example 12.2 In the system shown in Fig. 12.10, a three-phase static capacitive reactor of reactance 1 pu per phase is connected through a switch at motor bus bar. Calculate the limit of steady state power with and without

reactor switch closed. Recalculate the power limit with capacitive reactor replaced by an inductive reactor of the same value. Assume the internal voltage of the generator to be 1.2 pu and that of the motor to be 1.0 pu.

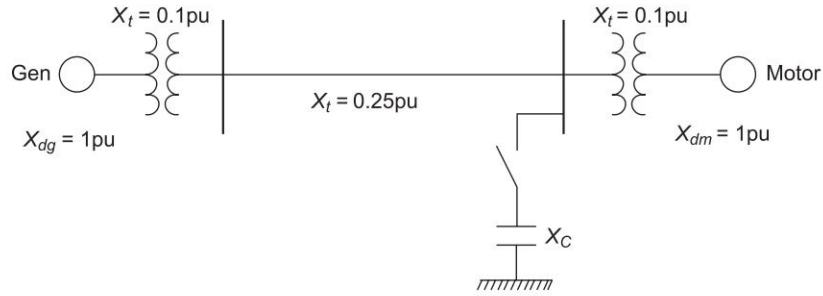

Fig. 12.10

Solution

(1) Steady state power limit without reactor

$$= \frac{|E_g||E_m|}{X(\text{total})} = \frac{1.2 \times 1}{1+0.1+0.25+0.1+1} = 0.49 \text{ pu}$$

(2) Equivalent circuit with capacitive reactor is shown in Fig. 12.11 (a).

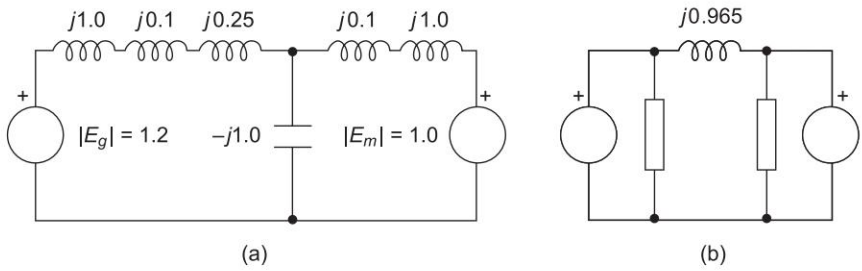

Fig. 12.11

Converting star to delta, the network of Fig. 12.11(a) is reduced to that of Fig. 12.11(b) where

$$jX(\text{transfer}) = \frac{j1.35 \times j1.1 + j1.1 \times (-j1.0) + (-j1.0) \times j1.35}{-j1.0}$$

$$= j0.965$$

$$\text{Steady state power limit} = \frac{1.2 \times 1}{0.965} = 1.244 \text{ pu}$$

(3) With capacitive reactance replaced by inductive reactance, we get the equivalent circuit of Fig. 12.12. Converting star to delta, we have the transfer reactance of

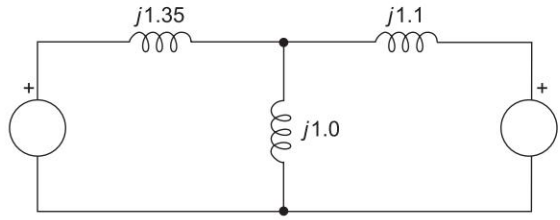

Fig. 12.12

$$jX(\text{transfer}) = \frac{j1.35 \times j1.1 + j1.1 \times j1.0 + j1.0 \times j1.35}{j1.0}$$

$$= j3.935$$

$$\text{Steady state power limit} = \frac{1.2 \times 1}{3.935} = 0.304 \text{ pu}$$

Example 12.3 The generator of Fig. 12.7(a) is delivering 1.0 pu power to the infinite bus ($|V| = 1.0$ pu), with the generator terminal voltage of $|V_t| = 1.0$ pu. Calculate the generator emf behind transient reactance. Find the maximum power that can be transferred under the following conditions:

(a) System healthy
(b) One line shorted (3-phase) in the middle
(c) One line open.

Plot all the three power angle curves.

Solution

Let $V_t = |V_t| \angle\alpha = 1\angle\alpha$

From power angle equation

$$\frac{|V_t||V|}{X} \sin\alpha = P_e$$

or $$\left(\frac{1 \times 1}{0.25 + 0.1}\right) \sin\alpha = 1$$

or $$\alpha = 20.5°$$

Current into infinite bus,

$$I = \frac{|V_t| \angle\alpha - |V| \angle 0°}{jX}$$

$$= \frac{1\angle 20.5° - 1\angle 0°}{j0.35}$$

$$= 1 + j0.18 = 1.016 \angle 10.3°$$

Voltage behind transient reactance,

$$E' = 1\angle 0° + j0.6 \times (1 + j0.18)$$
$$= 0.892 + j0.6 = 1.075\angle 33.9°$$

(a) System healthy

$$P_{\max} = \frac{|V||E'|}{X_{12}} = \frac{1 \times 1.075}{0.6} = 1.79 \text{ pu}$$

$$\therefore \quad P_e = 1.79 \sin\delta \qquad \text{(i)}$$

(b) One line shorted in the middle: As already calculated in this section,

$$X_{12} = 1.55$$

$$\therefore \quad P_{\max} = \frac{1 \times 1.075}{1.55} = 0.694 \text{ pu}$$

or $$P_e = 0.694 \sin\delta \qquad \text{(ii)}$$

(c) One line open:
It easily follows from Fig. 12.7(b) that

$$X_{12} = 0.25 + 0.1 + 0.5 = 0.85$$

$$\therefore \quad P_{\max} = \frac{1 \times 1.075}{0.85} = 1.265$$

or $$P_e = 1.265 \sin\delta \qquad \text{(iii)}$$

The plot of the three power angle curves (Eqs (i), (ii) and (iii)) is drawn in Fig. 12.13. Under healthy condition, the system is operated with $P_m = P_e = 1.0$ pu and $\delta_0 = 33.9°$, i.e., at the point P on the power angle curve 1.79 sin δ. As one line is shorted in the middle, P_m remains fixed at 1.0 pu (governing system acts instantaneously) and is further assumed to remain fixed throughout the transient (governing action is slow), while the operating point instantly shifts to Q on the curve 0.694 sin δ at $\delta = 33.9°$. Notice that because of machine inertia, the rotor angle can not change suddenly.

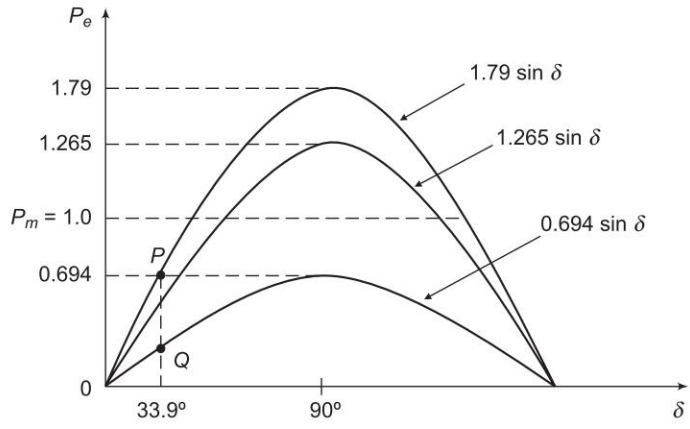

Fig. 12.13 Power angle curves

12.5 SIMPLE SYSTEMS

Machine Connected to Infinite Bus

Figure 12.14 is the circuit model of a single machine connected to infinite bus through a line of reactance X_e. In this simple case

$$X_{\text{transfer}} = X'_d + X_e$$

From Eq. (12.29b)

$$P_e = \frac{|E'||V|}{X_{\text{transfer}}} \sin \delta = P_{\max} \sin \delta \tag{12.36}$$

The dynamics of this system are described in Eq. (12.11) as

$$\frac{H}{\pi f} \frac{\mathrm{d}^2\delta}{\mathrm{d}t^2} = P_m - P_e \text{ pu} \tag{12.37}$$

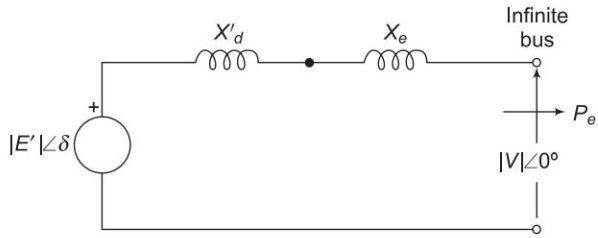

Fig. 12.14 Machine connected to infinite bus

Two Machine System

The case of two finite machines connected through a line (X_e) is illustrated in Fig. 12.15 where one of the machines must be generating and the other must be motoring. Under steady condition, before the system goes into dynamics,

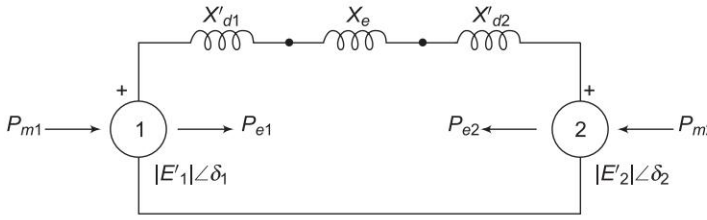

Fig. 12.15 Two-machine system

$$P_{m1} = -P_{m2} = P_m \tag{12.38a}$$

and the mechanical input/output of the two machines is assumed to remain constant at these values throughout the dynamics (governor action assumed slow). During steady state or in dynamic condition, the electrical power output of the generator must be absorbed by the motor (network being lossless). Thus at all time

$$P_{e1} = -P_{e2} = P_e \tag{12.38b}$$

The swing equations for the two machines can now be written as

$$\frac{d^2\delta_1}{dt^2} = \pi f\left(\frac{P_{m1} - P_{e1}}{H_1}\right) = \pi f\left(\frac{P_m - P_e}{H_1}\right) \tag{12.39a}$$

and

$$\frac{d^2\delta_2}{dt^2} = \pi f\left(\frac{P_{m2} - P_{e2}}{H_2}\right) = \pi f\left(\frac{P_e - P_m}{H_2}\right) \tag{12.39b}$$

Subtracting Eq. (12.39b) from Eq. (12.39a)

$$\frac{d^2(\delta_1 - \delta_2)}{dt^2} = \pi f\left(\frac{H_1 + H_2}{H_1 H_2}\right)(P_m - P_e) \tag{12.40}$$

or

$$\frac{H_{eq}}{\pi f}\frac{d^2\delta}{dt^2} = P_m - P_e \tag{12.41}$$

where

$$\delta = \delta_1 - \delta_2 \tag{12.42}$$

$$H_{eq} = \frac{H_1 H_2}{H_1 + H_2} \tag{12.43}$$

The electrical power interchange is given by expression

$$P_e = \frac{|E_1'||E_2'|}{X_{d1}' + X_e + X_{d2}'}\sin\delta \tag{12.44}$$

The swing equation, Eq. (12.41) and the power angle equation, Eq. (12.44) have the same form as for a single machine connected to infinite bus. Thus a two-machine system is equivalent to a single machine connected to infinite bus. Because of this, the single-machine (connected to infinite bus) system would be studied extensively in this chapter.

Example 12.4 In the system of Example 12.3, the generator has an inertia constant of 4 MJ/MVA, write the swing equation upon occurrence of the fault. What is the initial angular acceleration? If this acceleration can be assumed to remain constant for $\Delta t = 0.05$ s, find the rotor angle at the end of this time interval and the new acceleration.

Solution

Swing equation upon occurrence of fault,

$$\frac{H}{180f}\frac{d^2\delta}{dt^2} = P_m - P_e$$

$$\frac{4}{180 \times 50}\frac{d^2\delta}{dt^2} = 1 - 0.694 \sin\delta$$

or $$\frac{d^2\delta}{dt^2} = 2250\,(1 - 0.694 \sin \delta)$$

Initial rotor angle $\delta_0 = 33.9°$ (calculated in Example 12.3)

$$\left.\frac{d^2\delta}{dt^2}\right|_{t=0+} = 2250\,(1 - 0.694 \sin 33.9°)$$

$$= 1379 \text{ elect deg/s}^2$$

$$\left.\frac{d\delta}{dt}\right|_{t=0+} = 0;$$ rotor speed cannot change suddenly

$$\Delta\delta \text{ (in } \Delta t = 0.05\,\text{s)} = \frac{1}{2} \times 1379 \times (0.05)^2$$

$$= 1.7°$$

$$\delta_1 = \delta_0 + \Delta\delta = 33.9 + 1.7° = 35.6°$$

$$\left.\frac{d^2\delta}{dt^2}\right|_{t=0.05\ s} = 2250\,(1 - 0.694 \sin 35.6°)$$

$$= 1341 \text{ elect deg/s}^2$$

Observe that as the rotor angle increases, the electrical power output of the generator increases and so the acceleration of the rotor reduces.

12.6 STEADY STATE STABILITY

The steady state stability limit of a particular circuit of a power system is defined as the maximum power that can be transmitted to the receiving end without loss of synchronism.

Consider the simple system of Fig. 12.14 whose dynamics is described by equations

$$M\frac{d^2\delta}{dt^2} = P_m - P_e \text{ MW; Eq. (12.8)}$$

$$M = \frac{H}{\pi f} \text{ in pu system} \qquad (12.45)$$

and $$P_e = \frac{|E||V|}{X_d} \sin \delta = P_{\max} \sin \delta \qquad (12.46)$$

For determination of steady state stability, the direct axis reactance (X_d) and voltage behind X_d are used in the above equations.

The plot of Eq. (12.46) is given in Fig. 12.6. Let the system be operating with steady power transfer of $P_{e0} = P_m$ with torque angle δ_0 as indicated in the figure.

Assume a small increment ΔP in the electric power with the input from the prime mover remaining fixed at P_m (governor response is slow compared to the speed of energy dynamics), causing the torque angle to change to $(\delta_0 + \Delta\delta)$. Linearizing about the operating point Q_0 (P_{e0}, δ_0) we can write

$$\Delta P_e = \left(\frac{\partial P_e}{\partial \delta}\right)_0 \Delta\delta$$

The excursions of $\Delta\delta$ are then described by

$$M \frac{\mathrm{d}^2 \Delta\delta}{\mathrm{d}t^2} = P_m - (P_{e0} + \Delta P_e) = -\Delta P_e$$

or

$$M \frac{\mathrm{d}^2 \Delta\delta}{\mathrm{d}t^2} + \left[\frac{\partial P_e}{\partial \delta}\right]_0 \Delta\delta = 0 \tag{12.47}$$

or

$$\left[Mp^2 + \left(\frac{\partial P_e}{\partial \delta}\right)_0\right] \Delta\delta = 0$$

where $p = \dfrac{\mathrm{d}}{\mathrm{d}t}$.

The system stability to small changes is determined from the characteristic equation

$$Mp^2 + \left[\frac{\partial P_e}{\partial \delta}\right]_0 = 0$$

whose two roots are

$$p = \pm \left[\frac{-(\partial P_e/\partial \delta)_0}{M}\right]^{\frac{1}{2}}$$

As long as $(\partial P_e/\partial \delta)_0$ is positive, the roots are purely imaginary and conjugate and the system behaviour is oscillatory about δ_0. Line resistance and damper windings of machine, which have been ignored in the above modelling, cause the system oscillations to decay, the system is therefore stable for a small increment in power as long as

$$(\partial P_e/\partial \delta)_0 > 0 \tag{12.48}$$

When $(\partial P_e/\partial \delta)_0$ is negative, the roots are real, one positive and the other negative but of equal magnitude. The torque angle therefore increase without bound upon occurrence of a small power increment (disturbance) and the synchronism is soon lost. The system is therefore unstable for

$$(\partial P_e/\partial \delta)_0 < 0$$

$(\partial P_e/\partial d)_0$ is known as *synchronizing coefficient*. This is also called *stiffness* (electrical) of synchronous machine.

Assuming $|E|$ and $|V|$ to remain constant, the system is unstable, if

$$\frac{|E||V|}{X} \cos \delta_0 < 0$$

or
$$\delta_0 > 90^\circ \tag{12.49}$$

The maximum power that can be transmitted without loss of stability (steady state) occurs for

$$\delta_0 = 90^\circ \tag{12.50}$$

and is given by

$$P_{\max} = \frac{|E||V|}{X} \tag{12.51}$$

If the system is operating below the limit of steady stability condition (Eq. 12.48), it may continue to oscillate for a long time if the damping is low. Persistent oscillations are a threat to system security. The study of system damping is the study of dynamical stability.

The above procedure is also applicable for complex systems wherein governor action and excitation control are also accounted for. The describing differential equation is linearized about the operating point. Condition for steady state stability is then determined from the corresponding characteristic equation (which now is of order higher than two).

It was assumed in the above account that the internal machine voltage $|E|$ remains constant (i.e., excitation is held constant). The result is that, as loading increases, the terminal voltage $|V_t|$ dips heavily which cannot be tolerated in practice. Therefore, we must consider the steady state stability limit by assuming that excitation is adjusted for every load increase to keep $|V_t|$ constant. This is how the system will be operated practically. It may be understood that we are still not considering the effect of automatic excitation control.

Steady state stability limit with $|V_t|$ and $|V|$ constant is considered in Example 12.6.

Example 12.5 A synchronous generator of reactance 1.20 pu is connected to an infinite bus bar ($|V| = 1.0$ pu) through transformers and a line of total reactance of 0.60 pu. The generator no load voltage is 1.20 pu and its inertia constant is $H = 4$ MW-s/MVA. The resistance and machine damping may be assumed negligible. The system frequency is 50 Hz.

Calculate the frequency of natural oscillations if the generator is loaded to (i) 50% and (ii) 80% of its maximum power limit.

Solution

(i) For 50% loading

$$\sin \delta_0 = \frac{P_e}{P_{\max}} = 0.5 \text{ or } \delta_0 = 30^\circ$$

$$\left[\frac{\partial P_e}{\partial \delta}\right]_{30^\circ} = \frac{1.2 \times 1}{1.8} \cos 30^\circ$$

$$= 0.577 \text{ MW (pu)/elect rad}$$

$$M(\text{pu}) = \frac{H}{\pi \times 50} = \frac{4}{\pi \times 50} \text{ s}^2\text{/elect rad}$$

From characteristic equation

$$p = \pm j\left[\left(\frac{\partial P_e}{\partial \delta}\right)_{30^\circ} \Big/ M\right]^{\frac{1}{2}}$$

$$= \pm j\left(\frac{0.577 \times 50\,\pi}{4}\right)^{\frac{1}{2}} = \pm j4.76$$

Frequency of oscillations = 4.76 rad/sec

$$= \frac{4.76}{2\pi} = 0.758 \text{ Hz}$$

(ii) For 80% loading

$$\sin \delta_0 = \frac{P_e}{P_{\max}} = 0.8 \text{ or } \delta_0 = 53.1^\circ$$

$$\left(\frac{\partial P_e}{\partial \delta}\right)_{53.1^\circ} = \frac{1.2 \times 1}{1.8} \cos 53.1^\circ$$

$$= 0.4 \text{ MW (pu)/elect rad}$$

$$p = \pm j\left(\frac{0.4 \times 50\,\pi}{4}\right)^{\frac{1}{2}} = \pm j3.96$$

Frequency of oscillations = 3.96 rad/sec

$$= \frac{3.96}{2\pi} = 0.63 \text{ Hz}$$

Example 12.6 Find the steady state power limit of a system consisting of a generator equivalent reactance 0.50 pu connected to an infinite bus through a series reactance of 1.0 pu. The terminal voltage of the generator is held at 1.20 pu and the voltage of the infinite bus is 1.0 pu.

Solution

The system is shown in Fig. 12.16. Let the voltage of the infinite bus be taken as reference. Then

$$V = 1.0 \angle 0^\circ,\ V_t = 1.2 \angle \theta$$

Now
$$I = \frac{V_t - V}{jX} = \frac{1.2 \angle \theta - 1.0}{j1}$$

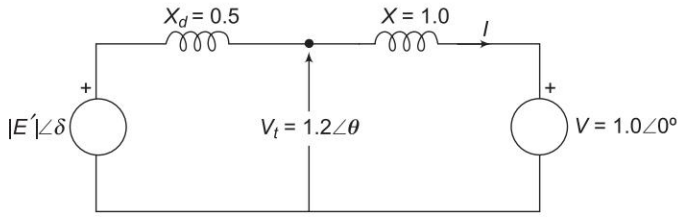

Fig. 12.16

$$E = V_t + jX_d I = 1.2 \angle \theta + j0.5 \left[\frac{1.2 \angle \theta - 1.0}{j1}\right]$$

or

$$E = 1.8 \angle \theta - 0.5 = (1.8 \cos \theta - 0.5) + j1.8 \sin \theta$$

Steady state power limit is reached when E has an angle of $\delta = 90^\circ$, i.e., its real part is zero. Thus,

$$1.8 \cos \theta - 0.5 = 0$$

or

$$\theta = 73.87^\circ$$

Now

$$V_t = 1.2 \angle 73.87^\circ = 0.332 + j1.152$$

$$I = \frac{0.332 + j1.152 - 1}{j1} = 1.152 + j0.668$$

$$E = 0.332 + j1.152 + j0.5\ (1.152 + j0.668)$$

$$= -0.002 + j1.728 \simeq 1.728 \angle 90^\circ$$

Steady state power limit is given by

$$P_{\max} = \frac{|E|\,|V|}{X_d + X} = \frac{1.728 \times 1}{1.5} = 1.152 \text{ pu}$$

If instead, the generator emf is held fixed at a value of 1.2 pu, the steady state power limit would be

$$P_{\max} = \frac{1.2 \times 1}{1.5} = 0.8 \text{ pu}$$

It is observed that regulating the generator emf to hold the terminal generator voltage at 1.2 pu raises the power limit from 0.8 pu to 1.152 pu; this is how the voltage regulating loop helps in power system stability.

Some Comments on Steady State Stability

A knowledge of steady state stability limit is important for various reasons. A system can be operated above its transient stability limit but not above its steady state limit. Now, with increased fault clearing speeds, it is possible to make the transient limit closely approach the steady state limit.

As is clear from Eq. (12.51), the methods of improving steady state stability limit of a system are to reduce X and increase either or both $|E|$ and $|V|$. If the transmission lines are of sufficiently high reactance, the stability limit can be raised by using two parallel lines which incidentally also increases the reliability of the system. Series capacitors are sometimes employed in lines to get better voltage regulation and to raise the stability limit by decreasing the line reactance. Higher excitation voltages and quick excitation system are also employed to improve the stability limit.

12.7 TRANSIENT STABILITY

It has been shown in Sec. 12.4 that the dynamics of a single synchronous machine connected to infinite bus bars is governed by the nonlinear differential equation

$$M \frac{\mathrm{d}^2\delta}{\mathrm{d}t^2} = P_m - P_e$$

where $$P_e = P_{\max} \sin\delta$$

or $$M \frac{\mathrm{d}^2\delta}{\mathrm{d}t^2} = P_m - P_{\max} \sin\delta \qquad (12.52)$$

As said earlier, this equation is known as the *swing equation*. No closed form solution exists for swing equation except for the simple case $P_m = 0$ (not a practical case) which involves elliptical integrals. For small disturbance (say, gradual loading), the equation can be linearized (see Sec. 12.6) leading to the concept of steady state stability where a unique criterion of stability ($\partial P_e/\partial d > 0$) could be established. No generalized criteria are available* for determining system stability with large disturbances (called transient stability). The practical approach to the transient stability problem is therefore to list all important severe disturbances along with their possible locations to which the system is likely to be subjected according to the experience and judgement of the power system analyst. Numerical solution of the swing equation (or equations for a multimachine case) is then obtained in the presence of such disturbances giving a plot of δ *v*. t called the *swing curve*. If δ starts to decrease after reaching a maximum value, it is normally assumed that the system is stable and the oscillation of δ around the equilibrium point will decay and finally die

* Recent literature gives methods of determining transient stability through Liapunov and Popov's stability criteria, but these have not been of partical use so far.

out. As already pointed out in the introduction, important severe disturbances are a short circuit or a sudden loss of load.

For ease of analysis certain assumptions and simplifications are always made (some of these have already been made in arriving at the swing equation (Eq. (12.52)). All the assumptions are listed, below along with their justification and consequences upon accuracy of results.

1. Transmission line as well as synchronous machine resistance are ignored. This leads to pessimistic result as resistance introduces damping term in the swing equation which helps stability. In Example 12.11, line resistance has been taken into account.
2. Damping term contributed by synchronous machine damper windings is ignored. This also leads to pessimistic results for the transient stability limit.
3. Rotor speed is assumed to be synchronous. In fact it varies insignificantly during the course of the stability transient.
4. Mechanical input to machine is assumed to remain constant during the transient, i.e., regulating action of the generator loop is ignored. This leads to pessimistic results.
5. Voltage behind transient reactance is assumed to remain constant, i.e., action of voltage regulating loop is ignored. It also leads to pessimistic results.
6. Shunt capacitances are not difficult to account for in a stability study. Where ignored, no greatly significant error is caused.
7. Loads are modelled as constant admittances. This is a reasonably accurate representation.

Note: Since rotor speed and hence frequency vary insignificantly, the network parameters remain fixed during a stability study.

A digital computer programme to compute the transient following sudden disturbance can be suitably modified to include the effect of governor action and excitation control.

Present day power systems are so large that even after lumping of machines (Eq. (12.17)), the system remains a multimachine one. Even then, a simple two-machine system greatly aids the understanding of the transient stability problem. It has been shown in Sec. 12.4 that an equivalent single-machine infinite bus system can be found for a two-machine system (Eqs (12.41) to (12.43)).

Upon occurrence of a severe disturbance, say a short circuit, the power transfer between the machines is greatly reduced, causing the machine torque angles to swing relatively. The circuit breakers near the fault disconnect the unhealthy part of the system so that power transfer can be partially restored, improving the chances of the system remaining stable. The shorter the time to breaker operating, called *clearing time*, the higher is the probability of the system being stable. Most of the line faults are transient in nature and get cleared on opening the line. Therefore, it is common practice now to employ *autoreclose breakers* which automatically close rapidly after each of the two

sequential openings. If the fault still persists, the circuit breakers open and lock permanently till cleared manually. Since in the majority of faults the first reclosure will be successful, the chances of system stability are greatly enhanced by using autoreclose breakers.

The procedure of determining the stability of a system upon occurrence of a disturbance followed by various switching 'off' and switching 'on' actions is called a *stability study*. Steps to be followed in a stability study are outlined below for a single-machine infinite bus bar system shown in Fig. 12.17. The fault is assumed to be a transient one which is cleared by the time of first reclosure. In the case of a permanent fault, this system completely falls apart. This will not be the case in a multimachine system. The steps listed, in fact, apply to a system of any size.

Fig. 12.17

1. From prefault loading, determine the voltage behind transient reactance and the torque angle δ_0 of the machine with reference to the infinite bus.
2. For the specified fault, determine the power transfer equation $P_e(\delta)$ during fault. In this system $P_e = 0$ for a three-phase fault.
3. From the swing equation starting with δ_0 as obtained in step 1, calculate δ as a function of time using a numerical technique of solving the non-linear differential equation.
4. After clearance of the fault, once again determine $P_e(\delta)$ and solve further for $\delta(t)$. In this case, $P_e(\delta) = 0$ as when the fault is cleared, the system gets disconnected.
5. After the transmission line is switched 'on', again find $P_e(\delta)$ and continue to calculate $\delta(t)$.
6. If $\delta(t)$ goes through a maximum value and starts to reduce, the system is regarded as stable. It is unstable if $\delta(t)$ continues to increase. Calculation is ceased after a suitable length of time.

An important numerical method of calculating $\delta(t)$ from the swing equation will be given in Sec. 12.9. For the single machine infinite bus bar system, stability can be conveniently determined by the equal area criterion presented in the following section.

12.8 EQUAL AREA CRITERION

In a system where one machine is swinging with respect to an infinite bus, it is possible to study transient stability by means of a simple criterion, without resorting to the numerical solution of a swing equation.

Consider the swing equation

$$\frac{d^2\delta}{dt^2} = \frac{1}{M}(P_m - P_e) = \frac{P_a}{M}; \; P_a = \text{accelerating power}$$

$$M = \frac{H}{\pi f} \text{ in pu system} \tag{12.53}$$

If the system is unstable δ continues to increase indefinitely with time and the machine loses synchronism. On the other hand, if the system is stable, $\delta(t)$ performs oscillations (nonsinusoidal) whose amplitude decreases in actual practice because of damping terms (not included in the swing equation). These two situations are shown in Fig. 12.18. Since the system is non-linear, the nature of its response $[\delta(t)]$ is not unique and it may exhibit instability in a fashion different from that indicated in Fig. 12.18, depending upon the nature and severity of disturbance. However, experience indicates that the response $\delta(t)$ in a power system generally falls in the two broad categories as shown in the figure. It can easily be visualized now (this has also been stated earlier) that for a stable system, indication of stability will be given by observation of the first swing where δ will go to a maximum and will start to reduce. This fact can be stated as a stability criterion, that the system is stable if at some time

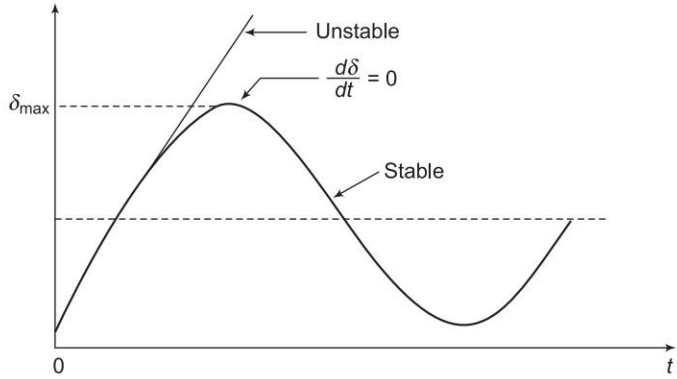

Fig. 12.18 Plot of δ *vs.* t for stable and unstable systems

$$\frac{d\delta}{dt} = 0 \tag{12.54}$$

and is unstable, if

$$\frac{d\delta}{dt} > 0 \tag{12.55}$$

for a sufficiently long time (more than 1 s will generally do).

The stability criterion for power systems stated above can be converted into a simple and easily applicable form for a single machine infinite bus system.

Multiplying both sides of the swing equation by $\left(2\frac{\mathrm{d}\delta}{\mathrm{d}t}\right)$, we get

$$2\,\frac{\mathrm{d}\delta}{\mathrm{d}t}\cdot\frac{\mathrm{d}^2\delta}{\mathrm{d}t^2}=\frac{2P_a}{M}\frac{\mathrm{d}\delta}{\mathrm{d}t}$$

Integrating, we have

$$\left(\frac{\mathrm{d}\delta}{\mathrm{d}t}\right)^2=\frac{2}{M}\int_{\delta_0}^{\delta}P_a\,\mathrm{d}\delta$$

or
$$\frac{\mathrm{d}\delta}{\mathrm{d}t}=\left(\frac{2}{M}\int_{\delta_0}^{\delta}P_a\,\mathrm{d}\delta\right)^{\frac{1}{2}} \tag{12.56}$$

where δ_0 is the initial rotor angle before it begins to swing due to disturbance.

From Eqs (12.55) and (12.56), the condition for stability can be written as

$$\left(\frac{2}{M}\int_{\delta_0}^{\delta}P_a\,\mathrm{d}\delta\right)^{\frac{1}{2}}=0$$

or
$$\int_{\delta_0}^{\delta}P_a\,\mathrm{d}\delta=0 \tag{12.57}$$

The condition of stability can therefore be stated as: the system is stable if the area under P_a (accelerating power) – δ curve reduces to zero at some value of δ. In other words, the positive (accelerating) area under $P_a-\delta$ curve must equal the negative (decelerating) area and hence the name 'equal area' criterion of stability.

To illustrate the equal area criterion of stability, we now consider several types of disturbances that may occur in a single machine infinite bus bar system.

Sudden Change in Mechanical Input

Figure 12.19 shows the transient model of a single machine tied to infinite bus bar. The electrical power transmitted is given by

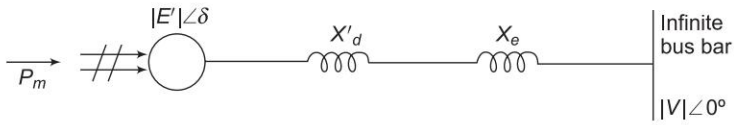

Fig. 12.19

$$P_e = \frac{|E'||V|}{X'_d + X_e} \sin\delta = P_{\max} \sin\delta$$

Under steady operating condition

$$P_{m0} = P_{e0} = P_{\max} \sin\delta_0$$

This is indicated by the point a in the $P_e - \delta$ diagram of Fig. 12.20.

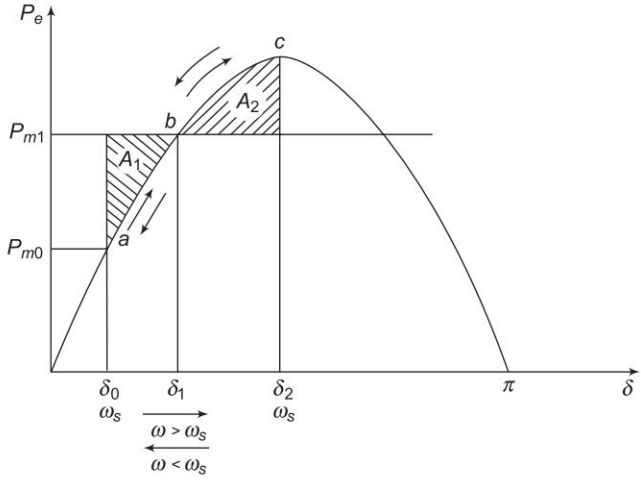

Fig. 12.20 $P_e = \delta$ diagram for sudden increase in mechanical input to generator of Fig. 12.19

Let the mechanical input to the rotor be suddenly increased to P_{m1} (by opening the steam valve). The accelerating power $P_a = P_{m1} - P_e$ causes the rotor speed to increase ($\omega > \omega_s$) and so does the rotor angle. At angle δ_1, $P_a = P_{m1} - P_e$ ($= P_{\max} \sin\delta_1$) = 0 (state point at b) but the rotor angle continues to increase as $\omega > \omega_s$. P_a now becomes negative (decelerating), the rotor speed begins to reduce but the angle continues to increase till at angle δ_2, $\omega = \omega_s$ once again (state point at c). At c, the decelerating area A_2 equals the accelerating area A_1 (areas are shaded), i.e., $\int_{\delta_0}^{\delta_2} P_a \, d\delta = 0$. Since the rotor is decelerating, the speed reduces below ω_s and the rotor angle begins to reduce. The state point now traverses the $P_e - \delta$ curve in the opposite direction as indicated by arrows in Fig. 12.20. It is easily seen that the system oscillates about the new steady state point b ($\delta = \delta_1$) with angle excursion up to δ_0 and δ_2 on the two sides. These oscillations are similar to the simple harmonic motion of an inertia–spring system except that these are not sinusoidal.

As the oscillations decay out because of inherent system damping (not modelled), the system settles to the new steady state where

$$P_{m1} = P_e = P_{\max} \sin \delta_1$$

From Fig. 12.20, areas A_1 and A_2 are given by

$$A_1 = \int_{\delta_0}^{\delta_1} (P_{m1} - P_e)\, \mathrm{d}\delta$$

$$A_2 = \int_{\delta_1}^{\delta_2} (P_e - P_{m1})\, \mathrm{d}\delta$$

For the system to be stable, it should be possible to find angle δ_2 such that $A_1 = A_2$. As P_{m1} is increased, a limiting condition is finally reached when A_1 equals the area above the P_{m1} line as shown in Fig. 12.21. Under this condition, δ_2 acquires the maximum value such that

$$\delta_2 = \delta_{\max} = \pi - \delta_1 = \pi - \sin^{-1} \frac{P_{m1}}{P_{\max}} \tag{12.58}$$

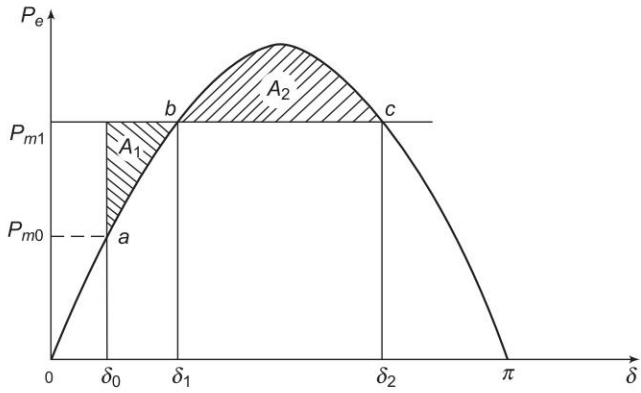

Fig. 12.21 Limiting case of transient stability with mechanical input suddenly increased

Any further increase in P_{m1} means that the area available for A_2 is less than A_1, so that the excess kinetic energy causes δ to increase beyond point c and the decelerating power changes over to accelerating power, with the system consequently becoming unstable. It has thus been shown by use of the equal area criterion that there is an upper limit to sudden increase in mechanical input $(P_{m1} - P_{m0})$, for the system in question to remain stable.

It may also be noted from Fig. 12.21 that the system will remain stable even though the rotor may oscillate beyond $\delta = 90^\circ$, so long as the equal area criterion is met. The condition of $\delta = 90^\circ$ is meant for use in steady state stability only and does not apply to the transient stability case.

Effect of Clearing Time on Stability

Let the system of Fig. 12.22 be operating with mechanical input P_m at a steady angle of δ_0 ($P_m = P_e$) as shown by the point a on the P_e–δ diagram of Fig. 12.23. If a three-phase fault occurs at the point P of the outgoing radial line, the electrical output of the generator instantly reduces to zero, i.e., $P_e = 0$ and the state point drops to b. The acceleration area A_1 begins to increase and so does the rotor angle while the state point moves along bc. At time t_c corresponding to angle δ_c the faulted line is cleared by the opening of the line circuit breaker. The values of t_c and δ_c are respectively known as *clearing time* and *clearing angle*. The system once again becomes healthy and transmits $P_e = P_{\max} \sin \delta$, i.e. the state point shifts to d on the original P_e–δ curve. The rotor now decelerates and the decelerating area A_2 begins while the state point moves along de.

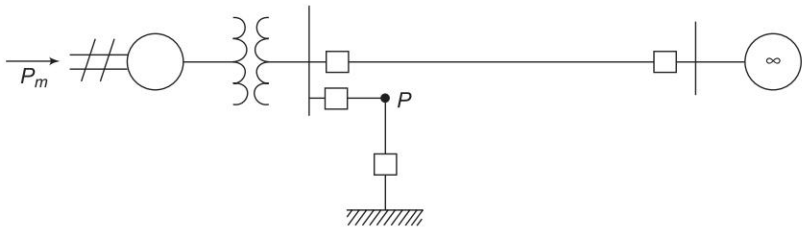

Fig. 12.22

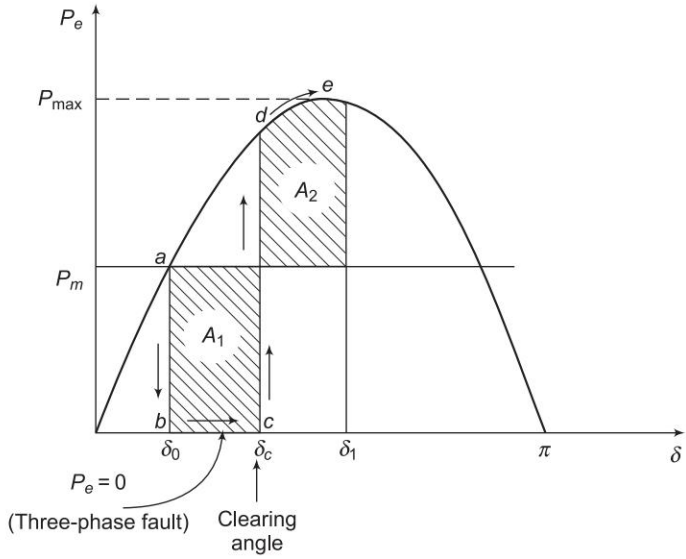

Fig. 12.23

If an angle δ_1 can be found such that $A_2 = A_1$, the system is found to be stable. The system finally settles down to the steady operating point a in an oscillatory manner because of inherent damping.

The value of clearing time corresponding to a clearing angle can be established only by numerical integration except in this simple case. The equal area criterion therefore gives only qualitative answer to system stability as the time when the breaker should be opened is hard to establish.

As the clearing of the faulty line is delayed, A_1 increases and so does δ_1 to find $A_2 = A_1$ till $\delta_1 = \delta_{\max}$ as shown in Fig. 12.24. For a clearing time (or angle) larger than this value, the system would be unstable as $A_2 < A_1$. The maximum allowable value of the clearing time and angle for the system to remain stable are known respectively as *critical clearing time* and *angle*.

For this simple case (P_e = 0 during fault), explicit relationships for δ_c (critical) and t_c (critical) are established below. All angles are in radians.

It is easily seen from Fig. 12.24 that

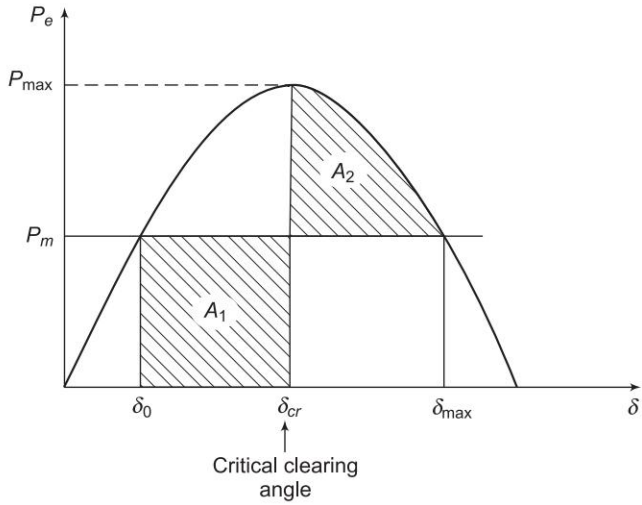

Fig. 12.24 Critical clearing angle

$$\delta_{\max} = \pi - \delta_0 \tag{12.59}$$

and

$$P_m = P_{\max} \sin \delta_0 \tag{12.60}$$

Now

$$A_1 = \int_{\delta_0}^{\delta_{cr}} (P_m - 0)\, \mathrm{d}\delta = P_m (\delta_{cr} - \delta_0)$$

and

$$A_2 = \int_{\delta_{cr}}^{\delta_{\max}} (P_{\max} \sin \delta - P_m)\, \mathrm{d}\delta$$

$$= P_{\max} (\cos \delta_{cr} - \cos \delta_{\max}) - P_m (\delta_{\max} - \delta_{cr})$$

For the system to be stable, $A_2 = A_1$, which yields

$$\cos \delta_{cr} = \frac{P_m}{P_{\max}} (\delta_{\max} - \delta_0) + \cos \delta_{\max} \tag{12.61}$$

where δ_{cr} = critical clearing angle

Substituting Eqs (12.59) and (12.60) in Eq. (12.61), we get

$$\delta_{cr} = \cos^{-1} [(\pi - 2\delta_0) \sin \delta_0 - \cos \delta_0] \tag{12.62}$$

During the period the fault is persisting, the swing equation is

$$\frac{d^2\delta}{dt^2} = \frac{\pi f}{H} P_m; P_e = 0 \tag{12.63}$$

Integrating twice

$$\delta = \frac{\pi f}{2H} P_m t^2 + \delta_0$$

or

$$\delta_{cr} = \frac{\pi f}{2H} P_m t^2_{cr} + \delta_0 \tag{12.64}$$

where t_{cr} = critical clearing time

δ_{cr} = critical clearing angle

From Eq. (12.64)

$$t_{cr} = \left(\frac{2H (\delta_{cr} - \delta_0)}{\pi f P_m} \right)^{\frac{1}{2}} \tag{12.65}$$

where δ_{cr} is given by the expression of Eq. (12.62)

An explicit relationship for determining t_{cr} is possible in this case as during the faulted condition P_e=0 and so the swing equation can be integrated in closed form. This will not be the case in most other situations.

Sudden Loss of one of Parallel Lines

Consider now a single machine tied to infinite bus through two parallel lines as in Fig. 12.25(a). Circuit model of the system is given in Fig. 12.25(b).

Let us study the transient stability of the system when one of the lines is suddenly switched off with the system operating at a steady load. Before switching off, power angle curve is given by

$$P_{eI} = \frac{|E'||V|}{X'_d + X_1 \| X_2} \sin \delta = P_{\max I} \sin \delta$$

Immediately on switching off line 2, power angle curve is given by

$$P_{eII} = \frac{|E'||V|}{X'_d + X_1} \sin \delta = P_{\max II} \sin \delta$$

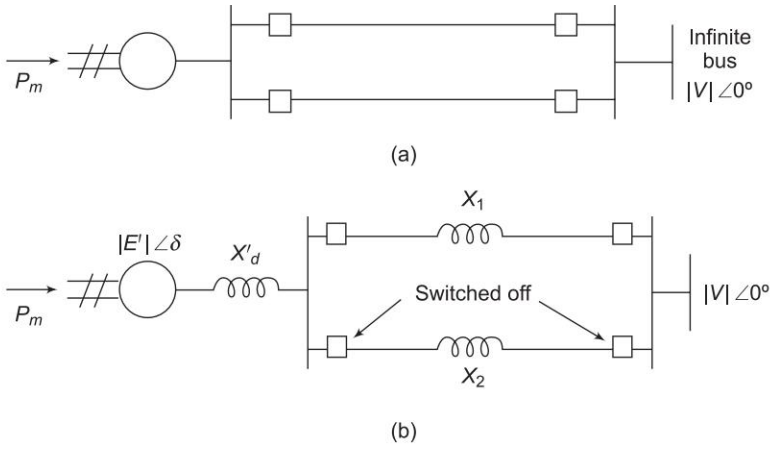

Fig. 12.25 Single machine tied to infinite bus through two parallel lines

Both these curves are plotted in Fig. 12.26, wherein $P_{\text{max II}} < P_{\text{max I}}$ as $(X'_d + X_1) > (X'_d + X_1 \parallel X_2)$. The system is operating initially with a steady power transfer $P_d = P_m$ at a torque angle δ_0 on curve I.

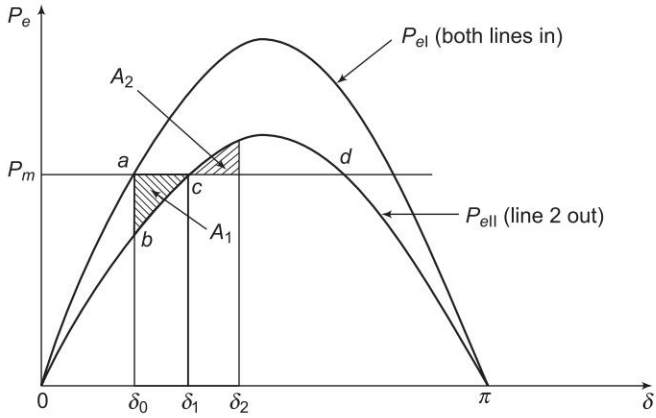

Fig. 12.26 Equal area criterion applied to the opening of one of the two lines in parallel

Immediately on switching off line 2, the electrical operating point shifts to curve II (point *b*). Accelerating energy corresponding to area A_1 is put into rotor followed by decelerating energy for $\delta > \delta_1$. Assuming that an area A_2 corresponding to decelerating energy (energy out of rotor) can be found such that $A_1 = A_2$, the system will be stable and will finally operate at *c* corresponding to a new rotor angle $\delta_1 > \delta_0$. This is so because a single line offers larger reactance and larger rotor angle is needed to transfer the same steady power.

It is also easy to see that if the steady load is increased (line P_m is shifted upwards in Fig. 12.26), a limit is finally reached beyond which decelerating area equal to A_1 cannot be found and therefore, the system behaves as an unstable one. For the limiting case of stability, δ_1 has a maximum value given by

$$\delta_1 = \delta_{\max} = \pi - \delta_c$$

which is the same condition as in the previous example.

Sudden Short Circuit on One of Parallel Lines

Case a: Short circuit at one end of line

Let us now assume the disturbance to be a short circuit at the generator end of line 2 of a double circuit line as shown in Fig. 12.27(a). We shall assume the fault to be a three-phase one.

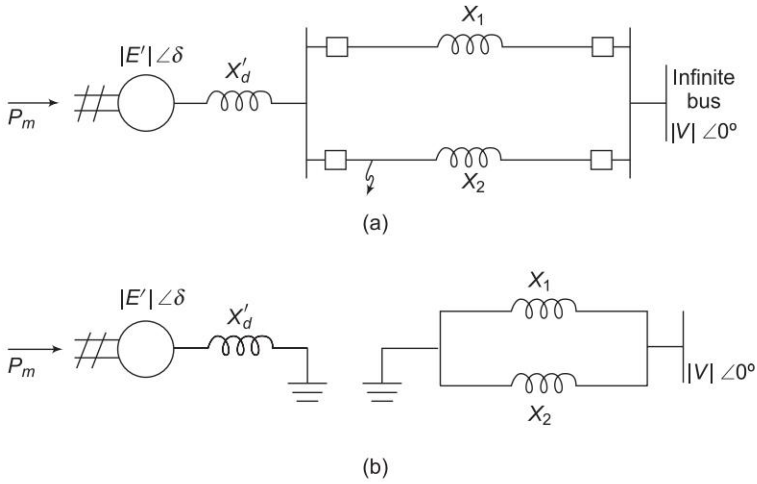

Fig. 12.27 Short circuit at one end of the line

Before the occurrence of a fault, the power angle curve is given by

$$P_{e\mathrm{I}} = \frac{|E'||V|}{X'_d + X_1 \| X_2} \sin\delta = P_{\max\mathrm{I}} \sin\delta$$

which is plotted in Fig. 12.25.

Upon occurrence of a three-phase fault at the generator end of line 2 (see Fig. 12.24(a)), the generator gets isolated from the power system for purposes of power flow as shown by Fig. 12.27(b). Thus during the period the fault lasts,

$$P_{e\mathrm{II}} = 0$$

The rotor therefore accelerates and angles δ increases. Synchronism will be lost unless the fault is cleared in time.

The circuit breakers at the two ends of the faulted line open at time t_c (corresponding to angle δ_c), the clearing time, disconnecting the faulted line. The power flow is now restored via the healthy line (through higher line reactance X_2 in place of $X_1 \parallel X_2$), with power angle curve

$$P_{e\text{III}} = \frac{|E'||V|}{X'_d + X_1} \sin\delta = P_{\max\text{ II}} \sin\delta$$

Obviously, $P_{\max\text{II}} < P_{\max\text{I}}$. The rotor now starts to decelerate as shown in Fig. 12.28. The system will be stable if a decelerating area A_2 can be found equal to accelerating area A_1 before δ reaches the maximum allowable value $\delta_{\max}$. As area A_1 depends upon clearing time t_c (corresponding to clearing angle δ_c), clearing time must be less than a certain value (critical clearing time) for the system to be stable. It is to be observed that the equal area criterion helps to determine critical clearing angle and not critical clearing time. Critical clearing time can be obtained by numerical solution of the swing equation (discussed in Sec. 12.8).

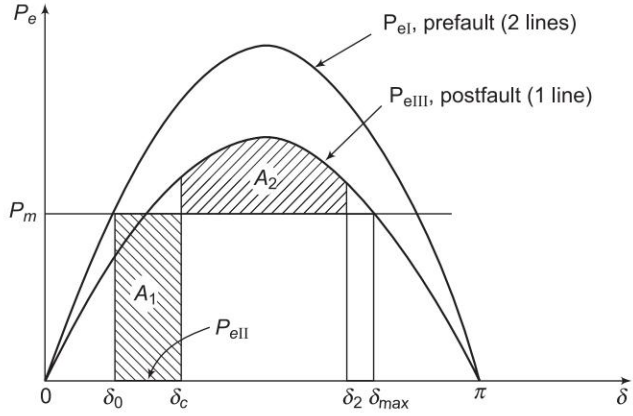

Fig. 12.28 Equal area criterion applied to the system of Fig. 12.24(a), I—system normal, II—fault applied, III—faulted line isolated

It also easily follows that larger initial loading (P_m) increases A_1 for a given clearing angle (and time) and therefore quicker fault clearing would be needed to maintain stable operation.

Case b: Short circuit away from line ends

When the fault occurs away from line ends (say in the middle of a line), there is some power flow during the fault though considerably reduced, as different from case *a* where $P_{e\text{II}} = 0$. Circuit model of the system during fault is now shown in Fig. 12.29(a). This circuit reduces to that of Fig. 12.29(c) through one delta-star and one star-delta conversion. Instead, node elimination technique of Sec. 12.3 could be employed profitably. The power angle curve during fault is therefore given by

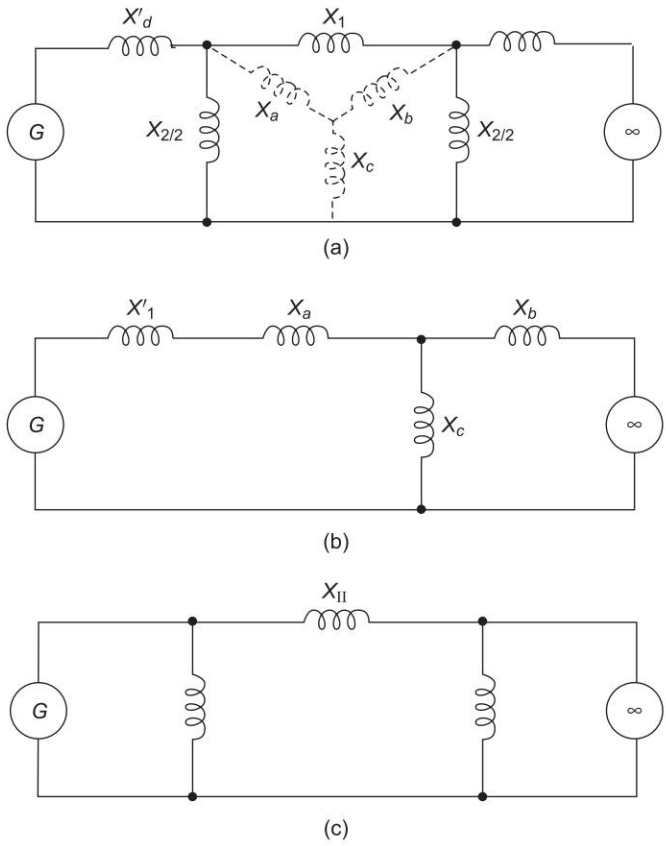

Fig. 12.29

$$P_{e\text{II}} = \frac{|E'||V|}{X_{\text{II}}} \sin \delta = P_{\max\text{II}} \sin \delta$$

$P_{e\text{I}}$ and $P_{e\text{III}}$ as in Fig. 12.28 and $P_{e\text{II}}$ as obtained above are all plotted in Fig. 12.30. Accelerating area A_1 corresponding to a given clearing angle δ_c is less in this case, than in case *a*, giving a better chance for stable operation. Stable system operation is shown in Fig. 12.30, wherein it is possible to find an area A_2 equal to A_1 for $\delta_2 < \delta_{\max}$. As the clearing angle δ_c is increased, area A_1 increases and to find $A_2 = A_1$, δ_2 increases till it has a value $\delta_{\max}$, the maximum allowable for stability. This case of critical clearing angle is shown in Fig. 12.31.

Applying equal area criterion to the case of critical clearing angle of Fig. 12.31, we can write

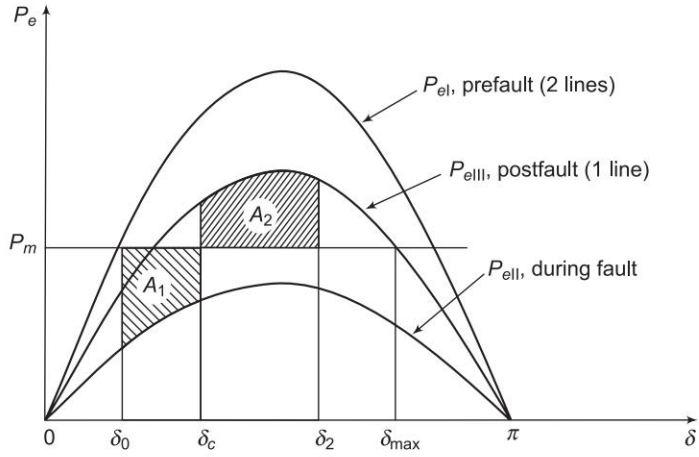

Fig. 12.30 Fault on middle of one line of the system of Fig. 12.24(a) with $\delta_c < \delta_{cr}$

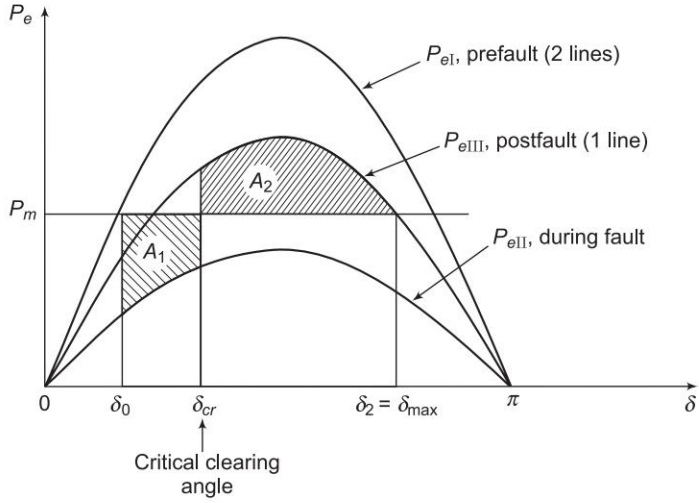

Fig. 12.31 Fault on middle of one line of the system of Fig. 12.24(a), case of critical clearing angle

$$\int_{\delta_0}^{\delta_{cr}} (P_m - P_{\max II} \sin \delta)\, d\delta = \int_{\delta_{cr}}^{\delta_{\max}} (P_{\max III} \sin \delta - P_m)\, d\delta$$

where

$$\delta_{\max} = \pi - \sin^{-1}\left(\frac{P_m}{P_{\max III}}\right) \tag{12.66}$$

Integrating, we get

$$(P_m\delta + P_{\max II}\cos\delta)\Big|_{\delta_0}^{\delta_{cr}} + (P_{\max III}\cos\delta + P_m\delta)\Big|_{\delta_{cr}}^{\delta_{\max}} = 0$$

or

$$P_m(\delta_{cr} - \delta_0) + P_{\max II}(\cos\delta_{cr} - \cos\delta_0) + P_m(\delta_{\max} - \delta_{cr}) + P_{\max III}(\cos\delta_{\max} - \cos\delta_{cr}) = 0$$

or

$$\cos\delta_{cr} = \frac{P_m(\delta_{\max} - \delta_0) - P_{\max II}\cos\delta_0 + P_{\max III}\cos\delta_{\max}}{P_{\max III} - P_{\max II}} \quad (12.67)$$

Critical clearing angle can be calculated from Eq. (12.67) above. The angles in this equation are in radians. The equation modifies as below if the angles are in degrees.

$$\cos\delta_{cr} = \frac{\frac{\pi}{180}P_m(\delta_{\max} - \delta_0) - P_{\max II}\cos\delta_0 + P_{\max III}\cos\delta_{\max}}{P_{\max III} - P_{\max II}}$$

Case c: Reclosure

If the circuit breakers of line 2 are reclosed successfully (i.e., the fault was a transient one and therefore vanished on clearing the faulty line), the power transfer once again becomes

$$P_{e\text{IV}} = P_{e\text{I}} = P_{\max I}\sin\delta$$

Since reclosure restores power transfer, the chances of stable operation improve. A case of stable operation is indicated by Fig. 12.32.

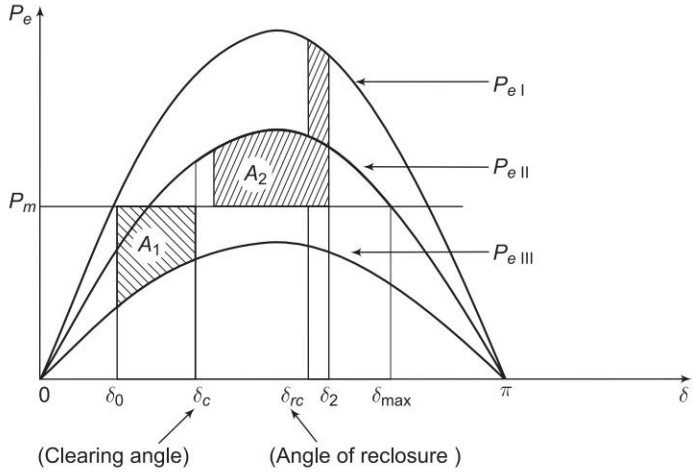

Fig. 12.32 Fault in middle of a line of the system of Fig. 12.27(a)

For critical clearing angle,

$$\delta_1 = \delta_{\max} = \pi - \sin^{-1}(P_m/P_{\max I})$$

$$\int_{\delta_0}^{\delta_{cr}} (P_m - P_{\max II}\sin\delta)\,d\delta = \int_{\delta_{cr}}^{\delta_{rc}} (P_{\max III}\sin\delta - P_m)\,d\delta + \int_{\delta_{rc}}^{\delta_{\max}} (P_{\max I}\sin\delta - P_m)\,d\delta$$

where

$$t_{rc} = t_{cr} + \tau;\ \tau = \text{time between clearing and reclosure.}$$

Example 12.7 Given the system of Fig. 12.33 where a three-phase fault is applied at the point *P* as shown.

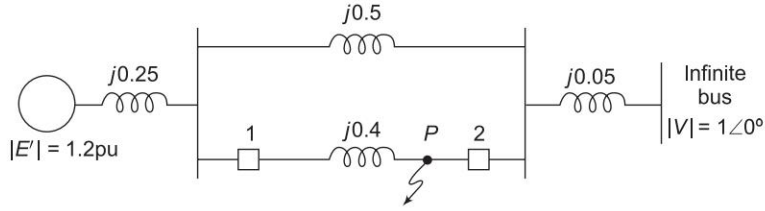

Fig. 12.33

Find the critical clearing angle for clearing the fault with simultaneous opening of the breakers 1 and 2. The reactance values of various components are indicated on the diagram. The generator is delivering 1.0 pu power at the instant preceding the fault.

Solution

With reference to Fig. 12.31, three separate power angle curves are involved.

I. Normal operation (prefault)

$$X_I = 0.25 + \frac{0.5 \times 0.4}{0.5 + 0.4} + 0.05$$

$$= 0.522 \text{ pu}$$

$$P_{eI} = \frac{|E'|\,|V|}{X_I}\sin\delta = \frac{1.2 \times 1}{0.522}\sin\delta$$

$$= 2.3 \sin\delta \qquad \text{(i)}$$

Prefault operating power angle is given by

$$1.0 = 2.3 \sin\delta_0$$

or

$$\delta_0 = 25.8^\circ = 0.45 \text{ radians}$$

II. During fault It is clear from Fig. 12.31 that no power is transferred during fault, i.e.,

$$P_{e\text{II}} = 0$$

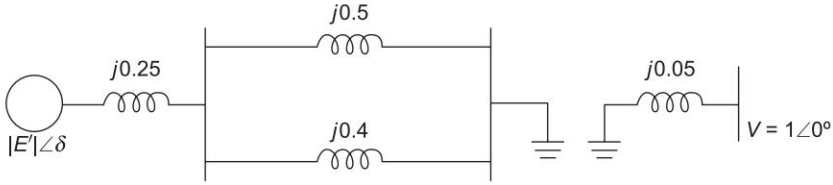

Fig. 12.34

III. Post fault operation (fault cleared by opening the faulted line)

$$X_{\text{III}} = 0.25 + 0.5 + 0.05 = 0.8$$

$$P_{e\text{III}} = \frac{1.2 \times 1.0}{0.8} \sin \delta = 1.5 \sin \delta \qquad \text{(iii)}$$

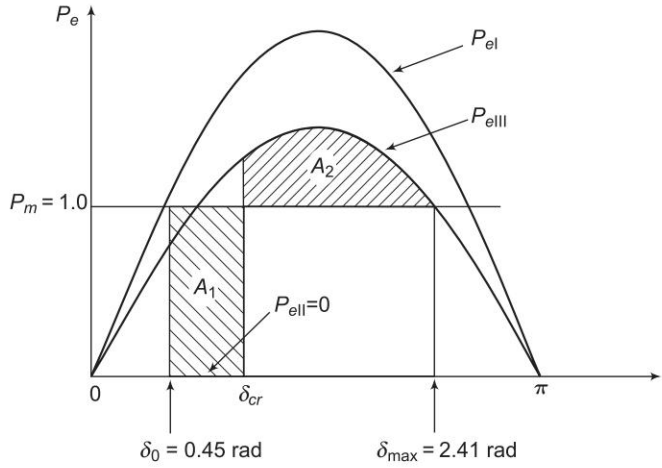

Fig. 12.35

The maximum permissible angle $\delta_{\max}$ for area $A_1 = A_2$ (see Fig. 12.35) is given by

$$\delta_{\max} = \pi - \sin^{-1} \frac{1}{1.5} = 2.41 \text{ radians}$$

Applying equal area criterion for critical clearing angle δ_c

$$A_1 = P_m(\delta_{cr} - \delta_0)$$
$$= 1.0(\delta_{cr} - 0.45) = \delta_{cr} - 0.45$$

$$A_2 = \int_{\delta_{cr}}^{\delta_{\max}} (P_{e\text{III}} - P_m)\, \mathrm{d}\delta$$

$$= \int_{\delta_{cr}}^{2.41} (1.5 \sin\delta - 1)\, \mathrm{d}\delta$$

$$= -1.5 \cos\delta - \delta \Big|_{\delta_{cr}}^{2.41}$$

$$= -1.5(\cos 2.41 - \cos\delta_{cr}) - (2.41 - \delta_{cr})$$
$$= 1.5 \cos\delta_{cr} + \delta_{cr} - 1.293$$

Setting $A_1 = A_2$ and solving

$$\delta_{cr} - 0.45 = 1.5 \cos\delta_{cr} + \delta_{cr} - 1.293$$

or $$\cos\delta_{cr} = 0.843/1.5 = 0.562$$

or $$\delta_{cr} = 55.8^\circ$$

The corresponding power angle diagrams are shown in Fig. 12.35.

Example 12.8 Find the critical clearing angle for the system shown in Fig. 12.36 for a three-phase fault at the point *P*. The generator is delivering 1.0 pu power under prefault conditions.

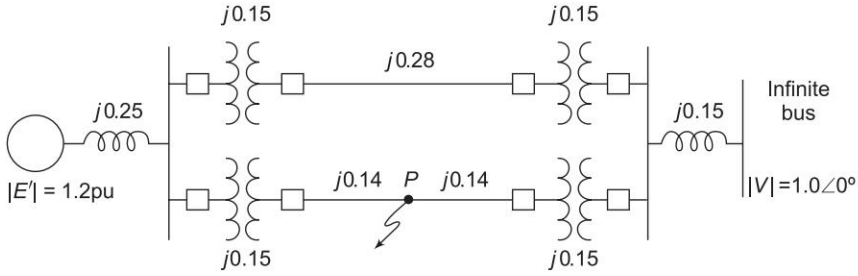

Fig. 12.36

Solution

I. Prefault operation Transfer reactance between generator and infinite bus is

$$X_{\text{I}} = 0.25 + 0.17 + \frac{0.15 + 0.28 + 0.15}{2} = 0.71$$

$$\therefore \quad P_{e1} = \frac{1.2 \times 1}{0.71} \sin \delta = 1.69 \sin \delta \qquad \text{(i)}$$

The operating power angle is given by

$$1.0 = 1.69 \sin \delta_0$$

or $$\delta_0 = 0.633 \text{ rad}$$

II. During fault The positive sequence reactance diagram during fault is presented in Fig. 12.37(a).

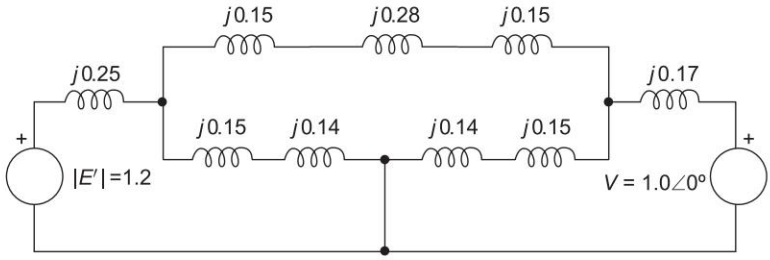

(a) Positive sequence reactance diagram during fault

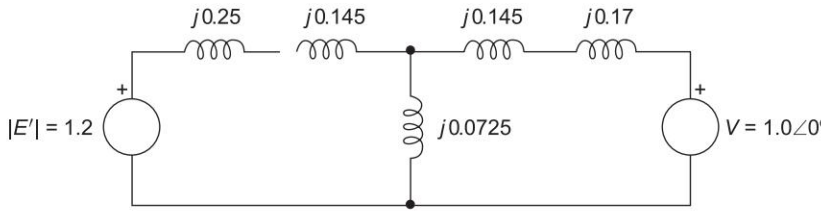

(b) Network after delta-star conversion

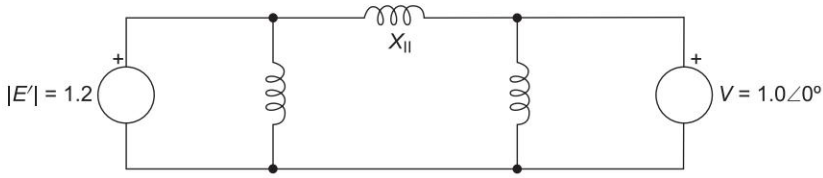

(c) Network after star-delta conversion

Fig. 12.37

Converting delta to star*, the reactance network is changed to that of Fig. 12.37(b). Further, upon converting star to delta, we obtain the reactance network of Fig. 12.37(c). The transfer reactance is given by

* Node elimination technique would be used for complex network.

$$X_{II} = \frac{(0.25+0.145)\,0.0725 + (0.145+0.17)\,0.0725 + (0.25+0.145)\,(0.145+0.17)}{0.075}$$

$$= 2.424$$

$$\therefore \quad P_{eII} = \frac{1.2 \times 1}{2.424} \sin\delta = 0.495 \sin\delta \qquad \text{(ii)}$$

III. Postfault operation (faulty line switched off)

$$X_{III} = 0.25 + 0.15 + 0.28 + 0.15 + 0.17 = 1.0$$

$$P_{eIII} = \frac{1.2 \times 1}{1} \sin\delta = 1.2 \sin\delta \qquad \text{(iii)}$$

With reference to Fig. 12.30 and Eq. (12.66), we have

$$\delta_{max} = \pi - \sin^{-1}\frac{1}{1.2} = 2.155 \text{ rad}$$

To find the critical clearing angle, areas A_1 and A_2 are to be equated.

$$A_1 = 1.0\,(\delta_{cr} - 0.633) - \int_{\delta_0}^{\delta_{cr}} 0.495 \sin\delta\, d\delta$$

and

$$A_2 = \int_{\delta_{cr}}^{\delta\,max} 1.2 \sin\delta\, d\delta - 1.0\,(2.155 - \delta_c)$$

Now

$$A_1 = A_2$$

or

$$\delta_{cr} = 0.633 - \int_{0.633}^{\delta_{cr}} 0.495 \sin\delta\, d\delta$$

$$= \int_{\delta_{cr}}^{2.155} 1.2 \sin\delta\, d\delta - 2.155 + \delta_{cr}$$

or

$$-0.633 + 0.495 \cos\delta \Big|_{0.633}^{\delta_{cr}} = -1.2 \cos\delta \Big|_{\delta_{cr}}^{2.155} - 2.155$$

or

$$-0.633 + 0.495 \cos\delta_{cr} - 0.399 = 0.661 + 1.2 \cos\delta_{cr} - 2.155$$

or

$$\cos\delta_{cr} = 0.655$$

or

$$\delta_{cr} = 49.1^{\circ}$$

Example 12.9 A generator operating at 50 Hz delivers 1 pu power to an infinite bus through a transmission circuit in which resistance is ignored. A fault takes place reducing the maximum power transferable to 0.5 pu whereas before the fault, this power was 2.0 pu and after the clearance of the fault, it is 1.5 pu. By the use of equal area criterion, determine the critical clearing angle.

Solution

All the three power angle curves are shown in Fig. 12.30. Here

$$P_{\text{maxI}} = 2.0 \text{ pu}, P_{\text{maxII}} = 0.5 \text{ pu and } P_{\text{maxIII}} = 1.5 \text{ pu}$$

Initial loading $P_m = 1.0$ pu

$$\delta_0 = \sin^{-1}\left(\frac{P_m}{P_{\text{max I}}}\right) = \sin^{-1}\frac{1}{2} = 0.523 \text{ rad}$$

$$\delta_{\max} = \pi \sin^{-1}\left(\frac{P_m}{P_{\text{max III}}}\right)$$

$$= \pi - \sin^{-1}\frac{1}{1.5} = 2.41 \text{ rad}$$

Applying Eq. (12.67)

$$\cos \delta_{cr} = \frac{1.0(2.41 - 0.523) - 0.5 \cos 0.523 + 1.5 \cos 2.41}{1.5 - 0.5} = 0.337$$

or $\delta_{cr} = 70.3^\circ$

12.9 NUMERICAL SOLUTION OF SWING EQUATION

In most practical systems, after machine lumping has been done, there are still more than two machines to be considered from the point of view of system stability. Therefore, there is no choice but to solve the swing equation of each machine by a numerical technique on the digital computer. Even in the case of a single machine tied to infinite bus bar, the critical clearing time cannot be obtained from equal area criterion and we have to make this calculation numerically through swing equation. There are several sophisticated methods now available for the solution of the swing equation including the powerful Runge-Kutta method. Here we shall treat the point-by-point method of solution which is a conventional, approximate method like all numerical methods but a well tried and proven one. We shall illustrate the point-by-point method for one machine tied to infinite bus bar. The procedure is, however, general and can be applied to every machine of a multimachine system.

Consider the swing equation

$$\frac{d^2\delta}{dt^2} = \frac{1}{M}(P_m - P_{\max}\sin\delta) = P_a/M;$$

$$\left(M = \frac{GH}{\pi} \text{ or in pu system } M = \frac{H}{\pi f}\right)$$

The solution $\delta(t)$ is obtained at discrete intervals of time with interval spread of Δt uniform throughout. Accelerating power and change in speed which are continuous functions of time are discretized as below:

1. The accelerating power P_a computed at the beginning of an interval is assumed to remain constant from the middle of the preceding interval to the middle of the interval being considered as shown in Fig. 12.38.

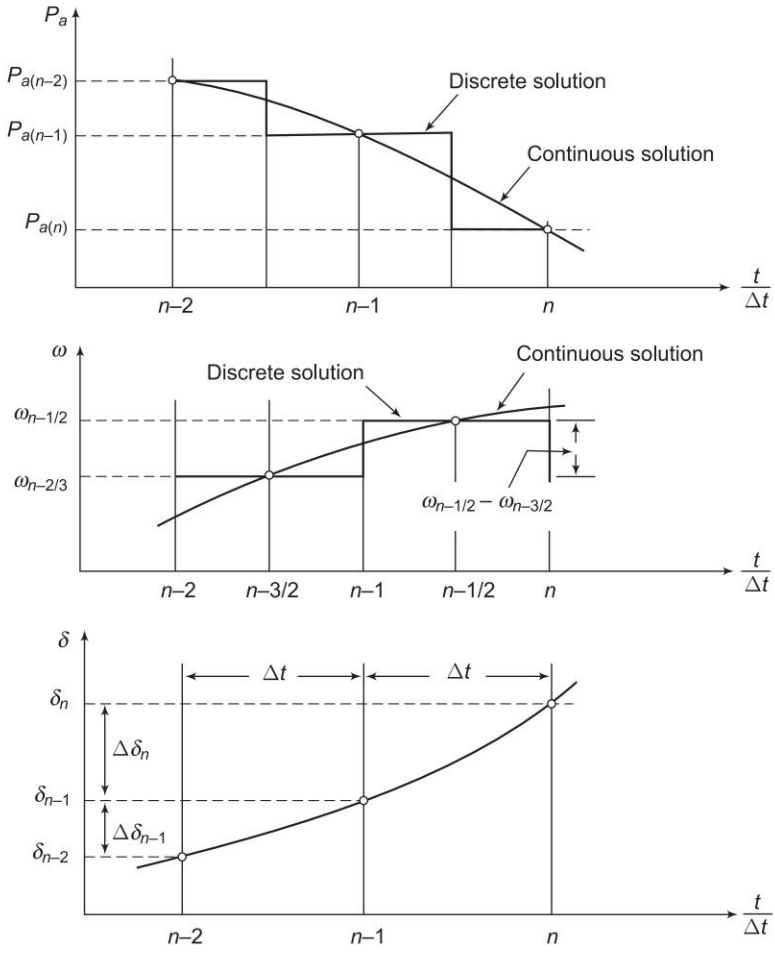

Fig. 12.38 Point-by-point solution of swing equation

2. The angular rotor velocity $\omega = \mathrm{d}\delta/\mathrm{d}t$ (over and above synchronous velocity ω_s) is assumed constant throughout any interval, at the value computed for the middle of the interval as shown in Fig. 12.38.

In Fig. 12.38, the numbering on $t/\Delta t$ axis pertains to the end of intervals. At the end of the $(n-1)$th interval, the acceleration power is

$$P_{a\,(n-1)} = P_m - P_{\max} \sin \delta_{n-1} \tag{12.68}$$

where δ_{n-1} has been previously calculated. The change in velocity ($\omega = \mathrm{d}\delta/\mathrm{d}t$), caused by the $P_{a(n-1)}$, assumed constant over Δt from $(n-3/2)$ to $(n-1/2)$ is

$$\omega_{n-1/2} - \omega_{n-3/2} = (\Delta t/M)\, P_{a(n-1)} \tag{12.69}$$

The change in δ during the $(n-1)$th interval is

$$\Delta\delta_{n-1} = \delta_{n-1} - \delta_{n-2} = \Delta t\, \omega_{n-3/2} \tag{12.70a}$$

and during the nth interval

$$\Delta\delta_n = \delta_n - \delta_{n-1} = \Delta t \omega_{n-1/2} \tag{12.70b}$$

Subtracting Eq. (12.70a) from Eq. (12.70b) and using Eq. (12.69), we get

$$\Delta\delta_n = \Delta\delta_{n-1} + \frac{(\Delta t)^2}{M} P_{a(n-1)} \tag{12.71}$$

Using this, we can write

$$\delta_n = \delta_{n-1} + \Delta\delta_n \tag{12.72}$$

The process of computation is now repeated to obtain $P_{a(n)}$, $\Delta\delta_{n+1}$ and δ_{n+1}. The time solution in discrete form is thus carried out over the desired length of time, normally 0.5 s. Continuous form of solution is obtained by drawing a smooth curve through discrete values as shown in Fig. 12.38. Greater accuracy of solution can be achieved by reducing the time duration of intervals.

The occurrence or removal of a fault or initiation of any switching event causes a discontinuity in accelerating power P_a. If such a discontinuity occurs at the beginning of an interval, then the average of the values of P_a before and after the discontinuity must be used. Thus, in computing the increment of angle occurring during the first interval after a fault is applied at $t = 0$, Eq. (12.71) becomes

$$\Delta\delta_1 = \frac{(\Delta t)^2}{M} + \frac{P_{a0+}}{2}$$

where P_{a0+} is the accelerating power immediately after occurrence of fault. Immediately before the fault the system is in steady state, so that $P_{a0-} = 0$ and δ_0 is a known value. If the fault is cleared at the beginning of the nth interval, in calculation for this interval one should use for $P_{a(n-1)}$ the value $\frac{1}{2}[P_{a(n-1)-} + P_{a(n-1)+}]$, where $P_{a(n-1)-}$ is the accelerating power immediately before clearing and $P_{a(n-1)+}$ is that immediately after clearing the fault. If the discontinuity occurs at the middle of an interval, no special procedure is

needed. The increment of angle during such an interval is calculated, as usual, from the value of P_a at the beginning of the interval.

The procedure of calculating solution of swing equation is illustrated in the following example.

Example 12.10 A 20 MVA, 50 Hz generator delivers 18 MW over a double circuit line to an infinite bus. The generator has kinetic energy of 2.52 MJ/MVA at rated speed. The generator transient reactance is $X'_d = 0.35$ pu. Each transmission circuit has $R = 0$ and a reactance of 0.2 pu on a 20 MVA base. $|E'| = 1.1$ pu and infinite bus voltage $V = 1.0 \angle 0^\circ$. A three-phase short circuit occurs at the mid point of one of the transmission lines. Plot swing curves with fault cleared by simultaneous opening of breakers at both ends of the line at 2.5 cycles and 6.25 cycles after the occurrence of fault. Also plot the swing curve over the period of 0.5 s if the fault is sustained.

Solution

Before we can apply the step-by-step method, we need to calculate the inertia constant M and the power angle equations under prefault and postfault conditions.

Base MVA = 20

$$\text{Inertia constant, } M(\text{pu}) = \frac{H}{180\, f} = \frac{1.0 \times 2.52}{180 \times 50}$$

$$= 2.8 \times 10^{-4} \text{ s}^2/\text{elect degree}$$

I. Prefault

$$X_{\text{I}} = 0.35 + \frac{0.2}{2} = 0.45$$

$$\therefore \quad P_{e\text{I}} = P_{\text{max I}} \sin \delta$$

$$= \frac{1.1 \times 1}{0.45} \sin \delta = 2.44 \sin \delta \qquad \text{(i)}$$

$$\text{Prefault power transfer} = \frac{18}{20} = 0.9 \text{ pu}$$

Initial power angle is given by

$$2.44 \sin \delta_0 = 0.9$$

or

$$\delta_0 = 21.64^\circ$$

II. During fault A positive sequence diagram is shown in Fig. 12.39(a). Converting star to delta, we obtain the network of Fig. 12.39(b), in which

$$X_{II} = \frac{0.35 \times 0.1 + 0.2 \times 0.1 + 0.35 \times 0.2}{0.1} = 1.25 \text{ pu}$$

$$\therefore \quad P_{eII} = P_{maxII} \sin \delta$$

$$= \frac{1.1 \times 1}{1.25} \sin \delta = 0.88 \sin \delta \qquad \text{(ii)}$$

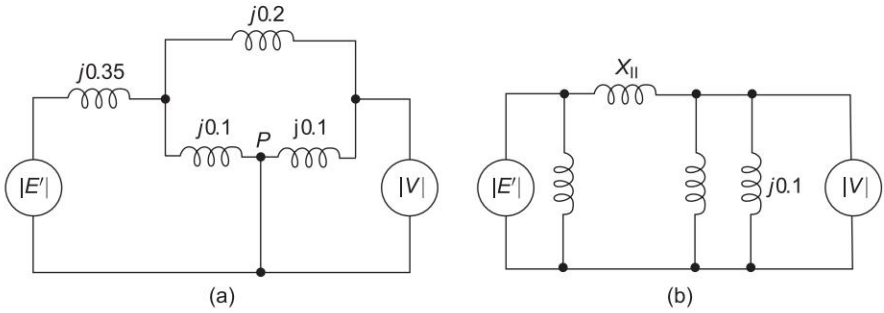

Fig. 12.39

III. Postfault With the faulted line switched off,

$$X_{III} = 0.35 + 0.2 = 0.55$$

$$\therefore \quad P_{eIII} = P_{maxIII} \sin \delta$$

$$= \frac{1.1 \times 1}{0.55} \sin \delta = 2.0 \sin \delta \qquad \text{(iii)}$$

Let us choose $\Delta t = 0.05$ s.

The recursive relationships for step-by-step swing curve calculation are reproduced below.

$$P_{a(n-1)} = P_m - P_{max} \sin \delta_{n-1} \qquad \text{(iv)}$$

$$\Delta\delta_n = \Delta\delta_{n-1} + \frac{(\Delta t)^2}{M} P_{a(n-1)} \qquad \text{(v)}$$

$$\delta_n = \delta_{n-1} + \Delta\delta_n \qquad \text{(vi)}$$

Since there is a discontinuity in P_e and hence in P_a, the average value of P_a must be used for the first interval.

$$P_a(0_-) = 0 \text{ pu and } P_a(0_+) = 0.9 - 0.88 \sin 21.64^\circ = 0.576 \text{ pu}$$

$$P_a(0_{\text{average}}) = \frac{0 + 0.576}{2} = 0.288 \text{ pu}$$

Sustained Fault

Calculations are carried out in Table 12.2 in accordance with the recursive relationship (iv), (v) and (vi) above. The second column of the table shows

P_{max} the maximum power that can be transferred at time t given in the first column. P_{max} in the case of a sustained fault undergoes a sudden change at $t = 0_+$ and remains constant thereafter. The procedure of calculations is illustrated below by calculating the row corresponding to $t = 0.15$ s.

Table 12.2 Point-by-point computations of swing curve for sustained fault, $\Delta t = 0.05$ s

t	P_{max}	$\sin\delta$	$P_e = P_{max}\sin\delta$	$P_a = 0.9 - P_e$	$\frac{(\Delta t)^2}{M} P_a = 8.929\, P_a$	$\Delta\delta$	δ
s	*pu*		*pu*	*pu*	*deg*	*deg*	*deg*
0_-	2.44	0.368	0.9	0.0	—	—	21.64
0_+	0.88	0.368	0.324	0.576	—	—	21.64
0_{avg}	—	0.368	—	0.288	2.57	2.57	21.64
0.05	0.88	0.41	0.361	0.539	4.81	7.38	24.21
0.10	0.88	0.524	0.461	0.439	3.92	11.30	31.59
0.15	0.88	0.680	0.598	0.301	2.68	13.98	42.89
0.20	0.88	0.837	0.736	0.163	1.45	15.43	56.87
0.25	0.88	0.953	0.838	0.06	0.55	15.98	72.30
0.30	0.88	0.999	0.879	0.021	0.18	16.16	88.28
0.35	0.88	0.968	0.852	0.048	0.426	16.58	104.44
0.40	0.88	0.856	0.754	0.145	1.30	17.88	121.02
0.45	0.88	0.657	0.578	0.321	2.87	20.75	138.90
0.50	0.88	—	—	—	—	—	159.65

$$(0.1\text{ s}) = 31.59^\circ$$

$$P_{max} = 0.88$$

$$\sin\delta(0.1\text{ s}) = 0.524$$

$$P_e(0.1\text{ s}) = P_{max}\sin\delta(0.1\text{ s}) = 0.88 \times 0.524 = 0.461$$

$$P_a(0.1\text{ s}) = 0.9 - 0.461 = 0.439$$

$$\frac{(\Delta t)^2}{M} P_a(0.1\text{ s}) = 8.929 \times 0.439 = 3.92^\circ$$

$$\delta(0.15\text{ s}) = \Delta\delta(0.1\text{ s}) + \frac{(\Delta t)^2}{M} P_a(0.1\text{ s})$$

$$= 7.38^\circ + 3.92^\circ = 11.33^\circ$$

$$\delta(0.15\text{ s}) = \delta(0.1\text{ s}) + \Delta\delta(0.15\text{ s})$$

$$= 31.59^\circ + 11.30^\circ = 42.89^\circ$$

$\delta(t)$ for sustained fault as calculated in Table 12.2 is plotted in Fig. 12.40 from which it is obvious that the system is unstable.

Fault Cleared in 2.5 Cycles

$$\text{Time to clear fault} = \frac{2.5}{50} = 0.05 \text{ s}$$

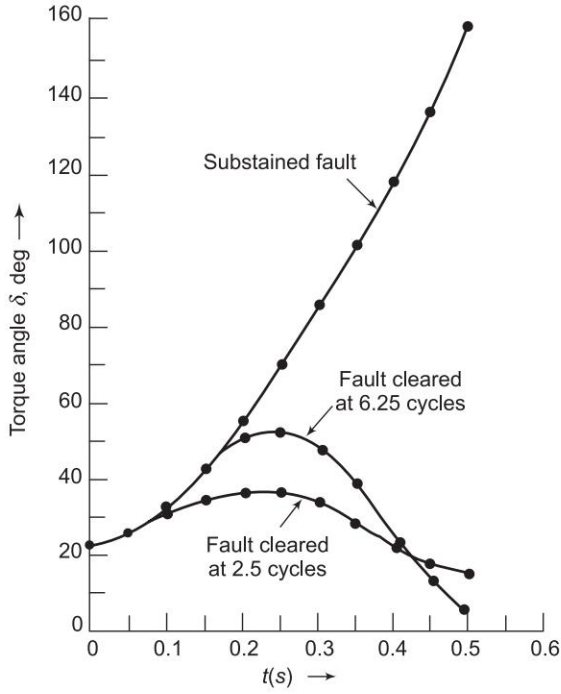

Fig. 12.40 Swing curves for Example 12.10 for a sustained fault and for clearing in 2.5 and 6.25 cycles

P_{max} suddenly changes from 0.88 at $t = 0.05_-$ to 2.0 at $t = 0.05_+$. Since the discontinuity occurs at the beginning of an interval, the average value of P_a will be assumed to remain constant from 0.025 s to 0.075 s. The rest of the procedure is the same and complete calculations are shown in Table 12.3. The swing curve is plotted in Fig. 12.40 from which we find that the generator undergoes a maximum swing of 37.5° but is stable as δ finally begins to decrease.

Fault Cleared in 6.25 Cycles

$$\text{Time to clear fault} = \frac{6.25}{50} = 0.125 \text{ s}$$

Since the discontinuity now lies in the middle of an interval, no special procedure is necessary, as in deriving Eqs (iv)–(vi) discontinuity is assumed to occur in the middle of the time interval. The swing curve as calculated in Table 12.4 is also plotted in Fig. 12.40. It is observed that the system is stable with a maximum swing of 52.5° which is much larger than that in the case of 2.5 cycle clearing time.

Table 12.3 Computations of swing curve for fault cleared at 2.5 cycles (0.05 s), $\Delta t = 0.05$ s

t s	P_{max} pu	$\sin\delta$	$P_e = P_{max}\sin\delta$ pu	$P_a = 0.9 - P_e$ pu	$\frac{(\Delta t)^2}{M} P_a = 8.929\, P_a$ deg	$\Delta\delta$ deg	δ deg
0_-	2.44	0.368	0.9	0.0	—	—	21.64
0_+	0.88	0.368	0.324	0.576	—	—	21.64
0_{avg}	—	0.368	—	0.288	2.57	2.57	21.64
0.05_-	0.88	0.41	0.36	0.54	—	—	24.21
0.05_+	2.00	0.41	0.82	0.08	—	—	24.21
0.05_{avg}				0.31	2.767	5.33	24.21
0.10	2.00	0.493	0.986	– 0.086	– 0.767	4.56	29.54
0.15	2.00	0.56	1.12	– 0.22	– 1.96	2.60	34.10
0.20	2.00	0.597	1.19	– 0.29	– 2.58	0.02	36.70
0.25	2.00	0.597	1.19	– 0.29	– 2.58	– 2.56	37.72
0.30	2.00	0.561	1.12	– 0.22	– 1.96	– 4.52	34.16
0.35	2.00	0.494	0.989	– 0.089	– 0.79	– 5.31	29.64
0.40	2.00	0.41	0.82	0.08	0.71	– 4.60	24.33
0.45	2.00	0.337	0.675	0.225	2.0	– 2.6	19.73
0.50							17.13

To find the critical clearing time, swing curves can be obtained, similarly, for progressively greater clearing time till the torque angle δ increases without bound. In this example, however, we can first find the critical clearing angle using Eq. (12.67) and then read the critical clearing time from the swing curve corresponding to the sustained fault case. The values obtained are:

Critical clearing angle = 118.62°

Critical clearing time = 0.38 s

12.10 MULTIMACHINES STABILITY

From what has been discussed so far, the following steps easily follow for determining multimachine stability.

1. From the prefault load flow data determine E'_k voltage behind transient reactance for all generators. This establishes generator emf magnitudes $|E_k|$ which remain constant during the study and initial rotor angle $\delta_k^0 = \angle E_k$. Also record prime mover inputs to generators, $P_{mk} = P_{Gk}^0$.
2. Augment the load flow network by the generator transient reactances. Shift network buses behind the transient reactances.
3. Find Y_{BUS} for various network conditions—during fault, post fault (faulted line cleared), after line reclosure.

4. For faulted mode, find generator outputs from power angle equations (generalized forms of Eq. (12.27)) and solve swing equations step by step (point-by-point method).
5. Keep repeating the above step for post fault mode and after line reclosure mode.
6. Examine $\delta(t)$ plots of all generators and establish the answer to the stability question.

The above steps are illustrated in the following example.

Table 12.4 Computations of swing curve for fault cleared at 6.25 cycles (0.125 s), $\Delta t = 0.05$ s

t	P_{max}	$\sin\delta$	$P_e = P_{max}\sin\delta$	$P_a = 0.9 - P_e$	$\frac{(\Delta t)^2}{M} P_a = 8.929\, P_a$	$\Delta\delta$	δ
s	*pu*		*pu*	*pu*	*deg*	*deg*	*deg*
0_-	2.44	0.368	0.9	0.0	–	–	21.64
0_+	0.88	0.368	0.324	0.576	–	–	21.64
0_{avg}	–	0.368	–	0.288	2.57	2.57	21.64
0.05	0.88	0.41	0.361	0.539	4.81	7.38	24.21
0.10	0.88	0.524	0.461	0.439	3.92	11.30	31.59
0.15	2.00	0.680	1.36	– 4.46	– 4.10	7.20	42.89
0.20	2.00	0.767	1.53	– 0.63	– 5.66	1.54	50.09
0.25	2.00	0.78	1.56	– 0.66	– 5.89	– 4.35	51.63
0.30	2.00	0.734	1.46	– 0.56	– 5.08	– 9.43	47.28
0.35	2.00	0.613	1.22	– 0.327	– 2.92	– 12.35	37.85
0.40	2.00	0.430	0.86	0.04	0.35	– 12.00	25.50
0.45	2.00	0.233	0.466	0.434	3.87	– 8.13	13.50
0.50	2.00						5.37

Example 12.11 A 50 Hz, 220 kV transmission line has two generators and an infinite bus as shown in Fig. 12.41. The transformer and line data are given in Table 12.5. A three-phase fault occurs as shown. The prefault load flow solution is presented in Table 12.6. Find the swing equation for each generator during the fault period.

Data are given below for the two generators on a 100 MVA base.

Generator 1 500 MVA, 25 kV, $X_d' = 0.067$ pu, H = 12 MJ/MVA

Generator 2 300 MVA, 20 kV, $X_d' = 0.10$ pu, H = 9 MJ/MVA

Plot the swing curves for the machines at buses 2 and 3 for the above fault which is cleared by simultaneous opening of the circuit breakers at the ends of the faulted line at (i) 0.275 s and (ii) 0.08 s.

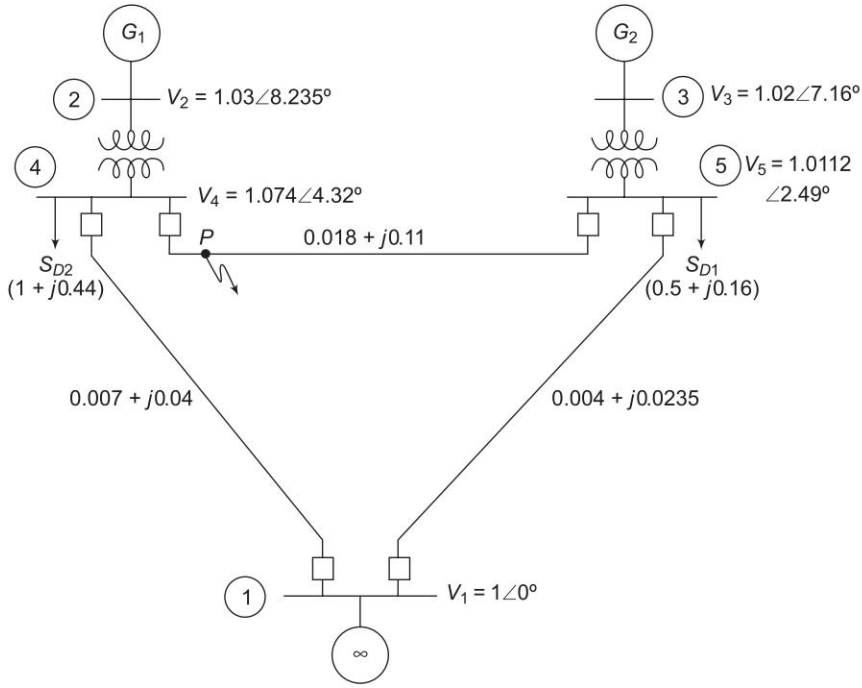

Fig. 12.41

Table 12.5 Line and transformer data for Example 12.11. All values are in pu on 220 kV, 100 MVA base

Bus to bus	*Series Z*		*Half line*
	R	*X*	*charging*
Line 4–5	0.018	0.11	0.113
Line 5–1	0.004	0.0235	0.098
Line 4–1	0.007	0.04	0.041
Trans: 2–4	—	0.022	—
Trans: 3–5	—	0.04	—

Solution

Before determining swing equation, we have to find transient internal voltages.

The current into the network at bus 2 based on the data in Table 12.6 is

$$I_2 = \frac{P_2 - jQ_2}{V_2^*} = \frac{3.25 - j0.6986}{1.03\angle -8.23519^\circ}$$

$$\therefore \quad I_2\, X'_{de} = \frac{3.25 - j0.6986}{1.03\angle -8.23519^\circ} \times 0.067\angle 90^\circ$$

$$E_2' = (1.0194 + j0.1475) + \frac{3.25 - j0.6986}{1.03 \angle -8.23519^\circ} \times 0.067 \angle 90^\circ$$

Table 12.6 Bus data and prefault load-flow values in pu on 220 kV, 100 MVA base

S.No. and Bus No.	Voltage Polar-Form	Bus type	Voltage		Generation		Load	
			Real e	Imaginary f	P	Q	P	Q
1	$1.0\angle 0^\circ$	Slack	1.00	0.0	– 3.8083	– 0.2799	0	0
2	$1.03\angle 8.35^\circ$	PV	1.0194	0.1475	3.25	0.6986	0	0
3	$1.02\angle 7.16^\circ$	PV	1.0121	0.1271	2.10	0.3110	0	0
4	$1.0174\angle 4.32^\circ$	PQ	1.0146	0.767	0	1.0	1.0	0.44
5	$1.0112\angle 2.69^\circ$	PQ	1.0102	0.0439	0	0	0.5	0.16

$$= 1.0340929 + j0.3632368$$

$$= 1.0960333 \angle 19.354398^\circ = 1.0960 \angle 0.3377 \text{ rad}$$

$$E_1' = 1.0 \angle 0^\circ \text{ (slack bus)}$$

$$E_3' = (1.0121 + j0.1271) + \frac{2.1 - j0.311}{1.02 \angle -7.15811^\circ} \times 0.1 \angle 90^\circ$$

$$= 1.0166979 + j0.335177 = 1.0705 \angle 18.2459^\circ$$

$$= 1.071 \angle 0.31845 \text{ rad}$$

The loads at buses 4 and 5 are represented by the admittances calculated as follows:

$$Y_{L4} = \frac{1.0 - j0.44}{(1.0174)^2}(0.9661 - j0.4251)$$

$$Y_{L5} = \frac{0.5 - j0.16}{(1.0112)^2}(0.4889 - j0.15647)$$

Prefault Bus Matrix

Load admittances, alongwith the transient reactances, are used with the line and transformer admittances to form the prefault augmented bus admittance matrix which contains the transient reactances of the machines. We will, therefore, now designate as buses 2 and 3, the fictitious internal nodes between the internal voltages and the transient reactances of the machines. Thus we get

$$Y_{22} = \frac{1}{(j0.067 + j0.022)} = -j11.236$$

$$Y_{24} = j11.236 = Y_{42}$$

$$Y_{33} = \frac{1}{j0.04 + j0.1} = -j7.143$$

$$Y_{35} = j7.143 = Y_{53}$$

$$Y_{44} = Y_{L4} + Y_{41} + Y_{45} + \frac{B_{41}}{2} + \frac{B_{45}}{2} + Y_{24}$$

$$= 0.9660877 - j0.4250785 + 4.245 - j24.2571 + 1.4488 - j8.8538 + j0.041 + j0.113 - j11.2359$$

$$= 6.6598977 - j44.6179$$

$$Y_{55} = Y_{L5} + Y_{54} + Y_{51} + \frac{B_{54}}{2} + \frac{B_{51}}{2} + Y_{35}$$

$$= 0.4889 - j0.1565 + 1.4488 - j8.8538 + 7.0391 - j41.355 + j0.113 + j0.098 - j7.1428$$

$$= 8.976955 - j57.297202$$

The complete augmented prefault Y_{BUS} matrix is shown in Table 12.7.

Table 12.7 The augmented prefault bus admittance matrix for Example 12.11, admittances in pu

Bus	*1*	*2*	*3*	*4*	*5*
1	11.284 – *j*65.473	0	0	– 4.245 + *j*24.257	– 7.039 + *j*41.355
2	0	– *j*11.2359	0	*j*11.2359	0
3	0	0	– *j*7.1428	0	*j*7.1428
4	– 4.245 + *j*24.257	*j*11.2359	0	6.6598 – *j*44.617	– 1.4488 + *j*8.8538
5	– 7.039 + *j*41.355	0	0 + *j*7.1428	– 1.4488 + *j*8.8538	8.9769 + *j*57.2972

During Fault Bus Matrix

Since the fault is near bus 4, it must be short circuited to ground. The Y_{BUS} during the fault conditions would, therefore, be obtained by deleting 4th row and 4th column from the above augmented prefault Y_{BUS} matrix. Reduced fault matrix (to the generator internal nodes) is obtained by eliminating the new 4th row and column (node 5) using the relationship

$$Y_{kj(\text{new})} = Y_{kj(\text{old})} - Y_{kn(\text{old})}\, Y_{nj(\text{old})} / Y_{nn(\text{old})}$$

The reduced faulted matrix (Y_{BUS} during fault) (3 × 3) is given in Table 12.8, which clearly depicts that bus 2 decouples from the other buses during the fault and that bus 3 is directly connected to bus 1, showing that the fault at bus 4 reduces to zero the power pumped into the system from the generator at bus 2 and renders the second generator at bus 3 to give its power radially to bus 1.

Post Fault Bus Matrix

Once the fault is cleared by removing the line, simultaneously opening the circuit breakers at the either ends of the line between buses 4 and 5, the

prefault Y_{BUS} has to be modified again. This is done by substituting $Y_{45} = Y_{54} = 0$ and subtracting the series admittance of line 4–5 and the capacitive susceptance of half the line from elements Y_{44} and Y_{55}.

Table 12.8 Elements of Y_{BUS} (during fault) and Y_{BUS} (post fault) for Example 12.11, admittances in pu

Reduced during fault $\mathbf{Y}_{BUS}$			
Bus	*1*	*2*	*3*
1	5.7986–*j*35.6301	0	– 0.0681 + *j*5.1661
2	0	– *j*11.236	0
3	– 0.0681 + *j*5.1661	0	0.1362 – *j*6.2737
Reduced post fault $\mathbf{Y}_{BUS}$			
1	1.3932 – *j*13.8731	– 0.2214 + *j*7.6289	– 0.0901 + *j*6.0975
2	– 0.2214 + *j*7.6289	0.5 – *j*7.7898	0
3	– 0.0901 + *j*6.0975	0	0.1591 – *j*6.1168

$$Y_{44(\text{post fault})} = Y_{44(\text{prefault})} - Y_{45} - B_{45}/2$$
$$= 6.65989 - j44.6179 - 1.448 + j8.853 - j0.113$$
$$= 5.2111 - j35.8771$$

Similarly,

$$Y_{55(\text{post fault})} = 7.5281 - j48.5563$$

The reduced post fault Y_{BUS} is shown in the lower half of Table 12.8. It may be noted that 0 element appears in 2nd and 3rd rows. This shows that, physically, the generators 1 and 2 are not interconnected when line 4–5 is removed.

During Fault Power Angle Equation

$$P_{e2} = 0$$
$$P_{e3} = \text{Re}\,[Y_{33}E_3'E_3'^* + E_3'^*\, Y_{31}E_1'], \text{ since } Y_{32} = 0$$
$$= |E_3'|^2\, G_{33} + |E_1'|\,|E_3'|\,|Y_{31}|\cos(\delta_{31} - \theta_{31})$$
$$= (1.071)^2\,(0.1362) + 1 \times 1.071 \times 5.1665 \cos(\delta_3 - 90.755^\circ)$$
$$P_{e3} = 0.1561 + 5.531 \sin(\delta_3 - 0.755^\circ)$$

Postfault Power Angle Equations

$$P_{e2} = |E_2'|^2\, G_{22} + |E_1'|\,|E_2'|\,|Y_{21}|\cos(\delta_{21} - \theta_{21})$$
$$= 1.096^2 \times 0.5005 + 1 \times 1.096 \times 7.6321 \cos(\delta_2 - 91.662^\circ)$$
$$= 0.6012 + 8.365 \sin(\delta_2 - 1.662^\circ)$$
$$P_{e3} = |E_3'|^2 G_{33} + |E_1'|\,|E_3'|\,|Y_{31}|\cos(\delta_{31} - \theta_{31})$$
$$= 1.071^2 \times 0.1591 + 1 \times 1.071 \times 6.098 \cos(\delta_3 - 90.8466^\circ)$$
$$= 0.1823 + 6.5282 \sin(\delta_3 - 0.8466^\circ)$$

Swing Equations—During Fault

$$\frac{d^2\delta_2}{dt^2} = \frac{180f}{H_2}(P_{m2} - P_{e2}) = \frac{180f}{H_2}P_{a_2}$$

$$= \frac{180f}{12}(3.25 - 0) \text{ elect deg/s}^2$$

$$\frac{d^2\delta_3}{dt^2} = \frac{180f}{H_3}(P_{m3} - P_{e3})$$

$$= \frac{180f}{9}[2.1 - \{0.1561 + 5.531 \sin(\delta_3 - 0.755^\circ)\}]$$

$$= \frac{180f}{9}[1.9439 - 5.531 \sin(\delta_3 - 0.755^\circ)] \text{ elect deg/s}^2$$

Swing Equations—Postfault

$$\frac{d^2\delta_2}{dt^2} = \frac{180f}{11}[3.25 - \{0.6012 + 8.365 \sin(\delta_2 - 1.662^\circ)\}] \text{ elect deg/s}^2$$

$$\frac{d^2\delta_3}{dt^2} = \frac{180f}{9}[2.10 - \{0.1823 + 6.5282 \sin(\delta_3 - 0.8466^\circ)\}] \text{elect deg/s}^2$$

It may be noted that in the above swing equations, P_a may be written in general as follows:

$$P_a = P_m - P_c - P_{\max} \sin(\delta - \gamma)$$

Digital Computer Solution of Swing Equation

The above swing equations (during fault followed by post fault) can be solved by the point-by-point method presented earlier or by the Euler's method presented in the later part of this section. The plots of δ_2 and δ_3 are given in Fig. 12.42 for a clearing time of 0.275 s and in Fig. 12.43 for a clearing time of 0.08 s. For the case (i), the machine 2 is unstable, while the machine 3 is stable but it oscillates wherein the oscillations are expected to decay if effect of damper winding is considered. For the case (ii), both machines are stable but the machine 2 has large angular swings.

If the fault is a transient one and the line is reclosed, power angle and swing equations are needed for the period after reclosure. These can be computed from the reduced Y_{BUS} matrix after line reclosure.

Consideration of Automatic Voltage Regulator (AVR) and Speed Governor Loops

This requires modelling of these two control loops in the form of differential equations. At the end of every step in the stability algorithm, the programme

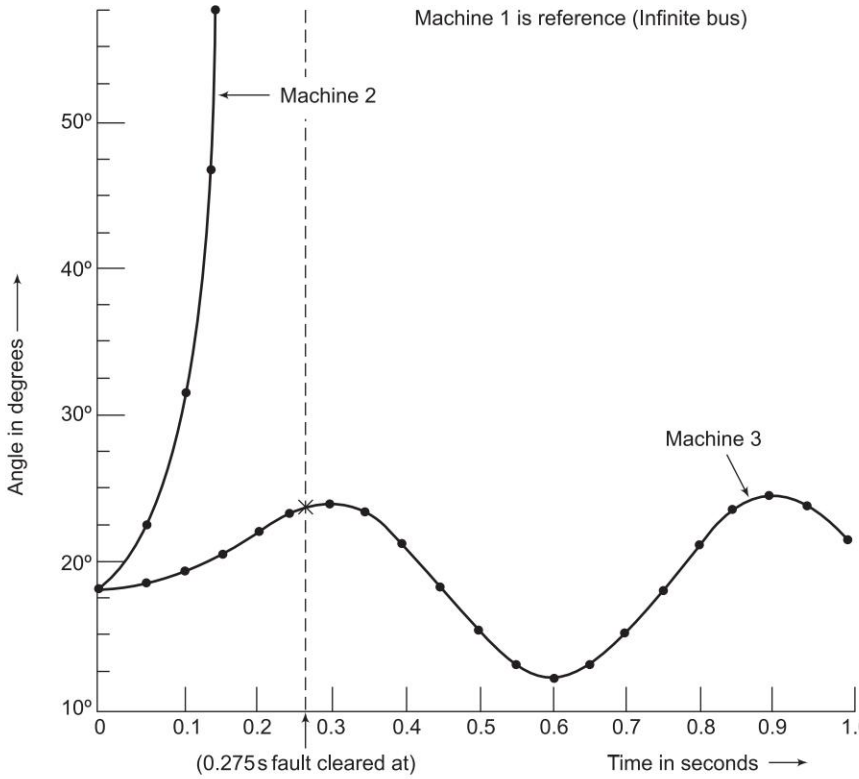

Fig. 12.42 Swing curves for machines 2 and 3 of Example 12.11 for clearing at 0.275 s

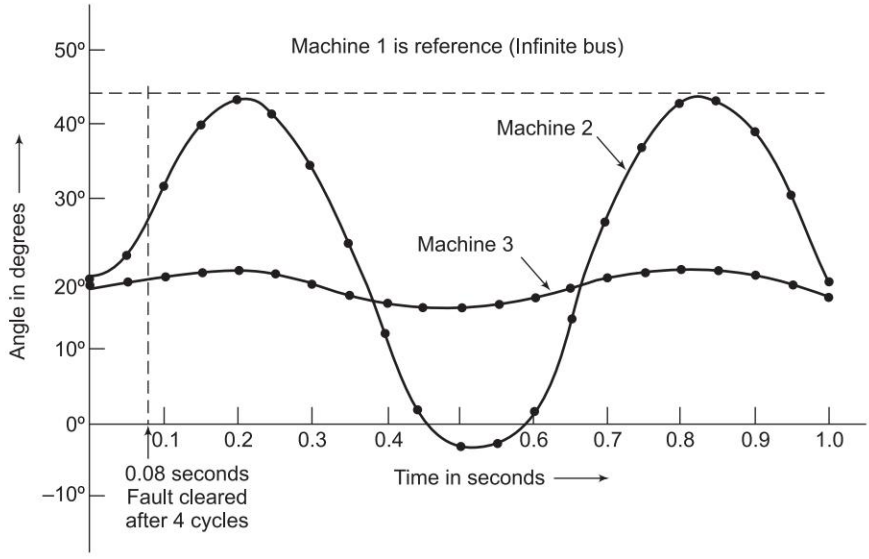

Fig. 12.43 Swing curves for machines 2 and 3 of Example 12.11 for clearing at 0.08 s

computes the modified values of E'_k and P_{mk} and then proceeds to compute the next step. This considerably adds to the dimensionality and complexity of stability calculations. To reduce the computational effort, speed control can continue to be ignored without loss of accuracy of results.

State Variable Formulation of Swing Equations

The swing equation for the kth generator is

$$\frac{d^2\delta_k}{dt^2} = \frac{\pi f}{H_k}(P^0_{Gk} - P_{Gk});\ k = 1, 2, ..., m \tag{12.73}$$

For the multimachine case, it is more convenient to organize Eq. (12.73) in state variable form. Define

$$x_{1k} = \delta_k = \angle E'_k$$

$$x_{2k} = \dot{\delta}_k$$

Then

$$\left.\begin{aligned} \dot{x}_{1k} &= x_{2k} \\ \dot{x}_{2k} &= \frac{\pi f}{H_k}(P^0_{Gk} - P_{Gk}),\ k = 1, 2, \ldots, m \end{aligned}\right\} \tag{12.74}$$

Initial state vector (upon occurrence of fault) is

$$x^0_{1k} = \delta^0_k = \angle E^0_k$$

$$x^0_{2k} = 0 \tag{12.75}$$

The state form of swing equations (Eq. (12.74)) can be solved by the many available integration algorithms (modified Euler's method is a convenient choice).

Computational Algorithm for Obtaining Swing Curves Using Modified Euler's Method

1. Carry out a load flow study (prior to disturbance) using specified voltages and powers.
2. Compute voltage behind transient reactances of generators (E^0_k) using Eq. (9.31). This fixes generator emf magnitudes and initial rotor angle (reference slack bus voltage V^0_1).
3. Compute Y_{BUS} (during fault, post fault, line reclosed).
4. Set time count $r = 0$.
5. Compute generator power outputs using appropriate Y_{BUS} with the help of the general form of Eq. (12.27). This gives $P^{(r)}_{Gk}$ for $t = t^{(r)}$.
   Note: After the occurrence of the fault, the period is divided into uniform discrete time intervals (Δt) so that time is counted as $t^{(0)}, t^{(1)}, \ldots$. A typical value of Δt is 0.05 s.

6. Compute $[(\dot{x}_{1k}^{(r)}, \dot{x}_{2k}^{(r)}), k = 1, 2, ..., m]$ from Eq. (12.74).
7. Compute the first state estimates for $t = t^{(r+1)}$ as

$$x_{1k}^{(r+1)} = x_{1k}^{(r)} + \dot{x}_{1k}^{(r)} \Delta t \qquad k = 1, 2, ..., m$$

$$x_{2k}^{(r+1)} = x_{2k}^{(r)} + \dot{x}_{2k}^{(r)} \Delta t$$

8. Compute the first estimates of $E_k^{(r+1)}$

$$E_k^{(r+1)} = E_k^0 (\cos x_{1k}^{(r+1)} + j \sin x_{1k}^{(r+1)})$$

9. Compute $P_{Gk}^{(r+1)}$ (appropriate Y_{BUS} and Eq. (12.72)).
10. Compute $[(\dot{x}_{1k}^{(r+1)}, \dot{x}_{2k}^{(r+1)}), k = 1, 2, ..., m]$ from Eq. (12.74).
11. Compute the average values of state derivatives

$$\dot{x}_{1k,\text{avg}}^{(r)} = \frac{1}{2}[\dot{x}_{1k}^{(r)} + \dot{x}_{1k}^{(r+1)}] \qquad k = 1, 2, ..., m$$

$$\dot{x}_{2k,\text{avg}}^{(r)} = \frac{1}{2}\left[\dot{x}_{2k}^{(r)} + \dot{x}_{2k}^{(r+1)}\right]$$

12. Compute the final state estimates for $t = t^{(r+1)}$.

$$x_{1k}^{(r+1)} = x_{1k}^{(r)} + \dot{x}_{1k,\text{avg}}^{(r)} \Delta t \qquad k = 1,2, ..., m$$

$$x_{2k}^{(r+1)} = x_{2k}^{(r)} + \dot{x}_{2k,\text{avg}}^{(r)} \Delta t$$

13. Compute the final estimate for E_k at $t = t^{(r+1)}$ using

$$E_k^{(r+1)} = |E_k^0|(\cos x_{1k}^{(r+1)} + j \sin x_{1k}^{(r+1)})$$

14. Print $(x_{1k}^{(r+1)}, x_{2k}^{(r+1)})$; $k = 1, 2, ..., m$
15. Test for time limit (time for which swing curve is to be plotted), i.e., check if $r > r_{\text{final}}$. If not, $r = r + 1$ and repeat from step 5 above. Otherwise print results and stop.

The swing curves of all the machines are plotted. If the rotor angle of a machine (or a group of machines) with respect to other machines increases without bound, such a machine (or group of machines) is unstable and eventually falls out of step.

The computational algorithm given above can be easily modified to include simulation of voltage regulator, field excitation response, saturation of flux paths and governor action.

Stability Study of Large Systems

To limit the computer memory and the time requirements and for the sake of computational efficiency, a large multi-machine system is divided into a study subsystem and an external subsystem. The study subsystem is modelled in

detail whereas approximate modelling is carried out for the external subsystem. The total study is rendered by the modern technique of dynamic equivalencing. In the external subsystem, number of machines is drastically reduced using various methods—coherency based methods being most popular and widely used by various power utilities in the world.

12.11 SOME FACTORS AFFECTING TRANSIENT STABILITY

We have seen in this chapter that the two-machine system can be equivalently reduced to a single machine connected to infinite bus bar. The qualitative conclusions regarding system stability drawn from a two-machine or an equivalent one-machine infinite bus system can be easily extended to a multimachine system. In the last article we have studied the algorithm for determining the stability of a multimachine system.

It has been seen that transient stability is greatly affected by the type and location of a fault, so that a power system analyst must at the very outset of a stability study decide on these two factors. In our examples we have selected a 3–phase fault which is generally more severe from the point of view of power transfer. Given the type of fault and its location let us now consider other factors which affect transient stability and therefrom draw the conclusions, regarding methods of improving the transient stability limit of a system and making it as close to the steady state limit as possible.

For the case of one machine connected to infinite bus, it is easily seen from Eq. (12.71) that an increase in the inertia constant M of the machine reduces the angle through which it swings in a given time interval offering thereby a method of improving stability but this cannot be employed in practice because of economic reasons and for the reason of slowing down the response of the speed governor loop (which can even become oscillatory) apart from an excessive rotor weight.

With reference to Fig. 12.30, it is easily seen that for a given clearing angle, the accelerating area decreases but the decelerating area increases as the maximum power limit of the various power angle curves is raised, thereby adding to the transient stability limit of the system. The maximum steady power of a system can be increased by raising the voltage profile of the system and by reducing the transfer reactance. These conclusions along with the various transient stability cases studied, suggest the following method of improving the transient stability limit of a power system.

1. Increase of system voltages, use of AVR.
2. Use of high speed excitation systems.
3. Reduction in system transfer reactance.
4. Use of high speed reclosing breakers (see Fig. 12.32). Modern tendency is to employ single-pole operation of reclosing circuit breakers.

When a fault takes place on a system, the voltages at all buses are reduced. At generator terminals, these are sensed by the automatic voltage regulators which help restore generator terminal voltages by acting within the excitation system. Modern exciter systems having solid state controls quickly respond to

bus voltage reduction and can achieve from one-half to one and one-half cycles ($\frac{1}{2}$–$1\frac{1}{2}$) gain in critical clearing times for three-phase faults on the HT bus of the generator transformer.

Reducing transfer reactance is another important practical method of increasing stability limit. Incidentally this also raises system voltage profile. The reactance of a transmission line can be decreased (i) by reducing the conductor spacing, and (ii) by increasing conductor diameter (see Eq. (2.37)). Usually, however, the conductor spacing is controlled by other features such as lightning protection and minimum clearance to prevent the arc from one phase moving to another phase. The conductor diameter can be increased by using material of low conductivity or by hollow cores. However, normally, the conductor configuration is fixed by economic considerations quite apart from stability. The use of bundled conductors is, of course, an effective means of reducing series reactance.

Compensation for line reactance by series capacitors is an effective and economical method of increasing stability limit specially for transmission distances of more than 350 km. The degree of series compensation, however, accentuates the problems of protective relaying, normal voltage profiles, and overvoltages during line-to-ground faults. Series compensation becomes more effective and economical if part of it is switched on so as to increase the degree of compensation upon the occurrence of a disturbance likely to cause instability. Switched series capacitors simultaneously decrease fluctuation of load voltages and raise the transient stability limit to a value almost equal to the steady state limit. Switching shunt capacitors on or switching shunt reactors off also raises stability limits (see Example 12.2) but the MVA rating of shunt capacitors required is three to six times the rating of switched series capacitors for the same increase in stability limit. Thus series capacitors are preferred unless shunt elements are required for other purposes, say, control of voltage profile.

Increasing the number of parallel lines between transmission points is quite often used to reduce transfer reactance. It adds at the same time to reliability of the transmission system. Additional line circuits are not likely to prove economical until after all feasible improvements have been carried out in the first two circuits.

As the majority of faults are transient in nature, rapid switching and isolation of unhealthy lines followed by reclosing has been shown earlier to be a great help in improving the stability margins. The modern circuit breaker technology has now made it possible for line clearing to be done as fast as in two cycles. Further, a great majority of transient faults are line-to-ground in nature. It is natural that methods have been developed for selective single pole opening and reclosing which further aid the stability limits. With reference to Fig. 12.17, if a transient LG fault is assumed to occur on the generator bus, it is immediately seen that during the fault there will now be a definite amount of power transfer, as different from zero power transfer for the case of a three-phase fault. Also when the circuit breaker pole corresponding to the faulty line is opened, the

other two lines (healthy ones) remain intact so that considerable power transfer continues to take place via these lines in comparison to the case of three-pole switching when the power transfer on fault clearing will be reduced to zero. It is, therefore, easy to see why the single pole switching and reclosing aids in stability problem and is widely adopted. These facts are illustrated by means of Example 12.12. Even when the stability margins are sufficient, single pole switching is adopted to prevent large swings and consequent voltage dips. Single pole switching and reclosing is, of course, expensive in terms of relaying and introduces the associated problems of overvoltages caused by single pole opening owing to line capacitances. Methods are available to nullify these capacitive coupling effects.

Recent Trends

Recent trends in design of large alternators tend towards lower short circuit ratio (SCR = $1/X_d$), which is achieved by reducing machine air gap with consequent savings in machine mmf, size, weight and cost. Reduction in the size of rotor reduces inertia constant, lowering thereby the stability margin. The loss in stability margin is made up by such features as lower reactance lines, faster circuit breakers and faster excitation systems as discussed already, and a faster system valving to be discussed later in this article.

A stage has now been reached in technology whereby the methods of improving stability, discussed above, have been pushed to their limits, e.g., clearing times of circuit breakers have been brought down to virtually irreducible values of the order of two cycles. With the trend to reduce machine inertias there is a constant need to determine availability, feasibility and applicability of new methods for maintaining and/or improving system stability. A brief account of some of the recent methods of maintaining stability is given below:

HVDC Links Increased use of HVDC links employing thyristors would alleviate stability problems. A DC link is asynchronous, i.e., the two AC system at either end do not have to be controlled in phase or even be at exactly the same frequency as they do for an AC link, and the power transmitted can be readily controlled. There is no risk of a fault in one system causing loss of stability in the other system.

Breaking Resistors For improving stability where clearing is delayed or a large load is suddenly lost, a resistive load called a breaking resistor is connected at or near the generator bus. This load compensates for at least some of the reduction of load on the generators and so reduces the acceleration. During a fault, the resistors are applied to the terminals of the generators through circuit breakers by means of an elaborate control scheme. The control scheme determines the amount of resistance to be applied and its duration. The breaking resistors remain on for a matter of cycles both during fault clearing and after system voltage is restored.

Short Circuit Current Limiters These are generally used to limit the short circuit duty of distribution lines. These may also be used in long transmission

lines to modify favourably the transfer impedance during fault conditions so that the voltage profile of the system is somewhat improved, thereby raising the system load level during the fault.

Turbine Fast Valving or Bypass Valving The two methods just discussed above are an attempt at replacing the system load so as to increase the electrical output of the generator during fault conditions. Another recent method of improving the stability of a unit is to decrease the mechanical input power to the turbine. This can be accomplished by means of fast valving, where the difference between mechanical input and reduced electrical output of a generator under a fault, as sensed by a control scheme, initiates the closing of a turbine valve to reduce the power input. Briefly, during a fast valving operation, the interceptor valves are rapidly shut (in 0.1 to 0.2 s) and immediately reopened. This procedure increases the critical switching time long enough so that in most cases, the unit will remain stable for faults with stuck-breaker clearing times. The scheme has been put to use in some stations in the USA.

Full Load Rejection Technique Fast valving combined with high-speed clearing time will suffice to maintain stability in most of the cases. However, there are still situations where stability is difficult to maintain. In such cases, the normal procedure is to automatically trip the unit off the line. This, however, causes several hours of delay before the unit can be put back into operation. The loss of a major unit for this length of time can seriously jeopardize the remaining system.

To remedy these situations, a full load rejection scheme could be utilized after the unit is separated from the system. To do this, the unit has to be equipped with a large steam bypass system. After the system has recovered from the shock caused by the fault, the unit could be resynchronized and reloaded. The main disadvantage of this method is the extra cost of a large bypass system.

Example 12.12 The system shown in Fig. 12.44 is loaded to 1 pu. Calculate the swing curve and ascertain system stability for:

(i) LG fault three pole switching followed by reclosure, line found healthy.
(ii) LG fault single pole switching followed by reclosure, line found healthy.

Switching occurs at 3.75 cycles (0.075s) and reclosure occurs at 16.25 cycles (0.325s). All values shown in the figure are in pu.

Solution

The sequence networks of the system are drawn and suitably reduced in Figs 12.45(a), (b) and (c).

For an LG fault at P the sequence networks will be connected in series as shown in Fig. 12.46. A star-delta transformation reduces Fig. 12.46 to that of Fig. 12.47 from which we have the transfer reactance

$$X_{12}(\text{LG fault}) = 0.4 + 0.4 + \frac{0.4 \times 0.4}{0.246} = 1.45$$

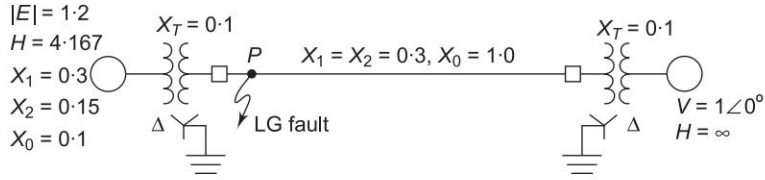

Fig. 12.44

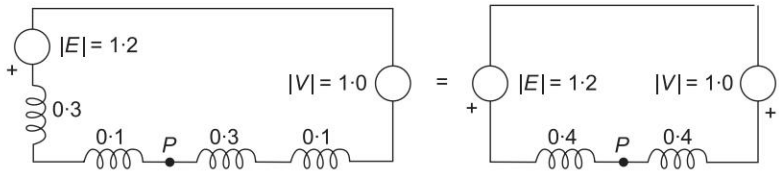

(a) Positive sequence network

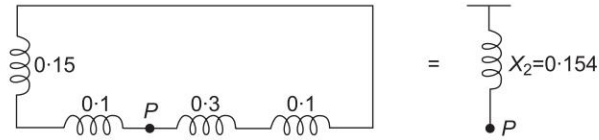

(b) Negative sequence network

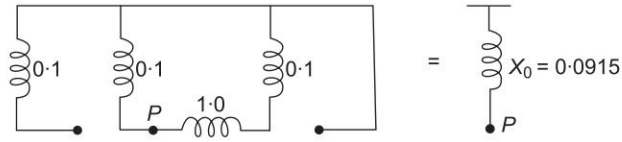

(c) Zero sequence network

Fig. 12.45

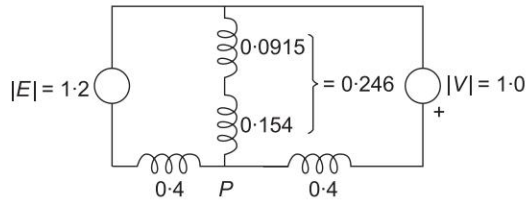

Fig. 12.46 Connection of sequence networks for an LG fault

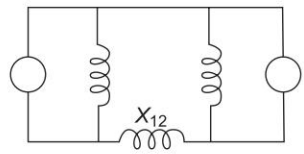

Fig. 12.47 Transfer impedance for an LG fault

When the circuit breaker poles corresponding to the faulted line are opened (it corresponds to a single-line open fault) the connection of sequence networks is shown in Fig. 12.48. From the reduced network of Fig. 12.49 the transfer reactance with faulted line switched off is

X_{12} (faulted line open) = 0.4 + 0.42 + 0.4 = 1.22

Under healthy conditions transfer reactance is easily obtained from the positive sequence network of Fig. 12.45(a) as

X_{12}(line healthy) = 0.8

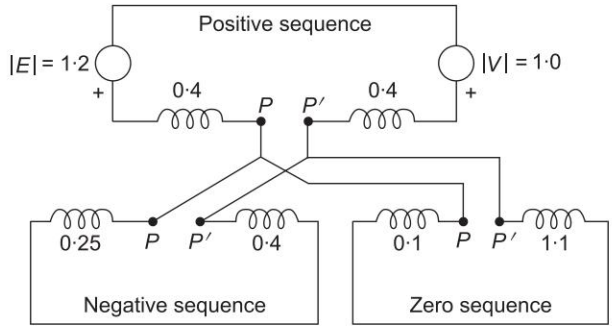

Fig. 12.48 Connection of sequence networks with faulted line switched off

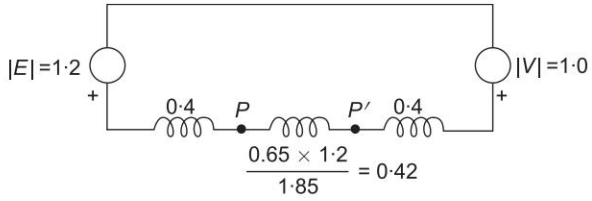

Fig. 12.49 Reduced network of Fig. 12.48 giving transfer reactance

Power angle equations

Prefault

$$P_{e\text{I}} = \frac{|E||V|}{X_{12}} \sin\delta = \frac{1.2 \times 1}{0.8} \sin\delta = 1.5 \sin\delta$$

Initial load = 1.0 pu

Initial torque angle is given by

$$1 = 1.5 \sin\delta_0$$

or $$\delta_0 = 41.8^\circ$$

During fault

$$P_{e\text{II}} = \frac{1.2 \times 1}{1.45} \sin\delta = 0.827 \sin\delta$$

During single pole switching

$$P_{e\text{III}} = \frac{1.2 \times 1}{1.22} \sin \delta = 0.985 \sin \delta$$

During three pole switching

$$P_{e\text{III}} = 0$$

Postfault

$$P_{e\text{IV}} = P_{e\text{I}} = 1.5 \sin \delta$$

Now

$$\Delta\delta_n = \Delta\delta_{n-1} + \frac{(\Delta t)^2}{M} P_{a(n-1)}$$

$$H = 4.167 \text{ MJ/MVA}$$

$$M = \frac{4.167}{180 \times 50} = 4.63 \times 10^{-4} \text{ s}^2/\text{electrical degree}$$

Taking $\Delta t = 0.05$ s

$$\frac{(\Delta t)^2}{M} = \frac{(0.05)^2}{4.63 \times 10^{-4}} = 5.4$$

Time when single/three pole switching occurs

= 0.075 s (during middle of Δt)

Time when reclosing occurs = 0.325 (during middle of Δt)

Table 12.9 Swing curve calculation—three pole switching

	t s	$P_{\max}$ (pu)	$\sin \delta$	P_e (pu)	P_a (pu)	5.4 P_a elec deg	$\Delta\delta$ elec deg	δ elec deg
	0_-	1.5	0.667	1.0	0.0			41.8
	0_+	0.827	0.667	0.552	0.448			41.8
	0_{avg}				0.224	1.2	1.2	41.8
	0.05	0.827	0.682	0.564	0.436	2.4	3.6	43.0
0.075→								
	0.10	0.0	0.726	0.0	1.0	5.4	9.0	46.6
	0.15	0.0		0.0	1.0	5.4	14.4	55.6
	0.20	0.0		0.0	1.0	5.4	19.8	70.0
	0.25	0.0		0.0	1.0	5.4	25.2	89.8
	0.30	0.0		0.0	1.0	5.4	30.6	115.0
0.325→								
	0.35	1.5	0.565	0.85	0.15	0.8	31.4	145.6
	0.40	1.5	0.052	0.078	0.922	5.0	36.4	177.0
	0.45	1.5	– 0.55	– 0.827	1.827	9.9	46.3	213.4
	0.50	1.5	– 0.984	– 1.48	2.48	13.4	59.7	259.7
	0.55	1.5	– 0.651	– 0.98	1.98	10.7	70.4	319.4
	0.60	1.5	0.497	0.746	0.254	1.4	71.8	389.8
	0.65							461.6

The swing curve is plotted in Fig. 12.50 from which it is obvious that the system is unstable.

Table 12.10 Swing curve calculation—single pole switching

	t s	P_{max} (pu)	$\sin\delta$	P_e (pu)	P_a (pu)	$5.4\,P_a$ elec deg	$\Delta\delta$ elec deg	δ elec deg
	0_-	1.5	0.667	1.0	0.0			41.80
	0_+	0.827	0.667	0.552	0.448			41.8
	0_{avg}				0.224	1.2	1.2	41.8
	0.05	0.827	0.682	0.564	0.436	2.4	3.6	43.0
0.075→								
	0.10	0.985	0.726	0.715	0.285	1.5	5.1	46.6
	0.15	0.985	0.784	0.77	0.230	1.2	6.3	51.7
	0.20	0.985	0.848	0.834	0.166	0.9	7.2	58.0
	0.25	0.985	0.908	0.893	0.107	0.6	7.8	65.2
	0.30	0.985	0.956	0.940	0.060	0.3	8.1	73.0
0.325→								
	0.35	1.5	0.988	1.485	– 0.485	– 2.6	5.5	81.1
	0.40	1.5	0.988	1.5	– 0.5	– 2.7	2.8	86.6
	0.45	1.5	1.0	1.5	– 0.5	– 2.7	0.1	89.4
	0.50	1.5	1.0	1.5	– 0.5	– 2.7	– 2.6	89.5
	0.55	1.5	0.9985	1.5	– 0.5	– 2.7	– 5.3	86.9
	0.60	1.5	0.989	1.485	– 0.485	– 2.6	– 7.9	81.6
	0.65	1.5	0.96	1.44	– 0.44	– 2.4	– 10.3	73.7
	0.70	1.5	0.894	1.34	– 0.34	– 1.8	– 12.1	63.4
	0.75	1.5	0.781	1.17	– 0.17	– 0.9	– 13.0	51.3
	0.80	1.5	0.62	0.932	0.068	0.4	– 12.6	38.3
	0.85	1.5	0.433	0.65	0.35	1.9	– 10.7	25.7
	0.90	1.5	0.259	0.39	0.61	3.3	– 7.4	15.0
	0.95	1.5	0.133	0.2	0.8	4.3	– 3.1	7.6
	1.00	1.5	0.079	0.119	0.881	4.8	1.7	4.5
	1.05	1.5	0.107	0.161	0.839	4.5	6.2	6.2
	1.10	1.5	0.214	0.322	0.678	3.7	9.9	12.4
	1.15	1.5	0.38	0.57	0.43	2.3	12.2	22.3
	1.20	1.5	0.566	0.84	0.16	0.9	13.1	34.5
	1.25	1.5	0.738	1.11	– 0.11	– 0.6	12.5	47.6
	1.30	1.5	0.867	1.3	– 0.3	– 1.6	10.9	60.1
	1.35	1.5	0.946	1.42	– 0.42	– 2.3	8.6	71.0
	1.40	1.5	0.983	1.48	– 0.48	– 2.6	6.0	79.6
	1.45	1.5	0.997	1.5	– 0.5	– 2.7	3.3	85.6
	1.50	1.5						88.9

The swing curve is plotted in Fig. 12.51 from which it follows that the system is stable.

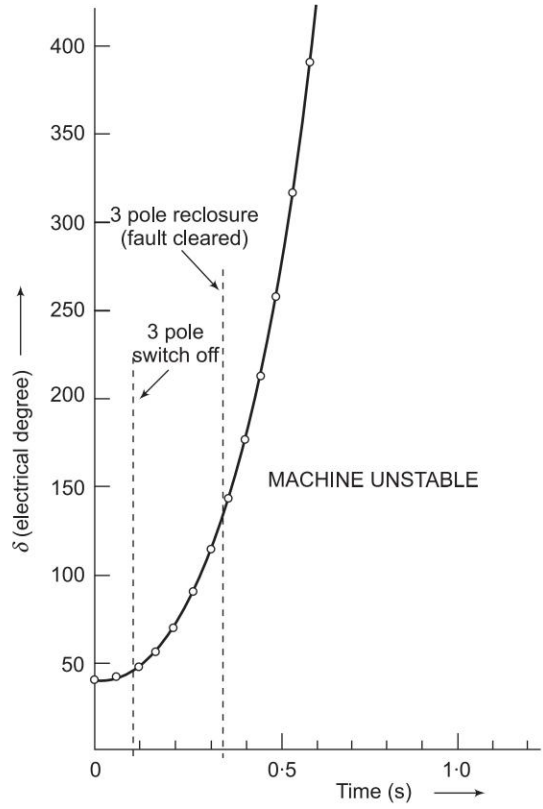

Fig. 12.50 Swing curve for three pole switching with reclosure

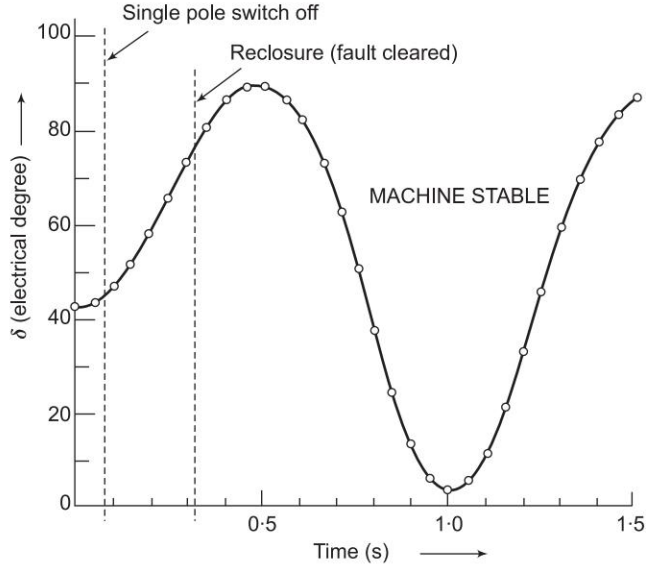

Fig. 12.51 Swing curve for single pole switching with reclosure

12.12 SUMMARY

This chapter deals with various types of power system stability, gives it dynamics, discusses equal area criterion, swing equation and its numerical solution is presented. Multimachine stability is also considered. Finally, various factors affecting transient stability are highlighted.

Problems

12.1 A two-pole, 50 Hz, 11 kV turboalternator has a rating of 100 MW, power factor 0.85 lagging. The rotor has a moment of inertia of a 10,000 kg-m^2. Calculate H and M.

12.2 Two turboalternators with ratings given below are interconnected via a short transmission line.
Machine 1: 4 pole, 50 Hz, 60 MW, power factor 0.80 lagging, moment of inertia 30,000 kg-m^2
Machine 2: 2 pole, 50 Hz, 80 MW, power factor 0.85 lagging, moment of inertia 10,000 kg-m^2
Calculate the inertia constant of the single equivalent machine on a base of 200 MVA.

12.3 Power station 1 has four identical generator sets each rated 80 MVA and each having an inertia constant 7 MJ/MVA; while power station 2 has three sets each rated 200 MVA, 3 MJ/MVA. The stations are located close together to be regarded as a single equivalent machine for stability studies. Calculate the inertia constant of the equivalent machine on 100 MVA base.

12.4 A 50 Hz transmission line 500 km long with constants given below ties up two large power areas:

$R = 0.11\ \Omega$/km $\qquad L = 1.45$ mH/km

$C = 0.009\ \mu$F/km $\qquad G = 0$

Find the steady state stability limit if $|V_S| = |V_R| = 200$ kV (constant). What will the steady state stability limit be if line capacitance is neglected? What will the steady state stability limit be if line resistance is also neglected? Comment on the results.

12.5 A power deficient area receives 50 MW over a tie line from another area. The maximum steady state capacity of the tie line is 100 MW. Find the allowable sudden load that can be switched on without loss of stability.

12.6 A synchronous motor is drawing 30% of the maximum steady state power from an infinite bus bar. If the load on motor is suddenly increased by 100 per cent, would the synchronism be lost? If not, what is the maximum excursion of torque angle about the new steady state rotor position.

12.7 The transfer reactances between a generator and an infinite bus bar operating at 200 kV under various conditions on the interconnector are:

Prefault	150 Ω per phase
During fault	400 Ω per phase
Postfault	200 Ω per phase

If the fault is cleared when the rotor has advanced 60 degrees electrical from its prefault position, determine the maximum load that could be transferred without loss of stability.

12.8 A synchronous generator is feeding 250 MW to a large 50 Hz network over a double circuit transmission line. The maximum steady state power that can be transmitted over the line with both circuits in operation is 500 MW and is 350 MW with any one of the circuits.

A solid three-phase fault occurring at the network-end of one of the lines causes it to trip. Estimate the critical clearing angle in which the circuit breakers must trip so that synchronism is not lost.

What further information is needed to estimate the critical clearing time?

12.9 A synchronous generator represented by a voltage source of 1.05 pu in series with a transient reactance of $j0.15$ pu and an inertia constant $H = 4.0$ s, is connected to an infinite inertia system through a transmission line. The line has a series reactance of $j0.30$ pu, while the infinite inertia system is represented by a voltage source of 1.0 pu in series with a transient reactance of $j0.20$ pu.

The generator is transmitting an active power of 1.0 pu when a three-phase fault occurs at its terminals. If the fault is cleared in 100 millisec, determine if the system will remain stable by calculating the swing curve.

12.10 For Problem 12.9 find the critical clearing time from the swing curve for a sustained fault.

12.11 A synchronous generator represented by a voltage of 1.15 pu in series with a transient reactance is connected to a large power system with voltage 1.0 pu through a power network. The equivalent transient transfer reactance X between voltage sources is $j0.50$ pu.

After the occurrence of a three-phase to ground fault on one of the lines of the power network, two of the line circuit breakers A and B operate sequentially as follows with corresponding transient transfer reactance given therein.

(i) Short circuit occurs at $\delta = 30^\circ$, A opens instantaneously to make $X = 3.0$ pu.

(ii) At $\delta = 60^\circ$, A recloses, $X = 6.0$ pu.

(iii) At $\delta = 75^\circ$, A reopens.

(iv) At $\delta = 90^\circ$, B also opens to clear the fault making $X = 0.60$ pu

Check if the system will operate stably.

12.12 A 50 Hz synchronous generator with inertia constant $H = 2.5$ s and a transient reactance of 0.20 pu feeds 0.80 pu active power into an infinite bus (voltage 1 pu) at 0.8 lagging power factor via a network with an equivalent reactance of 0.25 pu.

A three-phase fault is sustained for 150 millisec across generator terminals. Determine through swing curve calculation the torque angle δ, 250 millisec, after fault initiation.

12.13 A 50 Hz, 500 MVA, 400 kV generator (with transformer) is connected to a 400 kV infinite bus bar through an interconnector. The generator has

H = 2.5 MJ/MVA, voltage behind transient reactance of 450 kV and is loaded 460 MW. The transfer reactances between generator and bus bar under various conditions are:

Prefault	0.5 pu
During fault	1.0 pu
Postfault	0.75 pu

Calculate the swing curve using intervals of 0.05 s and assuming that the fault is cleared at 0.15 s.

12.14 Plot swing curves and check system stability for the fault shown on the system of Example 12.10 for fault clearing by simultaneous opening of breakers at the ends of the faulted line at three cycles and eight cycles after the fault occurs. Also plot the swing curve over a period of 0.6 s if the fault is sustained. For the generator assume H = 3.5 pu, G = 1 pu and carry out the computations in per unit.

12.15 Solve Example 12.10 for a LLG fault.

References

Books

1. Stevenson, W.D., *Elements of Power System Analysis*, 4th edn, McGraw-Hill, New York, 1982.
2. Elgerd, O.I., *Electric Energy Systems Theory: An Introduction*, 2nd edn, McGraw-Hill, New York, 1982.
3. Anderson, P.M. and A.A. Fouad, *Power System Control and Stability*, The Iowa State University Press, Ames, Iowa, 1977.
4. Stagg, G.W. and A.H. O-Abiad, *Computer Methods in Power System Analysis*, Chaps 9 and 10, McGraw-Hill, New York, 1968.
5. Crary, S.B., *Power System Stability*, vol. I (Steady State Stability), vol. II (Transient Stability), Wiley, New York, 1945–1947.
6. Kimbark, E.W., *Power System Stability*, vols 1, 2 and 3, Wiley, New York, 1948.
7. Venikov, V.A., *Transient Phenomena in Electrical Power System* (translated from the Russian), Mir Publishers, Moscow, 1971.
8. Byerly, R.T. and E.W. Kimbark (Eds), *Stability of Large Electric Power Systems*, IEEE Press, New York, 1974.
9. Neuenswander, J.R., *Modern Power Systems*, International Text Book Co., New York, 1971.
10. Pai, M.A., *Power System Stability Analysis by the Direct Method of Lyapunov*., North-Holland, System and Control Services, vol. 3, 1981.
11. Fouad, A.A. and V. Vittal, *Power System Transient Stability Analysis using the Transient Energy Function Method*, Prentice-Hall, Englewood Cliffs, New Jersey, 1992.
12. Kundur, P., *Power System Stability and Control*, McGraw-Hill, New York, 1994.

13. Chakrabarti, A., D.P. Kothari and A.K. Mukhopadhyay, *Performance, Operation and Control of EHV Power Transmission Systems*, Wheeler Publishing, New Delhi, 1995.
14. Padiyar, K.R., *Power System Dynamics: Stability and Control*, 2nd edn, B.S. Publications, Hyderabad, 2002.
15. Sauer, P.W. and M.A. Pai, *Power System Dynamics and Stability*, Prentice Hall, New Jersey, 1998.

Papers

16. Cushing, E.W., *et al*., "Fast Valving as an Aid to Power System Transient Stability and Prompt Resynchronization and Rapid Reload After Full Load Rejection", *IEEE Trans.*, 1972., PAS 91: 1624.
17. Kimbark, E.W., "Improvement of Power System Stability", *IEEE Trans.*, 1969, PAS-88: 773.
18. Dharma Rao, N., "Routh-Hurwitz Condition and Lyapunov Methods for the Transient Stability Problem", *Proc. IEE*, 1969, 116: 533.
19. Shelton, M.L., *et al*., "BPA 1400 MW Braking Resistor", *IEEE Trans.*, 1975, 94: 602.
20. Nanda, J., D.P. Kothari, P.R. Bijwe and D.L. Shenoy, "A New Approach for Dynamic Equivalents Using Distribution Factors Based on a Moment Concept", *Proc. IEEE Int. Conf. on Computers, Systems and Signal Processing*, Bangalore, Dec. 10–12, 1984.
21. Dillon, T.S., 'Dynamic Modelling and Control of Large Scale Systems", *Int. Journal of Electric Power and Energy Systems*, Jan. 1982, 4: 29.
22. Pai, M.A., *Energy Function Analysis for Power System Stability* 0-7923-9035-0.
23. Patel, R., T.S. Bhatti and D.P. Kothari, "Improvement of Power System Transient Stability using Fast Valving: A Review", *Int. J. of Electric Power Components and Systems*, vol. 29, Oct. 2001, pp. 927–938.
24. Patel, R., T.S. Bhatti and D.P. Kothari, "MATLAB/Simulink Based Transient Stability Analysis of a Multimachine Power System, *IJEEE*, vol. 39, no. 4, Oct. 2002, pp. 339–355.
25. Patel, R., T.S. Bhatti and D.P. Kothari, "A Novel Scheme of Fast Valving Control", *IEEE Power Engineering Review*, Oct. 2002, pp. 44–46.
26. Patel, R., T.S. Bhatti and D.P. Kothari, "Improvement of Power System Transient Stability by Coordinated Operation of Fast Valving and Breaking Resistor", To appear in *IEE proceedings-Gen*., Trans and Distribution.
27. Bhat, S., M. Glavic, M. Pavella, T.S. Bhatti and D.P. Kothari, "A Transient Stability Tool Combining the SIME Method with MATLAB and SIMULINK," *IJEEE*, vol. 43, no. 2 April 2006. pp. 119–133.
28. Arya, L.D., V.S. Pande and D.P. Kothari," A Technique for Load Shedding based on Voltage Stability Considerations", JEPES, vol. 27, 2005, pp. 506–517.

Chapter 13
Power System Transients

13.1 INTRODUCTION

In Chs 6–8, the types of problems studied can be classified as:

- The power system operating in steady-state, wherein the system models are nonlinear algebraic equations.
- Small-scale dynamic perturbations around the steady-state operating point, wherein the system models are *linear* differential equations with constant parametric values.

In this chapter we will discuss the abnormal situation, wherein the power system is in dynamic state with large scale perturbation caused by a fault, or opening or closing of a switch, or other large scale disturbances. This is the study of power system transients. Fault currents upon occurrence of a short circuit have already been studied in Chs 9 and 11.

Transient phenomenon lasts in a power system for a very short period of time, ranging from a few μs upto 1 s. Yet the study and understanding of this phenomenon is extremely important, as during these transients, the system is subjected to the greatest stress from excessive over-currents or voltages which, depending upon their severity, can cause extensive damage. In some extreme cases, there may be a complete shut-down of a plant, or even a black-out of a whole area. Because of this, it is necessary that a power system engineer should have a clear understanding of power system transients, to enable him to find out their impact on the system, to prevent them if possible, or at least control their severity or mitigate the damage caused. This chapter is devoted to the study of power system transients.

13.2 TYPES OF SYSTEM TRANSIENTS

The main causes of momentary excessive voltages and currents are:

(i) Lightning, (ii) switching, (iii) short-circuits and (iv) resonance conditions.

Out of these, lightning and switching are the most common, and usually the most severe causes. Transients caused by short-circuits or resonance conditions

usually arise as secondary effects, but may well lead to the plant breakdown in EHV (500–765 kV) systems. Also in EHV systems the voltage transients or surges caused by switching, i.e. opening and closing of circuit breakers, are becoming increasingly important. On cable systems, of course, lightning transients rarely occur and the other causes become more important.

Depending upon the speed of the transients, these can be classified as:

- Surge phenomena (extremely fast transients).
- Short-circuit phenomena (medium fast transients).
- Transient stability (slow transients).

Surge Phenomena

This type of transient is caused by lightning (atmospheric discharges on overhead transmission lines) and switching. Physically, such a transient initiates an electromagnetic wave (surge) travelling with almost the speed of light (3×10^8 m/s) on transmission lines. In a 150 km line, the travelling wave completes a round trip in 1 ms. Thus the transient phenomena associated with these travelling waves occur during the first few milli-seconds after their initiation. The ever-present line losses cause pretty fast attenuation of these waves, which die out after a few reflections.

The reflection of surges at open line ends, or at transformers which present high inductance, leads to multiplicative effect on voltage build-up, which may eventually damage the insulation of high-voltage equipment with consequent short-circuit (medium fast transient). The high inductance of the transformer plays the beneficial role of insulating the generator windings from transmission line surges. The travelling charges in the surges are discharged to ground via *lightning arresters* without the initiation of a line short-circuit, thereby protecting the equipment.

Selection of insulation level of various line equipment and transformers is directly related to the over-voltages caused by surge phenomena. Hence the importance of studying this class of transients.

Short-circuit Phenomena

About more than 50% short-circuits take place on exposed overhead lines, owing to the insulation failure resulting from over-voltages generated by surge phenomena described earlier, birds and other mechanical reasons. Short-circuits result from symmetrical (three-phase) faults, as well as unsymmetrical (LG, LL, LLG) faults. The occurrence of a symmetrical fault brings the power transfer across the line to zero immediately, whereas the impact is only partial in case of unsymmetrical faults. Like surge phenomena, short-circuits are also fully electric in nature. Their speed is determined by the time constants of the generator windings, which vary from a few cycles of 50 Hz wave for the damper windings to around 4 s for the field winding. Therefore, these transients will be sufficiently slower than the surge phenomena. The time range of practical importance to power system analyst is from 10 to 100 ms, i.e. the first few (5–10) cycles of the short-circuit currents.

The short-circuit currents may attain such high values that, if allowed to persist, they may result in *thermal damage* to the equipment. Therefore, the faulty section should be isolated as quickly as possible. Most of the short-circuits do not cause permanent damage. As soon as the fault is cleared, short-circuit path is deionized, and the insulation is restored. Reclosing breakers are, therefore, used in practice which automatically close periodically to find out if the line has recovered. If the fault continues for some time, then, of course, the breaker has to open permanently. This whole operation of successive closing–opening cycle may last for a second or so.

Transient Stability

Whenever a short-circuit takes place at any part of the integrated system, there is an instantaneous total or partial collapse of the bus voltages of the system. This also results in the reduction of the generator power output. Since initially for some instants the input turbine power remains constant, as there is always some time delay before the controllers can initiate corrective actions, each generator is subjected to a positive accelerating torque. This condition, if sustained for some time, can result in the most severe type of transients, namely the mechanical oscillations of the synchronous machine rotors. These *electromechanical* transients may, under extreme conditions, lead to loss of synchronism for some or all of the machines, which implies that the power system has reached its *transient stability limit*. Once this happens, it may take several hours for an electric system engineer to resynchronize such as "blacked-out" system. Thus, it is quite necessary to simulate this phenomenon on the computers and use the switching and load-management strategies that will avoid, or minimize, the ill effects of short-circuits.

The rotor swings are quite slow, as they are mechanical in nature. A transient stability study, thus, may confine itself for the time period of a few milliseconds to one minute in most of the cases. Power system stability has been the subject matter of Ch. 12.

In this chapter, we address ourselves to the problem of surge phenomena.

13.3 TRAVELLING WAVES AND PROPAGATION OF SURGES

The mathematical model used here assumes that the line is lossless, i.e. line resistance and shunt conductance are ignored (ωL and $\omega C >> R$ and G). The resulting equations have analytical solution and the results obtained are safe, i.e. pessimistic. Further, this simplification leads to better understanding of the phenomena involved. For advanced study the reader may refer to Bewley [1], Greenwood [3] and Bickford *et al*. [2].

As already modelled in Ch. 5, Fig. 13.1 shows the elemental section (length Δx) of a transmission line on per phase basis with R and G ignored.

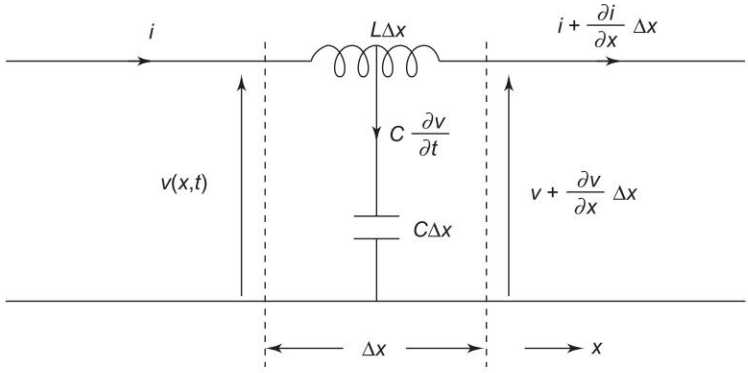

Fig. 13.1 Schematic diagram of an elemental section of a transmission line showing one phase and neutral

The series voltage rise over the element in the direction of x is

$$\frac{\partial v}{\partial x}\,\Delta x = -\,(L\Delta x)\,\frac{\partial i}{\partial t}$$

or

$$\frac{\partial v}{\partial x} = -\,L\,\frac{\partial i}{\partial t} \tag{13.1}$$

Also, the current, in passing through the element, increases by the negative of the current through shunt capacitance, i.e.,

$$\frac{\partial i}{\partial x}\,\Delta x = -\,(C\Delta x)\,\frac{\partial v}{\partial t}$$

or

$$\frac{\partial i}{\partial x} = -\,C\,\frac{\partial v}{\partial t} \tag{13.2}$$

Differentiating Eq. (13.1) w.r.t. x and Eq. (13.2) w.r.t. t, and eliminating the term $\partial_i^2/\partial x\,\partial t$ between these, finally yields

$$\frac{\partial^2 v(x,t)}{\partial x^2} = LC\,\frac{\partial^2 v(x,t)}{\partial t^2} \tag{13.3}$$

The general solution of this equation is given by

$$v(x,\,t) = v_f(x - vt) + v_b(x + vt) \tag{13.4}$$

where $v = \dfrac{1}{\sqrt{LC}}$ = speed of waves in m/s.

By differentiating Eq. (13.4) twice w.r.t. x and t, it can be verified that these satisfy Eq. (13.3).

In Eq. (13.4), v_f is the voltage wave which travels in the forward (positive) direction of x with speed γ, and v_b travels in the backward direction with the same speed. The actual wave shape of these functions is determined by the initial distribution of charges along line and at terminations.

At $t = t_1$, the forward travelling wave has a distribution $v_f(x - \gamma t_1)$, which bodily (as it is) moves forward by a distance $\Delta x = \gamma \Delta t$ at time $t_1 + \Delta t$ as shown in Fig. 13.2.

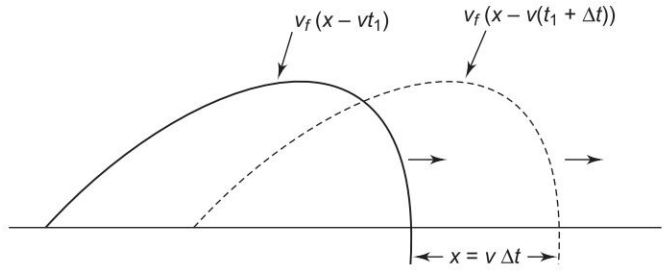

Fig. 13.2 A forward travelling voltage wave shown for values of time t_1 and $t_1 + \Delta t$

Current Solution

The current waves that are implied by the motion of the charges, and which accompany the voltage waves can be found as under.

Differentiating Eq. (13.4) w.r.t. x and using in Eq. (13.1), we have

$$\frac{\partial v}{\partial x} = v_f' + v_b' = -L\,\frac{\partial i}{\partial t} \tag{13.5}$$

where v_f' and v_b' are derivatives w.r.t. the total variables i.e. $(x - \gamma t)$ and $(x + \gamma t)$.

Integrating Eq. (13.5) w.r.t. t,

$$\int v_f'\,\mathrm{d}t + \int v_b'\,\mathrm{d}t = -Li(x, t) \tag{13.6}$$

But

$$\int v_f'\,\mathrm{d}t = \int \frac{\mathrm{d}v_f}{\mathrm{d}(x - vt)}\,\mathrm{d}t = \frac{1}{\gamma}\int \mathrm{d}v_f = -\frac{1}{\gamma}\,v_f\ (x - vt)$$

Similarly

$$\int v_b'\,\mathrm{d}t = \frac{1}{v}\,v_b\ (x + vt)$$

Hence from Eq. (13.6),

$$-\frac{1}{\gamma}\,v_f\ (x - vt) + \frac{1}{v}\,v_b(x + vt) = -Li(x, t)$$

or

$$i(x, t) = \frac{1}{\sqrt{L/C}} v_f(x - vt) - \frac{1}{\sqrt{L/C}} v_b(x + vt)$$

$$= \frac{v_f(x - vt)}{Z_c} - \frac{v_b(x + vt)}{Z_c} \quad (13.7a)$$

$$= i_f(x - vt) + i_b(x + vt) \quad (13.7b)$$

where $Z_c = \sqrt{L/C}$ = *characteristic (surge) impedance*.

The surge impedance has the dimensions of resistance for a lossless line. The negative sign in the backward component of current in Eq. (13.7a) is explained by the fact that current travelling in the backward direction has a negative value (w.r.t. positive direction of x).

Typical values of surge impedance of overhead transmission lines and cables are given below:

$$\left.\begin{aligned} Z_c(\text{TL}) &\approx 400 \\ Z_c(\text{Cable}) &\approx 80 \end{aligned}\right\} \quad (13.8)$$

This vast difference in their surge impedances is because of the fact that in a cable the conductors are much closer to each other compared to those in an overhead transmission line so that it possesses much smaller L (Eq. (2.25a)) and much larger C (Eq. (3.6)) (per unit length).

Physical Interpretation of Results

Consider an ideal charge distribution on a transmission line (uniform over 1 km length abruptly reducing to zero on each side). This charge distribution has its associated voltage distribution as shown in Fig. 13.3(a). The voltage distribution is equivalent to two voltage waves v_f and v_b of half the strength, identical in shape and travelling in opposite directions. The current waves associated with these voltage waves have opposite sign and these at this instant ($t = 0$) superimpose to zero resultant current as illustrated. At $t = t_1$ when each of the wave sets (voltage and current) have travelled 1/4 km (say) in opposite directions, the resultant picture is illustrated in Fig. 13.3(b). Again in Fig. 13.3(c) is illustrated the case when the wave sets have travelled so far that no parts of these overlap.

Reflection and Refraction of Travelling Waves

When a travelling wave arrives at a discontinuity in a line, where the Z_c of the line changes (abruptly), some adjustment must take place, if the proportionality between voltage and current wave (Z_c) is to be maintained. This adjustment takes the form of the initiation of two new wave pairs. The reflected voltage

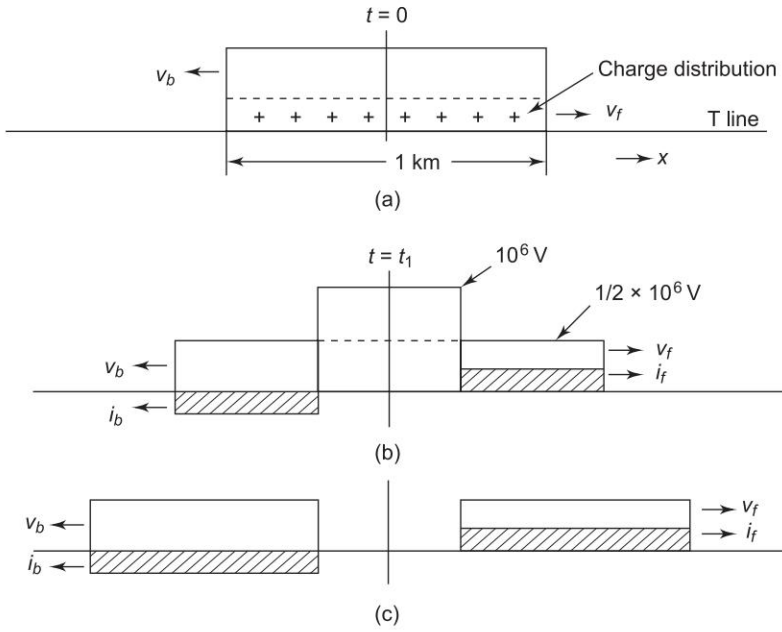

Fig. 13.3 Voltage and current travelling waves

wave and its companion current wave travel back down the line and are superimposed on the incident (incoming) wave. The *refracted* (continuing or transmitted) wave pair penetrates and travels beyond the discontinuity.

Figure 13.4 shows the junction of two lines (these could also be a line and a cable) with characteristic impedances of Z_{c1} and Z_{c2}. Here

v_i, i_i = incident wave pair

v_r, i_r = reflected wave pair

v_t, i_t = reflected (transmitted) wave pair

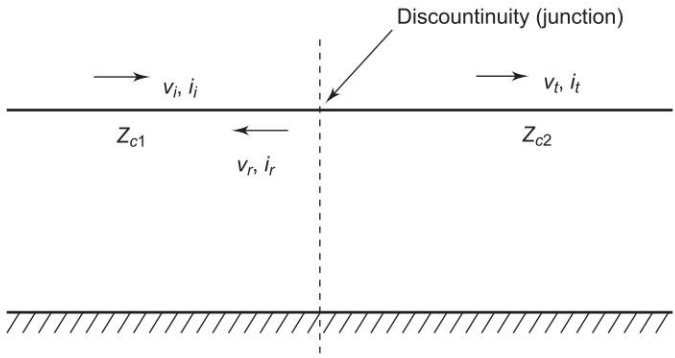

Fig. 13.4 Reflection and refraction of travelling waves

Applying the Kirchhoff's voltage and current laws at the junction

$$i_i + i_r = i_t \tag{13.9}$$

$$v_i + v_r = v_t \tag{13.10}$$

Equation (13.9) can be written in terms of voltage waves as

$$\frac{v_i}{Z_{c1}} - \frac{v_r}{Z_{c1}} = \frac{v_t}{Z_{c2}} \tag{13.11}$$

From Eqs (13.10) and (13.11), we get by elimination

$$v_r = \left(\frac{Z_{c2} - Z_{c1}}{Z_{c2} + Z_{c1}}\right) v_i \tag{13.12}$$

$$= \alpha v_i$$

where $\alpha = \dfrac{Z_{c2} - Z_{c1}}{Z_{c2} + Z_{c1}}$ = reflection coefficient (for voltage)

Also

$$v_t = \left(\frac{2Z_{c2}}{Z_{c2} + Z_{c1}}\right) v_i \tag{13.13}$$

$$= \beta v_i$$

where $\beta = \left(\dfrac{2Z_{c2}}{Z_{c2} + Z_{c1}}\right)$ = refraction (transmission) coefficient (for voltage). It may be easily noted that

$$\beta = 1 + \alpha \tag{13.14}$$

From Eq. (13.12),

$$-\left(-\frac{v_r}{Z_{c1}}\right) = \alpha \frac{v_i}{Z_{c1}}$$

or

$$i_r = -\alpha i_i \tag{13.15}$$

It means that the reflection coefficient for current is negative of the reflection coefficient for voltage.

For three special cases,

- Open-circuited line: $Z_{c2} = 0$ gives $\alpha = 1$, $\beta = 2$.
- Short-circuited line: $Z_{c2} = 0$ gives $\alpha = -1$, $\beta = 0$.
- Line terminated in its characteristic impedance (*matched termination*): $Z_{c2} = Z_{c1}$ gives $\alpha = 0$, $\beta = 1$.

It is seen from above that in the case of *matched termination*, there is no reflection and the line acts as if it is infinitely long. This thought is of importance in communication lines, but not in power lines.

Treatment of lines with lumped discontinuities (series lumped L or shunt lumped C) requires the use of the Laplace transform, and will be taken up at the end of this section.

Open-circuited Line As seen above

$$v_r = \alpha v_i = v_i$$

$$i_r = -\alpha v_i/Z_c = -v_i/Z_c = -i_i$$

Various stages in the process of reflection of a rectangular voltage wave and its associated current at the open-circuited end of a line are illustrated in Fig. 13.5. At $t = t_3$, voltage becomes double and current reduces to zero. At this stage all the energy stored in line inductance has been transferred to line capacitance, i.e.,

$$\frac{1}{2} Li_i^2 = \frac{1}{2} Cv_r^2$$

or

$$v_r = \sqrt{L/C}\ \ i_i = Z_c\, i_i = v_i$$

which is already indicated by the voltage reflection coefficient of $\alpha = 1$.

At $t = t_5$, it is seen that the voltage and current wave pair has been fully reflected (voltage positively and current negatively) at the open line end and are now travelling in the opposite direction.

Short-circuited Line At a short-circuited end

$$v_r = \alpha v_i = -v_i$$

$$i_r = -(-v_i/Z_c) = i_i$$

Various stages in the reflection process are now illustrated in Fig. 13.6. At $t = t_3$, line current has doubled, but line voltage has been reduced to zero (all the energy is transformed to electromagnetic form). Finally, at $t = t_5$, the voltage and current waves have been fully reflected and are now travelling in opposite directions (voltage reflected negatively and current positively).

Line Connected to Cable

A voltage wave upon entering a cable from a line gets modified as (Eq. (13.13))

$$v_t = \left(\frac{2Z_2}{Z_2 + Z_1}\right) v_i$$

As for a cable

$$Z_2 < Z_1$$

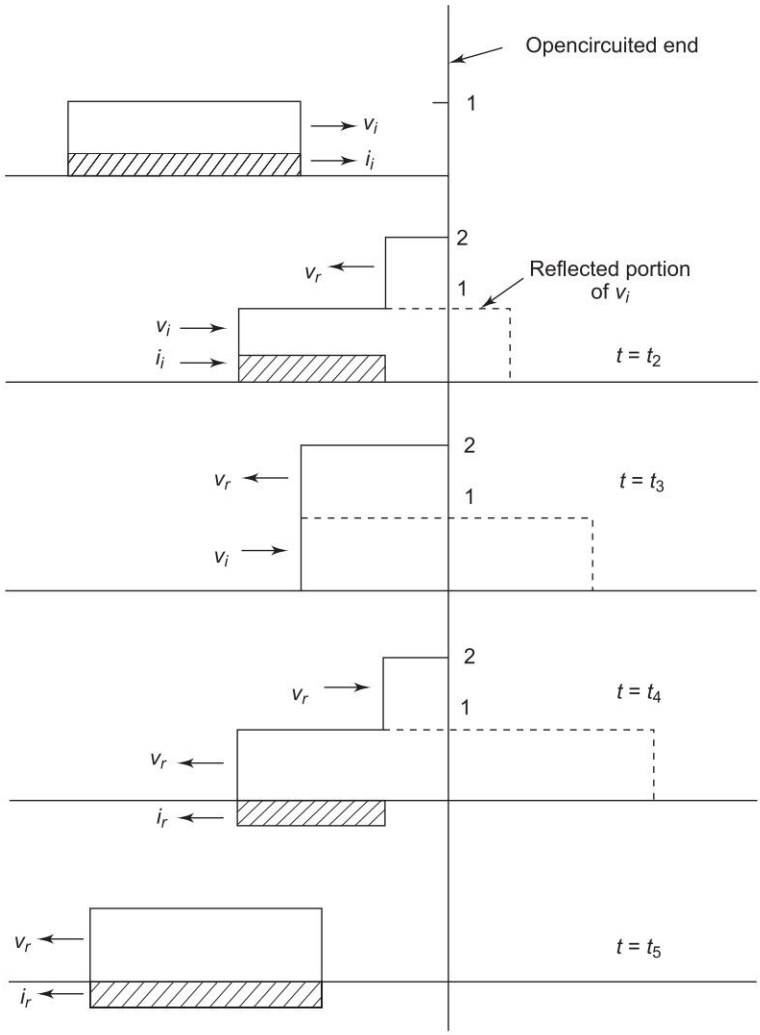

Fig. 13.5 Reflections of an open-circuited line

it follows that

$$v_t < v_i$$

It means that voltage wave travelling along a line reduces in strength upon entering a cable—a beneficial effect of connecting a line to transformer via a cable.

Reflection and Refraction at a T-junction

A travelling wave (E, I) travelling on a line of surge impedance Z_1 meets a junction with two lines having surge impedances respectively of Z_2 and Z_3 as shown in Fig. 13.8(a). On reaching the junction the wave sees the circuit as

shown in Fig. 13.8(b). It immediately follows that the reflection and refraction coefficients for voltage at the junction are

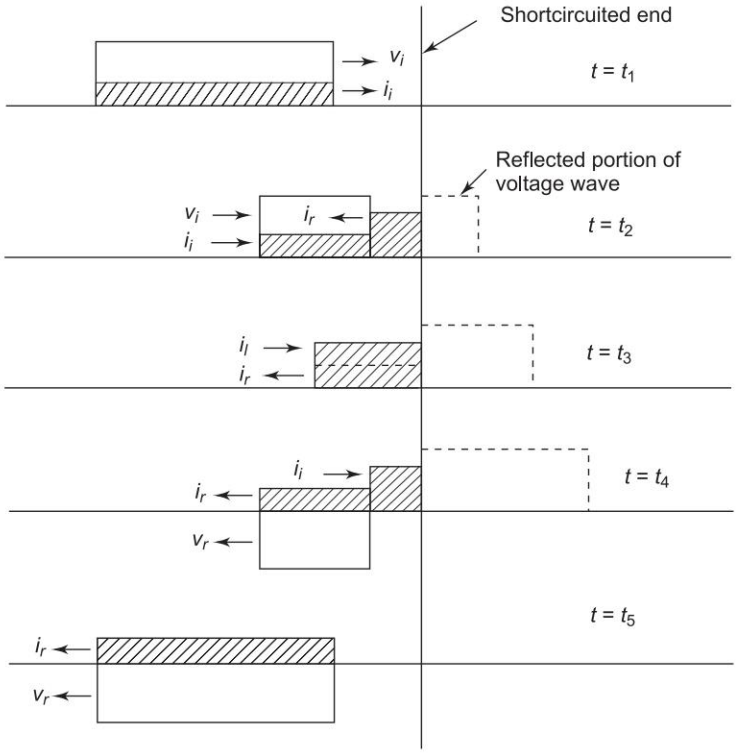

Fig. 13.6 Reflections at a short-circuited line

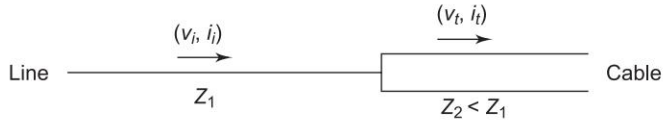

Fig. 13.7

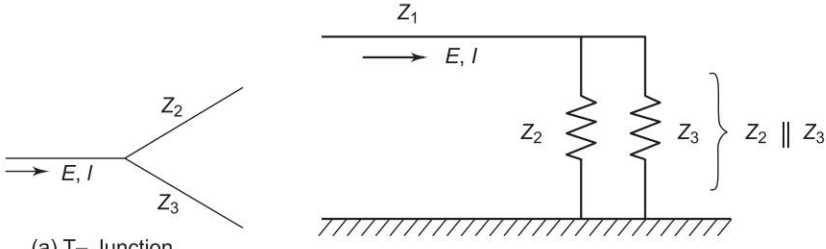

(a) T– Junction

(b) Circuit as seen by the wave pair at the junction

Fig. 13.8

Reflection coefficient, $\alpha = \dfrac{Z_2 \,||\, Z_3 - Z_1}{Z_2 \,||\, Z_3 + Z_1}$

$$= \frac{\dfrac{1}{Z_1} - \dfrac{1}{Z_2} - \dfrac{1}{Z_3}}{\dfrac{1}{Z_1} + \dfrac{1}{Z_2} + \dfrac{1}{Z_3}} \tag{13.16}$$

Refraction coefficient, $\beta = 1 + \alpha = \dfrac{\dfrac{2}{Z_1}}{\dfrac{1}{Z_1} + \dfrac{1}{Z_2} + \dfrac{1}{Z_3}}$ (13.17)

The wave pictures immediately following the reflection in terms of voltage and current waves are drawn in Fig. 13.9, which is self-explanatory (it is assumed that $\alpha < 0$).

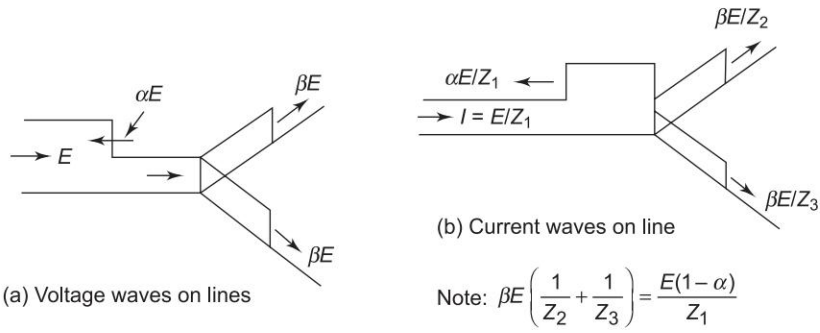

Fig. 13.9 Travelling waves on a T-junction

Lumped Reactive Junctions

When series or shunt lumped reactive elements are present on transmission line, recourse has to be taken to the Laplace transformation technique.

Shunt Capacitance

Figure 13.10(a) shows a line with a shunt capacitance and Fig. 13.10(b) is its equivalent circuit as seen by the travelling wave (e, i) as it reaches the junction J. Let the voltage wave be a step wave of strength E_0, i.e.,

$$e(x, t) = E_0\, u(\gamma t - x) \tag{13.18}$$

Let $t = 0$ when the wave front reaches the junction. It is observed at the junction as a time function

$$e(t) = E_0\, u(t) \tag{13.19}$$

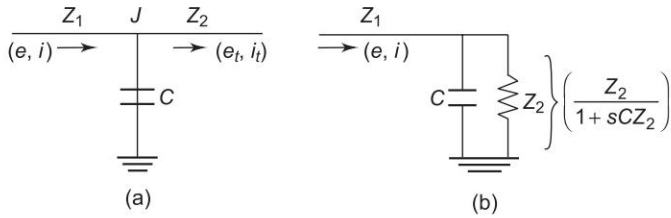

Fig. 13.10 Line with shunt capacitance

From Eq. (13.13), the junction voltage in the Laplace transform form is given by

$$E_J(\mathrm{s}) = \frac{2\left(\dfrac{Z_2}{1+sCZ_2}\right)}{Z_1 + \dfrac{Z_2}{1+sCZ_2}} E(\mathrm{s})$$

$$= \frac{2/Z_1C}{s + 2/Z'C} E(\mathrm{s});\ Z' = \frac{Z_1Z_2}{Z_1+Z_2} \tag{13.20}$$

For step incoming wave

$$E(s) = E_0/s$$

$$\therefore \quad E_J(s) = \frac{(2/Z_1C)\,E_0}{s\,(s+1/Z'C)} \tag{13.21}$$

Inverse Laplace transforming, we get

$$e_J(t) = E_{J0}\,(1 - e^{-t/Z'C})\,u(t) \tag{13.22}$$

where

$$E_{J0} = \left(\frac{2Z_2}{Z_2+Z_1}\right) E_0 \tag{13.23}$$

The junction voltage waveform is sketched in Fig. 13.11(a). This wave is injected into the line beyond C as shown in Fig. 13.11(b).

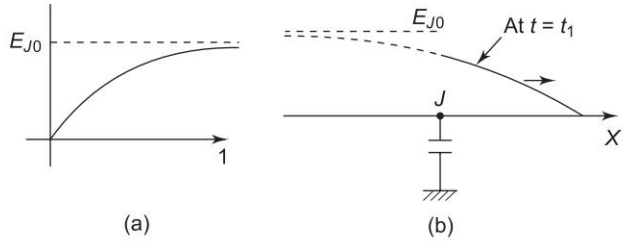

Fig. 13.11

The mathematical form of the onward travelling voltage wave is obtained by replacing

$$t \rightarrow (\gamma t - x)$$

in Eq. (13.21). Thus

$$e_t(x, t) = E_{J0}\,[1 - E^{-(\gamma t - x)/Z'C}]\,u(\gamma t - x) \tag{13.24}$$

The incoming and outgoing voltage waves are sketched in Fig. 13.12. It is observed from this figure that while the incoming voltage wave rises at infinite rate (step function), the outgoing voltage wave has a much reduced rate of rise. This is the wave front modifying property of a shunt capacitance. The rate of rise of voltage is an important factor in determining insulation failure of the terminal equipment. Thus a shunt capacitance hanging on a line protects the terminal equipment.

The reflected voltage wave seen as time function at J is

$$e_r(t) = e_J(t) - e(t)$$

$$= E_0 \left[\left(\frac{Z_2 - Z_1}{Z_2 + Z_1} \right) - \left(\frac{2Z_2}{Z_2 + Z_1} \right) e^{-t/Z'C} \right] u(t) \tag{13.25}$$

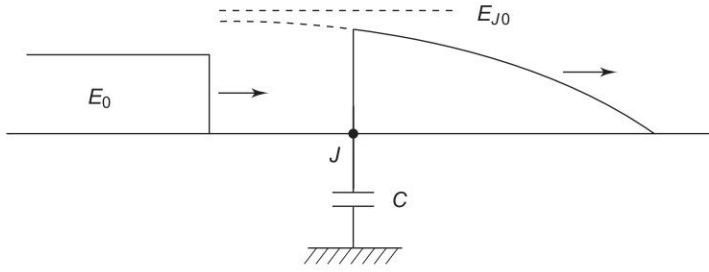

Fig. 13.12

Special Case

The results for the case when the capacitance C is at the termination end of a line, can be obtained by letting $Z_2 = \infty$ in Eqs (13.22) and (13.25). Thus

$$e_J(t) = 2E_0\,(1 - e^{-t/Z_1C})\,u(t) \tag{13.26}$$

and

$$e_r(t) = E_0\,(1 - 2\,e^{-t/Z_1C})\,u(t) \tag{13.27}$$

The incoming voltage wave, the reflected voltage wave, the resultant and the corresponding current waves as per the above results are shown in Fig. 13.13 at a particular instant of time. It is confirmed from this figure that the capacitance acts as a short-circuit as the wave just reaches it (voltage becomes zero, current

becomes double the incoming current wave), and as time elapses, it acts as an open-circuit (voltage becomes double the incoming voltage wave and current reduces to zero).

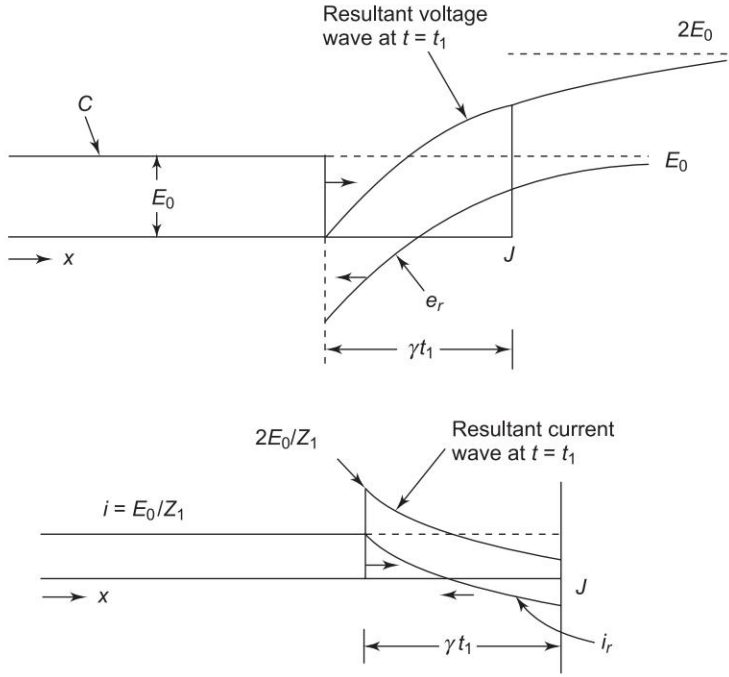

Fig. 13.13 Voltage and current waves on transmission line terminated in a capacitance

Series Inductance

Figure 13.14(a) is that of a line with series inductance and Fig. 13.14(b) shows the circuit seen by the incoming wave when it reaches the first junction J_1. The wave is assumed to be a step. (Eqs (13.18) and (13.19)).
From Eq. (13.13),

$$E_1(s) = \frac{2(sL + Z_2)}{(sL + Z_2) + Z_1} E(s) \tag{13.28}$$

Therefore

$$I_1(s) = \frac{E_1(s)}{sL + Z_2} = \frac{2E(s)}{sL + (Z_2 + Z_1)} \tag{13.29}$$

and

$$E_2(s) = Z_2\, I_1(s)$$

$$= \frac{2Z_2E_0}{s[sL + (Z_2 + Z_1)]} = \frac{(2Z_2 / L)E_0}{s\left(s + \dfrac{Z_2 + Z_1}{L}\right)} \tag{13.30}$$

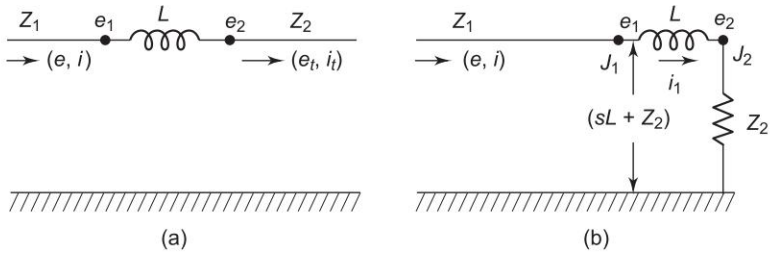

Fig. 13.14 Line with series inductance

Inverse Laplace transforming Eq. (13.30),

$$e_2(t) = \left(\frac{2Z_2}{Z_2 + Z_1}\right) E_0 \left[1 - \exp\left(-\frac{Z_2 + Z_1}{L}\, t\right)\right] u(t) \qquad (13.31)$$

The time voltage wave of Eq. (13.31) then travels along the line beyond L (with characteristic impedance Z_2). Its mathematical expression is

$$e^t(\gamma t - x) = \left(\frac{2Z_2}{Z_2 + Z_1}\right) E_0 \left[1 - \exp\left\{-\left(\frac{Z_2 + Z_1}{L}\right)(\gamma t - x)\right\}\right] u(\gamma t - x) \quad (13.32)$$

The incoming and outgoing voltage waves are sketched in Fig. 13.15. It is again observed that while the rate of rise of incoming wave is infinite (step function), the outgoing wave beyond L rises much more gradually—wave modifier effect of a series inductance. As in the case of a shunt capacitance, it helps to reduce the failure inducing stresses in the insulation of the terminal equipment.

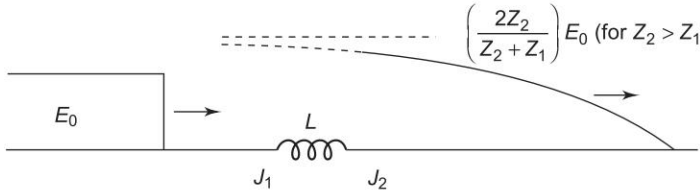

Fig. 13.15

Attenuation and Distortion of Travelling Waves

In this chapter so far lossless simple twin-conductor transmission lines have been considered. But the behaviour of travelling waves on multiconductor transmission lines is extremely complex [3]. Waves travel in more than one mode on multiconductor lines and these different modes may have different velocities.

In this section, we shall briefly deal with attenuation and distortion of travelling waves. Distortion is caused by losses and multiconductor effect. Except in a very special case where $R/L = G/C$, which does not occur in practical power lines, attenuation in travelling waves is accompanied by distortion. Distortionless lines are obviously very desirable in communication circuits and steps are taken to achieve it. But in power transmission lines, it is not a matter of any significance. Here resistive losses are always much greater than those due to leakage. A distortionless condition is hardly an incentive to artificially increase the leakage losses.

Attenuation is mainly caused by series resistance and leakage resistance, and these quantities are considerably larger (about 50 times) for travelling waves than their power frequency values. There are other phenomena that are responsible for attenuation and distortion, of which the most important is *corona*. Voltage surges on lines are unaffected by corona until their potential exceeds the corona threshold. Normally, lines are operated well below the corona threshold, but corona can be observed in wet whether when the corona voltage is lower. Corona reduces the initial peak considerably by the time the wave travels only 1–2 km. After that attenuation continues, but at a reduced rate.

Determination of attenuation is normally empirical, and use is made of the expression $v_x = v_i e^{-\alpha x}$, where v_x is the magnitude of the surge at distance x from the point of origination. Considering the power and losses over an incremental length dx of a line of resistance and shunt conductance per unit length of $R\,\Omega$ and $G\,\Omega$, the power loss

$$\mathrm{d}p = i^2 R\,\mathrm{d}x + v^2 G\,\mathrm{d}x \tag{13.33}$$

Also

$$p = vi = i^2\,Zc;\ \mathrm{d}p = -2i\,Z_c\,\mathrm{d}i \tag{13.34}$$

Here negative sign has been included in dp, as there is reduction in power as the wave travels with time.

From Eqs (13.33) and (13.34),

$$-2i\,Z_c\,\mathrm{d}i = (i^2 R + v^2 G)\,\mathrm{d}x$$

or

$$\frac{\mathrm{d}i}{i} = \frac{1}{2}\left(\frac{R + Z_c^2 G}{Z_c}\right)\mathrm{d}x$$

yielding

$$i = i_i \exp\left[-0.5\left(\frac{R}{Z_c} + GZ_c\right)x\right] \tag{13.35a}$$

where $i = i_i$ = surge amplitude at $x = 0$

or

$$i = i_i\, e^{-\alpha x} \tag{13.35b}$$

where

$$a = \frac{R + Z_c^2 G}{2Z_c}$$

Similarly it can be proved that

$$v = v_i \, e^{-\alpha x} \tag{13.36}$$

and the power at x

$$p_x = v_i \, i_i \exp\left[-\left(\frac{R}{Z_c} + GZ_c\right)\right] x \tag{13.37}$$

If R and G are correctly found out, including corona effect, attenuation may be accounted for in the travelling wave analysis.

From Eqs (13.35b) and (13.36), it is clear that the current and voltage waves get attenuated exponentially as they travel over the line, and the magnitude of attenuation depends on the line parameters. The value of line resistance depends not only on the size of the conductors but also on their shape and the length of waves. An empirical relation due to Foust and Menger relating the original voltage (V_0) to the voltage (V) at any point on the line after attenuation is given below:

$$V = \frac{V_0}{1 + kxV_0} \tag{13.38}$$

where x is the distance travelled in km, and V and V_0 in kV, and the attenuation constant k is given as

k = 0.00037 for chopped waves

= 0.00019 for short waves

= 0.0001 for long waves

In the estimation of transmission-line transients, the effects of attenuation and distortion are normally ignored for simplicity and ease of analysis. The results so obtained are pessimistic—voltages computed are higher than those obtained actually.

Determination of System Voltages Produced by Travelling Waves

As already seen in this chapter, switching operations, faults, lightning surges, and other intended or unintended disturbances cause temporary overvoltages and currents in power systems. The system must withstand these overvoltages with a certain probability, or their effects must be reduced and limited with protective devices. The simulation of transient phenomena is, therefore, important for coordination of the insulation, as well as the proper design of protection schemes. Such simulation is also needed to analyse unexpected

transient phenomena after their occurrence—such as ferro-resonance and subsynchronous resonance. By nature these phenomena are a combination of travelling wave effects on overhead lines and cables, and of oscillations in lumped-circuits of generators, transformers and other devices. It is practically impossible to study these electromagnetic transients using hand calculations, except for very simple cases. This complexity led to the development of transient network analyzers in the late 1930s [4] which are still widely used today.

Travelling waves problems were already studied with graphical methods in the 1920s and 1930s, long before digital computers became available. Basically two techniques became popular, namely, Bewley's lattice diagram technique and Bergeron's method. We will study only the former in detail in this section. Both techniques were later adopted for computer solutions, the lattice diagram technique [8] as well as Bergeron's method [9]. It appears that Bergeron's method is better suited for digital computer solutions, and most existing general-purpose programmes use it. Both these methods are only efficient for lossless, or distortionless, lines. Good accuracy is often obtained by lumping resistance at one or more points along the line. Most general-purpose programmes solve transients problems directly in the time domain. Although many mathematical techniques are available, and in fact used, the one due to Bewley [1] will only be described here as it clearly indicates the physical changes occurring in time.

Bewley Lattice Diagram

In order to keep track of the multiplicity of the successive reflections at the discontinuities in the system, Bewley has devised a time-space diagram which shows at a glance the position and direction of motion of every incident, reflected, and refracted wave on the system at every instant of time. The effect of attenuation and wave distortion can be accounted without much problem.

In the lattice diagram two axes are established, a horizontal one scaled in distance along the system, and a vertical one scaled in time. Lines showing the passage of surges are drawn such that their slopes give the time corresponding to distances travelled. At each point of change in impedance, the reflected and transmitted waves are obtained by multiplying the incidence wave magnitude by the proper reflection and refraction coefficients. Lattice diagrams for current may also be drawn. It should, however, be noted that the reflection coefficient for current is always the negative of the reflection coefficient for voltage.

To illustrate the method of constructing the Bewley lattice diagram, consider the simple system of Fig. 13.16, wherein a DC generator of unit voltage is switched 'on' to a lossless (no attenuation) line of characteristic impedance Z_c, with a load resistance R_c at its receiving end. For simplicity, it is assumed that the generator has zero impedance, such that a unit voltage wave is continuously fed to the line after the switching instant. The reflection coefficient at the receiving end is

$$\alpha_R = \frac{R_L - Z_c}{R_L + Z_c}$$

and that at the sending end is $\alpha_S = -1$, as the generator acts like a short-circuit with the assumption of zero impedance. Let the time of travel of surge from one end of the line to the other be T.

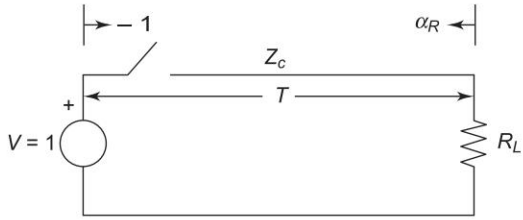

Fig. 13.16

Immediately upon switching a unit, step voltage surge (infinite length) travels down the line towards the receiving end. This fact is recorded diagrammatically by a line sloping downward (left to right) as shown in Fig. 13.17. When the surge reaches the line end (in T s), a surge of amplitude α_R is originated in the reflection process, which then travels towards the generator end reaching there at $t = 2T$ represented by a sloping line (right to left). The reflection at the generator end causes an outward surge of strength—α_R. This process continues indefinitely, and some of its steps are illustrated in the Bewley lattice diagram of Fig. 13.17.

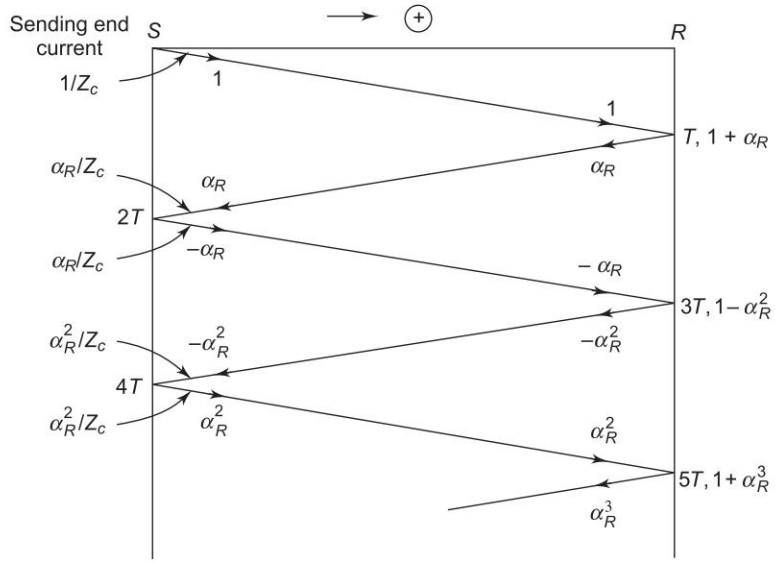

Fig. 13.17 Bewley lattice diagram

It is easily observed from the Bewley lattice diagram that, at the receiving-end, the increment of voltage at each reflection is the sum of the incident and reflected waves. The resultant voltages at various instants are written down in the right side of this diagram. In terms of series

$$V_R = (1 + \alpha_R) - (\alpha_R + \alpha_R^2) + (\alpha_R^2 + \alpha_R^3) - \ldots$$
$$= (1 + \alpha_R)\,[(1 + \alpha_R^2 + \alpha_R^4 + \ldots - (\alpha_R + \alpha_R^3 + \alpha_R^5 + \ldots)]$$

After infinite reflections, the voltage becomes

$$V_R = (1 + \alpha_R)\left[\frac{1}{1-\alpha_R^2} - \frac{\alpha_R}{1-\alpha_R^2}\right]$$
$$= 1$$

as it should be in the steady-state.

The receiving-end voltage is plotted against time in Fig. 13.18(a) and (b) for $\alpha_R > 0$ and $\alpha_R < 0$, respectively. In the former case the voltage settles to unit value in an oscillatory manner (square wave oscillations) and the latter case represents an overdamped situation.

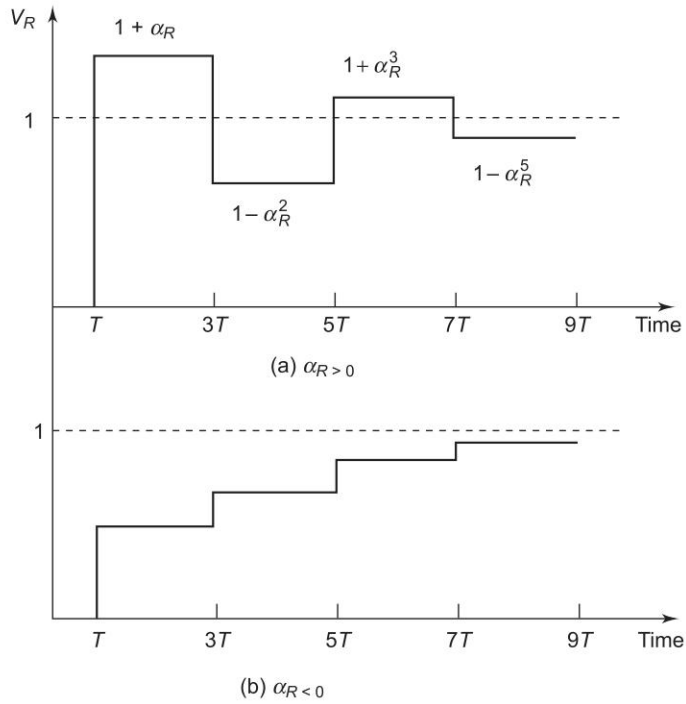

Fig. 13.18 Receiving end voltage vs. time

Let us now plot the sending end current. Each out-going surge is accompanied by a current wave of strength (voltage/Z_c) and each incoming wave is accompanied by a current wave (– voltage/Z_c). The plot of sending-

end current vs time is drawn in Fig. 13.19 for $\alpha_R > 0$. The steady value of the sending-end current is given by

$$I_S = \frac{1}{Z_c}\,[1 - 2\alpha_R + \alpha_R^2 - 2\alpha_R^3 + ...]$$

$$= \frac{1}{R_L} \text{ (the reader should prove this)}$$

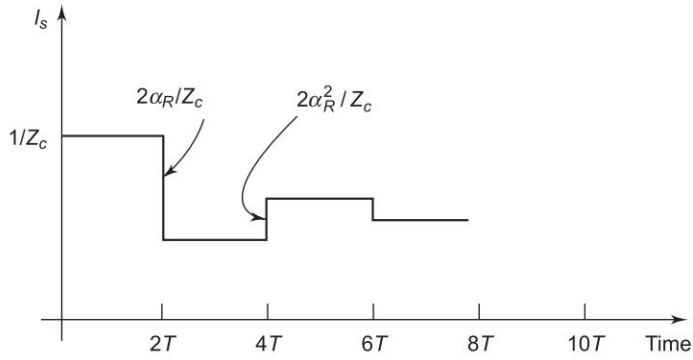

Fig. 13.19 Sending end current vs. time for $\alpha_R > 0$ (0.25)

Example 13.1 A unit-step voltage surge is travelling on a long line of surge impedance Z_1. It reaches the junction with a cable of finite length whose far end is open. The cable has a surge impedance of Z_2 and the time of one-way wave travel on it is T. Draw the Bewley lattice diagram and find from it the value of voltage at the junction at time $4T$ after the surge reaches the line-cable junction.

Given: $Z_1/Z_2 = 9$

Solution

Reflection coefficient line to cable, $\alpha_1 = \dfrac{1-9}{1+9} = -0.8$

Reflection coefficient cable to line, $\alpha_2 = \dfrac{9-1}{9+1} = +0.8$

Refraction coefficient line to cable, $\beta_1 = \dfrac{2\times 1}{1+9} = 0.2$

The Bewley lattice diagram is drawn in Fig. 13.20

Voltage at junction $4T^+$ (just after reflection has taken place)

$$= 1 - 0.8 + 0.36 + 0.288 = 0.848$$

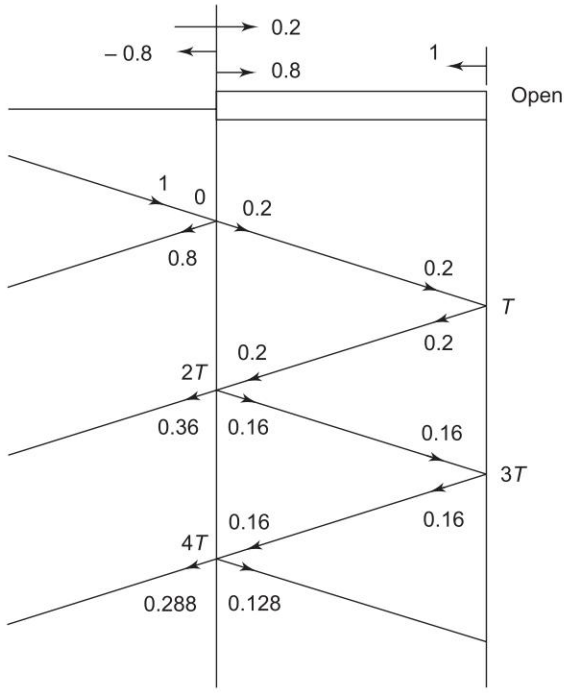

Fig. 13.20

Case of Finite Generator Impedance

With finite generator impedance Z_g, the voltage impressed on the line will be

$$\left(\frac{Z_c}{Z_g + Z_c}\right) V_g \tag{13.39}$$

where V_g is presented with the voltage divider circuit of Fig. 13.21.

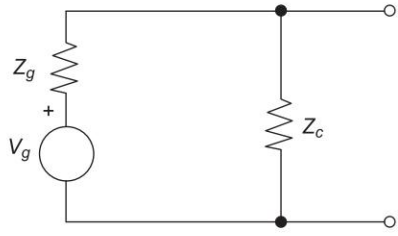

Fig. 13.21

13.4 GENERATION OF OVERVOLTAGES ON TRANSMISSION LINES

Transmission lines and power apparatus have to be protected from overvoltages. The overvoltages in a power system fall under three categories:

- Resonance overvoltages
- Switching overvoltages
- Lightning overvoltages

Overvoltages due to the latter two causes, though transient in nature, constitute the basis for selection of insulation level of lines and apparatus, and of devices for surge protection. Resonance overvoltages on the other hand decide the steady voltage rating of such devices. Resonance and switching overvoltages are directly related to the system operating voltage, but the level of lightning overvoltages caused by the natural phenomenon are independent of it. At transmission line voltages upto around 230 kV, the insulation level is dictated by the requirement of protection against lightning. For voltages from 230 kV to 700 kV, both switching transients and lightning overvoltages must be accounted for in deciding the insulation levels. In EHV (> 700 kV) switching surges cause higher overvoltages than lightning, and are therefore mainly responsible for insulation level decision. Fortunately cables are not exposed to lightning, and are automatically immune to the line surges which attenuate upon entering a cable (see Sec. 13.3). However, lines are preferred to cables for economic and technical reasons.

Resonance Overvoltages

Though it is unlikely that resonance in a supply network be obtained at normal supply frequencies, it is possible to have this condition at harmonic frequencies. Near resonance conditions may occur under certain type of unsymmetrical faults. Temporary overvoltages are also caused by inrush current, when transformers or reactors are energized (ferroresonance). Such overvoltages are important in choosing lightning arresters, which are not supposed to operate at these voltages. Thus they indirectly determine the insulation level of the network.

Switching Overvoltages

These overvoltages are caused by normal switchgear operation and/or power system faults, and their magnitudes are related to the system operating voltages. Further, these overvoltages have a very wide range of magnitudes and wave shapes and last for durations ranging from a few μs to several seconds. At EHV levels the most important causes of switching overvoltages are classified as:

- Sustained earth fault on phase conductors.
- Energization or reclosure of long lines.
- Load rejection at receiving end.
- Fault initiation and reclosure.

Switching transients are also classified as single-energy or double-energy transients. In a single-energy transient, energy is redistributed in the circuit inductance or capacitance while in a double-energy transient, one transient is interchanged between system inductance and capacitance, giving rise to natural frequency $\left(f_n = 1/2\pi\sqrt{L/C} \text{ with } R = 0\right)$ voltages and currents. Closing a circuit may result in excessive currents, and perhaps voltages also, while its opening normally results only in excessive transient voltages.

Among factors which decide the switching behaviour of power systems are the nature of source, characteristics of the transmission circuit, its length, the termination condition, the characteristic of earthing and shunt compensation. When the terminations are such that the energy is entirely or almost entirely reflected, high surge voltages are likely to build up (see Sec. 13.2).

The most important switching operations to be considered are line energization and reclosing. With the improvement of arc restriking performance of circuit breakers, the consequent surges—interruption of line charging current and chopping of magnetizing current are no longer of significance.

Attenuation of surges caused by line losses, and corona and reflection at the far end of the line from a loaded transformer help reduce the switching overvoltages, but mutual effects of sequential reclosing of the three phases tend to accentuate these.

The cost of EHV transmission system may be lowered by decreasing the switching overvoltages. This can be achieved by employing a circuit breaker, filled with a closing resistor of the order of the line surge impedance, in series with the breaker and the line which is subsequently short-circuited. The system is energized in two stages, producing two overvoltages, both of which are smaller than the overvoltage produced without the resistor.

Lightning Overvoltages

Lightning is a naturally occurring phenomenon (for theory of lightning consult reference [5]) wherein clouds get charged to several thousand kilovolts, and a discharge (stroke) can occur to high ground objects, or even to the ground. Transmission lines and towers being high objects attract lightning stroke, the underground cables being inherently immune to strokes. Lightning transients to which power system (lines, towers, substations and generating stations) are susceptible may occur on account of:

- Indirect strokes
- Direct strokes to phase conductors
- Direct strokes to towers
- Direct strokes to earth wires

Direct Stroke

A direct stroke occurs when a thunder cloud directly discharges on to transmission lines, tower or earth wires. This is the most severe and rarest form of stroke.

Indirect Stroke

When a thunder cloud passes over ground objects, it induces a positive charge in them. Over a period of hundreds of seconds, positive charges leak from the tower along the string insulators to the line conductors. This happens due to high field gradients involved. In the event the cloud discharges to some earth object, the line is left with a huge free concentration of positive charge, which cannot leak suddenly, but instead travels in the form of two identical surges in either line direction. This is called an indirect stroke.

Typical lightning voltage surge in waveform and amplitude that may be injected in direct stroke on line conductors in absence of ground wire is shown in Fig. 13.22(a). Typical lightning current on transmission line towers is shown in Fig. 13.22(b). High voltages of the form of Fig. 13.22(a) are known as *impulse voltages*. The standard test impulse voltage will be defined later in this section.

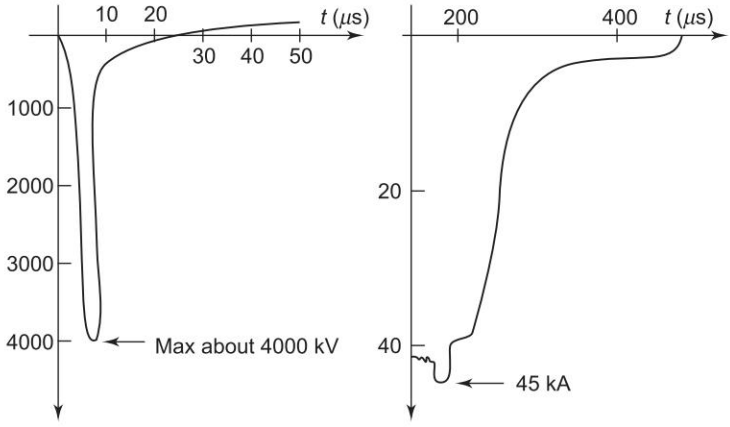

(a) Typical lightning stroke voltage on transmission line without ground wire

(b) Typical lightning current on a transmission line tower

Fig. 13.22

Back Flashover

A direct stroke to tower causes a high voltage to be set up across the tower inductance and tower footing resistance by the fast changing lightning current (say 10 kA/μs). This appears as an overvoltage between the tower top and conductors which are at lower voltage and can cause a flashover from tower to line conductor across the line insulator, called back flashover. The voltage wave caused on the line because of back flashover has a very high rate of rise which can cause damage to terminal equipment.

The amplitudes of voltages induced indirectly by lightning strokes to a tower, earth wire or nearby ground object, are normally much less than those caused by direct stroke to a line conductor. This voltage depends upon electrical nature of tower footing resistance and stroke characteristics. They are of

significance at lower voltages, such as 33 kV and below, and may even be important above this voltage.

13.5 PROTECTION OF TRANSMISSION LINES AGAINST LIGHTNING

Surges due to lightning are mostly injected into the power system through long cross-country transmission lines. Substation apparatus is always well shielded against direct lightning strokes. The protection of transmission lines against direct strokes requires a shield to prevent lightning from striking the electrical conductors. Adequate drainage facilities and adequate insulation structures must be provided so that the discharge can drain to ground without affecting the conductors. This prevents any arc from line conductor to ground.

Protection Using Shielding Wires or Ground Wires

The ground wire is a conductor run parallel to the main conductors of the transmission line. It is placed higher than the main conductors, is supported on the same towers and is earthed at equally and regularly spaced towers. It acts in two ways to protect the main conductors.

- The ground wire helps to increase the effective capacitance between the line conductor and ground, such that the voltage appearing between conductor and ground because of static cloud charge is reduced. This is illustrated by the capacitor equivalent of the cloud–conductor system shown in Fig. 13.23.

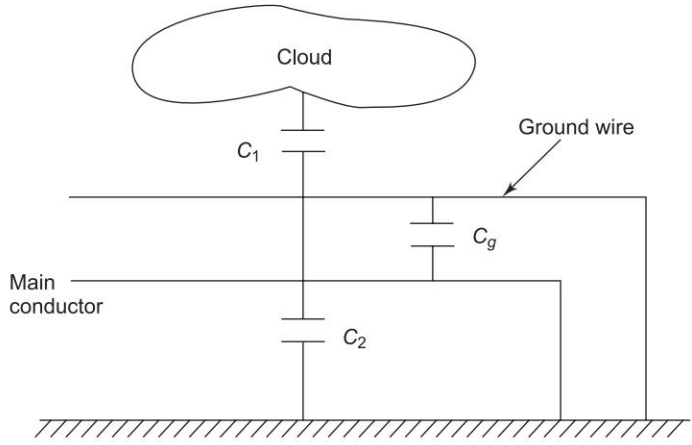

Fig. 13.23

- Being higher than the ground wire shields the main conductor against direct strokes, though it increases the probability of a direct stroke to itself (more than what it would be for the main conductor if the ground wire were absent). *The protection* (*or shielding*) angle of a ground wire is

found to be 30° for tower heights of 30 m or less. The protection zones of one and two ground wires are shown in Fig. 13.24(a) and (b), while Fig. 13.24(c) shows a double circuit line protected by a single ground wire. The height of the ground wire above the highest line conductor can be easily determined by the protection zone geometry. However, the present trend in fixing tower height and the shielding angle is by considering flashover rates and failure probabilities.

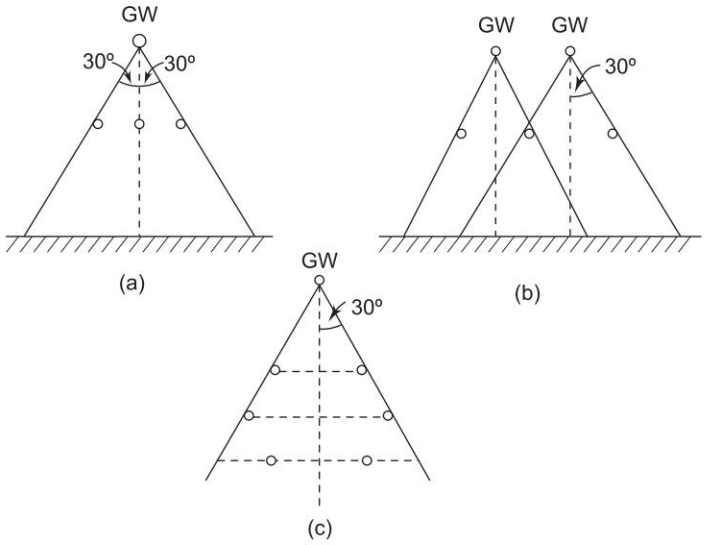

Fig. 13.24

- The presence of ground wire(s) helps reduce the rise of back flashover in the event of direct stroke to tower, as the instantaneous potential to which the tower top is raised is reduced by the fact that half the surge impedance ($Z_g/2$) of the ground wire appears in parallel to the tower surge impedance (Z_T). It follows from Fig. 13.25 that the tower top voltage is

$$V_T = \left(\frac{Z_T}{1 + \dfrac{2Z_T}{Z_g}} \right) I_i \qquad (13.40)$$

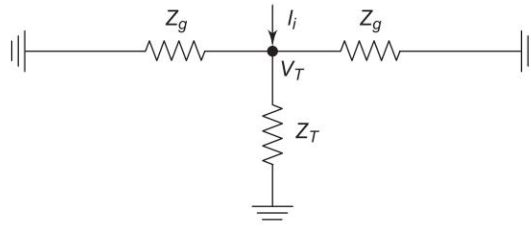

Fig. 13.25

where I_i is the impulse current injected into the tower. It is easily seen that Z_g (as low as possible) reduces V_T.

If the surge impedance of the tower which is the effective tower footing resistance, is reduced, the tower top surge voltage reduces to a considerable extent. Towers are grounded by providing driven ground rods and counterpoise wires [7] connected to tower legs at its foundations.

The standard value of this resistance is around 10 ohms for 66 kV lines, and increases with the operating voltage. For 400 kV it is approximately 80 ohms. The tower footing resistance is the value of the footing resistance when measured at 50 Hz. It is made as low as economically justifiable.

13.6 PROTECTION OF POWER SYSTEM APPARATUS AGAINST SURGES

In spite of the protection of transmission lines described earlier, sufficiently intense voltage surges can reach the substation and can damage the apparatus. The apparatus at substation (switchgear and transformer) is very expensive and outages can be prolonged, and must therefore be provided with almost 100% protection against surges. A two-pronged approach is followed in the protective scheme for apparatus. Surges before they reach the substation are modified to reduce the slope of their wave front. Upon reaching the substation, surges above a certain peak value are diverted into a shunt path to discharge their energies. As a result, the surges that finally reach the apparatus are so modified and reduced in strength as to be completely innocuous. The shunt discharge path for the surge must be autoclearing so as not to constitute a fault on the line.

Surge Modifiers

A surge modifier is nothing but a small shunt capacitor connected between the line and earth, or a series air-cored inductor. By temporary energy storage in them, the modifiers reduce the steepness of the surge wave front, which otherwise can be damaging to apparatus. Their theory has already been explained in Sec. 13.3. Damping resistors may be connected to reduce the oscillatory effects.

Corona on lines also removes some of the surge energy, thereby modifying the wave front.

Surge Diverters (Arresters)

Terminal equipment is protected against surges by surge diverters, also called surge arresters. A diverter is connected in shunt between the line and ground. Ideally it should

- become conducting at voltage above diverter rating;
- restrict the voltage across its terminals to the design value;

- become nonconducting again when the line-to-neutral voltage becomes lower than the design value. In other words it should not permit any *power follow-on current*;
- not conduct any current at normal or somewhat above normal power frequency voltages.

Three types of surge diverters are described below in principle, construction and application.

Rod gap

This is constituted of a plain air-gap between two square rods (1 cm^2) bent at right angles and connected between the line and earth as shown for the case of a transformer bushing in Fig. 13.26. The gap may also be in the form of horns or arcing rings.

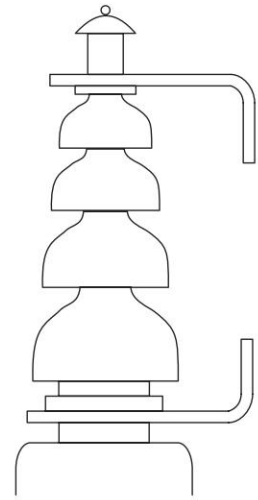

Fig. 13.26 Rod gap on bushing insulator

When the surge voltage reaches the design value of the gap, an arc appears in the gap providing an ionized path to ground, essentially a short-circuit. The gap suffers from the defect that after the surge has discharged, power frequency current continues to flow through the ionized path and the arc has to be extinguished by opening of circuit breakers resulting in outage. Rod gap is therefore generally used as back-up protection.

For a given gap the time to breakdown varies inversely with the applied voltage. It is normally recommended that a rod gap should be so set that it breaks down at a voltage no less than 30% below the voltage withstand level of the equipment to be protected.

Expulsion Type of Lightning Arrester (Protector Tube)

It is improvement over a rod gap. In Fig. 13.27 the series gap is set to arc over at a specified voltage lower than the withstand voltage of the equipment to be protected. The follow-on current is confined to the space inside the relatively small fibre tube. Part of the tube material vaporizes, and the high pressure gases so formed are expelled through the vent at the lower end of the tube, causing the power follow-in arc to be extinguished. The device, therefore, has the desired self-clearing property. Because of the vaporization of the tube material and weathering effect, the protector tube requires frequent replacement and

lack of proper maintenance may lead to occasional outage. It has not, therefore, found favour in application and is practically out of use now.

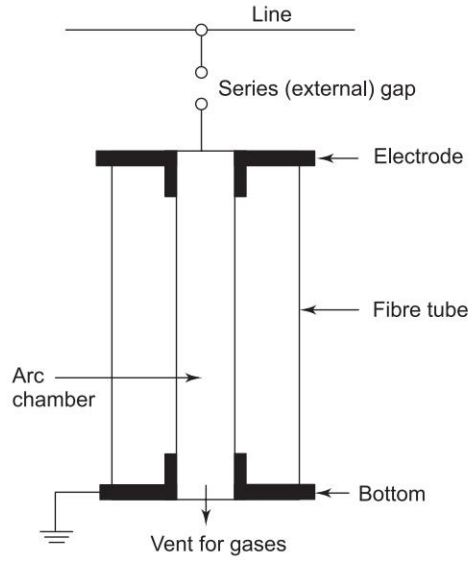

Fig. 13.27 Expulsion type lightning arrester

Valve Type (Nonlinear) Lightning Arrester (LA)

The valve type lightning arrester consists of nonlinear resistors in series with spark-gaps, as shown in Fig. 13.28. The spark-gap assembly acts as a fast switch, which gets ionized (conducting) at specified voltage. The nonlinear

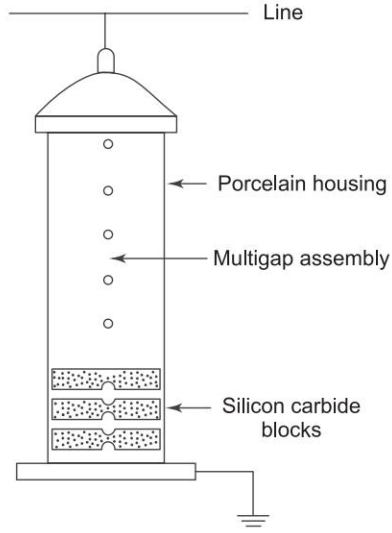

Fig. 13.28 Valve type lightning arrester (LA)

resistor elements are stacked, one over the other, in two or three sections. The problem of non-uniform voltage distribution across gap is solved by capacitors and non-linear resistors connected in parallel across each gap as shown in Fig. 13.29. As a result, the gap assembly has a high degree of consistency of breakdown (flashover) voltage. The entire assembly is placed in procelain housing, properly sealed to keep out dust and moisture.

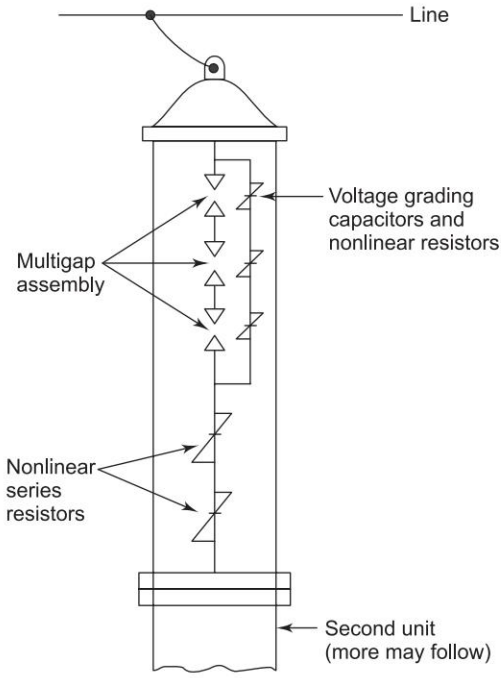

Fig. 13.29

The nonlinear resistors are made of loosely packed *silicon carbide*. The modern trend is to use *zinc oxide*, which gives more desirable characteristics. Because of loose packing of silicon carbide particles, the conduction process through it is mainly by means of short arcs and hence the nonlinear resistor characteristic. The static characteristic is empirically expressed as

$$I = KV^a \tag{13.41}$$

where I = discharge current
v = voltage across the element
a = an exponent more than unity (≈ 4)
K = constant

K and a depend upon the material, packing and dimensions of the element.

Because of the exponent a being close to 4, the current through the element rises more rapidly with the applied voltage than in the linear case which, in other words, means that the element offers a much lower resistance at higher currents. The dynamic characteristic of the diverter (several elements in series) for a surge current (rising and then falling) is shown in Fig. 13.30.

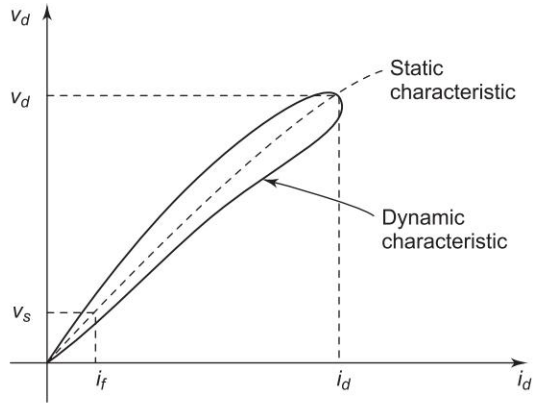

v_d = maximum voltage across the diverter during discharge of the surge current with peak value i_d
i_f = power frequency follow-on current at system voltage v_s

Fig. 13.30 Dynamic volt–ampere characteristic of surge diverter

Because of the nonlinear diverter characteristic, the power follow-on current at system voltage is so small that the cooling and deionizing effects of gap assembly are able to extinguish the arc. This gives the self-clearing property to the diverter, which is essential to its operation after the surge current has been discharged to ground.

As a voltage surge shown in Fig. 13.31 travelling on the line reaches the surge diverter, it breaks down at a specified voltage v_{bd}. The voltage across the diverter instantly dips and then, as the surge current shown discharges through it, a nearly constant voltage of value v_r, called *residual voltage* is maintained across it. After the surge current has discharged, the power follow-on current is interrupted by the gap assembly. The zinc oxide diverters maintain a practically

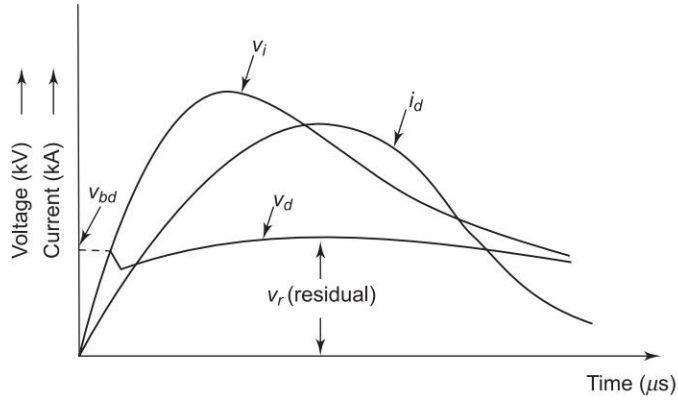

Fig. 13.31 Surge diverter operation

constant residual voltage over a very wide current range. Further their power follow-on current is so small that it is not essential to use a series air-gap to limit this current.

The important ratings of a surge diverter are:

- Rated system voltage (it should be able to withstand an overvoltage of 5%)
- Breakdown voltage
- Residual voltage
- Peak discharge current

13.7 INSULATION COORDINATION

Insulation coordination is the correlation of the insulation levels of various equipment of a high-voltage power system so as to minimize damage and loss of supply due to overvoltages. The insulation level of an equipment is defined as the combination of voltages (power-frequency and impulse) that characterize the insulation with regard to its ability to withstand various stresses. A proper insulation coordination has to ensure

- that the system insulation will withstand all normal, and most of the abnormal, stresses;
- that the overvoltages (generated internally or externally injected) are efficiently discharged to ground; and
- the external flashovers will protect equipment against failure, such as puncture or breakdown of insulation.

The problem of insulation coordination is that of a trade-off between the cost of equipment insulation sufficient to withstand overvoltages that are permitted to reach it by the protective devices (ground wire, LAs), the cost of the protective devices, the probability of equipment damage and the frequency and severity of outages.

The insulation coordination in a power system requires

- the determination of line insulation level;
- the selection of the basic insulation level (BIL) (defined later) and insulation level of other equipment; and
- that selection of proper protective devices, such as LAs, so as to provide to the equipment economically justifiable protection.

Before proceeding to tackle the coordination problem enunciated above, certain terms used in HV technology must be defined.

Basic Impulse Insulation Level or Basic Insulation Level (BIL)

Basic impulse insulation level or basic insulation level (BIL) is expressed as the impulse crest (peak) voltage of a standard wave not longer than $1.2 \times 50\ \mu s$ wave (defined later). Apparatus insulation levels as demonstrated by suitable tests should be equal to, or greater than, the BIL.

BIL measures the ability to withstand test voltages without disruptive discharge. For example, a transformer for 400 kV system tested successfully at 900 kV peak, is said to have a BIL of $\left(900 \div \frac{400\sqrt{2}}{\sqrt{3}}\right) = 2.76$ pu.

Critical Flashover (CFO) Voltage

Critical flashover (CFO) voltage is the peak voltage for a 50% probability of flashover or disruptive discharge.

Impulse Ratio

Impulse ratio (for flashover or puncture of insulation) is the impulse peak voltage divided by the peak value of the power frequency voltage to cause flashover or puncture.

Each equipment is normally tested for both the normal AC frequency and impulse strength.

Standard Impulse Test Wave

Impulse tests are generally carried out with typical impulse test wave called "1.2×50 μs standard test wave", which reaches 90% of its peak value in 1.2 μs and falls to half the peak value in 50 μs as shown in Fig. 13.32. This also typifies lightning surges. Mathematically, this wave can be expressed as the difference of two decaying exponentials i.e.,

$$v = V_0(e^{-\alpha t} - e^{-\beta t}) \tag{13.42}$$

with $\beta > \alpha$.

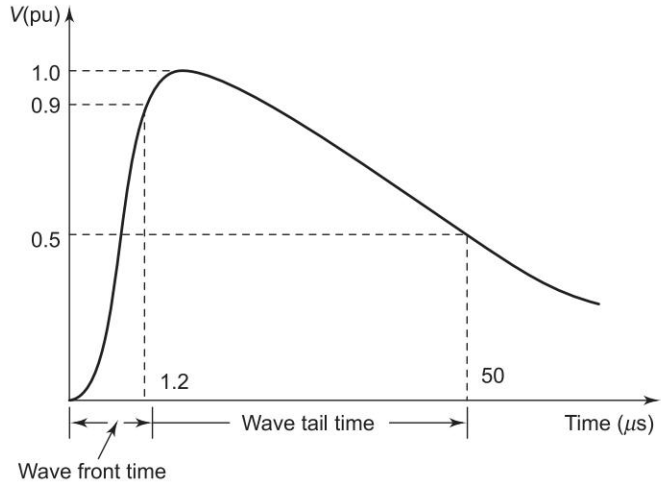

Fig. 13.32 Standard 1.2×5 μs test wave (time not to scale)

The standard test wave is obtained from an impulse generator, where capacitors are charged in parallel and discharged in series through resistors.

Switching surges comprise damped oscillatory waves, the frequency of which is given by system configuration and parameters. They are generally of amplitude 2–4 pu (base voltage – peak value of line to earth operating voltage).

Volt–time Characteristic (Curve)

For proper insulation coordination, one needs the understanding of the volt-time characteristic, apart from the meaning of BIL. It is a graphical indication of the relation between the crest flashover voltages and the time to flashover of an equipment for a series of impulse applications of a given wave shape. Figure 13.33 shows that keeping the wave front time as constant and raising in steps the peak voltage from relatively low values, a peak voltage is reached which is the highest at which the test object does not flashover. This peak value is the full wave impulse withstand voltage. If flashover occurs on the front of the wave, the flashover point is taken on the volt-time curve. If the flashover occurs on the tail side of the wave, in this case draw a horizontal line from the peak value of this wave and also draw a vertical line passing through the point where the flashover occurs. The intersection of the horizontal and vertical lines gives the point on volt-time curve.

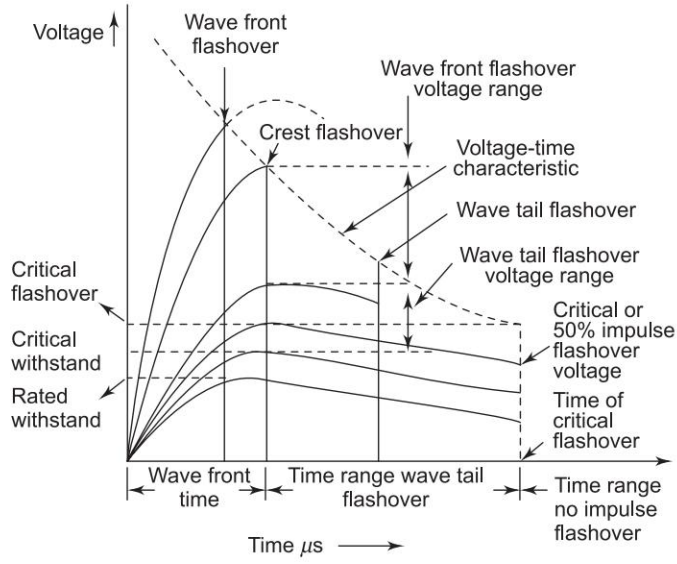

Fig. 13.33 Voltage–time characteristic of equipment under impulse voltage test

BIL of Equipment

To help in the process of insulation coordination, standard insulation levels are recommended and are summarized in Table 13.1. Reduced basic insulation

levels are employed while considering switching surges (see Table 13.1) or for solidly grounded systems.

The apparatus to be protected should have a withstand test value not less than the kV magnitude given in second column of Table 13.1 whatever may be the polarity of the wave and irrespective of the type of system grounding. At 345 kV, the switching voltage is considered to be 2.7 pu, i.e. 931.5 kV, which corresponds to the lightning level. At 500 kV, however, a 2.7 pu switching impulse would require 40% more tower insulation than that governed by lightning. The trend is, therefore, for another design of switching impulse level to be forced lower with increasing system operating voltage and controlling the surges by use of resistive switching in the circuit breakers. Thus for 500 kV network the level is 2 pu and, with further increase in system voltage, it is envisaged to decrease the level to 1.5 pu.

Table 13.1 Recommended standard BILs at various operating voltages

Reference Class (kV)	*Standard Basic Impulse Level (kV)*	*Reduced BIL (kV)*
23	150	
34.5	200	
46	250	
69	350	
92	450	
115	550	400
138	650	500
161	750	600
196	900	—
230	1050	900
287	1300	1050
345	1550	1300
500	1800	1550

Insulation Coordination

Proper insulation coordination should ensure that the volt-time curve of the weakest piece of equipment in the system will lie above the volt-time curve of the protective device such as lightning arrester, over the whole range of the volt-time curve as shown in Fig. 13.34. This weakest piece is always the transformer, the single most expensive equipment with intricately formed insulation. It is easily seen here that the incoming voltage surge which would have otherwise damaged the transformer insulation is reduced to that of the volt–time curve (residual voltage) of the lightning arrester such that the transformer is fully protected.

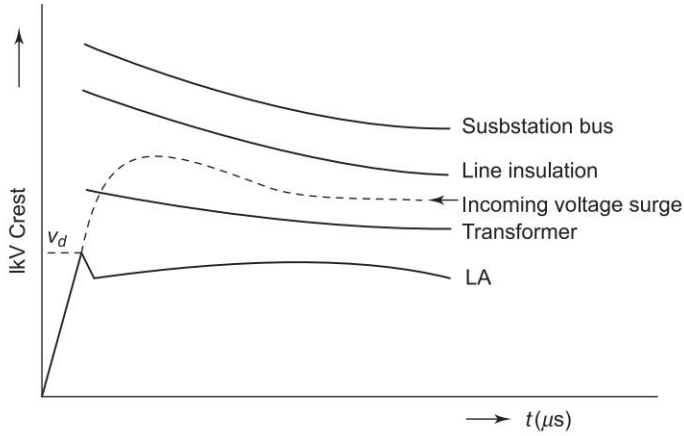

Fig. 13.34 Insulation coordination

In order that line insulators do not flashover, their volt-time curve should lie over that of possible strongest surge wave except for rare surges of extreme strength, in which case insulator failure is accepted as an economic design. Thus the line insulation is sufficient to prevent flashover for power frequency overvoltages and switching surges taking into account all the local unfavourable conditions, such as rain, dust, insulator pollution, which decrease their flashover voltage. The substation bus is always designed to have the highest located volt-time curve such that it can even withstand an occasional direct stroke.

Based on handbook data appropriate safety margins are provided among the various equipment volt-time curves as illustrated in Fig. 13.34. The modern practice, however, is to make use of probability theory and statistical procedures for close adjustment of insulation. These methods are, though tedious, proving useful and economical.

Location of Lightning Arrester Relative to Transformer

Figure 13.35 shows a lightning arrester (LA) located at distance L from the transformer it is protecting. The LA modifies the incoming surge to a rising wave front which, after reaching the residual voltage (v_r) of the LA, remains almost flat. This modified wave, as it approaches the transformer, gets positively reflected (transformer can be almost regarded as an open end). The voltage at the transformer, therefore, rises at twice the initial slope of the incoming wave front. The portion of the voltage wave reflected at the transformer gets negatively reflected at the LA which offers a low resistance shunt path. This negative voltage reaching the transformer does not allow the voltage at the transformer to build up to twice that of the incoming wave, as it otherwise would have. To what maximum does the voltage at the transformer build up, depends upon the time of travel or distance between the transformer

and LA. The smaller is this distance, the earlier this negatively reflected wave arrives and the smaller is the transformer voltage build up. This voltage is the least when the LA is located on the transformer and would equal the residual voltage of the LA. In conclusion therefore the LA should be located as close to the transformer as is physically possible.

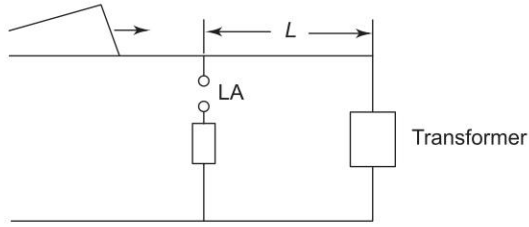

Fig. 13.35

13.8 LIGHTNING PHENOMENA

Lightning has always been attracting mankind since the early times. Franklin in 18th century was the first to initiate research on it. Lightning is a natural electrical phenomenon consisting of a high current, short time discharge that neutralizes an accumulation of charge in the atmosphere. The discharge path can be between two different locations in a cloud, two clouds, a cloud and the earth (or any structure connected to the earth). The mechanisms by which such charge accumulations take place is not yet fully known, but is related to the motions of large air masses that come across certain conditions of humidity, temperature and pressure. When the electric fields become excessive a breakdown or lightning flash takes place; this is normally a high current discharge. As explained earlier, lightning strokes that terminate on or near to power lines create problems for power engineers. The real incentive to obtain additional knowledge about lightning came from the necessity of the electrical industry to protect against its effects. It has been proved [3] that lightning is the greatest single cause of outages on transmission sector. A continuous effort has been made to improve the performance of power systems during thunderstorms. This has resulted in the development and application of ground wires, counter-poise, lightning arresters, etc.

Various theories [12] have been advanced explaining the charge formulation, such as Wilson's theory of charge separation and Simpson and Scarse's theory. We shall discuss these briefly below.

Wilson's Theory of Charge Separation

The theory assumes that many ions are present in the atmosphere which get themselves attached to tiny dust and water particles. It further assumes the presence of an electric field in the earths atmosphere during fair weather

directed towards the earth [Fig. 13.36 (a)]. The field intensity is roughly 1 V/cm at the earths surface, and progressively decreases with height so that at 10,000 m it is only about 0.02 V/cm.

Because of the atmospheric electric field, raindrops become polarized, the upper side gets a negative charge and the lower side a positive charge as shown in Fig. 13.36(a). Later, the lower part of the drops attracts negative ions from the atmosphere, acquiring an overall negative charge while leaving a propond-erance of positive charges in the air. The upward motion of air currents takes positively charged air and smaller drops to the top of the cloud. Heavier rain

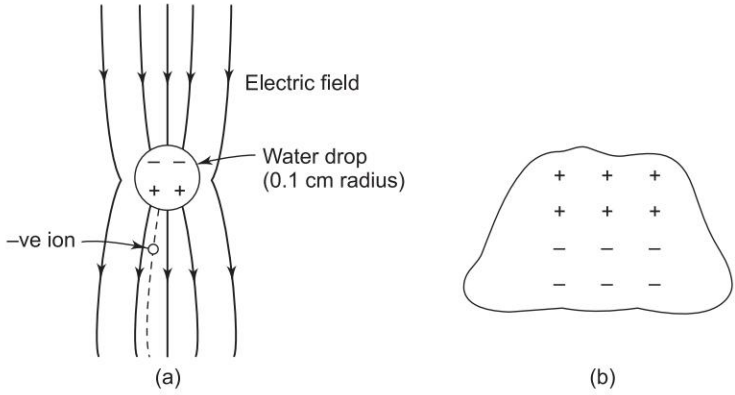

Fig. 13.36 (a) Capture of negative ions by large falling rains drops; (b) Charge separation in a thunder cloud

drops settle on the base of the cloud as shown in Fig. 13.36(b). Thus, according to Wilson's theory, a thundercloud is bipolar with positive charges at the top and negative at the bottom, normally separated by several kilometres. When the electric field strength becomes more than the breakdown value, a lightning discharge is commenced.

Simpson and Scarse's Theory

This theory is based on the temperature variations in the various regions of the cloud as shown in Fig. 13.37. In Fig. 13.37, a cloud is shown to be travelling from left to right along with the air currents. When these air currents collide with the water particles in the bottom of the cloud, the water drops are broken and carried upwards, unless they combine and remain in a small pocket of positive charges. With the collision of water drops the air is negatively charged and water particles positively charged. These negative charges in the air are at once absorbed by the cloud particles, which move upward with air currents. Figure 13.37 shows meteorological and electrical conditions within a thundercloud. A positive charge resides in the upper portion of the cloud above a region of separation from the negative charge in which the temperature is between – 10 and – 20°C. Thus a net positive charge will occur above the mid

level of the cloud, and the negative charge will be distributed more generally throughout the cloud body. This is how the charge is separated in a thunder cloud. Once this is done, the conditions are set for initiation of a lightning stroke.

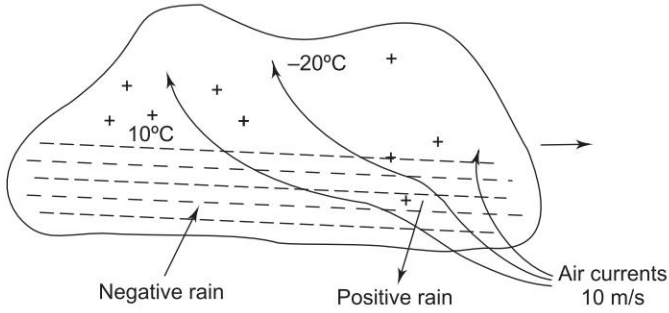

Fig. 13.37 Charge generation and separation in a thunder cloud as per Simpson's theory

Mechanism of Lightning Stroke

Lightning is the discharge of the cloud to the ground. The cloud and the ground form two plates of a gigantic capacitor, and the air is the dielectric between them. Since the lower part of the cloud is negatively charged, the earth gets positively charged by induction. Lightning discharge will need the puncture of the air between the cloud and the earth. Because of the high altitude, i.e. lower pressure and moisture, for the breakdown of air the electric field required is only 10 kV/cm.

When the electric field strength becomes more than the breakdown value, a lightning discharge begins. The first discharge travels towards the earth in steps (*stepped leader stroke*) as shown in Fig. 13.38. When near the earth, a much faster and more luminous *return stroke* travels upwards along the initial channel, and several such leaders and return strokes constitute a lightning flash. The ratio of negative to positive strokes is about 5 to 1 in temperature regions. The magnitude of the return stroke can be as high as 240 kA (average value of the order of 25 kA). A second stroke to the earth takes place in the ionized path formed by the original stroke after a very short interval from the initial stroke. Again a return stroke follows. Normally several such subsequent strokes (called *dart leaders*) take place. The complete sequence is known as a multiple stroke lightning flash and a typical representation of the strokes at various time intervals is shown in Fig. 13.38. Usually only the large current flowing over the first 50 μs is of significance, and the current-time relationship is generally of the form $i = i_{\max} (e^{-\alpha t} - e^{-\beta t})$ as stated earlier.

In conclusion we can say that thunderstorms appear to follow more or less definite paths as influenced by local terrain, which produces large localized variations in storm and lightning stroke density. Of the several proposed theories of charge formation (only two were discussed here), none explains

completely all the factors involved [9]. It is thus clear that though a lot of progress has been made in lightning research, there are still many questions that are left unanswered and these require further investigation.

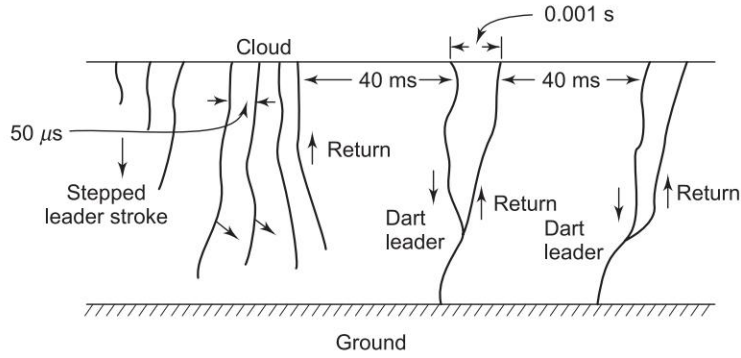

Fig. 13.38 Sequence of strokes at various time intervals in a multiple lightning stroke

13.9 NEUTRAL GROUNDING

From the unbalanced fault analysis, it has been seen that the neutral connections (transformer and generator) considerably influence the fault currents and voltages. Protective relaying and stability analysis are also influenced by neutral grounding. In most modern HV systems the system neutral is solidly (or effectively) grounded, i.e. connected directly to the ground. Of course the generators are grounded through a resistance to limit the stator fault currents, and also for stability considerations. The advantages of neutral grounding are:

(1) Voltages to ground are limited to the phase voltages.
(2) The high voltages due to arcing faults or transient line to ground faults are eliminated.
(3) Sensitive protective relays against line to ground faults can be employed.

The main advantage in operating with an isolated neutral is the possibility of maintaining a supply even with a fault on one line. Also interference with telephone lines is reduced due to the absence of zero sequence currents.

With normal balanced operation, the neutrals of an ungrounded or isolated system are held at ground voltage because of the system capacitance to earth as in Fig. 13.39(a). The phasor diagram for balanced operation is given in Fig. 13.39(b). For a fault on phase *C*, the phasor diagram is drawn in Fig. 13.39(c). A charging current thrice that of the per phase value flows. The voltage of healthy phases equals $\sqrt{3}\, V_{ph}$. The presence of inductance and capacitance in the system leads to what is called *arcing grounds*, and the system voltage may rise to dangerously high values. These voltages can be avoided by connecting

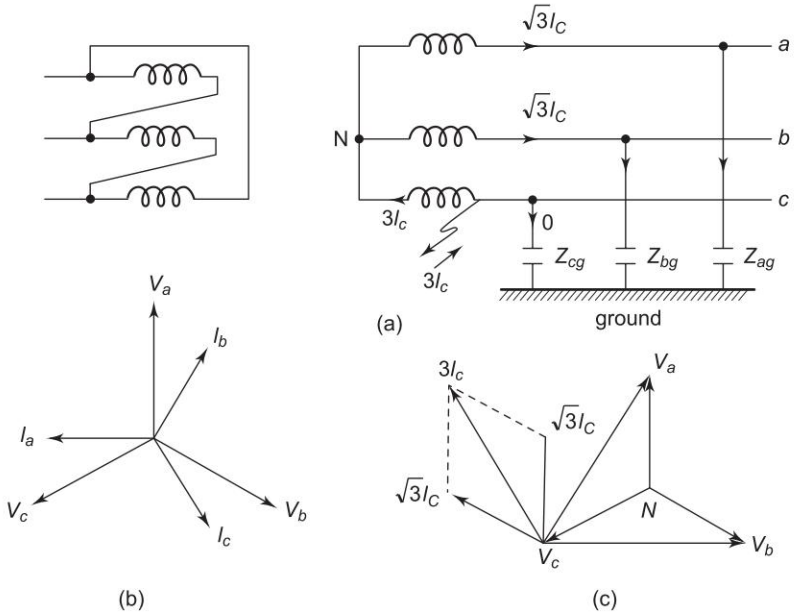

Fig. 13.39 (a) Isolated neutral system: fault on phase C, (b) Phasor diagram for balanced system, (c) Phasor diagram for fault on phase C

a suitable inductor between neutral and ground. If the value of the inductive reactance is such that the fault current I_c balances the charging current, then the grounding is known as *resonant grounding*, and the grounding inductor is known as *ground fault neutralizer* or *Peterson coil*. The reactance of this coil is in the range of 90–110% of the value required to neutralize the capacitive current. The phasor diagram for the resonant grounded system of Fig. 13.40(a) is shown in Fig. 13.40(b).

If V_{ph} is the line to ground voltage of the system, then voltage of the healthy phases will be $\sqrt{3}\, V_{ph}$. If C is the capacitance to ground of each phase, then charging current will be $3V_{ph}\ \omega C$. If L is the inductance of the Peterson coil, then

$$I_L = V_{ph}/\omega L$$

For balance condition

$$I_L = 3V_{ph}\ \omega C = V_{ph}/\omega L$$

or

$$L = \frac{1}{3\omega^2 C} \tag{13.43}$$

and

$$X_L = \frac{1}{3\omega C} \tag{13.44}$$

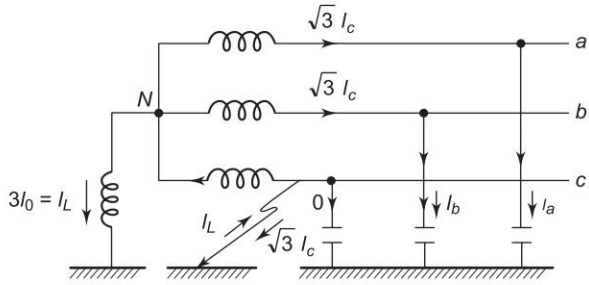

(a) System with Peterson coil; fault on phase *C*

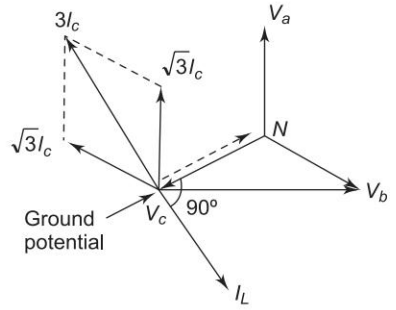

(b) Phasor diagram for the system of Fig. 13.39(a)

Fig. 13.40

This result may also be arrived at by analyzing the ground fault with the help of symmetrical components.

Normally ungrounded neutral systems lead to serious arcing fault voltages if the arc current exceeds the range 5–10 A for the systems operating above 33 kV. Peterson coils should be used for such systems operating with isolated neutrals. Because of the resonant condition, use of Peterson's coil leads to excessive overvoltages (voltage to ground of healthy phases rises to line voltage value) and, therefore, its use is not recommended in modern systems. Most of the systems at normal transmission voltages have grounded neutrals.

Methods of Neutral Grounding

Various methods of neutral grounding are:

(1) Solid or effective grounding
(2) Resistance grounding
(3) Reactance grounding
(4) Voltage transformer grounding
(5) Zig-zag transformer grounding

Resistance grounding is normally used where the charging current is small, i.e. for low voltage short lines. It facilitates relaying of ground faults. It helps in improving the system stability during ground fault. Whether a system is solidly

grounded or reactance grounded depends on the ratio of X_0/X_1. For reactance grounded system $X_0/X_1 > 3.0$, otherwise it is solidly grounded system for $X_0/X_1 < 3.0$. Reactance grounding lies between effective grounding and resonant grounding. This method may be employed for grounding the neutral of synchronous motors and capacitors, and systems having large charging currents.

For delta connection, busbar points, etc. a zig-zag transformer is used for neutral grounding as shown in Fig. 13.41. In the absence of such a transformer, a star-delta transformer can be used without loading the delta side.

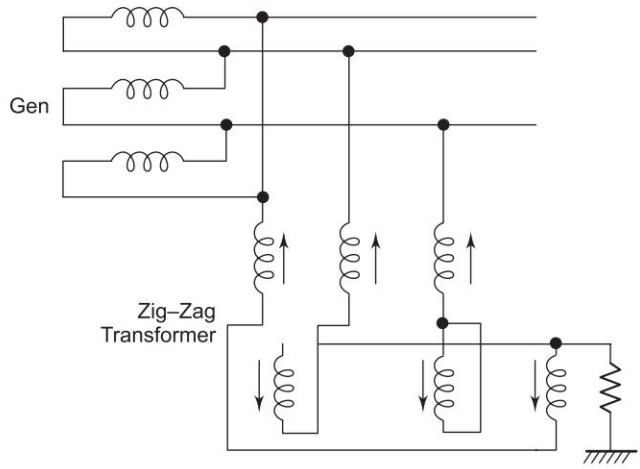

Fig. 13.41 Zig-zag transformer for neutral grounding

13.10 SUMMARY

In this chapter a detailed account on Power System Transients is presented along with insulation coordination, lightning phenomena and neutral grounding.

Problems

13.1 An overhead line, with inductance and capacitance per km of 1.2 mH and 0.9 μF, respectively, is connected in series with an underground cable having inductance and capacitance of 0.16 mH/km and 0.28 μF/km. Calculate the values of transmitted and reflected waves of voltage and current at the junction due to a voltage surge of 110 kV travelling to the junction (i) along the line towards the cable and (ii) along the cable towards the line.

13.2 An overhead line with surge impedance 500 ohm bifurcates into two lines of surge impedance 500 ohm and 50 ohm, respectively. If a surge of 25 kV is incident on the overhead line, determine the magnitudes of voltage and current which enter the bifurcated lines.

13.3 An overhead line is connected to terminal apparatus through a length of single-phase cable, the characteristic impedances being 500 and 25 ohms, respectively. A travelling wave of vertical front and infinite tail of 230 kV magnitude originates in the line and travels towards the junction with the cable. Calculate the energy transmitted into the cable during a period 5 μs after the arrival of the wave at the junction. What voltage is reflected back into the line?

13.4 A DC source of 100 V with negligible resistance is switched 'on' to a lossless line of characteristic impedance Z_c = 25 Ω terminated in a resistance of 75 Ω. Plot (i) the receiving-end voltage and (ii) sending end current versus time until $t = 5T$ where T is the time of wave travel on the line. Also find the steady values of the receiving-end voltage and the sending-end current.

13.5 Repeat Problem 13.4, if the receiving-end resistance is reduced to 25/3 Ω.

13.6 Solve Problem 13.4 if a resistance of 45 Ω is in series with the source.

13.7 A unit-step voltage is travelling on a long line of surge impedance Z_1. It reaches the junction with a cable of finite length whose far end is open. The cable has a surge impedance of Z_2, and the time of one-way wave travel on it is T. Draw the Bewley lattice diagram and find from it the value of voltage at the junction at time $4T$.
Given: $Z_1/Z_2 = 9$.

13.8 A DC voltage source of unit voltage is switched on to a lossless transmission line with surge impedance Z_s terminated in the far end by a lumped resistance R; the ratio $R/Z_s = 3$. The line length is 150 km. Draw the Bewley lattice diagram for voltage and current and, therefrom, plot the voltage vs. time at the far end of the line and current vs. time at the sending-end of line.

13.9 In Problem 13.8 plot voltage vs. time and current vs. time at a point one-third the line length from the sending-end.

13.10 A square wave voltage surge of magnitude E_0 and length D is travelling at speed γ on a transmission line of surge impedance Z_s. A capacitor C is connected between line and ground at the midpoint of the line. Derive analytically the expression for the voltage surge that travels along the line beyond the point where the capacitor is connected. Also sketch the voltage waveform.

13.11 A voltage pulse of magnitude E_0 and length D travels on a transmission line of characteristic impedance Z_c at speed γ. In the middle of the line it meets a series lumped inductance L. Find the expression for the voltage

wave as a function of time that will be injected into the line on the other side of the inductance. Also sketch the voltage wave form.

13.12 A unit-step voltage wave is travelling along a line of characteristic impedance Z_c. The line terminates in a shunt inductance L. Derive the expression for the voltage at the line and the inductance junction as a function of time.

13.13 Solve Problem 13.2 if the line terminals in a shunt capacitance C.

References

Books

1. Bewley, L.V., *Travelling Waves on Transmission Systems*, Dover Books, New York, 1963 (Reprint of 1951 edn).
2. Bickford, J.P., N. Mullineux and J.R. Reed, *Computation of Power System Transients*, IEE Monograph, 1976.
3. Greenwood, A., *Electrical Transients in Power Systems*, Wiley Interscience, New York, 1971.
4. Peterson, H.A., *Transients in Power Systems*, Dover Books, New York, 1966 (Reprint of 1951 edn).
5. Taylor, E.O. (Ed.), *Power System Transients*, George Newnes, London, 1954.
6. *Transmission Line Reference Book*, *345 kV and above*, Electric Power Research Institute, Palo Alto, Ca., 1975.
7. Indulkar, C.S. and D.P. Kothari, *Power System Transients*: *A Statistical Approach*, PHI, New Delhi, 1996.
8. Cotton, H. and H. Barber, *The Transmission and Distribution of Electrical Energy*, 3rd edn, B.I. Publishers, New Delhi, 1970.
9. *Electrical T & D. Ref. Book*, Westinghouse Elect. & Manufacturing Co., East Pittsburgh, Penn., 1964.
10. *EHV Transmission Line Reference Book*, Edison Electric Institute, New York, 1968.
11. Starr, A.T., *Generation, Transmission and Utilization of Electric Power*, Pitman, 1962.
12. Taylor, E.O. (Ed.), *Power System Transients*, George Newnes Ltd., London, 1954.
13. *Transmission Line Reference Book, 345 kV and Above*, Electric Power Research Institute, Palo Alto, Ca., 1975.
14. Dommel, H.W., *EMTP Theory Book*, BPA, August 1986.

Chapter 14

Circuit Breakers

14.1 CIRCUIT BREAKING TRANSIENTS

Figure 14.1 is illustrative of a three-phase symmetrical short-circuit on a generator with an intervening circuit breaker having three circuit opening poles, one in each phase. As explained in Secs 9.2 and 9.3, the short circuit current would comprise two components—DC offset current and symmetrical short-circuit current. The DC offset current is maximum in the phase whose voltage is zero at the instant of short circuit (say in phase B). Because of the time-varying synchronous reactance of the synchronous generator, the symmetrical short-circuit current decays reaching steady state after passing through subtransient and transient phases as shown in Fig. 9.4. The short-circuit current of phase B (i_B) is shown in Fig. 14.2.

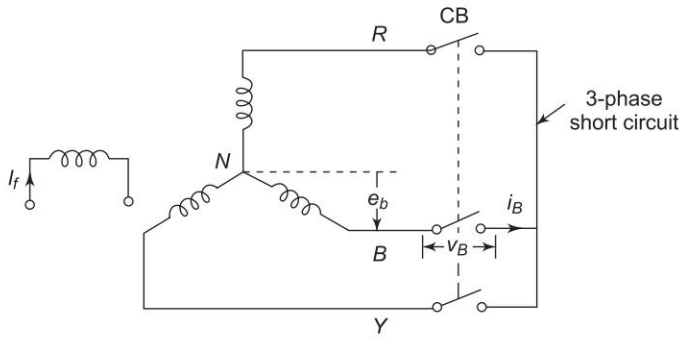

Fig. 14.1 Three-phase short circuit and circuit breaking

The heavy short-circuit current is sensed by protective relaying (Ch. 15), which energizes the trip circuit of the circuit breaker (CB) causing its moving poles to separate from the fixed poles at high speed. This is accomplished by a mechanical toggle mechanism. As the poles separate electric arc is struck across the intervening air-gap feeding the current. The arc would extinguish at current zero (of the AC current) and, if it does not restrike, the circuit opens successfully. The voltage across the poles is almost constant (about 80 V)

during the arcing phase (nonlinear nature of the arc phenomenon). After the arc is extinguished, AC voltage appears across the poles which builds up with passage of time as the air-gap flux in the generator recovers with the vanishing of the armature reaction.

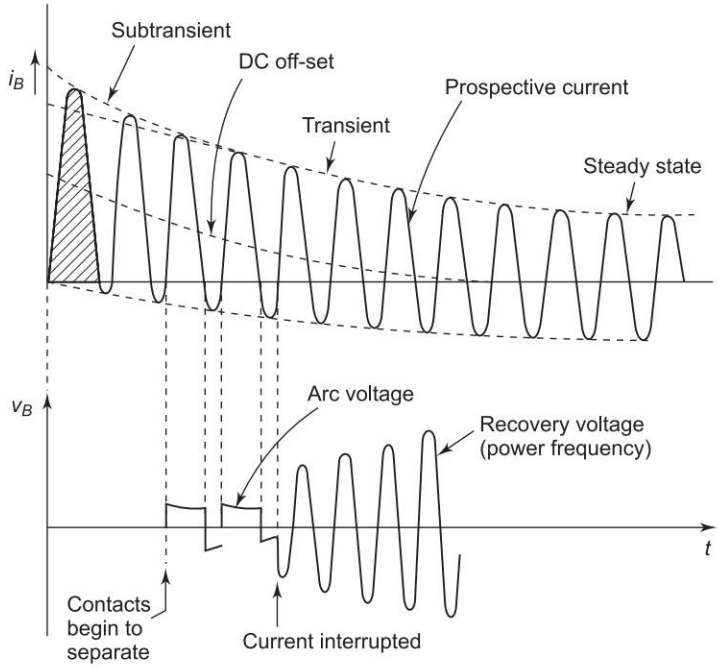

Fig. 14.2 Short-circuit current and recovery voltage

The waveforms of i_B and v_B are shown in Fig. 14.2. These phenomena also occur in other phases with a time phase difference of 120°. The voltage v_B will not be the phase voltage during the time phases when *R* and *Y* have not yet opened (see Fig. 14.8). The short-circuit current has an initial major loop (called *making current*), whose peak value is known as the *maximum momentary current*. The mechanical parts of the circuit breaker must be capable of withstanding forces released by this current (these are proportional to square of the current). The voltage appearing across the poles (v_B) when the arc extinguishes is known as *recovery voltage*. The current which would have flown if the breaker did not open is called the *prospective current*. At the instant of current interruption (arc extinction) an *LC* transient occurs involving generator inductance and stray capacitance causing high frequency damped oscillations as shown in Fig. 14.3. The recovery voltage with this transient is known as *transient recovery voltage* (TRV). Thus the voltage v_B across the breaker poles has a fast rate of rise and a peak value almost double the maximum voltage of the power-frequency component of the recovery voltage. These two phenomena in the recovery voltage tend to *restrike the arc* so that

the breaker would then open at a later current zero when larger pole separation has occurred. Restriking is detrimental to circuit breaking as it would damage the poles and delay the fault clearing in the power system.

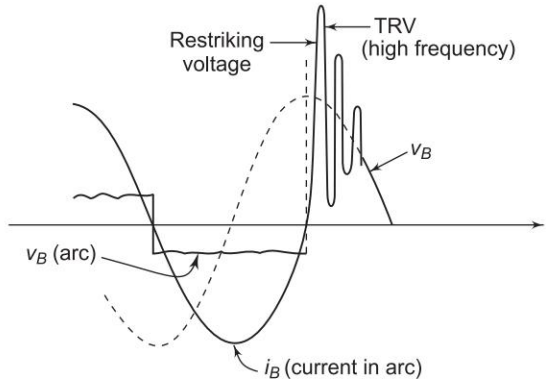

Fig. 14.3 Transient recovery voltage (TRV)

Transient Recovery Voltage

The per phase circuit of the short-circuit generator of Fig. 14.1 is drawn in Fig. 14.4 where ωL is the generator reactance and $1/\omega C$ the capacitive reactance of the stray generator capacitance. At power frequency $1/\omega C$ is negligible but becomes of significance at high frequency oscillations initiated by sudden opening of the current immediately following a current zero. This is equivalent to switching the generator voltage in the series LC circuit (resistance is so small that it can be ignored but its effect is later included).

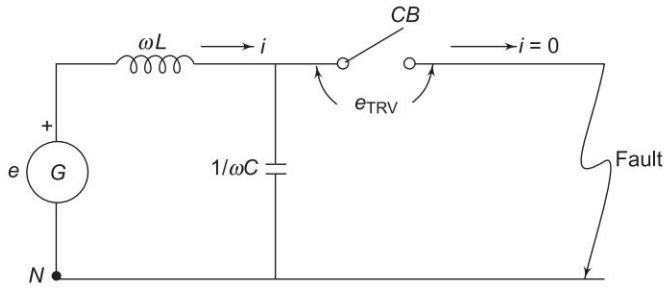

Fig. 14.4 Recovery voltage transient

The generator emf and short-circuit current are

$$e = E_m \cos \omega t \tag{14.1}$$

$$i = \frac{E_m}{\omega L}\cos(\omega t - 90°) = \frac{E_m}{\omega L}\sin \omega t \tag{14.2}$$

The CB opens at $t = 0$ (when $i = 0$). We need to solve LC transient when AC voltage $e = E_m \cos \omega t$ is switched 'on' at $t = 0$ with $i(0^+) = 0$. The frequency of the natural frequency oscillations initiated is of the order of kHz so that

$$\omega_n = \frac{1}{\sqrt{LC}} >> \omega \tag{14.3}$$

A simple way* to proceed would be to assume that the power frequency component in the circuit remains constant at its instantaneous value at $t = 0$, i.e.

$$e\,|_{\omega t = 0} = E_m$$

The governing differential equation of the circuit is then simplified to

$$L\frac{\mathrm{d}i}{\mathrm{d}t} + \frac{1}{C}\int i\,\mathrm{d}t = E_m u(t) \tag{14.4}$$

$$e_{\mathrm{TRV}} = \frac{1}{C}\int i\,\mathrm{d}t \tag{14.5}$$

Substituting Eq. (14.5) in Fig. 14.4,

$$LC\frac{\mathrm{d}^2 e_{\mathrm{TRV}}}{\mathrm{d}t^2} + e_{\mathrm{TRV}} = E_m u(t) \tag{14.6}$$

Solving, we get

$$e_{\mathrm{TRV}} = E_m\left(1 - \cos\frac{t}{\sqrt{LC}}\right);\ t \geq 0 \tag{14.7}$$

whose wave form is shown in Fig. 14.5.

With power frequency sinusoidal generator voltage and consideration of circuit damping, the wave form of TRV would be as shown in Fig. 14.3. Its mathematical form would be

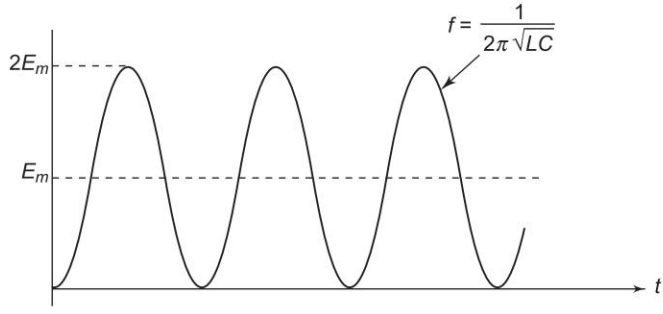

Fig. 14.5

$$e_{\mathrm{TRV}} = E_m\left(1 - \cos\frac{t}{\sqrt{LC}}\right) + E_m \cos\omega t\,;\ t \geq 0$$

* The reader should follow the procedure of Laplace transform and directly obtain the total solution.

with the understanding that at power frequency $\omega L << 1/\omega C$ and the generator voltage fully appears across the capacitor.

From the point of view of arc restriking two attributes of the recovery voltage are of importance, and must be limited for the restriking not to occur. These are

- maximum value of e_{TRV};
- maximum value of rate of rise of e_{TRV};

From Eq. (14.7),

$$e_{TRV}(\max) = 2E_m, \text{ (at } t = \pi\sqrt{LC}\text{)} \tag{14.8}$$

Differentiating Eq. (14.7), the rate of rise of recovery voltage is

$$\text{RRRV} = \frac{E_m}{\sqrt{LC}} \sin \frac{t}{\sqrt{LC}} \tag{14.9}$$

Its maximum value is

$$\text{RRRV}_{\max} = \frac{E_m}{\sqrt{LC}} \left(\text{at } t = \frac{\pi}{2}\sqrt{LC} \right) \tag{14.10}$$
$$= 2\pi f_n E_m$$

where $f_n = \dfrac{1}{2\pi\sqrt{LC}}$, the natural frequency of oscillations.

In the above discussion the pf of the short-circuit is assumed to be zero (Eqs (14.1) and (14.2)). In general, for pf angle θ,

$$e_{TRV}(\max) = 2E_m \sin\theta \tag{14.11}$$

$$(\text{RRRV})_{\max} = 2\pi f_n E_m \sin\theta \tag{14.12}$$

It is immediately observed from Eq. (14.10) or (14.12), that $(\text{RRRV})_{\max}$ can be reduced by reducing f_n, by introduction of damping into the circuit by addition of resistance as explained in what follows.

Resistance Switching

To introduce damping into the LC circuit at the time of CB opening with a view to reduce the oscillation frequency, a resistance is placed in parallel with the poles of the circuit breaker as shown in Fig. 14.6.

As the circuit breaker opens, the current continues to flow through the resistance. For determination of the natural frequency, the voltage source is assumed short circuited ($e = 0$). Thus

$$L\frac{\mathrm{d}i}{\mathrm{d}t} + \frac{1}{C}\int i_C \,\mathrm{d}t = 0 \tag{14.13}$$

$$i = i_C + i_r \tag{14.14}$$

$$\frac{1}{C}\int i_C \,\mathrm{d}t = r i_r \tag{14.15}$$

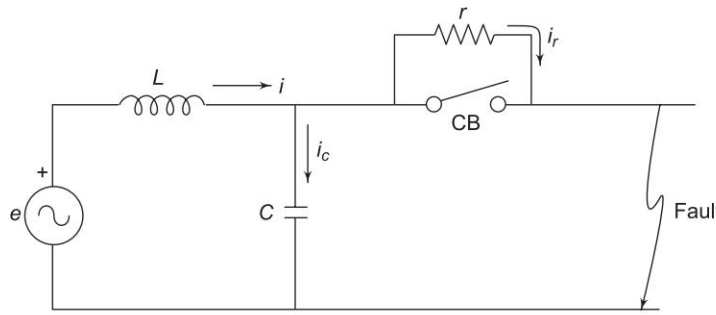

Fig. 14.6 Resistance switching

These equations yield

$$\frac{d^2 i_r}{dt^2} + \frac{1}{rC}\frac{di_r}{dt} + \frac{1}{LC} i_r = 0 \tag{14.16}$$

The natural frequency of oscillations is given by

$$f_n = \frac{1}{2\pi}\left(\frac{1}{LC} - \left(\frac{1}{2rC}\right)^2\right)^{1/2} \tag{14.17a}$$

It is seen from Eq. (14.17a) that the inclusion of r reduces the natural frequency and, therefore, $(RRRV)_{max}$. From Eq. (14.17a) it is also evident that if the resistance is given a value equal to, or less than, $\frac{1}{2}\sqrt{L/C}$, the oscillatory nature of the transient will vanish. Hence for critical damping

$$r = 0.5\sqrt{L/C} \tag{14.17b}$$

The resistance is brought into the circuit automatically by closing of the auxiliary resistor break shown in Fig. 14.7 before the main break opens. It opens after the main break and when the current has reduced because of inclusion of resistance in the short-circuit loop. The current required to be opened by the auxiliary break is of the order of 30% of the rated breaking

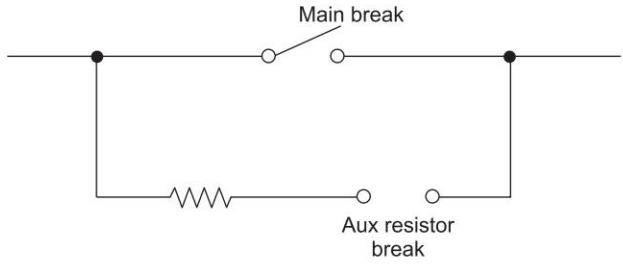

Fig. 14.7

current. The value of this resistance is of the order of 300 – 500 Ω in the case of 145 kV air-blast circuit breakers. In oil circuit breaker the opening resistance needs to carry only 5–10% of the rated current.

First Pole to Clear Factor

It has already been pointed out that in a three-phase circuit breaker one pole will open first and the other two will follow (these will open simultaneously). The power frequency recovery voltage appearing across the first pole to clear would, therefore, be not the phase voltage. This situation is like an open conductor fault (Sec. 11.6). Here the treatment will be on approximate basis.

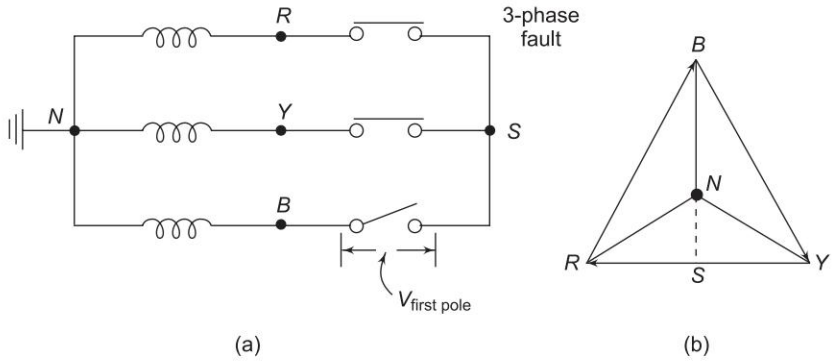

Fig. 14.8

In Fig. 14.8(a) the pole of *B* phase has just opened. The short-circuit point *S* is then at the mid-point potential of V_{RY} as shown in Fig. 14.8(b). Therefore,

$$V_{\text{first pole}} = V_{BS} = V_{BN} + V_{NS}$$
$$= 1.5\ V_{BN} \qquad (14.18)$$

It is seen from Eq. (14.18) that the power frequency voltage across the first pole to clear is 1.5 times the phase voltage. We define:

First pole to clear factor

$$= \frac{\text{rms voltage between healthy and faulty lines } (V_{BS} = V_{BR})}{\text{rms phase-to-neutral voltage with fault cleared}} \qquad (14.19)$$

Double Frequency Transient

L and *C* may be present on both sides of the circuit breaker as shown in Fig. 14.9, in which case each circuit oscillates at its own natural frequency and the difference of these two oscillating voltages appears across the circuit breaker poles as these open. This is illustrated in Fig. 14.10 and the phenomenon is called double frequency transient. Obviously the higher of the two frequencies governs the initial rate of rise of TRV.

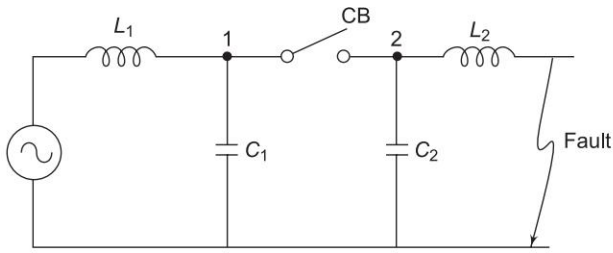

Fig. 14.9

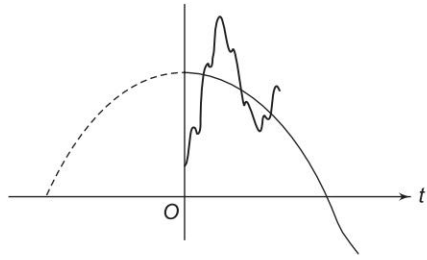

Fig. 14.10

Short-Line Fault–Kilometric Fault

The phenomenon of kilometric faults is analyzed in Ref. 2 using both travelling wave and Laplace transform techniques. The kilometric fault is shown in Fig. 14.11(a), wherein the fault is located a few kilometres from the circuit breaker. As the CB opens, a triangular voltage wave is present on the line. It is equivalent to two equal triangular waves—one travelling forward and the other backward. The forward travelling wave gets reflected at the short-circuit (SC) end and the backward wave gets reflected at the open end (CB side). These waves are illustrated in Fig. 14.11(b). As a result the voltage at the CB end oscillates triangularly through $\pm V$ (the original voltage at CB end of the line), the time of half oscillation being $2T$, i.e. twice the time of wave travel on the line from CB to SC. This time being very small (in μs), the voltage across the open CB poles has an extremely high rate of rise (V/T) which can result in arc restriking.

In order to cope up with the kilometric faults interruption, SF_6 gas circuit breakers (GCB) are experimented and GCB was considered to have excellent capability against SLF.

Interruption of Low Magnetizing Current—Current Chopping

The opening of magnetizing current of an unloaded transformer (or line reactor) leads to current chopping or sudden reduction of current to zero before the natural current zero. This is very likely to happen in fast acting air-blast circuit breakers. Current chopping has associated high rate of voltage rise phenomenon as illustrated below.

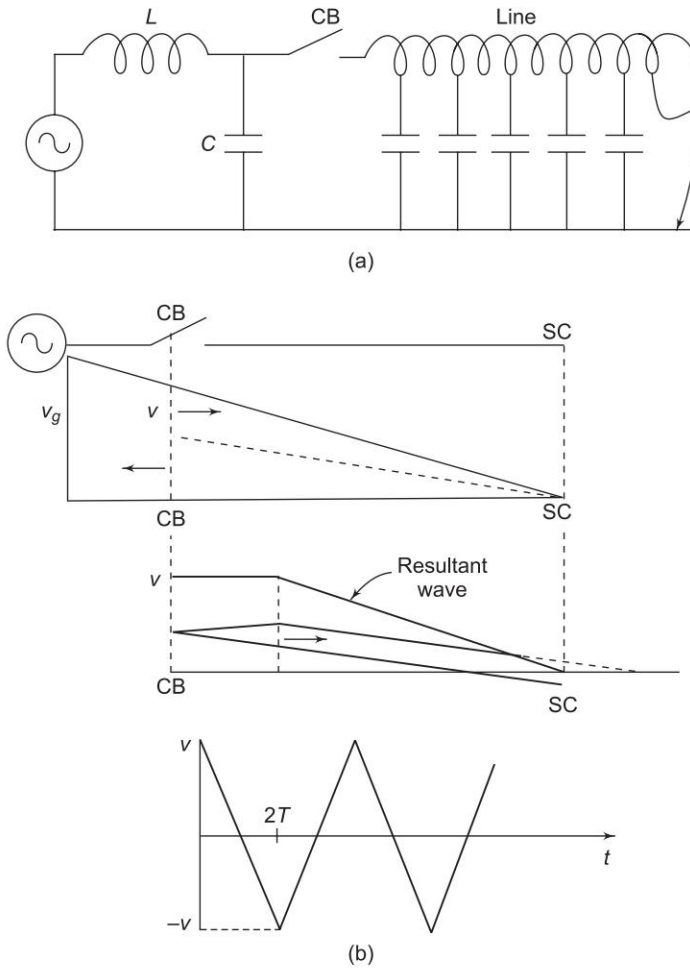

Fig. 14.11 Kilometric fault

Figure 14.12(a) shows the circuit diagram of a generator feeding an open-circuited transformer through a CB. The transformers stray capacitance shown in the figure plays an important role in high frequency oscillation upon CB opening. The magnetizing current drawn by the transformer is very low (2–5% of full-load current) and is almost purely reactive (lagging system voltage by 90°) as shown in Fig. 14.12(b) and (c). As the CB is opened, the current at value i_0 is suddenly reduced to zero by the arc extinguishing mechanism of the CB.

The energy trapped in the transformer inductance because of current chopping oscillates between this L and the transformer stray capacitance C. The peak of the oscillatory voltage is given by

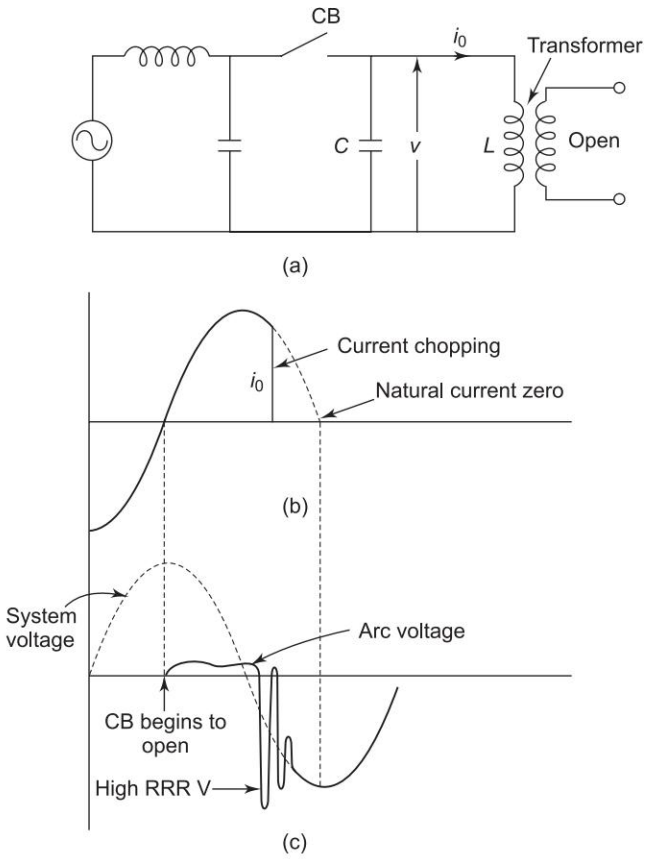

Fig. 14.12 Current chopping

$$\frac{1}{2}Li_0^2 = \frac{1}{2}Cv^2$$

or

$$v = i_0\sqrt{L/C} \qquad (14.20)$$

Consider 110 kV, 20 MVA transformer. For this transformer

$$\text{Rated current} = \frac{20\times10^3}{\sqrt{3}\times110} = 105 \text{ A}$$

Magnetizing current = 2 A (say)

$$X_0 = \frac{110\times10^3}{\sqrt{3}\times2} = 31.7\times10^3\ \Omega$$

$$L_0 = \frac{31.7 \times 10^3}{314} = 101 \text{ H}$$

Let the chopped current be $\sqrt{2} \times 2 = 2.82$ A. Then

$$v = 2.82\left(\frac{101}{5000 \times 10^{-12}}\right)^{1/2}; \; C = 5000 \text{ pf}$$

$$= 400 \text{ kV}$$

Thus the transformer phase rated $110/\sqrt{3} = 63.5$ kV is subjected to 400 kV, which is dangerous to transformer insulation. In fact, before the voltage reaches such high level, the arc restrikes (which protects the transformer). Several cycles of arc chopping and restriking may occur before the arc is finally extinguished. As already stated, current chopping is bound to occur in fast arc quenching air-blast and vacuum type circuit breakers. Current chopping is avoided by resistance switching (Fig. 14.7).

Switching of Capacitor Banks and Unloaded Lines

Switching of capacitive loads (capacitor banks or unloaded lines) can lead to arc restriking in breakers, in which the voltage level across the capacitor builds up in steps to dangerous levels. This situation is illustrated in Fig. 14.13 from circuit point of view.

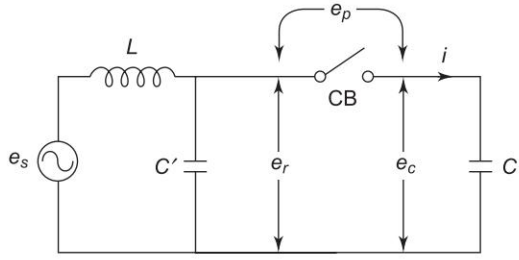

Fig. 14.13 Capacitor switching

Normally $C' << C$ so that with the CB open,

$$e_r \approx e_s \text{ (system voltage)} \tag{14.21}$$

Then the voltage across CB poles when the arc is interrupted is

$$e_p = e_c - e_r \tag{14.22}$$

The capacitive current (i) leads to voltage e_s by 90°, as shown in Fig. 14.14. The arc extinguishes at $i = 0$ when the capacitor C is charged to $-e_{max}$, and stays charged beyond this time. The voltage e_p rises to $2e_{max}$ when the arc would be most likely to restrike. Arc restriking is equivalent to switching a capacitor charged to $-e_{max}$ to voltage source of value $+e_{max}$ through the

inductance L. The amplitude of natural frequency oscillation would initially be $2e_{max}$, as indicated in the figure. The capacitor voltage would then rise to a peak value of $3e_{max}$, at which point the current i becomes zero and quenches once again. If this sequence of events repeats once again the capacitor voltage would rise to $5e_{max}$. It can lead to puncture of capacitor bank (or breakdown of line insulation). This phenomenon in capacitor switching is also avoided by resistance switching.

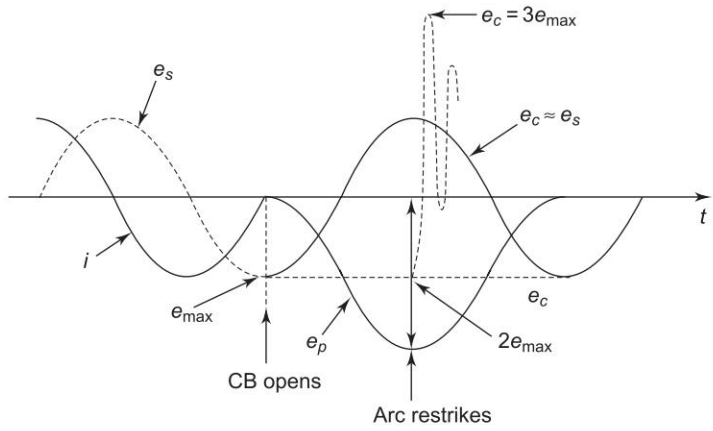

Fig. 14.14

Example 14.1 A 50 Hz, three-phase synchronous generator has an inductance per phase of 1.75 mH and its neutral is grounded. It feeds a line through a circuit breaker. The total stray capacitance to ground of the generator and circuit breaker is 0.0025 μF. A fault occurs just beyond the circuit breaker, which opens when the symmetrical SC current is 7500 A (rms). Ignoring the first pole to clear factor, determine the following:

(a) Natural frequency of oscillations.
(b) Peak value of TRV.
(c) Time at which peak value of TRV occurs.
(d) Maximum rate of rise of TRV.
(e) Time at which the maximum in part (a) occurs.

Solution

(a) $$f_n = \frac{1}{2\pi\sqrt{LC}} = \frac{1}{2\pi\sqrt{1.75\times10^{-3}\times0.0025\times10^{-6}}} = \frac{10^6}{2\pi\times2.092}$$

$$= 76.1 \text{ kHz}$$

(b) $$E = I\omega L$$

$$= 7500 \times 314 \times 1.75 \times 10^{-3} = 4.121 \text{ kV}$$

$$E_m = 4121\sqrt{2} = 5827 \text{ V}$$

Peak value of TRV $= 2E_m$

$$= 2 \times 5827 = 11655 \text{ V}$$

(c) Time to peak value of TRV is given by

$$\frac{t_p}{\sqrt{LC}} = \pi$$

or

$$t_p = \pi\sqrt{LC} = \pi \times 2.092 \times 10^{-6}$$

$$= 6.57 \ \mu\text{s}$$

(d) $(\text{RRRV})_{\max} = \dfrac{E_m}{\sqrt{LC}}$ (Eq. 14.10)

$$= \frac{5827 \times 10^6}{2.029} = 2785 \text{ V}/\mu\text{s}$$

(e) Time to $(\text{RRV})_{\max} = \dfrac{1}{2} t_p$

$$= 3.285 \ \mu\text{s}$$

14.2 CIRCUIT BREAKER RATING

Various circuit breaker ratings are defined below (consult IEC-56 and ISI-2516):

- Rated voltage—standard values.
- Rated insulation level—power-frequency withstand voltage and impulse withstand voltage.
- Rated frequency.
- Rated (normal) current—rms current the breaker can carry without overheating of its parts; standard values.
- Rated short-circuit (SC) breaking current or MVA—it has already been defined at length in Sec. 9.5.
- Rated SC making current = $1.8 \times \sqrt{2} \times$ subtransient SC current.
- Rated duration of SC—kA for a period of 1 s; the breaker should be able to carry rated breaking current for 1 s without damage to its parts.
- Rated operating sequence—

O (open)—t—CO (close-open)—T—CO

t = 0.3 s for rapid autoreclose CB

= 0.5 s for nonreclose CB

T = 3 m

- Rated TRV—basically this is specified in terms of gross slope up to the peak value (sometimes two slopes may be specified), peak value and time to reach the peak, which is a measure of frequency of oscillation. This is illustrated in Fig. 14.15(a) and (b).

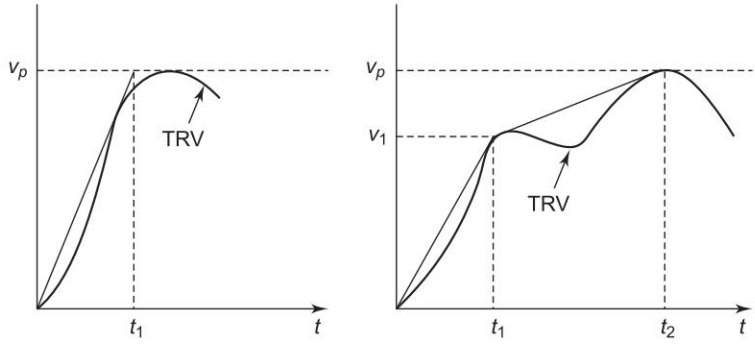

(a) Two-parameter method (b) Four-parameter method

Fig. 14.15 Specifying TRV

14.3 ARC AND ARC EXTINCTION

Under closed conditions the electrodes of a circuit breaker are maintained in conducting contact under pressure as shown in Fig. 14.16(a). As the pressure is released, the electrodes remain in contact at a small number of points causing contact resistance to increase considerably. As the same current is still to be conducted, large contact loss occurs leading to formation of hot spots and ionization of air voids. As the contacts separate, an arc is struck between the electrodes as in Fig. 14.16(b). The current is now conducted by ionized gas (plasma) with electrons moving towards the anode and slow-moving positive ions towards the cathode. The arc can be divided into three parts—arc core, plasma and hot gases. Temperature in the arc core can range from 6000°C to 25000°C. The temperature at the plasma boundary is of the order of 2000°C. Ionization in the arc is maintained by several processes enumerated below:

- Thermal ionization at temperatures above 6000°C.
- Ionization by collision of fast moving electrons with gas molecules.
- Thermal emission from the surface of contacts.
- Secondary emission from contact surface—heavy ions bombarding the cathode where a hot *cathode spot* is formed.
- Field emission from contact surfaces (for surface voltage gradient above 10^6 V/cm).
- Photo emission due to incidence of light energy (photons).

Simultaneously, deionization goes on in the arc path. In a stable arc, these two processes balance out. Various causes of deionization are:

- Recombination by collision of electrons with ions.
- Diffusion of ionized gas away from the arc.
- Conduction of heat—cooling.

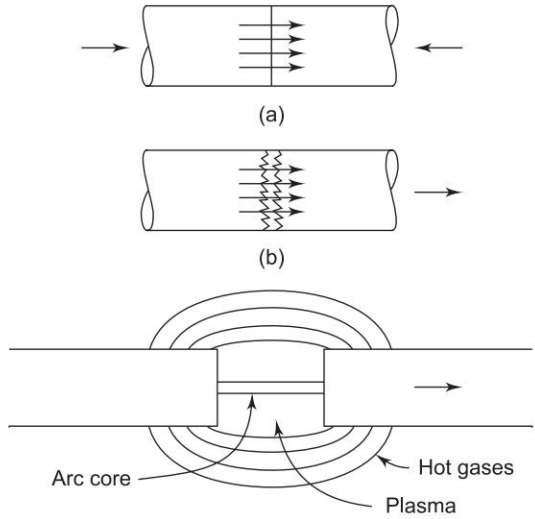

Fig. 14.16 Electric arc

Volt–ampere Characteristic of Arc

The voltage drop of arc can be divided into two components which can be expressed empirically as

$$A + \frac{C}{I_{\text{arc}}} \quad = \text{Cathode plus anode voltage drop}$$

and

$$\left(B + \frac{D}{I_{\text{arc}}}\right)d \quad = \text{voltage drop in arc length}$$

where A, B, C, D are constants and d = arc length.

Combining, the volt–ampere characteristic of the arc can be expressed as

$$V_{\text{arc}} = (A + Bd) + \left(\frac{C + Dd}{I_{\text{arc}}}\right) \tag{14.23}$$

As per Eq. (14.23), the arc voltage drop reduces with arc current (negative resistance characteristic) and becomes almost constant at large current as shown in Fig. 14.17.

The voltage drop in AC arc is illustrated in Fig. 14.18. Because of the random nature of ionization process, the voltage has high frequency components which also contribute radio frequency noise.

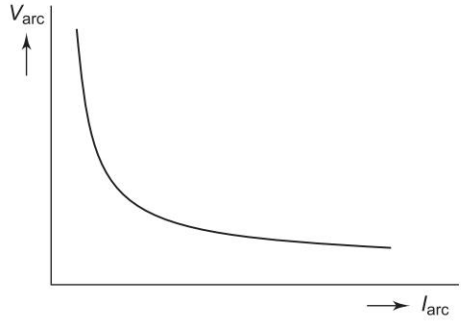

Fig. 14.17

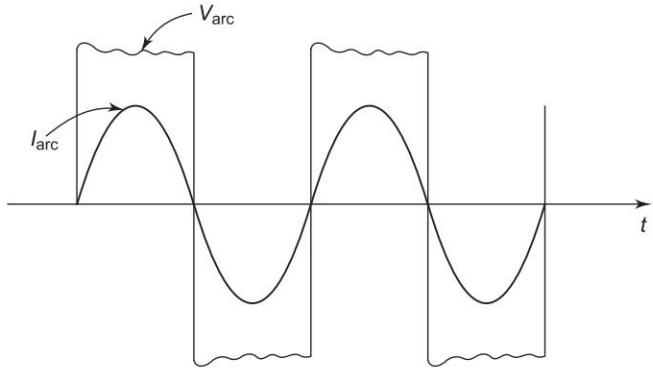

Fig. 14.18 Voltage drop in AC arc

Methods of Arc Extinction

High Resistance Interruption

The arc is elongated such that the voltage drop across it increases (Eq. 14.23) to such an extent that the system voltage cannot sustain the arc. The current reduces to zero earlier than the normal current zero (without elongating the arc). This method is employed in DC circuit breakers and in low and medium voltage AC circuit breakers.

The arc is elongated by

- magnetic blow-out coils used in conjunction with arc runners;
- pushing the arc against arc splitters. These are made of plates of resin bonded fibre glass.

Both these methods are used in conjunction, and are illustrated in Fig. 14.19. The magnetic field set up by the blow-out coils forces the arc current up the arc runner causing it to elongate. The arc finally strikes against the arc splits, gets split and extinguishes.

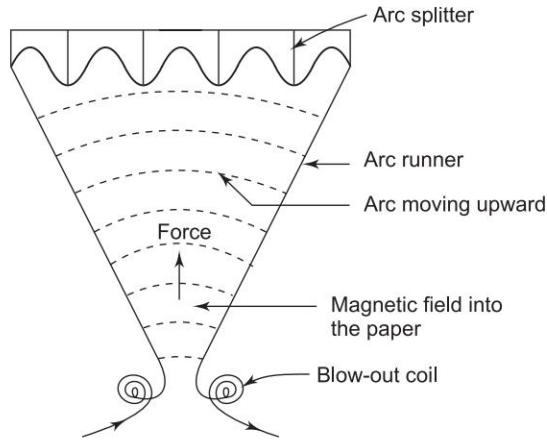

Fig. 14.19 Arc elongation and splitting

Low Resistance or Zero Point Extinction

At current zero the space between contacts left ionized is deionized by introducing fresh unionized medium like

- transformer coil;
- fresh air (may be at high pressure);
- SF_6 gas; or
- allowing metal vapour arc to extinguish in vacuum.

Prevention of Arc Restrike

Splepian Theory

After current zero TRV appears across the contacts of the breaker. The dielectric strength in the space intervening the contacts must build up faster than the TRV for the arc not to restrike. This is illustrated in Fig. 14.20. Fast

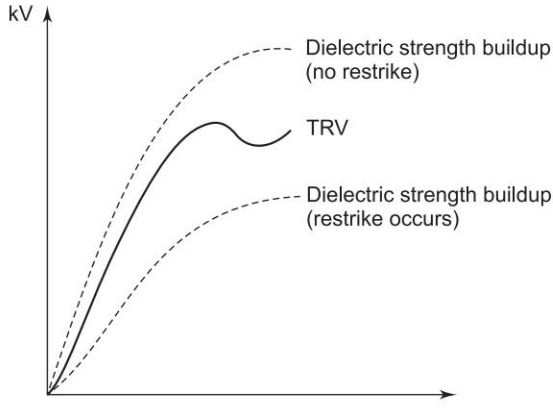

Fig. 14.20 TRV and dielectric strength race

dielectric strength build up is achieved by methods mentioned above in zero point extinction. Circuit breaker types are defined in accordance with the method adopted for replacement of the ionized medium—oil, air, SF_6 or vacuum.

Energy Balance Theory (Cassie Theory)

In gas-blast breakers, where very large amount of post-arc conductivity could exist with high rate of rise in TRV, an explanation that fits better the circumstance of arc extinction is the theory of energy balance due to Cassie.

Arc is assumed to be a uniform conducting column. Let

E = electric stress in volt/cm of arc length

I = total arc current

C = power loss due to cooling/cm of arc length

Q = energy content of arc/cm length

Then

$$\frac{dQ}{dt} = EI - C \tag{14.24}$$

The arc would extinguish (will not restrike) only if $\frac{dQ}{dt} < 0$, i.e., the arc energy continuously decreases.

Arc time Constant

It is the time required by the quenching medium to regain its original dielectric strength and is of the order of microseconds.

Arc Quenching Media

Various quenching media employed in circuit breakers are listed below. Each is employed over a range of voltages and capturing capacities required. Their regions of application tend to overlap. The present state of technology and future trends will be indicated in Sec. 14.4. The arc quenching media employed are

- Air at atmospheric pressure
- Oil
- Vacuum
- Air blast (air at high pressure)
- SF_6 gas

14.4 CIRCUIT BREAKER TYPES

A three-phase circuit breaker comprises the following sub-assemblies:

- three poles (set of contacts—one fixed, one movable);
- operating mechanism;
- control cabinet (indoor type breakers); and
- auxiliaries.

Operating Mechanism

The purpose of the operating mechanism is to change over the circuit breaker state from close to open, or vice versa. In closed position, sufficient pressure must hold the contacts together, overcoming all mechanical and electromagnetic force (caused by current flow). Opening must be fast, such that the operating time between the instant of the trip signal being received to the final contact separation is of the order of 0.03 s (i.e., 1/1/2 cycles) in EHV breakers, and about 3 cycles in distribution breakers. The opening is under the relays trip signal, which energises the CB trip coil from a battery source.

The mechanical energy required for the opening operation is obtained by one of the following means:

- spring charged during closing operation, or, in large breakers, the spring may be kept charged during closed condition by means of an electric motor;
- hydraulic pressure energy stored in accumulators; and
- high pressure compressed air stored in auxiliary air vessels—employed in air-blast circuit breakers.

In the first two methods toggle mechanism, or latches, are employed for achieving fast operating speed during operation. These mechanisms will not be described in this book. Stress will be laid on arc quenching mechanism and arrangement of contacts.

Various types of circuit breakers will now be described.

Air-break Circuit Breakers (ACB)

These are generally the indoor type, and are installed on vertical panels or indoor drawout type switch gear. These are used for DC circuits up to 12 kV, and for medium and low voltage AC circuits, usually up to 6.6 kV, 400–2400 A and rupturing currents of 13–20 kA.

The constructional details of an ACB are shown in Fig. 14.21. The arc is lengthened in the breaker by the magnetic field and arc runners, and is finally extinguished by arc splitters. There are two sets of contacts—main and arcing contacts. The main contacts are first to dislodge, while the arcing contacts are still closed under spring pressure. Thus the main contacts do not open any current and have long life. Arcing contacts made of hard copper alloy are easily replaceable.

Figure 14.22 shows the prospective current (current that would have flown), the let-through current, the arc voltage and recovery voltage when an ACB opens. Observe the current limiting feature of the lengthening arc with the current quenching much earlier than the normal current zero.

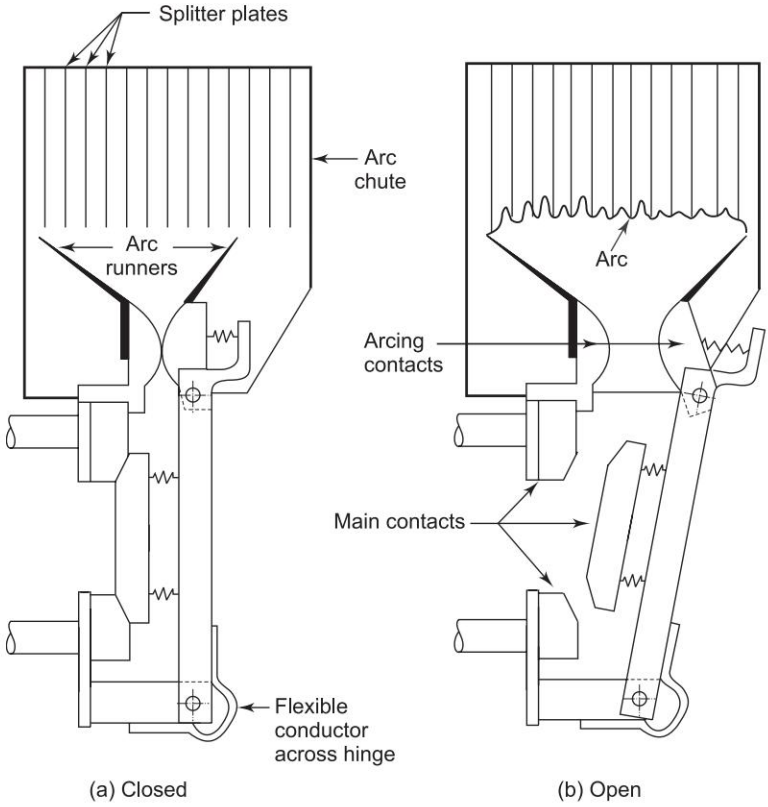

Fig. 14.21 Air-break circuit breaker

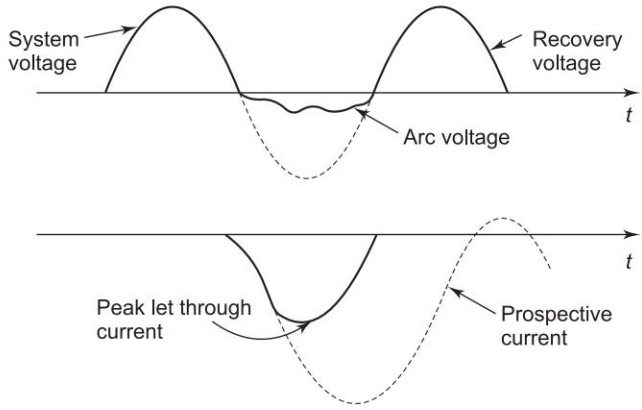

Fig. 14.22 Current limiting feature of air-break circuit breaker

Air-break DC Circuit Breaker

Figure 14.23 shows the circuit diagram of DC circuit breaking from which

$$V_{arc} = V_s - IR_s \tag{14.25}$$

where V_{arc} is a nonlinear function (Fig. 14.17) of the circuit current I. Equation (14.25) is a straight line, and is plotted in Fig. 14.24. If the VI characteristic of the arc intersects it, the arc would be sustained. However, as the arc is lengthened, its characteristic shifts to the right. When it no longer intersects the straight line, this condition corresponds to arc quenching in a DC circuit.

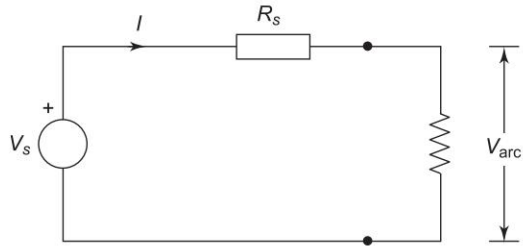

Fig. 14.23

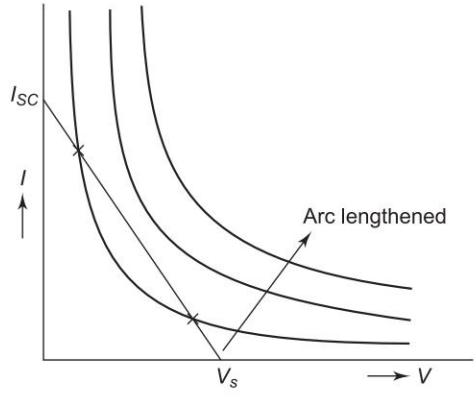

Fig. 14.24 Quenching of DC arc

Oil Circuit Breakers (OCB)

Here oil (transformer oil) is employed as the quenching medium. In earlier designs, bulk oil breakers, a large oil tank was used for quenching the arc. Modern practice is to use minimum-oil circuit breakers in which the arc is extinguished in a small arc control device filled with oil. These breakers have been developed for the following voltage ratings.

3.6 kV, 7.2 kV, 12 kV, 36 kV, 72.5 kV, 145 kV, 245 kV

In higher voltage ratings, air-blast and SF_6 breakers (to be described later) have now taken over. OCBs are still used for voltages up to 66 kV. Single interrupters suitable for draw-out type units are designed up to 12 kV.

The arc control devices are based on axial-flow and/or cross-flow principle. For higher current ratings cross-flow principle is preferred. Figure 14.25 shows the technique of arc quenching in a minimum oil circuit breaker. As the contacts separate, the heat of the arc causes the oil to decompose into hydrogen (70%),

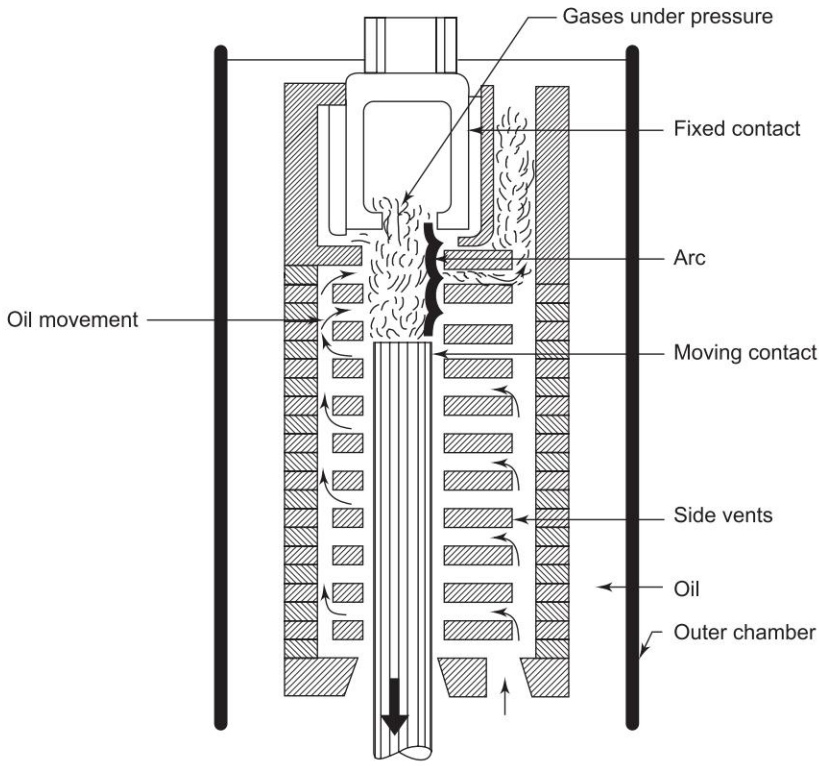

Fig. 14.25 Minimum oil circuit breaker

acetelyne etc. The gaseous formation causes the pressure inside the arc control device to rise and, as a result, the arc is pushed across the side vents, thereby somewhat elongating (crossflow). The movement of cool oil is also indicated in the figure. As the contacts move further apart lengthening the arc, it gets extinguished. For a given design and speed of contacts, the gas pressure generated is a function of arc current and arcing time, i.e., the arc energy. The time of final extinction of arc, therefore, is a function of arc current in an OCB as shown in Fig. 14.26, wherein smaller currents take longer breaking time in major part of the characteristic.

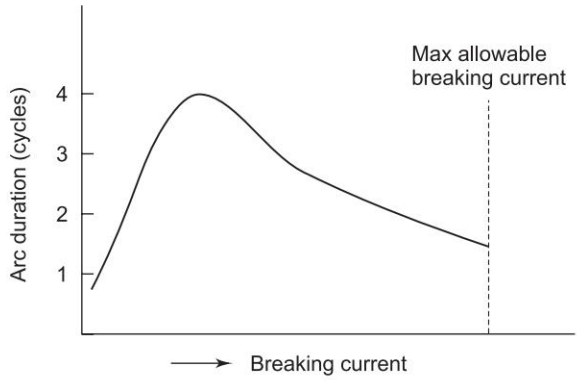

Fig. 14.26 Arc duration time in OCB

The contacts are allowed to travel well beyond the arc-control device, so that fresh dielectric oil fills the contact space after oil extinction.

Other techniques adopted to increase the rate of rise of dielectric strength after final current zero are:

- Flushing of contact space by fresh oil forced into contact space by piston-cylinder arrangement.
- Maintaining oil under pressure by means of inert gas; the pressure reduces the size of air bubbles, thereby increasing its dielectric strength.

Disadvantages of OCB

The main disadvantages of an OCB are as under:

- Arc products are inflammable.
- Oil is hygroscopic, and must be sealed air-tight in the chamber.
- Dielectric strength of oil is reduced by carbonization during the arcing process. Oil deteriorates over a period of time, and must be replaced at regular intervals.

Vacuum Circuit Breakers (VCB) (Fig. 14.27(a))

The vacuum as such is a dielectric medium and arc cannot persist in ideal vacuum. Vacuum employed in vacuum circuit breakers is of the order of 10^{-4} torr. The separation of current-carrying contacts causes the metal vapour to be released from the contacts giving rise to plasma—electrons and positive metal ions—which fills the space intervening the contacts and maintaining the arc. The vapour density depends upon the current in the arc. In the decreasing phase of the current the rate of release of metal vapour reduces. After the first current zero, the metal vapour quickly disperses and the medium regains its dielectric strength. The arc is thus extinguished in just half a cycle. The contact separation needed is of the order of a few millimetres—least among all circuit breaker types.

Technical Specification	
Rated voltage	12 kV
Rated continuous current	upto 1250 A
Rated frequency	50 Hz
Rated interrupting current	upto 26.3 kA (rms)
Rated making current	65.5 kA (p)
Rated short (3 sec.) current	26.3 kA (rms)
Operating duty	O-0.3 s-CO-3 m-CO (Rapid auto reclosing duty on request)
Applicable standard	IEC 60056 IEC 56 (1987)/IS 13118 (1991)
Power frequency withstand voltage	28/35 kV (rms)
Impulse withstand voltage	75 k(p)
Busbar rating	upto 2000 A

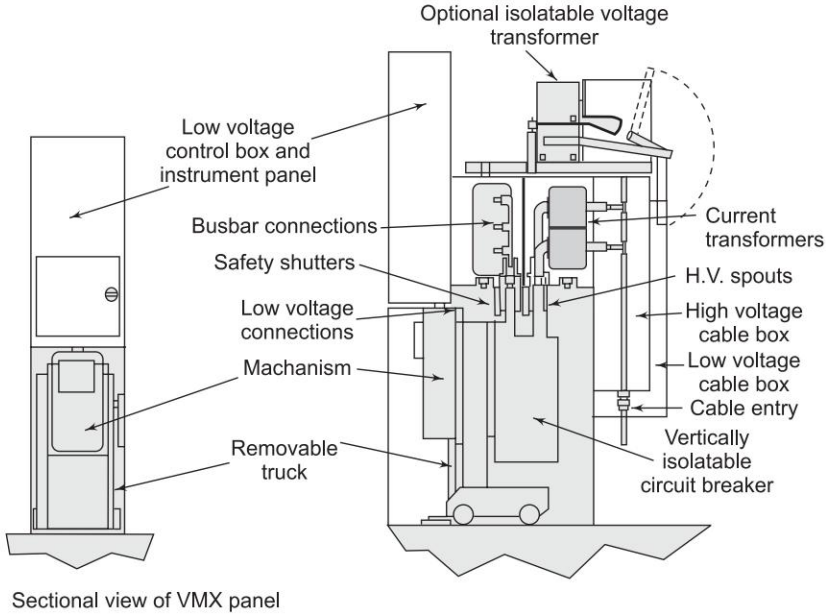

Fig. 14.27(a)

Upto 10 kA, plain-disc contacts are used. Several parallel arcs are formed, each sinking into a hot cathode spot (formed by bombardment by heavy metal ions). These parallel arcs repel* each other and quickly get diffused with consequent arc interruptions. Above 10 kA, these parallel arcs coalesce into a single arc with an extremely hot stationary cathode spot which cannot cool fast enough at current zero to prevent reignition of the arc. It also leads to erosion at a few spots on the contact surfaces reducing their life.

To overcome the above problem, special contact geometry is employed, wherein the current path is contrieved to achieve self-induced electromagnetic

* This differs from the case of two parallel conductions carrying current in the same direction, which attract each other.

movement of the arc. One type of contact geometry with deep forward curved fingers cut out on the contact surface as illustrated in Fig. 14.27(b) is commonly employed. This causes the root of the arc to keep moving round (retrograde motion), so that the temperature at any one spot cannot rise intolerably, with consequent uniform contact wear and a longer life.

The arc time constant is the least (a few μs) in vacuum circuit breakers compared to other breaker types. The rapid building up of dielectric strength after final arc extinction (20 kV/μs) is a unique feature of VCBs. These are, therefore, ideally suited for capacitor switching—restrike-free performance. The VCBs, because of this feature, tend to chop small currents.

Constructional Details

Figure 14.27(b) shows the constructional details of a VCB. The contacts are enclosed in a sealed glass or ceramic bottle whose space is evacuated to a high degree of vacuum (10^{-4} torr). The moving contact is attached to metal bellows, which permit the movement without loss of vacuum. To prevent the metal vapour from condensing on the bottle or bellows surfaces, metal shields *S* and *T* are provided. They also mask the high internal stress point and produce an almost linear axial grading of the external insulating surfaces. The contact geometry has already been described earlier. The interrupters are sealed for life and have a maintenance-free life of more than 20 years.

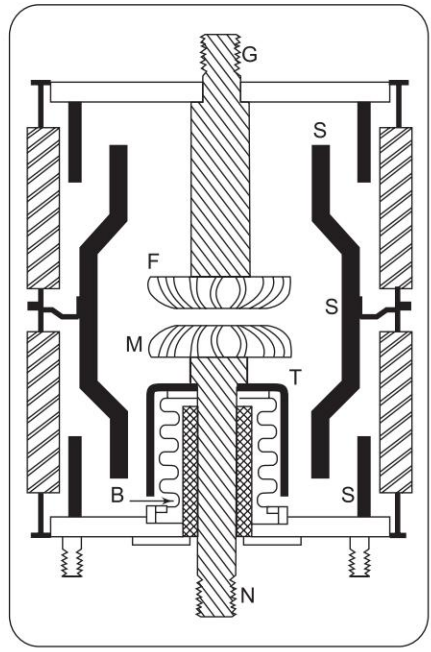

G—fixed electrode; N—moving electrode; F,M—arcing contacts; S—metal shield; E—ceramic or glass bottle; B—bellows; T—bellows shield

Fig. 14.27 (b) Typical vacuum interrupter

The properties required of contact material are:

- good mechanical strength and electrical conductivity;
- good thermal conductivity to assist rapid cooling of the arc;
- sufficient metal vapour from low-current arcing to control current chopping;
- limitation of metal vapour and thermionic emission from high-current arcing, to permit voltage recovery at current zero;
- low weld and cold adhesion strength at the contacting surfaces, to give easy and consistent separation; and
- low and uniform corrosion to give long operating life.

To achieve the above wide-ranging characteristics metal mixtures evolved from alloys and bulk interspersions, e.g. copper and bismuth, or chromium and copper, are used.

Application

Multi-unit VCBs have been employed at voltages upto 72.5 kV. These require smaller space than OCBs, and are employed both indoors and outdoors. Their advantages are being increasingly apparent over a widening application range. These will soon find favour on the Indian power distribution scenario.

Air-Blast Circuit Breakers (ABCB)

Blast of air at high speeds (supersonic) directed at the arc is very effective in cooling it, and in scavenging the products of ionization after current zero with consequent arc extinction within a cycle. The high speed air blast is produced by externally generated pressure (inside a pressure vessel), the pressure being of the order of 2–6 MN/m^2. The breaker is designed to direct a jet of air derived from the high pressure source to the contact space at the instant of contact separation. Various possible alternative arrangements for achieving this are shown in Fig. 14.28. Of these the axial blast, possibly using a hollow contact, is preferred for high power circuit breakers, since with the cross blast the arc is lengthened (requiring more breaker space). Cooling and, therefore, extinguishing takes place at the centre of the arc, which has been removed from the inter-contact space, and the ionized region which is left near each contact facilitates restriking.

Axial-blast breaker, being highly efficient, may cause current chopping to take place at low currents. But since the contact spacing is small (because of high efficiency of the interruption process), voltage surges generated would be limited by restriking. For the short break to withstand recovery voltage after final arc extinction, a series isolating switch is provided, which opens automatically after the arc is extinguished. This may not be necessary in breakers with pressurized arcing chambers.

As mentioned above most problems are obviated in present day designs by permanently pressurizing the system as shown in principle in Fig. 14.29. The blast value is located at the top of the column beyond the double interrupter

heads, so that air at full pressure constantly fills the receiver, the feed pipe through the support column and the interrupter heads right up to the blast valve.

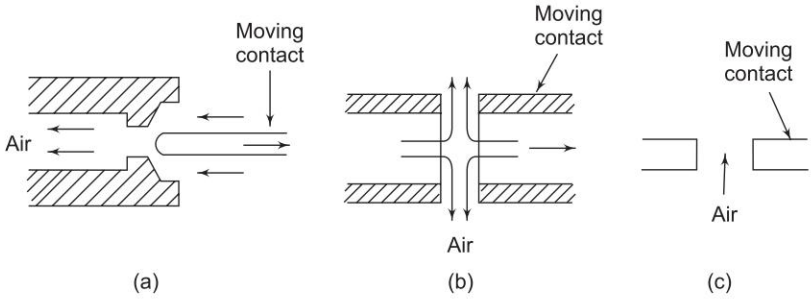

Fig. 14.28 (a) Axial blast with hollow fixed contact, (b) Radial blast, (c) Cross blast

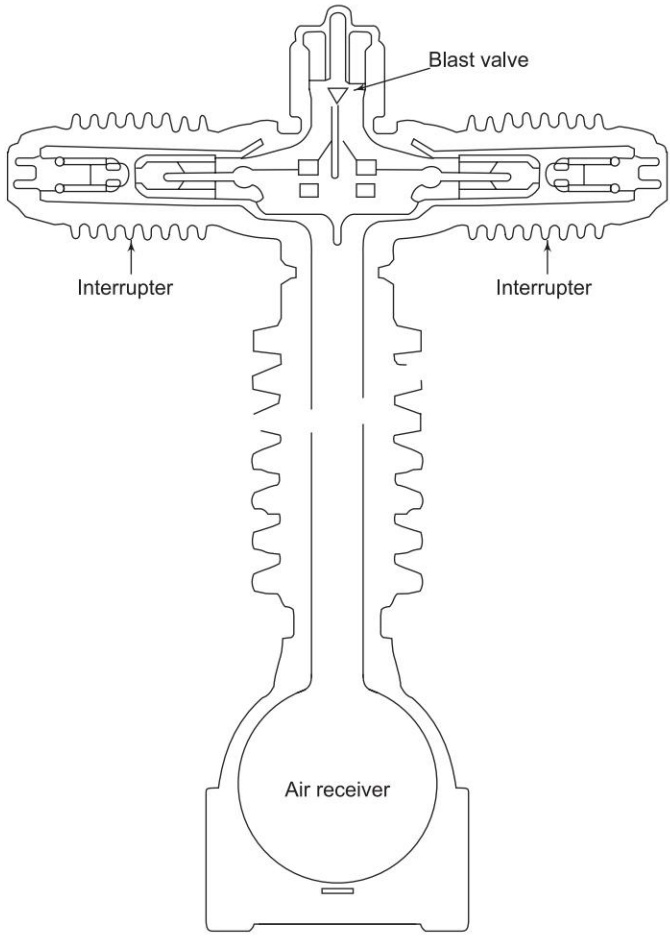

Fig. 14.29 Permanently pressurized air blast interrupter

The movement of contacts is controlled through a system of mechanical linkages from an operating mechanism at the base of the breaker, the contacts are held closed by a latch which is released by the trip signal, so that the contacts are free to move either mechanically or pneumatically or by a combination. The blast valve is closed after the interruption process is complete. The contacts remain open while the dielectric strength* of the high pressure air has the ability to withstand the recovery voltage, external isolator being not necessary.

For EHV circuit breakers, several interrupters have to be employed in series. In a modern 275 kV ABCB, four interrupters in series may be needed. On each interrupter are mounted in parallel resistor interrupters to limit the rate of rise of recovery voltage. Also capacitors in parallel to the interrupter are employed for voltage grading, equalizing voltages across the series interrupters. The action of grading capacitors is explained at the end. This type of construction is used for voltages of the order of 420 kV and higher with requisite number of interrupters.

Advantages of ABCB

The advantages of ABCBs are

- Reliable operation, because an external source of energy for arc extinction is employed.
- The ABCBs are clean, nondecomposable, and noninflammable.
- Fresh medium is used every time.
- There is faster contact travel because of pneumatic operation, no stored spring energy is needed, and these are suitable for repeated use.
- Small contact travel is involved.

Disadvantages of ABCB

The disadvantages of ABCBs are

- High air noise while operating, making them unsuitable for urban use.
- Chopping possibility.
- Independent pressure system needed for ABCB.

ABCB is receiving stiff competition from SF_6 breakers in all ranges of application, and may soon be superseded.

Grading Capacitors

Figure 14.30(a) shows the schematic diagram of several interrupters in series in an EHV system and Fig. 14.30(b) shows its capacitive equivalent circuit—series capacitances for each interrupter and shunt capacitances to ground for

* Air, at high pressure, acts as a good dielectric, as ionization by collision cannot occur due to high packing density of air molecules (free electrons cannot acquire sufficient velocity before striking a gas molecule).

each contact of the interrupters. This circuit applies at the instant the current goes through zero and the recovery voltage is appearing across the interrupters. Because of the circuit asymmetry, the capacitive current, and therefore the recovery voltage across interrupters, is unevenly distributed such that

$$V_{K1} < V_{K2} < V_{K3} < V_{K4} \tag{14.26}$$

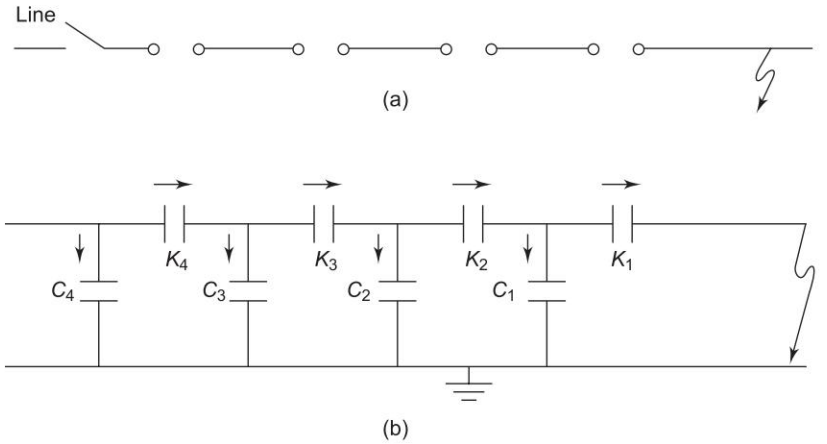

Fig. 14.30 Interrupters in series

The potential distribution will depend upon the kind of short circuit, and would be most uneven for line-to-ground fault. Because of this reason, the breaking capacity is unevenly shared by the series interrupters. Consequently, the breaking capacity of the system is less than the sum of the breaking capacities of individual interrupters; equivalently there is a loss in breaking capacity of the system.

The above discussed situation can be remedied by providing shunt grading capacitors with each interrupter. The equivalent capacitive circuit now becomes symmetrical as in Fig. 14.31. The capacitive current drawn by grounded capacitors is balanced by the grading capacitor current resulting in even distribution of recovery voltage across the interrupters.

Grading capacitors are used in series connected interrupters irrespective of the type of interrupters employed (air-blast or otherwise).

SF_6 Circuit Breakers

SF_6 is a heavy chemically inert nontoxic noninflammable gas. Its other properties, which make it ideal for circuit breaking are:

- At atmospheric pressure its dielectric strength is two to three times that of air. Because of excellent insulating properties of the gas, reduced electrical clearances are needed.
- Its heat transferrability at atmospheric pressure is 2 to $2\frac{1}{2}$ times that of air; therefore smaller conductor sizes needed.

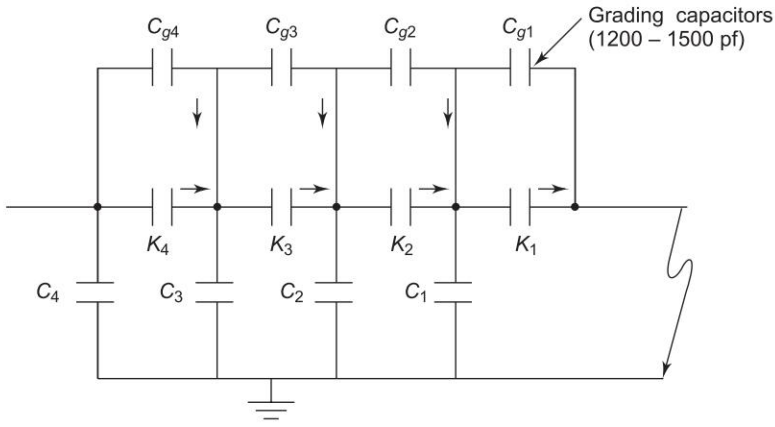

Fig. 14.31 Recovery voltage equalization by grading capacitors

- It is chemically stable at temperatures at which oil begins to decompose and oxidize; there are no carbon deposits and tracking.
- It is electronegative, its molecules rapidly absorb free electrons in the arc path forming heavy slow moving negative ions, which are ineffective as current carries. Hence its superior arc quenching ability.
- Its heat capacity below 6000°K is much larger than that of air and helps in continuous cooling of the arc zone.
- Its arc time constant is a few μs.

With the combination of superior insulating and arc-quenching properties, SF_6 breakers have a very wide range of application—6.6 kV to 765 kV and 20–60 kA rupturing capacity. These are becoming increasingly popular.

The properties of SF_6 are such that the gas blast speeds need not be as high as in ABCB. The gas is hermetically sealed inside the breaker body at a pressure of about 3 atm. High pressure needed to generate the gas blast of sufficient speed is obtained by a "puffer" mechanism at the time the breaker is opened. The puffer mechanism is a piston-cylinder arrangement, as illustrated in principle in Fig. 14.32. While the piston remains stationary, the cylinder is

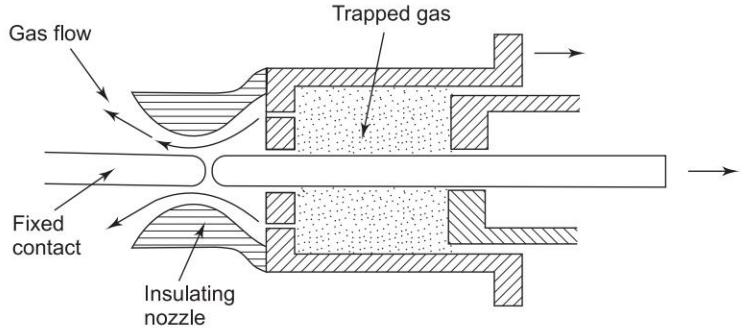

Fig. 14.32 Puffer principle

moved at high speed by means of the opening mechanism, creating a high pressure inside the enclosed space. The gas moves out through a convergent-divergent nozzle at high speed into the lower pressure region blowing the arc axially, and thereby quenching it.

The puffer mechanism and the arc quenching operation of a 145 kV circuit breaker is illustrated in Fig. 14.33. It is a latest design. Here combination of cross and axial blast is employed to quench the arc.

Advantages of SF_6 Circuit Breakers

The main advantages of SF_6 circuit breakers are as under:

- Low gas velocity and pressures employed prevent current chopping; capacitive currents are interrupted without restriking.
- There is no exhaust of high pressure gas to atmosphere, and their operation is silent.
- There is short time arc, low contact erosion and no contact replacement.
- No carbon deposition takes place and, as such, there is no insulation tracking.
- The smaller sizes of conductors and clearances lead to small overall breaker size; and these have ample overload margin.
- They are noninflammable.

14.5 HVDC CIRCUIT BREAKERS

The process of arc extinction in LVDC air-break circuit breakers was explained in Sec. 14.4. The arc is elongated till the arc voltage drop becomes in excess of the system voltage (Fig. 14.23), with consequent arc interruption. This method is not practical for HVDC circuit breaking. In this case the direct current must be reduced to zero by some auxiliary means.

Principle of Operation

The direct current to be opened is reduced to zero by the principle of commutation as illustrated in Fig. 14.34. Here L_1 and L_2 represent line inductances on either side of the circuit breaker (VCB). When the VCB begins to open, the switch S is immediately closed, causing the precharged capacitor C to discharge into the closed circuit. The current I_2 so produced is in a direction to oppose I_1 (SC current). As I_2 increases, the current $(I_1 - I_2)$ passes through zero giving opportunity to the VCB to interrupt the current. This is how the current is commutated to the auxiliary circuit.

Commutation Circuit

The interrupter has to be able to withstand the TRV which appears across it after current interruption. This duty is most severe in the DC circuit breaking.

A *figure of merit* commonly used in circuit breakers is the product $(\mathrm{d}I/\mathrm{d}t) \times (\mathrm{d}V/\mathrm{d}t)$, where $\mathrm{d}I/\mathrm{d}t$ is the rate of current decay before interruption and $\mathrm{d}V/\mathrm{d}t$ is the rate of rise of TRV. To achieve a high figure of merit, the vacuum interrupter is used for HVDC. Consider a 100 kV module capable of interrupting 5000 A.

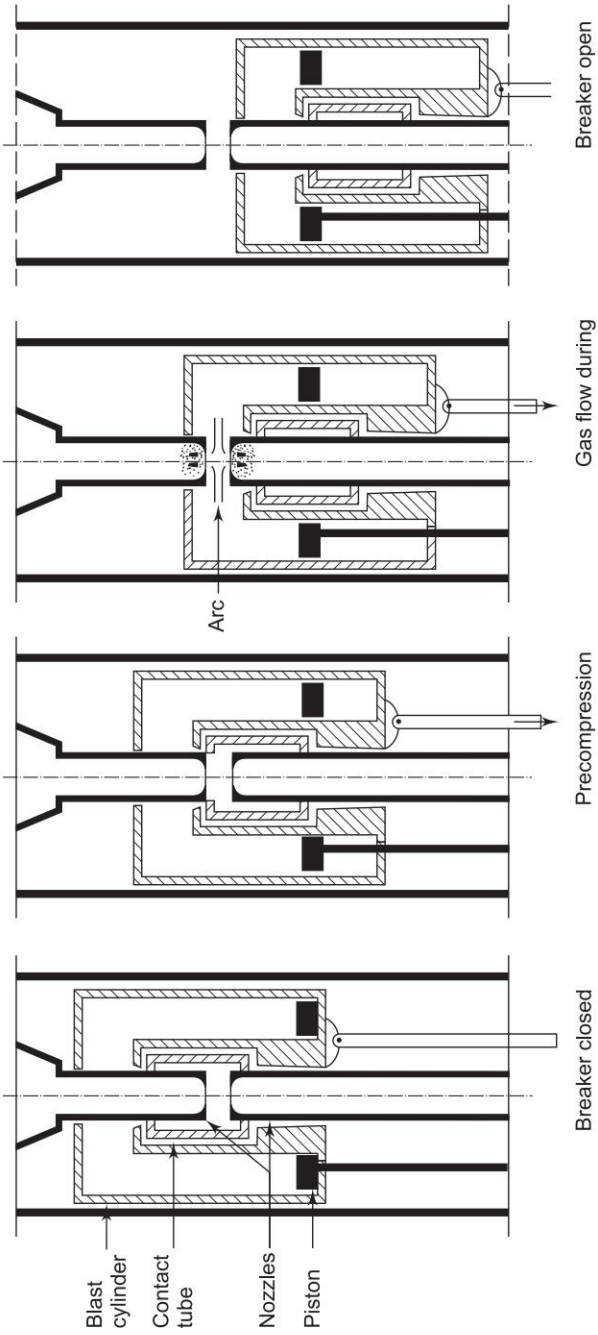

Fig. 14.33 Arc interrupting operation of a 145 kV SF_6 circuit breaker

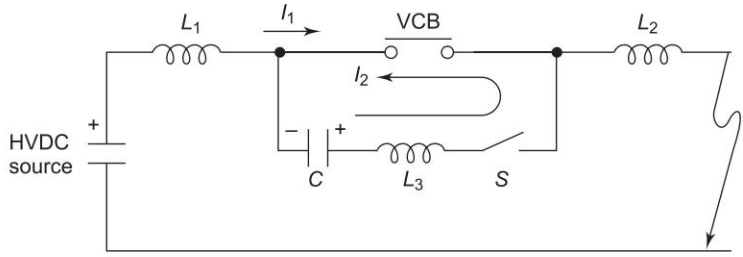

Fig. 14.34 Circuit diagram for direct current interruption

With the proposed circuit of Fig. 14.34, the current is brought to zero in about 5 μs, at a rate of 1000 A/μs. An AC circuit breaker interrupting a symmetrical 50 Hz current of 40,000 A experiences dI/dt of only 18 A/μs. The DC requirement is, therefore, quite extreme by this standard.

But as such, there is no interrupter which can match the HVDC requirements. Hence the circuit of Fig. 14.35 is modified to shape the current before interruption, and TRV after interruption, so as to match the capability of practical interrupting devices. In Fig. 14.35, a saturable core reactor L_4 has been added in series with VCB and a series RC_1 circuit in parallel to it. Normally when the power circuit is carrying current, the core is in saturated state, and offers a low inductance. When commutation is initiated, the current through L_4 begins to reduce, it comes out of saturated state and presents a very high inductance, slowing down the rate of current decay through VCB.

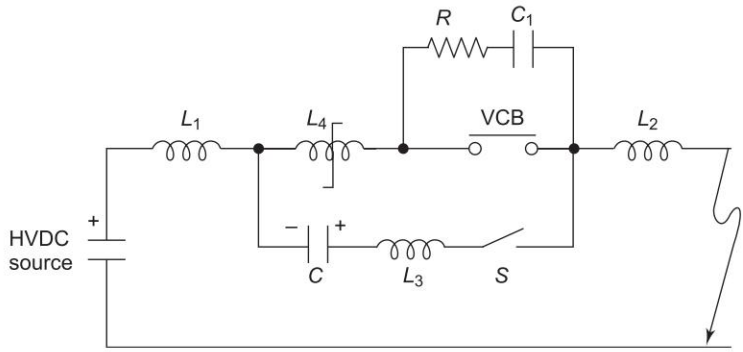

Fig. 14.35 Circuit of Fig. 14.34 modified to shape current and TRV

After VCB interrupts the current, the rate of rise of TRV across VCB is controlled by the charging of C_1 through R and L_4, which controls this rate of rise to an acceptable limit. The peak of TRV is also reduced, because charge is being removed from the commutating capacitor in this period.

For successful HVDC circuit breaking, it is necessary that breaker and commutation must be initiated as fast as possible. This calls for a high speed mechanism to part the contacts and a high speed switching device for the switch S. To achieve fast commutation, triggered vacuum gap is used for switching device.

14.6 TESTING OF HV AC CIRCUIT BREAKERS

Various tests to be performed on circuit breakers are:

- Mechanical tests
- Insulation tests, power frequency and impulse voltage
- Temperature rise tests
- Reliability tests under varying stress occurring in actual operation; ambient temperature, vibrations, dust, humidity, repeated operations
- SC tests

Here only SC tests will be described. Various SC tests are:

- Breaking current tests
- Making current tests
- Short time current tests
- Operating duty tests; basic short circuit test duties
- Test for short line fault
- Test for opening of small inductive current
- Test for breaking capacitive current

Short circuit testing is an experimental method for proving the ratings of circuit breakers and investigating the behaviour of circuit breakers for research and development work.

The two types of laboratory testing procedures used are:

- Direct tests, up to medium capacity circuit breakers
- Indirect tests, for large capacity circuit breakers

Direct Test

Full short circuit power is provided by a generator. The test plant in its simplest form is shown in Fig. 14.36. The functions of its various components are described below.

SC Generator

It has braced windings to repeatedly withstand full SC current. Also it has low reactance to give maximum short circuit current in the first half cycle. The stator windings can be connected star/delta; even two stator windings could be used to give a number of test voltages. It is driven by an AC motor which is cut off from the mains to prevent drawing of SC energy surge from the mains. The SC energy is provided by the inertia of the generator rotor. Instead a slip-ring motor with resistance included in rotor circuit at the time of short circuit could be employed. To prevent drop in generator voltage on short circuit, impulse excitation (about ten times normal excitation) is provided as shown.

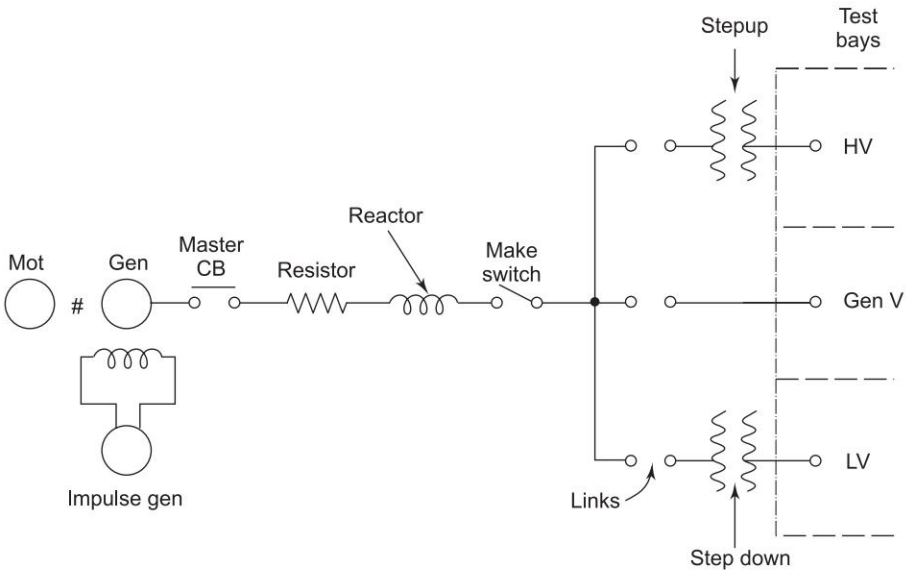

Fig. 14.36 Basic single-line diagram for SC test plant

Master CB

It provides protection against failure of the test breaker. This breaker must have interrupting capacity in excess of the short circuit MVA of the generator.

Resistor and Reactor

These control SC current and its power factor.

Make Switch

Controls the instant of short circuit on the voltage wave.

Sequence Switch (not shown in figure)

Controls the sequence of all switching operations.

The data recorded during a SC test are:

- SC current in each phase
- Voltage across each pole of test breaker before, during and after short circuit
- Oil pressure in case of OCBs
- Travel of moving contacts
- Current in trip coil circuit
- Generator voltage
- Timing marks

Indirect Tests

The short circuit testing capability of direct testing plant is not feasible beyond 4000 MVA. For testing larger rupturing capacity breakers (say 10,000 MVA at 245 kV), indirect testing must be employed. Various types of indirect tests are:

- Unit tests
- Synthetic tests
- Substitution tests
- Compensation tests
- Capacitance tests

Synthetic testing is the most popular. It permits testing of breaker capacity five times the short circuit capacity of the plant. This is the only one which will be described here.

Synthetic Testing

In this a low voltage current source provides short circuit current, and later a high voltage (low current) source supplies the transient recovery voltage. Two synthetic testing circuits are commonly employed and are described here.

Parallel Current-injection Method

Figure 14.37(a) shows the circuit used for parallel current-injection method. The three circuit breakers—master, auxiliary and test—are closed and then the make switch is switched 'on' to initiate the short circuit. The SC current is supplied by the generator (or generator and transformer) which is controlled by an inductance L_c while C_c eases the duty on the auxiliary breaker.

The voltage circuit comprises a source capacitor C_0 (charged to voltage V_0 by a separate DC source), a series spark gap and inductance L_v with a capacitance C_v in parallel with the test breaker.

At a certain time point t_0 of the SC current I_c (Fig. 14.37(b)) the auxiliary and test breakers are opened, and arc is struck in their contacts and they continue to conduct the current loop. At t_1 the spark gap is triggered (by irradiating it with ultraviolet light). It forces a current I_v through the test breaker as shown in Fig. 14.37(b). The source capacitance C_0 and inductance L_v are so adjusted that the current I_v oscillates at some frequency higher than the power frequency (i.e., the frequency of I_c).

From t_1 to t_2, the test breaker conducts the current $(I_c + I_v)$, when at t_2, I_c becomes zero and the auxiliary breaker opens. The test breaker opens at t_3 when I_v goes to zero. The voltage circuit oscillates at frequency $1/2\pi\sqrt{L_vC_v}$ ($C_0 >> C_v$), and a TRV of this frequency appears across the test breaker.

The SC current (I_c), the frequency and amplitude of TRV are easily controlled in this circuit to suit a range of circuit breakers.

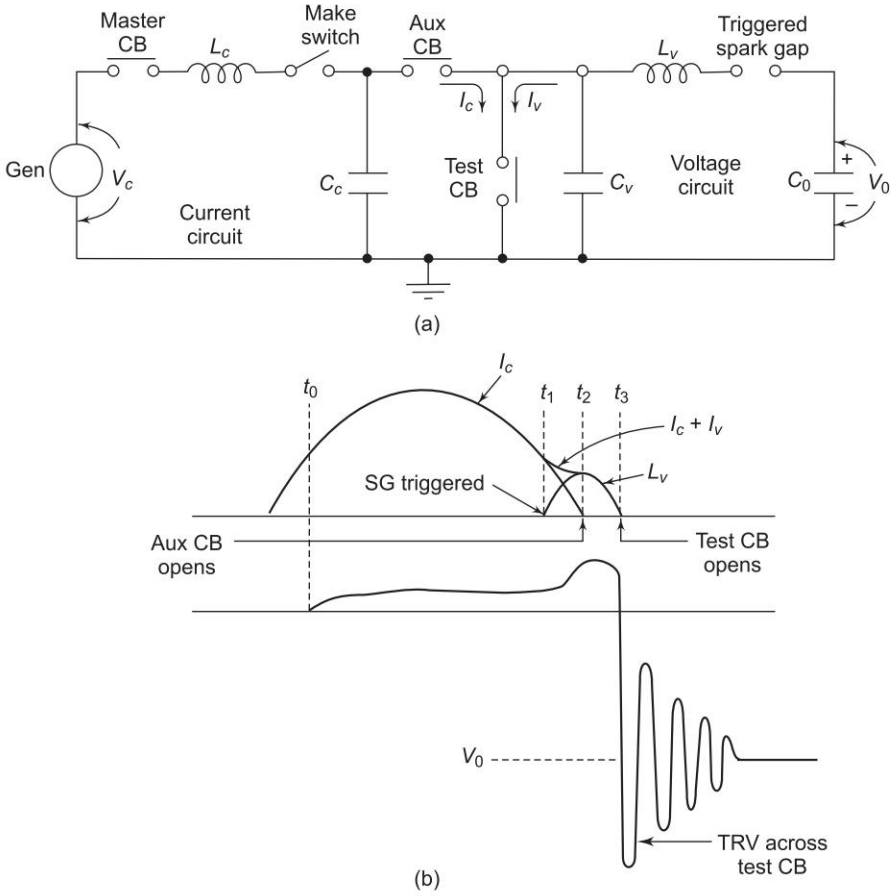

Fig. 14.37 Parallel current-injection method of synthetic testing

Series Current-injection Method

The circuit for this method is indeed the same as for the parallel current-injection method with the difference that the locations of the auxiliary and test breakers are interchanged as shown in Fig. 14.38(a).

With reference to Fig. 14.38(a), it is easily observed that when the spark gap is triggered at t_1, the current $(I_c - I_v)$ flows through the auxiliary breaker reaching zero at t_2 (Fig. 14.38(b)) before the normal current zero of the test breaker current (I_c). Except for the small shunting capacitances (C_c and C_v), the circuit becomes a series circuit, and a modified current I_v' flows through the test breaker coming to zero at t_3. If it opens, a TRV determined by voltage (V_0), inductance L_v and capacitance C_v will appear across it as shown in Fig. 14.38(b).

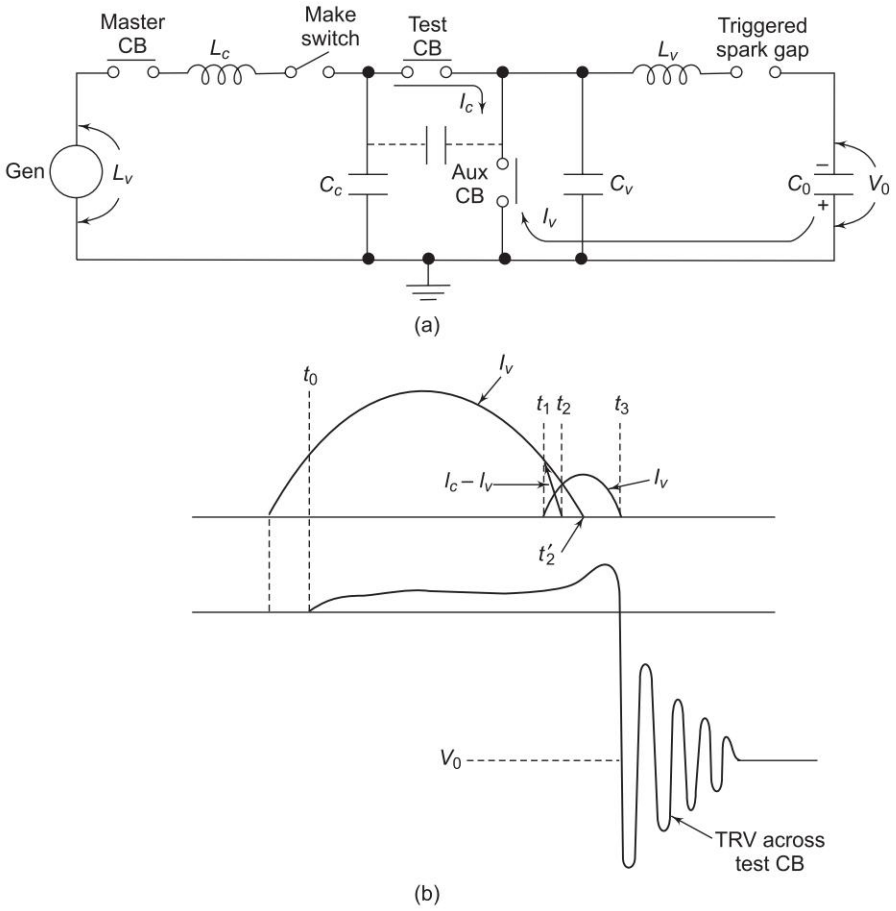

Fig. 14.38 Series current-injection method of synthetic testing

14.7 ISOLATORS

Isolators are used to disconnect the circuit breaker from live part of the system. An isolator is therefore also known as disconnecting-switch. It has no current-breaking and current making capacity. It operates under no load condition. For opening any circuit of the system, circuit breaker is opened first and then isolator is operated. As shown in Fig. 14.39, the isolators are used in combination with circuit breakers which can make and break circuit under normal and short-circuit conditions. (In addition to isolators and circuit-breakers, another device known as *load break switch* (or *load interrupting switch*) combines the functions of an isolator and switch. It is used for breaking the load current.

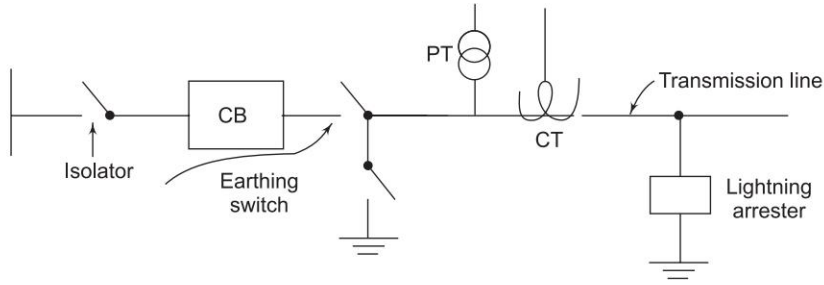

Fig. 14.39 Function of an isolator

14.8 FUSES

A fuse is the cheapest and simplest current-interrupting device for protection of 100 voltage (600 V) equipment against overloads and/or short circuits. High rupturing capacity cartridge (HRC) fuses are more reliable and give better discrimination and accurate characteristics. For safety reasons fuses are properly housed with iron clad cover.

In distribution circuits within a building individual circuit is protected against short circuits by microswitch which open magnetically on occurrence of accidental large current.

The fuse is expected to allow the flow of normal working current safely without overheating and during overloads/shortcircuits it gets heated up to melting point rapidly. The materials used normally are tin, lead, silver, zinc, aluminium, copper etc.

14.9 CONTACTORS

A **contactor** is an *electrical* device used for controlling power flow. A contactor is activated by a control input which is a lower *voltage*/*current* than that which the contactor is switching. Contactors come in many forms with varying capacities and features.

Contactors range from having a breaking current of several amps and 110 volts to thousands of amps and many kilovolts. There are highly specialized contactors which are as large as a small car and those which are almost subminiature.

A contactor is similar to, but different from an electrical *relay*. Although commonly both use a *magnetic coil* to draw a contact closed, a contactor differs in that it is designed to "break" a high current load—although relays are designed for switching loads 'on' or 'off' as well they tend to be of much lower capacity and are usually designed for both Normally Closed and Normally Open applications. Apart from optional auxiliary low current contacts, a contactor normally only has Normally Open contacts fitted.

Contactors are commonly fitted with overload protection to prevent damage to their loads. When an overload is detected the contactor is tripped removing power downstream from the contactor.

The contactor is commonly represented electrically with the symbol K.

A basic contactor will have a coil input (which may be driven by either an AC or DC supply depending on the contactor design) and generally a minimum of two poles which are controlled.

Some contactors are motor driven rather than relay driven and extremely high voltage contactors often have arc suppression systems fitted (such as an inert gas surrounding the contactor).

When a relay is used to switch a large amount of electrical power through its contacts, it is also designated as a *contactor*. Contactors typically have multiple contacts, and those contacts are usually (but not always) normally-open, so that power to the load is shut off when the coil is de-energized. Perhaps the most common industrial use for contactors is the control of electric motors. (see Fig. 14.40)

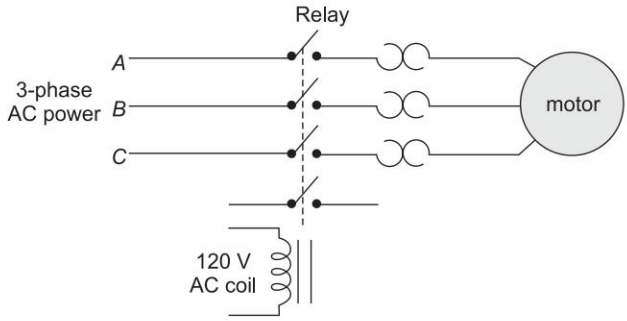

Fig. 14.40 Control of electric motor by a contactor

14.10 SUMMARY

This chapter discusses in detail about circuit breaker, transients, rating, types, HVDC CBs, and other protective devices such as fuses, isolators etc.

Problems

14.1 In a 220 kV system, the line to ground capacitance is 0.02 μF and inductance is 9 H. Find out the voltage appearing across the pole of a CB, if an instantaneous magnetizing current of 6 A is interrupted. Find the value of resistance to be used across the contacts to eliminate the restriking voltage.

14.2 In a short circuit test on a 220 kV, three-phase CB with earthed neutral the following results were obtained:

Fault pf = 0.4; recovery voltage = 0.9 of full line value; the breaking current is symmetrical and the restriking transient had a natural frequency of 18 kHz. Determine RRRV, assuming that the SC is an earthed fault.

14.3 A three-phase oil circuit breaker is rated at 1000 A, 1500 MVA 33 kV, 4 s. Find the rated normal current, symmetrical breaking current, making current and short time current rating.

14.4 A 50 Hz, 11 kV, three-phase synchronous generator with earthed neutral has a reactance of 4 Ω per phase and is connected to busbar through a CB. The capacitance to earth between the generator and the CB is 0.015 μF per phase and resistance may be ignored. Find
(a) Maximum voltage across the contacts of the CB.
(b) Frequency of the transient oscillations.
(c) The average rate of rise of restriking voltage up to the first peak of the oscillation.

References

Books

1. Dua, R., *Technology and Application of Vacuum Circuit Breakers*, M.Sc. Thesis, BITS, Pilani, 1984.
2. Greenwood, A., *Electrical Transients in Power System*, 2nd edn, John Wiley & Sons, 1991.
3. Lynthal, T.R., *J & P Switchgear Handbook*, 7th edn, Newnes Butterworth, London, 1972.
4. Wadhwa, C.L., *Electrical Power Systems*, 4th edn, New Age, New Delhi, 2005.
5. Rao, S.S., *Switchgear and Protection and Power Systems*, 11th edn, Khanna, Delhi, 1999.

Papers

6. Rowland, F.G., 'The Ins and Outs of Vacuum Circuit Breakers', *Electronics and Power*, May 1975.
7. Greenwood, A.N. and T.H. Loe, 'Theory and Application of the Commutation Principle for HVDC Circuit Breakers', *IEEE Trans*., *Power Apparatus and Systems*, vol. 91, no. 4, July/Aug. 1972, pp. 1570–1574.
8. *Electrical Transmission and Distribution Reference Book*, Westinghouse Electric Crop., East Pittsburgh, Penn., 1964.
9. Bhatia, C.M., D.P. Kothari and S.K. Agarwal, 'A Technique of Current Superposition for HVDC Circuit Breaker', *Proc., Int. Conf. on System Theory and Application*, vol. 1, Ludhiana, Dec. 1981, pp. B155–B160.
10. Saied, M.M., "The Kilometric Faults: Modelling and Normalized Relations for Line Transients and Breaker Recovery Voltage', *IEEE Trans., on P.D*, vol. 20, no. 2, April 2005.

Chapter 15

Power System Protection

15.1 INTRODUCTION

A fail-free power system is neither economically justifiable nor technically feasible. Faults can occur in any power system component—generators, transformers, buses, lines—though transmission lines being exposed to environment are the most vulnerable. Faults fall into two general categories—short-circuit faults and open-circuit faults. Short-circuit faults are the most severe kind, resulting in flow of abnormally high currents. If allowed to persist even for a short period of time, short circuits can lead to extensive damage to equipment. Undesirable effects of short-circuit faults are enumerated below:

- Arcing faults (most common) can vaporize equipment in the vicinity leading to, possibly, fire and explosion, e.g. in transformers and circuit breakers.
- Power system components carrying abnormal currents get overheated, with consequent reduction in the life span of their insulation.
- Operating voltages can go above or below their acceptable values, leading to development of another fault or damage to utilisation equipment.
- Consequent unbalanced system operation causes overheating of generator rotors.
- Power flow is severely restricted, or even completely blocked, while the short circuit lasts.
- As a consequence of blockage of power flow, power system areas can lose synchronism. The longer a fault lasts, the more is the possibility of loss of synchronism.

Open-circuit faults cause abnormal system operation and danger to personnel. Voltages tend to rise well beyond acceptable values in certain parts of the system with possibility of insulation failure and development of a short-circuit fault. While open-circuit faults can be tolerated for longer periods of time than short-circuit faults, these cannot be allowed to persist, and must be removed. We shall devote our attention to the more severe type of faults, i.e. the short-circuit faults. There are also other abnormal operating conditions which require remedying, but do not fall into the two categories of faults mentioned.

Two such important conditions are heavily unbalanced generator operation and loss of generator excitation.

Faults should be instantly detected and the faulty section isolated from the rest of the system in the shortest possible time. It is obviously not possible to do this manually, and it must, therefore, be accomplished automatically. Faults are *detected* automatically by means of *relays*, and the faulty section *isolated* by *circuit breakers* connected at the boundaries of the section (say, a line, transformer or generator). The combination of relays and circuit breakers is known as the protective system. The salient features of power system protection are:

- *Speed*: Faults at any point in the system must be detected and isolated in the shortest possible time. This time is of the order of 30–100 ms, depending upon the fault level of the section involved.
- *Sensitivity*: Relaying equipment must be sufficiently sensitive to operate reliably, when required, under conditions that produce the least operating tendency.
- *Selectivity*: Relaying equipment must clearly discriminate between normal and abnormal system conditions, so that it never operates unnecessarily.

Protective system must isolate a fault keeping as much of the system interconnected as possible.

- *Reliability*: Relaying equipment must be found in healthy operating condition when called upon to act, as years might elapse between two consecutive operations of relays at a particular station.
- On important lines the protective system, after once isolating the fault, must try to reclose the breakers restoring the system to its original configuration. This is necessary, as many faults (arcing faults) are self-clearing, and the system must be healthy in this respect.

The above objectives of a protective system are quite stringent, and some of these may conflict. Systems have, however, been devised and installed that work quite satisfactorily. The priorities of protective schemes differ from one organization to another, giving rise to a wide variation in relay application.*

15.2 PROTECTIVE ZONES

In order to delimit the number of elements disconnected by the protective system during a fault, the protective system is divided into a number of zones. Each protective zone has the primary responsibility to disconnect the element or elements in the zone in the event of a fault. For this purpose circuit breakers and relays are located at the zone boundaries. The protective zone concept is illustrated by means of Fig. 15.1. Certain features are observed here.

* It has been agreed by the users and consultants to adopt the following protection strategy for transmission lines for 400 kV and above:

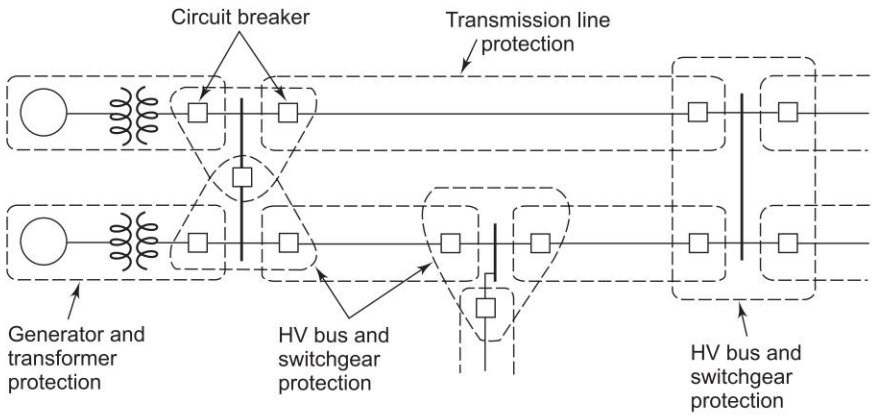

Fig. 15.1 Protective zones of a power system

- A separate zone of protection is established around each system element. Any failure within a zone will cause "tripping" (i.e. opening) of all circuit breakers of that zone, and only those breakers.
- The generator and transformer are lumped together in modern unit generation system (210 MW and above) and are protected by a single zone. However, separate protective schemes must be provided for the generator and transformer and both these schemes control the zone breaker. In older schemes, separate protective zones are employed for generator and transformer, necessitating two more circuit breakers and a low voltage bus.
- Adjoining protective zones are made to overlap. For a fault in the overlapping area of two zones, more circuit breakers will open than the minimum necessary to disconnect the faulty elements. Instead if there is no overlap, a small region between adjoining zones will remain unprotected. This is not acceptable.

The protection provided by each zone to its element(s) is known as *primary protection*. There may arise situations, however rare, that some components of a zone protection scheme fail to operate when called upon to do so. In order to almost 100% protect the power system elements and to prevent extensive damage, *backup protection* is provided which takes over only in the event of primary protection failure. Backup relays should not employ or control anything that is in common with primary relays that are to be backed up. This requires that the backup relays should be located at a different physical location

* To make the scheme reliable, active redundancy in the relays, current and potential transformers, battery supply and trip coil are provided. These are called MAIN I and MAIN II protection. Further, the type of relay is different in Main I and Main II. For example, if the relay in Main I is a carrier operated phase comparator relay, that for Main II shall be a carrier aided MHO relay. This approach eliminates to a very large extent the nonoperation of circuit breakers because of component failure of relay, current and potential transformers or battery.

(relaying station). Because of this requirement, a larger chunk of power system will get disconnected when backup relays operate. The principle of backup protection is illustrated by means of Fig. 15.2. Certain observations can immediately be made from this figure.

Fig. 15.2 Backup protection

- For a fault on line 1–2, if the primary protection fails to operate, backup relays will trip circuit breakers *ABIJ* opening 5 lines in place of one.
- For a fault on bus 1, backup protection is provided by relays located at *ABF*.

While remote backup concept is dealt above, mention needs to be made about *local backup*. This is widely used in present day 132 kV and above lines. Local backup relay trips all the breakers connected to the bus if a faulty line connected to the bus is not isolated by its breaker beyond a certain time. With reference to Fig. 15.2, a fault in the line 1–2 will be mainly isolated by *E* and *F*. If any of them fails e.g. *E*, a local backup relay, will isolate *C* and *D* after some time (obviously before the opening of *A* and *B*).

In general we conclude:

- Backup relaying should function with sufficient time delay so that first opportunity is given to primary relays to function in the event of a fault.
- When backup relaying functions, a larger part of the system is disconnected than when primary relaying operates correctly.
- Backup relaying is a must but is not a substitute for good maintenance.
- Backup relaying need to be provided for only the most severe kind of faults, i.e. short circuits. No backup relaying is employed for other abnormal conditions.

In the event of a fault on the line *AC* (Fig. 15.2), the backup relay at *A*, which controls the breaker *A*, provides a backup protection of sorts. In spite of this the line *AC* must be provided with its independent backup protection whose relays and breakers are located physically away from the stations *A* and *C*.

15.3 RELAYING ELEMENTS AND QUANTITIES

Currents and voltages at the two ends of a protected element are the basic quantities which are employed to recognize if the fault is in the protected zone. These quantities are fed to the relay which suitably processes these to produce a binary output—"trip" or "not trip (block)"—in the circuit breaker under its

control. In order that the relay (which indeed is a signal processor) be of small size and low-expense element, it must not be fed directly by the system currents and voltages whose level is tremendously high. This is further necessitated by the fact that the personnel working with the relay must be provided with a safe environment. Low-level samples of power system currents and voltages must, therefore, be extracted by means of transducers which are nothing but current and voltage transformers. It is seen with reference to Fig. 15.3 that at each relaying station, the protection system comprises three elements.

- Circuit breaker (CB)—to open the line.
- Transducers (T)—To provide low-level current and voltage samples to the relay.
- Relay (R)—to process the current and voltage signals to produce binary logic signal—'trip' or 'not trip'.

The power supply needed to trip the circuit breaker, or to provide the biasing signal in case of electronic relays, must be provided by an independent battery source, which must be regularly and thoroughly maintained. This is a must as during a fault, power system voltage would dip to very low levels.

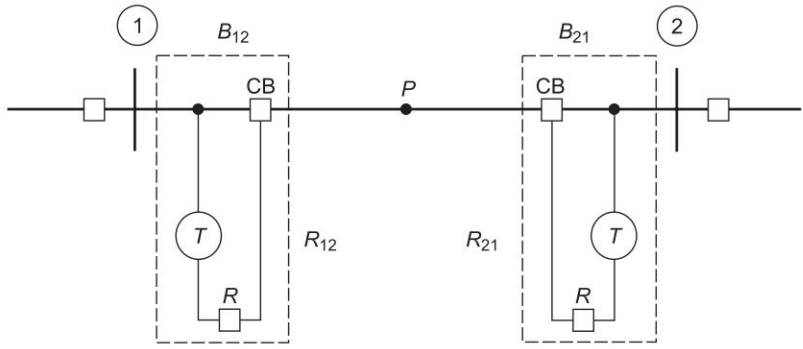

Fig. 15.3

In case of a fault at the point P of line 1–2 in Fig. 15.3, both relays R_{12} and R_{21} must recognize or see this fault and proceed to trip the respective breakers under their control. The area of responsibility of a relay is known as the *reach* of the relay.

The signal processing time to arrive at the logical decision is typically 8–40 ms, depending upon the type of relay employed. The total time that may elapse from the initiation of a fault to opening of the circuit breaker is between 30–100 ms depending upon the type of relay and circuit breaker employed. Intentional time delays may be included for coordination purposes.

For every type and location of a fault, there is some distinctive difference in the attributes of power system currents and voltages. Each relay is designed to recognize a particular difference and to operate in response to it. The differences are possible in one or more of the following attributes leading to various kinds of relays:

- Magnitude (of current or voltage)
- Direction (large change in phase angle)
- Ratio (impedance)
- Duration
- Rate of change
- Order of change
- Frequency
- Harmonics in wave shape.

15.4 CURRENT AND VOLTAGE TRANSFORMERS

These are also known as "instrument transformers". For obtaining low-level samples of power system currents and voltages, these offer certain distinct advantages.

- They are simple, economical and reliable.
- They provide electrical insulation from power system voltages.
- They are accurate and would tolerate overloading to some extent.

Figure 15.4 shows the representation of voltage (or potential) transformer (VT) and current transformer (CT) with zero loading—voltage transformer is open-circuited (infinite impedance) and current transformer is short-circuited (zero impedance). In a practical situation relays current element presents a small (but not zero) impedance to the secondary of a CT, and the relays voltage element presents a high (but not infinite) impedance to the secondary of a VT. The loading of an instrument transformer is commonly known as its "burden", and is expressed in terms of VA rather than impedance. VA for a VT expresses current at rated voltage and for a CT expresses voltage at rated current. Instrument secondaries are generally rated in the vicinity of 50 VA; this could be lower for transformers feeding electronic relays.

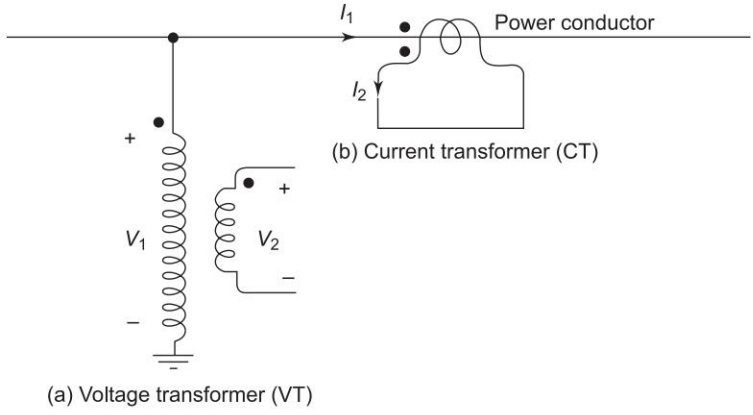

Fig. 15.4 Representation of instrument transformers

Voltage (Potential) Transformer (VT/PT)

Loading introduces error in voltage transformer because of voltage drops in leakage reactances of the windings. For system protection, extremely high accuracy in VTs is usually not required. It is, therefore, reasonable to model the VT as an ideal transformer, i.e.,

$$V_2 = \left(\frac{N_2}{N_1}\right) V_1$$

Thus V_2 is a scaled down version of V_1 in phase with it. A standard secondary voltage is 67 V (line-to-neutral) and $67 \times \sqrt{3}$ = 116 V (line-to-line). Commonly available voltage ratios are 1, 2, 2.5, 4, 5, 20, ..., 2,000, 3,000, 45,000 : 1.

For feeding 3-phase voltages to relays a commonly employed arrangement is the open-delta connection shown in Fig. 15.5, which requires only two VTs connected line-to-line.

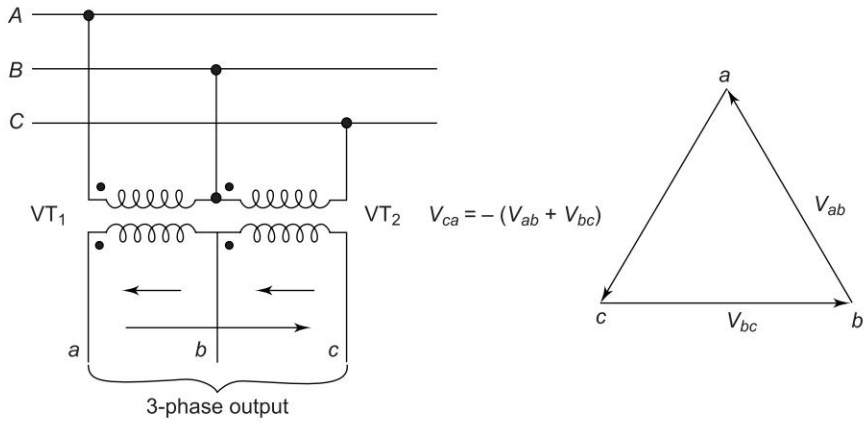

Fig. 15.5 Open-delta connection of VTs

Two types of voltage transformers are commonly found in relaying applications. For voltage upto about 11 kV, a VT is just like a multiwinding transformer. Such an arrangement becomes quite expensive for HV and EHV levels where a capacitance voltage divider is used as shown in Fig. 15.6. Capacitors C_1 and C_2 ($C_2 > C_1$) are adjusted such that a voltage of a few kV is obtained across C_2, which is then further stepped down by means of a two-winding transformer. Such an arrangement is known as capacitor voltage transformer (CVT).

The Thevenin equivalent across C_2 in Fig. 15.6 is a reduced voltage in series with capacitive reactance of $1/[\omega(C_1 + C_2)]$, which under loading would cause the voltage across C_2 to shift in phase from the line voltage. To nullify this effect a tuning inductance $\omega L = 1/[\omega(C_1 + C_2)]$ is included in series with the two-winding transformer.

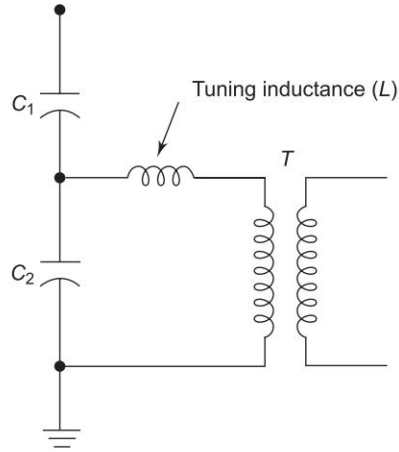

Fig. 15.6 Capacitor-coupled voltage transformer with tuning inductance

The Thevenin equivalent across C_2 in Fig. 15.6 is a reduced voltage in series with capacitive reactance of $1/[\omega(C_1 + C_2)]$, which under loading would cause the voltage across C_2 to shift in phase from the line voltage. To nullify this effect a tuning inductance $\omega L = 1/[\omega(C_1 + C_2)]$ is included in series with the two-winding transformer.

In HV and EHV systems, CVT is a free-standing device with its own supporting insulator. In case of a power transformer with bushing through which the conductor at system voltage passes, CVT could be located in the bushing with little additional cost. Bushing CVTs can supply smaller burden than free-standing CVTs.

Current Transformer (CT)

The schematic representation of a CT is shown in Fig. 15.4(b). The primary winding usually consists of a single turn which is the power conductor itself (along with its return circuit, it forms a single turn). The core is toroidal in shape through which is threaded the power conductor (primary), and on which are wound a few turns of the secondary. CTs are available in standard ratios given in Table 15.1, wherein the secondary current rating is 5 A. CTs are also available with the secondary current rating of 1 A.

Table 15.1 Standard CT ratios

Current ratio	*Current ratio*	*Current ratio*
50 : 5	300 : 5	800 : 5
100 : 5	400 : 5	900 : 5
150 : 5	450 : 5	1000 : 5
200 : 5	500 : 5	1200 : 5
250 : 5	600 : 5	

As the CTs have to carry currents as high as 10 to 20 times normal during short circuits, the error considerations are important because of core saturation. Figure 15.7 shows the equivalent circuit of a CT, with resistances and core loss neglected (a fair assumption for the sake of simplicity). The total leakage reactance is lumped on the secondary side, and the magnetizing reactance is referred to the secondary side. Again for ease of analysis, the load is considered to be purely reactive. As large current (short circuit case) flows through the load, the voltage developed across the magnetizing reactance is large enough for the core to go into saturating region of magnetization characteristic.

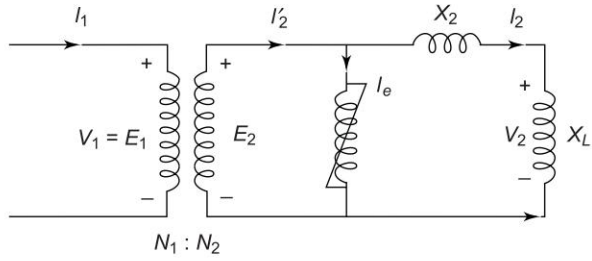

Fig. 15.7 Equivalent circuit of a CT

In Fig. 15.7

$$I_2' = \left(\frac{N_1}{N_2}\right) I_1 \tag{15.1}$$

$$E_2 = \left(\frac{N_2}{N_1}\right) V_1 \tag{15.2}$$

$$I_2 = I_2' - I_e \tag{15.3}$$

$$E_2 = jI_2(X_2 + X_L)$$

$$= j(X_2 + X_L)\left[\left(\frac{N_1}{N_2}\right) I_1 - I_e\right] \tag{15.4}$$

Since all the reactances are inductive, I_1 and I_e are in phase and, therefore, we can express the magnitude relationship corresponding to Eq. (15.4) as

$$|E_2| = (X_2 + X_L)\left[\left(\frac{N_1}{N_2}\right)|I_1| - |I_e|\right] \tag{15.5}$$

The magnetizing relationship is saturating type and can be expressed as

$$|E_2| = f(|I_e|) \tag{15.6}$$

Solving Eqs (15.5) and (15.6) graphically, we get $|I_e|$ for given $|I_1|$. Now

$$\text{CT error} = \frac{|I_2'| - |I_2|}{|I_2'|}$$

$$= \frac{|I_e|}{|I_2'|} \tag{15.7}$$

Certain conclusions can be drawn regarding CT errors from the above analysis.

- Large burden means large X_L. As a result, $|E_2|$ is large leading to large $|I_e|$, which indeed is the CT error and may exceed specified limit.
- For given burden, $|I_e|$ would be much larger for short circuit current than for normal load current. We must, therefore, check from the manufacturers data that this error is within acceptable values for relaying purpose.

CT error for given burden and input current can be calculated by means of Eqs (15.5), (15.6) and (15.7) as illustrated in Example 15.1.

In dead-tank type equipment—power transformers, oil circuit breakers, reactors—the power conductor passes through a bushing in which can be accommodated the CT—the bushing type CT. For EHV system where live-tank circuit breakers are employed, free-standing CTs are used.

Example 15.1 A CT has rated current of 250 : 5 A, $X_2 = 0.6\ \Omega$. Its magnetizing curve is given in Fig. 15.8. Compute $|I_2|$ and CT error for the following cases:

(1) Load current of 250 A; $X_L = 4\ \Omega$ and $X_L = 8\ \Omega$

(2) Fault current of 750 A; $X_L = 4\ \Omega$ and $X_L = 8\ \Omega$

Solution

(1) (a) Substituting values in Eq. (15.5),

$$|E_2| = (0.6 + 4)\left(\frac{5}{250} \times 250 - |I_e|\right)$$

$$|E_2| = 4.6\left(5 - |I_e|\right)$$

Intersection of this straight line with the magnetization curve (Fig. 15.8) gives

$$|I_e| = 0.2 \text{ A}$$

$$|I_2| = 5 - 0.2 = 4.8 \text{ A}$$

$$\text{CT error} = \frac{0.2}{5} = 4\%$$

(b) Equation (15.5) now becomes

$$|E_2| = 8.6\left(5 - |I_e|\right)$$

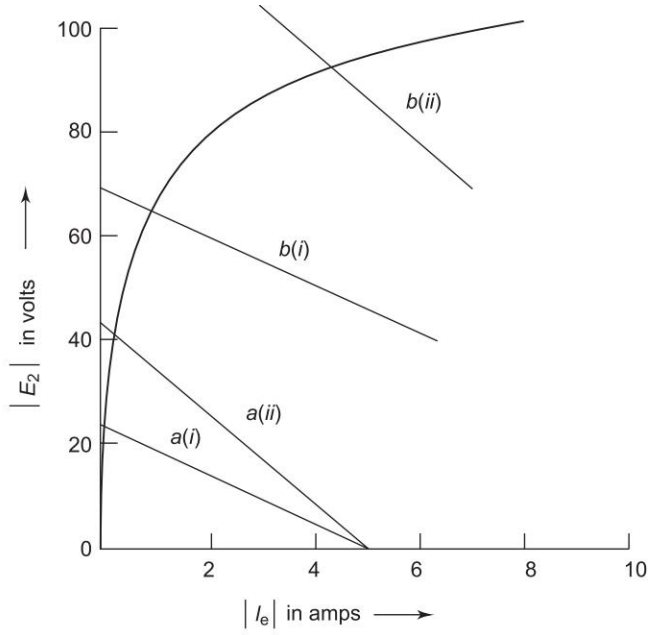

Fig. 15.8 Effect of CT saturation

We get from Fig. 15.8

$$|I_e| = 0.3 \text{ A}$$

$$|I_2| = 5 - 0.3 = 4.7 \text{ A}$$

$$\text{CT error} = \frac{0.3}{5} = 6\%$$

(2) (a) Equation (15.5) now becomes

$$|E_2| = 4.6\left(15 - |I_e|\right)$$

We get from Fig. 15.8

$$|I_e| = 0.9\text{A}$$

$$|I_2| = 15 - 0.9 = 14.1 \text{ A}$$

$$\text{CT error} = \frac{0.9}{15} = 6\%$$

(b) Equation (15.5) now becomes

$$|E_2| = 8.6\left(15 - |I_e|\right)$$

We get from Fig. 15.8

$$|I_e| = 4.3 \text{ A}$$

$$|I_2| = 15 - 4.3 = 10.7 \text{ A}$$

$$\text{CT error} = \frac{4.3}{15} = 28.7\%$$

Remark: The results of the example bear out the conclusions already drawn from the equivalent circuit. Notice that with large burden ($X_L = 8\ \Omega$), the CT error under fault condition (750 A) is unacceptable.

15.5 RELAY TYPES AND CHARACTERISTICS

Basic relay types most commonly used in power system are:

- Overcurrent relays
- Directional relays
- Impedance (distance) relays or modified impedance relays
- Differential relays
- Pilot relays

Amongst these overcurrent is the only single-quantity relay, which senses the current flowing in a particular element of the power system. Directional and impedance relays are two-quantity relays, which require both current and voltage samples as input quantities. The differential relays also require two inputs, but these are two current samples derived from two different physical locations. In fact, it is more a matter of connection than a new relay type—the relay itself is a sample modification of an overcurrent relay.

The general relay equation from which we can predict the operation of any of the first three relay types—overcurrent, directional, impedance—is given below:

$$Q = K_1 |I|^2 + K_2 |V|^2 + K_3 |V| |I| \cos(\theta - \tau) - K_4 \qquad (15.8)$$

where $|I|$ and $|V|$ are absolute values of current and voltage samples of the power system fed to the relay. θ is the phase angle between V and I, and τ is an adjustable parameter. The first two terms of this equation can also be absolute values of current and voltage rather than their square. K_1, K_2, K_3 and K_4 are scalar constants. The relay operates when

$$Q > 0 \qquad (15.9)$$

or the positive terms of Eq. (15.8) exceed K_4, a *threshold value* introduced for reliable relay operation.

The general relay Eqs (15.8) and (15.9) can be implemented analogously by (1) electromechanical devices or (2) electronic functional blocks, or digitally by using solid-state circuitry with no mechanically moving parts. Electromechanical relays are older, simpler and more widely used; solid-state relays are more versatile more reliable and faster. Solid state relays are fast gaining

ground compared to their electromechanical counterparts. They, of course, need very sound protection against over-voltage phenomena which is a common occurrence in power systems.

In the general relay equation Q will be a torque in an electromagnetic relay and it will be the voltage or current in a solid-state relay.

Overcurrent (OC) Relay

This relay employs the first and the last terms in the general relay equation, i.e., the relay operates when current through it (sample of power system current) satisfies the condition

$$Q = K_1 |I|^2 - K_4 > 0$$

or

$$|I| > \sqrt{K_4 / K_1} = |I_p| \tag{15.10}$$

where $|I_p|$ is said to be the *pickup* value of relay. Such a relay is an overcurrent relay and would operate in the shortest possible time (depending upon the type of hardware employed), and is called *instantaneous* overcurrent relay. Equation (15.10) could also be written as

$$|I| > |I_p| \text{ trip (relay trips circuit breaker)} \tag{15.11}$$

$$|I| < |I_p| \text{ block (relay does not trip circuit breaker)}$$

The value of pickup current can be easily adjusted by altering the constant K_1 by means of *plug setting** (PS); also known as tap setting. The plug setting current (pickup current) is expressed as % of relays current rating (5 A or 1 A). The standard PS available are:

50% to 200% adjustable in seven equal steps of 25%

20% to 80% adjustable in seven equal steps of 10%

10% to 40% adjustable in seven equal steps of 5%

For coordination of overcurrent relays, it is essential that these must have *inverse-time* characteristic where operating time (time to trip for a given current) decreases as the relay current increases, approaching a definite minimum value. Such relays are known as *inverse definite minimum time lag* (IDMTL) relays. Characteristics of an IDMTL relay are drawn in Fig. 15.9. The characteristic corresponding to TMS (explained below) = 1 can be expressed mathematically as

$$T_{op} = f\left(|I_{pu}| - 1\right) \text{ for } |I_{pu}| > 1 \tag{15.12a}$$

* In an electromechanical relay, the product of the coil current and the number of turns of current coil tapped i.e., the coil ampere-turns for the relay to just pickup is constant. So the relay pickup current is easily adjusted by tapping a suitable number of current coil turns. In a solid-state relay, plug setting is adjusted by means of a tapped plug bridge.

$$\left| I_{pu} \right| = \left| I \right| / \left| I_p \right|$$

= relay current in multiples of pickup current known as *plug setting multiplier* (PSM)

The operating time of an IDMTL relay can be adjusted by time multiplier setting (TMS). Thus

$$T_{op} = (\text{TMS})\, f\,(\text{PSM} - 1) \text{ for } \left| I \right| > \left| I_p \right| \qquad (15.12b)$$

TMS is continuously adjustable from 0.05 to 1.0 (for all three PS ranges specified earlier).

Figure 15.9 shows the characteristic of an IDMTL relay with $T_{op} = 1.3$ s for TMS = 1 and PSM = 10. For reliable relaying $\left| I_{\text{fault}} \right| > \left| 1.5 I_p \right|$, where $I_{\text{fault}} = I_f$ is the fault current sample on the secondary side of the CT (the current that flows through the relay).

Directional Relays

In a directional relay

$$Q = K_3 \,|\, V \,|\, |\, I \,|\, \cos(\theta - \tau) - K_4 \qquad (15.13)$$

where θ = angle by which $|\, I \,|$ leads $|\, V \,|$ and τ is an adjustable angle parameter. For small* K_4, the relay operates when

$$Q = K_3 \,|\, V \,|\, |\, I \,|\, \cos(\theta - \tau) > 0$$

or

$$\cos(\theta - \tau) > 0 \text{ trip}$$
$$\cos(\theta - \tau) < 0 \text{ block} \qquad (15.14)$$

The operating characteristic of such a relay in the complex plane is shown in Fig. 15.10. With reference to power system of Fig. 15.11, the relay will operate for fault to the left of bus 2 (current I_{21}) and will block for fault to the right of bus 2 (current I_{21}). The directional relay is thus able to discriminate between a fault on the protected zone and that outside it.

The relay characteristic will get slightly modified because of the term K_4 which is necessary for reliable relay operation—for a given V and θ the relay operates only above a certain minimum value of current.

In a directional relay, V is taken as the reference phasor as, under fault, it undergoes only a small change in phase angle (while the angle of the fault current can change by as large as 180°, depending on whether the fault is within or outside the protected zone). Such a phasor (V is this case) is called the *polarizing quantity* of the relay.

The relay characteristic of Fig. 15.10 can also be expressed by the inequalities

$$\theta_{\min} > \theta > \theta_{\max} \quad \text{trip}$$
$$\theta_{\min} < \theta < \theta_{\max} \quad \text{block} \qquad (15.15)$$

* Under fault conditions the left hand quantity in Eq. (15.13) is much larger than K_4 which does not effect relay operation.

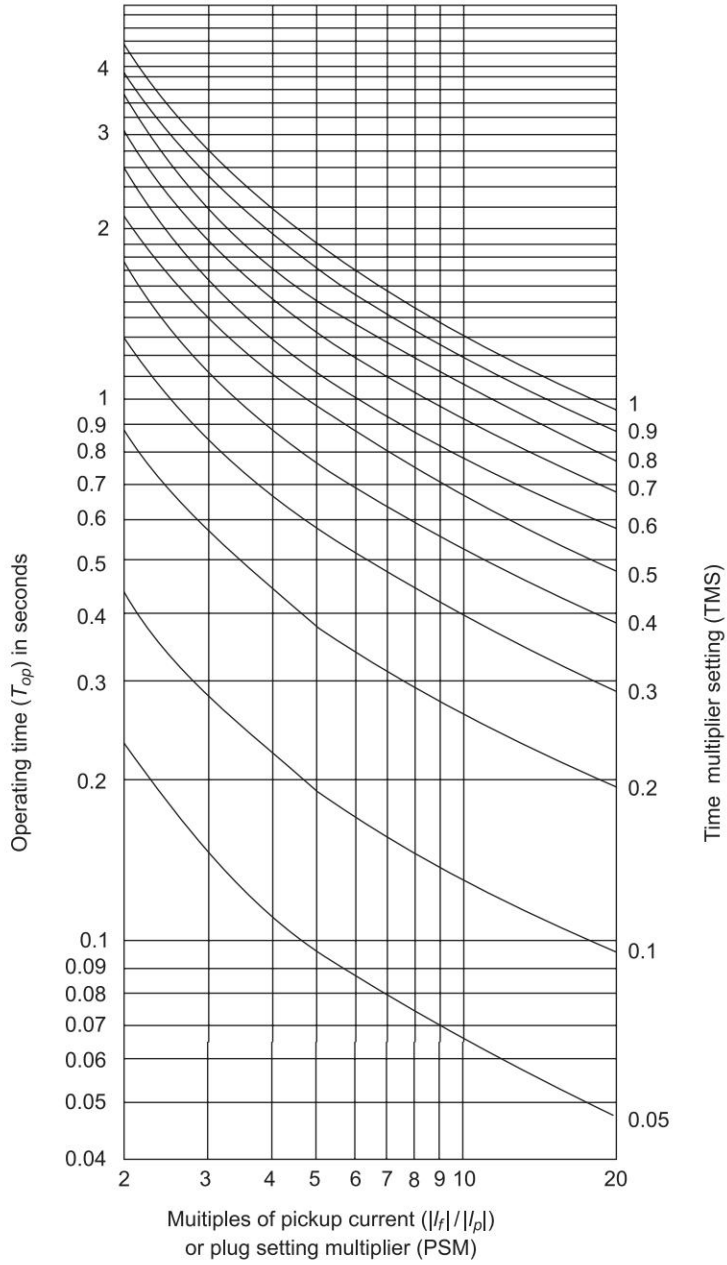

Fig. 15.9 Typical characteristics of IDMTL relays

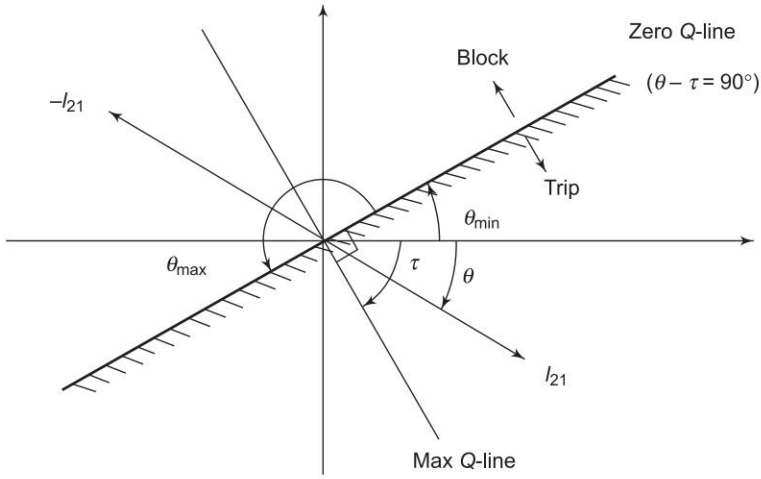

Fig. 15.10 Operating characteristic of a directional relay

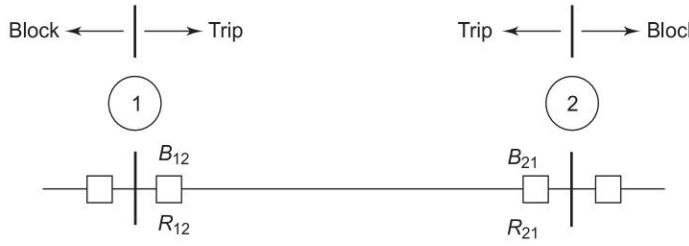

Fig. 15.11 Application of directional relay

An electromechanical directional relay senses sine of the phase angle (with reference to parameter τ) (Eq. 15.14)), while a solid-state relay would directly sense the phase angle (Eq. 15.15). Phase angle sensors in general are called *phase comparators*. An electromechanical relay is a sine phase comparator.

Impedance Relays

From the general relay equation (Eq. (15.8)), we have the special case

$$Q = K_1 | I |^2 + K_2 | V |^2 - K_4 \tag{15.16}$$

If effect of K_4 is neglected, the relay operates when

$$K_1 | I |^2 + K_2 | V |^2 > 0$$

or

$$\frac{|V|}{|I|} = |Z| < \left(\frac{K_1}{-K_2} \right)^{1/2} = | Z_{rs} | \tag{15.17}$$

If K_2 is made negative, such a relay senses impedance magnitude, and operates if the magnitude of impedance seen from its location (in any direction) is less than a specified value. Since $| V |$ prevents relay operation (K_2 negative) and $| I |$

tries to operate it, voltage is the *restraining* quantity of this relay and current is its *operating* quantity. A relay of this type is called an impedance relay or *distance relay* as line impedance is proportional to distance.

The characteristics of an impedance can in general be expressed as below and can be drawn in the *RX*-plane as in Fig. 15.12.

$$\begin{aligned} |Z| &< |Z_{rs}| \quad \text{trip} \\ |Z| &> |Z_{rs}| \quad \text{block} \end{aligned} \tag{15.18}$$

where $|Z_{rs}|$ = impedance setting of the relay.

Note that an impedance relay is inherently nondirectional, that is, it does not distinguish between $Z\angle\theta$ and $Z\angle(\theta + \pi)$. To make the impedance relay see in one direction only, it must be used in conjunction with a directional relay.

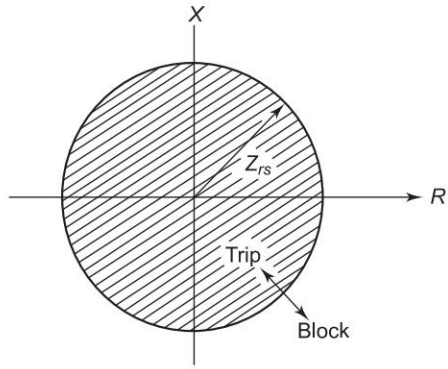

Fig. 15.12 *RX*-diagram of an impedance relay

A modified impedance relay called *mho* relay results if a directional relay is restrained by voltage. Thus

$$Q = K_3 \,|\, V \,|\, |\, I \,|\, \cos(\theta - \tau) - (-K_1) \,|\, V \,|^2 - K_4 \tag{15.19}$$

For relay operation neglecting K_4

$$K_3 \,|\, V \,|\, |\, I \,|\, \cos(\theta - \tau) - (-K_1) \,|\, V \,|^2 > 0$$

or

$$\frac{|V|}{|I|} = |Z| < \frac{K_3}{-K_1}\cos(\theta - \tau) \tag{15.20}$$

The right hand side of Eq. (15.20) is a circle with cente located on the line determined by the parameter τ and passing through, the origin as shown in Fig. 15.13. It is to be observed here that the characteristic is inherently directional. This characteristic can be alternatively expressed as

$$\begin{aligned} |Z - Z_{rs}| &< |Z_{rs}| \quad \text{trip} \\ |Z - Z_{rs}| &> |Z_{rs}| \quad \text{block} \end{aligned} \tag{15.21}$$

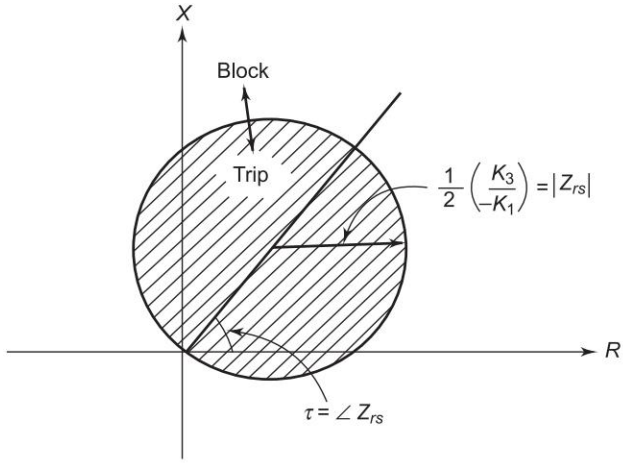

Fig. 15.13 *RX*-diagram of a mho relay

The centre of the impedance circle can, in general, be shifted to any point in the *RX*-plane by characterizing the relay as

$$\begin{aligned} |Z - Z_s| &< |Z_{rs}| \quad \text{trip} \\ |Z - Z_s| &> |Z_{rs}| \quad \text{block} \end{aligned} \tag{15.22}$$

Such a relay is called a *modified* impedance relay. The *RX*-diagram of such a relay is shown in Fig. 15.14.

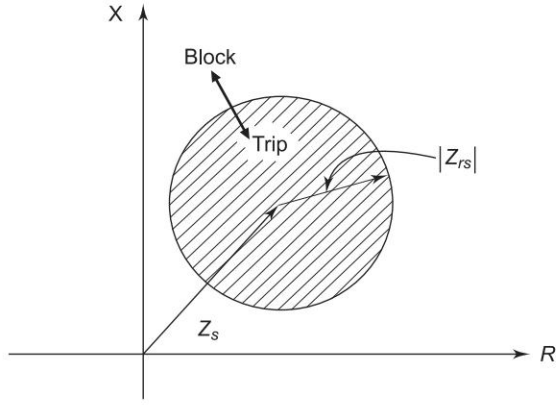

Fig. 15.14 *RX*-diagram of a modified impedance relay

A modified impedance relay characteristic is accomplished by the addition of a voltage, IZ_s, to the system voltage fed to the relay as shown in Fig. 15.15 from which we can write

$$V_r = V - IZ_s \tag{15.23}$$

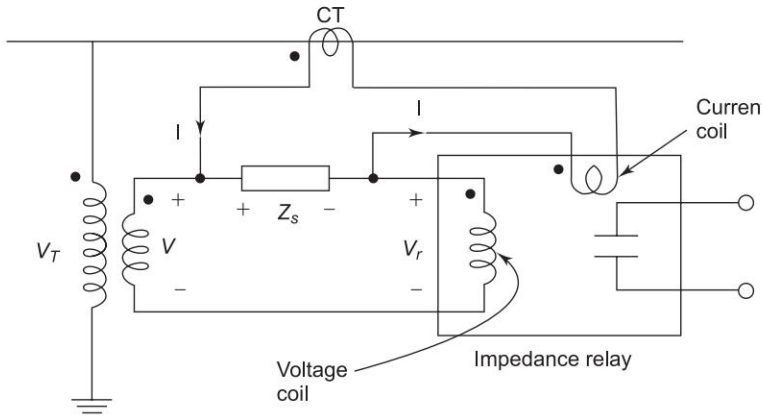

Fig. 15.15 Modified impedance relay

Let

$$V = |V| \angle 0° \tag{15.24a}$$

$$I = |I| \angle -\theta \tag{15.24b}$$

$$Z_s = |Z_s| < \theta_s \; ; \; -\pi/2 \le \theta_s \le \pi/2;$$

impedance setting of relay (15.24c)

$$= R_s + jX_s \tag{15.24d}$$

Now

$$V_r = |V| - |I||Z_s| \angle(\theta_s - \theta)$$

$$= |V| - |I||Z_s| \cos(\theta_s - \theta) - j|I||Z_s| \sin(\theta_s - \theta) \tag{15.25}$$

It immediately follows that

$$|V_r|^2 = \left[|V| - |I||Z_s| \cos(\theta_s - \theta)^2 + |I||Z_s| \sin(\theta_s - \theta)\right]^2$$

$$= |V|^2 - 2|I||Z_s| \cos(\theta_s - \theta) + |I|^2 |Z_s|^2 \tag{15.26}$$

From the impedance relay Eq. (15.17),

$$\frac{|V_r|^2}{|I|^2} = |Z_{rs}|^2, \text{ threshold of operation} \tag{15.27}$$

Substituting for $|V_r|^2$ from Eq. (15.3), we get

$$|Z_{rs}|^2 = \frac{|V|^2}{|I|^2} - 2|Z_s| \frac{|V|}{|I|} \cos(\theta_s - \theta) + |Z_s|^2$$

Recognizing that $|V|/|I| = |Z|$, the system impedance,

$$|Z_{rs}|^2 = |Z|^2 - 2|Z_s||Z|\cos(\theta_s - \theta) + |Z_s|^2 \quad (15.28)$$

Recalling $|Z|^2 = R^2 + X^2$ (15.29a)

$$R = |Z| \cos\theta \quad (15.29b)$$

$$X = |Z| \sin\theta \quad (15.29c)$$

Then

$$|Z_{rs}|^2 = R^2 + X^2 - 2|Z_s||Z|(\cos\theta_s \cos\theta + \sin\theta_s \sin\theta) + |Z_s|^2$$

$$= R^2 + X^2 - 2|Z_s|R\cos\theta_s - 2|Z_s|X\sin\theta_s + |Z_s|^2$$

which can be reorganized as

$$(R - |Z_s|\cos\theta_s)^2 + (X - |Z_s|\sin\theta_s)^2 = |Z_{rs}|^2$$

or

$$(R - R_s)^2 + (X - X_s)^2 = |Z_{rs}|^2 \quad (15.30)$$

Equation (15.30) is that of a circle in RX plane, with centre at (R_s, X_s) and of radius $|Z_{rs}|$ as shown in Fig. 15.14, which is the characteristic of a modified impedance relay.

If we set $R_s = R_{rs}$ and $X_s = X_{rs}$ (i.e. $Z_s = Z_{rs}$), a mho relay results with characteristic shown in Fig. 15.13. This is a simpler way to accomplish the characteristic of a mho relay than to use two elements as per Eqs (15.19) and (15.20).

A reactance relay is an overcurrent relay with directional restraint. The directional element is arranged to yield maximum Q contribution when its current lags its voltage by 90° (i.e. $\tau = 90°$). Thus

$$Q = K_1 |I|^2 - (-K_2)|V||I|\sin\theta - K_4$$

For relay operation neglecting K_4

$$K_1 |I|^2 - (-K_2)|V||I|\sin\theta > 0$$

or

$$\frac{|V|}{|I|}\sin\theta < \frac{K_1}{-K_2}$$

or

$$|Z| \sin\theta < \frac{K_1}{-K_2}$$

or

$$X < \frac{K_1}{-K_2} \quad (15.31)$$

Such a characteristic is represented in the *RX*-plane in Fig. 15.16. Notice that the relay does not sense resistance under fault condition, i.e., it is insensitive to the resistance of an arcing type fault.

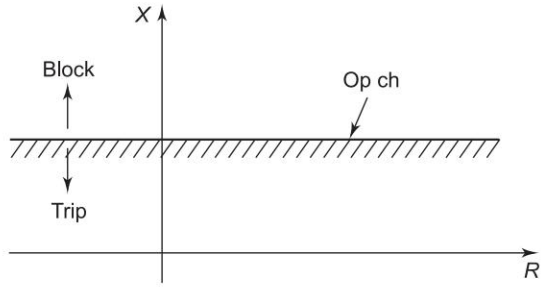

Fig. 15.16 *RX*-diagram of a reactance relay

Differential Relays

A differential relay is a suitably connected overcurrent relay operating on the difference of currents at the two ends of a protected element. For faults outside the protected element (*through fault*), the current in at one end equals the current out at the other, such that

$$I_1 - I_2 = 0$$

as is obvious from Fig. 15.17(a) which shows the differential protection of the phase winding of a generator. For a fault on the generator winding

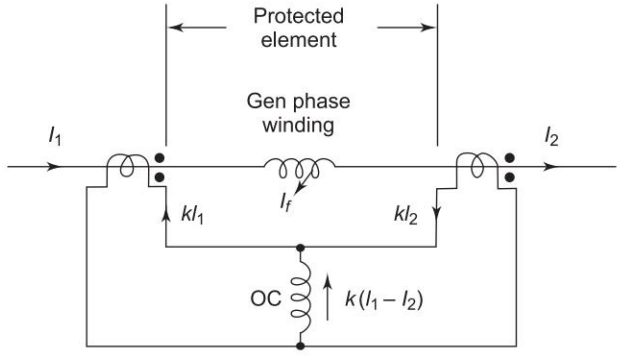

Fig. 15.17 (a) Differential relay protecting generator phase winding

$$I_1 - I_2 = I_f$$

and the relay operates to protect the element when

$$k\left|I_1 - I_2\right| = k\left|I_f\right| > \left|I_p\right| \qquad (15.32)$$

where k is the current transformation ratio of the two CTs.

In this simple arrangement of a differential relay (Fig. 15.17(a)), there is one snag. In case of a through fault, I_1 and I_2, though equal, are abnormally high, causing the CT ratios to have errors, i.e. CT ratio change, such that $k_1 \neq k_2$ and the relay operates erroneously when

$$\left| k_1 I_1 - k_2 I_2 \right|_{\text{Through fault}} > \left| I_p \right|$$

even though there is no fault on the generator winding, i.e. ($I_1 = I_2$).

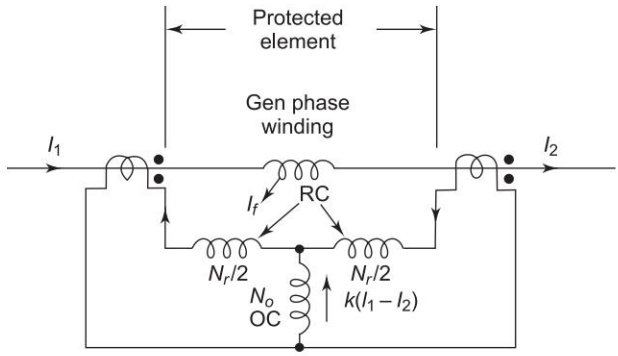

Fig. 15.17 (b) Percentage differential relay protecting generator phase winding

To remedy this difficulty, the differential relay is *restrained* by means of the sum of currents as shown in Fig. 15.17(b). Such a relay is called a *percentage* differential relay. Assuming electromechanical relays (see Sec. 15.6), which operate on comparison of AT and further assuming $\left| I_p \right|$ to be small, the percentage relay operates when

$$N_o k \left| I_1 - I_2 \right| > \frac{N_r}{2} k \left| I_1 + I_2 \right|$$

or

$$\left| I_1 - I_2 \right| > \frac{N_r}{N_o} \left| \frac{I_1 + I_2}{2} \right| \qquad (15.33a)$$

where N_o = number of turns of the *operating* coil

N_r = number of turns of the *restraining* coil

As per Eq. (15.26), the relay now operates when the magnitude of the difference (phasor) in the currents at the two ends of a protected element exceeds a certain percentage ($(N_r/N_o)/100$) of half the magnitude of their sum (phasor). Hence the name percentage differential relay. The relay actually operates when

$$k \left| I_1 - I_2 \right| - \left(\frac{N_r}{N_o} \right) k \left| \frac{I_1 + I_2}{2} \right| > \left| I_p \right| \qquad (15.33b)$$

Since the difference in currents in a percentage differential relay has to be much larger than $|I_p|$, under healthy conditions of the protected element the CT errors cannot cause undesired tripping, as always

$$|k_1 I_1 - k_2 I_2|_{\text{Through fault}} < \left(\frac{N_r}{N_o}\right) k \left|\frac{I_1 + I_2}{2}\right| \qquad (15.34)$$

Certain observations need to be made here.

- For such faults where I_f does not flow out of the protected element, $I_1 = I_2$, and the differential relay protection is ineffective. An example of this type of fault is an interturn fault on the generator phase winding. Other means have to be adopted to detect these type of faults.
- Wire connections to take the sum and difference of currents are only feasible where physical dimensions of the protected elements are small as in a generator and transformer. Differential protection scheme cannot be adopted, as such, for transmission lines.

Pilot Relays

As stated above long transmission lines (which may be hundreds of kilometres long) cannot be protected by simple differential scheme. In case of a through fault, the current magnitudes at the two ends of the line are equal and these have the same phase angle. This is illustrated in Fig. 15.18(a), where I_1 is the current into the protected zone at one end and I_2 is the current out of the zone at the other end. The magnitude and phase balance of I_1 and I_2 are upset for a fault on the protected line as shown in Fig. 15.18(b). This difference can be

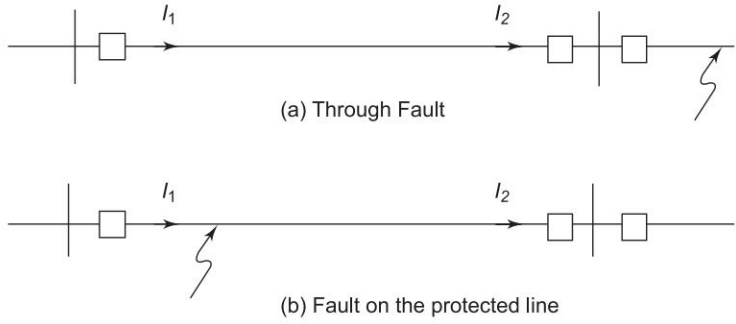

Fig. 15.18

detected by exchange of direction, or phase information, between the two ends of the line by means of carrier communication. These two schemes are known as *directional comparison* and *phase comparison* pilot protection. Carrier communication can be effected by means of telephone lines, or more reliably by the power lines themselves (known as power-line carriers). Wireless microwave channels can also be employed for pilot relaying. Since microwave transmission is limited to the line of sight, repeater stations have to be used along the pathway.

Example 15.2 Figure 15.19 shows the connections of a percentage differential relay to protect one phase of a generator. A high resistance fault occurs near the neutral end with the current distribution as shown in the figure. The relay has a slope of 10%, i.e., $N_r / N_o = 0.1$ as in Eq. (15.33a), and a pickup of 0.15 A. The CT ratio is 500/5.

(1) Would the relay operate under conditions indicated in the figure?
(2) Would the relay operate if this fault were to occur under no-load condition?

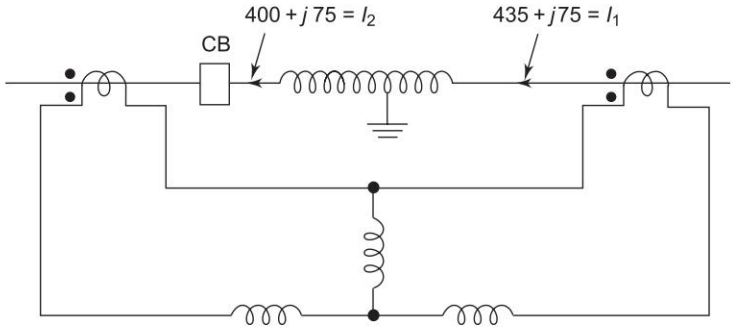

Fig. 15.19

Solution

(1) $\left|I_1 - I_2\right| = |(435 + j75) - (400 + j75)| = 35$ A

$$\left|\frac{I_1 + I_2}{2}\right| = \frac{1}{2}|(435 + j75) - (400 + j75)| = 424 \text{ A}$$

Since $35 < 0.1 \times 424 = 42.4$, the relay will not operate.

(2) Under no-load,

$$I_2 = 0$$
$$I_1 = 35 \text{ A}$$
$$\left|I_1 - I_2\right| = 35 \text{ A}$$
$$\left|\frac{I_1 + I_2}{2}\right| = 17.5 \text{ A}$$
$$\frac{5}{100} \times 7 - \frac{1}{100} \times 0.1 \times 17.5 = 0.3325 \text{ A}$$

Since this is more than the pickup value of 0.15 A, the relay will operate.

15.6 RELAY HARDWARE

To implement the relay function and characteristics discussed in Sec. 15.5, a variety of principles can be adopted. These are:

- Electromagnetic attraction
- Electromagnetic induction
- Solid-state relays (random logic)
- Sequential logic relays

How these principles can be adopted to discharge a particular relaying function (Eq. (15.8)) will be briefly outlined here without going into details of circuitry and operation.

Electromagnetic Attraction Type Relays

Figure 15.20 illustrates the basic operation of an electromagnetic attraction type relay. It is a single quantity relay, current in this case. The current causes a force, proportional to the square of its magnitude, to act on the armature which is restrained by a spring. The relay operates (to close its contacts in this case) when

$$Q \text{ (force)} = K_1 \mid I \mid^2 - K_4 > 0$$

or

$$\mid I \mid > \sqrt{K_4 / K_1} = \mid I_p \mid$$

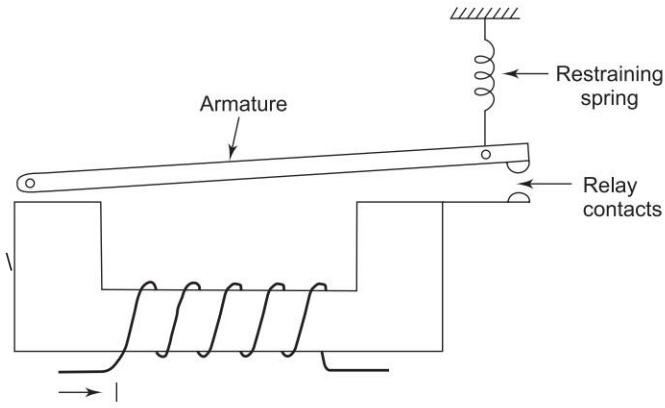

Fig. 15.20 Electromagnetic attraction type relay

- Such relays are instantaneous in operation. These suffer from chattering in AC operation, which can be inhibited by shading part of the core with a short-circuited coil. Once the relay has operated, because of reduction in air-gap in the magnetic circuit, the relay "drops out", i.e. armature begins to return to its normal (in this case open) position at a current smaller than the pickup value. Because of this undesirable feature, this type of relay is not adopted in AC relaying, and is restricted mainly to DC operation. It also cannot be adopted in two-quantity AC directional relays.

Electromagnetic Induction Type Relays

The relay operating torque is produced here by induction principle, so that these relays can only be applied in AC systems. It is basically a two-quantity relay which can be easily adopted for single-quantity operation.

Torque production

In Fig. 15.21 both fluxes ϕ_1 and ϕ_2 are piercing an aluminium (conducting) disc. These are sinusoidally varying fluxes with phase angle θ between them. Let

$$\phi_1 = |\Phi_1| \sin \omega t \tag{15.35a}$$

$$\phi_2 = |\Phi_2| \sin (\omega t + \theta) \tag{15.35b}$$

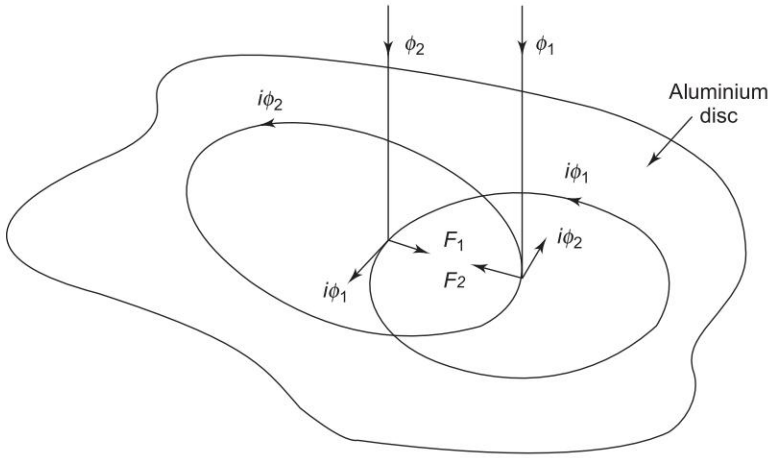

Fig. 15.21 Torque production in induction type relay

These fluxes induce currents i_{ϕ_1} and i_{ϕ_2} in the aluminium disc. With the positive direction of these currents shown in the figure as per Lenz's law.

$$i_{\phi_1} \propto \frac{d\phi_1}{dt} \propto |\Phi_1| \cos \omega t$$

$$i_{\phi_2} \propto \frac{d\phi_2}{dt} \propto |\Phi_2| \cos (\omega t + \theta)$$

The fluxes interacting with currents produce forces with directions indicated in the figure. These forces act along the line joining the points where the fluxes pierce the disc. The net force is given by

$$F = (F_1 - F_2) \propto (\phi_2 i_{\phi_1} - \phi_1 i_{\phi_2})$$

substituting for ϕ_1 and ϕ_2,

$$F \propto |\Phi_1||\Phi_2|[\sin(\omega t+\theta)\cos\omega t - \sin\omega t\cos(\omega t+\theta)]$$

$$\propto |\Phi_1||\Phi_2|[\sin\theta - \underbrace{\sin 2\omega t+\theta)}_{\text{Second harmonic torque}}]$$

It then follows that the average force is

$$F\,(\text{av}) \propto |\Phi_1||\Phi_2|\sin\theta \qquad (15.36)$$

The net (average) force is directed from the point where the leading flux pierces the disc (rotor) towards the point where the lagging flux pierces the rotor. It is as though the flux glides across the rotor dragging the rotor along.

Types of Actuating Structures

Shaded pole structure of Fig. 15.22 could be adopted for a single-quantity relay. The shading rings cause part of the flux created by the actuating quantity to lag the main flux by a fixed angle. The torque produced is given by

$$T \propto |I|^2 \text{ or } |V|^2$$

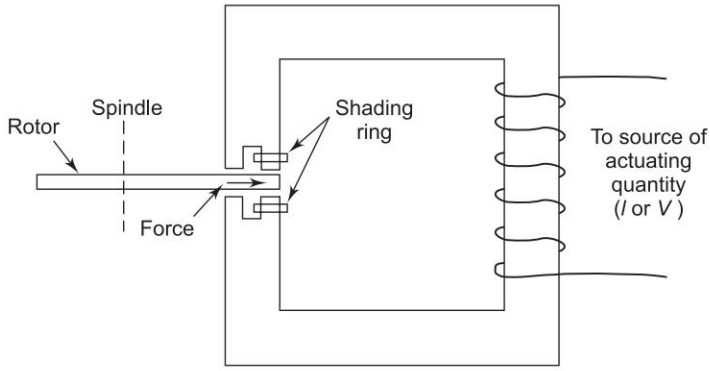

Fig. 15.22 Shaded-pole structure

Figure 15.23(a) shows an induction cup structure which can be employed for two-quantity or single-quantity relays. Suitable phase shifting networks are included in the two circuits to accomplish any desired feature (as in directional relays, explained shortly). Because of low inertia of induction cup construction, this structure admits of fast operation (less time lags). Double induction loop structure of Fig. 15.23(b) has even a smaller rotor inertia.

The flux created by each actuating current lags it by a small angle (as flux in a short-circuited transformer lags the primary current). In a symmetrical structure like in Fig. 15.23(a), this angle is the same for the currents through the two flux producing coils, and as a result the angle between the two fluxes is the same as between the coil currents.

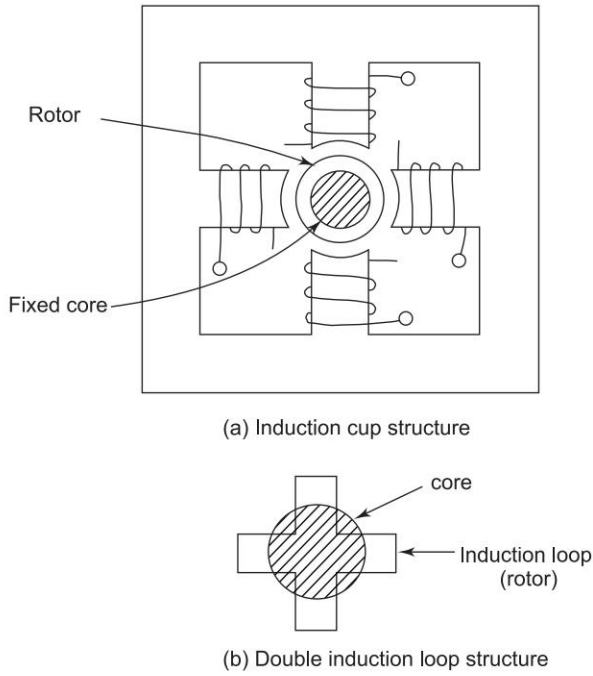

Fig. 15.23

A single-quantity relay results if both the coils are fed by the same actuating quantity with a fixed angle phase shifting network in one of the coils.

It may be remarked here that a current fed relay coil has a few turns with a resulting low impedance so as not to overburden the CT. On the other hand, a voltage fed relay coil has a large number of turns with resulting high input impedance so as not to overburden the VT.

Overcurrent Relay

Induction disc type relay of Fig. 15.22 with shaded-pole structure is employed for overcurrent relay. For a given angle θ through which the disc has to travel to close the relay contacts as shown in Fig. 15.24. Time inverseness is achieved by the saturation effect of relays magnetic circuit aided by the braking magnet. Time multiplier setting (TMS) is accomplished by adjusting the angle θ. Controlling torque is obtained by means of a spiral spring. Pickup current is easily adjusted by tapping different number of turns on the relay coil; pickup current is inversely proportional to the number of turns tapped. The characteristics of such a relay are given in Fig. 15.9.

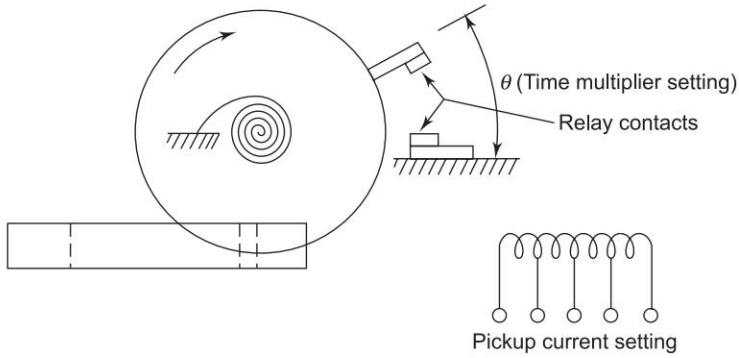

Fig. 15.24 Inverse-time overcurrent relay

Directional Relay

Induction cup or induction loop structure is employed for directional relay. One of the coils is current excited, while the other is voltage excited. Current setting can be adjusted by coil taps, while voltage setting is adjusted by means of series resistor or by auxiliary transformer taps. As in a short-circuited transformer, the flux produced by any coil lags its current by a certain angle. Because of structure symmetry, the angle between fluxes (which determines the relay torque as per Eq. (15.36) is the same as the angle between coil currents.

The phasor diagram of a directional relay is shown in Fig. 15.25. I_v, the voltage coil current lags the voltage applied by an angle depending upon the coil impedance. Since the fluxes are proportional to coil currents, and have the

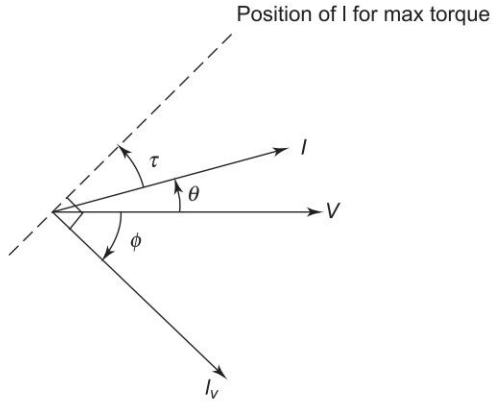

Fig. 15.25 Phasor diagram of directional relay

same angle separation as coil currents, the relay torque from Eq. (15.36) is found as

$$T = K_3 \mid V \mid \mid I \mid \sin(\theta - \phi) \qquad (15.37)$$

where ϕ = phase angle of voltage coil current I_v (shown lagging)

θ = angle by which the current applied to the relay leads its voltage

Taking the leading angle as positive and defining τ (a relay parameter) as the value of angle θ, when the relay develops maximum torque, then

$$\tau - \phi = 90^\circ$$

Substituting in Eq. (15.37),

$$T = K_3 \mid V \mid \mid I \mid \cos(\theta - \tau) \qquad (15.38)$$

which indeed is the directional characteristic. The parameter τ could be adjusted to any desired value by adjusting the angle of the voltage coil impedance without modifying its magnitude (see Example 15.3.).

Any Relay

Any type of the relays mentioned in Sec. 15.5 can be constructed by means of current and voltage actuated elements and the directional element described above.

Example 15.3 Figure 15.26 shows the connections of a directional relay. The voltage coil has an impedance of $210 + j450\ \Omega$. At what power factor will the relay develop maximum torque?

It is desired to modify the relay such that it develops the same maximum torque at a lagging power factor angle of 45°, the load being fed in the same direction. What modification would you recommend?

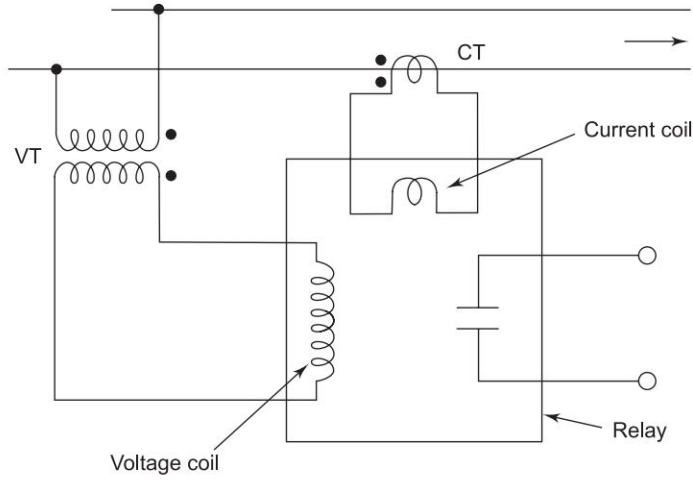

Fig. 15.26 Connection diagram of directional relay

Solution

With reference to the phasor diagram of Fig. 15.25

$$\phi = \tan^{-1}\frac{450}{210} = 65^\circ \text{ lagging}$$

At maximum torque

$$\theta = \tau = (90^\circ - \phi)$$
$$= 90^\circ - 65^\circ = 25^\circ \text{ leading}$$
$$\text{pf} = \cos 25^\circ = 0.906 \text{ leading}$$

For the relay to develop maximum torque at 45° lagging pf,

$$\tau = -45^\circ$$

$\therefore$ $\phi = +45^\circ$ leading $(\tau - \phi = -45^\circ - 45^\circ = -90^\circ)$

For the relay to develop the same maximum torque, the voltage coil current should remain the same while its angle modifies to $\phi = +45^\circ$. To achieve this, resistance and capacitance are added in series with the voltage coil as in Fig. 15.27.

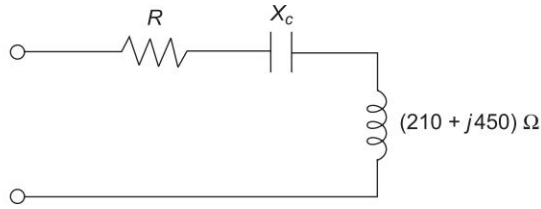

Fig. 15.27

For the conditions stated above,

$$\tan 45^\circ = \frac{X_c - 450}{R + 210} \quad \text{(i)}$$

and

$$(R + 210)^2 + (X_c - 450)^2 = (210)^2 + (450)^2 \quad \text{(ii)}$$

Solving, we get

$$X_c = 698.3\ \Omega$$
$$R = 908.3\ \Omega$$

Solid-state Relays

Apart from other electronic functional blocks, three main blocks of a solid-state relay are:

- Level detectors
- Time delay units
- Comparators

Level Detectors

Quite often level detectors are used to detect incoming or intermediate signal level with the purpose of giving an output if the input signal exceeds a fixed or a variable level.

The incoming signal in AC relaying is a rectified wave smoothed out by filtering which appears as V_{in} in the level detector of Fig. 15.28(a) (called Schmitt trigger). When the level of V_{in} exceeds $(V_A + V_{BE})$, the output voltage V_{out} goes high with a snap action as shown in Fig. 15.28(b). Snapping action can be improved with a positive feedback (not shown in Fig. 15.28(a)) from the collector of T_2 to the base of T_1. Hysteresis can be achieved by using high resistance for R_1 compared to that of R_2. Hysteresis is also influenced by the positive feedback resistance and R_4. Similar level detector can also be set up using OPAMP. The operation of the circuit of Fig. 15.28(a) is explained below.

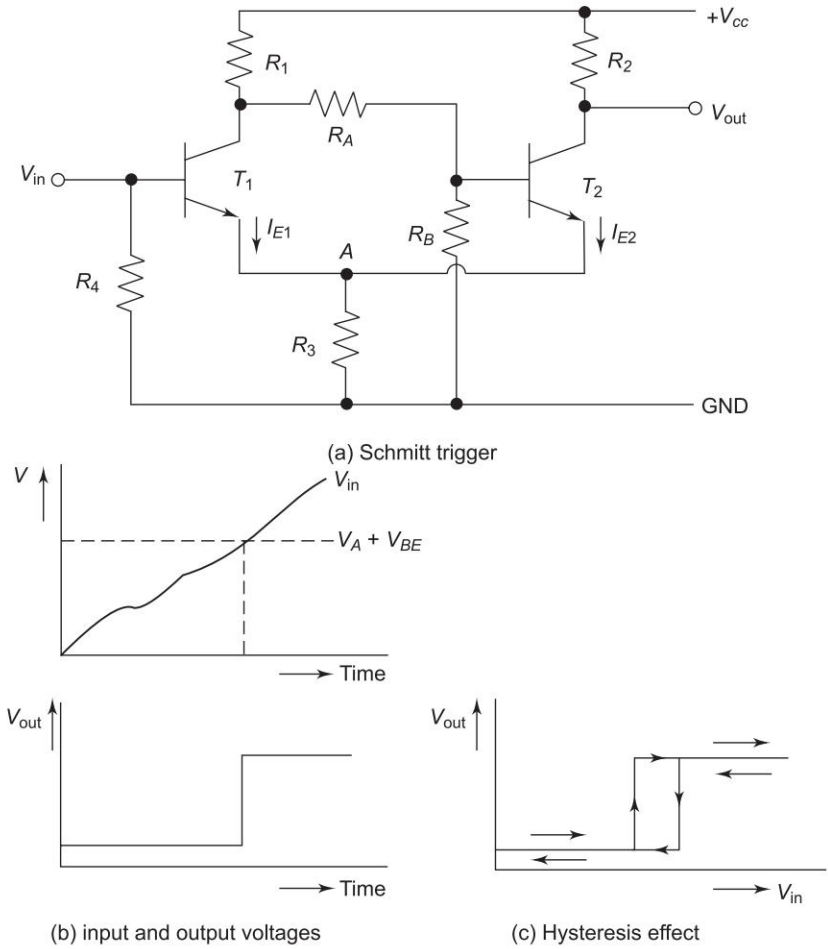

Fig. 15.28

Let the voltage V_{in} be sufficiently low so that the transistor T_1 is cut-off. The voltage at the base of T_2 (available through the potential divider consisting of R_1, R_A and R_B) will make the transistor T_2 conduct. The output voltage V_{out} will be at low level corresponding to this and the voltage at A will be $R_3 I_{E2}$. When V_{in} increases and passes through $R_3 I_{E2} + V_r$, where V_r is the cut-in voltage of the transistor (~0.5 V), the transistor T_1 goes low, which switches off T_2 and V_{out} goes high. Now the voltage at A will be $R_3 I_{E1}$. Any further increase in V_{in} will not affect V_{out}. If V_{in} is decreased, reverse transition occurs when it passes through $R_3 I_{E1} + V_r$. The transition points are not same in the two directions, which means the circuit exhibits hysteresis as illustrated in Fig. 15.18(c).

The value of V_{out} is easily adjusted by means of a potential divider at the output stage.

Time Delay Units

Intentional time delay could be introduced by several methods, the *RC* circuit shown in Fig. 15.29(a) being the most common. If

$$v_i = V_o u(t) \quad \text{and} \quad v_o = V_o(1 - e^{-t/\tau})\, u(t);\ \tau = RC$$

For a given pickup, the operating time can be adjusted by means of variable series resistance *R* as shown in Fig. 15.29(b). It is shown in Fig. 15.29(c) that, for a given V_{pu} and *R*, the operating time is inversely proportional to V_o which is

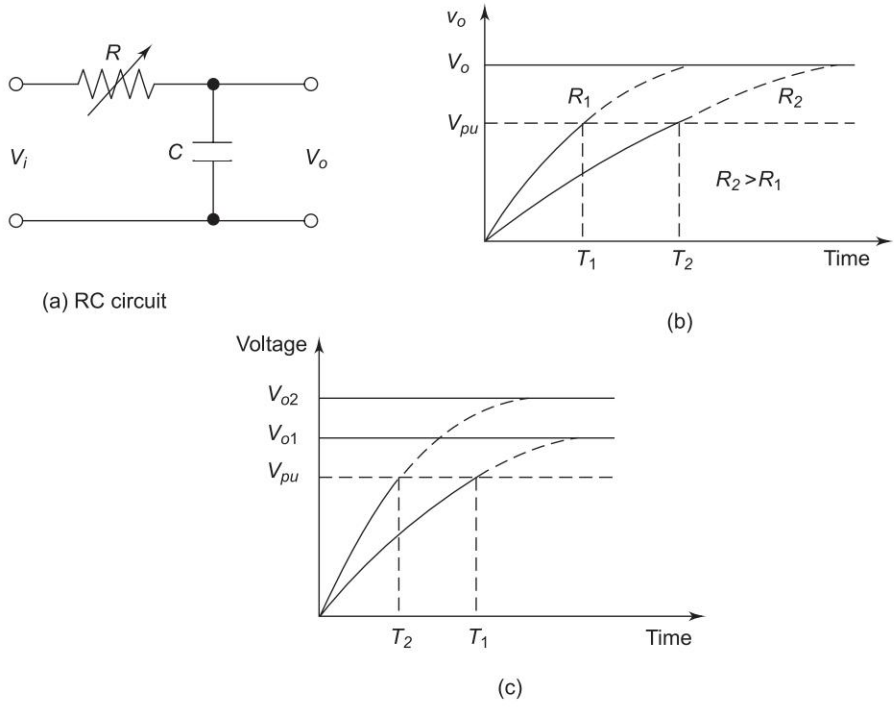

Fig. 15.29 RC time delay circuit

a replica of system current. Thus the level detector (Fig. 15.28) and time delay unit combination comprises an inverse-time overcurrent relay.

The inverse characteristics of IDMLT type relay is usually achieved not by the above type of integrating circuit, but by OP-AMP integrator.

Comparators

These form the heart of a solid-state relay and compare the amplitude or phase of two sinusoidal signals (of same frequency, i.e., power frequency). Accordingly these are classified as

- Amplitude comparators
- Phase comparators

Amplitude Comparators

Integrating comparator: Two sinusoidal quantities S_1 and S_2 to be compared in magnitude are rectified by bridge rectifiers as $|S_1|$ and $|S_2|$. Their difference $|S_1|-|S_2|$ is obtained by connecting the two rectifier bridges in antiparallel as shown in Fig. 15.30. The difference $|S_1|-|S_2|$ is then averaged to apply to a polarity detector which produces an output if $|S_1|>|S_2|$. S_1 and S_2 could be two currents or voltages. Where a voltage and a current area to be compared (as in an impedance relay), one of these has to be converted to the form of the other.

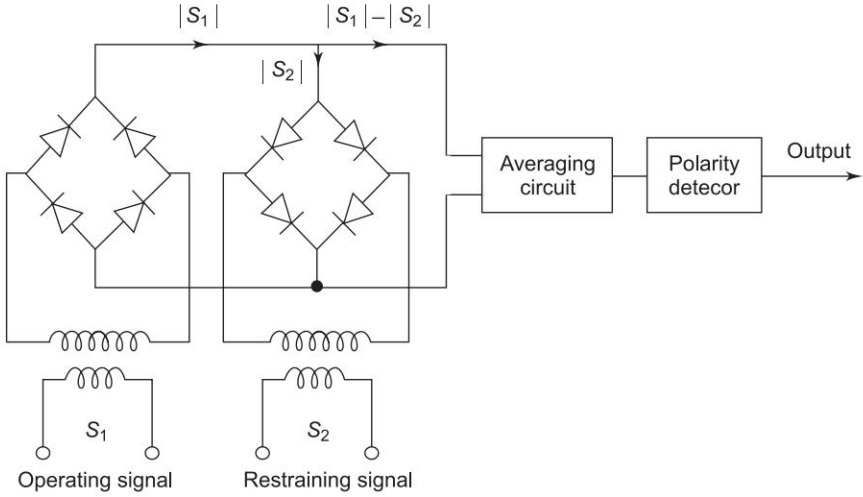

Fig. 15.30 Rectifier bridge comparator with static output circuit

Instantaneous comparator: Figure 15.31(a) shows the block diagram of averaging type instantaneous amplitude comparator. The restraining signal is rectified and smoothed to provide a level of restraint. The operating signal is

full-wave rectified and is compared with the restraint level. Output is produced when the peak of the operating signal exceeds the restraint level as shown in Fig. 15.31(b).

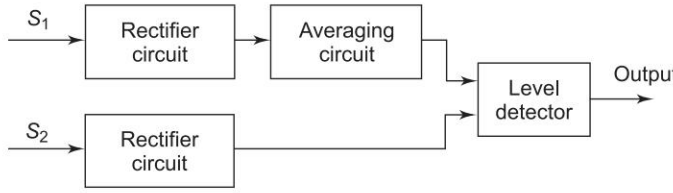

(a) Block diagram of averaging type instantaneous amplitude comparator

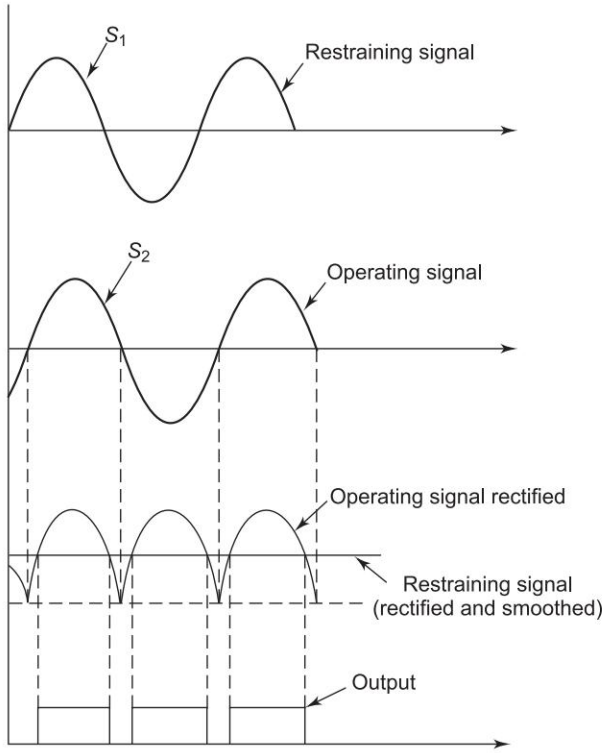

(b) Waveform for an instantaneous amplitude comparator

Fig. 15.31

Phase comparators: This type of comparator produces an output when the phase relationship between two inputs S_1 and S_2 satisfies the inequality

$$-\alpha_1 < \theta < \alpha_2$$

where θ is the angle by which S_1 lags S_2. If $\alpha_1 = \alpha_2 = 90°$, the comparator is known as cosine comparator and if $\alpha_1 = 0°$ and $\alpha_2 = 180°$, it is known as sine comparator.

There are two types of phase comparators:

- Coincidence type; and
- Vector-product type.
- There is quite a variety of circuits employed for either of these. Two types of coincidence phase comparators will be discussed here. Vector-product type are not generally employed and will not be discussed.

Phase splitting comparator: The two signals (sinusoidal) S_1 and S_2, whose phase is to be compared, are each shifted in phase by $\pm 45°$ to create $S_1 \angle 45°$, $S_1 \angle -45°$ and $S_2 \angle 45°$, $S_2 \angle -45°$ as shown in Fig. 15.32(a) and (b). The four components are fed into an AND circuit as shown in the block diagram of Fig. 15.33, which produces an output only when all the four signals are simultaneously positive. It can be seen from Fig. 15.32(b) and (c) that it is only possible if $-90° < \theta < 90°$.

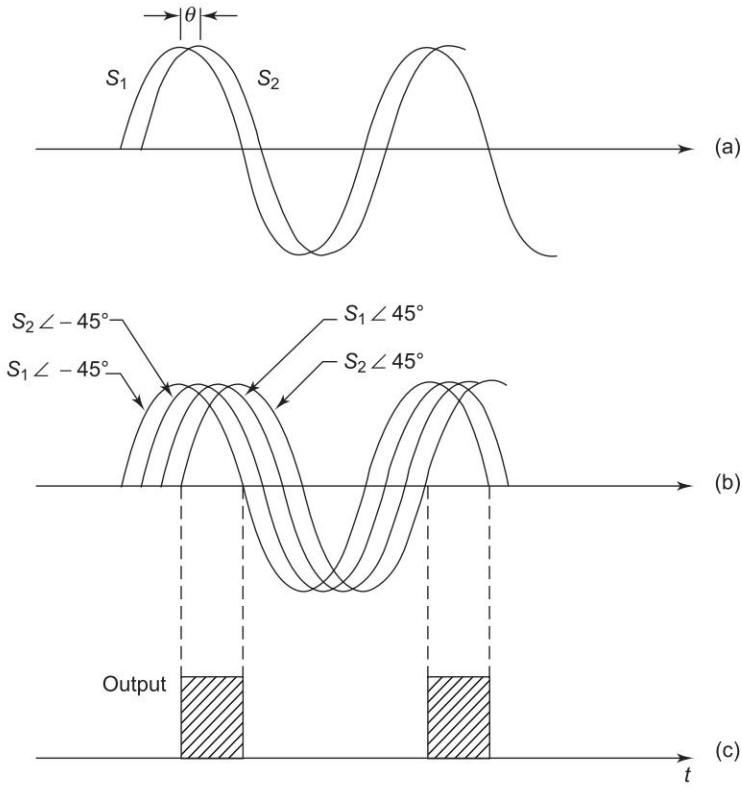

Fig. 15.32 Phase splitting technique

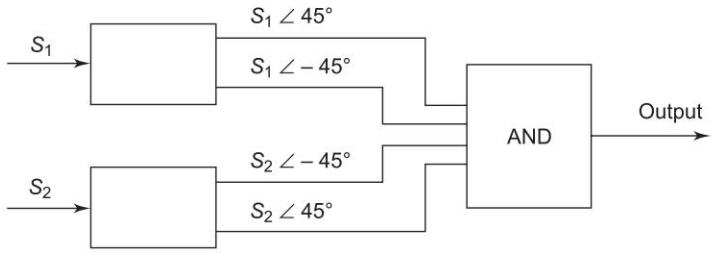

Fig. 15.33

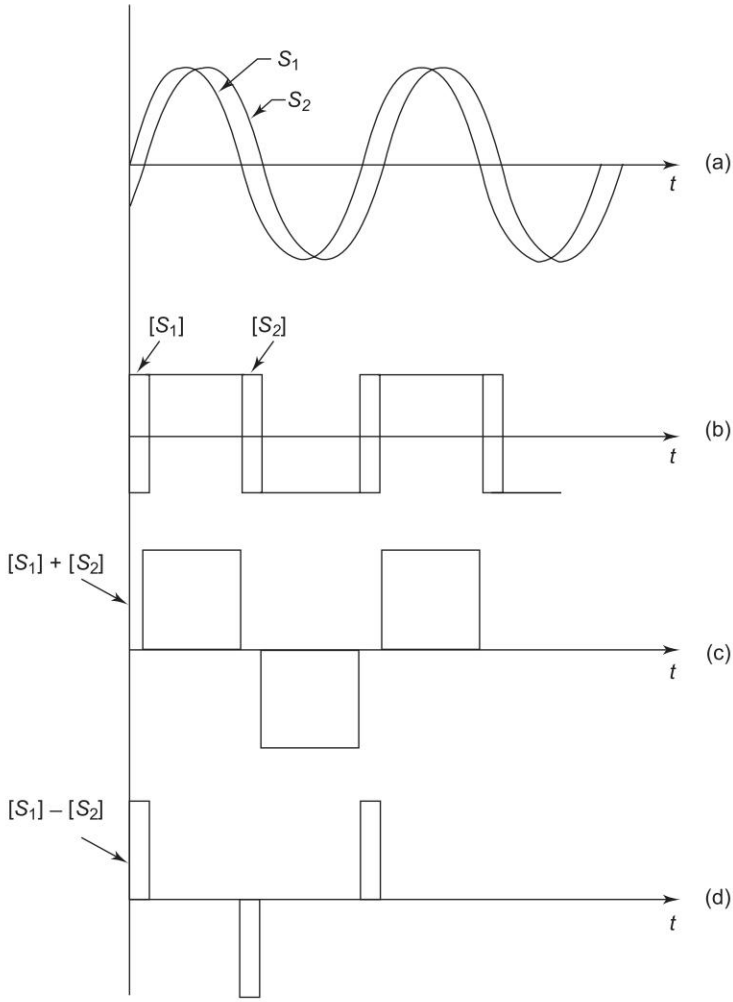

Fig. 15.34 Phase comparison by pulsed signals

Phase comparator based on pulsed signals: The signals S_1 and S_2 are converted to in-phase rectangular pulses before being fed to phase comparator as shown in Fig. 15.34(a) and (b). The pulsed signals $[S_1]$ and $[S_2]$ [Fig. 15.34(b)] are added and subtracted to produce $[S_1] + [S_2]$ and $[S_1] - [S_2]$ as in Fig. 15.34(c) and (d). These signals are then rectified, averaged and compared. It is easily seen from these figures that

$$\left|[S_1]+[S_2]\right| > \left|[S_1]-[S_2]\right|;\ -90° < \theta < 90°$$

and

$$\left|[S_1]+[S_2]\right| < \left|[S_1]-[S_2]\right|;\ 90° < \theta < -90°$$

A Directional Relay

A directional relay can be implemented by any of the methods described above. Another similar method along with its circuit illustration is described below.

Positive and Negative Coincidence Circuit

This circuit utilizes discrete devices to illustrate the underlying concepts. S_1 and S_2 represent sinusoidal wave forms whose "positive" and "negative" coincidence periods are to be measured.

The circuit shown in Fig. 13.35(a) consisting of transistor pairs T_1, T_2 and T_5, T_6 operates like AND gates, i.e. the output (V_o or V_o') shall be positive when

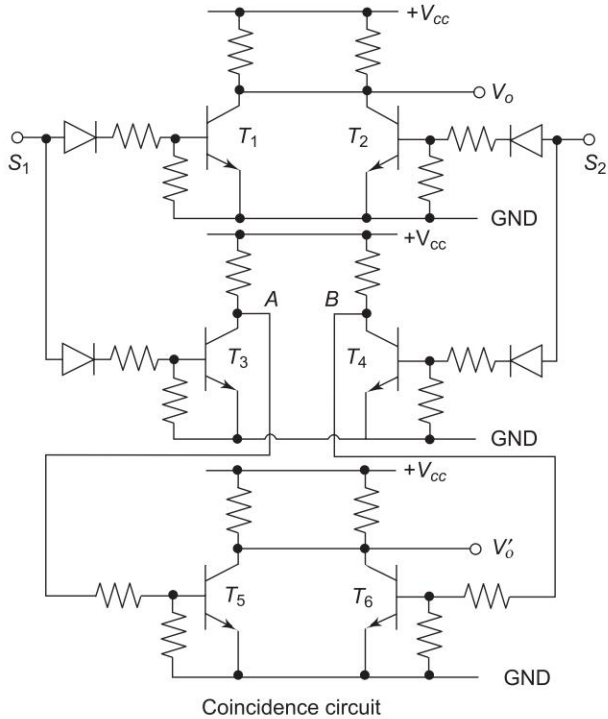

Coincidence circuit

Fig. 15.35 (a)

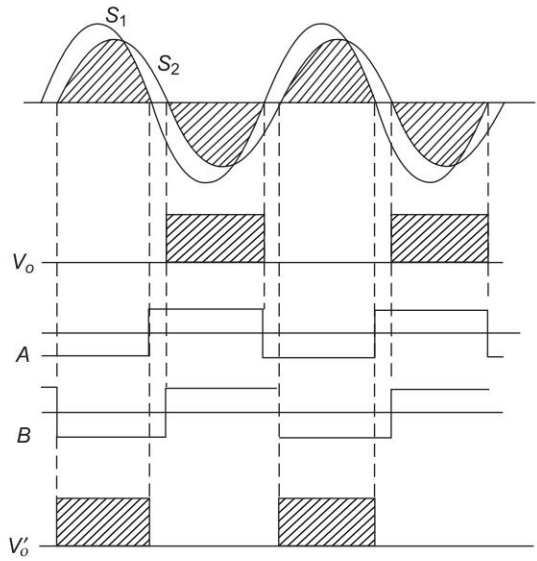

V_o = Measure negative coincidence
V_o' = Measure positive coincidence

Fig. 15.35 (b)

signals (S_1, S_2) are both simultaneously negative (or (A, B) are both positive) or when signals (S_1, S_2) are both simultaneously positive, or (A, B) are both negative.

Both V_o and V_o' are utilized to charge a linear integrator to produce a voltage across the integrator, which will be proportional to $(180^\circ - \theta)$, where θ is the desired limiting phase angle to be detected.

The circuit is applicable whenever a selected phase angle, or a range of phase angles, needs to be detected between any two sinusoidal signals, such as directional, mho, or quadrilateral phase comparator.

15.7 RELAY CONNECTIONS

Overcurrent Relays

The fault current is high for *phase faults* involving two or all the three lines. These faults are:

- Three-phase (3L) fault
- LL fault
- LLG fault

In faults involving one line and ground (LG) faults, the fault current is quite low because of the inclusion of zero sequence impedance in the connection of sequence networks. Sometimes this current may even be less than the load current.

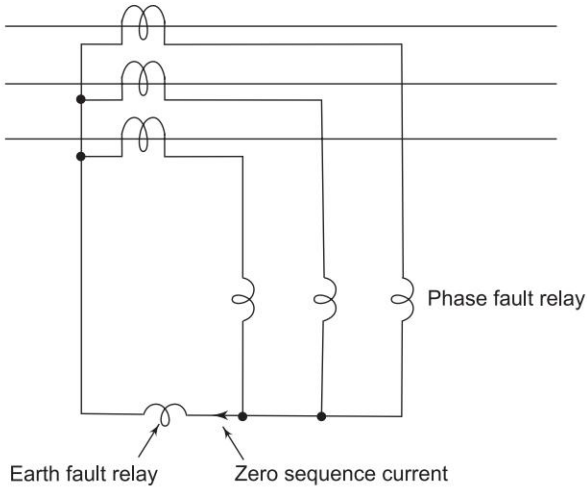

Fig. 15.36 Overcurrent relay connections

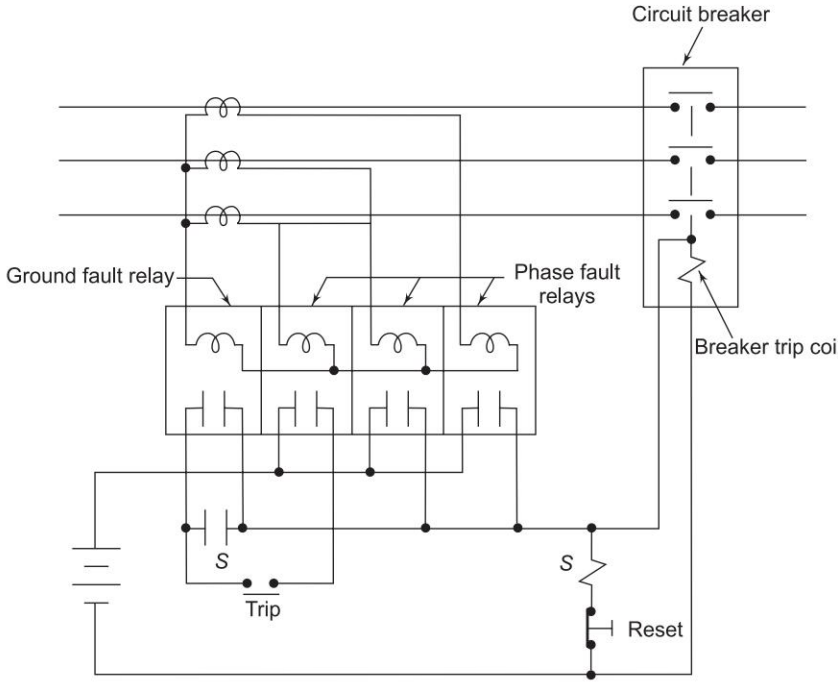

Fig. 15.37 Overcurrent relays and breaker connections

For the reasons enunciated above, separate sets of overcurrent relays are needed for detection of phase faults and ground faults. The CT connections for the two types of overcurrent relays are shown in Fig. 15.36. Since in a phase fault, fault current will flow in at least two lines, one of the phase fault relays could be omitted.

The connection of phase fault and ground fault overcurrent relays and the breaker tripping arrangement is shown in Fig. 15.37. It hardly requires any explanation. *S* is a seal-in relay. After the contacts of one of the overcurrent relays close, the seal-in relay gets energized closing contacts *S*, thereby shorting the contacts of the main relay, which then are relieved of carrying the trip coil current. This arrangement protects the contacts of the main relay.

Directional Relay

Power Relay

This relay senses the direction of real power flow. The relay connections and phasor diagram are shown in Fig. 15.38, wherein the relay is fed with voltage $V = V_{ab} + \frac{1}{2}V_{bc}$ and current I_a, which two would be in phase for unity power factor in the circuit. The relay is set to develop maximum actuating quantity (say torque) when V and I_a are in phase.

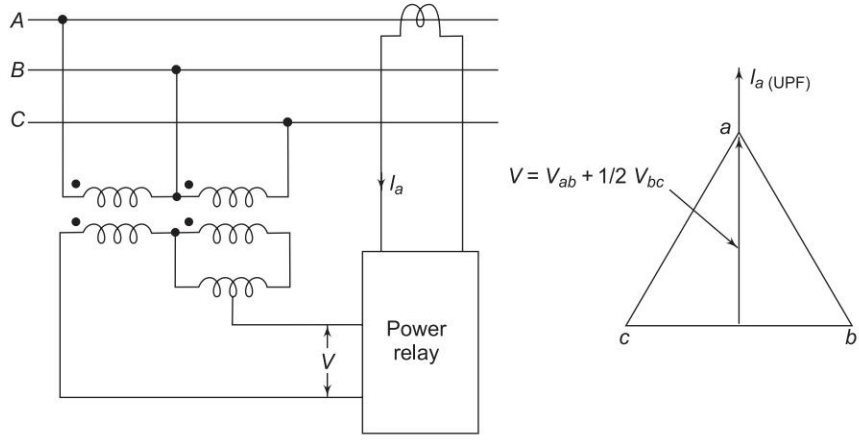

Fig. 15.38 Power relay-connection and phasor diagram

Directional Relays for Short Circuit Protection

Short circuit involves currents that lag the UPF position usually by large angles. It is desirable that directional relays for short circuit protection be arranged to develop maximum torque (or actuating quantity) under such lagging current condition.

Three conventional current and voltage combinations for short circuit directional relays are illustrated in Fig. 15.39. For the commonly used 30°-connection of Fig. 15.30(b), the voltage and current pairs are: (V_{ac}, I_a), (V_{ba}, I_b) and (V_{cb}, I_c).

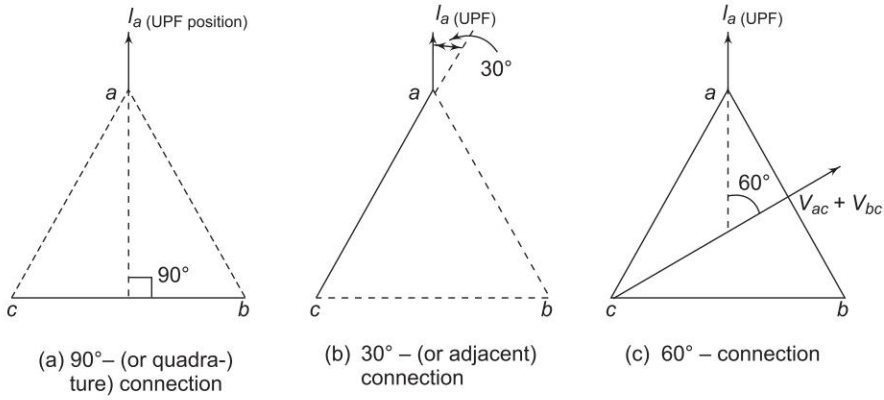

(a) 90°– (or quadra-) ture) connection

(b) 30° – (or adjacent) connection

(c) 60° – connection

Fig. 15.39 Current-voltage combination for SC protection

Observe that the voltages fed to the relays are line voltages, as these can be easily obtained by two open-delta connected VTs (see Fig. 15.5).

Also during the short circuit the phase of both line current and line voltage will shift (more in current than in voltage) and the angle between these must be determined by short circuit study for relay setting.

When directional relays are used in conjunction with other relays (may be overcurrent or impedance relays), the contacts of the combination must be in series with the trip coil of the CB for an AND operation, i.e. both relays must operate for the CB to trip.

Impedance Relays

Again because of the largely different impedances seen by the relays during phase and ground faults, separate sets of relays must be used for these faults.

For phase relays delta currents and voltages used are:

Relay	*Current*	*Voltage*
ab	$I_a - I_b$	$V_a - V_b = V_{ab}$
bc	$I_b - I_c$	$V_b - V_c = V_{bc}$
ca	$I_c - I_a$	$V_c - V_a = V_{ca}$

The ground fault relays use line currents and corresponding phase voltages ((I_a, V_a), (I_b, V_b) and (I_c, V_c)). The CT and VT connections of phase and ground relays are shown in Figs 15.40 (a) and (b).

Impedance Seen (Phase Relays)

For a line *XY* as shown in Fig. 15.41, with sequence impedances $Z_1 = Z_2$ and Z_0, consider an LL fault on phases *b* and *c* at point *F* located at fractional

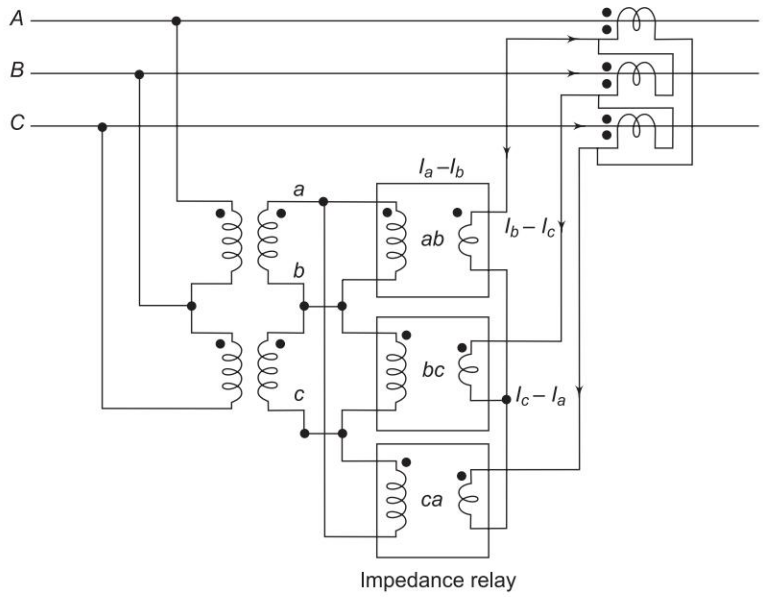

(a) Phase relay connections

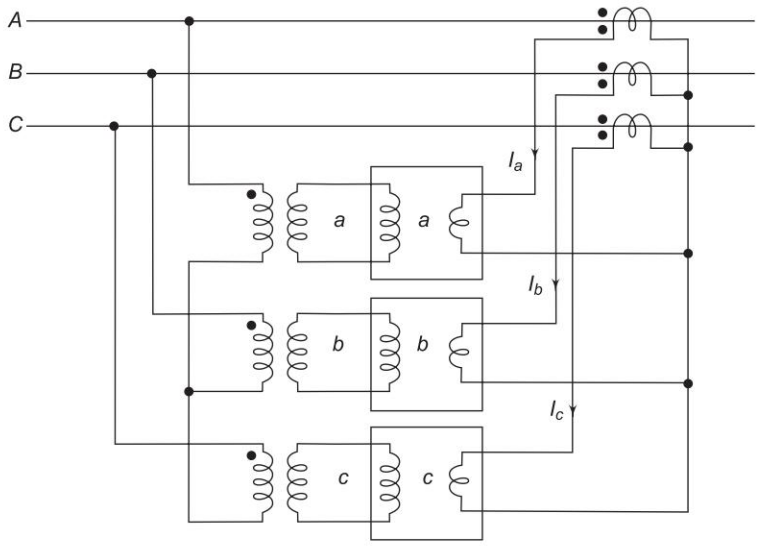

(b) Ground relay connections

Fig. 15.40 Impedance relay connections

distance k $(0 < k < 1)$ along the line. The positive and negative sequence voltages at the relay location are

$$V_{R1} = V_{F1} + k Z_1 I_1 \tag{15.39}$$

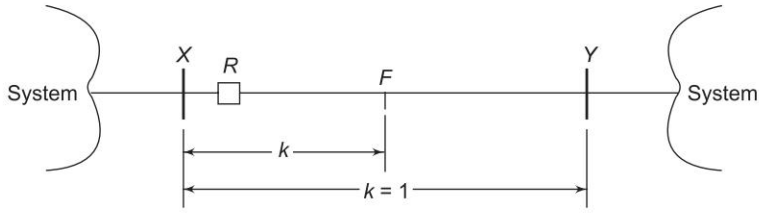

Fig. 15.41

$$V_{R2} = V_{F2} + k Z_2 I_2 \tag{15.40}$$

where V_{F1} and V_{F2} are positive and negative sequence voltages at F under fault. For an LL fault $V_{F1} = V_{F2}$, also for a line $Z_1 = Z_2$. Subtracting Eq. (15.40) from Eq. (15.39),

$$V_{R1} - V_{R2} = k(I_1 - I_2)Z_1$$

or

$$k Z_1 = \frac{V_{R1} - V_{R2}}{I_1 - I_2} \tag{15.41}$$

Now

$$V_{bR} = \alpha^2 V_{R1} + \alpha V_{R2} + V_{R0}$$

and

$$V_{cR} = \alpha V_{R1} + \alpha^2 V_{R2} + V_{R0}$$

$$V_{bR} - V_{cR} = (V_{R1} - V_{R2})(\alpha^2 - \alpha) \tag{15.42}$$

Similarly

$$I_b - I_c = (I_1 - I_2)(\alpha^2 - \alpha) \tag{15.43}$$

From Eqs (15.42) and (15.43), the impedance seen by the relay is

$$Z_R = \frac{V_{bR} - V_{cR}}{I_b - I_c} = \frac{V_{R1} - V_{R2}}{I_1 - I_2} = k Z_1 \tag{15.44}$$

Thus the impedance relay sees an impedance equal to the positive sequence impedance from the relay location to the fault, i.e. it senses *distance* to the fault.

Impedance Seen (Ground Relays)

For an LG fault on phase at F in line XY of Fig. 15.41

$$V_{aR} = V_1 + V_2 + V_0$$

$$= \underbrace{(V_{F1} + V_{F2} + V_{F0})}_{V_{aF} = 0} + k(Z_1 I_1 + Z_2 I_2 + Z_0 I_0)$$

or

$$V_{aR} = k(Z_1 I_1 + Z_2 I_2 + Z_0 I_0 + Z_1 I_0 - Z_1 I_0);\ Z_1 = Z_2$$

$$V_{aR} = kZ_1 I_a + k(Z_0 - Z_1)I_0$$

$$Z_{aR} = kZ_1 + k(Z_0 - Z_1)\frac{I_0}{I_a} \qquad (15.45)$$

It is observed that the impedance seen by the relay is a complicated function of k, but it can be shown by a numerical example that it is nearly proportional to distance. Observe that if $Z_1 = Z_0$, $Z_{aR} = kZ_1$, i.e. proportional to distance.

Assume $Z_0 = \beta Z_1$. From Eq. (15.45)

$$V_{aR} = kZ_1 I_a + kZ_1 (\beta - 1)I_0$$

or

$$kZ_1 = \frac{V_{aR}}{I_a + (\beta - 1)I_0} \qquad (15.46)$$

Equation 15.46 implies that the ground relay would see impedance proportional to distance provided it is fed with current sample of $I_a + (\beta - 1)\left(\frac{I_a + I_b + I_c}{3}\right)$. This can be accomplished by means of a suitably connected three-winding, three-phase CT, apart from the line CT. The reader is encouraged to draw the connection diagram.

In practice, however, only line CTs are used and the error is absorbed in relay setting.

Three-zone Impedance/Mho Relays

For transmission line protection, a single-phase distance relay of impedance/mho type consists of a single-phase directional unit and three high-speed impedance/mho relay units. This is necessary for providing back up protection as shall be explained in Sec. 15.8. The operating characteristics of three-zone distance relays of impedance/mho type are shown in Fig. 15.42(a) and (b). For impedance lying in zone 1, the operation is instantaneous (time T_1); for impedance in zones 2 and 3, there is delayed operation, with delay time of T_2 and T_3 ($T_3 > T_2$) respectively.

The control circuit for a 3-zone impedance relay is drawn in Fig. 15.43 which is self-explanatory. In this figure:

Z_1, Z_2, Z_3 = zones 1, 2, 3, distance relays
D = directional relay
T_2, T_3 = timers, zones 2, 3
S = seal-in relay
B = breaker trip relay

15.8 PROTECTION OF TRANSMISSION LINES

The power network comprising transmission lines and transformers transports electric energy from the generating stations to the load centres. This network

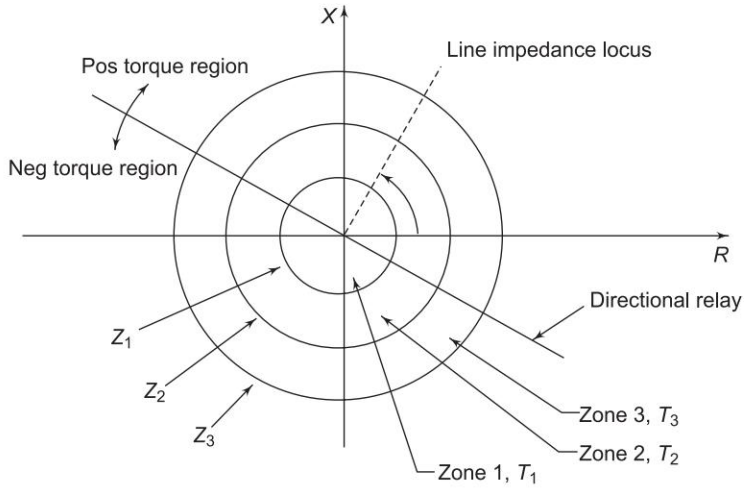

(a) 3-zone impedance relay

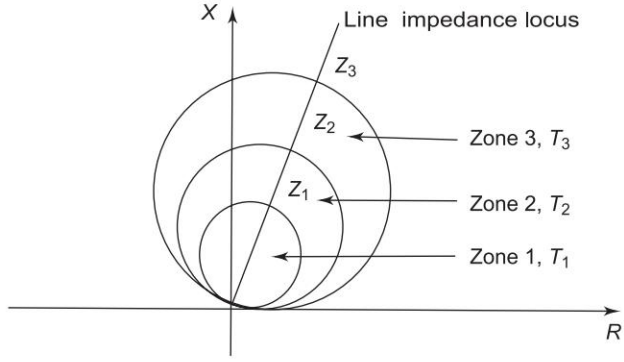

(b) 3-zone mho relay (no directional element necessary)

Fig. 15.42

extends over vast geographical areas and involves several voltage levels. The transmission lines span long distances and, being exposed to the elements—lightning, wind, snow, salt spray etc. are most prone to faults. These may also be subjected to man-made faults caused by aeroplanes, automobiles and sabotage. Therefore, compared to any other power system element, the protective relays of transmission lines are called upon to operate much more frequently. HV and EHV transmission lines, which transport large chunks of power, must be protected elaborately and with ample redundancy. Medium voltage subtransmission/distribution lines may be protected by simple and less expensive schemes—overcurrent protection. Low voltage distribution circuits are generally protected by fuses and autoreclosers. These will not be discussed here.

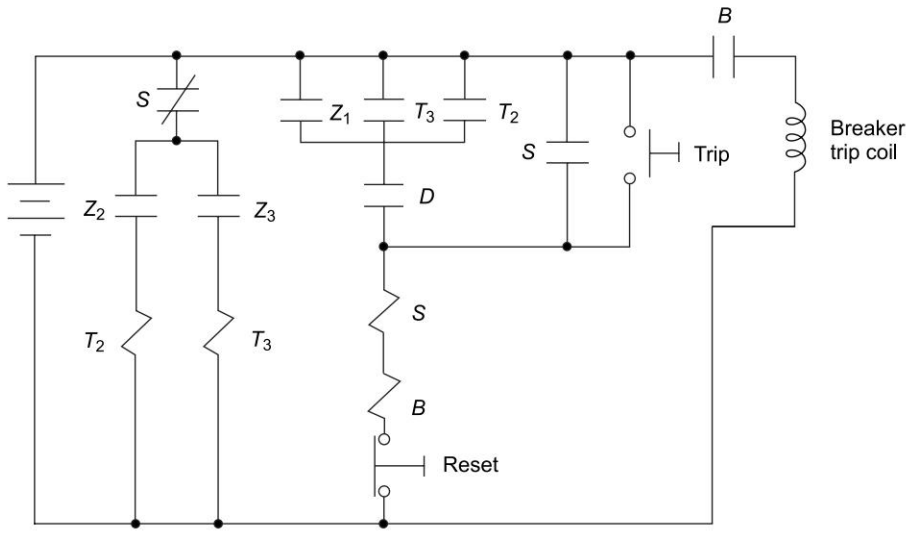

Z_1, Z_2, Z_3 = zones 1, 2, 3, distance relays
D = directional relay
T_2, T_3 = timers, zones 2, 3
S = seal-in relay
B = breaker trip relay

Fig. 15.43 Control circuit of three-zone impedance relay

Before discussing the protective schemes for transmission lines, it may be recalled here that an important objective of the scheme is to keep intact as much of the system as possible when clearing faults.

Overcurrent Protection of Subtransmission/Distribution Lines

Overcurrent relaying is the simplest and cheapest, yet most difficult to apply. In fact there is no way to coordinate overcurrent relays in a complex network. Further, as the system grows, the fault level rises demanding readjustment, or even replacement, of these relays.

Coordination of overcurrent relays is achieved by adjustment of pickup and time inverseness of their characteristics. To apply overcurrent relays, one must select the CT ratio for each relay and adjust for each relay its

- pickup current (plug setting (PS)), and
- time multiplier setting (TMS).

CT used for each relay must be so selected that under full-load conditions the relay carries less than its rated continuous current (5 A or 1 A). This is assured if the relay current for maximum fault current is close to the rated current.

As already discussed, a different set of relays will be employed for phase faults and for ground faults. Relay coordination will be discussed with reference to phase faults only.

Figure 15.44(a) shows a radial distribution system having three line sections with loads at each bus. Proper protection of this system requires that for a fault on any section only the relay nearest to its generator side end must act to open its breaker, and not the relay further towards the generator side. For example, for a fault on line section 2–3, the breaker B_{23} should open and not B_{12}, i.e. the relay R_{23} should operate faster than the relay R_{12}, even though both will be carrying the same current. Further, the relay R_{12} must provide backup protection in the event the relay R_{23} or its associated breaker fails to operate. As a result of proper operation of the relaying system, line sections 2–3 and 3–4 get disconnected interrupting loads 3 and 4, while loads 1 and 2 continue to be fed.

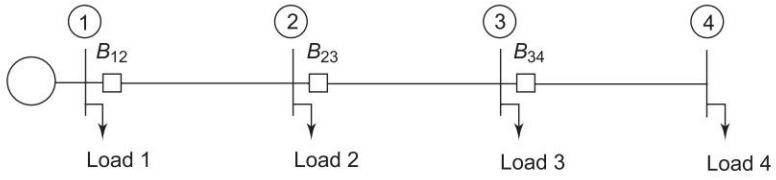

(a) Radial distribution system (fed from one end)

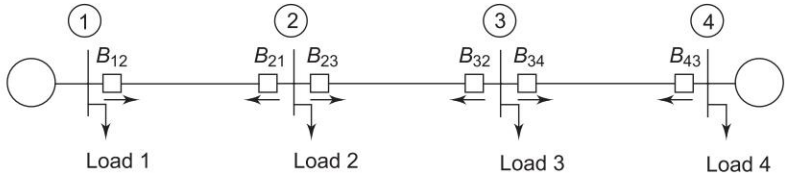

(b) Distribution system fed from both ends

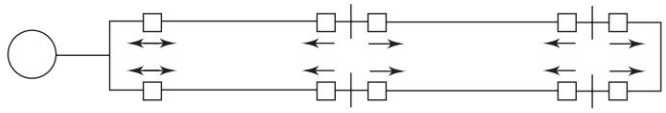

(c) Singly fed loop

Fig. 15.44

The above relaying philosophy can be extended to the system of Fig. 15.44(b) fed from both ends. For disconnecting only the faulted line section, relays at both line ends must operate to open their breakers. All the relays at the left ends of the line sections (B_{34}, B_{23}, B_{12}) must be coordinated, so that the relay nearest the fault operates faster than the relay next to it, which provides backup protection. Similarly the relays on the right ends of the lines (B_{21}, B_{32}, B_{43}) must be coordinated. For example, for fault on the line section 2–3, the relays R_{23} and R_{32} must operate to disconnect the faulted line, while the relays R_{12} and R_{43} provide backup protection for R_{23} and R_{32} respectively.

In relays other than those near the generator ends (R_{12} and R_{43}), the current during fault can flow in either direction depending on the location of the fault; but the relay must operate only for a fault on the line protected by it. To achieve this overcurrent relays in a doubly fed system must be used in conjunction with directional relays. The directional relays at each end of a line section must be directed inwards (Fig. 15.44(b)) to permit operation of the corresponding relays only for a fault on the protected line section. It may also be observed here that relays closest to generator ends (R_{12} and R_{43}) need not be directional as current in these can flow only in one direction by the very nature of the system.

Figure 15.34(c) shows a singly fed distribution loop with direction of directional relays marked by arrow. Double-headed arrow corresponds to a nondirectional overcurrent relay. A little reflection will show that this system is really no different from a doubly fed radial system (Fig. 15.44(b)). Starting with the relay at the generator end, relays are coordinated in two sets—clockwise and anticlockwise.

Pickup Adjustment

The pickup of a relay must be adjusted such that it will provide backup protection for short circuits on the adjoining line (further away from the source end for the coordinated relays). Since the fault currents reduce as the fault moves away from the source end, a relay that picks up for a fault on the adjoining line section, will pick up for fault on its own line. The relay pickup is, therefore, adjusted so that it picks up for minimum fault current. Minimum fault current occurs when

- the fault is farthest away from the line being back protected;
- the fault is a line-to-line fault (for setting phase relays)

$$(I^f(\text{LL}) = (\sqrt{3}/2)I^f(3-ph^*));$$

---

* Assume $Z_1 = Z_2$; this is practically true at a subtransmission/distribution level

For a 3-phase fault

$$I^f(\text{3-ph}) = \frac{E_a}{Z_1}$$

For LL fault on phases *b* and *c*

$$I_b = -I_c = \frac{-j\sqrt{3}E_a}{2Z_1}$$

or

$$I^f(\text{LL}) = \frac{\sqrt{3}E_a}{2Z_1}$$

Hence

$$I^f(\text{LL}) = (\sqrt{3}/2)I^f(\text{3-ph})$$

- generation is minimum (for a subtransmission/distribution system; it implies that minimum transformer capacity is feeding the line, it being validly assumed that the transformers are fed from an infinite system).

Figure 15.45 shows the location and the nature of the fault for pickup adjustment of the relay R_{12} which provides backup protection for R_{23}. To take care of errors in fault calculations, in CTs and in relay characteristics, the relay pickup must be so adjusted that the minimum fault current is at least 3 times relay pickup.

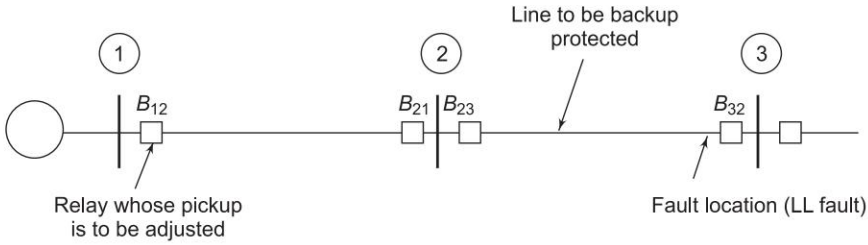

Fig. 15.45

Time Multiplier Setting (TMS)

With reference to Fig. 15.9 it can be easily seen that if two relays are time coordinated at a certain current (certain PSM), these always remain coordinated properly at lower values of current. Therefore, for time coordination, the fault current through the primary relay must be the maximum possible when its time is coordinated with the corresponding backup relay. For maximum possible fault current,

- the fault should be nearest the primary relay; and
- it should be a 3-phase fault (for phase relay).

These conditions are illustrated in Fig. 15.46. Under these conditions the operating times of relays R_{12} and R_{23} should be related as

$$T_{12} = T_{23} + B_{23} + O_{12} + F \qquad (15.47)$$

where T_{12} = operating time of relay R_{12}

T_{23} = operating time of relay R_{23}

B_{23} = short circuit interrupting time of breaker B_{23}

O_{12} = overtravel* time of relay R_{12}

F = factor of safety

* An electromechanical relay after it picks up continues to travel for some time even though the current through it reduces below the pickup value.

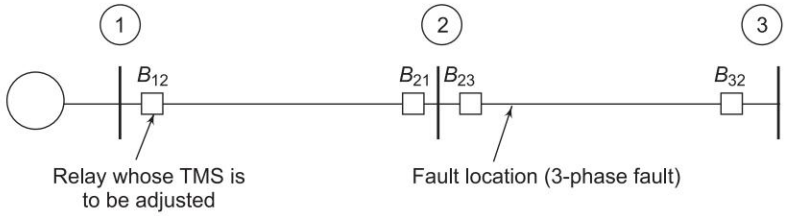

Fig. 15.46

Generally

$$\Delta T = T_{12} - T_{23} = B_{23} + O_{12} + F = 0.3 \text{ s} \qquad (15.48)$$

Under the assumption of maximum generation, the time coordination of relays is illustrated in Fig. 15.47. As we move further away from any particular relay

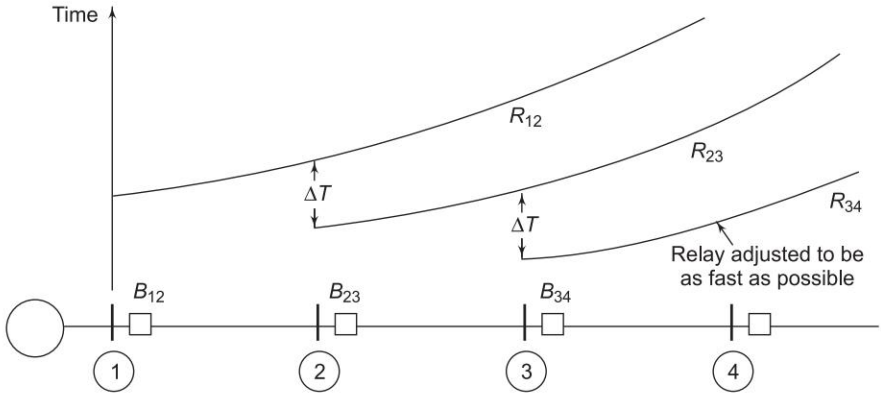

Fig. 15.47 Time coordination of overcurrent relays

location, the fault current decreases and the relay operating time increases. It is this time inverseness characteristic of the overcurrent relay which permits time coordination of relays.

Certain disadvantages of overcurrent relays are mentioned below:

- In a general network, overcurrent relay coordination, if at all possible, can be carried out by trial and error. For a multiply fed loop, or where loops have a common segment, it is not possible to coordinate overcurrent relays to be selective.
- As with load growth the system is fed with larger generation, or if the system configuration is modified, the system fault levels at relay locations modify (rise). The relays would then require resetting, or even replacement.

- For faults nearer the source end, the fault current is large, and so is the operating time, e.g. in Fig. 15.47 the fault current is largest for fault on the line section 12 and the relay R_{12} requires the longest time to operate. This is a serious drawback when a number of relays have to be time coordinated. Such long operating times cannot be tolerated in HV transmission lines.

Under the above circumstances, overcurrent relays cannot be applied. Instead, distance relays would be employed, which are insensitive to load growth and configuration changes.

Example 15.4 An 11 kV radial distribution system is shown in Fig. 15.48. Under emergency conditions the system has to be operated with one transformer. The high-voltage side of the system is assumed to be infinite bus. Shown in the figure are the reactances of the lines and the transformers all referred to the 11 kV side. Resistance may be neglected. The system is to be protected by means of overcurrent relays against phase faults. Compute the CT ratios, plug settings and time-multiplier settings for all the relays.

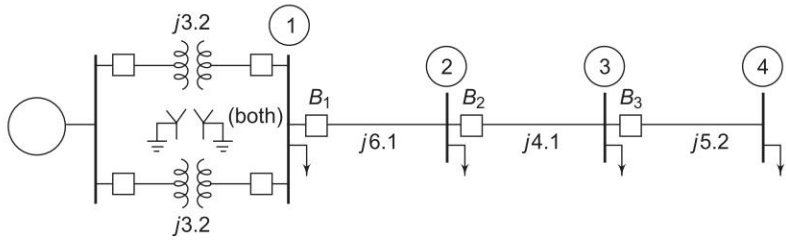

Fig. 15.48 Radial distribution system

Solution

Fault Calculations: For a fault on a bus, fault current is:

maximum with both transformers in and 3-phase fault;
minimum with one transformer in and LL fault.

For fault on bus 4

$$I^f(\max) = \frac{11 \times 1000/\sqrt{3}}{j3.2/2 + j6.1 + j4.1 + j5.2}$$

$$= 373.5 \text{ A}$$

$$I^f(\min) = \frac{\sqrt{3}}{2} \times 373.5$$

$$= 323.5 \text{ A}$$

Calculations can be made similarly for faults on other buses. Maximum and minimum fault currents are presented in Table 15.1.

Table 15.1*

Fault at bus	*1*	*2*	*3*	*4*
Max fault current	3969.3	824.8	538.2	373.5
Min fault current	1718.75	591.4	410.45	295.7

Relay setting

Relay R_3 : This relay must pickup for minimum fault current which from the table is 295.7 A. As already explained for reliable operation,

$$I_p' \text{ (on line side of CT)} = \frac{295.7}{3} = 98.64 \text{ A}$$

For a CT ratio of 100/5, relay must pick up at

$$I_p = \frac{98.6 \times 5}{100} = 4.9 \text{ A or } 5\text{A, i.e., PS} = 100\%$$

Since this is the last relay in the radial system, it must operate the fastest (it needs no coordination with any other relay). Hence its TMS = 0.05 (least possible).

Relay R_2 : This relay must provide backup protection to relay R_3, and therefore must pickup for minimum fault current conditions for R_3. It must have same CT ratio (100/5) and same PS (= 100%) as for R_3.

R_2 must time coordinate with R_3 for maximum fault current through R_3 which* from Table 15.1 is 538.2 A and for which

$$\text{PSM} = 538.2 \times \frac{5}{100} \times \frac{1}{5} = 5.38$$

Reading from Fig. 15.9 (overcurrent relay characteristics) for PSM = 5.38 and TMS = 0.05, the operating time of R_3 is 0.09 s. Under same conditions relay R_2 must operate in time

$$0.09 + 0.3 = 0.39 \text{ s}$$

Again reading from Fig. 15.9 for PSM = 5.38 and T_{op} = 0.39s, we get TMS = 0.22. Thus for relay R_2,

$$\text{CT ratio} = 100/5, \text{ PS} = 100\%, \text{ TMS} = 0.22$$

Relay R_1 : This relay must provide backup protection for minimum current through R_2 which from Table 15.1 is 410.45. Choosing a CT ratio of 150/5, the pickup current of relay R_1 should be

* Current through R_3 will be maximum for a 3-phase fault just to the right of it, which is equivalent to a 3-phase fault on bus 3.

$$\frac{1}{3} \times 410.45 \times \frac{5}{150} = 4.56 \text{ A or } 5 \text{ A, i.e., PS} = 100\%$$

To adjust the time-dial setting of R_1, consider the maximum current through R_2 which from Table 15.1 is 824.8 A for which

$$\text{PSM} = 824.8 \times \frac{5}{100} \times \frac{1}{5} = 8.25$$

From Fig. 15.9,

$$T_{op} \ (R_2 \text{ for max current}) = 0.3 \text{ s}$$

For same conditions

$$T_{op} \ (R_1) = 0.3 + 0.3 = 0.6 \text{ s}$$

Under these conditions (max current through R_2) current through R_1 in terms of multiplies of its pickup is

$$\text{PSM} = 824.8 \times \frac{5}{150} \times \frac{1}{5} = 8.25$$

Reading from Fig. 15.9 for $T_{op} = 0.6$ s and PSM = 0.25, the TMS of R_1 is 0.42. Thus for relay R_1

CT ratio = 150/5, PS = 100%, TMS = 0.42

In practice, the pickup setting of R_2 must be slightly above that of R_3, so that under heavy overload at bus 4 when relay R_3 current is near its pickup, R_2 has no chance of picking up owing to CT errors.

Protection of HV and EHV Lines by Distance Relaying

It has already been shown that in general networks prevailing at HV and EHV levels, overcurrent relays are impossible to coordinate and, therefore, cannot be employed. A relaying scheme, in a general network, must protect each line with full guarantee and must also back-protect adjoining lines, irrespective of how these lines are connected in the network. Distance relays, which operate by sensing impedance to fault or its suitable modification, can accomplish this because their operation does not depend upon the line current alone. The impedance to fault depends only upon distance to fault and the nature of fault, and is completely independent of how the faulted line is connected in the network. Also, as a consequence, the relay setting is insensitive to network modification and growth, a factor which is an additional handicap of overcurrent relays. In order that the line, which is general is fed from both ends, can be isolated, impedance relays must be employed at each end, and must be accompanied by directional relays which help the relay to recognize if the fault is on the protected line. Directional relays at each end of a line must be directed inwards. When mho relays are employed, no separate directional relays are needed as these are inherently directional (see Sec. 15.5). For achieving coordination between primary and backup protection, 3-zone distance relays

(Fig. 15.42) are employed. Further, because the impedance to fault as seen from the line end is entirely different for phase and ground faults, a separate set of distance relays must be employed for recognizing these faults.

Setting Impedance Relays

How to choose the impedance settings of the three zones will be explained with the help of the system of Fig. 15.49. The underlying basis of impedance setting being the same in either direction, it will be explained with reference to one direction only (left to right in Fig. 15.49).

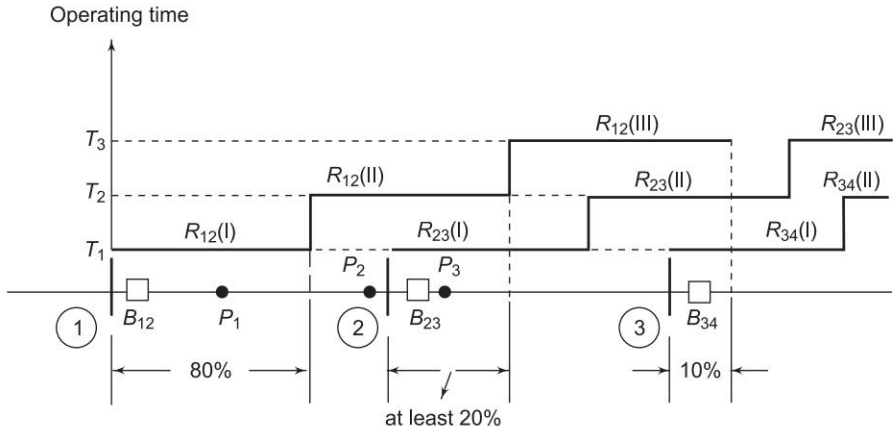

Fig. 15.49 Setting of impedance relays

Consider the setting of the first zone impedance of relay R_{12} in Fig. 15.49. If in an attempt to cover the whole line the impedance Z_1 is set to the full impedance of the line 1–2, this relay (R_{12}) will not be able to distinguish between faults at P_2 and P_3 on either side of the bus 2, as the impedance-to-fault for faults at either of these points is the same. To overcome this problem, the zone I (operating time T_1, instantaneous) impedance of the relay (R_{12}) is set to operate upto 80% of the line impedance ($Z_1 = 0.8\, Z_{12}$) as shown in the figure. The remaining 20% of the line is afforded protection by the zone II of R_{12} with operating time T_2 (i.e. with a time delay of $(T_2 - T_1)$). Thus in the direction left-to-right, only 80% of the line has fast (instantaneous) protection. The zone I of R_{23} is set similarly. To provide backup protection to R_{23}, the zone II of R_{12} must extend to at least 20% of the line 2–3 ($Z_2 = Z_{12} + 0.2\, Z_{23}$). In order not to clash with the zone II of R_{23}, the zone II of R_{12} cannot fully back protect the line 2–3. The remaining portion of the line 2–3 is back-protected by the zone III (operating time T_3 with time delay $(T_3 - T_1)$ of R_{12}, which must extend a little beyond the bus 3, say 10% ($Z_3 = Z_{12} + Z_{23} + 0.1Z_{34}$).

Relays in the other direction are set similarly. It must be observed here that only middle 60% of any line is fast protected while the remaining 40% is fast protected from one end, and slow (T_2) protected from the other end.

When multiple lines eminate from a bus as in Fig. 15.50(a), the zone II of R_{12} must extend to 20% of the shortest line and its zone III must extend just beyond the longest line (line 2–4 in Fig. 15.50(a)) in order to fully back-protect all the lines (lines 2–3 and 2–4). This is illustrated by the zone setting diagram of Fig. 15.50(b).

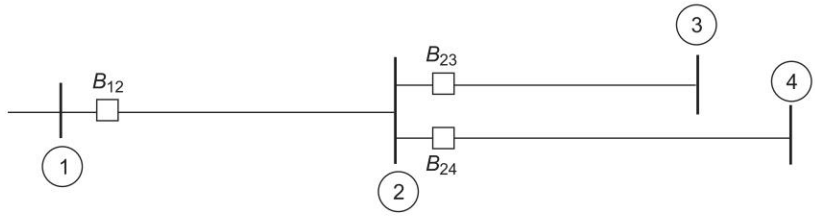

(a) Multiple lines outgoing from a bus

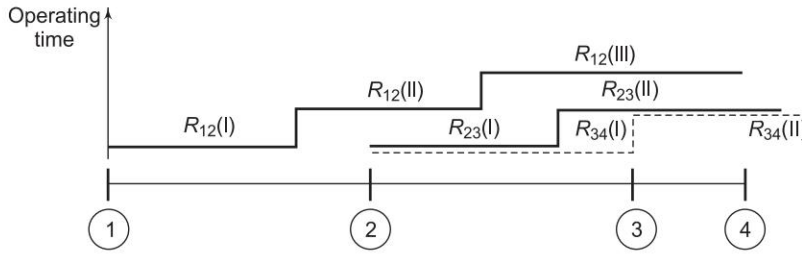

(b) Zone setting of relays

Fig. 15.50

Reactance and mho relays are set similarly. It must, however, be noted from Fig. 15.42(b) that the zone setting impedances relate to the *diameters* of zone circles.

Fault impedance (usually arc resistance) reduces the "reach" of distance relays (impedance seen is more than the impedance-to-fault), which can interfere with relay coordination particularly for short lines where fault resistance effect is most pronounced. Therefore, for short lines reactance type distance relays are recommended.

Effect of Power Swings

Under transient conditions when machines swing with respect to each other with their internal angles undergoing large changes, the impedances seen by distance relays protecting the interconnecting line can become much lower than under steady load conditions, so much so that the impedance seen may be lower than the relay setting, causing unwarranted line tripping. This is illustrated below for a two machine system.

Consider the impedance seen by the impedance relay R_{12} shown in Fig. 15.51. The relay current I_r is given by

$$I_r = \frac{E_1 - E_2}{Z_1 + Z_{12} + Z_2} = \frac{E_1 - E_2}{Z_T} \tag{15.49}$$

where $Z_T = Z_1 + Z_{12} + Z_2$.

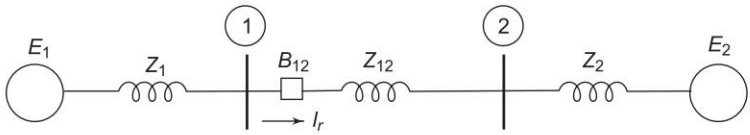

Fig. 15.51 A two-machine system

Phase voltage at the relay location is

$$V_r = E_1 - Z_1 I_r \tag{15.50}$$

Therefore, the impedance seen by the relay is

$$Z_r = \frac{V_r}{I_r} = \frac{(E_1 - Z_1 I_r) Z_T}{E_1 - E_2}$$

$$= \frac{E_1 Z_T}{E_1 - E_2} - Z_1$$

$$= \frac{Z_T}{1 - E_2 / E_1} - Z_1 \tag{15.51}$$

Now

$$\frac{E_2}{E_1} = \left|\frac{E_2}{E_1}\right| e^{-j\delta};\ \delta = \text{angle by which rotor of machine 1 is ahead of the rotor of machine 2}$$

$$\therefore \quad Z_r = \frac{Z_T}{1 - \left|\frac{E_2}{E_1}\right| e^{-j\delta}} - Z_1 \tag{15.52}$$

$|E_1|$ and $|E_2|$ are usually quite close to each other. Assuming $\left|\frac{E_2}{E_1}\right| = 1$ for simplicity,

$$Z_r = \left(\frac{e^{j\delta}}{e^{j\delta} - 1}\right) Z_T - Z_1$$

$$= \left(\frac{Z_T}{2} - Z_1\right) - j\frac{Z_T}{2} \cot \delta / 2 \tag{15.53}$$

The locus of the impedance seen by the relay as the angle increases is shown in the *RX*-diagram of Fig. 15.52. Shown in the figure are also the zone-1 impedance locus of the impedance, mho, and reactance relays for the same impedance setting. It is easily observed from this figure that as δ increases, Z_r-locus enters the tripping zone of the impedance relay at a particular δ causing it to trip. The Z_r-locus enters the tripping zone of the reactance relay upon crossing the *R*-axis at δ close to that of the impedance relay case. On the other hand the Z_r-locus enters the tripping zone of the mho relay at a much larger value of δ because the mho relay characteristic passes through origin and its radius is one half that of the impedance relay. It is, therefore, concluded that the mho relay is the least sensitive to power swings, and is hence preferred for long lines.

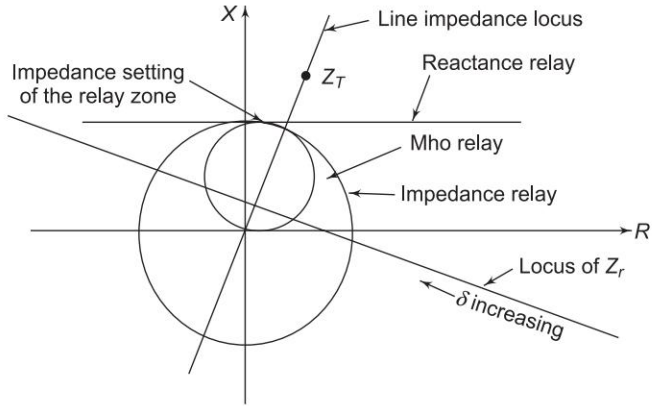

Fig. 15.52 Effect of power swing on impedance, mho and reactance relays

If the relay characteristic is shifted away from the origin so that its locus does not intersect the Z_r-locus, no unwarranted tripping at all will occur during power swings. Such a relay is called the *modified impedance relay* (see Fig. 15.15) and its characteristic in relation to the Z_r-locus is exhibited in Fig. 15.53.

Example 15.5 The portion of a 138 kV system is shown in Fig. 15.49. The lines 1–2, 2–3 and 3–4 are respectively 75, 75 and 106 km long. The positive sequence impedance of the transmission line is $0.05 + j0.4\ \Omega$ per km. The maximum load under emergency conditions carried by the line 1–2 is 60 MVA. Design a three-zone impedance relay system. You need only to determine the impedance setting on the secondary side of the relay R_{12}. Choose a suitable CT ratio and assume the CVT ratio as $138\ \text{kV}/67\sqrt{3}\ \text{V}$ connected between lines (relay is fed with delta currents and voltages).

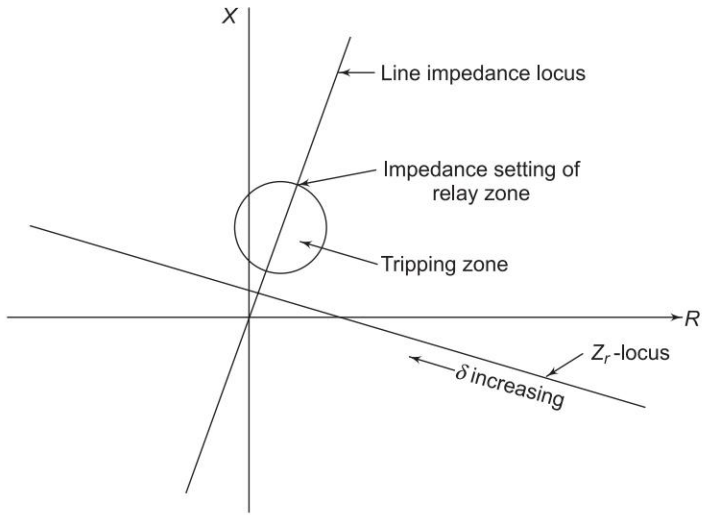

Fig. 15.53 Modified impedance relay unaffected by power swings

Solution

The positive sequence impedances of the three lines are

$$\text{Line 1–2} = 75(0.05 + j0.4) = 3.75 + j30\ \Omega$$
$$\text{Line 2–3} = 75(0.05 + j0.4) = 3.75 + \text{j}30\ \Omega$$
$$\text{Line 3–4} = 106(0.05 + j0.4) = 5.3 + j42.4$$

Maximum load current in the line 1–2 is

$$\frac{60 \times 10^6}{\sqrt{3} \times 138 \times 10^3} = 251 \text{ A}$$

We choose a CT ratio of 250/5 which will give a secondary current 5 A under condition of maximum load.

With delta connected secondaries

$$\frac{(V_a - V_b)}{(I_a - I_b)} = Z_{\text{line}}$$

or

$$\frac{(V_a - V_b)}{(I_a - I_b)} \times \frac{V_{\text{sec}} / V_{\text{line}}}{I_{\text{sec}} / I_{\text{line}}} = Z_{\text{line}} \times \frac{V_{\text{sec}}}{V_{\text{line}}} \times \frac{I_{\text{line}}}{I_{\text{sec}}}$$

$$= Z_{\text{line}} \times \frac{67\sqrt{3}}{138 \times 1000} \times \frac{250}{5}$$

$$= Z_{\text{line}} \times 0.042$$

Thus the line impedances as seen by the relay R_{12} are

$$\text{Line}_{1-2} = 0.158 + j\ 1.26\ \Omega$$
$$\text{Line}_{2-3} = 0.158 + j\ 1.26\ \Omega$$
$$\text{Line}_{3-4} = 0.223 + j\ 1.78\ \Omega$$

Impedance seen by the relay under condition of maximum load is

$$\frac{67\sqrt{3}}{251\times(5/250)} = 22.7 \ \ \Omega$$

Impedance setting of zone 1

$$0.8(0.158 + j1.26) = 1.016 \ \ \Omega, \text{ secondary}$$

Impedance setting of zone 2

$$(0.158 + j1.26) + 0.2(0.158 + j1.26) = 1.524 \ \ \Omega, \text{ secondary}$$

Impedance setting of zone 3

$$(0.158 + j1.26) + (0.158 + j1.26) + 0.1(0.223 + j1.78) = 2.72 \ \ \Omega, \text{ secondary}$$

It may be observed that the impedance seen by the relay under maximum load conditions is 22.7 Ω, which is far larger than the impedance setting of the zone 3, i.e. 2.72 Ω and there is no danger of line tripping under overload as well as under load swings.

Line Protection with Pilot Relays

Distance relays, while being much superior to overcurrent relays, suffer from the disadvantage that only 60% of the line is protected at high speed while the remaining 40% (20% at each end) is high speed protected from the near end and slow speed protected from the remote end. In modern HV and EHV systems, this delayed clearing from the remote end is unacceptable because of high fault levels and low stability margins. For high speed protection from both ends for the complete line, it is imperative that information about *phase* or *direction* of current flow must be exchanged between the two line ends. The information exchange is accomplished by means of a pilot, i.e. a communication channel. Three basic pilots are used.

- Separate electrical circuits, frequently telephone circuits. These are generally not preferred because of lower reliability of these circuits.
- Power line carrier—The power line itself is employed as a communication channel with carrier frequencies in the range of 30–200 kHz. The communication equipment at each end is coupled to power lines by means of LC voltage divider network. The signals are confined to the protected lines by resonant LC line traps (blocking filters) at each end. See Fig. 15.54.
- Microwave pilot—Relaying information is broadcast at microwave frequencies (900 MHz), thereby obviating the need for pilot line. Since microwave transmission is restricted to line-of-sight, intermediate repeater stations are required. This type of channel suffers from atmospheric disturbances and fading. It has the advantage that considerable information can be transmitted in a single beam.

Pilot relaying schemes are of two types as described below:

- *Phase comparison* Here the phase of the currents at the two ends of the line are compared to distinguish between an internal (on the protected line) fault and an external (outside the protected line) fault.
- *Directional comparison* Here the comparison is made between the direction of current at the two line ends to distinguish an internal fault from an external fault.

Pilot relays provide only primary protection and, therefore, a separate set of distance relays must be employed for the necessary backup protection.

Phase Comparison Pilot Relaying

Figure 15.54 shows the terminal equipment used at each end of a line protected by phase comparison relaying. The transmission line CTs feed a network (phase sequence filter) which transforms the CT output currents to a single-phase voltage which is representative of fault conditions on the network for any type of fault. The phase sequence network output is applied to control the output from the local carrier-current transmitter (T) and is also applied to a comparer. The output of the local carrier-current receiver (R), which receives the signal from the local transmitter as well as the signal over the line from the transmitter at the other end of the line, is also applied to the comparer, which in turn controls the operation of an auxiliary relay for tripping the local transmission line circuit breaker. The application of the network output to the

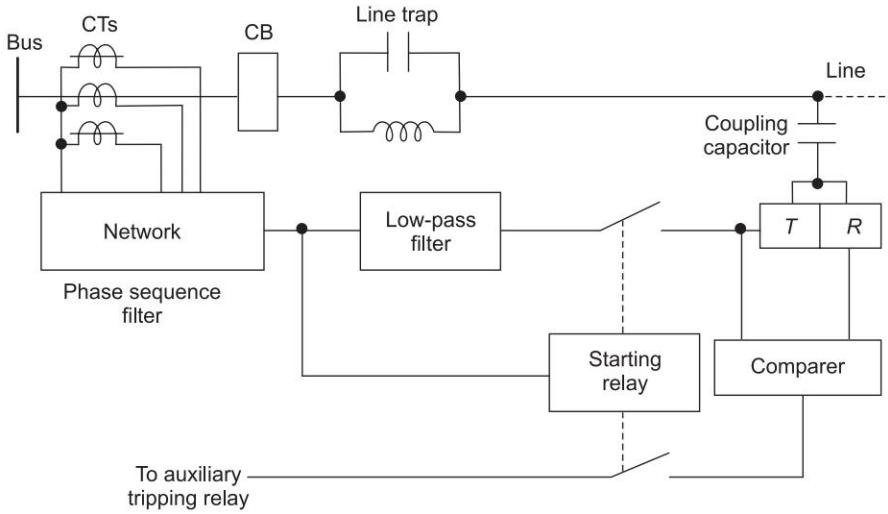

Fig. 15.54 Block diagram of power line carrier phase comparison relaying scheme

transmitter and the comparer output to the auxiliary relay are under control of a *starting relay** which in itself is governed by the network output. Therefore, it is only under fault conditions (internal or external) when the network output exceeds a preset limit that the starting relay operates to allow the application of the network output to the transmitter and the comparer output to the auxiliary relay. Thus under no fault conditions the transmitter and the receiver can be used for carrier-current telephony between the line ends.

The transmitter and receiver are coupled to the power line via an *LC* voltage divider shown in Fig. 15.55. Most of the 50 Hz power line voltage drops across *C*, and the 50 Hz voltage across *L* is small enough for safe operation and handling of the equipment. At the carrier frequency, *C* acts as a short circuit and the transmitter output appears on the line, and the receiver receives the line signal.

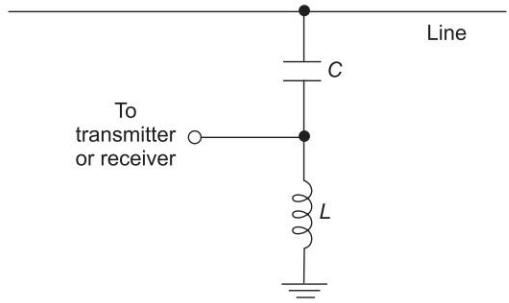

Fig. 15.55

It is assumed here that (1) the transmitter produces output signal when positive voltage is applied at its input, and does not produce any output when the input voltage is negative; and (2) the comparer blocks tripping (produces no output to operate the auxiliary relay) when it receives carrier signal at one or both of its input terminals, and permits tripping when it receives no carrier signal at any of its input terminals.

Consider the line 1–2 of Fig. 15.56 protected by means of phase comparison relaying. For a fault at F_2, external to the line, the line currents at the two ends of the line 1–2 are in phase, but the network voltages at the two buses are out of phase by 180°, because the CTs at the two ends of the line are reverse connected. So the carrier-current signals outputted by the transmitters at the two ends are out of phase by 180°. As a consequence, at each end a blocking carrier signal is received for one half cycle from the local transmitter, and during the other half cycle from the remote transmitter over the line. Since the

* In fact the starting relay has two sensitivity levels—when the line current is somewhat above the full-load current, it permits the network signal to be applied to the transmitter; and when the line current is much higher, it permits tripping, if called for by the comparer.

blocking signal is present all the time at both line ends, no tripping of circuit breakers takes place at either end. For an internal fault at point F_1, anywhere in the line 1–2, the line currents at the two ends are out of phase by almost 180° and the network voltages at each end are in phase. As a consequence, at each location the blocking carrier signal is present in one half cycle and the carrier signal is absent during the second half cycle, which permits tripping of circuit breakers at each end of the line. Wave forms and carrier signal at each end for external and internal faults are illustrated in Fig. 15.56.

Under blocking conditions (i.e. when the fault is external) phase shift less than 180° between network voltages is caused by the small angular difference between line currents owing to line charging (capacitive) component of current, and also by the length of time it takes for the carrier signal to travel from one end of the line to the other (this travel is at speed slightly less than that of light and causes a phase shift of about 12° per 160 km of line). This phase shift can be compensated by advancing the phase of the voltage applied by each network of its comparer.

Directional Comparison Pilot Relaying

Figure 15.57(b) shows the equipment at one end of the line for directional comparison pilot relaying. These are two directional relays at each station—D_i relay looks into the line, and D_o looks out of the line. These relays are respectively associated with normally open contacts D_i and D_o. When the receiver R receives a signal locally or over the line, the normally closed contact R opens.

Consider a fault at F_1, external to the line as shown in Fig. 15.57(a). This fault is detected by the directional relay D_o, but not D_i (at station 1). The contact D_o closes and the carrier-current is received by the local receiver (R) and by the remote receiver over the line. The normally closed R contacts, therefore, open blocking the operation of breakers (B_{12} and B_{21}) at both ends of the line. A fault at F_2, external to the line at the other end, produces similar action, with operations at the two ends reversed. A fault at F_3 within the protected zone is detected by both D_i relays and neither of D_o relays, blocking the carrier frequency and allowing tripping of B_{12} and B_{21}.

15.9 GENERATOR/MOTOR PROTECTION

Large 3-phase generators (synchronous) are major components of a power system, and must therefore be protected against a variety of hazards. Excessive heating can damage stator/rotor insulation, and can also cause structural damage, and must therefore be protected. Similarly, protection must be

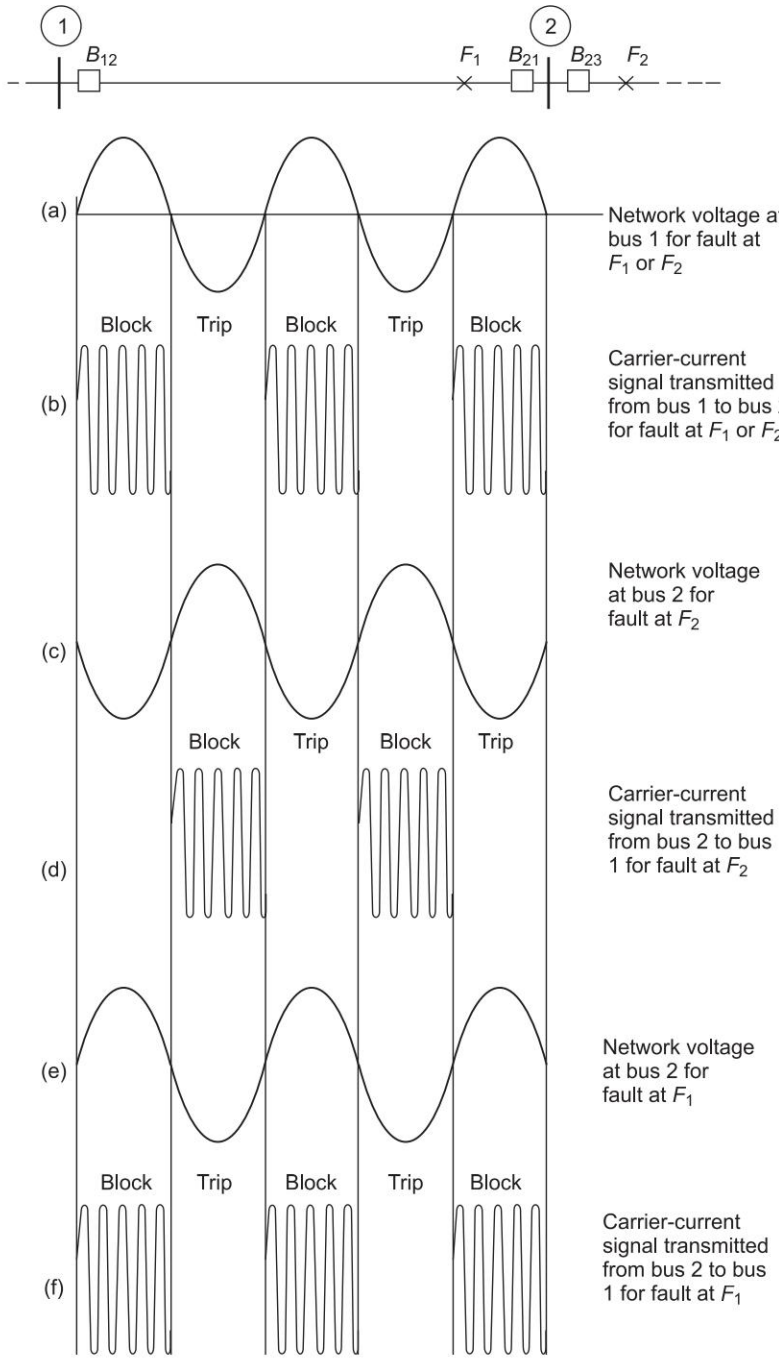

Fig. 15.56 External and internal fault behaviour of phase comparison relaying

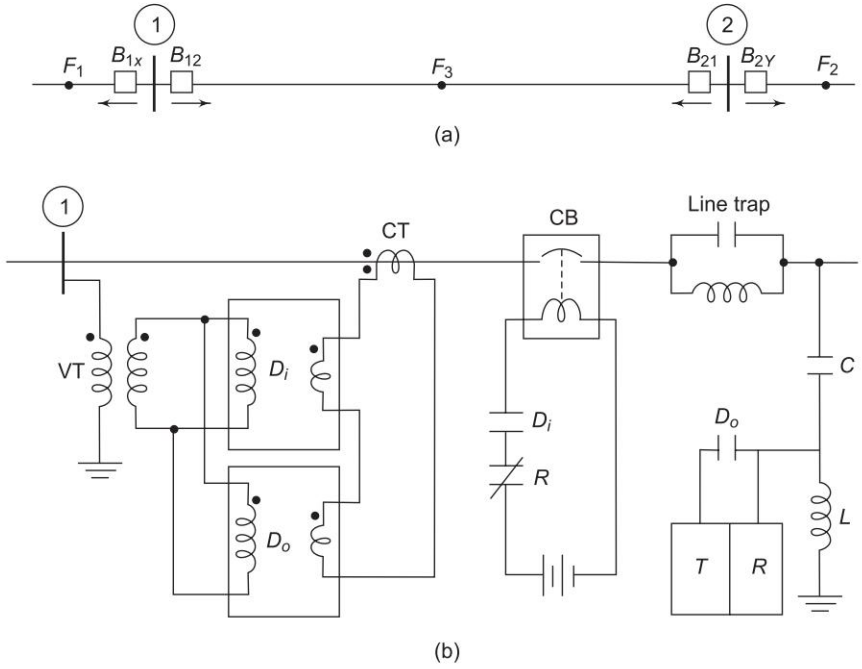

Fig. 15.57 Directional comparison pilot relaying equipment

provided against overvoltage and overspeed. Several items of protection and methods are common between motors and generators. Modern generators must be protected against the following hazards:

- Stator overload
- Stator winding short circuits
- Stator voltage/current unbalance
- Bearing overheating
- Loss of excitation
- Field faulted to ground
- Loss of synchronism
- Undervoltage
- External faults
- Loss of prime mover—motoring
- Overvoltage
- Overspeed

The motors do not require protection against the last three items.

Unbalanced operation of stator causes rotor overheating because of second harmonic field current induced by negative sequence rotating field (rotating at

synchronous speed in opposite direction to the main field). Protection is afforded by means of overcurrent relays used in conjunction with sequences filters sensitive to negative sequence voltages/currents.

We shall consider here mainly protection against short circuits (internal). These are of three kinds:

- Phase-to-phase fault
- Phase-to-ground fault
- Interturn faults (on a given phase)

Differential relaying techniques are adopted for these faults because of their selectivity and speed of response. The arrangement of CTs and percentage differential relays is shown in Fig. 15.58 for a star-connected generator, and in Fig. 15.59 for a delta-connected generator. In star connection, it is assumed that all three leads are available at the neutral end of the generator, and the neutral point is formed outside. If the neutral connection is made inside the generator, and only the neutral lead is brought outside and grounded through low impedance, percentage differential relaying can be provided only for ground faults as shown in Fig. 15.60, but the machine is not protected for phase-to-phase faults.

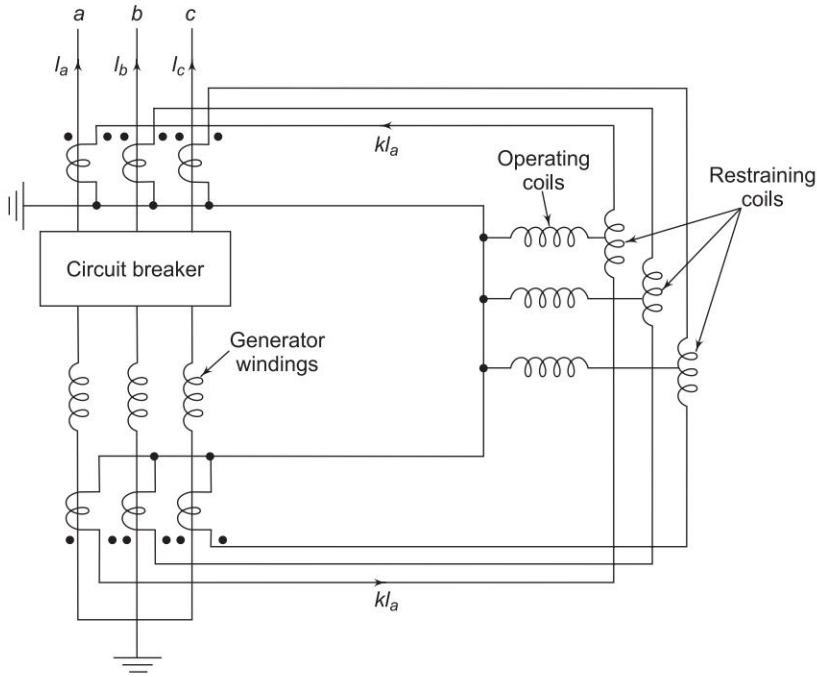

Fig. 15.58 Percentage differential relaying for a star-connected generator (currents are indicated for healthy conditions)

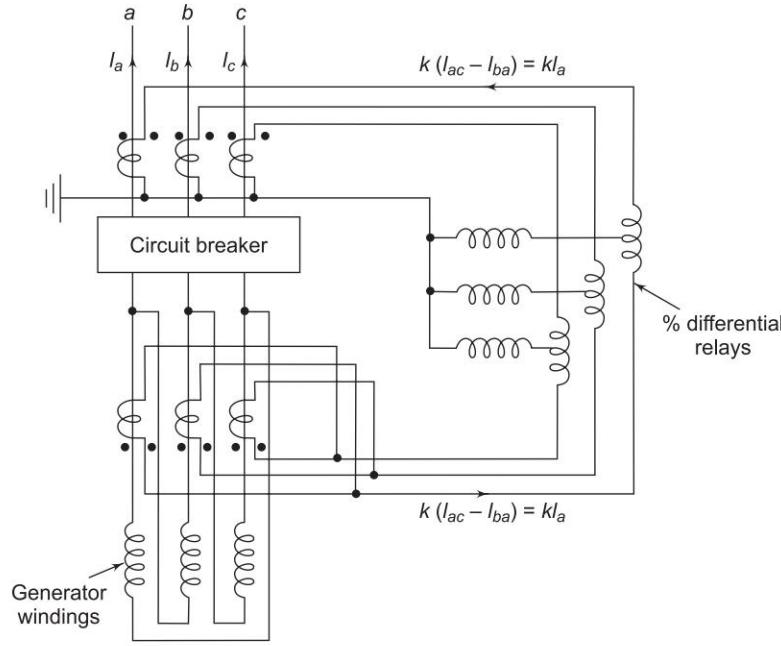

Fig. 15.59 Percentage differential relaying for delta-connected generator (currents are indicated under healthy conditions)

In Fig. 15.58 as the fault shifts closer to the neutral, the fault current which constitutes the difference of currents at the two ends of the windings gets considerably reduced, and as a result, the percentage differential relay cannot operate.* Hence a small percentage (about 20%) of the generator windings close to the neutral end indeed remains unprotected. This is not a serious drawback as the voltage of this winding section is small enough and faults in this section rarely occur.

None of the above schemes provide protection against interturn faults, as in this case the currents at the two ends of a winding remain equal, independent of the interturn fault. Interturn faults, thus, cannot be protected in the schemes described above. Differential protection against this fault is provided only for generators with multicircuit windings. The method used for protection is known as split-phase relaying as illustrated in Fig. 15.61. Notice that each phase is divided into two equal groups of parallel circuits with a CT for each group. If the number of parallel circuits per phase is odd, the current balance of two unequal groups is achieved by suitable CT ratios. Split-phase relaying will operate for any type of short-circuit in the generator winding.

* This is because the difference of currents at two ends must exceed a certain percentage of this sum by the pick up value of the relay (see Eq. 15.33b).

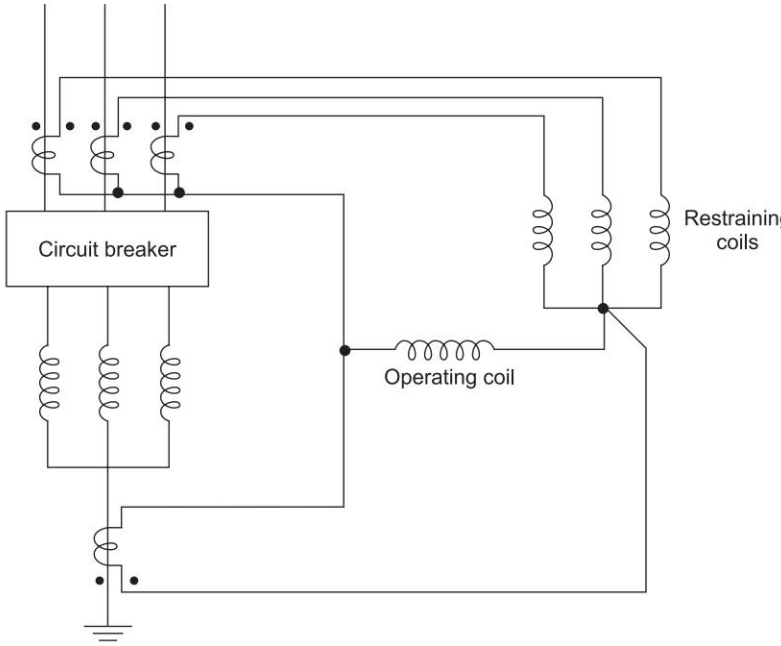

Fig. 15.60 Percentage differential relaying for star-connected generator with internally connected neutral—only neutral lead brought out

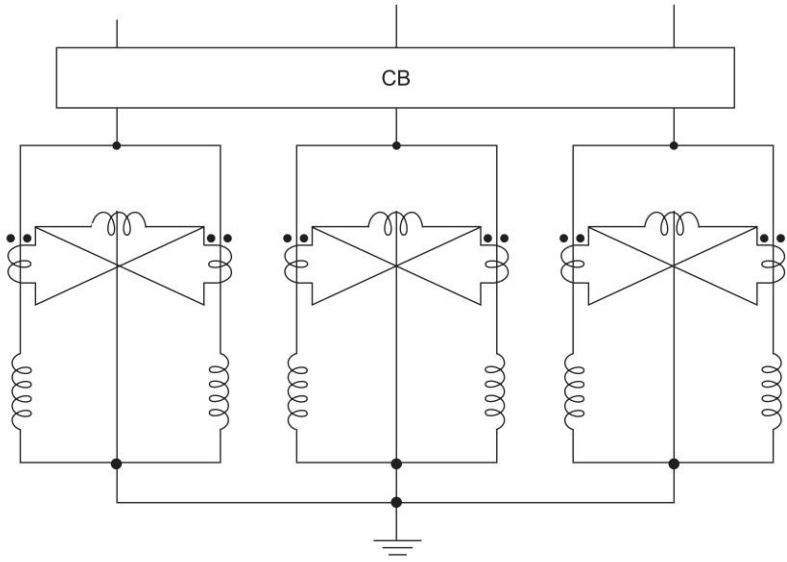

Fig. 15.61 Split-phase relaying for a multicircuit generator

Example 15.6 An 11 kV, 6 MVA star-connected generator has a reactance of 4.2 Ω per phase. The generator neutral is grounded through a resistance of 22 Ω. Determine what percent of the generator winding remains unprotected by the percentage differential relaying. Assume for simplicity that the percentage differential relay operates when out of balance current exceeds 25% of the full-load current.

Solution

Let x% of the winding be assumed to remain unprotected. The reactance of this portion of the winding is $4.2(x/100)^2$ Ω. For an LG fault at this distance along the winding, the total series impedance in the network connections will be

$$3 \times 22 + j\left[(4.2 + 4.2\,(\text{neg sequence}) + X_0\left(\frac{x}{100}\right)^2\right] \Omega$$

Because of the x^2 term the reactance component of this impedance can be neglected, so that fault calculations can be based on neutral resistance only.

$$\text{Phase voltage of } x\% \text{ of generator winding} = \left(\frac{11{,}000}{\sqrt{3}}\right)\frac{x}{100} \text{ V}$$

Fault current (= out of balance current) for fault

$$\text{at } x\% \text{ of winding away from neutral} = \frac{3 \times \dfrac{11{,}000}{\sqrt{3}}\dfrac{x}{100}}{3 \times 22}$$

$$\text{Full-load current} = \frac{6 \times 10^3}{\sqrt{3} \times 11} = 314.9 \text{ A}$$

Minimum out of balance current required for relay operation

$$= 0.25 \times 314.9 = 78.7 \text{ A}$$

Hence

$$\frac{\sqrt{3} \times 11{,}000\,(x/100)}{3 \times 22} = 78.7$$

or

$$x = 27.3\%$$

15.10 TRANSFORMER PROTECTION

In practice power transformers are protected against internal short circuits and overheating. No overload protection is provided. For transformers above 1 MVA capacity percentage differential relays are universally adopted for internal short-circuit protection. For smaller ratings overcurrent protection would suffice.

The currents on the two sides of a 3-phase transformer in general differ in both magnitude and phase. The CT connection must compensate for these differences, as a percentage relay must compare currents which, under normal conditions, are identical (in magnitude and phase). In star/star or delta/delta transformers the currents on the two sides have the same phase angle; the three CTs on both sides are, therefore, identically connected (star or delta) and an appropriate choice of CT ratios would be sufficient for magnitude equalization. In case of a star/delta transformer, the currents on the two sides also differ in phase by 30°. This is compensated by connecting CTs in delta on the star side, and in star on the delta side of the transformer.

Figure 15.62 shows a star/delta transformer with CTs connected in delta/star for feeding percentage differential relays under normal conditions

$$\frac{i_A - i_C}{N_{1s}} = \frac{i_a - i_c}{N_{2s}}$$

where N_{1s} and N_{2s} are standard CT ratios (primary/secondary current) which are selected such that

$$\frac{i_A - i_C}{N_{Is}} = \frac{i_a - i_c}{N_{2s}} \approx 5 \text{ A}$$

However,

$$\frac{i_a - i_c}{i_A - I_C} = N \quad \text{(the phase-to-phase voltage ratio of the transformer)}$$

$$\frac{N_{2s}}{N_{1s}} = N \tag{15.54}$$

The condition cannot always be met by using standard CT ratios. This mismatch is compensated by means of an auxiliary autotransformer type CT (3-phase) provided with a wide range of turn ratios. This autotransformer (start-connected) is interposed on one side of the percentage differential relays fed by the main CTs. Thus

$$\left(\frac{N_{2s}}{N_{1s}}\right) N_{\text{auto}} = N \tag{15.55}$$

Example 15.7 A 40 MVA, 3-phase, 345/34.5 kV transformer is star/delta connected. Select standard CT ratios on the two sides of the transformer for percentage differential protection of the transformer. Would an autotransformer be required? If so, what should be its current ratio?

Solution

$$\text{Line current on the star-side (345 kV)} = \frac{40 \times 10^3}{\sqrt{3} \times 345} = 66.9 \text{ A}$$

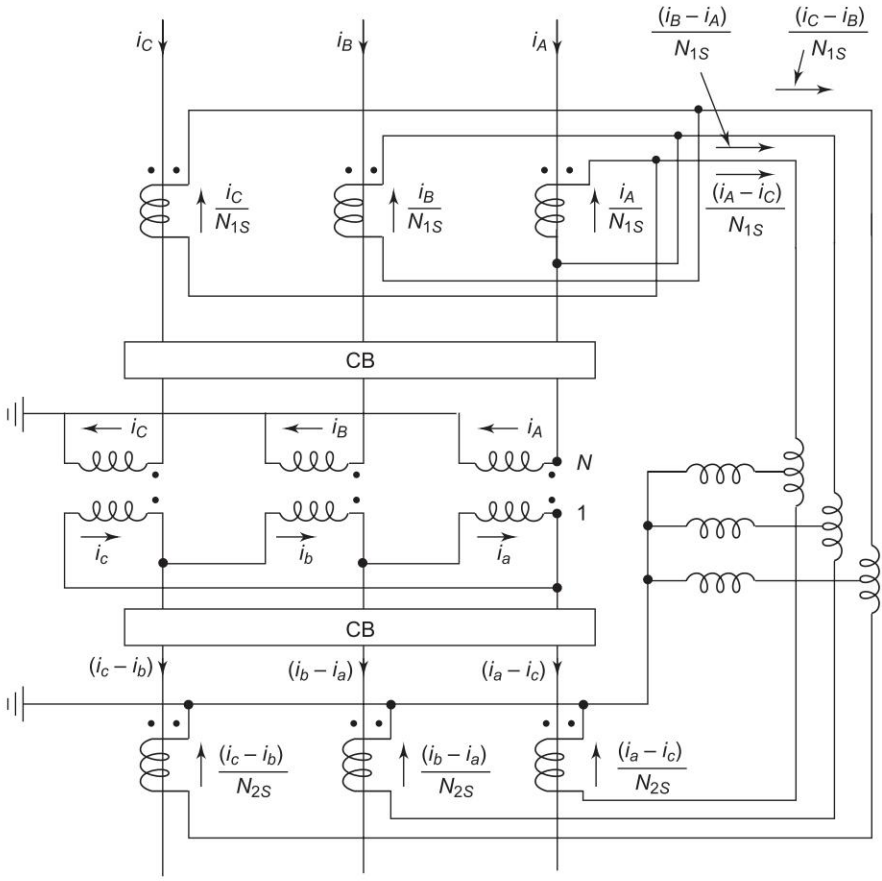

Fig. 15.62 CT connections for percentage differential protection of star/delta transformer

$$\text{Line current on the delta side (34.5 kV)} = \frac{40 \times 10^3}{\sqrt{3} \times 34.5} = 669 \text{ A}$$

Choosing a CT ratio of 800/5 on the 34.5 kV side, the current flowing to the differential relay from the star-connected CTs is

$$669 \times \frac{5}{800} = 4.18 \text{ A}$$

To balance this current from the delta-connected CTs on the 345 kV side, the current in the secondary windings of the CTs should be

$$\frac{4.18}{\sqrt{3}} = 2.41 \text{ A}$$

The CT ratio on the 345 kV side should, therefore, be

$$\frac{66.9}{2.41} = 27.8 \approx \frac{150}{5}$$

With this CT ratio the current fed to the differential relay from the delta-connected CTs of the 345 kV side is

$$66.9 \times \frac{5}{150} \times \sqrt{3} = 3.86 \text{ A}$$

This current mismatch (3.86 A against 4.18 A) must be removed by using an autotransformer CT ratio of

$$\frac{4.18}{3.86} = 1.1$$

as shown in Fig. 15.63

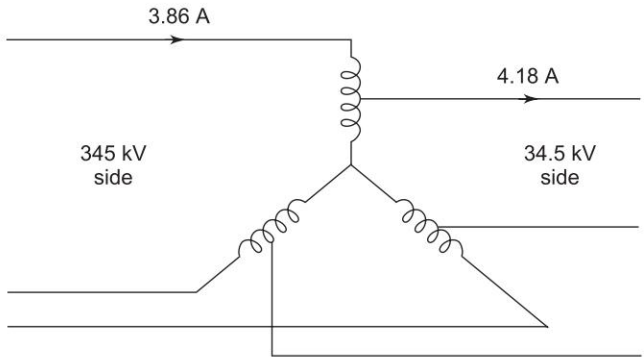

Fig. 15.63

Compensating for Magnetizing Current

In the above account it has been assumed that the transformer is ideal, so that under normal load conditions the primary and secondary currents flowing on the secondary sides of the CTs balance out. However, the magnetizing current, which flows only on the primary side, constitutes out-of-balance current. To prevent relay operation under normal conditions, the percentage differential relay must be compensated for this current. Figure 15.64 shows how magnetizing current compensation is carried out by the method of harmonic restraint. The magnetizing current is nonsinusoidal with a large third harmonic component. The filter F_1 is designed to pass the 50 Hz component to excite the operating coil R_o of the relay. The filter F_2 passes the third harmonic component through the restraining coil R_T (additional restraining coil) of the relay which provides sufficient restraint against the differential current resulting from the flow of the magnetizing current.

When a transformer is initially switched 'on', a large "in rush" (magnetizing) current flows, which appears as differential current and can trip the transformer. Since the inrush current has a large third harmonic component, undesired transformer tripping can be prevented by the method of harmonic restraint (Fig. 15.64).

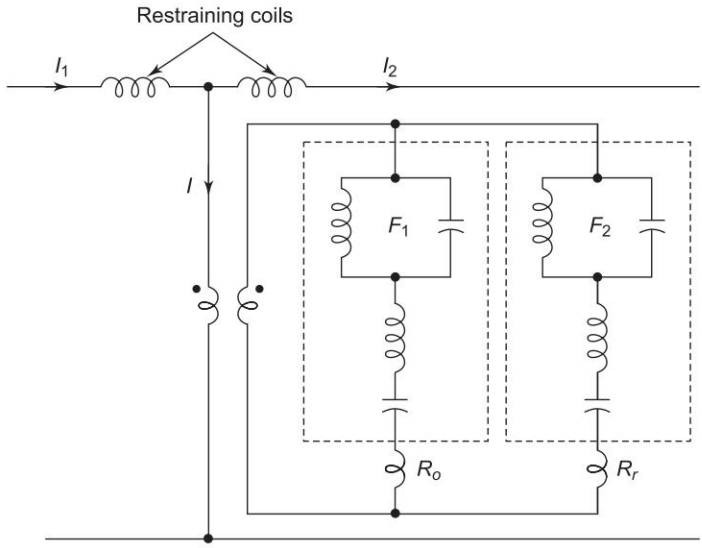

Fig. 15.64 Magnetizing current compensation—method of harmonic restraint

Another method of preventing false tripping upon flow of inrush current is to temporarily desensitize the differential relay, but only at full voltage. This method has the advantage of distinguishing inrush current from the fault current. The method is illustrated in Fig. 15.65. A shunt path to the operating

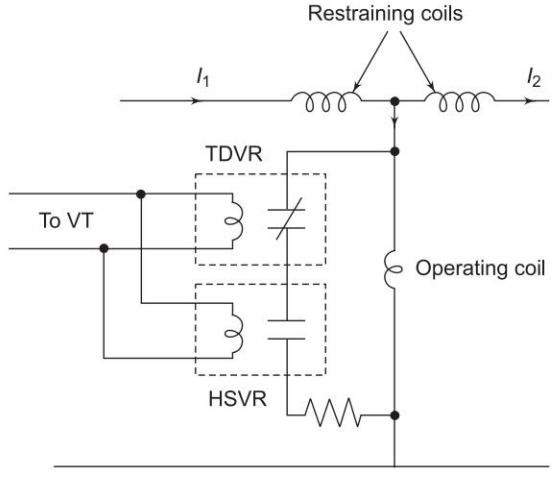

Fig. 15.65

coil of the differential relay is controlled by means of two voltage relays—TDVR (time delay voltage relay) with normally closed contacts and HSVR (high speed voltage relay) with normally open contacts. These relays are fed from the VT. When the transformer is switched 'on' (no fault), HSVR contacts close, and TDVR contacts do not open, so that the shunt path of the operating coil is closed, rendering it inoperative. After a small delay (at the end of which the inrush current has decayed to steady magnetizing current), HSVR contact opens, and consequently the differential relay, which was temporarily desensitized, becomes operative once again protecting the transformer against internal faults. If the transformer is switched on to a fault, the voltage is so low that HSVR does not pick up, and the shunt path remains open and the differential relay remains operative.

15.11 SEQUENCE FILTERS

It was seen earlier that certain type of relays respond to phase sequence quantities during conditions of fault (see Fig. 15.54 for phase comparison pilot relaying). Sequence quantities of line currents (or voltages) can be easily extracted analogically by means of CTs and certain network elements. Only current sequence filters will be described here.

Zero Sequence Current Filter

With three identical CTs connected in star as shown in Fig. 15.66, it easily follows that the current in the neutral connection is

$$3I_0 = I_a + I_b + I_c \tag{15.56}$$

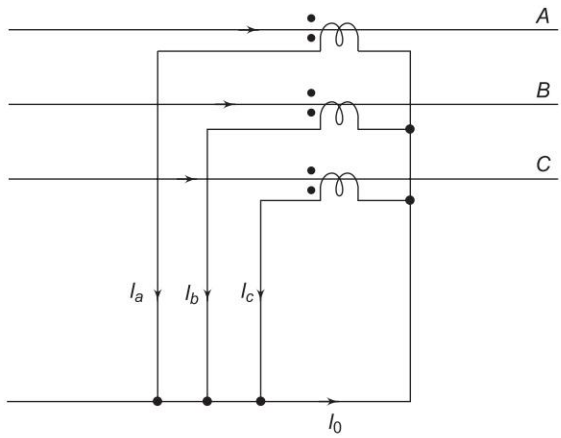

Fig. 15.66 Zero sequence current filter

Negative Sequence Current Filter

A simple negative sequence filter is shown in Fig. 15.67. Apart from CTs, it employs three mutually coupled inductors with self-reactances of kX and mutual reactances of $X_{ac} = X_{bc} = X$ with polarities as indicated. Assume that the filter is driven with "pure" positive sequence currents; $I_a = I_{a1}$, $I_b = \alpha^2 I_{a1}$, $I_c = \alpha I_{a1}$. Let the resistor R be so adjusted that the current I (in the inductor connected in phase C) is reduced to zero. Now $I_0 = 0$ and the current $I_c = \alpha I_{a1}$ flows through R. From circuit consideration,

$$\alpha I_{a1} R = jI_{a1}X - j\alpha^2 I_{a1}X$$

or

$$R = j\alpha^2 X - j\alpha X = j(\alpha^2 - \alpha)X$$

$$= \sqrt{3}\,X \qquad (15.57)$$

Equation (15.57) gives the condition necessary to make the filter "blind" to positive sequence currents.

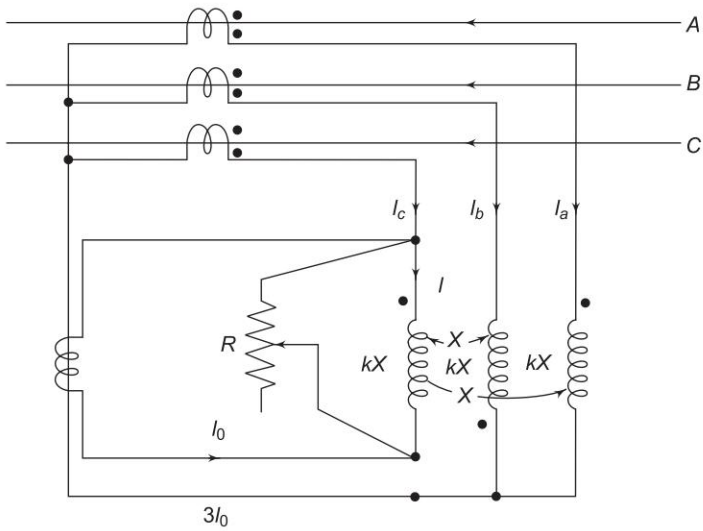

Fig. 15.67 Negative sequence current filter

Let the filter be now driven by any three currents, I_a, I_b, I_c. By KVL

$$(I_c - I_0 - I)R = jI_aX - jI_bX + IkX \qquad (15.58)$$

or

$$(I_0 + \alpha I_1 + \alpha^2 I_2 - I_0 - I)\sqrt{3}\,X = jX(I_0 + I_1 + I_2 - \alpha^2 I_1 - \alpha I_2 - I_0) + jIkX$$

or

$$\sqrt{3}\,(\alpha I_1 + \alpha^2 I_2 - I) = j(1 - \alpha^2)I_1 + j(1 - \alpha)I_2 + jkI$$

But

$$j(1 - \alpha^2) = \sqrt{3}$$

$$\therefore \quad \sqrt{3}\,\alpha^2 I_{a2} - \sqrt{3}\,I = j(1 - \alpha)I_2 + jkI$$

But

$$\sqrt{3}\,\alpha^2 - j(1 - \alpha) = 2\sqrt{3}\alpha^2$$

$$\therefore \quad (\sqrt{3} - jk)I = 2\sqrt{3}\alpha^2 I_2$$

or

$$I = \frac{2\sqrt{3}\alpha^2}{\sqrt{3} - jk} I_2 \tag{15.59}$$

As per Eq. (15.59) the current I is a measure of the negative sequence current I_2. An overcurrent relay connected in series to carry the current I would be sensitive to negative sequence currents flowing in the lines.

If current connections I_b and I_c are interchanged, the filter will sense positive sequence currents and would be blind to negative sequence currents.

15.12 MICROPROCESSOR-BASED RELAYING

The use of computers for real-time data acquisition and analysis of power system phenomena is now well established. Extensive development efforts are being devoted to the application of computers in relaying techniques. In fact some such computer-based relaying schemes have already been implemented in the US and Canada.

Computer-based relaying offers certain distinct advantages over the electromechanical, and more recent electronic relays. These are enumerated below.

- Multiprocessor architecture with parallel processing offers high speeds of fault detection at competitive price.
- Decentralized modular approach with a separate processor for each task admits of ease of modification or addition.
- Since relay settings are software governed, modifications can be made over a large dynamic range without any physical modification.
- Reliability and security are greatly enhanced by the use of parallel processing and software-based cross checking routines.
- Algorithm dependent performance of a computer-based relay is predictable to a high degree of accuracy.

Microprocessor-based Distance Relaying*

Figure 15.68 shows the general structure of transmission line distance relaying. To speed up the calculations, both sequential and parallel processing concept is employed. Eight 16 bit low-cost microprocessors are needed as shown in the figure with each processor performing a specific function. An analog interface samples the three line-voltages and the three-phase currents at a rate that may be set by the software (typically 16 samples/cycle). Two analog-to-digital interfaces (*A*/*D*) convert the voltages and currents into 12 bit words. This data is read by the voltage (*V*) and current (*I*) processors and converted into complex phasor values. Three impedance processors then operate on these results in parallel, to determine all the phase-to-ground and phase-to-phase impedances. The tripping logic (*T*) processor uses these impedances and the mode of relay operation (normal, line test, etc.) to establish the output command. The communication (*C*) and the local monitoring (*M*) processors are responsible for system state display via an oscilloscope and an alphanumeric display. Since the calculations are performed sequentially, and in parallel, all the data needed for one calculation (e.g. impedance) must pertain to the same sampling period. A special common memory system must be employed for this purpose (details will not be illustrated here).

In order to avoid false operation, the trip signals for the circuit breakers as generated by the *T* processor must be certified by signals from other processors using appropriate digital logic.

All operations from sampling to generation of the trip signals do not take more than one sampling period.

The tripping mode (three-phase opening with/without reclosing etc.) may be programmed into the system via input interface.

Relaying Functions

A multiprocessor-based distance relaying (Fig. 15.68) has been implemented by Hydro Québec Canada. It is provided with four impedance zones (one reverse) as shown in Fig. 15.69. The reactive and resistive reach and angle can be set by software. Tripping schemes and setting may be programmed depending on line configuration to be protected and the kind of tripping (single or three pole) required.

The *V* and *I* processors compute steady-state phase-to-ground voltages and phase currents using a full-cycle Fourier algorithm. The iterative equation for voltages is

$$\bar{V}_n = \bar{V}_{n-1} + (v_n - v_{n-N}) \exp(j2\pi\, n/N) \qquad (15.60)$$

* St. Jacques, A.L. and Santerre, Q., "A Multiprocessor-based Distance Relaying: Design Features and Test Results", *IEEE Trans*., PAS, vol. PAS-102, no. 12, Dec. 1983.

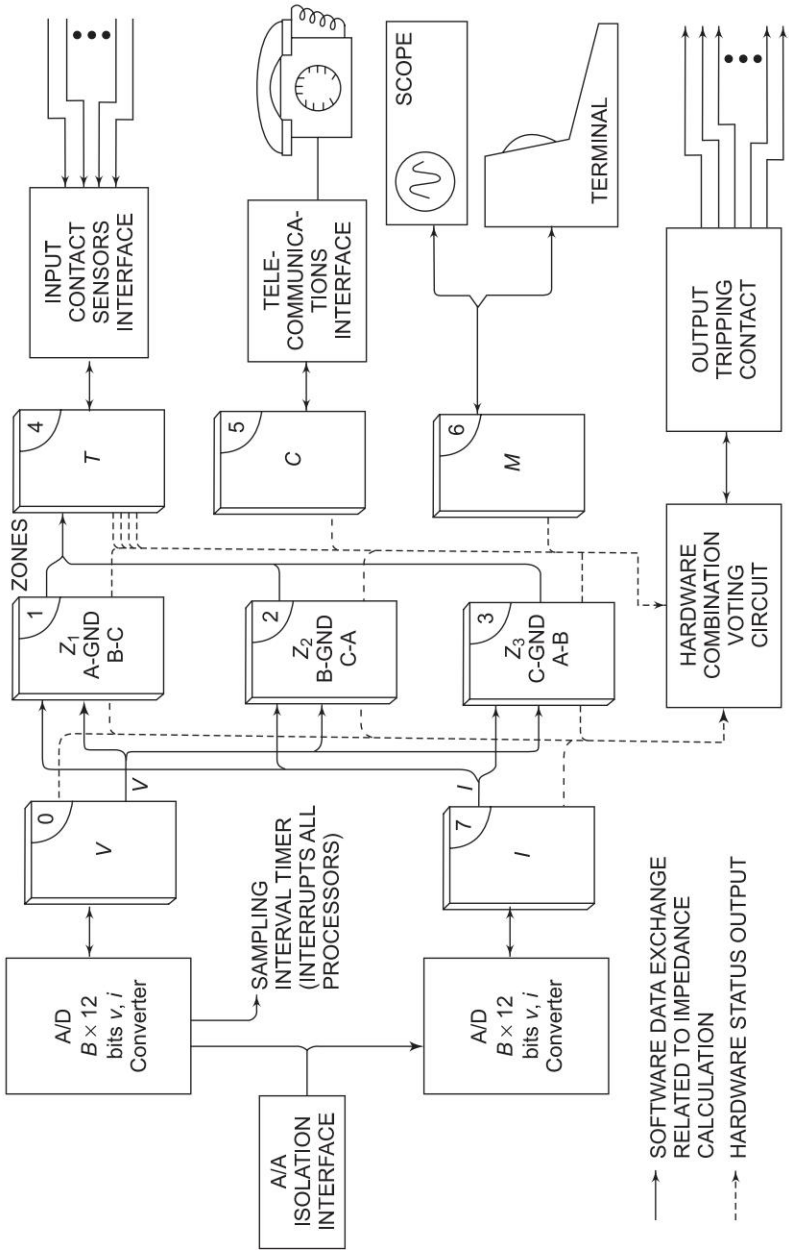

Fig. 15.68 Transmission line distance relaying—general structure

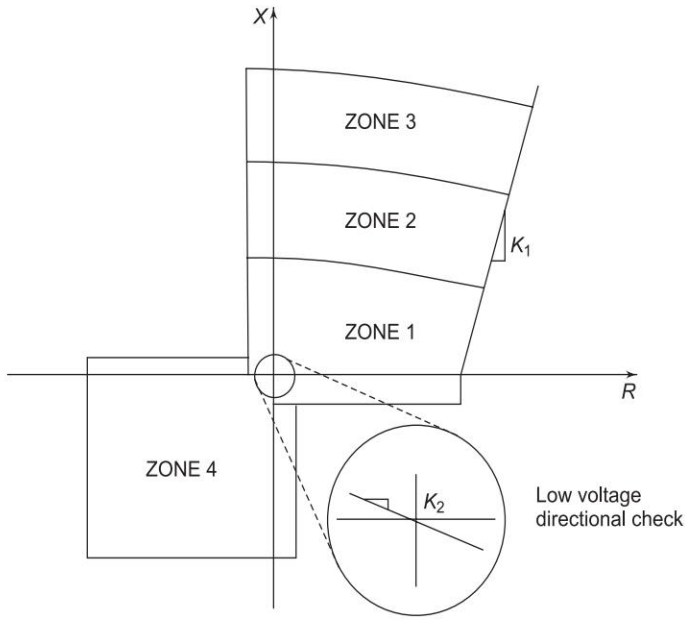

Fig. 15.69 Impedance zones

where $\bar{V}_n$ = complex phasor at sample n

N = number of samples per cycle.

The iterative equation for the currents is:

$$\bar{I}_n = \bar{I}_{n-1} + (i'_n - i'_{n-N})\,\gamma \exp\,(j2\,\pi(n/N)+ \phi) \qquad (15.61)$$

where $i'_n = i_n - i_{n-1}$, the numerical differentiation to minimize the effect of the decaying exponential of symmetrical currents.

and $\left.\begin{matrix}\gamma = 2(1-\cos 2\pi/n) \\ \phi = (\pi/2 - \pi/N)\end{matrix}\right\}$ Magnitude and phase of the compensation factor for numerical differentiation

(a) *Impedance:* All the six impedances—3 phase-to-phase and 3 phase-to-ground—are continuously calculated and compared with the four zone characteristics. When one of the impedances is detected within the characteristic boundaries, the corresponding zone timers are incremented. If the impedance is in zone 1, the zone 2 and 3 timers are also incremented. When a timer reaches a prescribed but adjustable value, a trip signal is permitted depending upon the zone and the tripping scheme. If, instead, the impedance moves out of the tripping zone, the zone timers are decremented. These are all set to zero when all the impedances stay outside the characteristic boundaries for a specified but adjustable time period.

The phase-to-phase impedances are calculated from delta voltages and currents, for example,

$$Z_{bc} = (V_b - V_c)/(I_b - I_c) \tag{15.62}$$

The equation for phase-to-ground impedance is

$$Z_{ag} = V_a/(I_a + KIN) \tag{15.63}$$

where K is a complex constant for zero sequence compensation.

The need for time consuming division indicated by Eqs (15.62) and (15.63) is obviated by computing compensated impedance Z'.

$$Z' = VI^* = Z\,|\,I\,|^2 \tag{15.64}$$

Then

$$Z_{\text{boundary}} = Z_{\text{setting}}\,|\,I\,|^2 \tag{15.65}$$

The line of slope K_2 passing through origin in Fig. 15.69 is the directional characteristic and is used to determine whether the fault lies in zone 1 or zone 4, when the fault voltage is too small for precise evaluation of the impedance.

(b) *Overcurrent:* For severe faults in zone 1, the voltage available is too low for impedance calculations. In such a case the overcurrent algorithms take over to trip the line. Since the current magnitudes are calculated from phasor current, the overcurrent response of the system is transient free. The detection time is made an inverse function of the ratio of fault current to the setting level.

(c) *Overvoltage:* Overvoltage detection algorithm is similar to the overcurrent algorithm. There are two levels of detection, each with an associated timer. An alarm is sounded above a certain voltage level, whereas when second (for still higher voltages) level is detected, a trip signal is outputted to isolate the line.

(d) *Line check:* The line check mode of operation permits fast tripping when a faulty line is energized. For a fault close to the relay end of the line, the line voltages are too low for detection by impedance or directional algorithm. Such faults are, therefore, covered by overcurrent protection. For distant faults, the three-zone fast impedance protection algorithm takes over.

The decision algorithm chooses between normal and line-check modes depending upon sustained value of the line voltage, for very low voltages the choice being the line-check mode.

Special features: A multiprocessor-based relaying scheme easily admits of some secondary features.

- Local and/or remote monitoring facility permits analysis and recording of data pertaining to any sample as well as the state of processors and interfaces.
- Data pertaining to any error in relaying system or a fault in the processor network is automatically despatched to a central computer for storage or debugging.
- The terminal attached to the relaying system indicates the rms voltages and currents during healthy state as well as upon occurence of a fault (phase, zone of operation etc.).

15.13 NUMERICAL (DIGITAL) RELAY

After monitoring currents and voltages using primary transducers (CTs and PTs), these analogue quantities are sampled and converted to digital form for numerical manipulation, analysis, display and recording. This gives a flexible and highly reliable relaying function, thereby enabling the same basic hardware units to be employed for more or less any kind of relaying scheme.

Digital relays are more suited to post-fault analysis since they can store data and therefore they can be used in a self-adaptive mode. They are also capable of self-monitoring and communicating with hierarchical controllers. Thus fast and selective fault clearance is possible and fault location can be revealed to mobile repair teams. Using a satellite-timing signal receiver with Global Positioning Satellite (GPS) to give a 1 μs synchronized signal, faults on lines can be found out to within 400 m.

Basic components of a numerical relay comprise (i) signal conditioning subsystem, (ii) conversion subsystem and (iii) digital processing relay subsystem.

Protective relays have undergone tremendous evolution over the years. Recent trend is the use of numerical relays in the protection system. A microprocessor-based relay, which works on numbers representing instantaneous values of the signals, is called *numerical relay*. Numerical relay is also known as digital relay, computer-based relay or microprocessor-based relay. Numerical relay is run through the software which runs in the background. Therefore a numerical relay is a combination of hardware and software. The conventional relays (Non-numerical relays) perform comparison rather than straight numerical computation. The numerical relay overcomes the limitation of conventional relays by performing real time computations.

A (Block diagram of) numerical relay is shown in Fig. (15.70).

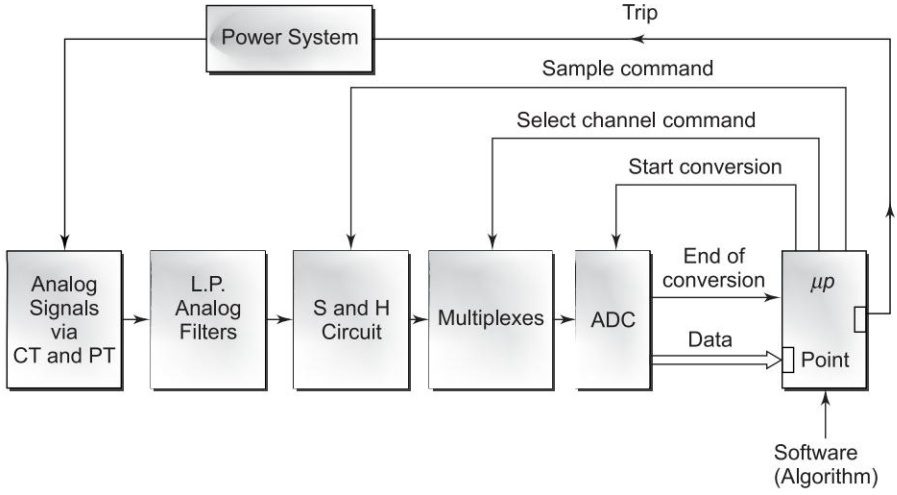

Fig. 15.70 A general block diagram of numerical relay

Before the sampling and conversion to digital form, we have to make sure that signals taken from CTs and PTs do not contain any frequency components having a frequency greater than one half of the sampling frequency.

The signals taken from CTs and PTs are first passed through a low pass analog filter to provide a proper shape to the frequency spectrum of the signal. The Sample and Hold Circuit (*S* and *H*) is used to sample the signal and to hold it constant during the time when the signal is converted to digital form. The multiplexes passes the signal from *S* and *H* circuit to the ADC so as to accommodate a large number of input signals.

Microprocessor controls the working of *S* and *H* circuit and ADC through control signals. The ADC converts the analogous signal into a digital signal i.e. 4, 8, 12, 16 or 32 bits or even higher order. The incoming digital signals from the ADC are stored in the RAM of the microprocessor and processed by the relay software in accordance with the background algorithm. The trip signal issued by the microprocessor is suitably processed so as to make it compatible with the trip coil of the CB. The same microprocessor can be used for other relays and supervisory controls.

Digital Transformer Differential Protection

A conceptual Block diagram for digital protection of a transformer is shown in Fig. (15.71).

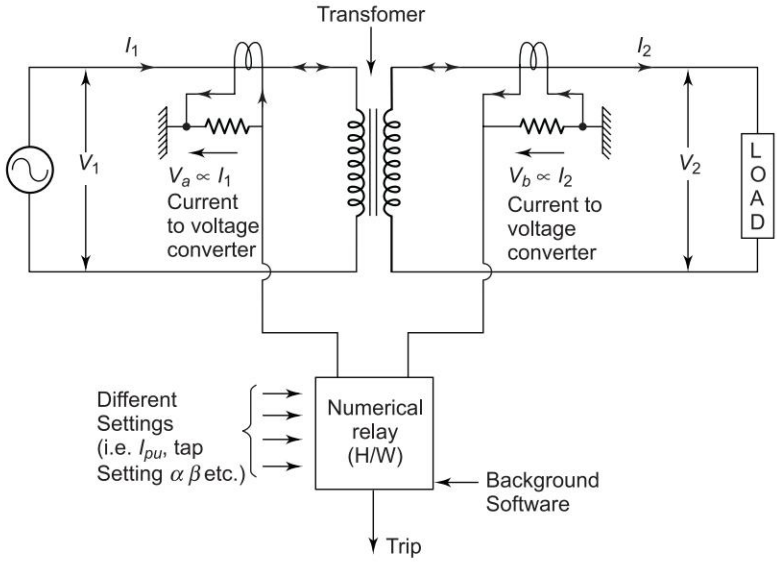

Fig. 15.71 A General Block diagram of numerical protection of transformer

The phasor values of the currents on both sides of the transformer and also the phasor difference between the two are computed. If the magnitude of this difference is substantial, an internal fault is indicated and the trip signal must

be sent. The numerical relay algorithm should be made to implement the percentage differential relay.

Algorithm

1. Read minimum pick-up I_{pu} and percentage Bias (B).
2. Compute the phasor value $\bar{I}_1$ by any method/technique.
3. Compute the phasor value $\bar{I}_2$ by any method/technique.
4. Compute spill current $I_{sp} = \bar{I}_1 - \bar{I}_2$.
5. Compute circulating current $I_{cir} = \dfrac{\left(\bar{I}_1 + \bar{I}_{sp}\right)}{2}$.
6. If $I_{sp} > (BI_{cir} + I_{pu})$ then trip, else restrain.

15.14 RECENT TRENDS

Recently developed relays employ travelling wave or harmonics. Other trends include

Dynamic relays: These are augmented by the first, second or both derivatives of the relay inputs. Use of these relays is called dynamically shaping the relay characteristics. Such as relay has different transient and steady state operating characteristics.

Adaptive relays: These adapt to variable fault characteristics, depending on the prefault power flow. These ensure minimum malfunction.

Harmonic-based relays: A ground-fault relay based on harmonics has been used for synchronous machines.

Statistical relays: They are used for overhead line protection against a high impedance ground fault.

For high-speed, single shot auto reclosure, the CBs must trip simultaneously and quickly from both ends of the high voltage line. It is usual practice to use either carrier-aided distance schemes or unit carrier schemes, both of which need a carrier (50 to 500 kHz) for transferring information from one end of the line to the other.

Relays based on Travelling Waves

Modern EHV lines require faults to be cleared rapidly and selectively. Ref. [12] describes a single-phase version of ultra high-speed directional relay, responding to the direction of travelling waves, created by a fault and thus suitable for a directional unit carrier scheme. The travelling wave directional relay derives its actuating quantity from a short stretch of conductor, called a coupler, mounted below the power line. The coupler, therefore, has simultaneous electric and magnetic coupling with the power conductor. This coupling replaces both current and voltage transformers.

Futuristic View

Artificial Neural Network

An ANN is a computer architecture inspired by research about the human brain. It attempts to build computing systems analogous to the biological nervous system. Its basic constituents are:

(i) The processing element, called neuron.
(ii) Network topology.
(iii) Learning (or training) method.
(iv) Recall method.

Complex pattern recognition problems occur when an incipient or broken conductor fault occurs. Then an ANN may be successfully applied. They do not replace conventional methods. They help us solve some tricky pattern recognition problems.

More research needs to be done on high-speed CBs. It appears that a half-cycle relay and a half-cycle breaker is the optimal solution.

The relaying field is still exciting and demanding. New frontiers are being opened to relaying engineers in the protection of EHU/UHV and HUDC lines demanding novel and creative approaches.

Central Computer Control and Protection

The advent of reliable cheap hardware, in terms of microprocessor and digital signal processing integrated circuits, enabled simpler tasks to be carried out at distribution levels. Its use has been widespread in protection and control functions. Hardware functions have now been transferred to very sophisticated software, thus enabling system adaptation and expansion by software configuration without much human intervention.

A major advantage of digital techniques is their ability to self monitor important circuits and functions all the time to ensure the nonstop availability of the devices and thus, quality of supply.

Electric utilities have to take a new look into integrating various functions such as control, measurement, protection, metering and plant diagnosis.

Adaptive Protection Systems

Adaptive protection systems allow protective functions to be adapted automatically, without manual intervention, in real time to changing system conditions. e.g. intelligent load-shedding program for the under frequency relay.

Expert Systems

An expert system is a computer program that employs knowledge and inference procedures to solve problems that are normally solved through human expertise.

The basic components of an expert system are knowledge base, inference procedures, data base and user interface.

15.15 SUMMARY

Power System Protection has been dealt in this chapter in sufficient details. Starting from basic principles, CT, VT, hardware, μp based relays, it ends with latest digital (numerical) relays highlighting finally the recent trends.

Problems

15.1 A single-phase 80 kVA 2000/200 V step-down transformer is to be differentially protected. Choose appropriate CT ratios. Also determine the ratio N_r/N_o if the relay is to tolerate a mismatch in current of upto 20% of I_1.

15.2 A 25 MVA transformer, which may be called upon to operate at 25% overload, feeds 11 kV busbars through a CB; other CBs supply outgoing feeders. The transformer circuit breaker is equipped with 1000/5 A CTs and feeder CBs with 400/5 A CTs and all sets of CTs feed induction type OC relays. The relays on feeder CBs have a 125% plug setting and a 0.3 time multiplier setting. If a 3-phase fault current of 5 kA flows from the transformer to one of the feeders, find the operating time of the feeder relay, the minimum plug setting of the transformer relay, and its time dial setting assuming a discriminative time margin of 0.5 s. IDMT relay characteristic is given in Fig. P-15.2.

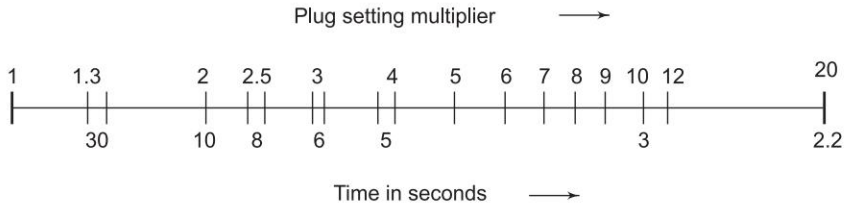

Fig. P-15.2 IDMT relay characteristic with TMS = 1

15.3 A 2 MVA 33/11 kV Δ/Y transformer is supplied from the 33 kV side and is earthed through a resistance R on the star side. It is protected by differential protection scheme, and the fault current for a single-phase to earth fault at the terminals of the star winding is to be limited to a full load value. Prepare a table showing percentage of winding protected to a base of fault setting (as a percentage of full load upto 40%). Calculate the setting which would be required to protect 70% of the star winding against earth faults under these circumstances. Comment on the suitability of the calculated setting for protecting 70% of the winding.

15.4 Determine the actual time of operation of an inverse time OC relay having TDS of 2.5 and rating 5 A, and having a plug setting of 125%. It is connected to a supply circuit through a CT of 400/5 ratio. The fault current is 5000 A.

15.5 A synchronous generator rated at 20 kV protected by the balanced circulating current system has its neutral grounded through a resistance of 15 ohms. The differential protection relay is set to operate when there is an out of balance current of 3.0 A. The CTs have a ratio of 1000/5 A. Determine: (1) the % winding which remains unprotected, and (2) the minimum value of the earthing resistance required to protect 75% of the winding.

15.6 Figure P-15.6 shows the % differential relay used for the protection of an alternator winding. The relay has a minimum pickup current of 0.25 A and has a % slope of 10%. A high resistance ground fault occurs near the grounded neutral and of the generator winding with the current distribution as shown. Assume a CT ratio of 400 : 5; determine if the relay will operate.

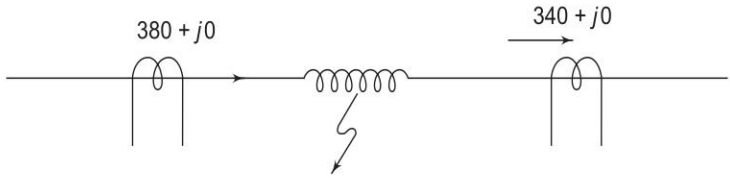

Fig. P-15.6

15.7 A three-phase transformer rated for 66 kV/11 kV is connected Y/Δ and the protecting CTs on the LV side have a ratio of 400/5. Determine the ratio of the CTs on the HV side.

15.8 A star connected, three-phase 12 MVA, 6.6 kV alternator is protected by a circulating current equipment, the star point being earthed via a resistor R. Show in a tabular form the effect of earthing resistance on the winding protected upto a 150% of full-load current through R showing the % of winding protected for an earth fault setting of 20%. Find the value of earth resistance if 80% of the winding is to be protected.

15.9 For the radial system of Example 15.4 design the settings (tap setting and time dial setting) for ground fault relays (LG fault)—R_1, R_2 and R_3. Assume that the zero sequence impedances of the lines are 2.5 times their positive sequence impedances. For an LG fault just to the left of the bus 3, how much time would the primary relay take to operate? If the primary relay fails, how much time would the appropriate backup relay take to operate?

References

Books

1. Mason, C.M., *The Art and Science of Protective Relaying*, Wiley, New York, 1956.
2. Warrington, A.R.C. Van, *Protective Relays*, vol. 1, 2nd edn, 1968, vol. 2, 3rd edn, 1978, Chapman and Hall, London.
3. Newark, N.J., Westinghouse Electric Corporation, *Applied Protective Relaying*, 1968.
4. Electricity Council (edited), *Power System Protection*, vols 1–3, MacDonald, London, 1969.
5. Stevenson, W.D., Jr. *Elements of Power System Analysis*, 4th edn, McGraw-Hill, New York, 1982.
6. Weedy, B.M. and B.J. Cory, *Electrical Power Systems*, 4th edn, Wiley, Singapore, 2002.
7. Guile, A.E. and W. Paterson, *Electrical Power Systems*, vols 1 and 2, Pergamon Press, New York, 1977.
8. Gross, C.A., *Power System Analysis*, Wiley, New York, 1979.
9. Singh, L.P., *Digital Protection*, Wiley Eastern, 1994.
10. Paithankar, Y.G. and S.R. Bhide, *Fundamentals of Power System Protection*, Prentice Hall of India, New Delhi, 2003.
11. Paithankar, Y.G., *Transmission Network Protection*: *Theory and Practice*, Marcel Dekker, New York, 1998.
12. Phadke, A.G. and J. Thorp, *Computer Relaying for Power Systems*, Institute of Physics Publishers, 2005.
13. Glaver, J.D. and M.S. Sharma, *Power System Analysis and Design*, 3rd edn, Thomson Asia, 2002.
14. Surge Protection in Power System, *IEEE Tutorial Course*, *79EH0144-6 PWR*.
15. RUS Bulletin 1724E-300.

Papers

16. Sekina, Y., M. Hatata and T. Yoshida, 'Recent Advances in Digital Protection', *Electric Power and Energy Systems*, July 1984, 6: 181.
17. IEEE Tutorial on Digital Computer Relaying, *IEEE Publication No. 79 EH 0148-7 PWR*, 1979.
18. Ahson, S.I. and D.P. Kothari, 'Testing of an Overcurrent Relay using a Microcomputer', *J.I.E.* (India), ET-1, Aug. 1982, 63: 55.
19. St. Jacques, A.L. and Q. Santerre, 'A Multiprocessor-based Distance Relaying: Design Features and Test Results', *IEEE Trans.*, *PAS*, Dec. 1983, 102: 3842–3848.
20. IEEE Tutorial Course on Microprocessor Relays and Protection Systems, *IEEE Publication No. 88 EH 0269-1 PWR*, 1988.

Chapter 16
Underground Cables

16.1 INTRODUCTION

In big cities and densely populated areas overhead lines become impractical owing to safety regulations. In such places insulated conductors are usually laid underground, and are called cables. Underground transmission and distribution is no doubt more expensive than the overhead alternative. Cables developed should be not only economically attractive, but physically they should be able to carry large chunks of power. The main constraint is the temperature rise of the insulating material used, the limit of conductor temperature being 90°C. For flexible cables, there exists an upper limit to overall diameter, and hence to the size of the conductor. The combination of paper and oil is still the most effective dielectric for HV cables. Cable installations are useful for submarine, crossings, railway yard, inside power station and in densely populated areas. Underground cables also provide greater safety, less interference with amenities and better outlook.

16.2 TYPES OF CABLES

Many types of cables are used depending upon the mechanical properties required, the transmission voltage range, and the type of insulation used. The insulating material used for cables should have good insulation resistance and high dielectric strength. It should be nonhygroscopic and should not react with acids and alkalies. The maximum current rating of a cable varies with the cable size, the insulation used, earth thermal resistivity and the method of laying the cable in the ground.

For LV (below 1 kV) applications, plastic cables are used. Aluminium is increasingly being used as both a conductor and sheath material. At lower voltages, oil-impregnated paper insulated cables are used mostly with the three conductors contained in a single sheath. Such a cable is called *belted* type cable (Fig. 16.1). For mechanical protection, steel armouring is employed. Jute is used for covering the cables. The tangential stresses are completely eliminated in case of the shielded construction.

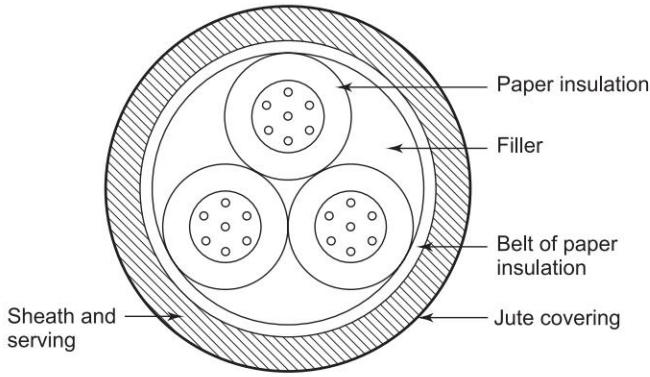

Fig. 16.1 A three-core belted type cable

For upto 11 kV HV systems, paper insulated cables are used, whereas for a 33 kV system, H-type M. Hochstadter cables are preferable. In 'SL' type cables, each core has its own lead sheath, with an additional lead sheath enclosing the three cores. In HSL type cables, there is a perforated screen, and a separate lead sheath is used for each core. For HV cables for 66 kV and more, single-core cables are used, since three-core cables would otherwise be too thick to bend.

For 220 kV (and higher) cables, it is necessary to avoid cable ionization by preventing the void formation. Voids are formed by cyclic heating and cooling of the impregnant. Void formation can be prevented by the use of a very thin film of oil under pressure. Such pressurized cables are known as *oil-filled cables*. In this type, a hollow conductor of soft drawn stranded copper, fed by oil reservoirs placed at intervals along the line, is used. The oil is maintained under pressure by these reservoirs. As the cable heats on load, oil is driven from the cable into the reservoirs and vice versa, hence the formation of voids is prevented. Impregnated paper is used for insulation, and a lead sheath and jute covering are employed to give water proofing. Figure 16.2 depicts a cross-section of a 220 kV oil filled cable. Oil-filled cables require relatively smaller amount of insulation as compared to the solid type for the same operating voltage, and, therefore, are used for higher voltages (66 kV–400 kV). At 500 kV, the oil-filled cable has a working stress of 15 kV/mm.

To counter the disadvantages of oil-filled cables in terms of expansion and contraction of oil during loading cycles, gas-filled cables are used. A gas-filled cable consists of a conductor supported in a rigid external pipe filled with a pressurized gas (usually SF_6 or nitrogen or air) at 3 atm pressure. The pressure makes the voids small by compression and reduces ionization. Because of the good thermal characteristic and high dielectric strength of SF_6, it is preferred for insulating cables.

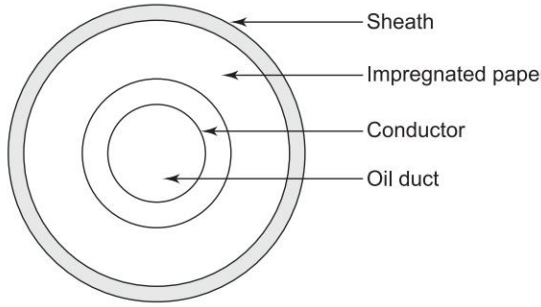

Fig. 16.2 Oil-filled cable

Gas pressure cable are mainly of two types, namely, impregnated-gas-pressure cables and gas-filled cables. A three-in-one earthed enclosure, filled with SF_6 gas is less costly as compared to the rigid isolated phase construction. Disc-type spacers [Fig. 16.3(a)] or column type spacers [Fig. 16.3(b)] may be used. A rigid tripolar compressed-gas insulated (C.G.I.) cable is shown in Fig. 16.3. Gas is maintained at a pressure of about 1.38 MN/m^2.

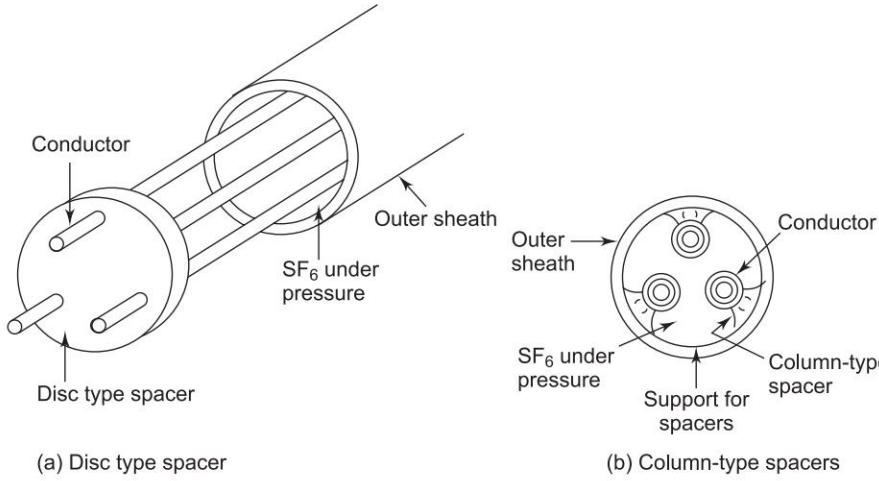

Fig. 16.3 Rigid tripolar C.G.I. cables

Flexible C.G.I cable has the advantages of a flexible form of a spacer cable. Another development which is promising is the use of two or more subconductors per phase. Development of a cable with lapped polyethylene pressurized with SF_6, has also been reported.

One advantage of the gas-filled cable is its better head dissipation by natural convection in the gas. More revolutionary are the cables incorporating cryogenic coolants. An alternative to the superconducting cable is the resistive operation of an Al or Cu conductor at *cryogenic temperatures*. Such a cable is called *cryoresistive*.

Oil filled and gas filled cables are used in the range of 132 kV to 500 kV. SF_6 filled cables can be used for transporting thousands of MVA even at UHV whereas conventional cables are confined to 1000 MVA and 500 kVA.

XLPE Cables (Cross Linked Polythene Cables)

Low density polythene, when vulcanized under controlled conditions results in cross linking of carbon atoms and produces cross-linked polythene. This new material has extremely high melting point with light weight, small dimension, low dielectric constant and high mechanical strength.

XLPE cable has high maximum continuous temperature rating of 90°C with dielectric strength of 20 kV/cm. Due to high temperature withstand capability and very low moisture absorption, these cables can be directly laid on soil bed and are suitable upto 33 kV.

Cables for HVDC Transmission

Due to absence of periodic charging current in HVDC system, cables play an effective role in DC transmission links. The dielectric loss is also low. There is no limitation of distance of transmission as there is no periodic charging current.

16.3 CAPACITANCE OF SINGLE-CORE CABLE

In a single-core cable, the conductor is surrounded by the dielectric material with an outer metallic sheath as shown in Fig. 16.4. The dielectric is stressed to about 1/5th of the breakdown value. It is easy to visualize that in this type of construction, the electric field is confined to the space between the conductor and the sheath, and has circular symmetry.

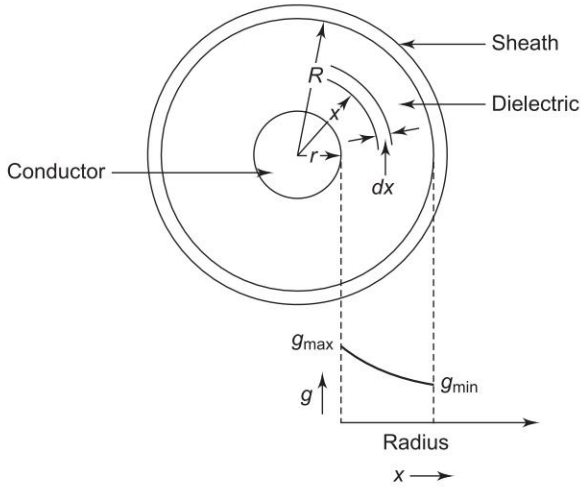

Fig. 16.4 Electric stress in a single-core cable

Let r be the radius of the conductor, R the inner radius of the sheath, k the permittivity of the dielectric, q the charge in c/m of axial length, V the potential of the conductor with respect to the sheath and g the electric field intensity (gradient) at a distance x from the centre of the conductor within the dielectric material.

$$g = \frac{q}{2\pi kx} \text{ V/m} \tag{16.1}$$

Now

$$V = \int_r^R g \cdot dx = \int_r^R \frac{q}{2\pi kx} dx = \frac{q}{2\pi k} \ln \frac{R}{r} \tag{16.2}$$

and the capacitance between core and sheath is

$$c = \frac{2\pi k_0 k_r}{\ln R/r} \text{ F/m} \tag{16.3}$$

From Eqs (16.1) and (16.2),

$$g = \frac{V}{x \ln R/r} \tag{16.4}$$

The maximum electric stress in the cable dielectric will occur at the surface of the conductor, i.e. at $x_{min} = r$ and is given by

$$g_{max} = \frac{V}{r \ln R/r} \tag{16.5}$$

and the gradient is minimum at $x_{max} = R$, i.e.

$$g_{min} = \frac{V}{R \ln R/r} \tag{16.6}$$

and

$$g_{max}/g_{min} = R/r \tag{16.7}$$

In order to keep a fixed overall size of the cable (R) for given V, there is a particular r which minimizes g_{max}, i.e. we have to maximize $r \ln R/r$, which occurs when $\ln R/r = 1$ or $R/r = e = 2.71882$.

Since the insulation can only be stressed to its limiting operating voltage gradient at the conductor surface, and is understressed as we move away from the conductor, it is advantageous to try to have a more uniform stress distribution across the dielectric. This will minimize the quantity of insulation (dielectric) needed for a given r and operating cable voltage. This technique is known as grading of cables.

16.4 GRADING OF CABLES

As stated above, in a cable with single homogeneous layer of insulation, much of the dielectric is being operated at a very much less than the maximum

allowable stress. The grading of cables means the subdivision of a cable in such a way that ($g_{max} \sim g_{min}$) is minimized, with the result that less dielectric is required and overall dia ($2R$) is reduced. It must be mentioned here that there is little application of methods of grading because of constructional reasons. However, we discuss them briefly here to illustrate important basic principles. There are two methods of grading.

Capacitive Grading

Here we use two or more insulating materials with those having the larger permittivities nearer to the conductor.

We know

$$g = \frac{q}{2\pi k_0 k_r x}$$

If the permittivity k_r could be varied continuously at different radii x in such a fashion that

$$k_r \frac{1}{x} = \frac{m}{x} \quad \text{(say)}$$

then for any x

$$g = \frac{q}{2\pi k_0 m} = \text{a constant}$$

An infinite gradation in k is, however, impossible, but practically two or three dielectrics with different values of k_r may be used.

Let there be three layers of dielectric of outer radii r_1, r_2 and R and of dielectric strength k_1, k_2 and k_3 as shown in Fig. 16.5.

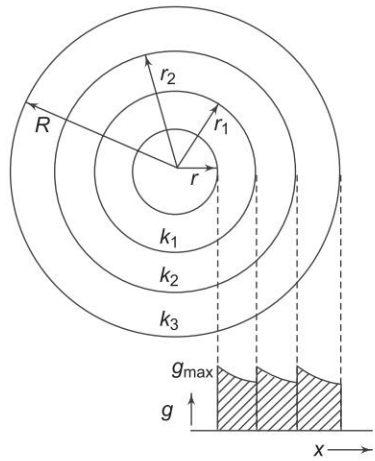

Fig. 16.5 Capacitive grading and voltage distribution

Let the dielectric strengths of the three materials be G_1, G_2 and G_3, respectively with the same factor of safety.

Gradient at $x = r$ is

$$\frac{q}{2\pi k_1 r} = \frac{G_1}{f}$$

Gradient at $x = r_1$ is

$$\frac{q}{2\pi k_2 r_1} = \frac{G_2}{f}$$

Gradient at $x = r_2$ is

$$\frac{q}{2\pi k_3 r_2} = \frac{G_3}{f}$$

where f = factor of safety.

From these three relations we get

$$q = 2\pi k_1 r \frac{G_1}{f} = 2\pi k_2 r_1 \frac{G_2}{f} = 2\pi k_3 r_2 \frac{G_3}{f}$$

or

$$k_1 r G_1 = k_2 r_1 G_2 = k_3 r_2 G_3$$

Since $r < r_1 < r_2$,

$$k_1 G_1 > k_2 G_2 > k_3 G_3 \tag{16.8}$$

This clearly shows that the material with the highest product of dielectric strength and permittivity should be placed nearest to the conductor, and other layers should be in the descending order of the product of dielectric strength and permittivity.

The second alternative is to subject all the materials to the same maximum stress.

Then

$$g_{max} = \frac{q}{2\pi k_1 r} = \frac{q}{2\pi k_2 r_1} = \frac{q}{2\pi k_3 r_2}$$

$$\therefore \quad k_1 r = k_2 r_1 = k_3 r_2$$

$$\therefore \quad k_1 > k_2 > k_3$$

The dielectric material with highest permittivity should be kept nearest to the conductor and so on.

Total operating voltage of the cable if g_{max} is the working stress (see Fig. 16.4)

$$V = g_{max} r \ln \frac{r_1}{r} + g_{max} r_1 \ln \frac{r_2}{r_1} + g_{max} r_2 \ln \frac{R}{r_2}$$

$$= g_{max}\left[r \ln \frac{r_1}{r} + r_1 \ln \frac{r_2}{r_1} + r_2 \ln \frac{R}{r_2}\right] \text{ V} \qquad (16.9)$$

Intersheath Grading

Here a single insulating material, i.e. homogeneous dielectric is separated into two or more layers by thin metallic intersheaths maintained at the appropriate potentials by being connected to tappings on the winding of an auxiliary transformer supplying the cable as shown in Fig. 16.6.

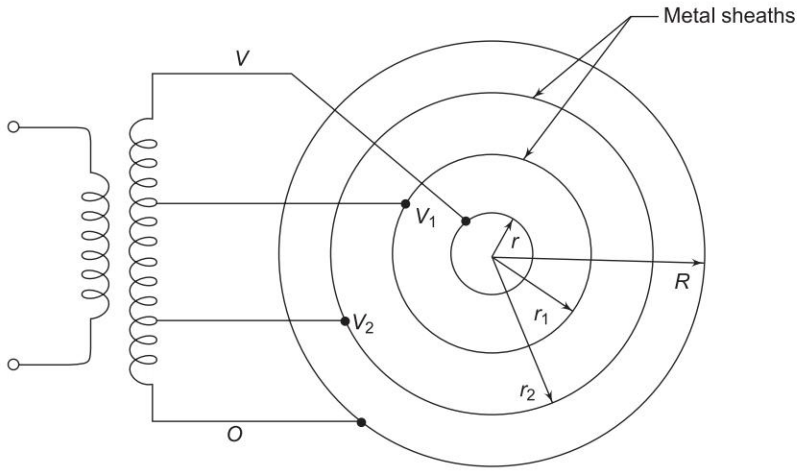

Fig. 16.6 Intersheath grading

There is thus a definite potential difference between the inner and outer radii of each sheath. Each sheath can, therefore, be considered as a homogeneous single-core cable. Let the various radii be r, r_1, r_2, ..., R as before. We can then write

$$g_{max\,1} = \frac{V_1}{r \ln r_1/r}, \; g_{max\,2} = \frac{V_2}{r_1 \ln r_2/r_1} \text{ and so on.}$$

But the condition of a homogeneous dielectric requires

$$g_{max\,1} = g_{max\,2} = g_{max\,3} = \ldots$$

or

$$\frac{V_1}{r \ln r_1/r} = \frac{V_2}{r_1 \ln r_2/r_1} = \ldots$$

We also have the condition (since all voltages are in phase)

$$V = V_1 + V_2 + V_3 + \ldots$$

If all the n layers have the same thickness t

$$\frac{V_1}{r \ln \frac{r+t}{r}} = \frac{V_2}{(r+t) \ln \frac{r+2t}{r+t}} = \ldots = \frac{V}{M} \tag{16.10}$$

where

$$M = r \ln \frac{r+t}{r} + (r+t) \ln \frac{r+2t}{r+t} + \ldots + [r + (n-1)t] \ln \frac{r+nt}{r+(n-1)t}$$

$\therefore$ Peak voltage across the mth layer for uniform g_{max} is

$$\therefore \quad V_m = \frac{V}{M}[r + (m-1)t] \ln \frac{r+mt}{r+(m-1)t} \tag{16.11}$$

Now let us consider a cable with one intersheath only. Let r and R be radii of core and outside of dielectric as earlier. Let r_1 be the radius of the intersheath as shown in Fig. 16.7.

$$g_{max} = \frac{V_1}{r \ln r_1/r} = \frac{V_2}{r_1 \ln R/r_1}$$

$$V_2 = V - V_1$$

$$\therefore \quad g_{max} r_1 \ln \frac{R}{r_1} = V - g_{max}\, r \ln \frac{r_1}{r}$$

$$\therefore \quad g_{max} = \frac{V}{r_1 \ln \frac{R}{r_1} + r \ln \frac{r_1}{r}}$$

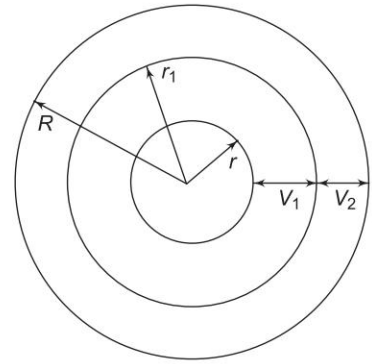

Fig. 16.7 One intersheath cable

To find the optimum placing of an intersheath,

$$\frac{d\, g_{max}}{d\, r_1} = 0$$

which gives

$$\frac{r_1}{r} \ln \frac{r_1}{r} = 1$$

Solving,

$$r_1 = 1.76\, r$$

$$\therefore \quad g_{max} \text{ for optimum } r_1 = \frac{V}{1.33r}$$

For a nonintersheath cable, the corresponding optimal condition is

$$g'_{max} = \frac{V}{r \ln R/r} = \frac{V}{r \ln e} = \frac{V}{r}$$

Hence for the same overall dimensions, the use of single intersheath has raised the maximum voltage the cable can withstand in the ratio

$$g'_{max}/g_{max} = \frac{V/r}{V/1.33r} = 1.33, \text{ an increase of } 33\%$$

The grading theory explained above is only of theoretical interset, as in practice none of the two methods are useful. Capacitance grading is difficult due to the nonavailability of materials in the different permittivities. Also with time the permittivities of the materials may change resulting in nonuniform potential gradient distribution, and may eventually lead to dielectric failure. In the case of intersheath grading, there is a possibility of damage of thin intersheath during the laying operation. The charging currents carried by the intersheaths may cause overheating. For these reasons, modern practice is to avoid grading and use instead the oil-filled and gas-filled cables.

Example 16.1 In a 66 kV lead-sheathed paper insulated cable with one intersheath, the insulating material has a permissible potential gradient of 40 kV/cm. Calculate the maximum overall diameter of the cable and the voltage at which the intersheath must be maintained. What is the economic conductor diameter and overall diameter of a similar cable with no intersheath?

Solution

Maximum stress in each layer

$$g_m = \frac{E_1}{r \log_e \frac{r_1}{r}} = \frac{E_2}{r_1 \ln \frac{r_2}{r_1}} \qquad \text{(i)}$$

For a given cable voltage E and g_m, minimum overall diameter r_2 is obtained when

$$E_1 = E/e, \quad r = \frac{E}{eg_m},$$

$$r_1 = \frac{E}{g_m} \qquad \text{(ii)}$$

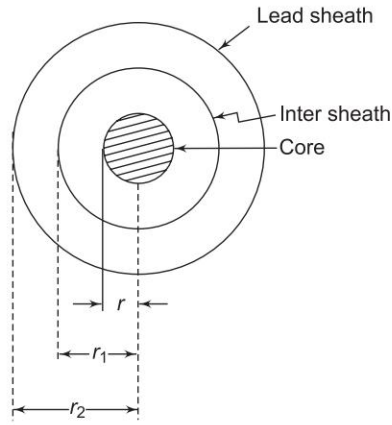

Fig. 16.8

Substituting (ii) in (i)

$$r_2 = r_1 e^{E_2/E}$$

$$g_m = 40 \text{ kV (peak)} \qquad E = 66\sqrt{2} \text{ kV (peak)}$$

From (ii)

$$40 = \frac{66\sqrt{2}}{2.718r} \qquad r = 0.86 \text{ cm}$$

$$r_1 = 0.86 \times 2.718 = 2.34 \text{ cm}$$

$$r_2 = 2.34 \times 2.718^{E_2/E}$$

$$E_2 = E - E_1$$

$$= 66 - \frac{66}{2.718} \text{ kV (rms)} = 41.7 \text{ kV}$$

$$\therefore \quad r_2 = 2.34 \times 2.718^{41.7/66} = 4.39 \text{ cm}$$

i.e. minimum overall diameter of the intersheathed cable 8.78 cm

For a similar cable with no intersheath

r = conductor radius, R = overall radius

For most economical conductor

$$\frac{R}{r} = e = 2.718$$

$$E = g_m r \ln R/r = g_m r$$

$$r = \frac{E}{g_m} = \frac{66\sqrt{2}}{40} = 2.33 \text{ cm} \quad \therefore \quad \textit{conductor dia} = 4.66 \text{ cm}.$$

$$R = 2.33 \times 2.718 = 6.33 \text{ cm}$$

$$\textit{overall dia} = 12.66 \text{ cm}$$

Example 16.2 The inner diameter of the lead sheath of a single-core cable is 10 cm, and the cable is to be used in a 3 phase 66 kV circuit. The permittivity of the dielectric is 4.5 Derive an expression for the voltage gradient at the surface of the conductor and determine the value of the conductor diameter which will minimize this voltage gradient. Using this diameter, determine the max voltage gradient and capacitance/km.

Solution

Reader is advised to see the text (Eqs 16.1 to 16.5) for the derivation.

In order to keep a fixed overall size of the cable (R) for given V, there is a particular 'r' which minimizes g_{max} i.e. we have to maximize $r \ln R/r$, which occurs when $\ln \frac{R}{r} = 1$ or $\frac{R}{r} = e = 2.71882$

$$\therefore \quad r = \frac{R}{e} = \frac{10/2}{2.71882} = 1.8390 \text{ cm}$$

Now, maximum voltage gradient will exist at conductor surface and is given by

$$g_{max} = \frac{V}{r} \Rightarrow \frac{66/\sqrt{3}}{1.839} = 20.6 \text{ kV/cm}$$

Capacitance/km $= 2\pi k_0 k_r$ F/m $= 2\pi \times 8.85 \times 10^{-12} \times 4.5 \times 10^{-6} \times 10^3$

$= 0.25 \ \mu$F/km

Example 16.3 For the cable with one intersheath shown in Fig. 16.9, obtain the condition under which the maximum values of the electric fields in the two regions are equal.

Solution

For conductor charge of q/m the electric field at radius x is given by

$$E = \frac{Q}{2\pi kx}$$

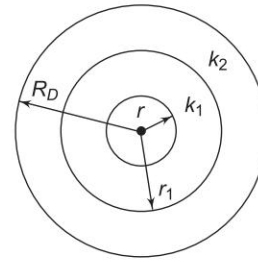

Fig. 16.9

In region 1 the electric field is maximum at $x = r$, surface of the conductor. In region 2 it is at the surface of the intersheath. The condition for the fields to be equal is

$$\frac{Q}{2\pi k_1 r} = \frac{Q}{2\pi k_2 r_1}$$

or $$k_1 r = k_2 r_1$$

Since $$r < r_1, \ k_1 > k_2$$

which means the dielectric constant of insulation closer to the conductor should be higher than the dielectric constant of the outer insulation.

Example 16.4 A single core cable, consisting of 1 cm diameter cable inside a 2.8 cm diameter sheath, is 20 km long and operates at 13 kV and 50 Hz. The relative permittivity of the dielectric is 5, and the open circuit power factor of the cable is 0.08. Calculate the capacitance of the cable and its charging current.

Solution

$$\mu = \frac{2\pi k_0 k_r}{\ln(R/r)} = \frac{2 \times \pi \times 8.854 \times 10^{-12} \times 5}{\ln(2.8/1)}$$

$= 0.270 \ \mu$F/km

Cable capacitance $C = 0.27 \times 20 = 5.4 \ \mu$F

Charging current $= \omega CV$

$= 2 \times \pi \times 50 \times 5.4 \times 10^{-6} \times 13 \times 10^3$

$= 22.05$ A

16.5 POWER FACTOR AND HEATING OF CABLES

For a single-core cable the insulation resistance is given by

$$R_i = \frac{\rho}{2\pi l} \ln \frac{R}{r} \ \Omega \tag{16.12}$$

Here ρ is the specific resistance of the material, and l length of the cable. Assuming ρ to remain constant, the impressed voltage V will send a current (in phase with V) through the insulation.

Capacitive current drawn from the supply = ωCV

where C is the cable capacitance.

The charging current leads V by 90°. The phasor diagram is shown in Fig. 16.10. The resultant current I leads V by ϕ ($\approx 90°$) where cos ϕ gives the power factor of the cable. But

$$\begin{aligned} \cos \phi &= \cos (\pi/2 - \delta) \\ &= \sin \delta \\ &= \delta \quad (\because \delta \text{ is very small}) \\ &= \tan \delta \end{aligned}$$

The cable power factor can be expressed as

$$\text{pf} = \delta = \frac{V / R_i}{\omega CV} = \frac{1}{\omega C R_i} \tag{16.13}$$

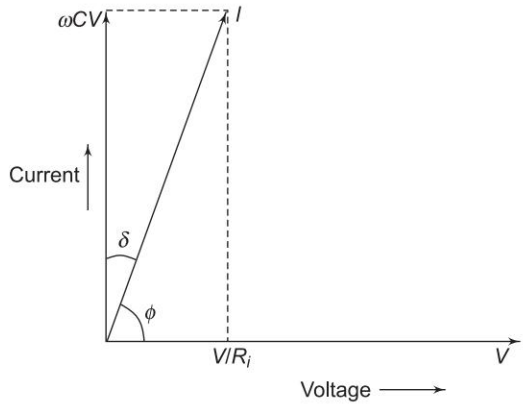

Fig. 16.10 The phasor diagram

Dielectric Loss

The breakdown of a cable may be owing to thermal or mechanical and electrical causes. Thermal breakdown is due to a rise in temperature owing to the losses in the cables, i.e. core loss (I^2R), dielectric loss and sheath loss. These losses cause heating of cables.

Dielectric loss is caused by dielectric absorption or polarization. It is small for voltages upto 33 kV, but for higher voltages has an increasingly important effect on the current rating. The cable is a sort of a capacitor, the phasor diagram is given in Fig. 16.10, the equivalent circuit being a parallel combination of leakage resistance R_i and a capacitance C. The loss in the dielectric is due to the loss in the equivalent leakage resistance.

$$\text{Dielectric loss} = VI \cos \delta = EI \sin \phi = EI\delta$$

But $$I = V\omega C$$

$$\therefore \quad \text{Dielectric loss} = V^2 \omega C \delta$$

$$= 2\pi f C V^2 \delta \text{ per phase at working voltage } V \qquad (16.14)$$

It is sufficient to assume that the loss occurs at conductor surface, and has to flow through the whole thermal resistance. The effect is to reduce the rated current of a 33 kV cable by about 1% and of a 400 kV cable by about 15%.

Sheath Loss

When single core cables are used for AC transmission, the current flowing through the core generates pulsating magnetic field which, linking the sheath, induces currents in it resulting in sheath losses. These are normally negligible as they are about 2% of the core losses.

Ionization

Power factor, and hence the dielectric loss, rises very steeply when ionization occurs. If voids are present due to imperfect impregnation, or as a result of the successive expansions and contractions which occur during a heating cycle, then discharges can take place. The effect of this ionization is a chemical action resulting in a gradual breakdown of the dielectric.

Stability

The term stability is used to denote the characteristic by which a cable will retain its freedom from ionization during worst conditions. Even if the cable is initially void-free (i.e. manufacturing is perfect), voids may be formed later when the heating cycle has repeated many times. The presence of voids with subsequent ionization is one of the chief causes of the deterioration of a cable dielectric.

16.6 CAPACITANCE OF 3-CORE BELTED CABLE

The expression of capacitance Eq. (16.3) is valid for circular conductor 3-core H-type cables, in which each core is separately screened or sheathed. A simple circuit of the belted cable is shown in Fig. 16.11. Since the conductor section is normally not circular, and conductors are not grounded by homogeneous

insulation of known permittivity, the capacitances C_c between cores and C_s between a core and sheath, cannot be easily calculated and are generally obtained by measurement.

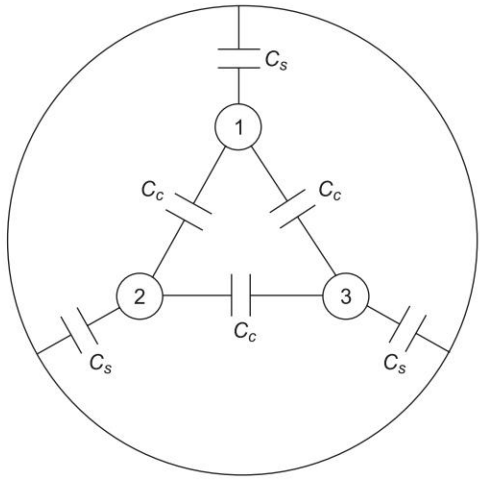

Fig. 16.11 Capacitances between cores and to sheath of a 3-core belted cable

The effective capacitances of each core to be earthed neutral is $C = (C_s + 3C_c)$ as shown in Fig. 16.12. To find C_s and C_c, two measurements are required.

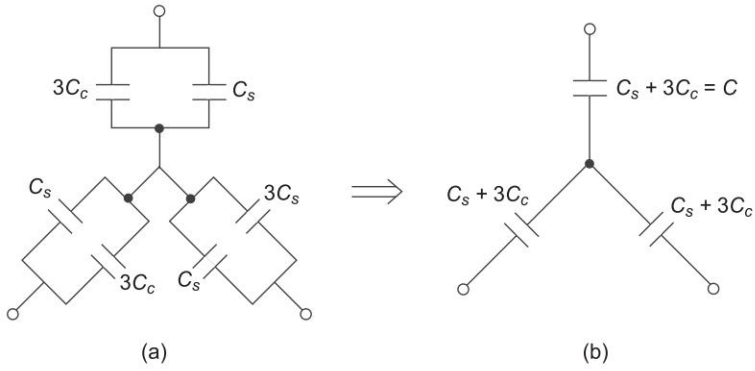

Fig. 16.12 Equivalent capacitance of a 3-core cable

(i) The capacitance between the three cores bunched together, and the sheath.
Let this be C_a given by $C_a = 3\ C_s$ as shown in Fig. 16.13.

(ii) The capacitance between any two cores bunched with sheath and the remaining core. Let this be C_b given in Fig. 16.14.

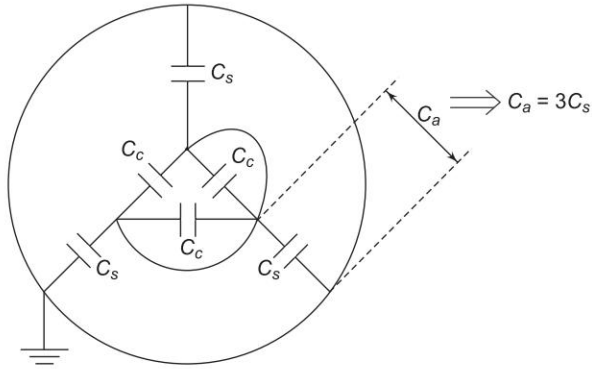

Fig. 16.13 Capacitance calculation between core and sheath (C_s)

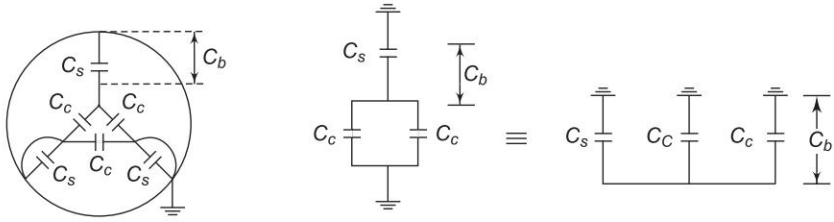

Fig. 16.14 Capacitance calculation between core (C_c)

From these two measurements

$$C_s = \frac{C_a}{3}$$

and

$$C_c = \frac{1}{2}(C_b - C_s)$$

$$= \frac{1}{2}\left[C_b - \frac{C_a}{3}\right]$$

From these values, the effective capacitance to neutral is:

$$C = C_s + 3C_c$$

$$= \frac{C_a}{3} + \frac{3}{2}\left(C_b - \frac{C_a}{3}\right)$$

$$\Rightarrow \quad \frac{C_a}{3} + \frac{3C_b}{2} - \frac{C_a}{2} \quad \Rightarrow \quad \frac{3C_b}{2} - \frac{C_a}{6}$$

$$= \frac{9C_b - C_a}{6} \qquad (16.15)$$

Example 16.5 The capacitance of the 3-core cable belted are measured and found to be as follows:

(i) between 3-cores bunched together and the sheath 10 μF.
(ii) between conductor and other two connected together to the sheath 6 μF.

Calculate the capacitance to neutral and the total charging kVA when the cable is connected to a 11 kV, 50 Hz 3-phase supply.

Solution

Here, $C_a = 10\ \mu F$

$C_b = 6\ \mu F$

$\therefore$ The effective capacitance to neutral

$$C = \frac{9C_b - C_a}{6}$$

$$\Rightarrow \frac{9 \times 6 - 10}{6} \Rightarrow 7.33\ \mu F$$

The total charging kVA = ωCV^2

$$\Rightarrow 2 \times \pi \times 50 \times 7.33 \times 10^{-6} \times (11 \times 10^3)^2$$

$$\Rightarrow 278.496 \text{ kVA}$$

16.7 D.C. CABLES

The losses in a DC cable are less than those with AC because, for a DC cable (1) there is no skin effect, (2) dielectric loss is small, since it is only due to leakage current, and (3) sheath losses are small as they are only due to leakage and ripple currents so that cross-bonding (similar to transposition in an overhead line case) equipment is not required. Further, there is no continuous charging current so that shunt compensation (reactors at the supply and load end of the cable) is not required. Due to these factors, the current carrying capacity is increased for DC by about 15% so that more power can be transmitted. DC cables are now available upto ±600 kV.

Joints and Terminations

The maximum length between joints is determined by the size of the reel or drum; for most cable circuits several lengths must be joined. At high voltages the design of the joint is complex and critical, especially as the splice must be applied by hand in situ and hence does not possess the electric strength of the cable insulation because of the presence of moisture. Both from an electrical and thermal standpoint, the joint represents a crucial part of a cable system.

16.8 SUMMARY

Various types of cables including oil and gas filled, HVDC are described in this chapter. Grading of cables is discussed in detail. Measurement of capacitance of cables is also given.

Problems

16.1 A 33 kV, three-phase 50 Hz underground feeder 4.5 km long, uses three single core cables. Each cable has a conductor diameter of 2.0 cm and the radial thickness of insulation is 0.8 cm. The relative permittivity of dielectric is 2.9. Calculate (i) capacitance of the cable per phase, (ii) charging current per phase, (iii) total charging kVAR, (iv) dielectric loss per phase if power factor of the unloaded cable is 0.025, (v) maximum stress in the cable.

16.2 The capacitances per kilometer of a three wire cables are 0.80 μF between the three bunched conductors and the sheath, and 0.35 μF between one conductor and the other two connected to the sheath. Determine the line to ground capacitance of a 30 km length of line.

16.3 Prove that for the same dimensions an insulating cable with an intersheath can withstand a working voltage 33% higher than a non-intersheath cable. Make suitable assumptions.

16.4 Find the minimum internal sheath diameter of a single core lead covered cable designed for 66 kV to earth. Its conductor diameter is 1.5 cm and three insulating materials *X*, *Y* and *Z* having relative permittivities of 3.5, 3 and 3.5 and peak permissible stress of 70.3, 55.5 and 61 kV/cm, respectively, are used.

References

Books

1. Anla, C.G. and A.F. Corry, 'Underground Transmission in the United States, *IEEE Spectrum*, Mar. 1970.
2. Barnes, C.C., *Electric Cables*, Pitman, London, 1964.
3. Cotton, H. and H. Barber, *The Transmission and Distribution of Electrical Energy*, 3rd edn, The English Universities Press, London, 1970.
4. *Electrical Transmission and Distribution Reference Book*, Westinghouse Electric Corp. Pennsylvania, 1964.
5. Guile, A.E. and W. Paterson, *Electrical Power Systems*, vol. 1, 2nd edn, Pergamon, Oxford, 1977.

6. King, S.Y. and N.A. Halfter, *Underground Power Cables*, Longman, London, 1982.
7. *Underground Systems Reference Book*, Edison Electric Institute, 1957.
8. Weedy, B.M. and B.J. Cory, *Electric Power Systems*, 4th edn, Wiley, N.Y. 1998.
9. Weedy, B.M., *Underground Transmission of Electric Power*, John Wiley, 1980.

Papers

10. Indulkar, C.S., P. Kumar and D.P. Kothari, Sensitivity Analysis of Modal Quantities for Underground Cables, *IEE Proc*., vol. 128, pt. C., no. 4, July 1981, pp. 229–234.
11. Indulkar, C.S., P. Kumar and D.P. Kothari, Modal Propagation and Sensitivity of Modal Quantities in Crossbonded Cables, *IEE Proc*., vol. 130, pt. C., no. 6, Nov. 1983, pp. 278–284.
12. Indulkar, C.S., M. Patrick and D.P. Kothari, Sensitivity Analysis of the Ampacities, Cable and System Losses of 135 kV Pipe Type Cable Systems, *Int. J. of Electric Machines and Power Systems*, vol. 13, no. 2, 1987, pp. 87–101.
13. Whitehead, S. and E.E. Hutchings, Current Ratings of Cables for Transmission and Distribution, *IEE*, vol. 83, 1938.
14. *EPRI's Underground Transmission Systems Reference Book.*

Chapter 17
Insulators for Overhead Lines

17.1 INTRODUCTION

Overhead lines are suspended from insulators, which in turn are supported by towers or poles. The span between two towers is dependent on the allowable sag in the line (span is normally 370 – 460 m). The successful operation of a transmission system mainly depends on the proper maintenance of the line insulation, and hence, on selection of suitable insulators which are normally made of either glazed porcelain or toughened glass. Insulators are designed and manufactured for a certain voltage range. The maximum voltage per insulator is about 33 kV. The types of insulator used for overhead lines are described below.

17.2 TYPES OF INSULATORS

(1) Pin-type insulators
(2) Suspension-type insulators
(3) Strain-type insulators

Pin-type insulators are made in one piece upto 25 kV, and above that voltage range, in more than one pieces. They are used for upto 50 kV only, since they become uneconomical for higher voltages. The pin-type insulator is shown in Fig. 17.1. It is seen from the diagram that the conductor is supported on the top of the insulator.

Suspension insulators are made in the form of discs, and a number of them are used together in a flexible string for the voltage range desired, the conductor being attached to the lower end. A typical suspension type insulator is shown in Fig. 17.2. For 400 kV lines, 19 discs of overall length 3.84 m are used. Owing to the capacitances existing between the discs, conductor, and tower and owing to the proximity of supporting structure, the distribution of voltage along the insulator string is not uniform, the disc (line unit) nearest the conductor being the most stressed. The advantage of using suspension type insulators on HV lines is that the working voltage can be increased at a small cost by adding extra insulator units.

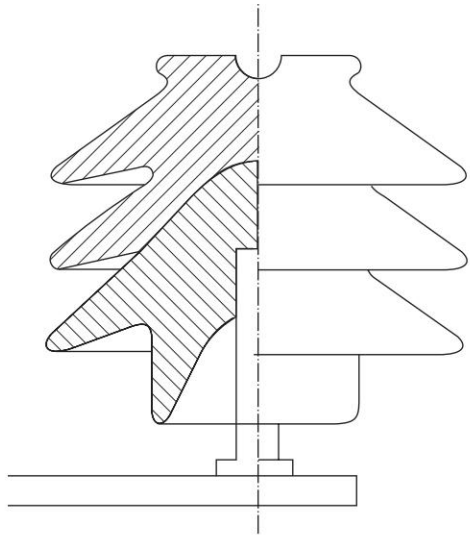

Fig. 17.1 A typical pin type insulator

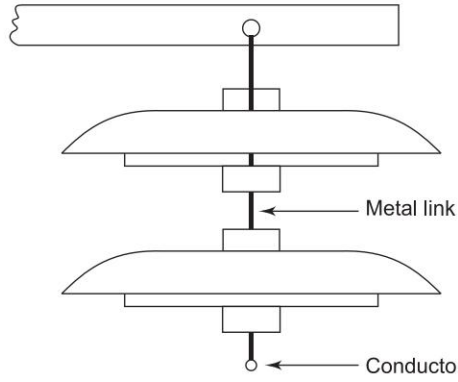

Fig. 17.2 A typical suspension type insulator

When a string of suspension insulators is used in a horizontal position, they can take the tension off the conductors also and, when used in such a position, are known as *strain insulators*. They are used at the line terminals or at the anchor towers where lines are dead ended, or at road or river crossings. Upto 11 kV *shackle* insulators are used for this purpose.

17.3 POTENTIAL DISTRIBUTION OVER A STRING OF SUSPENSION INSULATORS

As stated earlier, voltage does not divide equally across the various units of a string insulator. The capacitance between the metal parts of the insulators and the tower structure is the main reason for this. These capacitances could be

made very small by increasing the distance between the insulators and the tower, necessitating lengthier cross arms; but this is not economical. The capacitance of each unit is known as mutual capacitance. Figure 17.3 shows an equivalent circuit of a string of four identical insulator units (the capacitances between line conductor and metal work between insulators, being small, is ignored).

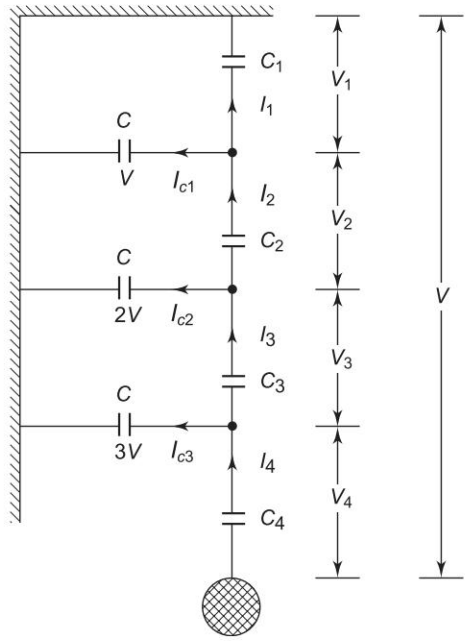

Fig. 17.3 Potential distribution across a string of four insulators

Let

$$m = \frac{\text{capacitance per insulator}}{\text{capacitance to ground}} = \frac{mC}{C}$$

where

$$C_1 = C_2 = C_3 = C_4 = mC$$

Let V be the operating voltage (line-to-ground) and V_1, V_2, V_3 and V_4 the voltage drops across the units

$$V = V_1 + V_2 + V_3 + V_4 \tag{17.1}$$

From Fig. 17.3, we can write

$$I_2 = I_1 + I_{C1}$$

$$\omega m C V_2 = \omega m C V_1 + \omega C V_1 \ (\omega = \text{supply angular frequency})$$

or

$$V_2 = V_1 \left(\frac{1+m}{m}\right) = V_1 \left(1 + \frac{1}{m}\right) \tag{17.2}$$

Also

$$I_3 = I_2 + I_{C2}$$

$$\omega m C V_3 = \omega m C V_2 + \omega C (V_1 + V_2)$$

Substituting for V_2 from Eq. (17.2) and simplifying, we get

$$V_3 = V_1 \left(\frac{m^2 + 3m + 1}{m^2} \right) = V_1 \left(1 + \frac{3}{m} + \frac{1}{m^2} \right) \tag{17.3}$$

Similarly V_4 can be expressed in terms of V_1 as follows:

$$V_4 = V_1 \left(\frac{m^2 + 3m + 1}{m^2} + \frac{3m^2 + 4m + 1}{m^3} \right)$$

$$= V_1 \left(1 + \frac{6}{m} + \frac{5}{m^2} + \frac{1}{m^3} \right) \tag{17.4}$$

V_1 can be expressed in terms of V and from this V_2, V_3 etc. can be obtained. Normally the value of $m > 1$. Let $m = 5$. Then

$$V_2 = 1.2V_1, \quad V_3 = 1.64V_1, \quad V_4 = 2.408V_1$$

This clearly shows that

$$V_1 < V_2 < V_3 < V_4$$

Thus the lowermost (line) unit is fully stressed or utilized. As 'm' increases, the division of voltage becomes more equalized. String efficiency is a measure of the utilization of material in the string and is defined as

$$\text{String efficiency} = \frac{\text{voltage across string}}{n \times \text{voltage across the unit adjacent to line}}$$

when n = total number of insulators in a string.

String efficiency is also defined as

$$= \frac{\text{SOV for the string}}{n \times \text{SOV of one disc}}$$

where SOV = the spark over voltage

If $V = 60$ kV, $m = 5$, then

$$V = V_1(1 + 1.2 + 1.64 + 2.408) = 6.248V_1$$

$$V_1 = 9.6 \text{ kV}, \; V_2 = 11.5 \text{ kV}, \; V_3 = 15.8 \text{ kV}, \; V_4 = 23.1 \text{ kV}$$

$$\eta = \frac{60}{4 \times 23.1} = 63.8\%$$

17.4 METHODS OF EQUALIZING POTENTIAL

The methods of equalizing potential are as under:

Selection of *m*

Performance of the string is dependent on the value of m, and as m is increased (by increasing length of cross arm which reduces C) the division of voltage becomes more equalized. But as stated earlier beyond a certain value of m, say $m = 10$, it is uneconomical.

Grading of the Units

Since the voltage for a given current is inversely proportional to the capacitance, the unit nearest to the cross arm should have the maximum capacitance in order to reduce the voltage across it. Further, as we move towards the power conductor the unit capacitance should progressively increase. By correct grading of the capacitances, complete equality of voltage can be achieved. This is called capacitance grading as shown in Fig. 17.4. Here, as before, we ignore the capacitance between the metal work and the power conductor. Let ground capacitances be C while mutual capacitances are C_1 to C_4 for a four insulator string.

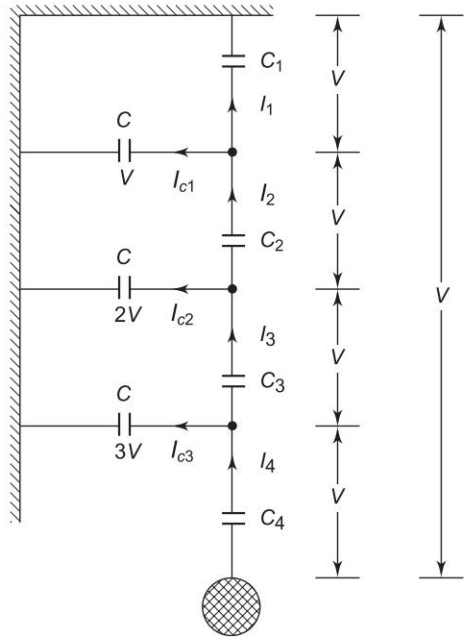

Fig. 17.4 Capacitance grading over a string of four insulators—unequal capacities

From Fig. 17.4, we can write

$$I_2 = I_1 + I_{c1} = \omega v(C + C_1) = \omega v C_2$$

or

$$\omega v(C_1 + C_2) = \omega v C_2$$

$$\therefore \quad C_2 = C + C_1 \tag{17.5}$$

Voltage producing I_{c2} is $2v$

$$I_{c2} = 2\omega\, Cv$$

Now

$$I_3 = I_{c2} + I_2$$

or

$$\omega C_3 v = 2\omega Cv + \omega(C + C_1)v$$

$$\therefore \quad C_3 = 3C + C_1 = C_1 + (1 + 2)C \tag{17.6}$$

Thus we can write capacity for the nth unit as

$$C_n = C_1 + (1 + 2 + 3 + \ldots + \overline{n-1})C \tag{17.7}$$

If $C_1 = 5C$, then

$$C_2 = 6C, \quad C_3 = 8C, \quad C_4 = 11C \text{ and so on}$$

From this, it is clear that if the capacitance of one unit is fixed, the capacitance of other units can be determined for equal distribution of voltage across the units of the string. This, however, requires units of different capacities, which is uneconomical and impractical and, therefore, this method is usually not employed except for very high voltage lines, where the string is graded in groups, may be two/three.

Static Shielding

The voltage distribution is equalized in this method by providing grading, or guard ring, in the form of a large metal ring surrounding the bottom unit and connected to the metal work at the bottom of this unit, and therefore to the line. This ring increases the capacitances between the string metal work and the line, which in fact, were neglected in our earlier analysis. The idea, thus, is to cancel exactly the pin to tower charging currents so that the same current flows through the units of identical capacities to produce equal voltage drops across each unit as shown in Fig. 17.5.

Denoting the capacities to the shield by x, y, z, ..., we can write

$$I_2 = I_1 + I_{c1} - I_x$$

$$I_3 = I_2 + I_{c2} - I_y \text{ etc.}$$

But if the voltage is v across each unit, and all n units are identical, the currents I_1, I_2, I_3, etc. must be equal.

Hence

$$I_x = I_{c1},\ I_y = I_{c2},\ I_z = I_{c3} \text{ etc.}$$

$$\therefore \quad vC\omega = (n = 1)vx\omega$$

$$2vC\omega = (n - 2)vy\omega$$

and

$$3vC\omega = (n - 3)vz\omega$$

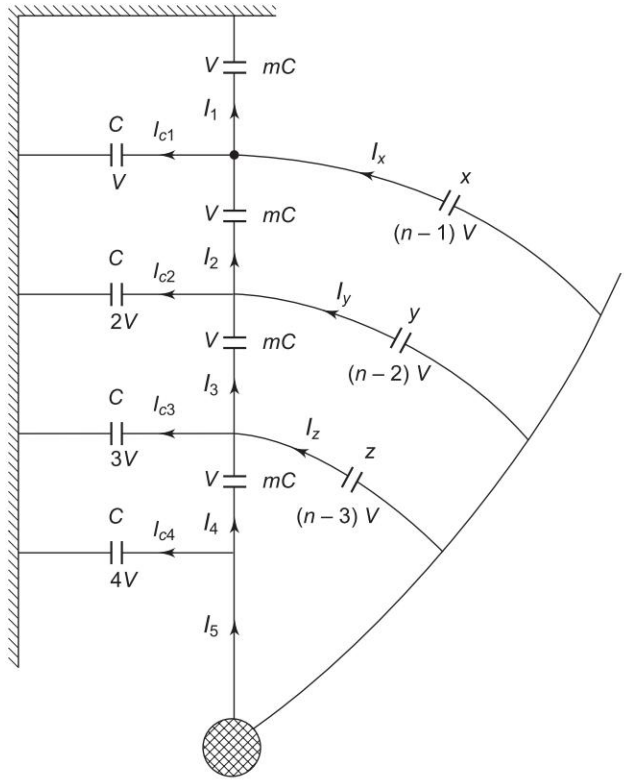

Fig. 17.5 Static shielding

which yield

$$x = \frac{C}{n-1}$$

$$y = \frac{2C}{n-2}$$

and

$$z = \frac{3C}{n-3}$$

In general, capacitance from the shield to the pth link from the top

$$C_p = \frac{pC}{n-p} \tag{17.8}$$

Remark: In practice, it is very difficult to achieve this condition; however, partial advantage can always be gained, and this method is normally used. Further, when used with arcing horn, it also protects the insulator string from flashover whenever overvoltage appears between the tower and conductor.

17.5 INSULATOR FAILURE

The failure of an insulator can be due to mechanical stresses, cracking, porosity, puncture and flashover. The failure due to mechanical stresses is very rare because defective pieces are weeded out in the routine factory tests. Cracking is due to continued action of alternate and sometimes rapidly varying heat and cold, dryness and dampness which produce high stresses on the porcelain and lead to failure. Porosity is due to under firing or other causes leads to failure because porous material absorbs water from atmosphere or cemrent and its electrical resistance decreases. A porosity test is a necessary routine factory test for insulators. The failure of an insulator by puncture is quite rare.

The most common reason of the insulator damage is the flashover of the insulator. The flashover voltage is the voltage which will cause an arc through the air surrounding the insulator. In practice insulators are often subjected to power frequency and impulse over voltages due to switching and lighting. If the overvoltage exceeds the flashover voltage of the insulator, an arc occurs between the line conductor and insulator base. As and when a flashover occurs the surrounding air is so ionized that there is virtually a follow through power arc due to system voltage, after the transient voltage has subsided. After a flashover an insulator continues to function properly unless it is shattered by the heat of the arc. For this reason insulators are often fitted with arcing horns to keep this power arc away from the insulator.

With time, the upper surface of an insulator can become damp and polluted by dirt, salt laden coastal spray, frost and fog to such an extent that these upper surfaces offer greatly reduced resistance to surface leakage current due to the system voltage. This has the effect of decreasing the voltage necessary to cause insulation flashover. The wet flashover voltage, is therefore, lower than the dry flashover voltage.

17.6 TESTING OF INSULATORS

An insulator should have good mechanical strength to withstand the load conditions. It should not have any pores or voids which may lead to breakdown. Its electrical strength should be large enough to withstand the normal voltage and usual overvoltages but the insulator should flashover at such voltages which are likely to cause damage to other equipment. The following tests are performed on the insulators:

(i) Mechanical strength, electrical insulation tests, environmental tests.
(ii) Porosity, galvanizing test
(iii) Power frequency dry flashover voltage
(iv) Power frequency wet flashover voltage
(v) Impulse voltage withstand flashover test
(vi) Puncture voltage test
(vii) Corona and radio interference test

Mechanical Tests

Tensile strength, compression test, torsional test, bending minimum test, mechanical vibration test.

Electrical Insulation Tests

The insulators are subjected to normal continuous power frequency over voltage and impulse voltage test. These voltages have different wave forms and durations.

For these standard test requirements and test procedures relevant standards are followed. For special requirements, the tests are decided jointly by customer and the supplier. The reader may refer to Sec. 13.6.

For systematizing the tests, the following categories are defined in the standards:

(i) Type tests: These are mechanical and electrical tests to prove the quality, material and mechanical properties.
(ii) Sample tests: These are mechanical tests to prove the quality, material and mechanical properties.
(iii) Routine tests: These are performed on every insulator.

Example 17.1 Calculate the string efficiency of a 3-unit suspension insulator of Fig. 17.6 if the capacitance of the link pins to earth and the line are respectively 25% and 10% of self C of each unit.

What should be the values of link pins to the line capacitance for 100% string efficiency?

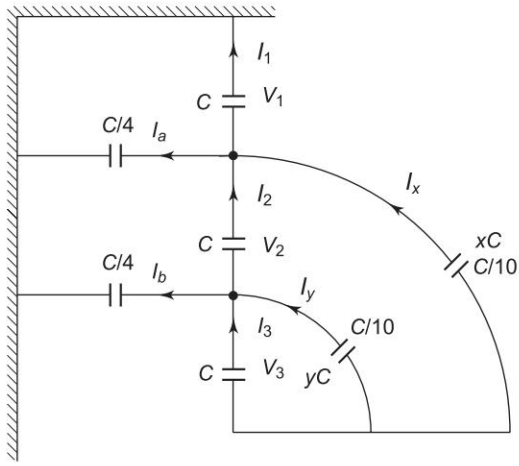

Fig. 17.6

Solution

$$I_2 = I_1 + I_a - I_x$$

$$\omega CV_2 = \omega CV_1 + \frac{1}{4}\ \omega CV_1 - \frac{1}{10}\ \omega C(V_2 + V_3)$$

ωC cancels out, on rearranging we get

$$25V_1 - 22V_2 - 2V_3 = 0 \qquad \text{(i)}$$

Similarly $I_3 = I_2 + I_b - I_y$

$$\omega CV_3 = \omega CV_2 + \frac{1}{4}\ \omega C(V_1 + V_2) - \frac{1}{10}\ \omega CV_3$$

$$5V_1 + 25V_2 - 22V_3 = 0 \qquad \text{(ii)}$$

$$V = V_1 + V_2 + V_3 \qquad \text{(iii)}$$

Solving Eqs (i), (ii) and (iii), we get

$$V_1 = \frac{466}{1809}\ \text{V},$$

$$V_2 = \frac{520}{1809}\ \text{V}$$

$$V_3 = \frac{735}{1809}\ \text{V} = 0.406\ \text{V}$$

String efficiency $\eta = \dfrac{V}{3 \times 0.406\, V} = 82.1\%$

For 100% η $V_1 = V_2 = V_3$, $I_1 = I_2 = I_3$

$$I_a = I_x$$

$$\frac{1}{4}\ \omega CV_1 = \omega xC\ 2V_1$$

$$\boxed{x = 1/8}$$

Also

$$I_b = I_y$$

$$\frac{1}{4}\ \omega C\ 2V_1 = \omega yCV_1$$

$$\boxed{y = 1/2}$$

Example 17.2 Determine the maximum voltage that the string of the suspension insulators in Fig. 17.7 can withstand if the maximum voltage per unit is 20 kV.

Solution

V_1, V_2 and V_3 are the voltages across the various units.

$$V = V_1 + V_2 + V_3$$

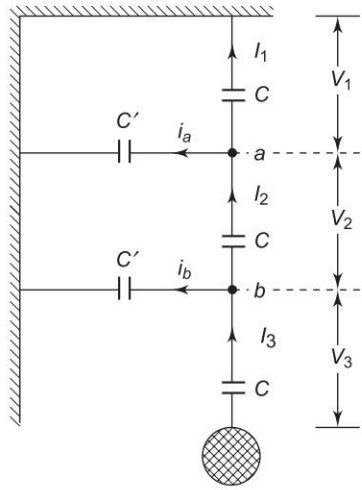

Fig. 17.7 Given $C' = C/6$

where V is withstand voltage of the string.

Applying KCL at "a"

$$I_2 = I_1 + I_a = V_1\omega C + V_1\omega C/6$$

$$V_2\omega C = \frac{7}{6}\ V_1\omega C$$

$$V_2 = \frac{7}{6}\ V_1 \qquad \text{(i)}$$

Applying KCL at "b"

$$I_3 = I_2 + I_b$$

$$V_3\omega C = V_2\omega C + (V_1 + V_2)\ \frac{\omega C}{6}$$

Substituting V_2 from Eq. (i) and simplifying yields

$$V_3 = \frac{55}{36}\ V_1 \qquad \text{(ii)}$$

The voltage V_3 across the unit near the power conductor is maximum

$$V_3 = \frac{55}{36}\ V_1 = 20 \text{ kV}$$

$$V_1 = 13.09 \text{ kV}$$

$$V_2 = \frac{7}{6}\ V_1 = 15.27 \text{ kV}$$

$$V = V_1 + V_2 + V_3 = 13.09 + 15.27 + 20$$

$$= 48.36 \text{ kV}$$

17.7 SUMMARY

The importance of insulators in power system transmission is explained along with different types of insulators, testing, string efficiency, insulation failure etc.

Problems

17.1 Each of the insulators forming a string has a self-capacitance of C Farads. The capacitance of the link pins to earth and the line are 20 C and 0.15 C respectively. Calculate the voltage across each insulator as a percentage of the line voltage to earth and also the string efficiency of the arrangement.

By how much does the string efficiency increases if a guard ring is provided increasing the capacitance to the line of the bottom most insulators to 0.35 C. Also find the redistribution of voltage caused by the guard ring.

17.2 Explain why the voltage does not divide equally across the units of a string insulator. Discuss the various methods by which the voltages across the units can be equalized and which of these methods is actually used in practice? Illustrate your answer by a string of 3-insulator units.

17.3 The potential across the 6 units of a string is equalized by using graded insulators. If the capacitance of the top insulator is 10 C and that of pin to earth is C, calculate the capacitance of the other units.

If instead of graded insulators, a guard ring is used to equalize the potential, calculate the capacitance of each link to conductor. Assume that the insulators used in the string are similar to that of the topmost unit.

References

1. Cotton, H. and H. Barber, *The Transmission and Distribution of Electrical Energy*, 3rd edn, B.I. Publishers, New Delhi, 1970.
2. Fink, D.G. and H.W. Beaty, *Standard Handbook of Electrical Engineers*, 11th edn, McGraw-Hill, New York, 1978.
3. Indulkar, C.S., *Electric Energy Systems Engineering*, Khanna, Delhi, 1976.
4. Wadhwa, C.L., *Electrical Power Systems*, 4th edn, New Age Int., New Delhi, 2005.
5. Kothari, D.P., *et al*., *Electrical Engineering*, Published by IETE (Study lessons), New Delhi, 1981.

Chapter 18

Mechanical Design of Transmission Lines

18.1 INTRODUCTION

In overhead transmission lines the conductors are supported at the towers or poles for low voltage lines). The conductors are pulled and stringing effected. When supported this way a conductor will *sag* or dip under its own weight. The distance between adjacent supporting towers is called the *span*. The conductors mechanical loading is due to its own weight (vertical load), weight of ice (vertical load) and wind load (horizontal). Under varying weather conditions of ambient temperature, the conductor tension (which is maximum near the tower ends) should not exceed the permissible limit (= breaking strength of conductor/safety factor (2–2.5)). The knowledge of maximum sag is essential in determining the ground clearance of the conductor, i.e. the least height of the conductor above ground which is 7 m for voltages more than 166 kV for a span of 300 m. The span is decided upon economic factors with due consideration to the line voltage and the conductor size. The number of towers for a given line length are determined by the span which also indirectly governs the sag and the tower height.

18.2 SAG AND TENSION CALCULATIONS

Figure 18.1 shows a conductor of weight w/unit length pulled between supports A and B with a certain tension with O as the lowest point of the conductor. The forces which act on the portion OP are the horizontal tension H at O, the tensions T_x and T_y at P and weight ws vertically downwards at the centre of the length OP.

Equating horizontal and vertical components, we get

$$H = T_x$$

$$T_y = ws$$

At point P' close to P, the direction of tension T is given by

$$\tan \psi = \mathrm{d}y/\mathrm{d}x = T_y/T_x = ws/H \qquad (18.1)$$

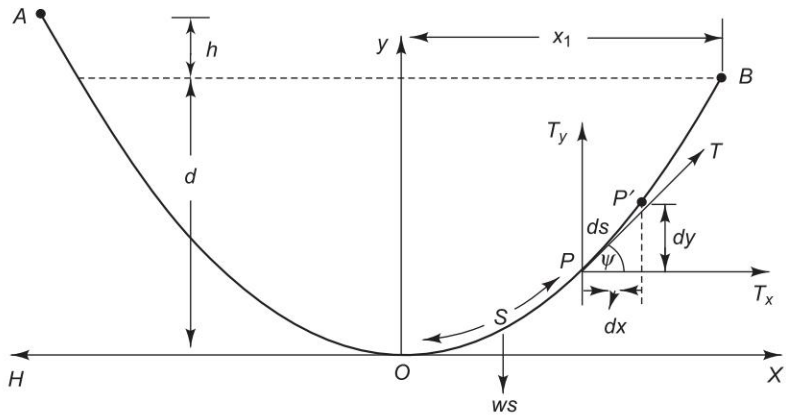

Fig. 18.1 A typical span of an overhead transmission line

Now

$$ds = \sqrt{dx^2 + dy^2}$$

or

$$\frac{ds}{dx} = \sqrt{1 + (dy/dx)^2} = \sqrt{1 + w^2 s^2 / H^2}$$

or

$$\int dx = \int \frac{ds}{\sqrt{1 + w^2 s^2 / H^2}}$$

which gives

$$x + c_1 = \frac{H}{w} \sinh^{-1}\left(\frac{ws}{H}\right);$$

where c_1 is a constant.

At the point $x = 0$, $s = 0$, $\therefore c_1 = 0$; hence

$$x = \frac{H}{w} \sinh^{-1}\left(\frac{ws}{H}\right)$$

or

$$s = \frac{H}{w} \sinh \frac{wx}{H} \tag{18.2}$$

From Eqs (18.1) and (18.2),

$$\frac{dy}{dx} = \frac{ws}{H} = \sinh\left(\frac{wx}{H}\right)$$

Integrating, we get

$$dy = \sinh \frac{wx}{H}\, dx$$

$$y = \frac{H}{w} \cosh\left(\frac{wx}{H}\right) + c_2$$

At O, $y = 0$ when $x = 0$.

$$\therefore \qquad 0 = \frac{H}{w} \cosh 0 + c_2 = \frac{H}{w} + c_2$$

or

$$c_2 = -H/w$$

Hence

$$y = \frac{H}{w}\left(\cosh \frac{wx}{H} - 1\right) \tag{18.3}$$

This is the equation of a *catenary*.

For tension at P,

$$T^2 = T_x^2 + T_y^2 = H^2 + w^2 s^2$$

$$= H^2 + H^2 \sinh^2\left(\frac{wx}{H}\right) = H^2 \cosh^2\left(\frac{wx}{H}\right)$$

or

$$T = H \cosh \frac{wx}{H} \tag{18.4}$$

Equations (18.2), (18.3) and (18.4) give the relations between the length, tension and the horizontal and vertical positions of the point P with respect to the lowest point O.

If the supports are at the same level and the span is $2l$ or half span is l, it then follows from Eq. (18.2) that the length of a line in half span is

$$S = \frac{H}{w} \sinh\left(\frac{wl}{H}\right) \tag{18.5}$$

$$y_A - y_B = \text{sag} = d = \frac{H}{w}\left(\cosh \frac{wl}{H} - 1\right) \tag{18.6}$$

and the tensions at end supports are:

$$T = T_A = T_B = H \cosh \frac{wl}{H} \tag{18.7}$$

Supports at Different Levels

If the supports are at unequal levels as shown in Fig. 18.1, and O is at a horizontal distance x_1 from B, then

$$y_B = \frac{H}{w}\left(\cosh\frac{wx_1}{H} - 1\right) \tag{18.8}$$

$$y_A = d + h = \frac{H}{w}\left(\cosh\frac{w(2l - x_1)}{H} - 1\right) \tag{18.9}$$

From Eqs (18.8) and (18.9) we get the difference in level between the supports as

$$h = \frac{H}{w}\left(\cosh\frac{w(2l - x_1)}{H} - \cosh\frac{wx_1}{H}\right)$$

$$= \frac{2H}{w}\sinh\frac{wl}{H}\sinh\frac{w(l - x_1)}{H} \tag{18.10}$$

Approximate Formulae

From Eq. (18.7)

$$\frac{T}{H} \approx 1 + \frac{w^2l^2}{2H^2} \tag{18.11}$$

From Eq. (18.3),

$$y = \frac{H}{w}\left(1 + \frac{w^2x^2}{2H^2} + \frac{w^4x^4}{24H^2} + \ldots - 1\right)$$

$$\approx \frac{wx^2}{2H} \tag{18.12}$$

$\therefore$ sag $d = wl^2/2T$ (assuming $T \approx H$)

Similarly

$$s \approx x + \frac{w^2x^3}{6T^2} \tag{18.13}$$

As $T \approx H$,

$$y = wx^2/2T \text{ (parabola)} \tag{18.14a}$$

$$d = wl^2/2T \tag{18.14b}$$

Half span conductor length, $S = 1 + w^2\, l^3/6T^2$ (18.14c)

Formulae (18.14) are quite accurate for sag < 10% of span.

Effect of Wind and Ice

The regulations insist that the effect of a thickness of 0.5 cm or more of ice may be considered. The effect of ice covering (w_i) is to increase the weight of the conductor (w_c), and thus increase the vertical sag. To guard against this, the tension on the conductors at the time of erection is suitably decreased.

If the wind pressure is also considered, the wind pressure acting on the projected area of the conductor per metre converted to load should be added to the weight. It is assumed that the wind pressure w_w acts horizontally.

Resultant weight, (pu conductor) $w = \sqrt{(w_c + w_i)^2 + w_w^2}$ (18.15)

If r is the radius of the conductor and t the radial thickness of ice, the volume of ice per unit length is

$$\pi\{(r + t)^2 - r^2\} \cdot 1 = \pi(t^2 + 2rt)$$

If ρ is the density of ice (915 kg/m^3), the weight of ice per unit length of conductor,

$$w_i = \pi\rho(t^2 + 2rt) \quad \text{kg/m} \tag{18.16}$$

The projected area/m on which wind is acting is

$$(r + t) \cdot 1 \quad \text{m}^2$$

If the wind pressure is p in kg/m^2,

$$\text{wind loading, } w_w = 2(r + t)p \quad \text{kg/m} \tag{18.17}$$

Stringing Chart

There are two factors which vary the sag and tension, viz. elasticity and temperature. Their combined effect is found in the following way. Let w_1, f_1, S_1, d_1 and θ_1 be the load per unit length, the stress (i.e. tension per mm^2), length of conductor over half span, sag and temperature at the maximum load conditions, and w_2, f_2, S_2, d_2 and θ_2 the values under stringing (erection) conditions. Let A be the area of cross section of the conductor, and α_1 the coefficient of linear expansion and E the Young's modulus.

Length of half the span under any conditions (from Eq. (18.13))

$$S = 1 + w^2 l^3 / 6\, A^2 f^2 \tag{18.18}$$

But

$$d = wl^2 / 2\, Af$$

$$\therefore \quad S = 1 + \frac{2}{3}\frac{d^2}{l} \tag{18.19}$$

The temperature rise from θ_1 to θ_2 causes an increase in half span length of $(\theta_2 - \theta_1)\alpha S \approx (\theta_2 - \theta_1)\alpha l$. At the same time, another effect of increase of temperature from θ_1 to θ_2 is the reduction in stress from f_1 to f_2.

The decrease in length due to this is

$$\left(\frac{f_1 - f_2}{E}\right) S \approx \left(\frac{f_1 - f_2}{E}\right) l$$

∴ New length,

$$S_2 = S_1 - \left(\frac{f_1 - f_2}{E}\right) l + (\theta_2 - \theta_1)\alpha l$$

but

$$S_2 = l + w_2^2 l^3 / 6 f_2^2 A^2$$

$$\therefore \quad l + \frac{w_2^2 l^3}{6 f_2^2 A^2} = l + \frac{w_1 l^3}{6 f_1^2 A^2} - \left(\frac{f_1 - f_2}{E}\right) l + (\theta_2 - \theta_1)\alpha l$$

Simplifying,

$$\frac{w_2^2 l^2 E}{6A^2} = f_2^2 \left[f_2 - f_1 + \frac{w_1^2 l^2 E}{6 f_1^2 A^2} + (\theta_2 - \theta_1)\alpha E \right] \qquad (18.20)$$

Equation (18.20) is a cubic equation in f_2, and knowing the value of f_2, d_2 can be found out as

$$d_2 = w_2 l^2 / 2 f_2 A$$

Thus it is possible to plot a graph between temperature (independent variable) and sag (dependent variable). Also f_2 or T_2 can be plotted against temperature. Figure 18.2 shows the plot of tension vs. temperature and sag vs. temperature. This is called the stringing chart.

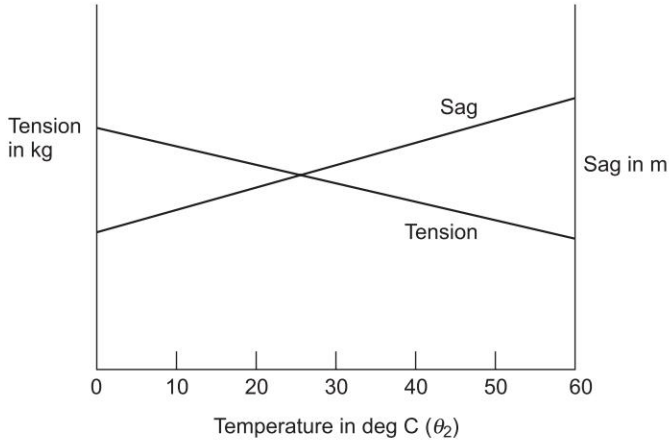

Fig. 18.2 Stringing chart

Sag Template

Two types of towers are used: (1) the standard or straight run or intermediate tower, and (2) the angle or anchor or tension tower. For normal or average

spans and for standard towers, the sag and the nature of the curve that the conductor will occupy under expected loading conditions is calculated and plotted as a template. The minimum ground clearance required can be plotted parallel to the conductor shape curve on the template. If the height of tower is standard and same, the tower footing line can also be drawn on the template as shown in Fig. 18.3, which is used for locating the position of towers so that the minimum ground clearance is maintained throughout.

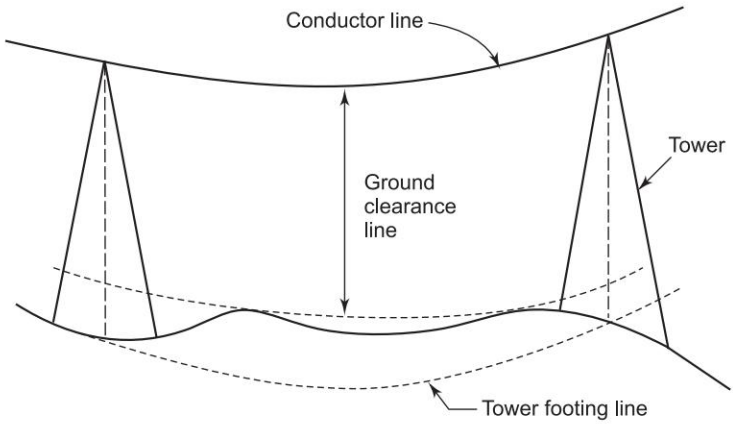

Fig. 18.3 Sag template used for locating towers

18.3 SPANS OF UNEQUAL LENGTH: RULING OR EQUIVALENT SPAN

When a line consists of unequal lengths each span should theoretically be tensioned according to its own length. However, this is not possible with suspension insulators since the insulator strings would swing so as to equalize the tension in each span. It is impractical to dead-end and erect each end span separately. However, it is possible to assume a uniform tension between dead-end supports by defining an *equivalent span*, which is called a *ruling span* (normally used for distribution lines).

If the actual spans are known, the ruling span can be calculated as

$$L_e = \sqrt{\frac{L_1^3 + L_2^3 + L_3^3 + \ldots + L_n^3}{L_1 + L_2 + \ldots + L_n}} \tag{18.21}$$

where L_e = ruling or equivalent span

L_i = each individual span in line

Also approximate ruling span is given by

$$L_e = L_{avg} + 2/3\ (L_{max} - L_{avg}) \tag{18.22}$$

where

L_{avg} = average span in line

L_{max} = maximum span in line

The line tension T can be estimated using this equivalent span length, and then the sag for each actual span can be calculated from

$$d = \frac{wl^2}{2T} \qquad (18.14b)$$

18.4 VIBRATION AND VIBRATION DAMPERS

The overhead transmission lines experience vibrations in the vertical plane and are of two types. However, if they are different than the much slower swings of conductors in the horizontal plane due to simple wind deflection are:

(i) Aeoline or Resonant vibration (high frequency 50–100 Hz and low amplitude upto 5 mm)

(ii) Galloping or Dancing of conductors (vibration) (low frequency 1–2 Hz, high amplitude 3 m).

These are normally caused by asymmetrical layers of ice formation.

In addition to the design of the clamp and accessories, the vibration problem has been solved by the use of special devices which will fall into two groups:

(a) Reinforcement or armour rods, (b) Dampers (a stock bridge damper is used).

To damp dancing of conductors (oscillations) it is required to make the conductor circular. For stranded conductors PVC tape is wrapped to make the conductor circular. Adoption of horizontal conductor configuration reduces the danger due to these vibrations.

Example 18.1 Calculate the maximum sag of a conductor having following data:

Span = 200 m, w = 0.8 kg/m,

maximum allowable tension 1600 kg.

Solution

$$T = H \cosh\left(\frac{wL}{H}\right) \approx H\left(1 + \frac{w^2l^2}{2H^2}\right)$$

or

$$\frac{T}{H} = \frac{2H^2 + w^2l^2}{2H^2}$$

$$H^2 - HT + \frac{w^2l^2}{2} = 0$$

Solving for H

$$H \approx T - \frac{w^2 l^2}{2T}$$

Substituting values,

$$H = 1600 - \frac{(0.8)^2\,(100)^2}{2 \times 1600}$$

$$= 1{,}598 \text{ kg m}$$

Example 18.2 In a transmission line, line conductor has an effective diameter of 0.0195 m, weighs 258.95 kg per 304.78 m and has an ultimate strength of 8037.18 kg. Calculate the height above ground at which a conductor with a span of 274.30 m must be supported in order that the total tension shall not exceed half the ultimate strength with a 0.0127 m radial coating of ice and a horizontal wind pressure of 39.056 kg/m^2 of projected area. The ground clearance required is 6.70, weight of 1 m^3 of ice = 953.63 kg.

Solution

The total loading is $w = 2.684$ kg/m

The maximum permissible tension $T = \frac{1}{2} \times 8037.18$

$$= 4018.59 \text{ kg}$$

$$l = 137.15 \text{ m}$$

$$d = \frac{wl^2}{2T} = \frac{2.684 \times (137.15)^2}{4018.59} = 12.50 \text{ m}$$

The more exactly $H = T - w^2 l^2 / 2T$

$$= 4018.59 - 33.55 = 3985.04$$

$$\frac{wl}{H} = \frac{2.684 \times 137.15}{3985.04} = 0.092$$

$$d = (H/w)\,[\cosh\,(wl/H) - 1]$$

$$= (3985.04/2.684)\,(\cosh\,(0.092) - 1)$$

$$= 6.349 \text{ m}$$

Height of support > 6.70 + 6.349 = 13.049

> 42′ 10″ = 43′

Safety factor = 2 (assumed)

Example 18.3 An overhead line comprises a copper conductor of 2.5 cm^2 cross sectional area and weighing 2.25 kg/m strung between the supports and equal height and 250 m apart. The conductor was strung to a tension of

3000 kg when the temperature was 20°C and there was no wind. Calculate the tension when the temperature is 0°C and the horizontal wind pressure is 1 kg/m of conductor length.

Given: $E = 1.27 \times 10^6$ kg/cm^2, $\alpha = 17 \times 10^{-6}$/°C.

Solution

$$d = \frac{wl^2}{8T}$$

$$d_1 = \frac{w_1 l^2}{8T_1} = \frac{2.25 \times (250)^2}{8 \times 3000} = 5.85 \text{ m}$$

$$\theta_1 = 20°\text{C}, \; w_1 = 2.25 \text{ kg/m}, \; T_1 = 3000 \text{ kg}$$

$$\theta_2 = 0°\text{C}, \; w_2 = \sqrt{(2.25)^2 + 1^2} = 2.46 \text{ kg/m}$$

$$T_2 = ?$$

$$d_2\left(d_2^2 - k\right) = \text{L}$$

$$\text{L} = \frac{3}{64}\frac{w_2 l^4}{AE} = \frac{3}{64} \times \frac{2.46 \times (250)^4}{2.5 \times 1.27 \times 10^6} = 142 \text{ m}$$

$$k = d_1^2 + \frac{3}{8}(\theta_2 - \theta_1)\alpha l^2 - \frac{3}{64}\frac{w_1 l^4}{AEd_1}$$

$$= \left[(5.85)^2 - \frac{3}{8} \times 20 \times 17 \times 10^{-6} \times (250)^2 - \frac{3}{64} \times \frac{2.25 \times (250)^4}{2.5 \times 1.27 \times 10^6 \times 5.85}\right]$$

$$= 34.3 - 7.5 \times 1.7 \times 0.625 - 22.2$$

$$= 4.1$$

$$d_2\left(d_2^2 - 4.1\right) = 142$$

Solving $d_2 = 5.5$ m $\quad T_2 = \frac{w_2 l^2}{8d_2} = \frac{2.46 \times (250)^2}{8 \times 5.5} = 3190$ kg

18.5 SUMMARY

In this chapter mechanical design of transmission line is described in detail. Sag and tension calculations are explained including the effect of wind and ice.

Problems

18.1 A transmission line conductor having a diameter of 19.5 mm weighs 850 kg per km. The span is 275 m. The wind pressure is 39 kg/m^2 of

projected area with ice coating of 13 mm. The ultimate strength of the conductor is 8000 kg. Calculate the maximum sag if the factor of safety is 2 and ice weighs 910 kg/m^3.

18.2 At a river crossing an overhead transmission line has a span of 600 m, with the two supports at 20 m and 100 m above water level. The weight of the conductor is 0.4 kg/m. If the tension of the conductor is adjusted to 1250 kg, determine the clearance of the conductor above water at a point 250 m from the base of the higher tower. Use approximate method.

18.3 An overhead line comprises a copper conductor of 2.5 cm^2 cross-sectional area and weighing 2.25 kg/m strung between the supports and equal height and 250 m apart. The conductor was strung to a tension of 3000 kg when the temperature was 20°C and there was no wind. Calculate the tension when the temperature is 0°C and the horizontal wind pressure is 1 kg/m of conductor length.

$$\textit{Given: } E = 1.27 \times 10^6 \text{ kg/cm}^2,\ \alpha = 17 \times 10^{-6}/^\circ\text{C}.$$

18.4 An overhead line at a river crossing is supported from two towers at height of 45.7 m and 91.4 m above water level, horizontal distance between the towers being 335.26 m. If the maximum tension is 1.93 kg and the weight per meter is 0.5. Find the clearance between the conductor and the water at a point midway between the towers.

References

1. *EHV Transmission Line Reference Book*, Edison Electric Institute, New York, 1968.
2. *Transmission Line Reference Book*, *345 kV and Above*, *EPRI*, Palo Alto, USA, 1975.
3. Cotton, H. and H. Barber, *The Transmission and Distribution of Electrical Energy*, 3rd edn, B.I. Publishers, New Delhi, 1970.
4. Starr, A.T., *Generation*, *Transmission and Utilization of Electric Power,* Pitman, 1962.
5. Woodruff, L.F., *Principles of Electric Power Transmission*, Wiley Eastern, New Delhi, 1968.
6. Turan Gönen, *Electric Power Transmission System Engineering: Analysis and Design,* John Wiley, New York, 1988.
7. Gupta, B.R., '*Power System Analysis and Design*', 3rd edn, Wheeler Publishing, 1998.

Chapter 19

Corona

19.1 INTRODUCTION

As the voltage on a line conductor system is raised beyond a certain limit, a point is reached when a pale violet glow appears on the conductor surface, together with a slight hissing noise and a smell of ozone. This phenomenon is called *corona*. The high voltages at which transmission lines operate produce electric field strengths of sufficient intensity to ionise the air near the phase conductors. The minimum potential difference required between the conductors, to start ionization, is called the *disruptive critical voltage* (V_d) for corona formation. For a visual corona the line voltage has to be somewhat higher than the disruptive critical voltage and is called *visual critical voltage* (V_v).

The potential gradient g_0 at which a dielectric, disrupts fully is called '*dielectric strength*' of the material. For air g_0 = 30 kV(max)/cm at NTP, i.e. 76 cm pressure of Hg and 25°C. The dielectric strength varies widely with the air density. The density of air at b cm (Hg) barometric pressure and t°C temperature is given by

$$\delta = \text{relative air density} = \frac{3.92\,b}{273 + t} \tag{19.1}$$

which takes into account atmospheric conditions.

19.2 CRITICAL DISRUPTIVE VOLTAGE

Consider a single-phase transmission line (Fig. 19.1). Let r_a and r_b be the radii of the conductors and D, the distance between the two conductors such that $D >> r_a, r_b$. Let q be the charge per unit length on the conductor a and hence $-q$ will be on conductor b.

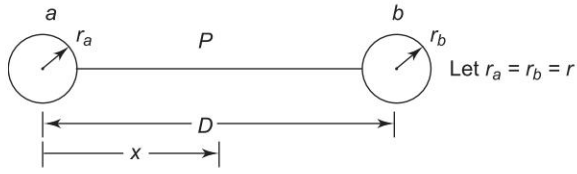

Fig. 19.1 One-phase transmission line

The electric field intensity at any point P at distance x for the centre of conductor a due to both the line charges will be

$$E_x = \frac{q}{2\pi \in_0 x} + \frac{q}{2\pi \in_0 (D-x)} = \frac{q}{2\pi \in_0}\left[\frac{1}{x} + \frac{1}{D-x}\right] \tag{19.2}$$

The potential difference between the conductors

$$V = -\int_{D-r}^{r} E_x \, dx = \int_{r}^{D-r} \frac{q}{2\pi \in_0}\left[\frac{1}{x} + \frac{1}{D-x}\right] dx$$

$$= \frac{q}{\pi \in_0} \ln D/r \tag{19.3}$$

Now the gradient at point P is given by

$$E_x = \frac{q}{2\pi \in_0}\left[\frac{1}{x} + \frac{1}{D-x}\right] = \frac{q}{2\pi \in_0} \frac{D}{x(D-x)}$$

Substituting for q from Eq. (19.3), we get

$$E_x = \frac{\pi \in_0 V}{\ln D/r} \frac{1}{2\pi \in_0} \frac{D}{x(D-x)}$$

$$= \frac{V}{2 \ln D/r} \frac{D}{x(D-x)}$$

$$= \frac{V' D}{x(D-x) \ln D/r}; \; V' = V/2 \tag{19.4}$$

where V' is the line to neutral voltage of the system.

For three-phase system, $V' = V_{\text{line}}/\sqrt{3}$.

It is easy to see from Eq. (19.4) that gradient increases as x decreases (point P is moved towards conductor a) and thus it is maximum when $x = r$ and is given by

$$g_{\max} = E_r = E_{\max} = \frac{V'D}{r(D-r) \ln D/r} \cong \frac{V'}{r \ln D/r}$$

$$V' = r g_{\max} \ln D/r \tag{19.5}$$

As $g_{\max}$ occurs at the conductor surface, the air medium breaks down when $g_{\max} = g_0$, the dielectric strength of air. At temperature conditions other than normal the dielectric strength of air modifies to

$$g_0' = g_0 \, \delta \tag{19.6}$$

where δ is given by Eq. (19.1)

$g_0 = 30$ kV/cm. For AC voltages $g_0 = \dfrac{30}{\sqrt{2}} = 21.2$ kV (rms)/cm

The critical disruptive voltage is then given by

$$V_d = r\, g_0\, \delta \ln \frac{D}{r} \quad \text{kV} \tag{19.7}$$

For 3-phase AC lines: V_d is in kV (rms)/phase and $g_0 = 21.2$ kV (rms)/cm

In arriving at this equation, an assumption is made that the conductor is solid and the surface is smooth. To account for surface irregularity due to stranding Eq. (19.7) is modified as

$$V_d = r\, g_0\, \delta\, m_0 \ln D/r \quad \text{kV rms line to neutral} \tag{19.8}$$

where m_0 = irregularity surface or stranding factor. It depends upon the shape of the cross-section of the conductor and on the state of its surface.

For smooth polished wires $m_0 = 1$;

For rough-surfaced conductors, $0.92 \le m_0 \le 0.98$;

For stranded conductors $0.82 \le m_0 \le 0.88$

When the voltage applied corresponds to the critical disruptive voltage, corona starts but it is not visible because the charged ions in the air must get some finite energy to cause further ionization by collisions.

It may be of interest to note that in the case of parallel wires the visual corona does not begin at voltage V_d but at a higher voltage V_{dv} called the visual critical voltage. The visual corona will occur when the breakdown value is attained at a distance $r\,(1 + 0.3/\sqrt{\delta r}\,)$ from the axis instead of r. This means that voltage to neutral should be $(1 + 0.3/\sqrt{\delta r}\,)$ times the disruptive critical voltage.

$$\therefore \quad V_{dv} = 21.1\, m_v\, \delta_r \left(1 + \frac{0.3}{\sqrt{\delta r}}\right) \ln D/r \quad \text{kV rms line to neutral} \tag{19.9}$$

According to Peek for visual corona

Surface factor m_v = 0.72 for stranded wires for local visual corona
= 0.82 for decided or general visual corona on stranded conductors
= 1 for polished wires

Since the surface of the conductor is irregular, the corona does not start simultaneously on the whole surface but it takes place at different points of the conductor which are pointed and this is called *local corona*. Using bundled conductors per phase reduces electric field intensity levels in the conductor vicinity because of the increase in effective phase radius.

19.3 CONDITIONS AFFECTING CORONA

As discussed earlier corona is owing to the bombardment of air molecules with subsequent dislodging of electrons, by ionized particles. Corona will thus be affected by the electrical state of the atmosphere, as well as by physical conditions and construction of the line.

Considering first the atmospheric conditions, of the factors are:

(i) Ion density in number/m^3
(ii) Size and charge per ion
(iii) Mean free path (dependent on density of air, rains, snow and hailstorm etc.)

In stormy weather ion density may be considerably greater than normal, and corona may then form at a voltage much less than the voltage required in fair weather. (≈ 80%).

Physical conditions of the line, the factors are:

(i) Line voltage
(ii) Ratio D/r
(iii) Contour and state of the surface

The effect of the dirt on the surface is to increase the irregularity and thereby cause a still further decrease in the breakdown value.

19.4 CORONA LOSS

Corona has three undesirable features: power loss, harmonic currents (causing non-sinusoidal voltage) and radio interference (RI) and these factors should be considered when evaluating a line design. Losses do somewhat affect efficiency of the line, but will not be of sufficient importance to have any appreciable effect on the voltage regulation. As in the case of critical voltage for corona, the power loss is affected both by atmospheric and line conditions.

Loss under fair weather conditions is given by Peek's formula as:

$$P_c = \frac{240}{\delta}(f + 25)\sqrt{r/D}\ (V - V_d)^2 \times 10^{-5}\ \text{kW/ph/km} \qquad (19.10)$$

where V = kV to neutral (rms), f = frequency in Hz;
when V/V_d is less than 1.8, Peterson's formula holds good, and is given by

$$P_c = \frac{21 \times 10^{-6} \times f V^2 F}{[\log_{10}(D/r)]^2}\ \text{kW/ph/km} \qquad (19.11)$$

Here F = corona factor determined by test.

The power loss is small varying from 1 to 2 kW/km for 500 kV, three conductors per phase bundle. It increases rapidly with bad weather, with frost being the worst situation.

The current in corona discharge has several high-frequency harmonics that interfere with a wide range of radio frequencies (0.2–4 MHz). In designing a HV line, the magnitude of RI (in μV/m), as well as its effect on the various communication services, e.g. amplitude-modulated broadcasting PLC, aviation and marine signals, etc. should be considered.

Corona loss can be reduced by using large dia conductors, hollow conductors and bundled conductors.

19.5 CORONA IN HVDC LINES

Ionization being the main cause of corona in EHV AC and DC transmission lines, the movements of charged particles differ around the conductor. In DC field negatively charged particles move from negative pole conductor to positive pole conductor continuously and steadily. Naturally they do not tend to remain near the surface of negative pole conductor. Thus the movement of charged particles will be characterized by electric field distribution rather than the surface gradient.

In HVDC lines, the corona loss is lesser due to the absence of factor $\sqrt{2}$ in the voltage waveform. Corona over insulators and metal surface are negligible.

However, the corona loss in HVDC system is an important factor and should be considered while designing a line. In bad weather conditions do not affect corona in DC lines as much as in AC lines. Also, the corona loss in monopolar HVDC line is minimum.

Additional Effect of DC Corona

Space charge field. This is only for DC lines. Other effects common with AC are corona loss. Radio and television interference and audible noise. The first effect involves movement of ions which results in the increase in the voltage gradient at the ground level. The 'electrostatic field' is defined as the field resulting from the charges on or near the conductor surface. The total 'electric field' results from the superposition of the electrostatic and space charge fields.

DC Corona Loss

$$P_{\text{loss}} = \left[2V\,(k+1)\,k_c\,n\,r\,2^{.25(g-g_0)}\right]\times 10^{-3}\ \text{kW/circuit km} \qquad (19.12)$$

where

V is the pole to ground voltage in kV
n is the number of subconductors with radius r in cm
g = max. conductor surface gradient at operating voltage (kV/cm)
$g_0 = 22\,\delta$ kV/cm where δ = relative air density
k_c = conductor surface coefficient (0.15 – 0.35)
$k = (2/\pi)\,\tan^{-1}\,(2H/S)$
H = mean height of conductors
S = pole spacing

The relative air density δ is given by

$$\delta = 2.94p/(273 + T) \qquad (19.13)$$

p = pressure in kilo-Pascal, T in °C.

The bipolar corona loss per pole is higher than the monopolar corona loss by a factor of 1.5 to 2.5. However, for a given voltage, the positive and negative polarity losses are nearly equal. DC corona loss normally increase with wind velocity in the range of 0 to 10 m/s.

19.6 PRACTICAL IMPORTANCE OF CORONA

Corona reduces the magnitude of high voltage steep fronted waves due to lightning or switching by partially dissipating them as corona loss. In this way, it acts as a safety valve, and use of lightning arrester is avoided to some extent.

19.7 SUMMARY

A very important phenomenon 'corona' has been explained in this chapter. How various factors affect it, its importance etc. have been fully explained.

Example 19.1 Determine the corona characteristics of a 3-phase line 200 km long, conductor dia 1 cm, 2.5 m delta spacing, air temperature 27°C, altitude 2440 m, corresponding to an approximate barometric pressure of 73.15 cm, operating voltage 110 kV at 50 Hz.

Solution

Radius of the conductor $r = 0.5$ cm

Relative air density

$$\delta = \frac{3.92\,b}{273+27} = \frac{3.92 \times 73.15}{273+27} = 0.9558$$

Assuming that the conductor is stranded and taking the stranding factor as 0.86

$$m_0 = 0.86$$

Disruptive critical voltage is given by:

$$V_d = g_0\, m_0\, r\, \delta \ln D/r \text{ kV rms line to neutral}$$

$$= 21.2 \times 0.86 \times 0.5 \times \left(\ln \frac{250}{0.5}\right) \times 0.9558$$

$$= 54.18 \text{ kV rms line to neutral}$$

Visual critical voltage

$$V_v = 21.2 \times m_v \delta r \left(1 + \frac{0.3}{\sqrt{\delta r}}\right) \ln D/r \text{ kV rms line to neutral}$$

$$= 21.2 \times 0.72 \times 0.9558 \times 0.5 \left(1 + \frac{0.3}{\sqrt{0.9558 \times 0.5}}\right) \ln \frac{250}{0.5}$$

$$= 64.50 \text{ kV rms to neutral.}$$

Fair weather loss using Peek's formula

$$P_c = \frac{240}{\delta}(f+25)\sqrt{\frac{r}{D}}\,(V - V_d)^2 \times 10^{-5} \text{ kW/ph/km}$$

$$= \frac{240}{0.9554} \times 75 \sqrt{\frac{0.5}{250}} \left(\frac{110}{\sqrt{3}} - 54.18\right)^2 \times 10^{-5}$$

$= 0.7332$ kW/ph/km

Approximate loss during storm conditions. The disruptive critical value is taken as 0.8 of the value for fair weather viz.

$$\therefore \quad \text{Loss} = \frac{240}{0.9554} \times 75 \times \sqrt{\frac{0.5}{250}} \left(\frac{110}{\sqrt{3}} - 0.8 \times 54.18 \right)^2 \times 10^{-5}$$

$= 3.427$ kW/ph/km

Example 19.2 A 3-phase 132 kV transmission line using stranded Cu conductors is to supply a load of 15 A for 10 hrs/day, 30 A for 8 hrs/day and 100 A for 6 hrs/day. The total cost of the line is Rs (50,000 + 32 A)/km; A = cross-sectional area of conductor in sq. mm. If interest and depreciation is 12% p.a. and cost of energy is 5 paise/unit, calculate the most economical section of the conductor. What conductor spacing should be used between conductors for the line to be corona free?

Given: specific R of Cu $= \frac{1}{58}$ ohm/m/mm^2 cross-section

Dia of stranded Cu conductor = 12% greater than that of a solid wire (because of stranding)

$\delta = 0.95$, $m_0 = 0.9$, breakdown strength of air = 30 kV/cm

Solution

$$\text{Daily losses} = 3\left[15^2 \times 10 + 30^2 \times 8 + 100^2 \times 6\right] \times \frac{\rho l}{A} \times \frac{1}{1000}$$

let $l = 1$ km

$$\therefore \quad \text{Daily losses} = \frac{3 \times 69450 \times 1000}{58 \times 1000 \times A} = \frac{3 \times 69450}{58 \times A} \text{ kWh/km of } 3\phi \text{ line}$$

$$\text{Total cost } C = 365 \times 0.05 \times \frac{3 \times 69450}{58 \times A} + 6000 + 3.84\,A$$

For the most economic cross-section

$$\frac{dC}{dA} = 0$$

$$3.84 = \frac{365 \times 0.05 \times 3 \times 69450}{58\,A^2}$$

$$\therefore \quad A^2 = 17072.5 \quad A = 130.66 \text{ mm}^2$$

$$\text{Radius of solid conductor} = \frac{\sqrt{130.66}}{\pi} = 6.45 \text{ mm}$$

$$\text{Radius of stranded conductor} = 1.12 \times 6.45 = 7.22 \text{ mm}$$

$$= 0.722 \text{ cm}$$

$$V_d = 21.1\, m_0\, \delta\, r \log_e D/r = 13.2/\sqrt{3} \text{ kV}$$

$$\frac{132}{\sqrt{3}} = 21.1 \times 0.9 \times 0.95 \times 0.722 \times \log_e D/r$$

$$\therefore \quad \log_e D/r = 5.82$$

$$\therefore \quad D/r = 336.88$$

$$\therefore \quad D = \frac{336.88 \times 0.722}{100} = 2.43 \text{ m}$$

Problems

19.1 In a three-phase line the conductors (with radii of 20 mm each) are arranged in the form of an equilateral triangle. Assuming fair weather conditions, air density factor of 0.95 and irregularity factor of 0.96. Find the minimum spacing between the conductors if the disruptive critical voltage is not to exceed 230 kV between lines. $g_0 = 30$ kV/cm (peak).

19.2 Find the corona characteristics of a 110 kV, 50 Hz, three-phase line 200 km long consisting of 1 cm dia stranded copper conductors spaced 3.5 m delta arrangement.

Temperature 27°C and barometric pressure 75 cm, $m_d = 0.85$, $m_v = 0.72$ and m_v for general corona = 0.81.

19.3 Determine the critical disruptive voltage and corona loss for a three-phase line operating at 110 kV which has conductor of 1.2 cm dia arranged in 3 m delta. Assume $\delta = 1.06$ and $g_0 = 21$ kV/cm.

19.4 A single-phase overhead line has two conductors of dia 1.5 cm with a spacing of 1.5 m between centres. If the dielectric strength of air is 21 kV/cm, determine the line voltage for which corona will commence on the line. ($\delta = 0.96$, $m_0 = 0.92$).

References

1. Cotton, H. and H. Barber, *The Transmission and Distribution of Electrical Energy*, 3rd edn, B.I. Publishers, New Delhi, 1970.
2. Wadhwa, C.L., *Electrical Power Systems*, 4th edn, New Age International, New Delhi, 2005.
3. Chakrabarti, A., M.L. Soni, P.V. Gupta and U.S. Bhatnagar, *A Text Book on Power System Engineering*, Dhanpat Rai and Co., New Delhi, 1997.
4. Padiyar, K.R., *HVDC Power Transmission Systems*, Wiley Eastern Ltd., New Delhi, 1990.

Chapter 20

High Voltage DC (HVDC) Transmission

20.1 INTRODUCTION

Application of electricity originally started with the use of direct current. The first Central Electric Station was installed by Edison in New York in 1882 supplying power at 110 V DC. The invention of transformer and induction motor and the concept of three-phase AC around 1890 initiated the use of AC. The advantages of three-phase AC almost eliminated the use of DC systems except for some special applications in electrolytic processes and adjustable speed motor drives.

Today DC transmission has staged a comeback in the form of HVDC transmission to supplement the HVAC transmission system. The first commercially used HVDC link (20 MW, 100 kV) in the world was built in 1954 between the Mainland of Sweden and the island of Gotland. This was a monopolar, 100 kV, 20 MW cable system making use of sea return.

Since then the technique of power transmission by HVDC has been continuously developing. In 1970, thyristor valves replaced the valves based on the mercury-arc technique. In 1961 an underwater DC link (cross-channel) of 2000 MW was set up between England and France. This was a bipolar, ±100kV, 160 MW cable system. Since 1972 all new HVDC systems are using thyristors. To date the biggest HVDC transmission is ITAIPU in Brazil (two bipoles, 6,300 MW and ±300 kV). DC transmission is an effective means to improve system performance. It is mainly used to complement AC systems rather than to displace these. In India, the first HVDC 810 km long distance OH line is Rihand-Delhi (±500 kV, 1500 MW) for bulk power transmission from Rihand/Singrauli complex to Delhi. The largest device rating is now in the range of 5 kV, 3 kA. The highest transmission voltage reached is ±600 kV. At present the world has over 60 HVDC schemes in operation for a total capacity of more than 66,000 MW and the growth of DC transmission capacity has reached an overage of 2,500 MW/year. HVDC is also used to interconnect systems of different frequency (e.g. the connection between north and south islands in Japan, which have 50 Hz and 60 Hz, respectively).

20.2 CONVERTOR BASICS

DC transmission requires a convertor at each end of the line. The sending end convertor act, as a rectifier converting AC to DC and the receiving end converter acts as an inverter converting DC to AC. The rectifier is fed from an AC source through a transformer and the inverter feeds AC load through a transformer. As we shall see later, the role of the converter is easily reversed from rectifier to inverter and vice versa, thereby, reversing the flow of DC power on the line.

Modern day converter are thyristor based. Some basic understanding of the thyristor converter–its operation and control—is essential at this stage.

Thyristor (Valve)

It is a three terminal solid-state device whose symbol is shown in Fig. 20.1. The three terminals are Anode, Cathode and Gate. When Anode is connected to positive polarity of a source and Cathode to its negative polarity and a short duration positive pulse is applied at the Gate, the current will be conducted from anode to cathode whose magnitude is dependent on the external circuit. If anode is negative and cathode positive, no current can flow irrespective of the gate pulse.

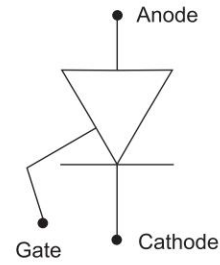

Fig. 20.1 Thyristor symbol

With proper anode and cathode polarities the conduction is initiated by the gate pulse after which the gate loses control over conduction.

The device will return to non-conducting state after anode to cathode current becomes zero (naturally or otherwise). It can pulsed (fired) again to start conduction, if the anode–cathode polarities are right.

Thyristor Converter

The connection diagram of a thyristor bridge converter is drawn in Fig. 20.2. The six thyristors are connected in three sets of two thyristors each across the DC terminals; in each set (or row) the thyristors have the same conduction direction.

Upon pulsing the gate of Th_1 it begins to conduct and the current which was being conducted by Th_4 shifts (commutes) to Th_1, which then conducts the current for 180°. This process keeps repeating between Th_1 and Th_4 every 180°. The same process occurs between Th_2 and Th_5 displaced by 120° from Th_1 and Th_4 and also between Th_3 and Th_6 displaced another 120°. In all there are 6 pulses per cycle of AC and the pulse rate is 6 times that of AC frequency.

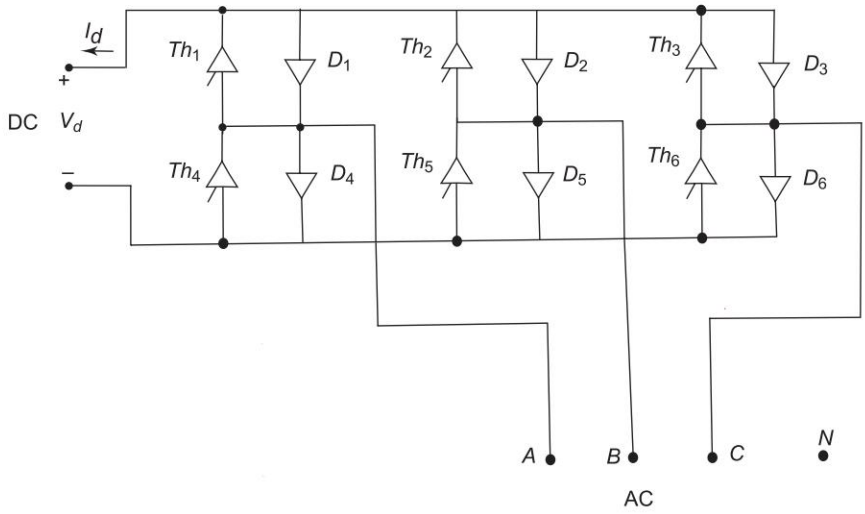

Fig. 20.2 Thyristor bridge converter

The basic control over DC voltage magnitude and polarity is achieved by the angle of thyristor firing (α). The waveform of voltage (line) v_{ab} is drawn in Fig. 20.3. This voltage appears across Th_1 and Th_5, where Th_5 is already conducting. Upon firing Th_1 at angle α it will conduct current I_d for 180° (upto $\pi + \alpha$). The average (DC) voltage V_d is positive.

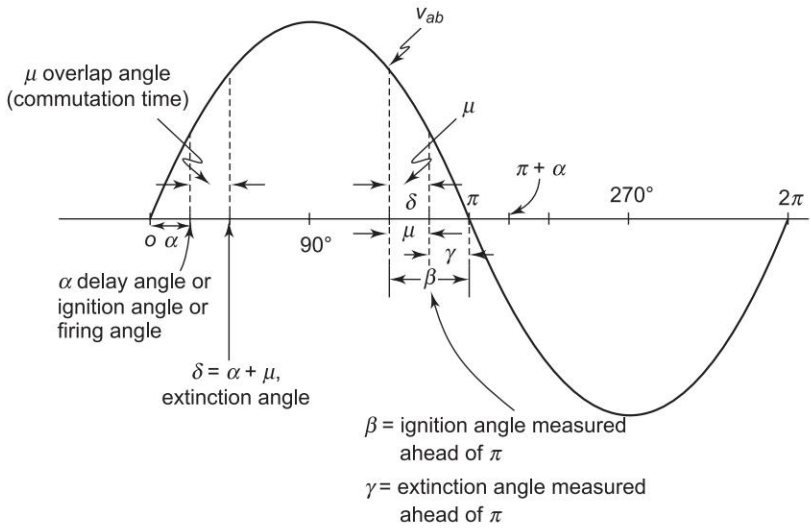

Fig. 20.3 Important angles for rectifier and inverter operation of a converter

The converter is therefore acting as a *rectifier*. As angle α is increased V_d reduces till at $\alpha = 90°$, $V_d = 0$. Of course from α the commutation occurs in

overlap angle μ and is completed at $\delta = \alpha + \mu$, the extinction angle. This overlap affects, (reduces) the value of V_d.

(I_d is flowing out of +ve terminal of V_d)

As angle α is increased beyond 90°, V_d (average voltage) becomes negative while I_d flows in the same direction. The DC power flows into the converter, while AC power flows out of it. The converter is therefore acting as an *inverter*.

To summarize:

$$\text{Rectifier } 0 < \alpha < 90°$$

$$\text{Inverter } 90° < \alpha < 180°$$

As from the firing angle onwards, the current flows for 180°, while voltage condition across thyristor change. This is because the current is out of phase with voltage. So for part of time current is conducted by diodes, called free wheeling diodes.

Thyristor Ratings

- Maximum current carrying capacity.
- Maximum inverse voltage above which the thyristor breaks down.

At present thyristor are available with current rating of 2.5 kA and voltage rating of 3 kV.

For higher current carrying and higher voltage rating converter each converter row (branch) is formed by series-parallel combination of thyristors.

The detailed derivation of converter performance equation will be carried out in Sec. 20.9.

Harmonics

The alternating current waveform injected by the inverter into the AC system have a high harmonic content. The rectifier draws nearly trapezoidal current which contains the fundamental sine wave and also harmonics of order depending upon the number (n) of thyristors (valves). For a six valve bridge the harmonic order is $6n \pm 1$ i.e. 5, 7, 11, ... 25.

By Fourier series it is found that

$$i = \frac{2\sqrt{3}}{\pi} I_d \left(\cos \omega t + \frac{1}{5} \cos 5\,\omega t - \frac{1}{7} \cos 7\,\omega t - \frac{1}{11} \cos 11\,\omega t\right)$$

The harmonics are affected by the two operating angles of the converters. These are

μ = commutation or overlap angle

α = delay angle

Harmonic magnitude decrease with decrease in μ. However, α for a given μ does cause any significant effect on harmonics. The largest variation in α is between 0 to 10°.

For normal operation α is less than 10° and $-\mu \approx 20°$, resulting in low harmonic content.

During faults, however, α may reach $\approx 90°$ while μ remains small, resulting in substantial increase in harmonic content.

Pulse Number (p): The number of pulsations (i.e., cycles of ripple) of the direct voltage per cycle of alternating voltage.

Ripple: The AC component from DC power supply arising from the conversion processes. It is expressed in peak, peak-to-peak, rms volts, or as % rms of DC voltage. Since HVDC converters have large DC smoothing reactors, approximately 1 H, the resultant DC is practically constant (ripple free). However, the direct voltage on the valve side of the smoothing reactor has ripple.

Ripple Amplitude: The maximum value of the instantaneous difference between the average and instantaneous value of a pulsating unidirectional wave.

Smoothing Reactor: An inductive reactor between the DC output of the converter and the load. It is used to smooth the ripple in the DC properly, to reduce harmonic voltages and currents in the DC line, and to limit the magnitude of the fault current (reduce the rate of rise of fault current on DC line).

20.3 TYPES OF DC LINKS (TRANSMISSION MODES)

The DC links can be classified into the following types:

(a) *Monopolar Link:* It has only one energized conductor normally of negative polarity and uses ground or sea water as the return path. It may be noted that earth has a much lower resistance to DC as compared to AC. The negative polarity is preferred on overhead lines due to lesser radio interference. Figure 20.4 (a) shows a monopolar link.

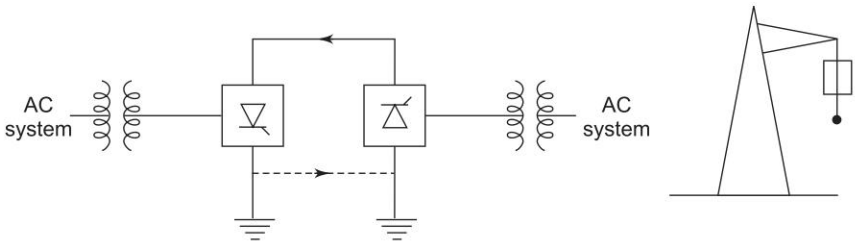

(a) Monopolar link (line) (b)

Fig. 20.4

(b) *Bipolar Link*: This link has two conductors, one positive and the other negative potential of the same magnitude (e.g. ±650 kV) (20.1 (b)). At each terminal, two converters of equal rated voltages are connected in series on the DC side. The neutral points (i.e. the junctions between converters) are grounded, at one or both ends. If both the neutrals are grounded, the two poles operate independently. If the currents in the two conductors are equal, the ground current is zero. If one conductor has a fault, the other conductor (alongwith ground return) can supply half the rated load. The rated voltage of bipolar link is given as (say) ±650 kV.

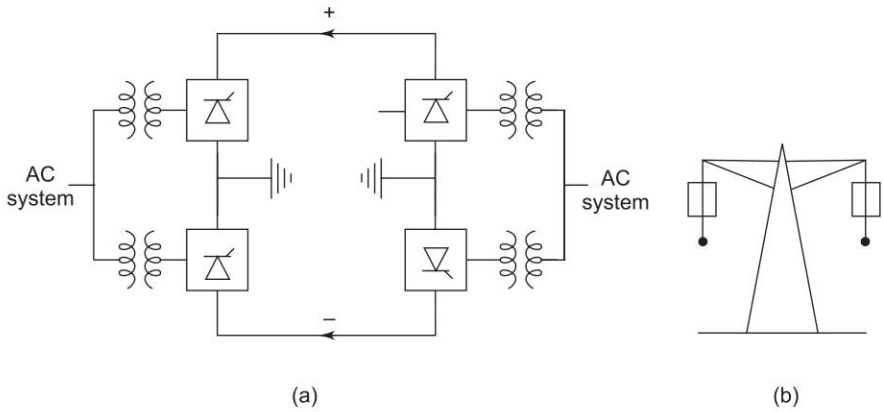

Fig. 20.5 Bipolar link (line)

A bipolar transmission has two circuits which are almost independent of each other A bipolar line can be operated as a monopolar line in an emergency.

In some applications continuous current through earth is not permitted, and a bipolar arrangement is the natural solution.

(c) *Homopolar Link*: A homopolar link shown in Fig. 20.6 has two or more conductors, all having the same polarity (usually negative), as the corona loss and radio interference get reduced, and it always operates with ground as the return. If one of the conductors develops a fault, the converter equipment can be reconnected so that the healthy conductor (with some overload capacity) can supply more than 50% of the rated power.

A two-conductor DC line is more reliable than a three-conductor AC line, because in the event of a fault on one conductor, the other conductor can continue to operate with ground return during the fault period. The same is not possible with the AC line.

Furthermore if a two pole (homopolar) DC line is compared with a double-circuit three-phase AC line, the DC line costs would be about 45% less than the AC line. In general, the cost advantage of the DC line increases at higher voltages.

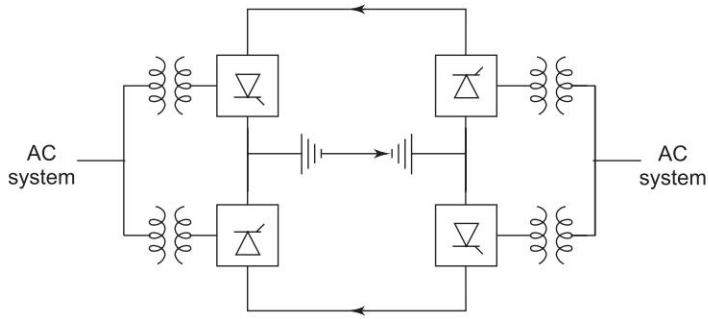

Fig. 20.6 Homopolar Link

20.4 STRUCTURE OF HVDC TRANSMISSION

HVDC transmission consists of two converter stations which are connected to each other by a DC cable or an overhead DC line. A typical arrangement of main components of an HVDC transmission is shown in Fig. 20.7.

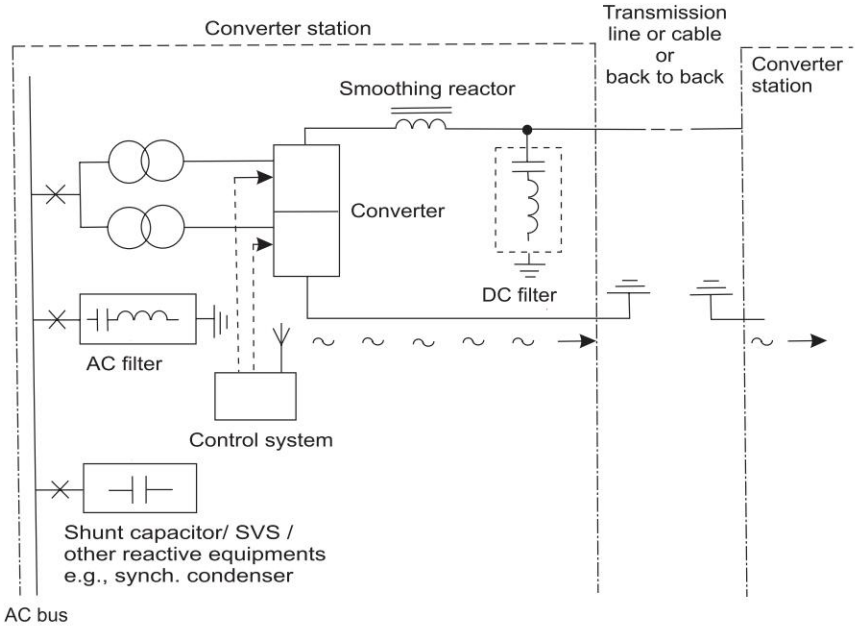

Fig. 20.7 Main components of a HVDC transmission—a typical arrangement

Two series connected 6-pulse converters (12-pulse bridge) consisting of valves and converter transformers are used. The valves convert AC to DC, and the transformers provide a suitable voltage ratio to achieve the desired direct voltage and galvanic separation of the AC and the DC systems. A smoothing

reactor in the DC circuit reduces the harmonic currents in the DC line, and possible transient overcurrents. Filters are used to take care of harmonics generated at the conversion. Thus we see that in an HVDC transmission, power is taken from one point in an AC network, where it is converted to DC in a converter station (rectifier), transmitted to another converter station (inverter) via line or a cable and injected into an AC system.

By varying the firing angle α (point on the voltage wave when the gating pulse is applied and conduction starts) the DC output voltage can be controlled between two limits, +ve and −ve. When α is varied, we get

Maximum DC voltage when $\alpha = 0°$
Rectifier operation when $0 < \alpha < 90°$
Inverter operation when $90° < \alpha < 180°$

While discussing inverter operation, it is common to define extinction (a chance) angle $\gamma = 180° - \alpha$.

Harmonics

The AC/DC converters are sources of harmonics on AC as well as DC sides. The harmful effects of harmonics are the possibility of resonance of the transmission circuit and the high frequency harmonics enhance interference with communication networks. To reduce the harmonic amplitude series and shunt filters are installed on both AC and DC sides as shown in Fig. 20.7. The shunt capacitors of the filter are helpful in supplying reactive power to the converters. A smoothing reactor (choke) is installed on the DC side to limit the harmonics.

Reactive Power Demand

The requirement of reactive power at converter stations is due to

1. The control of HVDC converter (α, γ) which introduces a phase shift between the fundamentals of AC current and voltage, and
2. The commutation process, in which the DC current is commutated from one valve to another, and which introduces further phase shift.

In addition to reactive power consumption by converters, converter transformers also consume reactive power. Considering normal values of α (rectifier) or γ (inverter), the reactive power demand usually is in the range of 50–60% of the transmitted active power. This figure is for each converter station.

The reactive power may be supplied from:

1. AC filters
2. Shunt capacitors (least costly)
3. AC network
4. Static compensators (SVS) (for fast voltage regulation), and
5. Synchronous condensers (if AC network is weak).

While choosing reactive power generation equipment, one must consider both economic and technical aspects.

20.5 PRINCIPLES OF HVDC CONTROL

One of the most important aspects of HVDC systems is its fast and stable controllability. In DC transmission the current and power flows from higher voltage (rectifier side) to lower voltage (inverter side) and is proportional to the voltage difference between the two sides as shown in Fig. 20.8. The amount of power transmitted is, therefore, easily controlled by adjusting the two voltages. For reversal of power flow the roles of rectifier and inverter are interchanged by adjusting their firing angles. This automatically causes the reversal of DC polarity.

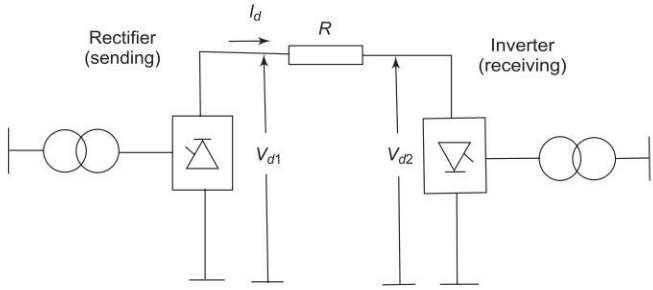

Fig. 20.8

In an HVDC transmission, one of the converter stations, generally the inverter station, is so controlled that the direct voltage of the system is fixed and has a rigid relation to the voltage on the AC side. Tap changers take care of the slow variations on the AC side. The other terminal station (rectifier) adjusts the direct voltage on its terminal so that the current is controlled to the desired transmitted power.

In Fig. 20.8

$$I_d = \frac{V_{d1} - V_{d2}}{R} \tag{20.1}$$

where R is the resistance of link and includes loop transmission resistance (if any), and resistance of smoothing reactors and converter valves. The power received is, therefore, given as

$$P = \left(\frac{V_{d1} - V_{d2}}{R}\right) V_{d2} = I_d V_{d2} \tag{20.2}$$

The rectifier and inverter voltages are given by

$$V_{d1} = n\left(\frac{3\sqrt{2}E_{L-L_r}}{\pi}\cos\alpha - \frac{3X_{cr}}{\pi} I_d\right) \tag{20.3}$$

$$V_{d2} = n\left(\frac{3\sqrt{2}E_{L-L_i}}{\pi}\cos\gamma - \frac{3X_{ci}}{\pi}I_d\right) \tag{20.4}$$

where n = number of series connected bridges.

E_{L-L_r}, E_{L-L_i} = line to line AC voltages at the rectifier and inverter bridges, respectively

X_{cr}, X_{ci} = commutation reactance at the rectifier and inverter, respectively.

From Eq. (20.2) it is clear that the DC power per pole is controlled by relative control of DC terminal voltages, V_{d1} and V_{d2}. Control on DC, voltage is exercised by the converter control angles α and γ as given by Eqs (20.3) and (20.4). Normal operating range of control angles is:

$$\alpha_{\min} = 5°,\ \alpha_{\max} = (15 \pm 3)°,\ \gamma_{\min} = 15°$$

The prime considerations in HVDC transmission are to minimize reactive power requirement at the terminals and to reduce the system losses. For this DC voltage should be as high as possible and α should be as low as possible.

20.6 ECONOMIC CONSIDERATIONS

Consider an AC line and a DC line employing the same number of conductors and insulators. Let us compare the power per conductor on the two lines. If in each case the current is limited by temperature rise, the direct current equals the rms alternating current. Assume also that the insulators withstand the same peak voltage to ground in each case. Then the direct voltage is $\sqrt{2}$ times the rms AC voltage

The DC power per conductor is

$$P_{dc} = V_{dc}I_{dc} \tag{20.5}$$

and the AC power per conductor is

$$P_{ac} = V_{ac}I_{ac}\cos\phi \tag{20.6}$$

where I_{dc} and I_{ac} are the currents per conductor, V_{dc} and V_{ac} the conductor-to-ground voltages, and cos ϕ the power factor. Now

$$\frac{P_{dc}}{P_{ac}} = \frac{V_{dc}I_{dc}}{V_{ac}I_{ac}\cos\phi} = \frac{\sqrt{2}}{\cos\phi} \tag{20.7}$$

taking

$$\cos\phi = 0.945,\ P_{dc}/P_{ac} = 1.5 \tag{20.8}$$

Now compare a three phase, three conductor AC line with a bipolar two conductor DC line. The power capabilities of the respective circuits are

$$P'_{dc} = 2P'_{dc} \text{ and } P'_{ac} = 3P'_{ac} \tag{20.9}$$

$$P'_{dc}/P'_{ac} = \frac{2}{3} \times 1.5 = 1 \qquad (20.10)$$

Both lines carry the same power. The DC line, however, is simpler, and cheaper, having two conductors instead of three. Further, an overhead line requires only 2/3 as many insulators, and the towers are simpler, cheaper and narrower. A narrower right of way would be required. Both lines have the same power loss per conductor. The percentage loss of the DC line is only two-thirds that of AC line.

If cables are used instead of line, the permissible working stress (voltage per unit thickness of insulation) is higher for DC than for AC, and, further, the power factor for DC is unity and, for AC, considerably lower than that used above. Both changes further favour DC as compared to AC by increasing the ratio of DC power to AC power per conductor. The resulting ratio may be between 5 and 10.

Since the power limit of an overhead AC line is normally fixed by factors other than conductor heating, the ratio of DC power per conductor to AC power per conductor may be as high as 4.

However, the cost of terminal equipment is much more in case of DC (converting stations) than in case of AC (transformer/substations). If we plot the variation of cost of power as a function of transmission distance it will be as shown in Fig. 20.9. The slope gives cost per unit length of the line and other accessories. The point of intersection *P* is called a *breakeven* point which shows that, if the transmission distance is more than 0_p, is preferable to use DC; otherwise AC should be used.

There is hardly any scope to reduce the cost of AC terminal equipment. But a lot of progress has been made in the development of converting devices, and the breakeven distances are reducing with further development of these devices.

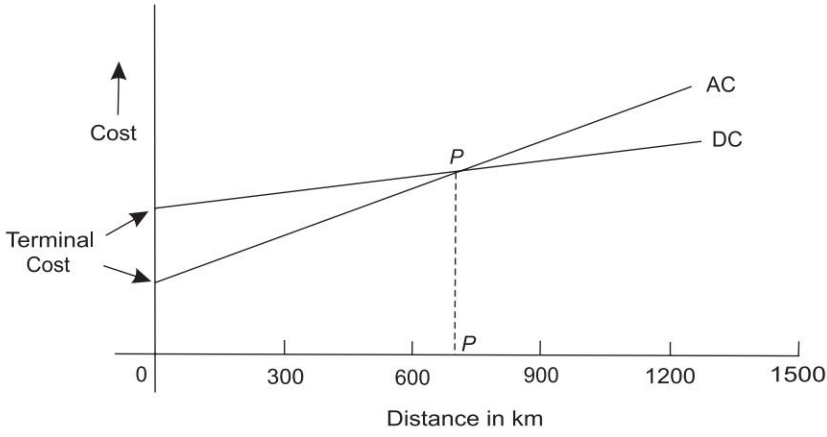

Fig. 20.9

Present day breakeven distance in favour of DC transmission is 7 km for overhead lines. However, the breakeven distance varies with each individual project and should always be checked. The difference installation costs between AC and DC submarine or underground cable is several times as high as the corresponding difference in overhead line costs. This means that the breakeven distance for a cable transmission is much shorter and is of the order of 30 – 50 km.

20.7 HVDC APPLICATIONS

The following modes of implanting a DC link in a predominant AC system may be used:

1. Interconnection of systems of the same frequency through a zero length DC link (back to back connection): This does not require any DC transmission line and AC lines terminate on the rectifier and inverter which are connected back to back (Fig. 20.10). A typical example is the Eel river scheme in Canada connecting the Québec hydro system with that of New Brunswick. This helps in interconnecting two AC systems without increasing their fault levels. In India a 400 kV, 500 MW Singrauli to Vindhyachal back to back link is working at Vindhyachal since 1991 (the breakeven distance concept is meaningless for such schemes).

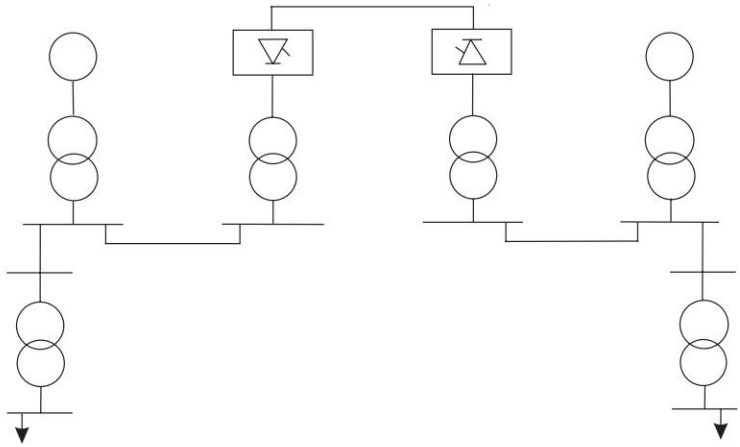

Fig. 20.10 Back-to-back connection

2. HVDC links are used to evacuate power from the remote super power stations to the load centres situated several hundred kilometres away. If there are faults in the AC network, this will not trip the units at the power station since the asynchronous DC link insulates the power station from the AC system.

3. *Interconnection between power systems or pools:* For smooth interchange of power between neighbouring grids irrespective of voltage and frequency fluctuations, such links ensure retention of the tie under the most stringent conditions of the constituent grids.
4. *High power underground (submarine) distribution system feeders:* Here it is found that DC may be cheaper at distances greater than approximately 50 km with a power level of 1000–2000 MW. With AC we need forced cooling due to the higher amount of heat produced. Also there are increased dielectric losses at EHV AC.
5. Stabilizing AC system by modulating DC power flow.

20.8 ADVANTAGES AND DISADVANTAGES OF HVDC SYSTEMS

Advantages

1. These systems are economical for long distance bulk power transmission by overhead lines (reduced tower and cable costs).
2. There is greater power per conductor and simpler line construction.
3. Ground return is possible.
4. There is no charging current and skin effect.
5. The voltage regulation problem is much less serious for DC, since only the IR drop is involved (IX = 0). For the same reason steady-state stability is no loner a major problem.
6. There is easy reversibility and controllability of power flow through a DC link.
7. The DC line is an asynchronous or flexible link (resynchronization is not required) and it can interconnect two rigid systems operating at different frequencies.
8. For a single DC line between two converter stations, circuit breakers are unnecessary since control of the converters can be used to block current flow during faulted conditions.
9. Each conductor can be operated as an independent circuit.
10. Smaller amount of right of way and narrower towers are required. The distance between two outside conductors of a 400 kV AC line is normally 20 m, whereas the same between a corresponding DC line is roughly half, i.e. 10 m only.
11. There is considerable insulation economy. The peak voltage of the 400 kV AC line is $\sqrt{2} \times 400$ = 564 kV. So the AC line requires more insulation between the tower and conductors, as well as greater clearance above the earth as compared to corresponding 400 kV DC line.
12. There is no technical limit to the distance over which power may be transmitted by lines or underground or undersea cables because of absence of both charging current and stability limitations.

13. Line losses are smaller.
14. It is possible to bring more power into an AC system via a DC link without raising the fault level and circuit breaker ratings.
15. No reactive compensation of DC lines is required.
16. Corona loss, radio interference and audible emissions are less as compared to AC.
17. HVAC line and HVDC link can be used in parallel as an AC–DC system.
18. The contribution of HVDC link to SCC of AC system is considerably less as compared to that of an alternative AC link.
19. DC cables can be worked at higher voltage gradient.
20. Low SC current is required on DC line.
21. Fast control of converters can be used to damp out connected AC system oscillations.

Disadvantages

1. The systems are costly since installation of complicated converters and DC switchgear is expensive.
2. Converters require considerable reactive power.
3. Harmonics are generated which required filters.
4. Converters do not have overload capability.
5. Lack of HVDC circuit breakers hampers multiterminal or network operation. There is no DC device which can perform excellent switching operations and ensure protection. (Simultaneous control at all converters is difficult).
6. There is nothing like DC transformer which can change the voltage level in a simple way. Voltage transformation has to be provided on the AC sides of the system.
7. Reactive power required by the load is to be supplied locally as no reactive power can be transmitted over a DC link.
8. Contamination of insulators is polluted in some areas or along the sea coast. Pollution affects DC more than AC. More frequent cleaning of insulators is required.

20.9 THREE-PHASE BRIDGE CONVERTER PERFORMANCE

The thyristor based three-phase bridge converter has been discussed in Sec. 20.2. It has been shown that the converter operates as rectifier for $0 < \alpha < 90°$ and as inverter for $90° < \alpha < 180°$
where α is the firing or delay angle.

The delay angle also controls the voltage magnitude in both type of converter operation. The results derived for converter as rectifier are valid for inverter in the range α as above.

20.10 RECTIFIER

If the commutation time i.e. overlap angle (μ) is ignored, the average direct voltage can be found from Fig. 20.2 as

$$V_d = \frac{3\sqrt{3}}{\pi} E_m \cos\alpha \tag{20.11}$$

$$= V_{d0} \cos \alpha \tag{20.12}$$

where $$V_{d0} = \frac{3\sqrt{3}}{\pi} E_m \tag{20.13}$$

E_m = maximum phase to neutral voltage

For $\alpha = 0$, $V_d = V_{d0}$

Equation (20.13) can be written as

$$V_{d0} = \frac{3\sqrt{6}}{\pi} E_{L-N} \text{ (rms)} \tag{20.14}$$

$$= 2.34\, E_{L-N}$$

Also $$V_{d0} = \frac{3\sqrt{2}}{\pi} E_{L-L} = 1.35\, E_{L-L} \tag{20.15}$$

where

E_{L-N} = rms line-to-neutral alternating voltage

E_{L-L} = rms line-to-line alternating voltage

We can now write $$V_{d0} = \frac{3\sqrt{6}}{\pi} E_{L-N} \cos\alpha \tag{20.16}$$

From Eq. (20.12) it is easy to see that the delay angle α can change the average direct voltage by the factor cos α. Since α can take values from 0 to almost 180°, the average direct voltage can take values from $+V_{d0}$ to $-V_{d0}$. However, the negative direct voltage V_d with positive current I_d causes the power to flow in the opposite direction. Hence, the converter operates as an inverter rather than as a rectifier. It may be noted that since the current can flow from anode to cathode, the direction of current I_d remains the same.

It can be shown that the rms value of the fundamental frequency component of AC is

$$I_{L1} = \frac{\sqrt{6}}{\pi} I_d \tag{20.17}$$

$$= 0.78\, I_d \tag{20.18a}$$

If losses are neglected

$$P_{ac} = P_{dc} \tag{20.18b}$$

where $$P_{ac} = 3\, E_{L-N}\, I_{L1} \cos \phi \quad (20.19a)$$

$$P_{dc} = V_d I_d \quad (20.19b)$$

Substituting Eq. (20.17) in Eq. (20.19a),

$$P_{ac} = \frac{3\sqrt{6}}{\pi} E_{L-N}\, I_d \cos\phi \quad (20.20)$$

Substituting Eq. (20.16) into (20.19b)

$$P_{dc} = \frac{3\sqrt{6}}{\pi} E_{L-N}\, I_d \cos\alpha \quad (20.21)$$

As $P_{ac} = P_{dc}$, we get from Eqs (20.20) and (20.21) that

$$\cos \phi = \cos \alpha \quad (20.22)$$

or displacement factor (vector pf) = cos (delay angle)

Thus, the converter draws reactive power from the AC system. In the words of Kimbark [3], the rectifier is said to take lagging current from the AC system, and the inverter is said either to deliver leading current to the AC system or draw lagging current from it.

An overlap angle (μ) causes the alternating current in each phase to lag behind its voltage. Hence, the corresponding decrease in direct voltage due to the commutation delay can be written as

$$\Delta V_d = \frac{V_{d0}}{2} [\cos \alpha - \cos (\alpha + \mu)] \quad (20.23)$$

The associated average direct voltage is then expressed as

$$V_d = V_{d0} \cos \alpha - \Delta V_d \quad (20.24)$$

or $$V_d = \frac{1}{2} V_{d0} [\cos \alpha + \cos l,\, \delta] \quad (20.25)$$

where extinction angle $\delta = \alpha + \mu$

From the above equations, we get

$$\Delta V_d = \frac{1}{2} V_{d0} (\cos \alpha - \cos \delta) \quad (20.26)$$

and $$V_d = \frac{1}{2} V_{d0} (\cos \alpha + \cos \delta) \quad (20.27)$$

The overlap angle μ is owing to the fact that the AC supply source has inductance. Therefore, the currents in it cannot change instantaneously. Hence, the current transfer from one phase to another takes a certain time, which is known as the commutation time or overlap time (μ/ω). In normal operation $0° < \mu < 60°$ holds good whereas in the abnormal operation mode $60° < \mu < 120°$. The commutation delay takes place when two phases of the supplying AC source are short circuited. Thus, it can be shown that at the end of the commutation,

$$I_d = I_s [\cos \alpha - \cos \delta] \tag{20.28}$$

but
$$I_s = \frac{\sqrt{3}\, E_m}{2\omega L_c} \tag{20.29}$$

Substituting Eq. (20.29) into Eq. (20.28),

$$I_d = \frac{\sqrt{3}\, E_m}{2\omega L_c} [\cos \alpha - \cos \delta] \tag{20.30}$$

where I_s = maximum value of current in line-to-line short circuit on AC source

L_c = series inductance per phase of AC source

Dividing Eq. (20.23) by Eq. (20.28), we get

$$\frac{\Delta V_d}{I_d} = \frac{V_{d0}}{2 I_s} \tag{20.31}$$

$$\therefore \quad \Delta V_d = \frac{I_d}{2 I_s} V_{d0} \tag{20.32}$$

Substituting ΔV_d in Eq. (20.24) gives

$$V_d = V_{d0}\left(\cos\alpha - \frac{I_d}{2 I_s}\right)$$

or
$$V_d = V_{d0} \cos \alpha - R_c I_d \tag{20.33}$$

where

R_c = equivalent commutation resistance per phase:

$$= \frac{3}{\pi} X_c \quad \text{or} \quad R_c = \frac{3}{\pi} \omega L_c \tag{20.34}$$

This does not consume any power and represents voltage drop due to commutation.

or
$$R_c = 6 f L_c \tag{20.35}$$

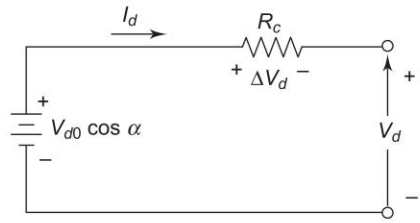

Fig. 20.11 Equivalent circuit representation of bridge rectifier

Figure 20.11 shows equivalent circuit of a bridge rectifier based on Eq. (20.33). The direct voltage V_d can be controlled by changing the delay angle α or by varying the no-load direct voltage using a transformer tap changer.

20.11 INVERTER

It has already been well explained as to how the converter operation can be changed from rectification to inversion resulting in change in the direction of power flow (DC to AC). The direction of DC current does not change but the DC voltage polarity reverse. It has already been shown that inversion operation result when delay angle α is in the range $90° < \alpha < 180°$.

AC line voltage wave forms and current wave forms for both rectifier and inverter are drawn in Fig. 20.12. Observe that the curvature of the front of a current wave form during commutation are different in rectification and inversion.

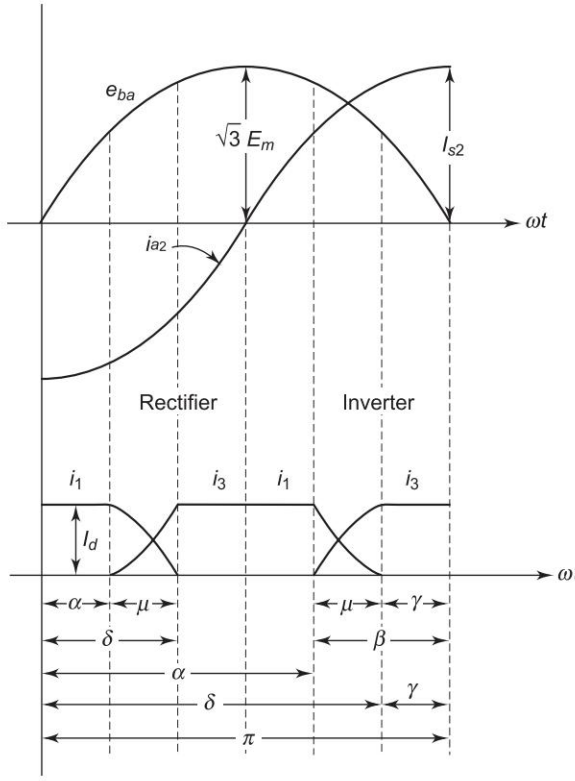

Fig. 20.12 Relations among angles employed in converter theory [3, 7]

References [3] and [7] give the following relationships among various inverter angles are:

$\beta = \pi - \alpha$; inverter ignition angle

$\gamma = \pi - \delta$; inverter extinction angle

$u = \delta - \alpha = \beta - \gamma$

To allow for sufficient time for charge carrier to move back, the extinction angle γ should be in the range 1°–10°. In adequate γ can cause *commutation failure*.

The rectifier equations can be employed for describing inverter operation by substituting α and δ by $\pi - \beta$ and $\alpha - \gamma$, respectively. To differentiate the inverter theory from the rectifier theory, it is normal practice to use the subscripts *i* and *r* to identify the inverter and rectifier operations, respectively. Hence, it can be put as

$$I_{di} = I_s (\cos \gamma - \cos \beta) \tag{20.36}$$

Substituting, the inverter equivalent of Eq. (20.30) into Eq. (20.36)

$$I_{di} = \frac{\sqrt{3} E_m}{2\omega L_c} (\cos \gamma - \cos \beta) \tag{20.37}$$

Correspondingly from Eq. (20.27), the inverter voltage is

$$V_{di} = \frac{1}{2} V_{d0i} (\cos \gamma + \cos \beta) \tag{20.38}$$

Whenever inverter voltage is used along with a rectifier voltage in a given equation, inverter voltage is expressed as negative. When used alone, it is positive.

Also, for inverters with constant-ignition-angle (CIA) control,

$$V_{di} = V_{d0i} \cos \beta + R_c I_d \tag{20.39}$$

or

$$V_{di} = V_{d0i} \cos \beta + \frac{3}{\pi} X_c I_d \tag{20.40}$$

and for inverters with constant-extinction-angle (CEA) control,

$$V_{di} = V_{d0i} \cos \gamma - R_c I_d \tag{20.41}$$

or

$$V_{di} = V_{d0i} \cos \gamma - \frac{3}{\pi} X_c I_d \tag{20.42}$$

It may be noted that it is better to operate inverters with CEA control rather than with CIA control. Figure 20.13 depicts the corresponding equivalent inverter circuits.

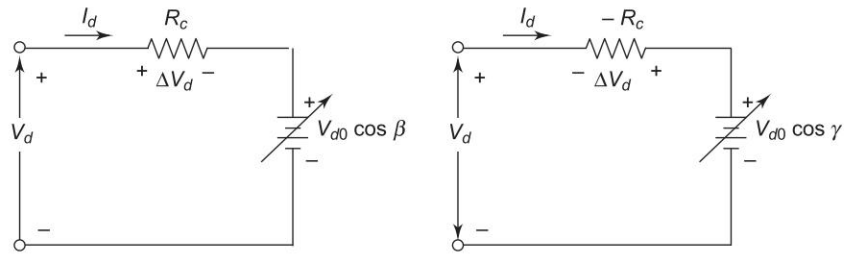

Fig. 20.13 Equivalent circuits of inverter (suffix *i* not used)

It may be seen that an inverter has a leading power factor, as against rectifier, which has a lagging power factor.

The required additional reactive power by the inverter is provided by the synchronous capacitors or by static shunt capacitors. Also, harmonic filters are required on both AC and DC sides of the converters to prevent the harmonics generated by the rectifier and inverter from entering into the AC and DC systems. The order of harmonics in the direct voltage are given by

$$N = pq \tag{20.43}$$

and the order of harmonics in the alternating current are given by

$$N = pq \pm 1 \tag{20.44}$$

where p = pulse number
q = integer number

Example 20.1 A transformer secondary line voltage to a 3-ϕ bridge converter rectifier is 38 kV (i.e. $E_{L-L} = 38$ kV).
Calculate the gross voltage O/P, when the overlap and commutation angle is 15° of delay angle is (a) 0°, (b) 15°, (c) 30°, (d) 45°

Solution

The average direct voltage V_d is given by

$$V_d = \frac{V_{d0}}{2} (\cos \alpha + \cos \delta) \; [\delta = \alpha + \mu]$$

α = delay angle

μ = overlap angle

δ = extinction angle

$$V_{d0} = \frac{3\sqrt{2}}{\pi} \times E_{L-L}$$

$$= \frac{3\sqrt{2}}{\pi} \times 38$$

$$= 51.31 \text{ kV}$$

$$V_d = \frac{V_{d0}}{2} (\cos \alpha + \cos \delta)$$

(a) $\alpha = 0°$, $\delta = 15°$

$$V_{dr} = \frac{81.31}{2} [\cos 0° + \cos 15°]$$

$$V_{dr} = 50.43 \text{ kV}$$

(b) $\alpha = 15°$, $\delta = 30°$

$$V_{dr} = \frac{81.31}{2} [\cos 15° + \cos 30°] = 47 \text{ kV}$$

(c) $\alpha = 30°$, $\delta = 30° + 15° = 45°$

$$V_d = \frac{51.31}{2}\,[\cos 30° + \cos 45°]$$

$$V_d = 40.35 \text{ kV}$$

(d) $\alpha = 45°$, $\delta = 45° + 15° = 60°$

$$V_{dr} = \frac{51.31}{2}\,[\cos 45° + \cos 60°]$$

$$V_{dr} = 30.96 \text{ kV}$$

Observe that V_{dr} reduce as α is advanced (increased).

Example 20.2 Assume for a 3-ϕ bridge rectifier the transformer secondary leakage reactance is 0.3 Ω and the line voltage is 440 V if the output current is 220 A. Find the angle of overlap and DC output voltage at a delay angle of 15°?

Solution

$$X_c = 0.3\ \Omega, \qquad E_{L-L} = 440 \text{ V}$$

$$I_d = 220 \text{ A}, \qquad \alpha = 15°$$

$$V_{d0} = \frac{3\sqrt{2}}{\pi} E_{L-L} = \frac{3\sqrt{2}}{\pi} \times 440 \quad \text{(Eq. (20.20))}$$

$$= 594.2 \text{ V}$$

Equivalent Commutation Resistance $R_c = \dfrac{3X_c}{\pi}$

$$= \frac{3 \times 0.3}{\pi} = 0.286\ \Omega$$

$$I_d = \frac{\sqrt{3}E_m}{2\omega L_c}(\cos\alpha - \cos\delta) \quad \text{Eq. (20.30)}$$

But $$V_{d0} = \frac{3\sqrt{3}E_m}{\pi} \text{ and } \omega L_c = \frac{\pi R_c}{3}$$

So

$$I_d = \frac{V_{d0}}{2R_c}\,(\cos\alpha - \cos\delta)$$

Substituting value, we have

$$220 = \frac{594.2}{2 \times 0.286}\,[\cos 15° - \cos\delta]$$

which gives

$$\cos\delta = 0.7541$$

or $$\delta = 41.05°$$

Overlap angle $$\mu = (\delta - \alpha) = 41.05° - 15°$$

or $$\mu = 26.05°$$

The average direct voltage is given by

$$V_d = \frac{V_{d0}}{2}[\cos\alpha + \cos\delta]; \quad \text{(Eq. (20.27)}$$

or $$V_d = \frac{594.2}{2}[\cos 15° + \cos 41.05°]$$

We find

$$V_d = 511.02 \text{ V}$$

Example 20.3 A 3-ϕ bridge invertor has commutation reactance of 100 Ω, the current and voltage at the DC side are 950 A and 245 kV, respectively. The AC line voltage is 325 kV. Calculate the extinction angle and the overlap angle.

Solution

General converter relationships

$$I_{L1} = \frac{\sqrt{6}}{\pi} I_d;$$

$$V_{d0} = \frac{3\sqrt{2}}{\pi} E_{L-L}$$

$$V_{d0} = \frac{3\sqrt{3}\, E_m}{\pi} = \frac{3\sqrt{2}\, E_{L-L}}{\pi}; \quad \text{Eq. (20.13)}$$

Given:

$$X_{Ci} = 100 \ \Omega$$
$$V_{di} = 245 \text{ kV}$$
$$I_{di} = 950 \text{ A}$$
$$V_{Li} = 325 \text{ kV}$$

For the inverter

$$V_{d0i} = \frac{3\sqrt{2}\, E_{(L-L_i)}}{\pi}$$

$$= \frac{3\sqrt{2}}{\pi} \times 325 = 438.90 \text{ kV}$$

From the equivalent circuit of Fig. 20.8 (b)

$$V_{di} = V_{d0i}\cos\gamma - RC_i I_{di}$$

$$245 \times 10^3 = 438.90 \times 10^3 \cos\gamma - \frac{3}{\pi} \times 100 \times 950 = 438.90 \cos\gamma - 907.8$$

Solving, we get

$$\cos\gamma = 0.7649 \quad \text{or} \quad \gamma = 40.1°$$

From Eq. (20.51)

$$V_{di} = \frac{V_{d0i}}{2}(\cos\beta + \cos\gamma)$$

or

$$V_{di} = \frac{V_{d0i}}{2}(\cos(\gamma + \mu) + \cos\gamma)$$

Substituting values

$$245 \times 10^3 = \frac{438.9 \times 10^3}{2} (\cos(\gamma + \mu) + 0.7649)$$

$$\cos(\gamma + \mu) = 0.3515$$

$$\gamma + \mu = 69.4°$$

$$\therefore \quad \mu = 69.4° - 40.1° = 29.3° \text{ (overlap angle)}$$

$$\therefore \quad \mu = 69.4° - 40.10$$

20.12 CIRCUIT BREAKING: SOME TOPICS IN HVDC

It is easy to interrupt AC currents because of their natural zeros. Since DC is a steady unidirectional current it does not have a natural zero and therefore it is difficult to interrupt large DC currents at high voltages. The faults on the DC line or in the converters are cleared by using the control grids of the converter valves to stop the DC temporarily.

In DC breakers the direct current is reduced to zero by some auxiliary means. A vaccum interrupter is used for circuit breaking in HVDC systems. The application of DC breakers is required mainly for fault clearing in MTDC systems. However, even for two terminal DC systems, the DC breakers can be useful in several situations e.g. when the converters feed two parallel DC lines; when parallel connected converters feed the same line.

AC–DC Link

At times it is required to put a DC link in parallel with an existing AC link. Such a scheme is employed to reinforce the AC link and to improve its stability. A DC link has an extremely fast speed of response (of the order of 50 ms) and

hence, it can change its transmitted power much more rapidly than (say) a turbine-generator can adjust its output. This feature can be used to improve the stability of an exiting AC link. Action can be taken to damp the oscillations within a system but inter area oscillations pose more severe problems and in such cases a DC link offers better solution.

The maximum transmitted power capability of an AC link may be set by its steady state stability limit or transient stability limit. It can be shown that connecting a DC link in parallel with AC link raises the steady-state and transient stability limits of the AC link. The 3100 MW, 1362 km pacific inter tie in USA is a typical example of this application.

Multi-Terminal DC Links

All large AC power systems are effectively of multi-terminal variety. However, most of the DC links are two terminal links. There is Kingsnorth-London multi-terminal DC link. A multi-terminal DC network has a number of rectifier and inverter stations. We need of course large DC circuit breakers, as mentioned earlier. A three-terminal HVDC link has been set up in Italy-Corsica-Sardina [8]. In the three terminal HVDC link, two converters can operate as rectifiers and the third as inverter. It can be reversed also i.e. 2 inverters and 1 rectifier. Thus there is a greater flexibility of operation.

20.13 RECENT ADVANCES

The basic element in an HVDC converter is thyristor. Thyristors using about 150 mm diameter wafers have been developed. This has reduced the costs of HVDC projects and increased the reliability. Light triggered thyristors are also being developed. Use of digital systems and microprocessors for control, protection and supervision is popular. Now GTOs are being used in some HVDC projects. Active AC and DC filters are also used for tackling harmonics. Finally advanced fully digital control systems are being used with optical fibres. MOS (metal oxide semiconductor) controlled thyristor or MCT (MOS controlled thyristor) appears to be a better technology [9].

Conversion of Existing AC Lines

The constraints on ROW are forcing some companies to look into the option of converting existing AC circuits to DC in order to increase the power transfer limit.

Recent Indian HVDC Projects

Talcher-Kolar HVDC System: A 2,000 MW, ±500 kV, bipolar HVDC system has been commissioned between Talcher and Kolar. It is a East-South interconnector to facilitate exchange of power between East India and South India (4 states and Pondicherry).

Chandrapur back to back project (2 × 500 MW), Chandrapur-Padghe bipolar system (±500 kV, 1,500 MW, 736 km) is operating successfully. Several back-to-back projects are also proposed besides around 2,000 circuit km of HVDC lines in next five years.

DC Reactor

A DC reactor is connected in series with each pole of a converter station. Inductance is around 0.4 to 1 H. It is used to

(i) prevent consequent commutation failures in the inverter,
(ii) decrease harmonic voltages and currents in the DC line,
(iii) decrease ripple factor,
(iv) limit the current in the rectifier when a short circuit occurs on the line.

The value of the inductance should be such that a resonance of the DC circuit does not occur at power frequency.

20.14 FUTURE TRENDS

Considerable research and development work is under way to provide a better understanding of the performance of HVDC links to achieve more efficient and economic designs of the thyristor valves and related equipment and to justify the use of alternative AC/DC system configurations.

Future power systems would include a transmission mix of AC and DC. Future controllers would be more and more microprocessor based, which can be modified or upgraded without requiring hardware changes, and without bringing the entire system down. While one controller is in action the duplicate controller is there as a 'hot standby' in case of a sudden need.

In the near future, it is expected that fibre optic system would be used to generate firing signal and the direct light fired thyristor would be employed for HVDC converters. Availability of 100 mm thyristors has eliminated the need of paralleling thyristors as these can handle currents of the order of 4 kA.

Although presently HVDC schemes operate perfectly well without the assistance of DC circuit breakers, it is clear that the prospective extension from point to point to other DC power system configurations can gain versatility and operational flexibility with the use of DC circuit breakers. The lack of current zero presents a difficult problem to the opening of DC circuits.

It is by now clear that HVDC transmission is already a reliable, efficient and cost-effective alternative to HVAC for many applications.

Currently a great deal of effort is being devoted to further research and development in solid-state technology due to which one can hope that HVDC converters and multi-terminal DC (MTDC) systems will play an even greater role in the power systems of the 21st century.

20.15 SUMMARY

In this chapter HVDC transmission, principles of AC/DC conversion and HVDC control, economic considerations applications, transmission modes, principles and working of converters, merits and demerits of HVDC have been fully explained in considerable details. Chapter ends with future trends and recent advances.

Problems

20.1 Calculate the necessary secondary line voltage of the T/F for a 3-ϕ bridge rectifier to provide a voltage of 110 kV. Assume $\alpha = 25°$ $\mu = 12°$. Calculate the effective reactance X_c if the rectifier is delivering a current $I_d = 750$ A.

20.2 The AC line voltage of a 3-ϕ bridge inverter is 140 kV, the extinction angle is 18° and with an overlap angle of 22°.
(i) Calculate the DC voltage at the inverter, (ii) Calculate the necessary extinction angle to maintain the AC line voltage at 140 kV, when DC voltage drops to 170 kV. Assume overlap angle to remain unchanged.

References

1. Adamson, C. and N.G. Hingorani, *High Voltage Direct Current Power Transmission*, Garraway, London, 1960.
2. Arrillaga, J., *High Voltage Direct Current Transmission*, Peter Peregrinus, London, 1983.
3. Kimbark, E.W., *Direct Current Transmission*, vol. 1, Wiley, New York, 1971.
4. Nanda, J. and D.P. Kothari, *Recent Trends in Electric Energy Systems*, Prentice-Hall, New Delhi, 1988.
5. Padiyar, K.R., *HVDC Power Transmission Systems*, Wiley Eastern Ltd., New Delhi, 1990.
6. Ullmann, E., *Power Transmission by Direct Current*, Springer-Verlag, Berlin, 1975.
7. Gönen, Turan, *Electric Power Transmission System Engineering*; *Analysis and Design*, John Wiley, NY, 1988.
8. Gupta, B.R., *Power System Analysis and Design*, S. Chand, New Delhi, 2006.
9. Kothari, D.P. and I.J. Nagrath, *Electric Machines*, 3rd edn, Tata McGraw-Hill, New Delhi, 2004. (Ch. 11).
10. Arrillaga, J., *et al*., *Computer Modelling of Electrical Power Systems*, John Wiley, NY, 1983.
11. Kothari, D.P. and I.J. Nagrath, *Modern Power System Analysis*, 3rd edn, Tata McGraw-Hill, New Delhi, 2003.
12. PSCAD/EMTDC, Manitoba HVDC Research Centre; www.hvdc.ca.

Chapter 21
Distribution Systems

21.1 INTRODUCTION

Though in this book there is a heavy bias for transmission systems and related topics, the general area of distribution cannot be considered to be of secondary importance. It is to be noted here that electric power is universally used for distribution.

An electric power system consists of three major components: (i) Generation (Ch. 1), (ii) Transmission (Ch. 5 and others) and (iii) Distribution*. A system may or may not have transmission component (like present day distributed and dispersed systems, specially autonomous non-conventional energy sources see Ch. 1 [15]), but distribution is an integral part of any electric power system. Like Transmission system (Ch. 1), distribution system based on voltage levels can be further classified as (i) primary distribution (33 kV and above), (ii) secondary distribution (11 kV/6.6 kV/3.3 kV) and (iii) tertiary distribution (400 V, 3-phase).

Distribution system has two components: (i) Feeder, (ii) Distributor. A feeder in a distribution network is a circuit carrying power from a main substation to a secondary substation such that the current loading is the same all along its length. Therefore, the main criterion for the design of a feeder is its current carrying capacity (thermal limits rather than voltage drops). A distributor on the other hand, has variable loading along its length due to the service conditions, tapping off at intervals by the individual consumers. The voltage variation at consumers terminals must be maintained within ± 5%. In order to avoid unsatisfactory operation of household lighting, fans and a variety of other appliances and excessive voltage variation may even lead to equipment failure. Thus, the main criterion for the design of a distributor is the limit on percentage voltage variations. A typical distribution system in a city area is shown in Fig. 21.1.

The effectiveness with which a distribution system achieves its objective of distributing electric energy to various consumers is measured in terms of voltage regulation, flexibility, security of supply efficiency and cost.

* Refs (5, 7) are books fully devoted to Distribution.

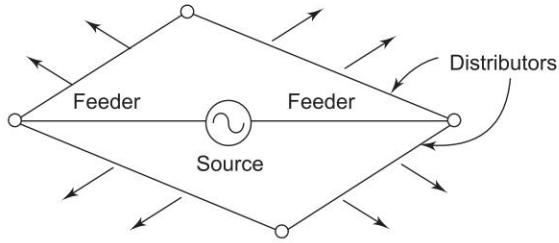

Fig. 21.1 A typical distribution system

21.2 TYPES OF DISTRIBUTION SYSTEMS

Distribution systems differ from transmission systems in several ways. The number of branches and sources is much higher in distribution networks, and the general structure or topology is quite different. A typical system consists of a step-down (e.g. 66/11 kV) on-load tap-changing transformer at a bulk supply point feeding a number of cables of different lengths. A series of step-down 3-phase transformers, e.g. 11 kV/415 V in India or 4.16 kV/240 V in the USA, are spaced along the route from where the consumers are supplied through 3-phase, 4-wire networks giving 230 V, or, in the USA, 120 V. Fig. 21.2 shows main parts of a distribution system.

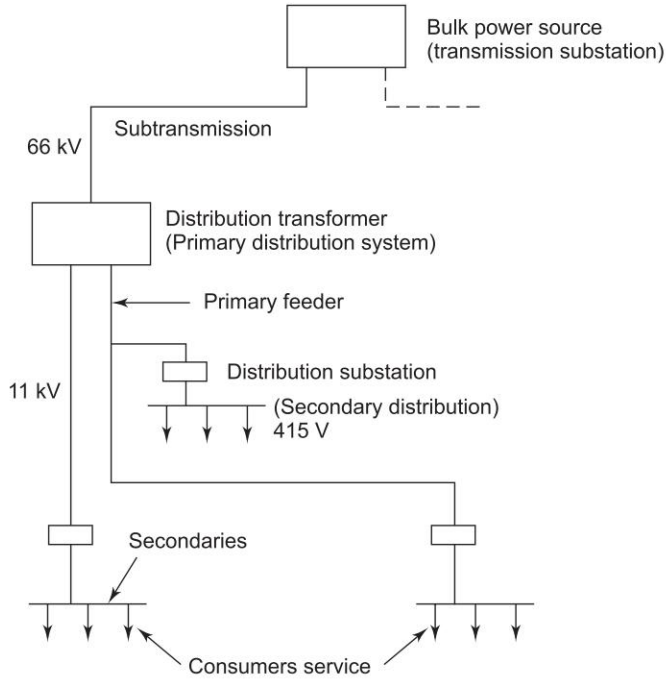

Fig. 21.2 A typical distribution system showing main parts

While designing a distribution system on has to keep in mind (1) service conditions, (2) electrical design, (3) mechanical design, and (4) various costs.

In service conditions, mainly load study is carried out, which tells us the type of load to be served, density of consumers, etc. Main loads are residential (domestic), commercial, industrial, municipal traction and so on.

The distribution system may be subdivided mainly into primary distribution, distribution transformers, secondary distribution and consumers service connections. The proper voltage, location, sizes and protective equipment must be chosen for the various components of the distribution system.

The distribution systems can be classified as follows:

Radial System

The radial type of distribution system, as shown in Fig. 21.3 is the most common.

This serves the light and medium density load areas. Feeders are not tapped in between the subtransmission substation and the distribution substations, while distributors are tapped throughout at several points to serve the consumers.

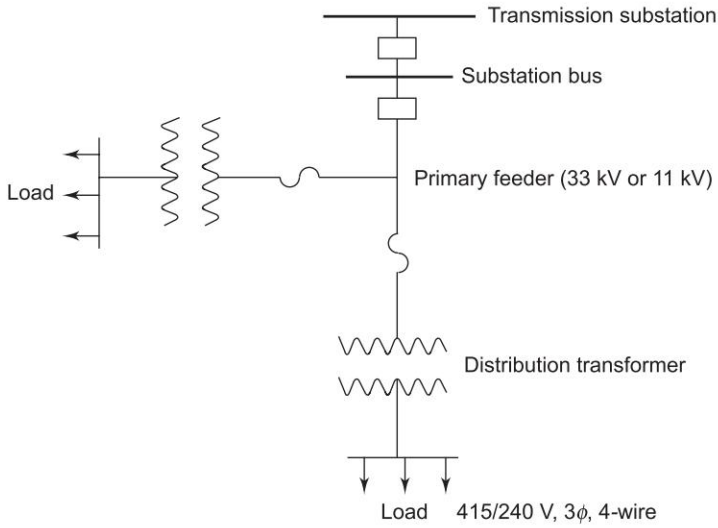

Fig. 21.3 Simple form of radial distribution system

Parallel or Loop System

In this system (Fig. 21.4) the circuit returns to the same point so that there is in effect one feeding point only. As the alternative path is available in case of fault, this system is more reliable than the radial system.

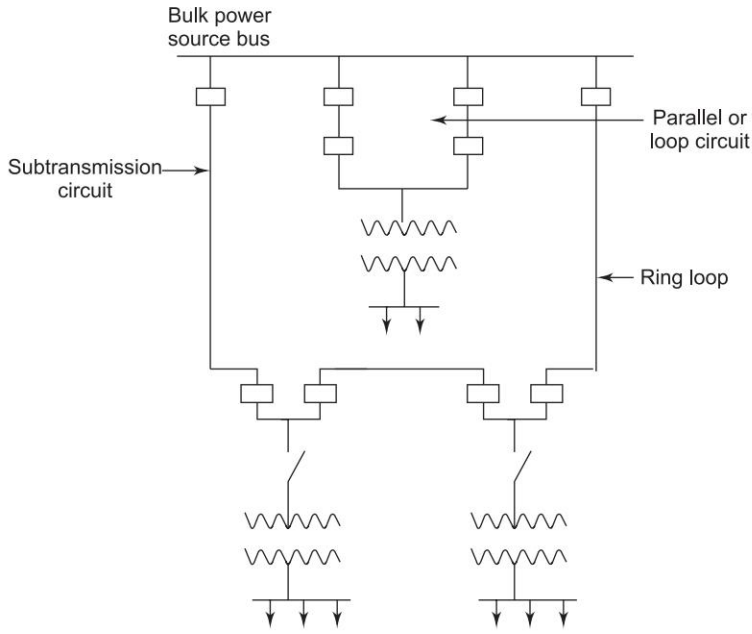

Fig. 21.4 A parallel or loop distribution layout

Network or Grid System of Distribution

This system as shown in Fig. 21.5 is preferred for large distribution areas for large loads which have to be supplied with greater reliability with all other advantages of grid (interconnected) system. This system gives better voltage regulation

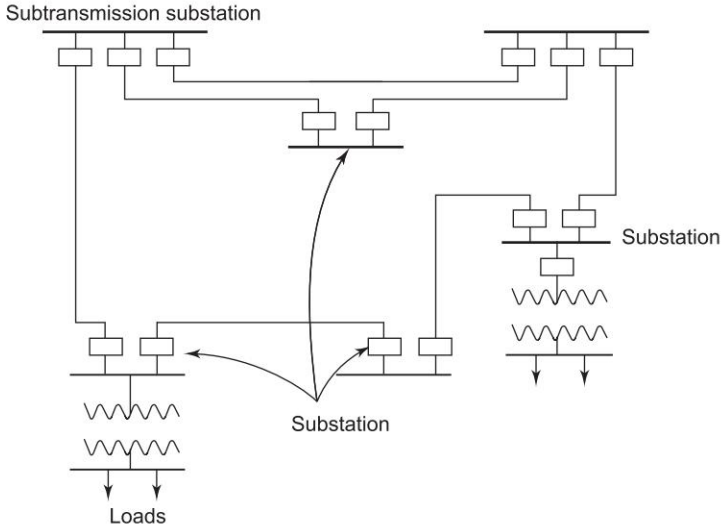

Fig. 21.5 Network or grid form of distribution

21.3 SECTION AND SIZE OF FEEDERS

Feeders carry current from one substation to another, or to transformer or a feeding point, and are not tapped in between. They are loaded at substations only. Voltage control can be done at the feeding points. Size of the cable conductors is chosen by application of Kelvin's law, which says that the most economical size of the conductor will be when the sum of the annual charge on the capital investment and the annual charge due to loss of energy in transmission would be minimum.

Annual charge on the cost of cable and distribution = $P_1 + P_2 A$

where

A = cross-sectional area of the conductor
P_1 = constant part of the annual charge
P_2 = part of the annual charge dependent on A

$3I^2 R \times 8760$ is the loss in kWh during the year, where I is the line current in a 3-phase line.

The cost of the energy loss/year = $\frac{P_3}{A}$ as $R \propto \frac{1}{A}$.

Kelvin's Law

$$\min_A \ (P_1 + P_2 A + P_3/A) \tag{21.1}$$

Differentiating with respect to A gives the economic condition as

$$P_2 A = P_3/A \tag{21.2}$$

Kelvin's law has several limitations and may not give the optimum result.

If a certain load is given and the length of line is given, the most economical voltage can be found out. In India, the standard voltages used for primary distribution are 3.3, 6.6, 11 kV, 3-phase 3-wire.

The most economical distance between the substations, and hence the number of substations in the system, is a function of the distribution voltage used.

The primary feeders may have a rating between 500 kVA to 2500 kVA. Often a distribution system is designed for total voltage drop of 8 to 10%.

The neutral of the distribution system is grounded properly and protection against lightning is provided.

In India design of rural distribution systems is very important. A distribution system has to serve consumers by long lines with low load density. Hence it should be least expensive, durable and reliable. The Rural Electrification Corporation (REC) has been set up to finance the rural electrification programmes by providing suitable loans for the projects.

Designing the industrial distribution system needs special care as the load groups and demands are concentrated. Industrial load in India consumes about

70% of the net energy produced. Loads are of high specific load density. Industrial distribution networks also differ from public supply networks as regards the degree of utilization. High utilization means high losses over a long period of time, and this must be considered while deciding the economic rating of the plant.

Comparison of Various Distribution Systems

Nowadays DC distribution system is phased out in almost every country. However some applications of DC power are still there; whereas in transmission both DC (Ch. 20) and AC exist. It is, therefore, necessary to analyze various possible distribution systems, given below:

(i) DC 2-wire system (monopolar operation)
(ii) DC 2-wire system with mid-point earthed (bipolar operation)
(iii) AC 1-phase 2-wire
(iv) AC 3-phase 3-wire
(v) AC 3-phase 4-wire

For comparison, following assumptions are made:

(a) The power transmitted is the same in all the cases.
(b) Distance and power loss are the same in all the cases.
(c) The lines should have the same insulation level. This requires that maximum potential difference between any conductor and earth are equal. Let V be the maximum potential difference between any conductor and the earth and I be the line current.

(a) DC 2-wire system

Figure 21.6 shows the 2-wire DC system without midpoint earthed. If R is the resistance of each conductor with a cross-sectional area, then

Power transmitted, $P = VI$

$$\text{Power loss} = 2I^2 R = \frac{2P^2R}{V^2} \qquad (21.3)$$

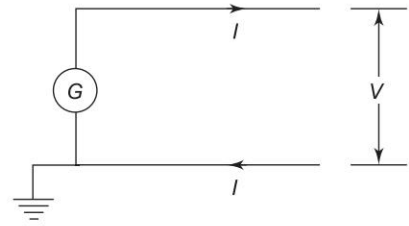

Fig. 21.6 DC 2-wire system

(b) DC 2-wire system mid-point earthed

Figure 21.7 shows the DC 2-wire mid-point earthed system. As no load is fed at voltage V, $I_1 = I_2$. Though the load voltage is 2 V, the insulation needed corresponds to V. If R_1 is the resistance of each conductor having cross-sectional area of a, then

Power transmitted $P = 2VI_1$

$$\text{Power loss } P_1 = 2I_1^2 R_1 = \frac{P^2R_1}{2V^2} \qquad (21.4)$$

If the power loss is same in both the cases, then from Eqs (21.3) and (21.4), we get

$$\frac{P^2R_1}{2V^2} = \frac{2P^2R}{V^2}$$

or
$$R = R_1/4 \tag{21.5}$$

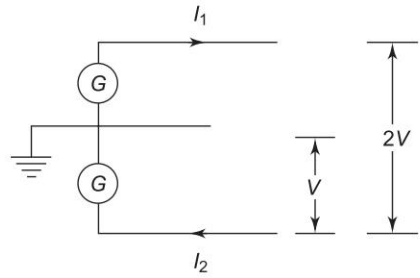

Fig. 21.7 DC 2-wire mid-point earthed system

Since the resistance is inversely proportional to the area of cross-section $\left(R = \rho \frac{l}{a}\right)$, Eq. (21.5) can be written in terms of area of cross-section as

$$a_1 = \frac{a}{4} \tag{21.6}$$

As the number of conductors used in both the cases is two, the ratio of volume of conductors will be

$$\frac{v_1}{v} = \frac{a_1 2l}{a2l} = \frac{1}{4} \tag{21.7}$$

Thus the volume of the conductor used in the case of DC 2-wire mid-point earthed is only 1/4th of that of the DC 2-wire system. As in the monopolar operation, ground is used as return path. If only one conductor is used in case (a), the saving of conductor volume will be 1/2 only. It is easy to see that

$$v_1/v = \frac{a_1 2l}{al} = \frac{1}{2} \tag{21.8}$$

(c) AC single-phase 2-wire

Figure 21.8 shows a single-phase 2-wire system with V middle point earthed. The maximum voltage between one of the outer wires and the earth is V volts.

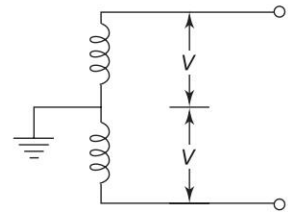

Fig. 21.8 Single-phase 2- wire AC system

$$\therefore \quad V_{rms} = V/\sqrt{2}$$

The voltage between the two outer conductors is $\frac{2V}{\sqrt{2}} = \sqrt{2}$ V.

$\therefore$ Current in outer wire $I = \frac{P}{\sqrt{2}\, V \cos\phi}$ ϕ = load pf angle. Let R_2 be the resistance of each wire, the copper loss = $2\left[\frac{P^2}{2V^2\cos^2\phi}\right] R_2$

$$= \frac{P^2}{V^2\cos^2\phi} R_2 \qquad (21.9)$$

(D) AC 3-phase 4-wire system

Figure 21.9 shows a 3-phase 4-wire, AC system.

The maximum voltage between one phase and grounded neutral is V volts.

$$V_{rms} = V/\sqrt{2}$$

$\therefore$ Current per phase under balanced condition = $\frac{P}{3 \times \frac{V}{\sqrt{2}} \cos\phi}$

where ϕ = load power factor angle

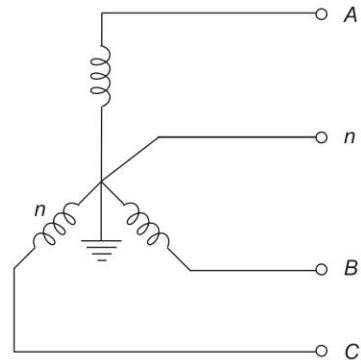

Fig. 21.9 3-phase 4-wire AC system

If R_3 is the resistance per conductor, copper loss is given by

$$\text{copper loss} = 3\,\frac{2P^2}{9V^2\cos^2\phi} R_3 = \frac{2}{3}\,\frac{P^2}{V^2\cos^2\phi} R_3 \qquad (21.10)$$

Equating the Eqs (21.4) and (21.10) copper loss due to 3 -phase 3-wire as calculated at with DC 2-wire system

$$\frac{P^2 R_1}{2V^2} = \frac{2P^2}{3V^2\cos^2\phi} R_3$$

or $$R_1/R_3 = 4/3\ \frac{1}{\cos^2\phi} \qquad (21.11)$$

or $$a_3/a_1 = 4/3\ \frac{1}{\cos^2\phi} \qquad (21.12)$$

In case of 3-phase 3-wire system there are 3-wires and in case of DC 2-wire system there are 2-wires. The ratio of volumes for the same conductor length l is

$$\frac{3a_3 l}{2a_1 l} = \frac{3}{2}\frac{a_3}{a_1} = \frac{3}{2}\frac{4}{3}\frac{1}{\cos^2\phi}$$

In case of 3-phase, 4-wire system the 4-wire is of the same size as the phase wire, and so the volume of copper required will be $4a_3 l$. The ratio of volumes is

$$\frac{4a_3 l}{2a_1 l} = \frac{2a_3}{a_1} = 2\frac{4}{3}\frac{1}{\cos^2\phi} = \frac{8}{3}\frac{1}{\cos^2\phi}$$

Similarly to compare the volume of copper required in case of AC single-phase 2-wire system with the DC two-wire system, we equate copper losses

$$\frac{P^2}{2V^2} R_1 = \frac{P^2}{V^2\cos^2\phi} R_2$$

$$\therefore \quad \frac{R_1}{R_2} = \frac{2}{\cos^2\phi} = \frac{a_2}{a_1} \tag{21.13}$$

Since the number of wires required is two in each case the ratio of copper volume is

$$1 : \frac{2}{\cos^2\phi}$$

We thus find that the ratio of copper volume required in the three cases discussed when DC 2-wire system is taken as a reference are (DC 2-wire): (1-phase, 2-wire); (3-phase, 4-wire)

$$1 : \frac{2}{\cos^2\phi} : \frac{8}{3}\frac{1}{\cos^2\phi} \tag{21.14}$$

If the system is single-phase 2-wire with neutral grounded, the reader can verify that the ratio of volume of copper w.r.t. DC 2-wire is

$$1 : \frac{8}{\cos^2\phi} \tag{21.15}$$

Remark: These figures workout to be in favour of DC 2-wire as for insulation $V_{dc} = \sqrt{2}\, V_{ac}$(rms). However DC distribution is no longer used because of inability to change voltage levels. DC would be used for very short distance for special need. However 3-phase, 4-wire AC system is universally used for distribution of power throughout the world.

21.4 VOLTAGE DROP IN DC DISTRIBUTORS

Voltage at the consumer premises must be within the permissible limits. It is very important and necessary to calculate the voltage drop in different parts of the power supply network. The voltage drop calculations in the distributors are

very lengthy because the loads are tapped at many points along the length of the distributors.

Distributor Fed at One End

Figure (21.10) shows a DC distributor fed at one end supplying concentrated loads. Let I_1, I_2, I_3 be the load currents tapped at different points. The resistance per unit length of the distributor (go and return) in r.

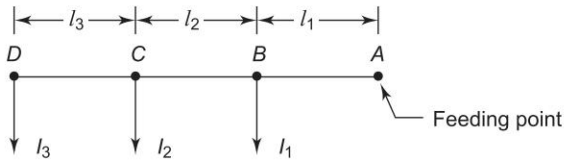

Fig. 21.10

Total voltage drop = (voltage drop in section AB + voltage drop in section BC + voltage drop in section CD)

$$= (I_1 + I_2 + I_3)l_1\, r + (I_2 + I_3)l_2\, r + I_3\, l_3\, r$$

$$= I_1\, l_1\, r + I_2\, (l_1 + l_2)\, r + I_3\, (l_1 + l_2 + l_3)\, r \qquad (21.16)$$

Distributor Fed at Both Ends

Figure (21.11) shows a DC distributor fed at both ends. Long distributors carrying large currents are supplied at both ends. If such a distributor is fed at only one end, the voltage drop at the far end may be unacceptable. The voltages at the feeding points may be equal or unequal. The load current is supplied from the both ends A and B. For the same voltage at both ends, this is nothing but ring distributor.

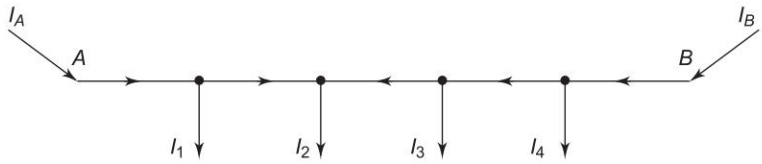

Fig. 21.11

The currents I_A and I_B can be calculated by the application of Kirchhoff's laws. The total voltage drop across the distributor must be equal to difference of voltages V_A and V_B.

Uniformly Distributed Load

Figure (21.12) shows a uniformly loaded distributor fed at one end. The total length of the distributor is taken l and i is the current tapped off per unit length. The voltage drop upto a distance x from the feeding point is

Voltage drop upto distance x

$$= \int_0^x r\, x\, i\, dx + i(l - x)dx$$

$$= i\, l\, r\, x - \frac{1}{2}\, i\, r\, x^2 \qquad (21.17)$$

Total voltage drop over the length l is obtained by substituting $x = l$.

$$\text{Total voltage drop} = \frac{1}{2}\, i\, r\, l^2 = \frac{1}{2}\, I\, r\, l$$

where $I = i\, l$, total current supplied by the distributor.
r = resistance per unit length of both wires of the distributor (go and return)

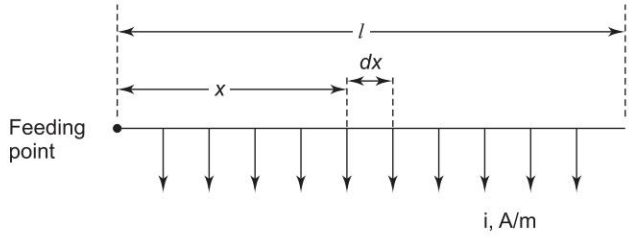

Fig. 21.12

Example 21.1 A 3-phase 3-wire line 50 km long supplies a balanced load of 6 MW at pf 0.8 lagging at 33 kV. Calculate the weight of copper required assuming the transmission efficiency to be 80%. In case of a 2-wire AC operating at the same voltage between the lines. What reduction of copper weight. will be possible? Given, specific resistance of copper $= 1.73 \times 10^{-8}\ \Omega$m and density = 8900 kg/m^3.

Solution

3-phase 3-wire system

$$P = 6000 \text{ kW}$$

$$V = 33 \text{ kV (line to line)}$$

$$\cos \phi = 0.8$$

$$I = \frac{6000 \times 1000}{\sqrt{3} \times 33 \times 1000 \times 0.8} = 131.21 \text{ A}$$

Efficiency of transmission

$$= \frac{\text{Power output}}{(\text{Power output} + \text{line loss})}$$

$$0.80 = \frac{6000}{6000 + \text{line losses}}$$

$$6000 + \text{line losses} = \frac{6000}{0.80}$$

$$\text{line losses} = 7500 - 6000$$

$$\text{line losses} = 1500 \text{ kW}$$

$$\text{line losses/phase} = \frac{1500}{3} = 500 \text{ kW/phase}$$

$$I^2R = 500 \times 1000$$

$$R = \frac{500 \times 10^3}{(131.21)^2} = 29.04 \ \Omega$$

Length of conductor $L = 50$ km
Conductor cross-sectional area

$$a = \frac{\rho L}{R} = \frac{1.73 \times 10^{-8} \times 50 \times 10^3}{29.04} = \frac{\rho l}{R}$$

$$= 2.9786 \times 10^{-5} \text{ m}^2$$

Volume of copper required = $3\ al$

$$= 3 \times 2.9786 \times 10^{-25} \times 50000$$

$$= 4.4679 \text{ m}^3$$

weight of the copper = Vol. × density

$$= 8900 \times 4.4679$$

$$= 3.9764 \times 10^4 \text{ kg m}$$

Single-phase system

$V = 33000$ volts

I = current per conductor

Power transmitted = 6000 kW

$$I \times 33{,}000 = 6000 \times 1000$$

$$I = \frac{6000}{33} = 181.81 \text{ A}$$

Copper loss = $2I^2 R$

$$= 2 \times (181.81)^2 \times R$$

If copper loss is to be same as in 3-phase systems

$$1500 \times 1000 = 2 \times (181.81)^2 \times R$$

$$R = 22.68 \ \Omega$$

Now $$R = \frac{\rho l}{A} \quad \text{or} \quad A = \frac{\rho l}{R}$$

$$A = \frac{1.73 \times 10^{-8} \times 50 \times 10^{3}}{22.68} = 3.8139 \times 10^{-5} \text{ m}^2$$

Volume of copper $= 2a \cdot l = 2 \times 3.8139 \times 10^{-5} \times 50 \times 1000$

$$= 3.8139$$

weight of copper $= 8900 \times 3.8139$

$$= 3.3943 \times 10^{4} \text{ kg}$$

% reduction in copper weights

$$= \frac{(3.9764 - 3.3943)}{3.9764} \times 100$$

$$= 17.1336\%$$

Example 21.2 A DC distributor is fed at both ends and two loads are tapped off from it as shown in Fig. 21.13. The line resistance valves are given on the figure. Calculate the load voltages.

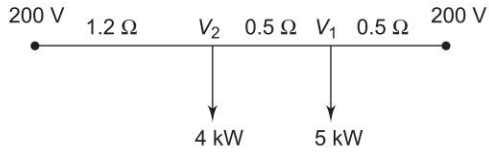

Fig. 21.13

Solution

As the load voltages are unknown but the load powers are known. We have to proceed iteratively.

To compute load currents we assume to start with V_1, $V_2 = 200$ V

$$4 \text{ kW} \longrightarrow \frac{4,000}{200} = 20 \text{ A}$$

$$5 \text{ kW} \longrightarrow \frac{5,000}{200} = 25 \text{ A}$$

From KCL, we can write the equation at nodes 1 (V_1) and node 2 (V_2)

$$\frac{200 - V_1}{0.5} + \frac{V_2 - V_1}{0.5} = 25$$

$$\frac{200 - V_2}{1.2} + \frac{V_1 - V_2}{0.5} = 20$$

Solving, we get

$$V_1 = 184.9 \text{ V}, \quad V_2 = 182.3 \text{ V}$$

With these values of V_1, V_2 we recalculate load current and calculate new values of V_1, V_2, continue till V_1 and V_2 converge in acceptable range (±).

In case of AC distributor, if the line resistance is neglected compared to its reactance, the DC solution will do for rms value otherwise each equation becomes two equation-one in magnitude and the other in angle and the task becomes complex.

21.5 SUMMARY

In this chapter a very important topic of power distribution systems is discussed. Various types of distribution systems are described. Their economics is also worked out. In India there is a huge network of several millions of circuit kms of distribution system. If it is properly planned, losses can be minimized to a great extent and better and more efficient operation can be ensured.

Problems

21.1 Calculate the percentage change in the volume of copper required with and without interconnection AC for the same voltage drop between points A and C. Assume all conductors have same cross section. The lengths of the cross sections are as shown in Fig. (P-21.1).

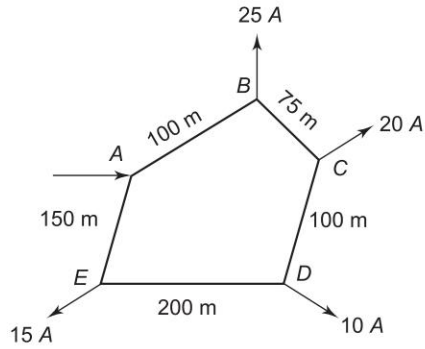

Fig. P-21.1

21.2 A DC 2-wire distribution system AB is 400 m long and it is fed at both ends at 250 V. The system is loaded as shown in Fig. (P-21.2). The resistance of each conductor is 0.04 ohm per km. Find the point of minimum potential at its potential.

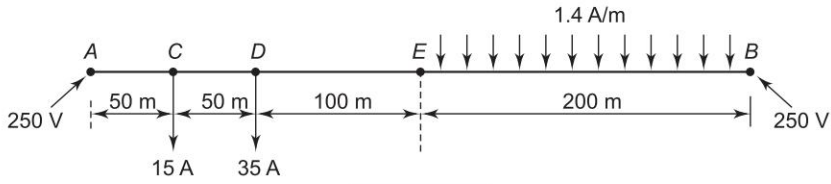

Fig. P-21.2

21.3 A train is running from station "*A*" and in crossing another train standing at 3 km from station *B*. The loading to running train is 600 *A*, while at standing it takes 60 *A* as shown in Fig. (P-21.3). What will be the position of the running train for having minimum potential at a point in the section having distance 8 km between stations *A* and *B*, if both the ends maintained at equal DC potential?

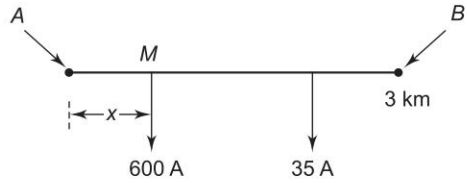

Fig. P-21.3

References

1. Deshpande, M.V., *Electrical Power System Design*, Tata McGraw-Hill, New Delhi, 1984.
2. *Planning and Design of Industrial Low Voltage Networks*, Siemens.
3. Rural Electrification Corporation (REC), *Specifications and Construction Standards*, 1971–1975.
4. Westinghouse Electric and Manufacturing Co., *Electrical Transmission and Distribution Reference Book*, 4th edn, 1950.
5. Turan Gonen, *Electric Power Distribution System Engineering*, McGraw-Hill, New York, 1986.
6. Das, D., H.S. Nagi and D.P. Kothari, "A New Load Flow Technique for Solving Radial Distribution Feeder—Main Feeder Case", *J.I.E.* (*India*), vol. 73, Oct. 1992, pp. 223–226.
7. Pabla, A.S., *Electric Power Distribution Systems*, 3rd edn, TMH, 1992.
8. Das, D., D. Tyagi and D.P. Kothari, "A New Load Flow Technique for Solving Radial Distribution Feeder", *Proc. XVI NSC '92*, Feb. 1993, pp. 143–147.
9. Sharma, H.K., J.C. Joshi and D.P. Kothari, 'Determination of optimum size and dynamic behaviour of single phase distribution systems of standalone PV system', *Published in New Dimensions in Renewable Energy*, Tata McGraw-Hill, New Delhi 1993, pp. 149–156.

10. Das, D., H.S. Nagi and D.P. Kothari, "A Novel Approach for Solving Radial Distribution Networks, *Proc. IEE* ptc, GTD vol. 141, no. 4, July 94, pp. 291–298.
11. Das, D., D.P. Kothari and A. Kalam, "A Simple and Efficient Method for Load Flow Solution of Radial Distribution Networks" *Int. J. of EPES*, 1995, pp. 335–346.
12. Ranjan, R., D. Das and D.P. Kothari, 'Voltage Improvement and Loss Minimization of Radial Distribution Networks by Optimal Conductor Grading', *Electrical India*, 15 June 1997, pp. 16–18.
13. Ranjan, R., D. Das and D.P. Kothari, 'Optimal Conductor Selection of Radial Distribution Feeders-Main Feeders Case', *Proceedings, All India Seminar on Efficient Use of Electric Motors, Generators and Drives for Industries and Utilities for Purpose of Achieving Saving in Energy*, Murthal (Sonepat) Feb. 1997, pp. 95–104.
14. Ranjan, R., D. Das and D.P. Kothari, 'Novel Computer Algorithm for Optimal Conductor Selection of Radial Distribution Feeders-Main Feeders Case', *International Conference on Computer Application in Electrical Engineering Recent Advances*, Roorkee, India, Sept. 1997, pp. 466–470.
15. Kothar, D.P. and I.J. Nagrath, *Modern Power System Analysis'*, 3rd edn, Tata McGraw-Hill, New Delhi, 2003.

Chapter 22

Voltage Stability

22.1 INTRODUCTION

Voltage control and stability problems are very much familiar to the electric utility industry but are now receiving special attention by every power system analyst and researcher. With growing size alongwith economic and environmental pressures, the possible threat of voltage instability is becoming increasingly pronounced in power system networks. In recent years, voltage instability has been responsible for several major network collapses in New York, France, Florida, Belgium, Sweden and Japan [4, 5]. Research workers, *R* and *D* organizations and utilities throughout the world, are busy in understanding, analyzing and developing newer and newer strategies to cope up with the menace of voltage instability/collapse.

Voltage stability* covers a wide range of phenomena. Because of this, voltage stability means different things to different engineers. Voltage stability is sometimes also called load stability. The terms voltage instability and voltage collapse are often used interchangeably. The voltage instability is a dynamic process wherein contrast to rotor angle (synchronous) stability, voltage dynamics mainly involves loads and the means for voltage control. Voltage collapse is also defined as a process by which voltage instability leads to very low voltage profile in a significant part of the system. Voltage instability limit is not directly correlated to the network maximum power transfer limit.

A CIGRE Task Force [25] has proposed the following definitions for voltage stability.

Small-disturbance voltage stability

A power system at a given operating state is *small-disturbance voltage stable* if, following any small disturbance, voltages near loads do not change or remain close to the pre-disturbance values. The concept of small-disturbance voltage stability is related to steady-state stability and can be analyzed using small-signal (linearized) model of the system.

* The problem of voltage stability has already been briefly tackled in Ch. 13. Here it is again discussed in greater details by devoting a full chapter.

Voltage Stability

A power system at a given operating state is voltage stable if on being subjected to a certain disturbance, the voltages near loads approach the post-disturbance equilibrium values.

The concept of voltage stability is related to transient stability of a power system. The analysis of voltage stability normally requires simulation of the system modelled by non-linear differential-algebraic equations.

Voltage Collapse

Following voltage instability, a power system undergoes voltage collapse if the post-disturbance equilibrium voltages near loads are below acceptable limits. Voltage collapse may be total (blackout) or partial.

Voltage security is the ability of a system, not only to operate stably, but also to remain stable following credible contingencies or load increases.

Although voltage stability involves dynamics, power flow based static analysis methods often serve the purpose of quick and approximate analysis.

22.2 COMPARISON OF ANGLE AND VOLTAGE STABILITY

The problem of rotor angle (synchronous) stability (covered in Ch. 12) is well understood and documented [3]. However, with power system becoming overstressed on account of economic and resource constraint on addition of generation, transformers, transmission lines and allied equipment, the voltage instability has become a serious problem. Therefore, voltage stability studies have attracted the attention of researchers and planners worldwide and is an active area of research.

Real power is related to rotor angle instability. Similarly reactive power is central to voltage instability analysis. Deficit or excess reactive power leads to voltage instability either locally or globally and any increase in loadings may lead to voltage collapse.

Voltage Stability Studies

The voltage stability can be studied either on static (slow time frame) or dynamic (over long time) considerations. Depending on the nature of disturbance and system/subsystem dynamics voltage stability may be regarded a slow or fast phenomenon.

Static Voltage Analysis

Load flow analysis reveals as to how system equilibrium values (such as voltage and power flow) vary as various system parameters and controls are changed. Power flow is a static analysis tool wherein dynamics is not explicitly considered. Many of the indices used to assess voltage stability are related to

NR load flow study. Details of static and dynamic voltage stability will be considered further in Sec. 22.5.

Some Counter Measures

Certain counter measures to avoid voltage instability are:

(i) generator terminal voltage increase (only limited control possible)
(ii) increase of generator transformer tap
(iii) reactive power injection at appropriate locations
(iv) load-end OLTC blocking
(v) strategic load shedding (on occurrence of undervoltage)

Counter measures to prevent voltage collapse will be taken up in Sec. 22.6.

22.3 REACTIVE POWER FLOW AND VOLTAGE COLLAPSE

Certain situations in power system cause problems in reactive power flow which lead to system voltage collapse. Some of the situations that can occur are listed and explained below:

(i) *Long Transmission Lines:* In power systems, long lines with voltage uncontrolled buses at the receiving ends create major voltage problems during light load or heavy load conditions.
(ii) *Radial Transmission Lines:* In a power system, most of the parallel EHV networks are composed of radial transmission lines. Any loss of an EHV line in the network causes an enhancement in system reactance. Under certain conditions the increase in reactive power delivered by the line(s) to the load for a given drop in voltage, is less than the increase in reactive power required by the load for the same voltage drop. In such a case a small increase in load causes the system to reach a voltage unstable state.
(iii) *Shortage of Local Reactive Power:* There may occur a disorganized combination of outage and maintenance schedule that may cause localized reactive power shortage leading to voltage control problems. Any attempt to import reactive power through long EHV lines will not be successful. Under this condition, the bulk system can suffer a considerable voltage drop.

22.4 MATHEMATICAL FORMULATION OF VOLTAGE STABILITY PROBLEM

The slower forms of voltage instability are normally analyzed as steady state problems using power flow simulation as the primary study method. "Snap-shots" in time following an outage or during load build up are simulated. Besides these post-disturbance power flows, two other power flow based methods are often used; *PV* curves and *VQ* curves (see also Sec. 13.6). These

two methods give steady-state loadability limits which are related to voltage stability. Conventional load flow programs can be used for approximate analysis.

PV curves are useful for conceptual analysis of voltage stability and for study of radial systems.

The model that will be employed here to judge voltage stability is based on a single line performance. The voltage performance of this simple system is qualitatively similar to that of a practical system with many voltage sources, loads and the network of transmission lines.

Consider the radial two bus system of Fig. 22.1. This is the same diagram as that of Fig. 5.26 except that symbols are simplified. Here E is V_S and V is V_R and E and V are magnitudes with E leading V by δ. Line angle $\phi = \tan^{-1} X/R$ and $|z| \approx X$.

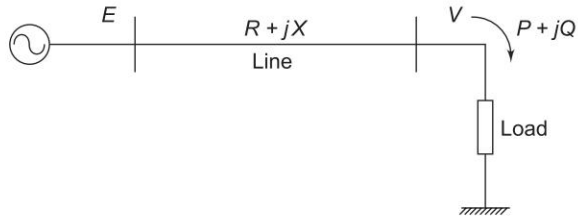

Fig. 22.1

In terms of P and Q, the system load end voltage can be expressed as [1]:

$$V = \left[\frac{-2QX + E^2}{2} \pm \frac{1}{2} \sqrt{(2QX - E^2)^2 - 4X^2(P^2 + Q^2)} \right]^{1/2} \tag{22.1}$$

It is seen from Eq. (22.1) that V is a double-valued function (i.e. it has two solutions) of P for a particular pf which determines Q in terms of P. The PV curves for various values of pf are plotted in Fig. 22.2. For each value of pf, the higher voltage solution indicates stable voltage case, while the lower voltage lies in the unstable voltage operation zone. The changeover occurs at V_{cri} (critical) and $P_{\max}$. The locus of V_{cri}–$P_{\max}$ points for various pfs is drawn in dotted line in the figure. Any attempt to increase the load above $P_{\max}$ causes a reversal of voltage and load. Reducing voltage causes an increasing current to be drawn by the load. In turn the larger reactive line drop causes the voltage to dip further. This being unstable operation causes the system to suffer voltage collapse. This is also brought out by the fact that in upper part of the curve $\frac{dP}{dV} < 0$ and in the lower part (unstable part) $\frac{dP}{dV} > 0$ (reducing load means reducing voltage and vice-versa). It may be noted here that the type of load assumed in Fig. 22.2 is constant impedance. In practical systems the type of loads are mixed or predominantly constant power type such that system voltage

degradation is more and voltage instability occurs much prior to the theoretical power limit.

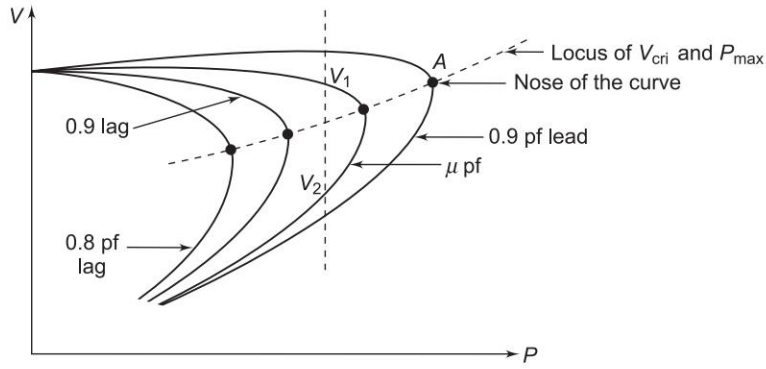

Fig. 22.2 *PV* curves for various power factors

As in the case of single line system, in a general power system, voltage instability occurs above certain bus loading and certain Q injections. This condition is indicated by the singularity of the Jacobian of Load Flow equations and level of voltage instability is assessed by the minimum singular value.

Certain results that are of significance for voltage stability are as under:

- Voltage stability limit is reached when

$$\left| \frac{S}{Y_{LL}^{*} V^2} \right| = 1 \tag{22.2}$$

where S = complex power at load bus

Y_{LL} = load bus admittance

V = load bus voltage

Nearer the magnitude in Eq. (22.2) to unity, lesser the stability margin.

- The loading limit of a transmission line can be determined from

$$|S| = V_{cri}^2 / X_{cri} \tag{22.3}$$

X_{cri} is the critical system reactance beyond which voltage stability is lost. It can be expressed as

$$X_{cri} = \frac{E^2}{2P} (-\tan \phi + \sec \phi) \tag{22.4}$$

We have so far considered how the *PV* characteristics with constant load power factor affect the voltage stability of a system. A more meaningful characteristic for certain aspects of voltage stability is the *QV* characteristic, which brings out the sensitivity and variation of bus voltage with respect to reactive power injections (+ve or –ve).

Consider once again the simple radial system of Fig. 22.1. For Q flow it is sufficiently accurate to assume $X \gg R$ i.e. $\phi \approx 90^\circ$. It then follows that

$$Q = \frac{EV}{X}\cos\delta - \frac{V^2}{X} \tag{22.5}$$

or
$$V^2 - EV\cos\delta + QX = 0 \tag{22.6}$$

Taking derivative w.r.t. V gives

$$\frac{dQ}{dV} = \frac{E\cos\delta - 2V}{X} \tag{22.7}$$

The QV characteristic on normalized basis (Q/P_{max}, V/E) for various values of P/P_{max} are plotted in Fig. 22.3. The system is voltage stable in the region where dQ/dV is positive, while the voltage stability limit is reached at $dQ/dV = 0$ which may also be termed as the critical operating point.

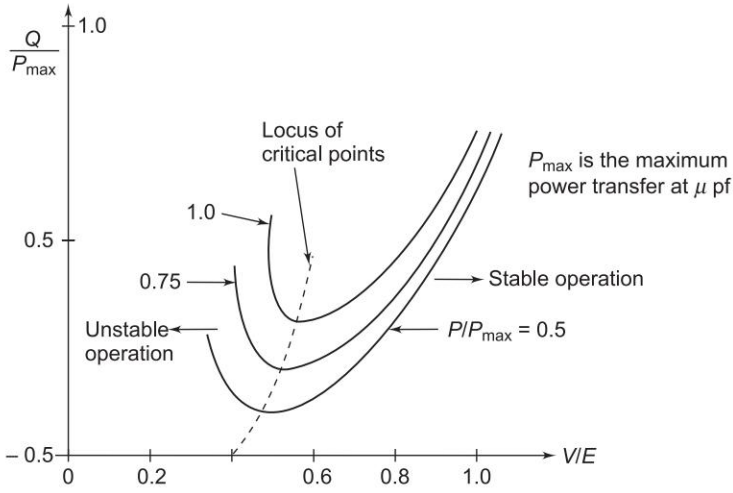

Fig. 22.3 *QV* characteristics for the system of Fig. 22.1 for various values of P/P_{max}

The limiting value of the reactive power transfer at the limiting stage of voltage stability is given by

$$Q_{lim} = \frac{V^2}{X}\cos 2\delta \tag{22.8}$$

The inferences drawn from the simple radial system qualitatively apply to a practical size system. Other factors that contribute to system voltage collapse are: strength of transmission system, power transfer levels, load characteristics, generator reactive power limits and characteristics of reactive power compensating devices.

Other Criteria of Voltage Stability

(i) $\frac{dE}{dV}$ criterion: (E = generator voltage; V = load voltage). Using this criterion, the voltage stability limit is reached when

$$\cos\delta\left\{\frac{dQ}{dV}+\frac{2V}{X}\right\}+\sin\delta\frac{dP}{dV}-\frac{E}{X}=0 \tag{22.9}$$

Using the decoupling principle i.e. $\frac{dP}{dV}=0$, we get

$$\frac{E}{X}=\cos\delta\left[\frac{dQ}{dV}+\frac{2V}{X}\right]$$

or $$I_{SC}=\cos\delta\left[\frac{dQ}{dV}+\frac{2V}{X}\right]$$

or $$EI_{SC}=E\cos\delta\left[\frac{dQ}{dV}+\frac{2V}{X}\right]$$

Voltage stability is achieved when

$$E\cos\delta\left(\frac{dQ}{dV}+\frac{2V}{X}\right)>EI_{SC}\ \text{(short circuit MVA of power source)} \tag{22.10}$$

(ii) $\frac{dZ}{dV}$ criterion

Voltage instability occurs when the system Z is such that

$$\frac{dV}{dZ}=\infty \text{ or } \frac{dZ}{dV}=0 \tag{22.11}$$

Application of this criterion gives value of Z_{cri}.

(iii) Ratio of source to load reactance is very important and for voltage stability

$$\frac{x_{\text{source}}}{x_{\text{load}}}<a^2 \tag{22.12}$$

a indicates the off-nominal tap ratio of the OLTC transformer at the load end.

22.5 VOLTAGE STABILITY ANALYSIS

The voltage stability analysis for a given system state involves examining following two aspects.

(i) *Proximity to voltage instability*: Distance to instability may be measured in terms of physical quantities, such as load level, real power flow through

a critical interface, and reactive power reserve. Possible contingencies such as a line outage, loss of a generating unit or a reactive power source must be given due consideration.

(ii) *Mechanism of voltage instability*: How and why does voltage instability take place? What are the main factors leading to instability? What are the voltage-weak areas? What are the most effective ways to improve voltage stability?

The static analysis techniques permit examination of a wide range of system conditions and can describe the nature of the problem and give the main contributing factors. Dynamic analysis is useful for detailed study of specific voltage collapse situations, coordination of protection and controls, and testing of remedial measures. Dynamic simulations further tell us whether and how the steady-state equilibrium point will be reached.

Modelling Requirements of Various Power System Components

Loads

Load modelling is very critical in voltage stability analysis. Detailed subtransmission system representation in a voltage-weak area may be required. This may include transformer ULTC action, reactive power compensation, and voltage regulators.

It is essential to consider the voltage and frequency dependence of loads. Induction motors should also be modelled.

Generators and their excitation controls

It is necessary to consider the droop characteristics of the AVR, load compensation, SVSs (static var system), AGC, protection and controls should also be modelled appropriately [4].

Dynamic Analysis

The general structure of the system model for voltage stability analysis is similar to that for transient stability analysis. Overall system equations may be expressed as

$$\dot{X} = f(X, V) \tag{22.13}$$

and a set of algebraic equations

$$I(X, V) = Y_N V \tag{22.14}$$

with a set of known initial conditions (X_0, V_0).

where X = system state vector

V = bus voltage vector

I = current injection vector

Y_N = network node admittance matrix.

Equations (22.13) and (22.14) can be solved in time domain by employing any of the numerical integration methods described in Ch. 12 and power flow analysis methods described in Ch. 6. The study period is of the order of several minutes. As the special models representing the "slow system dynamics" leading to voltage collapse have been included, the stiffness of the system differential equations is considerably higher than that of transient stability models. Stiffness is also called synchronizing coefficient as discussed in Ch. 12.

Static Analysis

The static approach captures *snapshots* of system conditions at various time frames along the time-domain trajectory. At each of these time frames, $\dot{X}$ in Eq. (22.13) is assumed to be zero, and the state variables take on values appropriate to the specific time frame. Thus, the overall system equations reduce to purely algebraic equations allowing the use of static analysis techniques.

In static analysis voltage stability is determined by computing *VP* and *VQ* curves at selected load buses. Special techniques using static analysis have been reported in literature. Methods based on *VQ* sensitivity such as eigenvalue (or modal) analysis have been devised. These methods give stability-related information from a system-wide perspective and also identify areas of potential problems [13–15].

Proximity to Instability

Proximity to small-disturbance voltage instability is determined by increasing load-generation in steps until the system becomes unstable or the load flow fails to converge. Refs [16–18] discuss special techniques for determining the point of voltage collapse and proximity to volage instability.

The Continuation Power-flow Analysis

The Jacobian matrix becomes singular at the voltage stability limit. As a result, conventional load-flow algorithms may have convergence problems at operating conditions near the stability limit. The continuation power-flow analysis overcomes this problem by reformulating the load-flow equations so that they remain well-conditioned at all possible loading conditions. This allows the solution of load-flow problem for both upper and lower portions of the *PV* curve [17].

The continuation method of power-flow analysis is robust and flexible and suited for solving load flow problems with convergence difficulties. However, the method is very slow and time-consuming. Hence the better approach is to use combination of conventional load flow method (NR/FDLF) and continuation method. Starting from the base case, LF is solved using a conventional method to compute power flow solutions for successively increasing load

levels until a solution cannot be obtained. Hereafter, the continuation method is resorted to obtain the load-flow solutions. Normally, the continuation method is required only if solutions are required exactly at and past the critical point.

Voltage Stability with HVDC Links

High voltage direct current (HVDC)* links are used for extremely long distance transmission and for asynchronous interconnections. An HVDC link can be either a back-to-back rectifier/inverter link or can include long distance DC transmission. Multi-terminal HVDC links are also feasible.

The technology has come to such a level that HVDC terminals can be connected even at voltage-weak points in power systems. HVDC links may present unfavourable "load" characteristics to the power system as HVDC converter consumes reactive power equal to 50–60% of the DC power.

HVDC-related voltage control (voltage stability and fundamental frequency temporary over voltages) may be studied using a transient stability program. Transient stability is often interrelated with voltage stability. Ref. [2] considers this problem in greater detail.

22.6 PREVENTION OF VOLTAGE COLLAPSE

(i) *Application of reactive power-compensating devices.*
Adequate stability margins should be ensured by proper selection of compensation schemes in terms of their size, ratings and locations.

(ii) *Control of network voltage and generator reactive output*
Several utilities in the world such as EDF (France), ENEL (Italy) are developing special schemes for control of network voltages and reactive power.

(iii) *Coordination of protections/controls*
Adequate coordination should be ensured between equipment protections/controls based on dynamic simulation studies. Tripping of equipment to avoid an overloaded condition should be the last alternative. Controlled system separation and adaptive or intelligent control could also be used.

(iv) *Control of transformer tap changers*
Tap changers can be controlled, either locally or centrally, so as to reduce the risk of voltage collapse. Microprocessor-based OLTC controls offer almost unlimited flexibility for implementing ULTC control strategies so as to take advantage of the load characteristics.

(v) *Under voltage load shedding*
For unplanned or extreme situations, it may be necessary to use undervoltage load-shedding schemes. This is similar to under frequency

* For detailed account of HVDC, the reader may refer to [Ch. 20].

load shedding, which is a common practice to deal with extreme situations resulting from generation deficiency.

Strategic load shedding provides cheapest way of preventing widespread voltage collapse. Load shedding schemes should be designed so as to differentiate between faults, transient voltage dips and low voltage conditions leading to voltage collapse.

(vi) *Operators' role*

Operators must be able to recognize voltage stability-related symptoms and take required remedial actions to prevent voltage collapse. On-line monitoring and analysis to identify potential voltage stability problems and appropriate remedial measures are extremely helpful.

22.7 STATE-OF-THE-ART, FUTURE TRENDS AND CHALLENGES

The present day transmission networks are getting more and more stressed due to economic and environmental constraints. The trend is to operate the existing networks optimally close to their loadability limit. This consequently means that the system operation is also near voltage stability limit (nose point) and there is increased possibility of voltage instability and even collapse.

Off-line and on-line techniques of determining state of voltage stability and when it enters the unstable state, provide the tools for system planning and real time control. Energy management system (EMS) provide a variety of measured and computer processed data. This is helpful to system operators in taking critical decisions *inter alia* reactive power management and control. In this regard automation and specialized software relieve the operator of good part of the burden of system management but it does add to the complexity of the system operation.

Voltage stability analysis and techniques have been pushed forward by several researchers and several of these are in commercial use as outlined in this chapter. As it is still hot topic, considerable research effort is being devoted to it.

Pai and Grady [8] considered an exponential type voltage dependent load model and a new index called condition number for static voltage stability prediction. Eigenvalue analyses has been used to find critical group of buses responsible for voltage collapse. Some researchers [26] have also investigated aspects of bifurcations (local, Hopf, global) and chaos and their implications on power system voltage stability. FACTS devices can be effectively used for controlling the occurrence of dynamic bifurcations and chaos by proper choice of error signal and controller gains.

Tokyo Electric Power Co. has developed a μP-based controller for coordinated control of capacitor bank switching and network transformer tap changing. HVDC power control is used to improve stability.

More systematic approach is still required for optimal siting and sizing of FACTS devices. The availability of FACTS controllers allow operation close

to the thermal limit of the lines without jeopardizing security. The reactive power compensation close to the load centres and at the critical buses is essential for overcoming voltage instability. Better and probabilistic load modelling [11] should be tried. It will be worthwhile developing techniques and models for study of non-linear dynamics of large size systems. This may require exploring new methods to obtain network equivalents suitable for the voltage stability analysis. AI is another approach to centralized reactive power and voltage control. An expert system [9] could assist operators in applying C-banks so that generators operate near μpf. The design of suitable protective measures in the event of voltage instability is necessary.

So far, computed PV curves are the most widely used method of estimating voltage security, providing MW margin type indices. Post-disturbance MW or MVAr margins should be translated to predisturbance operating limits that operators can monitor. Both control centre and power plant operators should be trained in the basics of voltage stability. For operator training simulator [10] a real-time dynamic model of the power system that interfaces with EMS controls such as AGC is of great help.

Voltage stability is likely to challenge utility planners and operators for the foreseable future. As load grows and as new transmission and load area generation become increasingly difficult to build, more and more utilities will face the voltage stability challenge. Fortunately, many creative researchers and planners are working on new analysis methods and an innovative solutions to the voltage stability challenge.

Example 22.1 A load bus is composed of induction motor where the nominal reactive power is 1 pu. The shunt compensation is K_{sh}. Find the reactive power sensitivity at the bus w.r.t. change in voltage.

Solution

$$Q_{load} = Q_{nom}\, V^2 \text{ [given]}$$

$$Q_{comp} = -K_{sh}\, V^2 \qquad \text{[–ve sign denotes inductive reactive power injection]}$$

$$Q_{net} = Q_{load} + Q_{comp}$$

$\therefore$ Here, $$Q_{net} = V^2 - K_{sh}\, V^2 \quad [Q_{nom} = 1.0 \text{ given}]$$

$\therefore$ $$\frac{dQ_{net}}{dV} = 2V - 2V\,K_{sh}$$

Sensitivity increases or decreases with K_{sh} as well as the magnitude of the voltage. Say at $V = 1.0$ pu, $K_{sh} = 0.8$

$\therefore$ $$\frac{dQ_{net}}{dV} = 2 - 1.6 = 0.4 \text{ pu}$$

Example 22.2 Find the capacity of a static VAR compensator to be installed at a bus with ± 5% voltage fluctuation. The short circuit capacity is 5,000 MVA.

Solution

For the switching of static shunt compensator,

Let ΔV = voltage fluctuation

ΔQ = reactive power variation

(i.e. the size of the compensator)

$S_{s/c}$ = system short circuit capacity

Then $$\Delta V = \frac{\Delta Q}{S_{s/c}}$$

$$\Delta Q = \Delta V S_{s/c}$$

$$= \pm (0.05 \times 5000)$$

$$= \pm 250 \text{ MVAR}$$

The capacity of the static VAR compensator is +250 MVAR.

22.8 SUMMARY

This chapter deals with yet another important problem of voltage stability, comparing with angle stability (Ch. 12). Finally state-of-art and future trends along with the challenges are highlighted.

Problems

22.1 A 100 km 400 kV line has a series reactance of 0.30 Ω/km and Power transmitted is 800 MW. It is connected to a source bus which has a short circuit capacity of 4000 MW. Find out the source voltage when the load is disconnected to (i) unity (ii) 0.9 lag.

22.2 A high voltage direct current (HVDC) transmission link connected to a Weak Power System is shown in Fig. P-22.2

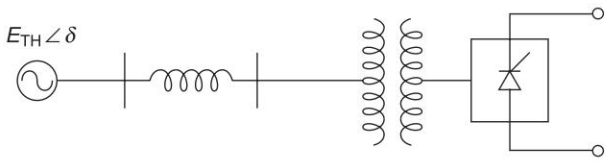

Fig. P- 22.2

The equivalent Thevenins reactance of the line is 0.5 pu. The converter consume reactive power of 50%. Assume converter commutating bus voltage ($V\angle 0^\circ$) to be 1 pu (per unit). Find out the AC system voltage when the DC system is disconnected.

22.3 A transmission line with a transfer rectance X has V_s and V_r as the sending and receiving voltages. Find the maximum power and the critical voltage (when power is maximum). If load power factor is (a) unity, (b) 0 p.f.

References

Books

1. Chakrabarti, A., D.P. Kothari and A.K. Mukhopadhyay, *Performance, Operation and Control of EHV Power Transmission Systems*, Wheeler Publishing, New Delhi, 1995.
2. Taylor, C.W., *Power System Voltage Stability*, McGraw-Hill, New York, 1994.
3. Bergen, A. and V. Vittal, *Power System Analysis*, 2nd edn, Prentice Hall, 1999.
4. Kundur, P., *Power System Stability and Control*, McGraw-Hill, New York, 1994.
5. Padiyar, K.R., *Power System Dynamics: Stability and Control*, John Wiley, Singapore, 1996.
6. Cutsem, T. Van and Costas Vournas, *Voltage Stability of Electric Power Systems*, Kluwer Int. Series, 1998.

Papers

7. Concordia, C. (Ed.), 'Special Issue on Voltage Stability and Collapse', *Int. J. of Electrical Power and Energy Systems*, vol. 15, no. 4, August 1993.
8. Pai, M.A. and M.G.O. Grady, 'Voltage Collapse Analysis with Reactive Generation and Voltage Dependent Constraints', *J. of Elect. Machines and Power Systems*, vol. 22, no. 6, 1989, pp. 379–390.
9. CIGRE′ Task Force 38–06–01, "Expert Systems Applied to Voltage and Var Control", 1991.
10. "Operator Training Simulator", *EPRI Final Report* EL–7244, May 1991, prepared by EMPROS Systems International.
11. Xu, W. and Y. Mansour, 'Voltage Stability using Generic Dynamic Load Models', *IEEE, Trans., on Power Systems*, vol. 9, no. 1, Feb. 1994, pp. 479–493.
12. Verma, H.K., L.D. Arya and D.P. Kothari, 'Voltage Stability Enhancement by Reactive Power Loss Minimization', *J.I.E. (I)*, vol. 76, May 1995, pp. 44–49.
13. *IEEE, special Publication 90 TH 0358–2 PWR*, 'Voltage Stability of Power Systems: Concepts, Analytical Tools, and Industry Experience'1990.
14. Flatabo, N., R. Ognedal and T. Carlsen, 'Voltage Stability Condition in a Power Transmission System Calculated by Sensitivity Methods', *IEEE Trans.,* vol. PWRS-5, no. 5, Nov. 1990, pp. 1286–1293.

15. Gao, B., G.K. Morison and P. Kundur, 'Voltage Stability Evaluation Using Modal Analysis', *IEEE Trans.,* vol. PWRS-7, no. 4, Nov. 1992, pp. 1529–1542.
16. Cutsem, and T. Van, "A Method to Compute Reactive Power Margins w.r.t. Voltage Collapse", *IEEE Trans*., vol. PWRS-6, no. 2, Feb. 1991, pp. 145–156.
17. Ajjarapu, V. and C. Christy, 'The Continuation Power Flow: A Tool for Steady State Voltage Stability Analysis', *IEEE PICA Conf. Proc*., May 1991, pp. 304–311.
18. Löf, A.-P., T. Sined, G. Anderson and D.J. Hill, 'Fast Calculation of a Voltage Stability Index', *IEEE Trans.*, vol. PWRS-7, no. 1, Feb. 1992, pp. 54–64.
19. Arya, L.D., S.C. Chaube and D.P. Kothari, 'Line Outage Ranking based on Estimated Lower Bound on Minimum Eigen Value of Load Flow Jacobian', *J.I.E. (I)*, vol. 79, Dec. 1998, pp. 126–129.
20. Bijwe, P.R., S.M. Kelapure, D.P. Kothari and K.K. Saxena, 'Oscillatory Stability Limit Enhancement by Adaptive Control Rescheduling', *Int J. of Electrical Power and Energy Systems*, vol. 21, no. 7, 1999, pp. 507–514.
21. Arya, L.D., S.C. Chaube and D.P. Kothari, 'Line Switching for Alleviating Overloads under Line Outage Condition taking Bus Voltage Limits into Account', *Int. J. of Electric Power and Energy System*, vol. 22, no. 3, 2000, pp. 213–221.
22. Bijwe, P.R., D.P. Kothari and S. Kelapure, 'An Efficient Approach to Voltage Security Analysis and Enhancement', *Int. J. of EP and ES*., vol. 22, no. 7, Oct. 2000, pp. 483–486.
23. Arya, L.D., S.C. Chaube and D.P. Kothari, 'Reactive Power Optimization using Static Stability Index (VSI)', *Int. J. of Electric Power Components and Systems*, vol. 29, no. 7, July 2001, pp. 615–628.
24. Arya, L.D., S.C. Chaube and D.P. Kothari, 'Line Outage Ranking for Voltage Limit Violations with Corrective Rescheduling Avoiding Masking', *Int. J. of EP and ES*, vol. 23, no. 8, Nov. 2001, pp. 837–846.
25. CIGRE Task Force 38–02–10, 'Cigre Technical Brochure: Modelling of Voltage Collapse Including Dynamic Phenomena', *Electra*, no. 147, April 1993, pp. 71–77.
26. Mark J. Laufenberg and M.A. Pai, 'Hopf Bifurcation Control in Power System with Static Var Compensators', *Electrical Power and Energy Systems*, vol. 19, no. 5, 1997, pp. 339–347.
27. Arya, L.D., V.S. Pande and D.P. Kothari, 'A Technique for Load Shedding based on Voltage Stability Considerations', *JEPES*, vol. 27, 2005, pp. 506–517.
28. Arya, L.D., D.K. Sakravdia and D.P. Kothari, 'Corrective Rescheduling for Static Voltage Stability Control', *JEPES*, vol. 27, Nov. 2005, pp. 3–12.

Appendix A

Introduction to Vector and Matrix Algebra

In this appendix, our aim is to present definitions and elementary operations of vectors and matrices necessary for power system analysis.

VECTORS

A vector x is defined as an ordered set of numbers (real or complex), i.e.

$$\boldsymbol{x} \triangleq \begin{bmatrix} x_1 \\ x_2 \\ \vdots \\ x_n \end{bmatrix} \tag{A-1}$$

$x_1, \ldots, x_n$ are known as the components of the vector x. Thus the vector x is a n-dimensional column vector. Sometimes transposed form of (A-1) is found to be more convenient and is written as the row vector.

$$\boldsymbol{x}^T \triangleq [x_1, x_2, \ldots, x_n] \tag{A-2}$$

Some Special Vectors

The null vector **0** is one whose each component is zero, i.e.

$$\mathbf{0} \triangleq \begin{bmatrix} 0 \\ 0 \\ \vdots \\ 0 \end{bmatrix}$$

The sum vector **1** has each of its components equal to unity, i.e.

$$\mathbf{1} \triangleq \begin{bmatrix} 1 \\ 1 \\ \vdots \\ 1 \end{bmatrix}$$

The unit vector e_k is defined as the vector whose kth component is unity and the rest of the components are zero, i.e.

$$e_k \triangleq \begin{bmatrix} 0 \\ \vdots \\ 0 \\ 1 \\ 0 \\ \vdots \\ 0 \end{bmatrix} \quad k\text{th component}$$

Some Fundamental Vector Operations

The two vectors $\boldsymbol{x}$ and $\boldsymbol{y}$ are known as equal if, and only if $x_k = y_k$ for $k = 1, 2, \ldots, n$. Then we say

$$\boldsymbol{x} = \boldsymbol{y}$$

The product of a vector by a scalar is carried out by multiplying each component of the vector by that scalar, i.e.

$$\alpha \boldsymbol{x} = \boldsymbol{x}\alpha \triangleq \alpha \begin{bmatrix} x_1 \\ x_2 \\ \vdots \\ x_n \end{bmatrix}$$

If a vector $\boldsymbol{y}$ is to be added to or subtracted from another vector $\boldsymbol{x}$ of the same dimension, then each component of the resulting vector will consist of addition or subtraction of the corresponding components of the vectors $\boldsymbol{x}$ and $\boldsymbol{y}$, i.e.

$$\boldsymbol{x} \pm \boldsymbol{y} \triangleq \begin{bmatrix} x_1 \pm y_1 \\ x_2 \pm y_2 \\ \vdots \\ x_n \pm y_n \end{bmatrix}$$

The following properties are applicable to the vector algebra:

$$\boldsymbol{x} + \boldsymbol{y} = \boldsymbol{y} + \boldsymbol{x}$$
$$\boldsymbol{x} + (\boldsymbol{y} + \boldsymbol{z}) = (\boldsymbol{x} + \boldsymbol{y}) + \boldsymbol{z}$$
$$\alpha_1(\alpha_2\, \boldsymbol{x}) = (\alpha_1\, \alpha_2)\boldsymbol{x}$$
$$(\alpha_1 + \alpha_2)\boldsymbol{x} = \alpha_1\boldsymbol{x} + \alpha_2\boldsymbol{x}$$
$$\alpha(\boldsymbol{x} + \boldsymbol{y} + \boldsymbol{z}) = \alpha\boldsymbol{x} + \alpha\boldsymbol{y} + \alpha\boldsymbol{z}$$
$$\mathbf{0}\boldsymbol{x} = \mathbf{0}$$

The multiplication of two vectors $\boldsymbol{x}$ and $\boldsymbol{y}$ of same dimensions results in a very important product known as *inner* or *scalar* product*, i.e.

$$\boldsymbol{x}^T\boldsymbol{y} \triangleq \sum_{i=1}^{n} x_i\, y_i \triangleq \boldsymbol{y}^T\boldsymbol{x} \tag{A-3}$$

Also, it is interesting to note that

$$\boldsymbol{x}^T\boldsymbol{x} = |\,\boldsymbol{x}\,|^2 \tag{A-4}$$

$$\cos\,\phi \triangleq \frac{\boldsymbol{x}^T\boldsymbol{y}}{|\,\boldsymbol{x}\,||\boldsymbol{y}|} \tag{A-5}$$

where ϕ is angle between vectors, $|\,\boldsymbol{x}\,|$ and $|\,\boldsymbol{y}\,|$ are the geometric lengths of vectors $\boldsymbol{x}$ and $\boldsymbol{y}$, respectively. Two non-zero vectors are said to be *orthogonal*, if

$$\boldsymbol{x}^T\,\boldsymbol{y} = 0 \tag{A-6}$$

MATRICES

Definitions

Matrix

An $m \times n$ (or m, n) matrix is an ordered rectangular array of elements which may be real numbers, complex numbers, functions or operators. The matrix

$$\boldsymbol{A} \triangleq \begin{bmatrix} a_{11} & a_{12} & \cdots & a_{1n} \\ a_{21} & a_{22} & \cdots & a_{2n} \\ \vdots & \vdots & & \vdots \\ a_{m1} & a_{m2} & \cdots & a_{mn} \end{bmatrix} = [a_{ij}] \tag{A-7}$$

is a rectangular array of mn elements.

a_{ij} denotes the (i, j)th element, i.e. the element located in the ith row and the jth column. The matrix $\boldsymbol{A}$ has m rows and n columns and is said to be of order $m \times n$.

* Sometimes inner product is also represented by the following alternative forms $x \times y$, (x, y), $<x, y>$.

When $m = n$, i.e. the number of rows is equal to that of columns, the matrix is said to be a *square matrix* of order n.

An $m \times 1$ matrix, i.e. a matrix having only one column is called a *column vector*. An $1 \times n$ matrix, i.e. a matrix having only one row is called a *row vector.*

Diagonal matrix

A diagonal matrix is a square matrix whose elements off the main diagonal are all zeros ($a_{ij} = 0$ for $i \neq j$).

Example

$$\boldsymbol{D} \triangleq \begin{bmatrix} 4 & 0 & 0 \\ 0 & 2 & 0 \\ 0 & 0 & 9 \end{bmatrix}$$

Null matrix

If all the elements of the square matrix are zero, the matrix is a *null* or *zero* matrix.

Example

$$\mathbf{0} \triangleq \begin{bmatrix} 0 & \cdots & 0 \\ \cdots & \cdots & \cdots \\ 0 & \cdots & 0 \end{bmatrix} \tag{A-8}$$

Unit (identity) matrix

A *unit matrix* $\boldsymbol{I}$ is a diagonal matrix with all diagonal elements equal to unity. If a unit matrix is multiplied by a constant (λ), the resulting matrix is a diagonal matrix with all diagonal elements equal to λ. This matrix is known as a *scalar* matrix.

Example

$$\boldsymbol{I} = \begin{bmatrix} 1 & 0 & 0 & 0 \\ 0 & 1 & 0 & 0 \\ 0 & 0 & 1 & 0 \\ 0 & 0 & 0 & 1 \end{bmatrix}; \quad 4 \begin{bmatrix} 1 & 0 & 0 \\ 0 & 1 & 0 \\ 0 & 0 & 1 \end{bmatrix} = \begin{bmatrix} 4 & 0 & 0 \\ 0 & 4 & 0 \\ 0 & 0 & 4 \end{bmatrix}$$

$= 4 \times 4$ unit matrix $\qquad\qquad$ $= 3 \times 3$ scalar matrix

Determinant of a matrix

For each square matrix, there exists a determinant which is formed by taking the determinant of the elements of the matrix.

For example, if

$$\boldsymbol{A} = \begin{bmatrix} 2 & -1 & 1 \\ -1 & 3 & 2 \\ 1 & 2 & 4 \end{bmatrix} \tag{A-9}$$

then

$$\det(\boldsymbol{A}) = |\boldsymbol{A}| = 2\begin{vmatrix} 3 & 2 \\ 2 & 4 \end{vmatrix} - (-1)\begin{vmatrix} -1 & 2 \\ 1 & 4 \end{vmatrix} + \begin{vmatrix} -1 & 3 \\ 1 & 2 \end{vmatrix}$$

$$= 2(8) + (-6) + (-5) = 5 \tag{A-10}$$

Transpose of a matrix

The transpose of matrix $\boldsymbol{A}$ denoted by $\boldsymbol{A}^T$ is the matrix formed by interchanging the rows and columns of $\boldsymbol{A}$.

Note that

$$(\boldsymbol{A}^T)^T = \boldsymbol{A}$$

Symmetric matrix

A square matrix is symmetric, if it is equal to its transpose, i.e.

$$\boldsymbol{A}^T = \boldsymbol{A}$$

Notice that the matrix $\boldsymbol{A}$ of Eq. (A-9) is a symmetric matrix.

Minor

The minor M_{ij} of an $n \times n$ matrix is the determinant of $(n-1) \times (n-1)$ matrix formed by deleting the ith row and the jth column of the $n \times n$ matrix.

Cofactor

The cofactor A_{ij} of element a_{ij} of the matrix $\boldsymbol{A}$ is defined as

$$A_{ij} = (-1)^{i+j}\boldsymbol{M}_{ij}$$

Adjoint matrix

The adjoint matrix of a square matrix $\boldsymbol{A}$ is found by replacing each element a_{ij} of matrix $\boldsymbol{A}$ by its cofactor $\boldsymbol{A}_{ij}$ and then transposing.

For example, if $\boldsymbol{A}$ is given by Eq. (A-9), then

$$\text{adj}\,\boldsymbol{A} = \begin{bmatrix} \begin{vmatrix} 3 & 2 \\ 2 & 4 \end{vmatrix} & -\begin{vmatrix} -1 & 2 \\ 1 & 4 \end{vmatrix} & \begin{vmatrix} -1 & 3 \\ 1 & 2 \end{vmatrix} \\ -\begin{vmatrix} -1 & 1 \\ 2 & 4 \end{vmatrix} & \begin{vmatrix} 2 & 1 \\ 1 & 4 \end{vmatrix} & -\begin{vmatrix} 2 & -1 \\ 1 & 2 \end{vmatrix} \\ \begin{vmatrix} -1 & 1 \\ 3 & 2 \end{vmatrix} & -\begin{vmatrix} 2 & 1 \\ -1 & 2 \end{vmatrix} & \begin{vmatrix} 2 & -1 \\ -1 & 3 \end{vmatrix} \end{bmatrix}^T$$

$$= \begin{bmatrix} 8 & 6 & -5 \\ 6 & 7 & -5 \\ -5 & -5 & 5 \end{bmatrix}^T = \begin{bmatrix} 8 & 6 & -5 \\ 6 & 7 & -5 \\ -5 & -5 & 5 \end{bmatrix} \quad \text{(A-11)}$$

Singular and non-singular matrices

A square matrix is called singular, if its associated determinant is zero, and non-singular, if its associated determinant is non-zero.

ELEMENTARY MATRIX OPERATIONS

Equality of matrices

Two matrices $\boldsymbol{A}(m \times n)$ and $\boldsymbol{B}(m \times n)$ are said to be equal, if and only if

$$a_{ij} = b_{ij} \text{ for } i = 1, 2, ..., m, j = 1, 2, ..., n$$

Then we write

$$\boldsymbol{A} = \boldsymbol{B}$$

Multiplication of a matrix by a scalar

A matrix is multiplied by a scalar α if all the mn elements are multiplied by α, i.e.

$$\alpha \boldsymbol{A} = \boldsymbol{A}\alpha = \begin{bmatrix} \alpha a_{11} & \cdots & \alpha a_{1n} \\ \cdots & \cdots & \cdots \\ \alpha a_{m1} & \cdots & \alpha a_{mn} \end{bmatrix} \quad \text{(A-12)}$$

Addition (or subtraction) of matrices

To add (or subtract) two matrices of the same order (same number of rows, and same number of columns), simply add (or subtract) the corresponding elements of the two matrices, i.e. when two matrices $\boldsymbol{A}$ and $\boldsymbol{B}$ of the same order are added, a new matrix C results such that

$$\boldsymbol{C} = \boldsymbol{A} + \boldsymbol{B};$$

whose ijth element equals

$$c_{ij} = a_{ij} + b_{ij}$$

Example Let

$$\boldsymbol{A} = \begin{bmatrix} 3 & 0 \\ 2 & -1 \end{bmatrix}; \boldsymbol{B} = \begin{bmatrix} 2 & -1 \\ 0 & 3 \end{bmatrix}$$

then

$$\boldsymbol{C} = \boldsymbol{A} + \boldsymbol{B} = \begin{bmatrix} 5 & -1 \\ 2 & 2 \end{bmatrix}$$

Addition and subtraction are defined only for matrices of the same order.

The following laws hold for addition:

(i) The *commutative law*: $\boldsymbol{A} + \boldsymbol{B} = \boldsymbol{B} + \boldsymbol{A}$

(ii) *The associative law*: $\boldsymbol{A} + (\boldsymbol{B} + \boldsymbol{C}) = (\boldsymbol{A} + \boldsymbol{B}) + \boldsymbol{C}$

Further

$$(\boldsymbol{A} \pm \boldsymbol{B})^T = \boldsymbol{A}^T \pm \boldsymbol{B}^T$$

Matrix Multiplication

The product of two matrices $\boldsymbol{A} \times \boldsymbol{B}$ is defined if $\boldsymbol{A}$ has the same number of columns as the number of rows in $\boldsymbol{B}$. The matrices are then said to be *conformable*. If a matrix $\boldsymbol{A}$ is of order $m \times n$ and $\boldsymbol{B}$ is an $n \times q$ matrix, the product $\boldsymbol{C} = \boldsymbol{AB}$ will be an $m \times q$ matrix. The element c_{ij} of the product is given by

$$c_{ij} = \sum_{k=1}^{n} a_{ik}\, b_{kj} \tag{A-13}$$

Thus the elements c_{ij} are obtained by multiplying the elements of the ith row of $\boldsymbol{A}$ with the corresponding elements of the jth column of $\boldsymbol{B}$ and then summing these elements products.

For example

$$\begin{bmatrix} a_{11} & a_{12} \\ a_{21} & a_{22} \end{bmatrix} \begin{bmatrix} b_{11} & b_{12} \\ b_{21} & b_{22} \end{bmatrix} = \begin{bmatrix} c_{11} & c_{12} \\ c_{21} & c_{22} \end{bmatrix}$$

where

$$\begin{aligned} c_{11} &= a_{11}\, b_{11} + a_{12}\, b_{21} \\ c_{12} &= a_{11}\, b_{12} + a_{12}\, b_{22} \\ c_{21} &= a_{21}\, b_{11} + a_{22}\, b_{21} \\ c_{22} &= a_{21}\, b_{12} + a_{22}\, b_{22} \end{aligned}$$

If the product $\boldsymbol{AB}$ is defined, the product $\boldsymbol{BA}$ may or may not be defined. Even if $\boldsymbol{BA}$ is defined, the resulting products of $\boldsymbol{AB}$ and $\boldsymbol{BA}$ are not, in general, equal. Thus, it is important to note that in general matrix multiplication is not commutative, i.e.

$$\boldsymbol{AB} \neq \boldsymbol{BA}$$

The associative and distributive laws hold for matrix multiplication (when the appropriate operations are defined), i.e.

Associative law: $(\boldsymbol{AB})\boldsymbol{C} = \boldsymbol{A}(\boldsymbol{BC}) = \boldsymbol{ABC}$

Distributive law: $\boldsymbol{A}(\boldsymbol{B} + \boldsymbol{C}) = \boldsymbol{AB} + \boldsymbol{AC}$

Example A-1 Given the two matrices

$$\boldsymbol{A} = \begin{bmatrix} 1 & 0 \\ 2 & 3 \\ 0 & 1 \end{bmatrix}; \boldsymbol{B} = \begin{bmatrix} 1 & -1 & 3 \\ 0 & 2 & 1 \end{bmatrix}$$

Find $\boldsymbol{AB}$ and $\boldsymbol{BA}$

$\boldsymbol{A}$ and $\boldsymbol{B}$ are conformable ($\boldsymbol{A}$ has two columns and $\boldsymbol{B}$ has two rows); thus we have

$$\boldsymbol{AB} = \begin{bmatrix} 1 & -1 & 3 \\ 2 & 4 & 9 \\ 0 & 2 & 1 \end{bmatrix}; \boldsymbol{BA} = \begin{bmatrix} -1 & 0 \\ 4 & 7 \end{bmatrix}$$

A matrix remains unaffected, if a null matrix, defined by Eq. (A-8) is added to it, i.e.

$$\boldsymbol{A} + \boldsymbol{0} = \boldsymbol{A}$$

If a null matrix is multiplied to another matrix $\boldsymbol{A}$, the result is a null matrix

$$\boldsymbol{A0} = \boldsymbol{0A} = \boldsymbol{0}$$

Also

$$\boldsymbol{A} - \boldsymbol{A} = \boldsymbol{0}$$

Note that equation $\boldsymbol{AB} = \boldsymbol{0}$ does not mean that either $\boldsymbol{A}$ or $\boldsymbol{B}$ necessarily has to be a null matrix, e.g.

$$\begin{bmatrix} 1 & 3 \\ 0 & 0 \end{bmatrix} \begin{bmatrix} 3 & 0 \\ -1 & 0 \end{bmatrix} = \begin{bmatrix} 0 & 0 \\ 0 & 0 \end{bmatrix}$$

Multiplication of any matrix by a unit matrix results in the original matrix, i.e.

$$\boldsymbol{AI} = \boldsymbol{IA} = \boldsymbol{A}$$

The transpose of the product of two matrices is the product of their transposes in reverse order, i.e.

$$(\boldsymbol{AB})^T = \boldsymbol{B}^T \boldsymbol{A}^T$$

The concept of matrix multiplication assists in the solution of simultaneous linear algebraic equations. Consider such a set of equations

$$\begin{aligned} a_{11}\, x_1 + a_{12}\, x_2 + \ldots + a_{1n}\, x_n &= c_1 \\ a_{21}\, x_1 + a_{22}\, x_2 + \ldots + a_{2n}\, x_n &= c_2 \\ &\vdots \\ a_{m1}\, x_1 + a_{m2}\, x_2 + \ldots + a_{mn}\, x_n &= c_m \end{aligned} \qquad \text{(A-14)}$$

or

$$\sum_{i=1}^{n} a_{ij}x_j = c_i; \quad i = 1, 2, \ldots, m$$

Using the rules of matrix multiplication defined above, Eqs (A-14) can be written in the compact notation as

$$\boldsymbol{Ax} = \boldsymbol{c} \tag{A-15}$$

where

$$\boldsymbol{A} = \begin{bmatrix} a_{11} & a_{12} & \cdots & a_{1n} \\ a_{21} & a_{22} & \cdots & a_{2n} \\ \vdots & \vdots & & \vdots \\ a_{m1} & a_{m2} & \cdots & a_{mn} \end{bmatrix}$$

$$\boldsymbol{x} = \begin{bmatrix} x_1 \\ x_2 \\ \vdots \\ x_n \end{bmatrix}; \quad \boldsymbol{c} = \begin{bmatrix} c_1 \\ c_2 \\ \vdots \\ c_m \end{bmatrix}$$

It is clear that the *vector-matrix* Eq. (A-15) is a useful shorthand representation of the set of linear algebraic equations (A-14).

Matrix Inversion

Division does not exist as such in matrix algebra. However, if $\boldsymbol{A}$ is a square non-singular matrix, its inverse ($\boldsymbol{A}^{-1}$) is defined by the relation

$$\boldsymbol{A}^{-1}\boldsymbol{A} = \boldsymbol{A}\boldsymbol{A}^{-1} = \boldsymbol{I} \tag{A-16}$$

The conventional method for obtaining an inverse is to use the following relation

$$\boldsymbol{A}^{-1} = \frac{\text{adj } \boldsymbol{A}}{\det \boldsymbol{A}} \tag{A-17}$$

It is easy to prove that the inverse is unique

The following are the important properties characterizing the inverse:

$$\begin{aligned} (\boldsymbol{AB})^{-1} &= \boldsymbol{B}^{-1}\boldsymbol{A}^{-1} \\ (\boldsymbol{A}^{-1})^T &= (\boldsymbol{A}^T)^{-1} \\ (\boldsymbol{A}^{-1})^{-1} &= \boldsymbol{A} \end{aligned} \tag{A-18}$$

Example If $\boldsymbol{A}$ is given by Eq. (A-9), then from Eqs (A-10), (A-11), (A-17), we get

$$\boldsymbol{A}^{-1} = \frac{\text{adj } \boldsymbol{A}}{\det \boldsymbol{A}} = \frac{1}{5}\begin{bmatrix} 8 & 6 & -5 \\ 6 & 7 & -5 \\ -5 & -5 & 5 \end{bmatrix} = \begin{bmatrix} 8/5 & 6/5 & -1 \\ 6/5 & 7/5 & -1 \\ -1 & -1 & 1 \end{bmatrix}$$

SCALAR AND VECTOR FUNCTIONS

A scalar function of n scalar variables is defined as

$$y \triangleq f(x_1, x_2, \ldots, x_n) \tag{A-19}$$

It can be written as a scalar function of a vector variable $\boldsymbol{x}$, i.e.

$$y = f(\boldsymbol{x}) \tag{A-20}$$

where $\boldsymbol{x}$ is an n-dimension vector,

$$\boldsymbol{x} = \begin{bmatrix} x_1 \\ x_2 \\ \vdots \\ x_n \end{bmatrix}$$

In general, a scalar function could be a function of several vector variables, e.g.

$$y = f(\boldsymbol{x}, \boldsymbol{u}, \boldsymbol{p}) \tag{A-21}$$

where $\boldsymbol{x}$, $\boldsymbol{u}$ and $\boldsymbol{p}$ are vectors of various dimensions.

A vector function is defined as

$$\boldsymbol{y} = \boldsymbol{f}(x) \triangleq \begin{bmatrix} f_1(\boldsymbol{x}) \\ f_2(\boldsymbol{x}) \\ \vdots \\ f_m(\boldsymbol{x}) \end{bmatrix} \tag{A-22}$$

In general, a vector function is a function of several vector variables, e.g.

$$\boldsymbol{y} = \boldsymbol{f}(\boldsymbol{x}, \boldsymbol{u}, \boldsymbol{p}) \tag{A-23}$$

DERIVATIVES OF SCALAR AND VECTOR FUNCTIONS

A derivative of a scalar function (A-20) with respect to a vector variable $\boldsymbol{x}$ is defined as

$$\frac{\partial \boldsymbol{f}}{\partial \boldsymbol{x}} \triangleq \begin{bmatrix} \dfrac{\partial f}{\partial x_1} \\ \dfrac{\partial f}{\partial x_2} \\ \vdots \\ \dfrac{\partial f}{\partial x_n} \end{bmatrix} \tag{A-24}$$

It may be noted that the derivative of a scalar function with respect to a vector of dimension n is a vector of the same dimension.

The derivative of a vector function (A-22) with respect to a vector variable $\boldsymbol{x}$ is defined as

$$\frac{\partial \boldsymbol{f}}{\partial \boldsymbol{x}} \triangleq \begin{bmatrix} \frac{\partial f_1}{\partial x_1} & \frac{\partial f_1}{\partial x_2} & \cdots & \frac{\partial f_1}{\partial x_n} \\ \frac{\partial f_2}{\partial x_1} & \frac{\partial f_2}{\partial x_2} & \cdots & \frac{\partial f_2}{\partial x_n} \\ \cdots & \cdots & \cdots & \cdots \\ \frac{\partial f_m}{\partial x_1} & \frac{\partial f_m}{\partial x_2} & \cdots & \frac{\partial f_m}{\partial x_n} \end{bmatrix} \tag{A-25}$$

$$= \begin{bmatrix} \left[\frac{\partial f_1}{\partial \boldsymbol{x}}\right]^T \\ \left[\frac{\partial f_2}{\partial \boldsymbol{x}}\right]^T \\ \vdots \\ \left[\frac{\partial f_m}{\partial \boldsymbol{x}}\right]^T \end{bmatrix} \tag{A-26}$$

Consider now a scalar function defined as

$$s = \lambda^T \boldsymbol{f}(\boldsymbol{x}, \boldsymbol{u}, \boldsymbol{p}) \tag{A-27}$$

$$= \lambda_1 f_1(\boldsymbol{x}, \boldsymbol{u}, \boldsymbol{p}) + \lambda_2 f_2(\boldsymbol{x}, \boldsymbol{u}, \boldsymbol{p}) + \cdot + \lambda_m f_m(\boldsymbol{x}, \boldsymbol{u}, \boldsymbol{p}) \tag{A-28}$$

Let us find $\frac{\partial s}{\partial \lambda}$. According to Eq. (A-24), we can write

$$\frac{\partial s}{\partial \lambda}. = \begin{bmatrix} f_1(\boldsymbol{x}, \boldsymbol{u}, \boldsymbol{p}) \\ f_2(\boldsymbol{x}, \boldsymbol{u}, \boldsymbol{p}) \\ \vdots \\ f_m(\boldsymbol{x}, \boldsymbol{u}, \boldsymbol{p}) \end{bmatrix} = \boldsymbol{f}(\boldsymbol{x}, \boldsymbol{u}, \boldsymbol{p}) \tag{A-29}$$

Let us now find $\frac{\partial s}{\partial \boldsymbol{x}}$. According to Eq. (A-24), we can write

$$\frac{\partial s}{\partial \boldsymbol{x}} = \begin{bmatrix} \frac{\partial s}{\partial x_1} \\ \frac{\partial s}{\partial x_2} \\ \vdots \\ \frac{\partial s}{\partial x_n} \end{bmatrix} = \begin{bmatrix} \lambda_1 \frac{\partial f_1}{\partial x_1} + \lambda_2 \frac{\partial f_2}{\partial x_1} + \ldots + \lambda_m \frac{\partial f_m}{\partial x_1} \\ \lambda_1 \frac{\partial f_1}{\partial x_2} + \lambda_2 \frac{\partial f_2}{\partial x_2} + \ldots + \lambda_m \frac{\partial f_m}{\partial x_2} \\ \ldots\ldots\ldots\ldots\ldots\ldots\ldots\ldots\ldots\ldots \\ \lambda_1 \frac{\partial f_1}{\partial x_n} + \lambda_2 \frac{\partial f_2}{\partial x_n} + \ldots + \lambda_m \frac{\partial f_m}{\partial x_n} \end{bmatrix}$$

$$\frac{\partial s}{\partial \boldsymbol{x}} = \begin{bmatrix} \frac{\partial f_1}{\partial x_1} & \frac{\partial f_2}{\partial x_1} & \cdots & \frac{\partial f_m}{\partial x_1} \\ \frac{\partial f_1}{\partial x_2} & \frac{\partial f_2}{\partial x_2} & \cdots & \frac{\partial f_m}{\partial x_2} \\ \cdots & \cdots & \cdots & \cdots \\ \frac{\partial f_1}{\partial x_n} & \frac{\partial f_2}{\partial x_n} & \cdots & \frac{\partial f_m}{\partial x_n} \end{bmatrix} \begin{bmatrix} \lambda_1 \\ \lambda_2 \\ \vdots \\ \lambda_n \end{bmatrix}$$

$$= \left[\frac{\partial \boldsymbol{f}}{\partial \boldsymbol{x}}\right]^T \lambda \qquad \text{(A-30)}$$

References

1. Shipley, R.B., *Introduction to Matrices and Power Systems*, Wiley, New York, 1976.
2. Hadley, G., *Linear Algebra*, Addison-Wesley Reading, Mass., 1961.
3. Bellman, R., *Introduction to Matrix Analysis*, McGraw-Hill New York, 1960.

Appendix B

Generalized Circuit Constants

We can represent, as we saw in Ch. 5, a three-phase transmission line* by a circuit with two input terminals (sending-end, where power enters) and two output terminals (receiving-end, where power exits). This two-terminal pair circuit is *passive* (since it does not contain any electric energy sources), *linear* (impedances of its elements are independent of the amount of current flowing through them), and *bilateral* (impedances being independent of direction of current flowing). It can be shown that such a two-terminal pair network can be represented by an equivalent T- or π-network.

Consider the unsymmetrical T-network of Fig. B-1, which is equivalent to the general two-terminal pair network.

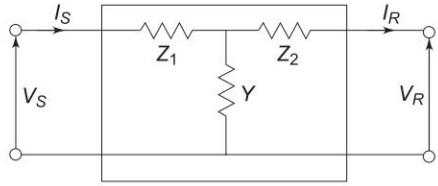

Fig. B-1 Unsymmetrical T-circuit equivalent to a general two-terminal pair network

For Fig. B-1, the following circuit equations can be written

$$I_S = I_R + Y(V_R + I_R Z_2)$$

or (B-1)

$$\begin{aligned} I_S &= YV_R + (1 + YZ_2)I_R \\ V_S &= V_R + I_R Z_2 + I_S Z_1 \\ &= V_R + I_R Z_2 + Z_1 Y V_R + I_R Z_1 + I_R Y Z_1 Z_2 \end{aligned}$$

or

$$V_S = (1 + YZ_1)\, V_R + (Z_1 + Z_2 + YZ_1Z_2)I_R \qquad \text{(B-2)}$$

Equations (B-1) and (B-2) can be simplified by letting

$$A = 1 + YZ_1 \quad B = Z_1 + Z_2 + YZ_1Z_2 \qquad \text{(B-3)}$$
$$C = Y \qquad D = 1 + YZ_2$$

* A transformer is similarly represented by a circuit with two input and two output terminals.

Using these, Eqs (B-1) and (B-2) can be written in matrix form as

$$\begin{bmatrix} V_S \\ I_S \end{bmatrix} = \begin{bmatrix} A & B \\ C & D \end{bmatrix} \begin{bmatrix} V_R \\ I_R \end{bmatrix} \tag{B-4}$$

This equation is the same as Eq. (5.1) and is valid for any linear, passive and bilateral two-terminal pair network. The constants A, B, C and D are called the *generalized circuit constants* or the *ABCD* constants of the network, and they can be calculated for any such two-terminal pair network.

It may be noted that *ABCD* constants of a two-terminal pair network are complex numbers in general, and always satisfy the following relationship:

$$AD - BC = 1 \tag{B-5}$$

Also, for any symmetrical network the constants A and D are equal. From Eq. (B-4) it is clear that A and D are dimensionless, while B has the dimensions of impedance (ohms) and C has the dimensions of admittance (mhos).

The *ABCD* constants are extensively used in power system analysis. A general two-terminal pair network is often represented as in Fig. B-2.

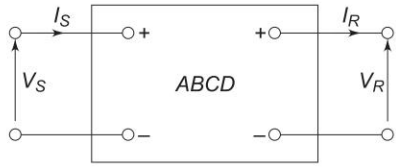

Fig. B-2 Schematic representation of a two-terminal pair network using *ABCD* constants

ABCD CONSTANTS FOR VARIOUS SIMPLE NETWORKS

We have already obtained the *ABCD* constants of an unsymmetrical *T*-network. The *ABCD* constants of unsymmetrical π-network shown in Fig. B-3 may be obtained in a similar manner and are given below:

$$\begin{aligned} A &= 1 + Y_2 Z \\ B &= Z \\ C &= Y_1 + Y_2 + Z Y_1 Y_2 \\ D &= 1 + Y_1 Z \end{aligned} \tag{B-6}$$

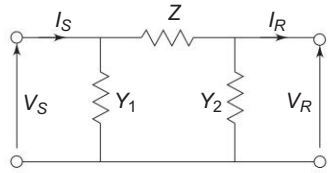

Fig. B-3 Unsymmetrical π-circuit

A series impedance often represents short transmission lines and transformers. The *ABCD* constants for such a circuit (as shown in Fig. B-4) can immediately be determined by inspection of Eqs (B-1) and (B-2), as follows:

$$\begin{aligned} A &= 1 \\ B &= Z \\ C &= 0 \\ D &= 1 \end{aligned} \tag{B-7}$$

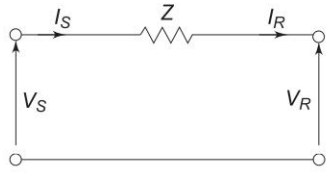

Fig. B-4 Series impedance

Another simple circuit of Fig. B-5 consisting of simple shunt admittance can be shown to possess the following *ABCD* constants:

$$\begin{aligned} A &= 1 \\ B &= 0 \\ C &= Y \\ D &= 1 \end{aligned} \tag{B-8}$$

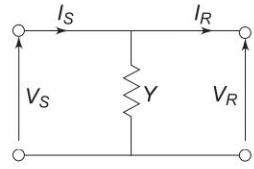

Fig. B-5 Shunt admittance

It may be noted that whenever *ABCD* constants are computed, it should be checked that the relation $AD-BC = 1$ is satisfied. For example, using Eq. (B-8) we get

$$AD - BC = 1 \times 1 - 0 \times Y = 1$$

If *ABCD* constants of a circuit are given, its equivalent *T*- or π-circuit can be determined by solving Eq. (B-3) or (B-6), respectively, for the values of series and shunt branches. For the equivalent π-circuit of Fig. B-3, we have

$$\begin{aligned} Z &= B \\ Y_1 &= \frac{D-1}{B} \\ Y_2 &= \frac{A-1}{B} \end{aligned} \tag{B-9}$$

ABCD CONSTANTS OF NETWORKS IN SERIES AND PARALLEL

Whenever a power system consists of series and parallel combinations of networks, whose *ABCD* constants are known, the overall *ABCD* constants for the system may be determined to analyze the overall operation of the system.

Consider the two networks in series, as shown in Fig. B-6. This combination can be reduced to a single equivalent network as follows:

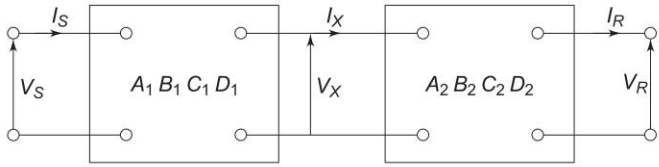

Fig. B-6 Networks in series

For the first network, we have

$$\begin{bmatrix} V_S \\ I_S \end{bmatrix} = \begin{bmatrix} A_1 & B_1 \\ C_1 & D_1 \end{bmatrix} \begin{bmatrix} V_X \\ I_X \end{bmatrix} \tag{B-10}$$

For the second network, we can write

$$\begin{bmatrix} V_X \\ I_X \end{bmatrix} = \begin{bmatrix} A_2 & B_2 \\ C_2 & D_2 \end{bmatrix} \begin{bmatrix} V_R \\ I_R \end{bmatrix} \tag{B-11}$$

From Eqs (B-10) and (B-11), we can write

$$\begin{bmatrix} V_S \\ I_S \end{bmatrix} = \begin{bmatrix} A_1 & B_1 \\ C_1 & D_1 \end{bmatrix} \begin{bmatrix} A_2 & B_2 \\ C_2 & D_2 \end{bmatrix} \begin{bmatrix} V_R \\ I_R \end{bmatrix}$$

$$= \begin{bmatrix} A_1A_2 + B_1C_2 & A_1B_2 + B_1D_2 \\ C_1A_2 + D_1C_2 & C_1B_2 + D_1D_2 \end{bmatrix} \begin{bmatrix} V_R \\ I_R \end{bmatrix} \tag{B-12}$$

If two networks are connected in parallel as shown in Fig. B-7, the *ABCD* constants of the combined network can be found out similarly with some simple manipulations of matrix algebra. The results are presented below:

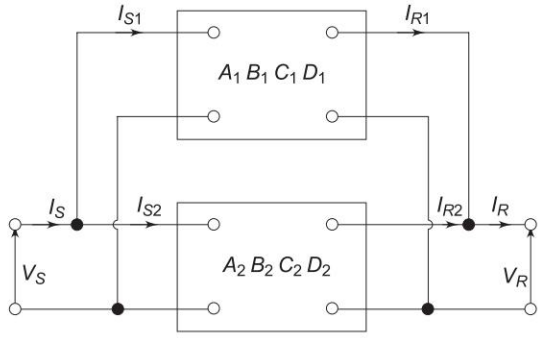

Fig. B-7 Networks in parallel

$$A = (A_1B_2 + A_2B_1)/(B_1 + B_2)$$
$$B = B_1B_2/(B_1 + B_2) \quad \text{(B-13)}$$
$$C = (C_1 + C_2) + (A_1 - A_2)\,(D_2 - D_1)/(B_1 + B_2)$$
$$D = (B_2D_1 + B_1D_2)/(B_1 + B_2)$$

Measurement of *ABCD* Constants

The generalized circuit constants may be computed for a transmission line which is being designed from a knowledge of the system impedance/admittance parameters using expressions such as those developed above. If the line is already built, the generalized circuit constants can be measured by making a few ordinary tests on the line. Using Eq. (B-4), these constants can easily be shown to be ratios of either voltage or current at the sending-end to voltage or current at the receiving-end of the network with the receiving-end open or short-circuited. When the network is a transformer, generator, or circuit having lumped parameters, voltage and current measurements at both ends of the line can be made, and the phase angles between the sending and receiving-end quantities can be found out. Thus the *ABCD* constants can be determined.

It is possible, also, to measure the magnitudes of the required voltages and currents simultaneously at both ends of a transmission line, but there is no simple method to find the difference in phase angle between the quantities at the two ends of the line. Phase difference is necessary because the *ABCD* constants are complex. By measuring two impedances at each end of a transmission line, however, the generalized circuit constants can be computed.

The following impedances are to be measured:

Z_{SO} = sending-end impedance with receiving-end open-circuited
Z_{SS} = sending-end impedance with receiving-end short circuited
Z_{RO} = receiving-end impedance with sending-end open-circuited
Z_{RS} = receiving-end impedance with sending-end short-circuited

The impedances measured from the sending-end can be determined in terms of the *ABCD* constants as follows:

From Eq. (B-4), with $I_R = 0$,

$$Z_{SO} = V_S/I_S = A/C \quad \text{(B-14)}$$

and with $V_R = 0$,

$$Z_{SS} = V_S/I_S = B/D \quad \text{(B-15)}$$

When the impedances are measured from the receiving-end, the direction of current flow is reversed and hence the signs of all current terms in Eq. (5.25). We can therefore rewrite this equation as

$$V_R = DV_S + BI_S \quad \text{(B-16)}$$
$$I_R = CV_S + AI_S$$

From Eq. (B-16), with $I_S = 0$,

$$Z_{RO} = V_R/I_R = D/C \tag{B-17}$$

and when $V_S = 0$,

$$Z_{RS} = V_R/I_R = B/A \tag{B-18}$$

Solving Eqs (B-14), (B-15), (B-17) and (B-18) we can obtain the values of the *ABCD* constants in terms of the measured impedances as follows:

$$Z_{RO} - Z_{RS} = \frac{AD - BC}{AC} = \frac{1}{AC} \quad \text{[using Eq. (B-5)]}$$

$$\frac{Z_{RO} - Z_{RS}}{Z_{SO}} = \frac{1}{AC} \cdot \frac{C}{A} = \frac{1}{A^2}$$

$$\therefore \quad A = \left(\frac{Z_{SO}}{Z_{RO} - Z_{RS}} \right)^{1/2} \tag{B-19}$$

By substituting this value of A in Eqs (B-14) and (B-18) and substituting the value of C so obtained in Eq. (B-17), we get

$$B = Z_{RS} \left(\frac{Z_{SO}}{Z_{RO} - Z_{RS}} \right)^{1/2} \tag{B-20}$$

$$C = \frac{1}{(Z_{RO}(Z_{SO} - Z_{RS}))^{1/2}} \tag{B-21}$$

$$D = \frac{Z_{RO}}{(Z_{SO}(Z_{RO} - Z_{RS}))^{1/2}} \tag{B-22}$$

Reference

1. Cotton, H. and H. Barber, *The Transmission and Distribution of Electrical Energy*, 3rd edn, B.I. Publishers, New Delhi, 1970.

Appendix C

Triangular Factorization and Optimal Ordering

We know that the nodal matrix $\boldsymbol{Y}_{\text{BUS}}$ and its associated Jacobian are very sparse, whereas their inverse matrices are full. For large power systems the sparsity of these matrices may be as high as 98% and must be exploited. Apart from reducing storage and time of computation, sparsity utilization limits the round-off computational errors. In fact, straight-forward application of the iterative procedure for system studies like load flow is not possible for large systems unless the sparsity of the Jacobian is dealt with effectively.

GAUSS ELIMINATION

One of the recent techniques of solving a set of linear algebraic equations, called *triangular factorization*, replaces the use of matrix inverse which is highly inefficient for large sparse systems. In triangularization, the elements of each row below the main diagonal are made zero and the diagonal element of each row is normalized as soon as the processing of that row is completed. It is possible to proceed columnwise but it is computationally inefficient and is therefore not used. After triangularization the solution is easily obtained by *back substitution*. The technique is illustrated in the example below.

Example C-1 Consider the linear vector-matrix equation

$$\begin{bmatrix} 2 & 1 \\ 3 & 5 \end{bmatrix} \begin{bmatrix} x_1 \\ x_2 \end{bmatrix} = \begin{bmatrix} 1 \\ 0 \end{bmatrix}$$

Procedure

1. Divide row 1 by the self-element of the row, in this case 2.
2. Eliminate the element (2, 1) by multiplying the modified row 1, by element (2, 1) and subtract it from row 2.
3. Divide the modified row 2 by its self-element $\left(\frac{7}{2}\right)$, and stop.

Following this procedure, we get the upper triangular equation as

$$\begin{bmatrix} 1 & \frac{1}{2} \\ 0 & \frac{\frac{7}{2}}{\frac{7}{2}} = 1 \end{bmatrix} \begin{bmatrix} x_1 \\ x_2 \end{bmatrix} = \begin{bmatrix} \frac{1}{2} \\ \frac{0 - \frac{3}{2}}{\frac{7}{2}} \end{bmatrix}$$

Upon back substituting, that is first solving for x_2 and then for x_1, we get

$$x_2 = \frac{0 - \frac{3}{2}}{\frac{7}{2}} = -\frac{3}{7}$$

$$x_1 = \frac{1}{2} - \frac{1}{2}x_2 = \frac{1}{2} - \frac{1}{2}\left(-\frac{3}{7}\right) = \frac{5}{7}$$

Check

$$2x_1 + x_2 = 2\left(\frac{5}{7}\right) - \frac{3}{7} = 1$$

$$3x_1 + 5x_2 = 3\left(\frac{5}{7}\right) - 5\left(\frac{3}{7}\right) = 0$$

Thus, we have demonstrated the use of the basic Gauss elimination and back substitution procedure for a simple system, but the same procedure applies to any general system of linear algebraic equations, i.e.

$$\boldsymbol{Ax = b} \tag{C-1}$$

An added advantage of row processing (elimination of row elements below the main diagonal and normalization of the self-element) is that it is easily amenable to use of the low storage compact storage schemes—avoiding storage of zero elements.

GAUSS ELIMINATION USING TABLE OF FACTORS

Where repeated solution of vector-matrix Eq. (C-1) with constant $\boldsymbol{A}$ but varying values of vector $\boldsymbol{b}$ is required, it is computationally advantageous to split the matrix $\boldsymbol{A}$ into triangular factor (termed as 'Table of factors' or 'LU decomposition') using the Gauss elimination technique. If the matrix $\boldsymbol{A}$ is sparse, so is the table of factors which can be compactly stored thereby not only reducing core storage requirements, but also the computational effort. Gauss elimination using the table of factors is illustrated in the following example.

Example C-2 Consider the following system of linear equations:

$$\begin{aligned}(2)x_1 + (1)x_2 + (3)x_3 &= 6\\ (2)x_1 + (3)x_2 + (4)x_3 &= 9\\ (3)x_1 + (4)x_2 + (7)x_3 &= 14\end{aligned} \tag{C-2}$$

For computer solution, maximum efficiency is attained when elimination is carried out by rows rather than the more familiar column order. The successive reduced sets of equations are as follows:

$$\begin{aligned}(1)x_1 + \left(\frac{1}{2}\right)x_2 + \left(\frac{3}{2}\right)x_3 &= \frac{6}{2}\\ (2)x_1 + (3)x_2 + (4)x_3 &= 9\\ (3)x_1 + (4)x_2 + (7)x_3 &= 14\end{aligned} \tag{C-3}$$

$$\begin{aligned}(1)x_1 + \left(\frac{1}{2}\right)x_2 + \left(\frac{3}{2}\right)x_3 &= 3\\ (2)x_2 + (1)x_3 &= 3\\ (3)x_1 + (4)x_2 + (7)x_3 &= 14\end{aligned} \tag{C-4}$$

$$\begin{aligned}(1)x_1 + \left(\frac{1}{2}\right)x_2 + \left(\frac{3}{2}\right)x_3 &= 3\\ (1)x_2 + \left(\frac{1}{2}\right)x_3 &= \frac{3}{2}\\ (3)x_1 + (4)x_2 + (7)x_3 &= 14\end{aligned} \tag{C-5}$$

$$\begin{aligned}(1)x_1 + \left(\frac{1}{2}\right)x_2 + \left(\frac{2}{3}\right)x_3 &= 3\\ (1)x_2 + \left(\frac{1}{2}\right)x_3 &= \frac{3}{2}\\ \left(\frac{5}{2}\right)x_2 + \left(\frac{5}{2}\right)x_3 &= 5\end{aligned} \tag{C-6}$$

$$\begin{aligned}(1)x_1 + \left(\frac{1}{2}\right)x_2 + \left(\frac{3}{2}\right)x_3 &= 3\\ (1)x_2 + \left(\frac{1}{2}\right)x_3 &= \frac{3}{2}\\ \left(\frac{5}{4}\right)x_3 &= \frac{5}{4}\end{aligned} \tag{C-7}$$

$$(1)x_1 + \left(\frac{1}{2}\right)x_2 + \left(\frac{3}{2}\right)x_3 = 3$$

$$(1)x_2 + \left(\frac{1}{2}\right)x_3 = \frac{3}{2} \qquad \text{(C-8)}$$

$$x_3 = 1$$

These steps are referred to as 'elimination' operations. The solution $\boldsymbol{x}$ may be immediately determined by 'back substitution' operation using Eq. (C-8).

The solution for a new set of values for $\boldsymbol{b}$ can be easily obtained by using a table of factors prepared by a careful examination of Eqs (C-3) to (C-8). We can write the table of factors $\boldsymbol{F}$ as below for the example in hand.

$$\boldsymbol{F} = \begin{bmatrix} f_{11} & f_{12} & f_{13} \\ f_{21} & f_{22} & f_{23} \\ f_{31} & f_{32} & f_{33} \end{bmatrix} = \begin{bmatrix} \frac{1}{2} & \frac{1}{2} & \frac{2}{3} \\ 2 & \frac{1}{2} & \frac{1}{2} \\ 3 & \frac{5}{2} & \frac{4}{5} \end{bmatrix} \qquad \text{(C-9)}$$

The row elements of $\boldsymbol{F}$ below the diagonal are the multipliers of the normalized rows required for the elimination of the row element, e.g. $f_{32} = 5/2$, the multiplier of normalized row 2 [Eq. (C-6)] to eliminate the element (3, 2), i.e. $(5/2)\,x_2$. The diagonal elements of $\boldsymbol{F}$ are the multipliers needed to normalize the rows after the row elimination has been completed, e.g. $f_{22} = \frac{1}{2}$, the factor by which row 2 of Eq. (C-4) must be multiplied to normalize the row. The elements of $\boldsymbol{F}$ above the diagonal can be immediately written down by inspection of Eq. (C-8). These are needed for the back substitution process.

In rapidly solving Eq. (C-1) by use of the table of factors $\boldsymbol{F}$, successive steps appear as columns (left to right) in Table C-1 below:

Table C-1

b	1, 1	2, 1	2, 2	3, 1	3, 2	3, 3	2, 3	1, 3	1, 2	*x*
6	3	3	3	3	3	3	3	5/2	1	1
9	9	3	3/2	3/2	3/2	3/2	3	1	1	1
14	14	14	14	5	5/4	1	1	1	1	1

The heading row (i, j) of Table C-1 represents the successive elimination and back substitution steps. Thus,

1, 1 represents normalization of row 1
2, 1 represents elimination of element (2, 1)
2, 2 represents normalization of row 2

3, 1; 3, 2	represent elimination of elements (3, 1) and (3, 2), respectively
3, 3	represents normalization of row 3
2, 3	represents elimination of element (2, 3) by back substitution
1, 3; 1, 2	represent elimination of elements (1, 3) and (1, 2) respectively by back substitution.

The solution vector at any stage of development is denoted by

$$[y_1\ y_2\ y_3]^T = \boldsymbol{y}$$

The modification of solution vector from column to column (left to right) is carried out for the heading (i, j) as per the operations defined below:

$$y_i = f_{ii} y_i, \qquad \text{if } j = i \tag{C-10}$$

$$y_i = y_i - f_{ij} y_i, \quad \text{if } j \neq i \tag{C-11}$$

Thus for heading 3, 2

$$y_3 = y_3 - f_{32} y_2$$

$$= 5 - \left(\frac{5}{2}\right)\left(\frac{3}{2}\right) = \frac{5}{4}$$

and for heading 3, 3

$$y_3 = f_{33} y_3$$

$$= \left(\frac{4}{5}\right)\left(\frac{5}{4}\right) = 1$$

In fact, operation (C-10) represents row normalization and (C-11) represents elimination and back substitution procedures.

Optimal Ordering

In power system studies, the matrix $\boldsymbol{A}$ is quite sparse so that the number of non-zero operations and non-zero storage required in Gauss elimination is very sensitive to the sequence in which the rows are processed. The row sequence that leads to the least number of non-zero operations is not, in general, the same as the one which yields least storage requirement. It is believed that the absolute optimum sequence of ordering the rows of a large network matrix (this is equivalent to renumbering of buses) is too complicated and time consuming to be of any practical value. Therefore, some simple yet effective schemes have been evolved to achieve near optimal ordering with respect to both the criteria. Some of the schemes of near optimal ordering the sparse matrices, which are fully symmetrical or at least symmetric in the pattern of non-zero off-diagonal terms, are described below [4].

Scheme 1

Number the matrix rows in the order of the fewest non-zero terms in each row. If more than one unnumbered row has the same number of non-zero terms, number these in any order.

Scheme 2

Number the rows in the order of the fewest non-zero terms in a row at each step of elimination. This scheme requires updating the count of non-zero terms after each step.

Scheme 3

Number the rows in order of the fewest non-zero off-diagonal terms generated in the remaining rows at each step of elimination. This scheme also involves an updating procedure.

The choice of scheme is a trade-off between speed of execution and the number of times the result is to be used. For Newton's method of load flow solution, scheme 2 seems to be the best. The efficiency of scheme 3 is not sufficiently established to offset the increased time required for its execution. Scheme 1 is useful for problems requiring only a single solution with no iteration.

Compact Storage Schemes

The usefulness of the Newton's method depends largely upon conserving computer storage and reducing the number of non-zero computations. To effect these ideas on the computer, elimination of lower triangle elements is carried out a row at a time using the concept of compact working row. The non-zero modified upper triangle elements and mismatches are stored in a compact and convenient way. Back substitution progresses backwards through the compact upper triangle table. A properly programmed compact storage scheme results in considerable saving of computer time during matrix operations.

Naturally, there are as many compact working rows and upper triangle storage schemes as there are programmers. One possible scheme for a general matrix stores the non-zero elements of successive rows in a linear array. The column location of these non-zero elements and the location where the next row starts (row index) is stored separately. The details of this and various other schemes are given in [2].

References

1. Singh, L.P., *Advanced Power System Analysis and Dynamics*, 2nd edn, Wiley Eastern, New Delhi, 1986.
2. Agarwal, S.K., 'Optimal Power Flow Studies', *Ph.D. Thesis*, B.I.T.S. Pilani, 1970.
3. Tinney, W.F. and J.W. Walker, 'Direct Solutions of Sparse Network Equations by Optimally Ordered Triangular Factorizations', *Proc. IEEE*, Nov. 1967, 55: 1801.
4. Tinney, W.F. and C.E. Hart, 'Power Flow Solution by Newton's Method', *IEEE Trans*., Nov. 1967, no. 11, PAS-86: 1449.

Appendix D

Elements of Power System Jacobian Matrix

Expressions to be used in evaluating the elements of the Jacobian matrix of a power system are derived below:

From Eq. (6.25b)

$$P_i - jQ_i = V_i^* \sum_{k=1}^{n} Y_{ik} V_k$$

$$= |V_i| \exp(-j\delta_i) \sum_{k=1}^{n} |Y_{ik}| \exp(j\theta_{ik}) |V_k| \exp(j\delta_k) \qquad \text{(D-1)}$$

Differentiating partially with respect to δ_m $(m \neq i)$

$$\frac{\partial P_i}{\partial \delta_m} - j\frac{\partial Q_i}{\partial \delta_m} = j|V_i| \exp(-j\delta_i) (|Y_{im}| \exp(j\theta_{im}) |V_m| \exp(j\delta_m))$$

$$= j(e_i - jf_i)(a_m + jb_m) \qquad \text{(D-2)}$$

where

$$Y_{im} = G_{im} + jB_{im}$$

$$V_i = e_i + jf_i$$

$$(a_m + jb_m) = (G_{im} + jB_{im})(e_m + jf_m)$$

Although the polar form of the NR method is being used, rectangular complex arithmetic is employed for numerical evaluation as it is faster.

From Eq. (D-2), we can write

$$\frac{\partial P_i}{\partial \delta_m} = (a_m f_i - b_m e_i) = H_{im}$$

$$\frac{\partial Q_i}{\partial \delta_m} = -(a_m e_i + b_m f_i) = J_{im}$$

For the case of $m = i$, we have

$$\frac{\partial P_i}{\partial \delta_i} - j\frac{\partial Q_i}{\partial \delta_i} = -j|V_i| \exp(-j\delta_i) \sum_{k=1}^{n} |Y_{ik}| \exp(j\theta_{ik}) |V_k| \exp(j\delta_k)$$
$$+ j|V_i| \exp(-j\delta_i) (|Y_{ii}| \exp(j\theta_{ii}) |V_i| \exp(j\delta_i))$$
$$= -j(P_i - jQ_i) + j|V_i|^2 (G_{ii} + jB_{ii}) \quad \text{(D-3)}$$

From Eq. (D-3), we can write

$$\frac{\partial P_i}{\partial \delta_i} = -Q_i - B_{ii}|V_i|^2 = H_{ii}$$

$$\frac{\partial Q_i}{\partial \delta_i} = P_i - G_{ii}|V_i|^2 = J_{ii}$$

Now differentiate Eq. (D-1) partially with respect to $|V_m|$ $(m \neq i)$. We have

$$\frac{\partial P_i}{\partial |V_m|} - j\frac{\partial Q_i}{\partial |V_m|} = |V_i| \exp(-j\delta_i) (|Y_{im}| \exp(j\theta_{im}) \exp(j\delta_m))$$

Multiplying by $|V_m|$ on both sides,

$$\frac{\partial P_i}{\partial |V_m|}|V_m| - j\frac{\partial Q_i}{\partial |V_m|}|V_m|$$
$$= |V_i| \exp(-j\delta_i) |Y_{im}| \exp(j\theta_{im}) |V_m| \exp(j\delta_m)$$
$$= (e_i - jf_i)(a_m + jb_m) \quad \text{(D-4)}$$

It follows from Eq. (D-4) that

$$\frac{\partial P_i}{\partial |V_m|}|V_m| = a_m e_i + b_m f_i = N_{im}$$

$$\frac{\partial Q_i}{\partial |V_m|}|V_m| = a_m f_i - b_m e_i = L_{im}$$

Now for the case of $m = i$, we have

$$\frac{\partial P_i}{\partial |V_i|} - j\frac{\partial Q_i}{\partial |V_i|} = \exp(-j\delta_i) \sum_{k=1}^{n} |Y_{ik}| \exp(j\theta_{ik}) |V_k| \exp(j\delta_k)$$
$$+ |V_i| \exp(-j\delta_i) |Y_{ii}| \exp(j\theta_{ii}) \exp(j\delta_i)$$

Multiplying by $|V_i|$ on both sides

$$\frac{\partial P_i}{\partial |V_i|}|V_i| - j\frac{\partial Q_i}{\partial |V_i|}|V_i|$$
$$= |V_i| \exp(-j\delta_i) \sum_{k=1}^{n} |Y_{ik}| \exp(j\theta_{ik}) |V_k| \exp(j\delta_k) + |V_i|^2 |Y_{ii}| \exp(j\theta_{ii})$$
$$= (P_i - jQ_i) + |V_i|^2 (G_{ii} + jB_{ii}) \quad \text{(D-5)}$$

It follows from Eq. (D-5) that

$$\frac{\partial P_i}{\partial |V_i|} |V_i| = P_i + G_{ii}|V_i|^2 = N_{ii}$$

$$\frac{\partial Q_i}{\partial |V_i|} |V_i| = Q_i - B_{ii}|V_i|^2 = L_{ii}$$

The above results are summarized below:

Case 1 $m \neq i$

$$\begin{aligned} H_{im} &= L_{im} = a_m f_i - b_m e_i \\ N_{im} &= -J_{im} = a_m e_i + b_m f_i \end{aligned} \tag{D-6}$$

where

$$\begin{aligned} Y_{im} &= G_{im} + jB_{im} \\ V_i &= e_i + jf_i \\ (a_m + jb_m) &= (G_{im} + jB_{im})\ (e_m + jf_m) \end{aligned} \tag{D-7}$$

Case 2 $m = i$

$$\begin{aligned} H_{ii} &= -Q_i - B_{ii}|V_i|^2 \\ N_{ii} &= P_i + G_{ii}|V_i|^2 \\ J_{ii} &= P_i - G_{ii}|V_i|^2 \\ L_{ii} &= Q_i - B_{ii}|V_i|^2 \end{aligned} \tag{D-8}$$

References

1. Tinney, W.F. and C.E. Hart, 'Power Flow Solution by Newton's Method', *IEEE Trans*., Nov 1967, no. 11, PAS-86: 1449.
2. Van Ness, J.E., 'Iteration Methods for Digital Load Flow Studies', *Trans., AIEE*, Aug. 1959, 78A: 583.

Appendix E

Kuhn-Tucker Theorem

The Kuhn-Tucker theorem makes it possible to solve the general non-linear programming problem with several variables wherein the variables are also constrained to satisfy certain equality and inequality constraints.

We can state the minimization problem with inequality constraints for the control variables as

$$\min_{\boldsymbol{u}} \; f(\boldsymbol{x}, \boldsymbol{u}) \tag{E-1}$$

subject to equality constraints

$$\boldsymbol{g}(\boldsymbol{x}, \boldsymbol{u}, \boldsymbol{p}) = \boldsymbol{0} \tag{E-2}$$

and to the inequality constraints

$$\boldsymbol{u} - \boldsymbol{u}_{\max} \leq \boldsymbol{0} \tag{E-3}$$

$$\boldsymbol{u}_{\min} - \boldsymbol{u} \leq \boldsymbol{0} \tag{E-4}$$

The Kuhn-Tucker theorem [1] gives the necessary conditions for the minimum, assuming convexity for the functions (E-1) – (E-4), as

$$\nabla \mathcal{L} = \boldsymbol{0} \text{ (gradient with respect to } \boldsymbol{u}, \boldsymbol{x}, \boldsymbol{\lambda}) \tag{E-5}$$

where $\mathcal{L}$ is the Lagrangian formed as

$$\mathcal{L} = f(\boldsymbol{x}, \boldsymbol{u}) + \boldsymbol{\lambda}^T \boldsymbol{g}(\boldsymbol{x}, \boldsymbol{u}, \boldsymbol{p}) + \alpha^T_{\max}(\boldsymbol{u} - \boldsymbol{u}_{\max}) + \alpha^T_{\min}(\boldsymbol{u}_{\min} - \boldsymbol{u}) \tag{E-6}$$

and

$$\left\{ \begin{array}{l} \alpha^T_{\max}(\boldsymbol{u} - \boldsymbol{u}_{\max}) = \boldsymbol{0} \\ \alpha^T_{\min}(\boldsymbol{u}_{\min} - \boldsymbol{u}) = \boldsymbol{0} \\ \alpha_{\max} \geq \boldsymbol{0}, \alpha_{\min} \geq \boldsymbol{0} \end{array} \right\} \tag{E-7}$$

Equations (E-7) are known as *exclusion equations.*

The multipliers $\alpha_{\max}$ and $\alpha_{\min}$ are the *dual variables* associated with the upper and lower limits on control variables. They are auxiliary variables similar to the Lagrangian multipliers λ for the equality constraints case.

If u_i violates a limit, it can either be upper or lower limit and not both simultaneously. Thus, either inequality constraint (E-3) or (E-4) is active at a time, that is, either $\alpha_{i,\max}$ or $\alpha_{i,\min}$ exists, but never both. Equation (E-5) can be written as

$$\frac{\partial \mathcal{L}}{\partial \boldsymbol{x}} = \frac{\partial f}{\partial \boldsymbol{x}} + \left(\frac{\partial g}{\partial \boldsymbol{x}}\right)^T \lambda = \mathbf{0} \tag{E-8}$$

$$\frac{\partial \mathcal{L}}{\partial \boldsymbol{u}} = \frac{\partial f}{\partial \boldsymbol{u}} + \left(\frac{\partial g}{\partial \boldsymbol{u}}\right)^T \lambda + \alpha = \mathbf{0} \tag{E-9}$$

In Eq. (E-9),

$$\alpha_i = \alpha_{i,\max} \quad \text{if } u_i - u_{i,\max} > 0$$
$$\alpha_i = -\alpha_{i,\min} \quad \text{if } u_{i,\min} - u_i > 0$$
$$\frac{\partial \mathcal{L}}{\partial \lambda} = \boldsymbol{g}(\boldsymbol{x}, \boldsymbol{u}, \boldsymbol{p}) = 0 \tag{E-10}$$

It is evident that α computed from Eq. (E-9) at any feasible solution, with λ from Eq. (E-8) is identical with negative gradient, i.e.

$$\alpha = -\frac{\partial \mathcal{L}}{\partial u} = \text{negative of gradient with respect to } \boldsymbol{u} \tag{E-11}$$

At the optimum, α must also satisfy the exclusion equations (E-7), which state that

$$\alpha_i = 0 \qquad \text{If } u_{i,\min} < u_i < u_{i,\max}$$
$$\alpha_i = \alpha_{i,\max} \geq 0 \qquad \text{If } u_i = u_{i,\max}$$
$$\alpha_i = -\alpha_{i,\min} \leq 0 \qquad \text{If } u_i = u_{i,\min}$$

which can be rewritten in terms of the gradient using Eq. (E-11) as follows:

$$\frac{\partial \mathcal{L}}{\partial u_i} = 0 \quad \text{if } u_{i,\min} < u_i < u_{i,\max}$$
$$\frac{\partial \mathcal{L}}{\partial u_i} \leq 0 \quad \text{if } u_i = u_{i,\max} \tag{E-12}$$
$$\frac{\partial \mathcal{L}}{\partial u_i} \geq 0 \quad \text{if } u_i = u_{i,\min}$$

Reference

1. Kuhn, H.W. and A.W. Tucker, "Nonlinear Programming", *Proceedings of the Second Berkeley Symposium on Mathematical Statistics and Probability,* University of California Press, Berkeley, 1951.

Appendix F

Real-time Computer Control of Power Systems

In developed countries the focus is shifting in the power sector from the creation of additional capacity to better capacity utilization through more effective management and efficient technology. This applies equally to developing countries where this focus will result in reduction in need for capacity addition.

Immediate and near future priorities now are better plant management, higher availability, improved load management, reduced transmission losses, revamps of distribution system, improved billing and collection, energy efficiency, energy audit and energy management. All this would enable an electric power system to generate, transmit and distribute electric energy at the lowest possible economic and ecological cost.

These objectives can only be met by use of information technology (IT) enabled services in power systems management and control. Emphasis is therefore, being laid on computer control and information transmission and exchange.

The operations involved in power systems require geographically dispersed and functionally complex monitoring and control system. The monitory and supervisory control that is constantly developing and undergoing improvement in its control capability is schematically presented in Fig. F-1 which is easily seen to be distributed in nature.

Starting from the top, control system functions are:

EMS Energy Management System—It exercises overall control over the total system.

SCADA Supervisory Control and Data Acquisition System—It covers generation and transmission system.

DAC Distribution Automation and Control System—It oversees the distribution system including connected loads.

Automation, monitoring and real-time control have always been a part of SCADA system. With enhanced emphasis on IT in power systems, SCADA has been receiving a lot of attention lately.

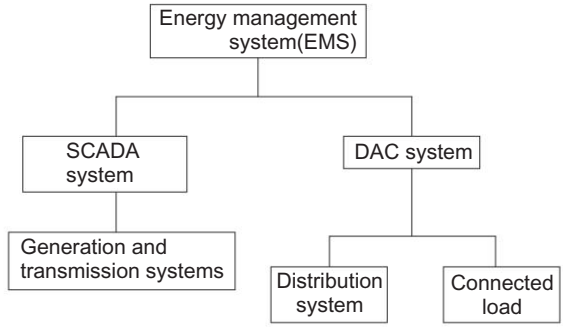

Fig. F-1 Real time monitoring and controlling of an electric power system

SCADA refers to a system that enables an electricity utility to remotely monitor, coordinate, control and operate transmission and distribution components, equipment and devices in a real-time mode from a remote location with acquisition of data for analysis and planning from one control location. Thus, the purpose of SCADA is to allow operators to observe and control the power system. The specific tasks of SCADA are:

- Data acquisition, which provides measurements and status information to operators.
- Trending plots and measurements on selected time scales.
- Supervisory control, which enables operators to remotely control devices such as circuit breakers and relays.

Capability of SCADA system is to allow operators to control circuit breakers and disconnect switches and change transformer taps and phase-shifter position remotely. It also allows operators to monitor the generation and high-voltage transmission systems and to take action to correct overloads or out-of-limit voltages. It monitors all status points such as switchgear position (open or closed), substation loads and voltages, capacitor banks, tie-line flows and interchange schedules. It detects through telemetry the failures and errors in bilateral communication links between the digital computer and the remote equipment. The most critical functions, mentioned above, are scanned every few seconds. Other noncritical operations, such as the recording of the load, forecasting of load, unit start-ups and shut-downs are carried out on an hourly basis.

Most low-priority programs (those run less frequently) may be executed on demand by the operator for study purposes or to initialize the power system. An operator may also change the digital computer code in the execution if a parameter changes in the system. For example, the MW/min capability of a generating unit may change if one of its throttle values is temporarily removed for maintenance, so the units share of regulating power must accordingly be decreased by the code. The computer software compilers and data handlers are designed to be versatile and readily accept operator inputs.

DAC is a lower level version of SCADA applicable in distribution system (including loads), which of course draws power from the transmission/ subtransmission levels. Obviously then there is no clear cut demarcation between DAC and SCADA.

In a distribution network, computerization can help manage load, maintain quality, detect theft and tampering and thus reduce system losses. Computerization also helps in centralization of data collection. At a central load dispatch centre, data such as current, voltage, power factor and breaker status are telemetered and displayed. This gives the operator an overall view of the entire distribution network. This enables him to have effective control on the entire network and issue instructions for optimizing flow in the event of feeder overload or voltage deviation. This is carried out through switching in/out of shunt capacitors, synchronous condensers and load management. This would help in achieving better voltage profile, loss reduction, improved reliability, quick detection of fault and restoration of service.

At a systems level, SCADA can provide status and measurements for distribution feeders at the substation. Distribution automation equipment can monitor selectionalizing devices like switches, interrupters and fuses. It can also operate switches for circuit reconfiguration, control voltage, read customers' meters, implement time-of-day pricing and switch customer equipment to manage load. This equipment significantly improves the functionality of distribution control centres.

SCADA can be used extensively for compilation of extensive data and management of distribution systems. Pilferage points too can be zeroed in on, as the flow of power can be closely scrutinized. Here again, trippings due to human errors can be avoided. Modern metering systems using electronic meters, automatic meter readers (AMRs), remote metering and spot billing can go a long way in helping electric utility. These systems can bring in additional revenues and also reduce the time lag between billing and collection.

Distribution automation through SCADA systems directly leads to increased reliability of power for consumers and lower operating costs for the utility. It results in forecasting accurate demand and supply management, faster restoration of power in case of a failure and alternative routing of power in an emergency.

A key feature of these systems is the remote control facility that allows faster execution of decisions. Manual errors and oversights are eliminated. Besides on line and real-time information, the system provides periodic reports that help in the analysis of performance of the power system. Distribution automation combines distribution network monitoring functions with geographical mapping, fault location, and so on, to improve availability. It also integrates load management, load despatch and intelligent metering.

DATA ACQUISITION SYSTEMS AND MAN–MACHINE INTERFACE

The use of computers nowadays encompasses all phases of power system operation: planning, forecasting, scheduling, security assessment and control. An energy control centre manages these tasks and provides optimal operation of the system. A typical control centre can perform the following functions:

(i) Short, medium and long-term load forecasting (LF)
(ii) System planning (SP)
(iii) Unit commitment (UC) and maintenance scheduling (MS)
(iv) Security monitoring (SM)
(v) State estimation (SE)
(vi) Economic dispatch (ED)
(vii) Load frequency control (LFC)

The above monitoring and control functions are performed in the hierarchical order classified according to time scales. The functions performed in the control centre are based on the availability of a large information base and require extensive software for data acquisition and processing.

At the generation level, the philosophy of 'distributed control' has dramatically reduced the cabling cost within a plant and has the potential of replacing traditional control rooms with distributed CRT/keyboard stations.

Data acquisition systems provide a supporting role to the application software in a control centre. The data acquisition system (DAS) collects raw data from selected points in the power system and converts these data into engineering units. The data are checked for limit violations and status changes and are sent to the data base for processing by the application software. The real-time data base provides structured information so that application programs needing the information have direct and efficient access to it.

The Man–Machine interface provides a link between the operator and the software/hardware used to control/monitor the power system. The interface generally is a colour graphic display system. The control processors interface with the control interface of the display system. The DAS and Man–Machine interface support the following functions:

(i) Load/Generation Dispatching
(ii) Display and CRT control
(iii) Data Base Maintenance
(iv) Alarm Handling
(v) Supervisory control
(vi) Programming functions
(vii) Data logging
(viii) Event logging
(ix) Real-time Network Analysis

With the introduction of higher size generating units, the monitoring requirements have gone up in power plants also. In order to improve the plant

performance, now all the utilities have installed DAS in their generating units of sizes 200 MW and above. The DAS in a thermal power station collects the following inputs from various locations in the plant and converts them into engineering units.

Analog inputs

(i) Pressures, flows, electrical parameters, etc.
(ii) Analog input of 0–10 V DC
(iii) Thermocouple inputs
(iv) RTD input

Digital inputs

(i) Contract outputs
(ii) Valve position, pressure and limit switches

All these process inputs are brought from the field through cables to the terminals. The computer processes the information and supplies to the Man–Machine interface to perform the following functions:

(i) Display on CRT screen
(ii) Graphic display of plant sub-systems
(iii) Data logging
(iv) Alarm generation
(v) Event logging
(vi) Trending of analogue variables
(vii) Performance calculation
(viii) Generation of control signals

Some of the above functions are briefly discussed as follows.

There are generally 2–3 CRTs in an operators console in the control room which facilitate the operator to have display of alarms, plant variables and other desired information simultaneously. To give a full view of the plant alongwith various real-time variables and status information, displays of mimic diagrams on a graphic CRT screen are very useful. The data can be logged on printers at a fixed interval automatically as well as on-demand. The limits of all the variables are checked by the software and if any of the variables is outside its pre-defined range, an alarm is raised to draw the operators attention. The selected important status changes are logged and a record of time of occurrences is maintained.

The DAS software contains programs to calculate periodically the efficiency of various equipment like boiler, turbine, generator, condenser, fans, heaters, etc.

The DAS can also carry out complete on-line control of power station equipment. The DAS for modern power plants employ distributed system configuration. The system is made up of a number of microcomputers each performing an assigned task and exchanging information among others through interconnection via a coaxial cable—the so-called Highway.

Distributed processing is a term that refers to any computing environment, in which multiple loosely coupled computer systems implement a given application. Automatic control by distributed intelligence has, among other advantages, great design flexibility together with improved reliability and performance. The information technology has now captured the imagination of power system engineers who are adopting the low-cost and relatively powerful computing devices in implementing their distributed DAS and control systems.

Computer control brings in powerful algorithms with the following advantages: (i) increase in capacity utilization in generation, (ii) savings in energy and so in raw materials due to increased operational efficiency, (iii) flexibility and modifiability, (iv) reduction in human drudgery, (v) improved operator effectiveness.

Intelligent database processors will become more common in power systems since the search, retrieval and updating activity can be speeded up. New functional concepts from the field of Artificial Intelligence (AI) will be integrated with power system monitoring, automatic restoration of power networks, and real-time control.

Personal computers (PCs) are being used in a wide range of power system operations including power station control, load management, SCADA systems, protection, operator training, maintenance functions, administrative data processing, generator excitation control and control of distribution networks. IT enabled systems thus not only monitor and control the grid, but also improve operational efficiencies and play a key part in maintaining the security of the power system.

References

1. *Power Line Magazine*, vol. 7, no. 1, October 2002, pp. 65–71.
2. Mahalanabis, A.K., D.P. Kothari and S.I. Ahson, *Computer Aided Power System Analysis and Control*, TMH, New Delhi, 1988.
3. IEEE Tutorial Course, *Fundamentals of Supervisory Control System*, 1981.
4. IEEE Tutorial Course, *Energy Control Centre Design*, 1983.
5. Handschin, E., *Real Time Control of Electric Power System*, Elsevier, New York, 1972.

Appendix G

Introduction to MATLAB and SIMULINK

MATLAB has been developed by MathWorks Inc. It is a powerful software package used for high performance scientific numerical computation, data analysis and visualization. MATLAB stands for MATrix LABoratory. The combination of analysis capabilities, flexibility, reliability and powerful graphics makes MATLAB the main software package for power system engineers. This is because unlike other programming languages where you have to declare matrices and operate on them with their indices, MATLAB provides matrix as one of the basic elements. It provides basic operations, as we will see later, like addition, subtraction, multiplication by use of simple mathematical operators. Also, we need not declare the type and size of any variable in advance. It is dynamically decided depending on what value we assign to it. But MATLAB is case sensitive and so we have to be careful about the case of variables while using them in our programs.

MATLAB gives an interactive environment with hundreds of reliable and accurate built-in functions. These functions help in providing the solutions to a variety of mathematical problems including matrix algebra, linear systems, differential equations, optimization, non-linear systems and many other types of scientific and technical computations. The most important feature of MATLAB is its programming capability, which supports both types of programming—object oriented and structured programming and is very easy to learn and use and allows user developed functions. It facilitates access to FORTRAN and C codes by means of external interfaces. There are several optional toolboxes for simulating specialized problems of different areas and extensions to link up MATLAB and other programs. SIMULINK is a program build on top of MATLAB environment, which along with its specialized products, enhances the power of MATLAB for scientific simulations and visualizations.

For a detailed description of commands, capabilities, MATLAB functions and many other useful features, the reader is referred to MATLAB Users Guide/Manual.

HOW TO START MATLAB?

You can start MATLAB by double clicking on MATLAB icon on your Desktop of your computer or by clicking on Start Menu followed by 'Programs' and then clicking appropriate program group such as 'MATLAB Release 12'. You will visualize a screen shown in Fig. G-1.

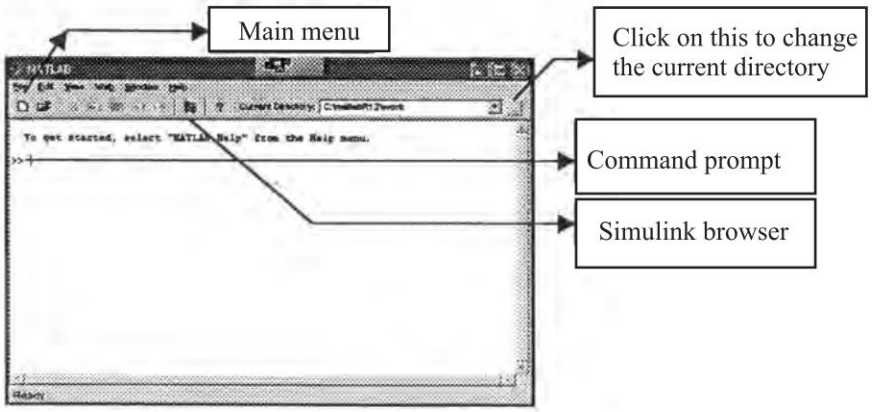

Fig. G-1

The command prompt (characterized by the symbol >>) is the one after which you type the commands. The main menu contains the submenus such as File, Edit, Help, etc. If you want to start a new program file in MATLAB (denoted by .m extension) one can click on **File** followed by **new** and select the desired **M-file**. This will open up a MATLAB File Editor/Debugger window where you can enter your program and save it for later use. You can run this program by typing its name in front of command prompt. Let us now learn some basic commands.

Matrix Initialization

A matrix can be initialized by typing its name followed by = sign and an opening square bracket after which the user supplies the values and closes the square brackets. Each element is separated from the other by one or more spaces or tabs. Each row of matrix is separated from the other by pressing Enter key at the end of each row or by giving semicolon at its end. Following examples illustrate this.

```
>>  A = [1 2 5]
```

>> $B = \begin{bmatrix} 1 & 5 & 7 \\ 7 & 2 & -9 \\ -3 & 2 & -5 \end{bmatrix}$

The above operation can also be achieved by typing

```
>>          B = [1 5 7; 7 2 –9; –3 2 –5]
```

If we do not give a semicolon at the end of closing square brackets, MATLAB displays the value of matrices in the command window. **If you do not want MATLAB to display the results, just type semicolon (;) at the end of the statement**. That is why you will find that in our programmes, whenever we want to display value of variables say voltages, we have just typed the name of the variable without semicolon at the end, so that user will see the values during the program. After the program is run with no values of the variables being displayed, if the user wants to see the values of any of these variables in the program he can simply type the variable name and see the values.

Common Matrix Operations

First let us declare some matrices

```
>>  A = [1 5; 6 9]
>>  B = [2 7; 9 –3]
```

Addition

```
>>  C = A + B
```

Add matrices A and B and stores them in matrix C.

Subtraction

```
>>  D = A – B
```

Subtract matrix B from matrix A and stores the result in D.

Multiplication

```
>>  E = A * B
```

Multiplies two conformable matrices A and B and stores the result in E.

Inverse

```
>>  F = inv(A)
```

This calculates the inverse of matrix A by calculating the co-factors and stores the result in F.

Transpose

Single quote (′) operator is used to obtain transpose of matrix. In case the matrix element is complex, it stores the conjugate of the element while taking the transpose, e.g.

```
>>  G = A′
```

or

```
>>  G1 = [1 3; 4 5; 6 3]′
```

also stores the transpose of matrix given in square brackets in matrix G1.

In case one does not want to take conjugate of elements while taking transpose of complex matrix, one should use . 'operator instead of' operator.

Determinant

```
>> H = det (A)
```
This stores determinant of matrix A in H.

Eigen Values

```
>> K = eig (A)
```
obtains eigenvalues of matrix A and stores them in K.

SPECIAL MATRICES AND PRE-DEFINED VARIABLES AND SOME USEFUL OPERATORS

MATLAB has some preinitialized variables. These variables can directly be used in programs.

pi

This gives the value of π

```
>> r = d*pi/180
```
converts degrees *d* into radians and stores it in variable *r*.

inf

You can specify a variable to have value as ∞.

```
>> gain = inf
```

i and j

These are predefined variables whose value is equal to sqrt (–1). This is used to define complex numbers. One can specify complex matrices as well.

```
>> P = 20
>> Q = – 10
>> S = P + j*Q
```
The above statement defines complex power S.

A word of caution here is that if we use *i* and *j* variables as loop counters then we cannot use them for defining complex numbers. Hence you may find that in some of the programs we have used *i*1 and *j*1 as loop variables instead of *i* and *j*.

eps

This variable is preinitialized to 2^{-52}.

Identity Matrix

To generate an identity matrix and store it in variable K, give the following command:

```
>> K = eye (3, 3)
```
So K after this becomes

$$K = \begin{bmatrix} 1 & 0 & 0 \\ 0 & 1 & 0 \\ 0 & 0 & 1 \end{bmatrix}$$

Zeros Matrix

```
>> L = zeros (3, 2)
```

generates a 3×2 matrix whose all elements are zero and stores them in L.

Ones Matrix

```
>> M = ones (3, 3)
```

generates a 3×2 matrix whose all elements are one and stores them in M.

: (Colon) operator

This is an important operator which can extract a submatrix from a given matrix. Matrix A is given as below

$$A = \begin{bmatrix} 1 & 5 & 7 & 8 \\ 2 & 6 & 9 & 10 \\ 5 & 4 & 3 & 1 \\ 9 & 3 & 1 & 2 \end{bmatrix}$$

```
>> B = A(2,:)
```

This command extracts all columns of matrix A corresponding to row 2 and stores them in B.
So B becomes [2 6 9 10]
Now try this command.

```
>> C = A (:, 3)
```

The above command extracts all the rows corresponding to column 3 of matrix A and stores them in matrix C.
So C becomes

$$\begin{bmatrix} 7 \\ 9 \\ 3 \\ 1 \end{bmatrix}$$

Now try this command

```
>> D = A(2 : 4, 1 : 3)
```

This command extracts a submatrix such that it contains all the elements corresponding to row number 2 to 4 and column number 1 to 3.

So

$$D = \begin{bmatrix} 2 & 6 & 9 \\ 5 & 4 & 3 \\ 9 & 3 & 1 \end{bmatrix}$$

ELEMENT BY ELEMENT MULTIPLICATION (.* OPERATOR)

This operation unlike complete matrix multiplication, multiplies element of one matrix with corresponding element of other matrix having same index. However in latter case both the matrices must have equal dimensions.

We have used this operator in calculating complex powers at the buses.

Say V = [0.845 + *j**0.307 0.927 + *j**0.248 0.966 + *j**0.410]′

And I = [0.0654 – *j**0.432 0.876 – *j**0.289 0.543 + *j**0.210]′

Then the complex power S is calculated as

```
>>  S = V.* conj  (I)
```

Here, **conj** is a built-in function which gives complex conjugate of its argument. So S is obtained as [– 0.0774 + 0.3851*i* 0.7404 + 0.4852*i* 0.6106 + 0.0198*i*] Note here, that if the result is complex MATLAB automatically assigns *i* in the result without any multiplication sign(*). But while giving the input as complex number we have to use multiplication (*) along with *i* or *j*.

COMMON BUILT-IN FUNCTIONS

sum

sum(A) gives the sum or total of all the elements of a given matrix A.

min

This function can be used in two forms

(a) For comparing two scalar quantities

```
>>  a = 4
>>  b = 7
>>  min (a, b) results in 4
```

if either *a* or *b* is complex number, then its absolute value is taken for comparison

(b) For finding minimum amongst a matrix or array

e.g. if A = [6 –3; 2 –5]

```
>>  min (A) results in – 5
```

abs

If applied to a scalar, it gives the absolute positive value of that element (magnitude). For example,

```
>>  x = 3 + j*4
```

abs(x) gives 5.

If applied to a matrix, it results in a matrix storing absolute values of all the elements of a given matrix.

CONTROL STRUCTURES

IF Statement

The general form of the IF statement is

```
IF expression
   statements
ELSE expression
   statements
ELSEIF
   statements
END
```

Expression is a logical expression resulting in an answer 'true' (1) or 'false'(0). The logical expression can consist of

(i) an expression containing relational operators tabulated along with their meanings in Table G-1.

Table G-1

Relational Operator	*Meaning*
>	Greater than
> =	Greater than or Equal to
<	Less than
< =	Less than or Equal to
= =	Equal to
~=	Not equal to

(ii) or many logical expressions combined with Logical Operators. Various logical operators and their meanings are given in Table G-2.

Table G-2

Logical Operator	*Meaning*
&	AND
|	OR
!	NOT

FOR Loops

This repeats a block of statements predetermined number of times.
The most common form of **FOR** loop used is

```
for  k = a : b : c,
   statements
end
```

where k is the loop variable which is initialized to value of initial variable a. If the final value (i.e. c) is not reached, the statements in the body for the loop are executed. The value of k is then incremented by step variable b. The process comes to an end when k reaches or exceeds the final value c. For example,

```
for i = 1:1:10,
   a (i)= 1
end
```

This initializes every element of *a* to 1. If increment is of 1, as in this case, then the increment part may as well be omitted and the above loop could be written as

```
for i = 1 : 10,
   a(i)= 1
end
```

While Loop

This loop repeats a block of statements till the condition given in the loop is true while expression

```
  statements
end
For example,
i = 1
while  i  < = 10
   a (i)  =  1
   i  =  i  +  1;
end
```

This loop makes first ten elements of array *a* equal to 1.

Break Statement

This statement allows one to exit prematurely from a **for** or **while** loop.

HOW TO RUN THE PROGRAMS GIVEN IN THIS APPENDIX?

1. Copy these programs into the work subfolder under MATLAB folder.
2. Just type the name of the program without '.m' extension and the program will run.
3. If you want to copy them in some other folder say c:\power, then after copying those files in c:\power, change the work folder to c:\power. You can do this by clicking on toolbar containing three periods—which is on the right side to the Current Directory on the top right corner.
4. You can see or edit these programs by going through File—Open menu and opening the appropriate file. However do not save those programs, unless you are sure that you want the changes you have made to these original files.
5. You can see which are the variables already defined by typing **whos** in front of command prompt. That is why you will normally find a **clear** command at the beginning of our programs. This clears all the variables defined so far from the memory, so that those variables do not interfere or maloperate our programs.

SIMULINK BASICS

SIMULINK is a software package developed by MathWorks Inc. which is one of the most widely used software in academia and industry for modelling and simulating dynamical systems. It can be used for modelling linear and nonlinear systems, either in continuous time frame or sampled time frame or even a hybrid of the two. It provides a very easy drag-drop type Graphical User Interface to build the models in block diagram form. It has many built-in block-library components that you can use to model complex systems. If these built-in models are not enough for you, SIMULINK allows you to have user defined blocks as well. However, in this short appendix, we will try to cover some of the very common blocks that one comes across while simulating a system. You can try to construct the models given in the examples.

HOW TO START?

You can start SIMULINK by simply clicking the simulink icon in the tools bar or by typing *Simulink* in front of the MATLAB command prompt >>. This opens up SIMULINK library browser, which should look similar to the one shown in Fig. G-2. There may be other tool boxes depending upon the license you have. The plus sign that you see in the right half of the window indicates that there are more blocks available under the icon clicking on the (+) sign will expand the library. Now for building up a new model click on File and select New Model. A blank model window is opened. Now all you have to do is to select the block in the SIMULINK library browser and drop it on your model window. Then connect them together and run the simulation. That is all.

AN EXAMPLE

Let us try to simulate a simple model where we take a sinusoidal input, integrate it and observe the output. The steps are outlined as below.

1. Click on the **Sources** in the SIMULINK library browser window.
2. You are able to see various sources that SIMULINK provides. Scroll down and you will see a Sine Wave sources icon.
3. Click on this sources icon and without releasing the mouse button drag and drop it in your model window which is currently named as 'untitled'.
4. If you double-click on this source, you will be able to see Block parameters for sine wave which includes amplitude, frequency, phase, etc. Let not change these parameters right now. So click on **cancel** to go back.
5. Similarly click on **continuous** library icon. You can now see various built-in blocks such as derivative, integrator, transfer-function, state-space etc. Select integrator block and drag-drop it in your model window.

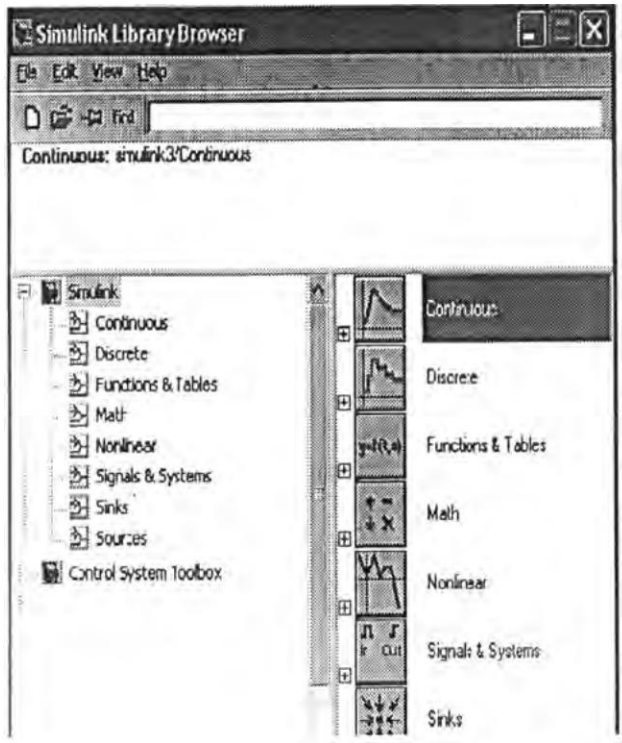

Fig. G-2

6. Now click on sinks and drag-drop scope block into your model. This is one of the most common blocks used for displaying the values of the blocks.
7. Now join output of sine-wave source to input of Integrator block. This can be done in two ways. Either you click the left button and drag mouse from output of sine-wave source to input of Integrator block and leave left button or otherwise click on right button and drag the mouse to form connection from input of integrator block to output of sine-wave source.
8. Now in the main menu, click on **Simulation** and click **Start**. The simulation runs and stops after the time specified by giving ready prompt at bottom left corner.
9. Now double-click on scope to see the output. Is something wrong? The result is a sine wave of magnitude 2. Is there something wrong with SIMULINK software?

   No, we have in fact forgotten to specify the integration constant! Integration of sin θ is $-\cos\theta + C$. At $\theta = 0$, $C = -1$. If we do not specify any initial condition for output of the integrator, simulink assumes it to be 0 and calculates the constant. So it calculates

– cos $\theta + C = 0$ at $t = 0$ giving $C = 1$. So the equation for output becomes – cos $\theta + 1$. Thus naturally, it starts from 0 at $t = 0$ and reaches its peak value of 2 at $\theta = \pi$, i.e. 3.14.

10. To rectify this error, double click on Integrator block and in the initial conditions enter – 1 which should be the output of the block at $t = 0$. Now run the simulation again and see for yourself that the result is correct.

Some Commonly used Blocks

1. *Integrator* We have already described its use in the above example.
2. *Transfer function* Using this block you can simulate a transfer function of the form $T(s) = N(s)/D(s)$, where $N(s)$ and $D(s)$ are polynomials in s. You can double click the block and enter the coefficients of s in numerator and denominator of the expression in ascending order of s which are to be enclosed inside square brackets and separated by a space.
3. *Sum* You can find this block under **Math** in **Simulink** block. By default, it has two inputs with both plus signs. You can modify it to have required number of inputs to be summed up by specifying a string of + or – depending upon the inputs. So if there are 3 inputs you can give the list of signs as + – – . This will denote one positive input and two inputs with – signs which are often used to simulate negative feedback.
4. *Gain* This block is also found under **Math** in **Simulink** block. It is used to simulate static gain. It can even have fractional values to act as attenuator.
5. *Switch* This block is available under **Non-linear** block in **Simulink**. It has 3 inputs with the top input being numbered 1. When the input number 2 equals or exceeds the threshold value specified in the properties of this block, it allows input number 1 to pass through, else it allows input number 3 to pass through.
6. *Mux and Demux* These blocks are available under **Signals and systems** block in **Simulink.** The Mux block combines its inputs into a single output and is mostly used to form a vector out of input scalar quantities. Demux block does the reverse thing. It splits the vector quantity into multiple scalar outputs.
7. *Scope* We have already described its use. However, if you are plotting a large number of points, click on properties toolbar and select **Data History** tab. Then uncheck the Limit data points box so that all points are plotted. Also when the waveform does not appear smooth, in the **general** tab of properties toolbar, select sample time instead of decimation in the sample time box and enter a suitable value like le – 3 (10^{-3}). The scope then uses the value at sample-time interval to plot.
8. *Clock* This block is used to supply time as a source input and is available in **Sources block** under **Simulink.**

9. *Constant* This block is used to provide constant input and is available in **Sources block** under **Simulink**. We have made use of this block in stability studies to provide constant mechanical input.
10. *Sinewave* This block we have already discussed. It can be used to generate a sine wave of any amplitude, frequency and phase.

The reader is encouraged to work out, the examples given in this Appendix to gain greater insight into the software.

SCRIPT AND FUNCTION FILES

Types of m-files

There are two types of m-files used in Matlab programming:

(i) *Script m-file*—This file needs no input parameters and does not return any values as output parameters. It is just a set of Matlab statements which is stored in a file so that one can execute this set by just typing the file name in front of the command prompt, e.g. programmes in G2 to G18 are script files.

(ii) *Function m-files*—This file accepts input arguments and return values as output parameters. It can work with variables which belong to the workspace as well as with the variables which are local to the functions. These are useful for making your own function for a particular application, e.g. PolarTorect.m in G1 is a function m-file.

The basic structure of function m-file is given below:

(i) *Function definition lin*e—This is the first line of a function. It specifies function name, number and order of input variables.
Its syntax is- function [output variables] = function-name (list of input variables).

(ii) *First line of hel*p—Whenever help is requested on this function or look for is executed MATLAB displays this line.
Its syntax is - % function-name help.

(iii) *Help text*—Whenever help is requested on the function-name help text is displayed by Matlab in addition to first help line.
Its syntax is - % function-name (input variables).

(iv) *Body of the function*—This consists of codes acting on the set of input variables to produce the output variables.

User can thus develop his/her own programs and functions and add them to the existing library of functions and blocks.

SOME SAMPLE EXAMPLES SOLVED BY MATLAB

In this Section, 18 solved examples of this book are solved again using MATLAB/SIMULINK to encourage the reader to solve more power system problems using MATLAB.

Ex G.1

```
% This function converts polar to rectangular coordinates
% The argument to this function is 1) Magnitude & 2)Angle is in degrees
% This function has been used in many problems which are solved in this
  appendix
function rect=polarTorect(a,b)
rect=a*cos(b*pi/180)+j*a*sin(b*pi/180);
```

Note: This function is used in solution of many of the examples solved later.

Ex G-2 (Example 5.6)

```
% This illustrates the Ferranti effect
% It simulates the effect by varying the length of line from
% zero(receiving-end) to 5000 km in steps of 10 km
% and plots the sending-end voltage phasor
% This corresponds to Fig. 5.13 and data from Example 5.6
clear
VR=220e3/sqrt(3);
alpha=0.163e-3;
beta=1.068e-3;
l=5000;
k=1;
for i=0:10:l,
   VS=(VR/2)*exp(alpha*i)*exp(j*beta*i)+(VR/2)*exp
      (-alpha*i)*exp(j*beta*i);
     X(k)=real(VS);
     Y(k)=imag(VS);
     k=k+1;
end
plot(X,Y)
```

Ex. G-3 (Example 5.7)

```
% This Program illustrates the use of different line models as
% in Example 5.7
clear
f=50
l=300
Z=40+j*125
Y=1e-3
PR=50e6/3
VR=220e3/(sqrt(3))
pfload=0.8
IR=PR/(VR*pfload)
z=Z/l
y=Y/l

% Now we calculate the sending-end voltage, sending-end current
% and sending-end pf by following methods for various lengths of line
```

```
% varying line lengths from 10 to 300 km in steps of 10 km
% and compare them as a function of line lengths.
% The methods are
% 1) Short Line approximatiom
% 2) Nominal-Pi method
% 3) Exact transmission line equations
% 4) Approximation of exact equations
i=1
for l=10:10:300,
    % Short line approximation
    Vs_shortline(i)=VR+(z*l)*IR
    Is_shortline(i)=IR
    Spf_shortline(i)=cos(angle(Vs_shortline(i)-angle(Is_shortline(i))))
    Spower_shortline(i)=real(Vs_shortline(i)*conj(Is_shortline(i)))

    %Nominal PI method
    A=1+(y*l)*(z*l)/2
    D=A
    B=z*l
    C=y*l*(1+(y*l)*(z*l)/4)
    Vs_nominalpi(i)=A*VR+B*IR
    Is_nominalpi(i)=C*VR+D*IR
    Spf_nominalpi(i)=cos(angle(Vs_nominalpi(i)-angle(Is_nominalpi(i))))
    Spower_nominalpi(i)=real(Vs_nominalpi(i)*conj(Is_nominalpi(i)))

    % Exact transmission Line Equations
    Zc=sqrt(z/y)
    gamma=sqrt(y*z)
    Vs_exact(i)=cosh(gamma*l)*VR + Zc*sinh(gamma*l)*IR
    Is_exact(i)=(1/Zc)*sinh(gamma*l) + cosh(gamma*l)*IR
    Spf_exact(i)=cos(angle(Vs_exact(i)-angle(Is_exact(i))))
    Spower_exact(i)=real(Vs_exact(i)*conj(Is_exact(i)))

     % Approximation of above exact equations
     A=1+(y*l)*(z*l)/2
     D=A
     B=(z*l)*(1+(y*l)*(z*l)/6)
     C=(y*l)*(1+(y*l)*(z*l)/6)
    Vs_approx(i)=A*VR+B*IR
    Is_approx(i)=C*VR+D*IR
    Spf_approx(i)=cos(angle(Vs_approx(i)-angle(Is_approx(i))))
    Spower_approx(i)=real(Vs_approx(i)*conj(Is_approx(i)))
    point(i)=i
    i=i+1

end
% The reader can uncomment any of the four plot statements given below
% by removing the percentage sign against that statement
% for ex. in the plot statement uncommented below
% it plots the sending-end voltages for short line model in red
```

```
% by nominal pi-model in green , by exact parameters model in black
% and by approx.  Pi model in blue
plot(point,abs(Vs_shortline),'r',point,abs(Vs_nominalpi),'g',point,abs…
(Vs_exact), 'b', point,abs(Vs_approx),'k')
% plot(point,abs(Is_shortline),'r',point,abs(Is_nominalpi),'g',point,abs…
(Is_exact),'b',point,abs(Is_approx),'k')
%plot(point,abs(Spf_shortline),'r',point,abs(Spf_nominalpi),'g',point,abs…
(Spf_exact),'b',point,abs(Spf_approx),'k')
plot(point,abs(Spower_shortline),'r',point,abs(Spower_nominalpi),'g',point,abs…
(Spower_exact),'b',point,abs(Spower_approx),'k')
```

Ex G-4 (Example 6.2)

```
% This program forms YBUS by Singular Transformation
% The data for this program is a primitive admittance matrix y
% which is to be given in the following format and stored in ydata.
% Ground is given as bus no 0.
% If the element is not mutually coupled with any other element,
% then the entry corresponding to 4th and 5th column of ydata
% has to be zero
% ------------------------------------------------------------------
% element no | connected  |    y (self)     |Mutually  |   y(mutual)   |
%            | From | To  |                 |coupled to|               |
%            |Busno |Busno|
% ------------------------------- ------------------------------
ydata=[ 1        1     2   1/(0.05+j*0.15)     0            0
        2        1     3   1/(0.1 +j*0.3 )     0            0
        3        2     3   1/(0.15+j*0.45)     0            0
        4        2     4   1/(0.10+j*0.30)     0            0
        5        3     4   1/(0.05+j*0.15)     0            0];
%  form primitive y matrix from this data and initialize it to zero.
% to start with
elements=max(ydata(:,1))
yprimitive=zeros(elements,elements)
% Process ydata matrix rowwise to form yprimitive
for i=1:elements,
    yprimitive(i,i)=ydata(i,4)
% Also if the element is mutually coupled with any other element
% (whose element no is indicated in 5th column of ydata above)
% the corresponding column no in the ith row is made equal to y(mutual)
    if (ydata(i,5) ~= 0 )
% j is the element no with which ith element is mutually coupled
       j=ydata(i,5)
       ymutual=ydata(i,6)
       yprimitive(i,j) = ymutual
    end
end
% Form Bus incidence matrix A from ydata
% this gives a matrix of size element x buses
buses=max(max(ydata(2,:)),max(ydata(3,:)))
```

```
A=zeros(elements,buses)

for i=1:elements,
% ydata(i,2) gives the 'from' bus no.
% The entry corresponding to column corresponding to this bus
% in A matrix is made 1 if this is not ground bus
    if ydata(i,2) ~= 0
    A(i,ydata(i,2))=1;
    end
% ydata(i,3) gives the 'to' bus no.
% The entry corresponding to column corresponding to this bus
% in A matrix is made 1 if this is not ground bus

   if ydata(i,3)~= 0
   A(i,ydata(i,3))=-1
   end
end

YBUS=A'*yprimitive*A
```

Ex G-5 (data same as Example 6.2)

```
% This program forms YBUS by adding one element at a time
% The data for this program is a primitive admittance matrix y
% which is to be given in the following format and stored in ydata
% Ground is given as bus no. 0
% If the element is not mutually coupled with any other element,
% then the entry corresponding to 4th and 5th column of ydata
% has to be zero
% The data must be arranged in ascending order of element no.
% ------------------------------------------------------------------
% element no | connected  |    y (self)     |Mutually  |   y(mutual)   |
%            | From | To  |                 |coupled to|               |
%            |Busno |Busno|
% ------------------------------- -------------------------------
ydata=[ 1        1     2   1/(0.05+j*0.15)     0            0
        2        1     3   1/(0.1 +j*0.3 )     0            0
        3        2     3   1/(0.15+j*0.45)     0            0
        4        2     4   1/(0.10+j*0.30)     0            0
        5        3     4   1/(0.05+j*0.15)     0            0];

% Following statement gives maximum no. of elements by calculating the
% maximum out of all elements (denoted by :) of first column of ydata
elements=max(ydata(:,1))
% this gives no. of buses which is nothing but the maximum entry
% out of 2nd and 3rd column of ydata which is 'from' and 'to' columns
buses=max(max(ydata(:,2)),max(ydata(:,3)));
YBUS=zeros(buses,buses);

for row=1:elements,
% if ydata(row,5) is zero that means the corresponding element
% is not mutually coupled with any other element

    if ydata(row,5) == 0
     i1 =ydata(row,2);
```

```
        j1 =ydata(row,3);
        if i1 ~= 0 & j1 ~= 0
            YBUS(i1,i1) = YBUS(i1,i1) + ydata(row,4);
            YBUS(i1,j1) = YBUS(i1,j1) - ydata(row,4);
            YBUS(j1,i1) = YBUS(i1,j1);
            YBUS(j1,j1) = YBUS(j1,j1) + ydata(row,4);
        end
        if i1 == 0 & j1 ~=0
            YBUS(i1,i1) = YBUS(i1,i1) + ydata(row,4);
        end
        if i1 == 0 & j1 ~=0
            YBUS(j1,j1) = YBUS(j1,j1) + ydata(row,4);
        end
    end
    % if ydata(row,5) is NOT zero that means the corresponding element
    % is mutually coupled with element given in ydata(row,5)
    if ydata(row,5) ~= 0
        i1 =ydata(row,2);
        j1 =ydata(row,3);
        % mutualwith gives the element no with which the current element
        % is mutually coupled with k and l give the bus nos between
        % which the mutually coupled element is connected
        mutualwith=ydata(i1,5);
        k=ydata(mutualwith,2);
        l=ydata(mutualwith,3);
        zs1=1/ydata(row,4);
        zs2=1/ydata(mutualwith,4);
        zm =1/ydata(row,6);
        zsm= [zs1 zm
            zm zs2];
        ysm=inv(zsm);
        % Following if block gives the necessary modifications in YBUS
        % when none of the buses is reference (ground) bus.
        if i1 ~= 0 & j1 ~= 0 & k ~=0 & l~=0
            YBUS(i1,i1) = YBUS(i1,i1) + ysm(1,1);
            YBUS(j1,j1) = YBUS(j1,j1) + ysm(1,1);
            YBUS(k,k) = YBUS(k,k) + ysm(2,2);
            YBUS(l,l) = YBUS(l,l) + ysm(2,2);
            YBUS(i1,j1) = YBUS(i1,j1) - ysm(1,1);
            YBUS(j1,i1) = YBUS(i1,j1);
            YBUS(k,l) = YBUS(k,l) - ysm(2,2);
            YBUS(l,k) = YBUS(k,l);
            YBUS(i1,k) = YBUS(i1,k) + ysm(1,2);
            YBUS(k,i1) = YBUS(i1,k);
            YBUS(j1,l) = YBUS(j1,l) + ysm(1,2);
            YBUS(l,j1) = YBUS(j1,l);
            YBUS(i1,l) = YBUS(i1,l) - ysm(1,2);
            YBUS(l,i1) = YBUS(i1,l);
            YBUS(j1,k) = YBUS(j1,k) - ysm(1,2);
            YBUS(k,j1) = YBUS(j1,k);
```

```
 end
 if i1 == 0 & j1 ~=0 & k~=0 & l~=0
      YBUS(j1,j1) = YBUS(j1,j1) + ysm(1,1);
      YBUS(k,k) = YBUS(k,k) + ysm(2,2);
      YBUS(l,l) = YBUS(l,l) + ysm(2,2);
      YBUS(k,l) = YBUS(k,l) - ysm(2,2);
      YBUS(l,k) = YBUS(k,l);
      YBUS(j1,l) = YBUS(j1,l) + ysm(1,2);
      YBUS(l,j1) = YBUS(j1,l);
      YBUS(j1,k) = YBUS(j1,k) - ysm(1,2);
      YBUS(k,j1) = YBUS(j1,k);
 end
 if i1~=0 & j1==0 & k~=0 & l~=0
      YBUS(i1,i1)= YBUS(i1,i1) + ysm(1,1);
      YBUS(k,k) = YBUS(k,k) + ysm(2,2);
      YBUS(l,l) = YBUS(l,l) + ysm(2,2);
      YBUS(k,l) = YBUS(k,l) - ysm(2,2);
      YBUS(l,k) = YBUS(k,l);
      YBUS(i1,k) = YBUS(i1,k) + ysm(1,2);
      YBUS(k,i1) = YBUS(i1,k);
      YBUS(i1,l) = YBUS(i1,l) - ysm(1,2);
      YBUS(l,i1) = YBUS(i1,l);
 end
 if i1~=0 & j1~=0 & k==0 & l~=0
      YBUS(i1,i1) = YBUS(i1,i1) + ysm(1,1);
      YBUS(j1,j1) = YBUS(j1,j1) + ysm(1,1);
      YBUS(l,l) = YBUS(l,l) + ysm(2,2);
      YBUS(i1,j1) = YBUS(i1,j1) - ysm(1,1);
      YBUS(j1,i1) = YBUS(i1,j1);
      YBUS(j1,l) = YBUS(j1,l) + ysm(1,2);
      YBUS(l,j1) = YBUS(j1,l);
      YBUS(i1,l) = YBUS(i1,l) - ysm(1,2);
      YBUS(l,i1) = YBUS(i1,l);
 end
 if i1~=0 & j1~=0 & k~=0 & l==0
      YBUS(i1,i1) = YBUS(i1,i1) + ysm(1,1);
      YBUS(j1,j1) = YBUS(j1,j1) + ysm(1,1);
      YBUS(k,k) = YBUS(k,k) + ysm(2,2);
      YBUS(i1,j1) = YBUS(i1,j1) - ysm(1,1);
      YBUS(j1,i1) = YBUS(i1,j1);
      YBUS(i1,k) = YBUS(i1,k) + ysm(1,2);
      YBUS(k,i1) = YBUS(i1,k);
      YBUS(j1,k) = YBUS(j1,k) - ysm(1,2);
      YBUS(k,j1) = YBUS(j1,k);
end
end
 end
YBUS
```

Ex G-6

```
% This is program for Gauss-Siedel Load flow. The data is from Example 6.5
clear
n=4
V=[1.04 1.04 1 1]

Y =[3 – j * 9     –2 + j * 6       –1 + j * 3       0
    – 2 + j * 6   3666 – j * 11    –0.666 + j * 2   –1 + j * 3
    – 1 + j * 3   –0.666 + j * 2   3.666 – j * 11   –2 + j * 6
    0             –1 + j * 3       –2 + j * 6       3 – j * 9 ]

type=ones(n,1)
typechanged=zeros(n,1)Qlimitmax=zeros(n,1)
Qlimitmin=zeros(n,1)
Vmagfixed=zeros(n,1)
type(2)=2
Qlimitmax(2)=1.0
Qlimitmin(2)=0.2
Vmagfixed(2)=1.04
diff=10;noofiter=1
Vprev=V;
while (diff>0.00001 | noofiter==1),
abs(V)
abs(Vprev)
%pause
Vprev=V;
P=[inf 0.5 -1  0.3];
Q=[inf 0  0.5 -0.1] ;
S=[inf+j*inf (0.5-j*0.2) (-1.0 + j*0.5) (0.3-j*0.1)];
for i=2:n,
    if type(i)==2 |typechanged(i)==1,
    if (Q(i)>Qlimitmax(i)| Q(i)<Qlimitmin(i)),
    if(Q(i)<Qlimitmin(i)),
        Q(i)=Qlimitmin(i);
    else
        Q(i)=Qlimitmax(i);
    end
    type(i)=1;
        typechanged(i)=1;
    else
        type(i)=2;
        typechanged(i)=0;
    end
    end
    end
    sumyv=0;
    for k=1:n,
        if(i ~= k)
        sumyv=sumyv+Y(i,k)*V(k);
    end
```

```
        end
         V(i)=(1/Y(i,i))*((P(i)-j*Q(i))/conj(V(i))-sumyv);
         if type(i)==2 & typechanged(i)~=1,
              V(i)=PolarTorect(Vmagfixed(i),angle(V(i))*180/pi);
              end
end
diff=max(abs(abs(V(2:n))-abs(Vprev(2:n))));
noofiter=noofiter+1;
end
V
```

Ex. G-7 (Example 6.6)

```
% Program for load flow by Newton-Raphson Method.
clear;
% n stands for number of buses
n=3;
% V ,voltages at those buses are initialized
V=[1.04 1.0 1.04];
% Y is YBus
Y=[ 5.88228-j*23.50514 -2.9427+j*11.7676   -2.9427+j*11.7676
    -2.9427+j*11.7676  5.88228-j*23.50514  -2.9427+j*11.7676
    -2.9427+j*11.7676  -2.9427+j*11.7676   5.88228-j*23.50514];
% Bus types are initialized in type array to code 1 which stands for PQ bus.
% code 2 stands for PV bus
type=ones(n,1);
% When Q limits are exceeded for a PV bus Bus type is changed to PQ
%temporarily
%an element i of typechanged is set to 1 in case its bus status
%is temporarily changed from PQ to PV. Otherwise it is zero
typechanged=zeros(n,1);
% Since max and min Q limits are checked only for PV buses,
% max & min  Q limits for other types of buses can be set to any values.
% here we have set them to zeros for convenience
Qlimitmax=zeros(n,1);
Qlimitmin=zeros(n,1);
Vmagfixed=zeros(n,1);
% Here we change type of PV buses to 2 and also set the Q limits for them
type(3)=2;
Qlimitmax(3)=1.5;
Qlimitmin(2)=0;
Vmagfixed(2)=1.04;
diff=10;noofiter=1;
Pspec=[inf 0.5 -1.5];
Qspec=[inf 1    0 ];
S=[inf+j*inf (0.5-j*0.2) (-1.0 + j*0.5) (0.3-j*0.1)];
% Here for all the buses depending on bustype, associated variables array
%element for each equation (deltaP or deltaQ) is initialized
%Also associated variables with each col( ddelta or dv) is formed
while (diff>0.00001 | noofiter==1),
```

```
eqcount=1;
for i=2:n,
        Scal(i)=0;
        sumyv=0;
        for k=1:n,
           sumyv=sumyv+Y(i,k)*V(k);
     end
       Scal(i)=V(i)*conj(sumyv);
       P(i)=real(Scal(i));
       Q(i)=imag(Scal(i));
% If the bus is a PV bus and the calculated Q is exceeding the
% limits, the bus type is temporarily changed to PQ and
% type changed is made 1 for that bus
% Otherwise its switched back to PV bus and
% type changed is resetted to zero for that bus
    if type(i)==2 |typechanged(i)==1,
       if (Q(i)>Qlimitmax(i)| Q(i)<Qlimitmin(i)),
       if(Q(i)<Qlimitmin(i)),
       Q(i)=Qlimitmin(i);
    else
       Q(i)=Qlimitmax(i);
     end
      type(i)=1;
      typechanged(i)=1;
   else
      type(i)=2;
      typechanged(i)=0;
   end
   end
% The mismatch equations are arranged and solved in matrix form
% as indicated below
% |dPi|               |dDelta|
% |dQi|       = [J]   |dVi|
% |dP(i + 1)|         |dDelta (i + 1)|
% |dQ(i + 1)|         |dV (i + 1)|
%  assoeqvar  (i)  [associated  equation  variable]  indicates  if  the
equationdeal % with  the mismatch for `P' real
% power or `Q' reactive power
% This decides the numerator quantity of the Jacobian element
% i.e. the quantity we want to differentiate will be dP/d* or dQ/d*
% where * may stand for either Delta or V
% mismatch array stores the mismatch quantities for P or Q
% assoeqbus (i) indicates which is the bus associated with equation i
% assocolvar (i) decides the denominator quantity of Jacobian element
% along each column of the Jacobian for a given equation
% i.e. for a Jacobian element in the ith column of a given equation
% with respect to what we are differentiating
% So we decide here if the element is d*/dDelta or d*/dV
% where * may be either P or Q
% assocolbus decides the bus associated
```

```
% with each element in the column corresponding to given equation
       if type(i)==1,
       assoeqvar(eqcount)='P';
       assoeqbus(eqcount)=i;
       mismatch(eqcount)=Pspec(i)-P(i);
       assoeqvar(eqcount+1)='Q';
       assoeqbus(eqcount+1)=i;
       mismatch(eqcount+1)=Qspec(i)-Q(i);
       assocolvar(eqcount)='d';
        assocolbus(eqcount)=i;
       assocolvar(eqcount+1)='V';
       assocolbus(eqcount+1)=i;
       eqcount=eqcount+2;
     else
     assoeqvar(eqcount)='P';
     assoeqbus(eqcount)=i;
     assocolvar(eqcount)='d';
     assocolbus(eqcount)=i;
     mismatch(eqcount)=Pspec(i)-P(i);
     eqcount=eqcount+1;
     end
end
mismatch
eqcount=eqcount-1;
noofeq=eqcount;
Update=zeros(eqcount,1);
Vprev=V
abs(V);
abs(Vprev)
pause
Vprev=V;
% ceq stands for current equation being processed, which is varied from
% 1 to total no. of equations (eqcount)
for ceq=1:eqcount,
   for ccol=1:eqcount,
        am=real(Y(assoeqbus(ceq),assocolbus(ccol))*V(assocolbus(ccol)));
        bm=imag(Y(assoeqbus(ceq),assocolbus(ccol))*V(assocolbus(ccol)));
        ei=real(V(assoeqbus(ceq)));
        fi=imag(V(assoeqbus(ceq)));
   if assoeqvar(ceq)=='P' & assocolvar(ccol)=='d',
   if assoeqbus(ceq)~=assocolbus(ccol),
   H=am*fi-bm*ei;
   else
   H=-Q(assoeqbus(ceq))imag(Y(assoeqbus(ceq),assocolbus(ceq))...
   *abs(V(assoeqbus(ceq)))^2);
   end
   Jacob(ceq,ccol)=H
   end
   if assoeqvar(ceq)=='P' & assocolvar(ccol)=='V',
```

```
    if assoeqbus(ceq)~=assocolbus(ccol),
    N=am*ei+bm*fi;
    else
    N=P assoeqbus(ceq))+real(Y(assoeqbus(ceq),assocolbus(ceq))...
    *abs(V(assoeqbus(ceq)))^2);
    end
    Jacob(ceq,ccol)=N
    end
    if assoeqvar(ceq)=='Q' & assocolvar(ccol)=='d',
    if assoeqbus(ceq)~=assocolbus(ccol),
    J=am*ei+bm*fi;
    else
     J=P(assoeqbus(ceq))real(Y(assoeqbus(ceq),assocolbus(ceq))
     *abs(V(assoeqbus(ceq)))^2);
     end
     Jacob(ceq,ccol)=J
     end
     if assoeqvar(ceq)=='Q' & assocolvar(ccol)=='V',
     if assoeqbus(ceq)~=assocolbus(ccol),
     L=am*fi-bm*ei;
     else
     L=Q(assoeqbus(ceq))-...
     imag(Y(assoeqbus(ceq),assocolbus(ceq))*abs(V(assoeqbus(ceq)))^2);
     end
     Jacob(ceq,ccol)=L
     end
     end
     end
     %New Update vector is calculated from Inverse of the Jacobian
     Jacob
     pause
     update=inv(Jacob)*mismatch';
     noofeq=1;
     for i=2:n,
     if type(i)==1
          newchinangV=update(noofeq);
          newangV=angle(V(i))+newchinangV;
          newchinmagV=update(noofeq+1)*abs(V(i));
          newmagV=abs(V(i))+newchinmagV;
          V(i)=polarTorect(newmagV,newangV*180/pi);
          noofeq=noofeq+2;
     else
          newchinangV=update(noofeq);
          newangV=angle(V(i))+newchinangV;
          V(i)=polarTorect(abs(V(i)),newangV*180/pi);
          noofeq=noofeq+1;
     end
     end
% All the following variables/arrays are cleared from
% memory. This is because their dimensions may change due to
% bus switched and once updates are calculated, the variables
```

```
% are of no use as they are being reformulated at the
% end of each iteration
clear mismatch Jacob update assoeqvar assoeqbus assocolvar assocolbus;
diff=min(abs(abs(V(2:n))-abs(Vprev(2:n))));
noofiter=noofiter+1;
end
```

Ex. G-8 (Table 7.1)

```
% MATLAB Program for optimum loading of generators
% The data are from Example 7.1
% It finds lamda by the algorithm given on the same page, once the demand
% is specified
% We have taken the demand as 231.25MW corresponding to the last but one
% row of Table 7.1 and calculated lamda and the load sharing
% n is no of generators
n=2
% Pd stands for load demand.
% alpha and beta arrays denote alpha beta coefficients
% for given generators.
Pd=231.25
alpha=[0.20
      0.25]
beta=[40
      30]
% initial guess for lamda
lamda=20
lamdaprev=lamda
% tolerance is eps and increment in lamda is deltalamda
eps=1
deltalamda=0.25
% the minimum and maximum limits of each generating unit
%are stored in arrays Pgmin and Pgmax.
% In real life large scale problems, we can first initialize the Pgmax
% array to inf using for loop and
% Pgmin array to zero using Pgmin=zeros(n,1) command
% Later we can change the limits individually
Pgmax=[125 125]
Pgmin=[20 20]
Pg=100*ones(n,1)
while abs(sum(Pg)-Pd)>eps
for i=1:n,
    Pg(i)=(lamda-beta(i))/alpha(i);
    if Pg(i)>Pgmax(i)
    Pg(i)=Pgmax(i);
    end
    if Pg(i)<Pgmin(i)
    Pg(i)=Pgmin(i);
    end
   end
    if (sum(Pg)-Pd )<0
```

```
    lamdaprev=lamda;
    lamda=lamda+deltalamda;
else
    lamdaprev=lamda;
    lamda=lamda-deltalamda;
end
end
disp('The final value of Lamda is')
lamdaprev
disp('The distribution of load shared by two units is')
Pg
```

Ex. G-9 (Table 7.2)

```
% MATLAB Program for optimum unit committment by Brute Force method
% The data for this program corresponds to Table 7.2
clear;
% alpha and beta arrays denote alpha beta coefficients for given generators
alpha=[0.77 1.60 2.00 2.50]';
beta=[23.5 26.5 30.0 32.0]';
Pgmin=[1 1 1 1]';
Pgmax=[12 12 12 12]';
  n=9
% n denotes total MW to be committed
min = inf;
cost=0;
for i=0:n,
    for j=0:n,
        for k=0:n,
        for l=0:n,
        unit = [0 0 0 0];
                % Here we eliminate straightaway those combinations which
                % dont make up the
                % n MW demand or such combinations where maximum generation
                % on individual
                % generation is exceeding the maximum capacity of any of the
                % generators
                 if(i+j+k+l)==n & i<Pgmax(1)& j<Pgmax(2) & k<Pgmax(3)&l<...
                 Pgmax(4)
   if i~=0
        unit(1,1)=i;
        % Find out the cost of generating these units and
        % add it up to total cost
        cost=cost+0.5*alpha(1)*i*i+beta(1)*i;
   end
   if j~=0
   unit(1,2)=j;
   cost=cost+0.5*alpha(2)*j*j+beta(2)*j ;
   end
   if k~=0
   unit(1,3)=k;
```

```
    cost=cost+0.5*alpha(3)*k*k+beta(3)*k ;
    end
    if l~=0
    unit(1,4)=l;
    cost=cost+0.5*alpha(4)*l*l+beta(4)*l;
    end
% If the total cost is coming out to be less than
% minimum of the cost in
% previous combinations then make min equal to cost and
% cunit (stand for committed units) equal to units
% committed in this iteration
% (denoted by variable units)
if cost < min
cunit = unit;
min=cost;
else
cost=0;
end
end
end
end
end
end
disp ('cunit display the no of committed units on each of the four genera-
tors')
disp(' If cunit for a particular generator is 0 it means the unit is not
committed')
disp (' The total no of units to be committed are')
cunit
```

Ex G-10 (Ex. 7.4)

```
clear
% MATLAB Program for optimum loading of generators
% This program finds the optimal loading of generators including
% penalty factors
% It implements the algorithm given just before Example 7.4.
% The data for this program are taken from Example 7.4
% Here we give demand Pd and alpha, beta and B-coefficients
% We calculate load shared by each generator
%  n is no of generators
n=2
% Pd stands for load demand
%  alpha  and  beta  arrays  denote  alpha  beta  coefficients  for  given
% generators
Pd=237.04;
alpha=[0.020
      0.04];
beta=[16
      20];
```

```
% initial guess for lamda
lamda=20;
lamdaprev=lamda;
% tolerance is eps and increment in lamda is deltalamda
eps=1;
deltalamda=0.25;
% the minimum and maximum limits of each generating unit
%are stored in arrays Pgmin and Pgmax.
% In actual large scale problems, we can first initialize the Pgmax array
% to inf using for loop
% and Pgmin array to zero using Pgmin=zeros(n,1) command
% Later we should can change the limits individually
Pgmax=[200 200];
Pgmin=[0 0];
B=[0.001 0
  [0 0];
Pg=zeros(n,1);
noofiter=0;
PL=0;
Pg=zeros(n,1);
while abs(sum(Pg)-Pd-PL)>eps
for i=1:n,
   sigma=B(i,:)*Pg-B(i,i)*Pg(i);
   Pg(i)=(1-(beta(i)/lamda)-(2*sigma))/(alpha(i)/lamda+2*B(i,i));
   PL=Pg'*B*Pg;
   if Pg(i)>Pgmax(i)
      Pg(i)=Pgmax(i);
      end
   if Pg(i)<Pgmin(i)
      Pg(i)=Pgmin(i);
   end
    end
    PL=Pg'*B*Pg;
if (sum(Pg)-Pd-PL )<0
    lamdaprev=lamda;
    lamda=lamda+deltalamda;
else
    lamdaprev=lamda;
    lamda=lamda-deltalamda;
end
noofiter=noofiter+1;
Pg;
end
disp('The no of iterations required are')
noofiter
disp('The final value of lamda is')
lamdaprev
disp('The optimal loading of generators including penalty factors is')
Pg
disp('The losses are')
PL
```

Ex. G-11

```
% In this example the parameters for all the blocks for the system in
% Fig. 8.8 are initialized. This program has to be run prior to the
simulation both for Figs G-3 and G-4.
Tsg=.4
Tt=0.5
Tps=20
Kps=100
R=3
Ksg=10
Kt=0.1
Ki=0.09
```

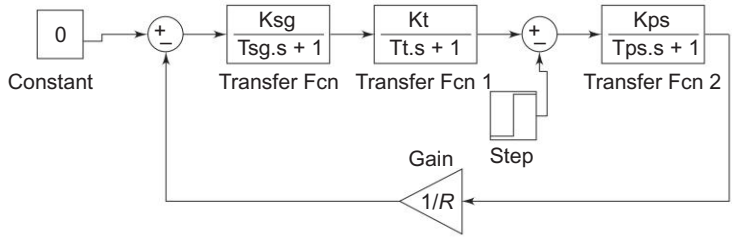

Fig. G-3 First order approximation for load frequency control

Ex. G-12

The system of Fig. 8.10 is simulated using Simulink as was done in Example G-11.

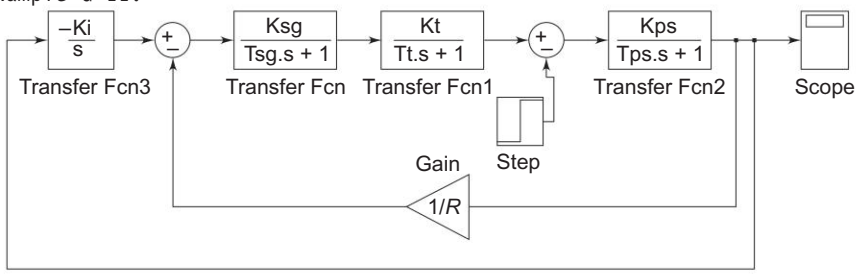

Fig. G-4 Proportional plus Integral load frequency control

Ex. G-13 (Example 9.8)

```
% Program for building of Zbus by addition of branch or link
% Zprimary=[elementno from  to  value
%            --       --   --   --
%            --       --   --   --
%            --       --   --   --
%            --       --   --   --]
% Here care should be taken that to begin with an element is added to
% reference and both from and to nodes should not be new nodes
clear
```

```
zprimary=[
    1 1 0 0.25
    2 2 1 0.1
    3 3 1 0.1
    4 2 0 0.25
    5 2 3 0.1]
[elements columns]=size(zprimary)
% To begin with zbus matrix is a null matrix
zbus=[]
% currentbusno indicates maximum no. of buses added until now
currentbusno=0
% Process each row of zprimary
for count=1:elements,
  [rows cols]=size(zbus)
  from=zprimary(count,2)
   to=zprimary(count,3)
   value=zprimary(count,4)
% newbus variable indicates the maximum of the two buses
% newbus bus may or may not already be a part of existing zbus
  newbus=max(from,to)
% ref variable indicates the minimum of the two buses
% & not necessarily the reference bus
% ref bus must always exist in the existing zbus
  ref=min(from,to)
% Modification of type1
% A new element is added from new bus to reference bus
if newbus >currentbusno & ref ==0
   zbus=[zbus zeros(rows,1)
        zeros(1,cols) value]
   currentbusno=newbus
   continue
end
% Modification of type2
% A new element  is added from new bus to old bus other than reference bus
if newbus >currentbusno & ref ~=0
    zbus=[zbus zbus(:,ref)
    zbus(ref,:) value+zbus(ref,ref)]
    currentbusno=newbus
    continue
end
% Modificaton of type3
% A new element is added between an old bus and reference bus
if newbus <=currentbusno & ref==0
   zbus=zbus-1/(zbus(newbus,newbus)+value)*zbus(:,newbus)*zbus(newbus,:)
   continue
end
% Modification of type4
% A new element is added betwen two old buses
if newbus <= currentbusno & ref ~=0
  zbus=zbus- 1/(value+zbus(from,from)+zbus(to,to)-
```

```
2*zbus(from,to))*((zbus(:,from)-zbus(:,to))*((zbus(from,:)-zbus(to,:))))
  continue
end
end
```

Ex. G-14 (Example 12.10)

```
% Program for transient stability of single machine connected to infinite
% bus this program simulates Example 12.10 using point by point method
clear
t=0
tf=0
tfinal=0.5
tc=0.125
tstep=0.05
M=2.52/(180*50)
i=2
delta=21.64*pi/180
ddelta=0
time(1)=0
ang(1)=21.64
Pm=0.9
Pmaxbf=2.44
Pmaxdf=0.88
Pmaxaf=2.00
while t<tfinal,
   if (t==tf),
     Paminus=0.9-Pmaxbf*sin(delta)
     Paplus=0.9-Pmaxdf*sin(delta)
     Paav=(Paminus+Paplus)/2
     Pa=Paav
   end
     if (t==tc),
     Paminus=0.9-Pmaxdf*sin(delta)
     Paplus=0.9-Pmaxaf*sin(delta)
     Paav=(Paminus+Paplus)/2
     Pa=Paav
   end
     if(t>tf & t<tc),
     Pa=Pm-Pmaxdf*sin(delta)
   end
     if(t>tc),
     Pa=Pm-Pmaxaf*sin(delta)
    end
      t,Pa
      ddelta=ddelta+(tstep*tstep*Pa/M)
      delta=(delta*180/pi+ddelta)*pi/180
      deltadeg=delta*180/pi
      t=t+tstep
      pause
```

```
      time(i)=t
       ang(i)=deltadeg
       i=i+1
   end
   axis([0 0.6 0 160])
   plot(time,ang,'ko-')
```

Ex. G-15

Here the earlier Example G-14 is solved again using SIMULINK.
Before running simulation shown in Fig. G-5 integrater 1 has to be initialized to prefault value of δ, i.e. δ_0. This can be done by double-clicking on integrater 1 block and changing the initial value from 0 to δ_0 (in radius). Also double click the switch block and change the threshold value from 0 to the fault clearing time (in sec.).

Ex. G-16 (Ex. 12.11)

```
% This program simulates transient stability of multimachine systems
% The data is from Example 12.11
clear all
format long
%Step 1 Initialization with load flow and machine data
f=50;tstep=0.01; H=[12 9]';
Pgnetterm=[ 3.25 2.10]';
Qgnetterm=[ 0.6986 0.3110]';
Xg=[0.067 0.10]';
% Note the use of .' operator here
% This does a transpose without taking the conjugate of each element

V0=[polarTorect(1.03, 8.235) polarTorect(1.02, 7.16)].'
% m is no of generators other than slack bus
m=2;
%Step 2
V0conj=conj(V0);
Ig0=conj((Pgnetterm+j*Qgnetterm)./V0);
Edash0=V0+j*(Xg.*Ig0);
Pg0=real(Edash0.*conj(Ig0));
x1_r=angle(Edash0);
% Initialization of state vector
Pg_r=Pg0;
% Pg_rplus1=Pg0;
x2_r=[0 0]';
x1dot_r=[0 0]';
x2dot_r=[0 0]';
x1dotrplus1=[0 0]';
x2dotrplus1=[0 0]';
%Step 3
% Here in this example we have not really calculated YBus But one
% can write separate program.
```

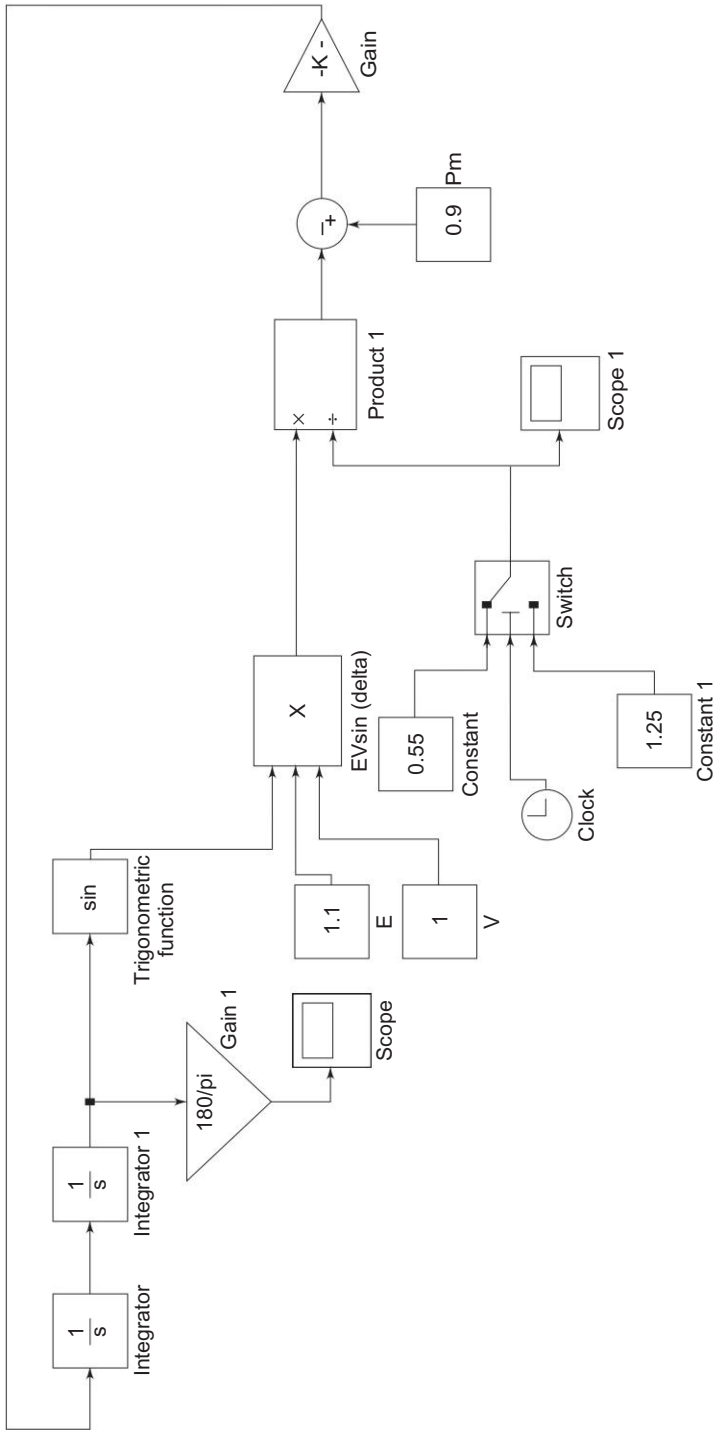

Fig. G-5 Transient stability for single machine connected to infinite Bus

```
YBusdf=[
5.7986-j*35.6301              0                    -0.0681+j*5.1661
     0                     -j*11.236                    0
 -0.0681+j*5.1661              0                     0.1362-j*6.2737];
YBuspf=[
1.3932-j*13.8731          -0.2214+j*7.6289        -0.0901+j*6.0975
 -0.2214+j*7.6289             0.5+j*7.7898               0
 -0.0901+j*6.0975                0                  0.1591-j*6.1168];
%Step 4
% Set the values for initial time t(occurence of fault) and
% tc is time at which fault is cleared
t=0;tc=0.08;tfinal=1.0;
r=1;
Edash_r=Edash0;Edash_rplus1=Edash0;
while t < tfinal,
%Step 5 Compute Generator Powers using appropriate YBus
% the YBus chosen in the following step is set according to the current
% time
if t <= tc YBus=YBusdf; else YBus=YBuspf;end
% Note that here we obtain the currents injected at generator bus
% by multiplying the corresponding row of the Ybus with the vector of
% voltages behind the transient reactances. This should also include
% slack bus voltage
% and hence the entry 1 appears in the bus voltage vector in addition to
% generator bus voltages
 I=YBus(2:m+1,:)*[1
                 Edash_r];
 Pg_r=real(Edash_r.*conj(I));
%Step 6 compute x1dot_r and x2dot_r
    x1dot_r=x2_r;
    for k=1:m,
    x2dot_r(k,1)=(pi*f/H(k))*(Pg0(k)-Pg_r(k));
    end
%Step 7 Compute first state estimates for t=t(r+1)
    x1_rplus1=x1_r+x1dot_r*tstep;
    x2_rplus1=x2_r+x2dot_r*tstep;
%Step 8 Compute first estimates of E'_r+1
Edash_rplus1=abs(Edash0).*(cos(x1_rplus1)+j*sin(x1_rplus1));
%Step 9 Compute Pg for t=t(r+1)
 I=YBus(2:m+1,:)*[1
                 Edash_rplus1];
 Pg_rplus1=real(Edash_rplus1.*conj(I));

%Step 10 Compute State derivatives at t=t(r+1)
x1dot_rplus1=[0 0]';
x2dot_rplus1=[0 0]';
for k=1:m,
x1dot_rplus1(k,1)=x2_rplus1(k,1);
x2dot_rplus1(k,1)=pi*f/H(k)*(Pg0(k)-Pg_rplus1(k));
end
```

```
%step 11 Compute average values of state derivatives
x1dotav_r=(x1dot_r+x1dot_rplus1)/2.0;
x2dotav_r=(x2dot_r+x2dot_rplus1)/2.0;
%step 12 Compute final state estimates for t=t(r+1)
x1_rplus1=x1_r+x1dotav_r*tstep;
x2_rplus1=x2_r+x2dotav_r*tstep;
%step 13 Compute final estimate for Edash at t=t(r+1)
Edash_rplus1=abs(Edash0).*(cos(x1_rplus1)+j*sin(x1_rplus1));
%Step 14 Print State Vector
    x2_r=x2_rplus1;
    x1_r=x1_rplus1;
    Edash_r=Edash_rplus1;
%Step 15
time(r)=t;
for k=1:m,
    ang(r,k)=(x1_r(k)*180)/pi;
end
t=t+tstep;
r=r+1;
end
plot(time,ang)
```

Ex. G-17 (Example 12.11)

```
%Example 12.11 is solved using SIMULINK
% The code given below should be run prior to simulation shown in
Fig. G-6.
clear all
global n r y yr
global Pm f H E  Y ngg
global rtd dtr %conversion factor rad/degree
global Ybf Ydf Yaf

f=50;
ngg=2;
r=5;
nbus=r;

rtd=180/pi;
dtr=pi/180;

%         Gen.  Ra    Xd'      H
gendata=[ 1     0     0       inf
          2     0   0.067    12.00
          3     0   0.100     9.00  ];
Ydf=[
5.7986-j*35.6301               0                   -0.0681+j*5.1661
       0                      -j*11.236             0
 -0.0681+j*5.1661                0                   0.1362-j*6.2737];
Yaf=[
1.3932-j*13.8731           -0.2214+j*7.6289        -0.0901+j*6.0975
  -0.2214+j*7.6289               0.5+j*7.7898              0
  -0.0901+j*6.0975                  0               0.1591-j*6.1168];
```

Fig. G-6 Multimachine transient stability

```
fct= input('fault clearing time fct = ');

%Damping factors
damp2=0.0;
damp3=0.0;

%Initial generator Angles
d2=0.3377*rtd;
d3=0.31845*rtd;

%Initial Powers
Pm2=3.25;
Pm3=2.10;

%Generator Internal Voltages
E1=1.0;
E2=1.03;
E3=1.02;

%Machine Inertia Constants;
H2=gendata(2,4);
H3=gendata(3,4);

%Machine Xd';
Xdd2=gendata(2,3);
Xdd3=gendata(3,3);
```

Note : For the simulation for multimachine stability the two summation boxes sum 2 & sum 3 give the net accelerating powers P_{a2} and P_{a3}. The gains of the gain blocks G1, G2 G3 and G4 are set equal to pi*f/H2, damp2, pi*f/H3 and damp3, respectively. The accelerating power P_a is then integrated twice for each mahcine to give the rotor angles δ_2 and δ_3. The initial conditions for integrator blocks integrator 1, integrator 2, integrator 3 and integrator 4 are set to 0, d2/rtd, 0 and d3/rtd, respectively. The gain blocks G5 and G6 convert the angles δ_2 and δ_3 into degrees and hence their gains are set to rtd. The electrical power P_{e2} is calculated by using two subsystems 1 and 2. The detailed diagram for subsystem 1 is shown in Fig. G-7. Subsystem 1 gives two outputs (i) complex voltage $E_2\angle\delta_2$ and (ii) current of generator I_2 which is equal to $E_1\angle\delta_1 * Y_{af}$ (2,1) + $E_2\angle\delta_2 * Y_{af}$(2,2) + $E_3\angle\delta_3 Y_{af}$ (2,3). The switches are used to switch between prefault and post fault conditions for each machine and their threshold values are adjusted to fct, i.e. the fault clearing time.

Ex. G-18

```
clear
% This Program finds the reduced matrix for stability studies
% which eliminates the load buses and retains only the generator buses
%  |Ig1|      |Y11  Y12 . . .  Y1n   Y1n+1   Y1n+2   . . .  Y1n+m|   |V1   |
%  |Ig2|      |Y21  Y21 . . .  Y2n   Y2n+1   Y2n+2   . . .  Y1n+m|   |V2   |
%  | . |      |                                                  |   | .   |
%  | . |      |                                                  |   | .   |
%  |Ign|  =   |Yn1  Yn2 . . .  Ynn   Ynn + 1 Ynn + 2     Ynn + m|   |Vn   |
%  |IL1|      |Yn+12 . . . .                                Yn+1m|   |Vn+1|
%  |IL2|      |                                                  |   |Vn+1|
```

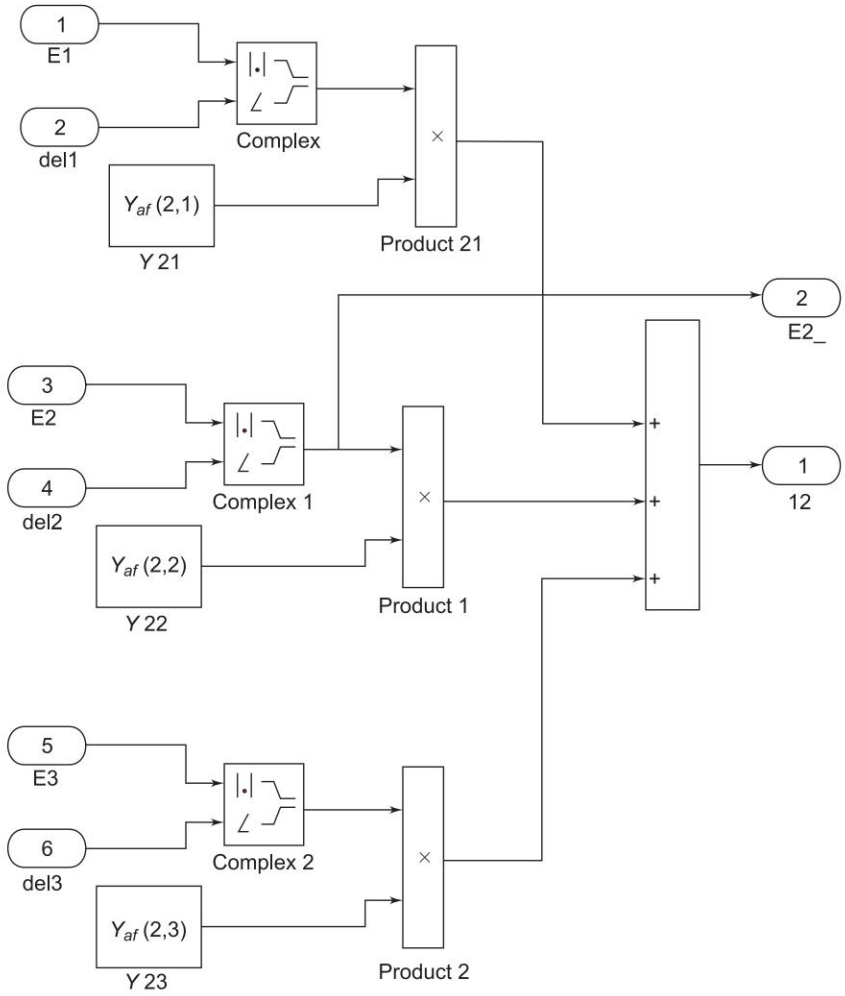

Fig. G-7 Multimachine transient stability: Subsystem 1

```
%  | . |      |                                                    |   | . |
%  | . |      |                                                    |   | . |
%  |ILm|      |Yn+m1  . . . .                          Yn+mn+m|   |Vn+m|
Yfull= -j*5       0       7*5
         0      -j*7.5    j*2.5
        j*5      j*2.5   -j*12.5]
[row columns]=size (Yfull)
n=2
YAA=Yfull (1:n,1:n)
YAB=Yfull (1:n, n+1;columns)
YBA=Yfull (n+1:rows,n+1:columns)
YBB=Yfull (n+1:rows,n+1:columns)
% This gives the reduced matrix

Yreduced=YAA-YAB*inv(YBB)*YBA
```

Appendix H
Substations

INTRODUCTION

The creation of huge power houses is the present need to meet the drastically increasing power demands. Usually large power-generating stations are built far away from load centres. Long transmission lines are necessary to transmit the bulk amount of power at higher voltage levels. In between the generating station and last consumer end, a number of transformation and switching stations have to be installed. These are generally known as substations. (Fig. H-1).

TYPES OF SUBSTATIONS

Substations may be classified as follows depending upon their purpose:

1. *Generating Substations* These are also known as step-up substations. These are associated with the generating stations. It is economical to generate the power at low value of voltage and to transmit at higher values. Generating units are connected to the step-up transformers to increase the voltage up to transmission voltage levels.
2. *Grid Substations* These substations are located in the intermediate points between the generating stations and load centres to provide connections of low-voltage lines.
3. *Secondary Substations* These substations are connected with secondary transmission lines. These substations are located at the load points where the voltage is further stepped down to sub-transmission and primary distribution voltage.
4. *Distribution Substations* These substations are located where the sub-transmission or primary distribution voltage is stepped down to supply voltage. These substations supply the power to the actual consumers through distributors and service lines.

Depending upon the constructional features, the substations may be further sub-divided into:

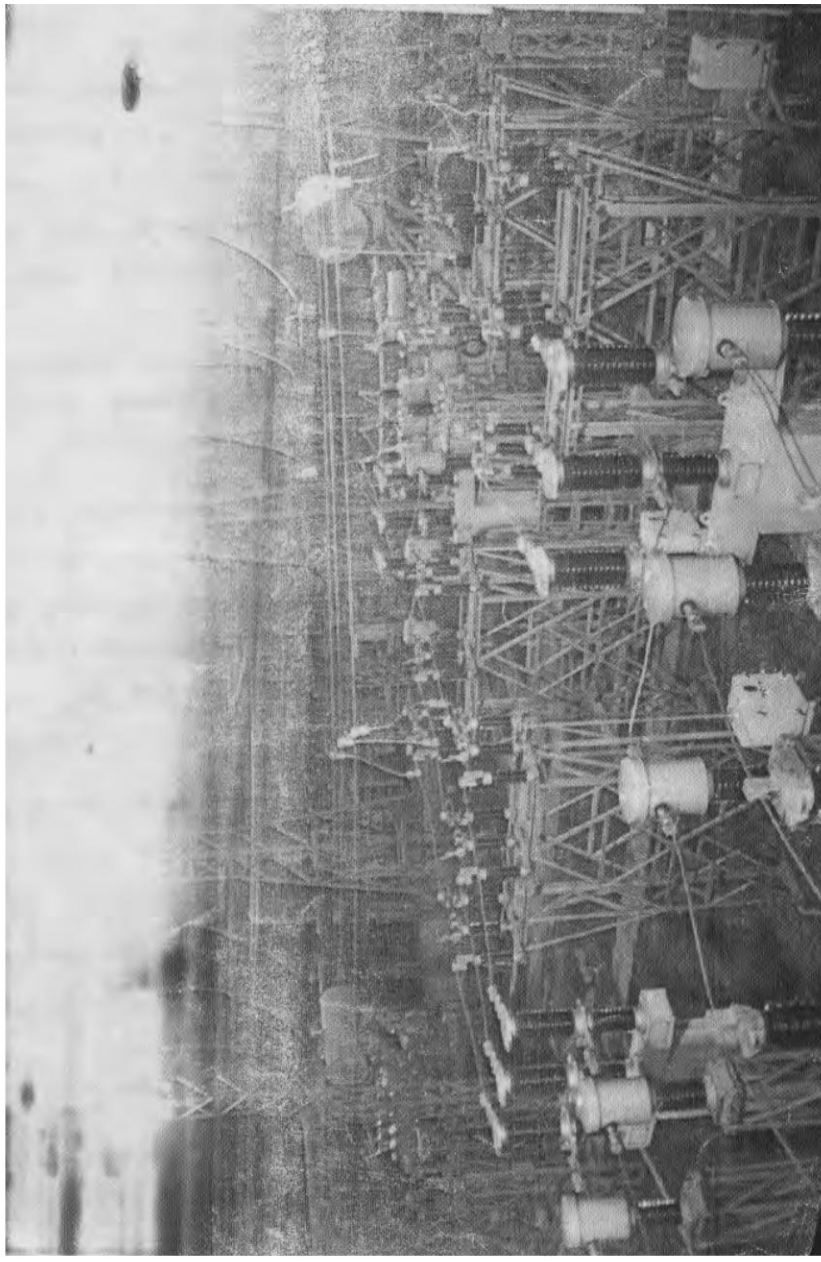

Fig. H-1 132 kV, photo 1 Substation

1. *Outdoor Substations* From the economy and safety point of view, the outdoor substations are used for 11 kV and above voltage levels. All equipments except control and monitoring equipments installed in open air.

2. *Indoor type* These substations are preferred in the big cities when the load centre lies in the heart of cities. The operating voltages are normally 400 V and 11 kV.
3. *Pole mounted* These substations are mounted on the poles. These substations are very simple in construction and economic as there is no need of any building.
4. *Underground type* Whole substation is made underground. These substations are used where the space is not available.

A substation comprises of several transformers and several incoming and outgoing lines.

SUBSTATION BUS BAR ARRANGEMENTS

There are numerous ways in which the switching equipment can be connected between the generating station and the receiving station or in a distribution system. The choice of the scheme mainly depends upon the following criteria:

1. Flexibility of operation
2. Continuity of supply
3. Economic aspects
4. The degree of maintenance required
5. Scope of extension
6. Safety and simplicity

With these basic requirements there are several combinations, some of them are briefly described below.

(a) Single Bus Bar Arrangement

This type of scheme is favoured for small and medium size stations where periodic shut downs can be permitted. It consists of a single (3-phase) to which various feeders are connected as shown in Fig. (H-2) of a fault or when the maintenance in case of the line is required, the whole bus bar has to be shut down.

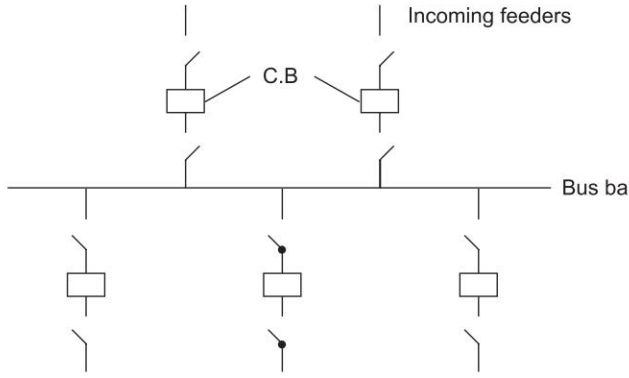

Fig. H-2 Outgoing feeders

(b) Duplicate Bus Bar Arrangement

For large systems, the technical aspects overcomes the economic considerations, since in these networks shut down results in disconnecting a large supply area.

The duplicate bus bar system incorporates flexibility, reliability and also permits periodic maintenance. A reserve bus can be used in case of a fault. Figure (H-3) shows a duplicate bus bar arrangement, there are two buses one main bus and a reserve bus. The coupler can be closed so as to connect the two buses. In more important stations the transfer bus is used to transfer the power from Bus I to Bus II.

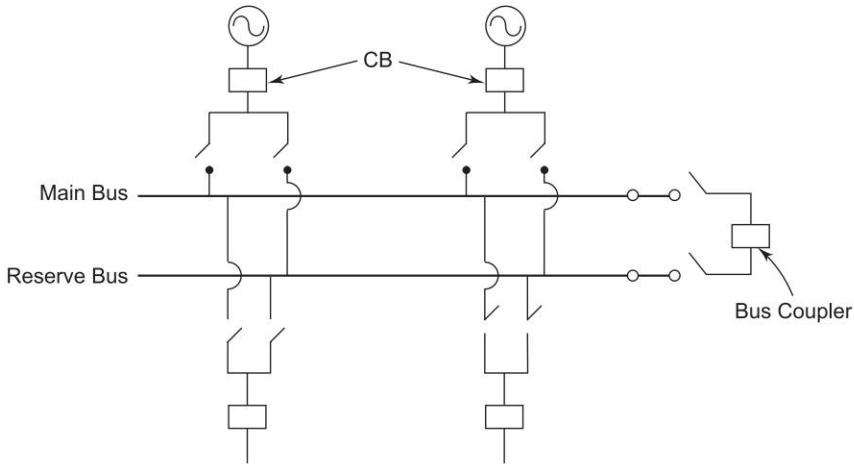

Fig. H-3 Duplicate bus bar arrangement (Single line diagram of 3-ϕ system)

(c) Sectionalizing of Bus (Fig. H-4)

The purpose of sectionalizing the bus bar arrangement is to incorporate some added advantages to the existing system. Firstly, the continuity of supply of one section is uninterrupted while the maintenance of other section is carried out; secondly, the fault MVA is reduced, by the addition of current limiting reactor, hence we can use CB of lesser capacity.

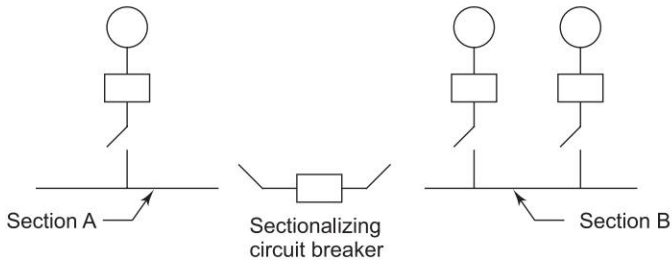

Fig. H-4 Sectionalizing of Bus

(d) Ring Bus (Fig. H-5)

This type of bus bar arrangement (Fig. H-5) adds more reliability to the power system. If a fault takes place in any one section no other adjacent sections are affected by it, and their continuity of supply is restored as shown in Fig. H-5. Also the supply can be taken from any adjacent section.

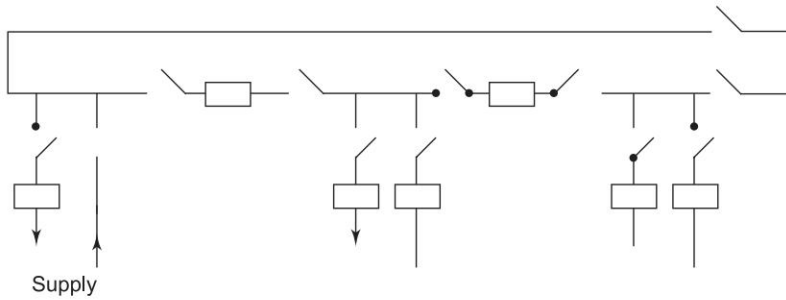

Fig. H-5 Ring bus system

(e) One and a Half Breaker arrangement (Fig. H-6)

This arrangement needs three circuit breaker for two circuits. By this arrangement if we require maintenance we can switch either circuit breaker without any by-pass.

This arrangement is used for the high power circuits, and gives a greater degree of security against loss of supply.

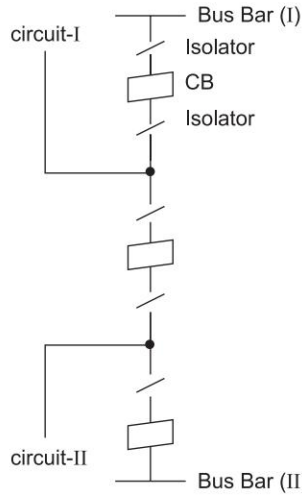

Fig. H-6 One and a half breaker arrangement

Appendix I

Convergence of Load Flow Methods

GAUSS–SIEDEL METHOD

The general form of Gauss–Siedel method involves the solution of n non-linear equations in n unknowns. The n equations in matrix form are given as

$$f(x) = 0 \tag{I-1}$$

where

$$f = (f_1(x) \ldots f_n(x))^T$$
$$x = (x_1 \ldots x_n)^T$$

The convergence property of GS method can be understood by considering the single variable problem

$$f(x) = 0 \tag{I-2}$$

Equation (I-2) is written in the form

$$x = g(x) \tag{I-3}$$

assuming that the initial approximate value of x, i.e. x_0 of Eq. (I-2) converges to the exact value after performing GS iteration on Eq. (I-3). Thus, the values of x at various iterations are given by

$$\begin{aligned} x_1 &= g(x_0) \\ x_2 &= g(x_1) \\ x_n &= g(x_n - 1) \end{aligned} \tag{I-4}$$

The iteration is continued till

$$x_n \cong \zeta = g(\zeta) \tag{I-5}$$

Figure (I-1) shows the graph of $g(x)$. In Fig. (I-1) ε_n and ε_{n+1} are the errors in the nth and $(n + 1)$th iteration.
Thus,

$$x_n = \zeta + \varepsilon_n \tag{I-6a}$$

$$x_{n+1} = \zeta + \varepsilon_{n+1} \tag{I-6b}$$

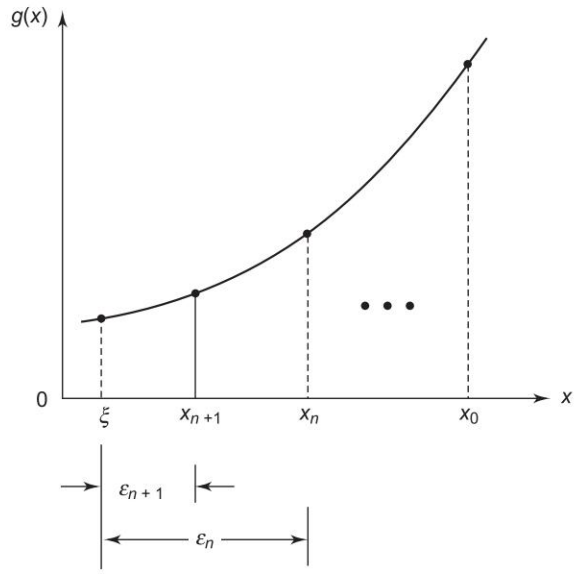

Fig. I-1

Also

$$x_{n+1} = g(x_n) \tag{I-6c}$$

Substituting Eq. (I-6a) in Eq. (I-6c),

$$x_{n+1} = g(\zeta + \varepsilon_n)$$

Expanding by Taylor's series about ζ, we get

$$x_{n+1} = \zeta + \varepsilon_{n+1} = g(\zeta) + \varepsilon_n g'(\zeta) + \frac{\varepsilon_n^2}{2} g''(\zeta) + \ldots$$

Neglecting higher order terms and substituting the value of $g(\zeta)$ from Eq. (I-5), we get

$$\zeta + \varepsilon_{n+1} = \zeta + \varepsilon_n g'(\zeta)$$

or

$$\varepsilon_{n+1} = g'(\zeta)\varepsilon_n \tag{I-7}$$

Since $g'(\zeta)$ is a constant, the error in the $(n+1)$th iteration is proportional to the previous error i.e. in the nth iteration. Hence, the convergence of GS method is linear. Depending on the value of $g'(\zeta)$, the GS method may or may not converge. Thus we must have

$$g'(\zeta) < 1 \tag{I-8}$$

for convergence, near $x = \zeta$.

Newton–Raphson Method

The Newton–Raphson method involves the solution of n equations (in general nonlinear) in n unknowns, written in the matrix form as,

$$f(x) = 0 \tag{I-9}$$

where

$$f = (f_1(x)\ f_2(x)\ \ldots\ f_n(x))^T$$

and

$$x = (x_1\ x_2\ \ldots\ x_n)^T$$

To understand the convergence properties of NR method we consider a single variable problem, such as $f(x) = 0$ where $f(x)$ can be an algebraic or transcendental function.

If we represent $y = f(x)$ graphically (Fig. I-2) the problem can be formulated so that we are looking for the intersection between the curve and the x-axis. We intend to start with a trivial value x_0, then construct better and better approximations of x such as $x_1, x_2, \ldots, x_n$, so that x_n is close to the actual value ζ for which $f(\zeta) = 0$.

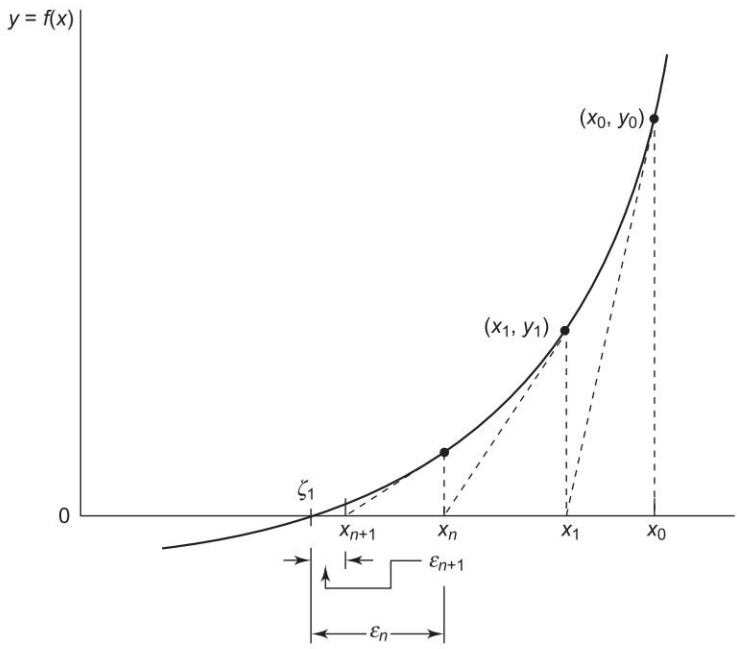

Fig. I-2

The basic idea is now to replace the curve by a suitable straight line, at the approximate point on the curve whose intersection with the x-axis can be easily computed. The direction of the line passing through the approximate point can be chosen in many ways. In NR method, the line passing through the point (x_n, y_n) has the slope given by $K = f'(x_n)$. The intersection of this line with the

x-axis gives the new approximate value of $x = x_{n+1}$ as shown in the Fig. I-2. The slope K is not constant, and is a function of the point x_n. Hence the NR method uses the variable tangent method (slope varies at each approximation). From Fig. (I-2), the slope is given by

$$f'(x_n) = \frac{y_n}{x_n - x_{n+1}} \quad (\neq 0) \tag{I-10}$$

$$x_{n+1} = x_n - \frac{y_n}{f'(x_n)} = x_n - \frac{f(x_n)}{f'(x_n)} \tag{I-11}$$

From the figure,

$$\begin{aligned} x_{n+1} &= \zeta + \varepsilon_{n+1} \\ x_n &= \zeta + \varepsilon_n \end{aligned} \tag{I-12}$$

where ε_n, ε_{n+1} are the errors

$$\zeta + \varepsilon_{n+1} = \zeta + \varepsilon_n - \frac{f(\zeta + \varepsilon_n)}{f'(\zeta + \varepsilon_n)}$$

$$\varepsilon_{n+1} = \frac{\varepsilon_n f'(\zeta + \varepsilon_n) - f(\zeta + \varepsilon_n)}{f'(\zeta + \varepsilon_n)}$$

$$= \frac{\varepsilon_n (f'(\zeta) + \varepsilon_n f''(\zeta) + \ldots) - (f(\zeta) + \varepsilon_n f(\zeta) + \varepsilon_{n/2}^2 f''(\zeta) + \ldots)}{f'(\zeta + \varepsilon_n)}$$

Considering only the significant terms,

$$\varepsilon_{n+1} = \frac{\varepsilon(f'(\zeta) + \varepsilon_n f''(\zeta)) - (\varepsilon_n f'(\zeta) + \varepsilon_{n/2}^2 f''(\zeta))}{f'(\zeta + \varepsilon_n)} \quad (\text{as } f(\zeta) = 0)$$

or

$$\varepsilon_{n+1} \cong \frac{f''(\zeta)}{2f'(\zeta + \varepsilon_n)} \varepsilon_n^2 \tag{I-13}$$

If x_n is sufficiently close to ζ and $f(x)$ is continuous at $x = \zeta$, we have

$$f'(\zeta + \varepsilon_n) \cong f'(\zeta)$$

Therefore,

$$\varepsilon_{n+1} \cong \frac{f''(\zeta)}{2f'(\zeta)} \varepsilon_n^2 \tag{I-14}$$

Thus, the error $C_{n+1} = (\zeta - x_{n+1})$ is proportional to the square of the previous error $\varepsilon_n^2 = (\zeta - x_n)^2$. This type of convergence is said to be quadratic. It is clear that $f''(\zeta)/2f'(\zeta)$ should not be large for fast convergence. For the cases where this term is low, the convergence is very fast if $|\varepsilon_n| < 1$.

Appendix J

Power Quality: An Overview

INTRODUCTION

Earlier times, the main concern of consumers of electricity were continuity of supply. But now, the consumers demand quality too. Even though power generation and transmission are reliable, the distribution is not so, even in most advanced countries. The electric power quality is also very important these days, because some of the consumer loads are sensitive to power quality and any outage or trip of the system may lead to huge financial loss. In a broader way, any deviation from the normal condition of the voltage and current is referred to as a power quality issue. Power quality means maintaining the voltage at its rated r.m.s value with negligible amount of harmonics and maintaining frequency within statutory limit and least amount of interruption [1]. A broad classification of power quality problem is as follows:

- Transient change in voltage (impulsive or oscillatory)
- Short duration voltage variation (sag, swell or interruption)
- Long duration voltage variation (Under, Over, sustained interruption)
- Voltage flicker (due to lightning etc.)
- Voltage imbalance (due to single phase loads)
- Waveform distortion and bad power factor (harmonics, notching, DC offset).

POWER QUALITY TERMS AND DEFINITIONS

(a) *Voltage sag:* A momentary voltage dip, lasting for a few seconds. Dips with duration of less than half a cycle are regarded as transients.
(b) *Voltage swells:* A momentary voltage rise which last for a few seconds.
(c) *Over voltage:* A steady state voltage rise lasting for several seconds. Sustained over voltage lasting for few hours may cause damage to appliances.
(d) *Under voltage:* A steady state voltage dip lasting for several seconds.
(e) *Outage:* A complete loss of voltage for a few seconds to several hours. The voltage sag, voltage swell, outage are as shown in Fig. J-1 (a).

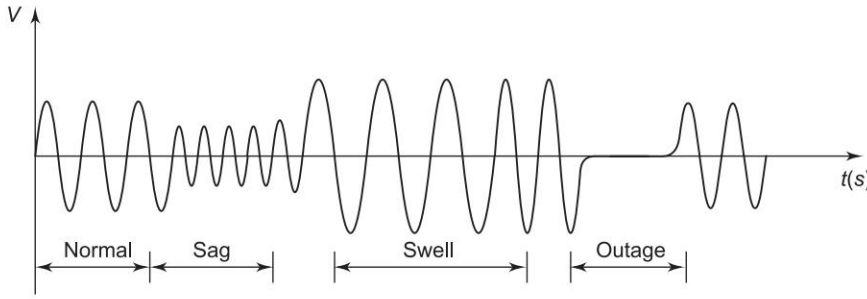

Fig. J-1 (a) Sag, swell and outage

(f) *Transients:* They are of high magnitude for extremely short duration as compared to voltage sag and swell. The transient behaviour is shown in Fig. J-1 (b).

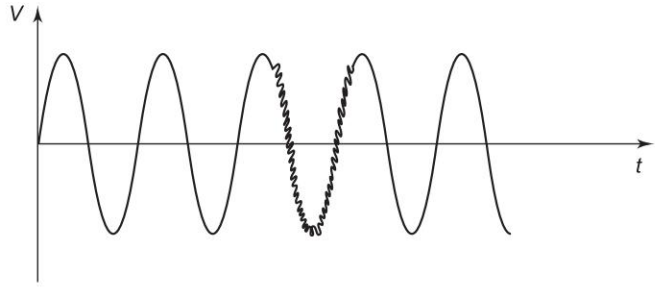

Fig. J-1 (b) Transient voltage (oscillatory)

(g) *Flicker:* Fluctuations in the system voltage can cause perceptible (low frequency) change in lamp output.

(h) *Harmonics:* The non-fundamental frequency components of a distorted power frequency waveform. THD (Total Harmonic Distortion) is the measure of harmonics in a system. The wave form distortion is shown in Fig. J-1 (c).

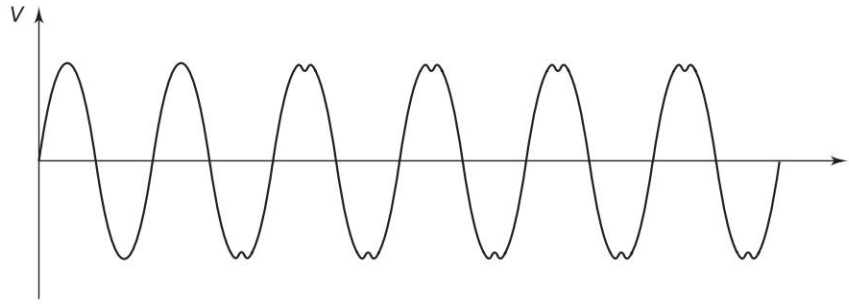

Fig. J-1 (c) Harmonic distortion

(i) *Voltage imbalance:* If the voltage magnitude is unequal in a three phase voltage sources or the phase difference between them is not equal to 120 electrical degrees or both, the situation is described as unbalanced. The transient behaviour is shown in Fig. J-1 (d).

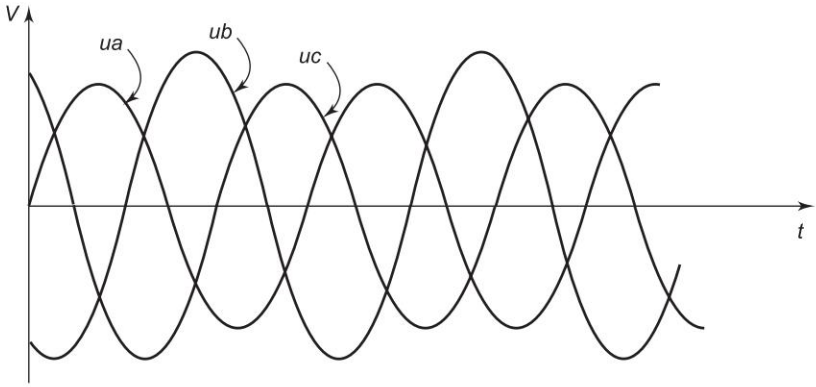

Fig. J-1 (d) Unbalanced voltages

CAUSES FOR POWER QUALITY (PQ) PROBLEMS

There are various causes for different power quality problem and some of them are capacitor switching, single line to ground fault, switching ON and OFF of loads, single phase loads, power electronic converters etc. But the main reason for wave form distortion is the non-linear load in the system. For example, in a power electronic controlled load, the current drawn from the system is not sinusoidal as shown in Fig. J-2.

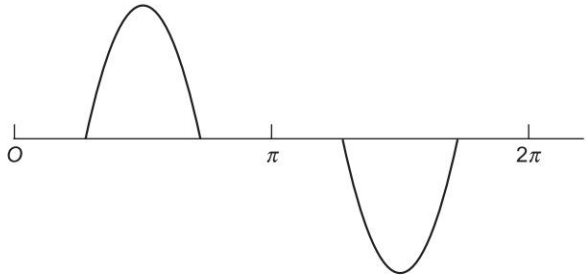

Current wave of switch mode power supply

Spectrum of Typical Switch Mode Power Supply

Harmonic	*Magnitude*	*Harmonic*	*Magnitude*
1	1.000	9	0.157
3	0.810	11	0.024
5	0.605	13	0.063
7	0.370	15	0.079

Fig. J-2 Typical current wave form of a power electronic converter and harmonic contents

It can be observed that the load current draws harmonic currents along with the fundamental component. This poor quality of current, pollute the voltage at the point where it is connected. So the individual customers are responsible for the poor quality of power. Hence the situation is severe as almost all loads are controlled by power electronic converters. Also, single phase loads cause unbalance in the system. And interestingly, these power electronic converters are mainly affected due to the poor power quality resulted from other power electronic equipment. The harmonics are the integer multiple of the fundamental frequency. The current drawn by any nonlinear load is non-sinusoidal in nature. This non-sinusoidal current flowing through network impedance cause the voltage also become non-sinusoidal, thus leading to a voltage distortion in the network. The 3rd, 5th and 7th harmonics are the most common harmonics that pollute the network. The 3rd harmonics are usually generated by single phase loads and the other harmonics by 3 phase load. Even harmonics cancel out and are negligible. A common PC generates 4 A/kW of 3rd harmonic and a discharge lamp will produce 1 A/kW 3rd harmonic. The sequence generated by harmonics and their effects are given in Table J-1.

Table J-1 Harmonics in power system

Sequence	*Harmonics*	*Direction of rotation*	*Effects*
+ ve	7th, 13th	Forward	Heating
– ve	5th, 11th	Backward	Heating and vibration in motors
zero	3rd	Insignificant	Over heating of neutral conductor due to accumulation

POWER QUALITY STANDARDS

There are international standards for the power quality. The Institute of Electrical and Electronics Engineers (IEEE) and International Electrotechnical Commission (IEC) have proposed power quality standards which are followed world over. An example is given below.

IEEE 519: Harmonic standards.

IEC 6100: Classification of power quality. Transients etc.

EFFECTS OF PQ PROBLEMS

The poor power quality affects the whole equipments connected to the electric power system adversely. Some of the cases are mentioned below.

Table J-2 Detrimental effect of harmonics in power system

Equipments	*Effects*
Transformers	Reduced capacity, increased loss
Motors	Reduced motor life, reduced rating, increased loss.
Conductors	Increased heating
Capacitors	Reduced life
Power electronic equipment	Malfunction
Meters	Malfunction
Relays	Malfunction
Digital equipment	Malfunction
Telephone/communication equipment	Interference
Lamps	Reduced life

REMEDIES FOR PQ PROBLEMS

There are two kinds of remedies for the PQ problems. One is through introducing devices with power quality that meet the standards and the other is to use the power conditioners which improve the power quality at the point of interconnection with the system.

Improved Power Quality Converters (IPQC)

These are the modifications proposed in the converters so that they draw current with minimum PQ problems. There are a number of converters developed based on this concept and one example with circuit diagram and waveforms showing power factor correction is given in Fig. J-3.

Retrofit Solutions

The harmonic currents can be prevented from entering into the utility system by means of filters. For the distribution systems, the harmonics and reactive power demand can be compensated using series or shunt filters. There are active and passive filters. Hybrid filters are also proposed which can perform both the shunt and series compensation. Another set of devices applied to the distribution system to enhance the quality and reliability of power supplied to customers are called custom power device. These devices are used for active filtering, load balancing, power factor correction and voltage regulation.

Customer Power Devices

The custom power devices are of three types based on the mode of connection with the system. The shunt connected device is DSTATCOM (distribution static compensator), the series connected device is DVR (Dynamic voltage restorer) and UPQC (unified power quality conditioner) has both shunt and series connection.

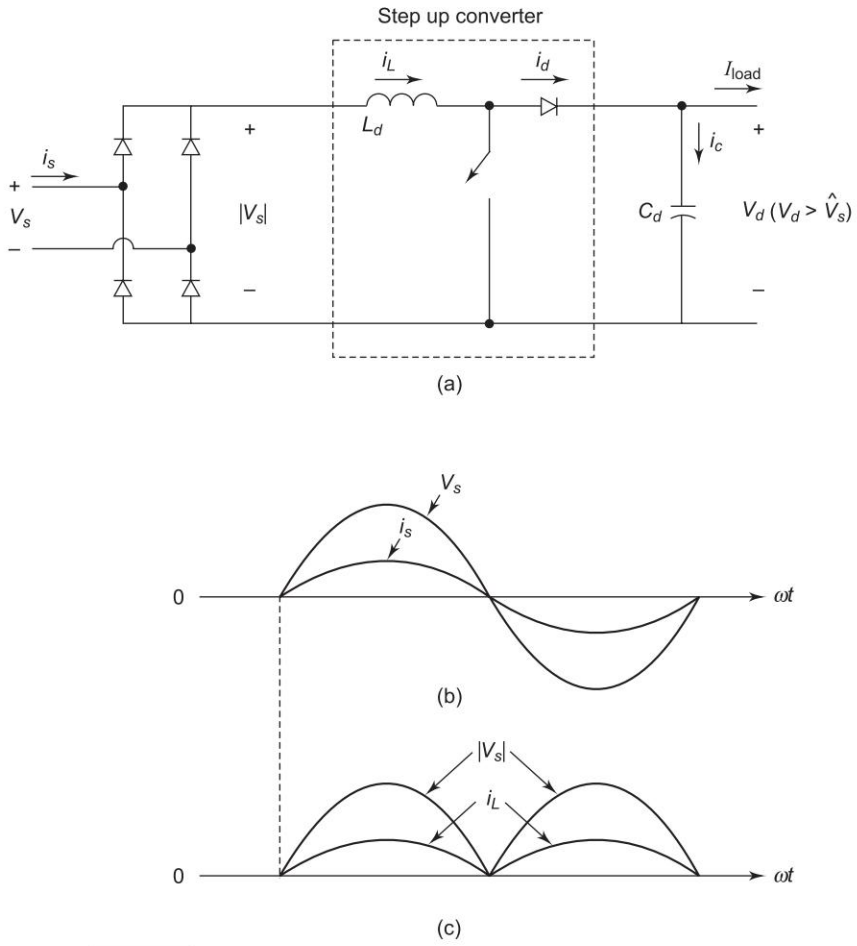

Fig. J-3 A power factor correction converter with waveforms

DSTATCOM (Distribution Static Compensator)

The instantaneous correction of harmonics is proposed in the VSI (Voltage source inverter) based DSTATCOM (Fig. J-4). This device compensates bad power factor, unbalance and voltage regulation along with harmonic compensation. It has a shunt connected structure which is able to inject an unbalanced and harmonically distorted current to eliminate unbalance or distortions in the load.

DVR (Dynamic Voltage Restorer)

This is a series connected device and its main purpose is to protect sensitive loads from sag/swell and interruptions in the supply side. These devices have a VSI (Voltage source inverter) with PWM switching connected in series with the load voltage and inject a distorted voltage to counteract with the harmonic voltage. Also, the voltage unbalance is reduced by injecting unbalanced voltages.

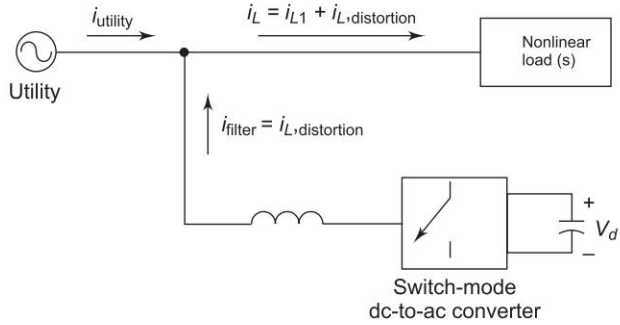

Fig. J-4 One line diagram of a DSTATCOM

UPQC (Unified Power Quality Conditioner)

This is a versatile device that can inject current in shunt and voltage in series simultaneously in a dual control mode. It must inject unbalanced and distorted voltages and currents to counteract harmonic current and harmonic voltage.

Custom Power Park

The concept is a park which supplies power of different power quality levels. High quality power can be supplied using the various custom power devices in a custom power park. Such a park gets its supply from two different feeders that are coupled together. There can be DSTATCOM, DVR or even a UPQC depending upon the grade of the customer. The higher grade customers are supplied power through a diesel-generator set when both incoming feeders are lost.

DISTRIBUTED POWER GENERATION

A trend is emerging currently, in which significantly smaller sized generating units are being connected at the distribution level (Refer chapter 1 for more details). Some of the factors that contribute to this trend are:

1. Renewable energy sources based smaller sized generating units are supported world-wide due to green house gas issues and aim for sustainable energy supply. The solar, wind, fuel cells and micro turbine-based power generation is increasing.
2. Co-generation is becoming more attractive in medium sized industrial plants. This effectively utilizes the byproduct, resulting in higher energy efficiency.
3. Power quality enhancement and reduction in distribution loss.

HARMONIC INDICES AND SOME EXAMPLES

The amplitude of current or voltage is characterized by the THD (Total Harmonic Distortion). It is defined as:

$$\text{THD} = \frac{\sqrt{\sum_{2}^{\infty} V_n^2}}{V_1} \tag{J-1}$$

where V_1 is the rms value of fundamental voltage, V_n is the rms harmonic voltage of nth harmonics. If V_s is the rms value of distorted voltage,

$$\text{THD} = \sqrt{\frac{V_s^2 - V_1^2}{V_1^2}} \tag{J-2}$$

In a similar way, for the current drawn,

$$\text{THD} = \sqrt{\frac{I_s^2 - I_1^2}{I_1^2}} \tag{J-3}$$

In the case of linear load, where there is no distortion in the current waveform, the power factor is

$$\text{PF} = \frac{\text{Real Power}}{V_s I_s} = \cos\phi \tag{J-4}$$

where V_s, I_s are the rms value of voltage and current and is the phase angle between voltage and current phasor.

In the presence of distortion in the current, the definition of power factor remains same. But here we take the real power as the power due to the fundamental frequency component only. Then,

$$\text{PF} = \frac{V_s I_1 \cos\phi}{V_s I_s}$$

$$= \frac{I_1}{I_s}\cos\phi \tag{J-5}$$

The ratio $\frac{I_1}{I_s}$ is defined as distortion factor (DF).

$$\text{DF} = \frac{I_1}{I_s} \tag{J-6}$$

Equation (J-5) shows that high distortion in the waveform leads to a low power factor. In terms of THD, Eq. (J-3), DF can be expressed as

$$\text{DF} = \frac{1}{\sqrt{1 + \text{THD}^2}} \tag{J-7}$$

Therefore, Eq. (J-5) becomes,

$$\text{PF} = \frac{1}{\sqrt{1+\text{THD}^2}} \cos\phi \qquad \text{(J-8)}$$

Example: The current drawn by a AC-DC converter is shown in Fig. J-5. Calculate the THD and power factor of the load.

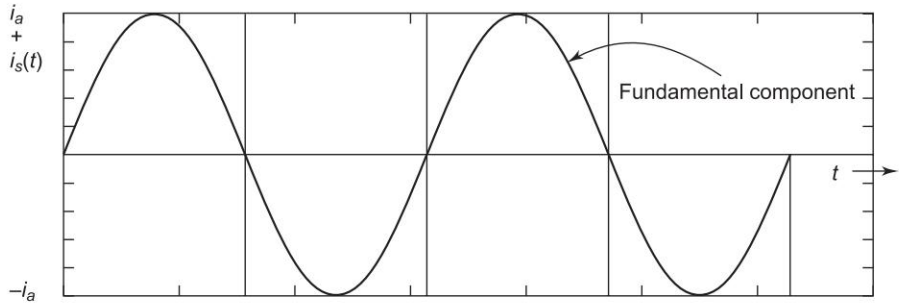

Fig. J-5

Solution

Using the Fourier analysis, the current is

$$i_s(t) = \frac{4I_a}{\pi}\left(\frac{\sin\omega t}{1} + \frac{\sin 3\omega t}{3} + \frac{\sin 5\omega t}{5} + \cdots\right)$$

The rms value of the fundamental component is

$$I_1 = \frac{4I_a}{\pi\sqrt{2}} = 0.9\, I_a$$

The rms value of the input current is

$$I_s = \frac{4I_a}{\pi\sqrt{2}}\left(\frac{1}{1} + \frac{1}{3^2} + \frac{1}{5^2}\cdots\right)^{1/2} = I_a$$

The total harmonic distortion (THD) is

$$\text{THD} = \sqrt{\left(\left(\frac{I_s}{I_1}\right)^2 - 1\right)} = \sqrt{\left(\left(\frac{1}{0.9}\right)^2 - 1\right)} = 0.484 \text{ or } 48.4\%$$

The displacement angle, which is the phase angle between the fundamental component of the current with the voltage is, $\Phi = 0$ and hence

$$\cos\Phi = 1.0$$

The power factor (PF) is

$$\text{PF} = \frac{I_1}{I_s} * 1.0 = 0.9 \ (\textit{lagging})$$

Note: The power factor is not unity because of the distortion in the current waveform.

SUMMARY

There are real costs from power quality. The sensitive loads like hospitals, semiconductor industries etc. require high quality power. So, the power quality conditioners are getting more and more importance. The expansion of distributed generation has the potential to significantly change the nature of the distribution system and the associated power quality issues. The future of energy delivery will be an integrated system of multiple sources where power quality as well as energy delivery are addressed.

References

1. Ghosh, A. and G. Ledwich, *Power Quality Enhancement Using Custom Power Devices*, Kluwer Academics, 2002.
2. Heydt, D.T., *Electric Power Quality*, Stars in a Circle Publications, 1991.
3. Arrillaga, J., N.R. Wattson and S. Chen, *Power System Quality Assessment*, John Wiley, 2000.
4. Ned Mohan, *First Course on Power System*, MNPERE, USA, 2006 edition.
5. Hingorani, N.G., Introducing Custom Power, *IEEE Spectrum*, vol. 32, Issue 6, June 1995, pp. 41–48.
6. Singh, B., B.N. Singh, A. Chandra, K. Al-Haddad, A. Pandey and D.P. Kothari, 'A Review of Single-Phase Improved Power Quality AC-DC Converters', *IEEE Transactions on Industrial Electronics*, vol. 50, Issue 5, Oct. 2003 pp. 962–981.
7. Singh, B., B.N. Singh, A. Chandra, K. Al-Haddad, A. Pandey and D.P. Kothari, 'A Review of Three-Phase Improved Power Quality AC-DC Converters', *IEEE Transactions on Industrial Electronics*, vol. 51, Issue 3, June 2004 pp. 641–660.
8. Singh, B., K. Al-Haddad and A. Chandra, 'A Review of Active Filters for Power Quality Improvement', *IEEE Transactions on Industrial Electronics*, vol. 46, Issue 5, Oct. 1999 pp. 960–971.
9. Singh, B., V. Verma, A. Chandra and K. Al-Haddad, 'Hybrid Filters for Power Quality Improvement', *IEE Proceedings Generation, Transmission and Distribution,* vol. 152, Issue 3, 6 May 2005, pp. 365–378.
10. Ghosh, A. and G. Ledwich, 'Load Compensating DSTATCOM in Weak AC Systems', *IEEE Transactions on Power Delivery*, vol. 18, Issue 4, Oct. 2003, pp. 1302–1309.
11. Muhammad H. Rashid, '*Power Electronics Circuits, Drives and Applications*', 2nd edn, Prentice Hall, April 1999.

Chapter 1

Introduction

1.1 Total installed generating capacity in India today (2006) is around
(a) 100,000 MW (b) 125,000 MW
(c) 50,000 MW (d) 200,000 MW

1.2 Load factor is defined as

(a) $\frac{\text{peak load}}{\text{average load}}$ (b) $\frac{\text{maximum load}}{\text{minimum load}}$

(c) $\frac{\text{average load}}{\text{peak load}}$ (d) $\frac{\text{peak load}}{\text{rated load}}$

1.3 Diversity factor is always
(a) 1 (b) 0
(c) greater than 1 (d) ∞

1.4 Nuclear power station is normally used for
(a) peak load (b) base load
(c) average load (d) any load

1.5 Theoretical power in a wind system is given by
(a) $P = 0.5\ \text{Av}^3$ W (b) $P = 0.5\ \rho\text{Av}^2$ W
(c) $P = 0.5\ \rho\text{Av}$ W (d) $P = 0.5\ \rho\text{Av}^3$ W

1.6 Electric power can be produced by solar energy
(a) By solar-thermal route (b) Photo voltaic route
(c) a and b both (d) Cannot be generated

1.7 Fuel cell
(a) converts chemical energy into electric energy
(b) mechanical energy into electric energy
(c) solar energy into electrical energy
(d) wind energy into electrical energy

1.8 Hydrogen can be used as a medium for
(a) energy transmission (b) for energy storage
(c) a and b both (d) for electrolysis

1.9 First nuclear power plant in India was started at
(a) Kota (b) Tarapur
(c) Kalpakam (d) Narora

1.10 Geothermal power plant was first started in
(a) New Zealand (b) Pakistan
(c) India (d) Italy

1.11 Low grade fuels have
(a) low ash content (b) low calorific value
(c) low carbon content (d) low moisture content

1.12 Which variety of coal has lowest calorific value?
(a) Lignite (b) Steam coal
(c) Bituminous coal (d) Anthracite

1.13 Betz law finds application in
(a) Wind mills (b) MHD
(c) Solar (d) Geothermal

1.14 Which plant can never have 100% load factor?
(a) Hydro (b) Nuclear
(c) Peak (d) Base load plant

1.15 During load shedding
(a) system voltage is reduced
(b) system frequency is reduced
(c) system power factor is changed
(d) some loads are switched off

Chapter 2

Inductance and Resistance of Transmission Lines

2.1 Bundled conductors in EHV transmission lines results to
(a) reduce capacitance (b) increase capacitance
(c) increase inductance (d) increase resistance

2.2 The internal flux linkage due to internal flux of a conductor is
(a) $I \times 10^{-7}$ Wb-T/m (b) $\frac{I}{4} \times 10^{-7}$ Wb-T/m
(c) $\frac{I}{2} \times 10^{-7}$ Wb-T/m (d) $\frac{1}{2} \times 10^{-7}$ Wb-T/m

2.3 A conductor of radius "r" will have the fictitious radius "r" for the inductance calculation
(a) $r' = 2r$ (b) $r' = r$
(c) $r' = 0.7788\, r$ (d) $r' = \frac{r}{0.7788}$

2.4 Aluminium is now most commonly employed conductor material in transmission lines than copper because
(a) It is more conductive (b) Its tensile strength is more
(c) Costlier (d) It is cheaper and lighter

2.5 A conductor is composed of seven identical copper strands each having a radius r, the self GMD of the conductor will be
(a) r (b) $3.177\, r$
(c) $2.177\, r$ (d) none of the above

2.6 The "skin effect" shows that
(a) The distribution of AC current is uniform through the cross section of the conductor.
(b) Current density is more at the centre of the conductor.
(c) Current density is lower at the surface of the conductor.
(d) Current density is highest at the surface of the conductor.

2.7 Apart from the "skin effect" the Non Uniformity of the current distribution is also caused by
(a) Faraday's effect (b) Bundled conductor
(c) Proximity effect (d) Ferranti effect

2.8 The total number of strands (N) in concentrically stranded cable with total annular space filled with strands of uniform diameter is given by (if x is the number of layers wherein the single central strand is counted as the first layer).
(a) $N = 3x^2 + 3x + 1$ (b) $N = 3x^2 - 2x + 1$
(c) $N = 3x^2 - 6x + 1$ (d) $N = 3x^2 - 3x + 1$

2.9 Which of the following are correct:
1. Bundle conductors reduce the corona loss.
2. Bundle conductor increases the inductance and reduces the capacitance.
3. Corona loss causes radio interference in adjoining telephone lines
(a) 1 (b) 1 and 2
(c) 2 (d) 1 and 3

2.10 Bundle conductors are used in transmission lines, the effective capacitance and inductance will respectively
(a) decrease and increase (b) increase and decrease
(c) remain same and increase (d) decrease and remain same

2.11 Transmission lines are transposed to
(a) reduce Ferranti effect
(b) reduce skin effect
(c) reduce transmission loss
(d) reduce interference with neighbouring communication lines

Chapter 3

Capacitance of Transmission Lines

3.1 The presence of earth in case of overhead lines
(a) increases the capacitance (b) decreases the capacitance
(c) increases the inductance (d) decreases the inductance

3.2 The term self GMD is used to calculate
(a) capacitance
(b) inductance
(c) both inductance and capacitance
(d) resistance

3.3 The presence of ground causes the line capacitance to
(a) increase by about 12% (b) decrease by about 12%
(c) increase by about 0.2% (d) none of the above

3.4 If we increase the spacing between the phase conductors, the line capacitance
(a) Decreases (b) Increases
(c) Remains the same (d) Not affected

3.5 If we increase the length of transmission line, the charging current
(a) Decreases (b) Increases
(c) Remains the same (d) Not affected

3.6 When an alternating voltage is applied to the line, the line capacitance draws a
(a) leading sinusoidal current
(b) lagging sinusoidal current
(c) a current in phase with voltage
(d) none of the above

3.7 The capacitance becomes increasingly important for
(a) short transmission lines (b) medium transmission lines
(c) both (a) and (b) (d) long transmission lines

3.8 An infinitely long straight conductor carries a uniform charge of q coulomb per metre length. If k is permitivity of the medium wherein two points are located at distance D_1 and D_2 respectively from the conductor axis. The potential difference V_{12} (between the two points) is given by

(a) $V_{12} = \dfrac{q}{\pi k} \ln D_2/D_1$ (b) $V_{12} = \dfrac{q}{2\pi k} \ln \dfrac{D_1}{D_2}$

(c) $V_{12} = \dfrac{q}{2\pi k} \ln \dfrac{D_2}{D_1}$ (d) $V_{12} = \dfrac{q}{2\pi k} \log_{10} D_2/D_1$

3.9 Consider a two-wire line shown in figure excited from a single-phase source.

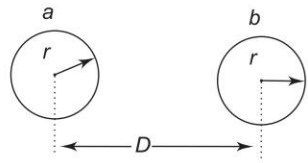

The line capacitance C_{ab} is given by

(a) $C_{ab} = \dfrac{0.0121}{\log(r/D)}$ μF/km (b) $C_{ab} = \dfrac{0.0121}{\log(D/r)}$ μF/km

(c) $C_{ab} = 0.0121 \log(D/r)$ μF/km(d) $C_{ab} = \dfrac{0.0121}{\log(D/r)}$ F/km

3.10 The method of images originally suggested by Lord Kelvin is used in

(a) calculation of inductance
(b) calculation of resistance
(c) effect of earth on line capacitance
(d) none of the above

Chapter 4

Representation of Power System Components

4.1 The per unit value of any quantity is defined as

(a) (The actual value in any units) × (The base value in the same units)

(b) $\dfrac{\text{The actual value in any units}}{\text{The base value in same units}}$

(c) $\dfrac{\text{The base value in any units}}{\text{The actual value in same units}}$

(d) $\dfrac{1}{\text{The base value in same units}}$

4.2 The per unit impedance Z(pu) is given by

(a) $\dfrac{Z(\text{ohms}) \times (\text{kVA})_B}{(\text{kV})_B^2}$ (b) $\dfrac{Z(\text{ohms}) \times (\text{MVA})_B}{(\text{kV})_B^2}$

(c) $\dfrac{Z(\text{ohms}) \times (\text{MVA})_B}{(\text{kV})_B^2 \times 100}$ (d) $\dfrac{Z(\text{ohms}) \times (\text{MVA})_B \times 100}{(\text{kV})_B^2}$

4.3 Which of the following is correct

(a) $Z(\text{pu})\text{new} = Z(\text{pu})\text{old} \times \dfrac{(\text{MVA})_{B,\text{old}}}{(\text{MVA})_{B,\text{new}}} \times \dfrac{(\text{kV})_{B,\text{old}}^2}{(\text{kV})_{B,\text{new}}^2}$

(b) $Z(\text{pu})\text{new} = Z(\text{pu})\text{old} \times \dfrac{(\text{MVA})_{B,\text{old}}}{(\text{MVA})_{B,\text{new}}} \times \dfrac{(\text{kV})_{B,\text{new}}^2}{(\text{kV})_{B,\text{old}}^2}$

(c) $Z(\text{pu})\text{new} = Z(\text{pu})\text{old} \times \dfrac{(\text{MVA})_{B,\text{new}}}{(\text{MVA})_{B,\text{old}}} \times \dfrac{(\text{kV})_{B,\text{old}}^2}{(\text{kV})_{B,\text{new}}^2}$

(d) $Z(\text{pu})\text{new} = Z(\text{pu})\text{old} \times \dfrac{(\text{MVA})_{B,\text{new}}}{(\text{MVA})_{B,\text{old}}} \times \dfrac{(\text{kV})_{B,\text{new}}^2}{(\text{kV})_{B,\text{old}}^2}$

4.4 If the transformer winding resistances and reactances are expressed in pu value then

(a) $R_1(\text{pu}) = R_2(\text{pu})$ and $X_1(\text{pu}) \neq X_2(\text{pu})$

(b) $R_1(\text{pu}) \neq R_2(\text{pu})$ and $X_1(\text{pu}) = X_2(\text{pu})$

(c) $R_1(\text{pu}) = \frac{1}{2} R_2(\text{pu})$ and $X_1(\text{pu}) = \frac{1}{2} X_2(\text{pu})$

(d) $R_1(\text{pu}) = R_2(\text{pu})$ and $X_1(\text{pu}) = X_2(\text{pu})$

4.5 If X_a is the armature reactance of a synchronous machine and X_l is the leakage reactance of the same machine then synchronous reactance X_s is

(a) $X_s = \frac{1}{2} X_a$ (b) $X_s = \frac{1}{2} (X_a - X_l)$

(c) $X_s = X_a + X_l$ (d) $X_s < X_a$

4.6 An Infinite bus in power system is

(a) a small system whose voltage varies with the power exchange between the synchronous machine and bus.

(b) a large system whose voltage and frequency varies with the power exchange between the synchronous machine and bus.

(c) a large system whose voltage and frequency remain constant independent of the power exchange between the synchronous machine and the bus.

(d) a large system with infinite voltage.

4.7 The per unit impedance of a circuit element is 0.30. If the base kV and base MVA are halved, then the new value of the per unit impedance of the circuit element will be

(a) 0.30 (b) 0.60

(c) 0.0030 (d) 0.0060

4.8 The power delivered by a synchronous generator to an infinite bus is given by

(a) $P = \frac{|N_t||E_f|}{R_a} \sin \delta$ (b) $P = \frac{|V_t||E_f|^2}{X_s} \sin \delta$

(c) $P = \frac{|V_t||E_f|}{X_s} \sin \delta$ (d) $P = \frac{|V_t||E_f|}{X_s} \cos \delta$

4.9 A synchronous machine is

(a) a single excited machine

(b) a doubly excited machine

(c) made to run at a speed less than N_s

(d) generally a lagging power factor machine

4.10 The per unit value of a 2 ohm resistor at 100 MVA base and 10 kV base voltage is

(a) 4 pu (b) 2 pu

(c) $\frac{1}{2}$ pu (d) 0.2 pu

4.11 The regulation of a line at full/load 08 pf lagging is 11.
A long line under no load conditions, for a good voltage profile needs
(a) Shunt resistance at receiving-end
(b) Shunt reactors at the receiving-end
(c) Shunt capacitors at receiving-end
(d) All of the above

4.12 For a 500 Hz frequency excitation, a 100 km long power line will be modelled as
(a) short line (b) medium line
(c) long line (d) none of the above

4.13 In a power system, the 3-phase fault MVA is always higher than the LG fault MVA at a bus.
(a) True (b) False

4.14 The charging current of a 400 kV line is more than that of a 220 kV line of the same length
(a) True (b) False

4.15 If in a line, resistance and reactance are found to be equal and regulation is zero, then load will have
(a) upf (b) zero pf
(c) 0.707 leading pf (d) 0.707 lagging pf

Chapter 5

Characteristic and Performance of Power Transmission Line

5.1 As the frequency of the system is increased, the charging MVAR.
(a) increases (b) decreases
(c) remains the same (d) none of the above

5.2 The receiving-end voltage for a long line under no load condition is
(a) less than the sending-end voltage
(b) more than the sending-end voltage
(c) equal to the sending-end voltage
(d) any of the above

5.3 For a given receiving-end voltage in a long transmission line, the sending-end voltage is more than the actual value calculated by
(a) Nominal-π method (b) Nominal-T method
(c) Load end capacitance method (d) None of the above

5.4 A short line with R/X ratio 1, the zero regulation is obtained when the power factor of the load is
(a) 0.5 (b) unity
(c) 0 leading (d) 0.707 leading

5.5 If the line is loaded with the surge impedance; the receiving-end voltage is
(a) less than the sending-end voltage
(b) equal to the sending-end voltage
(c) greater than the sending-end voltage
(d) none of these

5.6 The transfer of reactive power over a line mainly depends upon
(a) V_r (b) V_s
(c) $\mid V_s \mid - \mid V_r \mid$ (d) power angle

5.7 With 100% series compensation of lines
(a) low transient voltage
(b) high transient current
(c) the current is series resonant at power frequency
(d) (b) and (c)

5.8 The line constants of a transmission line are
(a) lumped (b) non-uniformly distributed
(c) uniformly distributed (d) none of these

5.9 Surge impedance of 400 Ω means
(a) line can be theoretically loaded upto 400 Ω
(b) line can be practically loaded upto 400 Ω
(c) open circuit impedance of 400 Ω
(d) short circuit impedance of 400 Ω

Chapter 6

Load Flow Studies

6.1 For load flow solutions, what are the quantities specified at load bus are
(a) P and $|V|$ (b) P and Q
(c) P and δ (d) Q and $|V|$

6.2 Load Flow study is carried out for
(a) Load frequency control (b) System planning
(c) Stability studies (d) Fault calculations

6.3 In the solution of load flow equation, Newton-Raphson (NR) method is superior to the Gauss-Seidel (GS) method, because the
(a) Convergence characteristic of the NR methods are not affected by selection of slack bus.
(b) Number of iterations required is not independent of the size of system in the NR method.
(c) Time taken to perform one iteration in the NR method is less when compared to the time taken in the GS method.
(d) Number of iteration required in the NR method is more than compared to that in the GS method.

6.4 At slack bus, which one of following combinations of variables is specified?
(a) $|V|, \delta$ (b) P, Q
(c) P, $|V|$ (d) Q, $|V|$

6.5 Normally Z_{Bus} matrix is a
(a) Null matrix (b) Sparse matrix
(c) Full matrix (d) Unity matrix

6.6 In loadflow analysis, the load at bus is represented as
(a) a voltage dependent impedance at bus.
(b) constant real and reactive powers drawn from bus.
(c) a constant impedance connected at bus.
(d) a constant current drawn from the bus.

6.7 In Gauss-Seidel method of power flow problem, the number of iterations may be reduced if the correction in voltage at each bus is multiplied by
(a) Gauss Constant (b) Acceleration constant
(c) Blocking factor (d) Deceleration constant

6.8 In load flow studies PV bus is treated as PQ bus when
(a) phase angle become high
(b) reactive power goes beyond limit
(c) voltage at the bus become high
(d) any of the above

6.9 In a power system the maximum number of buses are
(a) PV buses (b) Slack buses
(c) PQ buses (d) Any of the above

6.10 For accurate load flow calculations on large power systems, the best method is
(a) NR method (b) GS method
(c) Decoupled method (d) FDLR

Chapter 7

Optimal System Operations

7.1 In a two plant system, the load is connected to plant no 2. The loss coefficients.
(a) B_{11}, B_{12}, B_{22} are nonzero
(b) B_{11} is nonzero but B_{12} and B_{22} are zero
(c) B_{11} and B_{12} are nonzero but B_{22} is zero
(d) B_{11} and B_{22} are nonzero but B_{12} is zero

7.2 If the penalty factor of a plant is unity, its incremental transmission loss is
(a) 1.0 (b) – 1.0
(c) zero (d) none of above

7.3 Economic operation of power system is carried out on the basis of
(a) Equal incremental fuel cost (b) Equal area criterion
(c) Equal fuel cost criterion (d) All units sharing equal power

7.4 Unit Commitment is
(a) A must before we solve economic operation problem
(b) Is a short term problem of maintenance scheduling
(c) Is more meaningful for thermal units
(d) All above

7.5 For short term planning problem losses can be found out
(a) by using approximate loss formula
(b) by load flow studies
(c) by carrying out stability studies
(d) can be ignored

7.6 For long term hydrothermal problem
(a) head variation can be ignored
(b) transmission loss cannot be ignored
(c) unit commitment should be taken into account
(d) all above

7.7 For economic operation, the generator with highest positive incremental transmission loss will operate at
(a) The highest positive incremental cost of production
(b) The highest negative incremental cost of production
(c) The lowest positive incremental cost of production
(d) The lowest negative incremental cost of production

7.8 A two bus system has loss coefficient as

(a) $B_{11} = 0.03$ $B_{22} = 0.05$ $B_{12} = 0.001$, $B_{21} = -0.001$
(b) $B_{11} = 0.03$ $B_{22} = 0.005$ $B_{12} = -0.001$ $B_{21} = -0.001$
(c) $B_{11} = 0.02$ $B_{22} = 0.04$ $B_{12} = -0.01$ $B_{21} = 0.001$
(d) $B_{11} = 0.02$ $B_{22} = 0.05$ $B_{12} = 0.01$ $B_{21} = 0.015$

7.9 Incremental fuel cost in rupees per MWh for a plant consisting of two units are

$$\frac{dC_1}{dP_{G1}} = 0.20\, P_{G1} + 40.0$$

$$\frac{dC_2}{dP_{G2}} = 0.25\, P_{G2} + 30.0$$

where P_{G1} and P_{G2} (in MW) are power generated by both the units for a total demand of 250 MW The load shared by the two units are

(a) $P_{G1} = \frac{350}{3}$ MW and $P_{G2} = \frac{400}{3}$ MW
(b) $P_{G1} = 100$ MW and $P_{G2} = 250$ MW
(c) $P_{G1} = 125$ MW and $P_{G2} = 125$ MW
(d) $P_{G1} = 150$ MW and $P_{G2} = 100$ MW

7.10 Two plants generate power as given below. $P_{G1} = 50$ MW and $P_{G2} = 100$ MW respectively. If the loss coefficients of the two plants are given as $B_{11} = 0.002$, $B_{22} = 0.0015$, $B_{12} = -0.0011$. The power lost will be

(a) 20 MW (b) 15 MW
(c) 18 MW (d) 22 MW

Chapter 8

Automatic Generation and Voltage Control

8.1 Permissible change in power frequency is
(a) ± 0.5 Hz (b) ± 1 Hz
(c) ± 5 Hz (d) ± 10 Hz

8.2 Excitation voltage control is fast acting
(a) True (b) False

8.3 A control area constitutes coherent group of generators
(a) True (b) False

8.4 Transients in excitation control vanish very slowly
(a) True (b) False

8.5 Fill up the blanks
I. Turbine time constant lies in the range of _____ to _____

8.6 (a) $K_{sg} \times K_T$ is nearly equal to 1
(b) $K_{sg} \times K_T$ nearly equal to 0
(c) $K_{sg} \times K_T$ equal to ∞
(d) $K_{sg} \times K_T$ any value

8.7 Most of the Reheat units have a Generation Rate around
(a) 3% (b) 10%
(c) 0% (d) ∞

8.8 Zero steady state error can be achieved by using PI controller
(a) True (b) False

8.9 In central AGC of a given control area, the change in (error) in frequency
(a) Area control error (b) Volume control error
(c) Non linear control error (d) Optimal control error

8.10 Laplace transform of a impulse function is
(a) zero (b) one
(c) ∞ (d) undefined

Chapter 9

Symmetrical Fault Analysis

9.1 Transients in electric circuits normally disappears within a time equal to
(a) $4 \times$ time constant (b) $2 \times$ time constant
(c) $8 \times$ time constant (d) time constant

9.2 A short circuit occurs in a transmission line (neglect line capacitance) when the voltage wave is going through zero, the maximum possible momentary short circuit current corresponds to
(a) twice the maximum of symmetrical short circuit current
(b) the maximum of symmetrical short circuit current
(c) thrice the maximum of symmetrical short circuit current
(d) four times the maximum of symmetrical short circuit current

9.3 Which one of the following is correct
(a) $X''_d = X'_d = X_d$ (b) $X''_d < X'_d < X_d$
(c) $X''_d = \dfrac{X_d}{2}$ (d) $X''_d = \dfrac{X_d}{2}$

9.4 The pu synchronous reactance X_s (at rated MVA) of a turbo generator comes in the range
(a) 4.00 to 5.00 (b) 0.25 to 0.90
(c) 20 to 30 (d) 1.00 to 2.00

9.5 The three phase SC MVA to be interrupted by a circuit breaker in a power system is given by
(a) $\sqrt{3}$ × post fault line voltage in kV × SC current in kA
(b) $3 \times$ prefault line voltage in kV × SC current in kA
(c) $\sqrt{3}$ × prefault line voltage in kV × SC current in kA
(d) $\dfrac{1}{\sqrt{3}}$ × prefault line voltage in kV × SC current in kA

9.6 Fault level means
(a) voltage at the point of fault (b) fault current
(c) fault power factor (d) fault MVA

9.7 Fault calculations using computer are usually done by
(a) Y_{bus} Method (b) Z_{bus} Method
(c) None of the above (d) any of the above

9.8 When a line-to-ground fault occurs, the current in a faulted phase is 100 A. The zero sequence current in this case will be

(a) zero (b) 33.3 A

(b) 66.6 A (d) 100 A

9.9 The rated breaking capacity (MVA) of a circuit breaker is equal to

(a) the product of rate voltage (kV) and rated breaking current (kA)

(b) the product of rated voltage (kV) and rated symmetrical breaking current (kA)

(c) the product of breaking current (kA) and fault voltage (kV)

(d) twice the value of rated current (kA) and rated voltage (kV)

9.10 The following sequence currents were recorded in a power system under a fault condition

$$I_{\text{positive}} = j\ 1.753 \text{ pu}$$

$$I_{\text{negative}} = -j\ 0.6 \text{ pu}$$

$$I_{\text{zero}} = -j\ 1.153 \text{ pu}$$

The fault is

(a) line to ground (b) three phase

(c) line to line ground (d) line to line

Chapter 10
Symmetrical Components

10.1 For the fault analysis in power system, we use symmetrical components because
(a) the results are required in terms of symmetrical components
(b) the number of equations becomes smaller
(c) the sequence network do not have mutual coupling
(d) all the above

10.2 For a power transformer
(a) Positive sequence impedance is more than negative sequence and zero sequence impedances
(b) Positive, negative and zero sequence impedances are all equal
(c) Positive and negative sequence impedances are equal
(d) Positive sequence impedance is less

10.3 For measuring positive, negative and zero sequence voltages in a system, the reference is taken as
(a) Neutral of the system only
(b) Ground only
(c) For zero sequence neutral and for positive and negative the ground
(d) None of the above

10.4 The positive sequence component of voltage at the point of fault becomes zero when it is a
(a) three phase fault (b) line to line fault
(c) LLG fault (d) line to ground fault

10.5 Zero sequence currents can flow from a line into a transformer bank if the windings are in
(a) grounded star-delta (b) delta-star
(c) star-grounded star (d) delta-delta

10.6 Which of the following faults occurs most frequently
(a) Three phase (3L) faults (b) LLG faults
(c) Double line faults (d) Single line to ground faults

10.7 In the symmetrical component expression of voltages, we have

$$\begin{bmatrix} V_a \\ V_b \\ V_c \end{bmatrix} = [A] \begin{bmatrix} V_{a1} \\ V_{b2} \\ V_{a0} \end{bmatrix}$$

where matrix $[A]$ is

(a) $\begin{bmatrix} 1 & \alpha & 1 \\ \alpha^2 & \alpha & 1 \\ \alpha & \alpha^2 & 1 \end{bmatrix}$ (b) $\begin{bmatrix} 1 & \alpha & \alpha^2 \\ 1 & \alpha^2 & \alpha \\ 1 & \alpha & \alpha^2 \end{bmatrix}$

(c) $\begin{bmatrix} 1 & 1 & 1 \\ \alpha^2 & \alpha & 1 \\ \alpha & \alpha^2 & 1 \end{bmatrix}$ (d) $\begin{bmatrix} 1 & 1 & 1 \\ \alpha & \alpha^2 & 1 \\ \alpha^2 & \alpha & 1 \end{bmatrix}$

10.8 If X_s is self reactance of each line and X_n is mutual reactance of any line pair then positive sequence impedance of the transmission line is equal to

(a) $j(X_s + X_m)$ (b) $j(X_s - X_m)$
(c) jX_s (d) $-jX_m$

10.9 For a fully transposed transmission line

(a) equal positive and negative sequence impedances
(b) zero sequence impedance much larger than the positive sequence impedance
(c) both (a) and (b) are correct
(d) none of the above

10.10 The zero sequence impedance of a 3-ϕ transformer is shown below. The connection of its winding are

(a) delta-delta
(b) star-delta
(c) delta-star with neutral grounded
(d) star-star with both neutral grounded

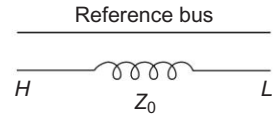

Chapter 11

Unsymmetrical Fault Analysis

11.1 The most frequently occurring fault in the power system are
(a) Single line to ground fault (b) Line to line (LL) fault
(c) Double line to ground fault (d) Symmetrical fault (3-ϕ fault)

11.2 In which type of faults given below, all the 3 components I_{a0}, I_{a1} and I_{a2} are equal
(a) Single line to ground fault (b) Line to line (LL) fault
(c) Double line to ground fault (d) None to the above

11.3 In which type of fault listed below, the positive and negative sequence voltages are equal ($V_{a1} = V_{a2}$)
(a) Line to line (LL) fault (b) Double line to ground fault
(c) Single line to ground fault (d) None of the above

11.4 In a transmission line there is a flow of zero sequence current when
(a) there is an occurrence of overvoltage on line due to a charged cloud
(b) line to line fault
(c) 3-phase fault
(d) double line to ground fault

11.5 Which of the following network gets affected by the method of neutral grounding
(a) zero sequence network
(b) positive sequence network
(c) negative sequence network
(d) all of the above

11.6 During the analysis of a fault, the symmetrical components are used because
(a) The results are required in terms of symmetrical components
(b) The sequence network do not have any mutual coupling
(c) The number of equations becomes smaller
(d) All of the above

11.7 Choose the correct one from the statement given below
(a) There is a minimum zero sequence voltage and maximum negative sequence voltage at the fault point and increase and decrease respectively towards the neutral

(b) The zero and negative sequence voltages are maximum at fault point toward neutral
(c) The zero and negative sequence voltages are minimum at fault point and increases towards neutral
(d) None of the above

11.8 For a single line to ground fault the zero sequence current is given by j 3.0 pu. The current carried by the neutral during the fault is
(a) j 1.0 pu (b) j 3.0 pu
(c) j 9.0 pu (d) j 6.0 pu

11.9 When a fault occurs in a power system the zero sequence component of current becomes zero. The type of fault is
(a) three phase to ground fault (b) double line fault
(c) double line to ground fault (d) single line to ground fault

11.10 When a fault occurs in a power system the following sequence currents are recorded.

$$I_{\text{zero}} = -j\ 1.246 \text{ pu}$$
$$I_{\text{positive}} = j\ 1.923 \text{ pu}$$
$$I_{\text{negative}} = -j\ 0.8 \text{ pu}$$

The fault is
(a) line to ground (b) line to line
(c) line to line to ground (d) three-phase

Chapter 12

Power System Stability

12.1 The study of steady state stability is concerned with the upper limit of machine loadings before losing synchronism when the load is gradually increased

(a) True (b) False

12.2 When there is a sudden disturbance in the power system, rotor speed, rotor angular difference and power transfer undergo fast changes whose magnitude depends upon the severity of disturbance, it comes under the study of

(a) dynamic stability (b) transient stability

(c) steady state stability (d) none of the above

12.3 When $\left(\frac{\partial P}{\partial \delta}\right)$ synchronizing coefficient is positive, the torque angle increases on small power increment and the synchronism is soon lost

(a) True (b) False

12.4 For transient stability analysis, as long as equal area criterion is satisfied, the maximum angle to which rotor angle can oscillate is

(a) 90° (b) 45°

(c) greater than 90° (d) less than 90°

12.5 For a turbo alternator of 100 MVA, the inertia constant is 5. The value of H for a alternator of 50 MVA is

(a) 8 (b) 12

(c) 10 (d) 15

12.6 By using the method of equal area criterion, we get the information about

(a) swing curves (b) stability region

(c) relative stability (d) absolute stability

12.7 For a power system we can improve the steady state stability limit by

(a) single pole switching

(b) reducing fault clearing time

(c) using double circuit line instead of single circuit line

(d) decreasing the generator inertia

12.8 For a fault in a power system, the term critical clearing time is related to
(a) reactive power limit (b) transient stability limit
(c) short circuit current limit (d) steady state stability limit

12.9 A shunt reactor is added at the infinite bus, which is fed by the synchronous generator. The stability limit will
(a) decrease (b) increase
(c) remains the same (d) any of the above

12.10 For stable operation, the normal value of δ normally lies between
(a) 0 to 30° (b) 0 to 90°
(c) 0 to 60° (d) 0 to 180°

Chapter 13

Power System Transients

13.1 Transient phenomenon last in a power system for a period ranging from
(a) few ms to 1 second (b) 1 second to 2 second
(c) 2 second to 3 second (d) greater than 3 second

13.2 The main cause of momentary excessive voltages and current are
1. Lightening 2. Switching
3. Short circuit 4. Resonance

Out of these the most common and most severe causes are
(a) 1 and 3 (b) 1 and 2
(c) 4 and 2 (d) 3 and 4

13.3 The reflection of surges at open line ends (transformer ends) leads to voltage build up, which may eventually damage the high voltage equipment.
(a) True (b) False

13.4 A major part of short circuit takes place on exposed overhead lines, due to the insulation failure caused by the surge phenomenon
(a) True (b) False

13.5 Lightening arrester should be located
(a) near the circuit breaker (b) away from the circuit breaker
(c) near the transformer (d) away from the transformer

13.6 In a power system lightening arresters are used to protect the electrical equipment against
(a) power frequency of over-voltages
(b) direct strokes of lightening
(c) overcurrent due to lightening stroke
(d) overvoltages due to indirect lightening stroke

13.7 In an Extra High Voltage overhead transmission line earth wire is provided to protect the line against
(a) switching surge (b) lightening surge
(c) corona effect (d) ensure fault voltages

13.8 During among faults in a power system severe overvoltages are produced with neutral
(a) solidly earthed
(b) isolated
(c) earthed through an inductive coil
(d) earthed through a low resistance

13.9 Consider the following statement about ground wires

1. Ground wire helps to increase the effective capacitance between the line conductor and ground
2. It shields the main conductor against direct strokes
3. It is placed higher than the main conductors and supported on the same tower
4. It helps to reduce the risk of back flash over in case of direct strokes

(a) 1 and 2 one correct (b) 2 and 3 are correct
(c) 1, 2 and 4 are correct (d) 1, 2, 3, 4 are correct

13.10 Switching over voltages may be caused by the

1. Sustained earth fault on phase conductors
2. Energization or reclosure of long lines
3. Load Rejection at the receiving-end
4. Fault initiation and

(a) 1 and 2 (b) 2 and 3
(c) 1, 2 and 3 (d) 1, 2, 3 and 4

Chapter 14

Circuit Breakers

14.1 The voltage that appears across the contacts after the circuit breaker is opened
(a) recovery voltage (b) arc voltage
(c) break open voltage (d) surge voltage

14.2 For circuit breaker the rated breaking capacity is equal to
(a) the product of breaking current and fault voltage
(b) the product of rated breaking current (kA) and rated voltage
(c) the product of rated symmetrical breaking current (kA) and rated voltage
(d) twice the value of rated current and rated voltage

14.3 The opening of magnetizing current of unloaded transformer (or line reactor) leads to current chopping, which has associated high rate of voltage rise
(a) True (b) False

14.4 Switching of capacitance loads (capacitor loads or unloaded lines) can lead to arc restriking in circuit breakers
(a) True (b) False

14.5 For an arc to be stable in vacuum it will depend upon
(a) circuit parameters only
(b) contact material only
(c) the contact material and its vapour pressure
(d) (a) and (b)

14.6 To minimize the current chopping tendency, the SF_6 gas is used at
(a) high velocity and low pressure
(b) low velocity and low pressure
(c) high velocity and high pressure
(d) low velocity and high pressure

14.7 The circuit breaker preferred when the current to be interrupted is low with high voltage arcs
(a) Oil circuit breaker (b) Air break circuit breaker
(c) Minimum oil circuit breaker (d) Vacuum circuit breaker

14.8 For a short line fault without switching resistor, the most suitable circuit breaker is

(a) Minimum oil circuit breaker (b) SF6 circuit breaker

(c) Air blast circuit breaker (d) None of the above

14.9 In air blast circuit breaker an internal source of energy for arc extinction is employed

(a) True (b) False

14.10 Which of the following properties are associated with SF6 circuit breaker

1. At atmospheric pressure its dielectric strength is 2 to 3 times of air.
2. Its molecules absorbs free electrons in the air path
3. Its arc time is few ms
4. Its heat capacity below 6000°K is much larger than that of air

(a) 1 and 3 (b) 2 and 3

(c) 3 and 4 (d) All the four properties

Chapter 15

Power System Protection

15.1 Mho relay is usually employed for the protection of
(a) short lines (b) medium lines
(c) long lines (d) any line

15.2 Reactance relay is normally used for protection against
(a) phase faults only (b) earth faults only
(c) any fault (d) series faults only

15.3 A large-size synchronous generator is protected against overloads by
(a) overcurrent relay, (b) mho relay
(c) temperature sensitive relay (d) Buchholz relay

15.4 A Buchholz relay is used for
(a) transformer (b) alternator
(c) induction motor (d) HVDC line

15.5 While energizing a transformer, to prevent the maloperation of a differentially connected relay, the relay restrained coil is biased with
(a) third harmonic current (b) second harmonic current
(c) seventh harmonic current (d) fifth harmonic current

15.6 Match list-I and list-II and select the correct answers. Using the codes below in the list

(I) (Relay used)	(II) (Equipment)
A. Mho Relay	1. Transformer
B. Negative sequence Relay	2. Motor
C. Thermal Relay	3. Generator
	4. Transmission Line

Codes:

(a)	A	B	C	(b)	A	B	C
	1	2	4		2	4	3
(c)	A	B	C	(d)	A	B	C
	4	2	2		3	1	2

15.7 A distance relay measures
(a) difference in voltage (b) difference in impedance
(c) difference in current (d) difference in phase

15.8 Under the poles of an induction disc relay the disc rotates from
(a) shaded pole to unshaded pole
(b) unshaded pole to shaded pole
(c) depends upon CT secondary connection
(d) depends upon magnitude of current

15.9 A series compensated overhead line is protected by using
(a) Reactance Relay (b) Impedance Relay
(c) Mho Relay (d) None of the above

15.10 For a 3-phase line, the complete protection is provided by
(a) Three phase and two earth fault relays
(b) Three phase and three earth fault relays
(c) Two phase and one earth fault relays
(d) Two phase and two earth fault relays are required

Chapter 16

Cables

16.1 The insulation resistance of a single core cable is 160 MΩ/km. The insulation resistance for 4 km length is
(a) 80 MΩ (b) 40 MΩ
(c) 120 MΩ (d) 320 MΩ

16.2 The electrostatic stress in a single core belted cable is
(a) same throughout the insulation layer
(b) minimum at conductor surface and maximum at sheath
(c) maximum at conductor surface and minimum at sheath
(d) none of the above

16.3 A cryoresistive cable works at
(a) normal temperature (b) zero temperature
(c) any temperature (d) cryogenic temperature

16.4 The surge impedance of an underground cable is around
(a) 400 ohms (b) 25 ohms
(c) 50 ohms (d) 100 ohms

16.5 When the diameter of the core and cable is doubled, the value of capacitance
(a) will be reduced to half (b) will be reduced to one-fourth
(c) will be doubled (d) remains unchanged

16.6 Copper as conductor for cables is used as
(a) hard drawn (b) hardened and tempered
(c) annealed (d) alloy with chromium

16.7 EHV cables are filled with thin oil under pressure
(a) to prevent entry of air and moisture
(b) to strengthen the cable conductor
(c) to provide extra insulation
(d) to avoid formation of voids

16.8 At bridge crossings and near the railway tracks ternary lead alloy cables are used since
(a) It has low specific gravity
(b) It has high tensile strength
(c) It has low coefficient of thermal expansion
(d) It can withstand shocks and vibrations

16.9 The insulating material most commonly used for power cable is
(a) paper (b) PVC
(c) rubber (d) oil

16.10 The loss angle of a cable is δ. The power factor is
(a) cos δ (b) tan δ
(c) δ (d) sin δ

Chapter 17
Insulators

17.1 A string insulator has 4 units. The voltage across the bottom most unit is 30% of the total voltage. Its string efficiency is
(a) 30% (b) 60%
(c) 75% (d) 83.33%

17.2 Grading ring is used to equalize the potential distribution across the units of the suspension insulator because it
(a) forms capacitances which help to cancel the charging current from link pins.
(b) forms capacitances with link pins to cancel the charging current from link pins.
(c) increases the capacitances of lower insulator units.
(d) decreases the capacitances of upper insulator units.

17.3 Which of the following insulators is used in transmission lines at the river and road crossings
(a) Pin type insulator (b) Suspension type insulator
(c) Strain type insulator (d) Both (a) and (b)

17.4 Pin type insulators are made in one piece upto
(a) 30 kV (b) 25 kV
(c) 11 kV (d) 50 kV

17.5 Which of the following is not a method of voltage equalization in a string insulator
(a) Increasing the length of cross arm
(b) Grading of the units
(c) Static shielding
(d) Connecting two discs in parallel

17.6 The materials used for porcelain are
(a) silica 40%, feldspar 20% and clay 40%
(b) silica 20%, feldspar 30% and clay 50%
(c) silica 20%, glass 30% and clay 50%
(d) none of the above

17.7 The pin type insulators are uneconomical beyond
(a) 11 kV (b) 33 kV
(c) 50 kV (d) 60 kV

17.8 The cost of a pin type insulator beyond 50 kV is given by (where $x > 2$)
(a) cost $\propto I^x$ (b) cost $\propto V$
(c) cost $\propto (VI)$ (d) cost $\propto V^x$

17.9 The design of insulation for power system above 400 kV, is based upon
(a) lightening overvoltages (b) switching surges
(c) system voltage level (d) system load level

17.10 A suspension type insulator has three units with self-capacitance C and ground capacitance of 0.2 C having a string efficiency of
(a) 78% (b) 80%
(c) 82% (d) 84%

Chapter 18

Mechanical Design of Transmission Lines

18.1 Temperature increase produces the following effect on a transmission line
(a) sag and tension of conductor decreases
(b) sag and tension of conductor increases
(c) sag increases and tension of the conductor decreases
(d) sag decreases and tension of the conductor increases

18.2 The knowledge of maximum sag is essential in determining the
(a) ground clearance of the conductor
(b) maximum span of the conductor
(c) maximum stress on the conductor
(d) none of the above

18.3 Stringing chart is used in transmission lines for
(a) for designing the tower
(b) for calculating the sag in the conductor
(c) determining the distance between the conductor
(d) in the design of insulator string

18.4 High voltage lines has a span of approximately
(a) 200 mt (b) 400 mt
(c) 300 mt (d) 800 mt

18.5 By increasing the sag on the transmission line, the tension
(a) increases (b) decreases
(c) not affected (d) may increase or decreases

18.6 The value of tower footing resistance is influenced by driven rods having
(a) larger length (b) good material
(c) larger cross-section (d) none of the above

18.7 The effect of ice covering is to increase the weight of the conductor and hence to increase the vertical sag
(a) True (b) False

18.8 The two factors which vary the sag and tension are temperature and elasticity
(a) True (b) False

18.9 The minimum clearance above the ground of the lowest conductor, for low and medium voltages lines, across a street may be

(a) 6 mt (b) 7.791 mt

(c) 8.591 mt (d) 6.791 mt

18.10 For the ground clearance required height is 7.5 mt with a sag of 2.5 mt, the height above the ground is

(a) 6.1 mt (b) 8.5 mt

(c) 10.591 mt (d) 9.9 mt

Chapter 19

Corona

19.1 At NTP, the breakdown strength of air is
(a) 30 kV rms/cm (b) 30 kV peak/cm
(c) 30 kV rms/m (d) 30 kV peak/m

19.2 As compared to plains, the corona loss in hilly areas is
(a) less (b) more
(c) remains the same (d) none of the above

19.3 The corona loss in a 50 Hz system is 0.3 kW/ph/km. At a frequency of 60 Hz the corona loss would be
(a) 0.3 kW/ph/km (b) 0.36 kW/ph/km
(c) zero (d) cannot be determined

19.4 Corona loss is less when the shape of the conductor is
(a) flat (b) circular
(c) oval (d) independent of shape

19.5 The effect of the bonding of the cable is
(a) to increase the effective R but reduce L
(b) to increase the effective R and L
(c) to decrease the effective R and L
(d) to decrease the effective R but increase the inductance L

19.6 During corona along with hissing noise a smell of following gas also comes
(a) O_2 (b) O_3
(c) H_2 (d) H_2S

19.7 Corona loss is directly proportional to
(a) f^2 (b) f^3
(c) f (d) f^{-1}

19.8 Corona also acts as a
(a) safety valve (b) transformer
(c) insulator (d) relay

19.9 Corona is affected by
(a) number of ions (b) size and charge per ion
(c) air density (d) all above

19.10 Relative air density δ_0 is given by

(a) $\dfrac{3.92b}{273+t}$ (b) $\dfrac{3.92}{273+b}$

(c) $\dfrac{3.92b}{273}$ (d) $\dfrac{3.92b}{t}$

Chapter 20

HVDC

20.1 The first commercially used HVDC link was built in
(a) 2006 (b) 1954
(c) 1886 (d) yet to be built

20.2 Reactive power to HVDC system may be supplied from
(a) AC filters (b) Shunt capacitors
(c) SVS (d) All above

20.3 Two AC systems can be connected through a zero length DC link
(a) True (b) False

20.4 Such a connection (Question 20.3) is called
(a) front to front connection (b) back to back connection
(c) front to back connection (d) back to front connection

20.5 Normal value of breakeven distance in DC transmission is around
(a) 70 km (b) 700 km
(c) 7000 km (d) any distance

20.6 HVDC transmission lines are more economical for
(a) short distance transmission (b) long distance transmission
(c) any distance transmission (d) interconnected systems

20.7 As compared to an HVAC line, the corona and radio interference on a HVDC line are
(a) lower (b) more
(c) the same (d) none of above

20.8 In 12 pulse valve group operation, the most troublesome harmonics on AC side are
(a) 24rd and 25th (b) 3rd and 5th
(c) 11th and 13th (d) none

20.9 Which one of the following in untrue for HVDC transmission?
(a) corona loss is much more than a HVAC
(b) back-to-back connection is possible
(c) distance limitation exists
(d) extra reactor power has to be supplied

20.10 In HVDC converter station equipment using thyristors, it is necessary to use a large number of thyristors in series because

(a) voltage ratings of thyristors are low
(b) current ratings of thyristors are low
(c) thyristors always fail to an internal open circuit
(d) none of the above

Chapter 21

Distribution

21.1 Which distribution system in more reliable
(a) tree (b) ring main
(c) radial (d) all above

21.2 A bus bar is rated by
(a) current and voltage only
(b) current only
(c) current, voltage and frequency
(d) any one of above

21.3 Which of the following equipment is not installed in a substation
(a) shunt reactors (b) excitors
(c) voltage transformers (d) series capacitors

21.4 For a given power delivered, if the working voltage of a distributor line is increased to m times, the cross sectional area 'a' of distributor line would be reduced to

(a) $\frac{1}{m^2}\ a$ (b) $\frac{1}{m}\ a$

(c) $\frac{1}{2m}\ a$ (d) m/a

21.5 Size of conductor in Distribution system is found out using
(a) Ohm's law (b) Kirchoff's law
(c) Kelvin's law (d) Faraday's law

21.6 Most commonly used distribution system is
(a) Radial (b) Parallel
(c) Ring (d) Mesh

21.7 If the power is transmitted in DC 2-wire system the volume of the two conductors used will be
(a) inversely proportional to the square of voltage
(b) directly proportional to the power transmitted
(c) directly proportional to the square of the length of conductor
(d) all of the above

21.8 In the radial distribution system the distributor is fed
(a) from the centre (b) from both ends
(c) at different points (d) from one end

21.9 In the ring main distribution system, the distributor is fed
(a) by two feeder (b) by one feeder
(c) by four feeder (d) at different points

21.10 The radial distribution system is adopted when
(a) the electrical energy is generated at low voltage
(b) the power station is situated at the centre of load
(c) the distributor end nearest to the supply is to be kept heavily loaded
(d) both (a) and (b)

Chapter 22

Voltage Stability

22.1 The highest transmission voltage used in India is
(a) 400 kV (b) 765 kV
(c) 220 kV (d) 500 kV

22.2 Allowed voltage variation is
(a) ± 10% (b) ± 5%
(c) ± 15% (d) any value

22.3 Which of the following leads to voltage instability
(a) transfer of reactive power (b) transfer of active power
(c) transfer of complex power (d) transfer of apparent power

22.4 A long line with no load
(a) generates capacitive reactive power
(b) generates inductive reactive power
(c) does not generate any power
(d) generates both active and reactive power

22.5 A synchronous condenser (dynamic compensator)
(a) decreases short circuit capacity
(b) increases short circuit capacity
(c) has no effect on short circuit capacity
(d) is nothing but synchronous motor running at no load

22.6 Voltage instability is also sometimes called voltage collapse
(a) True (b) False

22.7 Deregulation has increased the likelihood of voltage instability
(a) True (b) False

22.8 Voltage instability occurs when the system Z is such that
(a) $\frac{dv}{dz} = \infty$ (b) $\frac{dz}{dv} = 0$
(c) $\frac{dv}{dz} = 1$ (d) $\frac{dv}{dz}$ = any value

22.9 Strategic load shedding provides costliest way of preventing widespread voltage collapse
(a) True (b) False

22.10 Effect of HVDC transmission in power system
(a) improves voltage stability (b) causes voltage collapse
(c) has no effect (d) none of the above

Answers

CHAPTER 1

1.1 (b)	**1.2** (c)	**1.3** (c)	**1.4** (b)	**1.5** (d)
1.6 (c)	**1.7** (a)	**1.8** (c)	**1.9** (b)	**1.10** (d)
1.11 (b)	**1.12** (a)	**1.13** (a)	**1.14** (d)	**1.15** (d)

CHAPTER 2

2.1 (b)	**2.2** (c)	**2.3** (c)	**2.4** (d)	**2.5** (c)
2.6 (d)	**2.7** (c)	**2.8** (d)	**2.9** (d)	**2.10** (b)
2.11 (d)				

CHAPTER 3

3.1 (a)	**3.2** (b)	**3.3** (c)	**3.4** (a)	**3.5** (b)
3.6 (a)	**3.7** (d)	**3.8** (c)	**3.9** (b)	**3.10** (c)

CHAPTER 4

4.1 (b)	**4.2** (b)	**4.3** (c)	**4.4** (d)	**4.5** (c)
4.6 (c)	**4.7** (b)	**4.8** (c)	**4.9** (b)	**4.10** (b)
4.11 (b)	**4.12** (c)	**4.13** (a)	**4.14** (a)	**4.15** (c)

CHAPTER 5

5.1 (a)	**5.2** (b)	**5.3** (a)	**5.4** (d)	**5.5** (b)
5.6 (c)	**5.7** (d)	**5.8** (b)	**5.9** (a)	

CHAPTER 6

6.1 (b)	**6.2** (b)	**6.3** (a)	**6.4** (a)	**6.5** (c)
6.6 (b)	**6.7** (b)	**6.8** (b)	**6.9** (c)	**6.10** (a)

CHAPTER 7

7.1 (b)	**7.2** (c)	**7.3** (a)	**7.4** (d)	**7.5** (a)
7.6 (d)	**7.7** (c)	**7.8** (b)	**7.9** (a)	**7.10** (b)

CHAPTER 8

8.1 (a)	**8.2** (a)	**8.3** (a)	**8.4** (b)	**8.5** 0.2 to 2.5
8.6 (a)	**8.7** (a)	**8.8** (a)	**8.9** (a)	**8.10** (b)

CHAPTER 9

9.1 (a)	**9.2** (a)	**9.3** (b)	**9.4** (d)	**9.5** (c)
9.6 (d)	**9.7** (b)	**9.8** (b)	**9.9** (b)	**9.10** (c)

CHAPTER 10

10.1 (c)	**10.2** (b)	**10.3** (d)	**10.4** (a)	**10.5** (a)
10.6 (d)	**10.7** (c)	**10.8** (b)	**10.9** (c)	**10.10** (d)

CHAPTER 11

11.1 (a)	**11.2** (a)	**11.3** (b)	**11.4** (d)	**11.5** (a)
11.6 (b)	**11.7** (b)	**11.8** (c)	**11.9** (b)	**11.10** (c)

CHAPTER 12

12.1 (a)	**12.2** (b)	**12.3** (b)	**12.4** (c)	**12.5** (c)
12.6 (d)	**12.7** (c)	**12.8** (b)	**12.9** (c)	**12.10** (a)

CHAPTER 13

13.1 (a)	**13.2** (b)	**13.3** (a)	**13.4** (a)	**13.5** (c)
13.6 (d)	**13.7** (b)	**13.8** (b)	**13.9** (d)	**13.10** (d)

CHAPTER 14

14.1 (a)	**14.2** (c)	**14.3** (a)	**14.4** (a)	**14.5** (d)
14.6 (b)	**14.7** (d)	**14.8** (b)	**14.9** (b)	**14.10** (d)

CHAPTER 15

15.1 (c)	**15.2** (b)	**15.3** (c)	**15.4** (a)	**15.5** (b)
15.6 (c)	**15.7** (b)	**15.8** (b)	**15.9** (d)	**15.10** (c)

CHAPTER 16

16.1 (b) **16.2** (c) **16.3** (d) **16.4** (c) **16.5** (b)
16.6 (c) **16.7** (d) **16.8** (a) **16.9** (a) **16.10** (d)

CHAPTER 17

17.1 (d) **17.2** (a) **17.3** (c) **17.4** (b) **17.5** (d)
17.6 (b) **17.7** (b) **17.8** (d) **17.9** (b) **17.10** (a)

CHAPTER 18

18.1 (c) **18.2** (a) **18.3** (b) **18.4** (c) **18.5** (b)
18.6 (a) **18.7** (a) **18.8** (a) **18.9** (d) **18.10** (d)

CHAPTER 19

19.1 (b) **19.2** (b) **19.3** (b) **19.4** (b) **19.5** (a)
19.6 (b) **19.7** (c) **19.8** (a) **19.9** (d) **19.10** (a)

CHAPTER 20

20.1 (b) **20.2** (d) **20.3** (a) **20.4** (b) **20.5** (b)
20.6 (b) **20.7** (a) **20.8** (c) **20.9** (a) **20.10** (a)

CHAPTER 21

21.1 (b) **21.2** (a) **21.3** (b) **21.4** (a) **21.5** (c)
21.6 (a) **21.7** (d) **21.8** (d) **21.9** (a) **21.10** (b)

CHAPTER 22

22.1 (b) **22.2** (b) **22.3** (a) **22.4** (a) **22.5** (b) and (d)
22.6 (a) **22.7** (a) **22.8** (a) and (b) **22.9** (b) **22.10** (a)

Answers to Problems

CHAPTER 1

1.1 3360 MWh, 280 MW, 80 MW, 6720 MW, 96000 MW, 0.7142

1.2 (a) Rs 1400, Rs 2.8/kWh,
(b) Rs 1616.66, Rs 2.6944/kWh
(c) Rs 1277.6, Rs 2.552/kWh

CHAPTER 2

2.1 $L_{int} = \frac{1}{2} \times 10^{-7} \times \frac{1}{(r_2^2 - r_1^2)^2} \left[(r_2^4 - r_1^4) - 4r_1^2 (r_2^2 - r_1^2) + 4r_1^4 \ln \frac{r_2}{r_1} \right]$

2.2 0.658 ohm/km

2.3 $L = \frac{\mu}{2\pi} \ln (R/r)$ H/m

2.4 260.3 V/km

2.5 $H_P = \frac{-I}{3\pi d}$ AT/m^2 (directed upwards)

2.6 $X = \left[\frac{(X_1 - X_{12})(X_2 - X_{12})}{X_1 + X_2 - 2X_{12}} \right]$

2.7 0.00067 mH/km, 0.0314 V/km

2.8 0.0044 $\angle 140^\circ$ mH/km, 0.553 $\angle 140^\circ$ V/km

2.9 0.346 ohm/km

2.10 1.48 m

2.11 0.191 ohm/km/phase

2.12 0.455 mH/km/phase

2.13 2.38 m

2.14 (i) 0.557 $d^{1/2} A^{1/4}$
(ii) 0.633 $d^{2/3} A^{1/6}$
(iii) 0.746 $d^{3/4} A^{1/8}$

CHAPTER 3

3.1 $q_a = \dfrac{2\pi k\,|V|\left[\ln\dfrac{r}{2D}\angle 30^\circ - \ln\dfrac{D}{2r}\angle -30^\circ\right]}{2\ln\left(\dfrac{D}{r}\right)\ln\left(\dfrac{r}{2D}\right) - \ln\left(\dfrac{2D}{r}\right)\ln\left(\dfrac{D}{2r}\right)}$ F/m

$I_a = 2\pi f q_a \angle 90^\circ$ A

3.2 0.0204 μF/km
3.3 0.0096 μF/km
3.4 0.0103 μF/km to neutral
3.5 3.08×10^{-5} Coulomb/km
3.6 5.53×10^{-6} mho/km
3.7 8.54×10^{3} ohm/km
3.8 8.72×10^{-3} μF/km
3.9 71.24 kV

CHAPTER 4

4.1 12 kV

CHAPTER 5

5.1 (a) 992.75 kW (b) No solution possible
5.2 $A' = 0.9\angle 1.5^\circ$, $B' = 239.9\angle 66.3^\circ$, $C' = 0.001\angle 102.6^\circ$, $D' = 0.85\angle 1.96^\circ$
5.3 (a) $0.978\angle 0.5^\circ$, $86.4\angle 68.6^\circ$, $0.00056\angle 90.2^\circ$, $0.978\angle 0.5^\circ$
(b) 165.44 kV, $0.244\angle -28.3^\circ$ kA, 0.808 lagging, 56.49 MW
(c) 70.8%
(d) 28.15%
5.4 (a) 273.5 MVA
(b) 1174 A
(c) 467.7 MVA
5.5 133.92 kV, 23.12 MW
5.6 202.2 kV
5.7 At $x = 0$; $i_{x_1} = 0.314\cos(\omega t - 21.7^\circ)$, $i_{x_2} = 0.117\cos(\omega t + 109^\circ)$
At $x = 200$ km; $i_{x_1} = 0.327\cos(\omega t - 9.3^\circ)$, $i_{x_2} = 0.112\cos(\omega t + 96.6^\circ)$
5.8 $135.8\angle 7.8^\circ$ kV, $0.138\angle 15.6^\circ$ kA, 0.99 leading 55.66 MW, 89.8%, $373.1\angle -1.5^\circ$, 3338 km, 166900 km/s
5.9 $Z' = 128.3\angle 72.6^\circ$ $Y'/2 = 0.00051\angle 89.5^\circ$
5.10 7.12°, $pf_1 = 0.7$ lagging, $pf_2 = 0.74$ lagging
5.11 47.56 MVAR lagging

5.12 10.97 kV, 0.98 leading, – 0.27%, 86.2%

5.13 51.16 kV, 38.87 MVAR leading, 40 MW

5.14 238.5 kV, $P_s + j\,Q_s = 53 - j10$, pf = 0.983 leading

5.15 17.39 MVAR leading, 3.54 MW

CHAPTER 6

6.1 For this network tree is shown in Fig. 6.9; A is given by equation (6.20). The matrix is not unique. It depends upon the orientation of the elements.

6.2 $V_2^1 = 0.972 \angle -8.15^\circ$

6.3 $V_2^1 = 1.26 \angle -74.66^\circ$

6.4 (a)

$A =$

bus / e	1	2	3	4
1	1	0	0	0
2	0	1	0	0
3	0	0	1	0
4	0	0	0	1
—	—	—	—	—
5	0	0	1	–1
6	–1	0	0	1
7				
8	0	–1	0	1
9	–1	0	1	0

Note: Elements joining each bus to the ground node from the tree

(b)

$$Y = \begin{bmatrix} j\,0.3049 & & & & & & & & \\ & j\,0.1694 & & & & & & & \\ & & j\,0.1948 & & & & & & \\ & & & j\,0.3134 & & & & & \\ & & & & 0.807 - j\,5.65 & & & & \\ & & & & & 0.645 - j\,4.517 & & & \\ & & & & & & 0.968 - j\,6.776 & & \\ & & & & & & & 0.968 - j\,6.776 & \\ & & & & & & & & 0.88 - j\,6.16 \end{bmatrix}$$

(c)

$$\begin{bmatrix} 2.493 - j\,17.148 & |-0.968 + j\,6.776| & -0.880 + j\,6.610 & |-0.645 + j\,4.517| \\ 0.968 + j\,6.776 & |1.936 - j\,13.383| & 0 & |-0.968 + j\,6.776 \\ -0.880 + j\,6.160 & 0 & 1.687 - j\,11.615 & -0.807 + j\,5.650 \\ -0.645 + j\,4.517 & |-0.968 + j\,6.776| & -0.807 + j\,5.650 & |2.420 - j\,16.630 \end{bmatrix}$$

6.5 $P_{12} = -0.598$ pu; $P_{13} = 0.2$ pu; $P_{23} = 0.796$ pu
$Q_{12} = Q_{21} = 0.036$ pu; $Q_{13} = Q_{31} = 0.004$ pu;
$Q_{23} = Q_{32} = 0.064$ pu

6.6 (a) $P_{12} = -0.58$ pu; $P_{13} = 0.214$ pu; $P_{23} = 0.792$ pu
$Q_{12} = -0.165$ pu; $Q_{21} = 0.243$ pu; $Q_{13} = 0.204$ pu
$Q_{31} = -0.188$ pu; $Q_{23} = 0.479$ pu; $Q_{32} = -0.321$ pu

(b) $P_{12} = -0.333$ pu; $P_{23} = 0.664$ pu; $P_{31} = -0.333$ pu
$Q_{12} = Q_{21} = 0.011$ pu; $Q_{13} = Q_{31} = 0.011$ pu;
$Q_{23} = Q_{32} = 0.044$ pu

6.7 (a) (i) $\begin{bmatrix} -j10.1015 & j5.0505 & j5 \\ j5.0505 & -j10 & j5 \\ j5 & j5 & -j10 \end{bmatrix}$

(ii) $\begin{bmatrix} -j10 & 5\angle 93^\circ & j5 \\ 5\angle 87^\circ & -j10 & j5 \\ j5 & j5 & -j10 \end{bmatrix}$

(b) (i) $P_{12} = 0.600$ pu; $P_{13} = 0.202$ pu; $P_{23} = 0.794$ pu
$Q_{12} = 0.087$ pu; $Q_{21} = -0.0141$ pu;
$Q_{13} = Q_{31} = 0.004$ pu; $Q_{23} = Q_{32} = 0.064$ pu

(ii) $P_{12} = -0.685$ pu; $P_{13} = 0.287$ pu; $P_{23} = 0.711$ pu
$Q_{12} = 0.047$ pu; $Q_{13} = 0.008$ pu; $Q_{23} = 0.051$ pu

6.8 $V_3' = 1.025 - j\,0.095 = 1.029\angle -5.3^\circ$ pu

CHAPTER 7

7.1 Rs 22.5/hr

7.2 (a) $P_{G1} = 140.9$ MW $P_{G2} = 159.1$ MW
(b) Net Saving = Rs 218.16/day

7.3 (i) Generator A will share more load than Generator B
(ii) Generator A and Generator B will share load of P_G, and
(iii) Generator B will share more load than Generator A

7.4 $P_{G1} = 148$ MW, $P_{G2} = 142.9$ MW, $P_{G3} = 109.1$ MW

7.5 $(dC/dP_G) = 0.175\,P_G + 23$

7.6 (a) $P_{G1} = 138.89$ MW, $P_{G2} = 150$ MW, $P_D = 269.6$ MW
(b) $P_{G1} = 310.8$ MW, $P_{G2} = 55.4$ MW
(c) part (a): $C_T =$ Rs 6465.14/hr
(d) part (a): $C_T =$ Rs 7708.15/hr

7.7 $B_{11} = 0.03387$ pu or 0.03387×10^{-2} MW^{-1}
$B_{12} = 9.6073 \times 10^{-5}$ pu or 9.6073×10^{-7} MW^{-1}
$B_{22} = 0.02370$ pu or 0.02370×10^{-2} MW^{-1}

7.8 Economically optimum uc

Time	*Load(MW)*	*Unit Number*			
		1	2	3	4
0–4	20	1	1	1	1
4–8	14	1	1	1	0
8–12	6	1	1	0	0
12–16	14	1	1	1	0
16–20	4	1	0	0	0
20–24	10	1	1	0	0

7.9 Total operating cost (both units in service for 24 hrs) = Rs 1,47,960
Total operating cost (unit 1 put off in light-load period) = Rs 1,45,840

7.10 $P_{G1} = 168.495$ MW
$P_{G2} = 46.96$ MW

CHAPTER 8

8.1 Load on $G_1 = 123$ MW
Load on $G_2 = 277$ MW
System frequency = 50.77 Hz

No load frequencies $= f_{10} = 51\frac{1}{3}$ Hz

$$f_{20} = 51\frac{2}{3} \text{ Hz}$$

8.2 $\Delta f(t) = -0.029 - 0.04\, e^{-0.58t} \cos(1.254\, t + 137.8^\circ)$

8.3 $1/(50\, K_i)$ s

8.5 $$\Delta P_{\text{tie},1}(s) = \left[\frac{100(0.2s^2 + 0.9s + 1)}{80s^5 + 36s^4 + 458s^3 + 866s^2 + 1050s + 35}\right]$$

System is found to be unstable.

CHAPTER 9

9.1 $i_t = 3.14 \sin(314\, t - 66^\circ) + 2.87\, e^{-50t}$, $i_{mm} = 5$ A

9.2 (a) 81°
(b) – 9°

9.3 (i) $I_A = 2.386$ kA
$I_B = 1.75$ kA
(ii) $I_A = 4.373$ kA
$I_B = 1.75$ kA

9.4 8.87 kA, 4.93 kA

9.5 26.96 kA

9.6 6.97 kA

9.7 (a) 0.9277 kA
(b) 1.312 kA
(c) 1.4843 kA
(d) 1.0205 kA, 53.03 MVA
(e) 0.1959 kA

9.8 8.319 kA

9.9 2.39 pu

9.10 132.1, 47.9
136.9, 45.6

9.11 0.6 pu

9.12 $I^f = -j\,8.006$ pu
$I^f_{13} = -j\,4.004$ pu

CHAPTER 10

10.1 (i) $1.732 \angle 210^\circ$
(ii) $2 \angle 0^\circ$
(iii) $1.732 \angle 150^\circ$
(iv) $1 \angle 210^\circ$

10.2 $I_A = j\,1.16$ pu; $V_{AB} = 1.17 \angle 109.5^\circ$ pu;
$V_{BC} = 0.953 \angle -65.4^\circ$ pu; $V_{CA} = 0.955 \angle -113.1^\circ$ pu.

10.3 $V_{a1} = 197.8 \angle -3.3^\circ$ V
$V_{a2} = 20.2 \angle 158.1^\circ$ V
$V_{a0} = 21.61 \angle 10.63^\circ$ V

10.4 $I_{a1} = 19.23 \angle -30^\circ$ A
$I_{a2} = 19.23 \angle 150^\circ$ A
$I_{a0} = 0$ A

10.5 $I_{A1} = 27.87 \angle -30^\circ$ A
$I_{A2} = 13 \angle -44.93^\circ$ A
$I_{A0} = 0$
$I_{ab1} = 16.1$; $I_{ab2} = 7.5 \angle -75^\circ$; $I_{ab0} = 7.5 \angle 75^\circ$ A

10.6 $I_a = 16.16 + j\,1.335$ A
$I_b = -9.24 - j\,10.66$ A
$I_c = -6.93 + j\,9.32$ A
$|V_{n0}| = |V_{a0}| = 40.75$ V

10.7 1500.2 W

CHAPTER 11

11.1 $-j\,6.56$ kA,
$|V_{bc}| = 12.83$ kV, $|V_{ab}| = 6.61$ kV, $|V_{ca}| = 6.61$ kV

11.2 (a) $V_{ab} = V_{ac} = 1.8$ pu, $I_b = I_c = -2\sqrt{3}$ pu
(b) $V_{ab} = V_{ac} = 0.816$ pu, $|I_b| = 5.69$ pu

11.3 (i) $-j\,6.25$ (ii) -4.33 (iii) 6.01 (iv) $-j\,5$ pu
In order of decreasing magnitude of line currents the faults can be listed as
(a) LG (b) LLG (c) 3-phase (d) LL

11.4 0.1936 ohm, 0.581 ohm, -4.33 pu, $j\,5$ pu

11.5 (a) 3.51 pu (b) $V_b = 1.19\angle -159.5^\circ$ pu, $V_c = 1.68\angle 129.8^\circ$ pu
(c) 0.726 pu

11.6 $I_b = -I_G = -2.887$ pu

11.7 (a) $I_Y = -5.79 + j\,5.01$ kA, $I_B = 5.79 + j\,5.01$ kA, $I_G = j10.02$ kA
(b) $I_B = -I_Y = -6.111$ kA, $I_G = 0$

11.8 $I_{ag} = 0$ $\quad I_{am} = -j\,3.51$ pu
$I_{bg} = -j\,2.08$ pu $\quad I_{bm} = -j\,1.2$ pu
$I_{cg} = j\,2.08$ pu $\quad I_{cm} = -j\,1.2$ pu

11.9 5,266 A

11.10 $j\,2.0$ pu

11.11 $I^f = -j\,6.732$ pu, $I_a(\text{A}) = -j\,4.779$ pu,
$I_b(\text{A}) = -j\,0.255$ pu, $I_c(\text{A}) = -j\,0.255$ pu

11.12 0.42 pu, $-j\,9.256$ pu

11.13 $-j\,11.152$ pu, $-j\,2.478$ pu, $-j\,1.239$ pu

11.14 4.737 pu, 1 pu

11.15 $I_2 f = -j\,12.547$ pu, $I_{12} f\,(\text{b}) = -j\,0.0962$ pu

CHAPTER 12

12.1 4.19 MJ/MVA, 0.0547 MJ-s/elect deg

12.2 4.315 MJ/MVA

12.3 40.4 MJ/MVA

12.4 140.1 MW, 130.63 MW, 175.67 MW

12.5 72.54 MW

12.6 $\delta_3 = 58^\circ$

12.7 127.3 MW

12.8 53°. We need to know the inertia constant M to determine t_c.

12.9 The system is unstable

12.10 70.54°, 0.1725 s

12.11 The system is unstable

12.12 63.36°

12.13 The system is stable

12.14 The system is stable

12.15 The system is unstable for both three pole and single pole switching

CHAPTER 13

13.1 (i) $V_j = -72.3$ kV $v_t = 37.77$ kV
$j_r = 0.626$ kA
(ii) $V_r = 72.3$ kV $v_t = 182.3$ kV
$I_r = -3.03$ kV

13.2 $V_2 = V_3 = 4.17$ kV
$j_2 = 8.34$ A, 83.4 A

13.3 Energy transmitted = 88.2 J
$V_r = -199$ kV

13.4 (i) $\alpha_R = 0.5$ (ii) $\alpha_S = -1$
$V_R = 100$ V, $I_s = 1.33$ A

13.5 $\alpha_R = 0$
$V_R = 100$ V, $I_s = 4$ A

13.6 $\alpha_R = 0.5$, $\alpha_s = 0.286$
$V_R = 62.5$ V, $I_s = 0.83$ A

13.7 Junction voltage at 4 $T = 0.848$

CHAPTER 14

14.1 985 kV, 61.8 kΩ

14.2 $(RRRV)_{max} = 10.3$ kV/μs

14.3 1000 A, 26.24 kA, 66.8 kA, 26.24 kA for 4 s

14.4 (a) 18 kV
(b) 11.5 kHz
(c) 0.83 V/μs

CHAPTER 15

15.1 CT Ratio (primary side) 50:5
CT Ratio (secondary side) 500:5
Assuming $I_2 = 0.8\ I_1$, Then Nr/No = 0.222

15.2 Operating time of feeder relay = 0.9 s
Minimum plug setting = 175% (standard value)
Time setting = 0.222

15.3

% Setting	0	10	20	30	40
% Winding	0	41.6	58.9	72	83.2

(*Y* not protected)
The plug setting for 70% protection = 5.2%, which is too low; Restricted earth fault protection is needed

15.4 0.875 s

15.5 (i) 77.94%
(ii) 4.81 ohms

15.6 Relay will not operate
15.7 $200/\sqrt{3} : 5$
15.8 2.9 ohms
15.9 Design problem; no unique answer

CHAPTER 16

16.1 2.15 μF/ph, 12.86 A/ph, 735.04 kVAR, 6.11 kW, 5.62 kV/cm (rms)
16.2 11.73 μF
16.4 4.66 cm

CHAPTER 17

17.1 36.9%, 29.83%, 33.18%, 40.25%, 33%, 31.6% 35.4%, 100%

CHAPTER 18

18.1 57.60 m

CHAPTER 19

19.1 19.12 m
19.3 143.8 kV (line), no loss
19.4 147 kV

CHAPTER 20

20.1 $E_{\text{line-line}} = 95.54$ kV
$X_{cr} = 9.7\ \Omega$
20.2 162.32 kV, 12.63º

CHAPTER 21

21.1 25.5%
21.2 point '*E*'
21.3 $x = 4.08$ km

CHAPTER 22

22.1 (i) $E\text{th} = 1.0770 \angle 21.8º$
(ii) $E\text{th} = 1.2589 \angle 18.52º$
22.2 $E\text{th} = 1.346 \angle 21.801$
22.3 (a) $V_{cr} = 0.707$ pu; $P_{\max} = 0.5$, $\delta = 45º$
(b) $V_{cr} = 0.5$ pu; $V_R/V_S = 0.5$, $Q_{\max} = 0.25$ pu

Index